frontiers | Research Topics

Zoonotic diseases: epidemiology, multi-omics, and host-pathogen interactions

Edited by
Lei Deng, Hong Yin, Kevin S. W. Tan and Anastasios D. Tsaousis

Published in
Frontiers in Microbiology

FRONTIERS EBOOK COPYRIGHT STATEMENT

The copyright in the text of individual articles in this ebook is the property of their respective authors or their respective institutions or funders. The copyright in graphics and images within each article may be subject to copyright of other parties. In both cases this is subject to a license granted to Frontiers.

The compilation of articles constituting this ebook is the property of Frontiers.

Each article within this ebook, and the ebook itself, are published under the most recent version of the Creative Commons CC-BY licence. The version current at the date of publication of this ebook is CC-BY 4.0. If the CC-BY licence is updated, the licence granted by Frontiers is automatically updated to the new version.

When exercising any right under the CC-BY licence, Frontiers must be attributed as the original publisher of the article or ebook, as applicable.

Authors have the responsibility of ensuring that any graphics or other materials which are the property of others may be included in the CC-BY licence, but this should be checked before relying on the CC-BY licence to reproduce those materials. Any copyright notices relating to those materials must be complied with.

Copyright and source acknowledgement notices may not be removed and must be displayed in any copy, derivative work or partial copy which includes the elements in question.

All copyright, and all rights therein, are protected by national and international copyright laws. The above represents a summary only. For further information please read Frontiers' Conditions for Website Use and Copyright Statement, and the applicable CC-BY licence.

ISSN 1664-8714
ISBN 978-2-8325-5572-9
DOI 10.3389/978-2-8325-5572-9

About Frontiers

Frontiers is more than just an open access publisher of scholarly articles: it is a pioneering approach to the world of academia, radically improving the way scholarly research is managed. The grand vision of Frontiers is a world where all people have an equal opportunity to seek, share and generate knowledge. Frontiers provides immediate and permanent online open access to all its publications, but this alone is not enough to realize our grand goals.

Frontiers journal series

The Frontiers journal series is a multi-tier and interdisciplinary set of open-access, online journals, promising a paradigm shift from the current review, selection and dissemination processes in academic publishing. All Frontiers journals are driven by researchers for researchers; therefore, they constitute a service to the scholarly community. At the same time, the *Frontiers journal series* operates on a revolutionary invention, the tiered publishing system, initially addressing specific communities of scholars, and gradually climbing up to broader public understanding, thus serving the interests of the lay society, too.

Dedication to quality

Each Frontiers article is a landmark of the highest quality, thanks to genuinely collaborative interactions between authors and review editors, who include some of the world's best academicians. Research must be certified by peers before entering a stream of knowledge that may eventually reach the public - and shape society; therefore, Frontiers only applies the most rigorous and unbiased reviews. Frontiers revolutionizes research publishing by freely delivering the most outstanding research, evaluated with no bias from both the academic and social point of view. By applying the most advanced information technologies, Frontiers is catapulting scholarly publishing into a new generation.

What are Frontiers Research Topics?

Frontiers Research Topics are very popular trademarks of the *Frontiers journals series*: they are collections of at least ten articles, all centered on a particular subject. With their unique mix of varied contributions from Original Research to Review Articles, Frontiers Research Topics unify the most influential researchers, the latest key findings and historical advances in a hot research area.

Find out more on how to host your own Frontiers Research Topic or contribute to one as an author by contacting the Frontiers editorial office: frontiersin.org/about/contact

Zoonotic diseases: epidemiology, multi-omics, and host-pathogen interactions

Topic editors
Lei Deng — Massachusetts General Hospital, Harvard Medical School, United States
Hong Yin — Lanzhou Veterinary Research Institute, Chinese Academy of Agricultural Sciences, China
Kevin S. W. Tan — National University of Singapore, Singapore
Anastasios D. Tsaousis — University of Kent, United Kingdom

Citation
Deng, L., Yin, H., Tan, K. S. W., Tsaousis, A. D., eds. (2024). *Zoonotic diseases: epidemiology, multi-omics, and host-pathogen interactions*.
Lausanne: Frontiers Media SA. doi: 10.3389/978-2-8325-5572-9

Table of contents

06 Editorial: Zoonotic diseases: epidemiology, multi-omics, and host-pathogen interactions
Lei Deng, Hong Yin, Kevin S. W. Tan and Anastasios D. Tsaousis

09 Geographical distribution and pathogenesis of ticks and tick-borne viral diseases
Taif Shah, Qian Li, Binghui Wang, Zulqarnain Baloch and Xueshan Xia

27 Identification of novel Jingmen tick virus from parasitic ticks fed on a giant panda and goats in Sichuan Province, southwestern China
Lin Huang, Shunshuai Liu, Lu Chen, Fei Wang, Ping Ye, Luoyuan Xia, Baogui Jiang, Hao Tang, Qingyu Zhang, Xiangdong Ruan, Weijun Chen and Jiafu Jiang

36 Erratum: Identification of novel Jingmen tick virus from parasitic ticks fed on a giant panda and goats in Sichuan Province, southwestern China
Frontiers Production Office

37 Evaluation of *Leptospira interrogans* knockdown mutants for LipL32, LipL41, LipL21, and OmpL1 proteins
Luis G. V. Fernandes, Aline F. Teixeira and Ana L. T. O. Nascimento

53 Seroprevalence of human toxocariasis in Latin America and the Caribbean: a systematic review and meta-analysis
Juan R. Ulloque-Badaracco, Enrique A. Hernandez-Bustamante, Esteban A. Alarcón-Braga, Miguel Huayta-Cortez, Ximena L. Carballo-Tello, Rosa A. Seminario-Amez, Alejandra Rodríguez-Torres, Donovan Casas-Patiño, Percy Herrera-Añazco and Vicente A. Benites-Zapata

68 Isolation, characterization, and pathogenicity assessment of *Corynebacterium pseudotuberculosis* biovar equi strains from alpacas (*Vicugna pacos*) in China
Wanyu Meng, Shanyu Chen, Lin Huang, Jinpeng Yang, Wenqing Zhang, Zhijun Zhong, Ziyao Zhou, Haifeng Liu, Hualin Fu, Tingmei He and Guangneng Peng

82 Molecular detection of *Coxiella* spp. in ticks (Ixodidae and Argasidae) infesting domestic and wild animals: with notes on the epidemiology of tick-borne *Coxiella burnetii* in Asia
Abid Ali, Muhammad Kashif Obaid, Mashal M. Almutairi, Abdulaziz Alouffi, Muhammad Numan, Shafi Ullah, Gauhar Rehman, Zia Ul Islam, Sher Bahadar Khan and Tetsuya Tanaka

101 Exploring genetic variability of *Giardia duodenalis* and *Enterocytozoon bieneusi* in raw vegetables and fruits: implications for food safety and public health in Mozambique
Cátia Salamandane, Maria Luísa Lobo, Sónia Afonso, Lihua Xiao and Olga Matos

112 Corrigendum: Exploring genetic variability of *Giardia duodenalis* and *Enterocytozoon bieneusi* in raw vegetables and fruits: implications for food safety and public health in Mozambique
Cátia Salamandane, Maria Luísa Lobo, Sónia Afonso, Lihua Xiao and Olga Matos

113 Comparison of the pathological outcome and disease progression of two *Mycobacterium caprae* experimental challenge models in goats: endobronchial inoculation vs. intranasal nebulization
Cristian Melgarejo, Alex Cobos, Carles Planas, Jaume Fondevila, Maite Martín, Zoraida Cervera, Guillermo Cantero, Xavier Moll, Yvonne Espada, Mariano Domingo, Enric Vidal and Bernat Pérez de Val

125 Clinical characteristics and outcomes of acute kidney injury in patients with severe fever with thrombocytopenia syndrome
Zhongwei Zhang, Xue Hu, Qunqun Jiang, Wenjia Hu, Anling Li, Liping Deng and Yong Xiong

137 Emergence of Marburg virus: a global perspective on fatal outbreaks and clinical challenges
Shriyansh Srivastava, Deepika Sharma, Sachin Kumar, Aditya Sharma, Rishikesh Rijal, Ankush Asija, Suraj Adhikari, Sarvesh Rustagi, Sanjit Sah, Zahraa Haleem Al-qaim, Prashant Bashyal, Aroop Mohanty, Joshuan J. Barboza, Alfonso J. Rodriguez-Morales and Ranjit Sah

156 The two-component system CpxAR is required for the high potassium stress survival of *Actinobacillus pleuropneumoniae*
Jiajia Wan, Rui Zhang, Yizhen Jia, Tingting Xie, Lu Dai, Qing Yao, Wendie Zhang, Huasong Xiao, Xuejun Gao, Jing Huang, Weicheng Bei and Feng Liu

165 Molecular epidemiological investigation of piroplasms carried by pet cats and dogs in an animal hospital in Guiyang, China
Shengchun Wu, Jiao Meng, Fuxun Yu, Caomin Zhou, Bin Yang, Xingxing Chen, Guanghong Yang, Yi Sun, Wuchun Cao, Jiafu Jiang, Jiahong Wu and Lin Zhan

172 Progress of research on the diagnosis and treatment of bone cystic echinococcosis
Yibin Meng, Qian Ren, Jun Xiao, Haohao Sun, Yiping Huang, Yaqing Liu, Shan Wang and Sibo Wang

184 Description of *Mycobacterium pinniadriaticum* sp. nov., isolated from a noble pen shell (*Pinna nobilis*) population in Croatia
Silvio Špičić, Sanja Duvnjak, Bojan Papić, Irena Reil, Snježana Zrnčić, Željko Mihaljević, Šimun Naletilić, Ivana Giovanna Zupičić, Gordan Kompes, Boris Habrun, Ivana Mareković and Maja Zdelar-Tuk

193 First report of spotted fever group *Rickettsia aeschlimannii* in *Hyalomma turanicum*, *Haemaphysalis bispinosa*, and *Haemaphysalis montgomeryi* infesting domestic animals: updates on the epidemiology of tick-borne *Rickettsia aeschlimannii*
Abdul Majid, Mashal M. Almutairi, Abdulaziz Alouffi, Tetsuya Tanaka, Tsai-Ying Yen, Kun-Hsien Tsai and Abid Ali

209 Evaluation of the antibacterial effect of Epigallocatechin gallate on the major pathogens of canine periodontal disease and therapeutic effects on periodontal disease mice
Peijia Song, Yibing Hao, Degui Lin, Yipeng Jin and Jiahao Lin

222 Development and application of an indirect ELISA and nested PCR for the epidemiological analysis of *Klebsiella pneumoniae* among pigs in China
Zengshuai Wu, Na Li, Ziheng Li, Jianlong Wang, Mengmeng Liu, Mengzhu Qi, Shaopeng Wei, Tong Wu, Yu Guo, Junhui Zhu, Hexiang Jiang, Ruixue Xue, Changjiang Sun, Xin Feng, Jingmin Gu, Wenyu Han, Fengyang Li and Liancheng Lei

235 Molecular detection of Rickettsiales and a potential novel *Ehrlichia* species closely related to *Ehrlichia chaffeensis* in ticks (Acari: Ixodidae) from Shaanxi Province, China, in 2022 to 2023
Xue Zhang, Wen Lv, Zhongqiu Teng, Na Zhao, Yue Zhou, Di Ma, Lin Ma, Yuqing Cheng, Jianjun Wei, Jia He, Wenke Ma, Dongli Liu and Tian Qin

245 Discovery and vertical transmission analysis of Dabieshan Tick Virus in *Haemaphysalis longicornis* ticks from Chengde, China
Xiaofeng Xu, Zhihua Gao, Youhong Wu, Hong Yin, Qiaoyun Ren, Jie Zhang, Yongsheng Liu, Shunli Yang, Chimedtseren Bayasgalan, Ariunaa Tserendorj, Xiaolong Yang and Ze Chen

254 Tick-borne *Rickettsia, Anaplasma, Theileria*, and enzootic nasal tumor virus in ruminant, PET, and poultry animals in Pakistan
Anjum Jamil, Ze Yu, Yuxin Wang, Qing Xin, Shan Gao, Muhammad Abdul Wahab, Xiaohu Han and Zeliang Chen

267 *Anaplasma, Bartonella*, and *Rickettsia* infections in Daurian ground squirrels (*Spermophilus dauricus*), Hebei, China
Jing Xue, Si-Si Chen, Ze-Yun Xu, Fang-Ni Wang, Jiangli Wang, Danhong Diao, Luanying Du, Guang-Cheng Xie and Wen-Ping Guo

276 Epidemiological and clinical characteristics of death from hemorrhagic fever with renal syndrome: a meta-analysis
Wei Lu, Lin Kuang, Yuxing Hu, Jialing Shi, Qi Li and Wen Tian

frontiers | Frontiers in Microbiology

TYPE Editorial
PUBLISHED 04 October 2024
DOI 10.3389/fmicb.2024.1454659

Check for updates

OPEN ACCESS

EDITED AND REVIEWED BY
Axel Cloeckaert,
Institut National de recherche pour l'agriculture, l'alimentation et l'environnement (INRAE), France

*CORRESPONDENCE
Lei Deng
✉ cdl931023@163.com

RECEIVED 25 June 2024
ACCEPTED 20 September 2024
PUBLISHED 04 October 2024

CITATION
Deng L, Yin H, Tan KSW and Tsaousis AD (2024) Editorial: Zoonotic diseases: epidemiology, multi-omics, and host-pathogen interactions. *Front. Microbiol.* 15:1454659. doi: 10.3389/fmicb.2024.1454659

COPYRIGHT
© 2024 Deng, Yin, Tan and Tsaousis. This is an open-access article distributed under the terms of the Creative Commons Attribution License (CC BY). The use, distribution or reproduction in other forums is permitted, provided the original author(s) and the copyright owner(s) are credited and that the original publication in this journal is cited, in accordance with accepted academic practice. No use, distribution or reproduction is permitted which does not comply with these terms.

Editorial: Zoonotic diseases: epidemiology, multi-omics, and host-pathogen interactions

Lei Deng[1,2]*, Hong Yin[3], Kevin S. W. Tan[4] and Anastasios D. Tsaousis[5]

[1]Infectious Disease and Microbiome Program, Broad Institute of MIT and Harvard, Cambridge, MA, United States, [2]Center for Computational and Integrative Biology, Massachusetts General Hospital, Boston, MA, United States, [3]African Swine Fever Regional Laboratory, China (Lanzhou) and State Key Laboratory of Veterinary Etiological Biology and Key Laboratory of Veterinary Parasitology of Gansu Province, Lanzhou Veterinary Research Institute, Chinese Academy of Agricultural Sciences, Lanzhou, China, [4]Laboratory of Molecular and Cellular Parasitology, Healthy Longevity Translational Research Programme and Department of Microbiology and Immunology, Yong Loo Lin School of Medicine, National University of Singapore, Singapore, Singapore, [5]Laboratory of Molecular and Evolutionary Parasitology, School of Biosciences, University of Kent, Canterbury, United Kingdom

KEYWORDS

zoonotic diseases, epidemiology, multi-omics, host-pathogen interactions, global health

Editorial on the Research Topic
Zoonotic diseases: epidemiology, multi-omics, and host-pathogen interactions

Zoonotic diseases, which can be transmitted between humans and animals, pose a significant risk to global health. These infections, caused by various microorganisms such as viruses, bacteria, parasites, and fungi, often lead to severe and life-threatening illnesses. However, some infected individuals may remain asymptomatic. Remarkably, almost 60% of human diseases are zoonotic, and at least 75% of emerging infectious diseases are of zoonotic origin.

Despite their impact, many zoonotic diseases are neglected. This Research Topic aims to explore the pathogenesis, molecular evolution, transmission dynamics, and host interaction mechanisms of zoonotic pathogens, providing a platform for innovative research focused on preventing and controlling zoonotic diseases. Within this topic, 17 research articles and five reviews have been published that advanced our knowledge on zoonotic diseases.

Huang et al. investigated tick-borne viruses, particularly the Jingmen tick virus (JMTV), discovering a novel strain, the Sichuan tick virus, with implications for cross-species transmission and co-infection in multiple tick hosts. Through high-throughput sequencing, they identified whole virus genomes from four tick samples, revealing a novel JMTV-like virus with signals of reassortment with other JMTV strains, suggesting a complex interplay of viral evolution in ticks. Shah et al. reviewed several critical tick-borne viruses, such as Bourbon virus (BRBV), Dhori virus (DHOV), Powassan virus (POWV), Omsk hemorrhagic fever virus (OHFV), Colorado tick fever virus (CTFV), Crimean-Congo hemorrhagic fever virus (CCHFV), Heartland virus (HRTV), and Kyasanur forest disease virus (KFDV). They highlighted these viruses' eco-epidemiology, pathogenesis, and clinical manifestations, emphasizing the need for targeted preventive measures. Majid et al. identified *Rickettsia* pathogens in various tick species in Pakistan, highlighting

the need for comprehensive surveillance to assess potential health risks to humans and livestock. Their study revealed the presence of *Rickettsia* in ticks from domestic and wild hosts, underscoring the importance of monitoring tick populations to prevent zoonotic outbreaks.

Ali et al. conducted molecular screening of *Coxiella* spp. in various ticks from different hosts in Pakistan, identifying several new species and highlighting the need for proper surveillance to mitigate health risks. They confirmed the presence of *Coxiella burnetii* and *Coxiella* endosymbionts in multiple tick species, providing crucial insights into the ecology of these pathogens. Wu S. et al. investigated the prevalence and genetic diversity of piroplasmosis in pet dogs and cats in Guiyang. The study confirmed the presence of *Theileria uilenbergi* and *Theileria luwenshuni* in both cats and dogs, highlighting the importance of surveillance in pet populations to control the spread of these pathogens. They found a significant prevalence of these parasites, indicating a potential public health risk. Zhang X. et al. identified several tick-borne pathogens, including *Rickettsia, Anaplasma*, and *Ehrlichia* species, in ticks collected from domestic cattle and goats, emphasizing the need for comprehensive surveillance to mitigate the risk to human and animal health. Their findings provided a detailed genetic analysis of these pathogens, revealing the diversity and prevalence of tick-borne diseases in the region. Xu et al. identified a new Dabieshan tick virus strain, highlighting the need for expanded surveillance to understand its transmission and pathogenicity. Their study discovered the virus in multiple tick species, suggesting a widespread distribution and potential health impact. Jamil et al. investigated the prevalence of tick-borne pathogens (TBPs) in Pakistan. They collected 213 ticks from various animals, identifying five species: *Hyalomma anatolicum*, *Rhipicephalus microplus*, *Hyalomma scupense*, *Rhipicephalus turanicus*, and *Rhipicephalus sanguineus*. The study underscores a broader range of TBPs in Pakistan, highlighting the need for improved control measures to protect livestock and public health.

Fernandes et al. applied CRISPR interference (CRISPRi) to study the pathogenesis and virulence factors of Leptospira, providing insights into leptospiral biology and potential vaccine targets. They used CRISPRi to silence key leptospiral proteins, demonstrating the role of these proteins in bacterial virulence and host interactions. Meng W. et al. focused on *Corynebacterium pseudotuberculosis* strains isolated from alpacas, exploring their antibiotic resistance and genetic properties to understand their risk to livestock. Their study included antibiotic susceptibility tests and genome sequencing, revealing multiple antibiotic resistance genes and virulence factors.

Špičić et al. identified a novel *Mycobacterium* species in mollusks, contributing to the understanding of mycobacterial infections in marine environments. They used genomic and phenotypic analyses to characterize the new species, proposing *Mycobacterium pinniadriaticum* sp. nov. as the new species name.

The research by Wan et al. explores the role of the CpxAR system in *Actinobacillus pleuropneumoniae* under high potassium (K+) stress, which hinders bacterial growth. They found that CpxAR is crucial for cell division in these conditions by upregulating the cell division genes ftsE and ftsX. qRT-PCR showed positive regulation of these genes, and EMSA demonstrated CpxR-P binding to the ftsE promoter. This study is the first to detail the mechanism by which CpxAR confers high-K+ tolerance in *A. pleuropneumoniae*. Wu Z. et al. investigated the prevalence of *Klebsiella pneumoniae* in pigs. They infected mice and pigs with a human-derived *K. pneumoniae* strain and developed an indirect ELISA using KHE protein and a nested PCR method for detection. The ELISA was optimized, showing high sensitivity and specificity, with an infection rate of 27.28% (ELISA) and 19.13% (PCR) in 920 porcine samples. Infection rates correlated with population density, GDP, and tourism. The study highlights the significant prevalence of *K. pneumoniae* in Chinese pigs and its implications for pig health and disease prevention.

Srivastava et al. reviewed Marburg virus disease comprehensively, discussing its pathophysiology, transmission routes, and the need for effective treatments and vaccines. Their review included a detailed analysis of past outbreaks, virus structure, and the current state of clinical management and research.

Melgarejo et al. developed an experimental model of tuberculosis in goats to evaluate new vaccines and treatments. Their study compared intranasal and endobronchial routes of infection, providing insights into the pathogenesis and immune response in goats. It demonstrated the importance of route-specific inoculations to replicate natural infections. Xue et al. investigated the presence of zoonotic pathogens *Anaplasma*, *Bartonella*, and *Rickettsia*, in Daurian ground squirrels in Hebei Province, China. The study highlights the genetic diversity of these bacteria in ground squirrels and notes that six identified species are pathogenic to humans, posing a potential health risk to local populations, particularly herders who are in close contact with these animals.

Ulloque-Badaracco et al. performed a meta-analysis on the seroprevalence of human toxocariasis in Latin America and the Caribbean, offering valuable data for epidemiological surveillance and prevention strategies. Their analysis included over 31,000 participants, identifying key risk factors and providing a comprehensive overview of the disease's prevalence in the region. Salamandane et al. assessed the genetic patterns of *Giardia duodenalis* and *Enterocytozoon bieneusi* in vegetables and fruits in Mozambique, highlighting their public health importance and zoonotic transmission potential. They used nested-PCR methods to detect these pathogens, identifying multiple novel sequences with high zoonotic transmission potential. Meng Y. et al. reviewed the complexities of diagnosing and treating bone cystic echinococcosis, underlining the need for improved diagnostic and therapeutic strategies. Their review covered imaging techniques, serological tests, and treatment options, highlighting the challenges in managing this complex disease.

Song et al. explored the antibacterial and anti-inflammatory effects of epigallocatechin gallate (EGCG) in treating canine periodontal disease, suggesting its potential as a therapeutic agent. They conducted both *in vitro* and *in vivo* experiments, showing that EGCG significantly reduced bacterial load and inflammation in a mouse model of periodontal disease. Lu et al. conducted a meta-analysis of the clinical characteristics of patients who

died from hemorrhagic fever with renal syndrome (HFRS). They analyzed data from 37 articles involving 140,295 patients. The study found that those who died were typically older, more likely to smoke, and had hypertension and diabetes. These patients also exhibited severe symptoms like multiple organ dysfunction, shock, cerebral complications, heart and liver damage, and acute kidney injury. The findings highlight high-risk factors for mortality, aiding in clinical assessment and prognostication. Zhang Z. et al. examined the clinical characteristics and outcomes of acute kidney injury in patients with severe fever with thrombocytopenia syndrome (SFTS), identifying risk factors for poor prognosis. Their study provided detailed clinical data, highlighting the need for early identification and management of AKI in SFTS patients.

In conclusion, significant advances have been made in understanding zoonotic diseases through multi-omics and host-pathogen interaction studies. The research presented here emphasizes the importance of comprehensive surveillance, innovative diagnostic methods, and targeted prevention strategies. Several studies have revealed new insights into the genetic diversity, transmission dynamics, and ecological impacts of zoonotic pathogens. These findings underscore the necessity for larger-scale, interdisciplinary studies to fully understand the complexities of zoonotic diseases and their impact on public health. Future research should focus on integrating data from diverse ecosystems and host species within the One Health framework to develop more effective strategies for controlling zoonotic diseases.

Author contributions

LD: Writing – original draft, Writing – review & editing. HY: Conceptualization, Writing – review & editing. KT: Conceptualization, Writing – review & editing. AT: Conceptualization, Writing – review & editing.

Funding

The author(s) declare that no financial support was received for the research, authorship, and/or publication of this article.

Acknowledgments

ChatGPT, v. 4, a language model developed by OpenAI in San Francisco, CA, USA, helped in language editing and proofreading.

Conflict of interest

The authors declare that the research was conducted in the absence of any commercial or financial relationships that could be construed as a potential conflict of interest.

Publisher's note

All claims expressed in this article are solely those of the authors and do not necessarily represent those of their affiliated organizations, or those of the publisher, the editors and the reviewers. Any product that may be evaluated in this article, or claim that may be made by its manufacturer, is not guaranteed or endorsed by the publisher.

frontiers | Frontiers in Microbiology

TYPE Review
PUBLISHED 24 May 2023
DOI 10.3389/fmicb.2023.1185829

Check for updates

OPEN ACCESS

EDITED BY
Hong Yin,
Chinese Academy of Agricultural Sciences,
China

REVIEWED BY
Dasiel Obregon,
University of Guelph, Canada
Shu Shen,
Chinese Academy of Sciences, China

*CORRESPONDENCE
Xueshan Xia
✉ oliverxia2000@aliyun.com

RECEIVED 14 March 2023
ACCEPTED 04 May 2023
PUBLISHED 24 May 2023

CITATION
Shah T, Li Q, Wang B, Baloch Z and Xia X (2023) Geographical distribution and pathogenesis of ticks and tick-borne viral diseases.
Front. Microbiol. 14:1185829.
doi: 10.3389/fmicb.2023.1185829

COPYRIGHT
© 2023 Shah, Li, Wang, Baloch and Xia. This is an open-access article distributed under the terms of the Creative Commons Attribution License (CC BY). The use, distribution or reproduction in other forums is permitted, provided the original author(s) and the copyright owner(s) are credited and that the original publication in this journal is cited, in accordance with accepted academic practice. No use, distribution or reproduction is permitted which does not comply with these terms.

Geographical distribution and pathogenesis of ticks and tick-borne viral diseases

Taif Shah[1,2], Qian Li[1,2], Binghui Wang[1,2], Zulqarnain Baloch[1,2] and Xueshan Xia[1,2]*

[1]Faculty of Life Science and Technology, Kunming University of Science and Technology, Kunming, Yunnan, China, [2]Provincial Center for Molecular Medicine, Kunming, China

Ticks are obligatory hematophagous arthropods that harbor and transmit infectious pathogens to humans and animals. Tick species belonging to *Amblyomma*, *Ixodes*, *Dermacentor*, and *Hyalomma* genera may transmit certain viruses such as Bourbon virus (BRBV), Dhori virus (DHOV), Powassan virus (POWV), Omsk hemorrhagic fever virus (OHFV), Colorado tick fever virus (CTFV), Crimean-Congo hemorrhagic fever virus (CCHFV), Heartland virus (HRTV), Kyasanur forest disease virus (KFDV), etc. that affect humans and certain wildlife. The tick vectors may become infected through feeding on viraemic hosts before transmitting the pathogen to humans and animals. Therefore, it is vital to understand the eco-epidemiology of tick-borne viruses and their pathogenesis to optimize preventive measures. Thus this review summarizes knowledge on some medically important ticks and tick-borne viruses, including BRBV, POWV, OHFV, CTFV, CCHFV, HRTV, and KFDV. Further, we discuss these viruses' epidemiology, pathogenesis, and disease manifestations during infection.

KEYWORDS

ticks, tick-borne viruses, epidemiology, pathogenesis, manifestations

1. Overview

Ticks are obligatory hematophagous parasites, harboring and transmitting infectious pathogens to humans and animals in temperate North America, Europe, and Asia. Ticks are responsible for more than 95% of vector-borne diseases in the United States (Rosenberg et al., 2018). Tick-borne diseases have a significant economic impact, especially in developing countries (Estrada-Peña and Salman, 2013). Tick-borne diseases affect approximately 80% of the world's cattle population, with an estimated cost of around $13.9–18.7 billion (De Castro et al., 1997). For country like Tanzania, the economic losses due to tick-borne disease has been quantified to be $364 million, with an estimated mortality of 1.3 million cattle (Kivaria, 2006). In the United States, the Powassan virus (POWV) transmission has been seen as evidence of an emerging trend, spreading in new areas at a comparable rate (Hermance and Thangamani, 2017). Tick-borne diseases, particularly Crimean-Congo hemorrhagic fever (CCHF), are persistent problems at the One Health interface between humans, wildlife, and the environment (Anderson and Armstrong, 2012; Sorvillo et al., 2020). These conditions are often ignored, and receive less attention and dedicated public health funding than directly transmitted zoonotic viruses such as the recent COVID-19 pandemic (WHO, 2022b). Tick vector control's ability to reduce tick populations is limited by the availability of large-scale mitigation strategies and preventive control measures, demanding additional research to develop effective tick control strategies for human and wildlife (Eisen and Stafford, 2021). Current prevention and clinical

treatment are limited, despite their severe prognosis and high fatality rate. Many tick-borne infections in humans are also difficult to detect and diagnose, due to the broad clinical presentation of many tick-borne diseases, the lack of reliable diagnostic tests, and the multi-tiered approaches required to confirm pathogens (Fatmi et al., 2017; Bush and Vazquez-Pertejo, 2018). In brief, the expansion of tick populations and increasing incidence of tick-borne diseases are bringing ticks to the attention of public health professionals.

Among the tick families, i.e., hard ticks (Ixodidae), soft ticks (Argasidae), and Nuttalliellidae, Ixodidae is the most prominent family, including genera like *Amblyomma*, *Haemaphysalis*, *Ixodes*, *Rhipicephalus*, etc., and over 700 species worldwide (Brites-Neto et al., 2015; Dantas-Torres and Otranto, 2022). *Ixodes persulcatus* (Figure 1A) distribution has been reported in north-eastern Europe, some parts of Russia, China, Korea etc. (Topp et al., 2022); *I. ricinus* (Figure 1B) in Europe and northern Africa; *Dermacentor reticulatus* (Figure 1C) in some parts of Europe; *I. scapularis* (Figure 1D); *D. andersoni* (Figure 1E); and *Amblyomma americanum* (Figure 1F) in Northern America. Most members of the Ixodidae, particularly *I. scapularis* (Figure 2C), *A. americanum* (Figure 2D), *D. andersoni* (Figure 2E), and *Haemaphysalis spinigera* (Figure 2F) go through four different life stages, i.e., eggs, larvae, nymphs, and adult ticks (WHO, 2020). Among the two possible vertical transmission routes of tick-borne viruses (TBVs), transstadial transmission is the sequential passage that is critical for tick survival and life cycle completion, whereas transovarial transmission occurs when viruses are transmitted from an infected tick to their offspring, i.e., the virus remains in the egg after being laid by an infected female tick and eventually infects the offspring (Figures 2A,B; Barker and Reisen, 2019).

TBVs use a variety of mechanisms to evade host immune responses for successful tissue colonization in humans and animals (Charrel et al., 2004; Belikov et al., 2014; Brites-Neto et al., 2015). Despite low viremia in infected vertebrates, most organ damage is caused by host inflammatory responses; for example, induced inflammatory responses in TBV infections can increase vascular permeability, neurological complications, and even death in severe cases (Bente et al., 2013; Hermance et al., 2016; Bhatia et al., 2020; Campbell and Krause, 2020; Figure 3). Nonetheless, case reports and preliminary field studies published in the last decade indicate that TBVs present in different regions are underdiagnosed or misdiagnosed

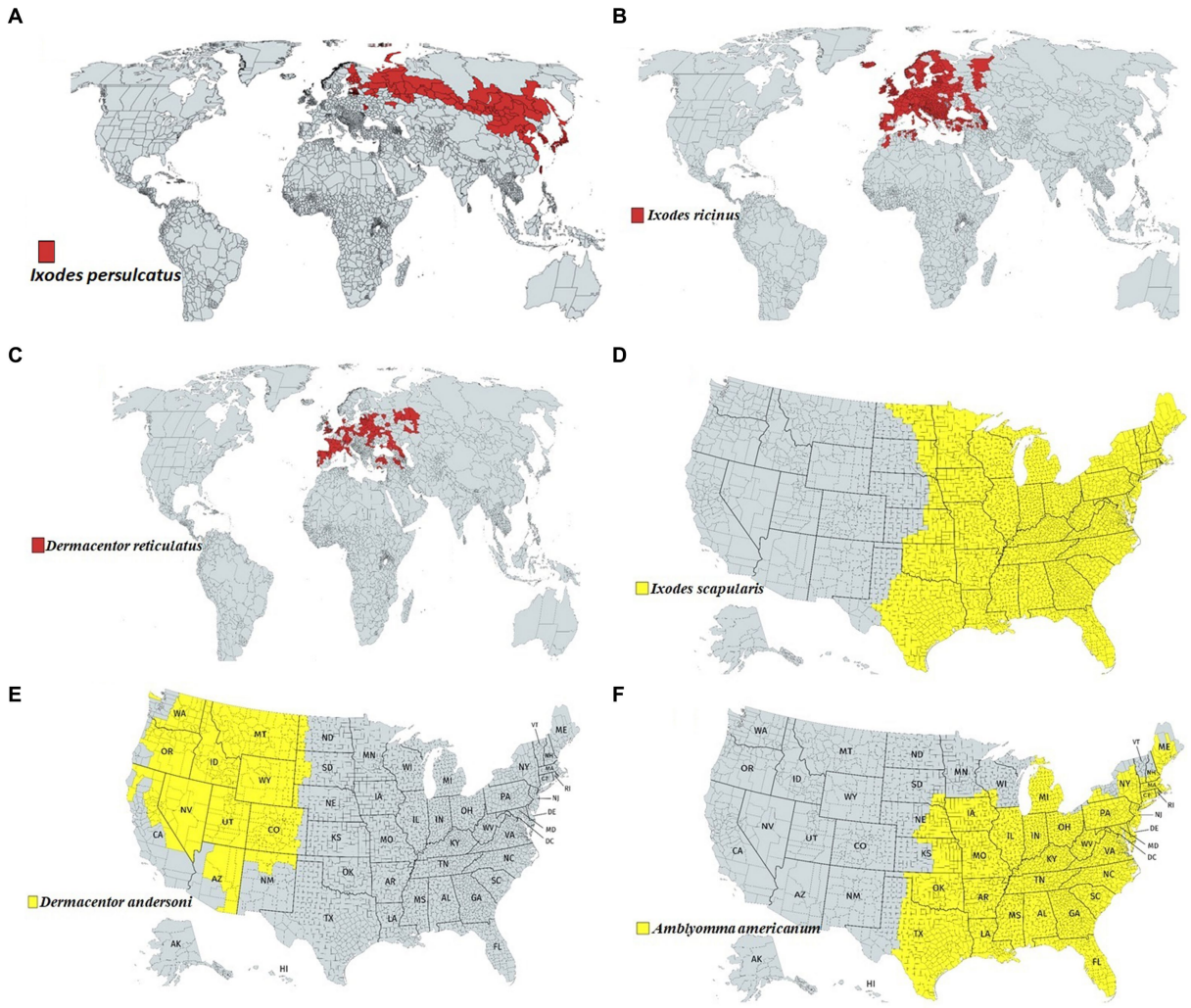

FIGURE 1
Approximate global distribution of some medically important ticks. **(A)** Ixodes persulcatus distribution in north-eastern Europe, some parts of Russia, China, Korea etc. **(B)** Ixodes ricinus in some parts of Europe and northern Africa. **(C)** Dermacentor reticulatus in some parts of Europe. **(D)** Ixodes scapularis, **(E)** Dermacentor andersoni and **(F)** Amblyomma americanum in Northern America.

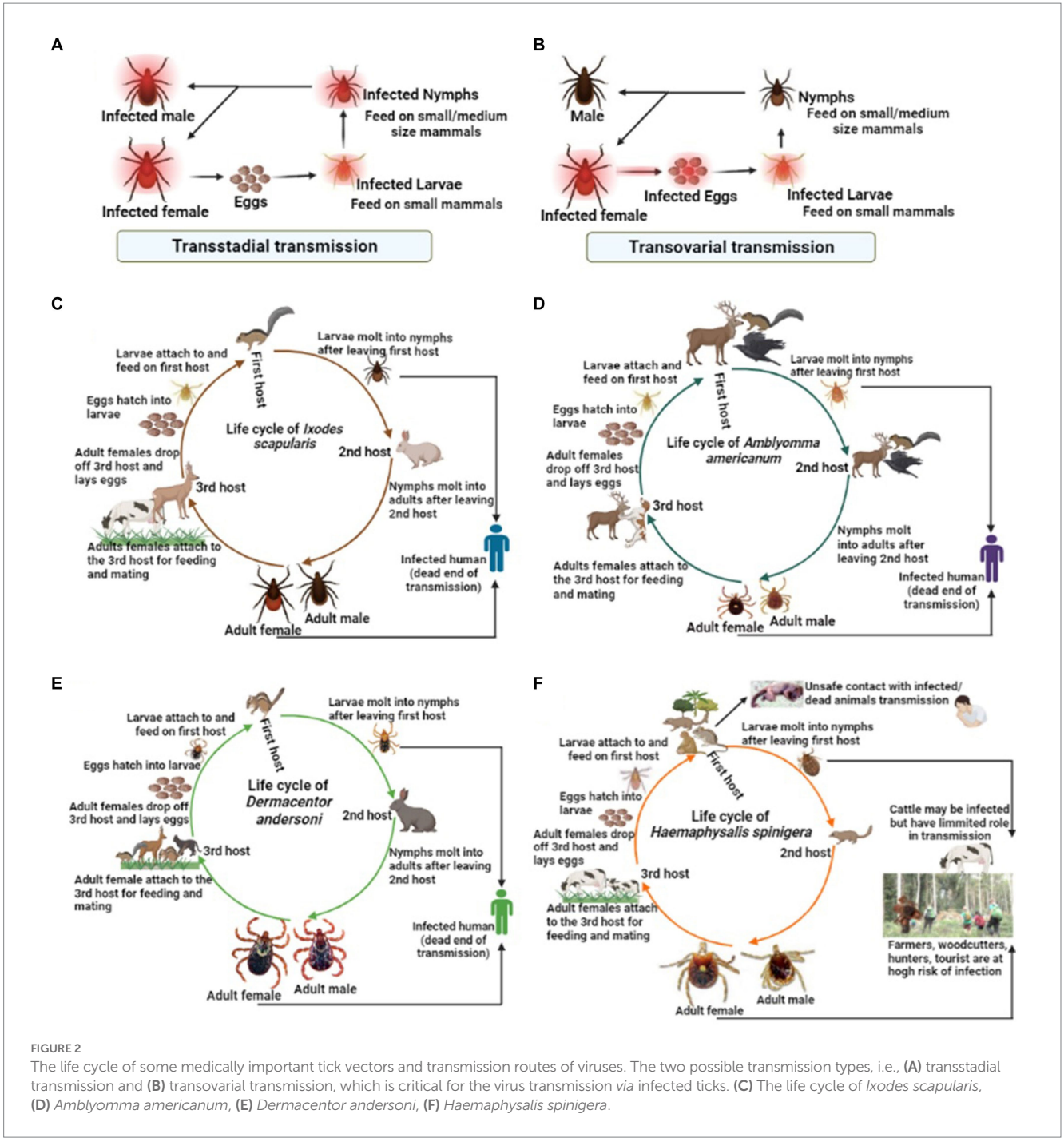

FIGURE 2
The life cycle of some medically important tick vectors and transmission routes of viruses. The two possible transmission types, i.e., **(A)** transstadial transmission and **(B)** transovarial transmission, which is critical for the virus transmission *via* infected ticks. **(C)** The life cycle of *Ixodes scapularis*, **(D)** *Amblyomma americanum*, **(E)** *Dermacentor andersoni*, **(F)** *Haemaphysalis spinigera*.

due to their complex behaviors. Although the epidemiological characteristics of ticks and TBVs are well documented, understanding pathogenesis, notably host immune responses to the virus and their impact on disease outcomes, is limited. The main focus of this review is to summarize the most recent advances in TBV diseases, with a focus on emerging diseases that pose a public health threat around the world.

This review thus emphasizes the epidemiological characteristics of some medically important tick vectors and TBVs, including Bourbon virus (BRBV), POWV, Omsk hemorrhagic fever virus (OHFV), Colorado tick fever virus (CTFV), Crimean-Congo hemorrhagic fever virus (CCHFV), Heartland virus (HRTV), and Kyasanur forest disease virus (KFDV) (Figure 4A). Details on TBVs' classification and distribution are shown in Table 1. For this review, we have drawn data from existing literature, our basic research, and public health experience with TBV diseases. Further, we discuss the epidemiology, pathogenesis, and disease manifestations of some medically important TBVs.

2. Bourbon virus

BRBV is a member of the *Orthomyxoviridae* family, genus *Thogotovirus*, infecting humans and animals *via* tick bites in most

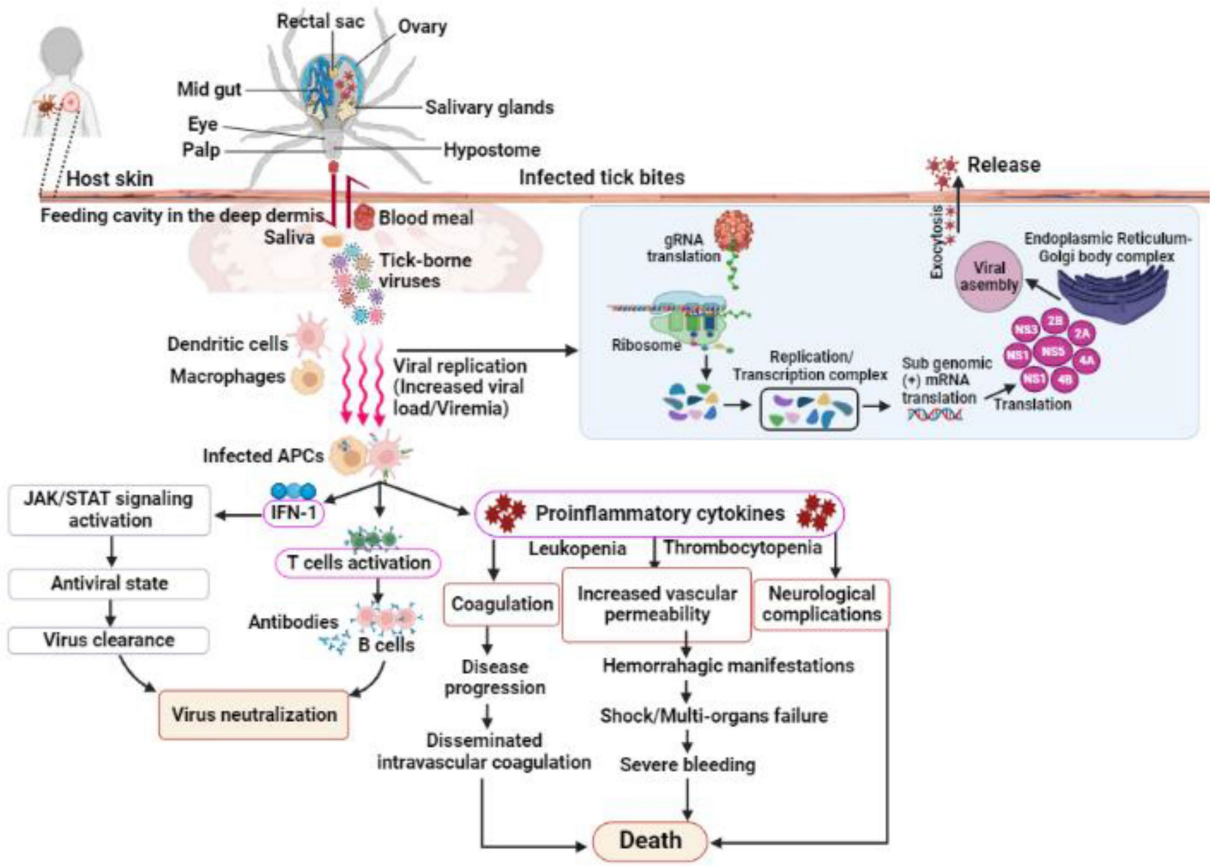

FIGURE 3
Shows the infection, replication and pathogenesis of TBVs in hosts taking *flavivirus* as an example. Ticks transmit the virus to susceptible host while feeding. TBVs enter the host cell *via* endocytosis or by fusing E protein to the heparan-sulfate and glycosaminoglycan receptors (found on vertebrates and tick cells). After entering the host cell, the virus fuses with the endosomal membrane and releases its capsid into the cytoplasm. In the infected cell cytoplasm, the viral RNA is unveiled and transcribed into proteases, which cleave the polypeptides into several NSPs, such as NS1, NS3, 2A, 2B, 4A, 4B, etc. RNA-dependent RNA polymerase and helicases work together to produce gRNA and RNAs, which are both required for viral replication and transcription. The newly synthesized viral RNA is translated, producing envelopes, capsids, membrane proteins, and other components that are then transported to the E.R-Golgi body complex for virion assembly. These virions coat the lipid bilayer completely, mature, and are exocytosed from the cytoplasm of the infected cell. Following transmission from an infected tick, the TBVs replicate and induces inflammatory responses in infected hosts, resulting in clinical signs and symptoms. These viruses use a variety of mechanisms to evade host immune responses and colonize host tissues. In some cases, the host immune responses to TBVs, particularly pro-inflammatory cytokines, can cause neurological and cardiovascular disorders during persistent infections.

parts of Africa, the Middle East, and Europe (Bai et al., 2019; Fuchs et al., 2019). Viruses in this family have filamentous, rounded, enveloped, segmented negative-sense ssRNA genomes comprising six genes, encoding viral polymerase basic protein 1 (PB-1), polymerase basic protein 2 (PB-2), polymerase acidic protein (PA), a matrix protein, a nucleoprotein, and a surface glycoprotein (Kosoy et al., 2015). The increased prevalence of BRBV in the last decade emphasizes the importance of tick surveillance; for example, *Haemaphysalis longicornis* is an important tick species in eastern Asia, transmitting viral pathogens to humans and animals (Rainey et al., 2018). In Ehime, Japan, researchers isolated a novel Oz virus (a close relative of BRBV) that efficiently replicated and caused a cytopathic effect in Vero cells. Furthermore, after intracerebral inoculation, OZV replicates in BHK-21 and DH82 cells and causes high mortality in suckling mice (Ejiri et al., 2018). The first sighting of the *H. longicornis* tick that transmits BRBV was on a sheep in New Jersey, and later on, the tick was reported in New Jersey, as well as in the eastern United States and Arkansas (Rainey et al., 2018). Advanced diagnostic methods, such as the IgM antibody capture-enzyme-linked immunosorbent assay (MAC-ELISA) (Martin et al., 2000; Piantadosi and Kanjilal, 2020) and microsphere immunoassay (MIA) coated with recombinant viral antigens (Johnson et al., 2007; Basile et al., 2013), are recommended for BRBV detection. In severe cases, no specific treatments or vaccines are available to prevent BRBV infection; however, disease symptoms can be treated with an intravenous fluid infusion. Because the symptoms overlap (coinfections acquired *via* tick bites carrying BRBV), proper diagnosis is required to understand preventive strategies. Future research into the transmission and underlying pathogenic mechanisms of BRBV would aid in our understanding of their ecology.

2.1. Epidemiology

The BRBV was first isolated from a hospitalized 50-year-old man's blood samples after he died in Kansas, United States (Kosoy et al.,

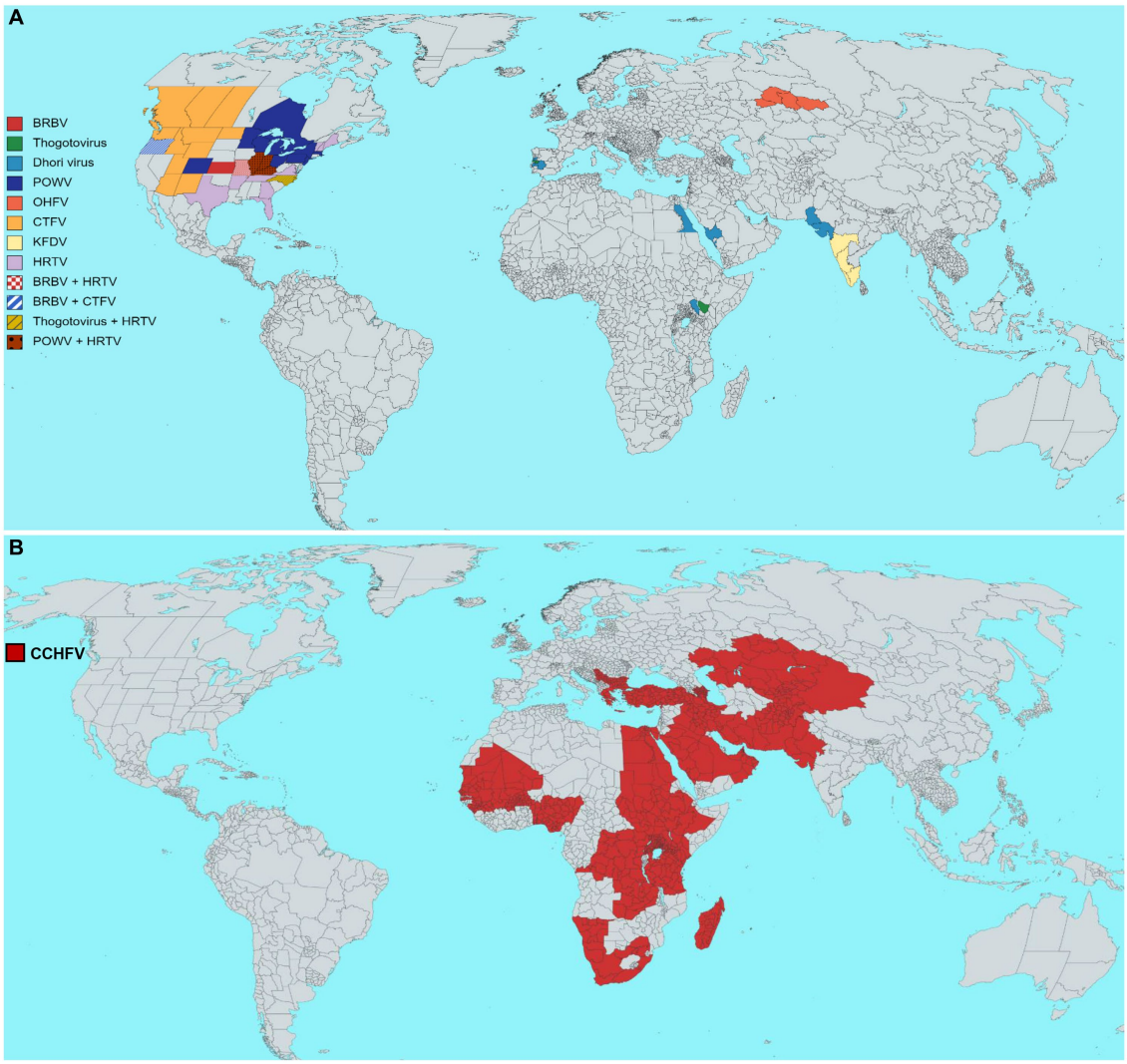

FIGURE 4
Estimated geographical distribution of selected tick-borne viruses (TBVs) of public health relevance. **(A)** Distribution of Bourbon virus (BRBV), *Dhori virus* (family *Orthomyxoviridae*, genus *Thogotovirus*), Powassan virus (POWV), Omsk hemorrhagic fever virus (OHFV), Colorado tick fever virus (CTFV), Kyasanur forest disease virus (KFDV), Heartland virus (HRTV). **(B)** The global distribution of the Crimean-Congo hemorrhagic fever virus (CCHFV). Each virus distribution has been shown according to the guidelines of WHO, the United States Centers for Disease Control and Prevention, and the European Center for Disease Prevention and Control.

2015). Subsequently, two more deaths were reported from the BRBV (Miller, 2018; Vallbracht et al., 2018), and two humans recovered after treatment (Savage et al., 2017; Miller, 2018). The BRBV is genetically similar to the DHOV, isolated from a man in India (Bricker et al., 2019). A new *Oz-virus* isolated in Japan (Ejiri et al., 2018) revealed a close association with the previously identified BRBV (Fuchs et al., 2022). A study reported a high BRBV prevalence in raccoons (50%) and white-tailed deer (86%) in Missouri, USA (Jackson et al., 2019). During tick surveillance in Bourbon County and neighboring southern Linn County, 20,639 host-seeking ticks were collected for the detection of BRBV, and it was found that the detection of BRBV in humans after lone star tick *A. americanum* bites lends support to the theory that *A. americanum* serves as a vector for BRBV transmission to humans and wildlife. In a study, nucleotide sequences revealed similarities among *Thogotovirus* European, Asian, and African isolates (Kuno et al., 2001). A survey in Missouri, United States, discovered BRBV-neutralizing antibodies in human sera. Only three of the 440 human sera tested for BRBV were positive, indicating BRBV circulation in the region (Bamunuarachchi et al., 2022). In North Carolina, the detection of BRBV antibodies in white-tailed deer (Komar et al., 2020) aids in identifying new TBVs in the area (Hubálek and Rudolf, 2012).

2.2. Pathogenesis, and disease manifestations

According to research findings, *A. americanum* may be infected with the BRBV at the larva or nymph stages (Spare et al., 2021; Aziati et al., 2022). Multiple BRBV detections in *A. americanum* indicate that these viruses have similar life cycles and routes of transmission (Miller, 2018; Savage et al., 2018). *Thogotovirus* replication begins with

TABLE 1 Characteristics of some medically important tick-borne viruses.

Virus name	Classification (family, genus)	Genome description	Distribution	Principal tick vector
Bourbon virus (BRBV)	*Orthomyxoviridae*, *Thogotovirus*	Segmented negative-stranded RNA	Eastern Asia, China, Japan	*Haemaphysalis longicornis*
Powassan virus (POWV)	*Flaviviridae*, *Flavivirus*	Positive stranded RNA	North America, Russian Federation	*Ixodes scapularis, Ixodes cookei*
Deer tick virus (DTV)	*Flaviviridae*, *Flavivirus*	Positive stranded RNA	North America	*Ixodes scapularis*
Omsk hemorrhagic fever virus (OHFV)	*Flaviviridae*, *Flavivirus*	Non-segmented positive ssRNA	Western Siberian regions	*D. reticulatus*, *Ixodes persulcatus*
Colorado tick fever virus (CTFV)	*Spinareoviridae*, *Coltivirus*	segmented double-stranded RNA	Western America, Canada	*Dermacentor andersoni*
Crimean Congo hemorrhagic fever virus (CCHFV)	*Bunyaviridae*, *Nairovirus*	Tri-segmented negative-stranded RNA	Asia, Africa, Eastern Europe	*Hyalomma marginatum*
Heartland virus (HRTV)	*Bunyaviridae*, *Phlebovirus*	Tri-segmented negative-stranded RNA	North America	*Amblyomma americanum*
Kyasanur forest disease virus (KFDV)	*Flaviviridae*, *Flavivirus*	Positive stranded RNA	Southern India	*Haemaphysalis spinigera*

the viral glycoprotein binding to the host cell's receptors, followed by virus entry *via* clathrin-mediated endocytosis. BRBV is then transported to the endosome, where low pH triggers the viral genome toward the nucleus for transcription and replication (SIB, 2022). Understanding the pathogenesis of BRBV and the protective immune responses of the host cell is critical for disease prevention and control. BRBV can infect polarized human airway epithelia but not foreskin fibroblast cells because these cells may have a strong IFN response against the viral infection (Ryu et al., 2010), therefore, may be resistant to such virus infection. In addition, IFN-α2a and IFN-γ treatment elicits antiviral immunity that suppresses BRBV propagation (Fuchs et al., 2019). MRI findings show basal ganglia, brainstem, and cerebellum involvement in POWV-infected patients (Piantadosi et al., 2016). In contrast, DHOV-infected Institute of Cancer Research (ICR) mice provided overall pathological and immunological reactions to DHOV infection (Li et al., 2008). After DHOV infection, increased levels of pro-inflammatory cytokines and chemokines were found in the liver, lungs, and sera of mice (Li et al., 2008), providing a true alternative animal model for studying virus pathophysiology and potential treatment (Li et al., 2008). Adult mice infected with the DHOV intranasally, subcutaneously, or intraperitoneally developed fatal illnesses with obvious clinical and pathologic findings. In addition, hepatocellular necrosis and steatosis were found outside of the lungs, and widespread fibrinous necrosis in lymphoid organs was marked by severe lymphocyte loss, karyorrhexis, and neuronal degeneration in the brain. Because of its biosafety level 2 status and its pathological effect in mice, the DHOV may provide a low-cost, relatively safe, and realistic animal model for revealing viral pathogenesis and management studies (Mateo et al., 2007). *In vitro,* growth shows increased BRBV replication in a variety of cell lines, including monkey kidney cells (LLC-MK2 and Vero E6), frog (XLK-WG), hamster (BHK21Cl-15), duck embryo (DE), human (HeLa and HUH-7), Aedes, Anopheles (AP-61, C6/36, CCL-125, C7/10,), *Dermacentor* ANE58, DAE15, *Hyalomma*, and *Amblyomma* RAE/CTVM1, HAE/CTVM9 AVL/CTVM17 (Lambert et al., 2015). Infected individuals have experienced fatigue, nausea, fever, headache, vomiting, leukopenia, maculopapular rashes, and thrombocytopenia (Miller, 2018; Savage et al., 2018). Recently, the effective use of favipiravir medication in mice (Bricker et al., 2019), suggests a possible treatment for BRBV infection.

3. Powassan virus

POWV is a type of *tick-borne flavivirus* (TBFV), first isolated from a human who died from encephalitis in Powassan, Ontario, Canada, in 1958 (Goethert et al., 2021). Later, POWV was classified into two genetically and ecologically distinct lineages: Lineage-I (the prototype POWV) and Lineage-II (also known as the *deer tick virus*) (Goethert et al., 2021). The *flavivirus* family has an ssRNA genome (about 11 kb) with a 5′ UTR (loops A and B) and a 3′ UTR that becomes infectious when it enters the host cell (Choi, 2021). *Flavivirus* attaches its surface glycoprotein to the host cell receptors, such as heparan-sulfate, laminin-binding protein, etc. The fusion of virus-containing vesicles with endosomes causes nucleocapsid release into the cytoplasm, where viral genomic RNA is translated into a single polypeptide at endoplasmic reticulum-associated ribosomes. Cellular and viral proteases process the newly synthesized structural and non-structural proteins into new virions. The mature virions exit from the cell cytoplasm *via* exocytosis. Except for some morphological differences between tick cells and the membranous structures of infected vertebrate cells, virus replication in mammals and ticks exhibits similar mechanisms in the cytoplasm and the formation of membranous replication compartments (Mackenzie, 2005; Bollati et al., 2010). Except for a few human isolates, the majority of lineage-I isolates from northern America have come from *Ixodes cookei* and their hosts (such as groundhogs, skunks, or red squirrels; Mostafa and Dean, 2022), suggesting the need for a deep molecular-level investigation to understand their underlying association with ticks and vertebrate hosts.

3.1. Epidemiology

POWV Lineage-II has been primarily associated with *Ixodes scapularis* ticks and white-footed mice in northern and north-central America (Ebel et al., 1999; Brackney et al., 2008; El Khoury et al., 2013) before transmission to humans and other vertebrates. Evidence of POWV incidence has been reported in the United States (Goethert et al., 2021), Canada, Primorsky krai of Russia (L'vov et al., 1974; Leonova et al., 2009), Alaska and New Mexico (Deardorff et al., 2013). Between 2003 and 2018, over 106 POWV meningoencephalitis cases were reported, with a 15% mortality rate. The recent emergence of Powassan encephalitis in North America (Campbell and Krause, 2020) was most likely attributed to the POWV lineage-II transmitted to humans *via I. scapularis* bites (Goethert et al., 2021). A 50 to 59-year-old male from Windham, Connecticut, United States, was hospitalized with a known tick bite history and a central nervous system (CNS) illness. Although POWV, particularly lineage II, is rare, with only a few dozen cases reported in the United States each year, it is considered a serious public health threat due to its potential for severe illness and death (Ebel, 2010; Piantadosi et al., 2016; Mlera et al., 2017). POWV has also been linked to human disease in eastern Russia (Deardorff et al., 2013). Other closely related POWV serogroups were reported in Siberia, India, the United Kingdom, Ireland, Norway, Spain, Malaysia, and Saudi Arabia (Calisher et al., 1989). The post-infection complications involve damage to the patient's CNS and other body organs (Goethert et al., 2021). Following the identification of the first human case, the geographic distribution of the POWV revealed high transmission with a higher fatality rate (over 30%) (Goethert et al., 2021). The adaptation of the POWV to invertebrate and vertebrate hosts directly influences the pathogen's transmission in a specific area. Other factors, such as climate change, global warming, and agricultural practices, influence POWV's geographic distribution (Lasala and Holbrook, 2010; Ostfeld and Brunner, 2015). Migratory birds may also aid in transmitting *Ixodes* species and their associated POWV over long distances (Waldenström et al., 2007).

3.2. Pathogenesis, and disease manifestations

POWV is transmitted through *Ixodes* species (*I. cookei*, *I. scapularis*, and *I. marxi*) after feeding on infected rodent blood (Ebel and Kramer, 2004). The primary POWV replication site is close to the tick bite, followed by the migration of the virus to lymph nodes *via* dendritic cells and macrophages, resulting in increased viral load/viremia in infected female BALB/c mice (Hermance et al., 2016). In the case of a neurotropic infection, POWVs can cross the blood–brain barrier and damage neurons (Belikov et al., 2014). A study investigated POWV pathogenesis using C57BL/6 mice. After footpad inoculation, infected mice exhibited severe infection with 100% mortality (Santos et al., 2016). In addition, immunofluorescence detected meningoencephalitis with mononuclear cell infiltration, activated microglia, and a polio-like disease. Moreover, the pathological analysis showed increased splenic macrophage counts, exploring the spleen's role in POWV pathogenesis (Santos et al., 2016). A biopsy was performed to investigate the skin at the POWV-positive tick bite site. The findings showed that increased neutrophils, macrophages, dendritic cells, and mononuclear cells infiltrated the infected areas, resulting in a transient viremia stage that led to multiple organ dissemination (Hermance et al., 2016). The virus crosses the blood–brain barrier during the viremia stage. TNF-α may also be important in modulating the permeability of the POWV blood–brain barrier (Suthar et al., 2013). Although the exact underlying molecular mechanism of this blood–brain barrier crossing is unknown; however, brain capillary endothelium's role in this mechanism cannot be ignored (Suthar et al., 2013). In the neurological stage of infection, POWV targets neurons and glial cells in the CNS (Kemenesi and Bányai, 2019). Surprisingly, rat astrocytes (a type of neuroglia in the CNS) resist POWV-mediated cell death by eliciting a pro-inflammatory IFN-α response, indicating dormant infection in rodent species (Potokar et al., 2019). The astrocyte's resistance capacity may keep the enzootic transmission cycle going through long-term illnesses. POWV hemorrhagic disease with liver and spleen tropism can cause viscerotropic disease (Kemenesi and Bányai, 2019). *I. ricinus*-associated POWV modulates dendritic cell responses, pro-inflammatory cytokines, TNF-α, IL6, and immune cells at the biting site (Kemenesi and Bányai, 2019). The pattern-recognition receptors (PRRs) (host cells express helicases that function similarly to PRRs) and toll-like receptors recognize the POWV pathogen (Diamond et al., 2009; Clarke et al., 2021). These PRRs induce pro-inflammatory cytokines, IFN-α, and dendritic cells to mount an immune response against the invading POWV (Kawai and Akira, 2006; Kemenesi and Bányai, 2019). Viral recognition by dendritic cells regulates multiple pathways, including increased expression of MHC-II, T-lymphocytes (T helper and T cytotoxic cells), pro-inflammatory cytokines, and chemokines *via* molecular signaling (Masson et al., 2008; Diamond et al., 2009; Clarke et al., 2021), as determined in acute human infections (Blom et al., 2015). Another study reported a significant response of natural killer cells against POWV infection in humans (Blom et al., 2016). The antibody response in POWV diseases appears at the end of the viremia phase when IgM levels rise within 1–2 days of infection. On the other hand, IgM titers show a slight increase in secondary infections, whereas the IgG response is rapid and effective in eliminating POWV infection (Kemenesi and Bányai, 2019). Infected individuals experience flu-like symptoms, i.e., chills, headache, mild fever, sore throat, neurological complications, apnea, cognitive deficits, dysarthria, encephalitis, memory impairment, spasticity, and psychosis. Clinical diagnosis is generally based on symptoms, signs, and a person's exposure history to ticks. According to serological diagnosis, a fourfold increase in POWV-specific IgG makes the presence of POWV in blood serum, tissue, or cerebrospinal fluid standard for laboratory diagnosis. IgM, which appears 6–14 days following infection, can be detected *via* ELISA (Kemenesi and Bányai, 2019). Further, the presence of POWV antibodies in patient serum at the CDC Laboratory in Ft. Collins, Colorado, emphasizes the need to adopt preventive measures to avoid infections (CDC, 2022). Due to the lack of effective medications/vaccines for Powassan virus prevention, people should be educated on how to avoid tick bites by treating their clothing with permethrin solution after outdoor activities in tick-endemic areas (Connally et al., 2019). People should also be educated on how domestic animals or pets can bring ticks into their homes, and a thorough tick inspection of animals after outdoor activities is recommended.

4. Omsk hemorrhagic fever virus

OHFV is a type of *flavivirus* that causes hemorrhagic fever primarily in the western Siberian region, including Omsk, Novosibirsk, Kurgan, and Tyumen (Růžek et al., 2010; Zhang et al., 2019). Ticks (*D. reticulatus*, *D. marginatus*, and *I. persulcatus*) transmit OHFV to humans and animals after feeding on infected hosts (Wagner et al., 2022). The *D. reticulatus* has evolved several extraordinary characteristics; for example, it has a high reproduction rate, a rapid life cycle completion, can survive underwater for months, and has a diverse host range (Földvári et al., 2016), which could enable OHFV transmission outside Russia (Wagner et al., 2022). In Russia, *Dermacentor* ticks serve as parasites that feed on small mammals, wild ungulates, domestic animals, and humans throughout their life cycle (Růžek et al., 2010), as shown in Figure 1C. According to evidence, ticks transmit OHFV to rodents (muskrats, narrow-skulled voles, and water voles) after feeding on an infected host. Moreover, OHFV has also been isolated from mosquitoes, *Coquilletidia richiardii*, *Ochlerotatus excruciates*, and yellow pygmy rice rat, *Oligoryzomys flavescens* (Wagner et al., 2022). Findings also show that OHFV isolated from different ticks and hosts differs from the early isolated strains (Růžek et al., 2010; Zhang et al., 2019).

4.1. Epidemiology

In mammalian cell lines, OHFV induces cytotoxic effects, i.e., changes in the cell through oxyphilic cytoplasmic inclusion formation (Růžek et al., 2010). It was speculated that the introduction of muskrats to Siberia might be responsible for the OHFV emergence, as the area was disease-free before (Růžek et al., 2010). Russians and Kazakhstanis have reportedly been aware of OFHV's chronic and fatal infections (Ruzek et al., 2013; Wagner et al., 2022). Recently, Wagner and researchers reported OHFV incidence outside Russia (i.e., in the Republic of Kazakhstan) (Wagner et al., 2022). It was speculated that the virus could spread outside of endemic areas due to several factors, particularly climate change, shifting/migrating mammals, or birds that may carry tick vectors.

4.2. Pathogenesis, and disease manifestations

Although OHFV is potentially pathogenic in endemic areas, little is known about its underlying pathogenic mechanism or the immune response in infected individuals. Research findings show that the virus has a high affinity for hemopoietic (hematopoietic tropism) and vascular tissues (vascular tropism). However, *in vivo,* studies have investigated OHFV pathogenesis in laboratory mice and non-human primates. A study's findings show that OHFV infection in BALB/c mice developed mild meningoencephalitis and significant cerebellar disorders (Holbrook et al., 2005), similar to symptoms previously described in OHFV-infected humans (Holbrook et al., 2005). The effects on the CNS and vascular systems were most prominent. Hemorrhages, focal glial cell proliferation, and perivascular inflammation infiltrate the brain parenchyma, causing CNS disorders (Holbrook et al., 2005). The OHFV infection did not cause paralysis or a fatal cerebrum infection. Distinct pathological findings in the OHFV-infected mice's spleens revealed different immune responses, supporting the BALB/c mouse as an OHFV disease model (Holbrook et al., 2005). Generally, information is scarce on the impact of a persistent OHFV infection on its natural hosts. Laboratory tests detect a fatal neuro-infection (Shestopalova et al., 1972) in the susceptible wild muskrat (*Ondathra zibethicus*) after an extraneural or intracerebral injection (Kharitonova and Leonov, 1986). Other wild vertebrates show mostly asymptomatic diseases with viremia (Kharitonova and Leonov, 1986; Růžek et al., 2010). Some infected animals showed poor mobility, weakness, and hyperpnoea. In addition, the cerebellum and brain hemispheres accumulated the highest viral load, followed by the lungs, kidneys, blood, feces, spleen, and liver (Shestopalova et al., 1972). The viral persistence in infected subcutaneous tissues and internal organs is a defining characteristic of the pathogenesis processes in mice. In severe infections, OHFV may cross the blood-barrier and infiltrate the brain, resulting in increased INF production in the CNS of baby mice (Hofmann et al., 1969). Further, edema in the infected mice causes sensory disturbances that may lead to collapse and shock (WHO, 1985), which may also increase the host's susceptibility to other pathogens (Novitskiy, 1948). In a study, OHFV-infected mice developed pneumonia, paralysis (Chumakov, 1948), meningoencephalitis with a high viral load in the cerebellum, and other pathological findings such as enlarged spleens and impaired gastrointestinal tracts, kidneys, and liver (Růžek et al., 2010; Li et al., 2021). In contrast, the infected macaques (*Macaca radiata*) showed no obvious pathological or histological symptoms, and no virus was isolated from their blood. Furthermore, high aminotransferase levels were observed, indicating viral replication in the liver (Kenyon et al., 1992). Direct contact with an infected animal's blood, body fluids, virus-carrying tick bites, or the feces/urine of an infected or dead rodent can result in chronic infection (Ruzek et al., 2013; Wagner et al., 2022). There has been no evidence of person-to-person transmission so far. High-grade fever, headache, cough, myalgia, moderate to severe hemorrhagic manifestations, pneumonia, nephrosis, and meningitis are all symptoms of OHF, with a mortality rate ranging from 0.4 to 3% (Kharitonova and Leonov, 1986; Růžek et al., 2010; Zhang et al., 2019). Currently, no specific treatment or vaccine is available to treat or prevent OHF; however, symptoms can be treated to minimize disease manifestations (Orlinger et al., 2011). Based on the antigenic similarity, available tick-borne encephalitis (TBE) vaccines were used as a preventive measure against OHFV during the 1991 outbreak. However, no clinical data support the vaccine's efficacy for complete prevention (Růžek et al., 2010). General disease management strategies include early hospitalization, drinking more water, and a nutritious diet supplemented with potassium, chloride, and vitamins K and C, which are recommended for quick recovery. OHF can be diagnosed based on clinical and epidemiological observations. ELISA is crucial for the accurate diagnosis of antibody titers in OHFV patients' serum samples following 1–3 weeks of infection (Růžek et al., 2010; Orlinger et al., 2011).

5. Kyasanur forest disease virus

The KFDV is a TBFV that spreads from infected mammals, notably monkeys, to humans *via H. spinigera* bites. The KFDV transmission cycle involves multiple *Haemaphysalis* species, notably *H. spinigera*, some *Ixodes* species, and hosts, such as bats, birds,

monkeys, rodents, and shrews (Pattnaik, 2006). KFD disproportionately impacts low-income rural communities in India, including forestry workers and smallholder farmers who harvest non-timber forest products (Pattnaik, 2006; Burthe et al., 2021), which may be attributed to their intervention in the natural ecosystem. However, no study confirms direct virus transmission from human to human (Shah et al., 2018; Bhatia et al., 2020). According to experimental evidence, adult female ticks transmit the KFDV to their offspring (Matser et al., 2009; Burthe et al., 2021).

5.1. Epidemiology

In southern India, this TBV causes a devastating, deadly hemorrhagic disease with approximately 500 cases and a 10% mortality rate per year (Pattnaik, 2006). KFDV was first isolated from a sick monkey in the Kyasanur Forest in Karnataka State, India, in 1957. KFDV is carried by ticks, Hemaphysalis spinigera, after being bitten by an infected tick, rodents, shrews, and monkeys, causing epizootics with high fatality in primates (Pattnaik, 2006; Burthe et al., 2021). Asymptomatic infections result in KFDV-specific antibody responses (Stone, 2014). Ticks also transmit the virus between the co-feeding ticks, i.e., without involving hosts (Randolph, 2011). Several reports have discussed the route of KFDV transmission from tick to human after being bitten or having direct contact with an infected *Haemaphysalis* species (becomes infected by feeding on viral reservoirs). Humans are merely incidental hosts for the KFDV and play no role in disease transmission (Matser et al., 2009), representing the KFDV as a spillover pathogen from wildlife reservoirs. However, no empirical data exist that describe the role of tick species that transmit KFDV to their hosts (Burthe et al., 2021). This virus affected those who visited the forests to cut wood, graze cattle, and engage in other agricultural-related activities. In the early stages of the disease, insect collectors on their way to investigating outbreaks become infected. Since 2005, KFD cases have increased, with recent outbreaks in neighboring Karnataka districts like Chikamagalur, Dakshina Kannada, Uttar Kannada, and Udupi, Karnataka, India (Gurav et al., 2018). The disease has now spread to Maharashtra, Kerala, Tamil Nadu, and Goa because of deforestation, agricultural use of forestlands, and subsequent displacement of land and animals (Burthe et al., 2021). A household survey of smallholder farmers, forest users, and native tribes in KFD-affected regions revealed that 69% of the respondents were concerned about the disease's repercussions, highlighting it as a major public health issue (Asaaga et al., 2021).

5.2. Pathogenesis, and disease manifestations

Humans, wild rodents (i.e., shrews, squirrels, white-bellied/white-tailed rats), bats, black-faced langurs, bonnet macaques, grey langurs, ground-nesting birds, Indian crested porcupines, cattle, and gerbils are all susceptible to the KFDV infection (Sreenivasan et al., 1986; Muraleedharan, 2016; Bhatia et al., 2020). Infected macaques exhibit leucopenia, thrombocytopenia, and high levels of alkaline phosphatase, alanine transaminase, and nuclear material phagocytosis in the peripheral-endothelial system. KFDV causes hemorrhagic disease, implying the presence of molecular determinants within the genome linked to viral pathogenicity. The E protein is a critical causal element of tissue tropism, mediating virus entry into the host cell and is responsible for virus immunogenic and phenotypic properties, thereby playing important roles in pathogenesis and immune evasion (Barker et al., 2009). The virus targets the endothelial cells lining the blood vessels, causing endothelial damage and leakage, bleeding, organ damage, and even shock in severe cases. High fever (lasting 6–11 days), anorexia, abdominal pain, cough, body ache, diarrhea, headache, insomnia, leucopenia, myalgia, thrombocytopenia, increased intravascular permeability, prolonged clotting time, bleeding from the gums/nose (Shah et al., 2018; Bhatia et al., 2020; Gupta et al., 2020), decreased heart rate, elevated creatinine phosphokinase, and elevated blood urea nitrogen levels are among the KFD symptoms (Bhatia et al., 2020). The infected person may also express reduced eosinophils, neutrophils, and lymphocyte counts within the first week of illness. About 10–20% of KFDV patients experience a secondary phase relapse (Muraleedharan, 2016), characterized by neurological disorders, including confusion, convulsions, drowsiness, tremors, etc. KFDV infection is diagnosed based on clinical symptoms and confirmed by laboratory tests. Virus isolation is the gold standard for diagnosing KFDV infection but it is risky and expensive. Molecular diagnosis, particularly the reverse transcription loop-mediated isothermal amplification (RT-LAMP) assay, is a quick, sensitive method for detecting KFDV infection and would be useful for high throughput screening of clinical samples (Kumar et al., 2021). The Indian Council of Medical Research developed the first vaccine to prevent KFDV (Bhatia et al., 2020); although the vaccine is safe, but has a low efficacy rate in humans (only 62%) (Kasabi et al., 2013). KFDV case is not treatable with antiviral medications; however, disease complications can be treated based on the signs and symptoms. Supportive therapies, such as intravenous electrolyte transfusions and maintaining oxygen levels and blood pressure, are suggested to manage patient health status (Bhatia et al., 2020).

6. Colorado tick fever virus

The CTFV member of the *Reovirales* order, *Spinareoviridae* family, and *Coltivirus* genus comprises a 12-segmented dsRNA genome (Owen et al., 2021). The CTFV genome is approximately 29,000 base pairs in size and contains an icosahedral capsid of about 80 nm in size (CDC, 2021a). CTF is a rare viral disease spread in humans by CTFV-infected Rocky Mountain wood tick (*D. andersoni*) bites (CDC, 2021a). Ticks become infected after feeding on the blood of host animals, such as rodents, squirrels, chipmunks, etc. Other animals, such as elk, marmots, and deer, can also be infected by *D. andersoni* (CDC, 2021a).

6.1. Epidemiology

Infected *D. albopictus*, *D. arumapertus*, *D. andersoni*, *D. occidentalis*, *Haemaphysalis leporispalustris*, *Otobius lagophilus*, *I. sculptus*, and *I. spinipalpis* may also transmit the CTFV to animals (Attoui et al., 2005); however, there is no evidence of CTFV transmission from person to person. Virus transmission *via* blood transfusion cannot be ignored due to the evidence that CTFV can live

for several months in human and animal red blood cells, suggesting that blood donation should be avoided for at least 6 months after CTFV infection (CDC, 2021a). Approximately 400 CTF cases have been reported each year, with 0.02 cases per 1 million people between 2002 and 2012 (Yendell et al., 2015), whereas only 59 cases were reported to the CDC from 2010 to 2019 (CDC, 2021a). As of September 2020, CTF cases were reported in Arizona, Colorado, Dakota, Idaho, New Mexico, Montana, Oregon, South Utah, and Wyoming (CDC, 2021a). In addition, CTFV has been reported in Canada (British Columbia and Alberta).

6.2. Pathogenesis, and disease manifestations

The incubation period, i.e., the time between a tick bite and the onset of illness, can range from 1 to 14 days (Romero and Simonsen, 2008; Burrell et al., 2016). Hospitalization is required in approximately 20% of severe CTF cases with hemorrhagic fever, meningitis, and meningoencephalitis (Romero and Simonsen, 2008; Burrell et al., 2016). In children, fatal CNS or hemorrhagic complications are commonly attributed to intravascular coagulopathy (Bennett et al., 2019), bleeding, and shock (Romero and Simonsen, 2008), with 5 to 10% of deaths. Persistent viremia is caused by virus replication in erythroblasts, reticulocytes, and CD34+ hematopoietic cells (Attoui et al., 2005). According to a survey, only 6.6% of *D. andersoni* in Western Montana were infected with CTFV (Williamson et al., 2019), indicating the virus's persistent infection by targeting skin endothelial cells (Owen et al., 2021). Endothelial cells play an essential role in homeostasis, regulation, and molecular trafficking by controlling vascular permeability and coagulation (Mai et al., 2013). In addition, endothelial cells facilitate immune cell trafficking, antigen presentation, and the production of increased pro-inflammatory cytokines and chemokines. In the case of severe infections, the induced pro-inflammatory cytokine/chemokine levels, innate immune response, and inflammatory response may cause endothelial cell injury, vascular dysfunction, or even patient death (Owen et al., 2021). *In vitro*, CTFV caused cytopathic effects on BHK21 cell lines, KB cell lines, glial progenitor cell lines, and hematopoietic stem cell lines (Owen et al., 2021). A study found that after CTFV infection, HMEC-1 human cell lines died *via* an apoptotic-like pathway that was not dependent on caspase-3/7 activity. Furthermore, in the presence of caspase inhibition, the HMEC-1 accumulated fewer viruses (Owen et al., 2021). CTF symptoms are typically flu-like, with fever, headache, muscle aches, and fatigue, but the illness can progress to more serious complications such as meningitis or encephalitis (Romero and Simonsen, 2008; Burrell et al., 2016). Serological tests are typically used in laboratory diagnosis, and supportive treatment is required. Although CTFV infection cannot be treated due to a lack of specific viral medications or vaccines, the risk of infection can be reduced by taking preventive measures (Burrell et al., 2016; CDC, 2021a), such as avoiding unnecessary exposure to tick-infested areas (WDH, 2022).

7. Crimean-Congo hemorrhagic fever virus

CCHFV, which causes CCHF, is one of the most severe viral diseases in humans. The virus is transmitted *via* ixodid ticks, particularly those of the genus *Hyalomma*, and is initially characterized by unspecific signs and symptoms (Rathore et al., 2021). The CCHFV genome is a tri-segmented, negative-sense ssRNA with a conserved 3′ and complementary 5′ ends, allowing the RNA to form a looped structure. The small (S) segment (~1.6 kb in size) encodes the multifunctional nucleocapsid (N) protein, which is an important virion structural component and is involved in viral infection. The medium (M) segment (~5.4 kb in size) encodes a glycoprotein precursor, which is further processed into glycoprotein-N (Gn), glycoprotein-C (Gc), and other non-structural proteins. CCHFV envelope glycoproteins have a crucial role in virus formation, RNA binding, oligomerization, and infectivity (Erickson et al., 2007). CCHFV invades the host cell through clathrin-mediated endocytosis and fuses with endosomal membranes (Bertolotti-Ciarlet et al., 2005). A recent study found that a single amino acid substitution in the CCHFV glycoprotein significantly reduced viral fusion with human cells, indicating that a glycoprotein variant in ticks may reduce viral infectivity in humans (Hua et al., 2020). This suggests that extensive CCHFV genome sequence variability may contribute to divergent clinical outcomes. In addition, to tick bites, CCHFV can be transmitted to humans through direct contact with infected animal tissues or other bodily fluids (i.e., during slaughter, handling of meat, or caring for infected patients). Furthermore, nosocomial outbreaks in healthcare settings have been reported in which infected blood or bodily fluids were handled incorrectly, resulting in human-to-human transmission (Tsergouli et al., 2020).

7.1. Epidemiology

CCHF transmitted *via Hyalomma* species, is widely distributed in Asia (Iraq, Iran, India, China, Pakistan, Afghanistan, Russia, Tajikistan, Uzbekistan, Kazakhstan, Kuwait, Oman, UAE, and Saudi Arabia) (Al-Abri et al., 2017), Africa (Sudan, Kenya, Egypt, Nigeria, Senegal, Chad, Uganda, Tanzania, South Africa, Mauritania, and Congo) (Temur et al., 2021), and Europe (Albania, Bulgaria, Turkey, Greece, Georgia, and Spain) (Maltezou et al., 2010; Figure 4B). In humans, the time required for the virus infection to cause hemorrhage is approximately 5–6 days. The first case of CCHFV was reported in a 51-year-old man in Tintane, Assaba, Mauritania, who had abdominal pain, diarrhea, vomiting, a 41°C body temperature, epistaxis, gingivorrhagia, diffuse ecchymosis, severe anemia, thrombocytopenia, etc. (Boushab et al., 2020). Later, an unusual CCHF case was reported in Nouakchott, Mauritania (Kleib et al., 2016), raising the prospect of the virus spreading from Mauritania to West Africa (Kleib et al., 2016). These findings, combined with CCHF cases and other findings in neighboring countries such as northwestern Senegal (Tall et al., 2009) and Mauritania (Kleib et al., 2016), suggest that CCHF is endemic in West Africa, emphasizing accurate disease diagnosis and raising awareness. CCHF was first described in Turkey in 2002, and more than 9,000 human cases were confirmed in 2015. During the COVID-19 pandemic, another CCHF outbreak occurred in Turkey (Leblebicioglu et al., 2016). Later, the Turkish Ministry of Health confirmed 243 CCHF human cases with 13 deaths (Infectiousdiseasenews, 2021). Most of the CCHF cases were reported in northern, eastern, and central Anatolia, where agricultural hubs exist, as well as the central Black Sea region (Daily-Sabah, 2022). Apart from disease awareness campaigns in

areas where cases are more common, the State Ministry of Agriculture and Forestry initiates programs to eradicate the tick *Hyalomma marginatum* in endemic regions. From January 1 to May 22, 2022, Iraq's health authorities notified the WHO of 212 cases of CCHF, of which 115 were suspected, and 97 polymerase chain reaction (PCR) confirmed cases, with an overall of 27 deaths (14 suspected and 13 PCR-confirmed cases). These reported cases are significantly higher than the 33 PCR-confirmed reported cases in 2021. Cases have been reported in several areas of Iraq, and the outbreak may put additional strain on an already overburdened healthcare system. Most confirmed cases had a history of direct contact with animals, including butchers and livestock breeders. Over half of the confirmed cases were among males aged 15–44 years (WHO, 2022c). Travelers from CCHF endemic countries were responsible for transmitting the virus to the non-endemic regions of the United Kingdom (for example, imported from Bulgaria and Afghanistan) (Chamberlain et al., 2013; Lumley et al., 2014), France (tourists from Senegal) (Tall et al., 2009), Germany (an American soldier returning from Afghanistan) (Conger et al., 2015), and a traveler from Bulgaria (Olschläger et al., 2011). In Iran, CCHF cases have been reported in almost every province. In a study, four sheep (three from Gachsaran and one from Dena regions) reported positive for CCHFV IgG, indicating virus circulation in Kohgiluyeh and Boyer-Ahmad Province, Iran. This finding suggests comprehensive monitoring programs to understand the CCHFV's circulation in ticks and host animals (Ghasemian et al., 2021). In 1998, 19 confirmed CCHF cases were reported in northeastern Afghanistan, making them the country's first documented cases. Later, an outbreak was reported in Afghanistan in 2008 (Mofleh and Ahmad, 2012). Regarding seasonal prevalence, the highest CCHF cases found from June to September probably coincide with Eid-al-Adha, with 13.7% of butchers and 11.8% of shepherds being two high-risk occupations in Afghanistan for CCHFV infection (Qaderi et al., 2021). ELISA and immunofluorescence assays detected CCHFV-specific IgG in 19% of sheep and 5% of goat serum samples in Balochistan, Pakistan (Kasi et al., 2020). In addition, this cross-sectional study also identified potential risk factors for CCHF seropositive sheep and goats. For example, open housing systems, grazing, vegetation in or around the yard, a lack of tick preventive measures, rural poultry absence, and tick-infested animals were all significant risk factors for CCHFV. Identifying risk factors may aid in lowering the CCHFV infection risk in cattle and humans (Kasi et al., 2020). A recent study examined the seroprevalence of CCHFV in sheep sera ($n = 176$) and found that CCHFV-specific antibodies were detected in 17 sera, indicating CCHFV circulation in the westernmost region of the Balkans, Bosnia and Herzegovina, which raises concerns about CCHFV transmission out of this region (Satrovic et al., 2022). A cross-sectional survey tested 800 humans, 666 cattle, 549 goats, and 32 dogs' sera samples from the Ugandan cattle corridor for CCHFV-specific IgG antibodies. Results show 221/800 CCHFV seropositivity in humans, 612/666 in cattle, 413/549 in goats and 18/32 in dogs. Human seropositivity was significantly associated with livestock farming, age, and collecting/eating engorged ticks. High CCHF seropositivity among livestock farmers, including collecting/eating engorged ticks, highlights the need for further surveillance and disease control strategies (Atim et al., 2022).

7.2. Pathogenesis, and disease manifestations

The first contact between the tick-host occurs during the tick's bite or feeding on the host. The tick secretes saliva into the feeding lesion, *via* which pathogens mediate vertebrate host inflammatory and immune responses (Kaufman, 1989). Despite the host's inflammatory and immune responses, the tick attaches to hosts for blood-feeding *via* the pharmacy located in its salivary glands (Connolly-Andersen et al., 2007). CCHFV Gn and Gc help their attachment to the target cell surface receptors. An interaction between viral Gn/Gc and target cell surface protein (i.e., nucleolin found within nucleoli may work as a putative entry factor) (Xiao et al., 2011) demands deep investigations to unveil the role of nucleolin in CCHFV internalization. CCHFV enters the cells using clathrin and the clathrin pit adaptor protein-2 complex (Simon et al., 2009; Garrison et al., 2013). CCHFV particles enter the cell and travel to endosomes and vesicular bodies, where the virus envelope fuses with cellular membranes. Cellular microtubulin and actin filaments are essential for CCHFV internalization, replication, and progeny production (Andersson et al., 2004; Simon et al., 2009). It has also been shown that the virus Gn interacts with cellular chaperones of the heat shock protein 70 families in association with DnaJ cofactor adapter proteins, which play roles in folding and transporting newly synthesized proteins (Surtees et al., 2016). Aquaporin 6 protein (a channel that facilitates water and small solutes across the plasma membrane) has also been shown to be involved in CCHFV replication (Molinas et al., 2016). DC-SIGN (C-type lectin) expressed on the surface of antigen-presenting dendritic cells probably acts as an entry factor for CCHFV (Suda et al., 2016). CCHFV highly replicates in epithelial cells, dendritic cells, and tissue-resident macrophages at the inoculation site. Apart from increased macrophage counts, more natural killer cells, CD4+, and CD8+ lymphocytes have been observed in CCHFV infections (Yilmaz et al., 2008; Akinci et al., 2009). As the disease progresses, the uncontrolled apoptosis of T lymphocytes contributes to lymphopenia (reduced lymphocyte count) in a STAT-1 knockout mouse model (Bente et al., 2010). These cells facilitate virus spread and infect local lymph nodes and peripheral blood-borne monocytes (Connolly-Andersen et al., 2007; Akıncı et al., 2013). The infection of endothelial cells and peripheral blood-borne monocytes results in extravasation into parenchymal tissue, enabling virus interaction with basolateral cell receptors (Connolly-Andersen et al., 2007). Secondary replication in these body parts facilitates systemic virus spread (Akıncı et al., 2013), as demonstrated by an experimental animal model: viral replication occurs in the blood on the first day of infection, then in the spleen and liver on the second day, and then spreads systemically to the lungs, kidneys, and brain (Bente et al., 2010). Endothelial cell damage is responsible for cellular hemostasis failure by platelet stimulation and degranulation as well as activation of the intrinsic coagulation cascade in host organs (Weber and Mirazimi, 2008; Bodur et al., 2010). It has been shown that CCHFV non-structural proteins may induce apoptosis *via* both intrinsic and extrinsic pathways (Barnwal et al., 2016). The induced apoptosis was attributed to releasing cytokines and chemokines from CCHFV-infected cells (Weber and Mirazimi, 2008; Barnwal et al., 2016). *In vitro* study showed that RIG-I acts as a PRR for CCHFV and mediates type I IFN response (Spengler et al., 2015). Tick cell lines enable CCHFV studies to offer an alternative approach to understanding tick cells' response to invading viruses (Bell-Sakyi

et al., 2012). *In vivo*, CCHFV transmission has been established using IFN knockout mice, an additional tool for studying tick-pathogen interactions(Gargili et al., 2013). CCHF manifestations include high fever, myalgia, dizziness, neck pain and stiffness, backache, headache, sore eyes, nausea, vomiting, diarrhea, abdominal pain, thrombocytopenia, leukopenia, and elevated liver enzyme levels. After a few days, the agitation may be replaced by sleepiness, depression, and lassitude, and the abdominal pain may localize to the upper right quadrant, with detectable liver enlargement. Patients may also experience a fast heart rate, enlarged lymph nodes, and a petechial rash on internal mucosal surfaces. There is usually evidence of hepatitis; severely ill patients may experience rapid kidney deterioration and sudden liver or pulmonary failure following an illness. The CCHF mortality rate is approximately 30%, with deaths occurring in the second week of illness (Yakut et al., 2021; WHO, 2022a). In brief, over the last decade, considerable progress has been made in exploring cellular components involved in tick-host-pathogen interactions; however, there is limited knowledge in the case of CCHFV due to its high-level containment requirement. Identifying the underlying molecular drivers that promote CCHFV survival in tick vectors may allow us to disrupt these processes and reduce tick populations and CCHF prevalence (de la Fuente et al., 2017). Moreover, the identification of the signaling pathways taking place during CCHFV-host interactions provides the opportunity to design novel control strategies for CCHF.

8. Heartland virus

The genus *Bandavirus*, classified under the order *Bunyavirales*, family *Phenuiviridae*, including HRTV, *Dabie bandavirus* (SFTSV), etc., poses threats to public health. The genus *Bandavirus* contains viruses that comprise three segments, i.e., small (S ~ 1.7 kb in size), medium (M ~ 3.2 kb in size), and large (L ~ 6.4 kb in size) (Adams et al., 2017). The M segment encodes Gn and Gc, which are crucial for the viral interaction with host receptors to neutralize host immune responses (Walter and Barr, 2011). The S segment encodes the structural protein nucleocapsid (N). In addition, the L segments synthesize NS proteins (RNA-dependent RNA polymerase). The viral Gn and Gc fused with the host cell's DC-SIGN, heparan-sulfate, and non-muscle myosin heavy-chain IIA receptors. This interaction is mediated by the viral Gc and is a critical step for pathogenesis. HRTV replication is complete in the host cell's cytoplasm and begins with the release of ribonucleoproteins, followed by the synthesis of new viral RNA. Ribonucleocapsids are formed in the Golgi apparatus, and progeny virions are exocytosed *via* the plasma membrane (Spiegel et al., 2016).

8.1. Epidemiology

HRTV transmitted by tick bites (*A. americanum*) was first reported in northwestern Missouri in 2009 (Pastula et al., 2014). In 2010, a tick-borne *phlebovirus* caused similar symptoms in China, Korea, and Japan, whereas a bat-borne, *Malsoor virus*, was responsible for HRTV-like symptoms in western India (Mourya et al., 2014). In 2018, two HRTV-infected cases were reported in Illinois, United States (McMullan et al., 2012). HRTV is closely related to the *Albatross Hunter Island virus*, isolated from *Ixodes* species and dying sea birds in Australia (Gauci et al., 2015). As of January 2021, more than 50 HRTV cases had been reported in midwestern regions (such as Illinois, Indiana, and Iowa), southwestern (Arkansas), southeastern (Georgia, Kentucky, North Carolina, and Tennessee), midwestern (Kansas and Missouri), and south-central (Oklahoma) of the United States. It has been shown that all local populations and visitors to HRTV endemic areas are at increased risk (Tuten et al., 2020; CDC, 2021b). Most patients reported seeing ticks (*A. americanum*) on their bodies 2 weeks before becoming ill (Brault et al., 2018). A study reported *A. americanum's* presence on the bodies of two HRTV-positive adult males (Tuten et al., 2020), indicating that the virus is widespread in these ticks in Illinois. The emergence of HRTV is a significant concern because of the geographic distribution and increased abundance of *A. americanum* (Tuten et al., 2020). Some HRTV patients have a high viral load in their bloodstream, indicating that healthy people in contact with patient blood are at an increased risk of getting infections (Brault et al., 2018). HRTV case mortality has ranged from 13 to 16%, with the highest rate occurring in 50-year-old men with sepsis and multiple organ failure (Fill et al., 2017). The first fatal case was an 80-year-old Tennessee man who died after being hospitalized with fever, leukopenia, thrombocytopenia, organ failure, and bleeding. In the post-mortem, HRTV was detected in the spleen and lymph node samples (Muehlenbachs et al., 2014).

8.2. Pathogenesis, and disease manifestations

HRTV disease symptoms are very similar to tick-borne ehrlichiosis, transmitted *via* the same tick (*A. americanum*). For example, two HRTV-infected farmers in northwestern Missouri developed ehrlichiosis-like mild fever, leukopenia, and thrombocytopenia (Pastula et al., 2014). A study injected HRTV into animals to assess potential vertebrate hosts and establish a tick-vertebrate model for evaluating vector competence. Seronegative raccoons from various fields in the Midwestern United States were challenged with HRTV and produced a high rate of neutralizing antibodies (Bosco-Lauth et al., 2015; Riemersma and Komar, 2015). None of the susceptible raccoons demonstrated disease signs or a detectable HRTV load (Bosco-Lauth et al., 2016). In a similar experiment, naive goats exposed to SFTSV experienced high viral loads (Jiao et al., 2015). In contrast, goats exposed to SFTSV-infected ticks and virus-infected needles failed to develop detectable viremia (Jin et al., 2012). In an experiment, goats were exposed to SFTSV-infected ticks, suggesting that a long-term vertebrate host's exposure to ticks could result in high viral loads sufficient to infect other ticks (Jin et al., 2012). A study also found that after being inoculated with HRTV, experimental mouse models failed to develop lesions or detectable viremia. In addition, HRTV-infected chickens, rabbits, and hamsters could not produce antibodies against the HRTV infection (Bosco-Lauth et al., 2016). This study further reports that when outbred CD-1 mouse models (immune-competent mice) were inoculated with HRTV, they failed to demonstrate neurovirulence (Bosco-Lauth et al., 2016). A dose-dependent response was observed in INF-type-I and -type-II deficient mice when a lethal dose of 50% of 10 plaque-forming units of HRTV was administered intraperitoneally, given that the low feeding efficiency of ticks in immune-compromised mice may differ from that of HRTV-infected vertebrates (Bosco-Lauth et al., 2016). On the other hand,

SFTSV-inoculated immune-competent mice exhibit pathological abnormalities similar to those seen in HRTV patients with leukopenia, thrombocytopenia, and elevated liver transaminases. These manifestations were mild, and the SFTSV replication was restricted to the spleen (Jin et al., 2012), indicating a protective INF response within mouse models. Hamsters deficient in INF type-I signaling were susceptible to HRTV lethality, indicating that rodents' protective INF response against HRTV infection was well-established (Westover et al., 2017). *Phleboviruses* infect mononuclear cells, eliciting strong INF-type-I reactions (Wuerth and Weber, 2016). More research is needed to determine these cells' direct and indirect roles in HRTV trafficking within hosts and their precise roles in pathological abnormalities in humans. Fever, fatigue, anorexia, diarrhea, leukopenia, thrombocytopenia, and elevated liver transaminases were all symptoms of HRTV infection (McMullan et al., 2012). Other disease symptoms are headaches, nausea, myalgia, arthralgia, and weakness. Some patients reported a local rash frequently associated with the initial tick bite (Brault et al., 2018). Patients with fever, leukopenia, and thrombocytopenia should seek laboratory testing in *A. americanum* endemic areas (Staples et al., 2020).

In brief, the evidence presented above shows that ticks transmit the most diverse array of infectious agents to animals and humans. Thus, there is a need to explore the global distribution of ticks that transmit infectious diseases to humans and animals. Further, there is a need to develop the latest novel diagnostic tools and treatment options to control these diseases. Interestingly, clinical manifestations in infected individuals highlight distinct features of each virus, such as thrombocytopenia in BRBV, CCHFV, HRTV, and KFDV. In some cases, TBV RNA and their associated induced IgM and IgG antibodies can be detected in infected individuals with leukopenia, thrombocytopenia, and mild to moderate elevations of liver transaminases (CDC, 2019; Madison-Antenucci et al., 2020). There is a need to develop novel *in vitro* and *in vivo* models to understand TBV's underlying pathogenic mechanisms, which will ultimately help with disease prevention and control measures.

9. Conclusions and future perspectives

Ticks transmit increased numbers of viral pathogens, such as BRBV, POWV, OHFV, CTFV, CCHFV, HRTV, and KFDV, which constantly threaten human and animal life worldwide, particularly those doing outdoor activities, increasing contact with ticks, their potential hosts. Ticks carrying viruses or their infected hosts' migration from endemic areas may increase the risk of infections in humans and animals. Therefore, identifying ticks and their associated pathogens will be of great importance in preventing TBV diseases.

Physicians should consider TBV infections in differential diagnostics in endemic regions, especially locally active TBVs, as most viruses are geographically restricted. Diseases occurring in remote areas should be reported to the local health department, which can issue preventive measures against ticks and their associated viruses. People should avoid contact with sick animals, particularly bats, muskrats, and monkeys, and avoid drinking non-pasteurized goat milk. The public should also be encouraged to report dead or sick animals, particularly muskrats or monkeys, as an early warning for TBV infections (WHO, 1985). In addition, short-term efforts should increase public awareness of the BRBV, POWV, CTFV, CCHFV, HRTV, and KFDV-associated illnesses. People should avoid unnecessary visits to tick-endemic areas. In case of visiting, certain preventive measures should be taken, such as wearing long-sleeved nylon clothes (WHO, 1985), apart from applying tick repellants containing n-n-diethylmetatoluamide and permethrin to the skin, clothes, and other items (Pages et al., 2014). Wearing light-colored clothing is suggested as an option for observing crawling ticks on the body before returning from tick-endemic areas. To prevent ticks from crawling up inside, pants legs should be tucked into socks, and long-sleeved shirts should be tucked into pants. Furthermore, spraying permethrin-containing repellents on boots and clothing can deter tick attachment (WDH, 2022). It has strongly encouraged people to seek medical attention when they notice a tick on their body parts or experience their first sign in endemic areas.

Improved healthcare infrastructure, new diagnostic tools, and trained personnel should be deployed in tick-endemic areas for disease control. Seasonal migratory birds, animals, or mammals may transmit ticks or TBVs across many regions and countries, suggesting that advanced research will aid in developing surveillance systems (such as radio-tracking) to track the emergence of TBVs. Surveillance programs should also identify relevant animals or mammals that help the tick vectors complete their life cycle. For example, birds and bats have gained attention due to their role in spreading ticks and their associated viruses during seasonal migration (Calisher et al., 2006; Buczek et al., 2020). Humans traveling with ticks or viruses from endemic areas have also gained attention for spreading TBV diseases (Tall et al., 2009; Lumley et al., 2014; Conger et al., 2015). Therefore, long-term efforts should be directed toward various parameters influencing the ecological distribution of ticks to investigate global disease circumstances and countermeasures. There is an urgent need to develop new vaccines/drugs and make them available to inaccessible remote tick endemic areas for public immunization and disease management.

Author contributions

TS and XX conceptualized the study. QL conducted the database search. TS, XX, BW, and ZB narratively screened the databases, then extracted their data and prepared the initial draft of the manuscript. TS prepared the final draft of the manuscript. XX supervised the project and critically assessed the manuscript. All authors contributed to the article and approved the submitted version.

Funding

This study was supported by the Yunnan Key R&D Program (No. 202103AQ100001) and Yunnan Major Scientific and Technological Project (No. 202202AG050013).

Conflict of interest

The authors declare that the research was conducted in the absence of any commercial or financial relationships that could be construed as a potential conflict of interest.

Publisher's note

All claims expressed in this article are solely those of the authors and do not necessarily represent those of their affiliated organizations, or those of the publisher, the editors and the reviewers. Any product that may be evaluated in this article, or claim that may be made by its manufacturer, is not guaranteed or endorsed by the publisher.

References

Adams, M. J., Lefkowitz, E. J., King, A. M. Q., Harrach, B., Harrison, R. L., Knowles, N. J., et al. (2017). Changes to taxonomy and the international code of virus classification and nomenclature ratified by the international committee on taxonomy of viruses (2017). *Arch. Virol.* 162, 2505–2538. doi: 10.1007/s00705-017-3358-5

Akıncı, E., Bodur, H., and Leblebicioglu, H. (2013). Pathogenesis of Crimean-Congo hemorrhagic fever. *Vector Borne Zoonotic Dis.* 13, 429–437. doi: 10.1089/vbz.2012.1061

Akinci, E., Yilmaz, M., Bodur, H., Ongürü, P., Bayazit, F. N., Erbay, A., et al. (2009). Analysis of lymphocyte subgroups in Crimean-Congo hemorrhagic fever. *Int. J. Infect. Dis.* 13, 560–563. doi: 10.1016/j.ijid.2008.08.027

Al-Abri, S. S., Abaidani, I. A., Fazlalipour, M., Mostafavi, E., Leblebicioglu, H., Pshenichnaya, N., et al. (2017). Current status of Crimean-Congo haemorrhagic fever in the World Health Organization eastern Mediterranean region: issues, challenges, and future directions. *Int. J. Infect. Dis.* 58, 82–89. doi: 10.1016/j.ijid.2017.02.018

Andersson, I., Simon, M., Lundkvist, A., Nilsson, M., Holmström, A., Elgh, F., et al. (2004). Role of actin filaments in targeting of Crimean Congo hemorrhagic fever virus nucleocapsid protein to perinuclear regions of mammalian cells. *J. Med. Virol.* 72, 83–93. doi: 10.1002/jmv.10560

Anderson, J. F., and Armstrong, P. M. (2012). Prevalence and genetic characterization of Powassan virus strains infecting Ixodes scapularis in Connecticut. *Am J Trop Med Hyg.* 87, 754–9. doi: 10.4269/ajtmh.2012.12-0294

Asaaga, F. A., Rahman, M., Kalegowda, S. D., Mathapati, J., Savanur, I., Srinivas, P. N., et al. (2021). 'None of my ancestors ever discussed this disease before!' how disease information shapes adaptive capacity of marginalised rural populations in India. *PLoS Negl. Trop. Dis.* 15:e0009265. doi: 10.1371/journal.pntd.0009265

Atim, S. A., Ashraf, S., Belij-Rammerstorfer, S., Ademun, A. R., Vudriko, P., Nakayiki, T., et al. (2022). Risk factors for Crimean-Congo Haemorrhagic fever (CCHF) virus exposure in farming communities in Uganda. *J. Infect.* 85, 693–701. doi: 10.1016/j.jinf.2022.09.007

Attoui, H., Mohd Jaafar, F., de Micco, P., and de Lamballerie, X. (2005). Coltiviruses and seadornaviruses in North America, Europe, and Asia. *Emerg. Infect. Dis.* 11, 1673–1679. doi: 10.3201/eid1111.050868

Aziati, I. D., McFarland, D., Antia, A., Joshi, A., Aviles-Gamboa, A., Lee, P., et al. (2022). Prevalence of Bourbon and heartland viruses in field collected ticks at an environmental field station in St. Louis County, Missouri, USA. *Ticks Tick Borne Dis.* 14:102080. doi: 10.1016/j.ttbdis.2022.102080

Bai, C., Qi, J., Wu, Y., Wang, X., Gao, G. F., Peng, R., et al. (2019). Postfusion structure of human-infecting Bourbon virus envelope glycoprotein. *J. Struct. Biol.* 208, 99–106. doi: 10.1016/j.jsb.2019.08.005

Bamunuarachchi, G., Harastani, H., Rothlauf, P. W., Dai, Y. N., Ellebedy, A., Fremont, D., et al. (2022). Detection of Bourbon virus-specific serum neutralizing antibodies in human serum in Missouri, USA. *mSphere* 7:e0016422. doi: 10.1128/msphere.00164-22

Barker, W. C., Mazumder, R., Vasudevan, S., Sagripanti, J. L., and Wu, C. H. (2009). Sequence signatures in envelope protein may determine whether flaviviruses produce hemorrhagic or encephalitic syndromes. *Virus Genes* 39, 1–9. doi: 10.1007/s11262-009-0343-4

Barker, C. M., and Reisen, W. K. (2019). "Epidemiology of vector-borne diseases" in *Medical and veterinary entomology*. eds. G. Mullen and L. Durden. *3rd* ed (Cambridge: Academic Press), 33–49.

Barnwal, B., Karlberg, H., Mirazimi, A., and Tan, Y. J. (2016). The non-structural protein of Crimean-Congo hemorrhagic fever virus disrupts the mitochondrial membrane potential and induces apoptosis. *J. Biol. Chem.* 291, 582–592. doi: 10.1074/jbc.M115.667436

Basile, A. J., Horiuchi, K., Panella, A. J., Laven, J., Kosoy, O., Lanciotti, R. S., et al. (2013). Multiplex microsphere immunoassays for the detection of IgM and IgG to arboviral diseases. *PLoS One* 8:e75670. doi: 10.1371/journal.pone.0075670

Belikov, S. I., Kondratov, I. G., Potapova, U. V., and Leonova, G. N. (2014). The relationship between the structure of the tick-borne encephalitis virus strains and their pathogenic properties. *PLoS One* 9:e94946. doi: 10.1371/journal.pone.0094946

Bell-Sakyi, L., Kohl, A., Bente, D. A., and Fazakerley, J. K. (2012). Tick cell lines for study of Crimean-Congo hemorrhagic fever virus and other arboviruses. *Vector Borne Zoonotic Dis.* 12, 769–781. doi: 10.1089/vbz.2011.0766

Bennett, J. E., Dolin, R., and Blaser, M. J. (2019). *Mandell, Douglas, and Bennett's principles and practice of infectious diseases E-book*. Amsterdam, Netherlands: Elsevier Health Sciences.

Bente, D. A., Alimonti, J. B., Shieh, W. J., Camus, G., Ströher, U., Zaki, S., et al. (2010). Pathogenesis and immune response of Crimean-Congo hemorrhagic fever virus in a STAT-1 knockout mouse model. *J. Virol.* 84, 11089–11100. doi: 10.1128/JVI.01383-10

Bente, D. A., Forrester, N. L., Watts, D. M., McAuley, A. J., Whitehouse, C. A., and Bray, M. (2013). Crimean-Congo hemorrhagic fever: history, epidemiology, pathogenesis, clinical syndrome and genetic diversity. *Antivir. Res.* 100, 159–189. doi: 10.1016/j.antiviral.2013.07.006

Bertolotti-Ciarlet, A., Smith, J., Strecker, K., Paragas, J., Altamura, L. A., McFalls, J. M., et al. (2005). Cellular localization and antigenic characterization of Crimean-Congo hemorrhagic fever virus glycoproteins. *J. Virol.* 79, 6152–6161. doi: 10.1128/JVI.79.10.6152-6161.2005

Bhatia, B., Feldmann, H., and Marzi, A. (2020). Kyasanur Forest disease and Alkhurma hemorrhagic fever virus-two neglected zoonotic pathogens. *Microorganisms* 8:1406. doi: 10.3390/microorganisms8091406

Blom, K., Braun, M., Pakalniene, J., Dailidyte, L., Béziat, V., Lampen, M. H., et al. (2015). Specificity and dynamics of effector and memory CD8 T cell responses in human tick-borne encephalitis virus infection. *PLoS Pathog.* 11:e1004622. doi: 10.1371/journal.ppat.1004622

Blom, K., Braun, M., Pakalniene, J., Lunemann, S., Enqvist, M., Dailidyte, L., et al. (2016). NK cell responses to human tick-borne encephalitis virus infection. *J. Immunol.* 197, 2762–2771. doi: 10.4049/jimmunol.1600950

Bodur, H., Akinci, E., Ongürü, P., Uyar, Y., Baştürk, B., Gözel, M. G., et al. (2010). Evidence of vascular endothelial damage in Crimean-Congo hemorrhagic fever. *Int. J. Infect. Dis.* 14, e704–e707. doi: 10.1016/j.ijid.2010.02.2240

Bollati, M., Alvarez, K., Assenberg, R., Baronti, C., Canard, B., Cook, S., et al. (2010). Structure and functionality in flavivirus NS-proteins: perspectives for drug design. *Antivir. Res.* 87, 125–148. doi: 10.1016/j.antiviral.2009.11.009

Bosco-Lauth, A. M., Calvert, A. E., Root, J. J., Gidlewski, T., Bird, B. H., Bowen, R. A., et al. (2016). Vertebrate host susceptibility to heartland virus. *Emerg. Infect. Dis.* 22, 2070–2077. doi: 10.3201/eid2212.160472

Bosco-Lauth, A. M., Panella, N. A., Root, J. J., Gidlewski, T., Lash, R. R., Harmon, J. R., et al. (2015). Serological investigation of heartland virus (Bunyaviridae: Phlebovirus) exposure in wild and domestic animals adjacent to human case sites in Missouri 2012-2013. *Am. J. Trop. Med. Hyg.* 92, 1163–1167. doi: 10.4269/ajtmh.14-0702

Boushab, B. M., Kelly, M., Kébé, H., Bollahi, M. A., and Basco, L. K. (2020). Crimean-Congo hemorrhagic fever, Mauritania. *Emerg. Infect. Dis.* 26, 817–818. doi: 10.3201/eid2604.191292

Brackney, D. E., Nofchissey, R. A., Fitzpatrick, K. A., Brown, I. K., and Ebel, G. D. (2008). Stable prevalence of Powassan virus in *Ixodes scapularis* in a northern Wisconsin focus. *Am. J. Trop. Med. Hyg.* 79, 971–973. doi: 10.4269/ajtmh.2008.79.971

Brault, A. C., Savage, H. M., Duggal, N. K., Eisen, R. J., and Staples, J. E. (2018). Heartland virus epidemiology, vector association, and disease potential. *Viruses* 10:498. doi: 10.3390/v10090498

Bricker, T. L., Shafiuddin, M., Gounder, A. P., Janowski, A. B., Zhao, G., Williams, G. D., et al. (2019). Therapeutic efficacy of favipiravir against Bourbon virus in mice. *PLoS Pathog.* 15:e1007790. doi: 10.1371/journal.ppat.1007790

Brites-Neto, J., Duarte, K. M., and Martins, T. F. (2015). Tick-borne infections in human and animal population worldwide. *Vet. World* 8, 301–315. doi: 10.14202/vetworld.2015.301-315

Buczek, A. M., Buczek, W., Buczek, A., and Bartosik, K. (2020). The potential role of migratory birds in the rapid spread of ticks and tick-borne pathogens in the changing climatic and environmental conditions in Europe. *Int. J. Environ. Res. Public Health* 17:2117. doi: 10.3390/ijerph17062117

Burrell, C. J., Howard, C. R., and Murphy, F. A. (2016). *Fenner and White's medical virology*. United States: Academic Press.

Burthe, S. J., Schäfer, S. M., Asaaga, F. A., Balakrishnan, N., Chanda, M. M., Darshan, N., et al. (2021). Reviewing the ecological evidence base for management of emerging tropical zoonoses: Kyasanur Forest disease in India as a case study. *PLoS Negl. Trop. Dis.* 15:e0009243. doi: 10.1371/journal.pntd.0009243

Bush, L. M., and Vazquez-Pertejo, M. T. (2018). Tick borne illness-Lyme disease. *Dis. Mon.* 64, 195–212. doi: 10.1016/j.disamonth.2018.01.007

Calisher, C. H., Childs, J. E., Field, H. E., Holmes, K. V., and Schountz, T. (2006). Bats: important reservoir hosts of emerging viruses. *Clin. Microbiol. Rev.* 19, 531–545. doi: 10.1128/CMR.00017-06

Calisher, C. H., Karabatsos, N., Dalrymple, J. M., Shope, R. E., Porterfield, J. S., Westaway, E. G., et al. (1989). Antigenic relationships between flaviviruses as determined by cross-neutralization tests with polyclonal antisera. *J. Gen. Virol.* 70, 37–43. doi: 10.1099/0022-1317-70-1-37

Campbell, O., and Krause, P. J. (2020). The emergence of human Powassan virus infection in North America. *Ticks Tick Borne Dis* 11:101540. doi: 10.1016/j.ttbdis.2020.101540

CDC (2019). *Tickborne diseases of the United States-heartland and Bourbon virus diseases*. Atlanta, Georgia: Centers for Disease Control and Prevention. Aavailable at: https://www.cdc.gov/ticks/tickbornediseases/heartland-virus.html. (Accessed April 26, 2022).

CDC (2021a). *Centers for Disease Control and Prevention: Colorado tick fever (CTF)-transmission*. Available at: https://www.cdc.gov/coloradotickfever/transmission.html. (Accessed March 31, 2022).

CDC (2021b). *Heartland virus: statistics and maps*. Available at: https://www.cdc.gov/heartland-virus/statistics/index.html. (Accesed March 22, 2022).

CDC (2022). *Connecticut department of public health confirms Year's first case of Powassan virus*. Press Releases: 05/04/2022. Available at: https://portal.ct.gov/DPH/Press-Room/Press-Releases---2022/POWV-illness. (Accessed June 27, 2022).

Chamberlain, J., Atkinson, B., Logue, C. H., Latham, J., Newman, E. N., and Hewson, R. (2013). Genome sequence of ex-Afghanistan Crimean-Congo hemorrhagic fever virus SCT strain, from an imported United Kingdom case in October 2012. *Genome Announc.* 1:e00161. doi: 10.1128/genomeA.00161-13

Charrel, R. N., Attoui, H., Butenko, A. M., Clegg, J. C., Deubel, V., Frolova, T. V., et al. (2004). Tick-borne virus diseases of human interest in Europe. *Clin. Microbiol. Infect.* 10, 1040–1055. doi: 10.1111/j.1469-0691.2004.01022.x

Choi, K. H. (2021). The role of the stem-loop A RNA promoter in Flavivirus replication. *Viruses* 13:1107. doi: 10.3390/v13061107

Chumakov, M. P. (1948). Results of a study made of Omsk hemorrhagic fever (OL) by an expedition of the institute of neurology. *Vestnik Acad. Med. Nauk SSSR* 2, 19–26.

Clarke, P., Leser, J. S., and Tyler, K. L. (2021). Intrinsic innate immune responses control viral growth and protect against neuronal death in an *ex vivo* model of West Nile virus-induced central nervous system disease. *J. Virol.* 95:e0083521. doi: 10.1128/JVI.00835-21

Conger, N. G., Paolino, K. M., Osborn, E. C., Rusnak, J. M., Günther, S., Pool, J., et al. (2015). Health care response to CCHF in US soldier and nosocomial transmission to health care providers, Germany, 2009. *Emerg. Infect. Dis.* 21, 23–31. doi: 10.3201/eid2101.141413

Connally, N. P., Rose, D. A., Breuner, N. E., Prose, R., Fleshman, A. C., Thompson, K., et al. (2019). Impact of wearing and washing/drying of Permethrin-treated clothing on their contact irritancy and toxicity for Nymphal *Ixodes scapularis* (Acari: Ixodidae) ticks. *J. Med. Entomol.* 56, 199–214. doi: 10.1093/jme/tjy138

Connolly-Andersen, A. M., Magnusson, K. E., and Mirazimi, A. (2007). Basolateral entry and release of Crimean-Congo hemorrhagic fever virus in polarized MDCK-1 cells. *J. Virol.* 81, 2158–2164. doi: 10.1128/JVI.02070-06

Daily-Sabah. (2022). *Daily-Sabah Zoonotic virus kills 13 since January in Turkey*. Available at: https://www.dailysabah.com/turkey/zoonotic-virus-kills-13-since-january-in-turkey/news. (Accessed June 27, 2022).

Dantas-Torres, F., and Otranto, D. (2022). "Ixodid and Argasid ticks," in *Encyclopedia of infection and immunity*. ed. N. Rezaei. *1st edn*. (United States: Elsevier), 1049–1063.

De Castro, J. J., James, A. D., Minjauw, B., Di Giulio, G. U., Permin, A., Pegram, R. G., et al. (1997). Long-term studies on the economic impact of ticks on Sanga cattle in Zambia. *Exp. Appl. Acarol.* 21, 3–19. doi: 10.1023/A:1018450824854

De la Fuente, J., Antunes, S., Bonnet, S., Cabezas-Cruz, A., Domingos, A. G., Estrada-Peña, A., et al. (2017). Tick-pathogen interactions and vector competence: identification of molecular drivers for tick-borne diseases. *Front. Cell. Infect. Microbiol.* 7:114. doi: 10.3389/fcimb.2017.00114

Deardorff, E. R., Nofchissey, R. A., Cook, J. A., Hope, A. G., Tsvetkova, A., Talbot, S. L., et al. (2013). Powassan virus in mammals, Alaska and New Mexico, U.S.A., and Russia, 2004-2007. *Emerg. Infect. Dis.* 19, 2012–2016. doi: 10.3201/eid1912.130319

Diamond, M. S., Mehlhop, E., Oliphant, T., and Samuel, M. A. (2009). The host immunologic response to West Nile encephalitis virus. *Front. Biosci. (Landmark Ed)* 14, 3024–3034. doi: 10.2741/3432

Ebel, G. D. (2010). Update on Powassan virus: emergence of a north American tick-borne flavivirus. *Annu. Rev. Entomol.* 55, 95–110. doi: 10.1146/annurev-ento-112408-085446

Ebel, G. D., Foppa, I., Spielman, A., and Telford, S. R. (1999). A focus of deer tick virus transmission in the northcentral United States. *Emerg. Infect. Dis.* 5, 570–574. doi: 10.3201/eid0504.990423

Ebel, G. D., and Kramer, L. D. (2004). Short report: duration of tick attachment required for transmission of Powassan virus by deer ticks. *Am. J. Trop. Med. Hyg.* 71, 268–271. doi: 10.4269/ajtmh.2004.71.3.0700268

Eisen, L., and Stafford, K. C. (2021). Barriers to effective tick management and tick-bite prevention in the United States (Acari: Ixodidae). *J. Med. Entomol.* 58, 1588–1600. doi: 10.1093/jme/tjaa079

Ejiri, H., Lim, C. K., Isawa, H., Fujita, R., Murota, K., Sato, T., et al. (2018). Characterization of a novel thogotovirus isolated from *Amblyomma testudinarium* ticks in Ehime, Japan: a significant phylogenetic relationship to Bourbon virus. *Virus Res.* 249, 57–65. doi: 10.1016/j.virusres.2018.03.004

El Khoury, M. Y., Hull, R. C., Bryant, P. W., Escuyer, K. L., St George, K., Wong, S. J., et al. (2013). Diagnosis of acute deer tick virus encephalitis. *Clin. Infect. Dis.* 56, e40–e47. doi: 10.1093/cid/cis938

Erickson, B. R., Deyde, V., Sanchez, A. J., Vincent, M. J., and Nichol, S. T. (2007). N-linked glycosylation of Gn (but not Gc) is important for Crimean Congo hemorrhagic fever virus glycoprotein localization and transport. *Virology* 361, 348–355. doi: 10.1016/j.virol.2006.11.023

Estrada-Peña, A., and Salman, M. (2013). Current limitations in the control and spread of ticks that affect livestock: a review. *Agriculture* 3, 221–235. doi: 10.3390/agriculture3020221

Fatmi, S. S., Zehra, R., and Carpenter, D. O. (2017). Powassan virus-A new reemerging tick-borne disease. *Front. Public Health* 5:342. doi: 10.3389/fpubh.2017.00342

Fill, M. A., Compton, M. L., McDonald, E. C., Moncayo, A. C., Dunn, J. R., Schaffner, W., et al. (2017). Novel clinical and pathologic findings in a heartland virus-associated death. *Clin. Infect. Dis.* 64, 510–512. doi: 10.1093/cid/ciw766

Földvári, G., Široký, P., Szekeres, S., Majoros, G., and Sprong, H. (2016). *Dermacentor reticulatus*: a vector on the rise. *Parasit. Vectors* 9:314. doi: 10.1186/s13071-016-1599-x

Fuchs, J., Lamkiewicz, K., Kolesnikova, L., Hölzer, M., Marz, M., and Kochs, G. (2022). Comparative study of ten Thogotovirus isolates and their distinct *in vivo* characteristics. *J. Virol.* 96:e0155621. doi: 10.1128/jvi.01556-21

Fuchs, J., Straub, T., Seidl, M., and Kochs, G. (2019). Essential role of interferon response in containing human pathogenic Bourbon virus. *Emerg. Infect. Dis.* 25, 1304–1313. doi: 10.3201/eid2507.181062

Gargili, A., Thangamani, S., and Bente, D. (2013). Influence of laboratory animal hosts on the life cycle of Hyalomma marginatum and implications for an in vivo transmission model for Crimean-Congo hemorrhagic fever virus. *Front. Cell. Infect. Microbiol.* 3:39. doi: 10.3389/fcimb.2013.00039

Garrison, A. R., Radoshitzky, S. R., Kota, K. P., Pegoraro, G., Ruthel, G., Kuhn, J. H., et al. (2013). Crimean-Congo hemorrhagic fever virus utilizes a clathrin- and early endosome-dependent entry pathway. *Virology* 444, 45–54. doi: 10.1016/j.virol.2013.05.030

Gauci, P. J., McAllister, J., Mitchell, I. R., St George, T. D., Cybinski, D. H., Davis, S. S., et al. (2015). Hunter Island group Phlebovirus in ticks, Australia. *Emerg. Infect. Dis.* 21, 2246–2248. doi: 10.3201/eid2112.141303

Ghasemian, S. O., Fazlalipour, M., Hosseini, G., Pouryaievali, M. H., Azad-Manjiri, S., Khakifirouz, S., et al. (2021). Serosurvey of Crimean-Congo hemorrhagic fever virus in livestock, Kohgiluyeh and Boyer-Ahmad, Iran, 2017. *J. Vector Borne Dis.* 58, 70–73. doi: 10.4103/0972-9062.313958

Goethert, H. K., Mather, T. N., Johnson, R. W., and Telford, S. R. (2021). Incrimination of shrews as a reservoir for Powassan virus. *Commun. Biol.* 4:1319. doi: 10.1038/s42003-021-02828-1

Gupta, N., Wilson, W., Neumayr, A., and Saravu, K. (2020). Kyasanur Forest disease: state-of-the-art review. *QJM*. doi: 10.1093/qjmed/hcaa119

Gurav, Y. K., Yadav, P. D., Gokhale, M. D., Chiplunkar, T. R., Vishwanathan, R., Patil, D. Y., et al. (2018). Kyasanur Forest disease prevalence in Western Ghats proven and confirmed by recent outbreak in Maharashtra, India, 2016. *Vector Borne Zoonotic Dis.* 18, 164–172. doi: 10.1089/vbz.2017.2129

Hermance, M. E., Santos, R. I., Kelly, B. C., Valbuena, G., and Thangamani, S. (2016). Immune cell targets of infection at the tick-skin Interface during Powassan virus transmission. *PLoS One* 11:e0155889. doi: 10.1371/journal.pone.0155889

Hermance, M. E., and Thangamani, S. (2017). Powassan Virus: An Emerging Arbovirus of Public Health Concern in North America. *Vector Borne Zoonotic Dis.* 17, 453–462. doi: 10.1089/vbz.2017.2110

Hofmann, H., Radda, A., and Kunz, C. (1969). Induction of interferon in the brain of baby mice by viruses of the tick-borne encephalitis (TBE) complex. *Arch. Gesamte Virusforsch.* 28, 197–202.

Holbrook, M. R., Aronson, J. F., Campbell, G. A., Jones, S., Feldmann, H., and Barrett, A. D. (2005). An animal model for the tickborne flavivirus--Omsk hemorrhagic fever virus. *J. Infect. Dis.* 191, 100–108. doi: 10.1086/426397

Hua, B. L., Scholte, F. E., Ohlendorf, V., Kopp, A., Marklewitz, M., Drosten, C., et al. (2020). A single mutation in Crimean-Congo hemorrhagic fever virus discovered in ticks impairs infectivity in human cells. *Elife* 9:e50999. doi: 10.7554/eLife.50999

Hubálek, Z., and Rudolf, I. (2012). Tick-borne viruses in Europe. *Parasitol. Res.* 111, 9–36. doi: 10.1007/s00436-012-2910-1

Infectiousdiseasenews. (2021). *Turkey records 13 Crimean-Congo hemorrhagic fever deaths year to date*. Available at: http://outbreaknewstoday.com/turkey-records-13-crimean-congo-hemorrhagic-fever-deaths-year-to-date-37034/. (Accessed on June 27, 2022).

Jackson, K. C., Gidlewski, T., Root, J. J., Bosco-Lauth, A. M., Lash, R. R., Harmon, J. R., et al. (2019). Bourbon virus in wild and domestic animals, Missouri, USA, 2012-2013. *Emerg. Infect. Dis.* 25, 1752–1753. doi: 10.3201/eid2509.181902

Jiao, Y., Qi, X., Liu, D., Zeng, X., Han, Y., Guo, X., et al. (2015). Experimental and natural infections of goats with severe fever with thrombocytopenia syndrome virus:

evidence for ticks as viral vector. *PLoS Negl. Trop. Dis.* 9:e0004092. doi: 10.1371/journal.pntd.0004092

Jin, C., Liang, M., Ning, J., Gu, W., Jiang, H., Wu, W., et al. (2012). Pathogenesis of emerging severe fever with thrombocytopenia syndrome virus in C57/BL6 mouse model. *Proc. Natl. Acad. Sci. U. S. A.* 109, 10053–10058. doi: 10.1073/pnas.1120246109

Johnson, A. J., Cheshier, R. C., Cosentino, G., Masri, H. P., Mock, V., Oesterle, R., et al. (2007). Validation of a microsphere-based immunoassay for detection of anti-West Nile virus and anti-St. Louis encephalitis virus immunoglobulin m antibodies. *Clin. Vaccine Immunol.* 14, 1084–1093. doi: 10.1128/CVI.00115-07

Kasabi, G. S., Murhekar, M. V., Sandhya, V. K., Raghunandan, R., Kiran, S. K., Channabasappa, G. H., et al. (2013). Coverage and effectiveness of Kyasanur forest disease (KFD) vaccine in Karnataka, South India, 2005-10. *PLoS Negl. Trop. Dis.* 7:e2025. doi: 10.1371/journal.pntd.0002025

Kasi, K. K., Sas, M. A., Sauter-Louis, C., von Arnim, F., Gethmann, J. M., Schulz, A., et al. (2020). Epidemiological investigations of Crimean-Congo haemorrhagic fever virus infection in sheep and goats in Balochistan, Pakistan. *Ticks Tick Borne Dis.* 11:101324. doi: 10.1016/j.ttbdis.2019.101324

Kaufman, W. R. (1989). Tick-host interaction: a synthesis of current concepts. *Parasitol. Today* 5, 47–56. doi: 10.1016/0169-4758(89)90191-9

Kawai, T., and Akira, S. (2006). Innate immune recognition of viral infection. *Nat. Immunol.* 7, 131–137. doi: 10.1038/ni1303

Kemenesi, G., and Bányai, K. (2019). Tick-borne Flaviviruses, with a focus on Powassan virus. *Clin. Microbiol. Rev.* 32:e00106. doi: 10.1128/cmr.00106-17

Kenyon, R. H., Rippy, M. K., McKee, K. T., Zack, P. M., and Peters, C. J. (1992). Infection of *Macaca radiata* with viruses of the tick-borne encephalitis group. *Microb. Pathog.* 13, 399–409. doi: 10.1016/0882-4010(92)90083-Z

Kharitonova, N. N., and Leonov, Y. A. (1986). *Omsk hemorrhagic fever. Ecology of the agent and Epizootiology*. Oxonian Press Pvt. Ltd., New Delhi, India.

Kivaria, F. M. (2006). Estimated direct economic costs associated with tick-borne diseases on cattle in Tanzania. *Trop. Anim. Health Prod.* 38, 291–299. doi: 10.1007/s11250-006-4181-2

Kleib, A. S., Salihy, S. M., Ghaber, S. M., Sidiel, B. W., Sidiya, K. C., and Bettar, E. S. (2016). Crimean-Congo hemorrhagic fever with acute subdural hematoma, Mauritania, 2012. *Emerg. Infect. Dis.* 22, 1305–1306. doi: 10.3201/eid2207.151782

Komar, N., Hamby, N., Palamar, M. B., Staples, J. E., and Williams, C. (2020). Indirect evidence of Bourbon virus (Thogotovirus, Orthomyxoviridae) infection in North Carolina. *N. C. Med. J.* 81, 214–215. doi: 10.18043/ncm.81.3.214

Kosoy, O. I., Lambert, A. J., Hawkinson, D. J., Pastula, D. M., Goldsmith, C. S., Hunt, D. C., et al. (2015). Novel thogotovirus associated with febrile illness and death, United States, 2014. *Emerg. Infect. Dis.* 21, 760–764. doi: 10.3201/eid2105.150150

Kumar, J. S., Yadav, P. D., Shete, A. M., Majumdar, T., Patil, S., and Dash, P. K. (2021). Development and evaluation of reverse transcription loop-mediated isothermal amplification for rapid and real-time detection of Kyasanur forest disease virus. *Int. J. Infect. Dis.* 112, 346–351. doi: 10.1016/j.ijid.2021.01.041

Kuno, G., Chang, G. J., Tsuchiya, K. R., and Miller, B. R. (2001). Phylogeny of Thogoto virus. *Virus Genes* 23, 211–214. doi: 10.1023/A:1011873028144

L'vov, D. K., Leonova, G. N., Gromashevskiĭ, V. L., Belikova, N. P., and Berezina, L. K. (1974). Isolation of the Powassan virus from *Haemaphysalis neumanni* Dönitz, 1905 ticks in the maritime territory. *Vopr. Virusol.* 5, 538–541.

Lambert, A. J., Velez, J. O., Brault, A. C., Calvert, A. E., Bell-Sakyi, L., Bosco-Lauth, A. M., et al. (2015). Molecular, serological and in vitro culture-based characterization of Bourbon virus, a newly described human pathogen of the genus *Thogotovirus*. *J. Clin. Virol.* 73, 127–132. doi: 10.1016/j.jcv.2015.10.021

Lasala, P. R., and Holbrook, M. (2010). Tick-borne flaviviruses. *Clin. Lab. Med.* 30, 221–235. doi: 10.1016/j.cll.2010.01.002

Leblebicioglu, H., Ozaras, R., Irmak, H., and Sencan, I. (2016). Crimean-Congo hemorrhagic fever in Turkey: current status and future challenges. *Antivir. Res.* 126, 21–34. doi: 10.1016/j.antiviral.2015.12.003

Leonova, G. N., Kondratov, I. G., Ternovoi, V. A., Romanova, E. V., Protopopova, E. V., Chausov, E. V., et al. (2009). Characterization of Powassan viruses from far Eastern Russia. *Arch. Virol.* 154, 811–820. doi: 10.1007/s00705-009-0376-y

Li, H., Jiang, X. M., Cui, N., Yuan, C., Zhang, S. F., Lu, Q. B., et al. (2021). Clinical effect and antiviral mechanism of T-705 in treating severe fever with thrombocytopenia syndrome. *Signal Transduct. Target. Ther.* 6:145. doi: 10.1038/s41392-021-00541-3

Li, G., Wang, N., Guzman, H., Sbrana, E., Yoshikawa, T., Tseng, C. T., et al. (2008). Dhori virus (Orthomyxoviridae: Thogotovirus) infection of mice produces a disease and cytokine response pattern similar to that of highly virulent influenza A (H5N1) virus infection in humans. *Am. J. Trop. Med. Hyg.* 78, 675–680. doi: 10.4269/ajtmh.2008.78.675

Lumley, S., Atkinson, B., Dowall, S., Pitman, J., Staplehurst, S., Busuttil, J., et al. (2014). Non-fatal case of Crimean-Congo haemorrhagic fever imported into the United Kingdom (ex Bulgaria), June 2014. *Euro Surveill.* 19:20864. doi: 10.2807/1560-7917.ES2014.19.30.20864

Mackenzie, J. (2005). Wrapping things up about virus RNA replication. *Traffic* 6, 967–977. doi: 10.1111/j.1600-0854.2005.00339.x

Madison-Antenucci, S., Kramer, L. D., Gebhardt, L. L., and Kauffman, E. (2020). Emerging tick-borne diseases. *Clin. Microbiol. Rev.* 33:e00083. doi: 10.1128/CMR.00083-18

Mai, J., Virtue, A., Shen, J., Wang, H., and Yang, X. F. (2013). An evolving new paradigm: endothelial cells--conditional innate immune cells. *J. Hematol. Oncol.* 6:61. doi: 10.1186/1756-8722-6-61

Maltezou, H. C., Andonova, L., Andraghetti, R., Bouloy, M., Ergonul, O., Jongejan, F., et al. (2010). Crimean-Congo hemorrhagic fever in Europe: current situation calls for preparedness. *Euro Surveill.* 15:19504. doi: 10.2807/ese.15.10.19504-en

Martin, D. A., Muth, D. A., Brown, T., Johnson, A. J., Karabatsos, N., and Roehrig, J. T. (2000). Standardization of immunoglobulin M capture enzyme-linked immunosorbent assays for routine diagnosis of arboviral infections. *J. Clin. Microbiol.* 38, 1823–1826. doi: 10.1128/JCM.38.5.1823-1826.2000

Masson, F., Mount, A. M., Wilson, N. S., and Belz, G. T. (2008). Dendritic cells: driving the differentiation programme of T cells in viral infections. *Immunol. Cell Biol.* 86, 333–342. doi: 10.1038/icb.2008.15

Mateo, R. I., Xiao, S. Y., Lei, H., DA Rosa, A. P., and Tesh, R. B. (2007). Dhori virus (Orthomyxoviridae: Thogotovirus) infection in mice: a model of the pathogenesis of severe orthomyxovirus infection. *Am. J. Trop. Med. Hyg.* 76, 785–790. doi: 10.4269/ajtmh.2007.76.785

Matser, A., Hartemink, N., Heesterbeek, H., Galvani, A., and Davis, S. (2009). Elasticity analysis in epidemiology: an application to tick-borne infections. *Ecol. Lett.* 12, 1298–1305. doi: 10.1111/j.1461-0248.2009.01378.x

McMullan, L. K., Folk, S. M., Kelly, A. J., MacNeil, A., Goldsmith, C. S., Metcalfe, M. G., et al. (2012). A new phlebovirus associated with severe febrile illness in Missouri. *N. Engl. J. Med.* 367, 834–841. doi: 10.1056/NEJMoa1203378

Miller, M. (2018). *Bourbon virus—now listed as emerging illness*. Missourian. Available at: http://www.emissourian.com/local_news/county/bourbon-virus-now-listedas-emerging-illness-new-case-in/article_5d67a0e6-bf55-5cfb-9e6c-9b73896fafad.html. (Accessed March 29, 2022).

Mlera, L., Meade-White, K., Saturday, G., Scott, D., and Bloom, M. E. (2017). Modeling Powassan virus infection in *Peromyscus leucopus*, a natural host. *PLoS Negl. Trop. Dis.* 11:e0005346. doi: 10.1371/journal.pntd.0005346

Mofleh, J., and Ahmad, Z. (2012). Crimean-Congo haemorrhagic fever outbreak investigation in the Western region of Afghanistan in 2008. *East Mediterr. Health J.* 18, 522–526. doi: 10.26719/2012.18.5.522

Molinas, A., Mirazimi, A., Holm, A., Loitto, V. M., Magnusson, K. E., and Vikström, E. (2016). Protective role of host aquaporin 6 against Hazara virus, a model for Crimean-Congo hemorrhagic fever virus infection. *FEMS Microbiol. Lett.* 363:fnw058. doi: 10.1093/femsle/fnw058

Mostafa, H. H., and Dean, A. B. (2022). Tick talk: Powassan, heartland, and Bourbon viruses. *Clin. Microbiol. Newsl.* 44, 13–21. doi: 10.1016/j.clinmicnews.2022.01.001

Mourya, D. T., Yadav, P. D., Basu, A., Shete, A., Patil, D. Y., Zawar, D., et al. (2014). Malsoor virus, a novel bat phlebovirus, is closely related to severe fever with thrombocytopenia syndrome virus and heartland virus. *J. Virol.* 88, 3605–3609. doi: 10.1128/JVI.02617-13

Muehlenbachs, A., Fata, C. R., Lambert, A. J., Paddock, C. D., Velez, J. O., Blau, D. M., et al. (2014). Heartland virus-associated death in Tennessee. *Clin. Infect. Dis.* 59, 845–850. doi: 10.1093/cid/ciu434

Muraleedharan, M. (2016). Kyasanur Forest disease (KFD): rare disease of zoonotic origin. *J Nepal Health Res Counc* 14, 214–218. doi: 10.33314/jnhrc.v14i3.881

Novitskiy, V. S. (1948). Pathologic anatomy of spring-summer fever in Omsk region. *Proc. OmGMI* 13, 97–134.

Olschläger, S., Gabriel, M., Schmidt-Chanasit, J., Meyer, M., Osborn, E., Conger, N. G., et al. (2011). Complete sequence and phylogenetic characterisation of Crimean-Congo hemorrhagic fever virus from Afghanistan. *J. Clin. Virol.* 50, 90–92. doi: 10.1016/j.jcv.2010.09.018

Orlinger, K. K., Hofmeister, Y., Fritz, R., Holzer, G. W., Falkner, F. G., Unger, B., et al. (2011). A tick-borne encephalitis virus vaccine based on the European prototype strain induces broadly reactive cross-neutralizing antibodies in humans. *J. Infect. Dis.* 203, 1556–1564. doi: 10.1093/infdis/jir122

Ostfeld, R. S., and Brunner, J. L. (2015). Climate change and Ixodes tick-borne diseases of humans. *Philos. Trans. R. Soc. Lond. Ser. B Biol. Sci.* 370:20140051. doi: 10.1098/rstb.2014.0051

Owen, S., Gaffney, C., Grado, L., Woodson, M. L., King, J. A., Balaraman, R. P., et al. (2021). Colorado tick fever virus induces apoptosis in human endothelial cells to facilitate viral replication. *Ticks Tick Borne Dis.* 12:101775. doi: 10.1016/j.ttbdis.2021.101775

Pages, F., Dautel, H., Duvallet, G., Kahl, O., de Gentile, L., and Boulanger, N. (2014). Tick repellents for human use: prevention of tick bites and tick-borne diseases. *Vector Borne Zoonotic Dis.* 14, 85–93. doi: 10.1089/vbz.2013.1410

Pastula, D. M., Turabelidze, G., Yates, K. F., Jones, T. F., Lambert, A. J., Panella, A. J., et al. (2014). Notes from the field: heartland virus disease - United States, 2012-2013. *MMWR Morb. Mortal. Wkly Rep.* 63, 270–271.

Pattnaik, P. (2006). Kyasanur forest disease: an epidemiological view in India. *Rev. Med. Virol.* 16, 151–165. doi: 10.1002/rmv.495

Piantadosi, A., and Kanjilal, S. (2020). Diagnostic approach for Arboviral infections in the United States. *J. Clin. Microbiol.* 58:19. doi: 10.1128/JCM.01926-19

Piantadosi, A., Rubin, D. B., McQuillen, D. P., Hsu, L., Lederer, P. A., Ashbaugh, C. D., et al. (2016). Emerging cases of Powassan virus encephalitis in New England: clinical presentation, imaging, and review of the literature. *Clin. Infect. Dis.* 62, 707–713. doi: 10.1093/cid/civ1005

Potokar, M., Jorgačevski, J., and Zorec, R. (2019). Astrocytes in Flavivirus infections. *Int. J. Mol. Sci.* 20:691. doi: 10.3390/ijms20030691

Qaderi, S., Mardani, M., Shah, A., Shah, J., Bazgir, N., Sayad, J., et al. (2021). Crimean-Congo hemorrhagic fever (CCHF) in Afghanistan: A retrospective single center study. *Int. J. Infect. Dis.* 103, 323–328. doi: 10.1016/j.ijid.2020.11.208

Rainey, T., Occi, J. L., Robbins, R. G., and Egizi, A. (2018). Discovery of *Haemaphysalis longicornis* (Ixodida: Ixodidae) parasitizing a sheep in New Jersey, United States. *J. Med. Entomol.* 55, 757–759. doi: 10.1093/jme/tjy006

Randolph, S. E. (2011). Transmission of tick-borne pathogens between co-feeding ticks: Milan Labuda's enduring paradigm. *Ticks Tick Borne Dis.* 2, 179–182. doi: 10.1016/j.ttbdis.2011.07.004

Rathore, S. S., Manju, A. H., Wen, Q., Sondhi, M., Pydi, R., Haddad, I., et al. (2021). Crimean-Congo haemorrhagic fever-induced liver injury: A systematic review and meta-analysis. *Int. J. Clin. Pract.* 75:e14775. doi: 10.1111/ijcp.14775

Riemersma, K. K., and Komar, N. (2015). Heartland virus neutralizing antibodies in vertebrate wildlife, United States, 2009-2014. *Emerg. Infect. Dis.* 21, 1830–1833. doi: 10.3201/eid2110.150380

Romero, J. R., and Simonsen, K. A. (2008). Powassan encephalitis and Colorado tick fever. *Infect. Dis. Clin. N. Am.* 22, 545–559. doi: 10.1016/j.idc.2008.03.001

Rosenberg, R., Lindsey, N. P., Fischer, M., Gregory, C. J., Hinckley, A. F., Mead, P. S., et al. (2018). Vital signs: trends in reported Vectorborne disease cases - United States and territories, 2004-2016. *MMWR Morb. Mortal. Wkly Rep.* 67, 496–501. doi: 10.15585/mmwr.mm6717e1

Ruzek, D., Holbrook, M. R., Yakimenko, V. V., Karan, L. S., and Tkachev, S. E. (2013). "Omsk hemorrhagic fever virus" in *Manual of Securtiy sensitive microbes and toxins*. ed. L. Dongyou (Boca Raton, FL, USA: CRC Press Inc), 193–200.

Růžek, D., Yakimenko, V. V., Karan, L. S., and Tkachev, S. E. (2010). Omsk haemorrhagic fever. *Lancet* 376, 2104–2113. doi: 10.1016/S0140-6736(10)61120-8

Ryu, J. H., Kim, C. H., and Yoon, J. H. (2010). Innate immune responses of the airway epithelium. *Mol. Cells* 30, 173–183. doi: 10.1007/s10059-010-0146-4

Santos, R. I., Hermance, M. E., Gelman, B. B., and Thangamani, S. (2016). Spinal cord ventral horns and lymphoid organ involvement in Powassan virus infection in a mouse model. *Viruses* 8:220. doi: 10.3390/v8080220

Satrovic, L., Softic, A., Zuko, A., Kustura, A., Koro, A., Goletic, S., et al. (2022). First evidence of Crimean-Congo haemorrhagic fever virus circulation in Bosnia and Herzegovina. *Vet. Med. Sci.* 8, 1271–1275. doi: 10.1002/vms3.781

Savage, H. M., Burkhalter, K. L., Godsey, M. S., Panella, N. A., Ashley, D. C., Nicholson, W. L., et al. (2017). Bourbon virus in Field-collected ticks, Missouri, USA. *Emerg. Infect. Dis.* 23, 2017–2022. doi: 10.3201/eid2312.170532

Savage, H. M., Godsey, M. S. Jr., Panella, N. A., Burkhalter, K. L., Manford, J., Trevino-Garrison, I. C., et al. (2018). Surveillance for tick-borne viruses near the location of a fatal human case of Bourbon virus (family Orthomyxoviridae: genus Thogotovirus) in eastern Kansas, 2015. *J. Med. Entomol.* 55, 701–705. doi: 10.1093/jme/tjx251

Shah, S. Z., Jabbar, B., Ahmed, N., Rehman, A., Nasir, H., Nadeem, S., et al. (2018). Epidemiology, pathogenesis, and control of a tick-borne disease- Kyasanur Forest disease: current status and future directions. *Front. Cell. Infect. Microbiol.* 8:149. doi: 10.3389/fcimb.2018.00149

Shestopalova, N. M., Reingold, V. N., Gagarina, A. V., Kornilova, E. A., Popov, G. V., and Chumakov, M. P. (1972). Electron microscopic study of the central nervous system in mice infected by Omsk hemorrhagic fever (OHF) virus. Virus reproduction in cerebellum neurons. *J. Ultrastruct. Res.* 40, 458–469. doi: 10.1016/S0022-5320(72)80035-2

SIB (2022). *Swiss Institute of Bioinformatics*. Thogotovirus. Available at: https://viralzone.expasy.org/79?outline=all_by_species. (Accessed on: June 2022).

Simon, M., Johansson, C., Lundkvist, A., and Mirazimi, A. (2009). Microtubule-dependent and microtubule-independent steps in Crimean-Congo hemorrhagic fever virus replication cycle. *Virology* 385, 313–322. doi: 10.1016/j.virol.2008.11.020

Sorvillo, T. E., Rodriguez, S. E., Hudson, P., Carey, M., Rodriguez, L. L., Spiropoulou, C. F., et al. (2020). Towards a Sustainable One Health Approach to Crimean-Congo Hemorrhagic Fever Prevention: Focus Areas and Gaps in Knowledge. *Trop Med Infect Dis.* 5:113. doi: 10.3390/tropicalmed5030113

Spare, M., Boorgula, G. D., Thomson, D., Bai, J., Goodin, D., Anderson, G., et al. (2021). Surveillance of host-seeking ticks in the Flint Hills region (USA) and associations with environmental determinants. *Parasitologia* 1, 137–147. doi: 10.3390/parasitologia1030015

Spengler, J. R., Patel, J. R., Chakrabarti, A. K., Zivcec, M., García-Sastre, A., Spiropoulou, C. F., et al. (2015). RIG-I mediates an antiviral response to Crimean-Congo hemorrhagic fever virus. *J. Virol.* 89, 10219–10229. doi: 10.1128/JVI.01643-15

Spiegel, M., Plegge, T., and Pöhlmann, S. (2016). The role of Phlebovirus glycoproteins in viral entry, assembly and release. *Viruses* 8. doi: 10.3390/v8070202

Sreenivasan, M. A., Bhat, H. R., and Rajagopalan, P. K. (1986). The epizootics of Kyasanur Forest disease in wild monkeys during 1964 to 1973. *Trans. R. Soc. Trop. Med. Hyg.* 80, 810–814. doi: 10.1016/0035-9203(86)90390-1

Staples, J. E., Pastula, D. M., Panella, A. J., Rabe, I. B., Kosoy, O. I., Walker, W. L., et al. (2020). Investigation of heartland virus disease throughout the United States, 2013-2017. *Open Forum Infect. Dis.* 7:ofaa125. doi: 10.1093/ofid/ofaa125

Stone, R. (2014). Monkey fever unbound. *Science* 345, 130–131. doi: 10.1126/science.345.6193.130

Suda, Y., Fukushi, S., Tani, H., Murakami, S., Saijo, M., Horimoto, T., et al. (2016). Analysis of the entry mechanism of Crimean-Congo hemorrhagic fever virus, using a vesicular stomatitis virus pseudotyping system. *Arch. Virol.* 161, 1447–1454. doi: 10.1007/s00705-016-2803-1

Surtees, R., Dowall, S. D., Shaw, A., Armstrong, S., Hewson, R., Carroll, M. W., et al. (2016). Heat shock protein 70 family members interact with Crimean-Congo hemorrhagic fever virus and Hazara virus Nucleocapsid proteins and perform a functional role in the Nairovirus replication cycle. *J. Virol.* 90, 9305–9316. doi: 10.1128/JVI.00661-16

Suthar, M. S., Aguirre, S., and Fernandez-Sesma, A. (2013). Innate immune sensing of flaviviruses. *PLoS Pathog.* 9:e1003541. doi: 10.1371/journal.ppat.1003541

Tall, A., Sall, A. A., Faye, O., Diatta, B., Sylla, R., Faye, J., et al. (2009). Two cases of Crimean-Congo haemorrhagic fever (CCHF) in two tourists in Senegal in 2004. *Bull. Soc. Pathol. Exot.* 102, 159–161.

Temur, A. I., Kuhn, J. H., Pecor, D. B., Apanaskevich, D. A., and Keshtkar-Jahromi, M. (2021). Epidemiology of Crimean-Congo hemorrhagic fever (CCHF) in Africa-underestimated for decades. *Am. J. Trop. Med. Hyg.* 104, 1978–1990. doi: 10.4269/ajtmh.20-1413

Topp, A. K., Springer, A., Dobler, G., Bestehorn-Willmann, M., Monazahian, M., and Strube, C. (2022). New and confirmed foci of tick-borne encephalitis virus (TBEV) in Northern Germany determined by TBEV detection in ticks. *Pathogens* 11:126. doi: 10.3390/pathogens11020126

Tsergouli, K., Karampatakis, T., Haidich, A. B., Metallidis, S., and Papa, A. (2020). Nosocomial infections caused by Crimean-Congo haemorrhagic fever virus. *J. Hosp. Infect.* 105, 43–52. doi: 10.1016/j.jhin.2019.12.001

Tuten, H. C., Burkhalter, K. L., Noel, K. R., Hernandez, E. J., Yates, S., Wojnowski, K., et al. (2020). Heartland virus in humans and ticks, Illinois, USA, 2018-2019. *Emerg. Infect. Dis.* 26, 1548–1552. doi: 10.3201/eid2607.200110

Vallbracht, M., Brun, D., Tassinari, M., Vaney, M. C., Pehau-Arnaudet, G., Guardado-Calvo, P., et al. (2018). Structure-function dissection of Pseudorabies virus glycoprotein B fusion loops. *J. Virol.* 92. doi: 10.1128/JVI.01203-17

Wagner, E., Shin, A., Tukhanova, N., Turebekov, N., Nurmakhanov, T., Sutyagin, V., et al. (2022). First indications of Omsk Haemorrhagic fever virus beyond Russia. *Viruses* 14:754. doi: 10.3390/v14040754

Waldenström, J., Lundkvist, A., Falk, K. I., Garpmo, U., Bergström, S., Lindegren, G., et al. (2007). Migrating birds and tickborne encephalitis virus. *Emerg. Infect. Dis.* 13, 1215–1218. doi: 10.3201/eid1308.061416

Walter, C. T., and Barr, J. N. (2011). Recent advances in the molecular and cellular biology of bunyaviruses. *J. Gen. Virol.* 92, 2467–2484. doi: 10.1099/vir.0.035105-0

WDH (2022). *Wyoming Department of Health. Infectious disease epidemiology unit-Colorado tick fever*. Available at: https://health.wyo.gov/publichealth/infectious-disease-epidemiology-unit/disease/colorado-tick-fever/. (Accessed April 6, 2022).

Weber, F., and Mirazimi, A. (2008). Interferon and cytokine responses to Crimean Congo hemorrhagic fever virus; an emerging and neglected viral zonoosis. *Cytokine Growth Factor Rev.* 19, 395–404. doi: 10.1016/j.cytogfr.2008.11.001

Westover, J. B., Rigas, J. D., Van Wettere, A. J., Li, R., Hickerson, B. T., Jung, K. H., et al. (2017). Heartland virus infection in hamsters deficient in type I interferon signaling: protracted disease course ameliorated by favipiravir. *Virology* 511, 175–183. doi: 10.1016/j.virol.2017.08.004

WHO (1985). *Viral hemorrhagic fevers*. Report of WHO Expert Committee: Geneva: World Health Organization. 128.

WHO (2020). *World Health Organization: vector-borne diseases*. Available at: https://www.who.int/news-room/fact-sheets/detail/vector-borne-diseases. (Accessed Oct 6, 2022).

WHO (2022a). *Crimean-Congo haemorrhagic fever*. WH0-Key facts. Available at: https://www.who.int/news-room/fact-sheets/detail/crimean-congo-haemorrhagic-fever. (Accessed at Jan 25, 2023).

WHO (2022b). *WHO coronavirus (COVID-19) dashboard*. Available at: https://covid19.who.int/. (Accessed Septemeber 05, 2022).

WHO (2022c). *World Health Organization. Crimean-Congo hemorrhagic fever–Iraq*. Available at: file:///C:/Users/leiwankeji/Downloads/Crimean-Congo%20Hemorrhagic%20Fever%20in%20Iraq.pdf.

Williamson, B. N., Fischer, R. J., Lopez, J. E., Ebihara, H., and Schwan, T. G. (2019). Prevalence and strains of Colorado tick fever virus in Rocky Mountain wood ticks in the Bitterroot Valley, Montana. *Vector Borne Zoonotic Dis.* 19, 694–702. doi: 10.1089/vbz.2018.2407

Wuerth, J. D., and Weber, F. (2016). Phleboviruses and the type I interferon response. *Viruses* 8:174. doi: 10.3390/v8060174

Xiao, X., Feng, Y., Zhu, Z., and Dimitrov, D. S. (2011). Identification of a putative Crimean-Congo hemorrhagic fever virus entry factor. *Biochem. Biophys. Res. Commun.* 411, 253–258. doi: 10.1016/j.bbrc.2011.06.109

Yakut, N., Kepenekli, E., and Dogru, O. (2021). Crimean-Congo hemorrhagic fever with hemophagocytic lymphohistiocytosis. *Rev. Soc. Bras. Med. Trop.* 54:e0438. doi: 10.1590/0037-8682-0438-2020

Yendell, S. J., Fischer, M., and Staples, J. E. (2015). Colorado tick fever in the United States, 2002-2012. *Vector Borne Zoonotic Dis.* 15, 311–316. doi: 10.1089/vbz.2014.1755

Yilmaz, M., Aydin, K., Akdogan, E., Sucu, N., Sonmez, M., Omay, S. B., et al. (2008). Peripheral blood natural killer cells in Crimean-Congo hemorrhagic fever. *J. Clin. Virol.* 42, 415–417. doi: 10.1016/j.jcv.2008.03.003

Zhang, Q., Li, N., Deng, C., Zhang, Z., Li, X., Yoshii, K., et al. (2019). Trans complementation of replication-defective Omsk hemorrhagic fever virus for antiviral study. *Virol. Sin.* 34, 412–422. doi: 10.1007/s12250-019-00109-0

frontiers | Frontiers in Microbiology

TYPE Original Research
PUBLISHED 14 June 2023
DOI 10.3389/fmicb.2023.1179173

Check for updates

OPEN ACCESS

EDITED BY
Hong Yin,
Chinese Academy of Agricultural Sciences,
China

REVIEWED BY
Guangyuan Liu,
Virginia Tech, United States;
Chinese Academy of Agricultural Sciences,
China

*CORRESPONDENCE
Xiangdong Ruan
✉ xdruan@163.com
Weijun Chen
✉ chenwj@genomics.cn
Jiafu Jiang
✉ jiangjf2008@139.com

†These authors have contributed equally to this work and share first authorship

RECEIVED 03 March 2023
ACCEPTED 12 May 2023
PUBLISHED 14 June 2023

CITATION
Huang L, Liu S, Chen L, Wang F, Ye P, Xia L, Jiang B, Tang H, Zhang Q, Ruan X, Chen W and Jiang J (2023) Identification of novel Jingmen tick virus from parasitic ticks fed on a giant panda and goats in Sichuan Province, southwestern China.
Front. Microbiol. 14:1179173.
doi: 10.3389/fmicb.2023.1179173

COPYRIGHT
© 2023 Huang, Liu, Chen, Wang, Ye, Xia, Jiang, Tang, Zhang, Ruan, Chen and Jiang. This is an open-access article distributed under the terms of the Creative Commons Attribution License (CC BY). The use, distribution or reproduction in other forums is permitted, provided the original author(s) and the copyright owner(s) are credited and that the original publication in this journal is cited, in accordance with accepted academic practice. No use, distribution or reproduction is permitted which does not comply with these terms.

Identification of novel Jingmen tick virus from parasitic ticks fed on a giant panda and goats in Sichuan Province, southwestern China

Lin Huang[1,2†], Shunshuai Liu[2,3†], Lu Chen[4], Fei Wang[5], Ping Ye[6], Luoyuan Xia[2], Baogui Jiang[2], Hao Tang[6], Qingyu Zhang[6], Xiangdong Ruan[7]*, Weijun Chen[8,9]* and Jiafu Jiang[1,2]*

[1]Department of Epidemiology and Biostatistics, School of Public Health, Anhui Medical University, Hefei, China, [2]State Key Laboratory of Pathogen and Biosecurity, Beijing Institute of Microbiology and Epidemiology, Beijing, China, [3]College of Life Sciences, Fujian Agriculture and Forestry University, Fuzhou, China, [4]Beijing Macro & Micro-test Bio-Tech Co., Ltd., Beijing, China, [5]Sichuan Forestry and Grassland Pest Control and Quarantine Station, Chengdu, China, [6]Wolong National Natural Reserve Administration Bureau, Wenchuan, China, [7]Academy of Inventory and Planning, National Forestry and Grassland Administration, Beijing, China, [8]BGI PathoGenesis Pharmaceutical Technology, BGI-Shenzhen, Shenzhen, China, [9]College of Life Sciences, University of Chinese Academy of Sciences, Beijing, China

Introduction: Tick-borne viruses (TBVs) pose a significant risk to the health of humans and other vertebrates. A class of multisegmented flavi-like viruses, Jingmen tick virus (JMTV) was first discovered in Rhipicephalus microplus ticks collected from Jingmen of Hubei Province, China in 2010. JMTV has been confirmed to have a relatively wide distribution in vectors and hosts and is associated with human diseases.

Methods: Parasitic and host-seeking ticks were collected in Wolong Nature Reserve, Sichuan Province. Total RNA was extracted and then enriched the viral RNA. The DNA library was constructed and then were sequenced with MGI High-throughput Sequencing Set (PE150). After the adaptor sequences,low-quality bases and host genome were removed, resulting reads classified as a virus were subsequently de novo assembled into contigs, which were then compared to the NT database. Those annotated under the kingdom virus were initially identified as potential virus-associated sequences. Phylogenetic and Reassortment analysis of sequences were performed using MEGA and SimPlot software, respectively.

Results and discussion: Two host-seeking ticks and 17 ticks that fed on giant pandas and goats were collected. Through high-throughput sequencing, whole virus genomes were attained from four tick samples (PC-13, PC-16, PC-18, and PC-19) that shared 88.7–96.3% similarity with known JMTV. Phylogenetic tree showed that it was a novel JMTV-like virus, referred to as Sichuan tick virus, which also had the signals of reassortment with other JMTV strains, suggesting a cross-species transmission and co-infection of segmented flavi-like viruses among multiple tick hosts.

Conclusion: We discovered and confirmed one new Jingmen tick virus, Sichuan tick virus. Further investigation is required to determine the pathogenicity of Sichuan tick virus to humans and animals, as well as its epidemiological characteristics in nature.

KEYWORDS

Jingmen virus group, tick borne disease, Sichuan tick virus, Sichuan Province, giant panda

1. Introduction

In recent decades, emerging tick-borne viruses (TBVs) has been increasing and widely distributed all over the world. Since the confirmation of the first TBV, the Louping ill virus found in Scottish sheep, over 80 years ago (Jeffries et al., 2014), at least 160 such viruses have been found to be transmitted by ticks (Bartíková et al., 2017). Among the confirmed TBVs are 9 families and at least 12 genera, as well as other unassigned members (Shi et al., 2018). TBVs feature a wide range of hosts, including cattle, sheep, humans, rodents, and horses, some of which can cause human diseases and losses in relation to animal husbandry and agriculture. Thus far, at least 5 families, namely *Nairoviridae, Phenuiviridae, Flaviviridae, Orthom-yxoviridae* and *Reoviridae*, and 15 species of TBVs that cause human diseases worldwide have been found (Liu et al., 2020; Ma et al., 2021). In China, emerging TBVs have been reported to cause multiple human diseases: tick-borne encephalitis virus (TBEV) (Xing et al., 2017), severe fever with thrombocytopenia syndrome virus (SFTSV) (Yu et al., 2011), Crimean-Congo hemorrhagic fever virus (CCHFV) (Sun et al., 2011), Jingmen tick virus (JMTV) (Qin et al., 2014; Jia et al., 2019), Alongshan virus (ALSV) (Wang et al., 2019), and Songling virus (SGLV) (Ma et al., 2021). The TBVs associated with human diseases are transmitted to humans through tick bites, causing varying degrees of symptoms, while other TVBs pose unclear risks to public health.

Jingmen tick virus (JMTV) is a novel tick-borne RNA virus that was identified in a pool of *Rhipicephalus microplus* collected from the Jingmen region of Hubei Province, China in 2010 (Qin et al., 2014). The viral genome of JMTV, the segmented flavi-like virus, consists of four segments. Two segments encode non-structural proteins that are genetically related to the NS3 and NS5 sequences of the genus *Flavivirus*, while the other two segments, which encode structural proteins, are completely unique suggesting that they might have originated from a yet uncharacterized virus (Qin et al., 2014). In 2014, partial protein sequences of Mogiana tick virus (MGTV) from Brazilian *Rhipicephalus microplus* were first reported as a novel tick-borne virus of the *Flaviviridae* family before JMTV was initially identified (Maruyama et al., 2014). Notably, the sequences of MGTV shared 92.4%-96.8% amino acid identity and 88%-90.3% nucleotide similarity with JMTV, which suggests they may be the same virus (Maruyama et al., 2014; Villa et al., 2017). Subsequently, JMTV has been detected in arthropods (ticks and mosquitoes) and vertebrates (rodents, humans, monkeys, cattle, and tortoises) from China, Uganda, Brazil, Kosovo, French, Turkey, and Kenya (Webster et al., 2015; Ladner et al., 2016; Shi et al., 2016; Emmerich et al., 2018; Souza et al., 2018; Temmam et al., 2019). More significantly, JMTV has been proven to infect human and cause mild to severe diseases through high-throughput sequencing of skin biopsies and blood samples (Jia et al., 2019).

The jingmenviruses group, which was identified recently, tentatively refers to segmented flavi-like viruses that have not been formally classified by the International Committee on Taxonomy of Viruses (ICTV) in 2015 (Shi et al., 2016; Temmam et al., 2019). This group is presently divided into two phylogenetic clades. The viruses of one clade are associated with ticks and vertebrates, such as JMTV, MGTV (from ticks in Brazil), ALSV (from ticks and humans in China, Finland, and Russia), and Yanggou tick virus (from ticks in China) (Qin et al., 2014; Shi et al., 2016; Wang et al., 2019; Colmant et al., 2022). The second clade comprises insect- and other host-associated jingmenviruses, such as Guaico Culex virus (GCXV) (from mosquitoes in Panama, Peru, and Trinidad), Wuhan aphid virus (WHAV) (from aphid in China), Wuhan flea virus (WHFV) (from flea in China), and Shuangao insect virus 7 (SAIV7) (from insects in China) (Sun et al., 2011; Colmant et al., 2022). Additionally, Heilongjiang tick virus (HLJTV), Amblyomma virus, Guangxi tick virus (GXTV), and *Rhipicephalus* associated flavi-like virus also classified as jingmenviruses and share a high similarity with JMTV strain SY84, with 93.06–94.39%, 92.81–94.52%, 92.8–94.5%, and 93–99% identity respectively (Liu, 2018; Shi et al., 2021). Therefore, it can be seen that jingmenviruses have been emerging around the world with a diversity of hosts, members of which lead to severe diseases. Thus, it is crucial to conduct jingmenviruses research in the coming years to deal with emerging related diseases.

In China, JMTV has been detected in various hosts, such as arthropods, humans, bats, rodents and mammals from Hubei, Fujian, Heilongjiang, Yunnan, Guizhou, Henan, Guangxi and Zhejiang provinces (Guo et al., 2020; Colmant et al., 2022). However, there is a lack of data regarding JMTV infections in Sichuan Province, where the national-level protected animal, giant pandas, is often parasitized by many ticks. To investigate the tick virome in Sichuan Wolong National Nature Reserve, host-seeking ticks and parasitic ticks from giant pandas and goats were collected in the area. High-throughput sequencing was then conducted in the collected ticks to determine the tick virome. The objectives of the study were to understand the potential threat of JMTV-like viruses on public health to local residents, as well as protected animals and livestock.

2. Materials and methods

2.1. Sample collection

Parasitic and host-seeking ticks were collected in Wolong Nature Reserve, Sichuan Province using different methods in 2020 (Figure 1). The parasitic ticks were carefully removed from giant pandas and goats by using tweezers, while host-seeking ticks were collected from vegetation by flagging. The collected ticks were stored in porous centrifuge tubes with moistened sterile filter paper. Subsequently, morphological identification was performed under a stereomicroscope. The collected ticks were kept in an artificial climate chamber at 20°C until further testing was conducted.

2.2. RNA extraction, library preparation, and sequencing

The RNA of collected live ticks was extracted using AllPrep DNA/RNA Mini Kit (cat.no.80204, QIAGEN) according to the manufacturer's instructions. The ticks were categorized into different groups, such as one engorged tick as a pool, 2–5 non-engorged ticks (around 20 mg) as one pool, and eggs of the engorged tick as one pool.

A Nucleic Acid Microbes Purification kit (KAPA RNA HyperPrep Kit with RiboErase, KK8561#, Roche) was also used to enrich the viral RNA from total RNA samples. The remaining RNA was fragmented to about 280 bp and then reverse-transcribed into cDNA. Next, a second strand synthesis was conducted by using a Reverse transcription kit (miScript II RT Kit, Cat.No.218161, QIAGEN). Through the synthetic double-stranded DNA, a DNA library was constructed through end-repair, UDI (unique dual-index) adaptor-ligation, and PCR amplification.

The constructed library was qualified with a Qubit® 4.0 Fluorometer (ThermoFisher, Foster City, CA, United States). The library fragment size

FIGURE 1
Location of sampling sites of ticks in Wolong Nature Reserve, Sichuan Province, 2020.

was analyzed with Qsep-100 (Hangzhou Houze Biotechnology Co., Ltd.). The Library Quant Kit (KAPA, Roche, Rotkreuz, Switzerland) was used to accurately quantify the library for screening qualified libraries. The qualified library was pooled at 3 nmol each. After circularization and generating DNA nanoballs (DNBs), the resulting libraries were sequenced with MGI High-throughput Sequencing Set (PE150) on MGISEQ-2000 platforms (MGI, Shenzhen, China).

2.3. Quantification of virus abundance

Adaptor sequences and low-quality bases were removed from raw sequencing reads by the fastp program (v0.23.1) to obtain clean data. The process of sequence mapping/alignment in the clean reads uses HISAT2 (v2.1.0) based on the hierarchical indexing of host genomes with default parameters to remove the host genome. The unaligned reads were used for microbial taxonomy *via* the Kraken2 program (v2.0.9-beta) taxonomic classifier based on a custom extended RefSeq database. The outputs generated by Kraken2 were transferred to the Bracken program to acquire more accurate estimations using abundance and diversity.

2.4. Viral contigs assembly and annotation

The resulting reads classified as a virus by Kraken2 were subsequently *de novo* assembled into contigs using the Megahit program (v1.2.9) (Vijaykrishna et al., 2015) with default parameters. The assembled contigs were then compared to the NT database using the blastn program (v0.9.21) (Ladner et al., 2016) with an *E*-value cut-off of 1×10^{-5} to identify viral sequences. Taxonomic lineage information was obtained for the top blast hit of each contig, and those annotated under the kingdom virus were initially identified as potential virus-associated sequences. To exclude false positives, these potential viral contigs were subjected to blastn comparisons against non-redundant nucleotide databases to distinguish viral sequences from non-viral host sequences, endogenous viral elements, and artificial vector sequences. Reference genomes of target species were selected based on blast results. Clean data aligned the reference genome of the target species using bwa (0.7.17-r1188). There were more than 50 bases aligning the reference genome defined as reads of the target species. An initial scaffold extension and reassembly from those reads were built using the *de novo* assembler SPAdes (v3.15.3). Reads aligned to the reference genome were returned to the assembled scaffold using bwa (0.7.17-r1188), and the scaffold was calibrated according to the sequencing depth of the aligned reads to output a complete sequence.

2.5. Phylogenetic analysis

Complete sequences obtained in this study were compared with all sequences in GenBank through blastn of NCBI, and appropriate reference sequences were selected for Phylogenetic analysis. Subsequently, MEGA_11.0.13 was used to align the sequences and reference sequences using the MUSCLE package and default parameters. The maximum-likelihood method of MEGA_11.0.13 was used to process the phylogenetic analyses with 1,000 bootstrap replicates.

2.6. Reassortment and variation analysis

Reassortment analysis of sequences for virus sequences was performed using SimPlot (v3.5.1). The schematic diagram of the genome structure was drawn on the basis of blastx comparison information of RNA sequence. Variation analysis was conducted through bwa, varscan, and snpeff bioinformatics software.

3. Results

3.1. Tick samples

A total of 19 live ticks were collected in Wolong Nature Reserve of Sichuan province from April 2020 to August 2020, including 17 parasitic ticks that fed on giant pandas or goats and 2 host-seeking ticks (Figure 1). These ticks were comprised of 19 adult ticks and 3 pools of tick eggs, including 4 *Ixodes acutitarsus*, 7 *Haemaphysalis longicornis*, and 8 *Ixodes ovatus*, of which 3 *Ixodes ovatus* ticks had laid eggs. Then 15 pools of tick samples, with 7 *Ixodes ovatus* from giant pandas (4 adult ticks and 3 groups of eggs), 2 *Ixodes acutitarsus* parasitizing on goats and 2 free *Ixodes acutitarsus*, and 4 *Haemaphysalis longicornis* from goats (Table 1) had total RNA extracted, followed by library preparation and sequencing for analysis.

10.3389/fmicb.2023.1179173

TABLE 1 Characteristics of tick samples collected from Sichuan Province in this study.

Pool ID	Tick species	Hosts	Developmental phase	Number of ticks/eggs
PC-5	*Ixodes acutitarsus*	Goat	♀ adult	1
PC-6	*Ixodes ovatus*	Giant panda	♀ adult	1
PC-7	*Ixodes ovatus*	Giant panda	Eggs	>200 From PC-6
PC-8	*Ixodes ovatus*	Giant panda	♀ adult	1
PC-9	*Ixodes ovatus*	Giant panda	Eggs	>200 From PC-7
PC-10	*Ixodes ovatus*	Giant panda	♀ adult	1
PC-11	*Ixodes ovatus*	Giant panda	Eggs	>200 From PC-8
PC-12	*Haemaphysalis longicornis*	Goat	♀ adult	1
PC-13	*Haemaphysalis longicornis*	Goat	♀ adult	1
PC-14	*Ixodes acutitarsus*	Free	♀ adult	1
PC-15	*Ixodes acutitarsus*	Free	♀ adult	1
PC-16	*Ixodes ovatus*	Giant panda	♀ adult	5
PC-17	*Haemaphysalis longicornis*	Goat	♀ adult	2
PC-18	*Haemaphysalis longicornis*	Goat	♀ adult	3
PC-19	*Ixodes acutitarsus*	Goat	♂ adult	1

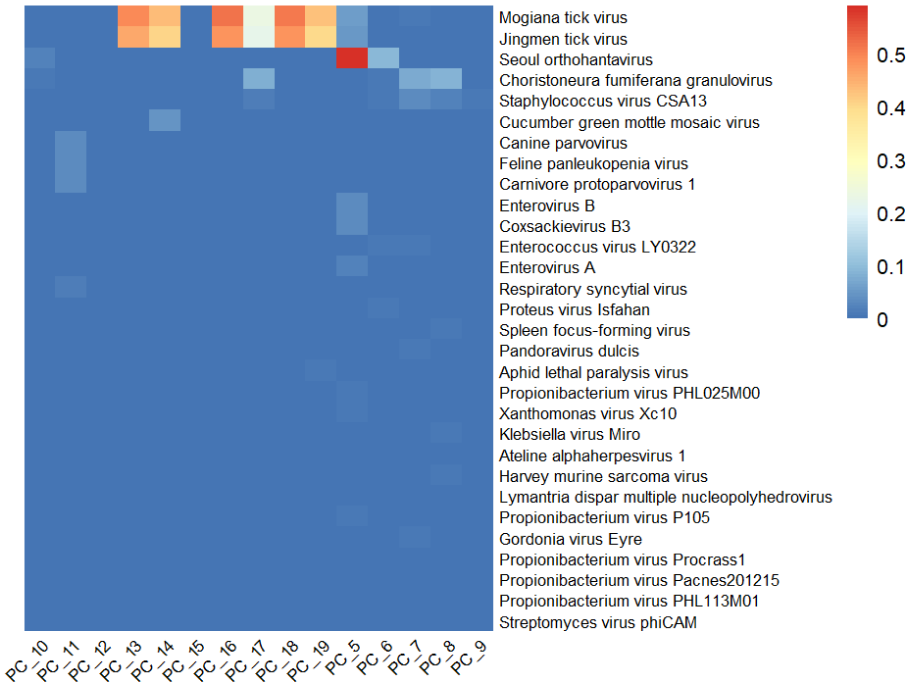

FIGURE 2
Overview of relative abundance of the top 30 virus species contained in the 15 tick sample pools from Wolong Nature Reserve of Sichuan Province.

3.2. Meta-transcriptomes analysis

Total RNA of 15 sample pools have been analyzed by meta-transcriptomes. A total of 165.15 GB nucleotide data was generated, which were assembled and annotated for identification and characteristic of virus groups. After quality control, removal of host gene and exclusion of reads with no significant similarity to any sequence in the NCBI, 110,846 valid reads for viruses were obtained.

3.3. Characteristics of viruses in the tick samples

The relative abundance of the first 30 viruses was shown in Figure 2, which represents the proportion of main viruses in every sample. According to relative abundance, the first five viruses of the tick samples were Mogiana tick virus, Jingmen tick virus, *Seoul orthohantavirus*, Choristoneura fumiferana

TABLE 2 Characteristics of complete nucleotide sequences from the following 4 tick samples.

Pool ID	Segment	Sequence length (nt)	GenBank accession No
PC-13	1	3,063	OQ320755
PC-13	2	2,796	OQ320756
PC-13	3	2,744	OQ320757
PC-13	4	2,737	OQ320758
PC-16	1	3,050	OQ320759
PC-16	2	2,672	OQ320760
PC-16	3	2,716	OQ320761
PC-16	4	2,736	OQ320762
PC-18	1	3,082	OQ158902
PC-18	2	2,679	OQ158903
PC-18	3	2,774	OQ158904
PC-18	4	2,750	OQ158905
PC-19	1	3,239	OQ320763
PC-19	2	2,753	OQ320764
PC-19	3	2,784	OQ320765
PC-19	4	2,759	OQ320766

granulovirus, and staphylococcus virus CSA13 virus from *Flaviviridae*, *Flaviviridae*, *Hantaviridae*, *Baculoviridae*, and *Rountreeviridae*, respectively. The genome of Mogiana tick virus and JMTV mainly existed in 4 tick samples, with 2 *Haemaphysalis longicornis* from goats (PC-13 and PC-18), 1 *Ixodes ovatus* from giant panda (PC-16) and 1 *Ixodes acutitarsus* from goats (PC-19), the relative abundance of which were more than 95%. Three other viruses were primarily distributed in 3 samples (PC-10, PC-5, and PC-6), 3 samples (PC-17, PC-7, and PC-8) and 3 sample (PC-17, PC-7, PC-8) separately.

Through comparison with all nucleotide sequences in GenBank database, it was found that the assembled RNA sequences in the 4 tick samples (PC-13, PC-16, PC-18, and PC-19) shared a higher similarity with JMTV, including four segments, which have been temporarily referred to as Sichuan tick virus. More significantly, the complete nucleotide sequences of the Sichuan tick viruses were obtained from the four tick samples (Table 2). These sequences have been deposited in the GenBank database with accession numbers OQ158902-OQ158905, OQ320755- OQ320766.

3.4. Phylogenetic analysis

The sequences of Sichuan tick virus from the four samples were extremely close to each other (99.82%–100% nucleotide identity) and had high similarity (93.96%–95.71%) with *Rhipicephalus* associated flavi-like virus and JMTV strains from Lao PDR. These sequences were also found to be similar to JMTV found in Lao PDR, Brazil, Kenya and some provinces of China, with an 88.73–96.28% identity. Subsequently, the analyzed Sichuan tick viruses had an 88.77–95% nucleotide identity with Heilongjiang tick virus, Guangxi tick virus, Mogiana tick virus, Amblyomma virus and Rhipicephalus-fassociated flavi-like virus deposited in GenBank. Through the maximum-likelihood method based on four segments of Sichuan tick viruses, the phylogenetic analyses revealed that every segment of the Sichuan tick viruses clustered together, and then formed a separate clade (Figures 3A–D). Segment 1 of the Sichuan tick viruses from the four tick samples was closest to *Rhipicephalus* associated flavi-like virus strain YNTV4 from Yunnan in terms of phylogeny, with 94.64–94.66% identity (Figure 3A). Yet segments 2, 3 and 4 of Sichuan tick viruses exhibited the closest evolutionary relationship with JMTV strain from Lao PDR, with 93.96%–94.26%, 95.71%, and 95.55%–95.56% similarity, respectively (Figures 3B–D). The structure of JMTV genome was relatively conserved among all JMTV strains in the GenBank database. Segment 1 and segment 3 of JMTV encoded NSP1 and NSP2 proteins respectively, non-structure proteins, which seem to have homology with NS5 and NS3 proteins of the genus flavivirus. Segment 2 and segment 4 of JMTV encoded VP1, VP2, and VP3 proteins, structure proteins, which have no known homologs.

3.5. Reassortment analysis

The signals of reassortment were observed between the four segments of the Sichuan tick viruses and other JMTV strains from *Amblyomma testudinarium* (Japan and Laos), *Bubalus bubalis* (China), *Myotis siligorensis* (China), *Haemaphysalis longicornis* (China). Especially, the signals of recombination between the four segments of the Sichuan tick viruses and GXTV (Guangxi tick virus) from *Amblyomma javanense* in China, MGTV (Mogiana tick virus) from *Amblyomma testudinarium* in China, suggested cross-species transmission and co-infection of segmented flavi-like viruses among multiple tick hosts (Figure 4). Reassortment has been frequently observed in segmented viruses and is considered a primary mechanism for interspecies transmission and the emergence of novel strains (Vijaykrishna et al., 2015; Ogola et al., 2022).

3.6. Variation analysis

The genome structure was drawn by taking the sample PC-19 strain as an example, which can be seen in Figure 5. Segment 3 encodes NS3-like protein; segment 2 encodes glycoprotein; segment 4 consists of putative capsid protein and putative membrane protein. Segment 1 comprises NS5-like protein. After comparison and statistics by bioinformatics software, PC-19 was used as the reference standard to obtain the unique variation results among the strains (Table 3 and Figure 6). PC-13 strain has 6 unique mutations, 2 insertions and 4 point mutations. PC-18 has only 2 point mutations. The result of PC-16 variation was consistent with PC-19.

4. Discussion

Since the discovery of Jingmen tick virus (JMTV), JMTV and Jingmenviruses group have been found to be distributed across the world, while there is little research on them in Sichuan Province. In this study, we described the discovery of Sichuan tick virus (SCTV), a

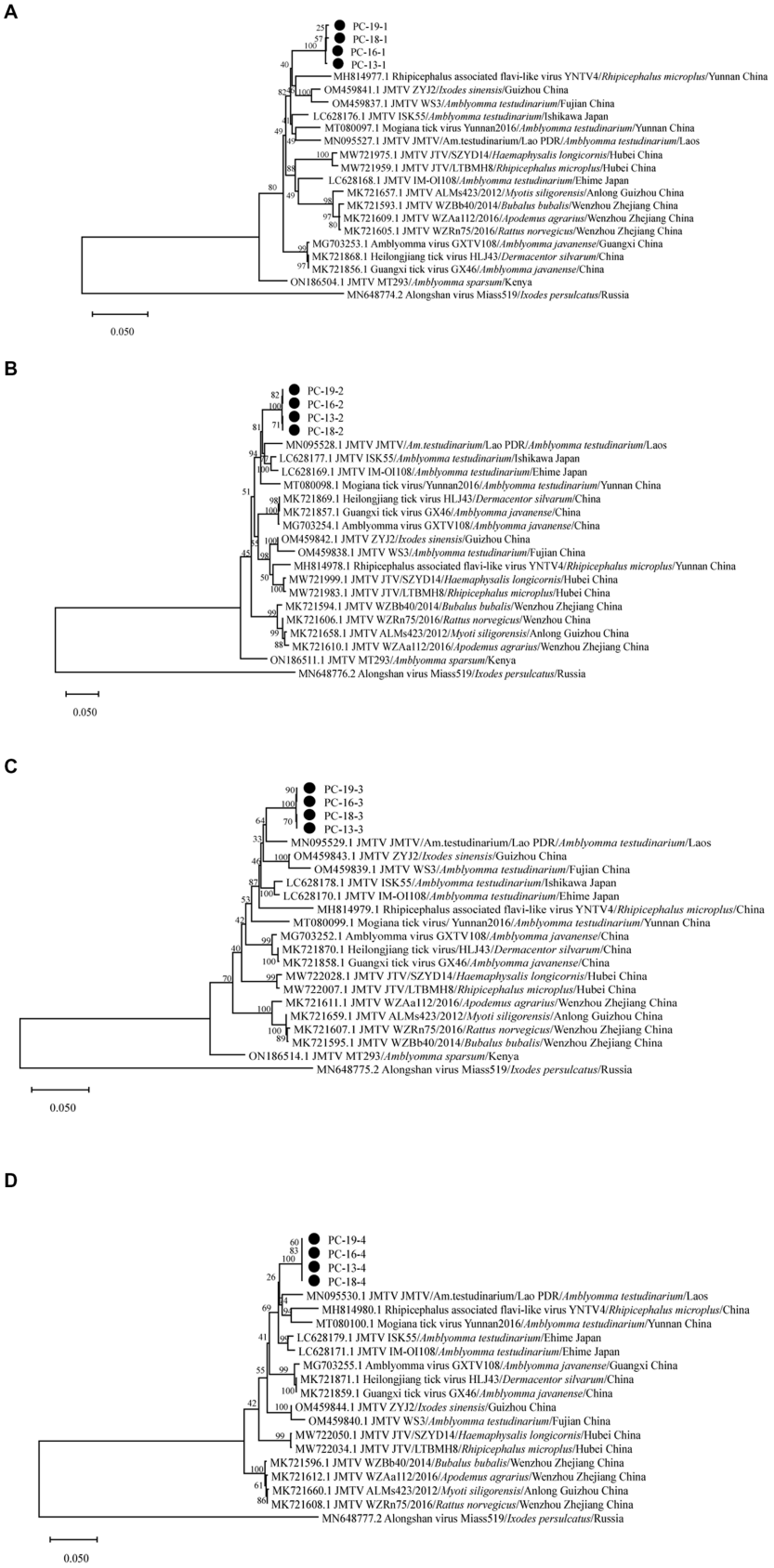

FIGURE 3
Phylogenetic analysis of the complete sequence of Sichuan tick virus in this study. Phylogenetic trees were constructed by the maximum-likelihood method using MEGA_11.0.13 with 1,000 bootstrap replicates: **(A)** (Segment 1), **(B)** (Segment 2), **(C)** (Segment 3), and **(D)** (Segment 4). The number on each branch shows the percent occurrence in 1000 bootstrap replicates.•stood for samples of Sichuan tick virus found in this study.

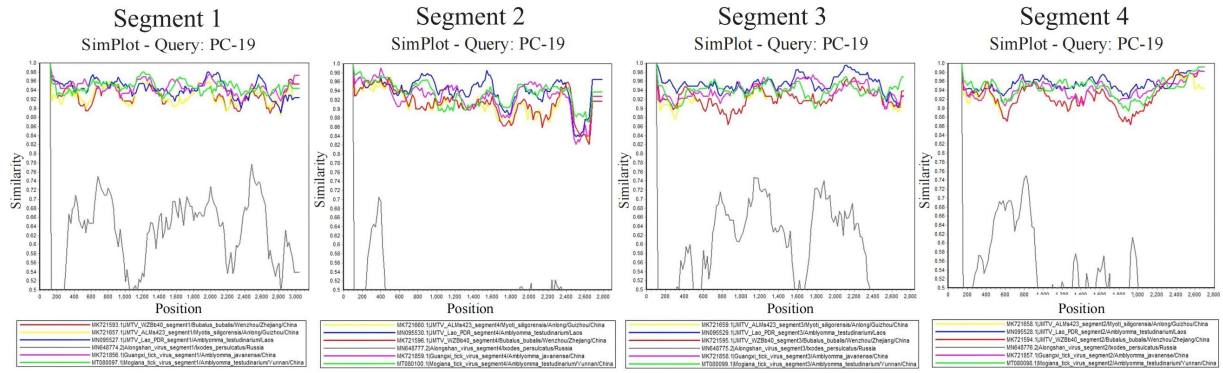

FIGURE 4
Recombination between Sichuan tick virus (PC-19) and reference sequences.

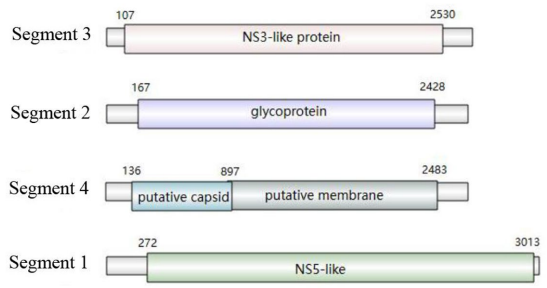

FIGURE 5
Genome structure of Sichuan tick virus (PC-19 strain).

TABLE 3 Results of variation among Sichuan tick viruses.

Virus	CHROM	POS	REF	ALT
PC-13	NC_024112.1	2,668	C	CAGAAAAAAAAAAA
PC-13	NC_024112.1	2,676	G	GA
PC-13	NC_024112.1	585	A	C
PC-13	NC_024112.1	2,677	G	A
PC-13	NC_024112.1	2,785	C	A
PC-13	NC_024114.1	776	T	C
PC-18	NC_024112.1	585	A	C
PC-18	NC_024114.1	776	T	C

novel JMTV-like virus, in three tick samples collected from goats and one from a giant panda. This is the first record of a JMTV-like virus in Sichuan Province.

To our knowledge, tick species that have been shown to carry JMTV are from 26 species in 6 genera: *Rhipicephalus, Amblyomma, Dermacentor, Haemaphysalis, Hyalomma,* and *Ixodes* (Shi et al., 2016). Remarkably, the SCTV genome showing strong similarity to JMTV in this study was first found in several tick species that were not previously associated with JMTV. The special tick species contained *Ixodes ovatus* parasitizing on a giant panda and *Ixodes acutitarsus* that fed on goats, which has expanded the range of tick hosts associated with JMTV. This in turn has increased the risk of human and wild animals infected with JMTV. When combined with earlier research, these results indicate that JMTV is an emerging tick-borne virus with an extensive geographical distribution and is capable of infecting a significant variety of tick species.

Meanwhile, SCTV was identified for the first time in all 3 tick species collected in Wolong Nature Reserve of Sichuan province, suggesting that SCTV exists in various hosts, may be widely distributed throughout southwestern China and form a stable ecological cycle in the Wolong Nature Reserve. Moreover, the 4 tick samples infected with SCTV were engorged ticks collected from a giant panda and goats, suggesting that SCTV also possibly infected parasitic animals. It would appear probable that the risk of SCTV transmission between ticks and parasitic animals could be increased by the act of co-feeding in different animals, especially national protected animals. More seriously, human contact with wild animals (such as giant pandas and goats) may increase the incidence of zoonosis related to SCTV and the hazard of human and wildlife infection with SCTV.

Phylogenetic analysis regarding Sichuan tick virus showed the four segments of SCTV had the closest evolutionary relationship with *Rhipicephalus* associated flavi-like virus strain YNTV4 from Yunnan province and JMTV strain from Lao PDR, illustrating that these jingmenviruses in special geographical locations (Laos, Sichuan and Yunnan provinces) manifested a consistent evolutionary direction under similar environmental factors (similar climate and ecological environment), or that they share a common virus ancestor. JMTV appears to be highly conserved in terms of its evolution as a concerned virus. However, reassortment analysis results demonstrated the sequence differences between SCTV and *Rhipicephalus* associated flavi-like virus, JMTV, were associated with gene recombination. In addition, although SCTV, a JMTV-like virus, showed the highest similarity with JMTV strains ISK55, IM-OI96, and IM-OI108 from Japan, SCTV phylogenetically displayed the closest relationship with *Rhipicephalus* associated flavi-like virus from Yunnan and JMTV from Laos, manifesting that may be the evolutionary consequences of different JMTV lineages or extensive mutations of the genome. Furthermore, the sequences of SCTV were remotely different from other jingmenviruses, with ALSV, HLJTV, *Amblyomma* virus, and Guangxi tick virus from China and Russia, suggesting that the gene recombination between flavivirus and other segmented flavi-like viruses was very common.

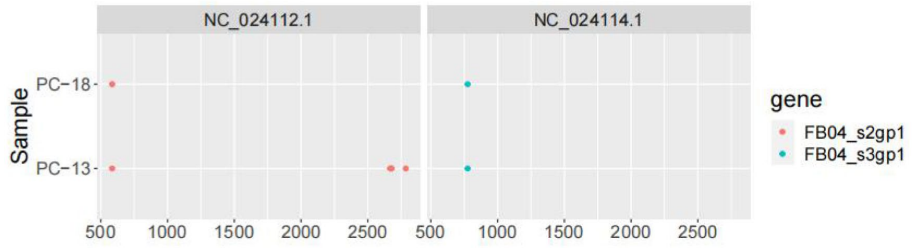

FIGURE 6
Variation of Sichuan tick virus (PC-13, PC-16, PC-18, and PC-19).

This study covered the discovery of Sichuan tick virus in Wolong Nature Reserve of Sichuan Province, which can increase our understanding of tick-borne viruses in the area, provide early warning and prediction of possible tick-borne diseases, reduce misdiagnosis and delay in treatment of tick-borne diseases. It can also improve the diagnostic rate and contribute to the survival of local residents. At the same time, tick-borne viruses in the area were investigated to prevent the occurrence of viral tick-borne infectious diseases, which is beneficial to the safety of residents and is also of great public health significance. Furthermore, early discovery of tick-borne viruses, their vectors, and hosts can provide support for the prevention and control of relevant tick-borne diseases, thereby protecting humans and wildlife, which is significant for public health.

Limitations of this study are as follows. Firstly, the study lacks PCR's validation of SCTV and its serological evidence in humans or animals. Secondly, Sichuan tick virus has not yet been isolated from ticks. Thirdly, the small number of ticks collected in this study is insufficient to indicate the prevalence of JMTV in Sichuan Province, China. In the future, a large-scale epidemiological survey of JMTV needs to be conducted in Sichuan Province to understand more relevant details, such as distribution, hosts, and prevalence. In addition, further serological testing is needed to assess Sichuan tick virus pathogenicity.

5. Conclusion

In summary, we discovered and confirmed one new Jingmen tick virus, Sichuan tick virus, in ticks parasitizing protected animals and livestock, in the Wolong Nature Reserve of Sichuan Province, and its complete nucleotide sequences have been obtained. However, further investigation is required to determine the pathogenicity of Sichuan tick virus to humans and animals, as well as its epidemiologi-cal characteristics in nature.

Data availability statement

The data presented in the study are deposited in the Genbank of National Center for Biotechnology Information, accession number OQ320755-OQ320766 and OQ158902-OQ158905.

Author contributions

JJ and XR conceived and designed the experiments. LH, BJ, and LX performed the experiments. WC, LC, SL, and LH analyzed the data. JJ, FW, PY, HT, and QZ were implemented sample collections. LH and JJ drafted and reviewed the manuscript. All authors contributed to the article and approved the submitted version.

Funding

This work was supported by the State Key Research Development Program of China (2019YFC1200501).

Acknowledgments

The authors wish to thank all the people who had collected samples in the field.

Conflict of interest

LC is employed by Beijing Macro & Micro-test Bio-Tech Co., Ltd.; WC is employed by BGI PathoGenesis Pharmaceutical Technology.

The remaining authors declare that the research was conducted in the absence of any commercial or financial relationships that could be construed as a potential conflict of interest.

Publisher's note

All claims expressed in this article are solely those of the authors and do not necessarily represent those of their affiliated organizations, or those of the publisher, the editors and the reviewers. Any product that may be evaluated in this article, or claim that may be made by its manufacturer, is not guaranteed or endorsed by the publisher.

References

Bartíková, P., Holíková, V., Kazimírová, M., and Štibrániová, I. (2017). Tick-borne viruses. *Acta Virol.* 61, 413–427. doi: 10.4149/av_2017_403

Colmant, A. M. G., Charrel, R. N., and Coutard, B. (2022). Jingmenviruses: Ubiquitous, understudied, segmented flavi-like viruses. *Front. Microbiol.* 13:997058. doi: 10.3389/fmicb.2022.997058

Emmerich, P., Jakupi, X., von Possel, R., Berisha, L., Halili, B., Günther, S., et al. (2018). Viral metagenomics, genetic and evolutionary characteristics of Crimean-Congo hemorrhagic fever orthonairovirus in humans, Kosovo. *Infect. Genet. Evol.* 65, 6–11. doi: 10.1016/j.meegid.2018.07.010

Guo, J. J., Lin, X. D., Chen, Y. M., Hao, Z. Y., Wang, Z. X., Yu, Z. M., et al. (2020). Diversity and circulation of Jingmen tick virus in ticks and mammals. *Virus Evol.* 6:veaa 051. doi: 10.1093/ve/veaa051

Jeffries, C. L., Mansfield, K. L., Phipps, L. P., Wakeley, P. R., Mearns, R., Schock, A., et al. (2014). Louping ill virus: an endemic tick-borne disease of Great Britain. *J. Gen. Virol.* 95, 1005–1014. doi: 10.1099/vir.0.062356-0

Jia, N., Liu, H. B., Ni, X. B., Bell-Sakyi, L., Zheng, Y. C., Song, J. L., et al. (2019). Emergence of human infection with Jingmen tick virus in China: a retrospective study. *EBioMedicine* 43, 317–324. doi: 10.1016/j.ebiom.2019.04.004

Ladner, J. T., Wiley, M. R., Beitzel, B., Auguste, A. J., Dupuis, A. P., Lindquist, M. E., et al. (2016). A multicomponent animal virus isolated from mosquitoes. *Cell Host Microbe* 20, 357–367. doi: 10.1016/j.chom.2016.07.011

Liu, H. B. (2018). Research on isolation, identification and monitoring of ticks infecting pathogens. [Doctoral thesis][Beijing(IL)]:Academy of MilitarySciences.

Liu, J., Dong, N., and Zhang, Y. (2020). Research advance on tick-borne viruses causing human diseases. *Chin. J. Public Health* 36, 646–649.

Ma, J., Lv, X. L., Zhang, X., Han, S. Z., Wang, Z. D., Li, L., et al. (2021). Identification of a new orthonairovirus associated with human febrile illness in China. *Nat. Med.* 27, 434–439. doi: 10.1038/s41591-020-01228-y

Maruyama, S. R., Castro-Jorge, L. A., Ribeiro, J. M. C., Gardinassi, L. G., Garcia, G. R., Brandão, L. G., et al. (2014). Characterisation of divergent flavivirus NS3 and NS5 protein sequences detected in *Rhipicephalus microplus* ticks from Brazil. *Mem. Inst. Oswaldo Cruz* 109, 38–50. doi: 10.1590/0074-0276130166

Ogola, E. O., Kopp, A., Bastos, A. D. S., Slothouwer, I., Marklewitz, M., Omoga, D., et al. (2022). Jingmen tick virus in ticks from Kenya. *Viruses* 14:1041. doi: 10.3390/v14051041

Qin, X. C., Shi, M., Tian, J. H., Lin, X. D., Gao, D. Y., He, J. R., et al. (2014). A tick-borne segmented RNA virus contains genome segments derived from unsegmented viral ancestors. *Proc. Natl. Acad. Sci. U. S. A.* 111, 6744–6749. doi: 10.1073/pnas.1324194111

Shi, J., Hu, Z., Deng, F., and Shen, S. (2018). Tick-Borne Viruses. *Virol. Sin.* 33, 21–43. doi: 10.1007/s12250-018-0019-0

Shi, M., Lin, X. D., Vasilakis, N., Tian, J. H., Li, C. X., Chen, L. J., et al. (2016). Divergent viruses discovered in arthropods and vertebrates revise the evolutionary history of the Flaviviridae and related viruses. *J. Virol.* 90, 659–669. doi: 10.1128/JVI.02036-15

Shi, J., Shen, S., Wu, H., Zhang, Y., and Deng, F. (2021). Metagenomic profiling of viruses associated with *Rhipicephalus microplus* ticks in Yunnan Province, China. *Virol. Sin.* 36, 623–635. doi: 10.1007/s12250-020-00319-x

Souza, W. M. D., Fumagalli, M. J., Torres Carrasco, A. D. O., Romeiro, M. F., Modha, S., Seki, M. C., et al. (2018). Viral diversity of *Rhipicephalus microplus* parasitizing cattle in southern Brazil. *Sci. Rep.* 8:16315. doi: 10.1038/s41598-018-34630-1

Sun, S. R., Meng, W. W., and Zhang, Y. J. (2011). Progress on the study of biological characteristic of Crimean-Congo hemorrhagic fever. *Chin. J. Epidemiol.* 32, 727–732.

Temmam, S., Bigot, T., Chrétien, D., Gondard, M., Pérot, P., Pommelet, V., et al. (2019). Insights into the host range genetic diversity, and geographical distribution of Jingmen viruses. *mSphere* 4, e00645–e00619. doi: 10.1128/mSphere.00645-19

Vijaykrishna, D., Mukerji, R., and Smith, G. J. D. (2015). RNA virus Reassortment: an evolutionary mechanism for host jumps and immune evasion. *PLoS Pathog.* 11:e1004902. doi: 10.1371/journal.ppat.1004902

Villa, E. C., Maruyama, S. R., De Miranda-Santos, I. K. F., Palacios, G., and Ladner, J. T. (2017). Complete coding genome sequence for Mogiana tick virus, a JINGMENVIRUS isolated from ticks in Brazil. *Genome Announc.* 5, e00232–e00217. doi: 10.1128/genomeA.00232-17

Wang, Z. D., Wang, B., Wei, F., Han, S. Z., Zhang, L., Yang, Z. T., et al. (2019). A new segmented virus associated with human febrile illness in China. *N. Engl. J. Med.* 380, 2116–2125. doi: 10.1056/NEJMoa1805068

Webster, C. L., Waldron, F. M., Robertson, S., Crowson, D., Ferrari, G., Quintana, J. F., et al. (2015). The discovery, distribution, and evolution of viruses associated with *Drosophila melanogaster*. *PLoS Biol.* 13:e1002210. doi: 10.1371/journal.pbio.1002210

Xing, Y., Schmitt, H.-J., Arguedas, A., and Yang, J. (2017). Tick-borne encephalitis in China: a review of epidemiology and vaccines. *Vaccine* 35, 1227–1237. doi: 10.1016/j.vaccine.2017.01.015

Yu, X.-J., Liang, M.-F., Zhang, S.-Y., Liu, Y., Li, J.-D., Sun, Y.-L., et al. (2011). Fever with thrombocytopenia associated with a novel bunyavirus in China. *N. Engl. J. Med.* 364, 1523–1532. doi: 10.1056/NEJMoa1010095

frontiers | Frontiers in Microbiology

TYPE Erratum
PUBLISHED 31 August 2023
DOI 10.3389/fmicb.2023.1279784

Check for updates

OPEN ACCESS

APPROVED BY
Frontiers Editorial Office,
Frontiers Media SA, Switzerland

*CORRESPONDENCE
Frontiers Production Office
✉ production.office@frontiersin.org

RECEIVED 18 August 2023
ACCEPTED 18 August 2023
PUBLISHED 31 August 2023

CITATION
Frontiers Production Office (2023) Erratum: Identification of novel Jingmen tick virus from parasitic ticks fed on a giant panda and goats in Sichuan Province, southwestern China. *Front. Microbiol.* 14:1279784. doi: 10.3389/fmicb.2023.1279784

COPYRIGHT
© 2023 Frontiers Production Office. This is an open-access article distributed under the terms of the Creative Commons Attribution License (CC BY). The use, distribution or reproduction in other forums is permitted, provided the original author(s) and the copyright owner(s) are credited and that the original publication in this journal is cited, in accordance with accepted academic practice. No use, distribution or reproduction is permitted which does not comply with these terms.

Erratum: Identification of novel Jingmen tick virus from parasitic ticks fed on a giant panda and goats in Sichuan Province, southwestern China

Frontiers Production Office*

Frontiers Media SA, Lausanne, Switzerland

KEYWORDS

Jingmen virus group, tick borne disease, Sichuan tick virus, Sichuan Province, giant panda

An Erratum on

Identification of novel Jingmen tick virus from parasitic ticks fed on a giant panda and goats in Sichuan Province, southwestern China

by Huang, L., Liu, S., Chen, L., Wang, F., Ye, P., Xia, L., Jiang, B., Tang, H., Zhang, Q., Ruan, X., Chen, W., and Jiang, J. (2023). *Front. Microbiol.* 14:1179173. doi: 10.3389/fmicb.2023.1179173

Due to a production error, an additional affiliation was erroneously listed for author Shunshuai Liu. The affiliation "Lanzhou Veterinary Research Institute, Chinese Academy of Agricultural Sciences, Lanzhou, China" has been removed from the list of author affiliations.

There was a missing affiliation for the Review Editor Guangyuan Liu. The following affiliation should be inserted "Chinese Academy of Agricultural Sciences, China."

The publisher apologizes for these mistakes. The original article has been updated.

frontiers | Frontiers in Microbiology

TYPE Original Research
PUBLISHED 23 June 2023
DOI 10.3389/fmicb.2023.1199660

Check for updates

OPEN ACCESS

EDITED BY
Kevin S. W. Tan,
National University of Singapore, Singapore

REVIEWED BY
André Alex Grassmann,
University of Connecticut Health Center,
United States
Raja Veerapandian,
Texas Tech University Health Sciences Center El Paso, United States
Chandan Shivamallu,
JSS Academy of Higher Education and Research, India

*CORRESPONDENCE
Luis G. V. Fernandes
✉ luisgui530@gmail.com
Ana L. T. O. Nascimento
✉ ana.nascimento@butantan.gov.br

RECEIVED 04 April 2023
ACCEPTED 05 June 2023
PUBLISHED 23 June 2023

CITATION
Fernandes LGV, Teixeira AF and Nascimento ALTO (2023) Evaluation of *Leptospira interrogans* knockdown mutants for LipL32, LipL41, LipL21, and OmpL1 proteins. *Front. Microbiol.* 14:1199660.
doi: 10.3389/fmicb.2023.1199660

COPYRIGHT
© 2023 Fernandes, Teixeira and Nascimento. This is an open-access article distributed under the terms of the Creative Commons Attribution License (CC BY). The use, distribution or reproduction in other forums is permitted, provided the original author(s) and the copyright owner(s) are credited and that the original publication in this journal is cited, in accordance with accepted academic practice. No use, distribution or reproduction is permitted which does not comply with these terms.

Evaluation of *Leptospira interrogans* knockdown mutants for LipL32, LipL41, LipL21, and OmpL1 proteins

Luis G. V. Fernandes[1]*, Aline F. Teixeira[1] and Ana L. T. O. Nascimento[1,2]*

[1]Laboratório de Desenvolvimento de Vacinas, Instituto Butantan, São Paulo, SP, Brazil, [2]Programa de Pos-Graduacao Interunidades em Biotecnologia, Instituto de Ciencias Biomedicas, São Paulo, Brazil

Introduction: Leptospirosis is a worldwide zoonosis caused by pathogenic and virulent species of the genus *Leptospira*, whose pathophysiology and virulence factors remain widely unexplored. Recently, the application of CRISPR interference (CRISPRi) has allowed the specific and rapid gene silencing of major leptospiral proteins, favoring the elucidation of their role in bacterial basic biology, host-pathogen interaction and virulence. Episomally expressed dead Cas9 from the *Streptococcus pyogenes* CRISPR/Cas system (dCas9) and single-guide RNA recognize and block transcription of the target gene by base pairing, dictated by the sequence contained in the 5′ 20-nt sequence of the sgRNA.

Methods: In this work, we tailored plasmids for silencing the major proteins of *L. interrogans* serovar Copenhageni strain Fiocruz L1-130, namely LipL32, LipL41, LipL21 and OmpL1. Double- and triple-gene silencing by in tandem sgRNA cassettes were also achieved, despite plasmid instability.

Results: OmpL1 silencing resulted in a lethal phenotype, in both *L. interrogans* and saprophyte *L. biflexa*, suggesting its essential role in leptospiral biology. Mutants were confirmed and evaluated regarding interaction with host molecules, including extracellular matrix (ECM) and plasma components, and despite the dominant abundance of the studied proteins in the leptospiral membrane, protein silencing mostly resulted in unaltered interactions, either because they intrinsically display low affinity to the molecules assayed or by a compensation mechanism, where other proteins could be upregulated to fill the niche left by protein silencing, a feature previously described for the LipL32 mutant. Evaluation of the mutants in the hamster model confirms the augmented virulence of the LipL32 mutant, as hinted previously. The essential role of LipL21 in acute disease was demonstrated, since the LipL21 knockdown mutants were avirulent in the animal model, and even though mutants could still colonize the kidneys, they were found in markedly lower numbers in the animals' liver. Taking advantage of higher bacterial burden in LipL32 mutant-infected organs, protein silencing was demonstrated *in vivo* directly in leptospires present in organ homogenates.

Discussion: CRISPRi is now a well-established, attractive genetic tool that can be applied for exploring leptospiral virulence factors, leading to the rational for designing more effective subunit or even chimeric recombinant vaccines.

KEYWORDS

CRISPR interference, knockdown mutants, virulence, host-pathogen interactions, LipL32, LipL41, LipL21, OmpL1

Introduction

Leptospirosis is a neglected zoonosis of global concern caused by pathogenic species of the genus *Leptospira,* which can infect a broad range of hosts directly after contact with the urine of infected animals or indirectly after exposure to contaminated water or soil (Bharti et al., 2003; Haake and Levett, 2015). Symptom presentation may vary, ranging from non-specific flu-like symptoms, such as fever, chills, headache, and myalgia, to severe leptospirosis, encompassing a potentially fatal condition known as Weil's disease (Levett, 2001) or severe pulmonary hemorrhage leptospirosis (SPHL) (McBride et al., 2005; Segura et al., 2005; Dolhnikoff et al., 2007), the latter recognized as an emerging clinical manifestation (Nally et al., 2004). Leptospirosis is responsible for more than 1 million cases and almost 60,000 human deaths per year worldwide (Costa et al., 2015; Torgerson et al., 2015).

The molecular basis of leptospiral pathogenesis, despite recent advances in functional genomics and mutagenesis, is still poorly understood (Murray, 2015; Daroz et al., 2021). After contact with damaged skin or mucosa, pathogenic leptospires can rapidly penetrate and breach host biological barriers and migrate across viscous environments (Picardeau, 2017), such as the extracellular matrix (ECM). Many leptospiral adhesins are capable of mediating bacterial adhesion to different elements on the surface of host cells and ECM (Fernandes et al., 2016b; Daroz et al., 2021).

When reaching the bloodstream for dissemination, leptospires need to overcome host natural defenses, such as the complement system and oxidative stress, and several research groups have elucidated the role of surface-exposed proteins in leptospiral immune evasion mechanisms by *in vitro* assays with recombinant proteins (Verma et al., 2006; Vieira et al., 2010a, 2018; Castiblanco-Valencia et al., 2012, 2016; Siqueira et al., 2016; Cavenague et al., 2019). Rapid tissue dissemination can also be related to the ability of pathogenic leptospires to impair the host coagulation cascade (Oliveira et al., 2013; Fernandes et al., 2015, 2016a).

Nevertheless, *in vitro* features of purified recombinant protein do not necessarily reflect the native counterpart role in *Leptospira* spp., and mutations in genes of interest are required to evaluate the resultant phenotype for function confirmation (Shapiro et al., 2018). Accordingly, *in vitro* evidence that leptospiral immunoglobulin-like (Lig) proteins LigA and LigB could play a pivotal role in complement evasion (Castiblanco-Valencia et al., 2012, 2016; Haake and Matsunaga, 2020) was further confirmed by evaluation of a double knockdown LigAB mutant obtained by CRISPR interference (CRISPRi) (Fernandes et al., 2021b), and this mutant was later shown to be avirulent in an animal model (Fernandes et al., 2021c).

The application of CRISPRi for leptospiral mutant generation has allowed the confirmation of native protein function in host–pathogen interaction and virulence. This novel genetic tool for gene silencing relies on the episomal expression of two components: a programmable DNA-binding protein, which is catalytically inactive Cas9 (dCas9), and a single-guide RNA, which dictates the target for gene silencing by base pairing (Qi et al., 2013; Fernandes et al., 2019).

It was previously shown that the silencing of the major outer membrane protein (OMP) LipL32 results in substantial changes in amounts of other lipoproteins and potential virulence factors expressed by *Leptospira*, including the virulence factors LigA and LigB. It was hypothesized that this global proteomic change occurred to fill a niche left by the silencing of LipL32 (Fernandes et al., 2021c). Moreover, the virulence evaluation of this mutant hinted at augmented virulence.

Outer membrane proteins (OMPs) are considered promising candidates for virulence factors because of their location, which enables direct interaction with host components and cells (Haake and Matsunaga, 2002; Ko et al., 2009). In leptospires, lipoproteins are the predominant OMPs, similar to *Borrelia* spp. (Haake and Matsunaga, 2010). Quantitative proteome analysis conducted by Malmström et al. (2009) revealed that LipL32, Loa22, LipL41, and LipL21 are the most abundant lipoproteins in *L. interrogans*. Notably, Loa22 was the first genetically defined virulence factor identified in *L. interrogans* (Ristow et al., 2007).

In this context, it is possible that other major proteins could also play a role in the virulence of leptospires. Exploring and validating leptospiral virulence factors could ultimately favor the design of more effective subunit or even chimeric recombinant vaccines (Barazzone et al., 2021). Directing the immune responses toward virulence determinants has historically proven to be a successful approach in interrupting the cycle of infection, leading to the generation of protective immunity (Delany et al., 2013).

LipL41, an abundant lipoprotein of pathogenic leptospires, is a 41 kDa protein first identified by Haake et al. (1991) and later described by Shang et al. (1996). Furthermore, LipL41 was previously reported to elicit a synergistic protection profile along with OmpL1 protein against lethal challenge in hamsters, inferring that OmpL1 protein could be relevant to pathogenesis (Haake et al., 1999). It was shown that LipL21 can contribute to leptospiral virulence as its binding to peptidoglycan allows leptospires to escape NOD1 and NOD2 (Ratet et al., 2017). In addition, LipL21 was shown to be a potent myeloperoxidase inhibitor, an enzyme stored in neutrophils (Vieira et al., 2018). A transposon mutant of *L. interrogans* serovar Manilae lacking LipL21 was found to be avirulent in a hamster model. However, complementation failed to restore the mutant's virulence. Thus, the contribution of LipL21 to the virulence of leptospires remains unclear (Ratet et al., 2017).

Hence, we were interested in evaluating the outcomes of the silencing of genes coding for these major proteins. For that, we used CRISPRi to create mutants of the major proteins LipL32, LipL41, LipL21, and OmpL1 in *L. interrogans* serovar Copenhageni, and mutant bacteria were evaluated regarding their interaction with host molecules and virulence in a hamster model.

Materials and methods

Bacterial strains and plasmids

Virulent low-passage *L. interrogans* serovar Copenhageni strain Fiocruz L1-130 and saprophytic *L. biflexa* serovar Patoc strain Patoc1 were cultured in EMJH medium (Difco, BD, Franklin Lakes,

TABLE 1 Primer sequences used in this study.

Primer	Sequence (5′ → 3′)	Purpose
sgLipL21 F	AACGTCTTTCGGATCGGATCGTTTTAGAGCTAGAAATAGC	Substitute the *lipL32* protospacer in the sgRNA cassette for the *lipL21* protospacer
sgLipL21 R	GATCCGATCCGAAAGACGTTGAAAATCACGGTATGAACTTAGG	
sgLipL41 F	CTACGTTACGAATGGTTCCGGTTTTAGAGCTAGAAATAGCAAG	Substitute the *lipL32* protospacer in the sgRNA cassette for the *lipL41* protospacer
sgLipL41 R	CGGAACCATTCGTAACGTAGGAAAATCACGGTATGAACTTAGG	
sgOmpL1 F	GCCGCCAGTAGTTCTATCGAGTTTTAGAGCTAGAAATAGCAAG	Substitute the *lipL32* protospacer in the sgRNA cassette for *ompL1* protospacer
sgOmpL1 R	TCGATAGAACTACTGGCGGCGAAAATCACGGTATGAACTTAGG	
sgOmpL1biflexa F	CGAAACGTACGTTTTCTTTGGTTTTAGAGCTAGAAATAGC	Substitute the *lipL32* protospacer in the sgRNA cassette for the *L. biflexa ompL1* protospacer
sgOmpL1biflexa R	CAAAGAAAACGTACGTTTCGGAAAATCACGGTATGAACTTAGG	
sgRNA F	TTAGGATCCCCCGGGGAACAAGAAAGAGTCAGAG	Amplification of whole sgRNA cassette for Gibson assembly
sgRNA R	ATCGAATTCCTGCAGAAAAAAGCACCGACTCGGTGC	
sgRNAsecond R	CTTTCTTGTTCCCGGAAAAAAGCACCGACTCGGTGC	
pMaOri2 F	ACGCAATGTATCGATACCGAC	Amplification flanking the sgRNA cassette
pMaOri2 R	ATAGGTGAAGTAGGCCCACCC	
qLipL32 F	AAGGATCTTTCGTTGCATCT	Quantification of bacterial load
qLipL32 R	TTACTTAGTCGCGTCAGAAG	

NJ, United States) supplemented with 10% (vol/vol) *Leptospira* Enrichment EMJH (Difco) (Turner, 1970) and 1% rabbit serum. Solid media were prepared by supplementing with 1.2% Noble agar (Difco). For transconjugant recovery, spectinomycin was added at a concentration of 40 μg/mL. *E. coli* strain β2163 auxotrophic for diaminopimelic acid (DAP) (Demarre et al., 2005; Picardeau, 2008) was used for general cloning and as conjugation donor cells and was grown in Luria–Bertani (LB, Difco) medium supplemented with DAP (0.3 mM, Sigma).

Macromolecules and antibodies

Murine laminin (Engelbreth-Holm-Swarm murine sarcoma basement membrane, L2020), collagen type IV (Engelbreth-Holm-Swarm murine sarcoma basement membrane, C0543), human cellular (foreskin fibroblasts, F2518) and plasma fibronectin (F2006), human fibrinogen (F4883), plasminogen (PLG) (P7999), recombinant E-cadherin (5085), thrombin (605190), and bovine serum albumin (BSA; A3912) were acquired from Sigma-Aldrich. Anti-laminin (L9393), anti-fibronectin (F3648), anti-fibrinogen (F8512), anti-collagen (SAB5500022), and anti-E-cadherin (SAB5500022) antibodies were acquired from Sigma-Aldrich, and anti-PLG antibody was produced *in house*. In brief, BALB/c female mice were immunized subcutaneously with 10 μg of human PLG mixed with 10% (v/v) Alhydrogel [2% Al(OH)3; Brenntag Biosector] as an adjuvant. Two subsequent boost immunizations were given at 2-week intervals. Horseradish peroxidase (HRP)-conjugated secondary anti-mouse (A9044), anti-goat (A8919), and anti-rabbit IgG (A0545) antibodies were also purchased from Sigma.

Plasmid construction and *Leptospira* spp. conjugation

Plasmid pMaOri.dCas9 (Fernandes et al., 2019) was used as a backbone for sgRNA cassette ligation by Gibson assembly (New England BioLabs, E2611S), according to manufacturer's instructions. The plasmid was digested at the *Xma*I site and sgRNA cassette targeting *lipL32* was amplified from previously described pMaOri.dCas9sgRNAlipL32 (Fernandes et al., 2021b), with primers sgRNA F and sgRNA R (Table 1) designed for the Gibson assembly reaction and for the specific reconstruction of the *Xma*I site at only the 5′ end of the inserted cassette. Thus, this newly obtained pMaOri.dCas9sgRNAlipL32 in this study differs from a previous one (Fernandes et al., 2021b), which was obtained by T4 ligase-mediated reaction and displayed *Xma*I sites at both ends of the cassette.

To generate plasmids containing a single sgRNA cassette targeting either *lipL41*, *lipL21*, or *ompL1* genes, we followed the protocol previously described by Fernandes and Nascimento (2020) to define protospacers (Table 2). The existing protospacer sequence in the template pMaOri.dCas9sgRNAlipL32 plasmid was substituted with the desired protospacer sequence by PCR. Specifically, primers flanking the 20-nt protospacer were used and included the new desired protospacer sequence at the 5' end to provide the required overhang. This resulted in a 9.5 kb amplicon, which was purified and used for subsequent Gibson assembly reactions to seal the plasmid backbone.

To create the double sRNA cassette plasmids, the pMaOri.dCas9sgLipL41 was digested with *Xma*I enzyme, and the desired cassettes for *lipL32* or *ompL1* were amplified from their respective single sgRNA plasmids with primers sgRNA F and

TABLE 2 Target genes and protospacers.

Target gene	Protospacer (5′ → 3′)	Species
lipL32	ACCACCGAAAGCACCACAAG	*L. interrogans*
lipL41	CTACGTTACGAATGGTTCCG	*L. interrogans*
lipL21	AACGTCTTTCGGATCGGATC	*L. interrogans*
ompL1	GCCGCCAGTAGTTCTATCGA	*L. interrogans*
ompL1	CGAAACGTACGTTTTCTTTG	*L. biflexa*

sgRNA second R (Table 1). Plasmid and inserts were mixed at 1:5 proportion for Gibson assembly. All the reactions were used to transform *E. coli* β2163 cells, which were further seeded onto LB plates containing DAP (0.3 mM) and spectinomycin (40 μg/mL) and individual colonies selected by PCR with pMaOri2 F and R primers flanking the sgRNA cassettes (Table 1). For the triple sgRNA plasmids, pMaOri.dCas9sgRNAlipL32sgRNAlipL41 was digested with *XmaI* enzyme, and the cassette for *lipL21* was obtained and ligated as described above. All the obtained plasmids were sequenced with pMaOri2 primers to confirm the correct sgRNA cassettes.

Leptospira spp. knockdown mutants were obtained by conjugation as previously described (Fernandes et al., 2021a).

Evaluation of mutants' binding to host ECM and plasma components

Before binding experiments, each component was serially diluted (1–0.008 μg in 100 μL) and coated onto ELISA plate wells (Costar High Binding; Corning) for detection with appropriate anti-component and secondary antibodies. The immobilized mass that gave a linear curve beyond that point was selected for incubation with the leptospiral mutant strains.

Knockdown mutants or control cells containing only pMaOri.dCas9 were brought to the same concentration (5×10^8/mL) and incubated with the previously defined components' mass for 2 h at 30°C; the bacterial suspensions were then centrifuged (10,000 × g, 15 min), and the supernatant was carefully removed and submitted to another round of centrifugation and supernatant collection. Next, 100 μL of each solution were used to coat the wells for 16 h at room temperature, in seven replicates, and a control without component was used as a blank to determine the baseline signal of the reaction. In parallel, a component mass curve was run in the experiment to determine the percentage of unbound components and, by consequence, indirectly infer the component bound to the leptospiral surface. Plates were washed with PBS containing 0.05% Tween-20 (PBS-T), blocked with 3% BSA in PBS-T for 1 h, and incubated with antibodies for each component (1 h 37°C) and secondary horseradish peroxidase (HRP)-conjugated secondary antibodies in 1% BSA in PBS-T. The wells were washed six times, and o-phenylenediamine (1 mg/mL) in citrate phosphate buffer (pH 5.0) plus 1 μL/mL H_2O_2 was added (100 μL per well).

The reaction proceeded for 10 min and was interrupted by the addition of 50 μL of 2 M H_2SO_4. Readings were taken at 492 nm with a microplate reader (Multiskan EX; Thermo Fisher Scientific, Helsinki, Finland), and absorbance values were compared with values generated from the component curve. The residual component mass in the supernatant was used to infer the mass bound to the leptospiral surface, statistical analysis was performed using one-way ANOVA, followed by the Tukey post-test for pairwise comparisons of each group against control dCas9, and a P-value of <0.05 was considered to be statistically significant.

Fibrin clot inhibition by mutant strains

Leptospires were recovered by centrifugation (10,000 × g, 15 min), washed twice with 0.9% NaCl, and resuspended in 0.9% NaCl to the standardized OD_{420nm} of 5; next, 60 μL of the leptospiral suspension were mixed with 540 μL of a human fibrinogen solution (1 mg/mL in 0.9% NaCl), resulting in a final leptospiral OD_{420nm} of 0.5. After 2 h incubation at 37°C, 90 μL of the incubation reaction were added to each well of a microdilution plate and mixed with 10 μL of 0.5 U/mL human thrombin. Experiments were performed with six replicates, and a control with no leptospires (maximal fibrin clot formation) or no thrombin (no fibrin clot formation) was included. Plates were read at 600 nm at 2-min intervals.

Plasmin formation

Plasmin formation was evaluated according to protocols described by Vieira et al. (2009), with slight modification. Leptospires were grown in EMJH medium without rabbit serum to avoid PLG contamination, recovered by centrifugation (10,000 × g, 15 min), washed twice, and resuspended in PBS. Bacterial suspensions were standardized to OD_{420nm} of 0.5 in 500 μL of PBS. Next, 2 μg of PLG were added followed by incubation for 2 h. Cells were pelleted by centrifugation, washed once, and resuspended in 250 μL of PBS, to which 50 ng of urokinase-type PLG activator (uPA) and 250 μL of plasmin (PLA) substrate D-Val-Leu-Lys-p-nitroanilide dihydrochloride (Sigma) were added to a final concentration of 0.4 mM for amidolytic activity determination. For experimental controls, either PLG, uPA, or leptospires were omitted from the reactions. After a 16-h reaction, bacteria were pelleted and the supernatant was collected for absorbance readings at 405 nm in microdilution plates, in quintuplicate.

Animal ethics statement

All animal experimentation was conducted in accordance with protocols as reviewed and approved by the Animal Care and Use Committee at Instituto Butantan under number 8790290422 and as approved by Institutional guidelines. Four- to six-week-old female hamsters were acclimated to the facility a week prior to the challenge and segregated in boxes of four animals with similar general weight average. The weight of each animal was considered 100% on the day of infection. Hamsters were monitored daily and always had *ad libitum* access to food and water.

Mutant *Leptospira* challenge

LipL32, LipL41, and LipL21 knockdown mutants were cultured to mid-late log phase in EMJH medium at 29°C. Groups of female Syrian gold hamsters (*Mesocricetus auratus*, group $n = 8$, two boxes of $n = 4$) were inoculated intraperitoneally with 5×10^7 leptospiral mutants at the same *in vitro* passage. Each animal was monitored daily and weighed for clinical signs of acute leptospirosis. Animals were humanely euthanized when weight loss (>10%) and/or additional clinical signs (blood on paws/nose/urogenital tract, lethargy, etc.) were observed (Zuerner et al., 2012) or on the basis of experimental time point. One kidney and one liver lobe were harvested and immediately macerated in 5 mL of EMJH medium plus 5-fluorouracil (5-FU). Suspensions were used at different dilutions to inoculate EMJH medium plus 5-FU, without or with spectinomycin, to confirm mutant identities and intact plasmids. Cultures were monitored daily by dark-field microscopy, and positivity scores were recorded depending on cell densities, with values of 0 (no cells observed), 1 (1–10 leptospires per field), 2 (10–100), and 3 (more than 100 leptospires per field). An additional section of the kidney and lobe of the liver was harvested and frozen at −80°C for bacterial burden analysis.

Once the virulence phenotypes of interest were established, a second animal experiment was conducted with additional and alternative experimental endpoints, with the challenge inoculum comprised of 5×10^7 mutant leptospires. One set of animals of each group ($n = 4$) were humanely euthanized on day 4 for synchronized comparison purposes, and the additional set ($n = 4$) was monitored daily for clinical symptoms.

Endpoints of animals inoculated with knockdown strains were compared to those displayed by animals infected with *L. interrogans* containing empty pMaOri.dCas9 plasmids by the log-rank test, and a p-value of <0.05 was considered to be statistically significant.

Quantification of bacterial load in target organs

A cross section of the kidney and liver tissue (15–20 mg) was used for DNA isolation using the DNeasy DNA Blood and Tissue isolation kit (Qiagen, MD, USA) following the manufacturer's specifications and using a final elution volume of 200 μL. The concentration curve of leptospiral genomic equivalent (GEq) was prepared with genomic DNA from *L. interrogans*. The bacterial load was quantified by quantitative PCR assay based on the protocol described by Wunder et al. (2021) using an CFX96 Real-Time System (Bio-Rad, Hercules, CA, USA). The *lipL32* gene was amplified in the samples (5 μL template/well) using primers qLipL32F (5′AAGGATCTTTCGTTGCATCT 3′) and qLipL32R (5′ TTACTTAGTCGCGTCAGAAG 3′), and amplicon was detected by SYBR Green PCR Master Mix (Applied Biosystems, Foster City, CA, USA). The total volume of PCR reactions was 20 μL containing 400 nM of each primer. The amplification protocol consisted of 10 min at 95°C, followed by 40 cycles of amplification (95°C for 15 s and 60°C for 1 min). A result was considered negative if the Ct was >40. The concentration of leptospires (GEq per gram of tissue) was calculated based on the standard curve equation.

Statistical differences between groups of interest were determined by one-tailed Mann–Whitney non-parametric test, and a p-value of <0.05 was considered to be statistically significant.

Evaluation of phenotype stability *in vivo* and *in vitro*

For evaluating target protein silencing in leptospires sheltered at the target organs, tissue macerates (5 mL) were transferred to 15-mL conical tubes and centrifuged at 1,150 × g for 10 min, and the supernatant (∼3 mL) was carefully recovered and transferred to two 1.5-mL microtubes. After centrifugation (10,000 × g, 15 min), pellets were washed twice with PBS and resuspended in 200 μL. Target protein expression in leptospires cultured out of EMJH medium after inoculation with organ macerates with or without spectinomycin (40 μg/mL) was also assessed. Bacteria were recovered from the medium by centrifugation (10,000 × g, 15 min) and washed twice with PBS, and suspensions were then counted. Protein samples were then processed for SDS-PAGE on 12% acrylamide gels (Bio-Rad) according to the manufacturer's guidelines. Cell lysates were applied to represent the total amount of 5×10^6 cells per lane. For comparing the extent of restored expression of target protein, lysates prepared from the control pMaOri.dCas9-containing leptospires were applied to generate different amounts of cells per lane. The immunoblots were performed to infer the maintenance of gene silencing, as previously described (Fernandes et al., 2021b).

Results

Transconjugant colony recovery suggests the essential role of OmpL1 porin in both *L. interrogans* and *L. biflexa*

Initially, aimed at the production of knockdown mutants for *L. interrogans* major membrane proteins, sgRNA cassettes were designed to target the coding strands of the *lipL41* and *ompL1* genes. As previous study suggested a synergetic effect on both proteins in an animal model (Haake et al., 1999), a plasmid containing the abovementioned sgRNA *in tandem* (see Material and Methods) was also constructed for concomitant silencing of LipL41 and OmpL1 proteins. Plasmid pMaOri.dCas9sgRNAlipL32 was also employed as a control for LipL32 silencing. As seen in Figures 1A–C, a markedly high number of transconjugant colonies could be recovered when *L. interrogans* cells carried pMaOri.dCas9 alone or containing the sgRNA for *lipL32* or *lipL41*. Surprisingly, no colonies were observed across the experiments when the plasmid constructions contained the sgRNA targeting *ompL1*, alone or in tandem with sgRNA for *lipL41*, suggesting that OmpL1 porin could be essential for leptospiral basic biology.

Since the double mutant for OmpL1 and LipL41 was unachievable, a plasmid containing sgRNA for *lipL32* and *lipL41* was created for the demonstration of multiple silencing by CRISPRi, and after conjugation, a substantial number of transconjugant colonies were observed (Figures 1C, D). Pushing the boundaries of multiple silencing, cassettes for concomitant

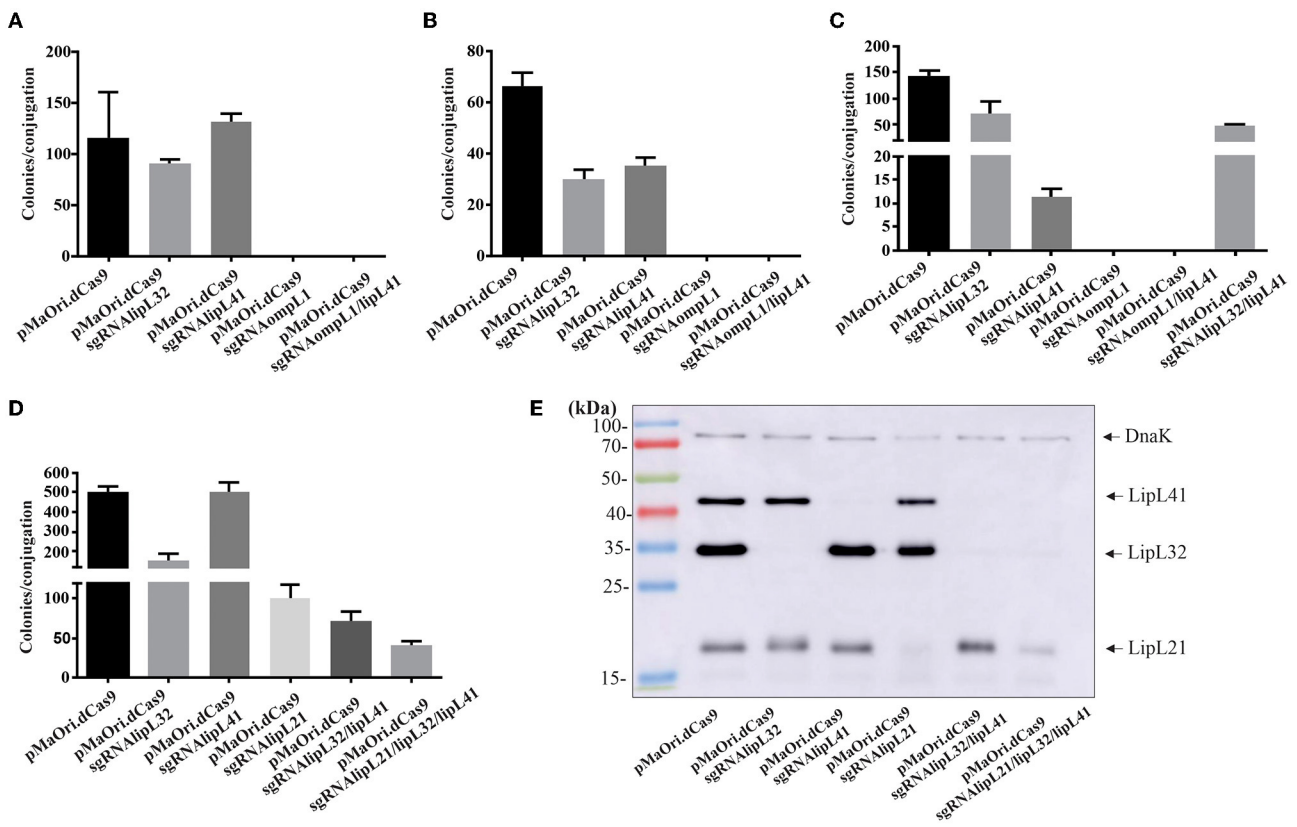

FIGURE 1
Transconjugant recovery and mutant validation. *E. coli* cells containing the plasmids of interest for gene silencing were used for *Leptospira* conjugation, and colonies formed on EMJH plus spectinomycin plates were counted. Graphics **(A–D)** refer to colony recovery in different experiments. Colonies were recovered from the plates, and leptospiral cells were released from the agar and inoculated in liquid media plus antibiotic. After growth, cells were harvested and whole-cell lysates were evaluated by immunoblotting with anti-LipL32, anti-LipL41, and anti-LipL21 antisera **(E)**. Polyclonal antiserum against DnaK chaperone was used as a loading control.

lipL21, *lipL32*, *lipL41*, and *lipL21* alone were used for the conjugation of *E. coli* cells to *L. interrogans* (Figure 1D). This last experiment was performed for the purpose of obtaining synchronized virulent mutants for downstream characterization and evaluation.

Transconjugants recovered were validated by immunoblotting, and gene silencing of the synchronized mutants (Figure 1D) is depicted in Figure 1E. As expected, when *L. interrogans* contained the plasmids for the expression of dCas9 and the sgRNA to *lipL32* and *lipL41* individually, no bands corresponding to the respective proteins were observed in the whole-cell lysates. For LipL21, a drastic reduction in protein expression was observed (>90%) when membranes were overexposed (Figure 1E), most possibly due to the selected protospacer location at the end of the *lipL21* gene. Aimed at demonstrating the applicability of multiple gene silencing by multiple sgRNA cassettes in the same plasmid, recombinant cells containing plasmid for dCas9 and sgRNA for both *lipL32* and *lipL41* or the triple cassette for *lipL21*, *lipL32*, and *lipL41* (Figure 1E) were also evaluated, indicating that the multiple one-step silencing strategy is suitable for *Leptospira*.

However, evaluation of double mutants after just one passage in a medium with antibiotic indicates an undesirable plasmid instability, which is denoted by the restored expression of the target proteins (Supplementary Figure 1); it is worth mentioning that the same difficulty was observed with the triple mutants. This phenomenon was observed with the mutants retrieved in every experiment and is most probably because of the repetitive elements due to the *in tandem* architecture of the sgRNA cassettes, favoring recombination events (Oliveira et al., 2009). Sequencing of the amplicons obtained after plasmid amplification with pMaOri2 primers in one of the clones for the double mutant indicated that recombination occurred resulting in the loss of the *lipL41* protospacer, which was replaced by another *lipl32* one. In addition, since recombination was confirmed to be happening, a complete loss of the whole sgRNA cassettes in the population cannot be ruled out.

To evaluate whether the *ompL1* gene is essential to *Leptospira* spp., a sgRNA targeting the *ompL1* gene in the saprophyte *L. biflexa* was designed, which shares 44% amino acid identity with the annotated *L. interrogans ompL1* ortholog. Confirming the findings in the pathogen *L. interrogans*, only a few (1st experiment) or no (2nd experiment) saprophyte colonies were retrieved when *ompL1* was silenced (Supplementary Figure 2A), in contrast to tens of thousands of colonies recovered when control pMaOri.dCas9

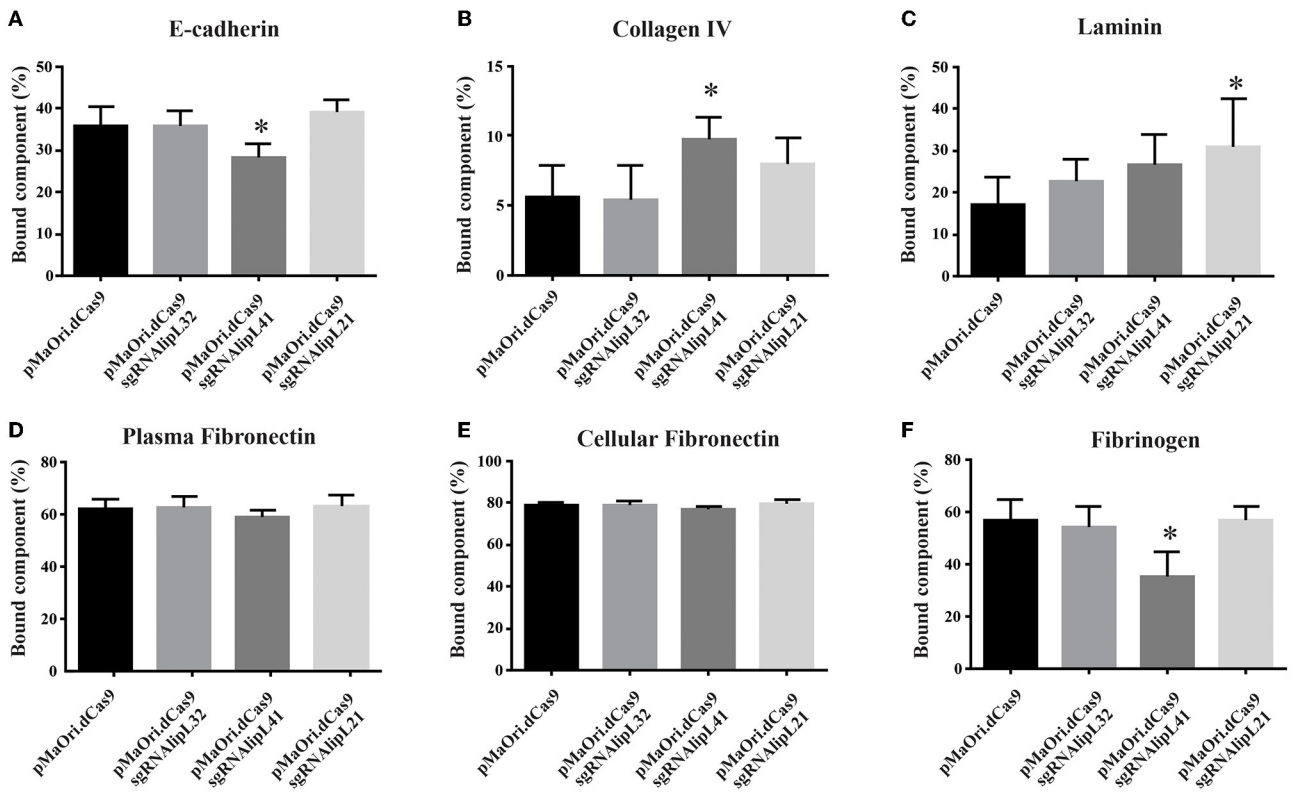

FIGURE 2
Interaction of *L. interrogans* mutant cells with host components. *L. interrogans* containing empty pMaOri.dCas9 (control) or knockdown mutants to LipL32 (pMaOri.dCas9sgRNAlipL32), LipL41 (sgRNAlipL41), and LipL21 (sgRNAlipL21) were incubated (5×10^8 cells/mL) with optimized concentrations of host components E-cadherin **(A)**, collagen type IV **(B)**, laminin **(C)**, plasma **(D),** and cellular **(E)** fibronectin and fibrinogen **(F)**. Bacterial suspensions after incubation were centrifuged, and the resulting supernatant was removed and submitted to a second round of centrifugation. The resulting supernatants were used to coat ELISA plates for component detection, along with a concentration curve. Plates were washed, blocked with 3% BSA in PBS-T, incubated with antibodies for each component and horseradish peroxidase (HRP)-conjugated secondary antibodies. Reactivity was revealed with o-phenylenediamine substrate, and the residual component mass in the supernatant was used to infer the mass bound to the leptospiral surface. Statistical analysis was performed using one-way ANOVA, followed by the Tukey post-test for pairwise comparisons of each group against control dCas9, and a *P*-value of <0.05 (*) was considered to be statistically significant.

plasmid was used, indicating the essential role of OmpL1 protein. Possibly, the few colonies observed in the first experiment are spontaneous mutants to spectinomycin, which has been shown to appear in conjugation and transformation assays (Poggi et al., 2010; Fernandes et al., 2019). Representative plates showing the colonies are depicted in Supplementary Figure 2B.

Effect of gene silencing on interaction with host components

Supernatants after interaction of E-cadherin (10 µg/mL), collagen IV (0.625 µg/mL), laminin (1 µg/mL), plasma (0.05 µg/mL), cellular fibronectin (0.2 µg/mL), and fibrinogen (0.1 µg/mL) with distinct *Leptospira* mutants were used to coat ELISA plates for component detection, along with a concentration curve for determining the percentage of component bound to the leptospiral surface.

In regard to E-cadherin binding, a significant decrease was achieved only for the LipL41 mutant in comparison with the control containing only dCas9 ($P < 0.05$) (Figure 2A), whereas an increase in binding was observed for the same mutant to collagen IV (Figure 2B); this increased binding might be due to an upregulation of leptospiral proteins that display higher affinity for the component. Major proteomic changes were previously demonstrated for the LipL32 knockdown mutant (Fernandes et al., 2021c). Accordingly, binding to laminin was also increased in the LipL21 mutant ($P < 0.05$) in comparison with the dCas9 control (Figure 2C). No differences were observed in binding to either plasma or cellular fibronectin (Figures 2D, E).

Even though binding to fibrinogen was affected when LipL41 protein was silenced ($P < 0.05$) (Figure 2F), no differential effect on fibrin clot inhibition was observed after incubation of fibrinogen with the mutants compared to the control cells containing only pMaOri.dCas9 plasmid (Supplementary Figure 3).

Overall, despite the statistical significances obtained, no substantial changes were observed in the differential interaction, indicating that despite their major abundance on leptospiral membrane, their role in the binding of the host components assayed was minimal, either intrinsically or because of the upregulation of other receptors to "fill the niche" left by protein silencing.

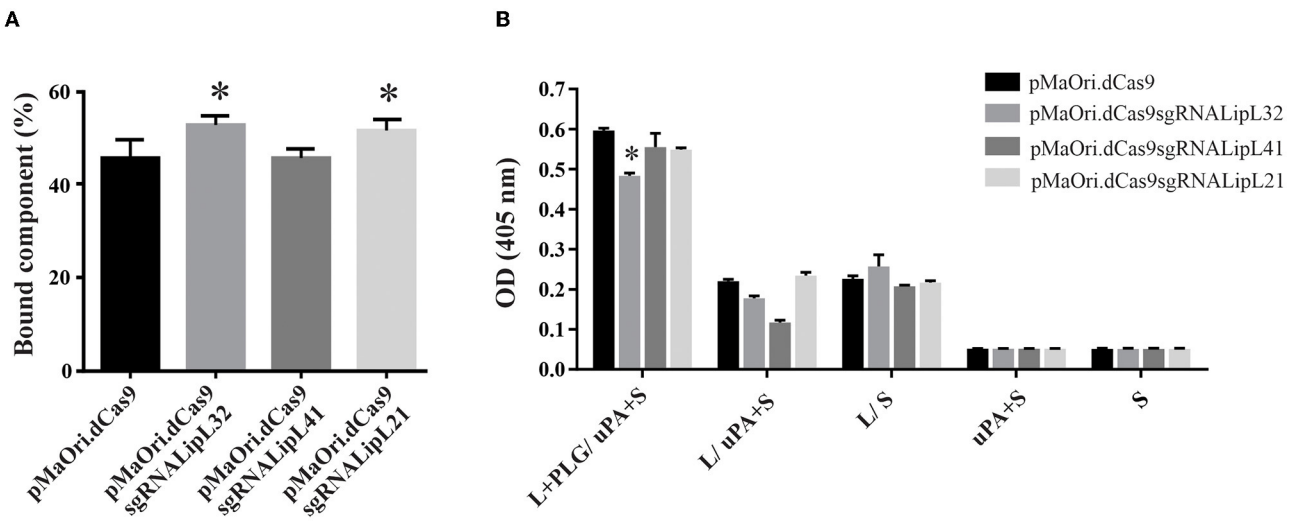

FIGURE 3
Interaction of leptospires with PLG and PLA formation. **(A)** Control or mutant *L. interrogans* cells were incubated with human plasminogen for binding evaluation by ELISA. The residual component mass in the supernatant was used to infer the mass bound to the leptospiral surface. **(B)** Leptospires (L) were incubated with human PLG, and cells were recovered by centrifugation and washed. Then, uPA along with the PLA substrate (S) was added. Controls lacking at least one component of the reaction or with no leptospires were included. Statistical analysis was performed using one-way ANOVA, followed by the Tukey post-test for pairwise comparisons of each group against control dCas9, and a *P*-value of <0.05 (*) was considered to be statistically significant.

Interaction of the mutants with PLG and PLA formation

Control and knockdown leptospires were allowed to interact with human PLG (1 μg/mL), and the supernatant was immobilized in ELISA plates for component quantification, as described above. A significant increase in binding was observed for LipL32 and LipL21 mutants ($P < 0.05$), and the binding of LipL41 mutant to PLG was unaffected (Figure 3A). Possibly, the overall proteomic change as a direct result of gene silencing in the LipL32 and LipL21 mutants favors binding affinity for PLG. However, plasmin formation from the surface-bound PLG, after the addition of exogenous uPA and substrate, was mostly unaffected despite statistical significance (Figure 3B), strengthening again the notion that, despite their major abundance in the leptospiral membrane, their overall participation in PLG binding is minimal, which is consistent with the numerous leptospiral PLG-receptors described to date (Daroz et al., 2021).

Evaluation of mutants' virulence in a hamster model

To assess mutants' phenotype in an animal model, each mutant or control pMaOri.dCas9-containing leptospires were re-validated by immunoblotting (Figure 4A) and then used to infect hamsters ($n = 8$) intraperitoneally. When endpoint criteria were met (Table 3), animals were humanely euthanized, and liver and kidney tissues were extracted. In this study, the acute disease is defined by the appearance of severe clinical symptoms in the first 7 days following experimental challenge. Tissue macerates were used to inoculate the medium without or with spectinomycin. All animals infected with the positive control, *L. interrogans* containing pMaOri.dCas9 only, exhibited clinical signs of acute leptospirosis, with prominent weight loss being observed first at day 4 (Figure 4B; Table 3). At day 7, seven out of eight animals (87.5%) had already met the endpoint criteria (Figure 4C), while for one animal, even though 10% weigh loss was observed at day 6, no evident clinical signs were observed, and this animal fully recovered.

Consistent with earlier findings (Fernandes et al., 2021c), the virulence of LipL32 was found to be significantly higher than that of the control group ($P < 0.05$). By day 5, all animals in the LipL32 group had met the endpoint criteria (Table 3) and exhibited more severe clinical signs of leptospirosis, including a higher number of moribund animals compared to the pMaOri.dCas9 only-infected group. The LipL32 mutant-infected group displayed lower average weight at day 3 ($P < 0.05$) in comparison with the other groups. Contrarily, no apparent sign of disease or weight loss in the animals challenged with the LipL21 mutant strain was observed ($P < 0.05$) (Figures 4B), even though the protein was not completely silenced (>90% silencing), and two animals were euthanized at day 6 for comparing the bacterial burden in a "acute" time frame. For the LipL41 mutant-infected animals, no statistical difference was observed in comparison with the pMaOri.dCas9 only-infected group, and animals first met endpoint criteria at day 6 (contrasting with day 4 in control and LipL32 mutant groups). On day 7, five animals (62.5%) had already met endpoint criteria, and the remaining animals, which displayed slight weight loss, could fully recover. Individual weight measurements are presented in Supplementary Figure 4.

In a subsequent experiment, a new set of virulent leptospiral mutants was generated, validated (Figure 4D), and used to infect animals. Given that the increased virulence of the LipL32 mutant

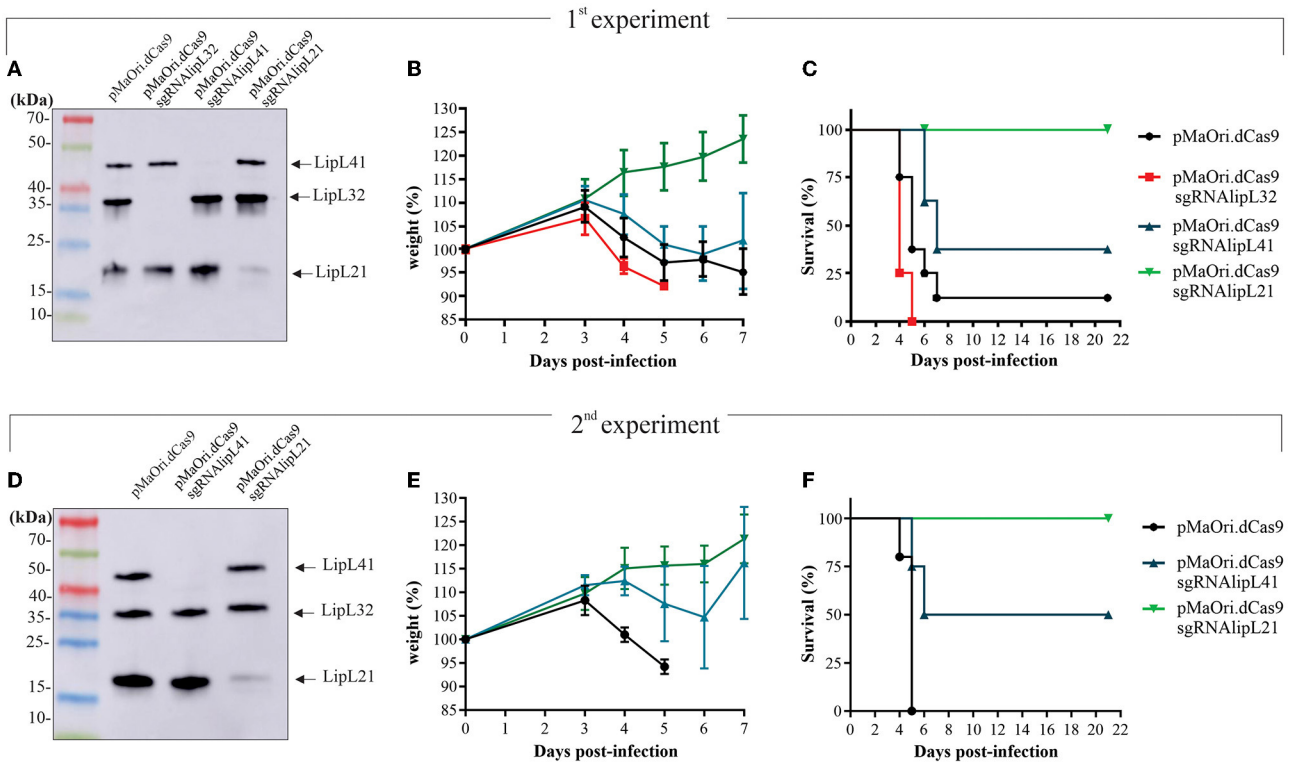

FIGURE 4
Virulence of leptospiral mutants in hamster model of infection. LipL32, LipL41, and LipL21 knockdown mutants and control cells containing pMaOri.dCas9 only were validated prior to animal infection **(A, D)**, and groups of recently weaned female Syrian gold hamsters ($n = 8$ in the first experiment and $n = 4$ in the second) were inoculated intraperitoneally with 5×10^7 distinct and passage-synchronized leptospires. Each animal was monitored daily and weighed **(B, E)** for clinical signs of acute leptospirosis. Animals were humanely euthanized when weight loss (>10%) and/or additional clinical signs (blood on paws/nose/urogenital tract, lethargy) was observed **(C, F)**.

had already been established, only the LipL41 and LipL21 knockdown mutants were included in comparison with the control group infected with pMaOri.dCas9-containning leptospires. In this experiment, one set of animals from each group ($n = 4$) was euthanized on day 4 to compare the bacterial burden in target organs, while the other set ($n = 5$ or 4) was monitored until meeting the endpoint criteria.

The relative weight of dCas9 only-infected animals dropped at day 4 (Figure 4E; Table 3), consistent with all animals ($n = 5$) meeting endpoint criteria at day 5 (Figure 4F). In agreement with the first experiment, all LipL21 mutant-infected animals neither met endpoint criteria ($P < 0.01$) nor displayed weight loss, confirming the attenuation due to LipL21 silencing and the role of this protein in acute disease. The animals infected with the LipL41 mutant had delayed weight loss (Figure 4E; Table 3), and only 50% met endpoint criteria ($P < 0.05$).

Mutant recovery from target organs and bacterial burden quantification

In the first experiment, kidneys and livers from four animals that were euthanized in the acute time frame were used to prepare homogenates followed by inoculation in a liquid medium with or without spectinomycin. Cultures were monitored daily for the presence of motile leptospires, and a positivity score was given depending on their presence and abundance in the medium with antibiotics (mutant cells only). All kidney and liver cultures from the pMaOri.dCas9 only and LipL32 mutant were positive for the presence of leptospires; interestingly and consistent with the increased virulence of LipL32 mutant, positive cultures were recorded as soon as day 1 for all cultures from kidney and three out of four liver homogenates of this group (Figures 5A, B; Supplementary Figure 5). LipL32 mutant-derived cultures also reached higher cell densities earlier than those from the control group. In all cases, similar growth profile was observed in cultures with or without spectinomycin, indicating that most of the cells were still harboring the plasmids for gene silencing.

Liver macerate cultures from LipL41 and LipL21 mutants were negative for leptospires (Figure 5A), most probably because of the later time point when these animals met endpoint criteria (for LipL41 mutant-infected animals) or when animals were taken for "acute time point" comparative purposes (LipL21 mutant). Although kidney cultures were positive, they first turned positive at days 5 and 7 for LipL41 and LipL21 mutant groups (Figure 5B; Supplementary Figure 5), respectively, indicating lower bacterial burden and/or cell viability of these mutants in regard to pMaOri.dCas9 only control group.

10.3389/fmicb.2023.1199660

TABLE 3 Animal experiment results.

	Endpoints/total	Endpoint day	Average weight (%)[a]		
			3	4	5
1st experiment					
pMaOri.dCas9	7/8	4,4,5,5,5,6,7	109.1	102.6	97.1
pMaOri.dCas9sgRNAlipL32	8/8	4,4,4,4,4,4,5,5	106.5	96.4	92.52
pMaOri.dCas9sgRNAlipL41	5/8	6,6,6,7,7	110.4	107.4	101.1
pMaOri.dCas9sgRNAlipL21	0/8	6,6*	110.8	116.3	117.5
2nd experiment					
pMaOri.dCas9	5/5	4,5,5,5,5	108.3	101	94.2
pMaOri.dCas9sgRNAlipL41	2/4	5,6	111.5	112.4	107.6
pMaOri.dCas9sgRNAlipL21	0/4	–	109.7	115.0	115.7

[a]Compared to day 0 (100%).
*Animals taken for comparative purposes.

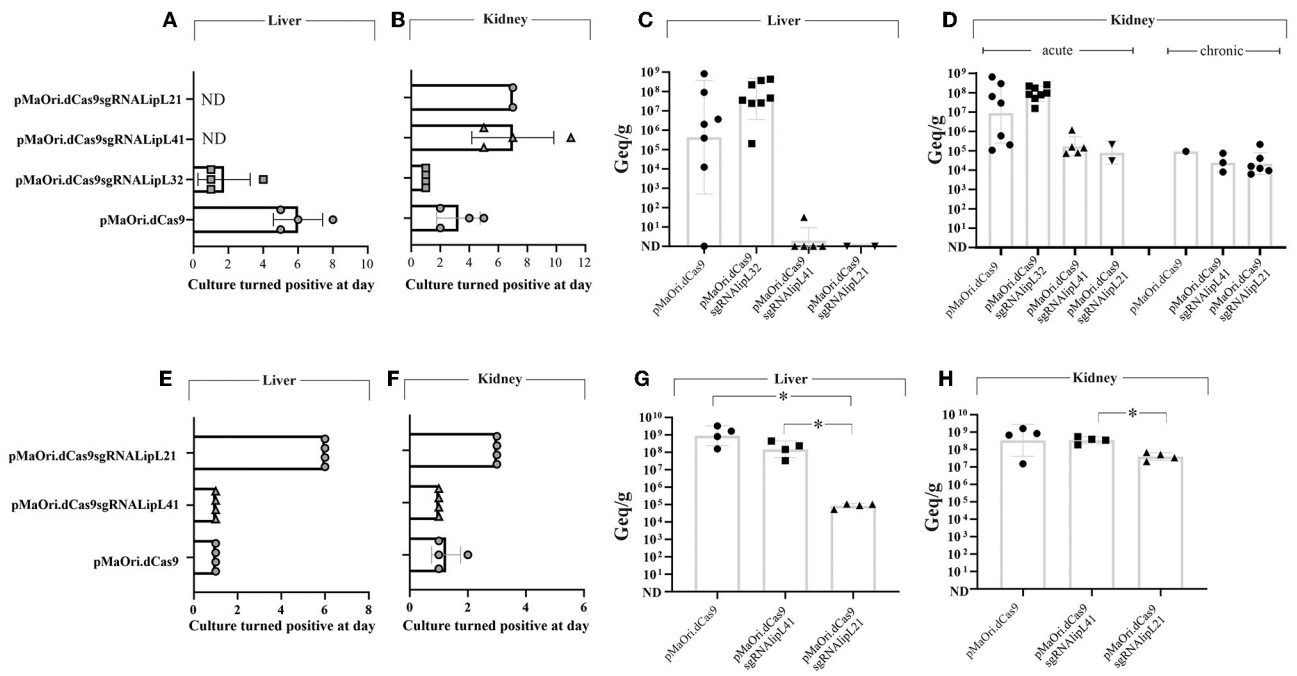

FIGURE 5
Leptospiral mutant isolation in a liquid medium and bacterial load quantification in target organs from infected animals. Kidney and liver from euthanized animals were macerated and homogenates used to inoculate liquid EMJH medium plus spectinomycin (recovery of only mutant cells), cultures were monitored daily regarding the presence of leptospires, and the day where they turned positive in the presence of antibiotics was recorded [**(A, B)**, first experiment, **(E, F)**, second one]. Organs were also used for total DNA extraction and bacterial burden quantification by quantitative PCR [**(C, D)**, first experiment, **(G, H)**, second one]. Bacterial loads are expressed in genome equivalents (Geq) per gram of tissue. Statistical analysis was performed using one-way ANOVA, followed by the Tukey post-test for pairwise comparisons and a *P*-value of <0.05 (*) was considered to be statistically significant.

The results of bacterial quantification in the liver (Figure 5C) and kidney (Figure 5D) confirmed the higher bacterial load in animals infected with LipL32 mutant, with a geometric mean of 4 $\times$ 10^7 in the liver, compared to 4.3 $\times$ 10^5 in the control animals, and 9.1 $\times$ 10^7 in the kidneys, compared to 8.9 $\times$ 10^6 in control animals. Because of animal variability in the pMaOri.dCas9 group, statistical significance was not achieved between these groups. Liver loads were reduced or not found in LipL41 mutant- and LipL21 mutant-infected animals. Kidney loads in the "acute time frame" were reduced in these groups, with an average of 1.7 $\times$ 10^5 and 7.9 $\times$ 10^4 for LipL41 and LipL21 mutant-infected animals, contrasting with 8.9 $\times$ 10^6 in pMaOri.dCas9 only-infected group. Kidney loads in the surviving animals were similar between groups (Figure 5D).

When acute time frame-synchronized animals were euthanized (day 4) in the second challenge experiment, liver macerates were positive for LipL41 mutant and pMaOri.dCas9 group at day 1 of growth, the latter reaching higher cell densities earlier, and in contrast, growth was observed at day 6 for the LipL21 mutant group (Figure 5E). Cultures from kidney macerates turned positive at day 1 for all LipL41 mutant group and for three

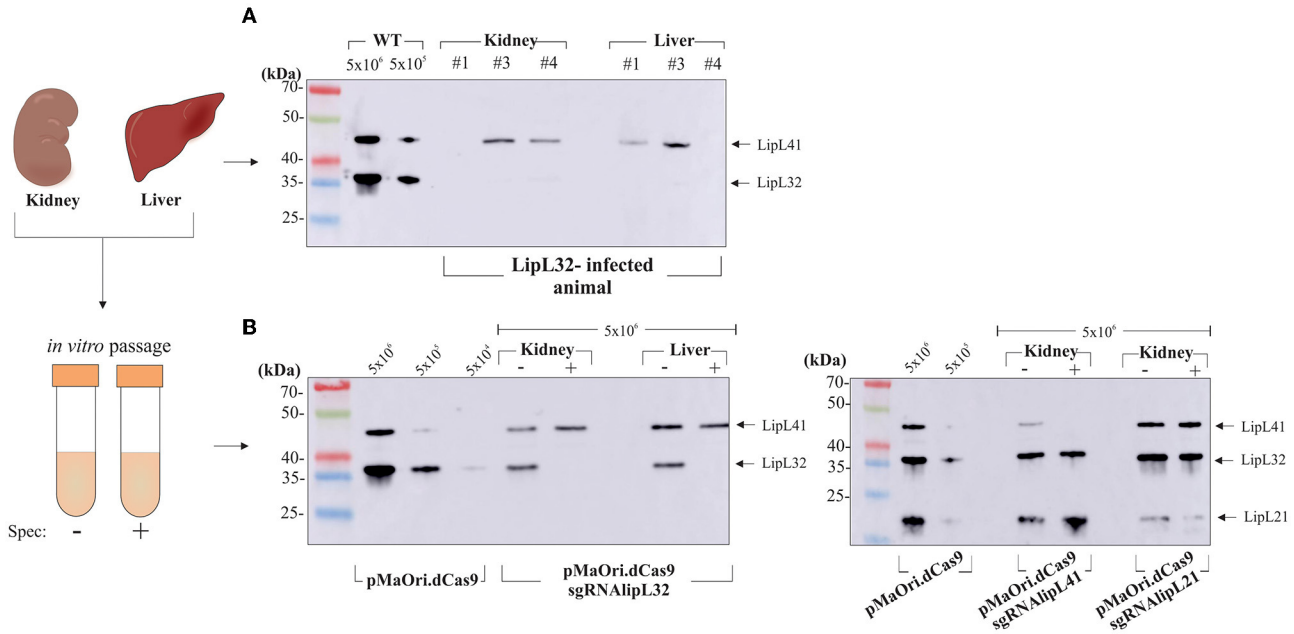

FIGURE 6
In vivo and *in vitro* silencing phenotype stability. **(A)** Protein silencing in leptospires sheltered at the target organs. Tissue macerates from kidney and liver sections were centrifuged at low speed, and the supernatant was carefully recovered. After centrifugation, pellets were washed and resuspended for preparation of cell lysates, which were evaluated by immunoblotting. Different numbers of control leptospires were also used for comparison purposes. **(B)** Target protein expression in leptospires cultured out of EMJH medium after inoculation of organ macerate, with (+) or without (−) spectinomycin (40 μg/mL), was also assessed. Bacteria were recovered from the medium and washed, and suspensions were then counted. Whole-cell lysates corresponding to 5×10^6 leptospiral cells were evaluated by immunoblotting. For comparative purposes, various amounts of wild-type (WT) leptospires or leptospires containing the control pMaOri.dCas9 were included in the experiment.

out of four in pMaOri.dCas9 control since the presence of leptospires was only observable at day 2 in one of these cultures (Figure 5F). Compatible with previous results, LipL21 mutant cultures from kidney homogenates were positive at day 3 of incubation (Figure 5F). Bacterial quantification results agreed with macerates' cultures, whereas liver loads were drastically reduced in the LipL21 mutant-infected animals, which displayed an average of 8.4×10^4 Geq/g of tissue, contrasting with 9×10^8 ($P < 0.05$) and 1.5×10^8 ($P < 0.05$) for dCas9 only and LipL41 mutant-infected animals, respectively (Figure 5G). Lesser extent contrasts were found in the kidneys, with the similar number of leptospires found in the dCas9 only and LipL41 mutant groups (3.4×10^8) and 3.9×10^7 in the LipL21 mutant-infected animals (Figure 5H).

Demonstration of phenotype stability *in vivo* and *in vitro*

Exploiting the higher bacterial burden in target organs of LipL32-infected animals, silencing profiles were assessed directly from the tissue macerates from three animals, normalized by volume. Lysates were separated by SDS-PAGE and proteins were evaluated by immunoblotting. As depicted in Figure 6A, when leptospires were detected in the macerates by co-incubation with anti-LipL41 and anti-LipL32, only the LipL41 protein could be detected, contrasting with intense LipL32 reactivity in wild-type control at a different number of leptospires per well, directly demonstrating the plasmid upkeep *in vivo*, and by consequence, gene silencing. It is worth mentioning that leptospires from the pMaOri.dCas9 only-infected organs could not be detected in the lysates (data not shown), most probably due to lower bacterial loads.

Tissue macerates were also used to inoculate EMJH medium (50 μL in 5 mL) with (+) or without (−) spectinomycin, the latter to recover only mutant cells. For the acute time frame, cell lysates from knockdown or control *Leptospira* after one *in vitro* passage were compared. Regarding the mutants isolated from the kidney and liver (in the case of LipL32 mutant), only a minor target protein expression band was observed when leptospires grew in medium without antibiotic (Figure 6B), whereas the presence of the antibiotic resulted in the retrieval of only mutant cells. Kidney macerate cultures from the LipL41 and LipL21 mutant-infected animals confirmed the silencing in the presence of spectinomycin, with only minor target protein reappearance when no antibiotic was added to the medium (Figure 5B), confirming phenotype stability.

Discussion

Extensive literature exists that focuses on understanding how pathogenic *Leptospira* interact with their hosts (reviewed by Daroz et al., 2021). This was primarily accomplished through analyzing

the entire genome sequences, mainly of *L. interrogans*, resulting in the creation of recombinant proteins that have been extensively studied to determine their interaction with host components. These studies have shed light on leptospiral surface-exposed proteins that may be involved in colonization (Barbosa et al., 2006; Pinne et al., 2010; Vieira et al., 2010b; Fernandes et al., 2012; Siqueira et al., 2013; Teixeira et al., 2015; Silva et al., 2016), invasion (Vieira et al., 2010a; Oliveira et al., 2013; Pereira et al., 2017; Santos et al., 2018; Takahashi et al., 2021), and immune evasion processes (Verma et al., 2006; Stevenson et al., 2007; Barbosa et al., 2010; Castiblanco-Valencia et al., 2012, 2016; Siqueira et al., 2016; Cavenague et al., 2019). Although *in vitro* experiments have yielded promising results, researchers often encounter frustration when the antigens fail to be protective in vaccine tests or when mutants still prove to be virulent in animal infection models.

The development and application of CRISPRi allowed easy, specific, and one-step generation of knockdown mutants in several pathogenic *Leptospira,* including the newly described *L. sanjuanensis* (Fernandes et al., 2022) and *L. borgpetersenii* (Fernandes et al., unpublished data), making it feasible to evaluate virulence factors in an animal model (Fernandes et al., 2021c). This scenario has brought the spotlight back to the evaluation of the role of major OMPs in leptospiral pathogenicity, which could ultimately guide the rationale for the generation of subunits and/or chimeric vaccines.

LipL32 protein was first characterized by Haake et al. (2000), when the authors concluded that this protein could be relevant to *Leptospira* pathogenesis. However, a transposon mutant was still capable of causing both acute and chronic disease as effectively as the wild-type strain (Murray et al., 2009). Recently, a knockdown LipL32 mutant obtained by CRISPRi was re-evaluated in a hamster model, and the results consistently suggested that the silencing of this protein leads to a more perceptible virulence phenotype, with the presentation of early (and more severe) symptoms and higher liver bacterial burden (Fernandes et al., 2021c).

To further confirm this interesting finding, a new batch of LipL32 knockdown mutant was obtained and used to infect hamsters. Accordingly, we demonstrated that LipL32 silencing results in more virulent *Leptospira* cells, culminating in early and more severe symptom presentation in hamsters, accompanied by higher liver and kidney loads. Remarkably, taking advantage of this higher organ load, we could demonstrate LipL32 silencing directly from organ macerates, proving that silencing is maintained *in vivo,* at least in the "acute" time frame.

The interaction of LipL32 mutant with host components was unaffected, except for a slight increase in PLG binding, which could be explained by minor participation of this protein in *Leptospira*–host interactions or by a compensation mechanism due to the upregulation of proteins with more affinity for host ligands to fill the niche left by LipL32 silencing. Our results agree with the ones from Murray et al. (2009) that showed that the LipL32 mutant binding to laminin was unaffected. Previous whole-cell proteome analysis performed on the LipL32 mutant cells showed an overall change in protein abundance profile, with 84 proteins being upregulated, including the now well-established cooperative virulence factors LigA and LigB, which could help explain the increased virulence of this mutant. In addition, LipL41 and LipL21 proteins were significantly up- and downregulated in the LipL32 mutant, respectively (Fernandes et al., 2021c). However, these differential expressions were not perceivable in our immunoblots.

LipL41 protein has been widely studied since it was first described, including its interaction with host molecules (Takahashi et al., 2021). Recombinant LipL41 protein could efficiently bind to elastin, collagen IV, laminin, E-cadherin, cellular fibronectin, PLG, and fibrinogen. In our results, the LipL41 knockdown mutant displayed slight and significant decreased binding to E-cadherin and fibrinogen (but fibrin clot formation was unaffected), whereas an increase was observed for collagen IV binding.

When a transposon mutant for LipL41 (*L. interrogans* serovar Pomona) was assessed in a hamster model of infection, it was still virulent as no animals survived the infection (King et al., 2013). Our animal infection results indicated that, even though the LipL41 knockdown mutant was still virulent, some animals could still survive the lethal challenge, with less severity observed in those that succumbed to infection and later endpoint dates, suggesting that a slight attenuation in virulence could occur by LipL41 silencing in *L. interrogans* strain Fiocruz L1-130. It is possible that attenuation could be more distinguishable by different infection routes or inoculum sizes. By comparing liver and kidney loads in time-synchronized animals, only a minor reduction in liver burden was observed in comparison with control leptospires containing only the pMaOri.dCas9 plasmid.

Supported by the data that LipL41 elicited a synergistic protection profile along with the porin OmpL1 against lethal challenge in hamsters (Haake et al., 1999), a double knockdown mutant was pursued but no colonies could be recovered; silencing of OmpL1 alone, in both pathogenic *L. interrogans* and saprophytic *L. biflexa,* was also not possible, suggesting the essentiality of OmpL1 protein.

OmpL1 protein is a unique porin encoded by *Leptospira* spp., and its topological model contains ten amphipathic transmembrane β-strands (Haake et al., 1993; Shang et al., 1995). The outer face of the β-strand is characterized by its hydrophobic nature, facilitating interactions with the lipid bilayer. On the contrary, the inner face exhibits hydrophilic properties, allowing it to interact with the aqueous pore within the protein (Haake et al., 1993). The porin superfamily is composed of proteins that form membrane-spanning, water-filled channels permitting the diffusion of hydrophilic molecules into the periplasmic space (Jeanteur et al., 1991). Some exception can occur since it was previously described that outer membrane protein OmpW from *E. coli* (Hong et al., 2006) and OprG from *Pseudomonas aeruginosa* (Touw et al., 2010) form an eight-stranded beta-barrel with the hydrophobic channel. Major outer membrane porin (PorB), which mediates ion exchange between *Neisseria gonorrhoeae* and the environment (Chen and Seifert, 2014), was shown to be essential to these bacteria, likely due to its ability to allow nutrients access to the periplasm (Haines et al., 1988). In this sense, OmpL1 protein could be mechanistically involved in nutrient uptake or membrane integrity in *Leptospira* spp.

LipL21 has been shown to be a surface-exposed protein in *L. interrogans* by previous studies (Cullen et al., 2003; Techawiwattanaboon et al., 2021). Seeking to explore the potential

role of native LipL21 in virulence and host–pathogen interactions, a knockdown LipL21 mutant was obtained. LipL21 mutant *Leptospira* binding to host components was mostly unaltered, with only a modest increase in laminin and PLG binding; however, when used to infect hamster, the LipL21 mutant was consistently unable to cause acute disease.

Evaluation of target organ loads in time-synchronized "acute phase" animals revealed remarkably decreased liver loads (∼4 logs) in LipL21 mutant-infected animal in comparison with the control, whereas kidney loads were only slightly reduced. These results agree with the animal phenotype displayed by the LigA/B knockdown mutant (Fernandes et al., 2021c), which also causes asymptomatic infections in hamster with renal colonization and with drastically reduced liver loads, hinting that bacterial hepatic concentration in the early time point of infection could be a feature of acute leptospirosis, which is also in agreement with the higher liver loads of the more severe LipL32 mutant.

There are several mechanisms that could explain this virulence attenuation. It has been previously shown that LipL21 protein is tightly bound to the leptospiral peptidoglycan, protecting it from degradation into muropeptides, thereby blocking signaling through nucleotide oligomerization domain (NOD)-like receptors (NOD1 and NOD2) proteins, potentially helping *L. interrogans* to circumventing innate host responses (Ratet et al., 2017). Even though both interactions with periplasmic peptidoglycan and surface-exposure could be mutually exclusive features due to LipL21 size, it has been proposed that this protein could coexist in two forms, one residing in the periplasm and another free in the outer membrane (Ratet et al., 2017), similar to the Lpp protein from *E. coli* (Cowles et al., 2011).

In addition, Kumar et al. (2022) demonstrated that recombinant LipL21 interacts with complement negative regulator C4bp and FH, favoring serum resistance, and displays *in vitro* nuclease activity toward neutrophil extracellular trap (NET); LipL21 protein can modulate neutrophil function by inhibiting myeloperoxidase (MPO) activity (Vieira et al., 2018).

The virulence phenotype of double or triple mutants remains to be evaluated since the multiple mutants obtained in this study displayed genetic instability during *in vitro* cultivation. The usage of different promoters for different sgRNA cassettes for avoiding recombination or pursuing gene silencing in the genetic background of a recently obtained *L. interrogans* knockout for LipL32 (Fernandes and Nascimento, 2022) are interesting strategies and are being evaluated by our group.

In conclusion, we demonstrated augmented bacterial virulence as a result of LipL32 silencing, and a subtle attenuation of acute disease presentation in the LipL41 mutant. LipL21 silencing resulted in the inability of leptospires to cause acute disease, even though they could still colonize the kidney. The participation of OmpL1 porin in virulence and host–pathogen interaction could not be determined, since its silencing was lethal to both saprophyte and pathogenic *Leptospira,* indicating its essentiality to leptospiral basic biology. CRISPRi is now a well-established genetic tool for exploring leptospiral pathogenic mechanisms that will increase our knowledge of this fascinating microorganism and add new pieces to the complex puzzle of leptospirosis.

Data availability statement

The original contributions presented in the study are included in the article/Supplementary material, further inquiries can be directed to the corresponding authors.

Ethics statement

The animal study was reviewed and approved by Animal Care and Use Committee at Instituto Butantan.

Author contributions

LGVF, AFT, and ALTON: literature revision, manuscript preparation, and experimental design. LGVF and AFT: experimental manipulation. LGVF: figures. All authors reviewed and approved the manuscript, participated in the literature revision, discussion, and preparation of manuscript.

Funding

The following Brazilian agencies: FAPESP (grant 2019/17488-2), CNPq (grant 304445/2021-5), and Fundação Butantan, financially supported this study. LGVF and AFT have FAPESP fellowships 2017/06731-8 and 2016/11541-0, respectively. The funders had no role in the study design, analysis, decision to publish, or preparation of the manuscript.

Acknowledgments

The authors are deeply indebted to Dr. Al Leyva, BS, for his critical reading and English editing of this manuscript.

Conflict of interest

The authors declare that the research was conducted in the absence of any commercial or financial relationships that could be construed as a potential conflict of interest.

Publisher's note

All claims expressed in this article are solely those of the authors and do not necessarily represent those of their affiliated organizations, or those of the publisher, the editors and the reviewers. Any product that may be evaluated in this article, or claim that may be made by its manufacturer, is not guaranteed or endorsed by the publisher.

Supplementary material

The Supplementary Material for this article can be found online at: https://www.frontiersin.org/articles/10.3389/fmicb.2023.1199660/full#supplementary-material

SUPPLEMENTARY FIGURE 1
Phenotype instability in the double LipL32/LipL41 mutants. After colony formation, distinct colonies (a to d) were selected and grown in a liquid medium plus spectinomycin (P1) and then re-inoculated in the same medium and monitored until mid-log phase (P2). Cell lysates from both P1 and P2 cultures were evaluated by immunoblotting with anti-LipL32, anti-LipL41, and anti-LipL21 antisera.

SUPPLEMENTARY FIGURE 2
OmpL1 silencing is lethal to *L. biflexa* cells. Plasmids pMaOri.dCas9 alone or containing a sgRNA cassette targeting the *ompL1* gene were delivered by conjugation to *L. biflexa* cells. Colonies recovered in EMJH plates plus spectinomycin were counted in two independent experiments **(A)**, and representative images of the plates were taken **(B)**.

SUPPLEMENTARY FIGURE 3
Fibrinogen binding and fibrin clot inhibition by leptospires. **(A)** *L. interrogans* containing empty pMaOri.dCas9 (control) or knockdown mutants to LipL32 (pMaOri.dCas9sgRNAlipL32), LipL41 (sgRNAlipL41), and LipL21 (sgRNAlipL21) were incubated with human fibrinogen for binding evaluation by ELISA. Reactivity was revealed with o-phenylenediamine substrate, and the residual component mass in the supernatant was used to infer the mass bound to the leptospiral surface. Statistical analysis was performed using one-way ANOVA, followed by the Tukey post-test for pairwise comparisons of each group against control dCas9, and a P-value of < 0.05 (*) was considered to be statistically significant. **(B)** Leptospires were resuspended in a human fibrinogen solution (1 mg/mL) to a final OD_{420nm} of 0.5. After 2 h incubation at 37°C, 90 μL of the incubation reactions were added to each well of a microdilution plate and mixed with 10 μL of 0.5 U/mL human thrombin. Experiments were performed with six replicates, and controls with no leptospires (maximal fibrin clot formation) or no thrombin (no fibrin clot formation) were included. Plates were read at 600 nm at 2-min intervals. The results are expressed in percentage of clot formation, where clot turbidity in the control with no leptospires was considered 100%.

SUPPLEMENTARY FIGURE 4
Daily measurements of hamsters' weight. Animals' weight from the first and second experiments were recorded daily. For each animal, individual weight displayed at day 0 was considered 100%. LipL32 mutant was not included in the second experiment.

SUPPLEMENTARY FIGURE 5
Daily observation and positivity scores from medium inoculated with tissue macerates. Cultures containing spectinomycin (retrieval of only mutant leptospires) were monitored daily for the presence and abundance of leptospires, and positivity scores were recorded. 1: 1 to 10 leptospires per field; 2: 10 to 100; 3: >100 leptospires per field. LipL32 mutant was not included in the second experiment.

References

Barazzone, G. C., Teixeira, A. F., Azevedo, B. O. P., Damiano, D. K., Oliveira, M. P., Nascimento, A. L. T. O., et al. (2021). Revisiting the development of vaccines against pathogenic. *Front. Immunol.* 12, 760291. doi: 10.3389/fimmu.2021.760291

Barbosa, A. S., Abreu, P. A., Neves, F. O., Atzingen, M. V., Watanabe, M. M., Vieira, M. L., et al. (2006). A newly identified leptospiral adhesin mediates attachment to laminin. *Infect. Immun.* 74, 6356–6364. doi: 10.1128/IAI.00460-06

Barbosa, A. S., Monaris, D., Silva, L. B., Morais, Z. M., Vasconcellos, S. A., Cianciarullo, A. M., et al. (2010). Functional characterization of LcpA, a surface-exposed protein of Leptospira spp. that binds the human complement regulator C4BP. *Infect. Immun.* 78, 3207–3216. doi: 10.1128/IAI.00279-10

Bharti, A. R., Nally, J. E., Ricaldi, J. N., Matthias, M. A., Diaz, M. M., Lovett, M. A., et al. (2003). Leptospirosis: a zoonotic disease of global importance. *Lancet Infect. Dis.* 3, 757–771. doi: 10.1016/S1473-3099(03)00830-2

Castiblanco-Valencia, M. M., Fraga, T. R., Breda, L. C., Vasconcellos, S. A., Figueira, C. P., Picardeau, M., et al. (2016). Acquisition of negative complement regulators by the saprophyte Leptospira biflexa expressing LigA or LigB confers enhanced survival in human serum. *Immunol. Lett.* 173, 61–68. doi: 10.1016/j.imlet.2016.03.005

Castiblanco-Valencia, M. M., Fraga, T. R., Silva, L. B., Monaris, D., Abreu, P. A., Strobel, S., et al. (2012). Leptospiral immunoglobulin-like proteins interact with human complement regulators factor H, FHL-1, FHR-1, and C4BP. *J. Infect. Dis.* 205, 995–1004. doi: 10.1093/infdis/jir875

Cavenague, M. F., Teixeira, A. F., Filho, A. S., Souza, G. O., Vasconcellos, S. A., Heinemann, M. B., et al. (2019). Characterization of a novel protein of *Leptospira interrogans* exhibiting plasminogen, vitronectin and complement binding properties. *Int. J. Med. Microbiol.* 309, 116–129. doi: 10.1016/j.ijmm.2018.12.005

Chen, A., and Seifert, H. S. (2014). Saturating mutagenesis of an essential gene: a majority of the Neisseria gonorrhoeae major outer membrane porin (PorB) is mutable. *J. Bacteriol.* 196, 540–547. doi: 10.1128/JB.01073-13

Costa, F., Hagan, J. E., Calcagno, J., Kane, M., Torgerson, P., Martinez-Silveira, M. S., et al. (2015). Global morbidity and mortality of leptospirosis: a systematic review. *PLoS Negl. Trop. Dis.* 9, e0003898. doi: 10.1371/journal.pntd.0003898

Cowles, C. E., Li, Y., Semmelhack, M. F., Cristea, I. M., and Silhavy, T. J. (2011). The free and bound forms of Lpp occupy distinct subcellular locations in *Escherichia coli*. *Mol. Microbiol.* 79, 1168–1181. doi: 10.1111/j.1365-2958.2011.07539.x

Cullen, P. A., Haake, D. A., Bulach, D. M., Zuerner, R. L., and Adler, B. (2003). LipL21 is a novel surface-exposed lipoprotein of pathogenic Leptospira species. *Infect. Immun.* 71, 2414–2421. doi: 10.1128/IAI.71.5.2414-2421.2003

Daroz, B. B., Fernandes, L. G. V., Cavenague, M. F., Kochi, L. T., Passalia, F. J., Takahashi, M. B., et al. (2021). A review on host-leptospira interactions: what we know and future expectations. *Front. Cell. Infect. Microbiol.* 11, 777709. doi: 10.3389/fcimb.2021.777709

Delany, I., Rappuoli, R., and Seib, K. L. (2013). Vaccines, reverse vaccinology, and bacterial pathogenesis. *Cold Spring Harb. Perspect. Med.* 3, a012476. doi: 10.1101/cshperspect.a012476

Demarre, G., Guérout, A. M., Matsumoto-Mashimo, C., Rowe-Magnus, D. A., Marlière, P., Mazel, D., et al. (2005). A new family of mobilizable suicide plasmids based on broad host range R388 plasmid (IncW) and RP4 plasmid (IncPalpha) conjugative machineries and their cognate *Escherichia coli* host strains. *Res. Microbiol.* 156, 245–255. doi: 10.1016/j.resmic.2004.09.007

Dolhnikoff, M., Mauad, T., Bethlem, E. P., and Carvalho, C. R. (2007). Pathology and pathophysiology of pulmonary manifestations in leptospirosis. *Braz. J. Infect. Dis.* 11, 142–148. doi: 10.1590/S1413-86702007000100029

Fernandes, L. G., de Morais, Z. M., Vasconcellos, S. A., and Nascimento, A. (2015). *Leptospira interrogans* reduces fibrin clot formation by modulating human thrombin activity via exosite I. *Pathog. Dis.* 73, 13. doi: 10.1093/femspd/ftv001

Fernandes, L. G., Filho, A. F., Souza, G. O., Vasconcellos, S. A., Romero, E. C., Nascimento, A. L., et al. (2016a). Decrease in antithrombin III and prothrombin serum levels contribute to coagulation disorders during leptospirosis. *Microbiology* 162, 1407–1421. doi: 10.1099/mic.0.000318

Fernandes, L. G., Siqueira, G. H., Teixeira, A. R., Silva, L. P., Figueredo, J. M., Cosate, M. R., et al. (2016b). Leptospira spp.: novel insights into host-pathogen interactions. *Vet. Immunol. Immunopathol.* 176, 50–57. doi: 10.1016/j.vetimm.2015.12.004

Fernandes, L. G., Vieira, M. L., Kirchgatter, K., Alves, I. J., Morais, Z. M., d. e., et al. (2012). OmpL1 is an extracellular matrix- and plasminogen-interacting protein of Leptospira spp. *Infect. Immun.* 80, 3679–3692. doi: 10.1128/IAI.00474-12

Fernandes, L. G. V., Guaman, L. P., Vasconcellos, S. A., Heinemann, M. B., Picardeau, M., Nascimento, A. L. T. O., et al. (2019). Gene silencing based on RNA-guided catalytically inactive Cas9 (dCas9): a new tool for genetic engineering in Leptospira. *Sci. Rep.* 9, 1839. doi: 10.1038/s41598-018-37949-x

Fernandes, L. G. V., Hornsby, R. L., Nascimento, A. L. T. O., and Nally, J. E. (2021a). Application of CRISPR interference (CRISPRi) for gene silencing in pathogenic species of leptospira. *J. Vis. Exp.* 14, e62631. doi: 10.3791/62631-v

Fernandes, L. G. V., Hornsby, R. L., Nascimento, A. L. T. O., and Nally, J. E. (2021b). Genetic manipulation of pathogenic Leptospira: CRISPR interference (CRISPRi)-mediated gene silencing and rapid mutant recovery at 37°C. *Sci. Rep.* 11, 1768. doi: 10.1038/s41598-021-81400-7

Fernandes, L. G. V., and Nascimento, A. L. T. O. (2020). Specific gene silencing in *leptospira biflexa* by rna-guided catalytically inactive cas9 (dCas9). *Methods Mol. Biol.* 2134, 109–122. doi: 10.1007/978-1-0716-0459-5_10

Fernandes, L. G. V., and Nascimento, A. L. T. O. (2022). A novel breakthrough in Leptospira spp. mutagenesis: knockout by combination of CRISPR/Cas9 and non-homologous end-joining systems. *Front. Microbiol.* 13, 915382. doi: 10.3389/fmicb.2022.915382

Fernandes, L. G. V., Putz, E. J., Stasko, J., Lippolis, J. D., Nascimento, A. L. T. O., Nally, J. E., et al. (2021c). Evaluation of LipL32 and LigA/LigB knockdown mutants in *leptospira interrogans* serovar copenhageni: impacts to proteome and virulence. *Front. Microbiol.* 12, 799012. doi: 10.3389/fmicb.2021.799012

Fernandes, L. G. V., Stone, N. E., Roe, C. C., Goris, M. G. A., van der Linden, H., Sahl, J. W., et al. (2022). *Leptospira sanjuanensis* sp. nov., a pathogenic species of

the genus leptospira isolated from soil in Puerto Rico. *Int. J. Syst. Evol. Microbiol.* 72, 005560. doi: 10.1099/ijsem.0.005560

Haake, D. A., Champion, C. I., Martinich, C., Shang, E. S., Blanco, D. R., Miller, J. N., et al. (1993). Molecular cloning and sequence analysis of the gene encoding OmpL1, a transmembrane outer membrane protein of pathogenic Leptospira spp. *J. Bacteriol.* 175, 4225–4234. doi: 10.1128/jb.175.13.4225-4234.1993

Haake, D. A., Chao, G., Zuerner, R. L., Barnett, J. K., Barnett, D., Mazel, M., et al. (2000). The leptospiral major outer membrane protein LipL32 is a lipoprotein expressed during mammalian infection. *Infect. Immun.* 68, 2276–2285. doi: 10.1128/IAI.68.4.2276-2285.2000

Haake, D. A., and Levett, P. N. (2015). Leptospirosis in humans. *Curr. Top. Microbiol. Immunol.* 387, 65–97. doi: 10.1007/978-3-662-45059-8_5

Haake, D. A., and Matsunaga, J. (2002). Characterization of the leptospiral outer membrane and description of three novel leptospiral membrane proteins. *Infect. Immun.* 70, 4936–4945. doi: 10.1128/IAI.70.9.4936-4945.2002

Haake, D. A., and Matsunaga, J. (2010). Leptospira: a spirochaete with a hybrid outer membrane. *Mol. Microbiol.* 77, 805–814. doi: 10.1111/j.1365-2958.2010.07262.x

Haake, D. A., and Matsunaga, J. (2020). Leptospiral Immunoglobulin-Like Domain Proteins: Roles in Virulence and Immunity. *Front. Immunol.* 11, 579907. doi: 10.3389/fimmu.2020.579907

Haake, D. A., Mazel, M. K., McCoy, A. M., Milward, F., Chao, G., Matsunaga, J., et al. (1999). Leptospiral outer membrane proteins OmpL1 and LipL41 exhibit synergistic immunoprotection. *Infect. Immun.* 67, 6572–6582. doi: 10.1128/IAI.67.12.6572-6582.1999

Haake, D. A., Walker, E. M., Blanco, D. R., Bolin, C. A., Miller, M. N., Lovett, M. A., et al. (1991). Changes in the surface of *Leptospira interrogans* serovar grippotyphosa during in vitro cultivation. *Infect. Immun.* 59, 1131–1140. doi: 10.1128/iai.59.3.1131-1140.1991

Haines, K. A., Yeh, L., Blake, M. S., Cristello, P., Korchak, H., Weissmann, G., et al. (1988). Protein I, a translocatable ion channel from *Neisseria gonorrhoeae*, selectively inhibits exocytosis from human neutrophils without inhibiting O2- generation. *J. Biol. Chem.* 263, 945–951. doi: 10.1016/S0021-9258(19)35444-4

Hong, H., Patel, D. R., Tamm, L. K., and van den Berg, B. (2006). The outer membrane protein OmpW forms an eight-stranded beta-barrel with a hydrophobic channel. *J. Biol. Chem.* 281, 7568–7577. doi: 10.1074/jbc.M512365200

Jeanteur, D., Lakey, J. H., and Pattus, F. (1991). The bacterial porin superfamily: sequence alignment and structure prediction. *Mol. Microbiol.* 5, 2153–2164. doi: 10.1111/j.1365-2958.1991.tb02145.x

King, A. M., Bartpho, T., Sermswan, R. W., Bulach, D. M., Eshghi, A., Picardeau, M., et al. (2013). Leptospiral outer membrane protein LipL41 is not essential for acute leptospirosis but requires a small chaperone protein, lep, for stable expression. *Infect. Immun.* 81, 2768–2776. doi: 10.1128/IAI.00531-13

Ko, A. I., Goarant, C., and Picardeau, M. (2009). Leptospira: the dawn of the molecular genetics era for an emerging zoonotic pathogen. *Nat. Rev. Microbiol.* 7, 736–747. doi: 10.1038/nrmicro2208

Kumar, A., Varma, V. P., and Faisal, S. M. (2022). Screening of surface-exposed lipoproteins of Leptospira involved in modulation of host innate immune response. *Front. Microbiol.* 13, 761670. doi: 10.3389/fmicb.2022.761670

Levett, P. N. (2001). Leptospirosis. *Clin. Microbiol. Rev.* 14, 296–326. doi: 10.1128/CMR.14.2.296-326.2001

Malmström, J., Beck, M., Schmidt, A., Lange, V., Deutsch, E. W., Aebersold, R., et al. (2009). Proteome-wide cellular protein concentrations of the human pathogen *Leptospira interrogans*. *Nature* 460, 762–765. doi: 10.1038/nature08184

McBride, A. J., Athanazio, D. A., Reis, M. G., and Ko, A. I. (2005). Leptospirosis. *Curr. Opin. Infect. Dis.* 18, 376–386. doi: 10.1097/01.qco.0000178824.05715.2c

Murray, G. L. (2015). The molecular basis of leptospiral pathogenesis. *Curr. Top. Microbiol. Immunol.* 387, 139–185. doi: 10.1007/978-3-662-45059-8_7

Murray, G. L., Srikram, A., Hoke, D. E., Wunder, E. A., Henry, R., Lo, M., et al. (2009). Major surface protein LipL32 is not required for either acute or chronic infection with *Leptospira interrogans*. *Infect. Immun.* 77, 952–958. doi: 10.1128/IAI.01370-08

Nally, J. E., Chantranuwat, C., Wu, X. Y., Fishbein, M. C., Pereira, M. M., Silva, J. J. D., et al. (2004). Alveolar septal deposition of immunoglobulin and complement parallels pulmonary hemorrhage in a guinea pig model of severe pulmonary leptospirosis. *Am. J. Pathol.* 164, 1115–1127. doi: 10.1016/S0002-9440(10)63198-7

Oliveira, P. H., Prather, K. J., Prazeres, D. M., and Monteiro, G. A. (2009). Structural instability of plasmid biopharmaceuticals: challenges and implications. *Trends Biotechnol.* 27, 503–511. doi: 10.1016/j.tibtech.2009.06.004

Oliveira, R., Domingos, R. F., Siqueira, G. H., Fernandes, L. G., Souza, N. M., Vieira, M. L., et al. (2013). Adhesins of *Leptospira interrogans* mediate the interaction to fibrinogen and inhibit fibrin clot formation in vitro. *PLoS Negl. Trop. Dis.* 7, e2396. doi: 10.1371/journal.pntd.0002396

Pereira, P. R. M., Fernandes, L. G. V., de Souza, G. O., Vasconcellos, S. A., Heinemann, M. B., Romero, E. C., et al. (2017). Multifunctional and redundant roles of *Leptospira interrogans* proteins in bacterial-adhesion and fibrin clotting inhibition. *Int. J. Med. Microbiol.* 307, 297–310. doi: 10.1016/j.ijmm.2017.05.006

Picardeau, M. (2008). Conjugative transfer between *Escherichia coli* and Leptospira spp. as a new genetic tool. *Appl. Environ. Microbiol.* 74, 319–322. doi: 10.1128/AEM.02172-07

Picardeau, M. (2017). Virulence of the zoonotic agent of leptospirosis: still terra incognita? *Nat. Rev. Microbiol.* 15, 297–307. doi: 10.1038/nrmicro.2017.5

Pinne, M., Choy, H. A., and Haake, D. A. (2010). The OmpL37 surface-exposed protein is expressed by pathogenic Leptospira during infection and binds skin and vascular elastin. *PLoS Negl. Trop. Dis.* 4, e815. doi: 10.1371/journal.pntd.0000815

Poggi, D., Oliveira de Giuseppe, P., and Picardeau, M. (2010). Antibiotic resistance markers for genetic manipulations of Leptospira spp. *Appl. Environ. Microbiol.* 76, 4882–4885. doi: 10.1128/AEM.00775-10

Qi, L. S., Larson, M. H., Gilbert, L. A., Doudna, J. A., Weissman, J. S., Arkin, A. P., et al. (2013). Repurposing CRISPR as an RNA-guided platform for sequence-specific control of gene expression. *Cell* 152, 1173–1183. doi: 10.1016/j.cell.2013.02.022

Ratet, G., Santecchia, I., Fanton d'Andon, M., Vernel-Pauillac, F., Wheeler, R., Lenormand, P., et al. (2017). LipL21 lipoprotein binding to peptidoglycan enables *Leptospira interrogans* to escape NOD1 and NOD2 recognition. *PLoS Pathog.* 13, e1006725. doi: 10.1371/journal.ppat.1006725

Ristow, P., Bourhy, P., McBride, F. W. D. C., Figueira, C. P., Huerre, M., Ave, P., et al. (2007). The OmpA-like protein Loa22 is essential for leptospiral virulence. *PLoS Pathog.* 3, e97. doi: 10.1371/journal.ppat.0030097

Santos, J. V., Pereira, P. R. M., Fernandes, L. G. V., Siqueira, G. H., Souza, G. O., d. e., et al. (2018). Binding of human plasminogen by the lipoprotein LipL46 of *Leptospira interrogans*. *Mol. Cell. Probes* 37, 12–21. doi: 10.1016/j.mcp.2017.10.004

Segura, E. R., Ganoza, C. A., Campos, K., Ricaldi, J. N., Torres, S., Silva, H., et al. (2005). Clinical spectrum of pulmonary involvement in leptospirosis in a region of endemicity, with quantification of leptospiral burden. *Clin. Infect. Dis.* 40, 343–351. doi: 10.1086/427110

Shang, E. S., Exner, M. M., Summers, T. A., Martinich, C., Champion, C. I., Hancock, R. E., et al. (1995). The rare outer membrane protein, OmpL1, of pathogenic Leptospira species is a heat-modifiable porin. *Infect. Immun.* 63, 3174–3181. doi: 10.1128/iai.63.8.3174-3181.1995

Shang, E. S., Summers, T. A., and Haake, D. A. (1996). Molecular cloning and sequence analysis of the gene encoding LipL41, a surface-exposed lipoprotein of pathogenic Leptospira species. *Infect. Immun.* 64, 2322–2330. doi: 10.1128/iai.64.6.2322-2330.1996

Shapiro, R. S., Chavez, A., Porter, C. B. M., Hamblin, M., Kaas, C. S., DiCarlo, J. E., et al. (2018). A CRISPR-Cas9-based gene drive platform for genetic interaction analysis in Candida albicans. *Nat. Microbiol.* 3, 73–82. doi: 10.1038/s41564-017-0043-0

Silva, L. P., Fernandes, L. G., Vieira, M. L., Souza, G. O., d. e., Heinemann, M. B., et al. (2016). Evaluation of two novel leptospiral proteins for their interaction with human host components. *Pathog. Dis.* 74, ftw040. doi: 10.1093/femspd/ftw040

Siqueira, G. H., Atzingen, M. V., Alves, I. J., Morais, Z. M., d. e., Vasconcellos, S. A., et al. (2013). Characterization of three novel adhesins of *Leptospira interrogans*. *Am. J. Trop. Med. Hyg.* 89, 1103–1116. doi: 10.4269/ajtmh.13-0205

Siqueira, G. H., Atzingen, M. V., de Souza, G. O., Vasconcellos, S. A., and Nascimento, A. L. (2016). *Leptospira interrogans* Lsa23 protein recruits plasminogen, factor H and C4BP from normal human serum and mediates C3b and C4b degradation. *Microbiology* 162, 295–308. doi: 10.1099/mic.0.000217

Stevenson, B., Choy, H. A., Pinne, M., Rotondi, M. L., Miller, M. C., Demoll, E., et al. (2007). *Leptospira interrogans* endostatin-like outer membrane proteins bind host fibronectin, laminin and regulators of complement. *PLoS ONE* 2, e1188. doi: 10.1371/journal.pone.0001188

Takahashi, M. B., Teixeira, A. F., and Nascimento, A. L. T. O. (2021). The leptospiral LipL21 and LipL41 proteins exhibit a broad spectrum of interactions with host cell components. *Virulence* 12, 2798–2813. doi: 10.1080/21505594.2021.1993427

Techawiwattanaboon, T., Thaibankluay, P., Kreangkaiwal, C., Sathean-Anan-Kun, S., Khaenam, P., Makjaroen, J., et al. (2021). Surface proteomics and label-free quantification of *Leptospira interrogans* serovar Pomona. *PLoS Negl. Trop. Dis.* 15, e0009983. doi: 10.1371/journal.pntd.0009983

Teixeira, A. F., Morais, Z. M., d. e., Kirchgatter, K., Romero, E. C., Vasconcellos, S. A., et al. (2015). Features of two new proteins with OmpA-like domains identified in the genome sequences of *Leptospira interrogans*. *PLoS ONE* 10, e0122762. doi: 10.1371/journal.pone.0122762

Torgerson, P. R., Hagan, J. E., Costa, F., Calcagno, J., Kane, M., Martinez-Silveira, M. S., et al. (2015). Global burden of leptospirosis: estimated in terms of disability adjusted life years. *PLoS Negl. Trop. Dis.* 9, e0004122. doi: 10.1371/journal.pntd.0004122

Touw, D. S., Patel, D. R., and van den Berg, B. (2010). The crystal structure of OprG from Pseudomonas aeruginosa, a potential channel for transport of hydrophobic molecules across the outer membrane. *PLoS ONE* 5, e15016. doi: 10.1371/journal.pone.0015016

Turner, L. H. (1970). Leptospirosis. 3. Maintenance, isolation and demonstration of leptospires. *Trans. R. Soc. Trop. Med. Hyg.* 64, 623–646. doi: 10.1016/0035-9203(70)90087-8

Verma, A., Hellwage, J., Artiushin, S., Zipfel, P. F., Kraiczy, P., Timoney, J. F., et al. (2006). LfhA, a novel factor H-binding protein of *Leptospira interrogans*. *Infect. Immun.* 74, 2659–2666. doi: 10.1128/IAI.74.5.2659-2666.2006

Vieira, M. L., Atzingen, M. V., Oliveira, T. R., Oliveira, R., Andrade, D. M., Vasconcellos, S. A., et al. (2010a). In vitro identification of novel plasminogen-binding receptors of the pathogen *Leptospira interrogans*. *PLoS ONE* 5, e11259. doi: 10.1371/journal.pone.0011259

Vieira, M. L., de Morais, Z. M., Gonçales, A. P., Romero, E. C., Vasconcellos, S. A., Nascimento, A. L. (2010b). Lsa63, a newly identified surface protein of *Leptospira interrogans* binds laminin and collagen IV. *J. Infect.* 60, 52–64. doi: 10.1016/j.jinf.2009.10.047

Vieira, M. L., Teixeira, A. F., Pidde, G., Ching, A. T. C., Tambourgi, D. V., Nascimento, A. L. T. O., et al. (2018). *Leptospira interrogans* outer membrane protein LipL21 is a potent inhibitor of neutrophil myeloperoxidase. *Virulence* 9, 414–425. doi: 10.1080/21505594.2017.1407484

Vieira, M. L., Vasconcellos, S. A., Gonçales, A. P., Morais, Z. M., d. e., and Nascimento, A. L. (2009). Plasminogen acquisition and activation at the surface of leptospira species lead to fibronectin degradation. *Infect. Immun.* 77, 4092–4101. doi: 10.1128/IAI.00353-09

Wunder, E. A., Adhikarla, H., Hamond, C., Owers Bonner, K. A., Liang, L., Rodrigues, C. B., et al. (2021). A live attenuated-vaccine model confers cross-protective immunity against different species of the Leptospira genus. *Elife* 10, e64166. doi: 10.7554/eLife.64166

Zuerner, R. L., Alt, D. P., and Palmer, M. V. (2012). Development of chronic and acute golden Syrian hamster infection models with Leptospira borgpetersenii serovar Hardjo. *Vet. Pathol.* 49, 403–411. doi: 10.1177/0300985811409252

frontiers | Frontiers in Public Health

TYPE Systematic Review
PUBLISHED 27 June 2023
DOI 10.3389/fpubh.2023.1181230

Check for updates

OPEN ACCESS

EDITED BY
Lei Deng,
Harvard Medical School, United States

REVIEWED BY
Priyadarshi Sahu,
Medical University of the Americas–Nevis, United States
Shuai Wang,
Xinxiang Medical University, China

*CORRESPONDENCE
Vicente A. Benites-Zapata
✉ vbenites@usil.edu.pe

RECEIVED 07 March 2023
ACCEPTED 30 May 2023
PUBLISHED 27 June 2023

CITATION
Ulloque-Badaracco JR, Hernandez-Bustamante EA, Alarcón-Braga EA, Huayta-Cortez M, Carballo-Tello XL, Seminario-Amez RA, Rodríguez-Torres A, Casas-Patiño D, Herrera-Añazco P and Benites-Zapata VA (2023) Seroprevalence of human toxocariasis in Latin America and the Caribbean: a systematic review and meta-analysis.
Front. Public Health 11:1181230.
doi: 10.3389/fpubh.2023.1181230

COPYRIGHT
© 2023 Ulloque-Badaracco, Hernandez-Bustamante, Alarcón-Braga, Huayta-Cortez, Carballo-Tello, Seminario-Amez, Rodríguez-Torres, Casas-Patiño, Herrera-Añazco and Benites-Zapata. This is an open-access article distributed under the terms of the Creative Commons Attribution License (CC BY). The use, distribution or reproduction in other forums is permitted, provided the original author(s) and the copyright owner(s) are credited and that the original publication in this journal is cited, in accordance with accepted academic practice. No use, distribution or reproduction is permitted which does not comply with these terms.

Seroprevalence of human toxocariasis in Latin America and the Caribbean: a systematic review and meta-analysis

Juan R. Ulloque-Badaracco[1], Enrique A. Hernandez-Bustamante[2,3], Esteban A. Alarcón-Braga[1], Miguel Huayta-Cortez[1], Ximena L. Carballo-Tello[1], Rosa A. Seminario-Amez[1], Alejandra Rodríguez-Torres[4,5], Donovan Casas-Patiño[4,5], Percy Herrera-Añazco[6,7] and Vicente A. Benites-Zapata[8]*

[1]Escuela de Medicina, Universidad Peruana de Ciencias Aplicadas, Lima, Peru, [2]Sociedad Cientifica de Estudiantes de Medicina de la Universidad Nacional de Trujillo, Trujillo, Peru, [3]Grupo Peruano de Investigación Epidemiológica, Unidad Para la Generación y Síntesis de Evidencias en Salud, Universidad San Ignacio de Loyola, Lima, Peru, [4]Universidad Autónoma del Estado de México, CU Amecameca, Mexico, [5]Red Internacional en Salud Colectiva y Salud Intercultural, Amecameca, Mexico, [6]Universidad Privada del Norte, Trujillo, Peru, [7]Red Peruana de Salud Colectiva, Lima, Peru, [8]Unidad de Investigación Para la Generación y Síntesis de Evidencias en Salud, Vicerrectorado de Investigación, Universidad San Ignacio de Loyola, Lima, Peru

Introduction: The current study aimed to quantitatively synthesize available evidence regarding the seroprevalence of human toxocariasis in Latin America and the Caribbean.

Methods: A systematic research involving six electronic databases was conducted using a research strategy that combined MeSH terms with free terms. Article selection and information extraction were performed using a double and independent approach. The Newcastle-Ottawa tool was used to assess the risk of bias in the included articles. The meta-analysis used the random-effects approach, with subgroup analysis and sensitivity analysis for risk of bias also being performed.

Results: We included 101 articles with a total of 31,123 participants. The studies were conducted between 1990 and 2022, with Brazil accounting for the largest number of studies (n = 37). The overall seroprevalence of human toxocariasis was 31.0% (95% CI: 27.0-35.0%, I^2=99%). The prevalence of the main characteristics observed in seropositive patients were as follows: ocular toxocariasis (30.0%), asymptomatic (26.0%), and presence of dogs at home (68.0%). In addition, the seroprevalence was lower in studies including only adults than in those including children or both. In contrast, no differences in seroprevalences were found between studies conducted in the community and hospital.

Conclusion: The overall seroprevalence of human toxocariasis in Latin America and the Caribbean was high. Notably, our findings showed that the seroprevalence was increased among populations who kept a dog at home but was decreased in populations comprising only adults. Our findings can be used to establish epidemiological surveillance strategies for the prevention and early identification of toxocariasis.

KEYWORDS

toxocariasis, zoonoses, seroepidemiologic studies, systematic review, metaanalysis

1. Introduction

Toxocariasis is a zoonosis caused by the larvae of two main species of *Toxocara*, *Toxocara canis* found in dogs and *Toxocara cati* found in cats (1, 2). Although other species, such as *Toxocara leonina* found in foxes, can also cause toxocariasis, *T. canis* has been most associated with human toxocariasis (3). Toxocariasis is a prevalent parasitic disease with a significant socioeconomic impact in symptomatic patients, especially among poor communities, and at the governmental level, with the need for investments in animal deworming campaigns (4, 5). Although infected humans may be asymptomatic, toxocariasis in human always causes extraintestinal pathologies (5). As such, toxocariasis has been associated with various short- and medium-term diseases, such as ocular disease (4), heart disease, stroke, heart failure (6), childhood asthma (7), allergic skin disorders (8), epilepsy (9), or diseases of the urinary system (10), although evidence for this remains inconclusive. Hence, health care systems should prioritize the diagnosis and adequate treatment of this condition.

Toxocariasis is particularly prevalent in the tropics, subtropics, and in low- and middle-income countries where treatment and canine population control is limited (11). However, the prevalence of toxocariasis has varied. Studies estimating the prevalence of specific serum anti-*Toxocara* antibodies found that it was 0.7% in New Zealand, 1.6% in Japan, 2.4% in Denmark, 6.3% in Austria, 7% in Sweden, 14% in the United States, and 31% in Ireland (12). Nevertheless, higher prevalence rates were observed in some ethnic and socioeconomically disadvantaged groups, such as Iran (22%) and Nepal (81%) (12). This suggests that in countries with large socioeconomically disadvantaged groups, better measures are needed to prevent the complications of this disease, including determination of its prevalence based on which future prevention and/or control programs can be implemented (12).

Latin America and the Caribbean are heterogeneous regions with inequities that impact various health indicators (13, 14), including some coexisting conditions that are associated with increased risk of toxocariasis. These include warm, humid regions where eggs survive better in the soil; low levels of education; and areas with a lower human development index and poor environmental sanitation and hygiene (4). Hence, a systematic review found that the prevalence of specific anti-*Toxocara* antibodies was 27.8% in South American countries and 12.8% in North American countries, suggesting potentially frequent infections at the population level (12).

Despite the numerous studies on seroprevalence, to the best of our knowledge, no study has yet synthesized available evidence regarding the seroprevalence of human toxocariasis in Latin American countries according to certain clinical and sociodemographic conditions. Therefore, the present study aimed to synthesize evidence on the seroprevalence of human toxocariasis in Latin America and the Caribbean through a systematic review and meta-analysis.

2. Methods

2.1. Registration and reporting

A short version of the protocol for this systematic review was uploaded to the International Prospective Register of Systematic Reviews (PROSPERO) [CRD42023389135]. The manuscript follows the Preferred Reporting Items for Systematic Reviews and Meta-Analyzes (PRISMA) statement for reporting results (15).

2.2. Search strategy and databases

The search strategy used MeSH, Emtree, and free terms following the Peer Review of Electronic Search Strategies (PRESS) Checklist (16). A search formula was created to retrieve studies assessing the seroprevalence of *T. canis* in humans. Afterwards, it was adopted for all employed databases, without date or language restrictions. Preprint databases and reference lists of the included studies were also manually searched. A systematic search of the following databases was performed simultaneously on December 23, 2022: PubMed, Scopus, Embase, LILACS, Scielo, and Web of Science. The complete search strategy is detailed in Supplementary Table S1 attached as Supplementary material.

2.3. Study selection and data extraction

All phases of study selection were independently performed by two authors (E.A.A-B and E.A.H-B). The eligibility criteria were (1) cross-sectional studies assessing the (2) seroprevalence of *T. canis* in humans. We excluded narrative reviews, scoping reviews, systematic reviews, and conference abstracts. Duplicates were removed using EndNote 20.1 ©. The remaining studies were then exported to Rayyan QCRI © for screening according to titles and abstracts (17). After identifying potential studies for inclusion, the authors independently assessed the full text of each one. Any conflict or discrepancy in any phase of the study selection process was resolved via consensus. Data extraction was independently performed by four authors (J.R.U-B, X.L.C-T, R.A.S-A and M.A.H-C) using a standardized data extraction sheet created using Microsoft Excel ©. The following pieces of information were extracted: author names, publication date, country, type population, sample size, survey modality, and seroprevalence of human toxocariasis in Latin America and the Caribbean.

2.4. Risk of bias and publication bias

Quality assessment was performed independently by four authors (J.R.U-B, X.L.C-T, R.A.S-A and M.A.H-C). We used the Newcastle-Ottawa Scale (NOS) for cohort/case–control studies and the adapted version of the Newcastle-Ottawa Scale for cross-sectional studies (NOS-CS) (18). Studies with a score of ≥7 stars were considered to have a low risk of bias (high quality), whereas those with a score of <7 stars were considered to have a high risk of bias (low quality). Publication bias was not assessed given that it is not recommended for proportional meta-analyzes considering the lack of evidence that proportions are adjusted correctly (19, 20).

2.5. Data synthesis

Statistical analysis was performed using STATA 17.0 ©. We conducted a pooled analysis of the seroprevalences of human infections according to *T. canis*. The 95% confidence intervals (CI) for

the proportions reported in each study were calculated using the Clopper–Pearson method. The Freeman–Tukey double arcsine transformation was used as the variance stabilizer. A random-effects model (Dersimonian and Laird) was created for quantitative analysis. Between-study heterogeneity was assessed using the Cochran's Q test and I^2 statistic. Values ≥60% indicated high heterogeneity for the I^2 statistic, whereas *p* values <0.1 indicated heterogeneity in Cochran's Q test. In addition, we conducted a subgroup analysis according to continent and population groups and a sensitivity analysis excluding studies with high risk of bias.

3. Results

3.1. Search results

The systematic search identified a total of 4,355 studies. After removing 1,620 duplicate studies, 2,735 studies remained for further screening. Subsequently, screening according to abstracts and titles was performed, after which 230 studies remained. Finally, the full texts of the remaining studies were evaluated, and 101 studies were found to satisfy all eligibility criteria (21–121). This selection process is summarized in the PRISMA flow diagram (Figure 1).

3.2. Study characteristics

A total of 101 studies with 31,123 participants were included. The studies were conducted between 1990 and 2022 and were developed in the following countries: Brazil (35 studies), Argentina (13 studies), Venezuela (10 studies), Mexico (10 studies), Peru (11 studies), Colombia (5 studies), Bolivia (3 studies), Cuba (3 studies), Chile (2 studies), Ecuador (2 studies), Puerto Rico (1 study), Trinidad and Tobago (1 study), Saint Lucia (1 study), Paraguay (1 study), Honduras (1 study), Jamaica (1 study), and multiple Caribbean countries (1 study). In all studies, seroprevalence was assessed using ELISA method (Table 1).

During the quality assessment of the studies using NOS and NOS-CS, 5 studies were found to have a high risk of bias, whereas the remaining 96 were found to have a low risk of bias (Supplementary Table S2).

3.3. Seroprevalence of human toxocariasis

Some meta-analyzes results are summarized in Table 2 given the large number of studies involved, which diminish the quality of the images. All 101 studies were included in the meta-analysis. Notably, the seroprevalence of human toxocariasis in Latin America and the Caribbean was 31.0% (95% CI: 27.0–35.0%) with high heterogeneity across all studies ($I^2 = 99\%$). Subgroup analysis according to country showed no decrease in heterogeneity in any of the countries: Brazil (28%), Argentina (37%), Venezuela (22%), Mexico (19%), Peru (34%), Colombia (39%), Bolivia (19%), Cuba (28%), Chile (26%), and Ecuador (64%). Analysis according to age group revealed no decrease in heterogeneity in any of the groups: Children and adults (31%), adults (20%), and children (32%). Subgroup analysis according to sample collection site found no decrease in heterogeneity in any of the groups: Community (30%) and Hospital (31%). Finally, sensitivity analysis revealed no evidence of a decrease in heterogeneity with a seroprevalence of 30.0% (95% CI: 26.0–34.0%, $I^2 = 99.03$).

3.4. Characteristics of patients seropositive for human toxocariasis

Ocular toxocariasis in patients with human toxocariasis was evaluated in 17 studies (Figure 2), revealing a prevalence of 30.0% (95% CI: 15.0–45.0%) with a high heterogeneity among studies ($I^2 = 98.49\%$). Meanwhile, the number of asymptomatic patients with human toxocariasis was evaluated in 9 studies (Figure 3), revealing a prevalence of 26.0% (95% CI: 2.0–50.0%) with a high heterogeneity among studies ($I^2 = 99.02\%$). Finally, the seroprevalence of toxocariasis in patients with dogs at home was evaluated in 36 studies, revealing a prevalence 68.0% (95% CI: 61.0–75.0%; Figure 4) with a high heterogeneity among studies ($I^2 = 96.15\%$).

4. Discussion

The main findings of the current study show that 3 out of 10 participants were seropositive for *T. canis*, with the same findings obtained at the community and hospital levels. A comparison between children and adults showed that 3 out of 10 children and 2 out of 10 adults were seropositive for *T. canis*. Meanwhile, two-thirds of patients living with dogs in homes were seropositive. Variations in seroprevalence had been noted among countries, with Honduras and Puerto Rico showing an increased and decreased seroprevalence, respectively. One-fourth of the seropositive patients were asymptomatic and one-third of them had ocular involvement.

The worldwide prevalence of *Toxocara* in humans is influenced, at the population level, by environmental, geographic, cultural, and socioeconomic factors and, at the individual level, by susceptibility to infection, which is consequently influenced by immunity, co-infection, genetics, age, nutrition, or the sex of the host (11). These factors, along with population growth, global migration, and rural–urban migration, have promoted increasingly close human–host interactions, making toxocariasis a dynamic public health problem (11). However, some systematic reviews have attempted to determine its seroprevalence.

A systematic review that calculated the overall prevalence of serum anti-*Toxocara* antibodies in humans found that one-fifth of the world's population is seropositive for *Toxocara*, with Africa showing increased seropositive rates with a mean of 37.7% and the Eastern Mediterranean region showing decreased rates with a mean of 8.2%. Evidencing in South American countries, specifically in Latin America and the Caribbean, showed an average seroprevalence of 27.8% (range 23.1–32.7%) and was 12.8% in North American countries (range 10.0–15.8%) (122). These results show the heterogeneity of prevalence in the countries within the region, similar to that observed herein and in various systematic reviews involving other regions globally.

In fact, a systematic review that determined the burden of toxocariasis in North America found that prevalence estimates ranged from 0.6% in a Canadian Inuit community to 30.8% in Mexican children with asthma (123). In Africa, another systematic review found that, despite underdiagnosis, human exposure to *Toxocara* is widespread in various geographical areas and different populations in

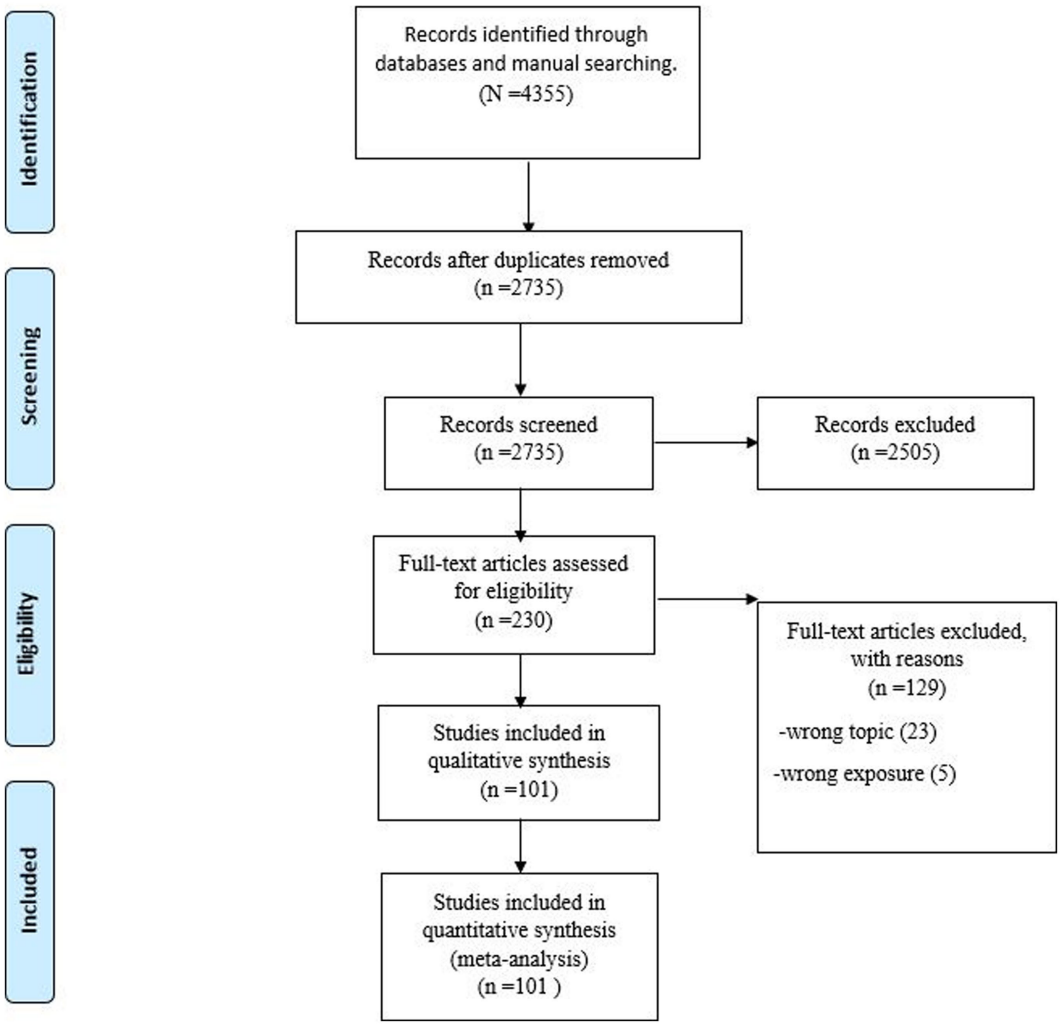

FIGURE 1
PRISMA flow diagram.

Africa and occurs in virtually all climatic zones, with seroprevalences greater than 80% in some populations such as in Makoko, Nigeria, or La Réunion (124). Finally, the seroprevalence among the general European population was 6.2%, although no significant differences were observed among the combined prevalence rates of the European subregions (125).

These differences may be due to the varying proportion of risk factors in the studies, which also vary among the regions studied and, in some cases, are common in Latin American and Caribbean countries. Globally, areas with a low human development index and income levels, those located within the low-latitude regions, those having high ambient temperature, and those with increased precipitation have been associated with a high prevalence of serum anti-*Toxocara* antibodies (122). Other risk factors include male sex; living in rural areas; young age; close contact with dogs, cats, or soil; consumption of raw meat; and consumption of untreated drinking water (122). In North America, commonly cited risk factors include African American race, poverty, male sex, pet ownership, or environmental contamination by animal feces (123). Additionally, apart from the differences in serodiagnostic methods used, other systematic reviews likely included other types of *Toxocara*, unlike our research, which only evaluated the seroprevalence of *T. canis*, precluding direct comparisons between our results (5). Likewise, a limitation of *T. canis* antigen tests, which is their cross-reactivity with other helminths such as *Ascaris lumbricoides*, needs to be considered, particularly in endemic areas (5) given the potential for overestimating the seroprevalence of *T. canis* in Latin America and the Caribbean (126).

Our study, which evaluated not only overall seroprevalence but also differences according to site of evaluation and age group, found that around 3 out of 10 seropositive patients were asymptomatic. In most patients, *Toxocara* infections were not severe, and several people, especially adults infected with a small number of larvae, may remain asymptomatic or have mild or nonspecific symptoms that go undiagnosed, with more severe cases being rare (4). In this sense, the similarity in seroprevalence at the hospital and community levels could be attributed the low disease severity in majority of the cases. Similarly, although the percentage of asymptomatic patients in our study is important, we emphasize that positive results in serological test for antibodies against *Toxocara*,

TABLE 1 Characteristics of the included studies.

Author	Year	Country	Type of population	Sample collection site	Participants (male/female)	Number of seropositive participants	Seroprevalence of *Toxocara* infection	Ocular toxocariasis in seropositive participants	Seropositive participants with dogs at home	Asymptomatic seropositive participants
Acero M et al.	2001	Colombia	Children	Community	193 (114/79)	14	7.30%	NR	8	NR
Agudelo C et al.	1990	Colombia	Children and Adult	Community	202 (NR/NR)	95	47.50%	NR	NR	NR
Aguiar-Santos AM et al.	2004	Brazil	Children	Hospital	386 (269/117)	152	39.40%	NR	NR	NR
Alderete J et al.	2003	Brazil	Children	Community	399 (196/203)	155	38.80%	NR	NR	NR
Alonso JM et al.	2004	Argentina	Children and adult	Hospital	355 (30/325)	138	38.00%	NR	NR	NR
Alvarado-Esquivel C et al. (A)	2013	Mexico	Adults	Hospital	90 (34/56)	12	13%	4	1	NR
Alvarado-Esquivel C et al. (B)	2014	Mexico	Children and Adult	Community	126 (53/73)	33	26.20%	NR	NR	NR
Alvarado-Esquivel C et al. (C)	2014	Mexico	Children and Adult	Community	336 (306/30)	6	1.80%	NR	NR	NR
Anaruma Filho F et al.	2002	Brazil	Children and Adult	Community	138 (87/51)	33	23.90%	NR	9	NR
Araujo Z et al.	2015	Venezuela	Children and Adult	Community	50 (21/29)	5	10%	NR	NR	NR
Archelli S et al. (A)	2014	Argentina	Children	Community	120 (NR/NR)	46	38.33%	NR	NR	NR
Archelli S et al. (B)	2018	Argentina	Children and Adult	Community	98 (NR)	40	40.80%	NR	NR	NR
Baboolal S et al.	2002	Trinidad and Tobago	Children	Community	1,009 (498/511)	629	62.33%	NR	NR	NR
Berrocal J et al.	1980	Puerto Rico	Children and Adult	Hospital	671 (NR/NR)	44	6.50%	NR	NR	NR
Bojanich MV et al.	2008	Argentina	Children	Community	273 (144/129)	168	61.54%	NR	153	NR
Cabral M et al.	2022	Brazil	Children	Community	412 (NR/NR)	234	56.80%	NR	179	NR
Campos-Junior D et al.	2003	Brazil	Children	Hospital	602 (NR/NR)	75	12.45%	NR	NR	NR
Cancrini G et al.	1998	Bolivia	Adults	Community	216 (NR/NR)	73	34%	NR	NR	NR
Cermeño J et al.	2016	Venezuela	Children	Community	146 (73/73)	43	32.20%	1	43	29
Chieffi P et al.	1990	Brazil	Children and Adult	Community	2025 (1,219 /806)	70	3.46%	NR	NR	NR
Chiodo P et al.	2006	Argentina	Children and Adult	Community	100 (46/54)	23	23%	NR	23	NR
Coelho LM et al.	2004	Brazil	Children	Community	180 (92/88)	69	38.33%	NR	53	NR
Colli C et al.	2010	Brazil	Children	Community	376 (NR/NR)	194	51.60%	NR	NR	NR
Cook J et al.	2016	Jamaica	Children and Adult	Community	1,447 (738/709)	304	21%	NR	NR	NR
Correa C et al.	2009	Brazil	Children	Community	100 (NR/NR)	28	28%	NR	NR	28/28

(Continued)

10.3389/fpubh.2023.1181230

TABLE 1 (Continued)

Author	Year	Country	Type of population	Sample collection site	Participants (male/female)	Number of seropositive participants	Seroprevalence of *Toxocara* infection	Ocular toxocariasis in seropositive participants	Seropositive participants with dogs at home	Asymptomatic seropositive participants
Damian M et al.	2007	Brazil	Children and Adult	Community	100 (NR/NR)	52	52%	NR	NR	NR
Dattoli V et al.	2011	Brazil	Adults	Community	306 (108/198)	124	46.30%	NR	NR	NR
De Abreu A et al.	2011	Venezuela	Children	Community	215 (112/103)	74	34.40%	NR	NR	NR
Devera R et al.	2015	Venezuela	Children	Community	547 (223/3244)	269	58.90%	NR	206	NR
Díaz-Suárez O et al.	2010	Venezuela	Children and Adult	Community	83 (42/41)	18	21.68%	NR	NR	NR
Espinoza Y et al. (B)	2008	Peru	Children	Community	182 (NR/NR)	59	32.40%	36	58	1
Espinoza Y et al. (A)	2010	Peru	Children and Adult	Community	303 (128/175)	62	20.46%	11	NR	NR
Espinoza Y et al. (C)	2003	Peru	Children and Adult	Hospital	553 (NR/NR)	129	23.32%	NR	NR	NR
Figuereido S et al.	2005	Brazil	Children	Hospital	208 (NR/NR)	114	54.80%	NR	NR	NR
Fillaux J et al.	2007	Argentina	Children and Adult	Hospital	114 (45/69)	36	31.57%	NR	14	NR
García-Pedrique ME et al.	2004	Venezuela	Children	Community	72 (45/27)	7	9.72%	NR	NR	NR
Gétaz-Schaller L et al.	2007	Peru	Children	Hospital	150 (72/78)	24	16%	NR	15	NR
Guilherme E et al.	2013	Brazil	Children	Hospital	167 (NR/NR)	7	4.20%	NR	5	0
Guo F et al.	2016	Multiple Caribbean countries	Adults	Hospital	435 (0/435)	63	14.50%	NR	NR	NR
Heredia R et al.	2014	Mexico	Adults	Community	200 (NR/NR)	20	10%	NR	15	NR
Hernández S et al.	2020	Honduras	Children and Adult	Community	88 (43/45)	80	90.90%	NR	NR	NR
Kanobana K et al.	2013	Cuba	Children	Hospital	958 (504/454)	384	40.10%	NR	NR	NR
Lescano S et al.	1998	Peru	Children and Adult	Community	1,023 (740/283)	75	7.33%	NR	NR	NR
Lima-Coêlho R et al.	2005	Brazil	Children	Community	215 (NR/NR)	26	12.09%	NR	NR	NR
Lopez MA et al.	2010	Argentina	Children	Hospital	100 (NR/NR)	55	55%	NR	NR	NR
Lozano-Beltrán D et al.	2011	Bolivia	Children	Hospital	82 (NR/NR)	5	6.50%	NR	5	NR
Lynch NR et al. (A)	1988	Venezuela	Children	Hospital	476 (NR/NR)	56	11.7%	NR	37	NR
Lynch NR et al. (B)	1993	Venezuela	Children	Hospital	368 (NR/NR)	74	20.10%	NR	NR	NR
Manini M et al.	2012	Brazil	Children	Community	90 (NR/NR)	16	17.80%	NR	NR	NR
Marchioro A et al.	2015	Brazil	Children	Community	544 (299/245)	136	25%	NR	NR	NR
Martín U et al. (A)	2014	Argentina	Children	Community	857 (NR/NR)	335	59.70%	NR	NR	NR
Martín U et al. (B)	2008	Argentina	Children	Community	100 (62/38)	59	59%	5	NR	NR

(Continued)

10.3389/fpubh.2023.1181230

TABLE 1 (Continued)

Author	Year	Country	Type of population	Sample collection site	Participants (male/female)	Number of seropositive participants	Seroprevalence of *Toxocara* infection	Ocular toxocariasis in seropositive participants	Seropositive participants with dogs at home	Asymptomatic seropositive participants
Martínez M et al.	2018	Venezuela	Children	Hospital	259 (148/111)	37	14.30%	5	25	NR
Mattia S et al.	2011	Brazil	Children	Community	353 (NR/NR)	130	36.80%	NR	78	NR
Meza D et al.	2010	Colombia	Children	Community	133 (57–76)	56	42.10%	1	38	NR
Minvielle M et al.	2000	Argentina	Adults	Hospital	180 (47/133)	19	10.60%	NR	NR	NR
Miranda-Choque E et al.	2014	Peru	Children	Hospital	242 (92/150)	148	61.20%	16	NR	NR
Montalvo A et al.	1994	Cuba	Children	Community	152 (NR/NR)	8	5.20%	NR	NR	NR
Morocoima A et al.	2021	Venezuela	Children	Hospital	118 (50/68)	22	18.60%	14	NR	NR
Muñoz-Guzmán M et al.	2010	Mexico	Children	Hospital	437 (NR)	118	27%	NR	NR	NR
Muradian V et al.	2005	Brazil	Children	Community	338 (NR/NR)	89	26–9%	NR	NR	NR
Nava-Cortés N et al.	2015	Mexico	Children	Community	183 (97/86)	22	12.02%	NR	8	NR
Negri E et al.	2013	Brazil	Adults	Community	253 (148/105)	22	8.70%	NR	14	NR
Nicoletti A et al.	2002	Bolivia	Children and Adult	Community	346 (NR/NR)	56	24.80%	NR	NR	NR
Oliart-Guzmán H et al.	2014	Brazil	Children	Community	539 (NR/NR)	106	19.66%	NR	NR	NR
Orlando-Indacochea N et al.	2018	Ecuador	Children	Community	50 (NR)	18	36%	NR	NR	NR
Ortega-Pacheco A et al.	2015	Mexico	Adults	Community	84 (8/76)	19	22.60%	16	NR	NR
Oviedo-Vera A et al.	2021	Ecuador	Children	Hospital	290 (NR)	200	69%	NR	NR	NR
Paludo M et al.	2007	Brazil	Children	Hospital	130 (NR/NR)	36	28.80%	NR	78	NR
Paranhos-Fragoso et al.	2011	Brazil	Children	Hospital	391(NR/NR)	202	51.60%	NR	78	NR
Pereira L et al.	2016	Brazil	Adults	Hospital	311 (0/311)	23	7.20%	NR	NR	NR
Prestes-Carneiro L et al. (A)	2008	Brazil	Children	Community	79 (NR/NR)	17	21.50%	NR	NR	NR
Prestes-Carneiro L et al. (B)	2009	Brazil	Children and Adult	Community	182 (64/118)	25	13.73%	8	20	4
Prestes-Carneiro L et al. (C)	2013	Brazil	Children and Adult	Community	194 (101/93)	102	52.60%	NR	67	NR
Pulcha-Ugarte R et al.	2021	Peru	Children	Community	61 (33/28)	22	36.10%	NR	7	NR

(Continued)

10.3389/fpubh.2023.1181230

TABLE 1 (Continued)

Author	Year	Country	Type of population	Sample collection site	Participants (male/female)	Number of seropositive participants	Seroprevalence of *Toxocara* infection	Ocular toxocariasis in seropositive participants	Seropositive participants with dogs at home	Asymptomatic seropositive participants
Radman NE et al.	2000	Argentina	Children and Adult	Hospital	156 (NR/NR)	61	39.10%	4	NR	10
Ramírez-Bustamante C et al.	2010	Peru	Children and Adult	Hospital	41 (21/20)	31	75.60%	31	NR	NR
Ribeiro L et al.	2012	Brazil	Children	Community	1,445 (NR/NR)	540	47%	NR	NR	NR
Rivarola M et al.	2009	Paraguay	Children	Community	68 (NR)	53	78%	NR	NR	NR
Rodriguez C et al.	2006	Brazil	Children	Hospital	242 (NR/NR)	21	8.70%	NR	NR	NR
Roldan W et al. (A)	2008	Peru	Children	Community	200 (96/104)	62	31%	13	43	NR
Roldan W et al. (B)	2009	Peru	Adults	Community	256 (NR/NR)	115	44.92%	16	109	27
Roldan W et al. (C)	2010	Peru	Children and Adult	Community	300 (112/188)	107	35.66%	39	89	5
Romero R et al.	2017	Colombia	Children	Community	165 (77/88)	30	18.20%	NR	NR	NR
Romero-Nuñez C et al.	2013	Mexico	Children	Community	108 (52/56)	24	22.22%	NR	18	NR
Rubinsky-Elefant G et al.	2008	Brazil	Children and Adult	Community	403 (NR/NR)	108	26.80%	NR	31	NR
Santarem V et al.	2011	Brazil	Children	Community	252 (NR/NR)	28	11.10%	NR	18	NR
Santos P et al.	2015	Brazil	Children and Adult	Community	280 (0/280)	18	6.40%	NR	16	NR
Sariego I et al.	2012	Cuba	Children	Community	1,011 (525/486)	392	38.80%	NR	NR	NR
Schoenardie E et al.	2013	Mexico	Children	Hospital	427 (NR/NR)	216	50.58%	NR	NR	NR
Silva-Cadore P et al.	2016	Brazil	Children	Hospital	208 (113/95)	24	11.53%	NR	NR	NR
Souza RF et al.	2011	Brazil	Children and Adult	Community	338 (NR/NR)	201	59.46%	NR	120	NR
Taranto NJ et al. (A)	2000	Argentina	Children	Community	98 (NR/NR)	20	20.40%	NR	NR	NR
Taranto NJ et al. (B)	2003	Argentina	Children and Adult	Community	154 (NR/NR)	34	22.10%	NR	NR	NR
Thompson DE et al.	1986	Saint Lucía	Children	Hospital	203 (NR/NR)	170	84%	NR	NR	NR
Tinoco-Gracias L et al.	2008	Mexico	Children	Hospital	288 (153/135)	25	8.68%	NR	10	NR
Triviño X et al.	1999	Chile	Children	Hospital	24 (NR)	8	33.30%	1	8	0
Urbano-Ferreira M et al.	2007	Brazil	Children	Community	606 (NR/NR)	133	21.50%	NR	NR	NR
Vargas C et al.	2016	Chile	Children and Adult	Hospital	355 (NR/NR)	90	25.40%	NR	80	NR
Virginia P et al.	1991	Brazil	Children	Hospital	54 (NR/NR)	21	40%	NR	NR	NR
Waindok P et al.	2021	Colombia	Children and Adult	Hospital	483 (232/247)	383	79.30%	NR	NR	NR

NR, not reported.

10.3389/fpubh.2023.1181230

TABLE 2 Results of seroprevalence meta-analyzes.

	Number of studies	Pooled seroprevalence (%)	95% CI	*n*	I^2	*p*
Overall seroseroprevalence	101	31.0%	27.0–35.0%	31,123	99%	<0.001
Central America and Caribbean Islands	19	–	–	8,253		
Mexico	10	19.0%	10.0–29.0%	2,279	98.23%	<0.001
Cuba	3	28.0%	7.0–49%	2,121	99.23%	<0.001
Puerto Rico	1	6.0%	4.0–9.0%	671	–	<0.001
Trinidad and Tobago	1	62.0%	59.0–65.0%	1,009	–	<0.001
Saint Lucia	1	83.0%	78.0–88.0%	203		<0.001
Honduras	1	90.0%	83.0–86.0%	88	–	<0.001
Jamaica	1	21.0%	18.0–23.0%	1,447	–	<0.001
Multiple Caribbean Countries	1	14.0%	11.0–18.0%	435	–	<0.001
South America	82	–	–	22,870		
Brazil	35	28.0%	22.0%–34.0%	12,508	98.89%	<0.001
Argentina	13	37.0%	28.0–45.0%	2,409	95.76%	<0.001
Venezuela	10	22.0%	13.0–31.0%	2035	96.57%	<0.001
Peru	11	34.0%	23.0%–46.0%	3,311	98.34%	<0.001
Colombia	5	39.0%	6.0–71.0%	1,176	99.51%	<0.001
Bolivia	3	19.0%	5.0–32.0%	644	95.49%	<0.001
Chile	2	26.0%	21.0–30.0%	379	-	<0.001
Ecuador	2	64.0%	59.0–69.0%	340	-	<0.001
Paraguay	1	78.0%	66.0–87.0%	68	-	<0.001
Type of population						
Children	61	32.0%	27.0–37.0%	17,786	98.48%	<0.001
Adults	10	20.0%	13.0–28.0%	2,293	96.54%	<0.001
Childrens and adults	30	31.0%	25.0–38.0%	1,104	99.26%	<0.001
Sample collection site						
Community	66	30.0%	26.0–35.0%	10,439	98.98%	<0.001
Hospital	36	31.0%	24.0–38.0%	5,144	99.02%	<0.001
Sensitivity analysis	96	30.0%	26.0–34%	30,436	99.03%	<0.001

which have been available, are not necessarily correlated with any clinical symptoms and cannot differentiate between current active disease and past infection (4).

Another significant finding of our study was that 3 out of 10 seropositive patients had ocular involvement. Ocular involvement in toxocariasis occurs when *Toxocara* larvae migrate to the eyes, promoting symptoms and signs that include vision loss, ocular inflammation, or retinal damage, usually in a single eye (127). As of 2018, a total of 823 cases of ocular toxocariasis had been reported, including 282 cases in Europe, 317 cases in Asia, five cases in Australia, 218 cases in Latin America, and 1 documented case in Tunisia (4). The highest number of ocular toxocariasis cases had been reported in Japan, Korea, France, Brazil, and the US (4). Our results showed that up to 133 Peruvian patients alone were seropositive, which warrants special follow-up by the Peruvian health authorities. Ocular involvement is more common among children aged 5 to 10 years (128–130), which could explain the higher prevalence of toxocariasis among children. However, studies in Europe show otherwise such that the pooled seroprevalence was higher among people over 50 years of age than among younger people (18). A systematic review found that the pooled estimate of the worldwide prevalence of *T. canis* in the pediatric population was 30%, with Asian populations showing higher rates than the European, American, and African populations (131). One study in America showed a seroprevalence of 31%; however, given that this study included North American countries and both *T. canis* and *T. cati*, our results cannot be compared (131).

Our findings showed that the seroprevalence was higher in patients who had a dog in the household. This is consistent with the results of a systematic review in the Americas, Middle East, and Western Pacific Region, which found a statistically significant association between seropositivity for *Toxocara* and contact with pets, although only in younger people with both dogs and cats (132). Toxocariasis has a fecal–oral route of transmission where domestic

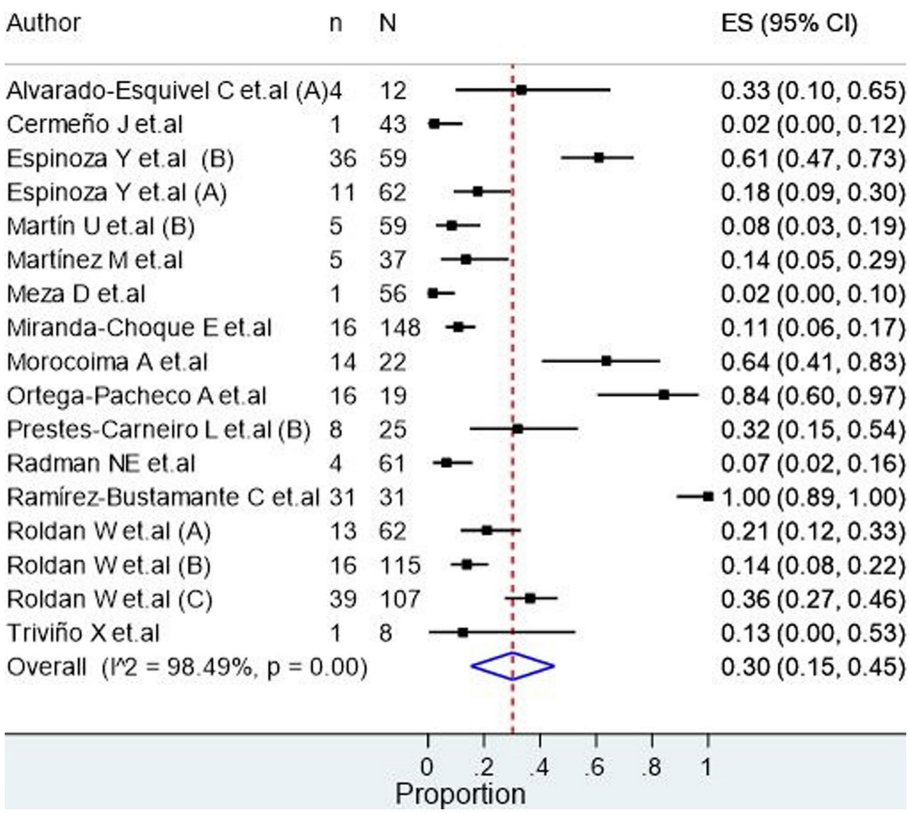

FIGURE 2
Seroprevalence of ocular toxocariasis in seropositive participants.

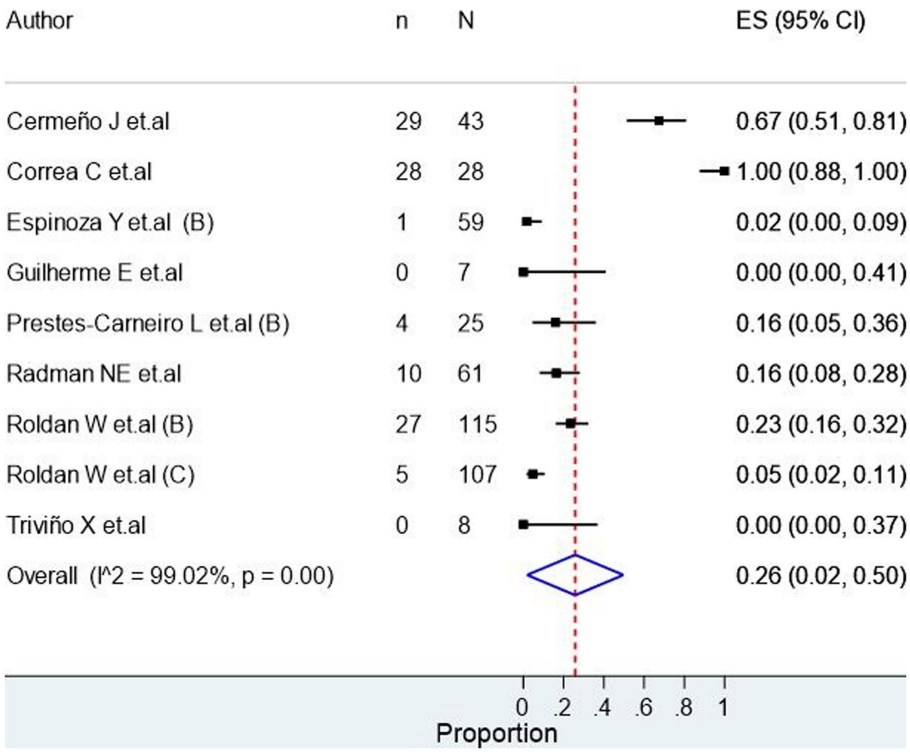

FIGURE 3
Seroprevalence of asymptomatic seropositive participants.

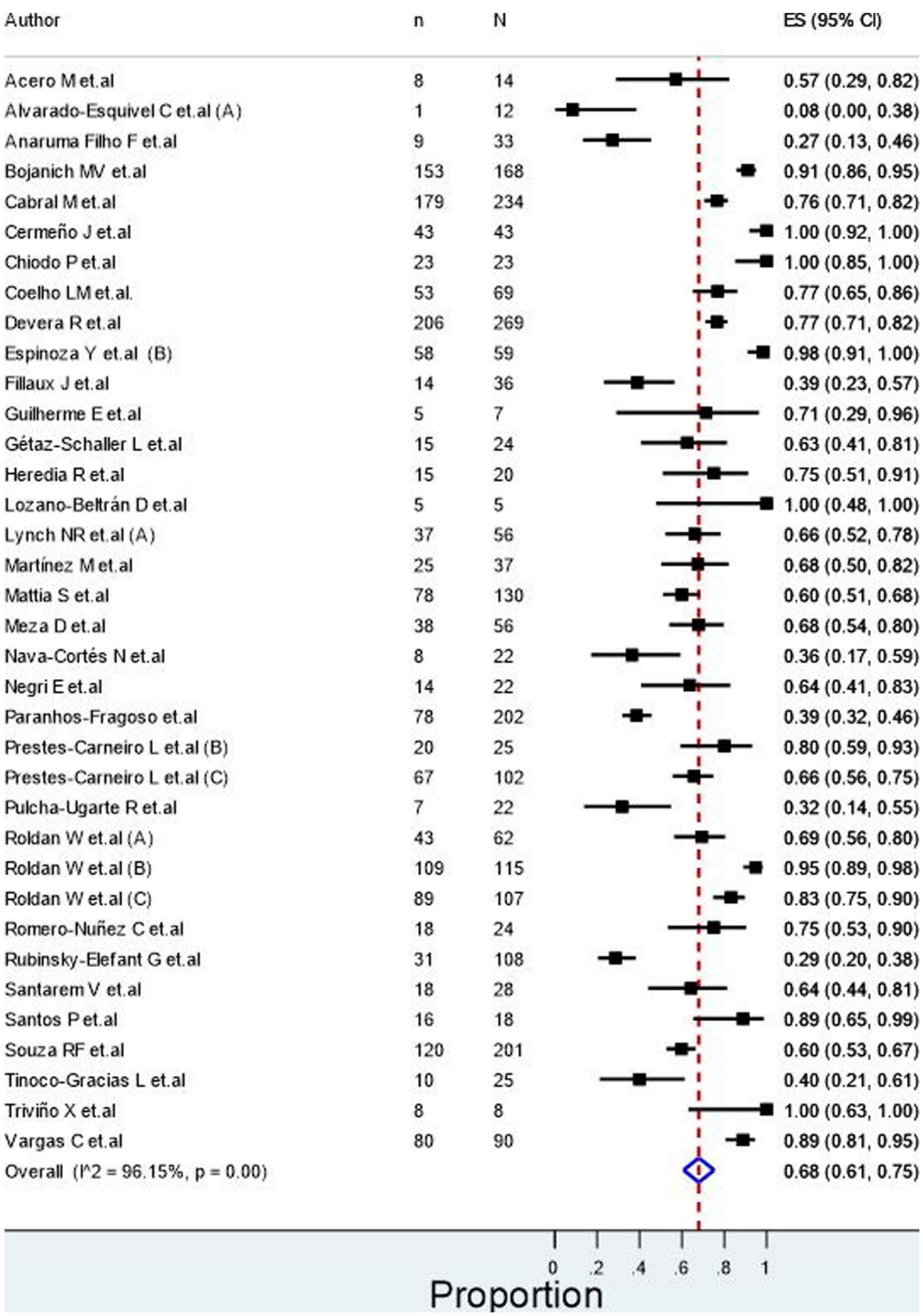

FIGURE 4
Seroprevalence of seropositive participants with dogs in home.

dogs accounted for 39% of the total egg production, followed by feral cats, domestic cats, and foxes (4). However, in some urban areas, egg production may be dominated by feral cats (4). Therefore, some health care systems include mass deworming of dogs and cats as a strategy for disease control. However, attention has been drawn to harmful effects of parasiticides on a wide range of invertebrates, which could be very detrimental to wildlife and ecosystems and could impact public health. Another important strategy could be the use of molecular tests (polymerase chain reaction) for the identification of various types of *Toxocara* eggs in parks and recreational areas for better monitoring and control.

To avoid these problems, one study in the United Kingdom suggest promoting regular health checks and providing information on all approaches to prevent animals from contracting parasites, explaining the symptoms, informing owners regarding the risks associated with infections, and reminding them to always collect and dispose of feces responsibly (4). Likewise, the same study suggested providing an explanation to patients and animal owners regarding the

potential risks of parasiticides to animals, humans, and the environment. Finally, the mentioned study suggests adopting a risk-based approach to prescribing in which parasiticide prescriptions and frequency of administration are tailored to the needs and risk level of the animal (4). These recommendations could also be applied to the countries studied herein.

4.1. Limitations

This study has several limitations that warrant discussion. Firstly, performing many more subgroup analysis (according to comorbidities, sex, age, etc.) would have been ideal in order to explain the high heterogeneity of our study. Secondly, many of the included studies have non-probabilistic sampling and small sample sizes, which could exaggerate the weighting representation in the random-effects method and alter the confidence interval values. Thirdly, future studies are needed to analyze more associated factors or compare different environmental (humidity, altitude, temperature, soil acidity), economic, and sociodemographic variables.

5. Conclusion

The current study found a high seroprevalence of human toxocariasis in Latin America and the Caribbean. Moreover, we observed differences in seroprevalence across Latin American and Caribbean countries probably attributed to sociodemographic and economic variables. Our findings can be used to establish epidemiological surveillance strategies for the prevention and early identification of this pathology. However, more factors associated with human toxocariasis seropositivity need to be analyzed in future studies.

Author contributions

JU-B, AR-T, DC-P, PH-A, and VB-Z: conceptualization and writing review and editing. JU-B, EA-B, EH-B, XC-T, RS-A, and MH-C: data curation. JU-B, EA-B, and VB-Z: formal analysis. JU-B, EA-B, EH-B, and VB-Z: methodology. JU-B, EA-B, EH-B, XC-T, RS-A, MH-C, AR-T, DC-P, PH-A, and VB-Z: writing—original draft. All authors have read and agreed to the published version of the manuscript.

Conflict of interest

The authors declare that the research was conducted in the absence of any commercial or financial relationships that could be construed as a potential conflict of interest.

Publisher's note

All claims expressed in this article are solely those of the authors and do not necessarily represent those of their affiliated organizations, or those of the publisher, the editors and the reviewers. Any product that may be evaluated in this article, or claim that may be made by its manufacturer, is not guaranteed or endorsed by the publisher.

Supplementary material

The Supplementary material for this article can be found online at: https://www.frontiersin.org/articles/10.3389/fpubh.2023.1181230/full#supplementary-material

References

1. Woodhall DM, Fiore AE. Toxocariasis: a review for pediatricians. *J Pediatr Infect Dis Soc*. (2014) 3:154–9. doi: 10.1093/jpids/pit066

2. Maciag L, Morgan ER, Holland C. *Toxocara*: time to let cati 'out of the bag'. *Trends Parasitol*. (2022) 38:280–9. doi: 10.1016/j.pt.2021.12.006

3. Lee AC, Schantz PM, Kazacos KR, Montgomery SP, Bowman DD. Epidemiologic and zoonotic aspects of ascarid infections in dogs and cats. *Trends Parasitol*. (2010) 26:155–61. doi: 10.1016/j.pt.2010.01.002

4. Patterson J. Toxocarosis in humans: how much of a problem is it in the UK? *Drug Ther Bull*. (2023) 61:7–11. doi: 10.1136/dtb.2022.000052

5. Chen J, Liu Q, Liu GH, Zheng WB, Hong SJ, Sugiyama H, et al. Toxocariasis: a silent threat with a progressive public health impact. *Infect Dis Pover*. (2018) 7:59. doi: 10.1186/s40249-018-0437-0

6. Kuenzli E, Neumayr A, Chaney M, Blum J. Toxocariasis-associated cardiac diseases--a systematic review of the literature. *Acta Trop*. (2016) 154:107–20. doi: 10.1016/j.actatropica.2015.11.003

7. Aghaei S, Riahi SM, Rostami A, Mohammadzadeh I, Javanian M, Tohidi E, et al. *Toxocara* spp. infection and risk of childhood asthma: a systematic review and meta-analysis. *Acta Trop*. (2018) 182:298–304. doi: 10.1016/j.actatropica.2018.03.022

8. Mohammadzadeh I, Riahi SM, Saber V, Darvish S, Amrovani M, Arefkhah N, et al. The relationship between Toxocara species seropositivity and allergic skin disorders: a systematic review and meta-analysis. *Trans R Soc Trop Med Hyg*. (2018) 112:529–37. doi: 10.1093/trstmh/try094

9. Quattrocchi G, Nicoletti A, Marin B, Bruno E, Druet-Cabanac M, Preux PM. Toxocariasis and epilepsy: systematic review and meta-analysis. *PLoS Negl Trop Dis*. (2012) 6:e1775. doi: 10.1371/journal.pntd.0001775

10. Ardekani A, Roshanshad A, Hosseini SA, Magnaval JF, Abdollahi A, Rostami A. Toxocariasis-associated urinary system diseases: a systematic review of reported cases. *Trans R Soc Trop Med Hyg*. (2022) 116:668–72. doi: 10.1093/trstmh/trab177

11. Macpherson CN. The epidemiology and public health importance of toxocariasis: a zoonosis of global importance. *Int J Parasitol*. (2013) 43:999–1008. doi: 10.1016/j.ijpara.2013.07.004

12. Rostami A, Ma G, Wang T, Koehler AV, Hofmann A, Chang BCH, et al. Human toxocariasis–a look at a neglected disease through an epidemiological 'prism'. *Infect Genet Evol*. (2019) 74:104002. doi: 10.1016/j.meegid.2019.104002

13. Cardona D, Acosta LD, Bertone CL. Inequities in health among Latin American and Caribbean countries (2005–2010). *Gac Sanit*. (2013) 27:292–7. doi: 10.1016/j.gaceta.2012.12.007

14. Cavalcanti AUA, Boccolini CS. Social inequalities and complementary feeding in Latin America and the Caribbean. *Cien Saude Colet*. (2022) 27:619–30. doi: 10.1590/1413-81232022272.31862020

15. Liberati A, Altman DG, Tetzlaff J, Mulrow C, Gøtzsche PC, Ioannidis JPA, et al. The PRISMA statement for reporting systematic reviews and meta-analyses of studies that evaluate healthcare interventions: explanation and elaboration. *BMJ*. (2009) 339:b2700. doi: 10.1136/bmj.b2700

16. McGowan J, Sampson M, Salzwedel DM, Cogo E, Foerster V, Lefebvre C. PRESS peer review of electronic search strategies: 2015 guideline statement. *J Clin Epidemiol*. (2016) 75:40–6. doi: 10.1016/j.jclinepi.2016.01.021

17. Ouzzani M, Hammady H, Fedorowicz Z, Elmagarmid A. Rayyan–a web and mobile app forsystematic reviews. *Syst Rev*. (2016) 5:210. doi: 10.1186/s13643-016-0384-4

18. Alarcón-Braga EA, Hernandez-Bustamante EA, Salazar-Valdivia FE, Valdez-Cornejo VA, Mosquera-Rojas MD, Ulloque-Badaracco JR, et al. Acceptance towards COVID-19 vaccination in Latin America and the Caribbean: a systematic review and meta-analysis. *Travel Med Infect Dis*. (2022) 49:102369. doi: 10.1016/j.tmaid.2022.102369

19. Barker TH, Migliavaca CB, Stein C, Colpani V, Falavigna M, Aromataris E, et al. Conducting proportional meta-analysis in different types of systematic reviews: a guide for synthesisers of evidence. *BMC Med Res Methodol*. (2021) 21:189. doi: 10.1186/s12874-021-01381-z

20. Hunter JP, Saratzis A, Sutton AJ, Boucher RH, Sayers RD, Bown MJ. In meta-analyses of proportion studies, funnel plots were found to be an inaccurate method of assessing publication bias. *J Clin Epidemiol*. (2014) 67:897–903. doi: 10.1016/j.jclinepi.2014.03.003

21. Ramírez Bustamante CE, Hernández Peña A, Breña Chávez JP, Yoshiyama Sasaki C, Lu L, Alzamora Barrios B, et al. Pacientes con toxocariosis ocular atendidos en el Hospital Nacional Cayetano Heredia, el Hospital Nacional Arzobispo Loayza y el Instituto Nacional de Salud del Niño entre los años 1997 y 2010. *Acta Med Peru*. (2010) 27:250–6.

22. Agudelo C, Villareal E, Cáceres E, López C, Eljach J, Ramírez N, et al. Human and dogs *Toxocara canis* infection in a poor neighborhood in Bogota. *Mem Inst Oswaldo Cruz*. (1990) 85:75–8. doi: 10.1590/S0074-02761990000100012

23. Romero Núñez C, Mendoza Martínez GD, Yañez Arteaga S, Ponce Macotela M, Bustamante Montes P, Ramírez DN. Prevalence and risk factors associated with *Toxocara canis* infection in children. *ScientificWorldJournal*. (2013) 2013:572089. doi: 10.1155/2013/572089

24. Heredia R, Romero C, Mendoza GE, Ponce M, Portal A, González L, et al. Ocurrence of *Toxocara canis* in students of veterinary and graphic design in a Mexican university. *Acta Sci Vet*. (2014) 42:1–6.

25. Bojanich M, López M, Fernández G, Azula L, Alonso J, Por I. *Toxocara canis* en población infantil vulnerable del noreste de Argentina. *Enferm Emerg*. (2008) 10:84–7.

26. Cortés NN, Núñez CR, Guiliana BG, García PA, Cárdenas RH. Presence of anti-*Toxocara canis* antibodies and risk factors in children from the Amecameca and Chalco regions of México. *BMC Pediatr*. (2015) 15:65. doi: 10.1186/s12887-015-0385-9

27. Schoenardie ER, Scaini CJ, Brod CS, Pepe MS, Villela MM, McBride AJ, et al. Seroprevalence of *Toxocara* infection in children from southern Brazil. *J Parasitol*. (2013) 99:537–9. doi: 10.1645/GE-3182

28. Espinoza YA, Huapaya PE, Roldán WH, Jiménez S, Abanto EP, Rojas CA, et al. Seroprevalence of human toxocariasis in Andean communities from the northeast of Lima, Peru. *Rev Inst Med Trop Sao Paulo*. (2010) 52:31–6. doi: 10.1590/S0036-46652010000100005

29. Fillaux J, Santillan G, Magnaval JF, Jensen O, Larrieu E, Sobrino-Becaria CD. Epidemiology of toxocariasis in a steppe environment: the Patagonia study. *Am J Trop Med Hyg*. (2007) 76:1144–7. doi: 10.4269/ajtmh.2007.76.1144

30. Radman NE, Archelli SM, Fonrouge RD, Del Guardis M, Linzitto OR. Human toxocarosis. Its seroprevalence in the City of La Plata. *Mem Inst Oswaldo Cruz*. (2000) 95:281–5. doi: 10.1590/S0074-02762000000300001

31. Espinoza YA, Huapaya PH, Roldán WH, Jiménez S, Arce Z, Lopez E. Clinical and serological evidence of *Toxocara* infection in school children from Morrope district, Lambayeque, Peru. *Rev Inst Med Trop Sao Paulo*. (2008) 50:101–5. doi: 10.1590/S0036-46652008000200007

32. Chiodo P, Basualdo J, Ciarmela L, Pezzani B, Apezteguía M, Minvielle M. Related factors to human toxocariasis in a rural community of Argentina. *Mem Inst Oswaldo Cruz*. (2006) 101:397–400. doi: 10.1590/S0074-02762006000400009

33. Lescano SA, Chieffi PP, Peres BA, de Mello EO, Velarde CN, Salinas AA, et al. Soil contamination and human infection by *Toxocara* sp. in the urban area of Lima, Peru. *Mem Inst Oswaldo Cruz*. (1998) 93:733–4. doi: 10.1590/S0074-02761998000600005

34. Díaz-Suárez O, García ME, Meléndez F, Estévez J. Seroepidemiología de la toxocariasis en una comunidad indígena yucpa de la Sierra de Perijá al occidente de Venezuela. *Kasmera*. (2010) 38:138–46.

35. Baboolal S, Rawlins SC. Seroprevalence of toxocariasis in schoolchildren in Trinidad, in: trans R soc trop med Hyg Trinidad. *Trans Soc Trop Med Hyg*. (2002) 96:139–43. doi: 10.1016/s0035-9203(02)90281-6

36. Archelli S, Santillan GI, Fonrouge R, Céspedes G, Burgos L, Radman N. Toxocariasis: seroprevalence in abandoned-institutionalized children and infants. *Rev Argent Microbiol*. (2014) 46:3–6. doi: 10.1016/S0325-7541(14)70040-9

37. Cadore PS, Zhang L, Lemos L, Lorenzi C, Telmo L, Dos Santos PC, et al. Toxocariasis and childhood asthma: a case-control study. *J Asthma*. (2016) 53:601–6. doi: 10.3109/02770903.2015.1064951

38. Ticono-Gracia L, Barreras-Serrano A, Lopez-Valencia G, Tamayo-Sosa AR, Quiroz-Romero H, Melgarejo T. Seroprevalence of larva migrans of *Toxocara canis* and evaluation of associated risk factors among children in a Mexico-United States border region. *Intern J Appl Res Vet Med*. (2008) 6:130–6.

39. Coelho LM, Silva MV, Dini CY, Giacon Neto AA, Novo NF, Silveira EP. Human toxocariasis: a seroepidemiological survey in schoolchildren of Sorocaba, Brazil. *Mem Inst Oswaldo Cruz*. (2004) 99:553–7.

40. Rubinsky-Elefant G, da Silva-Nunes M, Malafronte RS, Muniz PT, Ferreira MU. Human toxocariasis in rural Brazilian Amazonia: seroprevalence, risk factors, and spatial distribution. *Am J Trop Med Hyg*. (2008) 79:93–8. doi: 10.4269/ajtmh.2008.79.93

41. Alvarado-Esquivel C. Toxocariasis in waste pickers: a case control seroprevalence study. *PLoS One*. (2013) 8:e54897. doi: 10.1371/journal.pone.0054897

42. Fragoso RP, Monteiro MBM, Lemos EM, Pereira FEL. Anti-Toxocara antibodies detected in children attending elementary school in Vitoria, state of Espírito Santo, Brazil: prevalence and associated factors. *Rev Soc Bras Med Trop*. (2011) 44:461–6. doi: 10.1590/S0037-86822011000400012

43. Anaruma Filho F, Chieffi PP, Correa CRS, Camargo ED, Silveira EPRD, Aranha JJB, et al. Human toxocariasis: a seroepidemiological survey in the municipality of Campinas (SP), Brazil. *Rev Inst Med Trop Sao Paulo*. (2002) 44:303–7. doi: 10.1590/S0036-46652002000600002

44. Alonso JM, Lopez MDL, Bojanich MV, Marull J. Infección por *Toxocara canis* en población adulta sana de un área subtropical de Argentina. *Parasitol Latin*. (2004) 59:61–4. doi: 10.4067/S0717-77122004000100012

45. Martínez M, Montero J, Pineda A, Mijares V, Lares M, Catalano E, et al. Epidemiological, clinical and laboratory features of toxocariasis in school children from Aragua state, Venezuela. *Trans R Soc Trop Med Hyg*. (2018) 112:255–63. doi: 10.1093/trstmh/try051

46. Lynch NR, Eddy K, Hodgen AN, Lopez RI, Turner KJ. Seroprevalence of *Toxocara canis* infection in tropical Venezuela. *Trans R Soc Trop Med Hyg*. (1988) 82:275–81. doi: 10.1016/0035-9203(88)90446-4

47. Thompson DE, Bundy DA, Cooper ES, Schantz PM. Epidemiological characteristics of *Toxocara canis* zoonotic infection of children in a Caribbean community. *Bull World Health Organ*. (1986) 64:283–90.

48. Waindok P, Kann S, Aristizabal A, Dib JC, Strube C. *Toxocara* seroprevalence and risk factor analysis in four communities of the Wiwa, an indigenous tribe in Colombia. *Microorganisms*. (2021) 9:1768. doi: 10.3390/microorganisms9081768

49. Vargas C, Torres P, Jercic MI, Lobos M, Oyarce A, Miranda JC, et al. Frequency of anti- *Toxocara* spp. antibodies in individuals attended by the centro de salud familiar and environmental contamination with *Toxocara canis* eggs in dog feces, in the coastal Niebla town, Chile. *Rev Inst Med Trop Sao Paulo*. (2016) 58:62. doi: 10.1590/S1678-9946201658062

50. Hernández SA, Gabrie JA, Rodríguez CA, Matamoros G, Rueda MM, Canales M, et al. An integrated study of *Toxocara* infection in Honduran children: human seroepidemiology and environmental contamination in a coastal community. Trop med. *Infect Dis*. (2020) 5:135. doi: 10.3390/tropicalmed5030135

51. Gétaz Schaller L, Samalvides Cuba F, Breña Chavez J, Torrejon D, Maguiña VC. Relación entre toxocariosis y asma: estudio prospectivo en niños del hospital Nacional Cayetano Heredia. *Acta Med Peru Lima*. (2007) 24:11–20.

52. Lozano Beltran DF, Suarez Barrientos E, Ortuño UE, Cruz Torrico M, Cordova Rojas M, Gisela GJ, et al. Relación entre asma y toxocariasis en pacientes pediátricos en Cochabamba, Bolivia. *Gac Med Boliv*. (2011) 34:76–9.

53. Oliart-Guzmán H, Delfino BM, Martins AC, Mantovani SA, Braña AM, Pereira TM, et al. Epidemiology and control of child toxocariasis in the western Brazilian Amazon - a population-based study. *Am J Trop Med Hyg*. (2014) 90:670–81. doi: 10.4269/ajtmh.13-0506

54. Espinoza Y, Huapaya P, Sevilla C, Huiza A, Jiménez S, Náquira C. *Toxocariosis humana*: seroprevalencia en población de Lima mediante la técnica de ELISA. *An Fac Med*. (2003) 64:228–32. doi: 10.15381/anales.v64i4.1420

55. Cabral Monica T, Evers F, Souza Lima Nino B, Pinto-Ferreira F, Breganó JW, Ragassi Urbano M, et al. Socioeconomic factors associated with infection by toxoplasma gondii and *Toxocara canis* in children. *Transbound Emerg Dis*. (2022) 69:1589–95. doi: 10.1111/tbed.14129

56. Berrocal J. Prevalence of *Toxocara canis* in babies and in adults as determined by the ELISA test. *Trans Am Ophthalmol Soc*. (1980) 78:376–413.

57. Chieffi PP, Ueda M, Camargo ED, de Souza AM, Guedes ML, Gerbi LJ, et al. Visceral larva migrans: a seroepidemiological survey in five municipalities of São Paulo state, Brazil. *Rev Inst Med Trop Sao Paulo*. (1990) 32:204–10. doi: 10.1590/S0036-46651990000300010

58. Virginia P, Nagakura K, Ferreira O, Tateno S. Serologic evidence of toxocariasis in Northeast Brazil. *Jpn J Med Sci Biol*. (1991) 44:1–6. doi: 10.7883/yoken1952.44.1

59. Lynch NR, Hagel I, Vargas V, Rotundo A, Varela MC, Di Prisco MC, et al. Comparable seropositivity for ascariasis and toxocariasis in tropical slum children. *Parasitol Res*. (1993) 79:547–50. doi: 10.1007/BF00932238

60. Cancrini G, Bartoloni A, Zaffaroni E, Guglielmetti P, Gamboa H, Nicoletti A, et al. Seroprevalence of *Toxocara canis*-IgG antibodies in two rural Bolivian communities. *Parassitologia*. (1998) 40:473–5.

61. Minvielle MC, Taus MR, Raffo A, Ciarmela ML, Basualdo JA. Seroprevalence of toxocariasis in blood donors of Gualeguaychú, Argentina. *Trans R Soc Trop Med Hyg*. (2000) 94:373–5. doi: 10.1016/s0035-9203(00)90108-1

62. Taranto NJ, Passamonte L, Marinconz R, de Marzi MC, Cajal SP, Malchiodi EL. Zoonotic parasitosis transmitted by dogs in the Chaco Salteño, Argentina. *Med (B Aires)*. (2000) 60:217–20.

63. Nicoletti A, Bartoloni A, Reggio A, Bartalesi F, Roselli M, Sofia V, et al. Epilepsy, cysticercosis, and toxocariasis: a population-based case-control study in rural Bolivia. *Neurology*. (2002) 58:1256–61. doi: 10.1212/WNL.58.8.1256

64. Campos Júnior D, Elefant GR, Silva EOM, Gandolfi L, Jacob CMA, Tofeti A, et al. Freqüência de soropositividade para antígenos de *Toxocara canis* em crianças de classes sociais diferentes. *Rev Soc Bras Med Trop*. (2003) 36:509–13. doi: 10.1590/S0037-86822003000400013

65. Taranto NJ, Cajal SP, De Marzi MC, Fernández MM, Frank FM, Brú AM, et al. Clinical status and parasitic infection in a Wichí aboriginal community in Salta,

Argentina. *Trans R Soc Trop Med Hyg*. (2003) 97:554–8. doi: 10.1016/s0035-9203(03)80026-3

66. Alderete JMS, Jacob CMA, Pastorino AC, Elefant GR, Castro APM, Fomin ABF, et al. Prevalence of *Toxocara* infection in schoolchildren from the Butantã region, São Paulo. *Brazil Mem Inst Oswaldo Cruz*. (2003) 98:593–7. doi: 10.1590/S0074-02762003000500002

67. García-Pedrique ME, Díaz-Suárez O, Estévez J, Cheng-Ng R, Araujo-Fernández M, Castellano J, et al. Prevalencia de Infección por *Toxocara en* Pre-Escolares de una Comunidad Educativa de el Moján, Estado Zulia, Venezuela: Resultados Preliminares. *Investig Clin*. (2004) 45:347–54.

68. Aguiar-Santos AM, Andrade LD, Medeiros Z, Chieffi PP, Lescano SZ, Perez EP. Human toxocariasis: frequency of anti-*Toxocara* antibodies in children and adolescents from an outpatient clinic for lymphatic filariasis in Recife, Northeast Brazil. *Rev Inst Med Trop Sao Paulo*. (2004) 46:81–5. doi: 10.1590/S0036-46652004000200005

69. Figueiredo SD, Taddei JA, Menezes JJ, Novo NF, Silva EO, Cristóvão HL, et al. Clinical-epidemiological study of toxocariasis in a pediatric population. *J Pediatr*. (2005) 81:126–32. doi: 10.2223/1317

70. Aoki T, de Carvalho LB, Takeuchi T, Yamasaki H, Ito A, Perez EP, et al. Prevalence of toxocariasis in northeastern Brazil based on serology using recombinant *Toxocara canis* antigen. *Am J Trop Med Hyg*. (2005) 72:103–7. doi: 10.4269/ajtmh.2005.72.103

71. Muradian V, Gennari SM, Glickman LT, Pinheiro SR. Epidemiological aspects of visceral larva migrans in children living at São Remo community, São Paulo (SP). *Brazil Vet Parasitol*. (2005) 134:93–7. doi: 10.1016/j.vetpar.2005.05.060

72. Teixeira CR, Chieffi PP, Lescano SA, de Melo Silva EO, Fux B, Cury MC. Frequency and risk factors for toxocariasis in children from a pediatric outpatient center in southeastern Brazil. *Rev Inst Med Trop Sao Paulo*. (2006) 48:251–5. doi: 10.1590/S0036-46652006000500003

73. Ferreira MU, Rubinsky-Elefant G, de Castro TG, Hoffmann EH, da Silva-Nunes M, Cardoso MA, et al. Bottle feeding and exposure to *Toxocara* as risk factors for wheezing illness among under-five Amazonian children: a population-based cross-sectional study. *J Trop Pediatr*. (2007) 53:119–24. doi: 10.1093/tropej/fml083

74. Paludo ML, Falavigna DL, Elefant GR, Gomes ML, Baggio ML, Amadei LB, et al. Frequency of *Toxocara* infection in children attended by the health public service of Maringá, South Brazil. *Rev Inst Med Trop Sao Paulo*. (2007) 49:343–8. doi: 10.1590/S0036-46652007000600002

75. Damian MM, Martins M, Sardinha JF, Souza LO, Chaves A, Tavares AM. Freqüência de anticorpo anti-*Toxocara canis* em comunidade do Rio Uatumã, no Estado do Amazonas. *Rev Soc Bras Med Trop*. (2007) 40:661–4. doi: 10.1590/S0037-86822007000600013

76. Prestes-Carneiro LE, Santarém V, Zago SC, Miguel NA, Zambelli F, Villas R, et al. Sero-epidemiology of toxocariasis in a rural settlement in São Paulo state. *Brazil Ann Trop Med Parasitol*. (2008) 102:347–56. doi: 10.1179/136485908x278801

77. Roldán WH, Espinoza YA, Atúncar A, Ortega E, Martinez A, Saravia M. Frequency of eosinophilia and risk factors and their association with *Toxocara* infection in schoolchildren during a health survey in the north of Lima, Peru. *Rev Inst Med Trop Sao Paulo*. (2008) 50:273–8. doi: 10.1590/S0036-46652008000500005

78. Prestes-Carneiro LE, Souza DH, Moreno GC, Troiani C, Santarém V, Zago SC, et al. Toxocariasis/cysticercosis seroprevalence in a long-term rural settlement, São Paulo. *Brazil Parasitology*. (2009) 136:681–9. doi: 10.1017/S0031182009005769

79. Roldán WH, Espinoza YA, Huapaya PE, Huiza AF, Sevilla CR, Jiménez S. Frequency of human toxocariasis in a rural population from Cajamarca, Peru determined by DOT-ELISA test. *Rev Inst Med Trop Sao Paulo*. (2009) 51:67–71. doi: 10.1590/S0036-46652009000200002

80. Correa CRS, Bismarck CM. Toxocariasis: incidence, prevalence and the time serum remains positive in school children from Campinas, SP. *Brazil J Trop Pediatr*. (2010) 56:215–6. doi: 10.1093/tropej/fmp095

81. Colli CM, Rubinsky-Elefant G, Paludo ML, Falavigna DL, Guilherme EV, Mattia S, et al. Serological, clinical and epidemiological evaluation of toxocariasis in urban areas of South Brazil. *Rev Inst Med Trop Sao Paulo*. (2010) 52:69–74. doi: 10.1590/S0036-46652010000200002

82. Roldán WH, Cavero YA, Espinoza YA, Jiménez S, Gutiérrez CA. Human toxocariasis: a seroepidemiological survey in the Amazonian city of Yurimaguas, Peru. *Rev Inst Med Trop Sao Paulo*. (2010) 52:37–42. doi: 10.1590/S0036-46652010000100006

83. Santarém VA, Leli FN, Rubinsky-Elefant G, Giuffrida R. Protective and risk factors for toxocariasis in children from two different social classes of Brazil. *Rev Inst Med Trop Sao Paulo*. (2011) 53:66–72. doi: 10.1590/S0036-46652011000200002

84. Souza RF, Dattoli VC, Mendonça LR, Jesus JR, Baqueiro T, Santana C, et al. Prevalence and risk factors of human infection by *Toxocara canis* in Salvador, state of Bahia. *Brazil Rev Soc Bras Med Trop*. (2011) 44:516–9. doi: 10.1590/S0037-86822011000400024

85. Dattoli VC, Freire SM, Mendonça LR, Santos PC, Meyer R, Alcantara-Neves NM. *Toxocara canis* infection is associated with eosinophilia and total IgE in blood donors from a large Brazilian Centre. *Tropical Med Int Health*. (2011) 16:514–7. doi: 10.1111/j.1365-3156.2010.02719.x

86. Mattia S, Colli CM, Adami CM, Guilherme GF, Nishi L, Rubinsky-Elefant G, et al. Seroprevalence of *Toxocara* infection in children and environmental contamination of urban areas in Paraná state. *Brazil J Helminthol*. (2012) 86:440–5. doi: 10.1017/S0022149X11000666

87. Manini MP, Marchioro AA, Colli CM, Nishi L, Falavigna-Guilherme AL. Association between contamination of public squares and seropositivity for *Toxocara* spp. in children. *Vet Parasitol*. (2012) 188:48–52. doi: 10.1016/j.vetpar.2012.03.011

88. Mendonça LR, Veiga RV, Dattoli VC, Figueiredo CA, Fiaccone R, Santos J, et al. *Toxocara* seropositivity, atopy and wheezing in children living in poor neighbourhoods in urban Latin American. *PLoS Negl Trop Dis*. (2012) 6:e1886. doi: 10.1371/journal.pntd.0001886

89. Guilherme EV, Marchioro AA, Araujo SM, Falavigna DL, Adami C, Falavigna-Guilherme G, et al. Toxocariasis in children attending a public health service pneumology unit in Paraná state, Brazil. *Rev Inst Med Trop S Paulo*. (2013) 55:189. doi: 10.1590/S0036-46652013000300009

90. Negri EC, Santarém VA, Rubinsky-Elefant G, Giuffrida R. Anti-*Toxocara* spp. antibodies in an adult healthy population: serosurvey and risk factors in Southeast Brazil. *Asian Pac J Trop Biomed*. (2013) 3:211–6. doi: 10.1016/s2221-1691(13)60052-0

91. Prestes-Carneiro LE, Rubinsky-Elefant G, Ferreira AW, Araujo PR, Troiani C, Zago SC, et al. Seroprevalence of toxoplasmosis, toxocariasis and cysticercosis in a rural settlement, São Paulo state, Brazil. *Ann Trop Med Parasitol*. (2013) 107:88–95. doi: 10.1179/2047773213Y.0000000079

92. Martiń UO, Giraldez E, Demonte MA, Mendicino D, Contini L, Barco M. Toxocariosis in different vulnerable groups of children in Argentina. *Salud(i) Ciencia*. (2014) 20:592–7.

93. Marchioro AA, Colli CM, Ferreira ÉC, Viol BM, Araújo SM, Falavigna-Guilherme AL. Risk factors associated with toxoplasmosis and toxocariasis in populations of children from nine cities in southern Brazil. *J Helminthol*. (2015) 89:428–32. doi: 10.1017/S0022149X14000212

94. Araujo Z, Brandes S, Pinelli E, Bochichio MA, Palacios A, Wide A, et al. Seropositivity for ascariosis and toxocariosis and cytokine expression among the indigenous people in the Venezuelan Delta region. *Rev Inst Med Trop Sao Paulo*. (2015) 57:47–55. doi: 10.1590/S0036-46652015000100007

95. Santos PC, Lehmann LM, Lorenzi C, Hirsch C, Telmo PL, Mattos GT, et al. The seropositivity of *Toxocara* spp. antibodies in pregnant women Attented at the University Hospital in Southern Brazil and the factors associated with infection. *PLoS One*. (2015) 10:e0131058. doi: 10.1371/journal.pone.0131058

96. Cermeño J, Houda S, Salvador N, Salaverria C. Seroprevalencia y factores de riesgos asociados con la infección por *Toxocara canis* en la población de la laguna, estado Anzoátegui, Venezuela. *Saber*. (2016) 28:62–72.

97. Pereira LC, Elefant GR, Nóbrega YM, Vital T, Nitz N, Gandolfi L, et al. *Toxocara* spp. seroprevalence in pregnant women in Brasília. *Brazil. Rev Soc Bras Med Trop*. (2016) 49:641–3. doi: 10.1590/0037-8682-0106-2016

98. Sariego I, Kanobana K, Junco R, Vereecken K, Núñez FA, Polman K, et al. Frequency of antibodies to *Toxocara* in Cuban schoolchildren. *Tropical Med Int Health*. (2012) 17:711–4. doi: 10.1111/j.1365-3156.2012.02996.x

99. Alvarado-Esquivel C. Seroepidemiology of toxocariasis in a rural Tepehuanos population from Durango. *Mexico J Helminthol*. (2014) 88:173–6. doi: 10.1017/S0022149X12000880

100. Muñoz-Guzmán MA, del Río-Navarro BE, Valdivia-Anda G, Alba-Hurtado F. The increase in seroprevalence to *Toxocara canis* in asthmatic children is related to cross-reaction with ascaris suum antigens. *Allergol Immunopathol (Madr)*. (2010) 38:115–21. doi: 10.1016/j.aller.2009.09.007

101. Kanobana K, Vereecken K, Junco Diaz R, Sariego I, Rojas L, Bonet Gorbea M, et al. Toxocara seropositivity, atopy and asthma: a study in Cuban schoolchildren. *Tropical Med Int Health*. (2013) 18:403–6. doi: 10.1111/tmi.12073

102. Alvarado-Esquivel C, Hernández-Tinoco J, Sánchez-Anguiano LF. *Toxocara* infection in gardeners: a case control seroprevalence study. *Asian Pac J Trop Med*. (2014) 7S1:S79–81. doi: 10.1016/S1995-7645(14)60207-8

103. Ortega-Pacheco A, Torres-Acosta JFJ, Alzina-López A, Gutiérrez-Blanco E, Bolio-González ME, Aguilar-Caballero AJ, et al. Parasitic zoonoses in humans and their dogs from a rural Community of Tropical Mexico. *J Trop Med*. (2015) 2015:481086. doi: 10.1155/2015/481086

104. Cook J, Hardie R, Bailey K, Tapper M, Vickers I, Calder D, et al. Seroprevalence of human toxocariasis, Jamaica. *Trop Biomed*. (2016) 33:88–94.

105. Guo F, Forde MS, Werre SR, Krecek RC, Zhu G. Seroprevalence of five parasitic pathogens in pregnant women in ten Caribbean countries. *Parasitol Res*. (2017) 116:347–58. doi: 10.1007/s00436-016-5297-6

106. Oviedo-Vera AY, Chis Ster I, Chico ME, Silva MB, Salazar-Garcés LF, Alcantara-Neves NM, et al. A prospective seroepidemiological study of toxocariasis during early childhood in coastal Ecuador: potential for congenital transmission and risk factors for infection. *Parasit Vectors*. (2021) 14:95. doi: 10.1186/s13071-020-04575-4

107. Orlando-Indacochea NF, Osejos-Merino MA, Jaramillo-Véliz JJ, Saltos-Bury MA, Alcívar-Cobeña JL. Prevalencia de *Toxocara canis* y su incidencia zoonótica ambiental en niños de la ciudad de Jipijapa. *P Del C*. (2018) 3:29–57. doi: 10.23857/pc.v3i8.591

108. Pulcha-Ugarte R, Figueroa-Vásquez V, Lazo-Porras M, Maguiña-Vargas C. *Toxocara canis* infection in children from a public school in Iquitos, Peru. *Rev Peru Med Exp Salud Publica*. (2021) 38:363–4. doi: 10.17843/rpmesp.2021.382.7580

109. Rivarola CME, Vuyk AIN, Riveros MM, Canese A, Micó VGA. *Toxocara canis* en Población Pediátrica Rural. *Pediatría*. (2018) 36:122–6.

110. Montalvo AM, Espino AM, Escalante G, Finlay CM. Study of the seroprevalence of toxocariasis in an infantile population in the City of Havana. *Rev Cuba Med Trop*. (1994) 46:156–8.

111. Mendoza Meza DL, Lozano Socarras S, Jaimes MB. Exposición al parásito *Toxocara canis* en una población escolar de la comuna 7 del Distrito de Santa Marta, Colombia. *Duazary*. (2010) 7:183–90.

112. Acero M, Muñoz MM, Flórez AC, Nicholls RS. Seroprevalencia de anticuerpos contra *Toxocara canis* y factores de riesgo en niños, Ciudad Bolívar, Bogotá, D.C., 2000. *Biomédica*. (2001) 21:256–63. doi: 10.7705/biomedica.v21i3.1116

113. Romero Bernal RI, Muñoz O. Factores epidemiológicos relacionados con la seropositividad anti *Toxocara canis* en niños de pamplona N.S., 2015. C.E.S. *Salud Publ*. (2019) 8:3–12.

114. Devera R, Blanco Y, Amaya I, Requena I, Tutaya R, González A, et al. Infección por *Toxocara canis*: seroepidemiología. *Saber*. (2015) 27:537–46.

115. Archelli SM, Kozubsky LE, Gamboa MI, Osen BA, Costas ME, López MA, et al. *Toxocara canis* en humanos, perros y suelos en ribera del Río de la Plata, provincia de Buenos Aires. *Acta Bioquim Clin Latinoam*. (2018) 52:441–9.

116. Morocoima A, Herrera L, Ruiz E, Córdova M, Ferrer E. Manifestaciones oculares de la toxocariasis en escolares del estado Anzoátegui en Venezuela. *Rev Peru Med Exp Salud Publica*. (2021) 38:621–6. doi: 10.17843/rpmesp.2021.384.9322

117. Triviño X, Bedregal P, Torres M, Canales M, Alvarado C, Hernandez R. Toxocarosis en Chile: serie clínica en un centro de pediatría ambulatoria. *Parasitol Día*. (1999) 23:113–7. doi: 10.4067/S0716-07201999000300008

118. De Abreu A, Delgado R, Díaz D, Garrido N, López Y, Medina Z, et al. Seroprevalencia contra *Toxocara canis* en niños de 1 a 6 años con y sin síntomas respiratorios de Barquisimeto, Venezuela. *Arch Venez Pueric Pediatr*. (2011) 74:100–4.

119. Miranda CE. Alta frecuencia de serología positiva contra toxocara en un Hospital Pediátrico del Perú. *An Fac Med.* (2014) 75:223–6. doi: 10.15381/anales.v75i3.9774

120. Martín UO, Machuca PB, Demonte MA, Contini L. Estudio en niños con diagnóstico presuntivo de toxocariasis en Santa Fe, Argentina. *Med (B Aires)*. (2008) 68:353–7.

121. López DLA, Bojanich MV, Jacobacci JM, Sercic C, Michelini A, Alonso JM. Toxocara canis and bronchial asthma. *Med (B Aires)*. (2010) 70:75–8.

122. Rostami A, Riahi SM, Holland CV, Taghipour A, Khalili-Fomeshi M, Fakhri Y, et al. Seroprevalence estimates for toxocariasis in people worldwide: a systematic review and meta-analysis. *PLoS Negl Trop Dis*. (2019) 13:e0007809. doi: 10.1371/journal.pntd.0007809

123. Lee RM, Moore LB, Bottazzi ME, Hotez PJ. Toxocariasis in North America: a systematic review. *PLoS Negl Trop Dis*. (2014) 8:e3116. doi: 10.1371/journal.pntd.0003116

124. Lötsch F, Vingerling R, Spijker R, Grobusch MP. Toxocariasis in humans in Africa - a systematic review. *Travel Med Infect Dis*. (2017) 20:15–25. doi: 10.1016/j.tmaid.2017.10.009

125. Strube C, Raulf MK, Springer A, Waindok P, Auer H. Seroprevalence of human toxocarosis in Europe: a review and meta-analysis. *Adv Parasitol*. (2020) 109:375–418. doi: 10.1016/bs.apar.2020.01.014

126. Chammartin F, Scholte RG, Guimarães LH, Tanner M, Utzinger J, Vounatsou P. Soil-transmitted helminth infection in South America: a systematic review and geostatistical meta-analysis. *Lancet Infect Dis*. (2013) 13:507–18. doi: 10.1016/S1473-3099(13)70071-9

127. Fan CK, Holland CV, Loxton K, Barghouth U. Cerebral toxocariasis: silent progression to neurodegenerative disorders? *Clin Microbiol Rev*. (2015) 28:663–6. doi: 10.1128/CMR.00106-14

128. Cruz-Cruz C, López-Hernández D, Hernández-Shilón JA, Luna-Cazáres LM, Vidal JE, Gutiérrez-Jiménez J. Stunting and intestinal parasites in school children from high marginalized localities at the Mexican southeast. *J Infect Dev Ctries*. (2018) 12:1026–33. doi: 10.3855/jidc.10481

129. Peréz Cordón G, Cordova Paz Soldan O, Vargas Vásquez F, Velasco Soto JR, Sempere Bordes L, Sánchez Moreno M, et al. Prevalence of enteroparasites and genotyping of *Giardia lamblia* in Peruvian children. *Parasitol Res*. (2008) 103:459–65. doi: 10.1007/s00436-008-1007-3

130. Celestino AO, Vieira SCF, Lima PAS, Rodrigues LMCL, Lopes IRS, França CM, et al. Prevalence of intestinal parasitic infections in Brazil: a systematic review. *Rev Soc Bras Med Trop*. (2021) 54:e00332021. doi: 10.1590/0037-8682-0033-2021

131. Abedi B, Akbari M, KhodaShenas S, Tabibzadeh A, Abedi A, Ghasemikhah R, et al. The global prevalence of *Toxocara* spp. in pediatrics: a systematic review and meta-analysis. *Clin Exp Pediatr*. (2021) 64:575–81. doi: 10.3345/cep.2020.01039

132. Merigueti YFFB, Giuffrida R, da Silva RC, Kmetiuk LB, Santos APD, Biondo AW, et al. Dog and cat contact as risk factor for human toxocariasis: systematic review and meta-analysis. *Front Public Health*. (2022) 10:854468. doi: 10.3389/fpubh.2022.854468

frontiers | Frontiers in Microbiology

TYPE Original Research
PUBLISHED 03 July 2023
DOI 10.3389/fmicb.2023.1206187

Check for updates

OPEN ACCESS

EDITED BY
Lei Deng,
Harvard Medical School, United States

REVIEWED BY
Michael John Calcutt,
University of Missouri, United States
Yuwei Gao,
Chinese Academy of Agricultural Sciences (CAAS), China
Hualei Wang,
Jilin University, China

*CORRESPONDENCE
Tingmei He
✉ 248109505@qq.com
Guangneng Peng
✉ pgn.sicau@163.com

†These authors have contributed equally to this work

RECEIVED 15 April 2023
ACCEPTED 15 June 2023
PUBLISHED 03 July 2023

CITATION
Meng W, Chen S, Huang L, Yang J, Zhang W, Zhong Z, Zhou Z, Liu H, Fu H, He T and Peng G (2023) Isolation, characterization, and pathogenicity assessment of *Corynebacterium pseudotuberculosis* biovar equi strains from alpacas (*Vicugna pacos*) in China. *Front. Microbiol.* 14:1206187. doi: 10.3389/fmicb.2023.1206187

COPYRIGHT
© 2023 Meng, Chen, Huang, Yang, Zhang, Zhong, Zhou, Liu, Fu, He and Peng. This is an open-access article distributed under the terms of the Creative Commons Attribution License (CC BY). The use, distribution or reproduction in other forums is permitted, provided the original author(s) and the copyright owner(s) are credited and that the original publication in this journal is cited, in accordance with accepted academic practice. No use, distribution or reproduction is permitted which does not comply with these terms.

Isolation, characterization, and pathogenicity assessment of *Corynebacterium pseudotuberculosis* biovar equi strains from alpacas (*Vicugna pacos*) in China

Wanyu Meng[1†], Shanyu Chen[1†], Lin Huang[1†], Jinpeng Yang[1†], Wenqing Zhang[1], Zhijun Zhong[1], Ziyao Zhou[1], Haifeng Liu[1], Hualin Fu[1], Tingmei He[2]* and Guangneng Peng[1]*

[1]The Key Laboratory of Animal Disease and Human Health of Sichuan Province, College of Veterinary Medicine, Sichuan Agricultural University, Chengdu, Sichuan, China, [2]Sichuan Wolong National Natural Reserve Administration, Wenchuan, Sichuan, China

Corynebacterium pseudotuberculosis is a zoonotic pathogen that causes lymphadenitis in humans, livestock, and wildlife. In this study, *C. pseudotuberculosis* biovar equi strains were isolated from three alpacas. Antibiotic susceptibility tests and pathogenicity tests were also conducted. Moreover, one strain was sequenced using DNBSEQ and Oxford Nanopore technology. The three strains exhibited resistance to aztreonam, fosfomycin, and nitrofurantoin. The median lethal doses (LD_{50}) of strains G1, S2 and BA3 in experimentally infected mice was 1.66×10^5 CFU, 3.78×10^5 CFU and 3.78×10^5 CFU, respectively. The sequencing of strain G1 resulted in the assembly of a chromosomal scaffold comprising 2,379,166 bp with a G+C content of 52.06%. Genome analysis of strain G1 revealed the presence of 48 virulence genes and 5 antibiotic resistance genes (ARGs). Comparative genomic analysis demonstrates a high degree of genetic similarity among *C. pseudotuberculosis* strains, in contrast to other *Corynebacterium* species, with a clear delineation between strains belonging to the two biovars (ovis and equi). The data of the present study contribute to a better understanding of the properties of *C. pseudotuberculosis* biovar equi strains and the potential risk they pose to alpacas and other livestock, as well as the necessity of ongoing surveillance and monitoring of infectious diseases in animals.

KEYWORDS

alpaca, *Corynebacterium pseudotuberculosis*, biovar equi, virulence, antibiotic resistance, pathogenicity, genomic sequencing

1. Introduction

Corynebacterium pseudotuberculosis is a facultative intracellular pathogen, which belongs to the *Corynebacterium*, *Mycobacterium*, *Nocardia*, and *Rhodococcus* (CMNR) group of the *Actinomycetota* (Mills et al., 1997; Dorella et al., 2006). It is a non-motile, non-capsulated, and non-sporulating Gram-positive bacterium, with fimbriae (Hard, 1969). This zoonotic pathogen

is the main cause of caseous lymphadenitis (CLA) and can infect humans (Peel et al., 1997), livestock (Oliveira et al., 2014), and wildlife (Oliveira et al., 2016) worldwide through respiratory, digestive and wound transmission. *C. pseudotuberculosis* causes (Kinne, 2016) serious economic losses, including reduced reproductive efficiency and losses in wool, meat, and milk production, as well as increased expenses for the drugs and labor required for treatment (de Sá Guimarães et al., 2011). It is classified by host preference and nitrate reduction into two biovars: ovis (serotype I, nitrate-negative) causes lymphadenitis in small ruminants, mainly sheep and goats; equi (serotype II, nitrate-positive) results in ulcerative lymphangitis in equines (Bernardes et al., 2021) and oedematous skin disease (OSD) in buffaloes (Barakat et al., 1984; Moussa et al., 2016). However, *C. pseudotuberculosis* exhibits phenotypic intra-species variation, with certain strains isolated from sheep exhibiting nitrate reduction capability, and some equine isolates displaying nitrate negativity (Costa et al., 1998; Connor et al., 2000; Retamal et al., 2011). Considering the potential discrepancies due to mutations, genotypic tests have proven to be a more reliable and sensitive diagnostic tool compared to phenotypic tests (Asfour and Darwish, 2014; Almeida et al., 2017) The *narG* (nitrate reductase gene) gene was also included in PCR assays along with the 16S rRNA, *pld* (Phospholipase D) and *rpoB* (RNA polymerase beta subunit region) genes to improve the accuracy of multiplex PCR at the biovar level (Almeida et al., 2017).

CLA is one of the most serious infectious diseases in alpacas and has been reported in Germany (Sting et al., 2022), USA (Anderson et al., 2004), and Peru (Braga et al., 2006). In China, case of *C. pseudotuberculosis* infection have been documented in sheep (Liu, 2021), goats (Wang R. et al., 2021), Bactrian camels (Liu et al., 1986; Guo et al., 1988), buffaloes (Zhang et al., 1989), chickens (He et al., 1991), deer (Zhu and Lei, 2001), and humans (Du, 1997). Among these, the strains isolated from goats were identified as biovar ovis through phenotypic and genotypic tests, while strains isolated from other hosts were characterized only phenotypically, without fully determining their biovars. Strains isolated from chickens and deer were nitrate-negative, whereas strains isolated from humans were nitrate-positive. Both nitrate-positive and nitrate-negative strains have been reported in Bactrian camels. However, to the best of our knowledge, there have been no documented cases of CLA in alpacas in China.

The pathogenic mechanism of *C. pseudotuberculosis* is closely associated with its virulence factors, including several virulence genes, such as *pld*, iron uptake and regulation (*fagA*, *fagB*, *fagC*, *fagD*), mycolic acid, σ factor, and oligopeptide permease (*oppA*, *oppB*, *oppC*, *oppD*, *oppF*) (Billington et al., 2002). PLD is a highly potent exotoxin secreted by *C. pseudotuberculosis*, known for its necrotic and hemolytic activities (Sutherland et al., 1989). It is widely regarded as the most critical virulence factor produced by the bacterium, and the *pld* gene has been found to be widely detected in all *C. pseudotuberculosis* strains isolated from mammals (Songer, 1997; Aquino De Sá et al., 2013). Selective extracytoplasmic function (ECF) sigma factor family proteins, such as *sigE*, mainly regulate cell surface stress and control the expression of virulence-associated genes in various pathogenic bacteria (Kazmierczak et al., 2005). The Opp transporters are not only essential for nutrient accumulation but also contribute to the regulation of diverse intercellular signaling processes. One notable aspect of their regulatory function is the control they exert over the expression of virulence genes in pathogenic bacteria (Samen et al., 2004).

With the continuous advancement of sequencing technology, the number of available whole genome sequences for *C. pseudotuberculosis* has been growing. At present, a total of 125 *C. pseudotuberculosis* strains from 19 countries and regions have been fully sequenced (as of April 1, 2023). This abundance of genomic data provides a valuable resource for conducting comprehensive comparative genomics studies. Of these, only one isolate was yielded from camel (biovar ovis) and one isolate from llama (biovar equi), while the majority of *C. pseudotuberculosis* isolates were from goats (28%), sheep (24%), and horses (22%). Notably, the whole genome sequencing of *C. pseudotuberculosis* strain isolated from alpacas has not yet been reported (Data source: https://www.ncbi.nlm.nih.gov/genome/. The whole genome sequencing statistics of *C. pseudotuberculosis* are presented in Supplementary Table S1 and Supplementary Figure S1). All strains that infect sheep and goats are biovar ovis (strain PA02 was mistakenly labeled as biovar equi and is actually lacking the *narG* gene, as shown in Supplementary Figure S2). In contrast, all strains that infect horses and buffalo are biovar equi, while strains that infect cattle include both biovars ovis and equi. Seven *C. pseudotuberculosis* biovar equi strains that were isolated from equine were subjected to pan-genomic analysis, which revealed one of the smallest core genomes ever recorded and considerable genetic variability. There were no discernible genetic distinctions among the strains responsible for the three distinct types of infection, including those causing external abscesses, infections with abscess formation in the internal organs, and ulcerative lymphangitis (Barauna et al., 2017). The clustered regularly interspaced short palindromic repeats (CRISPR)-Cas (CRISPR-associated proteins) cluster is only seen in the biovar equi strains, while the methylation type III cluster is only found in biovar ovis strains (Parise et al., 2018).

The main objective of this study was to identify the causative bacteria responsible for the disease in three alpacas and investigate their biological characteristics, with a focus on pathogenicity assessed through mouse infection tests. Furthermore, it entailed the whole genome sequencing of the *C. pseudotuberculosis* biovar equi strain isolated from an alpaca, and this genome was compared to other *C. pseudotuberculosis* strains of both biovars ovis and equi.

2. Materials and methods

2.1. Sample collection

In November 2021, two diseased alpacas (G1 and S2) and a dead alpaca (BA3) from a local alpaca farm were brought to the Animal Hospital of Sichuan Agricultural University (Chengdu, Sichuan, China) for consultation. Tests for *Brucella* antibodies were negative for alpacas G1 and S2. Despite receiving careful medical attention, alpaca G1's condition deteriorated, and it died on the third day of treatment. Necropsies were performed on the dead alpacas, and extremity pus from one diseased alpaca (S2) and liver abscesses from two dead alpacas (G1 and BA3) were aseptically collected.

2.2. Bacteriological examination

Samples were subjected to routine bacteriological examination using Luria-Bertani (LB) broth (Hopebio, Qingdao, China), including

cultivation under both aerobic and anaerobic conditions. Three mono-colony isolates from one sick alpaca and two dead alpacas were marked as S2, G1, and BA3, respectively. The hemolytic ability of the strains was determined by inoculating them onto blood agar plates (Solarbio, Beijing, China) containing 5% sheep blood. Morphological and biochemical properties of the bacteria were characterized through gram staining and standard biochemical tests, according to the manufacturer's instructions (Hopebio). The resulting isolates were stored at −80°C in 25% glycerol for subsequent experiments.

2.3. Molecular identification

The genomic DNA from the isolates was extracted using the Bacterial DNA Kit (Tiangen, Beijing, China) and stored at −80°C. For bacterial species identification, the partial 16S rRNA gene was amplified using the primers 27-F (5'-GATGGTCATAGGGATGAAG AGCTT-3′) and 1492-R (5'-AGGGATGAAGAGCTTCGGCTCTG-3′) (Fredriksson et al., 2013). Additionally, the *narG* gene was amplified using the primers F (5′-ACCCGTACTTGCACTCTTTC-3′) and R (5′-AGTCAGTACTTCCGCAGGTC′) (Almeida et al., 2017). Each PCR reaction (25 μL) contained 12.5 μL 2× *Pro Taq* Master Mix (Accurate Biology, Hunan, China), 8.5 μL RNase-free H_2O (Sangon Biotech, Shanghai, China), 1 μL forward and reverse primers (Sangon Biotech), and 2 μL template DNA. In the PCR test for amplifying the partial 16S rRNA gene, RNase-free water was used instead of template DNA as a negative control. For other PCR tests, *Staphylococcus aureus* ATCC 25923 was used as a negative control strain. The reaction conditions included predenaturation at 94°C for 5 min, followed by 35 cycles of 94°C for 1 min, annealing temperature for 50 s, and 72°C for 1 min, with a final extension at 72°C for 10 min. The PCR products were validated by 1% agarose gel electrophoresis with TS-GelRed (Tsingke Biotechnology, Beijing, China) and sent to Tsingke Biotechnology Co., Ltd. for Sanger sequencing. A homology search was performed in the GenBank database using the BLAST tool,[1] and Clustal X2.0[2] for sequence alignment.

2.4. Antibiotic susceptibility testing

The Kirby-Bauer disk diffusion method (Oxoid, Basingstoke, UK) was utilized to test the antimicrobial susceptibility of the isolates. Representative drugs from 12 major classes of antibiotics, including β-lactams, carbapenems, polyphosphates, glycopeptides, aminoglycosides, tetracyclines, macrolides, amide alcohols, quinolones, sulfonamides, nitrofurans, and rifampicin, were selected. The bacterial solution cultured to 0.5 McFarland turbidity was evenly spread on Muller-Hinton (MH) solid medium (Hopebio) using a spreader stick. Disks were then placed on the medium and the culture was incubated at 37°C for 24–48 h. *S. aureus* ATCC 25923 was employed as the quality control strain in our study. The zone diameters for each drug were interpreted based on the Clinical and Laboratory Standards Institute (CLSI, 2019) and recorded as sensitive (S), intermediate (I), or resistant (R).

2.5. Pathogenicity test

The animal study was reviewed and approved by the Sichuan Agricultural University Animal Ethical and Welfare Committee. Female Specific Pathogen Free (SPF) Kunming mice were obtained from Chengdu Dossy Experimental Animals CO., LTD. (Chengdu, China). The mice were housed in clean cages at 23 ± 2°C and a relative humidity of 50 ± 10%. The mice were 6 weeks old at the start of the study.

Preliminary experiments were conducted to determine the infection range of three *C. pseudotuberculosis* strains (6×10^4 to 10^7 CFU/mL) (CFU: Colony Forming Unit). Healthy mice ($n = 78$) were randomly divided into 13 groups of 6 mice each. Groups 1–4, 5–8, and 9–12 were intraperitoneally injected with 0.2 mL of G1, S2, and BA3 bacterial solutions (with normal saline and diluted to 6×10^4 to 10^7 CFU/mL), respectively. Group 13 served as the control group and received 0.2 mL of saline intraperitoneally.

Clinical signs and mortality were recorded every 2 h within 12 h post-injection and every day for 7 consecutive days. The median lethal dose (LD_{50}) was calculated. Histopathological analysis was performed on the initial three mice that died following infection with strains G1, S2, and BA3, respectively. The liver, heart, spleen, lung, kidney, and intestines of dead mice were fixed in 10% formaldehyde for histopathological examination. On day 14, the organs of the remaining mice were collected and weighed to compare changes in organ index after infection with different concentrations of bacterial solutions.

2.6. Whole genome sequencing

2.6.1. Genome sequencing and assembly

The genome of a *C. pseudotuberculosis* strain was sequenced using a combination of the DNBSEQ platform (BGI, Shenzhen, China) and the Oxford Nanopore technology (ONT, Oxford, UK) at the Beijing Genomics Institute. The program Canu was utilized for self-correction. Draft genomic unitigs were assembled using Canu, a high-quality assembler that employs a corrected circular consensus sequence subread set. To improve the accuracy of the genome sequences, GATK[3] was used to make single-base corrections.

2.6.2. Gene prediction and annotation

The functional annotation of the *C. pseudotuberculosis* strain genome for open reading frame (ORF) prediction was performed using glimmer3[4] with Hidden Markov models. tRNA, rRNA and sRNA recognition made use of tRNAscan-SE,[5] RNAmmer, and the Rfam database. The tandem repeat annotation was obtained using the Tandem Repeat Finder,[6] and the minisatellite DNA and microsatellite DNA were selected based on the number and length of repeat units.

1 http://www.ncbi.nlm.nih.gov/BLAST
2 http://www.clustal.org/
3 https://www.broadinstitute.org/gatk/
4 http://www.cbcb.umd.edu/software/glimmer/
5 http://gtrnadb.ucsc.edu/
6 http://tandem.bu.edu/trf/trf.html

The Genomic Island Suite of Tools (GIST) was used for genomic island analysis[7] with IslandPath DIOMB, SIGI-HMM, IslandPicker method. Prophage regions were predicted using the PHAge Search Tool (PHAST) web server[8] and CRISPR-Cas identification using the CRISPRCasFinder.[9]

The best hit was extracted using the BLAST alignment tool for function annotation. Virulence factors and antibiotic resistance genes (ARGs) were identified based on the core datasets in the VFDB (Virulence Factors of Pathogenic Bacteria) and ARDB (Antibiotic Resistance Genes Database) databases. Additionally, general function annotation was performed using three databases: COG (Clusters of Orthologous Groups), GO (Gene Ontology), and KEGG (Kyoto Encyclopedia of Genes and Genomes).

2.6.3. Comparative genomics

(i) Structural Variation (Synteny). The genome sequence of the *C. pseudotuberculosis* strain was compared with that of the reference bacteria. (ii) FastANI (version 1.32) software was used to conduct the Average Nucleotide Identity (ANI) analysis. (iii) CD-HIT clustering analysis was conducted on the protein gene sets of the *C. pseudotuberculosis* strain investigated in this study and other *Corynebacterium* strains to obtain the core/specific/dispensable gene set. (iv) Gene families were constructed by pairwise aligning the protein sequences of multiple target genomes using the BLAST, eliminating redundancy with Solar (BGI), and clustering the alignment results using the Hcluster_sg software. (v) The phylogenetic tree was constructed by the TreeBeST[10] using the method of neighbor-joining (NJ).

2.7. Statistical analysis

The *in vitro* experiment was performed in triplicate and the data were analyzed using SPSS software (IBM, Armonk, NY, USA). Statistical significance was determined by one-way ANOVA, and differences were considered significant at $p < 0.05$ and extremely significant at $p < 0.01$. The LD_{50} values were calculated by Probit analysis (Xiong et al., 2013). The difference in LD_{50} among the three *C. pseudotuberculosis* strains were examined by the Kruskal-Wallis test. All graphical presentations were generated by Adobe Illustrator 2020 (Adobe Inc., San Jose, CA, USA) and GraphPad Prism 9.0 (GraphPad Software, San Jose, CA, USA).

3. Results

3.1. Postmortem examination

All three alpacas exhibited purulent infections in the skin and subcutaneous tissue, with some abscesses that developed in "beaded" pattern. White, yellowish pus or caseous pus masses were observed after incision of the pustules. Additionally, skin ulceration and necrosis were observed (Supplementary Figure S3). Upon necropsy of dead alpaca (G1, BA3), multiple abscesses were found in subcutaneous tissue, anterior shoulder lymph nodes, and inguinal lymph nodes. Alpaca G1 was found to have abscesses in the liver and mesenteric lymph nodes, as well as hemorrhagic spots in the lung (Supplementary Figure S4).

3.2. Bacteriological examination

Dry, friable, and opaque porcelain white colonies were grown on LB solid medium under both anaerobic and aerobic conditions (Figure 1A). A narrow and transparent hemolytic ring formed on the blood plate, which is β-hemolysis (Figure 1B). Microscopic examination of Gram-stained samples showed a large number of blue-purple globular or rod-shaped Gram-positive bacteria that were arranged singly and sporadically (Figure 1C).

Biochemical identification was consistent for the three strains (Table 1), and was in accordance with the biochemical properties of *C. pseudotuberculosis* previously summarized (Dorella et al., 2006). These three strains were further identified as *C. pseudotuberculosis* biovar equi by nitrate reduction experiments (+).

3.3. Molecular identification

Identification analysis of the partial 16S rRNA gene confirmed that all three isolates were *C. pseudotuberculosis* (accession numbers OQ980206, OP903368 and OP903369). These sequences exhibited 100% similarity to the sequences MT649220 (dromedary, equi, India) and LC549531 (goat, ovis, Malaysia), suggesting a high degree of similarity between the three strains.

The *narG* gene was successfully amplified and identified in all three isolates as *C. pseudotuberculosis* biovar equi (accession numbers OQ817706, OQ817707 and OQ817708). These sequences displayed 100% identity to both the sequences CP003652 (strain Cp162, equi, camel) and CP017384 (strain I37, equi, cattle).

3.4. Antibiotic susceptibility testing

The antibiotic susceptibility test showed that the three *C. pseudotuberculosis* strains were sensitive to all antibiotics tested except aztreonam, fosfomycin and nitrofurantoin. Specific results are shown in Table 2.

3.5. Pathogenicity test

After artificial infection with *C. pseudotuberculosis* for 5–6 h, the mice began to develop abnormal symptoms, including disheveled coat, depression, accelerated respiration, slow reaction, slow movement, and inappetence. Survival curves were plotted according to the time of death in each group (Figure 2). The LD_{50} values for mice infected with strains G1, S2 and BA3 were 1.66×10^5 CFU, 3.78×10^5 CFU and 3.78×10^5 CFU, respectively ($p > 0.05$). The LD_{50} of strain G1 was less than that of the strains S2 and BA3, but the difference is not significant ($p > 0.05$).

7 http://www5.esu.edu/cpsc/bioinfo/software/GIST/
8 http://phast.wishartlab.com/
9 https://crisprcas.i2bc.paris-saclay.fr//CrisprCasFinder/Index
10 http://treesoft.svn.sourceforge.net/viewvc/treesoft/trunk/treebest/

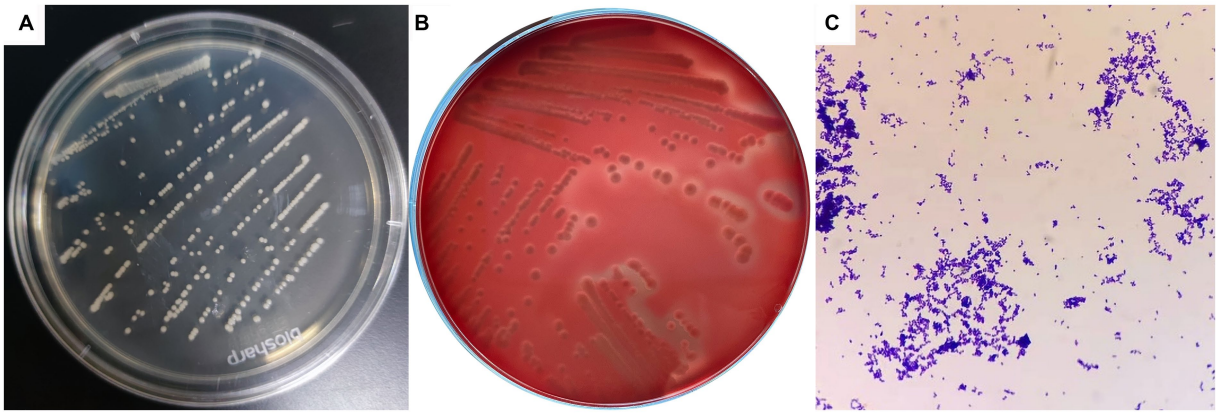

FIGURE 1
Colony morphology and bacterial morphology observation of *C. pseudotuberculosis*. **(A)** Colony morphology (LB solid medium). **(B)** Colony morphology (5% sheep blood). **(C)** Bacterial morphology (1000 ×).

TABLE 1 Biochemical characteristics of *C. pseudotuberculosis* in this study.

Category	Result	Category	Result	Category	Result	Category	Result
Glucose	+	Sucrose	–	Hydrogen sulfide	–	Esculin hydrolysis	–
Mannose	+	Arabinose	–	Citrate	–	Urease test	+
Fructose	+	Xylose	–	Voges-Proskauertest	–	Catalase	+
Lactose	–	Raffinose	–	Gelatin liquefaction	–	Nitrate reduction	+
Maltose	–	Melibiose	–	Inositol	–		

+, positive; –, negative.

Necropsy of dead mice (10^7 CFU/mL group) showed dilatation of the gastrointestinal tract with significant fluid accumulation, hemorrhagic spots in the liver, and a congested and enlarged spleen. The dead mice did not show typical CLA or suppuration symptoms, which may be explained by acute death of mice post-injection and the fact that the infected organs lacked the time to develop the organ lesions. Sterile collection was performed on the liver, spleen, and kidneys of the dead mice, and after streaking and incubation, *C. pseudotuberculosis* was isolated from all organs. The pathological sections revealed that there was pronounced central vein congestion (red arrow) and diffuse hepatic cell lipid degeneration (black arrow) in the liver tissue (Figure 3A). Heart tissue (Figure 3B) showed no apparent abnormalities. Spleen tissue (Figure 3C) showed irregularities in the white pulp, along with numerous small vacuoles (black arrow) and a large area of extramedullary hematopoietic foci in the red pulp (red arrow), with a significant amount of neutrophil infiltration (blue arrow). Lung tissue (Figure 3D) exhibited extensive alveolar interstitial congestion and expansion (red arrow), with only a few lymphocyte infiltrates observed around blood vessels (blue arrow). Kidney tissue (Figure 3E) displayed a small number of epithelial cells that underwent cellular hydropic degeneration and cytoplasmic relaxation (black arrow), and a large portion of renal tubular interstitial congestion and expansion (red arrow). Intestine tissue (Figure 3F) showed a considerable amount of villous epithelial cells that experienced necrosis and shedding (yellow arrow), and there was also necrosis or atrophy of the basal intestinal glands in the lamina propria, resulting in a reduced structure (orange arrow), together with a small amount of lymphocyte infiltration (blue arrow).

14 days after intraperitoneal injection of *C. pseudotuberculosis*, enlarged spleens of the mice were observed at necropsy. Changes in organ indices were consistent with necropsy findings. After intraperitoneal injection of strain G1, the spleen organ index of mice in 10^5 CFU/mL group was significantly higher than in the control group and 10^4 CFU/mL group ($p < 0.01$), and 10^4 CFU/mL group was significantly higher than the control group ($p < 0.05$). After intraperitoneal injection of S2 or BA3 strains, the spleen organ index of mice in 10^5 CFU/mL group was significantly higher than the control group ($p < 0.01$) and 10^4 CFU/mL group ($p < 0.05$), while there was no significant difference between 10^4 CFU/mL group and the control group ($p > 0.05$). There was no significant difference in the organ index of other organs (liver, heart, lung and kidney) ($p > 0.05$) (Figure 4). The spleen is an important immune organ in the host, and when exposed to external infections, immune cell infiltration, hypersplenism and portal hypertension can cause splenomegaly (Wang X. et al., 2021).

3.6. Whole genome sequencing

Based on the consistent biochemical properties, biovars identification, and antibiotic sensitivity test results of these three *C. pseudotuberculosis* strains, and no significant difference in LD_{50} among them, only one strain was specifically chosen for whole genome sequencing and comparative genomics analysis. The strain G1 was chosen due to its lower LD_{50} compared to the other two strains.

3.6.1. Genome sequencing and assembly of *Corynebacterium pseudotuberculosis* strain G1

Initially, a total of 1,314 Mb of raw data were produced from the DNBSEQ sequencing platform, from 8,764,210 reads (Supplementary Table S2). After single-molecule nanopore DNA

sequencing and data clean-up, 2,331,063,777 bp of sequence data were obtained, with reads mean length of 6,908 bp (Supplementary Table S3). The final assembly was composed of a chromosomal scaffold of 2,379,166 bp (52.06% G + C) (Supplementary Table S4; Supplementary Figure S5) without any plasmid. The genome has been uploaded to the NCBI (National Center for Biotechnology Information) database with accession number CP121342.

3.6.2. Gene prediction and annotation of *Corynebacterium pseudotuberculosis* strain G1

A total of 49 tRNA-encoding genes and 4 rRNA operons (four 5S rRNAs, four 16S rRNAs and four 23S rRNAs) were identified in the chromosome (Supplementary Table S5). The results of tandem repeat prediction are presented in Supplementary Table S6. Phages were not predicted in this study. Three different CRISPR clusters were detected in the chromosome of *C. pseudotuberculosis* strain G1, and details are shown in Supplementary Table S7.

After comparing the ORFs to the ARDB database, we annotated that the strain G1 contains five ARGs, including *rpoB*, *rbpA*, EF-Tu mutant, *thyA*, and *murA* (identity >60%), and is predicted to be resistant to rifamycin, elfamycin, salicylic acid, and fosfomycin. In addition, we compared the strain G1 with the VFDB database and annotated 43 genes related to virulence factors, including adherence (such as *spaC* and *spaI*), exotoxin (*pld*), immune modulation (*rfbB* and *ndk*), nutritional/metabolic factor (such as *fagA-D* and *ciuA-E*), and stress survival (such as *sigE*, *sigH*, and *sigA/rpoV*). Specific virulence genes are shown in Supplementary Table S8 (identity >60%). Furthermore, we aligned the strain G1 with the I37 strain (accession number: CP017384) to annotate the virulence factor-related genes *oppA*, *oppB*, *oppC*, *oppD*, and *oppF* (identity >98%).

After comparing the predicted gene set with the COG database, the homologous gene annotation was completed, and the COG functional clustering was obtained. The genome of strain G1 has been annotated with 1538 genes that have known functions and 55 genes that have unknown functions. The highest number of genes is related to metabolism ($n = 896$), followed by cellular and information. There are 98 genes predicted for general function prediction only (Supplementary Figure S6A). Through the annotation in the GO database, we can determine the potential function of a gene based on its annotation in various categories. Supplementary Figure S6B displays the statistical results of the annotation findings for the strain G1 in the three categories (cellular component, molecular function, and biological process) of the GO database. The KEGG database divides biological pathways into eight categories, with each category further subdivided and labeled with the relevant genes. This allows for easy identification of all annotated genes associated with a specific function. Supplementary Figure S6C shows the histogram resulting from the KEGG secondary classification statistics of the strain G1.

3.6.3. Comparative genomics

As shown in Figure 5, strain G1 clusters with the other 12 strains of *C. pseudotuberculosis*, with intraspecies ANI values greater than 98.6. The highest ANI values (> 99.94) were observed between strain G1 and strain Cp162 (equi, camel), followed by >99.93 with strain I37 (equi, cattle). ANI values were greater than 98.9 between strains of the

TABLE 2 Antibiotic susceptibility of *C. pseudotuberculosis* in this study.

Classification	Antibiotics	Judgment		
		G1	S2	BA3
β-lactams	Amoxicillin-clavulanate	S	S	S
	Ampicillin-sulbactam	S	S	S
	Cephazolin	S	S	S
	Aztreonam	R	R	R
	Penicillin	S	S	S
	Ceftriaxone	S	S	S
Carbapenems	Imipenem	S	S	S
	Meropenem	S	S	S
Polyphosphates	Fosfomycin	R	R	R
Glycopeptides	Vancomycin	S	S	S
Aminoglycosides	Amikacin	S	S	S
	Gentamicin	S	S	S
Tetracyclines	Tetracycline	S	S	S
Macrolides	Clarithromycin	S	S	S
	Azithromycin	S	S	S
	Erythromycin	S	S	S
Amide alcohols	Chloramphenicol	S	S	S
Quinolones	Ciprofloxacin	S	S	S
Sulfonamides	Sulfamethoxazole	S	S	S
Nitrofurans	Nitrofurantoin	R	R	R
Rifamycins	Rifampicin	S	S	S

R, resistant; S, sensitive.

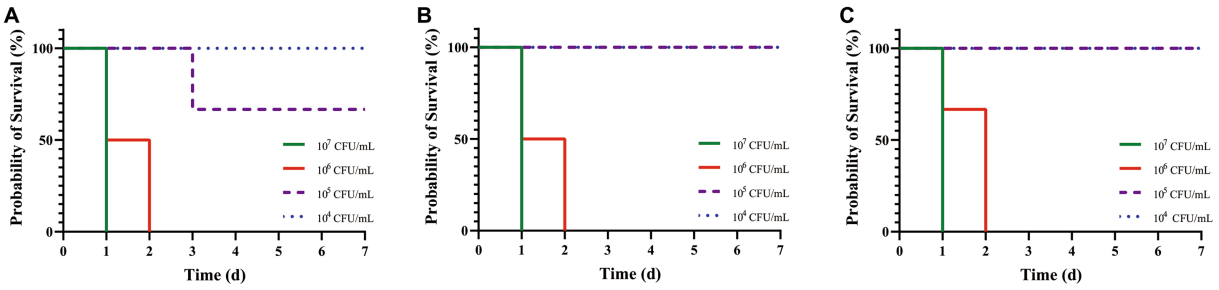

FIGURE 2
Survival curves of mice challenged with *C. pseudotuberculosis* strains at different concentrations. **(A)** G1 strain. **(B)** S2 strain. **(C)** BA3 strain.

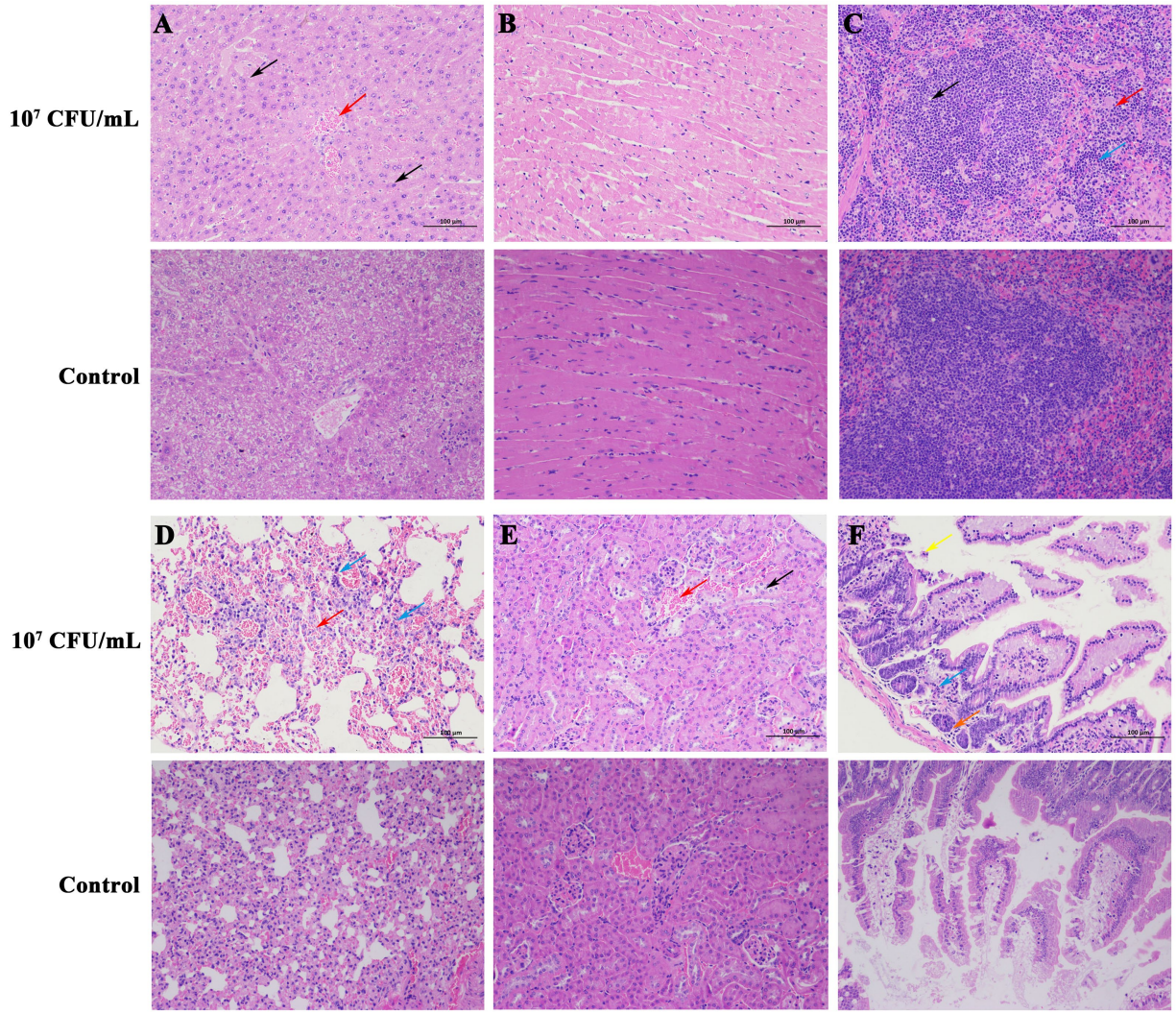

FIGURE 3
Histopathologic changes in mice killed by *C. pseudotuberculosis* (200×). **(A)** Liver. **(B)** Heart. **(C)** Spleen. **(D)** Lung. **(E)** Kidney. **(F)** Intestine.

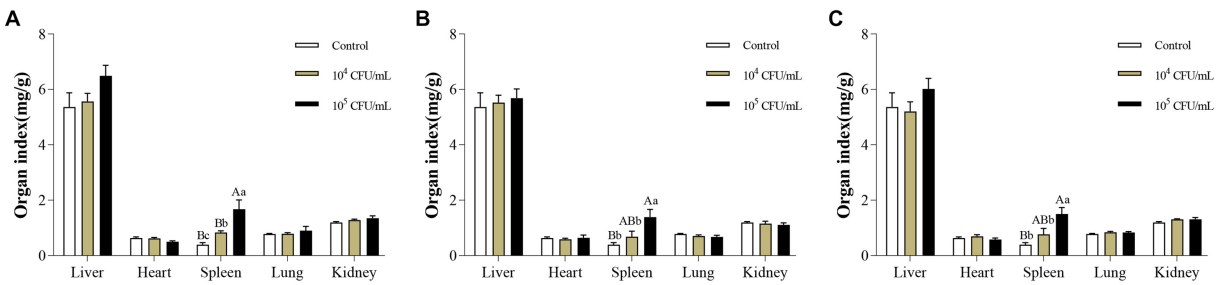

FIGURE 4
Changes of organ index in mice infected with different concentrations of *C. pseudotuberculosis*. **(A)** G1 strain. **(B)** S2 strain. **(C)** BA3 strain. Significant differences were observed among the different letter marks. Uppercase letters indicate $p < 0.01$, while lowercase letters indicate $p < 0.05$. The absence of any letter mark, or the presence of the same letter mark, indicates no significant difference ($p > 0.05$).

same biovars of *C. pseudotuberculosis*, and ranged from 98.6 to 98.9 between strains of different biovars of *C. pseudotuberculosis*. The interspecies ANI values between *C. pseudotuberculosis* and *C. ulcerans* ranged from 84.8 to 85.0. Interspecies ANI values were less than 80 for strains of *C. pseudotuberculosis* versus *C. diphtheriae*, *C. glutamicum* and *C. pseudopelargi*.

Gene family statistics for the 21 strains of *Corynebacterium* are presented in Supplementary Table S9 and Supplementary Figure S8.

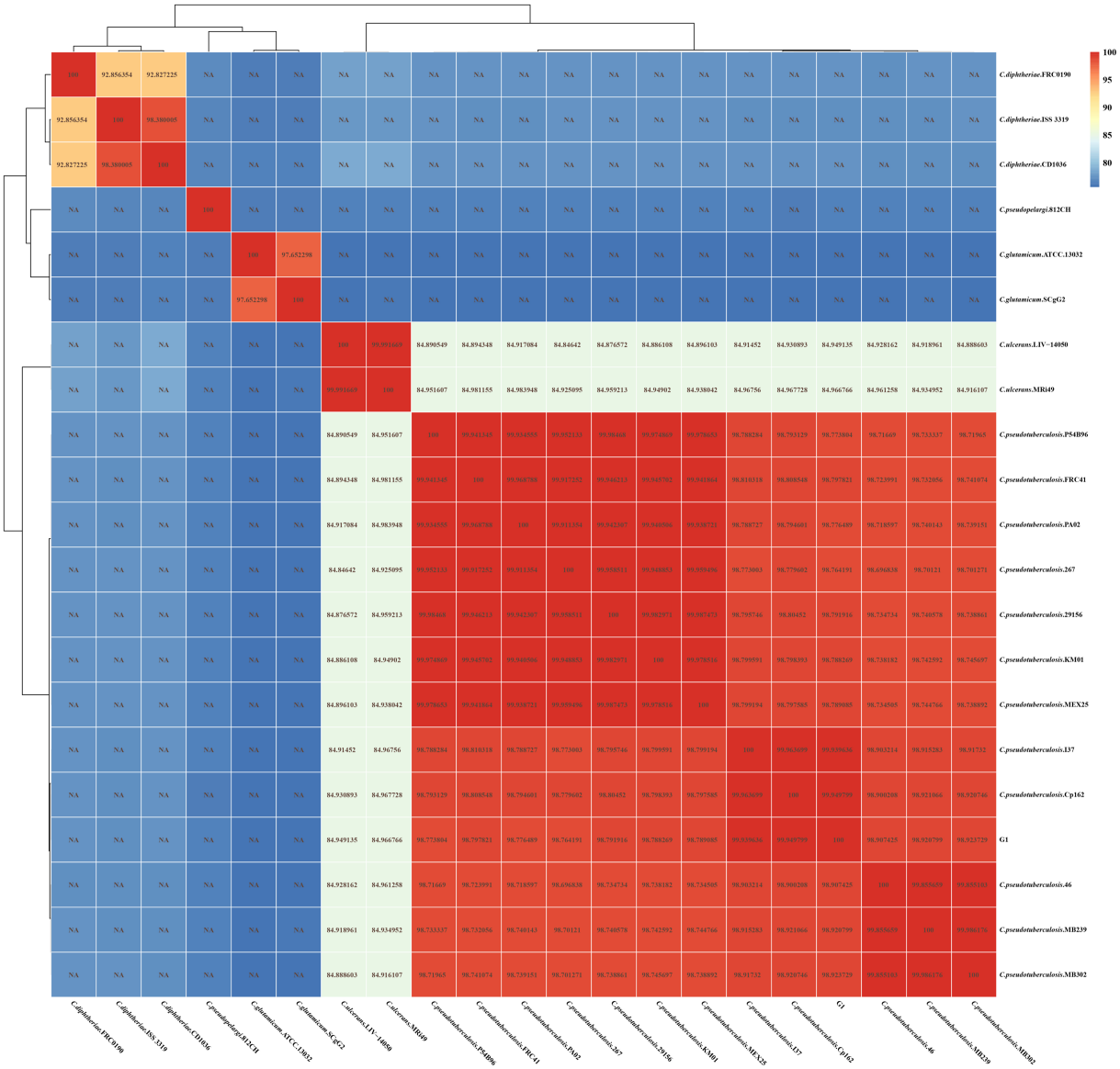

FIGURE 5
ANI heat map of 21 *Corynebacterium* strains. The horizontal and vertical axes represent the strain names. Each value in the heat map represents the ANI value.

The analysis revealed a total of 1,080 homologous gene families, with 762 Single Copy Orthologs identified among all 20 strains of *Corynebacterium*. Notably, the strain G1 showed 8 unique paralogs and 2 unique families.

The protein coding DNA sequences (CDSs) of strain G1, 12 strains of *C. pseudotuberculosis* and 8 strains of other *Corynebacterium* were clustered, and the number of pan genes was 6224, the number of core genes was 931, and the number of dispensable genes was 3277 (Figure 6A). Analyses of the core gene set and pan gene set of different numbers of strain combinations, resulted in the core gene and pan gene dilution curves (Figure 6B). According to the distribution of dispensable genes in different samples, a heat map was drawn to show the clustering among samples (Figure 6C). Different species of *Corynebacterium* were clustered separately, but different biovars of *C. pseudotuberculosis* were not clustered.

Mapped sequence library genes of the core genes, dispensable genes, and specific genes to the corresponding functions of the COG database are shown in Supplementary Figure S7. Of the 128 specific genes in *C. pseudotuberculosis* strain G1, only one gene (Cell wall/membrane/envelope biogenesis) matched the COG database. In the core and dispensable gene sequence libraries of the 21 *Corynebacterium* strains, 850 and 1934 genes, respectively, matched the COG database, with the majority of core genes (91.30%, $n = 931$) and dispensable genes (59.02%, $n = 3277$) having COG classification information. Translation, ribosomal structure and biogenesis genes had the largest proportion among the core genes (16.00%), while inorganic ion transport and metabolism genes had the highest proportion among the dispensable genes (7.93%).

To infer the phylogenetic relationships of strain G1 and 20 strains of *Corynebacterium*, we constructed phylogenetic trees based on gene family and core-pan genome (Figure 7).

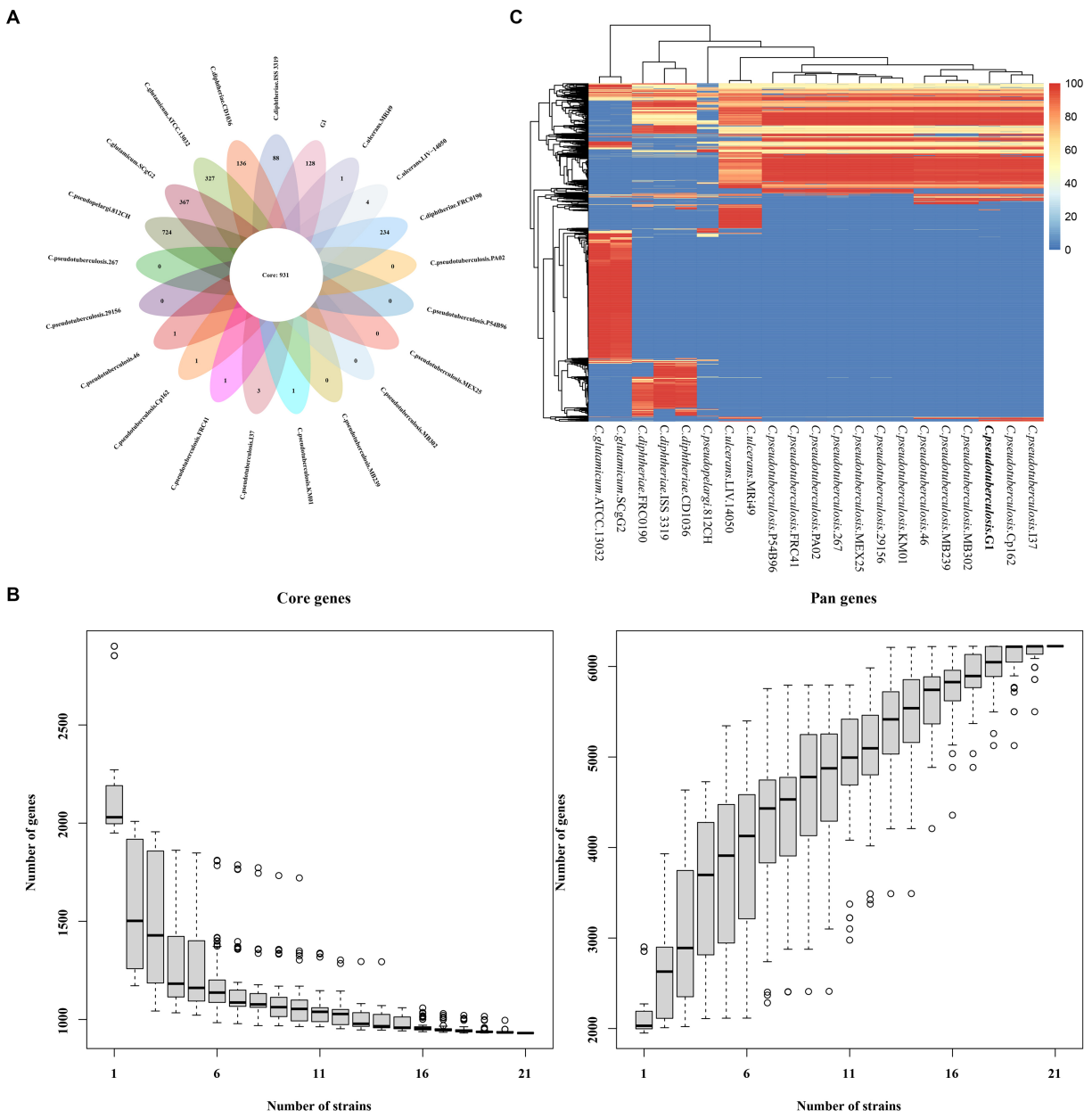

FIGURE 6
The core and pan-genome of 21 *Corynebacterium* strains. **(A)** Venn plots showing the number of core genes and strain-specific genes in 21 the *Corynebacterium* strains. **(B)** Dilution curve of the pan-genome and core genome of the 21 *Corynebacterium* strains. **(C)** Heat map displaying the dispensable genes.

The phylogenetic tree shows that different species of *Corynebacterium* clustered separately, while 13 *C. pseudotuberculosis* strains were divided into two biovars with clear demarcation, and strain G1 with *C. pseudotuberculosis* biovar equi clustered in the same clade. On the phylogenetic tree, *C. pseudotuberculosis* strain G1 was the closest relative to Cp162 and I37, and this result was consistent with the ANI analysis. The phylogenetic trees constructed based on the results of the two analyses showed the same branching structure, indicating good conservation of core-pan genes and gene families among these *Corynebacterium* strains.

Synteny analysis was conducted between strain G1 and other *C. pseudotuberculosis* strains. The analysis revealed that strain G1 has a chromosomal inversion compared with strain Cp162 (equi, camel), a chromosomal translocation with four biovar equi (I37, MB302, MB239, and 46) and three biovar ovis (267, FRC41, and PA02) strains, and four chromosomal translocations with two biovar ovis (29,156 and MEX25) strains (Figure 8). No host or biovar-specific patterns were observed.

4. Discussion

CLA, caused by *C. pseudotuberculosis*, is one of the most important bacterial infectious diseases in camelids. This disease is

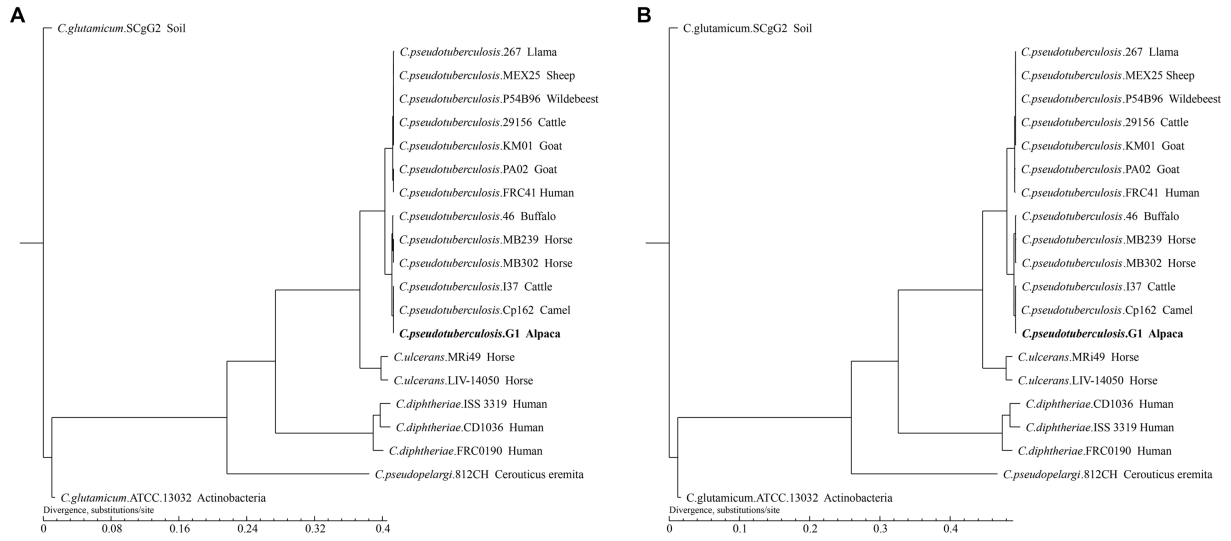

FIGURE 7
Phylogenetic tree of the 21 *Corynebacterium* strains. The tree was constructed using TreeBeST and PHYML based on **(A)** Core-pan gene. **(B)** Gene family. The numbers on the branches represent percent bootstrapping values from 1000 replicates. Each sequence is identified by its species, strain name, and host. Sequences obtained in this study are shown in bold.

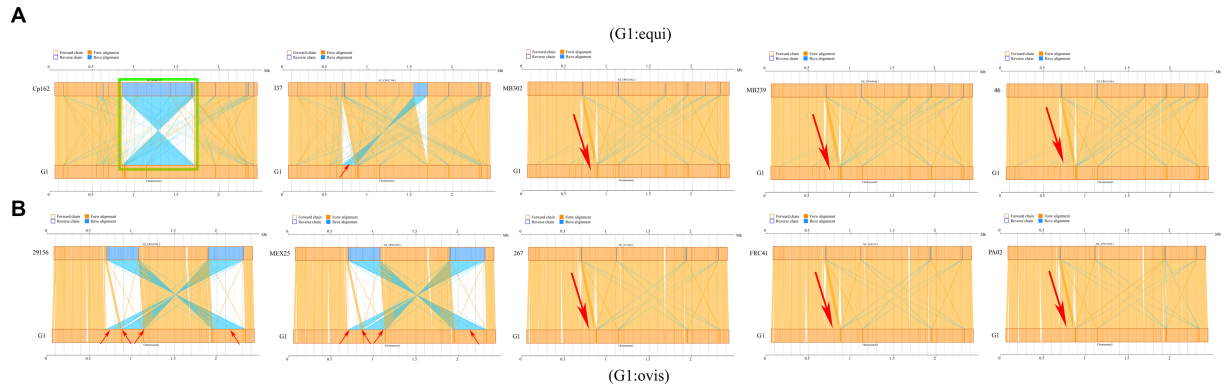

FIGURE 8
Synteny analysis. **(A)** Comparison of strain G1 with *C. pseudotuberculosis* biovar equi strains (Cp162 - camel, I37 - cattle, MB302 - horse, MB239 - horse, 46 - buffalo). **(B)** Comparison of strain G1 with *C. pseudotuberculosis* biovar ovis strains (29156 - cattle, MEX25 - sheep, 267 - llama, FRC41 - human, PA02 - goat). Green box indicates chromosome inversion, while red arrow represents chromosome translocation.

characterized by abscesses of one or more superficial lymph nodes, and it can also infect internal organs such as the liver, lungs, and mammary glands, causing great losses to the breeding industry and attracting the attention of many scholars (Kinne, 2016). CLA has been reported in Old World Camels (Bactrian camel and dromedary camel) from several countries, such as China (Mullali et al., 2017), Russia, India (Purohit et al., 1985), Iran (Esterabadi et al., 1975), Saudi Arabia (Radwan et al., 1989), United Arab Emirates (Afzal et al., 1996), Oman, Jordan (Hawari, 2008), Kazakhstan (Samartsev, 1950), Egypt (Nashed and Mahmoud, 1987), Ethiopia (Domenech, 1980), Kenya (Wernery, 2012), Spain (Tejedor-Junco et al., 2008), as well as in Australia (Wernery et al., 2014). CLA has also been reported in New World Camels (alpaca and llama) from the USA (Lopes et al., 2012), Peru (Braga et al., 2006), Sweden, Germany (Sting et al., 2022) and Italy. Specifically, there have been reports of a llama in USA (Lopes et al., 2012) and 130 alpacas in Germany (Sting et al., 2022) being infected with biovar ovis strains. CLA by *C. pseudotuberculosis* biovar equi has not previously been reported in alpacas. Previous reports have solely documented the infection of goats with *C. pseudotuberculosis* biovar ovis strains in Sichuan Province, China (Zhang et al., 2015). While the alpacas in this study were imported from Chile and the Netherlands, it is worth noting that in Chile, cases of *C. pseudotuberculosis* biovar equi strains infection in horses have been reported (Cavalcante et al., 2015). Therefore, the pathogenic bacteria isolated in this study may have originated from the country from where the alpacas were introduced. Horses can only be infected by *C. pseudotuberculosis* biovar equi strains, while cattle and camelids can be infected by both biovars. It is crucial to be vigilant, as the outbreak of this pathogen in Chinese farms would pose a significant threat to the cattle, horse, and camelid

breeding industries, resulting in economic losses such as death of farmed animals and reduced production. Therefore, effective prevention and control measures must be taken to prevent the spread and infection of this pathogen.

The genome of strain G1 is approximately 2.379 Mb, which is smaller than the genomes of biovar equi strains isolated from buffaloes (strains 31–36, 38, 39, and 48) and camel (strain 267). The GC content is 52.06%, which is lower than that of previously sequenced whole genomes of *C. pseudotuberculosis* strains (Supplementary Table S1). Three CRISPR clusters were detected on the chromosome of the strain G1, which were only detected in biovar equi strains (Parise et al., 2018). The gene set was subjected to COG functional annotation, and the categorical statistics were similar to those of six biovar equi strains (MEX1, MEX9, MEX25, MEX29, MEX30, and MEX31) isolated from equines in Mexico, except for strain MEX30 which harbors a gene related to chromatin structure and dynamics gene (Parise et al., 2018).

The widespread prevalence and significant economic impact of this disease have prompted investigations into the molecular mechanisms of virulence in this pathogen (Dorella et al., 2009). In sheep and goats, the virulence factor-related genes *pld* and *fagA*, *B* were detected in 100% of isolates, and *fagC*, *D* genes were detected in more than 95% (Aquino De Sá et al., 2013). Notably, all *fagD*-negative isolates were obtained from superficial abscesses, suggesting variations in the virulence potential of the clinical isolates (Aquino De Sá et al., 2013). A mutation in *fagB* (*C*) can reduce the pathogenicity of *C. pseudotuberculosis* in goat infections (Billington et al., 2002). To study the role of Opp in *C. pseudotuberculosis*, an OppD-deficient strain was created, and it was observed that the mutant strain had impaired growth when exposed to the toxic glutathione peptide, similar to the wild-type strain. The *ΔoppD* strain also showed a reduced ability to adhere to and infect macrophages compared to the wild-type strain, but both strains had similar potential to colonize spleens and cause injury and death to infected mice (Moraes et al., 2014).The above ten virulence genes (*pld*, *fagA-D*, *oppA-F*) were detected in the strain LY20 isolated from a goat in China (Wang R. et al., 2021). Whole genome sequencing of *C. pseudotuberculosis* strain I37 isolated from cattle (accession number CP017384, Israel) also revealed the presence of these ten virulence genes. At present, there are few reports related to *C. pseudotuberculosis* from alpaca, and the results of whole genome sequencing of *C. pseudotuberculosis* isolated from llama showed the presence of the *pld* and *fagA-D* (Lopes et al., 2012). In this study, we annotated 48 genes related to virulence factors in five categories (adherence, exotoxin, immune modulation, nutritional/metabolic factor, and stress survival). Among them, *pld* is the only exotoxin-related virulence gene. Other genes include σ factors (*sigE*, *sigH*, *sigA/rpoV*), iron uptake and regulation-related genes (*fagA-D*, *ciuA-E*), oligopeptide permease (*oppA-F*), minor pilin proteins (*spaC*, *spaI*), and superoxide dismutase (*sodA*).

The success of antimicrobial treatment to CLA is poor (Kinne, 2016). Performing resistance testing of isolates can provide guidance for the use of antibiotics. At present, there have been limited studies on antibiotic susceptibility of *C. pseudotuberculosis* in alpaca, with most research focusing on horse (Foley et al., 2004; Rhodes et al., 2015), sheep (Gallardo et al., 2019), and goat (Connor et al., 2000; Abebe and Sisay, 2015) isolates. The minimum inhibitory concentration (MIC) of the antimicrobial agent showed no significant differences between the isolates from horses and cows compared to those from sheep and goats, except in the case of amikacin (Costa et al., 1998). The MIC of equine *C. pseudotuberculosis* isolates demonstrated that several commonly used antimicrobials are effective against *C. pseudotuberculosis in vitro*. Abscess location was not associated with different MIC patterns in cultured isolates (Rhodes et al., 2015). It has been determined that 59 *C. pseudotuberculosis* isolates from sheep and goats were primarily susceptible to norfloxacin (77.97%), doxycycline HCl (72.88%), and kanamycin (72.88%), while mainly resistant to ampicillin (28.81%), clindamycin (25.42%), and doxycycline HCl (22.04%) (Abebe and Sisay, 2015). Strain XH02 (Boer goat, China) exhibited high sensitivity to 13 antibacterial agents, including chloromycetin, tetracycline, norfloxacin, minocycline, cefoxitin, clarithromycin, roxithromycin, and ceftriaxone, but completely resistant to nitrofurantoin and furazolidone (Zhou et al., 2016). However, the susceptibility of five alpaca isolates to gentamicin, sulfonamide, oxacillin, neomycin, and ceftiofur varied (Anderson et al., 2004). In this study, 21 antibiotics in 12 categories commonly used in clinical practice were selected for antibiotic susceptibility testing. The three strains were sensitive to penicillin, cefotaxime, meropenem, erythromycin and other antibiotics, resistant to aztreonam, fosfomycin, and nitrofurantoin. Combined with the antibiotic sensitivity results and clinical manifestations of the sick alpaca (S2), meropenem with high sensitivity was selected for treatment, and the sick alpaca symptoms improved, and gradually recovered.

Horizontal gene transfer (HGT) of drug-resistance genes leads to global infections of multi-drug resistant (MDR) microorganisms in hospitals and communities, posing a serious potential hazard to public health safety (Warnes et al., 2012). PCR amplification of the ARGs in *C. pseudotuberculosis* strains obtained from goats and sheep from Egypt indicated the presence of the β-lactams resistance gene (*bla*) in 40% of the isolates, and the aminoglycoside resistance gene (*aadA2*) in 42% of the isolates (Tawab et al., 2019). Upon analyzing the complete genome sequence of the *C. pseudotuberculosis* strain Cp267 isolated from llama (accession number CP003407, USA), we discovered that it carries 12 ARGs, mainly expressed as MRD protein (*marR*, *norM*, and *emrB*), lincomycin resistance protein (*lmrB*), bleomycin resistance protein and glycopeptide antibiotic resistance protein, and no β-lactam resistance gene was found (Lopes et al., 2012). In this study, the complete genome sequence of the *C. pseudotuberculosis* strain G1 isolated from alpaca was annotated with five ARGs, including rifamycin resistance genes *rpoB* and *rbpA*, elfamycin antibiotic gene EF-Tu mutant, fosfomycin antibiotic gene *murA*, and pyrazine antibiotic gene *pncA*. Our findings indicate that these ARGs exhibited a low correlation with the resistance phenotype, suggesting that detection of ARGs cannot replace routine antibiotic susceptibility testing. The expression of ARGs is influenced by various factors, including gene expression level, drug resistance mechanism, and bacterial adaptability to the environment. Therefore, the presence of a certain ARG does not necessarily imply that the bacterium will exhibit resistance to the corresponding antibiotic. Lastly, the difference in the carriage of resistance genes between the strains analyzed in this study and previous studies may be attributed to the variation in antibiotic usage in different regions to combat bacterial infectious diseases.

Several different serological tests (haemagglutination, haemagglutination inhibition, and ELISAs) have been tried for the diagnosis of CLA but, with the exception of ELISA, are rarely used on camelids (Kinne, 2016). An in-house ELISA was developed based on commercially available ELITEST, using protein A substituted anti-goat/sheep conjugate, is currently routinely used to detect CLA antibodies in dromedaries with good results (Berlin et al., 2015). Serologic testing was performed on 232 alpacas using a commercially

available ELISA based on PLD as antigen and an in-lab ELISA based on whole cell antigens (WCA), and showed a substantial degree of agreement of 89.5% for both tests (Sting et al., 2022). Further comparative studies showed that the immunoblot had a sensitivity superior to both ELISAs (Sting et al., 2022). In conclusion, serological testing using ELISA combined with validation by immunoblot should be considered as critical methods to control CLA in alpaca herds.

5. Conclusion

To our knowledge, this is the first report of infection with *C. pseudotuberculosi* from alpaca in China, and the first whole genome sequencing of *C. pseudotuberculosis* biovar equi strain in alpaca. Comparative genomics analysis based on ANI value, gene families, core-pan genome, and synteny analysis demonstrated a high degree of genetic similarity among *C. pseudotuberculosis* strains, in contrast to other *Corynebacterium* species, with a clear delineation between strains belonging to the two biovars (ovis and equi). This study provides fundamental information for further exploration of the pathogenic mechanisms of *C. pseudotuberculosis* in alpaca and practical guidance for the prevention, diagnosis, and treatment of CLA in this species.

Data availability statement

The original contributions presented in the study are included in the article/Supplementary material, further inquiries can be directed to the corresponding authors.

Ethics statement

The animal study was reviewed and approved by the Sichuan Agricultural University Animal Ethical and Welfare Committee. Written informed consent was obtained from the owners for the participation of their animals in this study.

Author contributions

WM: methodology, data analysis and visualization, and writing – original draft. SC: clinical case handling. LH: writing – original draft. JY: data analysis and visualization. WZ: investigation. ZhZ and ZiZ: resources. HL and HF: writing – review and editing. TH: project administration. GP: conceptualization and supervision. All authors have read and approved the manuscript.

Funding

This research was supported by Sichuan Wolong National Nature Reserve Administration (510000-02-064387), and the State Forestry and Grassland Administration (2022-2222219002).

Acknowledgments

The authors thank Zhiyou Dong and Qianlan Li for their invaluable assistance in the feeding and management of experimental animals. Additionally, we extend our heartfelt appreciation to Cao Deng for his expert guidance in the partial data analysis of the whole genome.

Conflict of interest

The authors declare that the research was conducted in the absence of any commercial or financial relationships that could be construed as a potential conflict of interest.

Publisher's note

All claims expressed in this article are solely those of the authors and do not necessarily represent those of their affiliated organizations, or those of the publisher, the editors and the reviewers. Any product that may be evaluated in this article, or claim that may be made by its manufacturer, is not guaranteed or endorsed by the publisher.

Supplementary material

The Supplementary material for this article can be found online at: https://www.frontiersin.org/articles/10.3389/fmicb.2023.1206187/full#supplementary-material

References

Abebe, D., and Sisay, T. T. (2015). Determination of *Corynebacterium pseudotuberculosis* prevalence and antimicrobial susceptibility pattern of isolates from lymph nodes of sheep and goats at an organic export abattoir, Modjo. *Ethiopia. Lett Appl. Microbiol.* 61, 469–476. doi: 10.1111/lam.12482

Afzal, M., Sakir, M., and Hussain, M. M. (1996). *Corynebacterium pseudotuberculosis* infection and lymphadenitis (taloa or mala) in the camel. *Trop. Anim. Hlth. Prod.* 28, 158–162. doi: 10.1007/BF02299568

Almeida, S., Dorneles, E. M. S., Diniz, C., Abreu, V., Sousa, C., Alves, J., et al. (2017). Quadruplex PCR assay for identification of *Corynebacterium pseudotuberculosis* differentiating biovar Ovis and Equi. *BMC Vet. Res.* 13:290. doi: 10.1186/s12917-017-1210-5

Almeida, S., Sousa, C., Abreu, V., Diniz, C., Dorneles, E. M. S., Lage, A. P., et al. (2017). Exploration of nitrate Reductase metabolic pathway in *Corynebacterium pseudotuberculosis*. *Int. J. Genomics* 2017, 1–12. doi: 10.1155/2017/9481756

Anderson, D. E., Rings, D. M., and Kowalski, J. (2004). Infection with *Corynebacterium pseudotuberculosis* in five alpacas. *J. Am. Vet. Med. Assoc.* 225, 1743–1747. doi: 10.2460/javma.2004.225.1743

Aquino De Sá, M. D. C., Gouveia, G. V., Krewer, C. D. C., Veschi, J. L. A., de Mattos-Guaraldi, A. L., and Da Costa, M. M. (2013). Distribution of PLD and FagA, B, C and D genes in *Corynebacterium pseudotuberculosis* isolates from sheep and goats with caseus lymphadenitis. *Genet. Mol. Biol.* 36, 265–268. doi: 10.1590/S1415-47572013005000013

Asfour, H. A. E., and Darwish, S. F. (2014). Evaluation of phenotypic methods versus molecular methods for differentiation of coagulase positive staphylococci causing bovine mastitis with a special reference to atypical *Staphylococcus aureus*. *Int. J. Curr. Microbiol. App. Sci.* 3, 543–558.

Barakat, A. A., Selim, S. A., Atef, A., Saber, M. S., Nafie, E. K., and El-Edeeby, A. A. (1984). Two serotypes of *Corynebacterium pseudotuberculosis* isolated from different animal species. *Rev. Sci. Tech.* 3, 151–163. doi: 10.20506/rst.3.1.147

Barauna, R. A., Ramos, R. T., Veras, A. A., Pinheiro, K. C., Benevides, L. J., Viana, M. V., et al. (2017). Assessing the genotypic differences between strains of *Corynebacterium pseudotuberculosis* biovar equi through comparative genomics. *PLoS One* 12:e170676. doi: 10.1371/journal.pone.0170676

Berlin, M., Joseph, M., Jose, S., Raghavan, R., and Wernery, U. (2015). Production of a caseous lymphadenitis vaccine for dromedaries. *J. Camel. Pract. Res.* 22:163. doi: 10.5958/2277-8934.2015.00026.0

Bernardes, J. S., Eberle, R. J., Vieira, F. R. J., and Coronado, M. A. (2021). A comparative pan-genomic analysis of 53 *C. pseudotuberculosis* strains based on functional domains. *J. Biomol. Struct. Dyn.* 39, 6974–6986. doi: 10.1080/07391102.2020.1805017

Billington, S. J., Esmay, P. A., Songer, J. G., and Jost, B. H. (2002). Identification and role in virulence of putative iron acquisition genes from *Corynebacterium pseudotuberculosis*. *FEMS Microbiol. Lett.* 208, 41–45. doi: 10.1111/j.1574-6968.2002.tb11058.x

Braga, W. U., Chavera, A., and Gonzalez, A. (2006). *Corynebacterium pseudotuberculosis* infection in highland alpacas (*Lama pacos*) in Peru. *Vet. Rec.* 159, 23–24. doi: 10.1136/vr.159.1.23

Cavalcante, A. L. Q., Dias, L. M., Alves, J. T. C., Veras, A. A. O., Guimarães, L. C., Rocha, F. S., et al. (2015). Complete genome sequence of *Corynebacterium pseudotuberculosis* strain E19, isolated from a Horse in Chile. *Genome Announc.* 3, e1315–e1385. doi: 10.1128/genomeA.01385-15

CLSI (2019). *Performance Standards for Antimicrobial Susceptibility Testing. 29th ed. CLSI supplement M100.* Wayne, PA: Clinical and Laboratory Standards Institute.

Connor, K. M., Quirie, M. M., Baird, G., and Donachie, W. (2000). Characterization of United Kingdom isolates of *Corynebacterium pseudotuberculosis* using pulsed-field gel electrophoresis. *J. Clin. Microbiol.* 38, 2633–2637. doi: 10.1128/JCM.38.7.2633-2637.2000

Costa, L. R. R., Spier, S. J., and Hirsh, D. C. (1998). Comparative molecular characterization of *Corynebacterium pseudotuberculosis* of different origin. *Vet. Microbiol.* 62, 135–143. doi: 10.1016/S0378-1135(98)00202-8

de Sá Guimarães, A., Carmo, F. B. D., Pauletti, R. B., Seyffert, N., Ribeiro, D., Lage, A. P., et al. (2011). Caseous lymphadenitis: epidemiology, diagnosis, and control. *IIOAB J.* 2, 33–43.

Domenech, J. (1980). Etube bactériologique de Corynebacterium pseudotuberculosis et de Corynebacterium pyogenes isolés chez le deomadaire en Ethiopie. *Revue d'elevage et de medecine veterinaire des pays tropicaux.* 33, 123–126. doi: 10.19182/remvt.8220

Dorella, F. A., Pacheco, L. G. C., Oliveira, S. C., Miyoshi, A., and Azevedo, V. (2006). *Corynebacterium pseudotuberculosis*: microbiology, biochemical properties, pathogenesis and molecular studies of virulence. *Vet. Res.* 37, 201–218. doi: 10.1051/vetres:2005056

Dorella, F. A., Pacheco, L. G., Seyffert, N., Portela, R. W., Meyer, R., Miyoshi, A., et al. (2009). Antigens of *Corynebacterium pseudotuberculosis* and prospects for vaccine development. *Expert Rev. Vaccines* 8, 205–213. doi: 10.1586/14760584.8.2.205

Du, Y. (1997). A case of thyroid abscess induced by *Corynebacterium pseudotuberculosis*. *Labor Med.* 12:123.

Esterabadi, A. H., Entessar, F., Hedayati, H., Narimani, A. A., and Sadri, M. (1975). Isolation of *Corynebacterium pseudotuberculosis* from camel in Iran. *Arch Razi Inst.* 27, 61–66. doi: 10.22092/ARI.1975.108778

Foley, J. E., Spier, S. J., Mihalyi, J., Drazenovich, N., and Leutenegger, C. M. (2004). Molecular epidemiologic features of *Corynebacterium pseudotuberculosis* isolated from horses. *Am. J. Vet. Res.* 65, 1734–1737. doi: 10.2460/ajvr.2004.65.1734

Fredriksson, N. J., Hermansson, M., and Britt-Marie, W. (2013). The choice of PCR primers has great impact on assessments of bacterial community diversity and dynamics in a wastewater treatment plant. *PLoS One* 8:e76431. doi: 10.1371/journal.pone.0076431

Gallardo, A. A., Toledo, R. A., González Pasayo, R. A., Azevedo, V., Robles, C., Paolicchi, F. A., et al. (2019). *Corynebacterium pseudotuberculosis* biovar ovis: evaluación de la sensibilidad antibiótica in vitro. *Rev. Argent. Microbiol.* 51, 334–338. doi: 10.1016/j.ram.2018.12.001

Guo, Z., Sun, J., Cheng, J., Zheng, L., and Bao, Z. (1988). Diagnosis of *Corynebacterium pseudotuberculosis* in camels. *Vet. Orien.*, 101–103.

Hard, G. C. (1969). Electron microscopic examination of *Corynebacterium ovis*. *J. Bacteriol.* 97, 1480–1485. doi: 10.1128/jb.97.3.1480-1485.1969

Hawari, A. D. (2008). *Corynebacterium pseudotuberculosis* infection (*Caseous lymphadenitis*) in camels (*Camelus Dromedarius*) in Jordan. *Am. J. Anim. Vet. Sci.* 3, 68–72. doi: 10.3844/ajavsp.2008.68.72

He, W., Liu, H., and Wei, D. (1991). Diagnosis report of Pseudotuberculosis in chicken. *Chin. J. Vet. Med.* 17:16.

Kazmierczak, M. J., Wiedmann, M., and Boor, K. J. (2005). Alternative sigma factors and their roles in bacterial virulence. *Microbiol. Mol. Biol. Rev.* 69, 527–543. doi: 10.1128/mmbr.69.4.527-543.2005

Kinne, U. W. A. J. (2016). Caseous lymphadenitis (Pseudotuberculosis) in Camelids: a review. *Austin J. Vet. Sci. Anim. Husb.* 3:1022.

Liu, M. (2021). *Isolation of Corynebacterium pseudotuberculosis and its specific bacteriophage*. Master Northwest A&F University, Xianyang

Liu, H., Zhang, Y., Huang, Z., Wang, Y., and Shen, M. (1986). Study on *Corynebacterium pseudotuberculosis* from camels. *J. Ningxia Agric. For Sci. Technol.* 46–48.

Lopes, T., Silva, A., Thiago, R., Carneiro, A., Dorella, F. A., Rocha, F. S., et al. (2012). Complete genome sequence of *Corynebacterium pseudotuberculosis* strain Cp267, isolated from a Llama. *J. Bacteriol.* 194, 3567–3568. doi: 10.1128/JB.00461-12

Mills, A. E., Mitchell, R. D., and Lim, E. K. (1997). *Corynebacterium pseudotuberculosis* is a cause of human necrotising granulomatous lymphadenitis. *Pathology* 29, 231–233. doi: 10.1080/00313029700169944

Moraes, P. M. R. O., Seyffert, N., Silva, W. M., Castro, T. L. P., Silva, R. F., Lima, D. D., et al. (2014). Characterization of the Opp peptide transporter of *Corynebacterium pseudotuberculosis* and its role in virulence and pathogenicity. *Biomed. Res. Int.* 2014, 1–7. doi: 10.1155/2014/489782

Moussa, I. M., Ali, M. S., Hessain, A. M., Kabli, S. A., Hemeg, H. A., and Selim, S. A. (2016). Vaccination against *Corynebacterium pseudotuberculosis* infections controlling caseous lymphadenitis (CLA) and oedematousskin disease. *Saudi J. Biol. Sci.* 23, 718–723. doi: 10.1016/j.sjbs.2016.06.005

Mullali, Wulsbai, Y. W., Uang, B., and Hazibai, H. (2017). Diagnosis and treatment of camel impetigo (*Corynebacterium pseudotuberculosis*). *Vet. Clin. Sci.* 10:68. doi: 10.3969/j.issn.2096-3637.2017.10.060

Nashed, S. M., and Mahmoud, A. Z. (1987). Microbiological and histopathological studies for rare cases of *Corynebacterium* infection in camel. *AVMJ* 18, 82–85.

Oliveira, M., Barroco, C., Mottola, C., Santos, R., Lemsaddek, A., Tavares, L., et al. (2014). First report of *Corynebacterium pseudotuberculosis* from caseous lymphadenitis lesions in Black Alentejano pig (*Sus scrofa domesticus*). *BMC Vet. Res.* 10:218. doi: 10.1186/s12917-014-0218-3

Oliveira, A., Teixeira, P., Azevedo, M., Jamal, S. B., Tiwari, S., Almeida, S., et al. (2016). *Corynebacterium pseudotuberculosis* may be under anagenesis and biovar Equi forms biovar Ovis: a phylogenic inference from sequence and structural analysis. *BMC Microbiol.* 16:100. doi: 10.1186/s12866-016-0717-4

Parise, D., Parise, M. T. D., Viana, M. V. C., Muñoz-Bucio, A. V., Cortés-Pérez, Y. A., Arellano-Reynoso, B., et al. (2018). First genome sequencing and comparative analyses of *Corynebacterium pseudotuberculosis* strains from Mexico. *Stand. Genomic Sci.* 13:21. doi: 10.1186/s40793-018-0325-z

Peel, M. M., Palmer, G. G., Stacpoole, A. M., and Kerr, T. G. (1997). Human lymphadenitis due to *Corynebacterium pseudotuberculosis*: report of ten cases from Australia and review. *Clin. Infect. Dis.* 24, 185–191. doi: 10.1093/clinids/24.2.185

Purohit, N., Chouhan, D., and Choudhary, R. (1985). Lymphangitis in the camel. *Agri. Pract.* 6, 23–24.

Radwan, A. I., El-Magawry, S., Hawari, A., Al-Bekairi, S. I., and Rebleza, R. M. (1989). *Corynebacterium pseudotuberculosis* infection in camels (*Camelus dromedarius*) in Saudi Arabia. *Trop. Anim. Health Prod.* 21, 229–230.

Retamal, P., Ríos, M., Cheuquepán, F., Abalos, P., Pizarro-Lucero, J., Borie, C., et al. (2011). Host associated polymorphisms in the *Corynebacterium pseudotuberculosis* rpoB gene sequence. *Vet. Microbiol.* 151, 400–403. doi: 10.1016/j.vetmic.2011.03.012

Rhodes, D. M., Magdesian, K. G., Byrne, B. A., Kass, P. H., Edman, J., and Spier, S. J. (2015). Minimum inhibitory concentrations of equine *Corynebacterium pseudotuberculosis* isolates (1996-2012). *J. Vet. Intern. Med.* 29, 327–332. doi: 10.1111/jvim.12534

Samartsev, A. (1950). Infectious pustular dermatitis in camels. *Proc. Kazakh Res. Vet. Inst.* 5, 190–197.

Samen, U., Gottschalk, B., Eikmanns, B. J., and Reinscheid, D. J. (2004). Relevance of peptide uptake systems to the physiology and virulence of *Streptococcus agalactiae*. *J. Bacteriol.* 186, 1398–1408. doi: 10.1128/JB.186.5.1398-1408.2004

Songer, J. G. (1997). Bacterial phospholipases and their role in virulence. *Trends Microbiol.* 5, 156–161. doi: 10.1016/S0966-842X(97)01005-6

Sting, R., Geiger, C., Rietschel, W., Blazey, B., Schwabe, I., Rau, J., et al. (2022). *Corynebacterium pseudotuberculosis* infections in Alpacas (*Vicugna pacos*). *Animals* 12:1612. doi: 10.3390/ani12131612

Sutherland, S. S., Speijers, E. J., and Andres, B. (1989). Comparison of the exotoxins of four strains of *Corynebacterium pseudotuberculosis*. *Res. Vet. Sci.* 47, 190–194.

Tawab, A. A. A. E., Rizk, A. M., Afifi, S. E., and Mohamed, S. R. (2019). *Corynebacterium pseudotuberculosis* infection in small ruminant and molecular study of virulence and resistance genes in Beni-Suef governorate. *Benha Vet. Med. J.* 37, 122–127. doi: 10.21608/BVMJ.2019.18710.1125

Tejedor-Junco, M. T., Lupiola, P., Schulz, U., and Gutierrez, C. (2008). Isolation of nitrate-reductase positive *Corynebacterium pseudotuberculosis* from dromedary camels. *Trop. Anim. Health Prod.* 40, 165–167. doi: 10.1007/s11250-007-9077-2

Wang, X., Li, J., and Wang, L. (2021). Effect of *Mycobacterium tuberculosis* infection on the expression of IL-12 in mouse spleen and its correlation with body mass ratio and

organ index of mice. *Int. J. Clin. Exp. Med.* 20, 1132–1135. doi: 10.3969/j.issn.1671-4695.2021.11.004

Wang, R., Lin, C., Chi, X. L., Chen, S., and Zhang, X. (2021). Isolation and identification of *Corynebacterium pseudotuberculosis* from goats and histopathological observation of infected mice. *Chin. J. Vet. Sci.* 41, 413–422. doi: 10.16303/j.cnki.1005-4545.2021.12.18

Warnes, S. L., Highmore, C. J., and Keevil, C. W. (2012). Horizontal transfer of antibiotic resistance genes on abiotic touch surfaces: implications for public health. *MBio* 3, e412–e489. doi: 10.1128/mBio.00489-12

Wernery, U. (2012). Caseous lymphadenitis (Pseudotuberculosis) in camelids. *J. Camel Pract. Res.* 19, 21–27.

Wernery, U., Kinne, J, and Schuster, R. (2014). *Camelid infectious disorders* Paris OIE Book.

Xiong, H., Wei, B., Wei, R., Yang, N., and Qi, M. (2013). Calculation of median lethal dose (LD50) for Yersinia pestis by SPSS package. *Chin. J. Zoonoses.* 29, 1127–1130. doi: 10.3969/cjz.j.issn.1002-2694.2013.11.020

Zhang, M., Li, H., and Zhou, Z. (2015). Diagnosis and drug sensitivity test of *Corynebacterium pseudotuberculosis* in Goats in Dazhou, Sichuan. *Chin. J. Vet. Med.* 51, 54–56. doi: 10.3969/j.issn.0529-6005.2015.12.019

Zhang, Z., Teng, Z., Ye, B., Yang, Z., and Zhu, C. (1989). Diagnosis of cutaneous *Corynebacterium pseudotuberculosis* infection in Buffalo. *Chin. J. Pre. Vet.* 1, 20–21.

Zhou, Z., Li, H., Zhang, M., Wang, Z., Zhou, R., Hu, S., et al. (2016). Genome sequence of *Corynebacterium pseudotuberculosis* strain XH02 isolated from a Boer Goat in Xuanhan, China. *Genome Announc.* 4, e1316–e1329. doi: 10.1128/genomeA.01329-16

Zhu, L., and Lei, L. (2001). Diagnosis and treatment of psuedotuberculosis in deer. *Chin. Vet. Sci.* 31, 42–43. doi: 10.3969/j.issn.1673-4696.2001.12.022

frontiers | Frontiers in Microbiology

TYPE Original Research
PUBLISHED 27 July 2023
DOI 10.3389/fmicb.2023.1229950

Check for updates

OPEN ACCESS

EDITED BY
Hong Yin,
Chinese Academy of Agricultural Sciences (CAAS), China

REVIEWED BY
Rosa Estela Quiroz Castañeda,
Instituto Nacional de Investigaciones Forestales, Agrícolas y Pecuarias (INIFAP), Mexico
Zhijie Liu,
Chinese Academy of Agricultural Sciences (CAAS), China

*CORRESPONDENCE
Abid Ali
✉ uop_ali@yahoo.com
Tetsuya Tanaka
✉ k6199431@kadai.jp

RECEIVED 30 May 2023
ACCEPTED 03 July 2023
PUBLISHED 27 July 2023

CITATION
Ali A, Obaid MK, Almutairi MM, Alouffi A, Numan M, Ullah S, Rehman G, Islam ZU, Khan SB and Tanaka T (2023) Molecular detection of *Coxiella* spp. in ticks (Ixodidae and Argasidae) infesting domestic and wild animals: with notes on the epidemiology of tick-borne *Coxiella burnetii* in Asia.
Front. Microbiol. 14:1229950.
doi: 10.3389/fmicb.2023.1229950

COPYRIGHT
© 2023 Ali, Obaid, Almutairi, Alouffi, Numan, Ullah, Rehman, Islam, Khan and Tanaka. This is an open-access article distributed under the terms of the Creative Commons Attribution License (CC BY). The use, distribution or reproduction in other forums is permitted, provided the original author(s) and the copyright owner(s) are credited and that the original publication in this journal is cited, in accordance with accepted academic practice. No use, distribution or reproduction is permitted which does not comply with these terms.

Molecular detection of *Coxiella* spp. in ticks (Ixodidae and Argasidae) infesting domestic and wild animals: with notes on the epidemiology of tick-borne *Coxiella burnetii* in Asia

Abid Ali[1]*, Muhammad Kashif Obaid[1], Mashal M. Almutairi[2], Abdulaziz Alouffi[3], Muhammad Numan[1], Shafi Ullah[1], Gauhar Rehman[1], Zia Ul Islam[4], Sher Bahadar Khan[5] and Tetsuya Tanaka[6]*

[1]Department of Zoology, Abdul Wali Khan University Mardan, Mardan, Khyber Pakhtunkhwa, Pakistan, [2]Department of Pharmacology and Toxicology, College of Pharmacy, King Saud University, Riyadh, Saudi Arabia, [3]King Abdulaziz City for Science and Technology, Riyadh, Saudi Arabia, [4]Department of Biotechnology, Abdul Wali Khan University Mardan, Mardan, Khyber Pakhtunkhwa, Pakistan, [5]College of Animal Husbandry and Veterinary Sciences, Abdul Wali Khan University Mardan, Mardan, Khyber Pakhtunkhwa, Pakistan, [6]Laboratory of Infectious Diseases, Joint Faculty of Veterinary Medicine, Kagoshima University, Kagoshima, Japan

Tick-borne *Coxiella* spp. are emerging in novel regions infecting different hosts, but information regarding their occurrence is limited. The purpose of this study was the molecular screening of *Coxiella* spp. in various ticks infesting goats, sheep, camels, cattle, wild mice, and domestic fowls (*Gallus gallus domesticus*) in various districts of Khyber Pakhtunkhwa, Pakistan. Morphologically identified tick species were confirmed by obtaining their *cox1* sequences and were molecularly screened for *Coxiella* spp. by sequencing *GroEL* fragments. Almost 345 out of 678 (50.9%) hosts were infested by nine tick species. Regarding the age groups, the hosts having an age >3 years were highly infested (192/345, 55.6%), while gender-wise infestation was higher in female hosts (237/345, 68.7%). In collected ticks, the nymphs were outnumbered (613/1,119, 54.8%), followed by adult females (293/1,119, 26.2%) and males (213/1,119, 19.7%). A total of 227 ticks were processed for molecular identification and detection of *Coxiella* spp. The obtained *cox1* sequences of nine tick species such as *Hyalomma dromedarii, Hyalomma anatolicum, Haemaphysalis cornupunctata, Haemaphysalis bispinosa, Haemaphysalis danieli, Haemaphysalis montgomeryi, Rhipicephalus haemaphysaloides, Rhipicephalus microplus*, and *Argas persicus* showed maximum identities between 99.6% and 100% with the same species and in the phylogenetic tree, clustered to the corresponding species. All the tick species except *Ha. danieli* and *R. microplus* were found positive for *Coxiella* spp. (40/227, 17.6%), including *Coxiella burnetii* (15/40, 6.7%), *Coxiella* endosymbionts (14/40, 6.3%), and different *Coxiella* spp. (11/40, 4.9%). By the BLAST results, the *GroEL* fragments of *Coxiella* spp. showed maximum identity to *C. burnetii*, *Coxiella* endosymbionts, and *Coxiella* sp., and phylogenetically clustered to the corresponding species. This is the first comprehensive report regarding the genetic characterization of *Coxiella* spp. in Pakistan's ticks infesting domestic and wild hosts. Proper surveillance and management measures should be undertaken to avoid health risks.

KEYWORDS

ticks, *cox1*, *Coxiella burnetii*, *GroEL*, domestic and wild animals, Pakistan

Introduction

Ticks are hematophagous ectoparasites, actively contributing to transmitting infectious agents to wild and domestic animals and humans (De la Fuente et al., 2017). Numerous ticks act as distinguished vectors and reservoirs for various pathogens, including bacteria causing rickettsiosis, anaplasmosis, Lyme disease, viruses such as Powassan, and protozoan agents such as *Theileria* spp. and *Babesia* spp. (De la Fuente et al., 2017; Karim et al., 2017; Rochlin and Toledo, 2020; Ali et al., 2021). Aside from transmitting various infectious agents, ticks are hosts to many endosymbionts and a diversified microbiome (Špitalská et al., 2018).

Among the bacterial genus *Coxiella* having one pathogenic species, *Coxiella burnetii* is a Gram-negative obligate intracellular bacterium distributed worldwide except in New Zealand and French Polynesia (Musso et al., 2014; Eldin et al., 2017). Common reservoirs of *C. burnetii* are domestic mammals, including cattle, sheep, goats, and camels as well as reptiles, birds, and ticks (Anderson et al., 2013; Abdel-Moein and Hamza, 2017), and have the potential to cause query (Q) fever (Musso et al., 2014). The Q-fever was reported for the first time in 1935 from Australia as an outbreak of febrile illness with flu-like symptoms (Derrick, 1937), and its causative agent was initially named *Rickettsia burnetii*, but later on renamed as *C. burnetii* (Philip, 1948). *Coxiella* spp. have been isolated from almost 40 tick species, and hence considered as its tick-borne transmission to animals and humans (Eklund et al., 1947; Beaman and Hung, 1989; Duron et al., 2014). Tick species, including *Hyalomma dromedarii, Hyalomma anatolicum, Hyalomma scupense, Rhipicephalus microplus*, and *Rhipicephalus annulatus*, may serve as vector reservoirs for the transmission of *C. burnetii* in Pakistan (Karim et al., 2017). *Coxiella*-like endosymbionts were also found in various tick species, and an obligatory mutualism between this bacteria and host ticks has been proven (Smith et al., 2015).

Ticks can transmit *Coxiella* spp. both transovarially and transstadially to their offspring. Infected ticks excrete enormous amounts of *Coxiella* spp. in their feces, contaminating the skin of host animals and playing a significant role in the spread of *Coxiella* infection (Cong et al., 2015; Seo et al., 2016). *Coxiella burnetii* may resist harsh environmental factors, for instance, dry and hot weather, desiccation, and other antiseptics. As it may affect the productive and reproductive abilities, humans and animals could face long-term infection risks (Ullah et al., 2019). Various techniques have been effectively followed for the surveillance of *C. burnetii* infection. Still, ELISA is considered an effective technique for its serological diagnosis. In combination with sequencing, PCR is believed to be the best technique for the molecular identification and genetic characterization of *C. burnetii* (Niemczuk et al., 2014; Bontje et al., 2016).

Coxiella spp. have been detected in different tick species, animals, humans, and soil samples in Asia that have been reported in various studies. *Coxiella burnetii* is the causative agent of Q-fever, one of the ignored zoonoses in developing countries, including Pakistan. To the best of our knowledge, approximately 24 studies from 1955 to 2022 regarding this infection have been reported in Pakistan, and Q-fever in humans, goats, sheep, cattle, buffaloes, as well as rodents has been serologically documented (Ahmed, 1987; Ullah et al., 2019; Ali et al., 2022a; Hussain et al., 2022). The *C. burnetii* is also considered a soil-borne pathogen as its isolation has been confirmed from soil samples (Shabbir et al., 2015). Due to the information dearth regarding numerous tick-borne pathogens (TBPs) that infect ruminants and other animals in Pakistan, substantial research is required to investigate the genetic composition of various TBPs, specifically *Coxiella* spp. Hence, this study aimed to molecularly characterize different tick species infesting domestic and wild animals and screen out the associated *Coxiella* spp. in Pakistan and summarize the association of *Coxiella* spp. with ticks infesting various hosts in Asia.

Materials and methods

Ethical considerations

The Advance Studies and Research Board (ASRB: Dir/A&R/AWKUM/2022/9396) of the Department of Zoology, Abdul Wali Khan University Mardan, Pakistan, approved prior consent for this study. Additionally, permission was taken from the owners of the animals to observe hosts and ticks collection. All the rules regarding animal welfare regulations were followed while handling the animals.

Description of the study area and sampling sites

Different districts including Lakki Marwat (32.5993° N, 70.9160° E), Mansehra (34.3271° N, 73.1992° E), Bajaur (34.7522° N, 71.5162° E), Dir Upper (35.3274° N, 72.0907° E), Dir Lower (34.8364° N, 71.8964° E), Abbottabad (34.1534° N, 73.2215° E), Buner (34.459129° N, 72.557252° E), Charsadda (34.161297° N, 71.755377° E), Chitral (35.727064° N, 71.759794° E), and Nowshera (33.998608° N, 71.999144° E) of Khyber Pakhtunkhwa were selected for the current study. These study locations have desertic plains, arid plains, arid hilly, humid plains, and hilly areas with variations in their climatic conditions, altitude, and seasons (winter, spring, summer, and autumn). The summer season is comparatively hot and longer in district Lakki Marwat than in other districts; however, snowfall occurs in winter in the districts of Chitral, Mansehra, Buner, Bajaur, Dir Upper, Dir Lower, and Abbottabad (climate-data.org; accessed on 20 February 2023). Goats, sheep, camels, and cattle are the livestock of the region that are intended for producing dairy products and transportation. These transhumant animals move from one place to another within the district for food and natural pastures. Their diet and resources depend upon climatic conditions that remarkably vary spatiotemporally. The Global Positioning System was used for the geographical coordinates of the districts as mentioned above and designed the study map through ArcGIS v 10.3.1 (Figure 1).

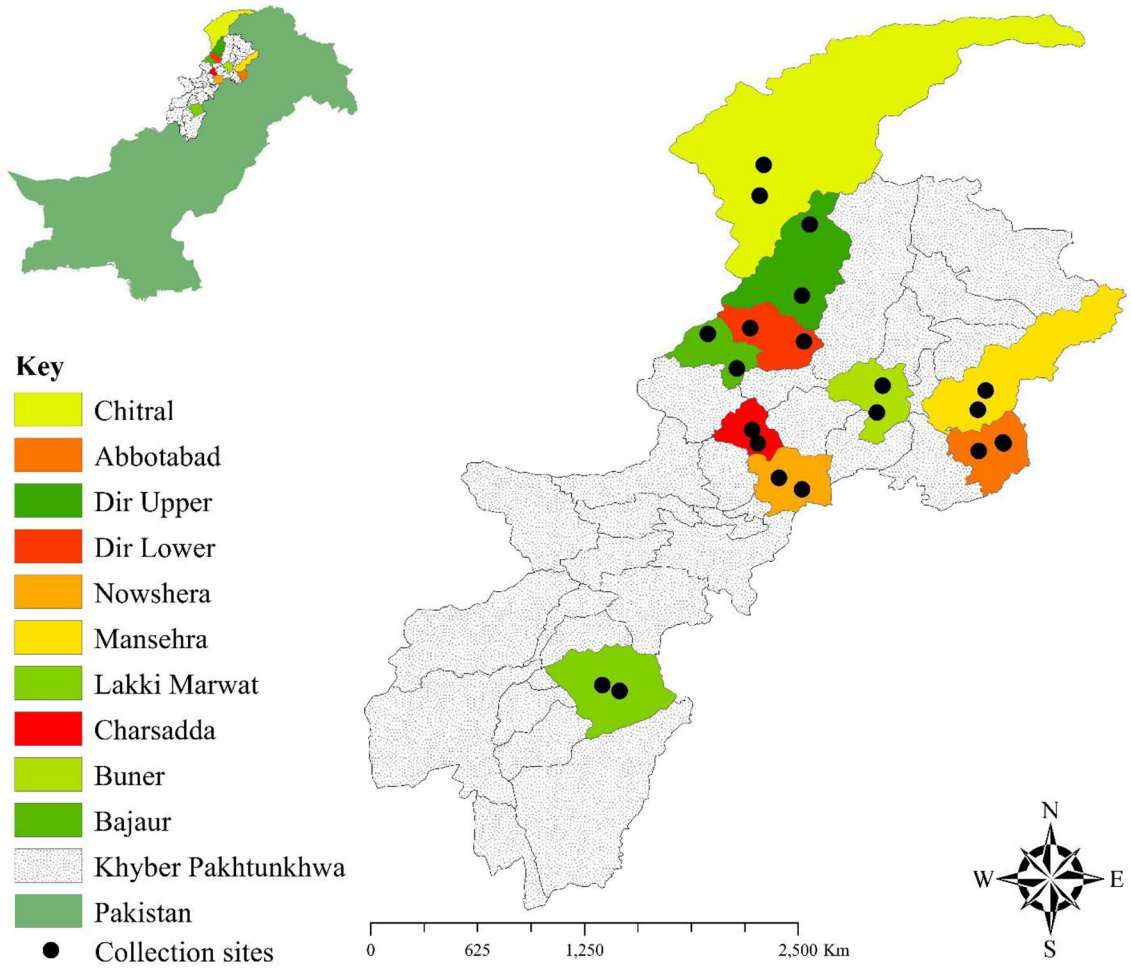

FIGURE 1
Map showing the collection sites where ticks were collected.

Tick collection and their morphological identification

The herds of goats, sheep, camels, and cattle were visited for tick collection from September 2021 to August 2022. Moreover, wild mice captured by local farmers on agricultural land and domestic fowls (*Gallus gallus domesticus*) were also examined for tick specimens. Tick specimens were collected manually from different hosts in the study districts. The collected ticks were morphologically identified under a stereomicroscope (SZ61, Olympus, Japan) using available standard morphological keys (Hoogstraal and Kaiser, 1959; Hoogstraal and Varma, 1962; Hoogstraal and Trapido, 1966; Dhanda and Kulkarni, 1969; Kohls et al., 1970; Cerný and Hoogstraal, 1977; Apanaskevich, 2003; Apanaskevich et al., 2008; Ahmad et al., 2022; Ali et al., 2022b). The identified tick species were categorized according to species, gender, and nymph stage or adult stage, and then preserved in 100% ethanol at room temperature before further analyses.

DNA extraction and molecular screening

The preserved ticks were washed with 70% ethanol, followed by their immersion in distilled water for 10 min to eliminate the external contamination, and subsequently dried on a sterile filter paper. A subset of 227 (137 N, 49 F, and 41 M) ticks including 65 *Ha. cornupunctata* (41 N, 14 F, and 10 M), 28 *Ha. montgomeryi* (17 N, 6 F, and 5 M), 28 *Hy. anatolicum* (17 N, 6 F, and 5 M), 27 *A. persicus* (17 N, 6 F, and 4 M), 23 *R. haemaphysaloides* (15 N, 5 F, and 3 M), 19 *R. microplus* (9 N, 5 F, and 5 M), 19 *Ha. bispinosa* (11 N, 4 F, and 4 M), 12 *Hy. dromedarii* (7 N, 1 F, and 4 M), and 6 *Ha. danieli* (3 N, 2 F, and 1 M) were randomly selected and used individually for DNA extraction. Each stage of the morphologically identified tick species was individually crushed using sterile scissors to extract genomic DNA through the standard protocol of the phenol–chloroform method (Sambrook et al., 1989).

The whole extracted genomic DNA of each morphologically identified tick species (each stage) was individually used to amplify *cox1* fragments by utilizing species-specific primers in a

TABLE 1 Primers and PCR cycling conditions used in the current study.

Gene	Sequence (5-3)	Amplicon size	Cycling conditions	References
cox1	HCO2198: TAAACTTCAGGGTGACCAAAAAATCA	710 bp	$\frac{98^\circ C}{30\ sec} \rightarrow 40X\left[\frac{98^\circ C}{10\ sec} \rightarrow \frac{63^\circ C}{20\ sec} \rightarrow \frac{72^\circ C}{25\ sec}\right] \rightarrow \frac{72^\circ C}{5\ min} \rightarrow 10^\circ C$	Folmer et al., 1994
	LCO1490: GGTCAACAAATCATAAAGATATTGG			
GroEL	CoxGrF1: * TTTGAAAAYATGGGCGCKCAAATGGT	655 bp	$\frac{95^\circ C}{3\ min} \rightarrow 30X\left[\frac{95^\circ C}{30\ sec} \rightarrow \frac{56^\circ C}{30\ sec} \rightarrow \frac{72^\circ C}{1.5\ min}\right] \rightarrow \frac{72^\circ C}{7\ min} \rightarrow 10^\circ C$	Duron et al., 2014
	CoxGrR2: * CGRTCRCCAAARCCAGGTGC			
	CoxGrF2: ** GAAGTGGCTTCGCRTACWTCAGACG	619 bp		
	CoxGrFR1: ** CCAAARCCAGGTGCTTTYAC			

*First run of nested PCR. **Second run of nested PCR.

conventional PCR (Table 1). Nested PCR was performed to amplify the *GroEL* fragment of *Coxiella* spp. (GE-96G, BIOER, Hangzhou, China). In nested PCR, two pairs of primers were used for the said purpose (Table 1). PCR reaction mixtures were performed in 25 μL, comprised of 1 μL of each primer at a concentration of 10 pmol/μL (first pair of primers in case of *GroEL*), 8.5 μL PCR water, 2 μL (100 ng/μL) genomic DNA, and 12.5 μL Dream*Taq* MasterMix (2×) (Thermo Fisher Scientific, Inc., Waltham, MA, USA). However, 2 μL of PCR product from the first PCR amplified reaction was used instead of genomic DNA in the second PCR run (in the case of *GroEL*) along with the second pair of primers at the same concentration. In each PCR reaction, PCR water was taken as a negative control, while *Hyalomma scupense* and *Rickettsia massiliae* DNA were taken as a positive control for ticks and *Coxiella*, respectively. The amplified products were loaded in 2% agarose gel to observe the expected band through the Gel Documentation System (BioDoc-It™ Imaging Systems, UVP, LLC, Upland, CA, USA). PCR amplified products were purified *via* GeneClean II Kit (Qbiogene, Il-lkirch, France) following the manufacturer's protocol. The amplified amplicons were sequenced bidirectionally through the Sanger-based sequencing method (Macrogen, Inc., Seoul, South Korea).

Sequences and phylogenetic analyses

The chromatograms of all the obtained sequences were manually observed and trimmed for purification purposes to remove the contaminated and poor reading regions through SeqMan V. 5 (DNASTAR, Inc., Madison, WI, USA). Final trimmed sequences were subjected to Basic Local Alignment Search Tool (BLAST) (Altschul et al., 1990) at National Center for Biotechnology Information to get the high identity sequences in FASTA format. ClustalW multiple alignments (Thompson et al., 1994) were used to align all the downloaded sequences along with the obtained and selected outgroup sequences in BioEdit Sequence Alignment Editor V.7.0.5 (Raleigh, NC, USA) (Hall et al., 2011). The phylogenetic trees based on partial fragments of *cox1* and *GroEL* were constructed in MEGA-X (Molecular Evolutionary Genetics Analysis) (Kumar et al., 2018) through the neighbor-joining method (Tamura-Nei model) and the Maximum Parsimony method (Tamura-Nei model) (Tamura and Nei, 1993) with support of 1000 bootstrapping replicons, respectively. The coding fragments (*cox1* and *GroEL*) were aligned using MUSCLE (Edgar, 2004).

Literature search

The literature search was conducted using databases such as PubMed, Google Scholar, and Web of Sciences, to overview the published studies regarding the detection of *C. burnetii* in different ticks, animals, humans, or soil in Asia. The keywords used for the search were as follows: tick(s), small ruminant(s), livestock, *C. burnetii*, Coxiellosis, and Q-fever. Combinations of the aforementioned various keywords were used to retrieve full-text research articles, review articles, short communications, and conference papers. Reference lists of retrieved articles were screened to identify relevant articles (accessed on 16 April 2023) (Table 2).

Results

Hosts prevalence

The highest number of observed hosts (374/678, 55.2%) were included in a group having age > 3 years, followed by various hosts (192/678, 28.3%) having age 1–3 years, and the lowest numbers of observed hosts (112/678, 16.5%) belonging to the age group having age <1 year. Different hosts having age >3 years were highly infested (192/345, 55.6%), while animals having age ≤1 year were least infested (62/345, 18.0%). The examined and infested female hosts were more predominant in number (486/678; 71.7%, 237/345; 68.7%) than male hosts (192/678; 28.3%, 108/345; 31.3%). The highest number of infested hosts was recorded in summer (June–August) (146/345, 42.3%), followed by spring (March–May) (99/345, 28.7%), autumn (September–November) (65/345, 18.8%), and winter (December–February) (35/345, 10.4%), respectively (Table 3).

TABLE 2 *Coxiella burnetii* detected in different ticks, animals, humans, or soil samples in Asia.

Country/year	Tick spp./source	Detected/infested host	Serologically/molecularly	Reference
Abu Dhabi/2021	Blood	Camels	Serologically	El Tigani-Asil et al., 2021
Afghanistan/2012–2013	Blood	Humans	Serologically	Akbarian et al., 2015
		Livestock		
Armenia/1971-1974	Blood	Humans	Serologically	Tarasevič et al., 1976
		Cattle		
Azerbaijan/2018	Milk	Goats, sheep	Molecularly (PCR)	Khademi et al., 2020
Bangladesh/2018-2021	Blood	Cattle and goats, Humans	Serologically	Chakrabartty et al., 2021
	Milk samples	Cattle	Molecularly (PCR)	
Bhutan/2014-2015	Blood	Humans (patients)	Serologically and Molecularly (PCR)	Tshokey et al., 2018
Bhutan/2015		Goats	Serologically	Tshokey et al., 2019
Bangladesh/2007-2008	Blood	Cattle, goats, sheep	Serologically	Rahman et al., 2016
	Placenta	Sheep	Molecularly (PCR)	
Cambodia/2019	Blood	Goats	Serologically	Siengsanan-Lamont et al., 2023
China	Blood	Humans	Serologically and Molecularly (PCR)	El-Mahallawy et al., 2016
China/2018	Tissue (spleens)	Hedgehogs	Molecularly (PCR and sequencing)	Gong et al., 2020
China/2018-2019	*D. nuttalli*	Cattle, sheep	Molecularly (PCR and sequencing)	Ni et al., 2020
	D. pavlovskyi			
	D. silvarum			
	D. niveus			
	Hy. rufipes			
	Hy. anatolicum			
	Hy. asiaticum			
	R. sanguineus			
	Ha. punctata			
Cyprus	Blood	Humans	Serologically	Psaroulaki et al., 2006
		Goats and sheep		
	R. sanguineus and *Hyalomma* spp.	Goats and sheep	Molecularly (PCR)	
Hong Kong/2008	Blood	Humans	Serologically	Chan et al., 2010
India	Blood	Humans	Serologically	Sahu et al., 2018
India/2018-2019	Blood	Goats	Serologically and Molecularly (PCR and sequencing)	Patra et al., 2020
	R. microplus			
Iran/2013-2016	Blood	Humans	Molecularly (PCR)	Esmaeili et al., 2019
Iran/2017–2018	Aborted samples	Cattle, sheep, and goats	Molecularly (PCR)	Mohabati Mobarez et al., 2021
	Spleen, liver, and cotyledons			
Iraq/2019	Blood	Camels	Serologically and Molecularly (PCR and sequencing)	Al-Graibawi et al., 2021
Iraq/2007	Topsoil and airborne dust		Molecularly (PCR)	Leski et al., 2011
Iraq/2018-2019	Blood and milk	Cows	Serologically and Molecularly (PCR and sequencing)	Gharban and Yousif, 2020

(Continued)

TABLE 2 (Continued)

Country/year	Tick spp./source	Detected/infested host	Serologically/molecularly	Reference
Iraq/2005	Blood	Humans (US military)	Serologically	Royal et al., 2013
Israel/2005	Blood	Humans	Serologically and Molecularly (PCR)	Amitai et al., 2010
Israel	*Hy. dromedarii*	Camels	Molecularly (PCR)	Mumcuoglu et al., 2022
	Hy. aegyptium	Tortoises		
Indonesia/2017	Tissue	Cows, goats, sheep	Molecularly (PCR and sequencing)	Rini et al., 2022
Japan/1996–1997	Blood	Humans	Molecularly (PCR)	Kato et al., 1998
Jordan/2015–2016	Blood	Humans	Serologically	Obaidat et al., 2019
Jordan/2015–2017	Blood	Goats, sheep	Serologically	Lafi et al., 2020
Kazakhstan/2021–2022	*D. marginatus* and *Hy. anatolicum*	Cattle	Molecularly (PCR and sequencing)	Sultankulova et al., 2022
Korea/2016	Blood	Humans	Molecularly (PCR and sequencing)	Lee et al., 2020
Kuwait/2007	Topsoil and airborne dust		Molecularly (PCR)	Leski et al., 2011
Lebanon/2015	Blood	Humans	Serologically	Dabaja et al., 2018
Lebanon/2014	*R. annulatus*	Cattle, sheep, goats	Molecularly (PCR)	Dabaja et al., 2020
	R. turanicus			
	Hy. anatolicum			
	R. sanguineus			
	R. bursa			
	Milk		Serologically	
Laos/2016–2017	Blood	Goats	Serologically	Burns et al., 2018
Malaysia/2012–2013	Blood	Humans	Serologically	Khor et al., 2018
Malaysia/2013	Blood and vaginal sample	Cattle	Molecularly (PCR and sequencing)	Nurkunasegran et al., 2017
	Amblyomma and *Dermacentor* spp.	Rodents		
	Haemaphysalis spp.	Vegetation		
	R. sanguineus and *Dermacentor* spp.	Dogs		
Mongolia/2008–2015	Blood	Snow leopards	Serologically	Esson et al., 2019
	Ticks		Molecularly (PCR)	
Nepal/2016	Blood	Cattle	Serologically	Panth et al., 2017
Oman/2019	Blood/bone	Humans	Serologically	Al-Kindi et al., 2022
Pakistan	Blood	Humans, goats, sheep, buffaloes, cows, Rodents	Serologically	Ahmed, 1987
Pakistan	Soil	Soil	Molecularly (PCR)	Shabbir et al., 2015
Pakistan	Blood	Camels	Serologically	Hussain et al., 2022
Pakistan/2016	Ticks and blood	Goats and sheep	Serologically and Molecularly (PCR)	Ullah et al., 2019
Pakistan	Blood	Humans	Serologically	Ali et al., 2022a
Palestine/2016	Blood	Rams	Serologically	Jalboush and Alzuheir, 2017
Qatar/2005–2006	Blood	Humans (US military)	Serologically	Royal et al., 2013
Saudi Arabia	Blood, milk, feces, and urine	Camels, cattle, and goats	Molecularly (PCR)	Mohammed et al., 2014

(Continued)

TABLE 2 (Continued)

Country/year	Tick spp./source	Detected/infested host	Serologically/molecularly	Reference
Saudi Arabia/2011–2013	Blood	Humans	Serologically	Almogren et al., 2013
South Korea/2007–2013	Blood	Horses	Serologically	Seo et al., 2016
Taiwan/2007	Blood	Humans	Serologically	Chang et al., 2010
Taiwan/2009–2011	Blood	Dogs	Molecularly (PCR and sequencing)	Chou et al., 2014
Thailand/2012–2013	Blood	Humans	Serologically and Molecularly (PCR)	Doung-Ngern et al., 2017
		Cattle		
	Milk	Cattle		
Turkey	Blood	Cows, sheep, goats	Serologically	Ozgen et al., 2022
Turkey/2007	Blood	Humans	Serologically	Kilic et al., 2008
Tunisia/2015–2017	*Hy. impeltatum*	Camels	Molecularly (PCR and sequencing)	Selmi et al., 2019
	Hy. dromedarii			
United Arab Emirates	Blood	Goats, sheep	Serologically	Barigye et al., 2022
Vietnam	Bone marrow	Humans (patient)	Molecularly (PCR)	Thi Vinh An et al., 2022

TABLE 3 Age, gender, and season-wise infestation rate of hosts.

Variables		Observed host (%)	Infested hosts (%)	Total infested/total observed (%)
Age	<1 year	112 (16.5)	62 (18.0)	345/678 (52.1)
	1–3 years	192 (28.3)	91 (26.4)	
	>3 years	374 (55.2)	192 (55.6)	
Gender	Female	486 (71.7)	237 (68.7)	345/678 (52.1)
	Male	192 (28.3)	108 (31.3)	
Seasons	Spring (March–May)	163 (24.0)	99 (28.7)	345/678 (52.1)
	Summer (June–August)	191 (28.2)	146 (42.3)	
	Autumn (September–November)	165 (24.3)	65 (18.8)	
	Winter (December–February)	159 (23.4)	35 (10.1)	

A total of 678 different hosts such as goats, sheep, camels, cattle, wild mice, and domestic fowls were examined for tick collection in the selected localities, of which other hosts (number = 345/678, 50.9%), including goats (78/149, 52.3%), sheep (75/136, 55.1%), camels (36/93, 38.7%), cattle (69/129, 53.5%), wild mice (15/48, 31.2%), and domestic fowls (72/123, 58.5%) were found tick infested. The highest prevalence of infested hosts was recorded in district Lakki Marwat (44/351, 12.5%), followed by Charsadda (36/351, 10.3%), Nowshera, Buner, Mansehra, and Abbottabad (35/351, 9.7%), Chitral (34/351, 9.7%), Dir Upper and Dir Lower (33/351, 9.4%), while least infestation rate was recorded in district Bajaur (31/351, 8.8%) (Table 4).

Ticks and their molecular analyses

Altogether, 1,119 ticks including nymphs (613/1,119, 54.8%), adult females (293/1,119, 26.2%), and males (213/1,119, 19.0%) were collected from infested hosts and were categorized into four genera (*Haemaphysalis, Hyalomma, Rhipicephalus*, and *Argas*). The highest number of collected tick species was *Ha. cornupunctata* (258/1,119, 23.1%), followed by *Hy. anatolicum* (209/1,119, 18.7%), *A. persicus* (146/1,119, 13.0%), *R. microplus* (137/1,119, 12.2%), *Ha. montgomeryi* (119/1,119, 10.6%), *R. haemaphysaloides* (97/1,119, 8.7%), *Ha. bispinosa* (92/1,119, 8.2%), *Hy. dromedarii* (47/1,119, 4.2%), and *Ha. danieli* (14/1,119, 1.2%). Genomic DNA was extracted from 227 morphologically identified ticks (137 N, 49 F, and 41 M), and all identified tick species were molecularly confirmed *via* sequencing of the *cox1* partial fragment (Table 4).

Screening of *Coxiella* in various ticks

Extracted DNA of 227 (20.3%) was used to amplify the fragments of *GroEL* of *Coxiella* spp. A total of 40/227 (17.6%) ticks were found positive for *Coxiella* spp., including *C. burnetii*

TABLE 4 Occurrence of ticks and molecular detection of *Coxiella* spp. in different districts of Khyber Pakhtunkhwa.

Districts	Hosts			Tick species	Ticks life stages	Molecularly analyzed (DNA extraction and PCR)	Molecularly screened *Coxiella* spp.							
	Animal type	Observed	Infested		(N, F, M) Total	(N, F, M) Total	*Coxiella burnetii* (OQ883856)	*Coxiella* endosymbiont (OQ883857)	*Coxiella* endosymbiont (OQ883858)	*Coxiella* sp. (OQ883859)	*Coxiella* sp. (OQ883860)	*Coxiella* sp. (OQ883861)	*Coxiella* sp. (OQ883862)	*Coxiella* sp. (OQ883863)
Lakki Marwat	Goats	19	8	*R. haemaphysaloides*	(5 N, 3 F, 1 M) 9	(1 N, 1 F) 2	–	–	–	–	–	–	–	–
				Hy. anatolicum	(7 N, 3 F, 2 M) 12	(1 N, 1 M) 2	–	–	–	–	–	–	–	–
				Ha. bispinosa	(6 N, 2 F, 3 M) 11	(1 N, 1 M) 2	–	–	–	–	–	–	–	–
	Sheep	18	7	*R. haemaphysaloides*	(5 N, 2 F, 1 M) 8	(2 N, 1 F) 3	–	–	–	–	–	–	–	–
				Ha. montgomeryi	(7 N, 2 F, 3 M) 12	(1 N, 1 M) 2	–	–	–	–	–	–	–	–
				Ha. cornupunctata	(5 N, 1 F, 3 M) 9	(1 N) 1	–	–	–	–	–	–	–	–
	Camels	31	13	*Hy. dromedarii*	(6 N, 3 F, 3 M) 12	(3 N, 1 F, 2 M) 6	2 N, 1 F	–	–	–	–	–	–	–
				Hy. anatolicum	(8 N, 4 F, 3 M) 15	(2 N, 1 F, 1 M) 4	1 N, 1 F	–	–	–	–	–	–	–
	Cattle	17	8	*R. microplus*	(10 N, 3 F, 4 M) 17	(1 N, 1 M) 2	–	–	–	–	–	–	–	–
				Hy. anatolicum	(6 N, 4 F, 1 M) 11	(1 N) 1	–	–	–	–	–	–	–	–
	Wild mice	4	2	*Ha. cornupunctata*	(4 N, 3 F) 7	(2 N, 1 F) 3	–	–	–	–	–	–	–	–
	Domestic fowls	17	6	*A. persicus*	(8 N, 4 F, 2 M) 14	(2 N, 1 F, 1 M) 4	–	–		–				
Charsadda	Goats	17	7	*Ha. cornupunctata*	(5 N, 3 F, 1 M) 9	(1 N, 1 F) 2	–	–	–	–	–	–	–	–
				Hy. anatolicum	(6 N, 3 F, 3 M) 12	(1 N, 1 M) 2	–	–	–	–	–	–	–	–
				Ha. bispinosa	(5 N, 2 F, 2 M) 9	(1 N, 1 F, 1 M) 3	–	–	–	–	–	–	–	–
	Sheep	15	5	*R. haemaphysaloides*	(4 N, 2 F, 2 M) 8	(1 N) 1	–	–	–	–	–	–	–	–
				Ha. montgomeryi	(7 N, 3 F, 2 M) 12	(1 N, 1 F, 1 M) 3	–	–	–	–	–	–	–	–
				Ha. cornupunctata	(5 N, 2 F, 2 M) 9	(1 N, 1 F) 2	–	–	–	–	–	–	–	–
	Camels	26	8	*Hy. dromedarii*	(7 N, 3 F, 2 M) 12	(1 N, 1 M) 2	–	–	–	–	–	–	–	–
				Hy. anatolicum	(5 N, 4 F, 2 M) 11	(1 N) 1	–	–	–	–	–	–	–	–

(Continued)

10.3389/fmicb.2023.1229950

TABLE 4 (Continued)

Districts	Hosts			Tick species	Ticks life stages	Molecularly analyzed (DNA extraction and PCR)	Molecularly screened *Coxiella* spp.							
	Animal type	Observed	Infested		(N, F, M) Total	(N, F, M) Total	*Coxiella burnetii* (OQ883856)	*Coxiella* endosymbiont (OQ883857)	*Coxiella* endosymbiont (OQ883858)	*Coxiella* sp. (OQ883859)	*Coxiella* sp. (OQ883860)	*Coxiella* sp. (OQ883861)	*Coxiella* sp. (OQ883862)	*Coxiella* sp. (OQ883863)
	Cattle	15	7	*R. microplus*	(10 N, 6 F, 1 M) 17	(1 N, 1 F, 1 M) 3	–	–	–	–	–	–	–	–
				Hy. anatolicum	(8 N, 4 F, 3 M) 15	(1 N, 1 F) 2	–	–	–	–	–	–	–	–
	Wild mice	11	3	*Ha. cornupunctata*	(4 N, 3 M) 7	(4 N, 1 F) 5	3 N, 1 F	–	–	–	–	–	–	–
	Domestic fowls	13	6	*A. persicus*	(9 N, 4 F, 3 M) 16	(1 N, 1 M) 2	–	–	–	–	–	–	–	–
Nowshera	Goats	19	7	*Ha. bispinosa*	(5 N, 3 F, 1 M) 9	(1 N, 1 F) 2	–	–	–	–	–	–	–	–
				Ha. cornupunctata	(6 N, 3 F, 3 M) 12	(1 N, 1 F, 1 M) 3	–	–	–	–	–	–	–	–
	Sheep	11	6	*R. haemaphysaloides*	(5 N, 4 F, 1 M) 10	(1 N) 1	–	–	–	–	–	–	–	–
				Ha. montgomeryi	(4 N, 2 F, 2 M) 8	(2 N) 2	–	–	–	–	–	–	–	–
	Camels	21	8	*Hy. dromedarii*	(7 N, 2 F, 3 M) 12	(1 N, 1 M) 2	–	–	–	–	–	–	–	–
	Cattle	13	6	*R. microplus*	(8 N, 4 F, 2 M) 14	(1 N, 1 F) 2	–	–	–	–	–	–	–	–
	Wild mice	3	1	*Ha. cornupunctata*	(4 N, 1 F, 1 M) 6	(1 N, 1 F) 2	–	–	–	–	–	–	–	–
	Domestic fowls	15	7	*A. persicus*	(9 N, 2 F, 3 M) 14	(2 N, 1 F) 3	–	–	–	–	–	–	–	–
Dir Upper	Goats	16	9	*Ha. cornupunctata*	(7 N, 3 F, 3 M) 13	(1 N, 1 F, 1 M) 3	–	–	–	–	–	–	–	–
				Ha. bispinosa	(6 N, 2 F, 3 M) 11	(1 N, 1 M) 2	–	–	–	–	–	–	–	1 N, 1 M
				Ha. danieli	(8 N, 4 F, 2 M) 14	(3 N, 2 F, 1 M) 6	–	–	–	–	–	–	–	–
	Sheep	15	7	*R. haemaphysaloides*	(5 N, 3 F, 2 M) 10	(1 N, 1 F) 2	–	–	–	–	–	–	–	–
				Ha. montgomeryi	(6 N, 2 F, 1 M) 9	(1 N, 1 F) 2	–	–	–	–	–	–	–	–
				Ha. cornupunctata	(7 N, 3 F, 2 M) 12	(1 N) 1	–	–	–	–	–	–	–	–
	Cattle	12	10	*R. microplus*	(9 N, 2 F, 4 M) 15	(1 N, 1 M) 2	–	–	–	–	–	–	–	–
	Wild mice	2	1	*Ha. cornupunctata*	(4 N, 2 F, 2 M) 8	(1 N) 1	–	–	–	–	–	–	–	–

(Continued)

10.3389/fmicb.2023.1229950

TABLE 4 (Continued)

Districts	Hosts			Tick species	Ticks life stages	Molecularly analyzed (DNA extraction and PCR)	Molecularly screened *Coxiella* spp.							
	Animal type	Observed	Infested		(N, F, M) Total	(N, F, M) Total	*Coxiella burnetii* (OQ883856)	*Coxiella* endosymbiont (OQ883857)	*Coxiella* endosymbiont (OQ883858)	*Coxiella* sp. (OQ883859)	*Coxiella* sp. (OQ883860)	*Coxiella* sp. (OQ883861)	*Coxiella* sp. (OQ883862)	*Coxiella* sp. (OQ883863)
	Domestic fowls	10	6	*A. persicus*	(7 N, 3 F, 2 M) 12	(1 N) 1	–	–	–	–	–	–	–	–
Dir Lower	Goats	13	10	*Ha. cornupunctata*	(5 N, 2 F, 2 M) 9	(5 N, 2 F, 1 M) 8	1 N, 1 F	2 N, 1 F	–	1 N, 1 M	–	–	–	–
				Ha. bispinosa	(6 N, 3 F, 3 M) 12	(1 N) 1	–	–	–	–	–	–	–	–
	Sheep	14	9	*Ha. montgomeryi*	(4 N, 2 F, 2 M) 8	(1 N) 1	–	–	–	–	–	–	–	–
				Ha. cornupunctata	(8 N, 3 F, 3 M) 14	(2 N, 1 F, 2 M) 5	1 N, 1 F, 2 M	–	–	–	–	–	–	–
	Cattle	13	5	*R. microplus*	(7 N, 4 F, 2 M) 13	(1 N) 1	–	–	–	–	–	–	–	–
				Hy. anatolicum	(9 N, 4 F, 2 M) 15	(1 N, 1 F) 2	–	–	–	–	–	–	–	–
	Wild mice	5	1	*Ha. cornupunctata*	(5 N, 5 F) 10	(1 N, 1 F) 2	–	–	–	–	–	–	–	–
	Domestic fowls	11	8	*A. persicus*	(8 N, 3 F, 3 M) 14	(1 N, 1 M) 2	–	–	–	–	–	–	–	–
Buner	Goats	14	7	*Ha. cornupunctata*	(5 N, 4 F, 2 M) 11	(2 N) 2	–	–	–	–	–	–	–	–
				Hy. anatolicum	(8 N, 3 F, 5 M) 16	(1 N) 1	–	–	–	–	–	–	–	–
				Ha. bispinosa	(6 N, 4 F) 10	(1 N) 1	–	–	–	–	–	–	–	–
	Sheep	13	10	*R. haemaphysaloides*	(5 N, 2 F, 2 M) 9	(1 N, 1 F) 2	–	–	–	–	–	–	–	–
				Ha. montgomeryi	(6 N, 5 F, 1 M) 12	(2 N, 1 F) 3	–	–	2 N, 1 F	–	–	–	–	–
				Ha. cornupunctata	(5 N, 4 F, 1 M) 10	(1 N) 1	–	–	–	–	–	–	–	–
	Cattle	11	9	*R. microplus*	(8 N, 4 F, 3 M) 15	(1 N, 1 F) 2	–	–	–	–	–	–	–	–
				Hy. anatolicum	(7 N, 3 F, 3 M) 13	(1 N, 1 M) 2	–	–	–	–	–	–	–	–
	Wild mice	3	1	*Ha. cornupunctata*	(5 N, 3 F, 1 M) 9	(1 N) 1	–	–	–	–	–	–	–	–
	Domestic fowls	13	8	*A. persicus*	(6 N, 5 F, 2 M) 13	(1 N, 1 F) 2	–	–	–	–	–	–	–	–

(Continued)

10.3389/fmicb.2023.1229950

TABLE 4 (Continued)

Districts	Hosts			Tick species	Ticks life stages	Molecularly analyzed (DNA extraction and PCR)	Molecularly screened *Coxiella* spp.							
	Animal type	Observed	Infested		(N, F, M) Total	(N, F, M) Total	*Coxiella burnetii* (OQ883856)	*Coxiella* endosymbiont (OQ883857)	*Coxiella* endosymbiont (OQ883858)	*Coxiella* sp. (OQ883859)	*Coxiella* sp. (OQ883860)	*Coxiella* sp. (OQ883861)	*Coxiella* sp. (OQ883862)	*Coxiella* sp. (OQ883863)
Mansehra	Goats	12	8	*Ha. cornupunctata*	(5 N, 2 F, 1 M) 8	(2 N, 1 F) 3	–	–	–	–	–	–	–	–
				Hy. anatolicum	(7 N, 3 F, 4 M) 14	(1 N) 1	–	–	–	–	–	–	–	–
	Sheep	10	9	*R. haemaphysaloides*	(6 N, 2 F, 3 M) 11	(3 N, 1 F, 2 M) 6	–	2 N, 1 F, 1 M	–	–	–	–	–	–
				Ha. montgomeryi	(4 N, 3 F) 7	(1 N, 1 F) 2	–	–	–	–	–	–	–	–
				Ha. cornupunctata	(6 N, 2 F, 2 M) 10	(2 N) 2	–	–	–	–	–	–	–	–
	Cattle	14	9	*R. microplus*	(9 N, 4 F, 3 M) 16	(1 N, 1 F) 2	–	–	–	–	–	–	–	–
				Hy. anatolicum	(7 N, 3 F, 4 M) 14	(1 N, 1 M) 2	–	–	–	–	–	–	–	–
	Wild mice	5	2	*Ha. cornupunctata*	(5 N, 2 F, 3 M) 10	(1 N) 1	–	–	–	–	–	–	–	–
	Domestic fowls	9	7	*A. persicus*	(9 N, 3 F, 4 M) 16	(2 N, 1 F) 3	–	–	–	–	–	–	–	–
Bajaur	Goats	16	6	*Ha. bispinosa*	(5 N, 4 F, 3 M) 12	(1 N) 1	–	–	–	–	–	–	–	–
				Ha. montgomeryi	(9 N, 3 F, 4 M) 16	(3 N, 1 F, 1 M) 5	–	–	–	–	–	–	–	–
				Ha. cornupunctata	(4 N, 5 F) 9	(2 N, 1 F) 3	–	–	–	1 F	–	–	–	–
	Sheep	17	7	*R. haemaphysaloides*	(6 N, 3 F, 3 M) 12	(2 N) 2	–	–	–	–	–	–	–	–
				Ha. montgomeryi	(8 N, 2 F, 4 M) 14	(3 N, 1 F, 1 M) 5	–	–	–	–	2 N	1 F	–	–
	Cattle	12	8	*Hy. anatolicum*	(7 N, 4 F, 3 M) 14	(1 N) 1	–	–	–	–	–	–	–	–
	Wild mice	8	1	*Ha. cornupunctata*	(5 N, 4 F, 1 M) 10	(1 N, 1 M) 2	–	–	–	–	–	–	–	–
	Domestic fowls	14	9	*A. persicus*	(8 N, 3 F, 3 M) 14	(1 N) 1	–	–	–	–	–	–	–	–
Abbottabad	Goats	13	9	*Ha. cornupunctata*	(6 N, 2 F, 4 M) 12	(1 N, 1 F, 1 M) 3	–	–	–	–	–	–	–	–
				Hy. anatolicum	(5 N, 2 F, 3 M) 10	(1 N) 1	–	–	–	–	–	–	–	–

(Continued)

10.3389/fmicb.2023.1229950

TABLE 4 (Continued)

Districts	Hosts			Tick species	Ticks life stages	Molecularly analyzed (DNA extraction and PCR)	Molecularly screened *Coxiella* spp.							
	Animal type	Observed	Infested		(N, F, M) Total	(N, F, M) Total	*Coxiella burnetii* (OQ883856)	*Coxiella* endosymbiont (OQ883857)	*Coxiella* endosymbiont (OQ883858)	*Coxiella* sp. (OQ883859)	*Coxiella* sp. (OQ883860)	*Coxiella* sp. (OQ883861)	*Coxiella* sp. (OQ883862)	*Coxiella* sp. (OQ883863)
				Ha. bispinosa	(4 N, 3 F, 1 M) 8	(3 N, 1 F, 1 M) 5	–	–	–	–	–	–	2 N, 1 F	–
	Sheep	12	6	*R. haemaphysaloides*	(7 N, 2 F, 3 M) 12	(1 N, 1 M) 2	–	–	–	–	–	–	–	–
				Ha. montgomeryi	(5 N, 3 F, 1 M) 9	(1 N) 1	–	–	–	–	–	–	–	–
				Ha. cornupunctata	(6 N, 4 F, 2 M) 12	(1 N, 1 M) 2	–	–	–	–	–	–	–	–
	Camels	15	7	*Hy. dromedarii*	(6 N, 4 F, 1 M) 11	(2 N) 2	–	–	–	–	–	–	–	–
				Hy. anatolicum	(9 N, 5 F, 14	(1 N, 1 F) 2	–	–	–	–	–	–	–	–
	Cattle	9	7	*R. microplus*	(9 N, 4 F, 3 M) 16	(1 N, 1 M) 2	–	–	–	–	–	–	–	–
	Wild mice	3	1	*Ha. cornupunctata*	(5 N, 2 M) 7	(2 N, 1 M) 3	–	–	–	–	–	–	–	–
	Domestic fowls	9	5	*A. persicus*	(8 N, 4 F, 3 M) 15	(1 N, 1 F) 2	–	–	–	–	–	–	–	–
Chitral	Goats	10	7	*Ha. cornupunctata*	(5 N, 2 F, 2 M) 9	(1 N, 1 M) 2	–	–	–	–	–	–	–	–
				Hy. anatolicum	(8 N, 3 F, 1 M) 12	(1 N, 1 F) 2	–	–	–	–	–	–	–	–
				Ha. bispinosa	(6 N, 2 F, 2 M) 10	(1 N, 1 F) 2	–	–	–	–	–	–	–	–
	Sheep	11	9	*R. haemaphysaloides*	(5 N, 3 F) 8	(2 N) 2	–	–	–	–	–	–	–	–
				Ha. montgomeryi	(7 N, 3 F, 2 M) 12	(1 N, 1 M) 2	–	–	–	–	–	–	–	–
				Ha. cornupunctata	(5 N, 3 F, 1 M) 9	(1 N) 1	–	–	–	–	–	–	–	–
	Cattle	13	6	*Hy. anatolicum*	(5 N, 3 F, 3 M) 11	(1 N, 1 F) 2	–	–	–	–	–	–	–	–
				R. microplus	(7 N, 4 F, 3 M) 14	(1 N, 1 F, 1 M) 3	–	–	–	–	–	–	–	–
	Wild mice	4	2	*Ha. cornupunctata*	(4 N, 2 F, 1 M) 7	(1 N) 1	–	–	–	–	–	–	–	–
	Domestic fowls	12	10	*A. persicus*	(9 N, 5 F, 4 M) 18	(5 N, 1 F, 1 M) 7	–	2 N, 1 F, 1 M	–	–	–	–	–	–
Total		**678**	**345** (50.9%)		(613 N, 293 F, 213 M) **1,119**	(137 N, 49 F, 41 M) **227**	**15** (6.7%)	**14** (6.3%)	**11** (4.9%)					

10.3389/fmicb.2023.1229950

(15, 6.7%), *Coxiella* endosymbionts (14, 6.3%), and *Coxiella* sp. (11, 4.9%). *Coxiella burnetii* was detected in ticks collected from camels (*Hy. dromedarii* and *Hy. anatolicum*) in the district of Lakki Marwat, wild mice (*Ha. cornupunctata*) in Charsadda, and goats and sheep (*Ha. cornupunctata*) in Dir Lower. *Coxiella* endosymbionts were detected in ticks collected from goats (*Ha. cornupunctata*) in district Dir Lower sheep (*Ha. montgomeryi* and *R. haemaphysaloides*) in Buner and Mansehra, and domestic fowls (*A. persicus*) in Chitral. *Coxiella* spp. were detected in ticks collected from goats (*Ha. bispinosa*) in the district of Dir Upper, from goats (*Ha. cornupunctata*) in Dir Lower, from goats and sheep (*Ha. cornupunctata* and *Ha. montgomeryi*) in Bajaur, and from goats (*Ha. bispinosa*) in Abbottabad (Table 4).

Phylogenetic analyses of the obtained sequences

All amplified PCR products were separately sequenced. The identical sequences were considered as a single consensus sequence. Trimmed and purified sequences of *cox1* fragments were obtained from nine tick species, including *Ha. cornupunctata, Ha. bispinosa, Ha. danieli, Ha. montgomeryi, Hy. anatolicum, Hy. dromedarii, R. haemaphysaloides, R. microplus*, and *A. persicus*. The BLAST results showed that the *cox1* fragments of the nine tick species were 99.6–100% identical to the corresponding species. Additionally, these sequences were phylogenetically clustered to the corresponding species reported from Pakistan, China, India, Bangladesh, Kazakhstan, Kenya, and Iran (Figure 2).

Based on the *GroEL* fragment, eight *GroEL* fragments of *Coxiella* spp. were detected in the aforementioned tick species except for *Ha. danieli* and *R. microplus*. By the BLAST results, the obtained *GroEL* fragment of *Coxiella* sp. (detected in *Ha. cornupunctata, Hy. dromedarii,* and *Hy. anatolicum*) showed maximum identity (99.8–100%) with the *C. burnetii* and phylogenetically clustered with the corresponding species reported from Slovakia (MG860513), China (ON455116), Russia (EF627450), USA (CP040059), and Thailand (MZ327921).

The obtained *GroEL* fragment of *Coxiella* spp. (detected in *Ha. cornupunctata*, *A. persicus*, and *R. haemaphysaloides*) showed 100% identity with the *Coxiella* endosymbiont reported from China (MZ367034 and MZ367036). Another *GroEL* fragment of *Coxiella* sp. (detected in *Ha. montgomeryi*) showed 99.8% maximum identity with the *Coxiella* endosymbiont reported from France (KP985488) and China (KP985490). Both partial fragments clustered with the corresponding *Coxiella* endosymbiont in the phylogenetic tree.

The BLAST results of the obtained *GroEL* fragments of *Coxiella* sp. OQ883859 (detected in *Ha. cornupunctata*) showed 88–90% maximum identity with *Coxiella* endosymbiont reported from the United Kingdom (KP985492), *Coxiella* sp. OQ883860 (detected in *Ha. montgomeryi*) showed 90.23% identity with *Coxiella* sp. reported from France (KP985502 and KP985500), Tunisia (KP985456), and Algeria (KP985472). The *Coxiella* sp. OQ883861 (detected in *Ha. montgomeryi*) showed 95.4% identity with *Coxiella* sp. reported from Chile (KJ459055) and Spain (MW287611), while *Coxiella* sp. OQ883862 (detected in *Ha. bispinosa*) showed 93.9% identity with *Coxiella* sp. reported from China (OK625731 and OK625732), and *Coxiella* sp. OQ883863 (detected in *Ha. bispinosa*) showed 91.3% identity with *Coxiella* sp. reported from China (OK625731 and OK625732). In the phylogenetic tree, all the obtained aforementioned *Coxiella* sp. sequences were clustered to the corresponding *Coxiella* sp. sequences (Figure 3).

The obtained *cox1* partial fragments of ticks were submitted to GenBank under accession numbers: OQ860250 (*Ha. cornupunctata*), OQ860248 (*Ha. bispinosa*), OQ860704 (*Ha. danieli*), OQ860705 (*Ha. montgomeryi*), OQ860706 (*Hy. anatolicum*), OQ860725 (*Hy. dromedarii*), OQ861058 (*R. haemaphysaloides*), OQ861080 (*R. microplus*), and OQ860245 (*A. persicus*). The obtained *GroEL* partial fragments of *Coxiella* spp. were submitted to GenBank under accession numbers: OQ883856 (*C. burnetii*), OQ883857 (*Coxiella* endosymbiont), OQ883858 (*Coxiella* endosymbiont), OQ883859 (*Coxiella* sp.), OQ883860 (*Coxiella* sp.), OQ883861 (*Coxiella* sp.), OQ883862 (*Coxiella* sp.).

Discussion

Various ticks and their associated pathogens ideally propagate in Pakistan's humid and variable climatic conditions (Karim et al., 2017; Ali et al., 2019, 2020, 2021; Obaid et al., 2023). Microbiota belonging to different bacterial genera have been detected in different tick species in Pakistan (Karim et al., 2017; Ali et al., 2021; Alam et al., 2022; Khan Z. et al., 2022; Khan S. M. et al., 2023; Numan et al., 2022). Some serological surveys of Q-fever in small ruminants, large ruminants, rodents, and humans have been reported from Pakistan (Ahmed, 1987; Ali et al., 2022a). There is limited information available regarding the molecular characterization of *C. burnetii* and thus it remains an ignored zoonotic disease in the country. The association of *Coxiella* spp. with different ticks infesting various hosts has been reviewed globally (Guatteo et al., 2011); therefore, in this study, we summarized this association of *Coxiella* spp. with different ticks in Asia. Nine tick species including *Ha. cornupunctata, Ha. bispinosa, Ha. montgomeryi, Ha. danieli, Hy. anatolicum, Hy. dromedarii, R. haemaphysaloides, R. microplus*, and *A. persicus* infesting goats, sheep, camels, cattle, wild mice, and domestic fowls were genetically characterized. In addition, this is the first report regarding the molecular detection and phylogenetic positioning of *Coxiella* spp. associated with ticks in Pakistan. Overall, *C. burnetii*, two *Coxiella* endosymbionts, and five undetermined *Coxiella* sp. were genetically characterized based on *GroEL* fragments in various tick species.

Environmental factors such as humidity and temperature mainly affect the distribution of ticks, TBDs, and their zoonotic threats to human and animal health (Léger et al., 2013). Since the current study area's existing environmental and climatic conditions are favorable for tick infestation and propagation of various pathogens (Aiman et al., 2022; Ali et al., 2023), many ticks were collected during this survey. Contrary to previous studies, *Ha. cornupunctata* tick was more prevalent than other tick species such as *R. microplus* and *Hy. anatolicum* in Pakistan (Karim et al., 2017; Ali et al., 2019, 2021; Khan Z. et al., 2022). It may be due to examining different hosts, such as goats, sheep, and wild mice attributing a closed association with this species.

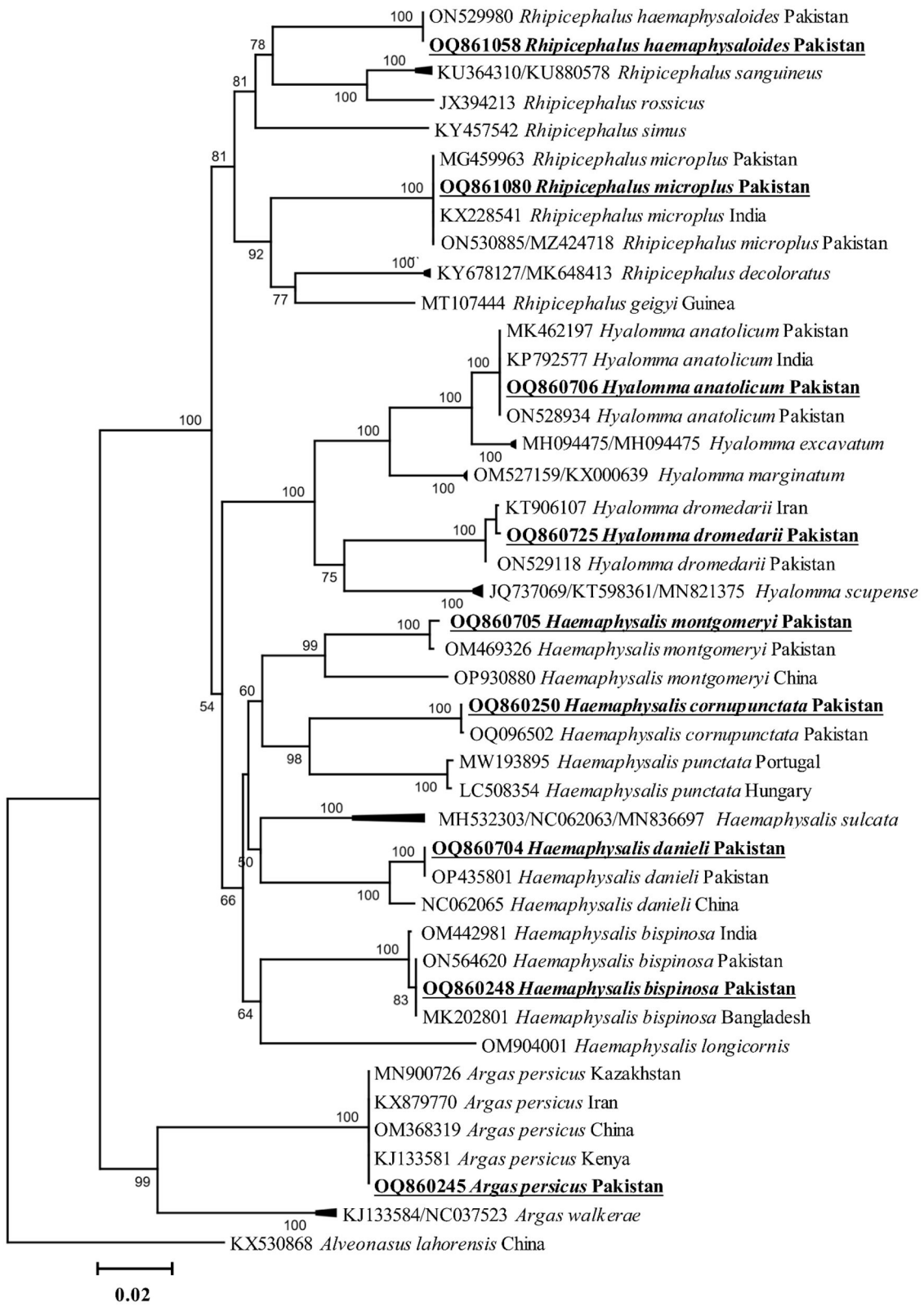

FIGURE 2
Phylogenetic tree based on *cox1* fragments of tick species. The sequence of *Alveonasus lahorensis* (KX530868) was used as an outgroup. The levels of bootstrap support (≥60%) for phylogenetic groupings are given at each node. The obtained sequences are represented with bold and underlined fonts.

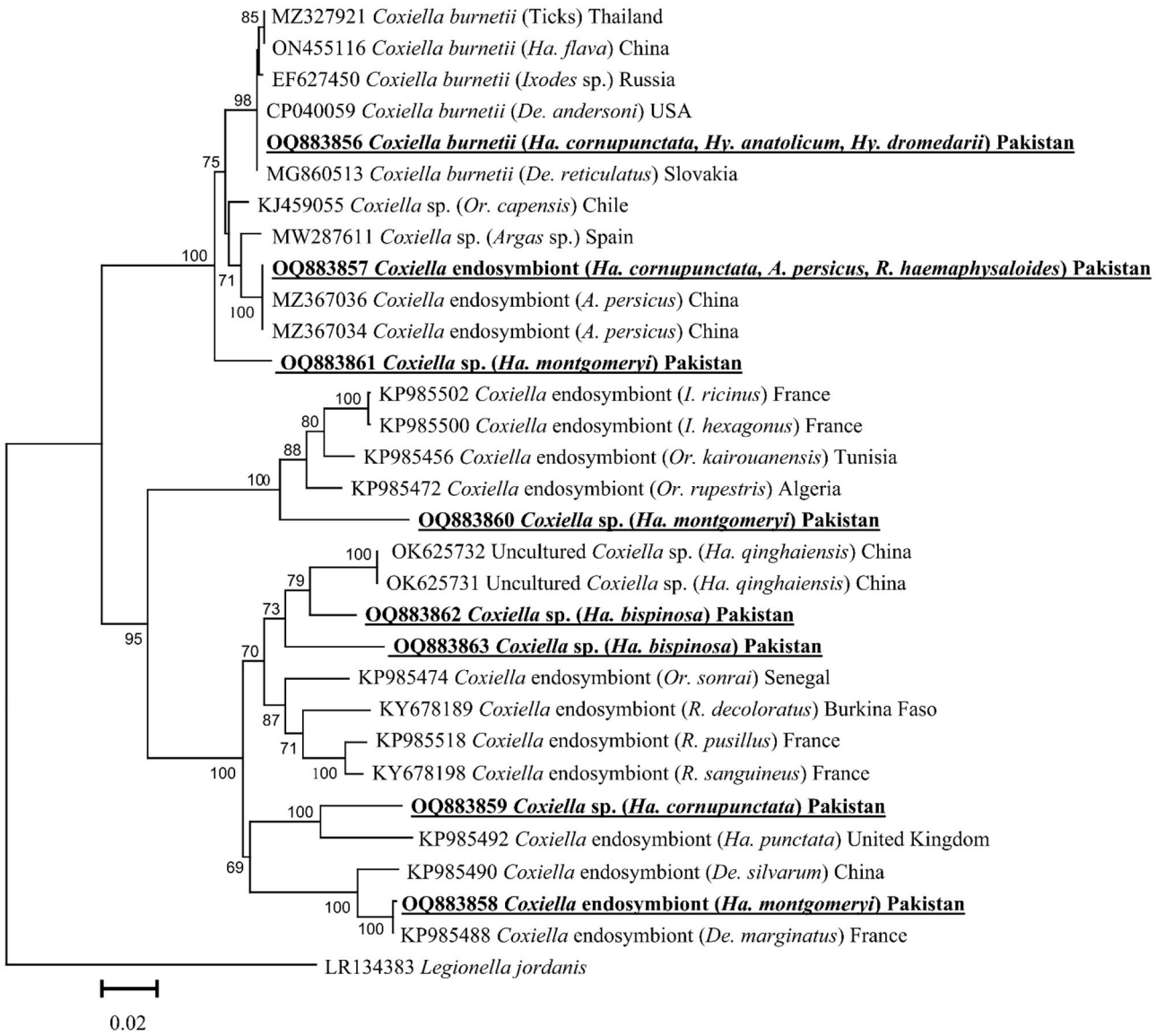

FIGURE 3
Phylogenetic tree based on *GroEL* fragments of *Coxiella* spp. detected in tick species. The sequence of *Legionella jordanis* (LR134383) was used as an outgroup. The levels of bootstrap support (≥ 60%) for phylogenetic groupings are given at each node. The obtained sequences are represented with bold and underlined fonts.

The age of the host is a significant factor to tick infestation. According to previous reports, a high tick burden was recorded on adult hosts compared with young ones (Ali et al., 2021; Kamran et al., 2021; Khan Z. et al., 2022). Large body surfaces and free grazing practices of adult animals make them more vulnerable due to high tick infestation. In contrast, the robust immune system, less grazing, and low body surface of the younger hosts contribute to less tick infestation (Swai et al., 2005). Female hosts were highly tick infested compared with the male hosts, which is consistent with previous findings (Ullah et al., 2023). Higher levels of progesterone and prolactin hormones in females make them susceptible to tick infestation (Anderson et al., 2013; Ahmed et al., 2023). The higher levels of progesterone and prolactin hormones may increase the susceptibility of females to tick's infections (Lloyd, 1983; Ahmed et al., 2023). Additionally, in the current study, ticks were predominantly reported in summer (June–August) compared with other seasons because the warm and humid climatic conditions in the region provide a suitable environment for the development of all stages of ticks (Ali et al., 2019, 2021). The comparatively wide host range noted for different *Haemaphysalis, Hyalomma*, and *Rhipicephalus* ticks may be due to frequent practices such as putting various hosts in the same shelter and over-crowded livestock and concurrent grazing in the survey area.

Major consequences have been revealed in the epidemiology of Q-fever upon the molecular detection of *C. burnetii* DNA in ticks collected from the environment, domestic and wild animals (Yessinou et al., 2022). It has been observed that ticks may transmit the Q-fever agent and pollute the environment as well as the host's body in Pakistan (Ullah et al., 2019). The association between different ticks and *C. burnetii* and its transstadially and transovarially transmission has been reported, suggesting the Q-fever transmission from infected to healthy animals through blood

meal (Gong et al., 2020). In this study, molecular detection of *Coxiella* spp. varied in the aforementioned seven tick species collected from various hosts. A high prevalence of Q-fever in camels in this study may be attributable to the camels' vulnerability regarding *C. burnetii* infection or camel tick competence as a reservoir for this pathogen (Gumi et al., 2013). Common reservoirs for *C. burnetii* are small ruminants that may excrete a diverse number of these bacteria in their birth byproducts (placenta). *Coxiella* spp. were highly detected in ticks collected from small ruminants (goats and sheep), and these findings agreed with the previous serosurvey conducted in Pakistan (Ullah et al., 2019). *Coxiella* sp. detected in *A. persicus* ticks collected from domestic fowls suggest that different soft ticks may also be investigated as host reservoirs for various undetermined *Coxiella* spp., as reported in other studies (Trinachartvanit et al., 2018).

In the current study, phylogenetic analysis *via cox1* fragments of nine different tick species revealed a close evolutionary relationship with the same species reported from Pakistan, China, India, Bangladesh, and Iran, and these findings were supported by previous studies (Ahmad et al., 2022; Alam et al., 2022; Ali et al., 2022a; Khan S. M. et al., 2023). Phylogenetic analysis of *Coxiella* spp., detected in different tick species, showed close association with their respective species reported from the same or different tick species and humans. This association of *Coxiella* spp. may be due to the close interaction of infested animals with humans, which enhances zoonotic infections such as Q-fever in humans. So-far neglected surveillance of *Coxiella* spp. in the region demands immediate attention to its pathogenic consequences.

Conclusion

Coxiella spp. were molecularly detected in ticks infesting goats, sheep, camels, cattle, wild mice, and domestic fowls and were confirmed through sequencing for the first time in Pakistan. Further research is essential to investigate any potential health risks due to these agents. The veterinarian livestock holders and farm workers lack knowledge regarding the epidemiology of Q-fever and its causative agents in Pakistan. Livestock holders should be adequately educated regarding Q-fever prevention and management practices because the occurrence of this agent can lead to long-term environmental contamination, which is a potential threat to animals and humans. Consequently, effective measures associated with Q-fever must be implemented, including limiting contact between herds, quarantining newly purchased animals, and using disinfectants that can reduce the spread of infection and possible transmission to humans.

Institutional review board statement

The Advance Studies and Research Board (ASRB: Dir/A&R/AWKUM/2022/9396) of the Department of Zoology, Abdul Wali Khan University Mardan, Pakistan, approved prior consent for this study. Additionally, permission was taken from the owners of the animals to observe hosts and ticks collection. All the rules regarding animal welfare regulations were followed while handling the animals.

Data availability statement

The datasets presented in the study have been deposited to the NCBI GenBank repository, accession numbers OQ860250 (*Ha. cornupunctata*), OQ860248 (*Ha. bispinosa*), OQ860704 (*Ha. danieli*), OQ860705 (*Ha. montgomeryi*), OQ860706 (*Hy. anatolicum*), OQ860725 (*Hy. dromedarii*), OQ861058 (*R. haemaphysaloides*), OQ861080 (*R. microplus*), OQ860245 (*A. persicus*), OQ883856 (*C. burnetii*), OQ883857 (*Coxiella* endosymbiont), OQ883858 (*Coxiella* endosymbiont), OQ883859 (*Coxiella* sp.), OQ883860 (*Coxiella* sp.), OQ883861 (*Coxiella* sp.), and OQ883862 (*Coxiella* sp.).

Ethics statement

The animal study was reviewed and approved by the Advance Studies and Research Board (ASRB: Dir/A&R/AWKUM/2022/9396) of the Department of Zoology, Abdul Wali Khan University Mardan, Pakistan, approved prior consent for this study. Written informed consent was obtained from the owners for the participation of their animals in this study.

Author contributions

AAli designed the study. AAli, MMA, TT, SBK, and AAlo carried out the experiments of the study. AAli, MN, ZUI, GR, MKO, SBK, and SU collected the tick samples and performed the experiments. AAli, MKO, and MN performed the phylogenetic and statistical analyses. All authors have read and agreed to the published version of the manuscript.

Funding

The authors acknowledge the financial support provided by the Higher Education Commission of Pakistan and the Pakistan Science Foundation. The researchers support project number (RSP2023R494), King Saud University, Riyadh, Saudi Arabia. This work was supported by JSPS KAKENHI Grant Numbers JP20KK0154 and JP22H02522, JSPS Bilateral Program (Grant number JPJSBP120239937).

Conflict of interest

The authors declare that the research was conducted in the absence of any commercial or financial relationships that could be construed as a potential conflict of interest.

Publisher's note

All claims expressed in this article are solely those of the authors and do not necessarily represent those of their affiliated organizations, or those of the publisher, the editors and the reviewers. Any product that may be evaluated in this article, or claim that may be made by its manufacturer, is not guaranteed or endorsed by the publisher.

References

Abdel-Moein, K. A., and Hamza, D. A. (2017). The burden of *Coxiella burnetii* among aborted dairy animals in Egypt and its public health implications. *Acta Trop.* 166, 92–95. doi: 10.1016/j.actatropica.2016.11.011

Ahmad, I., Ullah, S., Alouffi, A., Almutairi, M. M., Khan, M., Numan, M., et al. (2022). Description of male, redescription of female, host record, and phylogenetic position of *Haemaphysalis danieli*. *Pathogens.* 11, 1495. doi: 10.3390/pathogens11121495

Ahmed, I. P. (1987). A serological investigation of Q fever in Pakistan. *J. Pak. Med. Assoc.* 37, 126–129.

Ahmed, M., Ibrahim, A., and Mahamed, S. (2023). Study on prevalence of one humped camel mange and its associated risk factors in selected kebeles of Kebribeyah District of Fafan Zone, Somali Regional State, Ethiopia. *Res. Squ. [Preprint].* doi: 10.21203/rs.3.rs-2619682/v1

Aiman, O., Ullah, S., Chitimia-Dobler, L., Nijhof, A. M., and Ali, A. (2022). First report of *Nosomma monstrosum* ticks infesting Asian water buffaloes (*Bubalus bubalis*) in Pakistan. *Ticks Tick-Borne Dis.* 13, 101899. doi: 10.1016/j.ttbdis.2022.101899

Akbarian, Z., Ziay, G., Schauwers, W., Noormal, B., Saeed, I., Qanee, A. H., et al. (2015). Brucellosis and *Coxiella burnetii* infection in householders and their animals in secure villages in Herat province, Afghanistan: a cross-sectional study. *PLoS Negl. Trop. Dis.* 9, e0004112. doi: 10.1371/journal.pntd.0004112

Alam, S., Khan, M., Alouffi, A., Almutairi, M. M., Ullah, S., Numan, M., et al. (2022). Spatio-temporal patterns of ticks and molecular survey of *Anaplasma marginale*, with notes on their phylogeny. *Microorganisms.* 10, 1663. doi: 10.3390/microorganisms10081663

Al-Graibawi, M. A., Yousif, A. A., Gharban, H. A., and Zinsstag, J. (2021). First serodetection and molecular phylogenetic documentation of *Coxiella burnetii* isolates from female camels in Wasit governorate, Iraq. *Iraqi J. Vet. Sci. 35*, 47–52. doi: 10.33899/ijvs.2021.130888.1890

Ali, A., Khan, M. A., Zahid, H., Yaseen, P. M., Qayash Khan, M., Nawab, J., et al. (2019). Seasonal dynamics, record of ticks infesting humans, wild and domestic animals and molecular phylogeny of *Rhipicephalus microplus* in Khyber Pakhtunkhwa Pakistan. *Front. Physiol. 10*, 793. doi: 10.3389/fphys.2019.00793

Ali, A., Mulenga, A., and Vaz, I. S. Jr. (2020). Tick and tick-borne pathogens: molecular and immune targets for control strategies. *Front. Physiol.* 11, 744. doi: 10.3389/fphys.2020.00744

Ali, A., Numan, M., Ullah, S., Khan, M., and Kamran, K. (2023). Genetic characterization of *Haemaphysalis (Rhipistoma) indica* and *Haemaphysalis (Segalia) montgomeryi* ticks (Ixodoidea: Ixodidae). *Ticks Tick Borne Dis.* 14, 102105. doi: 10.1016/j.ttbdis.2022.102105

Ali, A., Shehla, S., Zahid, H., Ullah, F., Zeb, I., Ahmed, H., et al. (2022a). Molecular survey and spatial distribution of *Rickettsia* spp. in ticks infesting free-ranging wild animals in Pakistan (2017–2021). *Pathogens.* 11, 162. doi: 10.3390/pathogens11020162

Ali, A., Zahid, H., Zeb, I., Tufail, M., Khan, S., Haroon, M., et al. (2021). Risk factors associated with tick infestations on equids in Khyber Pakhtunkhwa, Pakistan, with notes on *Rickettsia massiliae* detection. *Parasit. Vectors.* 14, 1–12. doi: 10.1186/s13071-021-04836-w

Ali, S., Saeed, U., Rizwan, M., El-Adawy, H., Mertens-Scholz, K., and Neubauer, H. (2022b). Serological prevalence of and risk factors for *Coxiella burnetii* infection in women of Punjab Province, Pakistan. *Int. J. Environ. Res. Public Health.* 19, 4576. doi: 10.3390/ijerph19084576

Al-Kindi, N., Al-Yaaqoubi, M., Al-Rashdi, Y., Al-Rashdi, A., Al-Ajmi, A., and Al-Maani, A. (2022). The first confirmed pediatric chronic osteomyelitis due to *Coxiella burnetii* in Oman. *Oman Med. J.* 37, e449. doi: 10.5001/omj.2023.03

Almogren, A., Shakoor, Z., Hasanato, R., and Adam, M. H. (2013). Q fever: a neglected zoonosis in Saudi Arabia. *Ann. Saudi Med.* 33, 464–468. doi: 10.5144/0256-4947.2013.464

Altschul, S. F., Gish, W., Miller, W., Myers, E. W., and Lipman, D. J. (1990). Basic local alignment search tool. *J. Mol. Biol.* 215, 403–410. doi: 10.1016/S0022-2836(05)80360-2

Amitai, Z., Bromberg, M., Bernstein, M., Raveh, D., Keysary, A., David, D., et al. (2010). A large Q fever outbreak in an urban school in central Israel. *Clin. Infect. Dis.* 50, 1433–1438. doi: 10.1086/652442

Anderson, K., Ezenwa, V. O., and Jolles, A. E. (2013). Tick infestation patterns in free ranging African buffalo (*Syncercus caffer*): effects of host innate immunity and niche segregation among tick species. *Int. J. Parasitol. Parasites Wildl.* 2, 1–9. doi: 10.1016/j.ijppaw.2012.11.002

Apanaskevich, D. A. (2003). Differentiation of closely related species *Hyalomma anatolicum* and *H. excavatum* (Acari: Ixodidae) based on a study of all life cycle stages, throughout entire geographical range. *Parazitologiia.* 37, 259–280.

Apanaskevich, D. A., Schuster, A. L., and Horak, I. G. (2008). The genus *Hyalomma*: VII. Redescription of all parasitic stages of *H. (Euhyalomma) dromedarii* and *H. (E.) schulzei* (Acari: Ixodidae). *J. Med. Entomol. 45*, 817–831. doi: 10.1093/jmedent/45.5.817

Barigye, R., Hassan, N. A. D., Abdalla-Alfaki, I. M., Al Alawi, H. K. K., Aldhaheri, A. M. B., Ghanim, F. M., et al. (2022). Pilot serosurvey of *Coxiella burnetii* in domesticated small ruminants in the United Arab Emirates. *Trop. Anim. Health Prod.* 54, 1–6. doi: 10.1007/s11250-022-03150-6

Beaman, M. H., and Hung, J. (1989). Pericarditis associated with tick-borne Q fever. *Intern. Med.* 19, 254–256. doi: 10.1111/j.1445-5994.1989.tb00258.x

Bontje, D. M., Backer, J. A., Hogerwerf, L., Roest, H. I. J., and Van Roermund, H. J. W. (2016). Analysis of Q fever in Dutch dairy goat herds and assessment of control measures by means of a transmission model. *Prev. Vet. Med.* 123, 71–89. doi: 10.1016/j.prevetmed.2015.11.004

Burns, R. J., Douangngeun, B., Theppangna, W., Khounsy, S., Mukaka, M., Selleck, P. W., et al. (2018). Serosurveillance of Coxiellosis (Q-fever) and Brucellosis in goats in selected provinces of Lao People's Democratic Republic. *PLoS Negl. Trop. Dis.* 12, e0006411. doi: 10.1371/journal.pntd.0006411

Cerný, V., and Hoogstraal, H. (1977). *Haemaphysalis (Allophysalis) danieli*, sp. n. (Ixodoidea: Ixodidae), female and tentatively associated immature stages from high mountains of northern Pakistan and Afghanistan. *J. Parasitol.* 567-574. doi: 10.2307/3280022

Chakrabartty, A., Nahar, A., Rahman, M. S., Rahman, A. K. M. A., Sarker, A. S., Hasan, M. M., et al. (2021). Sero-molecular investigation of *Coxiella burnetii* infection in domestic ruminants and humans and associated risk factors based on "One Health" approach in Bangladesh. *J. Vet. Med. OH Res*, 3, 93–117. doi: 10.36111/jvmohr.2021.3(1).0027

Chan, J. F., Tse, H., To, K. K., Li, I. W., Tang, B. S., Cheng, V. C., et al. (2010). Q fever: underdiagnosed in Hong Kong. *Hong Kong Med. J.* 16, 56–58.

Chang, C. C., Lin, P. S., Hou, M. Y., Lin, C. C., Hung, M. N., Wu, T. M., et al. (2010). Identification of risk factors of *Coxiella burnetii* (Q fever) infection in veterinary-associated populations in southern Taiwan. *Zoonoses Public Health.* 57, e95–e101. doi: 10.1111/j.1863-2378.2009.01290.x

Chou, C. H., Yeh, T. M., Lu, Y. P., Shih, W. L., Chang, C. D., Chien, C. H., et al. (2014). Prevalence of zoonotic pathogens by molecular detection in stray dogs in central Taiwan. *Thai J. Vet. Med.* 44, 363–375.

Cong, W., Meng, Q. F., Shan, X. F., Sun, W. W., Kang, Y. H., Chen, L., Wang, W. L., and Qian, A. D. (2015). *Coxiella burnetii* (Q fever) infection in farmed ruminants in three northeastern provinces and Inner Mongolia autonomous region, China. V*ector Borne Zoonotic Dis*. 15, 512–514. doi: 10.1089/vbz.2015.1789

Dabaja, M. F., Greco, G., Blanda, V., Tempesta, M., Bayan, A., Torina, A., et al. (2020). Multispacer sequence typing of *Coxiella burnetii* from milk and hard tick samples from ruminant farms in Lebanon. *Vet. Ital.* 56, 289–296. doi: 10.12834/VetIt.1799.13290.1

Dabaja, M. F., Greco, G., Villari, S., Bayan, A., Vesco, G., Gargano, V., et al. (2018). The first serological study of Q fever in humans in Lebanon. *Vector Borne Zoonotic Dis.* 18, 138–143. doi: 10.1089/vbz.2016.2102

De la Fuente, J., Antunes, S., Bonnet, S., Cabezas-Cruz, A., Domingos, A. G., Estrada-Peña, A., et al. (2017). Tick-pathogen interactions and vector competence: identification of molecular drivers for tick-borne diseases. *Front. Cell. Infect. Microbiol.* 7, 114. doi: 10.3389/fcimb.2017.00114

Derrick, E. H. (1937). "Q" fever, a new fever entity: clinical features, diagnosis and laboratory investigation. *Med. J. Aust.* 2, 43743. doi: 10.5694/j.1326-5377.1937.tb43743.x

Dhanda, V., and Kulkarni, S. M. (1969). Immature stages of *Haemaphysalis cornupunctata* Hoogstraal and Varma, 1962 (Acarina: Ixodidae) with new host and locality records, and notes on its ecology. *Orient. Insects.* 3, 15–21. doi: 10.1080/00305316.1969.10433891

Doung-Ngern, P., Chuxnum, T., Pangjai, D., Opaschaitat, P., Kittiwan, N., Rodtian, P., et al. (2017). Seroprevalence of *Coxiella burnetii* antibodies among ruminants and occupationally exposed people in Thailand, 2012–2013. *Am. J. Trop. Med. Hyg.* 96, 786. doi: 10.4269/ajtmh.16-0336

Duron, O., Jourdain, E., and McCoy, K. D. (2014). Diversity and global distribution of the *Coxiella* intracellular bacterium in seabird ticks. *Ticks tick-borne Dis.* 5, 557–563. doi: 10.1016/j.ttbdis.2014.04.003

Edgar, R. C. (2004). MUSCLE: a multiple sequence alignment method with reduced time and space complexity. *BMC Bioinform.* 5, 113. doi: 10.1186/1471-2105-5-113

Eklund, C. M., Parker, R. R., Lackman, D. B., Ecklund, C. M., and Lockman, D. B. (1947). A case of Q fever probably contracted by exposure to ticks in nature. *Public Health Rep.* 1896–1970, 1413–1416. doi: 10.2307/4586287

El Tigani-Asil, E. T. A., Blanda, V., Abdelwahab, G. E., Hammadi, Z. M. A., Habeeba, S., Khalafalla, A. I., et al. (2021). Molecular investigation on tick-borne hemoparasites and *Coxiella burnetii* in dromedary camels (*Camelus dromedarius*) in Al Dhafra Region of Abu Dhabi, UAE. *Animals.* 11, 666. doi: 10.3390/ani11030666

Eldin, C., Mélenotte, C., Mediannikov, O., Ghigo, E., Million, M., Edouard, S., et al. (2017). From Q fever to *Coxiella burnetii* infection: a paradigm change. *Clin. Microbiol. Rev.* 30, 115–190. doi: 10.1128/CMR.00045-16

El-Mahallawy, H. S., Kelly, P., Zhang, J., Yang, Y., Wei, L., Tian, L., et al. (2016). Serological and molecular evidence of *Coxiella burnetii* in samples from humans and animals in China. *Ann. Agric. Environ. Med.* 23, 1196859. doi: 10.5604/12321966.1196859

Esmaeili, S., Mohabati Mobarez, A., Khalili, M., Mostafavi, E., and Moradnejad, P. (2019). Genetic evidence of *Coxiella burnetii* infection in acute febrile illnesses in Iran. *Plos Neg. Trop. Dis.* 13, e0007181. doi: 10.1371/journal.pntd.0007181

Esson, C., Skerratt, L. F., Berger, L., Malmsten, J., Strand, T., Lundkvist, Å., et al. (2019). Health and zoonotic infections of snow leopards *Panthera unica* in the South Gobi Desert of Mongolia. *Infect. Ecol. Epidemiol.* 9, 1604063. doi: 10.1080/20008686.2019.1604063

Folmer, O., Hoeh, W. R., Black, M., and Vrijenhoek, R. C. (1994). Conserved primers for PCR amplification of mitochondrial DNA from different invertebrate phyla. *Mol. Marine Biol. Biotechnol.* 3, 294–299.

Gharban, H. A., and Yousif, A. A. (2020). Serological and molecular phylogenetic detection of *Coxiella burnetii* in lactating cows, Iraq. *Iraqi J.Vet.Med.* 44, 42–50. doi: 10.30539/ijvm.v44i(E0).1020

Gong, X. Q., Xiao, X., Liu, J. W., Han, H. J., Qin, X. R., Lei, S. C., et al. (2020). Occurrence and genotyping of *Coxiella burnetii* in hedgehogs in China. *Vector Borne Zoonotic Dis.* 20, 580–585. doi: 10.1089/vbz.2019.2589

Guatteo, R., Seegers, H., Taurel, A. F., Joly, A., and Beaudeau, F. (2011). Prevalence of *Coxiella burnetii* infection in domestic ruminants: a critical review. *Vet. Microbiol.* 149, 1–16. doi: 10.1016/j.vetmic.2010.10.007

Gumi, B., Firdessa, R., Yamuah, L., Sori, T., Tolosa, T., Aseffa, A., et al. (2013). Seroprevalence of brucellosis and Q-fever in southeast Ethiopian pastoral livestock. *J. Vet. Sci. Med. Diagn.* 2, 109. doi: 10.4172/2325-9590.1000109

Hall, T., Biosciences, I., and Carlsbad, C. J. (2011). BioEdit: an important software for molecular biology. *GERF Bull Biosci.* 2, 60–61.

Hoogstraal, H., and Kaiser, M. (1959). Observations on Egyptian *Hyalomma* ticks (Ixodoidea, Ixodidae). 5. Biological notes and differences in identity of *H. anatolicum* and its subspecies *anatolicum* Koch and *excavatum* Koch among Russian and other workers. Identity of *H. lusitanicum* Koch. *Ann. Entomol. Soc. Am.* 52, 3 243–261. doi: 10.1093/aesa/52.3.243

Hoogstraal, H., and Trapido, H. (1966). Redescription of the type materials of *Haemaphysalis (Kaiseriana) bispinosa* Neumann (India), *H. (K.) neumanni* Dönitz (Japan), *H. (K.) lagrangei* Larrousse (Vietnam), and *H. (K.) yeni* Toumanoff (Vietnam) (Ixodoidea, Ixodidae). *J. Parasitol.* 52, 1188–1198. doi: 10.2307/3276366

Hoogstraal, H., and Varma, M. G. R. (1962). *Haemaphysalis cornupunctata* sp. n. and H. kashmirensis sp. n. from Kashmir, with Notes on *H. sundrai* Sharif and *H. sewelli* Sharif of India and Pakistan (Ixodoidea, Ixodidae). *J. Parasitol.* 48, 185–194. doi: 10.2307/3275561

Hussain, S., Saqib, M., El-Adawy, H., Hussain, M. H., Jamil, T., Sajid, M. S., et al. (2022). Seroprevalence and molecular evidence of *Coxiella burnetii* in dromedary camels of Pakistan. *Front. Vet. Sci.* 9, 908479. doi: 10.3389/fvets.2022.908479

Jalboush, N., and Alzuheir, I. (2017). Serosurvey of Q fever in active reproductive rams in northern Palestine. *Iraqi J. Vet. Sci.* 31, 87–90. doi: 10.33899/ijvs.2017.145602

Kamran, K., Ali, A., Villagra, C., Siddiqui, S., Alouffi, A. S., and Iqbal, A. (2021). A cross-sectional study of hard ticks (acari: ixodidae) on horse farms to assess the risk factors associated with tick-borne diseases. *Zoonoses Public Health.* 68, 247–262. doi: 10.1111/zph.12809

Karim, S., Budachetri, K., Mukherjee, N., Williams, J., Kausar, A., Hassan, M. J., et al. (2017). A study of ticks and tick-borne livestock pathogens in Pakistan. *PLoS Negl. Trop. Dis.* 11, e0005681. doi: 10.1371/journal.pntd.0005681

Kato, K., Arashima, Y., Asai, S., Furuya, Y., Yoshida, Y., Murakami, M., et al. (1998). Detection of *Coxiella burnetii* specific DNA in blood samples from Japanese patients with chronic nonspecific symptoms by nested polymerase chain reaction. *FEMS Immunol. Med. Microbiol.* 21, 139–144. doi: 10.1111/j.1574-695X.1998.tb01159.x

Khademi, P., Ownagh, A., Ataei, B., Kazemnia, A., Enferadi, A., Khalili, M., et al. (2020). Prevalence of *C. burnetii* DNA in sheep and goats milk in the northwest of Iran. *Int. J. Food Microbiol.* 331, 108716. doi: 10.1016/j.ijfoodmicro.2020.108716

Khan, S. M., Khan, M., Alouffi, A., Almutairi, M. M., Numan, M., Ullah, S., et al. (2023). Phylogenetic position of *Haemaphysalis kashmirensis* and *Haemaphysalis cornupunctata*, with Notes on *Rickettsia* spp. *Genes.* 14, 360. doi: 10.3390/genes14020360

Khan, Z., Shehla, S., Alouffi, A., Kashif Obaid, M., Zeb Khan, A., Almutairi, M. M., et al. (2022). Molecular survey and genetic characterization of *Anaplasma marginale* in ticks collected from livestock hosts in Pakistan. *Animals.* 12, 1708. doi: 10.3390/ani12131708

Khor, C. S., Mohd-Rahim, N. F., Hassan, H., Chandren, J. R., Nore, S. S., Johari, J., et al. (2018). Seroprevalence of Q fever among the indigenous people (Orang Asli) of Peninsular Malaysia. V*ector Borne Zoonotic Dis.* 18, 131–137. doi: 10.1089/vbz.2017.2153

Kilic, S., Yilmaz, G. R., Komiya, T., Kurtoglu, Y., and Karakoc, E. A. (2008). Prevalence of *Coxiella burnetii* antibodies in blood donors in Ankara, Central Anatolia, Turkey. *New Microbiol.* 31, 527–534

Kohls, G. M., Hoogstraal, H., Clifford, C. M., and Kaiser, M. N. (1970). The subgenus Persicargas (Ixodoidea, Argasidae, *Argas*). 9. Redescription and New World records of *Argas (P.) persicus* (Oken), and resurrection, redescription, and records of *A. (P.) radiatus* Railliet, *A. (P.) sanchezi* Dugès, and *A. (P.) miniatus* Koch, New World ticks misidentified as *A. (P.) persicus*. *Ann. Entomol. Soc. Am.* 63, 590–606. doi: 10.1093/aesa/63.2.590

Kumar, S., Stecher, G., Li, M., Knyaz, C., and Tamura, K. (2018). MEGA X: molecular evolutionary genetics analysis across computing platforms. *Mol. Biol. Evol.*, 35, 1547. doi: 10.1093/molbev/msy096

Lafi, S. Q., Talafha, A. Q., Abu-Dalbouh, M. A., Hailat, R. S., and Khalifeh, M. S. (2020). Seroprevalence and associated risk factors of *Coxiella burnetii* (Q fever) in goats and sheep in northern Jordan. *Trop. Anim. Health Prod. 52*, 1553–1559. doi: 10.1007/s11250-019-02153-0

Lee, S. H., Lee, J. H., Park, S., Lee, H. K., Do Hwang, S., Jeong, H. W., et al. (2020). Isolation of *Coxiella burnetii* in patients with nonspecific febrile illness in South Korea. *BMC Infect. Dis.* 20, 1–5. doi: 10.1186/s12879-020-05130-3

Léger, E., Vourc'h, G., Vial, L., Chevillon, C., and McCoy, K. D. (2013). Changing distributions of ticks: causes and consequences. *Exp. Appl. Acarol.* 59, 219–244. doi: 10.1007/s10493-012-9615-0

Leski, T. A., Malanoski, A. P., Gregory, M. J., Lin, B., and Stenger, D. A. (2011). Application of a broad-range resequencing array for detection of pathogens in desert dust samples from Kuwait and Iraq. *Appl. Environ. Microbiol.* 77, 4285–4292. doi: 10.1128/AEM.00021-11

Lloyd, S. (1983). Effect of pregnancy and lactation upon infection. *Vet. Immunol. Immunopathol.* 4, 153–176. doi: 10.1016/0165-2427(83)90057-0

Mohabati Mobarez, A., Khalili, M., Mostafavi, E., and Esmaeili, S. (2021). Molecular detection of *Coxiella burnetii* infection in aborted samples of domestic ruminants in Iran. *PLoS ONE.* 16, e0250116. doi: 10.1371/journal.pone.0250116

Mohammed, O. B., Jarelnabi, A. A., Aljumaah, R. S., Alshaikh, M. A., Bakhiet, A. O., Omer, S. A., et al. (2014). *Coxiella burnetii*, the causative agent of Q fever in Saudi Arabia: molecular detection from camel and other domestic livestock. *Asian Pac. J. Trop. Med.* 7, 715–719. doi: 10.1016/S1995-7645(14)60122-X

Mumcuoglu, K. Y., Arslan-Akveran, G., Aydogdu, S., Karasartova, D., Kosar, N., Gureser, A. S., et al. (2022). Pathogens in ticks collected in Israel: I. Bacteria and protozoa in *Hyalomma aegyptium* and *Hyalomma dromedarii* collected from tortoises and camels. *Ticks Tick-Borne Dis.* 13, 101866. doi: 10.1016/j.ttbdis.2021.101866

Musso, D., Broult, J., Parola, P., Raoult, D., and Fournier, P. E. (2014). Absence of antibodies to *Rickettsia* spp., *Bartonella* spp., *Ehrlichia* spp. and *Coxiella burnetii* in Tahiti, French Polynesia. *BMC Infect. Dis.* 14, 1–4. doi: 10.1186/1471-2334-14-255

Ni, J., Lin, H., Xu, X., Ren, Q., Aizezi, M., Luo, J., et al. (2020). *Coxiella burnetii* is widespread in ticks (Ixodidae) in the Xinjiang areas of China. *BMC Vet. Res.* 16, 1–9. doi: 10.1186/s12917-020-02538-6

Niemczuk, K., Szymańska-Czerwińska, M., Smietanka, K., and Bocian, Ł. (2014). Comparison of diagnostic potential of serological, molecular and cell culture methods for detection of Q fever in ruminants. *Vet. Microbiol.* 171, 147–152. doi: 10.1016/j.vetmic.2014.03.015

Numan, M., Islam, N., Adnan, M., Zaman Sa, fi, S., Chitimia-Dob and ler, L., Labruna, M. B., et al. (2022). First genetic report of *Ixodes kashmiricus* and associated *Rickettsia* sp. *Parasi. Vectors.* 15, 1–12. doi: 10.1186/s13071-022-05509-y

Nurkunasegran, M., Kho, K., Koh, F., Tan, P., Nizam, Q., Ong, B., et al. (2017). Molecular detection of *Coxiella burnetii* from farm animals and ticks in Malaysia. *Trop. Biomed.* 34, 675–680.

Obaid, M. K., Almutairi, M. M., Alouf, A., Sa, S. Z., Tanaka, T., and Ali, A. (2023). Assessment of cypermethrin and amitraz resistance and molecular profiling of voltage-gated sodium channel and octopamine tyramine genes of *Rhipicephalus microplus*. *Front. Cell. Infect. Microbiol.* 13, 1176013. doi: 10.3389/fcimb.2023.1176013

Obaidat, M. M., Malania, L., Imnadze, P., Roess, A. A., Salman, A. E. B., and Arner, R. J. (2019). Seroprevalence and risk factors for *Coxiella burnetii* in Jordan. *Am. J. Trop. Med. Hyg.* 101, 40. doi: 10.4269/ajtmh.19-0049

Ozgen, E. K., Kilicoglu, Y., Yanmaz, B., Ozmen, M., Ulucan, M., Bagatir, P. S., et al. (2022). Molecular epidemiology of *Coxiella burnetii* detected in humans and domestic ruminants in Turkey. *Vet. Microbiol.* 273, 109519. doi: 10.1016/j.vetmic.2022.109519

Panth, Y., Shrestha, S., and Bastola, R. (2017). Demonstration of circulating antibodies of *Coxiella burnetii* in dairy cattle of Rupandehi district, Nepal. *Int. J. Inno. Res. Multi. Field.* 3, 46–49.

Patra, G., Ghosh, S., Priyanka, E.fimova, M. A., Sahara, A., Al-Awsi, G. R. L., Polley, S., et al. (2020). Molecular detection of *Coxiella burnetii* and *Borrelia burgdorferi* in ticks infesting goats in North-Eastern States of India. *Int. J. Acarol.* 46, 431–438. doi: 10.1080/01647954.2020.1805000

Philip, C. B. (1948). Comments on the Name of the Q fever organism. *Public Health Rep.* 63, 402. doi: 10.2307/4586402

Psaroulaki, A., Hadjichristodoulou, C., Loukaides, F., Soteriades, E., Konstantinidis, A., Papastergiou, P., et al. (2006). Epidemiological study of Q fever in humans, ruminant animals, and ticks in Cyprus using a geographical information system. *Eur. J. Clin. Microbiol. Infect. Dis.* 25, 576–586. doi: 10.1007/s10096-006-0170-7

Rahman, M., Alam, M., Islam, M., Bhuiyan, A. K., and Rahman, A. K. M. (2016). Serological and molecular evidence of Q fever in domestic ruminants in Bangladesh. *Vet. Med. Int.* 2016, 9098416. doi: 10.1155/2016/9098416

Rini, E. P., Sasaki, M., Astuti, D., Juniantito, V., Wibawan, I. W. T., Sawa, H., et al. (2022). First molecular detection of *Coxiella burnetii* in beef cattle in West Java, Indonesia. *Jpn. J. Infect. Dis.* 75, 83–85. doi: 10.7883/yoken.JJID.2020.769

Rochlin, I., and Toledo, A. (2020). Emerging tick-borne pathogens of public health importance: a mini-review. *J. Med. Microbiol.* 69, 781. doi: 10.1099/jmm.0.001206

Royal, J., Riddle, M. S., Mohareb, E., Monteville, M. R., Porter, C. K., and Faix, D. J. (2013). Seroepidemiologic survey for *Coxiella burnetii* among US military personnel deployed to Southwest and Central Asia in 2005. *Am. J. Trop. Med. Hyg.* 89, 991. doi: 10.4269/ajtmh.12-0174

Sahu, R., Kale, S. B., Vergis, J., Dhaka, P., Kumar, M., Choudhary, M., et al. (2018). Apparent prevalence and risk factors associated with occurrence of *Coxiella burnetii* infection in goats and humans in Chhattisgarh and Odisha, India. *Comp. Immunol. Microbiol. Infect. Dis.* 60, 46–51. doi: 10.1016/j.cimid.2018.08.004

Sambrook, J., Fritsch, E. F., and Maniatis, T. E. (1989). *Molecular Cloning: A Laboratory Manual (No. Ed. 2)*. Cold Spring Harbor Laboratory Press, New York, NY, United States.

Selmi, R., Said, M. B., Mamlouk, A., Yahia, H. B., and Messadi, L. (2019). Molecular detection and genetic characterization of the potentially pathogenic *Coxiella burnetii* and the endosymbiotic *Candidatus* Midichloria mitochondrii in ticks infesting camels (*Camelus dromedarius*) from Tunisia. *Microb. Pathog.* 136, 103655. doi: 10.1016/j.micpath.2019.103655

Seo, M. G., Lee, S. H., VanBik, D., Ouh, I. O., Yun, S. H., Choi, E., et al. (2016). Detection and genotyping of *Coxiella burnetii* and *Coxiella*-like bacteria in horses in South Korea. *PLoS ONE.* 11, e0156710. doi: 10.1371/journal.pone.0156710

Shabbir, M. Z., Jamil, T., Ali, A. A., Ahmad, A., Naeem, M., Chaudhary, M. H., et al. (2015). Prevalence and distribution of soil-borne zoonotic pathogens in Lahore district of Pakistan. *Front. Microbiol.* 6, 917. doi: 10.3389/fmicb.2015.00917

Siengsanan-Lamont, J., Kong, L., Heng, T., Khoeun, S., Tum, S., Selleck, P. W., et al. (2023). Risk mapping using serologic surveillance for selected One Health and transboundary diseases in Cambodian goats. *PLoS Negl. Trop. Dis.* 17, e0011244. doi: 10.1371/journal.pntd.0011244

Smith, T. A., Driscoll, T., Gillespie, J. J., and Raghavan, R. (2015). A *Coxiella*-like endosymbiont is a potential vitamin source for the Lone Star tick. *Genome Biol. Evol.* 7, 831–838. doi: 10.1093/gbe/evv016

Špitalská, E., Sparagano, O., Stanko, M., Schwarzová, K., Špitalský, Z., Škultéty, L., et al. (2018). Diversity of *Coxiella*-like and *Francisella*-like endosymbionts, and *Rickettsia* spp., *Coxiella burnetii* as pathogens in the tick populations of Slovakia, Central Europe. *Ticks Tick Borne Dis.* 9, 1207–1211. doi: 10.1016/j.ttbdis.2018.05.002

Sultankulova, K. T., Shynybekova, G. O., Issabek, A. U., Mukhami, N. N., Melisbek, A. M., Chervyakova, O. V., et al. (2022). The Prevalence of Pathogens among Ticks Collected from Livestock in Kazakhstan. *Pathogens.* 11, 1206. doi: 10.3390/pathogens11101206

Swai, E. S., Mbise, A. N., Kessy, V., Kaaya, E., Sanka, P., and Loomu, P. M. (2005). Farm constraints, cattle disease perception and tick management practices in pastoral Maasai community-Ngorongoro, Tanzania. *Livest. Res. Rural. Dev.* 17, 17–20. Available online at: https://www.lrrd.cipav.org.co/lrrd17/2/swai17017.htm

Tamura, K., and Nei, M. (1993). Estimation of the number of nucleotide substitutions in the control region of mitochondrial DNA in humans and chimpanzees. *Mol. Biol. Evol.* 10, 512–526.

Tarasevič, I. V., Plotnikova, L. F., Fetisova, N. F., Makarova, V. A., Jablonskaja, V. A., Reháček, J., et al. (1976). Rickettsioses studies: 1. natural foci of rickettsioses in the Armenian Soviet Socialist Republic. *Bull. World Health Organ.* 53, 25.

Thi Vinh An, D., Thi Viet Ha, B., Xuan Co, D., Minh Tam, V., Thi Diem Tuyet, L., and Van Truong, V. (2022). The first case of *Coxiella burnetii* infection detected through bone marrow biopsy in Vietnam. *Clin. Pathol.* 15, 397. doi: 10.1177/2632010X221096397

Thompson, J. D., Higgins, D. G., and Gibson, T. J. (1994). CLUSTAL W: improving the sensitivity of progressive multiple sequence alignment through sequence weighting, position-specific gap penalties and weight matrix choice. *Nucleic Acids Res.* 22, 4673–4680. doi: 10.1093/nar/22.22.4673

Trinachartvanit, W., Maneewong, S., Kaenkan, W., Usananan, P., Baimai, V., and Ahantarig, A. (2018). *Coxiella*-like bacteria in fowl ticks from Thailand. *Parasit. Vectors.* 11, 1–6. doi: 10.1186/s13071-018-3259-9

Tshokey, T., Stenos, J., Durrheim, D. N., Eastwood, K., Nguyen, C., Vincent, G., et al. (2018). Rickettsial infections and Q fever amongst febrile patients in Bhutan. *Trop. Med. Infect. Dis.* 3, 12. doi: 10.3390/tropicalmed3010012

Tshokey, T., Stenos, J., Tenzin, T., Drukpa, K., Gurung, R. B., and Graves, S. R. (2019). Serological evidence of *Rickettsia*, *Orientia*, and *Coxiella* in domestic animals from Bhutan: preliminary findings. *Vector Borne Zoonotic Dis.* 19, 95–101. doi: 10.1089/vbz.2018.2336

Ullah, Q., El-Adawy, H., Jamil, T., Jamil, H., Qureshi, Z. I., Saqib, M., et al. (2019). Serological and molecular investigation of *Coxiella burnetii* in small ruminants and ticks in Punjab, Pakistan. *Int. J. Environ. Res. Public Health.* 16, 4271. doi: 10.3390/ijerph16214271

Ullah, S., Alouffi, A., Almutairi, M. M., Islam, N., Rehman, G., Islam, Z. U., et al. (2023). First report of *Rickettsia conorii* in *Hyalomma kumari* ticks. *Animals.* 13, 1488. doi: 10.3390/ani13091488

Yessinou, R. E., Katja, M. S., Heinrich, N., and Farougou, S. (2022). Prevalence of *Coxiella*-infections in ticks-review and meta-analysis. *Ticks Tick Borne Dis.* 2022, 101926. doi: 10.1016/j.ttbdis.2022.101926

frontiers | Frontiers in Microbiology

TYPE Original Research
PUBLISHED 04 August 2023
DOI 10.3389/fmicb.2023.1223151

Check for updates

OPEN ACCESS

EDITED BY
Anastasios D. Tsaousis,
University of Kent, United Kingdom

REVIEWED BY
Panagiotis Karanis,
University of Nicosia, Cyprus
David Carmena,
Carlos III Health Institute (ISCIII), Spain

*CORRESPONDENCE
Olga Matos
✉ omatos@ihmt.unl.pt
Maria Luísa Lobo
✉ luisalc@ihmt.unl.pt

†These authors have contributed equally to this work and share first authorship

RECEIVED 15 May 2023
ACCEPTED 17 July 2023
PUBLISHED 04 August 2023

CITATION
Salamandane C, Lobo ML, Afonso S, Xiao L and Matos O (2023) Exploring genetic variability of *Giardia duodenalis* and *Enterocytozoon bieneusi* in raw vegetables and fruits: implications for food safety and public health in Mozambique. *Front. Microbiol.* 14:1223151. doi: 10.3389/fmicb.2023.1223151

COPYRIGHT
© 2023 Salamandane, Lobo, Afonso, Xiao and Matos. This is an open-access article distributed under the terms of the Creative Commons Attribution License (CC BY). The use, distribution or reproduction in other forums is permitted, provided the original author(s) and the copyright owner(s) are credited and that the original publication in this journal is cited, in accordance with accepted academic practice. No use, distribution or reproduction is permitted which does not comply with these terms.

Exploring genetic variability of *Giardia duodenalis* and *Enterocytozoon bieneusi* in raw vegetables and fruits: implications for food safety and public health in Mozambique

Cátia Salamandane[1,2,3†], Maria Luísa Lobo[1*†], Sónia Afonso[4], Lihua Xiao[5] and Olga Matos[1,6*]

[1]Group of Opportunistic Protozoa/HIV and Other Protozoa, Global Health and Tropical Medicine, Medical Parasitology Unit, Instituto de Higiene e Medicina Tropical, Universidade Nova de Lisboa, Lisboa, Portugal, [2]Nova School of Business and Economics, Universidade Nova de Lisboa, Carcavelos, Portugal, [3]Faculdade de Ciências de Saúde, Universidade Lúrio, Nampula, Mozambique, [4]Parasitology Department of Veterinary Faculty, Universidade Eduardo Mondlane, Maputo, Mozambique, [5]College of Veterinary Medicine, South China Agricultural University, Guangzhou, Guangdong, China, [6]Environmental Health Institute, Faculdade de Medicina da Universidade de Lisboa, Lisboa, Portugal

Giardia duodenalis and *Enterocytozoon bieneusi* are etiological agents of enteric diseases characterized by diarrhea that can progress to chronicity in humans, especially in children and in immunocompromised patients. This study aims to assess the genetic pattern of *G. duodenalis* and *E. bieneusi* detected in vegetables and fruits commercialized in Maputo markets, Mozambique and determine their public health importance. Eight study points were sampled: a farmer zone, a wholesale, four retail markets, and two supermarkets in Maputo city, where eight types of horticultural products were purchased. Using nested-PCR methods, 2.8% (9/321) and 1.3% (4/321) of samples monitored were positive for *G. duodenalis* and *E. bieneusi*, respectively. Based on the analysis of the β-giardin and ITS rRNA sequences of *G. duodenalis* and *E. bieneusi* detected, respectively, four different sequences of *G. duodenalis* (three novel sequences: BgMZ1, BgMZ2, and BgMZ3, and one known sequence) all from assemblage B and three genotypes of *E. bieneusi* (two novel sequences: EbMZ4 and EbMZ5, and one known sequence: KIN-1) from group 1. These microorganisms were found and characterized for the first time in horticultural products in Maputo markets. All identified *G. duodenalis* and *E. bieneusi* display high genetic similarity within their β-giardin and ITS rRNA sequences, respectively, having been clustered into assemblages and genotypes with high zoonotic transmission potential. Our study may represent a relevant step in the understanding of these intestinal pathogens in association with fresh vegetables and fruits for human consumption, for a better and broader "One Health" approach.

KEYWORDS

intestinal protozoa, microsporidia, raw horticultural products, foodborne diseases, zoonotic transmission, Maputo, One Health

1. Introduction

Giardia duodenalis and *Enterocytozoon bieneusi* are etiological agents of acute and chronic disorders including diarrhea, malabsorption, and severe debilitation illnesses in humans and animals, particularly in children and immunocompromised patients (Lobo et al., 2014; Xiao and Feng, 2017; Stentiford et al., 2019; Junaidi et al., 2020; Rafiei et al., 2020). Human infections by the pathogens *G. duodenalis* and *E. bieneusi* may be acquired through direct contact with infected persons (person-to-person transmission) or animals (zoonotic transmission) or even ingestion of contaminated water (waterborne transmission; Baldursson and Karanis, 2011; Efstratiou et al., 2017a; Ahmed et al., 2018) and food (foodborne transmission; Li et al., 2012; Matos et al., 2012; Stentiford et al., 2016; Squire and Ryan, 2017; Rodrigues et al., 2020). As *G. duodenalis* cysts and *E. bieneusi* spores are robust and resistant to environmental conditions, some waterborne and foodborne outbreaks mostly for human giardiasis have been reported (Thompson et al., 2008; Ahmed et al., 2018; Javanmard et al., 2020; Bahramian et al., 2021; Hassan et al., 2021). Relatively less is known about the occurrence and molecular epidemiology of these two pathogenic species in water and food in Africa.

Giardia duodenalis has eight genetic assemblages (A-H): A, B, C, D, E, and F can infect humans (mostly A and B) and other animals, and assemblages C to H have a narrower host range (Yaoyu and Xiao, 2011; Cai et al., 2021; Dixon, 2021). *Enterocytozoon bieneusi* is mentioned as the most prevalent among the 17 human-infecting microsporidia species (Lobo et al., 2012; Matos et al., 2012; Stentiford et al., 2019). The genetic variability of this pathogenic species is based on the analysis of single-nucleotide polymorphisms (SNPs) in the internal transcribed spacer (ITS) region of the ribosomal RNA (rRNA; Santin and Fayer, 2009; Lobo et al., 2014; Li et al., 2019b). To date, over 600 genotypes of *E. bieneusi* have been identified (Cunha et al., 2017; Chen et al., 2019; Zhang et al., 2020; Cao et al., 2021), clustered in 11 phylogenetic groups (Matos et al., 2012; Xiao and Feng, 2017; Cacciò et al., 2018; Cao et al., 2021). Within Group 1, genotypes D, Ebp C, and Type IV are those most frequently found not only in humans but also in domestic and wild animals worldwide, suggesting a low level of host specificity and the potential for zoonotic or cross-species transmission. Also, Group 1 genotypes, such as Peru 6, Peru 8, and Peru 11, have been regularly identified in both humans and animals. Group 2 genotypes were once considered to be adapted to ruminants but have subsequently been found in other animals and humans. Group 3 to Group 11 genotypes seem to have a clear and strong host specificity although few information is available for those groups (Santin and Fayer, 2009; Wang et al., 2016; Li et al., 2019a,b, 2020b; Wu et al., 2020a). However, the lack of information on risk factors or epidemiology associated with its transmission limits the full understanding and implications of *E. bieneusi*'s zoonotic potential.

Several studies (Lobo et al., 2014; Li et al., 2020b; Salamandane et al., 2021b; Mozer et al., 2022) for the molecular characterization of *G. duodenalis* and *E. bieneusi* have been carried out, but in Africa, studies on *G. duodenalis* are more abundant than studies on *E. bieneusi*. More precisely, there are studies done mainly in humans and livestock (Akinbo et al., 2012; Samra et al., 2012; Lobo et al., 2014; Laatamna et al., 2015; Wegayehu et al., 2020). In Mozambique, the first study on *E. bieneusi* genotyping was recently carried out in young children, in which a novel subtype, HhMzEb1, was reported (Muadica et al., 2020).

In southern Africa, some of the few studies on these two pathogenic microorganisms were also performed in water (Dalu et al., 2011; Mtapuri-Zinyowera et al., 2014; Archer et al., 2020; Siwila et al., 2020). Globally, the occurrence of protozoan parasitic contamination in vegetables and fruits ranges from 1.9 to 9.3% (Li et al., 2019a). Thus, this study aims to carry out the genetic characterization of *G. duodenalis* and *E. bieneusi* detected in vegetables and fruits commercialized in Maputo markets, Mozambique and determine their public health importance.

2. Materials and methods

2.1. Sampling

This study was carried out in the rainy (February to March) and in the dry seasons (August to October) of 2019, in eight points of study, and according to the markets' typology, namely, a producer zone (Infulene Valley), one wholesale market (Zimpeto), four retail markets (Xipamanine, Benfica, Central da Baixa, and Fajardo), and two supermarkets (LMC and LSP) in Maputo city. In each selected study point, we randomly purchased three specimens of each of the eight types of raw and fresh horticultural products, namely, coriander (*Coriandrum sativum*), parsley (*Petroselinum crispum*), Portuguese cabbage (*Brassica Oleracea costata*), pointed white cabbage (*Brassica oleracea capitata*), carrot (*Daucus carota*), tomato (*Solanum lycopersicum*), green pepper (*Capsicum annuum*), and lettuce (*Lactuca sativa cea*). The products were placed in individual plastic bags, encoded with a unique number and the date of collection, and transported in a container at 4°C. Several detaching and concentrating *G. duodenalis* cysts and *E. bieneusi* spores protocols reported in the literature were reviewed (Monge and Chinchilla, 1996; Cook et al., 2007; Mozer et al., 2022), and the more consensual approach was selected for this study, taking into account the distinct size and food matrices of the products studied and the field work conditions.

A total of 321 samples collected (153 in the rainy season and 168 in the dry season) were transported to the laboratory for processing. At the laboratory, we first weighed the fruits and vegetables according to their sizes: for the large ones, we weighed 150–250 g (lettuce, pointed white cabbage, and Portuguese cabbage), and for the small ones, we weighed 80–100 g (coriander, parsley, carrot, tomato, and green pepper). Then, they were washed in 200 ml and 50 ml of a solution of NaCl (0.85%) in distillate water, for large and small fruits/vegetables, respectively, in a plastic bag. They were shaken vigorously on an orbital shaker (SK-300 Lab Companion, Woburn, Massachusetts, USA) at 150 rpm for 20 min and brined overnight. The next morning, the solution was collected in 50 ml Falcon tubes and centrifuged at 8,000 × *g* for 15 min. Finally, 5–8 ml of the concentrated vegetable extracts was saved for DNA extraction and direct microscopy analysis, and the remainder was used to make smears for staining (Salamandane et al., 2021b). The samples were stored in a cooler at 4°C for DNA extraction.

2.2. Molecular detection of *Giardia duodenalis* and *Enterocytozoon bieneusi* using nested-PCR methods

Genomic DNA was extracted from concentrated vegetable/fruit extracts for the molecular detection of *G. duodenalis* and *E. bieneusi*, using the QIAamp Fast DNA Stool Mini Kit according to the manufacturer's instructions. The extracted DNA (100 µl/sample) was kept at −20°C.

A nested-PCR analysis (Cacciò et al., 2002; Lalle et al., 2005) targeting the β-giardin (*bg*) gene was used to detect *G. duodenalis*. The primary reactions were carried out using the primers GiaFW1 (5′-AAGCCCGACGACCTCACCCGCAGTGC-3′) and GiaRV1 (5′-GAGGCCGCCCTGGATCTTCGAGAC GAC-3′) for the 753-bp fragment amplification. For the secondary reactions, the primers GiaFW2 (5′-GAACGAACGAGATCGAGGTCCG-3′) and GiaRV2 (5′-CTCGACGAGCTTCGTGTT-3′) were used to amplify the 511-bp fragment.

The detection of *E. bieneusi* was performed by nested-PCR analysis targeting the entire internal transcribed spacer (ITS) region of the rRNA gene, and its genotyping was conducted by sequence analysis of amplified fragments of the ITS rRNA gene (Lobo et al., 2012). Primary and secondary reactions were carried out using the primers MLLF1 (5′-CGCCCGTCACTATTTCAGAT-3′) and MLLR1 (5′-GCTTAAGTCCAGGGAGTATCCA-3′) to amplify a 514-bp fragment, and MLLF2 (5′-AGTCGTAACAAGGTTTCAGTTGG-3′) and MLLR2 (5′-GGACTTTTCGCATTCTTTCG−3′) to amplify a 386-bp fragment, respectively.

Successively, the PCR products were loaded on 1.5% agarose gel stained with ethidium bromide and subjected to electrophoresis and finally visualized under UV light on a proper device.

2.3. *Giardia duodenalis* and *Enterocytozoon bieneusi* sequencing and data analysis

The products of the expected size were purified using a PureLink™ Quick Gel Extraction and PCR Purification Combo kit (Invitrogene, Carlsbad, Califórnia, EUA), as described on the manufacturer's instructions, and were submitted to Sanger sequencing in both directions on an ABI3100 automated sequencer (Applied Biosystem, Foster City, CA) at STABVIDA Company (Lisbon, Portugal). Three PCR products of each positive sample obtained from different PCRs were submitted to DNA sequencing. The authors analyzed all three sets of sequencing chromatograms obtained for each of the positive samples. Next, the individual sequences were subsequently aligned against reference sequences from the GenBank database using the BLASTN (www.ncbi.nlm.nih.gov) and ClustalX (ftp://ftp-igbmc.u-strasbg.fr/pub/ClustalX/) programs to determine *G. duodenalis* and *E. bieneusi* genetic variability.

Representative nucleotide sequences of *bg* and ITS genes of *G. duodenalis* and *E. bieneusi* are available in the NCBI GenBank database under the accession numbers ON924995, ON924996, OP066417-OP066422, and OP076835-OP076838, respectively.

2.4. *Giardia duodenalis* and *Enterocytozoon bieneusi* phylogenetic analysis

Phylogenetic analysis based on the β-giardin and ITS rRNA sequences dataset of *G. duodenalis* and *E. bieneusi*, respectively, was performed using the maximum likelihood method based on the general time reversible model conducted in MEGA 7.

3. Results

After nested-PCR analysis, *G. duodenalis* and *E. bieneusi* were detected in 2.8% (9/321) and 1.3% (4/321), respectively, of the samples monitored. According to the distinct seasons, *G. duodenalis* was found in three (1.96%) samples (lettuce, green pepper, and tomato) in the rainy season and in six (3.6%) samples (Portuguese cabbage, lettuce, parsley/2, and pointed white cabbage/2) in the dry season. *Enterocytozon bieneusi* DNA was detected in one (0.7%) sample (pointed white cabbage) in the rainy season and in three (1.8%) samples (lettuce, tomato, and coriander) in the dry season, among four different markets. *Giardia duodenalis* was detected in products from four markets and one supermarket, and *E. bieneusi* was found in products from three markets and in products from the same supermarket as *Giardia*. The distribution of *G. duodenalis* assemblages and *E. bieneusi* genotypes identified in the horticultural products among the markets monitored, during dry and rainy seasons, in Maputo City is summarized in Table 1.

DNA Sanger sequencing was successfully achieved for all nine and four specimens diagnosed as positive for *G. duodenalis* and *E. bieneusi*, respectively, using nested-PCR methods. The authors analyzed the three sets of sequencing chromatograms obtained for each positive sample, which were found to be consistent, indicating the reliability of the identified new sequences. No instances of mixed infection were identified.

Sequencing and alignment of our nine nucleotide sequences with others of known identity deposited in the GenBank database showed the presence of four different *G. duodenalis bg* sequences all from assemblage B in the samples studied. One of them was a known *bg* sequence, and three were novel *bg* sequences. Of the nine sequences obtained, three (BGMZ69, BGMZ71, and BGMZ90 samples) had 100% similarity with the *G. duodenalis* nucleotide sequence MK033096, one (BGMZ7) constitutes a novel sequence (BgMZ2) and differs from the previous three by a single nucleotide at 356 (G→ A) displaying 99.81% homology with sequence MK033096. The remaining five sequences generated in this study are also new *G. duodenalis bg* sequences and have 99% homology with *G. duodenalis* nucleotide sequences previously reported: three (BGMZ54, BGMZ60, and BGMZ64; BgMZ3) had one substitution to isolate KY320578 at 456 (C→ T), and two (BGMZ3, BGMZ25; BgMZ1) had three substitutions to isolate MG736246 at 99 (T→ C), at 136 (A→ G), and at 356 (G→ A).

The four *E. bieneusi* ITS sequences characterized in the four positive samples obtained in this study revealed high genetic diversity: two (EBMZ86 and EBMZ95) sequences with the genotype KIN-1 (e.g., identified in humans and livestock, such as cattle, pig, goat, horse, wild animals, and non-human primates), one (EBMZ30; EbMZ4 genotype) of the sequences characterized is a novel genotype displaying 99.71% homology with KIN-1 and

TABLE 1 Genetic characterization of *Giardia duodenalis* and *Enterocytozoon bieneusi* by nested-PCR and DNA sequencing analysis according to horticultural product, market, and seasons monitored in Maputo city.

Sample code	Market	Season	Horticultural product	Species	Assemblage or genotype
BGM Z3	Zimpeto	Rainy	Lettuce	*G. duodenalis*	B[a]
BGM Z7	Zimpeto	Rainy	Green pepper	*G. duodenalis*	B[b]
BGMZ 25	Benfica	Rainy	Tomato	*G. duodenalis*	B[a]
BGMZ 54	Zimpeto	Dry	Portuguese cabbage	*G. duodenalis*	B[c]
BGMZ 60	Xipamanine	Dry	Lettuce	*G. duodenalis*	B[c]
BGMZ 64	Xipamanine	Dry	Parsley	*G. duodenalis*	B[c]
BGMZ 69	LMC	Dry	Pointed white cabbage	*G. duodenalis*	B
BGMZ 71	LMC	Dry	Parsley	*G. duodenalis*	B
BGMZ 90	Fajardo	Dry	Pointed white cabbage	*G. duodenalis*	B
EBMZ 30	Central da baixa	Rainy	Pointed white cabbage	*E. bieneusi*	EbMZ4[d]
EBMZ 73	LMC	Dry	Lettuce	*E. bieneusi*	EbMZ5[e]
EBMZ 86	Benfica	Dry	Tomato	*E. bieneusi*	KIN-1
EBMZ 95	Fajardo	Dry	Coriander	*E. bieneusi*	KIN-1

[a]BgMZ1.
[b]BgMZ2.
[c]BgMZ3: new *G. duodenalis* bg sequences identified in this study.
[d,e]New *E. bieneusi* genotypes identified in this study.

Peru8 genotypes, with one substitution at 139 (T→ C) and one substitution at 159 (C→ T), respectively. The remaining novel one (EBMZ73; EbMZ5 genotype) had 99.44% similarity with KIN-1 and had two substitutions at 124 (G→ A) and at 182 (G→ A).

To obtain information on the β-giardin and ITS rRNA sequences in this study and the respective reference sequences published in previous studies, two phylogenetic trees were constructed.

Phylogenetic analysis revealed that the nine *G. duodenalis* sequences from this study were clustered within assemblage B and formed three genetic clusters comprising species mostly infecting humans and several other domestic and wild mammals (Figure 1).

The two novel and the two known *E. bieneusi* genotypes detected in this research were all clustered into zoonotic group 1 (Figure 2).

4. Discussion

Several pathogens are responsible for causing human diarrheal diseases, among which *G. duodenalis* and the microsporidian *E. bieneusi* are important contributors worldwide. Both species can be transmitted by ingestion of contaminated food and water. Contact and ingestion of contaminated water are considered important risk factors related to both *G. duodenalis* and *E. bieneusi* infection in epidemiological studies (Santin and Fayer, 2009; Li et al., 2012; Squire and Ryan, 2017; Stentiford et al., 2019; Dixon, 2021). Either *G. duodenalis* cysts or microsporidian spores are robust and can be highly resistant to external environmental conditions and to several physical and chemical disinfection methods used in drinking water plants, swimming pools, and irrigation systems. Moreover, as the other human-infecting microsporidia, *E. bieneusi* spores are microscopic in size and have low specific gravity, which facilitates their easy dissemination (Matos et al., 2012; Stentiford et al., 2019; Dixon, 2021).

Fresh vegetables and fruits, despite the health benefits of their human consumption, can be an important source of some foodborne pathogenic microorganisms, including *G. duodenalis* and *E. bieneusi* (Rafael et al., 2017; Utaaker et al., 2017; Ferreira et al., 2018; Li et al., 2019a, 2020a; Archer et al., 2020; Salamandane et al., 2020; Siwila et al., 2020). This study showed the occurrence of these two important human pathogenic species and their genotypes among raw and fresh horticultural products in different markets of different typologies in Maputo city. Using nested-PCR techniques, 2.8 and 1.3% of the samples monitored were positive for *G. duodenalis* and *E. bieneusi*, respectively. Based on the *bg* and ITS rRNA sequences analysis of *G. duodenalis* and *E. bieneusi*, respectively, four different *G. duodenalis* sequences (three novel and one known) all from assemblage B and three *E. bieneusi* genotypes (two novel and one known) from group 1 were characterized for the first time in fruits and vegetables from Maputo markets in Mozambique.

Much higher prevalence rates of *G. duodenalis* human infection are observed in developing countries in comparison to the developed regions (Dixon, 2021). The prevalence of *G. duodenalis* in Africa has been reported between rates from 0.3 to 62.2% according to the population studied (age, gender, symptoms, and immunological status) and the methodology used (Squire and Ryan, 2017; Damitie et al., 2018; Miambo et al., 2019; Yu et al., 2019; Belkessa et al., 2021; Messa et al., 2021). It is estimated that this protozoan causes about 28.2 million cases of diarrhea annually due to the ingestion of contaminated food (Ryan et al., 2019). *Giardia duodenalis* human infections are often associated with the consumption of contaminated raw fruits and vegetables, and the

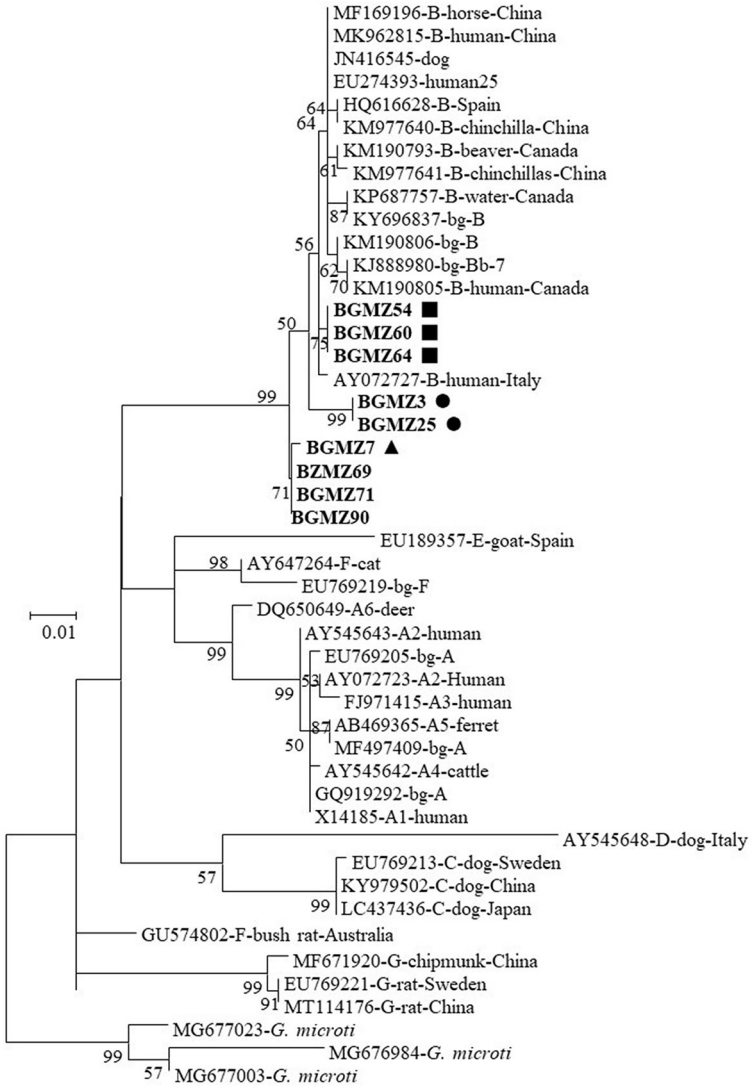

FIGURE 1
Phylogenetic relationship between *Giardia duodenalis* characterized in this study and other sequences in GenBank by analysis of β-giardin sequences. The evolutionary history was inferred by using the maximum likelihood method based on the general time reversible model. The tree with the highest log likelihood (−1,638.69) is shown. The percentage of trees in which the associated taxa clustered together is shown next to the branches. Initial tree(s) for the heuristic search were obtained automatically by applying Neighbor-Join and BioNJ algorithms to a matrix of pairwise distances estimated using the maximum composite likelihood (MCL) approach and then selecting the topology with superior log likelihood value. A discrete gamma distribution was used to model evolutionary rate differences among sites [five categories (+*G*, parameter = 0.2391)]. The rate variation model allowed for some sites to be evolutionarily invariable [[+*I*], 58.88% sites]. The tree is drawn to scale, with branch lengths measured in the number of substitutions per site. The analysis involved 48 nucleotide sequences. Codon positions included were 1st+2nd+3rd+Non-coding. All positions containing gaps and missing data were eliminated. There were a total of 472 positions in the final dataset. Evolutionary analyses were conducted in MEGA7. The *G. duodenalis* β-giardin sequences from this study are in boldface. The circles (BgMZ1), triangles (BgMZ2), and squares (BgMZ3) filled in black indicate new *bg* sequences identified in this study.

occurrence of the parasite cysts in these products has been reported in many countries with an average prevalence estimated of 4.8% (Li et al., 2020a). The 2.8% of *G. duodenalis* occurrence in the samples analyzed in our study is in accordance with the few available data from African countries that described 0–17.8% rates of this parasite in contaminated vegetables and fruits, reported in Morocco, Egypt, Libya, Ghana, Ethiopia, and Nigeria (Eraky et al., 2014; Istifanus and Panda, 2018; Kudah et al., 2018; Alemu et al., 2019; Berrouch et al., 2020; Li et al., 2020a; Sripanompong et al., 2021), mainly the leafy ones (Badri et al., 2022). Although the rate of incidence for *G. duodenalis* has been described as 0.11 in Africa (Hald et al., 2016), other studies mentioned the prevalence of *G. duodenalis* higher in developing countries (0.9–40.7%) when compared with developed countries (0.4–7.0%; Ryan and Cacciò, 2013; Wu et al., 2020b; Mozer et al., 2022).

As observed for *G. duodenalis*, the potential zoonotic pathogen *E. bieneusi* is described as a cause of symptomatic and asymptomatic infections in humans and other animals worldwide. There is limited information on *E. bieneusi* occurrence and genetic characterization in African countries, but the reported frequency

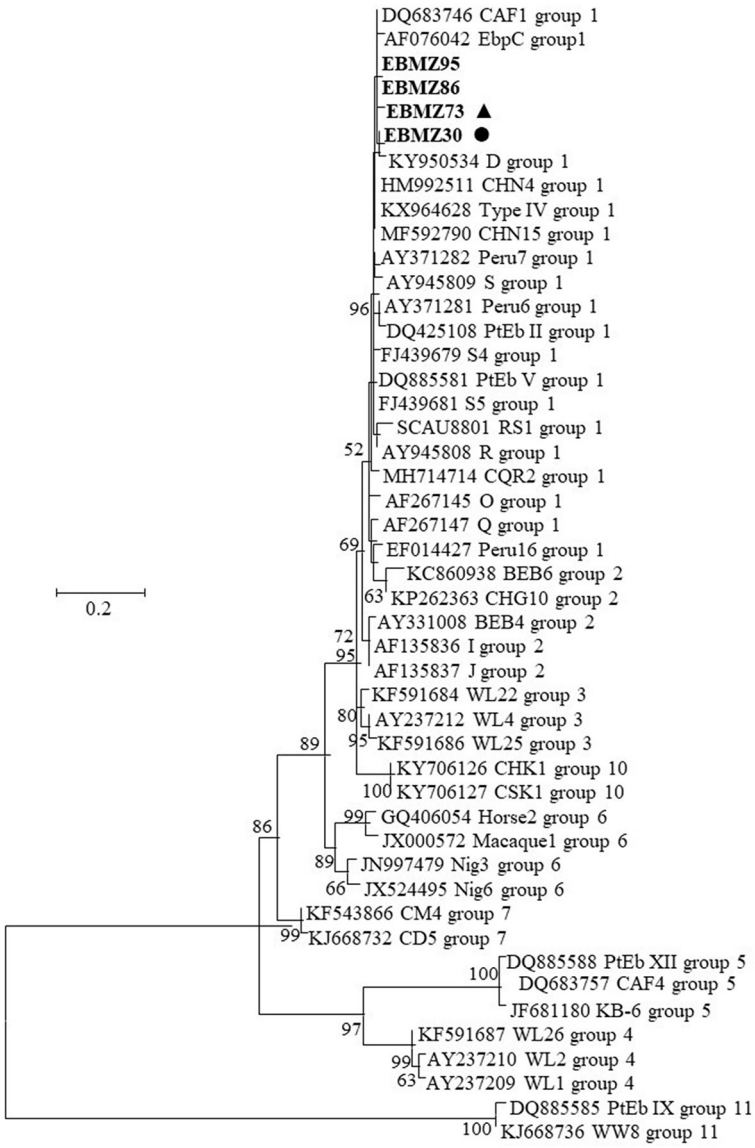

FIGURE 2
Phylogenetic relationship between *Enterocytozoon bieneusi* characterized in this study and other sequences in GenBank by analysis of ITS rRNA sequences. The evolutionary history was inferred by using the maximum likelihood method based on the general time reversible model. The tree with the highest log likelihood (−1,808.47) is shown. The percentage of trees in which the associated taxa clustered together is shown next to the branches. Initial tree(s) for the heuristic search were obtained automatically by applying Neighbor-Join and BioNJ algorithms to a matrix of pairwise distances estimated using the maximum composite likelihood (MCL) approach and then selecting the topology with superior log likelihood value. A discrete gamma distribution was used to model evolutionary rate differences among sites [five categories (+*G*, parameter = 1.4711)]. The rate variation model allowed for some sites to be evolutionarily invariable [[+*I*], 4.58% sites]. The tree is drawn to scale, with branch lengths measured in the number of substitutions per site. The analysis involved 47 nucleotide sequences. All positions containing gaps and missing data were eliminated. There was a total of 215 positions in the final dataset. Evolutionary analyses were conducted in MEGA7. The *E. bieneusi* sequences from this study are in boldface. The circle (EbMZ4) and triangle (EbMZ5) filled in black indicate the new genotypes identified in this study.

rates of infection can range from 0.5 to 76.9%, mostly among HIV-infected patients, by PCR techniques (Muadica et al., 2020). More recently, Muadica et al. detected 0.7% (9/1,247) of *E. bieneusi*-positive samples in symptomatic and asymptomatic children in Mozambique (Muadica et al., 2020). Most human infections with *E. bieneusi* are thought to result from fecal-oral transmission of infectious spores through ingestion of contaminated food or water (Qiu et al., 2019). For instance, *E. bieneusi* has been identified in milk, raspberries, beans, and lettuce (Lee, 2008; Decraene et al., 2012), and the first foodborne outbreak caused by this species was reported in Sweden in 2009 (Decraene et al., 2012). More recently, a study mentioned a foodborne outbreak of *E. bieneusi* in Denmark (Michlmayr et al., 2022). Thus, foodborne transmission of *E. bieneusi* has been documented, and the contamination of vegetables and fruits with this pathogen was reported in China (PCR), Costa Rica (Ziehl-Nielsen stain), and Poland (staining or with fluorescence *in situ* hybridization). The average prevalence of the reported contamination among these studies was estimated

as 3.6% (Li et al., 2020a). A lower frequency of contamination by *E. bieneusi* (1.3%) was detected in the vegetables and fruits analyzed in this study. Although this low rate may be associated with the difficulty in recovering these tiny microsporidia spores from the horticultural products analyzed, limiting their molecular detection, this finding may also constitute a positive indicator of safer products commercialized in these markets compared to others from different regions.

The presence of *G. duodenalis* was observed in fresh vegetables purchased in four municipal markets and *E. bieneusi* in fresh vegetables purchased in three markets and one supermarket. The higher occurrence of these pathogenic species in the main markets (open-air markets with limited or even absent proper sanitary conditions) than in the supermarkets monitored was expected and is certainly associated with their specific structural and environmental characteristics, which contribute to the contamination of food products in those former markets. However, in the other markets of different typologies surveyed, namely, in Central da Baixa market (a covered, well-structured market) and especially in the supermarket that have all the guaranteed resources, availability of water, market stalls and toilets, transport, handling and display of products for their safety, the produce contamination by one or both pathogenic species observed were not expected. The vegetables and fruits handled during preparation for display in the supermarket or even by the consumer can be one of the factors for the contamination that we observed (Salamandane et al., 2020, 2021b).

Both pathogens were mostly found in leafy vegetables (lettuce, point white cabbage, and parsley). Usually, high contamination rates of lettuce and other types of leafy vegetables (cabbage, parsley, and coriander) are also reported by other authors due to the uneven external surface of their leaves, which enables the easy entry and adherence of the *G. duodenalis* and *E. bieneusi* resistant forms (Rodrigues et al., 2020; Salamandane et al., 2020, 2021b; Badri et al., 2022).

In reports of contaminated vegetables and fruit worldwide, among the eight genetically distinct *G. duodenalis* assemblages (A–H) described to date, the zoonotic assemblages A and B were commonly detected (Li et al., 2020a). A few *Giardia* genotyping studies have been carried out in Africa; however, available reports show that five *G. duodenalis* assemblages (A, B, C, E, and F) have been identified in humans (Cai et al., 2021). In African countries, assemblage B was the most frequent among genotyped samples (19.5–100%) in 18 of 28 human population studies with assemblage A dominant (1.4–100%) in the remaining 10 reports (Cai et al., 2021). Recently, a study performed in Mozambique (Messa et al., 2021), in children aged under 5 years, reported a very low prevalence for assemblage A (10%) when compared with assemblage B (90%), following the normal tendency in sub-Saharan Africa. β-giardin sequence analysis from all nine *G. duodenalis* sequences identified in this study belong exclusively to assemblage B. Within the assemblage B sequences, four distinct *bg* sequences were formed: *bg* one sequence is an identical *bg* sequence to one previously reported; and the other three (BgMZ1, BgMZ2, and BgMZ3) display 99% of similarity to other *bg* sequences deposited in the reference database. The four different *bg* sequences identified were very similar with a mild difference between them and were relative to the reference sequences only from one to three single-nucleotide polymorphisms (SNP). Phylogenetic analysis of all nine *G. duodenalis* isolates, from the vegetables and fruits included in this study, indicates that all of them clustered closer to other sequences (Figure 1) previously detected in humans, other animals, and water, corroborating their potential role as a source of human infection and environmental contamination. In this study, the observed heterogeneity of assemblage B among *G. duodenalis bg* sequences was somewhat expected. This assemblage typically exhibits more genetic variability than assemblage A, as reported in the literature (Cai et al., 2021).

Genotyping tools and the phylogenetic analysis of *E. bieneusi* genotypes inferred by the genetic diversity of their ITS rRNA region recognized 11 genetic groups (Groups 1–11), figuring out their host specificity and zoonotic potential. Molecular studies on *E. bieneusi* worldwide stated that the occurrence of genotypes from Groups 1 (D, EbpC, and Type IV) and 2 (BEB4, BEB6, I, and J) are the most commonly identified (Li et al., 2019b, 2020b; Rahimi et al., 2021), where pigs and cattle are the main zoonotic reservoir of *E. bieneusi* (Li et al., 2019b; Zang et al., 2021). Despite the few studies on *E. bieneusi* in vegetables and water, some authors reported that D, BEB6, and E genotypes are the most frequent and with high zoonotic potential. In fact, the D genotype was identified also in chicken, water, humans, and vegetables (Javanmard et al., 2018; Cao et al., 2020; Rahimi et al., 2021). In Africa, molecular characterization remains rare and connected with livestock or clinical environments, performed only in a few countries such as Algeria, Ethiopia, Nigeria, South Africa, and recently in Mozambique (Akinbo et al., 2012; Samra et al., 2012; Laatamna et al., 2015; Stentiford et al., 2019; Muadica et al., 2020; Wegayehu et al., 2020). In another study working with stool specimens (Muadica et al., 2020), some known genotypes (Peru 11, Type IV and S2) were identified and described a new one HhMzEb1 (from Group 1) in Mozambique. None of the studies was associated with food or water or horticultural products. Nucleotide sequence analysis of the ITS region revealed a high degree of genetic diversity with a total of three distinct genotypes including one known (KIN-1) and two novel (EbMZ4 and EbMZ5) genotypes in the four *E. bieneusi* sequences obtained from the horticultural products monitored in this study. Phylogenetic analysis showed that both the known and the novel genotypes clustered within the previously designated zoonotic Group 1 include genotypes with low host specificity and the potential for zoonotic and cross-species transmission (Figure 2). All the genotypes identified in this study clustered very closer with other genotypes (e.g., D, Ebp C; Figure 2) that display a high zoonotic transmission potential (Li et al., 2020b).

The contamination of fresh horticultural products with the infectious stages of parasites may occur at any of the distinct points from the farm level to the food handler/consumer level. At the farm level, the contamination of fresh vegetables and fruits may occur during production, harvesting, packaging, transport, or selling. Contamination with *Giardia* cysts and *E. bieneusi* spores can occur directly from the hands of infected farm workers (or their equipment) or those who are in close contact with infected individuals; through the use of animal or human feces as manure for farmland; or direct access to infected cattle and other animals to crops. Indirect contamination of horticultural products at the

production zone can occur by using irrigation water contaminated with feces; mixing pesticides; or washing horticultural products, hands, or equipment (Dixon, 2021). The direct contamination of fresh produce by infected food handlers, or who have been in close contact with infected persons, is probably a main contributor and has been identified as the direct cause of a number of outbreaks (Dixon, 2021). Although, in this study, *G. duodenalis* and *E. bieneusi* were not detected in the production zone (Infulene Valley) by the molecular techniques, it does not mean for sure that the products were not contaminated at this point. For instance, *G. duodenalis*, like other intestinal parasites, were detected in this zone by the authors (Salamandane et al., 2021b), in a previous study with microscopic methods. In this study, different *G. duodenalis bg* sequences from assemblage B, as well as similar *E. bieneusi* genotypes or *G. duodenalis* assemblage B, were detected in the same market/supermarket. Also, similar *E. bieneusi* genotypes/*G. duodenalis bg* sequences from assemblage B were identified in distinct markets (Table 1). All this reflection leads us to think that the possible contamination of horticultural products in markets and supermarkets in our study may have a similar origin, which is in agreement with other authors who report that post-harvest contamination can occur mainly during packaging, transport, and handling of the products (Vizon et al., 2019; Salamandane et al., 2021a).

The recognition of these intestinal pathogens in fresh vegetables and fruits not only allows this study to be framed within the strict scope of zoonotic diseases, helping to clarify the epidemiology of *G. duodenalis* and *E. bieneusi* in the country but also opens doors to other dimensions. There is a particular emphasis on the environmental dimension and its role in global homeostasis, as advocated in the context of the One Health approach. In addition to alerting to the risk for human consumption of these products, directly improving health population outcomes, this study suggests the existence of contamination at an environmental level. Such contamination may occur through animals and wastewater polluted with human and animal waste during various processes of production, transport, and sale of these products. Therefore, our findings indirectly reinforce the need to develop better epidemiological surveillance systems for enteric pathogens in the area and to adopt measures such as improving sanitary conditions and ensuring safe water and food to prevent and control these diseases. These measures will bring benefits to the health of people, animals, and ecosystems.

5. Strengths and limitations of the study

Our research, to the best of our knowledge, represents a groundbreaking study on the detection of *G. duodenalis* and *E. bieneusi*, as well as the assessment of their genetic heterogeneity. We isolated these organisms from raw horticultural products obtained from eight different types of markets in Maputo, Mozambique. Additionally, this study included a significant number of horticultural products with two different food matrices (leafy vegetables and fruits) that were randomly purchased in triplicate from the most popular and frequently visited markets in Maputo city, during the two main seasons of the year. By employing molecular tools, we not only demonstrated the presence of potential zoonotic assemblages/genotypes of *G. duodenalis* and *E. bieneusi* among the fresh fruits and vegetables examined but also highlighted the usefulness of these tools in tracing the sources of food contamination.

However, our study has certain limitations associated with the methodology we adopted, particularly the protocols used for recovering cysts/spores from horticultural product extracts and the molecular tools employed. These limitations are primarily due to the unavailability of certain technical resources, such as a fluorescent microscope, and the constraints of working in the field. The only standardized method currently available for detecting intestinal protist parasites in food matrices is ISO 18744:2016, which was developed and optimized for the detection and enumeration of *Cryptosporidium* and *Giardia* in fresh leafy green vegetables and berry fruits. However, this method is neither suitable for routine analysis or monitoring in a hazard analysis plan and critical control points (Chalmers et al., 2020) nor does it enable the determination of species or genotypes (Efstratiou et al., 2017b). Therefore, to overcome this limitation, we reviewed several protocols described in the literature for detaching and concentrating the transmissive stages of intestinal pathogens from vegetable matrices. Then, we selected the most widely accepted approach, considering the specific size and food matrices of the products studied and the conditions under which the fieldwork was conducted. Additionally, it is important to mention that the concentration and purification processes for the main protist transmissive stages recommend conducting initial spiking experiments with known amounts of (oo)cysts/spores to evaluate the median percentage recovery of the chosen method. However, this study was unable to perform such a procedure, and as a result, the recovery rates of these methodologies were not estimated. This strongly suggests that the reported PCR-positive rate here is likely an underestimate of the true rate. Furthermore, due to limitations in resources and technical conditions, it was not possible to perform a multilocus sequence genotyping of *G. duodenalis*. If a multi-copy marker, such as the SSU rRNA gene, had been selected, it would have increased the sensitivity of detecting parasite cysts in vegetable product extracts. Instead, we utilized the *bg* locus, which is a single-copy gene but strikes a balance between very specific detection and genetic discrimination. While these methodology choices were made based on the available resources and technical conditions in the field, certainly, they may have led to an underestimation of both the positivity rate for *Giardia* and *E. bieneusi* reported in this study.

Even though it was not within the scope of this study, the absence of available technical conditions represents another limitation. Specifically, we were unable to conduct viability and infectivity assays on the transmissive stages of the detected protists in the horticultural products. Consequently, by solely focusing on the detection and genotyping of these microorganisms without assessing their viability and infectivity, the true impact of these agents on public health may have been underestimated. However, it is important to note that the transmissive stages of these important pathogens were found in raw products that had not undergone any cooking or freezing processes prior to ingestion by humans

or other animals. Considering the high resistance of cysts and spores to adverse environmental conditions, as well as the endemic nature of both microorganisms in the country, these findings undoubtedly suggest concerns regarding public health and warrant further investigation in future studies.

6. Conclusion

To the best of our knowledge, this study presents the first data on the detection and genetic characterization of the pathogenic *G. duodenalis* and *E. bieneusi* in horticultural products collected in dry and rainy seasons from different typology markets in Maputo city, Mozambique. In addition, this study suggests the presence of potential zoonotic assemblages or genotypes of these two important pathogens in vegetables and fruits, commercialized in the markets most used by the population of the city and therefore can be a source of human infection by gastrointestinal parasitic pathogens. Another major concern is the fact that many people tend to consume these horticultural products raw, in salads, and other typical street food available in markets and/or nearby. Although no viability or infectivity assays were conducted to assess the actual impact of these protists on public health, this study suggests a risk associated with consuming raw horticultural products contaminated with these pathogenic intestinal species. It emphasizes the importance of implementing improved safety practices throughout the production, transport, and handling of these products. These measures should be adopted by producers, vendors, and consumers to minimize the potential for foodborne outbreaks.

Data availability statement

The original contributions presented in the study are included in the article/supplementary material, further inquiries can be directed to the corresponding authors.

Author contributions

ML and OM: conceptualization, project administration, and supervision. CS, ML, SA, and OM: investigation. CS, SA, LX, and ML: methodology. CS, ML, and LX: software. CS and ML: writing—original draft. LX and OM: writing—review and editing. All authors have read and agreed to the published version of the manuscript.

Funding

This research was funded by Fundação para a Ciência e a Tecnologia (FCT) with a scholarship reference SFRH/BD/135355/2017 from TropikMan Doctoral Program, Lisboa, Portugal and the funds to GHTM – UID/04413/2020 and LA – REAL – LA/P/0117/2020.

Acknowledgments

The authors would like to thank all those who contributed to this study.

Conflict of interest

The authors declare that the research was conducted in the absence of any commercial or financial relationships that could be construed as a potential conflict of interest.

Publisher's note

All claims expressed in this article are solely those of the authors and do not necessarily represent those of their affiliated organizations, or those of the publisher, the editors and the reviewers. Any product that may be evaluated in this article, or claim that may be made by its manufacturer, is not guaranteed or endorsed by the publisher.

References

Ahmed, S. A., Guerrero Flórez, M., Karanis, P., Efstratiou, A., Ongerth, J., and Karanis, P. (2018). The impact of water crises and climate changes on the transmission of protozoan parasites in Africa. *Water Res.* 112, 96–112. doi: 10.1080/20477724.2018.1523778

Akinbo, F. O., Okaka, C. E., Omoregie, R., Dearen, T., Leon, E. T., and Xiao, L. (2012). Molecular epidemiologic characterization of *Enterocytozoon bieneusi* in HIV-infected persons in Benin City, Nigeria. *Am. J. Trop. Med. Hyg.* 86, 441–445. doi: 10.4269/ajtmh.2012.11-0548

Alemu, G., Mama, M., Misker, D., and Haftu, D. (2019). Parasitic contamination of vegetables marketed in Arba Minch town, southern Ethiopia. *BMC Infect. Dis.* 19. doi: 10.1186/s12879-019-4020-5

Archer, J., O'Halloran, L., Al-Shehri, H., Summers, S., Bhattacharyya, T., Kabaterine, N. B., et al. (2020). Intestinal *Schistosomiasis* and *Giardiasis* co-infection in Sub-Saharan Africa: can a One Health approach improve control of each waterborne parasite simultaneously? *Trop. Med. Infect. Dis.* 5, 137. doi: 10.3390/tropicalmed5030137

Badri, M., Olfatifar, M., Karim, M. R., Modirian, E., Houshmand, E., Abdoli, A., et al. (2022). Global prevalence of intestinal protozoan contamination in vegetables and fruits: a systematic review and meta-analysis. *Food Control* 133, 108656. doi: 10.1016/j.foodcont.2021.108656

Bahramian, B., Afshari, A., Kiani, B., Sani, M. A., and Hashemi, M. (2021). The prevalence of foodborne parasites in raw vegetables in Iran: a comprehensive systematic review and meta-analysis. *J. Environ. Heal. Sci. Eng.* 19, 2027–2045. doi: 10.1007/s40201-021-00714-w

Baldursson, S., and Karanis, P. (2011). Waterborne transmission of protozoan parasites: review of worldwide outbreaks—An update 2004-2010. *Water Res.* 45, 6603–6614. doi: 10.1016/j.watres.2011.10.013

Belkessa, S., Thomas-Lopez, D., Houali, K., Ghalmi, F., and Stensvold, C. R. (2021). Molecular characterization of giardia duodenalis in children and adults sampled in algeria. *Microorganisms* 9, 1–11. doi: 10.3390/microorganisms9010054

Berrouch, S., Escotte-Binet, S., Harrak, R., Huguenin, A., Flori, P., Favennec, L., et al. (2020). Detection methods and prevalence of transmission stages of *Toxoplasma gondii*, *Giardia duodenalis* and *Cryptosporidium* spp. in fresh vegetables: a review. *Parasitology* 147, 516–532. doi: 10.1017/S0031182020000086

Cacciò, S. M., De Giacomo, M., and Pozio, E. (2002). Sequence analysis of the β-giardin gene and development of a polymerase chain reaction-restriction fragment length polymorphism assay to genotype *Giardia duodenalis* cysts from human faecal samples. *Int. J. Parasitol.* 32, 1023–1030. doi: 10.1016/S0020-7519(02)00068-1

Cacciò, S. M., Lalle, M., and Svärd, S. G. (2018). Host specificity in the *Giardia duodenalis* species complex. *Infect. Genet. Evol.* 66, 335–345. doi: 10.1016/j.meegid.2017.12.001

Cai, W., Ryan, U., Xiao, L., and Feng, Y. (2021). Zoonotic giardiasis: an update. *Parasitol. Res.* 120, 4199–4218. doi: 10.1007/s00436-021-07325-2

Cao, S., Xu, M., Jiang, Y., Liu, H., Yuan, Z., Sun, L., et al. (2020). Prevalence and genetic characterization of *Cryptosporidium*, *Giardia* and *Enterocytozoon* in chickens from Ezhou, Hubei, China. *Front. Vet. Sci.* 7, 30. doi: 10.3389/fvets.2020.00030

Cao, Y., Tong, Q., Zhao, C., Maimaiti, A., Chuai, L., Wang, J., et al. (2021). Molecular detection and genotyping of *Enterocytozoon bieneusi* in pet dogs in Xinjiang, Northwestern China. *Parasite* 28, 2021057. doi: 10.1051/parasite/2021057

Chalmers, R. M., Robertson, L. J., Dorny, P., Jordan, S., Kärssin, A., Katzer, F., et al. (2020). Parasite detection in food: current status and future needs for validation. *Trends Food Sci. Technol.* 99, 337–350. doi: 10.1016/j.tifs.2020.03.011

Chen, L., Zhao, J., Li, N., Guo, Y., Feng, Y., Feng, Y., et al. (2019). Genotypes and public health potential of Enterocytozoon bieneusi and Giardia duodenalis in crab-eating macaques. *Parasit. Vect.* 12, 1–11. doi: 10.1186/s13071-019-3511-y

Cook, N., Nichols, R. A. B., Wilkinson, N., Paton, C. A., Barker, K., and Smith, H. V. (2007). Development of a method for detection of *Giardia duodenalis* cysts on lettuce and for simultaneous analysis of salad products for the presence of *Giardia* cysts and *Cryptosporidium oocysts*. *Appl. Environ. Microbiol.* 73, 7388–7391. doi: 10.1128/AEM.00552-07

Cunha, M. J. R., Cury, M. C., and Santín, M. (2017). Molecular identification of *Enterocytozoon bieneusi*, *Cryptosporidium*, and *Giardia* in Brazilian captive birds. *Parasitol. Res.* 116, 487–493. doi: 10.1007/s00436-016-5309-6

Dalu, T., Barson, M., and Nhiwatiwa, T. (2011). Impact of intestinal microorganisms and protozoan parasites on drinking water quality in Harare, Zimbabwe. *J. Water Sanit. Hyg. Dev.* 1, 153–163. doi: 10.2166/washdev.2011.049

Damitie, M., Mekonnen, Z., Getahun, T., Santiago, D., and Leyns, L. (2018). Molecular epidemiology of *Giardia duodenalis* infection in humans in Southern Ethiopia: a triosephosphate isomerase gene-targeted analysis. *Infect. Dis. Poverty* 7, 1–10. doi: 10.1186/s40249-018-0397-4

Decraene, V., Lebbad, M., Botero-Kleiven, S., Gustavsson, A. M., and Löfdahl, M. (2012). First reported foodborne outbreak associated with microsporidia, Sweden, October 2009. *Epidemiol. Infect.* 140, 519–527. doi: 10.1017/S095026881100077X

Dixon, B. R. (2021). Giardia duodenalis in humans and animals—Transmission and disease. *Res. Vet. Sci.* 135, 283–289. doi: 10.1016/j.rvsc.2020.09.034

Efstratiou, A., Ongerth, J., and Karanis, P. (2017b). Evolution of monitoring for *Giardia* and *Cryptosporidium* in water. *Water Res.* 123, 96–112. doi: 10.1016/j.watres.2017.06.042

Efstratiou, A., Ongerth, J. E., and Karanis, P. (2017a). Waterborne transmission of protozoan parasites: review of worldwide outbreaks—An update 2011–2016. *Water Res.* 114, 36. doi: 10.1016/j.watres.2017.01.036

Eraky, M. A., Rashed, S. M., Nasr, M. E. S., El-Hamshary, A. M. S., and Salah El-Ghannam, A. (2014). Parasitic contamination of commonly consumed fresh leafy vegetables in Benha, Egypt. *J. Parasitol. Res.* 2014, 7. doi: 10.1155/2014/613960

Ferreira, F. P., Caldart, E. T., Freire, R. L., Mitsuka-Breganó, R., de Freitas, F. M., Miura, A. C., et al. (2018). The effect of water source and soil supplementation on parasite contamination in organic vegetable gardens. *Rev. Bras. Parasitol. Vet.* 27, 327–337. doi: 10.1590/s1984-296120180050

Hald, T., Aspinall, W., Devleesschauwer, B., Cooke, R., Corrigan, T., Havelaar, A. H., et al. (2016). World Health Organization estimates of the relative contributions of food to the burden of disease due to selected foodborne hazards: a structured expert elicitation. *PLoS ONE* 11, 1–35. doi: 10.1371/journal.pone.0145839

Hassan, E. M., Örmeci, B., DeRosa, M. C., Dixon, B. R., Sattar, S. A., and Iqbal, A. (2021). A review of *Cryptosporidium* spp. and their detection in water. *Water Sci. Technol.* 83, 1–25. doi: 10.2166/wst.2020.515

Istifanus, W. A., and Panda, S. M. (2018). Parasitic agents in fresh fruits and vegetables sold in open markets in Bauchi, Nigeria. *J. Food Qual. Hazards Control* 5, 84–88. doi: 10.29252/jfqhc.5.3.84

Javanmard, E., Mirjalali, H., Niyyati, M., Jalilzadeh, E., Seyed Tabaei, S. J., Asadzadeh Aghdaei, H., et al. (2018). Molecular and phylogenetic evidences of dispersion of human-infecting microsporidia to vegetable farms via irrigation with treated wastewater: one-year follow up. *Int. J. Hyg. Environ. Health* 221, 642–651. doi: 10.1016/j.ijheh.2018.03.007

Javanmard, E., Mirsamadi, E. S., Olfatifar, M., Ghasemi, E., Saki, F., Mirjalali, H., et al. (2020). Prevalence of *Cryptosporidium* and *Giardia* in vegetables in Iran: a nineteen-years meta-analysis review. *J. Environ. Heal. Sci. Eng.* 18, 1629–1641. doi: 10.1007/s40201-020-00493-w

Junaidi, J., Cahyaningsih, U., Purnawarman, T., Latif, H., Sudarnika, E., Hayati, Z., et al. (2020). "*Entamoeba histolytica* Neglected Tropical Diseases (NTDs) agents that infect humans and some other mammals: a review," in *E3S Web of Conferences* (Banda Aceh). doi: 10.1051/e3sconf/202015101019

Kudah, C., Sovoe, S., and Baiden, F. (2018). Parasitic contamination of commonly consumed vegetables in two markets in Ghana. *Ghana Med. J.* 52, 88–93. doi: 10.4314/gmj.v52i2.5

Laatamna, A. E., Wagnerová, P., Sak, B., Květonová, D., Xiao, L., Rost, M., et al. (2015). Microsporidia and *Cryptosporidium* in horses and donkeys in Algeria: detection of a novel *Cryptosporidium hominis* subtype family (Ik) in a horse. *Vet. Parasitol.* 208, 135–142. doi: 10.1016/j.vetpar.2015.01.007

Lalle, M., Pozio, E., Capelli, G., Bruschi, F., Crotti, D., and Cacciò, S. M. (2005). Genetic heterogeneity at the β-giardin locus among human and animal isolates of *Giardia duodenalis* and identification of potentially zoonotic subgenotypes. *Int. J. Parasitol.* 35, 207–213. doi: 10.1016/j.ijpara.2004.10.022

Lee, J. H. (2008). Molecular detection of *Enterocytozoon bieneusi* and identification of a potentially human-pathogenic genotype in milk. *Appl. Environ. Microbiol.* 74, 1664–1666. doi: 10.1128/AEM.02110-07

Li, J., Shi, K., Sun, F., Li, T., Wang, R., Zhang, S., et al. (2019a). Identification of human pathogenic *Enterocytozoon bieneusi*, *Cyclospora cayetanensis*, and *Cryptosporidium parvum* on the surfaces of vegetables and fruits in Henan, China. *Int. J. Food Microbiol.* 307, 108292. doi: 10.1016/j.ijfoodmicro.2019.108292

Li, J., Wang, Z., Karim, M. R., and Zhang, L. (2020a). Detection of human intestinal protozoan parasites in vegetables and fruits: a review. *Parasit. Vect.* 13, 380. doi: 10.1186/s13071-020-04255-3

Li, N., Xiao, L., Wang, L., Zhao, S., Zhao, X., Duan, L., et al. (2012). Molecular surveillance of *Cryptosporidium* spp., *Giardia duodenalis*, and *Enterocytozoon bieneusi* by genotyping and subtyping parasites in wastewater. *PLoS Negl. Trop. Dis.* 6, 1809. doi: 10.1371/journal.pntd.0001809

Li, W., Feng, Y., and Santin, M. (2019b). Host specificity of *Enterocytozoon bieneusiand* public health implications. *Trends Parasitol.* 35, 436–451. doi: 10.1016/j.pt.2019.04.004

Li, W., Feng, Y., and Xiao, L. (2020b). Diagnosis and molecular typing of *Enterocytozoon bieneusi*: the significant role of domestic animals in transmission of human microsporidiosis. *Res. Vet. Sci.* 133, 251–261. doi: 10.1016/j.rvsc.2020.09.030

Lobo, M. L., Augusto, J., Antunes, F., Ceita, J., Xiao, L., Codices, V., et al. (2014). *Cryptosporidium* spp., *Giardia duodenalis*, *Enterocytozoon bieneusi* and Other intestinal parasites in young children in Lobata Province, Democratic Republic of São Tomé and Principe. *PLoS ONE* 9, e97708. doi: 10.1371/journal.pone.0097708

Lobo, M. L., Xiao, L., Antunes, F., and Matos, O. (2012). Microsporidia as emerging pathogens and the implication for public health: a 10-year study on HIV-positive and -negative patients. *Int. J. Parasitol.* 42, 197–205. doi: 10.1016/j.ijpara.2011.12.002

Matos, O., Lobo, M. L., and Xiao, L. (2012). Epidemiology of *Enterocytozoon bieneusi* infection in humans. *J. Parasitol. Res.* 2012, 981424. doi: 10.1155/2012/981424

Messa, A., Köster, P. C., Garrine, M., Gilchrist, C., Bartelt, L. A., Nhampossa, T., et al. (2021). Molecular diversity of *Giardia duodenalis* in children under 5 years from the manhiça district, southern mozambique enrolled in a matched case-control study on the aetiology of diarrhoea. *PLoS Negl. Trop. Dis.* 15, 1–24. doi: 10.1371/journal.pntd.0008987

Miambo, R. D., Laitela, B., Malatji, M. P., Afonso, S. M. S., Junior, A. P., Lindh, J., et al. (2019). Prevalence of *Giardia* and *Cryptosporidium* in young livestock and dogs in magude district of Maputo Province, Mozambique. *Onderstepoort J. Vet. Res.* 86, a1709. doi: 10.4102/ojvr.v86i1.1709

Michlmayr, D., Alves de Sousa, L., Müller, L., Jokelainen, P., Ethelberg, S., Vestergaard, L. S., et al. (2022). Incubation period, spore shedding duration, and symptoms of *Enterocytozoon bieneusi* genotype C infection in a foodborne outbreak in Denmark, 2020. *Clin. Infect. Dis.* 75, 468–475. doi: 10.1093/cid/ciab949

Monge, R., and Chinchilla, M. (1996). Presence of *Cryptosporidium oocysts* in fresh vegetables. *J. Food Prot.* 59, 202–203. doi: 10.4315/0362-028X-59.2.202

Mozer, S., Abdulwahhab, I. G., and Azaawie, A. L. A. F. (2022). Extraction of the DNA of *Giardia lamblia* isolated from vegetables and fruits in a simplified way and its diagnosis using Nested-PCR. *J. Parasit. Dis.* 46, 771–775. doi: 10.1007/s12639-022-01484-4

Mtapuri-Zinyowera, S., Ruhanya, V., Midzi, N., Berejena, C., Chin'Ombe, N., Nziramasanga, P., et al. (2014). Human parasitic protozoa in drinking water sources in rural Zimbabwe and their link to HIV infection. *Germs* 4, 86–91. doi: 10.11599/germs.2014.1061

Muadica, A. S., Messa, A., Dashti, A., Balasegaram, S., Santin, M., Manjate, F., et al. (2020). First identification of genotypes of *Enterocytozoon bieneusi* (Microsporidia) among symptomatic and asymptomatic children in mozambique. *PLoS Negl. Trop. Dis.* 14, 1–19. doi: 10.1371/journal.pntd.0008419

Qiu, L., Xia, W., Li, W., Ping, J., Ding, S., and Liu, H. (2019). The prevalence of microsporidia in China: a systematic review and meta-analysis opeN. *Sci. Rep.* 9, 3174. doi: 10.1038/s41598-019-39290-3

Rafael, K., Marchioro, A. A., Colli, C. M., Tiyo, B. T., Evangelista, F. F., Bezagio, R. C., et al. (2017). Genotyping of *Giardia duodenalis* in vegetables cultivated with organic and chemical fertilizer from street markets and community vegetable gardens in a region of Southern Brazil. *Trans. R. Soc. Trop. Med. Hyg.* 111, 540–545. doi: 10.1093/trstmh/try013

Rafiei, A., Baghlaninezhad, R., Köster, P. C., Bailo, B., de Mingo, M. H., Carmena, D., et al. (2020). Multilocus genotyping of *Giardia duodenalis* in Southwestern Iran. A community survey. *PLoS ONE* 15, 228317. doi: 10.1371/journal.pone.0228317

Rahimi, H. M., Mirjalali, H., and Zali, M. R. (2021). Molecular epidemiology and genotype/subtype distribution of *Blastocystis* sp., *Enterocytozoon bieneusi*, and *Encephalitozoon* spp. in livestock: concern for emerging zoonotic infections. *Sci. Rep*. 11, 17467. doi: 10.1038/s41598-021-96960-x

Rodrigues, A. C., da Silva, M. D. C., Pereira, R. Â. S., and Pinto, L. C. (2020). Prevalence of contamination by intestinal parasites in vegetables (*Lactuca sativa* L. and *Coriandrum sativum* L.) sold in markets in Belém, northern Brazil. *J. Sci. Food Agric*. 100, 2859–2865. doi: 10.1002/jsfa.10265

Ryan, U., and Cacciò, S. M. (2013). Zoonotic potential of *Giardia*. *Int. J. Parasitol*. 43, 943–956. doi: 10.1016/j.ijpara.2013.06.001

Ryan, U., Hijjawi, N., Feng, Y., and Xiao, L. (2019). *Giardia*: an under-reported foodborne parasite. *Int. J. Parasitol*. 49, 1–11. doi: 10.1016/j.ijpara.2018.07.003

Salamandane, A., Silva, A. C., Brito, L., and Malfeito-Ferreira, M. (2021a). Microbiological assessment of street foods at the point of sale in Maputo (Mozambique). *Food Qual. Saf*. 5, 1–9. doi: 10.1093/fqsafe/fyaa030

Salamandane, C., Fonseca, F., Afonso, S., Lobo, M. L., Antunes, F., and Matos, O. (2020). Handling of fresh vegetables: knowledge, hygienic behavior of vendors, public health in maputo markets, Mozambique. *Int. J. Environ. Res. Public Health* 17, 6302. doi: 10.3390/ijerph17176302

Salamandane, C., Lobo, M. L., Afonso, S., Miambo, R., and Matos, O. (2021b). Occurrence of intestinal parasites of public health significance in fresh horticultural products sold in Maputo markets and supermarkets, Mozambique. *Microorganisms* 9, 1806. doi: 10.3390/microorganisms9091806

Samra, N. A., Thompson, P. N., Jori, F., Zhang, H., and Xiao, L. (2012). *Enterocytozoon bieneusi* at the wildlife/livestock interface of the Kruger National Park, South Africa. *Vet. Parasitol*. 190, 587–590. doi: 10.1016/j.vetpar.2012.06.031

Santin, M., and Fayer, R. (2009). *Enterocytozoon bieneusi* genotype nomenclature based on the internal transcribed spacer sequence: a consensus. *J. Eukaryot. Microbiol*. 56, 34–38. doi: 10.1111/j.1550-7408.2008.00380.x

Siwila, J., Mwaba, F., Chidumayo, N., and Mubanga, C. (2020). Food and waterborne protozoan parasites: the African perspective. *Food Waterborne Parasitol*. 20, e00088. doi: 10.1016/j.fawpar.2020.e00088

Squire, S. A., and Ryan, U. (2017). *Cryptosporidium* and *Giardia* in Africa: current and future challenges. *Parasit. Vect*. 10, 1–32. doi: 10.1186/s13071-017-2111-y

Sripanompong, J., Tipayamongkholgul, M., Mahittikron, A., and Kosaisavee, V. (2021). *Giardia duodenalis* contamination of fresh vegetables in a wholesale market. *Thai J. Public Heal*. 51, 276–283.

Stentiford, G. D., Bass, D., and Williams, B. P. (2019). Ultimate opportunists—the emergent enterocytozoon group microsporidia. *PLoS Pathog*. 15, e1007668. doi: 10.1371/journal.ppat.1007668

Stentiford, G. D., Becnel, J. J., Weiss, L. M., Keeling, P. J., Didier, E. S., Williams, B. A. P. P., et al. (2016). Microsporidia—Emergent pathogens in the global food chain. *Trends Parasitol*. 32, 336–348. doi: 10.1016/j.pt.2015.12.004

Thompson, R. C. A., Palmer, C. S., and O'Handley, R. (2008). The public health and clinical significance of *Giardia* and *Cryptosporidium* in domestic animals. *Vet. J*. 177, 18–25. doi: 10.1016/j.tvjl.2007.09.022

Utaaker, K., Kumar, A., Joshi, H., Chaudhary, S., and Robertson, L. (2017). Checking the detail in retail: occurrence of *Cryptosporidium* and *Giardia* on vegetables sold across different counters in Chandigarh, India. *Int. J. Food Microbiol*. 263, 1–8. doi: 10.1016/j.ijfoodmicro.2017.09.020

Vizon, K. C. C., Battad, Z. G., and Castillo, D. S. C. (2019). Contamination of food-borne parasites from green-leafy vegetables sold in public markets of San Jose City, Nueva Ecija, Philippines. *J. Parasit. Dis*. 43, 651–657. doi: 10.1007/s12639-019-01144-0

Wang, X. T., Wang, R. J., Ren, G. J., Yu, Z. Q., Zhang, L. X., Zhang, S. Y., et al. (2016). Multilocus genotyping of *Giardia duodenalis* and *Enterocytozoon bieneusi* in dairy and native beef (Qinchuan) calves in Shaanxi province, northwestern China. *Parasitol. Res*. 115, 1355–1361. doi: 10.1007/s00436-016-4908-6

Wegayehu, T., Li, J., Karim, M. R., and Zhang, L. (2020). Molecular characterization and phylogenetic analysis of *Enterocytozoon bieneusi* in lambs in Oromia Special Zone, Central Ethiopia. *Front. Vet. Sci*. 7, 6. doi: 10.3389/fvets.2020.00006

Wu, Y., Chen, Y., Chang, Y., Zhang, X., Li, D., Wang, L., et al. (2020a). Genotyping and identification of *Cryptosporidium* spp., *Giardia duodenalis* and *Enterocytozoon bieneusi* from free–range Tibetan yellow cattle and cattle–yak in Tibet, China. *Acta Trop*. 212, 105671. doi: 10.1016/j.actatropica.2020.105671

Wu, Y., Gong, B., Liu, X., Jiang, Y., Cao, J., Yao, L., et al. (2020b). Identification of uncommon *Cryptosporidium* viatorum (a novel subtype XVcA2G1c) and *Cryptosporidium andersoni* as well as common *Giardia duodenalis* assemblages A and B in humans in Myanmar. *Front. Cell. Infect. Microbiol*. 10, 614053. doi: 10.3389/fcimb.2020.614053

Xiao, L., and Feng, Y. (2017). Molecular epidemiologic tools for waterborne pathogens *Cryptosporidium* spp. and *Giardia duodenalis*. *Food Waterborne Parasitol*. 2, 8–9. doi: 10.1016/j.fawpar.2017.09.002

Yaoyu, F., and Xiao, L. (2011). Zoonotic potential and molecular epidemiology of *Giardia* species and giardiasis. *Clin. Microbiol. Rev*. 24, 110–140. doi: 10.1128/CMR.00033-10

Yu, F., Amer, S., Qi, M., Wang, R., Wang, Y., Zhang, S., et al. (2019). Multilocus genotyping of *Giardia duodenalis* isolated from patients in Egypt. *Acta Trop*. 196, 66–71. doi: 10.1016/j.actatropica.2019.05.012

Zang, M., Li, J., Tang, C., Ding, S., Huang, W., Qin, Q., et al. (2021). Prevalence and phylogenetic analysis of microsporidium *Enterocytozoon bieneusi* in diarrheal patients. *Pathogens* 10, 1–10. doi: 10.3390/pathogens10020128

Zhang, Y., Mi, R., Yang, J., Wang, J., Gong, H., Huang, Y., et al. (2020). *Enterocytozoon bieneusi* genotypes in farmed goats and sheep in Ningxia, China. *Infect. Genet. Evol*. 85, 104559. doi: 10.1016/j.meegid.2020.104559

frontiers | Frontiers in Microbiology

TYPE Correction
PUBLISHED 28 August 2023
DOI 10.3389/fmicb.2023.1275235

Check for updates

OPEN ACCESS

APPROVED BY
Frontiers Editorial Office,
Frontiers Media SA, Switzerland

*CORRESPONDENCE
Olga Matos
omatos@ihmt.unl.pt
Maria Luísa Lobo
luisalc@ihmt.unl.pt

†These authors have contributed equally to this work and share first authorship

RECEIVED 09 August 2023
ACCEPTED 15 August 2023
PUBLISHED 28 August 2023

CITATION
Salamandane C, Lobo ML, Afonso S, Xiao L and Matos O (2023) Corrigendum: Exploring genetic variability of *Giardia duodenalis* and *Enterocytozoon bieneusi* in raw vegetables and fruits: implications for food safety and public health in Mozambique.
Front. Microbiol. 14:1275235.
doi: 10.3389/fmicb.2023.1275235

COPYRIGHT
© 2023 Salamandane, Lobo, Afonso, Xiao and Matos. This is an open-access article distributed under the terms of the Creative Commons Attribution License (CC BY). The use, distribution or reproduction in other forums is permitted, provided the original author(s) and the copyright owner(s) are credited and that the original publication in this journal is cited, in accordance with accepted academic practice. No use, distribution or reproduction is permitted which does not comply with these terms.

Corrigendum: Exploring genetic variability of *Giardia duodenalis* and *Enterocytozoon bieneusi* in raw vegetables and fruits: implications for food safety and public health in Mozambique

Cátia Salamandane[1,2,3†], Maria Luísa Lobo[1*†], Sónia Afonso[4], Lihua Xiao[5] and Olga Matos[1,6*]

[1]Group of Opportunistic Protozoa/HIV and Other Protozoa, Global Health and Tropical Medicine, Medical Parasitology Unit, Instituto de Higiene e Medicina Tropical, Universidade Nova de Lisboa, Lisboa, Portugal, [2]Nova School of Business and Economics, Universidade Nova de Lisboa, Carcavelos, Portugal, [3]Faculdade de Ciências de Saúde, Universidade Lúrio, Nampula, Mozambique, [4]Parasitology Department of Veterinary Faculty, Universidade Eduardo Mondlane, Maputo, Mozambique, [5]College of Veterinary Medicine, South China Agricultural University, Guangzhou, Guangdong, China, [6]Environmental Health Institute, Faculdade de Medicina da Universidade de Lisboa, Lisboa, Portugal

KEYWORDS

intestinal protozoa, microsporidia, raw horticultural products, foodborne diseases, zoonotic transmission, Maputo, One Health

A corrigendum on
Exploring genetic variability of *Giardia duodenalis* and *Enterocytozoon bieneusi* in raw vegetables and fruits: implications for food safety and public health in Mozambique

by Salamandane, C., Lobo, M. L., Afonso, S., Xiao, L., and Matos, O. (2023). *Front. Microbiol.* 14:1223151. doi: 10.3389/fmicb.2023.1223151

In the published article, there was an error in the **Funding statement**. An incorrect grant number was inserted and a funding source was omitted. The correct funding statement appears below:

This research was funded by Fundação para a Ciência e a Tecnologia (FCT) with a scholarship reference SFRH/BD/135355/2017 from TropikMan Doctoral Program, Lisboa, Portugal and the funds to GHTM – UID/04413/2020 and LA – REAL – LA/P/0117/2020.

The authors apologize for this error and state that this does not change the scientific conclusions of the article in any way. The original article has been updated.

Publisher's note

All claims expressed in this article are solely those of the authors and do not necessarily represent those of their affiliated organizations, or those of the publisher, the editors and the reviewers. Any product that may be evaluated in this article, or claim that may be made by its manufacturer, is not guaranteed or endorsed by the publisher.

frontiers | Frontiers in Microbiology

TYPE Original Research
PUBLISHED 11 August 2023
DOI 10.3389/fmicb.2023.1236834

Check for updates

OPEN ACCESS

EDITED BY
Hong Yin,
Chinese Academy of Agricultural Sciences, China

REVIEWED BY
Heike Uta Köhler,
Friedrich-Loeffler-Institut, Germany
Elisabeth M. Liebler-Tenorio,
Friedrich-Loeffler-Institut, Germany

*CORRESPONDENCE
Bernat Pérez de Val
✉ bernat.perez@irta.cat
Enric Vidal
✉ enric.vidal@irta.cat

†These authors have contributed equally to this work and share last authorship

RECEIVED 08 June 2023
ACCEPTED 25 July 2023
PUBLISHED 11 August 2023

CITATION
Melgarejo C, Cobos A, Planas C, Fondevila J, Martín M, Cervera Z, Cantero G, Moll X, Espada Y, Domingo M, Vidal E and Pérez de Val B (2023) Comparison of the pathological outcome and disease progression of two *Mycobacterium caprae* experimental challenge models in goats: endobronchial inoculation vs. intranasal nebulization.
Front. Microbiol. 14:1236834.
doi: 10.3389/fmicb.2023.1236834

COPYRIGHT
© 2023 Melgarejo, Cobos, Planas, Fondevila, Martín, Cervera, Cantero, Moll, Espada, Domingo, Vidal and Pérez de Val. This is an open-access article distributed under the terms of the Creative Commons Attribution License (CC BY). The use, distribution or reproduction in other forums is permitted, provided the original author(s) and the copyright owner(s) are credited and that the original publication in this journal is cited, in accordance with accepted academic practice. No use, distribution or reproduction is permitted which does not comply with these terms.

Comparison of the pathological outcome and disease progression of two *Mycobacterium caprae* experimental challenge models in goats: endobronchial inoculation vs. intranasal nebulization

Cristian Melgarejo[1,2], Alex Cobos[1,2,3], Carles Planas[4], Jaume Fondevila[2], Maite Martín[2], Zoraida Cervera[2], Guillermo Cantero[1,2], Xavier Moll[4,5], Yvonne Espada[4,5], Mariano Domingo[1,2,3], Enric Vidal[1,2*†] and Bernat Pérez de Val[1,2*†]

[1]Unitat Mixta d'Investigació IRTA-UAB en Sanitat Animal, Centre de Recerca en Sanitat Animal, Campus de la Universitat Autònoma de Barcelona, Bellaterra, Spain, [2]IRTA, Programa de Sanitat Animal, Centre de Recerca en Sanitat Animal, Campus de la Universitat Autònoma de Barcelona, Bellaterra, Spain, [3]Departament de Sanitat i Anatomia Animals, Universitat Autònoma de Barcelona, Bellaterra, Spain, [4]Fundació Hospital Clínic Veterinari, Universitat Autònoma de Barcelona, Bellaterra, Spain, [5]Departament de Medicina y Cirugía Animals, Universitat Autònoma de Barcelona, Bellaterra, Spain

Background: Goats are natural hosts of tuberculosis (TB) and are a valid animal model to test new vaccines and treatments to control this disease. In this study, a new experimental model of TB in goats based on the intranasal nebulization of *Mycobacterium caprae* was assessed in comparison with the endobronchial route of infection.

Methods: Fourteen animals were divided into two groups of seven and challenged through the endobronchial (EB) and intranasal (IN) routes, respectively. Clinical signs, rectal temperature, body weight, and immunological responses from blood samples were followed up throughout the experiment. All goats were euthanized at 9 weeks post-challenge. Gross pathological examination, analysis of lung lesions using computed tomography, and bacterial load quantification in pulmonary lymph nodes (LNs) by qPCR were carried out.

Results: The IN-challenged group showed a slower progression of the infection: delayed clinical signs (body weight gain reduction, peak of temperature, and apparition of other TB signs) and delayed immunological responses (IFN-γ peak response and seroconversion). At the end of the experiment, the IN group also showed significantly lower severity and dissemination of lung lesions, lower mycobacterial DNA load and volume of lesions in pulmonary LN, and higher involvement of the nasopharyngeal cavity and volume of the lesions in the retropharyngeal LN.

Conclusion: The results indicated that the IN challenge with *M. caprae* induced pathological features of natural TB in the lungs, respiratory LN, and extrapulmonary organs but extremely exaggerating the nasopharyngeal TB pathological features. On the other hand, the EB route oversized and accelerated the pulmonary TB lesion progression. Our results highlight the need to refine the inoculation routes in the interest of faithfully reproducing the natural TB infection when evaluating new vaccines or treatments against the disease.

KEYWORDS

tuberculosis, *Mycobacterium caprae*, goat, experimental infection, intranasal, endobronchial

1. Introduction

Tuberculosis (TB) is an infectious disease caused by mycobacteria belonging to the *Mycobacterium tuberculosis* complex (MTBC) that affects humans and a wide range of domestic animals and wildlife. TB in domestic goats is mainly caused by *Mycobacterium caprae*, a member of the MTBC (Aranaz et al., 2003). The disease has an economic impact resulting from production losses (Seva et al., 2002; Daniel et al., 2009), and infected goats pose a risk of infection to other animal species (Napp et al., 2013; Cano-Terriza et al., 2018; Vidal et al., 2018) and humans (Rodríguez et al., 2011).

TB in goats is usually transmitted through the aerogenous route, and it is common to find lesions mainly in the respiratory tract (Domingo et al., 2014). Goats develop caseous-necrotizing cavitary lesions similar to those observed in human TB (Pérez de Val et al., 2011; Sanchez et al., 2011), whereas these lesions are rarely developed in cattle (Buddle et al., 2016). Different approaches exist to control livestock TB, and the test and slaughter strategy is the most widely implemented, particularly in cattle. Vaccination against TB could be considered as an alternative approach. However, cattle vaccination against TB is currently forbidden in the EU (Council Directive 78/52/EEC) due to interference with currently used TB diagnostic tools. The goat model of TB has proven to be a suitable one to study new TB vaccines for ruminants and humans and for a better understanding of the pathogenesis of the disease (Ramirez et al., 2003; Pérez de Val et al., 2011, 2013; Wedlich et al., 2022).

In the different TB studies using the goat model, the infection has typically been carried out through the endobronchial route (Pérez de Val et al., 2011, 2012, 2013; Arrieta-Villegas et al., 2018, 2020; Melgarejo et al., 2022), intratracheal aerosolization (Gonzalez-Juarrero et al., 2013), and transthoracic injection (Bezos et al., 2010, 2015), all of them inducing primarily pulmonary TB lesions. In particular, the endobronchial approach allows for an accelerated progression of pulmonary TB, which is positive in terms of reducing the duration of the experiments. However, if the infectious dose is not well-adjusted, exaggeratedly large lung lesions may be produced. These large lesions do not only differ from the common natural presentation of the disease but also might preclude a proper evaluation of the vaccine effect (Arrieta-Villegas et al., 2020). A completely different experimental approach is the "natural" infection by long-term direct-contact exposure of experimental goats with infected animals in controlled conditions (Bezos et al., 2017; Roy et al., 2018, 2019). The advantage of this approach is that it induces all the natural features of the infection, but other aspects such as infection dose or infection time point remain uncontrolled, and it dramatically increases the duration of the experiment. Nowadays, *in vitro/ex vivo* and *in silico* experimental models are being developed to replace or reduce animal models in preclinical studies of vaccine candidates against TB (Tanner et al., 2016; Català et al., 2020). However, the optimization of these approaches requires a comparison to well-characterized animal models that can be used as "gold standard". Altogether, an accurate standardization of a goat model of TB is critical to predicting the efficacy of new vaccine candidates. This study aimed to evaluate and characterize the experimental infection of goats with *M. caprae* by intranasal nebulization in comparison with the endobronchial route. The rationale was to use a more natural access path of mycobacteria to the respiratory tract than the endobronchial route to reproduce more precisely the spectrum of lesions of goat TB found in field cases.

2. Materials and methods

2.1. Animals and experimental infections

Fourteen 3–4 months old female Pyrenean goats, from an officially tuberculosis-free herd, located in the Catalan Pyrenees (Spain), were chosen for this study. Experimental animals were transferred to the IRTA-CReSA Biosafety Level 3 (BSL-3) facility (Catalonia, Spain), where they were weighted and randomly divided into two experimental groups of seven animals each, challenged by the endobronchial (EB) and intranasal (IN) routes, respectively. According to body weights, corrections to ensure homogenous distribution between the groups were applied, and then, the animals were housed in two experimental boxes with animals 4–3 and 3–4 from the EB and IN groups in each box, respectively. The animals were fed hay, alfalfa, feed, and mineral salt and had access to water *ad libitum* throughout the experiment.

After 1 week of acclimatization, the animals were sedated intramuscularly with acepromazine maleate (0.05 mg/kg) and butorphanol (0.2 mg/kg) and subsequently anesthetized with intravenous administration of propofol (5 mg/kg) and midazolam (0.2 mg/kg). Afterward, the animals were challenged with 0.5 ml of a *M. caprae* field strain (Balseiro et al., 2017) at a suspension of 2×10^3 CFU/ml. Animals of the EB group were challenged through the endobronchial route as previously described (Pérez de Val et al., 2011).

The animals of the IN group were challenged by using a syringe-adapted device for atomized spraying (MADgic®, Wolfe Tory Medical, Inc., Salt Lake City, USA). This device consists of a flexible cannula measuring 21.6 cm in length and 4.82 mm in width with a nebulizer located at its end that generates droplets of 30–100 μm in diameter, according to the manufacturer's instructions. The cannula was inserted into the nasal cavity ~10–15 cm depending on the size of the animal. Each side of the nasal cavity received 0.5 ml of the same *M. caprae* strain at a suspension of 10^3 CFU/ml without anesthesia.

After the challenge, all animals were daily monitored for clinical signs by a veterinarian to assess whether any of the animals reached the endpoint criteria. The clinical evaluation included 0–3 scoring of each of the following five parameters: body condition, mental state/behavior, weight loss, fever, and the presence of respiratory signs (0: absence of respiratory signs; 1: mild dyspnea and/or occasional cough; 2: moderate dyspnea and continued coughing; and 3: marked dyspnea, continued coughing, and/or severe nasal discharge). Any global score higher than 11 and/or the presence of qualitative criteria such as prostration, lack of movement, or severe respiratory distress resulted in euthanasia. Rectal temperature and body weight were measured each week. Heparinized blood samples were collected at weeks 0 (before challenge), 3, 5, 7, and 9 (endpoint) for immunological assays.

2.2. Ethics statement

All the procedures with experimental animals carried out during the study were approved by the Animal Welfare Committee of the *Generalitat de Catalunya* (Project Ref. #10794), in accordance with the European Union legislation for the protection of experimental animals (86/609/CEE, 91/628/EEC, 92/65/EEC, and 90/425/EEC).

2.3. Antigens and reagents

M. bovis tuberculin (PPD-B, 2,500 IU/ml) was obtained from CZ vaccines (Porriño, Spain). The specific recombinant antigens of MTBC ESAT-6, CFP-10, and MPB83 were obtained from Lionex (Braunschweig, Germany) at a concentration of 500 μg/ml each. ESAT-6 and CFP-10 were mixed 1:1 in an antigenic (E/C) cocktail. The P22 antigenic complex was produced by immunopurification of PPD-B (CZ vaccines) as described previously (Infantes-Lorenzo et al., 2017) and was supplied by the *Carlos III Research Institute* (Madrid, Spain) at a concentration of 500 μg/ml.

2.4. Whole blood IFN-γ release assay

Approximately 10 ml of whole blood was collected at the abovementioned time points from the jugular vein using heparinized tubes. Blood samples were maintained at room temperature for <1 h when they were stimulated in 96-well cell culture plates (Eppendorf, Hamburg, Germany) with PPD-B, P22 (except at week 7), and E/C at a final concentration of 20 μg/ml each. Phosphate-buffered saline was used as an unstimulated control. The samples were incubated at 37°C and 5% CO_2 for 18 ± 2 h. Plasma supernatants were collected after centrifugation at 18 *g* for 10 min, and the released IFN-γ was measured by ELISA (ID Screen® Ruminant IFN-g kit, ID.vet, Grabels, France). Optical densities of the ELISA plates were read at 450 nm (OD_{450nm}) using a spectrophotometer (Biotek Power Wave XS®, Agilent, Santa Clara, USA). Antigen-specific IFN-γ responses were calculated as OD_{450nm} of the antigen-stimulated well minus OD_{450nm} of the unstimulated well ($\Delta OD_{450\ nm}$).

2.5. Antibody detection assays

Plasma samples from all experimental animals were analyzed in duplicate to follow antibody responses against MTBC after the challenge. Indirect ELISAs were used to detect total IgG against MPB83 antigen and P22 antigenic complex, respectively. The two ELISAs were performed as previously described (Pérez de Val et al., 2017; Infantes-Lorenzo et al., 2019). MPB83-IgG levels were calculated as OD_{450nm} of the antigen-coated well minus OD_{450nm} of the uncoated well (ΔOD_{450nm}). A sample was considered positive when $\Delta OD_{450nm} \geq 0.05$. P22-IgG levels were calculated as a percentage of ELISA (E%) = [mean OD_{450nm} of the antigen-coated well/(2 × mean negative control OD_{450nm})] × 100. A sample was considered negative when E% ≤ 100%, non-conclusive when E% was between 110 and 150%, and positive (seroconversion) when E% ≥ 150%.

2.6. Necropsy, pathological examination, and computed tomography

At week 9 post-challenge, all goats were sedated intramuscularly by an injection of acepromazine maleate (0.1 mg/kg) and butorphanol (0.2 mg/kg) and subsequently euthanized with an intravenous overdose of sodium pentobarbital. At necropsy, the size of TB-compatible lesions in the retropharyngeal (right and left), mediastinal (cranial and caudal), and tracheobronchial (LN) lymph nodes was measured, and the volume of lesions was inferred using the volume formula of the most similar 3D-geometrical morphology (including sphere, cylinder, or prism), as previously described (Balseiro et al., 2017). Other visible lesions in extrapulmonary tissues were also recorded and fixed in 10% buffered formalin to be confirmed by histopathology and Ziehl–Neelsen staining to detect acid-resistant bacilli. The lungs were fixed by airway instillation followed by immersion in formalin, as previously described (Pérez de Val et al., 2011), and then scanned by computed tomography (CT) using a 16-slice multidetector scanner (Brivo CT-385, General Electric Healthcare, Madrid, Spain). CT analysis was performed as previously described (Balseiro et al., 2017). In brief, total volumes of the lungs and TB lesions were measured using volume representation images with different density patterns (i.e., solid, mineralized, and cavitary lesions), and the total volume of mineralization was calculated using 100–300 Hounsfield units.

2.7. Quantification of bacterial DNA

After macroscopic pathological evaluation, mediastinal and tracheobronchial LNs were collected and stored at −20°C until they were processed for bacteriology. The whole LNs were then thawed and homogenized in 10 ml of sterile-distilled water using a homogenizer (Masticator, IUL Instruments, Barcelona, Spain). An aliquot of 1 ml of each homogenate was inactivated at 75°C for 1 h for bacterial DNA quantification. In parallel, an aliquot of 100 ml of the master seed *of M. caprae* (∼10^8 CFU/ml), used for the challenged inoculum, was inactivated and then diluted in eight 10-fold dilutions to establish the standard curve. DNA samples were extracted using an ID Gene™ spin universal extraction kit (ID.vet) and amplified with the *Mycobacterium tuberculosis* complex duplex kit (ID.vet), following the manufacturer's instructions. The amplification was performed in a 7500 fast real-time PCR system (Applied Biosystems, Waltham, MA, USA). The genomic equivalents of CFU were calculated as previously described (Vidal et al., 2022).

2.8. Data analysis

A completely randomized design was performed to compare the effects of *M. caprae* infection (primary factor) by the EB and

IN routes. First, all data distributions were analyzed by using the Shapiro–Wilk normality test. Temperature and body weight were compared using a unidirectional unpaired *t*-test. Antigen-specific immune responses (measured by IGRA, IgG-ELISA), lesion volumes, and mycobacterial DNA load were compared using the non-parametric Mann–Whitney test. GraphPad Prism version 8.0.0 (San Diego, CA, USA) was used for statistical analyses.

3. Results

3.1. Endobronchial challenge induced earlier and stronger immune responses

Mean antigen-specific IFN-γ responses in whole blood before and after the challenge for each treatment group are presented in Figure 1. An increase in IFN-γ-specific responses to PPD-B, P22, and E/C antigens was detected in both groups after the challenge (week 0, Figures 1A–C). Animals of the EB group showed a peak-up response of IFN-γ to the three antigens at weeks 3 and 5, which was significantly higher than in animals of the IN group ($P < 0.01$; except $P < 0.05$ for PPD-B at week 5). IFN-γ-specific responses in intranasally challenged animals increased progressively over weeks, while IFN-γ levels elicited after the endobronchial challenge decreased at the end of the experiment when responses in both groups tended to converge (no significant differences at weeks 7 and 9).

IgG levels to the MPB83 antigen and the P22 antigenic complex, as well as individual seroconversion, were studied using two ELISAs throughout the study (Figure 2). Endobronchial challenge induced an early increase in MPB83 IgG-specific responses (a peak-up response at weeks 5 and 7), and all EB animals seroconverted at week 5 p.c. On the contrary, only a mild response was detected in IN animals, seroconversion was not detected in 2 of them throughout the experiment, and the other five animals seroconverted between weeks 5 and 9 (Figure 2A). In comparison with MPB83, IgG responses to P22 were more progressive in the EB group, reaching a peak at the end of the experiment (week 9), but seroconversion was detected in six of seven animals. IgG responses to P22 were practically undetectable in the IN group throughout the experiment, and only one animal showed a clear seroconversion (Figure 2B).

3.2. Disease-related clinical signs appeared later in intranasally challenged goats

Rectal temperature, body weight, and clinical signs of TB were weekly recorded throughout the experiment (Figure 3).

In the EB group, a peak of mean rectal temperature was observed between weeks 2 and 4 p.c., being statistically significantly higher compared with the IN group ($P < 0.01$, weeks 2 and 4; $P < 0.05$, week 3; Figure 3A). A mild peak was also observed in the IN group between weeks 5 and 7, although still remained slightly lower than the EB group, and decreased at week 8 to be significantly lower than the EB group again ($P < 0.05$).

The mean body weight gain was greater in the IN group compared with the EB group since week 4, being statistically significant at week 5 ($P < 0.05$, Figure 3B), although a stagnation in body weight increase was observed from week 5 onward. In contrast, animals belonging to the EB group showed a mild increase in mean body weight from week 6 to the end of the experiment, where the difference in mean cumulative weight gain (ΔKg, Kg at weeks 9–0) between the IN and EB groups was minimal (4.2 ± 3.3 95% CI and 3.5 ± 2.9 95%CI, respectively).

The presence or absence of clinical signs, other than weight loss or fever, compatible with TB was recorded in all challenged animals until the end point of the experiment (Figure 3C). The observed signs included cough, dyspnea, eye discharge, enlarged lymph nodes, runny nose, and anorexia. An animal of the EB group showed clinical signs at week 1, 4 at week 2, and 6 from week 3 to the endpoint, whereas a 2-week delay in the onset of clinical signs was observed in the IN group: 1, 4, and 6 animals at weeks 3, 4, and from 5 to the endpoint, respectively (Figure 3C). The proportion of animals with clinical signs was significantly higher in the EB group at weeks 2 ($P < 0.01$), 3 ($P < 0.01$), and 4 ($P < 0.05$) compared with the IN group. All experimental animals showed clinical signs at weeks 8 and 9.

3.3. Endobronchially challenged animals showed more severe lung lesions

All goats showed TB lesions at necropsy. Lung lesions were quantitatively assessed by CT. All animals challenged by the EB route (7/7) had lung lesions, while only 4/7 animals of the IN group presented lung lesions, and the severity and dissemination of these lesions were very much lower compared with those found in the EB group. Figure 4 shows the extension of lung TB granulomas expressed as the volume of lung lesions, the intrapulmonary spread of TB lesions expressed as the number of affected lung lobes, and the degree of development of lung TB lesions expressed as the volume ratio between mineralization and lesion of each group. The EB group showed a significantly larger median volume of lung lesions compared with the IN group ($P < 0.001$, Figure 4A). In addition, the EB group showed a higher number of affected lobes compared with the IN group ($P < 0.01$, Figure 4B). Five out of seven EB animals showed TB lesions in all seven pulmonary lobes, while only one IN animal showed lesions in six pulmonary lobes. The EB group also showed a significantly greater median volume of lung mineralization (18.36 cm^3, 95% CI: 2. 634–84.53, $P < 0.001$) compared with the IN group (0 cm^3, 95% CI: 0–0.72), as well as higher median proportion of mineralization of lung lesions ($P < 0.01$; Figure 4C) indicative of a faster progression of pulmonary TB infection.

3.4. Intranasal challenge caused more severe lesions in the head but less generalized TB forms

All intranasally challenged animals showed lesions in retropharyngeal (RF) LNs, while these lesions were only detected in 2/7 animals of the EB group, and the median volume of lesions in the RF LNs was significantly higher in the IN group compared

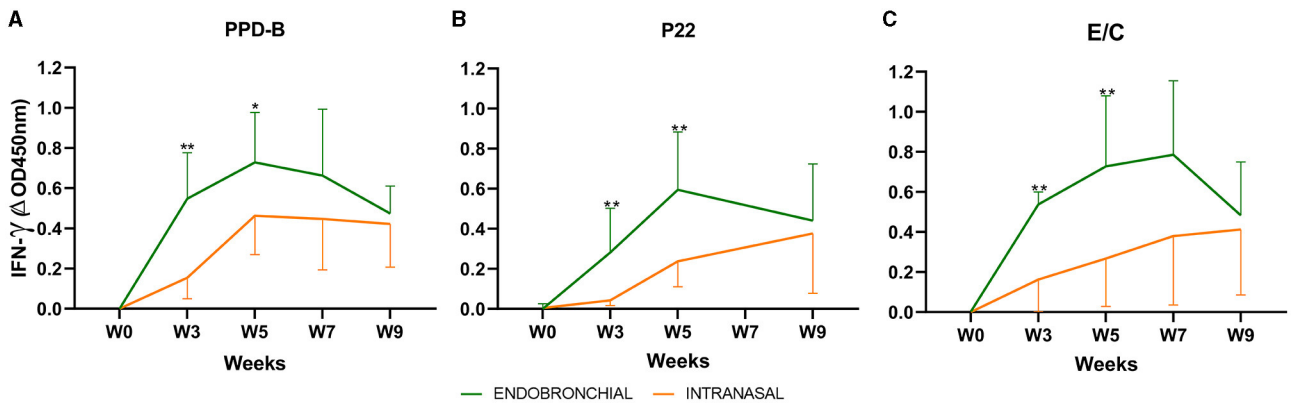

FIGURE 1
Whole blood IFN-γ responses before and after challenge: the graph shows the IFN-γ levels measured by ELISA. The results are expressed as ΔOD450mn ± 95% CI. **(A)** Response against bovine tuberculin (PPD-B). **(B)** Response to the P22 complex. **(C)** Response against E/C antigen cocktail. $^{*}P < 0.05$, $^{**}P < 0.01$, Mann–Whitney test. Groups: Endobronchial ($n = 7$, green) and Intranasal ($n = 7$, orange). Two animals of the endobronchial group were humanely sacrificed at week 7 and one animal of the group Intranasal.

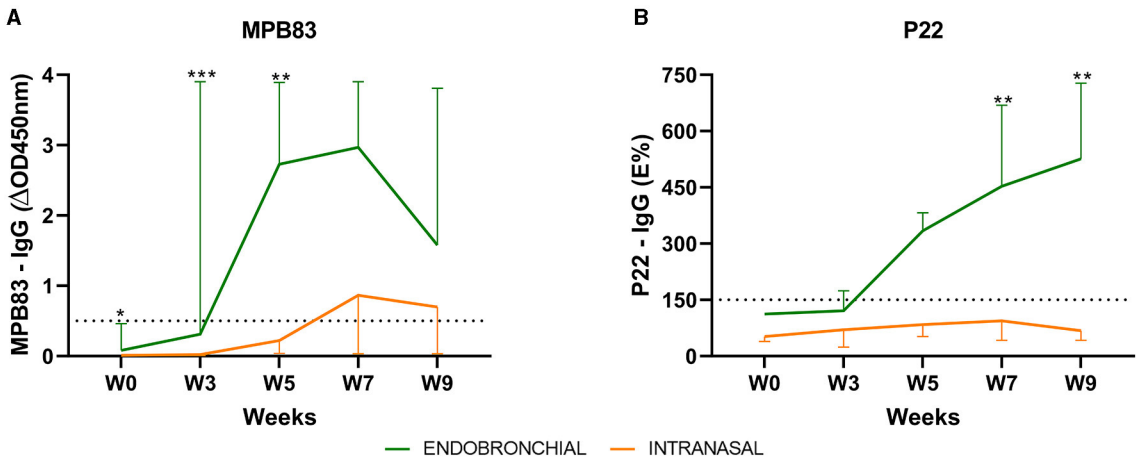

Group	W0	W3	W5	W7	W9
EB	6/1/0	3/1/3	0/0/7	0/0/7	0/0/5[a]
IN	7/0/0	7/0/0	3/1/3	2/0/5	2/1/3[b]

Group	W0	W3	W5	W7	W9
EB	3/4/0	2/4/1	3/0/4	1/0/6	1/0/4[a]
IN	6/1/0	5/1/1	4/2/1	4/2/1	6/0/0[b]

FIGURE 2
Antibody responses before and after the challenge. The figure shows the mean levels of IgG against MPB83 and P22 antigens measured by ELISA throughout the study. **(A)** MPB83-ELISA results are expressed as ΔOD450mn ± 95% CI. A sample was considered positive when ΔOD450nm ≥ 0.05. **(B)** P22-ELISA results are expressed as E%. E% = [mean OD450nm of the antigen-coated well/(2 × mean negative control OD450nm)] × 100. A sample is considered negative when it is ≤100%, inconclusive between 110 and 150% and seroconverted when the percentage is ≥150%. The dashed horizontal line shows the cutoff point for positivity. $^{*}P < 0.05$, $^{**}P < 0.01$, $^{***}P < 0.001$. Mann–Whitney test. The table indicates the numbers of animals and their seroconversion status: negative/inconclusive/positive. Groups: endobronchial (EB, $N = 7$, $^{a}N = 5$ at W9) and intranasal (IN, $N = 7$, $^{b}N = 6$ at W9).

with the EB group ($P < 0.01$, Figure 5C). In contrast, only 3/7 animals that received the IN challenge developed TB lesions in pulmonary LNs, whereas these lesions were macroscopically found in all EB-challenged ones. The median volume of TB lesions in pulmonary LN was significantly higher in the EB group compared with the IN group ($P < 0.001$, Figure 5A), and the bacterial DNA load in pulmonary LNs, estimated as CFU equivalents by qPCR, was also significantly higher in the EB group ($P < 0.05$, Figure 5B).

All extrapulmonary lesions macroscopically compatible with TB were confirmed as such by histopathological examination. In general, the IN group presented major affectation of the head, whereas more severe TB-compatible lesions in the thoracic and abdominal cavities were found in the EB group. Four out of seven animals of the IN group had an intense granulomatous inflammatory infiltrate in the nasal cavity (see Figures 6E, F), and the three animals had lesions in the retropharyngeal and/or submandibular lymph nodes.

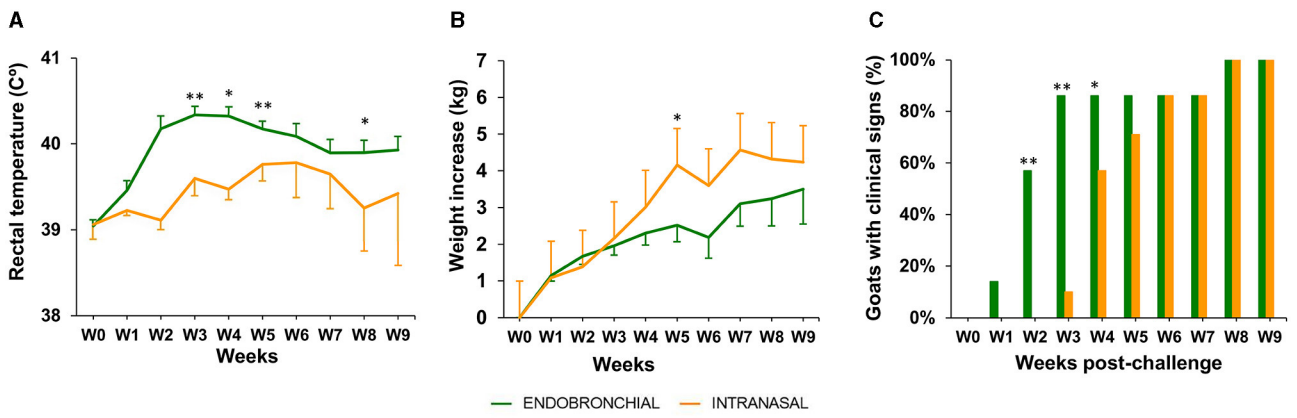

FIGURE 3
Rectal temperature, body weight, and clinical signs post-challenge. **(A)** The weekly mean rectal temperature of each group expressed in °C ± 95% CI. **(B)** Weekly mean cumulative body weight increases of each group expressed in ΔKg (Kg at each week post-challenge minus Kg at week 0) ± 95% CI. **(C)** The percentage of animals with the presence of TB-related clinical signs in each group. The clinical signs observed were cough, dyspnea, eye discharge, enlarged lymph nodes, nasal discharge, and anorexia (the groups were compared using the chi-square test). Groups: endobronchial (green, $N = 7$; $N = 5$ at weeks 8 and 9) intranasal (orange, $N = 7$; $N = 6$ at weeks 8 and 9). Body temperature and weight were compared using the one-way unpaired *t*-test. $^{*}P < 0.05$, $^{**}P < 0.01$.

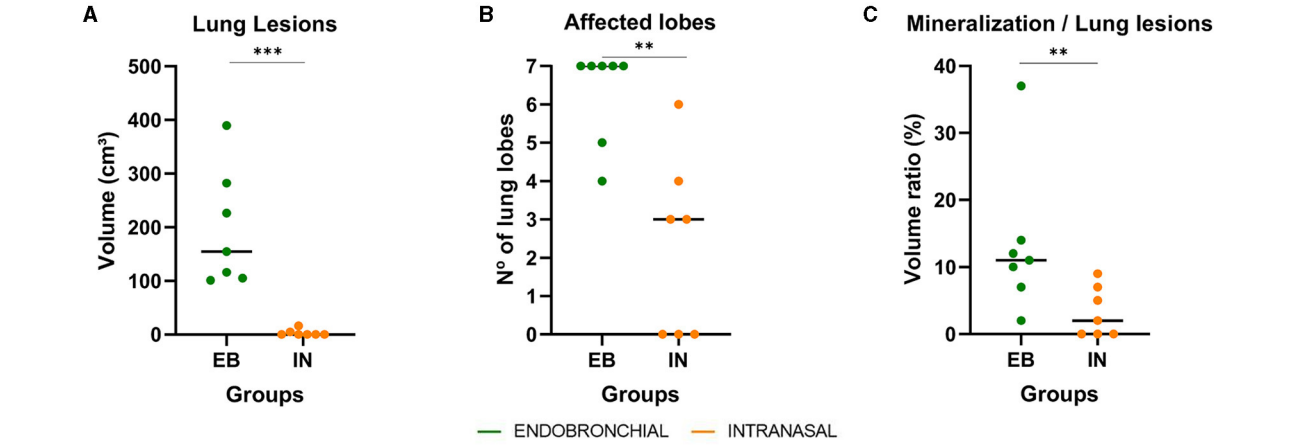

FIGURE 4
Lung pathological findings in endobronchially (EB) and intranasally (IN) *M. caprae*-challenged goats. **(A)** Volumes of lung TB lesions expressed in cm^3 measured by computed tomography (CT) scan. **(B)** Number of lung lobes with TB lesions. **(C)** The ratio between the volume of mineralization and the volume of lung lesions expressed in %. Groups: endobronchial ($n = 7$, green) and intranasal ($n = 7$, orange). $^{**}P < 0.01$, $^{***}P < 0.001$, Mann–Whitney test.

Figures 6, 7 show examples of TB lesions developed in representative IN- and EB-challenged animals in the head and lungs, respectively. The longitudinal section of the head of intranasally challenged goats evidenced bilateral extensive multifocal to coalescent granulomatous lesions in the nasal cavity of 4/7 goats; the endoturbinates and the middle nasal concha (on the caudal aspect of the nasal cavity) were always the most affected, while the dorsal and ventral nasal concha and the nasal septum were more variably involved (Figure 6E). Microscopically, granulomas of variable extension were observed in the nasal turbinates (Figure 6F) and nasopharyngeal mucosa (Figure 6G), while the EB-challenged animals did not present visible lesions in this localization (Figures 6A, B). Lesions in the head lymph nodes were more severe in the IN group (Figure 6H) while minimal or absent in the EB group (Figure 6D). Microscopically, the lesional patterns observed were equivalent in both groups, differing only in their extension and location. On the other hand, the rendered images of the lungs obtained by CT disclosed more extensive lung lesions and a higher total volume of lung mineralization in the EB-challenged animals (Figure 7).

Figure 8 presents the distribution of TB lesions in all the animals of each group. The animals of the EB group have minimal involvement in the head structure whereas all animals of the IN group had lesions in the head (all of them in the retropharyngeal LNs). On the other hand, all animals of the EB group had lesions in the thorax but also in the abdominal cavity (especially in the spleen), indicative of early hematogenous generalization.

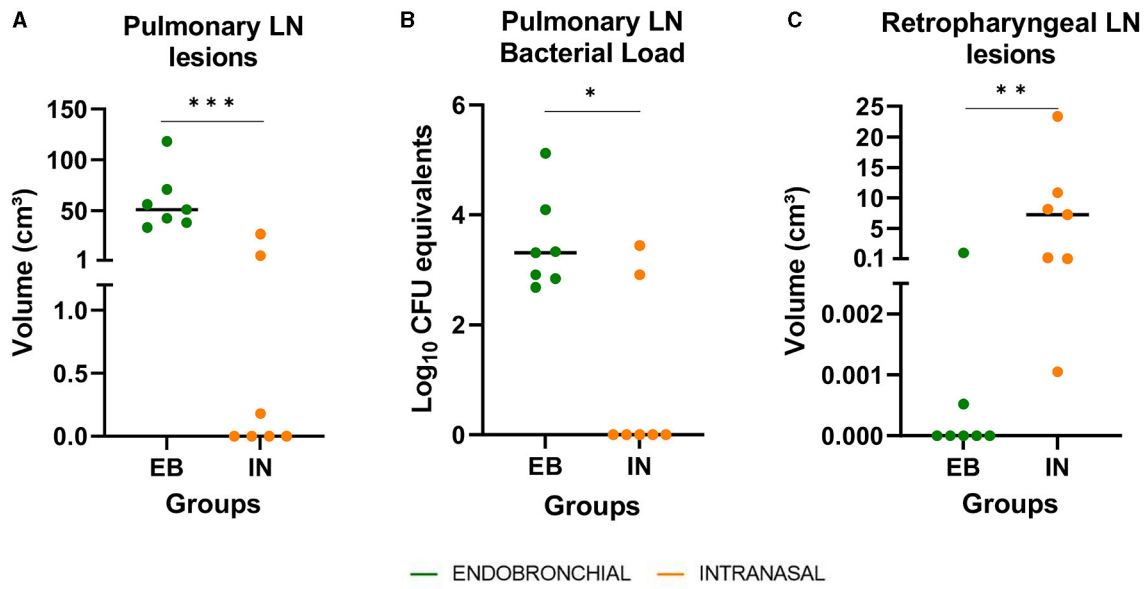

FIGURE 5
Post-mortem results in respiratory lymph nodes (LN). **(A)** The volume of lesions in pulmonary LN (tracheobronchial and mediastinal) expressed in cm^3. **(B)** *M. caprae* DNA load in pulmonary LN, measured by quantitative PCR and expressed as Log_{10} CFU equivalents. **(C)** The volume of lesions in retropharyngeal LN expressed in cm^3. Groups: endobronchial (EB, green)-challenged and intranasal (IN, orange)-challenged. $^*P < 0.05$, $^{**}P < 0.01$, $^{***}P < 0.001$, Mann–Whitney test.

4. Discussion

Since vaccination of cattle against TB is currently forbidden in the EU due to its interference with the current diagnostic tools used in eradication programs, the goat represents an excellent translational model to investigate the effect of vaccines against TB, which can be tested under field conditions (Pérez de Val et al., 2012, 2013; Bezos et al., 2017; Arrieta-Villegas et al., 2018; Roy et al., 2018; Melgarejo et al., 2022). Additionally, goats are also a suitable animal model for human TB because they resemble more closely than small laboratory animals and possess key anatomical features such as the complex bronchial tree (Mclaughlin et al., 1961) and lung parenchyma organized in a net of interlobular septa that tend to encapsulate the lesions (Gil et al., 2010), the respiratory tract and lung vascularization (Magno et al., 1990), and the respiratory lymphoid tissues (Liebler-Tenorio and Pabst, 2006).

The present study aimed to evaluate the IN nebulization of *M. caprae* as a field-like infection entrance pathway. The rationale was to better reproduce the features of the natural progression of TB infection but in a controlled manner, in order to improve the monitoring of clinical, immunological, bacteriological, and pathological parameters that could be used as predictors of vaccine efficacy in further studies. The new approach was compared with the well-established experimental infection through endobronchial inoculation (Pérez de Val et al., 2011). The severity and the progression of the disease were not only compared by the different distribution of lesions in the EB and IN groups but also they were holistically evaluated considering all the parameters mentioned above, according to previous investigations on TB pathogenicity in goats (Pérez de Val et al., 2013; Domingo et al., 2014).

The results showed that IN infection slowed the progression of the disease in comparison with the EB route in terms of cell-mediated immune response kinetics (antigen-specific IFN-γ responses) and the onset of clinical signs (body weight gain, rectal temperature, and respiratory signs). The delay of proinflammatory responses (determined by IFN-γ levels) in the IN group may be explained by a slower development of granulomatous lesions that normally show a direct correlation with antigen-specific IFN-γ responses (Vordermeier et al., 2002; Pérez de Val et al., 2012). The kinetics and intensity of proinflammatory responses in the IN group are consistent with the more progressive, less intense, and delayed rectal temperature peaks (weeks 5–7 p.c in the IN group instead of weeks 2–4 p.c. in the EB group). The delayed seroconversion rates (MPB83) or absence of detectable humoral responses (P22) in most animals of the IN group are also indicative of a slower progression of the disease. The lower intensity of MPB83-specific IgG responses in the IN group can also be associated with a lower severity of TB lesions and bacterial burden, as previously described in cattle and goats (Lyashchenko et al., 2004; Pérez de Val et al., 2011).

However, at the end of the study, all IN-challenged animals showed TB-compatible clinical signs indicating that the infection was well-established. This was also supported by the fact that the cumulative body weight gains of the IN and EB groups tended to converge at the end of the experiment. Previous studies, carried out by our research group, demonstrated that body weight increase in goat kids, experimentally challenged with *M. caprae,* inversely correlates with pathological TB outcome (Melgarejo et al., 2022).

From the pathological point of view, the EB infection induces faster disease progression with the early development of large-extensive pulmonary lesions similar to those found in certain

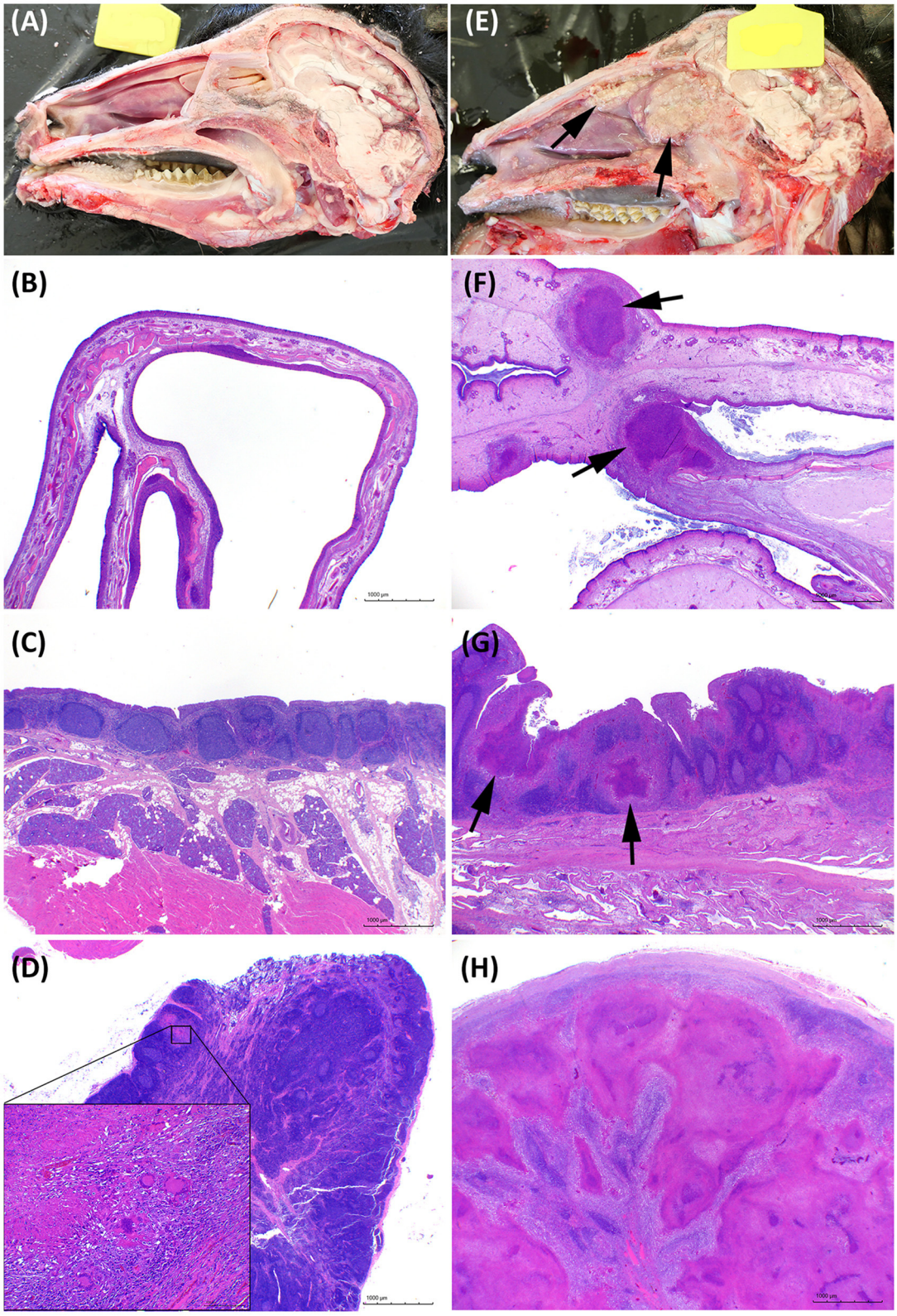

FIGURE 6
Pathological features in the head. **(A–D)** Representative images of goats challenged by the endobronchial route (EB). **(E–H)** Representative images of goats challenged by the intranasal route (IN). **(A, E)** Longitudinal section of the head. Granulomatous lesions are marked with arrows in the IN-challenged goat. **(B, F)** Transversal histological section of a normal nasal turbinate compared with an enlarged edematous nasal turbinate with multifocal granulomatous lesions (arrows). Hematoxylin and Eosin stain (H&E), bars 1,000 μm. **(C, G)** Nasopharyngeal mucosa with mucosal-associated lymphoid tissue. Noticeable multiple granulomas (arrows) in the IN animal in G. H&E, bars 1,000 μm. **(D, H)** Tuberculous lesions in the retropharyngeal lymph nodes of the EB-challenged group were absent or minimal as the one shown in the insert in **(B)**, or extensive and obliterating the whole lymph node in the IN group as shown in H. H&E, bars 1,000 μm.

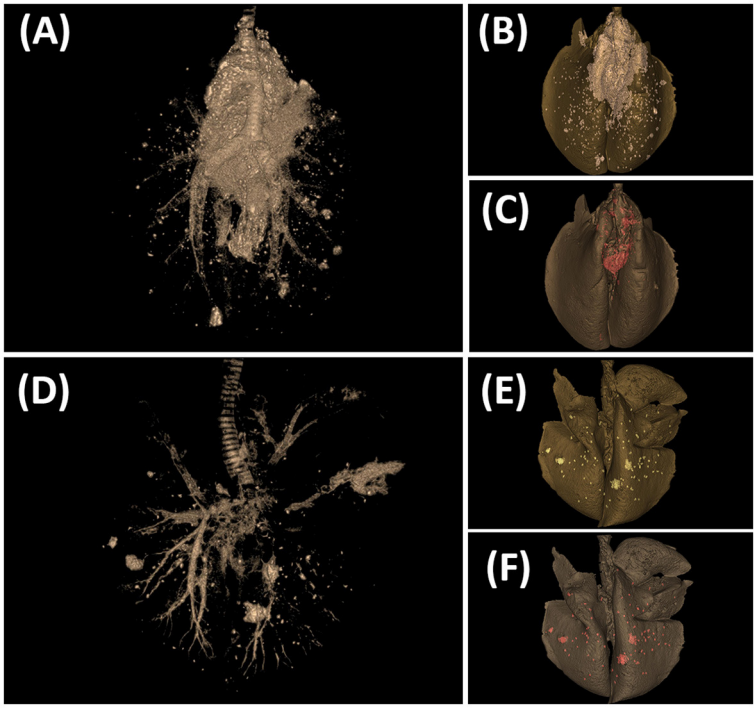

FIGURE 7
Tuberculosis lesions evidenced by computed tomography (CT) scan in the lungs. **(A–C)** Goat challenged by the endobronchial route. **(D–F)** Goat challenged by the intranasal route. **(A, D)** CT scan image showing the tracheobronchial tree and TB lesions. **(B, E)** CT-rendered image of TB lesions (whitish) on the total volume of the lung (dark gray). **(C, F)** CT-rendered image of mineralization (red) on the total volume of the lung (dark gray).

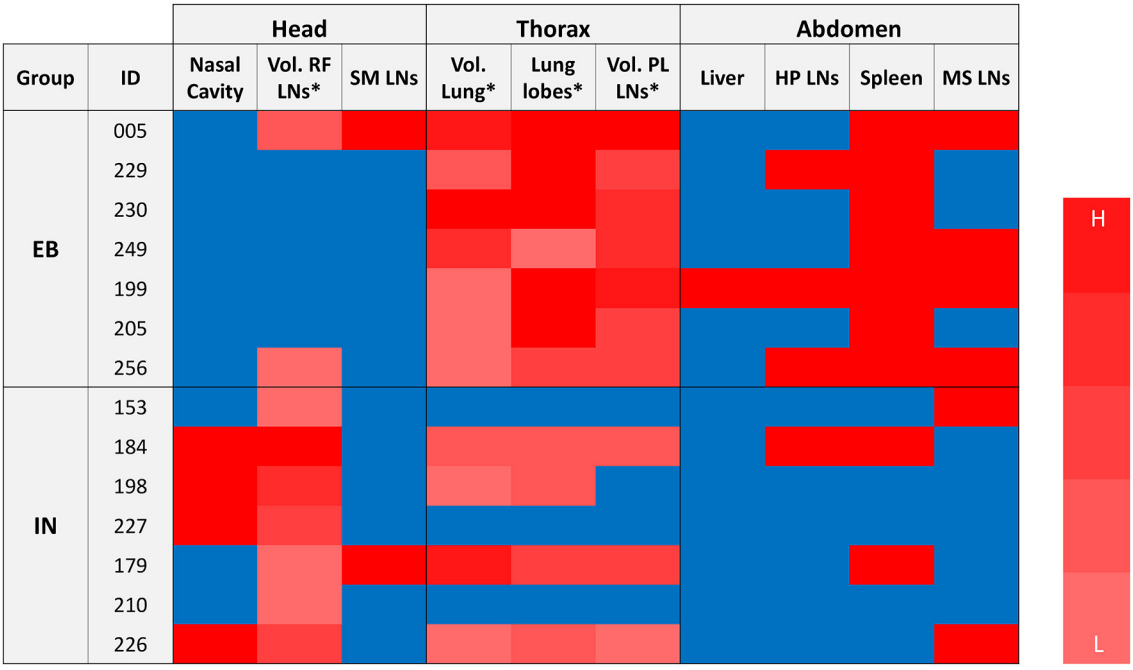

FIGURE 8
Distribution of TB lesions. Blue and red cells indicate the absence and presence of lesions, respectively. (*) In the case of RF LN, pulmonary LN, and lungs, a gradation of red levels represents the quintile distribution of volumes of lesions or number of affected lobes (scale: L -Low: 1- to H -High: 5-). Groups: endobronchial (EB)-challenged ($N = 7$) and intranasal (IN)-challenged ($N = 7$). LN, lymph node; SM, submandibular; RF, retropharyngeal; PL, pulmonary; HP, hepatic; MS, mesenteric.

chronic advanced cases of caprine TB in the field (Domingo et al., 2014). In contrast, after 9 weeks, goats infected through the IN route showed moderate pulmonary lesions similar to those usually obtained in natural infections, characterized by small to medium, multifocal lung nodular granulomatous lesions with a varying degree of encapsulation, variable presence of satellite granulomas, and occasionally, bigger coalescing lesions with central cavitation. These lung lesions are often associated with lesions in the thoracic lymph nodes (Domingo et al., 2014). The main drawback of the IN route is the intense granulomatous lesions found in the nasal cavity and head LN in some animals, which were artificially induced by the nebulization platform used to inoculate the mycobacteria. These lesions are not usually observed in field cases (Sanchez et al., 2011). This might be explained by the fact that during the challenge, a considerable proportion of the droplets containing mycobacteria bulk delivered into the nasal cavity was not inhaled and remained in the upper airways, thus generating local granulomatous lesions. In contrast, airborne aerosols transporting mycobacteria in field conditions are likely to access the lung parenchyma directly and in discrete installments, thus bypassing the upper airways (Daniel et al., 2009).

In an experimental infection conducted in calves inoculated intranasally with *M. bovis*, most animals (11/12) developed TB granulomatous lesions in LNs associated with the upper respiratory tract, and only four of them had lesions in the lungs or tracheobronchial LN (McCorry et al., 2005). In the present study, we investigated not only the head LNs but also performed a longitudinal section of the skull to investigate the nasal cavity. We found macroscopic intranasal granulomas in 4/7 animals that partially obstructed the upper airways and, in one case, provoked severe dyspnea that led to the humane euthanasia of one animal at week 8 before the completion of the experiment. Putative variations of the location of the cannula in the dorsal or middle nasal meatus vs. the ventral nasal meatus could explain the location of lesions in the caudal aspect of the nasal cavity in 4/7 animals, while in the 3/7 animals with no lesions, the cannula was likely introduced in the ventral meatus. In one of these animals, the lesions in the lung were the most severe in the group (animal 179, suggestive of an effective delivery of the inoculum to the lung), while the other two only developed lesions in the retropharyngeal lymph nodes. In addition, two animals of the IN group had lesions in the mesenteric LN, and this could be explained by the partial ingestion of the inoculum (in the case of animal 153, no lesion was observed in the nose), by swallowing the mycobacteria from the granulomatous lesions developing in the nasal cavity and/or associated lymph nodes (in the case of animal 226) or, less likely, due to lymphohematogenous dissemination to the abdominal cavity. The involvement of mesenteric LN was a frequent finding in natural settings in a field study carried out in a goat herd, where the most likely transmission pathway was the shared feeders between infected and susceptible animals (Vidal et al., 2017). Spread of TB lesions beyond the upper airways and thoracic cavity also occurred in all EB-challenged animals (i.e., all of them showed lesions in the spleen), most likely due to a lymphohematogenous spreading from the primary complex generated in the lungs and pulmonary LN, similar to that reported in previous studies (Arrieta-Villegas et al., 2018; Melgarejo et al., 2022). This phenomenon could also have occurred in two IN-challenged animals that showed lesions in the spleen (suggestive of hematogenous dissemination), one of which had the most extensive lung TB lesions in the IN-challenged group, without nasal cavity affectation.

To properly develop a suitable infection model to measure the efficacy of TB treatments, it would be necessary to refine the nebulization procedure to ensure that most of the inoculum enters into the trachea, avoiding the biased involvement of the nasal cavity. This could be accomplished by introducing the cannula directly into the ventral nasal meatus. Another explanation for the skewed distribution of lesions in the IN-challenged goats could be the fact that the animals might not have inhaled normally when inoculated and even tried to reject or swallow the inoculum. Thus, sedation of the goats before the experimental challenge could also facilitate a more direct delivery to the lungs.

To date, different approaches to MTBC experimental infections have been modelized in goats: transthoracic (Bezos et al., 2010, 2015), endobronchial (Pérez de Val et al., 2011; Wedlich et al., 2022), aerosolization (Gonzalez-Juarrero et al., 2013), and the infection by contact approach, i.e., the exposure of susceptible goats to infected ones by close contact (Bezos et al., 2017; Roy et al., 2019). The latter has the advantage to mimic natural infection in the herd but has the disadvantage of not controlling critical points such as the infection time point, infection dose, and infection route, which hinder the monitorization of the infection progress and, most critically, comparison between treatment groups. Similarly, the use of aerosolizers enables the inhalation of mycobacteria (Gonzalez-Juarrero et al., 2013) but does not allow to deposit the inoculum in a defined site of the respiratory tract at the start-point of the experiment, to compare the pathological evolution from the infection site among the treatment groups. The atomizing device used in the present study sprays droplets > 30 mm in diameter that resemble those excreted by sneezing or coughing. With the IN nebulization one can control the infection time point and infection dose conditions but still not ensure the infection site within the respiratory tract, resulting in moderate pulmonary TB lesions in only 4/7 animals, probably because a significant fraction of the inoculum was retained in the nasal cavity, whereas all goats infected by EB inoculation showed pulmonary TB lesions as previously described in all experimental infections of goats with *M. caprae* or *M. bovis* by this route (Pérez de Val et al., 2011, 2012, 2013; Arrieta-Villegas et al., 2018, 2020; Melgarejo et al., 2022; Wedlich et al., 2022). However, the EB model, as does the transthoracic one, can induce advanced caseous-necrotizing lesions even in vaccinated individuals, limiting the capacity to predict the protective effect of vaccinated candidates (Arrieta-Villegas et al., 2020). In contrast, the IN infection induced low-to-moderate pulmonary lesions with a low degree of mineralization, suggesting a more initial developmental stage that may facilitate the evaluation of the containment of TB lesions spreading in immunized animals. Optimization of the model is required to reach a compromise among (A) conditions control (dose, inoculation point), (B) duration of the experiment, and (C) reproducibility of TB field phenotype in order to precisely evaluate the efficacy of the tested vaccines.

Data availability statement

The original contributions presented in the study are included in the article/supplementary material, further inquiries can be directed to the corresponding authors.

Ethics statement

The animal studies were approved by Animal Welfare Committee of the Generalitat de Catalunya. The studies were conducted in accordance with the local legislation and institutional requirements. Written informed consent was not obtained from the owners for the participation of their animals in this study because the animals were purchased for these studies.

Author contributions

BP and EV conceived and planned the study. CM, AC, CP, MM, ZC, GC, XM, YE, MD, EV, and BP performed the experiments and contributed to data collection. CM, AC, JF, CP, YE, EV, and BP analyzed and interpreted the data. BP and MD acquired funding and were in charge of project administration. CM, EV, and BP wrote the original draft. MD contributed to writing, reviewing, and editing the final version of the manuscript. All authors contributed to the article and approved the submitted version.

Funding

This study was funded through a grant from the Spanish Ministry of Science and Innovation (Ref. PID2019-105155RB-C32/AEI/10.13039/501100011033). IRTA was supported by CERCA Programme/*Generalitat de Catalunya*. CM is the recipient of a pre-doctoral grant from the program Don Carlos Antonio López of the Republic of Paraguay (Ref. 88/2020).

Acknowledgments

The authors are grateful to Abel Muñoz, Mónica Pérez, Rosa López, Anna Barceló, and the staff of the BLS-3 Unit of IRTA-CReSA for their outstanding technical support.

Conflict of interest

The authors declare that the research was conducted in the absence of any commercial or financial relationships that could be construed as a potential conflict of interest.

Publisher's note

All claims expressed in this article are solely those of the authors and do not necessarily represent those of their affiliated organizations, or those of the publisher, the editors and the reviewers. Any product that may be evaluated in this article, or claim that may be made by its manufacturer, is not guaranteed or endorsed by the publisher.

References

Aranaz, A., Cousins, D., Mateos, A., and Domínguez, L. (2003). Elevation of *Mycobacterium tuberculosis* subsp. caprae Aranaz et al. 1999 to species rank as *Mycobacterium caprae* comb. nov., sp. nov. *Int. J. Syst. Evol. Microbiol.* 53, 1785–1789. doi: 10.1099/ijs.0.02532-0

Arrieta-Villegas, C., Allepuz, A., Grasa, M., Martín, M., Cervera, Z., Mercader, I., et al. (2020). Long-term efficacy of BCG vaccination in goat herds with a high prevalence of tuberculosis. *Sci. Rep.* 10, 20369. doi: 10.1038/s41598-020-77334-1

Arrieta-Villegas, C., Perálvarez, T., Vidal, E., Puighibet, Z., Moll, X., Canturri, A., et al. (2018). Efficacy of parenteral vaccination against tuberculosis with heat-inactivated *Mycobacterium bovis* in experimentally challenged goats. *PLoS ONE* 13, e0196948. doi: 10.1371/journal.pone.0196948

Balseiro, A., Altuzarra, R., Vidal, E., Moll, X., Espada, Y., Sevilla, I. A., et al. (2017). Assessment of BCG and inactivated *Mycobacterium bovis* vaccines in an experimental tuberculosis infection model in sheep. *PLoS ONE* 12, e0180546. doi: 10.1371/journal.pone.0180546

Bezos, J., Casal, C., Álvarez, J., Roy, A., Romero, B., Rodríguez-Bertos, A., et al. (2017). Evaluation of the *Mycobacterium tuberculosis* SO2 vaccine using a natural tuberculosis infection model in goats. *Vet. J.* 223, 60–67. doi: 10.1016/j.tvjl.2017.04.006

Bezos, J., Casal, C., Díez-Delgado, I., Romero, B., Liandris, E., Álvarez, J., et al. (2015). Goats challenged with different members of the *Mycobacterium tuberculosis* complex display different clinical pictures. *Vet. Immunol. Immunopathol.* 167, 185–189. doi: 10.1016/j.vetimm.2015.07.009

Bezos, J., de Juan, L., Romero, B., Álvarez, J., Mazzucchelli, F., Mateos, A., et al. (2010). Experimental infection with *Mycobacterium caprae* in goats and evaluation of immunological status in tuberculosis and paratuberculosis co-infected animals. *Vet. Immunol. Immunopathol.* 133, 269–275. doi: 10.1016/j.vetimm.2009.07.018

Buddle, B. M., Martin Vordermeier, H., and Hewinson, R. G. (2016). Experimental infection models of tuberculosis in domestic livestock. *Microbiol. Spectr.* 4, 44–66. doi: 10.1128/microbiolspec.TBTB2-0017-2016

Cano-Terriza, D., Risalde, M. A., Rodríguez-Hernández, P., Napp, S., Fernández-Morente, M., Moreno, I., et al. (2018). Epidemiological surveillance of *Mycobacterium tuberculosis* complex in extensively raised pigs in the south of Spain. *Prev. Vet. Med.* 159, 87–91. doi: 10.1016/j.prevetmed.2018.08.015

Català, M., Prats, C., López, D., Cardona, P. J., and Alonso, S. (2020). A reaction-diffusion model to understand granulomas formation inside secondary lobule during tuberculosis infection. *PLoS ONE* 15, 1–20. doi: 10.1371/journal.pone.0239289

Daniel, R., Evans, H., Rolfe, S., De La Rua-Domenech, R., Crawshaw, T., Higgins, R. J., et al. (2009). Papers: outbreak of tuberculosis caused by *Mycobacterium bovis* in golden Guernsey goats in great britain. *Vet. Rec.* 165, 335–342. doi: 10.1136/vr.165.12.335

Domingo, M., Vidal, E., and Marco, A. (2014). Pathology of bovine tuberculosis. *Res. Vet. Sci.* 97, S20–S29. doi: 10.1016/j.rvsc.2014.03.017

Gil, O., Díaz, I., Vilaplana, C., Tapia, G., Díaz, J., Fort, M., et al. (2010). Granuloma encapsulation is a key factor for containing tuberculosis infection in minipigs. *PLoS ONE* 5, e10030. doi: 10.1371/journal.pone.0010030

Gonzalez-Juarrero, M., Bosco-Lauth, A., Podell, B., Soffler, C., Brooks, E., Izzo, A., et al. (2013). Experimental aerosol *Mycobacterium bovis* model of infection in goats. *Tuberculosis* 93, 558–564. doi: 10.1016/j.tube.2013.05.006

Infantes-Lorenzo, J. A., Moreno, I., Risalde, M. D. L. Á., Roy, Á., Villar, M., Romero, B., et al. (2017). Proteomic characterisation of bovine and avian purified protein derivatives and identification of specific antigens for serodiagnosis of bovine tuberculosis. *Clin. Proteom.* 14, 36. doi: 10.1186/s12014-017-9171-z

Infantes-Lorenzo, J. A., Moreno, I., Roy, A., Risalde, M. A., Balseiro, A., de Juan, L., et al. (2019). Specificity of serological test for detection of tuberculosis in cattle,

goats, sheep and pigs under different epidemiological situations. *BMC Vet. Res.* 15, 70. doi: 10.1186/s12917-019-1814-z

Liebler-Tenorio, E., and Pabst, R. (2006). MALT structure and function in farm animals. *Vet. Res.* 37, 257–280. doi: 10.1051/vetres:2006001

Lyashchenko, K., Whelan, A. O., Greenwald, R., Pollock, J. M., Andersen, P., Hewinson, R. G., et al. (2004). Association of tuberculin-boosted antibody responses with pathology and cell-mediated immunity in cattle vaccinated with *Mycobacterium bovis* BCG and infected with *M. bovis*. *Infect. Immun.* 72, 2462–2467. doi: 10.1128/IAI.72.5.2462-2467.2004

Magno, M., Long Nadel, J., Wanner, A., and Lockhart, A. (1990). Comparative anatomy of the tracheobronchial circulation. *Eur. Respir. J.* 13, 557S−563S.

McCorry, T., Whelan, A. O., Welsh, M. D., McNair, J., Walton, E., Bryson, D. G., et al. (2005). Shedding of *Mycobacterium bovis* in the nasal mucus of cattle infected experimentally with tuberculosis by the intranasal and intratracheal routes. *Vet. Rec.* 157, 613–618. doi: 10.1136/vr.157.20.613

Mclaughlin, R. F., Tyler, W. S., and Canada, R. (1961). A study of the subgross pulmonary anatomy in various mammals. *Am. J. Anat.* 108, 149–165. doi: 10.1002/aja.1001080203

Melgarejo, C., Planas, C., Cobos, A., Arrieta-Villegas, C., Sevilla, I. A., Bezos, J., et al. (2022). A proof-of-conclept study to investigate the efficacy of heat-inactivated autovaccines in *Mycobacterium caprae* experimentally challenged goats. *Sci. Rep.* 12, 22132. doi: 10.1038/s41598-022-26683-0

Napp, S., Allepuz, A., Mercader, I., Nofrarias, M., Lopez-Soria, S., Domingo, M., et al. (2013). Evidence of goats acting as domestic reservoirs of bovine tuberculosis. *Vet. Rec.* 172, 663. doi: 10.1136/vr.101347

Pérez de Val, B., López-Soria, S., Nofrarías, M., Martín, M., Vordermeier, H. M., Villarreal-Ramos, B., et al. (2011). Experimental model of tuberculosis in the domestic goat after endobronchial infection with *Mycobacterium caprae*. *Clin. Vacc. Immunol.* 18, 1872–1881. doi: 10.1128/CVI.05323-11

Pérez de Val, B., Napp, S., Velarde, R., Lavín, S., Cervera, Z., Singh, M., et al. (2017). serological follow-up of tuberculosis in a wild boar population in contact with infected cattle. *Transbound. Emerg. Dis.* 64, 275–283. doi: 10.1111/tbed.12368

Pérez de Val, B., Vidal, E., Villarreal-Ramos, B., Gilbert, S. C., Andaluz, A., Moll, X., et al. (2013). A multi-antigenic adenoviral-vectored vaccine improves BCG-induced protection of goats against pulmonary tuberculosis infection and prevents disease progression. *PLoS ONE* 8, e81317. doi: 10.1371/journal.pone.0081317

Pérez de Val, B., Villarreal-Ramos, B., Nofrarías, M., López-Soria, S., Romera, N., Singh, M., et al. (2012). Goats primed with *Mycobacterium bovis* BCG and boosted with a recombinant adenovirus expressing Ag85A show enhanced protection against tuberculosis. *Clin. Vacc. Immunol.* 19, 1339–1347. doi: 10.1128/CVI.00275-12

Ramirez, I. C., Santillan, M. A., and Dante, V. (2003). The goat as an experimental ruminant model for tuberculosis infection. *Small Rumin. Res.* 47, 113–116. doi: 10.1016/S0921-4488(02)00243-2

Rodríguez, S., Bezos, J., Romero, B., de Juan, L., Álvarez, J., Castellanos, E., et al. (2011). *Mycobacterium caprae* infection in livestock and wildlife, Spain. *Emerg. Infect. Dis.* 17, 532–535. doi: 10.3201/eid1703.100618

Roy, Á., Risalde, M. A., Bezos, J., Casal, C., Romero, B., Sevilla, I., et al. (2018). Response of goats to intramuscular vaccination with heat-killed Mycobacterium bovis and natural challenge. *Comp. Immunol. Microbiol. Infect. Dis.* 60, 28–34. doi: 10.1016/j.cimid.2018.09.006

Roy, A., Tomé, I., Romero, B., Lorente-Leal, V., Infantes-Lorenzo, J. A., Domínguez, M., et al. (2019). Evaluation of the immunogenicity and efficacy of BCG and MTBVAC vaccines using a natural transmission model of tuberculosis. *Vet. Res.* 50, 1–3. doi: 10.1186/s13567-019-0702-7

Sanchez, J., Tomás, L., Ortega, N., Buendía, A. J., del Rio, L., Salinas, J., et al. (2011). Microscopical and immunological features of tuberculoid granulomata and cavitary pulmonary tuberculosis in naturally infected goats. *J. Comp. Pathol.* 145, 107–117. doi: 10.1016/j.jcpa.2010.12.006

Seva, J., Menchén, V., Navarro, J. A., Pallarés, F. J., Villar, D., Vásquez, F., et al. (2002). Caprine tuberculosis eradication program: an immunohistochemical study. *Small Rumin. Res.* 46, 107–114. doi: 10.1016/S0921-4488(02)00174-8

Tanner, R., O'Shea, M. K., Fletcher, H. A., and McShane, H. (2016). *In vitro* mycobacterial growth inhibition assays: a tool for the assessment of protective immunity and evaluation of tuberculosis vaccine efficacy. *Vaccine* 34, 4656–4665. doi: 10.1016/j.vaccine.2016.07.058

Vidal, E., Arrieta-Villegas, C., Grasa, M., Mercader, I., Domingo, M., and Pérez de Val, B. (2017). Field evaluation of the efficacy of Mycobacterium bovis BCG vaccine against tuberculosis in goats. *BMC Vet. Res.* 13, 252. doi: 10.1186/s12917-017-1182-5

Vidal, E., Burgaya, J., Michelet, L., Arrieta-Villegas, C., Cantero, G., de Cruz, K., et al. (2022). Experimental *Mycobacterium microti* infection in bank voles (*Myodes glareolus*). *Microorganisms* 10, 135. doi: 10.3390/microorganisms10010135

Vidal, E., Grasa, M., Perálvarez, T., Martín, M., Mercader, I., and Pérez de Val, B. (2018). Transmission of tuberculosis caused by *Mycobacterium caprae* between dairy sheep and goats. *Small Rumin. Res.* 158, 22–25. doi: 10.1016/j.smallrumres.2017.11.010

Vordermeier, H. M., Chambers, M. A., Cockle, P. J., Whelan, A. O., Simmons, J., and Hewinson, R. G. (2002). Correlation of ESAT-6-specific gamma interferon production with pathology in cattle following *Mycobacterium bovis* BCG vaccination against experimental bovine tuberculosis. *Infect. Immun.* 70, 3026–3032. doi: 10.1128/IAI.70.6.3026-3032.2002

Wedlich, N., Figl, J., Liebler-Tenorio, E. M., Köhler, H., von Pückler, K., Rissmann, M., et al. (2022). Video endoscopy-guided intrabronchial spray inoculation of *Mycobacterium bovis* in goats and comparative assessment of lung lesions with various imaging methods. *Front. Vet. Sci.* 9, 877322. doi: 10.3389/fvets.2022.877322

frontiers | Frontiers in Microbiology

TYPE Original Research
PUBLISHED 13 September 2023
DOI 10.3389/fmicb.2023.1236091

Check for updates

OPEN ACCESS

EDITED BY
Lei Deng,
Massachusetts General Hospital and Harvard Medical School, United States

REVIEWED BY
Masaki Yasukawa,
Ehime Prefectural University of Health Sciences, Japan
Hao Li,
Beijing Institute of Microbiology and Epidemiology, China

*CORRESPONDENCE
Anling Li
✉ anling888@126.com
Liping Deng
✉ dengliping@whu.edu.cn
Yong Xiong
✉ yongxiong64@163.com

†These authors have contributed equally to this work and share first authorship

RECEIVED 09 June 2023
ACCEPTED 30 August 2023
PUBLISHED 13 September 2023

CITATION
Zhang Z, Hu X, Jiang Q, Hu W, Li A, Deng L and Xiong Y (2023) Clinical characteristics and outcomes of acute kidney injury in patients with severe fever with thrombocytopenia syndrome.
Front. Microbiol. 14:1236091.
doi: 10.3389/fmicb.2023.1236091

COPYRIGHT
© 2023 Zhang, Hu, Jiang, Hu, Li, Deng and Xiong. This is an open-access article distributed under the terms of the Creative Commons Attribution License (CC BY). The use, distribution or reproduction in other forums is permitted, provided the original author(s) and the copyright owner(s) are credited and that the original publication in this journal is cited, in accordance with accepted academic practice. No use, distribution or reproduction is permitted which does not comply with these terms.

Clinical characteristics and outcomes of acute kidney injury in patients with severe fever with thrombocytopenia syndrome

Zhongwei Zhang[1†], Xue Hu[2†], Qunqun Jiang[1], Wenjia Hu[1], Anling Li[3]*, Liping Deng[1]* and Yong Xiong[1]*

[1]Department of Infectious Disease, Zhongnan Hospital of Wuhan University, Wuhan, China, [2]Department and Institute of Infectious Disease, Tongji Hospital, Tongji Medical College, Huazhong University of Science and Technology, Wuhan, China, [3]Department of Clinical Laboratory, Center for Gene Diagnosis, and Program of Clinical Laboratory Medicine, Zhongnan Hospital of Wuhan University, Wuhan, China

Background: Severe fever with thrombocytopenia syndrome (SFTS) is an emerging zoonosis caused by a novel bunyavirus. Until recently, the SFTS related acute kidney injury (AKI) was largely unexplored. This study aimed to investigate the clinical characteristics and outcomes of AKI in patients with SFTS.

Methods: The non-AKI and AKI groups were compared in terms of general characteristics, clinical features, laboratory parameters and cumulative survival rate. The independent risk factors for in-hospital mortality in patients with SFTS were analyzed by multivariate logistic regression to identify the population with poor prognosis.

Results: A total of 208 consecutive patients diagnosed with SFTS were enrolled, including 153 (73.6%) patients in the non-AKI group and 55 (26.4%) patients in the AKI group. Compared with patients without AKI, patients with AKI were older and had a higher frequency of diabetes. Among these laboratory parameters, platelet count, albumin and fibrinogen levels of patients with AKI were identified to be significantly lower than those of patients without AKI, while ALT, AST, ALP, triglyceride, LDH, BUN, uric acid, creatine, Cys-C, β2-MG, potassium, AMY, lipase, CK-MB, TnI, BNP, APTT, thrombin time, D-dimer, CRP, IL-6, PCT and ESR levels were significantly higher in patients with AKI. A higher SFTS viral load was also detected in the AKI patients than in the non-AKI patients. The cumulative survival rates of patients at AKI stage 2 or 3 were significantly lower than those of patients without AKI or at AKI stage 1. However, there was no significant difference in the cumulative survival rates between patients without AKI and those with stage 1 AKI. Univariate and multivariate binary logistic regression analyses demonstrated that stage 2 or 3 AKI was an independent risk factor for in-hospital mortality in patients with SFTS.

Conclusion: AKI is associated with poor outcomes in patients with SFTS, especially patients at AKI stage 2 or 3, who generally have high mortality. Our findings support the importance of early identification and timely treatment of AKI in patients with SFTS.

KEYWORDS

severe fever with thrombocytopenia syndrome, acute kidney injury, clinical characteristics, risk factor, mortality

Introduction

Severe fever with thrombocytopenia syndrome (SFTS) is an emerging infectious disease caused by a novel bunyavirus that was reported in rural areas of China in 2009 (Yu et al., 2011). SFTS is mainly transmitted by contact with ticks, and can be transmitted among humans (Bao et al., 2011), even direct infection of SFTS virus from cats and dogs to humans has been reported, which is recognized as a social problem (Park et al., 2019; Yamanaka et al., 2020). Patients with mild SFTS can present with fever, thrombocytopenia, anorexia, dizziness, headache, nausea, vomiting and diarrhea, while patients with serious SFTS might develop multiple organ dysfunction syndrome including encephalopathy, cardiac failure, acute respiratory distress syndrome, severe pancreatitis, acute kidney injury (AKI), and disseminated intravascular coagulation, with a reported mortality rate ranging from 2.5% to 30% in various epidemic areas (Zhang et al., 2012; Liu S. et al., 2014; Li et al., 2018). The extensive distribution, and high morbidity and mortality of SFTS make it a significant newly emerging infectious disease in China.

Critically ill patients with SFTS always have a high mortality rate, and the clinical manifestations and laboratory parameters could be used to predict the outcomes of patients with SFTS, which have been explored with high interest (Wen et al., 2014; Xu et al., 2018). Among these definite predictors, elevated serum creatinine (sCr) levels have been frequently demonstrated to be closely related to poor prognosis (Cui et al., 2015; Nie et al., 2020; He et al., 2021). The elevated sCr levels in a short time typically represent AKI. It suggests that AKI may be closely related to the adverse outcomes of patients with SFTS. Hence, a comprehensive understanding of the clinical characterization of AKI and its associated outcomes is crucial for formulating personalized treatment strategies to improve the prognosis of patients with SFTS. However, until recently, the data for AKI in SFTS were limited. We performed a study to investigate the incidence, clinical manifestations and outcomes of AKI in a retrospective cohort of hospitalized patients with SFTS.

Methods

Patients

A total of 208 consecutive patients with SFTS admitted to the Department of Infectious Disease, Zhongnan Hospital of Wuhan University between August 2016 and June 2023 were included in a retrospective cohort. The patients were then divided into the AKI ($n = 153$) and non-AKI groups ($n = 55$) according to the presence of AKI. According to the current Kidney Disease: Improving Global Outcomes (KDIGO) staging criteria for AKI, patients in the AKI group were further divided into three subgroups: stage 1 AKI group ($n = 23$), stage 2 AKI group ($n = 17$) and stage 3 AKI group ($n = 15$).

The criteria of diagnosing SFTS were as follows (Liu Q. et al., 2014): (1) acute fever (temperature >37.3°C for over 24 h) with thrombocytopenia; (2) laboratory-confirmed SFTS virus infection by detection of viral RNA through polymerase chain reaction assay. Patients were excluded if they fulfilled one or more of the following criteria: (1) age ≤18 years or ≥80 years, (2) reduced glomerular filtration rate or chronic kidney disease had been confirmed before admission, (3) previous kidney transplantation; (4) the presence of preterminal comorbidities (heart disease New York Heart Association III–IV, severe chronic obstructive pulmonary disease), (5) any other types of immunodeficiency. (6) history of malignant tumor.

Diagnosis of AKI was based on the KDIGO guidelines (Palevsky et al., 2013): (1) increase in sCr by ≥26.5 μmol/L (or ≥50%) within 48 h; or (2) increase in sCr to ≥1.5 times the baseline value, which is known or presumed to have within the previous 7 days; or (3) urine volume <0.5 mL/kg/h for 6 h. The KDIGO criteria for AKI staging were as follows: (1) AKI stage 1, increase in sCr by 1.5–1.9 times the baseline value, or increase in sCr by 26.5 μmol/L within 48 h, or urine volume <0.5 mL/kg/h and >0.3 mL/kg/h for 6–12 h; (2) AKI stage 2, increase in sCr by 2.0–2.9 times the baseline value, or urine volume <0.5 mL/kg/h and >0.3 mL/kg/h for ≥12 h; (3) AKI stage 3, increase in sCr by 3.0 times the baseline value, or increase in sCr to 353.6 μmol/L, or start of renal replacement therapy, or urine volume <0.3 mL/kg/h for ≥24 h.

During hospitalization, all patients received routine supportive treatment, including bed rest, adequate nutritional support, intensive care and monitoring. Complications including coagulation disorders, thrombocytopenia crisis, neutropenia, acute respiratory distress syndrome, septic shock and AKI were closely monitored and managed immediately.

Data collection

The medical records of patients with SFTS were reviewed, demographic details, comorbid conditions, symptoms, signs and laboratory tests data including white blood cell (WBC) count and percentage, neutrophil count and percentage, lymphocyte count and percentage, hemoglobin, platelet (PLT) count, alanine aminotransferase (ALT), aspartate aminotransferase (AST), total bilirubin (TBIL), albumin, alkaline phosphatase (ALP), gamma glutamyl transpeptidase (GGT), lactate dehydrogenase (LDH), total cholesterol (TC), triglyceride (TG), blood urea nitrogen (BUN), uric acid, sCr, cystatin C (Cys-C), β2-microglobulin (β2-MG), sodium, potassium, calcium, magnesium, chlorine, phosphorus, amylase (AMY), lipase, creatinine kinase (CK), creatinine kinase myocardial B fraction (CK-MB), troponin I (TnI), brain natriuretic peptide (BNP), prothrombin time (PT), international normalized ratio (INR), prothrombin activity (PTA), activated partial thromboplastin time (APTT), thrombin time (TT), fibrinogen, D-dimer, C-reactive protein (CRP), procalcitonin (PCT), interleukin-6 (IL-6), erythrocyte sedimentation rate (ESR), SFTS viral load, fecal occult blood test (OBT), urine protein test (UPT), urine occult blood test (UOBT) and survival time were collected at the time of AKI diagnosis.

Statistical analysis

All data were analyzed with IBM SPSS statistical analysis software (version 23.0, Chicago, United States), and $p < 0.05$ (two-sided) was considered statistically significant. Categorical variables were shown as numbers (percentages) and were compared by the Chi-square test or Fisher's exact test. Continuous variables were shown as the means ± standard deviations for data with a normal distribution or medians with interquartile ranges

TABLE 1 Comparison of demographics, comorbid conditions and clinical symptoms between the non-AKI and AKI groups.

	All (n = 208)	Non-AKI (n = 153)	AKI (n = 55)	p-value
Male, n (%)	110 (52.9)	81 (52.9)	29 (52.7)	0.978
Age (years)	65 ± 8	64 ± 8	67 ± 7	0.024
Diabetes, n (%)	15 (7.2)	7 (4.6)	8 (14.5)	0.028
Hypertension, n (%)	53 (25.5)	36 (23.5)	17 (30.9)	0.281
Days from onset to admission	7 (6–9)	6 (5–7)	8 (7–10)	0.033
Clinical manifestations, n (%)				
Fever >38°C	50 (24.0)	33 (21.6)	17 (30.9)	0.164
Headache	40 (19.5)	24 (15.7)	16 (29.1)	0.031
Dizziness	62 (29.8)	43 (28.1)	19 (34.5)	0.370
Cough	55 (26.4)	39 (25.5)	16 (29.1)	0.604
Sputum	41 (19.7)	29 (19.0)	12 (21.8)	0.647
Chest distress	42 (20.2)	28 (18.3)	14 (25.5)	0.257
Anorexia	153 (73.6)	106 (69.3)	47 (85.5)	0.020
Nausea	160 (76.9)	116 (75.8)	44 (80.0)	0.528
Vomiting	53 (25.5)	41 (26.8)	12 (21.8)	0.467
Abdominal pain	55 (26.4)	34 (22.2)	21 (38.2)	0.021
Diarrhea	33 (15.9)	20 (13.1)	13 (23.6)	0.012
Petechia	22 (10.6)	10 (6.5)	12 (21.8)	0.032
Encephalopathy	32 (15.4)	14 (9.2)	18 (32.7)	<0.001
Hepatosplenomegaly	23 (11.1)	12 (7.8)	11 (20.0)	0.014

(P25–P75) for data with a non-normal distribution, which were compared by the student's t-test or Mann–Whitney U test, respectively. Correlations between numerical laboratory parameters were analyzed using Spearman correlation analysis. The cumulative survival rates of patients were evaluated using the Kaplan–Meier method and were compared by the log-rank test. Logistic regression analysis was conducted to identify the risk factors for fatal outcome of patients. All clinical data including demographic, comorbid conditions, clinical symptoms and laboratory indicators were included for univariate analysis, from which biologically plausible variables with p-value <0.05 were entered into the multivariate model by a stepwise method.

Results

Demographic and clinical manifestations

A total of 208 consecutive patients diagnosed with SFTS were enrolled, including 153 patients in the non-AKI group and 55 patients in the AKI group. Among these patients, 48 patients were diagnosed with AKI at admission, and seven patients were diagnosed with AKI during hospitalization. The time between symptom onset and diagnosis of AKI was 8 (7–12) days. Compared with patients without AKI, patients with AKI were older, and had a higher frequency of diabetes and more days from onset to admission. No difference was observed in the frequency of sex or hypertension between the two groups. Among all these clinical manifestations, headache, anorexia, abdominal pain, diarrhea, petechia, encephalopathy and hepatosplenomegaly were significantly overrepresented in patients in the AKI group compared with patients in the non-AKI group. However, there was no significant difference in other clinical features including dizziness, cough, sputum, chest distress, nausea, vomiting and the frequency of fever >38°C (Table 1).

Laboratory test results

Among these laboratory parameters, PLT count, albumin and fibrinogen levels of patients with AKI were identified to be significantly lower than those of patients without AKI, while ALT, AST, ALP, LDH, TG, BUN, uric acid, sCr, Cys-C, β2-MG, potassium, phosphorus, AMY, lipase, CK-MB, TnI, BNP, APTT, TT, D-dimer, CRP, IL-6, PCT and ESR levels were significantly higher in patients with AKI. A higher SFTS viral load was also detected in the AKI patients than in the non-AKI patients. In terms of routine urine test examinations, the urine RBC count in the AKI patients was significantly higher than that in the non-AKI patients. No significant difference was observed for WBC, neutrophil and lymphocyte counts, TBIL, TC, sodium, PT, INR, APTT or frequency of OBT positivity between the two groups (Table 2).

Spearman correlation analysis was conducted to analyze the correlation between sCr and other laboratory parameters. The results indicated that sCr was positively correlated with ALT, AST, TBIL, GGT, ALP, BUN, uric acid, Cys-C, AMY, lipase, CK, CK-MB, TnI, PT, INR, APTT and TT, but was negatively correlated with PLT count, albumin, urine volume and fibrinogen (Figure 1).

10.3389/fmicb.2023.1236091

TABLE 2 Comparison of laboratory parameters in the two study groups.

Variables	Normal range	All (*n* = 208)	Non-AKI (*n* = 153)	AKI (*n* = 55)	*p*-value
WBC (10^9/L)	3.5–9.5	4.1 (2.3–6.7)	4.0 (2.1–6.9)	4.2 (2.6–6.4)	0.778
Neutrophil (%)	40.0–75.0	70.1 (54.0–82.4)	68.9 (51.6–82.3)	72.7 (60.5–82.9)	0.160
Neutrophil (10^9 /L)	1.8–6.3	2.7 (1.2–5.1)	2.6 (1.1–5.0)	3.1 (1.5–5.3)	0.375
Lymphocyte (%)	20.0–50.0	20.8 (11.6–31.2)	20.6 (11.4–32.6)	20.9 (12.4–27.5)	0.590
Lymphocyte (10^9/L)	1.1–3.2	0.7 (0.5–1.1)	0.7 (0.5–1.1)	0.7 (0.5–1.1)	0.511
Hemoglobin (g/L)	130–175	122 ± 23	124 ± 23	118 ± 24	0.140
PLT (10^9/L)	125–350	41 (28–57)	42 (31–57)	34 (22–58)	0.050
ALT (U/L)	9–50	74 (45–130)	69 (45–113)	92 (48–204)	0.022
AST (U/L)	15–40	187 (91–419)	152 (85–315)	402 (134–825)	<0.001
TBIL (μmol/L)	5–21	11.7 (8.6–17.2)	10.8 (8.3–16.1)	13.7 (9.4–20.8)	0.084
Albumin (g/L)	40–55	29.9 ± 5.1	30.5 ± 4.7	28.0 ± 5.6	0.001
ALP (U/L)	30–120	74 (58–103)	71 (55–88)	106 (65–159)	<0.001
GGT (U/L)	8–57	40 (24–97)	33 (22–79)	48 (32–128)	<0.001
LDH (U/L)	125–243	708 (402–1,000)	634 (391–961)	925 (562–1,622)	0.002
TC (mmol/L)	0–5.18	2.94 (2.41–3.57)	2.91 (2.40–3.54)	3.07 (2.42–3.66)	0.459
TG (mmol/L)	0–1.70	2.23 (1.53–3.05)	2.01 (1.49–2.94)	2.65 (1.96–3.52)	0.026
BUN (mmol/L)	2.8–7.6	5.3 (4.0–8.0)	4.9 (3.6–6.1)	8.5 (6.2–15.8)	<0.001
Uric acid (μmol/L)	119–417	305 (243–397)	270 (227–326)	444 (387–513)	<0.001
sCr (μmol/L)	64–104	75 (64–110)	69 (61–79)	197 (146–299)	<0.001
Cys-C (mg/L)	0–1.2	1.26 (1.01–1.58)	1.16 (0.95–1.43)	1.68 (1.37–2.75)	<0.001
β2-MG (μg/L)	1,000–3,000	4,067 (3422–5,410)	3,616 (3073–4,210)	5,432 (4565–14,821)	<0.001
Sodium (mmol/L)	137–147	135 (132–138)	135 (132–138)	134 (131–139)	0.868
Potassium (mmol/L)	3.5–5.3	3.6 (3.3–4.2)	3.5 (3.2–3.9)	4.0 (3.6–4.5)	<0.001
Calcium (mmol/L)	2.0–2.7	1.93 (1.82–2.03)	1.93 (1.88–2.02)	1.95 (1.76–2.06)	0.425
Magnesium (mmol/L)	0.85–1.15	0.93 (0.81–1.09)	0.93 (0.81–1.03)	0.95 (0.80–1.15)	0.249
Chlorine (mmol/L)	96–106	103.0 (99.0–105.1)	103.2 (98.9–105.4)	102.3 (99.3–104.3)	0.320
Phosphorus (mmol/L)	0.8–1.5	1.09 (0.87–1.43)	0.98 (0.82–1.17)	1.52 (1.40–1.60)	<0.001
AMY (U/L)	0–90	146 (94–227)	130 (85–204)	192 (134–318)	<0.001
Lipase (U/L)	0–70	164 (78–315)	129 (67–260)	266 (117–465)	0.001
CK (U/L)	0–171	444 (147–1,197)	429 (132–997)	512 (182–1,582)	0.156
CK-MB (U/L)	0–25	32 (15–49)	28 (14–45)	39 (22–89)	0.004
TnI (pg/mL)	0–26.2	96.6 (34.7–218.5)	72.1 (40.9–207.0)	126.9 (75.8–432.5)	0.012
BNP (pg/mL)	0–1800	78.0 (128.3–192.5)	73.7 (58.4–120.5)	142.7 (123.5–280.8)	0.034
PT (s)	9.4–12.5	11.4 (10.7–12.0)	11.3 (10.6–12.0)	11.7 (11.1–12.7)	0.111
INR	0.85–1.15	1.04 (0.98–1.10)	1.03 (0.97–1.10)	1.06 (1.01–1.14)	0.107
PTA (%)	80–130	98 (88–109)	100 (90–109)	95 (85–108)	0.126
APTT (s)	25.1–36.5	42.1 (36.2–49.0)	41.0 (35.7–45.4)	48.0 (39.6–57.4)	<0.001
TT (s)	10.3–16.6	18.3 (16.6–22.3)	17.3 (16.1–19.9)	20.7 (17.1–24.7)	0.001
Fibrinogen (mg/dL)	238–498	237 (185–290)	249 (198–295)	223 (147–280)	0.017
D-dimer (ng/mL)	0–500	1,063 (472–2,230)	900 (403–1913)	1810 (612–3,340)	0.003
CRP (mg/L)	0–10.0	7.1 (2.4–17.5)	4.9 (1.6–14.9)	10.7 (6.4–28.0)	0.033
PCT (ng/mL)	0–0.05	0.26 (0.08–0.72)	0.18 (0.06–0.40)	0.89 (0.34–2.42)	<0.001
IL-6 (pg/mL)	0–7	41.0 (15.1–115.3)	33.3 (13.1–86.9)	113.4 (26.7–557.6)	<0.001
ESR (mm/h)	0–20	8 (4–14)	7 (4–12)	10 (7–23)	0.038
Urine RBC count	0–13.1	19.3 (8.5–65.4)	16.7 (7.4–40.9)	33.9 (14.1–146.0)	0.009
Viral load (log_{10} copies/mL)		4.2 (3.2–5.4)	4.0 (3.1–4.5)	5.5 (3.8–6.9)	0.002
OBT positive, *n* (%)		49 (23.6)	31 (20.3)	18 (32.8)	0.062
UPT positive, *n* (%)		171 (82.2)	125 (81.6)	46 (83.6)	0.747
UOBT positive, *n* (%)		163 (78.4)	118 (77.1)	45 (81.8)	0.468

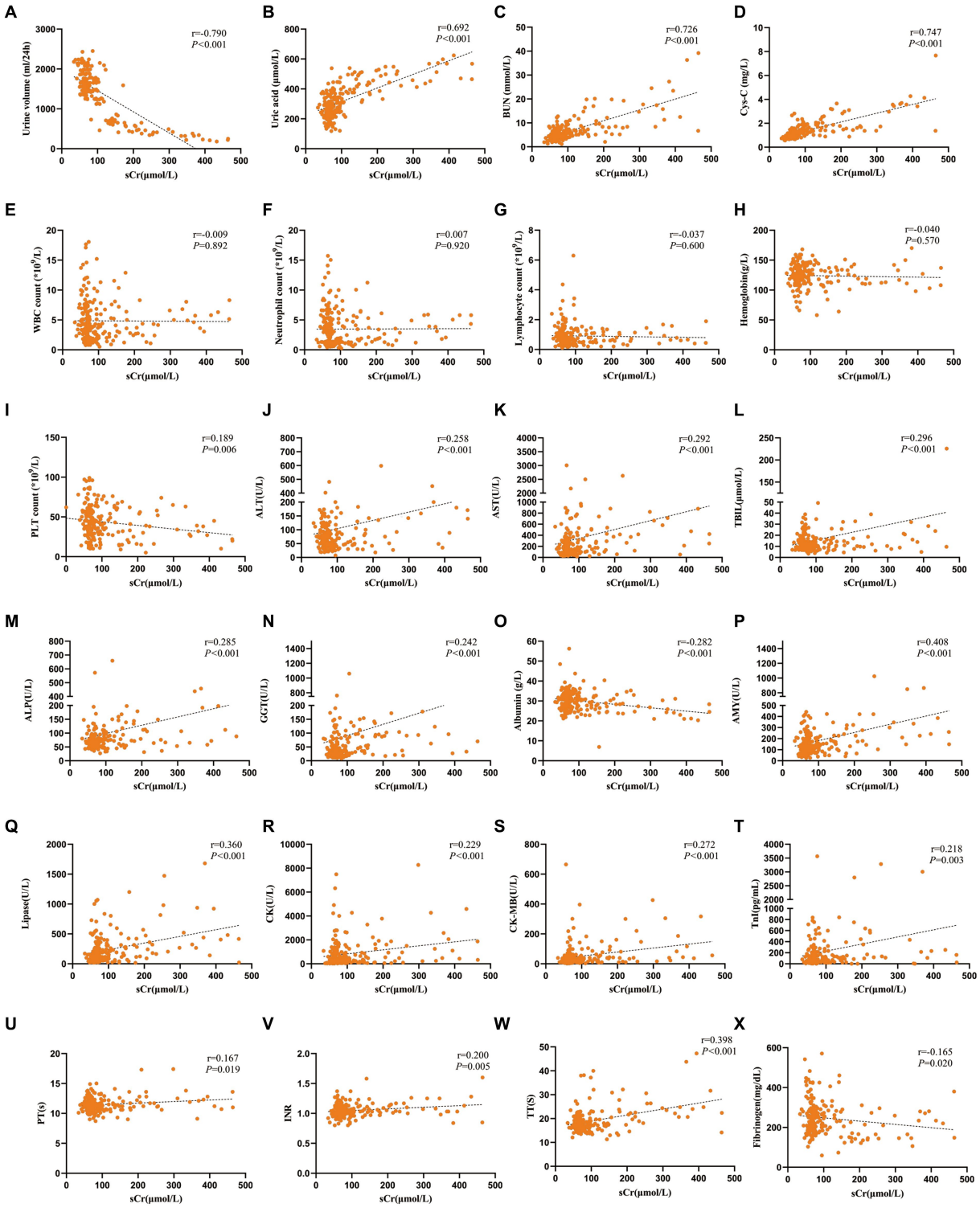

FIGURE 1
Spearman correlation analysis was carried out to analyze the relationship between the levels of sCr and other laboratory parameters in patients with SFTS. **(A)** Correlation analysis between sCr and urine volume. **(B)** Correlation analysis between sCr and uric acid. **(C)** Correlation analysis between sCr and BUN. **(D)** Correlation analysis between sCr and Cys-C. **(E)** Correlation analysis between sCr and WBC count. **(F)** Correlation analysis between sCr and neutrophil count. **(G)** Correlation analysis between sCr and lymphocyte count. **(H)** Correlation analysis between sCr and hemoglobin. **(I)** Correlation analysis between sCr and PLT count. **(J)** Correlation analysis between sCr and ALT. **(K)** Correlation analysis between sCr and AST. **(L)** Correlation analysis between sCr and TBIL. **(M)** Correlation analysis between sCr and ALP. **(N)** Correlation analysis between sCr and GGT. **(O)** Correlation analysis between sCr and albumin. **(P)** Correlation analysis between sCr and AMY. **(Q)** Correlation analysis between sCr and lipase. **(R)** Correlation analysis between sCr and CK. **(S)** Correlation analysis between sCr and CK-MB. **(T)** Correlation analysis between sCr and TnI. **(U)** Correlation analysis between sCr and PT. **(V)** Correlation analysis between sCr and INR. **(W)** Correlation analysis between sCr and TT. **(X)** Correlation analysis between sCr and Fibrinogen.

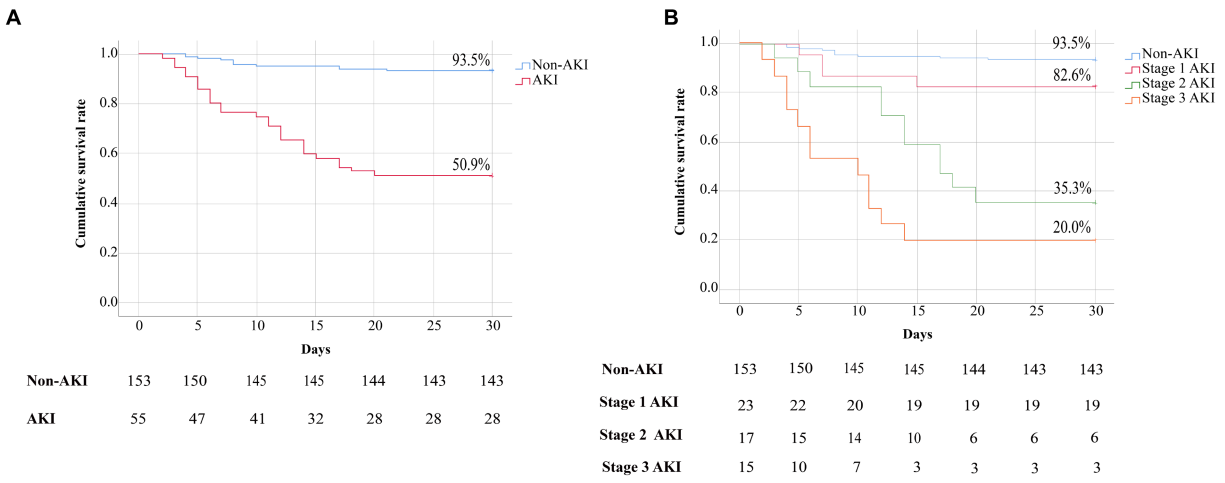

FIGURE 2
(A) Kaplan–Meier curves showing the cumulative survival rates of patients in the non-AKI and AKI groups. Comparison of the survival estimates was performed using the log rank test, non-AKI group vs. AKI group, $p < 0.001$. **(B)** Kaplan–Meier curves showing the cumulative survival rates of patients with SFTS based on AKI stage. Comparison of the survival estimates was performed using the log rank test, non-AKI group vs. stage 1 AKI group, $p = 0.481$; non-AKI group vs. stage 2 AKI or stage 3 AKI group, all $p < 0.001$; stage 1 AKI group vs. stage 2 AKI or stage 3 AKI group, $p = 0.003$, $p < 0.001$, respectively.

Prognosis classification of patients with SFTS

As shown in Figure 2A, the cumulative survival rate of patients in the AKI group was significantly lower than that in the non-AKI group (93.4% vs. 50.9%, $p < 0.001$). As shown in Figure 2B, patients in the AKI group were divided into three subgroups, and the cumulative survival rates of patients at AKI stages 1, 2 and 3 were 82.6%, 35.3% and 20.0%, respectively. Both the cumulative survival rates of patients at AKI stage 2 or 3 were significantly lower than those of patients without AKI (all $p < 0.001$). However, there was no significant difference in the cumulative survival rates between the stage 1 AKI and non-AKI groups ($p = 0.066$). Moreover, compared with patients at AKI stage 1, patients at AKI stage 2 or 3 also had significantly lower cumulative survival rates ($p = 0.003$, $p < 0.001$, respectively). Moreover, the clinical features and laboratory parameters of patients at AKI stages 1, 2 and 3 were compared. We revealed that patients with stage 2 or 3 AKI had more days from onset to admission, and higher serum levels of ALT, AST, LDH, uric acid, Cys-C, β2-MG, AMY, lipase, CK-MB, TnI, BNP, D-dimer, CRP, PCT, IL-6, ESR, viral load and urine RBC count than patients with stage 1 AKI (Supplementary Table S1).

Risk factors for fatal outcomes

Univariable logistic regression analyses revealed that the presence of petechia, encephalopathy, hepatosplenomegaly and stage 2 or 3 AKI, old age, and decreased albumin, low fibrinogen, and elevated levels of AST, ALP, GGT, LDH, TG, uric acid, AMY, lipase, CK-MB, PT, APTT, TT, IL-6 and viral load were risk factors for fatal outcomes in patients with SFTS. The above variables were used for multivariable logistic regression analyses. It demonstrated that stage 2 or 3 AKI (OR, 10.329; 95% CI, 4.815–21.244), encephalopathy (OR, 5.935; 95% CI, 3.056–13.903), elevated levels of LDH (OR, 1.002; 95% CI, 1.001–1.003) and viral load (OR, 2.415; 95% CI, 1.702–4.026) were independent risk factors for mortality in patients with SFTS (Table 3).

Longitudinal changes in laboratory parameters in patients without AKI or at AKI stages 1, 2 and 3

Subgroup patients with longitudinal laboratory test results were analyzed to investigate their serial changes with respect to disease severity. Levels of 22 laboratory parameters at four time points were collected and presented. Compared with patients without AKI or with stage 1 AKI, patients with stage 2 or 3 AKI showed a significant increase in serum concentrations of sCr, BUN, Cys-C, β2-MG, AST, TBIL, ALP, GGT, LDH, BUN, AMY, lipase, CK-MB, TnI, TT, D-dimer, CRP, IL-6, and PCT and significantly reduced serum levels of albumin and PLT count during the course of hospitalization (see Figure 3).

Discussion

AKI is a clinical syndrome caused by a sudden decrease in renal excretory function, with the accumulation of nitrogen metabolism waste such as creatinine and urea. Other common clinical and laboratory presentations include reduced urine output, resulting in the accumulation of metabolic acids, potassium and phosphate. It is a frequent complication in hospital patients and very common in critically ill patients (Bellomo et al., 2012; Gonsalez et al., 2019). AKI in patients with SFTS was also observed in previous studies (Cui et al., 2015; Jia et al., 2017; Wang et al., 2019; He et al., 2021), yet with very little information on its incidence, clinical characteristics and prognosis.

10.3389/fmicb.2023.1236091

TABLE 3 Univariable and multivariable logistic regression analyses of in-hospital mortality in patients with SFTS.

	Univariable analysis		Multivariable analysis	
	OR (95% CI)	*p*-value	OR (95% CI)	*p*-value
Male	1.436 (0.704–2.931)	0.320		
Age	1.057 (1.008–1.108)	0.022		
Diabetes	2.516 (0.806–7.855)	0.112		
Hypertension	1.012 (0.494–2.462)	0.812		
Days from onset to admission	1.036 (0.921–1.164)	0.560		
Fever >38°C	2.649 (0.946–5.632)	0.052		
Headache	2.072 (0.921–4.658)	0.078		
Anorexia	2.075 (0.815–5.285)	0.126		
Abdominal pain	1.429 (0.661–3.086)	0.364		
Diarrhea	1.301 (0.517–3.274)	0.576		
Petechia	3.094 (1.191–8.037)	0.020		
Encephalopathy	7.381 (3.220–16.917)	<0.001	5.935 (3.056–13.903)	0.012
Hepatosplenomegaly	4.501 (1.794–11.294)	0.001		
Stage 2 or 3 AKI	12.536 (8.454–23.178)	<0.001	10.329 (4.815–21.244)	<0.001
WBC (10^9/L)	1.014 (0.916–1.122)	0.787		
Neutrophil (%)	0.999 (0.992–1.007)	0.831		
Neutrophil (10^9 /L)	0.999 (0.885–1.127)	0.987		
Lymphocyte (%)	0.986 (0.959–1.014)	0.311		
Lymphocyte (10^9/L)	1.120 (0.711–1.762)	0.625		
Hemoglobin (g/L)	0.991 (0.977–1.005)	0.206		
PLT (10^9/L)	0.982 (0.964–1.001)	0.059		
ALT (U/L)	1.002 (0.999–1.004)	0.131		
AST (U/L)	1.002 (1.001–1.003)	<0.001		
TBIL (μmol/L)	1.016 (0.998–1.034)	0.077		
Albumin (g/L)	0.903 (0.834–0.977)	0.011		
ALP (U/L)	1.006 (1.002–1.009)	0.002		
GGT (U/L)	1.003 (1.001–1.005)	0.008		
LDH (U/L)	1.003 (1.001–1.004)	<0.001	1.002 (1.001–1.003)	0.006
TC (mmol/L)	0.712 (0.410–1.239)	0.230		
TG (mmol/L)	1.276 (1.000–1.628)	0.050		
BUN (mmol/L)	1.000 (0.990–1.010)	0.816		
Uric acid (μmol/L)	1.009 (1.005–1.012)	<0.001		
Cys-C (mg/L)	1.132 (0.931–1.375)	0.214		
Sodium (mmol/L)	0.984 (0.926–1.046)	0.604		
Potassium (mmol/L)	4.349 (2.282–8.290)	<0.001		
AMY (U/L)	1.002 (1.001–1.003)	0.002		
Lipase (U/L)	1.002 (1.000–1.003)	0.007		
CK (U/L)	1.000 (1.000–1.000)	0.040		
CK-MB (U/L)	1.009 (1.004–1.014)	<0.001		
TnI (pg/mL)	1.001 (1.000–1.001)	0.069		
PT (s)	1.474 (1.118–1.944)	0.006		
INR	1.003 (0.990–1.017)	0.627		
PTA (%)	0.984 (0.963–1.005)	0.140		

(Continued)

TABLE 3 (Continued)

	Univariable analysis		Multivariable analysis	
	OR (95% CI)	*p*-value	OR (95% CI)	*p*-value
APTT (s)	1.073 (1.039–1.108)	<0.001		
TT (s)	1.075 (1.022–1.131)	0.005		
Fibrinogen (mg/dL)	0.988 (0.982–0.995)	<0.001		
D-dimer (ng/mL)	1.001 (1.000–1.003)	0.397		
CRP (mg/L)	1.025 (0.983–1.069)	0.254		
PCT (ng/mL)	1.118 (0.981–1.274)	0.096		
IL-6 (pg/mL)	1.008 (1.002–1.014)	0.012		
ESR (mm/h)	1.025 (0.996–1.056)	0.096		
Viral load	3.309 (1.855–5.902)	<0.001	2.415 (1.702–4.026)	0.026
OBT positive	1.769 (0.794–3.940)	0.163		
UPT positive	1.144 (0.439–2.978)	0.783		
UOBT positive	1.629 (0.635–4.180)	0.310		
Urine RBC count	1.000 (1.000–1.001)	0.692		

To our knowledge, this is the first report of the clinical features and outcomes of AKI in SFTS. In the present study, we demonstrated the incidence of AKI in 26.4% of hospitalized SFTS patients. We also revealed that the patients with AKI showed higher decreased levels of albumin and fibrinogen, and elevated levels of AST, TBIL, ALP, LDH, BUN, uric acid, sCr, AMY, lipase, CKMB, TnI, APTT, TT and D-dimer than patients without AKI during hospitalization. Spearman correlation analysis also showed that sCr was closely correlated with these laboratory parameters. They are generally associated with fatal outcomes, and are commonly used to reflect the heart, liver, pancreas, kidney and coagulation functions, and their extremely abnormal levels reveal severe organ injury and dysfunction, which usually occur in critically ill patients, who should receive more attention, specifically by developing new therapeutic and prevention strategies to be used in clinical practice. Furthermore, we revealed that nonspecific symptoms including abdominal pain, diarrhea, encephalopathy and hepatosplenomegaly were more frequent in patients with AKI. Some studies have reported that encephalopathy and hepatosplenomegaly are independent predictors of mortality in patients with SFTS (Liu et al., 2013; Gong et al., 2021). It revealed that AKI was often linked with other severe complications, leading to poor prognosis.

A number of studies have revealed that a high viral load is generally associated with poor outcome. Which can be used to predict the mortality of patients with SFTS (Liu et al., 2016; Yang et al., 2016; Jo et al., 2022; Wang et al., 2022). We also found that the viral load was an independent risk factor for the prognosis of patients with SFTS. In the present study, the viral load was significantly higher in the AKI group than in the non-AKI group. At least in part, it could explain why patients in the AKI group have a higher mortality rate. Although the mechanisms of AKI in patients with SFTS are unclear, some studies reported that the SFTS virus was detected in the kidneys (Chen et al., 2012; Jin et al., 2012). Recently, a report showed that SFTS viral load in urine is an independent predictor of the incidence of AKI (Zhang et al., 2023). It implies that the SFTS virus may directly induce renal damage. Moreover, a large number of studies have shown that the SFTS virus can substantially produce inflammatory cytokines and chemokines, leading to cytokine storms (Khalil et al., 2021; Wang et al., 2021; Gao et al., 2022). It can promote kidney vascular permeability, and even microcirculatory dysfunction, and it can induce thrombosis and capillary leak syndrome, resulting in disseminated intravascular coagulation. In addition, these high serum levels of cytokines can directly cause the death of renal endothelial and tubular epithelial cells (Ahmadian et al., 2021; Legrand et al., 2021).

In the present study, we used the less sensitive sCr-based criteria to identify AKI. Although inulin clearance and radionuclide renal imaging are more sensitive, they are inconvenient and costly. Nonetheless, sCr measurement is still the most practical and widely accepted method for evaluating renal function in patients with AKI at present (Moledina et al., 2017; Moledina and Parikh, 2018). Some biomarkers of AKI including Cys-C and β2-MG were also evaluated in patients with SFTS. Cys-C is an elegant indicator of glomerular filtration rate because it is not affected by factors such as muscle mass, diet, drugs, sex and tubular secretion, and it is a reliable parameter for evaluating and predicting AKI in critically ill patients (Mårtensson et al., 2012; Luft, 2021). β2-MG has also traditionally been used to evaluate renal tubular function, and elevated β2-MG is typically accompanied by kidney injury (Bagshaw et al., 2007). Our results also showed that the serum levels of Cys-C and β2-MG in the AKI group were significantly higher than those in the non-AKI group.

Importantly, our findings confirmed that stage 2 or 3 AKI was a strong independent risk factor for the prognosis in patients with SFTS, and patients at AKI stage 2 or 3 showed a significantly higher in-hospital mortality than patients without AKI or at AKI stage 1. Some previous studies of other diseases also had yielded similar results. A large observational study demonstrated that the mortality of hospitalized patients at AKI stage 2 or 3 was approximately 2 or 4 times higher than that of patients at AKI stage 1, respectively (Khadzhynov et al., 2019). A retrospective analysis of the cohort of patients from the North American Consortium for the Study of

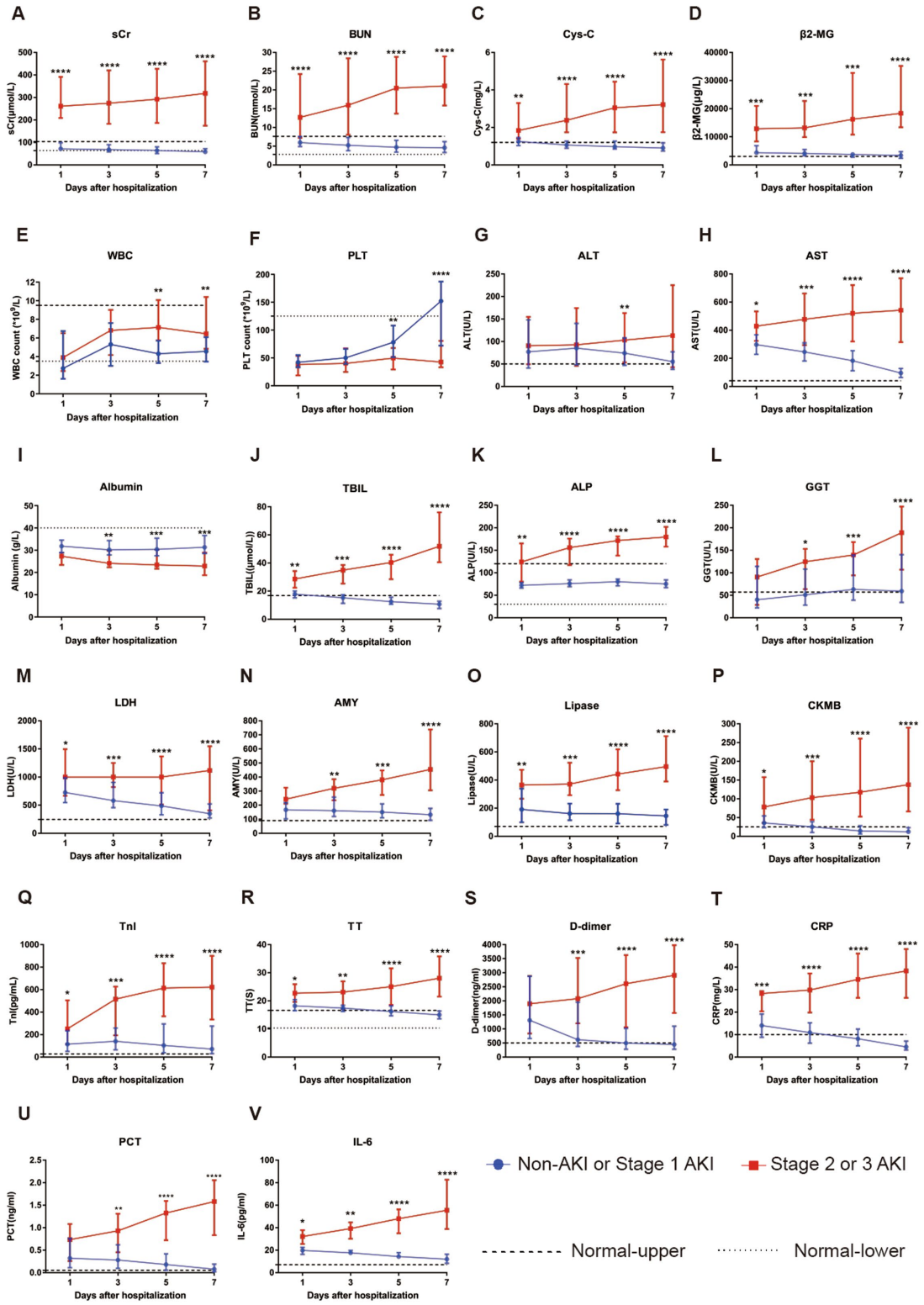

FIGURE 3
Evaluation of serial laboratory parameters for the non-AKI or stage 1 AKI group (n = 51) vs. stage 2 or 3 group (n = 16) of SFTS patients during hospitalization. **(A)** The longitudinal changes in sCr between the two groups. **(B)** The longitudinal changes in BUN between the two groups. **(C)** The longitudinal changes in Cys-C between the two groups. **(D)** The longitudinal changes in β2-MG between the two groups. **(E)** The longitudinal changes in WBC count between the two groups. **(F)** The longitudinal changes in PLT count between the two groups. **(G)** The longitudinal changes in ALT between the two groups. **(H)** The longitudinal changes in AST between the two groups. **(I)** The longitudinal changes in albumin between the two groups. **(J)** The longitudinal changes in TBIL between the two groups. **(K)** The longitudinal changes in ALP between the two groups. **(L)** The longitudinal changes in GGT between the two groups. **(M)** The longitudinal changes in LDH between the two groups. **(N)** The longitudinal changes in

(Continued)

FIGURE 3 (Continued)
AMY between the two groups. **(O)** The longitudinal changes in lipase between the two groups. **(P)** The longitudinal changes in CKMB between the two groups. **(Q)** The longitudinal changes in TnI between the two groups. **(R)** The longitudinal changes in TT between the two groups. **(S)** The longitudinal changes in D-dimer between the two groups. **(T)** The longitudinal changes in CRP between the two groups. **(U)** The longitudinal changes in PCT between the two groups. **(V)** The longitudinal changes in IL-6 between the two groups. All data are presented as medians with interquartile ranges (P25–P75). $*p < 0.05$, $**p < 0.01$, $***p < 0.001$, and $****p < 0.0001$. Normal-upper: the upper limit of the normal value range. Normal-lower: the lower limit of the normal value range.

End-Stage Liver Disease study on the complications of patients with decompensated cirrhosis revealed that patients at AKI stage 2 or 3 had higher model for end-stage liver disease scores, presence of systemic inflammatory response syndrome and second infections, resulting in a lower survival rate (Wong et al., 2021). Moreover, we compared the longitudinal changes in laboratory parameters of patients in the non-AKI, stage 1, 2 and 3 AKI groups. It revealed that laboratory indicators reflecting organ injury and inflammation returned to the normal range in patients without AKI or at AKI stage 1, but these parameters were aggravated continuously in patients at AKI stage 2 or 3 during hospitalization. These results could explain the higher mortality of patients at AKI stage 2 or 3.

Limitations of our study include the observational and retrospective study design. Additionally, the sample size of this study was relatively small. Therefore, the subsequent analysis of risk factors for AKI development in SFTS was not conducted.

At the same time, due to the limited laboratory resources in our hospital, some other AKI biomarkers including neutrophil gelatinase-associated lipocalin, kidney injury molecule-1 and interleukin-18 could not be measured. Finally, because this was a single-center study, the observations made here could not be extrapolated to other centers.

Conclusion

In conclusion, we found a high incidence of AKI in patients with SFTS, and AKI was associated with poor prognosis. Most importantly, we revealed that patients at AKI stage 2 or 3 had higher mortality. These results provide strong evidence to emphasize that patients with SFTS should be carefully monitored for the development of AKI and corresponding measures should be taken to prevent it, and further explorations are required to identify the risk factors for the development of AKI.

Data availability statement

The original contributions presented in the study are included in the article/Supplementary material, further inquiries can be directed to the corresponding authors.

Ethics statement

The studies involving humans were approved by Ethics Committee of Zhongnan Hospital of Wuhan University. The studies were conducted in accordance with the local legislation and institutional requirements. The ethics committee/institutional review board waived the requirement of written informed consent for participation from the participants or the participants' legal guardians/next of kin because the written informed consent was waived due to the nature of the retrospective study and pandemic nature of the disease.

Author contributions

ZZ and XH were involved in patient data analysis and wrote the manuscript drafting. QJ and WH were mainly responsible for the data collection. AL, LD, and YX were responsible for the study design and critical revision. All authors contributed to the article and approved the submitted version.

Funding

This work was supported by grants from Key Research and Development Program of Hubei Province, China (2020BCB025).

Acknowledgments

The authors wish to thank the patient for participating in this study and all the staff members at our institution.

Conflict of interest

The authors declare that the research was conducted in the absence of any commercial or financial relationships that could be construed as a potential conflict of interest.

Publisher's note

All claims expressed in this article are solely those of the authors and do not necessarily represent those of their affiliated organizations, or those of the publisher, the editors and the reviewers. Any product that may be evaluated in this article, or claim that may be made by its manufacturer, is not guaranteed or endorsed by the publisher.

Supplementary material

The Supplementary material for this article can be found online at: https://www.frontiersin.org/articles/10.3389/fmicb.2023.1236091/full#supplementary-material

References

Ahmadian, E., Hosseiniyan Khatibi, S. M., Razi Soofiyani, S., Abediazar, S., Shoja, M. M., Ardalan, M., et al. (2021). Covid-19 and kidney injury: pathophysiology and molecular mechanisms. *Rev. Med. Virol.* 31:e2176. doi: 10.1002/rmv.2176

Bagshaw, S. M., Langenberg, C., Haase, M., Wan, L., May, C. N., and Bellomo, R. (2007). Urinary biomarkers in septic acute kidney injury. *Intensive Care Med.* 33, 1285–1296. doi: 10.1007/s00134-007-0656-5

Bao, C. J., Guo, X. L., Qi, X., Hu, J. L., Zhou, M. H., Varma, J. K., et al. (2011). A family cluster of infections by a newly recognized bunyavirus in eastern China, 2007: further evidence of person-to-person transmission. *Clin. Infect. Dis.* 53, 1208–1214. doi: 10.1093/cid/cir732

Bellomo, R., Kellum, J. A., and Ronco, C. (2012). Acute kidney injury. *Lancet* 380, 756–766. doi: 10.1016/S0140-6736(11)61454-2

Chen, X., Cong, M., Li, M., Kang, Y., Feng, Y., Plyusnin, A., et al. (2012). Infection and pathogenesis of Huaiyangshan virus (a novel tick-borne bunyavirus) in laboratory rodents. *J. Gen. Virol.* 93, 1288–1293. doi: 10.1099/vir.0.041053-0

Cui, N., Liu, R., Lu, Q., Wang, L., Qin, S., Yang, Z., et al. (2015). Severe fever with thrombocytopenia syndrome bunyavirus-related human encephalitis. *J. Infect.* 70, 52–59. doi: 10.1016/j.jinf.2014.08.001

Gao, C., Yu, Y., Wen, C., Li, Z., Ding, H., Qi, X., et al. (2022). Nonstructural protein NSs activates inflammasome and pyroptosis through interaction with NLRP3 in human microglial cells infected with severe fever with thrombocytopenia syndrome bandavirus. *J. Virol.* 96:e0016722. doi: 10.1128/jvi.00167-22

Gong, L., Zhang, L., Wu, J., Lu, S., Lyu, Y., Zhu, M., et al. (2021). Clinical progress and risk factors for death from severe fever with thrombocytopenia syndrome: a multihospital retrospective investigation in Anhui, China. *Am. J. Trop. Med. Hyg.* 104, 1425–1431. doi: 10.4269/ajtmh.20-0270

Gonsalez, S. R., Cortês, A. L., Silva, R. C. D., Lowe, J., Prieto, M. C., and Silva Lara, L. D. (2019). Acute kidney injury overview: from basic findings to new prevention and therapy strategies. *Pharmacol. Ther.* 200, 1–12. doi: 10.1016/j.pharmthera.2019.04.001

He, F., Zheng, X., and Zhang, Z. (2021). Clinical features of severe fever with thrombocytopenia syndrome and analysis of risk factors for mortality. *BMC Infect. Dis.* 21:1253. doi: 10.1186/s12879-021-06946-3

Jia, B., Yan, X., Chen, Y., Wang, G., Liu, Y., Xu, B., et al. (2017). A scoring model for predicting prognosis of patients with severe fever with thrombocytopenia syndrome. *PLoS Neglect. Trop. Dis.* 11:e5909. doi: 10.1371/journal.pntd.0005909

Jin, C., Liang, M., Ning, J., Gu, W., Jiang, H., Wu, W., et al. (2012). Pathogenesis of emerging severe fever with thrombocytopenia syndrome virus in C57/BL6 mouse model. *Proc. Natl. Acad. Sci. U.S.A.* 109, 10053–10058. doi: 10.1073/pnas.1120246109

Jo, H., Kim, J., Hwang, S., Seo, J., Kim, D. Y., Yun, N., et al. (2022). Viral load as a factor affecting the fatality of patients suffering from severe fever with thrombocytopenia syndrome. *Viruses* 14:881. doi: 10.3390/v14050881

Khadzhynov, D., Schmidt, D., Hardt, J., Rauch, G., Gocke, P., Eckardt, K. U., et al. (2019). The incidence of acute kidney injury and associated hospital mortality. *Dtsch. Arztebl. Int.* 116, 397–404. doi: 10.3238/arztebl.2019.0397

Khalil, J., Yamada, S., Tsukamoto, Y., Abe, H., Shimojima, M., Kato, H., et al. (2021). The nonstructural protein NSs of severe fever with thrombocytopenia syndrome virus causes a cytokine storm through the hyperactivation of NF-κb. *Mol. Cell. Biol.* 41:e0054220. doi: 10.1128/MCB.00542-20

Legrand, M., Bell, S., Forni, L., Joannidis, M., Koyner, J. L., Liu, K., et al. (2021). Pathophysiology of COVID-19-associated acute kidney injury. *Nat. Rev. Nephrol.* 17, 751–764. doi: 10.1038/s41581-021-00452-0

Li, S., Li, Y., Wang, Q., Yu, X., Liu, M., Xie, H., et al. (2018). Multiple organ involvement in severe fever with thrombocytopenia syndrome: an immunohistochemical finding in a fatal case. *Virol. J.* 15:97. doi: 10.1186/s12985-018-1006-7

Liu, S., Chai, C., Wang, C., Amer, S., Lv, H., He, H., et al. (2014). Systematic review of severe fever with thrombocytopenia syndrome: virology, epidemiology, and clinical characteristics. *Rev. Med. Virol.* 24, 90–102. doi: 10.1002/rmv.1776

Liu, Q., He, B., Huang, S. Y., Wei, F., and Zhu, X. Q. (2014). Severe fever with thrombocytopenia syndrome, an emerging tick-borne zoonosis. *Lancet Infect. Dis.* 14, 763–772. doi: 10.1016/S1473-3099(14)70718-2

Liu, M., Lei, X., and Yu, X. (2016). Meta-analysis of the clinical and laboratory parameters of SFTS patients in China. *Virol. J.* 13:198. doi: 10.1186/s12985-016-0661-9

Liu, W., Lu, Q., Zhuang, L. U., Hu, C., Yuan, C., And Fan, X., et al. (2013). Case-fatality ratio and effectiveness of ribavirin therapy among hospitalized patients in China who had severe fever with thrombocytopenia syndrome. *Clin. Infect. Dis.* 57, 1292–1299. doi: 10.1093/cid/cit530

Luft, F. C. (2021). Biomarkers and predicting acute kidney injury. *Acta Physiol.* 231:e13479. doi: 10.1111/apha.13479

Mårtensson, J., Martling, C. R., and Bell, M. (2012). Novel biomarkers of acute kidney injury and failure: clinical applicability. *Brit. J. Anaesth.* 109, 843–850. doi: 10.1093/bja/aes357

Moledina, D. G., Hall, I. E., Thiessen-Philbrook, H., Reese, P. P., Weng, F. L., Schröppel, B., et al. (2017). Performance of serum creatinine and kidney injury biomarkers for diagnosing histologic acute tubular injury. *Am. J. Kidney Dis.* 70, 807–816. doi: 10.1053/j.ajkd.2017.06.031

Moledina, D. G., and Parikh, C. R. (2018). Phenotyping of acute kidney injury: beyond serum creatinine. *Semin. Nephrol.* 38, 3–11. doi: 10.1016/j.semnephrol.2017.09.002

Nie, Q., Wang, D., Ning, Z., Li, T., Tian, X., Bian, P., et al. (2020). Analysis of severe fever with thrombocytopenia syndrome in critical ill patients in central China. *Shock* 54, 451–457. doi: 10.1097/SHK.0000000000001527

Palevsky, P. M., Liu, K. D., Brophy, P. D., Chawla, L. S., Parikh, C. R., Thakar, C. V., et al. (2013). KDOQI US commentary on the 2012 KDIGO clinical practice guideline for acute kidney injury. *Am. J. Kidney Dis.* 61, 649–672. doi: 10.1053/j.ajkd.2013.02.349

Park, E., Shimojima, M., Nagata, N., Ami, Y., Yoshikawa, T., Iwata-Yoshikawa, N., et al. (2019). Severe fever with thrombocytopenia syndrome phlebovirus causes lethal viral hemorrhagic fever in cats. *Sci. Rep.* 9:11990. doi: 10.1038/s41598-019-48317-8

Wang, Y., Han, S., Ran, R., Li, A., Liu, H., Liu, M., et al. (2021). A longitudinal sampling study of transcriptomic and epigenetic profiles in patients with thrombocytopenia syndrome. *Nat. Commun.* 12:5629. doi: 10.1038/s41467-021-25804-z

Wang, Y., Song, Z., Wei, X., Yuan, H., Xu, X., Liang, H., et al. (2022). Clinical laboratory parameters and fatality of severe fever with thrombocytopenia syndrome patients: a systematic review and meta-analysis. *PLoS Neglect. Trop. Dis.* 16:e10489. doi: 10.1371/journal.pntd.0010489

Wang, L., Wan, G., Shen, Y., Zhao, Z., Lin, L., Zhang, W., et al. (2019). A nomogram to predict mortality in patients with severe fever with thrombocytopenia syndrome at the early stage—a multicenter study in China. *PLoS Neglect. Trop. Dis.* 13:e7829. doi: 10.1371/journal.pntd.0007829

Wen, H., Zhao, L., Zhai, S., Chi, Y., Cui, F., Wang, D., et al. (2014). Severe fever with thrombocytopenia syndrome, Shandong province, China, 2011. *Emerg. Infect. Dis.* 20, 1–5. doi: 10.3201/eid2001.120532

Wong, F., Reddy, K. R., Tandon, P., O'Leary, J. G., Garcia-Tsao, G., Vargas, H. E., et al. (2021). Progression of stage 2 and 3 acute kidney injury in patients with decompensated cirrhosis and ascites. *Clin. Gastroenterol. Hepatol.* 19, 1661–1669. doi: 10.1016/j.cgh.2020.08.025

Xu, X., Sun, Z., Liu, J., Zhang, J., Liu, T., Mu, X., et al. (2018). Analysis of clinical features and early warning indicators of death from severe fever with thrombocytopenia syndrome. *Int. J. Infect. Dis.* 73, 43–48. doi: 10.1016/j.ijid.2018.05.013

Yamanaka, A., Kirino, Y., Fujimoto, S., Ueda, N., Himeji, D., Miura, M., et al. (2020). Direct transmission of severe fever with thrombocytopenia syndrome virus from domestic cat to veterinary personnel. *Emerg. Infect. Dis.* 26, 2994–2998. doi: 10.3201/eid2612.191513

Yang, Z., Hu, J., Lu, Q., Guo, C., Cui, N., Peng, W., et al. (2016). The prospective evaluation of viral loads in patients with severe fever with thrombocytopenia syndrome. *J. Clin. Virol.* 78, 123–128. doi: 10.1016/j.jcv.2016.03.017

Yu, X. J., Liang, M. F., Zhang, S. Y., Liu, Y., Li, J. D., Sun, Y. L., et al. (2011). Fever with thrombocytopenia associated with a novel bunyavirus in China. *N. Engl. J. Med.* 364, 1523–1532. doi: 10.1056/NEJMoa1010095

Zhang, Y., He, Y., Dai, Y., Xiong, Y., Zheng, H., Zhou, D., et al. (2012). Hemorrhagic fever caused by a novel bunyavirus in China: pathogenesis and correlates of fatal outcome. *Clin. Infect. Dis.* 54, 527–533. doi: 10.1093/cid/cir804

Zhang, Q., Zhao, J., Dai, Y., Jiang, Z., Chen, T., Hu, N., et al. (2023). A high viral load in urine correlates with acute kidney injury and poor outcomes in hospitalized patients with severe fever with thrombocytopenia syndrome: a noninvasive and convenient prognostic marker. *Open Forum Infect. Dis.* 10:ofad085. doi: 10.1093/ofid/ofad085

Glossary

AKI	acute kidney injury
ALT	alanine aminotransferase
AST	aspartate aminotransferase
ALP	alkaline phosphatase
AMY	amylase
APTT	activated partial thromboplastin time
BNP	brain natriuretic peptide
BUN	blood urea nitrogen
CK	creatinine kinase
CK-MB	creatinine kinase myocardial B fraction
CRP	C-reactive protein
Cys-C	cystatin C
ESR	erythrocyte sedimentation rate
GGT	gamma glutamyl transpeptidase
INR	international normalized ratio
IL-6	interleukin-6
LDH	lactate dehydrogenase
β2-MG	β2-microglobulin
OBT	occult blood test
PLT	platelet
PT	prothrombin time
PTA	prothrombin activity
PCT	procalcitonin
sCr	serum creatinine
SFTS	severe fever with thrombocytopenia syndrome
TBIL	total bilirubin
TC	total cholesterol
TG	triglyceride
TT	thrombin time
TnI	troponin I
UPT	urine protein test
UOBT	urine occult blood test
WBC	white blood cell

frontiers | Frontiers in Microbiology

TYPE Review
PUBLISHED 13 September 2023
DOI 10.3389/fmicb.2023.1239079

Check for updates

OPEN ACCESS

EDITED BY
Lei Deng,
Massachusetts General Hospital and Harvard Medical School, United States

REVIEWED BY
Wakako Furuyama,
Nagasaki University, Japan
Md. Aminul Islam,
President Abdul Hamid Medical College, Bangladesh

*CORRESPONDENCE
Shriyansh Srivastava
✉ shriyanshsrivastav@gmail.com
Joshuan J. Barboza
✉ jbarbozame@ucvvirtual.edu.pe

RECEIVED 12 June 2023
ACCEPTED 25 August 2023
PUBLISHED 13 September 2023

CITATION
Srivastava S, Sharma D, Kumar S, Sharma A, Rijal R, Asija A, Adhikari S, Rustagi S, Sah S, Al-qaim ZH, Bashyal P, Mohanty A, Barboza JJ, Rodriguez-Morales AJ and Sah R (2023) Emergence of Marburg virus: a global perspective on fatal outbreaks and clinical challenges.
Front. Microbiol. 14:1239079.
doi: 10.3389/fmicb.2023.1239079

COPYRIGHT
© 2023 Srivastava, Sharma, Kumar, Sharma, Rijal, Asija, Adhikari, Rustagi, Sah, Al-qaim, Bashyal, Mohanty, Barboza, Rodriguez-Morales and Sah. This is an open-access article distributed under the terms of the Creative Commons Attribution License (CC BY). The use, distribution or reproduction in other forums is permitted, provided the original author(s) and the copyright owner(s) are credited and that the original publication in this journal is cited, in accordance with accepted academic practice. No use, distribution or reproduction is permitted which does not comply with these terms.

Emergence of Marburg virus: a global perspective on fatal outbreaks and clinical challenges

Shriyansh Srivastava[1,2]*, Deepika Sharma[2], Sachin Kumar[1], Aditya Sharma[2], Rishikesh Rijal[3], Ankush Asija[4], Suraj Adhikari[5], Sarvesh Rustagi[6], Sanjit Sah[7,8], Zahraa Haleem Al-qaim[9], Prashant Bashyal[10], Aroop Mohanty[11], Joshuan J. Barboza[12]*, Alfonso J. Rodriguez-Morales[13,14] and Ranjit Sah[15,16,17]

[1]Department of Pharmacology, Delhi Pharmaceutical Sciences and Research University (DPSRU), New Delhi, India, [2]Department of Pharmacy, School of Medical and Allied Sciences, Galgotias University, Greater Noida, India, [3]Division of Infectious Diseases, University of Louisville, Louisville, KY, United States, [4]WVU United Hospital Center, Bridgeport, WV, United States, [5]Manipal College of Medical Sciences, Pokhara, Nepal, [6]School of Applied and Life Sciences, Uttaranchal University, Dehradun, Uttarakhand, India, [7]Global Consortium for Public Health and Research, Datta Meghe Institute of Higher Education and Research, Jawaharlal Nehru Medical College, Wardha, India, [8]Department of Anesthesia Techniques, SR Sanjeevani Hospital, Siraha, Nepal, [9]Al-Mustaqbal University College, Hilla, Iraq, [10]Lumbini Medical College and Teaching Hospital, Kathmandu University Parvas, Palpa, Nepal, [11]Department of Clinical Microbiology, All India Institute of Medical Sciences, Gorakhpur, Uttar Pradesh, India, [12]Escuela de Medicina, Universidad César Vallejo, Trujillo, Peru, [13]Master Program on Clinical Epidemiology and Biostatistics, Universidad Científica del Sur, Lima, Peru, [14]Gilbert and Rose-Marie Chagoury School of Medicine, Lebanese American University, Beirut, Lebanon, [15]Department of Microbiology, Tribhuvan University Teaching Spital, Institute of Medicine, Kathmandu, Nepal, [16]Department of Microbiology, Dr. D. Y. Patil Medical College, Hospital and Research Centre, Dr. D. Y. Patil Vidyapeeth, Pune, Maharashtra, India, [17]Department of Public Health Dentistry, Dr. D. Y. Patil Dental College and Hospital, Dr. D. Y. Patil Vidyapeeth, Pune, Maharashtra, India

The Marburg virus (MV), identified in 1967, has caused deadly outbreaks worldwide, the mortality rate of Marburg virus disease (MVD) varies depending on the outbreak and virus strain, but the average case fatality rate is around 50%. However, case fatality rates have varied from 24 to 88% in past outbreaks depending on virus strain and case management. Designated a priority pathogen by the National Institute of Allergy and Infectious Diseases (NIAID), MV induces hemorrhagic fever, organ failure, and coagulation issues in both humans and non-human primates. This review presents an extensive exploration of MVD outbreak evolution, virus structure, and genome, as well as the sources and transmission routes of MV, including human-to-human spread and involvement of natural hosts such as the Egyptian fruit bat (*Rousettus aegyptiacus*) and other *Chiroptera species*. The disease progression involves early viral replication impacting immune cells like monocytes, macrophages, and dendritic cells, followed by damage to the spleen, liver, and secondary lymphoid organs. Subsequent spread occurs to hepatocytes, endothelial cells, fibroblasts, and epithelial cells. MV can evade host immune response by inhibiting interferon type I (IFN-1) synthesis. This comprehensive investigation aims to enhance understanding of pathophysiology, cellular tropism, and injury sites in the host, aiding insights into MVD causes. Clinical data and treatments are discussed, albeit current methods to halt MVD outbreaks remain elusive. By elucidating MV infection's history and mechanisms, this review seeks to advance MV disease treatment, drug development, and vaccine creation. The World Health Organization (WHO) considers MV a high-concern filovirus causing severe and fatal hemorrhagic fever, with a death rate ranging from 24 to 88%. The virus often spreads through contact with infected individuals, originating from animals. Visitors to bat habitats like caves or mines face higher risk. We tailored this search strategy for four databases: Scopus, Web

of Science, Google Scholar, and PubMed. we primarily utilized search terms such as "Marburg virus," "Epidemiology," "Vaccine," "Outbreak," and "Transmission." To enhance comprehension of the virus and associated disease, this summary offers a comprehensive overview of MV outbreaks, pathophysiology, and management strategies. Continued research and learning hold promise for preventing and controlling future MVD outbreaks.

KEYWORDS

filovirus, pathogenesis, Marburg virus, epidemic, vaccine, treatment

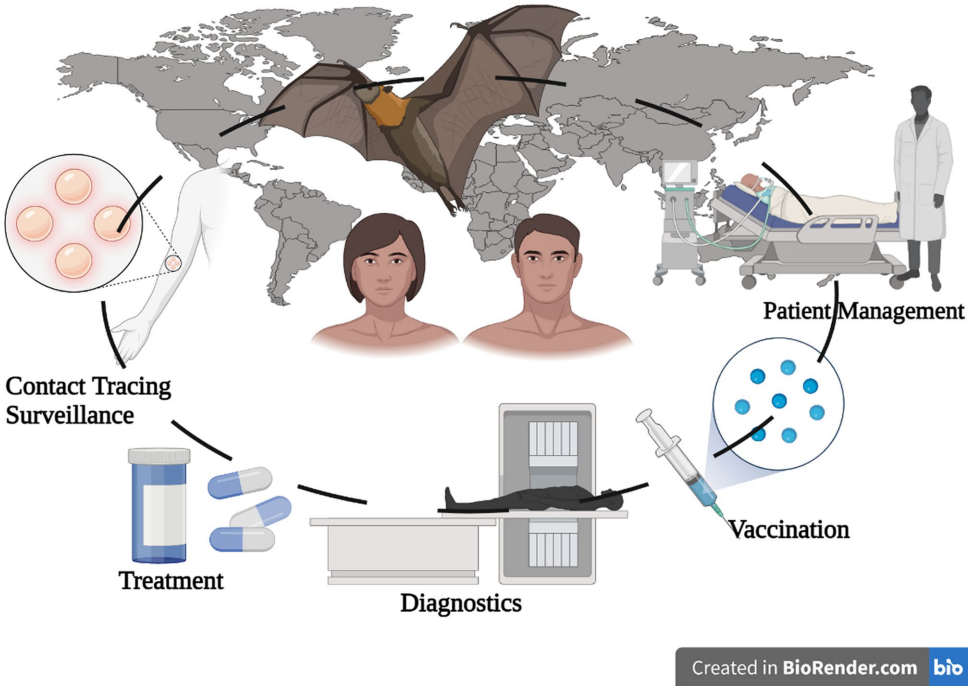

GRAPHICAL ABSTRACT

1. Introduction

The Marburg virus (MV) has emerged as a significant global threat, instigating multiple fatal outbreaks with a considerable mortality rate since its discovery and characterization in 1967. Its initial appearance spanned regions including Marburg, Frankfurt (Germany), Yugoslavia (now Serbia), and Belgrade, with Africa primarily bearing the brunt of its impact (Brauburger et al., 2012). According to the National Institute of Allergy and Infectious Diseases, the main cause of MVD is Marburg virus (Bente et al., 2009). The virus's nomenclature stems from the city where it is devastating effects were most pronounced, resulting in seven deaths among 31 early patients (Brauburger et al., 2012). Investigation subsequently unveiled the virus's origin in imported Ugandan green African monkeys (Gear et al., 1975). Contrary to the belief that MV posed a lesser threat, significant outbreaks in the Democratic Republic of the Congo (DRC) from 1998 to 2000 and in Angola from 2004 to 2005 demonstrated a fatality rate of 83% and 90%, respectively, dispelling this notion (Bausch et al., 2006; Qiu et al., 2014). Different variants were connected to the outbreak in the DRC, but just one version spread from person to person in Angola (Bertherat et al., 1999; Bausch et al., 2006). By 2008, reported MV cases surged to 452, with 368 confirmed deaths, raising concerns of underreporting (Brauburger et al., 2012). Despite receiving less media attention than its *Filoviridae* counterparts, MV's elevated fatality rates underscore its significance. Recent cases in Guinea, Ghana, and the ongoing Equatorial Guinea outbreak accentuate the necessity for continuous surveillance and containment. The latter reported a swift succession of deaths, and Tanzania also reported fatalities attributed to the virus, highlighting the ongoing threat

Abbreviations: CIRMF, Centre Interdisciplinaire de Recherches Médicales de Franceville; DRC, Democratic Republic of Congo; EBOV, Ebola virus; EUNID, European Network for Infectious Diseases; GP, Glycosylated protein; HLIU, High-level isolation unit; HPV, Human papillomavirus; IFN, Interferons; L, Large protein; MV, Marburg virus; MVD, Marburg virus disease; NHPs, Non-human primates; NIAID, The National Institute of Allergy and Infectious Diseases; PPE, Personal protective equipment; RT-PCR, Real-time polymerase chain reaction; VSV, Vesicular stomatitis virus; WHO, World Health Organization.

(Manohar et al., 2023). MVD's impact spans hemorrhagic fever and organ dysfunction in both humans and non-human primates, affecting the liver, spleen, brain, kidneys, and causing coagulation anomalies (Mehedi et al., 2011; van Paassen et al., 2012). As a member of the Marburg virus genus within the *Filoviridae* family and *Mononegavirales* order, MV comprises a distinct species (Bukreyev et al., 2014). Its zoonotic connection to the Egyptian fruit bat (*Rousettus aegyptiacus*) and human-to-human transmission parallel other Ebola viruses, such as Sudan virus, *Bundibugyo virus*, and EBOV. Ongoing research has elucidated MV's natural sources, including *Hipposideros caffer*, in tandem with *Rousettus aegyptiacus* (Towner et al., 2009). With an average incubation period of 5 to 10 days, ranging from 3 to 21 days, the virus infiltrates immune cells like monocytes, macrophages, and dendritic cells via compromised skin or mucosal surfaces. It initiates replication in the spleen, liver, and secondary lymphoid organs before propagating to hepatocytes, endothelial cells, fibroblasts, and epithelial cells. Additionally, it thwarts interferon type I (IFN-1) production (Yu et al., 2021). This review explores the evolutionary course of MVD outbreaks, succinctly delineating the virus's structure and genome, elucidating MV's origins, and detailing its diverse transmission modes among humans and non-human sources. We comprehensively examine MVD's genesis through scrutinizing pathophysiology, cellular tropism, immune evasion, and critical host injury sites. Additionally, this overview encompasses current clinical data and treatments, underscoring the vital need for robust research to foster effective drugs and vaccines. By deepening comprehension of the virus's historical progression and infection mechanisms, this review strengthens defenses against MV disease, driving the innovation of therapeutic agents and vaccines, thus supporting future researchers in countering this enduring health threat.

2. Mutational analysis and genome composition

The Marburg virus (MV) exhibits an enveloped and pleomorphic structure, displaying uniform diameter but variable length filamentous, non-segmented, rod-like, cobra-like, circular/annular, and branched particles (Chakraborty et al., 2022; Islam et al., 2023a). Its viral genome encompasses seven open reading frames (ORFs), namely nucleoprotein (NP), virion protein 35 (VP35), VP40, VP30, VP24, glycoprotein (GP), and large viral polymerase, all characterized as single-stranded negative-sense RNA (-ssRNA; Zhao et al., 2022). The non-coding regions of these seven genes contain cis-acting elements implicated in DNA replication, transcription, and packaging (Feldmann et al., 1992; Sanchez et al., 1993). The 3′ and 5′ ends of these genes possess unusually long non-coding nucleotide sequences and highly conserved transcription start and stop signals (Feldmann et al., 1992; Sanchez et al., 1993). Intergenic regions separate all MV genes except two, ranging from 4 to 97 nucleotides in length, and the transcription start and stop signals of the VP24 and VP30 genes share an overlapping sequence of five nucleotides (UAAUU). The nucleocapsid complex, comprising structural proteins NP, VP35, VP30, and L, envelops the MV genome (Becker et al., 1998). VP35, acting as a polymerase cofactor, and L, functioning as an RNA-dependent RNA polymerase, are essential for replication and transcription of viral genomes (Mühlberger et al., 1999). The host-derived membrane layer of MV is regularly spiked, where highly glycosylated protein (GP) plays a key role in binding to receptive host cells (Feldmann et al., 1991). VP40, responsible for budding and binding to the matrix and nucleocapsid, constitutes the inner matrix of a virion (Kolesnikova et al., 2004; Swenson et al., 2004). The interaction of the protein VP24 with the membrane NP and other cell membranes is vital for the release of virion progeny. Table 1 provides an overview of the characteristics and functions of the proteins in MV (Bamberg et al., 2005). Phylogenetic analysis of Marburg virus sequences has been conducted to ascertain sequence cohesion and identify splits between sequences of particular interest and well-known sequences that exhibit unexpectedly deep divergence (Peterson and Holder, 2012). From cDNA clones made from genomic RNA and mRNA, the first 3,000 nucleotides of the Marburg virus genome were identified (Sanchez et al., 1992). There is up to 21% nucleotide diversity among previously characterized East African strains of the Marburg virus, according to partial Marburg virus RNA sequence study (Towner et al., 2006). Serial passages of Marburg virus resulted in a single mutation in the region encoding the glycoprotein (GP; Alfson et al., 2018). To clarify the relationship between various Marburg virus strains, phylogenetic analysis of full-length or partial genomes of Marburg viruses obtained from people or bats has been carried out (Towner et al., 2009). Phylogenetic analysis showed the 2021 Guinean Marburg virus' relationship to strains from the 2004–2005 Marburg virus outbreak in Angola, which are related to Marburg virus sequences obtained from bats in Sierra Leone (2017–2018). The viral genome sequence of the 2021 Guinean Marburg virus was recovered to 99.3% (Magassouba, 2021). Sequential mouse passaging and cell-culture adaption during deep sequencing of the Marburg virus genome have shown significant changes over time (Wei et al., 2017). An analysis was performed on the sequencing data to identify sites in viral mRNAs (Shabman et al., 2014). Structural and functional studies on the Marburg virus GP2 fusion loop have also been conducted (Liu et al., 2015). Marburg virus has been subjected to mutational and phylogenetic analysis, and the genome has been sequenced to identify changes over time shown in Figure 1 (Mühlberger, 2007).

3. Epidemiology

3.1. MVD outbreak in 1967

In the European outbreak, most patients between 2 and 7 days after the onset of symptoms had non-itchy rash. The diseases were linked to three laboratories in different cities that had each received an infected cargo of African green monkeys. The first MVD outbreak, which was documented in 1967 and was brought on by laboratory workers in Germany and Serbia handling green African monkeys called grivets (*Chlorocebusaethiops*), was brought on by these imports. According to grivets' reports, staff employees were primarily exposed to these sick wild animals' meat and organs, which caused them to contract MV (Mehedi et al., 2011; Languon and Quaye, 2019). Seven patients died as a result of the sickness, which affected a total of 31 patients and was caused by 25 primary and 6 secondary infections (Deb et al., 2023).

TABLE 1 Marburg virus: genes, proteins, characteristics, and functions.

S. no	Gene (sequence)	Protein (abbreviation)	Description	Amino acid	Functions	Gene length	References
1.	NP	Nucleoprotein (NP)	Binds to VP35 protein, VP40, VP30, and VP24, and is a component of the RNP complex. It also undergoes phosphorylation and homo-oligomerizes to form a helical polymer. Additionally, it is the second-most prevalent protein found in virions.	695	Creation of NC and cellular inclusion body; Encapsidation of RNA genome as well as antigenome; Replication and transcription; Budding	2,796/2,088	DiCarlo et al. (2011), Brauburger et al. (2015), and Liu et al. (2017)
2.	VP35	Viral protein 35	RNP complex components that bind to dsRNA, NP, and L and homo-oligomerize. They are also weakly phosphorylated.	329	Formation of NC; RdRp cofactor; Replicase transcriptase cofactor; IFN antagonist	1,557/990	Bale et al. (2012), Brauburger et al. (2015), Edwards et al. (2016), and Bruhn et al. (2017)
3.	VP40	Viral Protein 40	It homo-oligomerizes to form dimers, circular hexamers, and octamers, binds ssRNA and VP35, and is one of the most common proteins in virions and infected cells.	303	Matrix component: Negative regulator of transcription and replication; Budding and host adaption; regulation of the morphogenesis of the virion and egress; hinders JAK–STAT pathway	1,405/912	Kolesnikova et al. (2012), Brauburger et al. (2015), Koehler et al. (2018), and Amiar et al. (2021)
4.	GP	Glycoprotein (GP1,2)	Uses GP_1 and GP_2 subunits to create heterodimers; the mature protein is found as a trimer of $GP_{1,2}$ heterodimers; can insert into membranes; Acylated, substantially N- and O-glycosylated and phosphorylated. Class I fusion and type I transmembrane protein, along with ADAM17, convert $GP_{1,2}$ into soluble $GP_{1,2.}$	681	Attachment of virions to susceptible cells using cellular attachment factor: determination of cell and tissue tropism; Receptor binding; induction of virus-cell membrane; Tetherin antagonist;	2,846/2,046	Carette et al. (2011) and Brauburger et al. (2015)
5.	VP30	Viral protein 30 activator	RNP complex components with high phosphorylation, ssRNA, NP, and L binding, as well as a zinc binding domain.	281	Formation of NC; Initiation, reinitiation and antitermination and enhancement of transcription	1,249/846	Enterlein et al. (2006), Wenigenrath et al. (2010), and Wan et al. (2017)
6.	VP24	Viral protein 24	Components of the RNP complex; homo-tetramerizes; connected with the hydrophobic membrane.	253	Formation and maturation of NC; Negative regulation of transcription; regulation of replication; virion morphogenesis regulatory function	1,287/762	Edwards et al. (2014), Page et al. (2014), Zhang et al. (2014), Brauburger et al. (2015), and Wan et al. (2017)
7.	L	Large protein (L)	RNP complex components that bind to VP35, VP30, genomic, and antigenomic RNA, as well as mRNA capping enzymes, and homodimerize.	2,331	Catalytic domain of RdRp; Replication of genome; Transcription of mRNA	7,745/69,96	Koehler et al. (2016) and Kirchdoerfer et al. (2017)

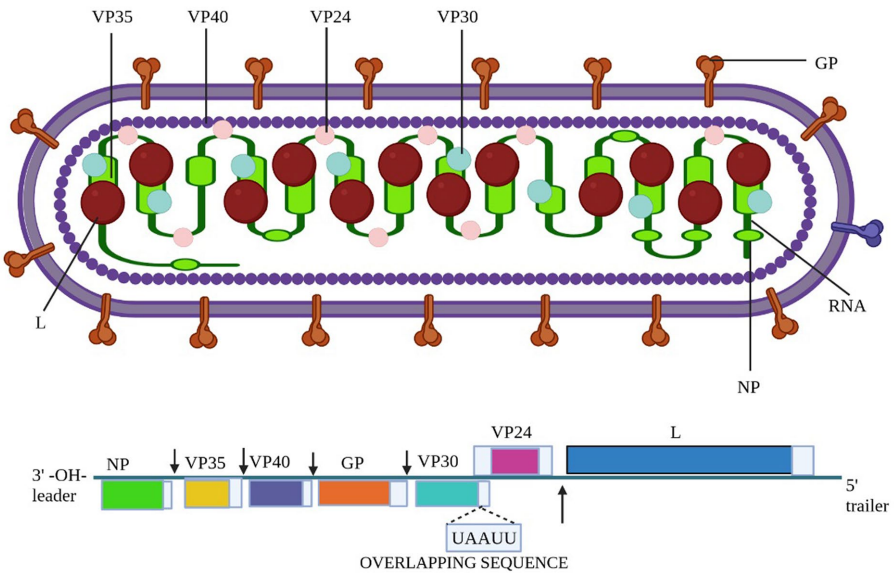

FIGURE 1
The structure of the Marburg virus and the organization of its genome are depicted in the figure. The upper portion of the figure shows the structure of the virus and identifies the structural proteins. The genomic organization of the seven-gene Marburg virus strain is depicted in the lower section of the figure, which has been crudely scaled. Light blue boxes indicate non-coding regions, whereas colored boxes depict the coding sections of genes. Except for the overlap between VP24 and VP30, which is depicted as a black triangle, the genes are separated by intergenic regions, as shown by the black arrows. At the ends, the 3′ and 5′ trailer sequences are also displayed. Bio render software was used to create this figure (Abir et al., 2022).

3.2. MVD outbreak in 1975

In 1975, the MVD outbreak marked the second recorded instance of the disease and the initial occurrence in Africa. It took place in Johannesburg, South Africa, involving three cases and resulting in one fatality. The outbreak originated from a 20-year-old Australian man who had journeyed to Zimbabwe (then Rhodesia) and explored several bat-inhabited caves. After his return to Johannesburg, he exhibited symptoms such as fever, headache, myalgia, and vomiting, ultimately succumbing on 5 February 1975. His travel companion and a nurse who cared for him were secondary cases, both of whom survived through supportive treatment. Swift case isolation and contact tracing successfully contained the outbreak. While the source of infection remained unconfirmed, suspicion centered on the index case acquiring the virus through exposure to bats or their droppings within the caves (Gear et al., 1975; Abir et al., 2022).

3.3. MVD outbreak in 1980

In 1980, Kenya experienced the third documented outbreak of Marburg-virus disease. The initial patient contracted the infection in western Kenya, leading to the subsequent infection of a doctor in Nairobi who had close contact with the patient, ultimately resulting in severe haematemesis. However, no additional instances of transmission within medical settings were observed. Surveillance efforts in western Kenya did not uncover evidence of Marburg-virus disease, but they did indicate the potential existence of Ebola hemorrhagic fever (Smith et al., 1982).

3.4. MVD outbreak in 1987

In 1987, a single case of MVD outbreak emerged in Kenya, centering around a 15-year-old Danish boy who fell victim to the infection and subsequently passed away. The boy had encountered the virus within a cave inhabited by Egyptian fruit bats. This marked the inaugural documented instance of Ravn virus transmission, a near kin of the Marburg virus responsible for MVD. Effective containment measures were enacted through patient isolation and contact tracing, successfully preventing the emergence of secondary cases (Johnson et al., 1996).

3.5. MVD outbreak in 1998 and 2000

In both 1998 and 2000, there was a single MVD outbreak situated in Durba, Democratic Republic of the Congo (DRC). The affected individuals were gold miners who toiled within a mine known to be home to Egyptian fruit bats, the virus's natural reservoir. This outbreak encompassed a total of 154 cases and tragically led to 128 fatalities, resulting in an 83% case fatality rate. Remarkably, this marked the initial occurrence of a substantial MVD outbreak and the primary instance of a combined outbreak involving Marburg virus and Ravn virus. These two closely related viruses both contribute to causing MVD (Colebunders et al., 2007; Towner et al., 2009).

3.6. MVD outbreak in 2004 and 2005

A second significant MV outbreak in the Uige region of Angola began in October 2004 and lasted until July 2005. The root cause of

the epidemic, which later spread to other provinces, was discovered to be the death of a hospital employee in Uige. This epidemic has the highest number of illnesses and deaths linked to a single outbreak to date, with 252 cases of infection and 227 fatalities (a 90% mortality rate). An epidemic that occurred in Uganda in 2007 only resulted in four confirmed cases. The patients were Ibanda district workers at the Kitaka mine. The two workers contracted the disease after sharing a tent camp with the index case in the Kashoya-Kitomi Central Forest Reserve close to the mine. The fourth patient was working at the mine when the epidemic started, without any personal protective equipment (PPE). The mining adit was surrounded by bats, and the only personal protective equipment (PPE) accessible was a pair of gloves; masks, respirators, or goggles were not. The main source of infection was direct contact with bats or bat excretions. During this epidemic, MV was isolated from *Rousettus aegyptiacus*, and the first definite filovirus reservoir was discovered by sampling bats (Languon and Quaye, 2019).

3.7. MVD outbreak in 2012 and 2017

On 29 November 2012, the Ugandan Ministry of Health declared MV infection in Uganda. The Ugandan districts of Kabale, Ibanda, Mbarara, and Kampala have recorded about 15 fatalities and 8 probable cases (Deb et al., 2023). This outbreak in the Ibanda district occurred concurrently with the 2007 MV disease outbreak in the Kitaka mining region. As a result, *Rousettus aegyptiacus* bats were once more connected to the outbreak in 2012. It is interesting to note that the epidemic hit the *Rousettus aegyptiacus* bat population during the second half of the yearly viral cycle (Languon and Quaye, 2019). Additionally, the genome sequences of this MV strain and the MV strain that had previously been identified in Egyptian fruit bats were similar. A health worker contracted the disease and succumbed to it in Kampala, Uganda in 2014, where an epidemic also occurred (Nyakarahuka et al., 2017). In 2017, a new MV outbreak occurred in the Kween region of Uganda. The four family members who became MV-infected during this outbreak only had one survivor (Nyakarahuka et al., 2019). Nevertheless, extensive studies are still being conducted because the clinical evidence for this outbreak is still insufficient.

3.8. MVD outbreak in 2021

Last but not least, Guinea saw its most recent outbreak in August 2021, which was eventually contained in September 2021. One man became ill and died during this time, but the strain is still unclear (Aborode et al., 2022; Makenov et al., 2023; WHO, 2023a).

3.9. MVD outbreak in 2023

Between 7 January and 7 February 2023, two villages in the Nsock Nsomo district of the Ro Muni area in the eastern Kie-Ntem province experienced at least eight fatalities. The affected individuals presented symptoms such as fever, weakness, vomiting, and bloody diarrhea. In two cases, skin lesions and otorrhagia were also observed. On 9 February 2023, health authorities collected blood samples from eight contacts and submitted them to the Centre Interdisciplinary de Recherches Médicales de Franceville (CIRMF) in Gabon. However, real-time polymerase chain reaction (RT-PCR) testing at CIRMF yielded negative results for the presence of Marburg and Ebola viruses (WHO, 2023a). On 12 February 2023, additional blood samples were obtained from different contacts and sent to the Institute Pasteur in Dakar, Senegal. RT-PCR testing confirmed one of these samples to be positive for the Marburg virus. The patient associated with this confirmed case displayed symptoms of fever, bloodless vomiting, bloody diarrhea, and convulsions, ultimately succumbing to the infection on 10 February 2023, at Ebebiyin District Hospital. This case was linked to four other deceased cases originating from one of the villages in the Nsoc-Nsomo District. As of 21 February 2023, a total of nine cases have been reported, consisting of one confirmed, four probable, and four suspected cases, all of which resulted in fatalities. Health workers have not been affected, and 34 contacts remain under surveillance. After the initial outbreak, on 13 March 2023, two individuals from Kié-Ntem province, and on 15 March 2023, one person from Litoral province, tested positive for the Marburg virus through RT-PCR. On 18 and 20 March, three more laboratory-confirmed cases were reported from Litoral province, and on 20 March, two additional cases were identified in Centre Sur province. The extensive geographical spread of the infections and the uncertain epidemiological situation in Centre Sur Province raise concerns that the virus may be spreading undetected within the community (WHO, 2023a). Table 2 represents different outbreak of Marburg (Figure 2).

3.10. Socioeconomic impact of MVD outbreaks

The socioeconomic impact of MVD outbreaks can significantly affect countries with weaker economies, leading to inadequate containment and management (Manohar et al., 2023). Epidemics can interact at the host population, influencing one another's severity and trajectories when they co-occur (Reuben and Abunike, 2023). MVD outbreaks can result in fatalities and socioeconomic consequences, including loss of tourism (Nyakarahuka et al., 2017). Comprehensive research of MVD is necessary given its link to MV infection and the disease's high fatality rate of up to 90% (Abir et al., 2022). The Filoviridae family, including MV, has caused significant loss of human and animal lives (Languon and Quaye, 2021). Past outbreaks have exhibited varying case fatality rates, ranging from 24% to 88%, contingent upon virus strain and case management (WHO, 2021a). According to the World Health Organization (WHO), MVD is a highly contagious disease that can cause hemorrhagic fever and has a death rate of up to 88%. The WHO advises treatment of symptoms, oral or intravenous rehydration, and supportive care to increase survival. Although continuing analyses of prospective remedies, such as blood products, immunological therapies, and pharmacological therapies, are being conducted, there is currently no known cure for MVD (WHO, 2023b). Case management, surveillance, contact tracing, a well-functioning laboratory service, safe and respectable burials, and social mobilization are only a few of the actions that are needed to suppress outbreaks. Community involvement is also essential for effective epidemic control (WHO, 2021a).

TABLE 2 Outbreaks of Marburg virus (MV).

MVD outbreak	Location	Transmission	Number of deaths	Number of cases	Case fatality rate	Mortality rate	References
1967	Germany, Serbia	Contact with grivets	7	31	22%	22.6%	Mehedi et al. (2011), Languon and Quaye (2019), and Deb et al. (2023)
1975	South Africa	Person-to-person	3	3	100%	100.0%	Gear et al. (1975) and Abir et al. (2022)
1980	Kenya	Person-to-person	1	1	100%	100.0%	Smith et al. (1982)
1987	Kenya	Unknown	1	1	100%	100.0%	Johnson et al. (1996)
1998 and 2000	Democratic Republic of the Congo	Unknown	128	154	83%	83.1%	Towner et al. (2009) and Colebunders et al. (2007)
2004–2005	Angola	Person-to-person	227	252	90%	90.1%	Languon and Quaye (2019)
2012	Uganda	Contact with *Rousettus aegyptiacus* bats	15	23	60%	65.2%	Deb et al. (2023)
2017	Uganda	Unknown	3	4	75%	75.0%	Languon and Quaye (2019) and Nyakarahuka et al. (2019)
2021	Guinea	Unknown	1	1	100%	100.0%	Nyakarahuka et al. (2019) and WHO (2023a)
2023	Equatorial Guinea, Tanzania,	Unknown	27	29	93%	86.0%	WHO (2023a)

4. Source and transmission of Marburg virus

The fruit bat species *Rousettus aegyptiacus* is the most important natural source of MV infection. In addition, some *Chiroptera and Hipposideros caffer* may act as infectious agents. There are several ways in which MV strains can be transmitted from bat to bat. Recent research found MV in rectal, oral, and urine samples from infected bats as well as in blood and oral samples from bats that had come into contact with humans. According to this research, MV is horizontally transmitted from infected bats to bat contacts (Schuh et al., 2017). The findings of the previous study showed that MV was present in the tissues of the lungs, intestines, kidneys, bladder, salivary glands, and female reproductive tract of immunized bats, supporting the hypothesis that MV transmission might occur (Amman et al., 2012) both vertically and horizontally in reservoirs. It has also been suggested that bats could spread the illness to one another by bites (Amman et al., 2015), sexual contact (Amman et al., 2012), or hematophagous arthropods (Schuh et al., 2017). Direct contact (injured skin or mucous membranes) with the blood and other bodily fluids of infected people (urine, saliva, feces, vomit, breast milk, amniotic fluid, and semen) or indirect contact with contaminated surfaces and materials, such as contaminated clothing, bedding, and medical equipment, are the two main methods of interpersonal transmission after infection. Infection may happen if sick people are buried (Schwartz, 2019). Infected animals, particularly bushmeat (such as monkeys, chimpanzees, forest antelopes, and bats), whether alive or dead, can also spread the disease to humans (Figure 3; WHO, 2021a). Bushmeat consumption has been linked to Ebola virus (EBOV) outbreaks (Malik et al., 2023). Because numerous bushmeat species, including chimpanzees and forest antelope, are vulnerable to virus multiplication and consumption following infection (Heeney, 2015), they are regarded as intermediate hosts. There is growing concern about the persistence of filovirus in the testis as a potential route of transmission. Experimental trials have identified persistent MV infection of the immunoprivileged testicular tubules in male monkeys (Coffin et al., 2018). During the 1967 MV outbreak, the first possible case of sexual transmission was found. Two months after the recovery of a male patient, symptoms appeared in his wife, which were confirmed by the detection of MV antigen in his semen (Feldmann, 2018). Simultaneous testing of nine other convalescents for MV did not detect virus or viral antigen (Slenczka, 2017). In pregnant women, filovirus infection is usually more severe than in nonpregnant women, which may be due to decreased immune function or placental involvement (Brainard et al., 2016). Based on case reports, viral titers have been found in placental tissue, suggesting that hematogenous transplacental transmission is the most typical route of fetal infection (Bebell and Riley, 2015). Despite the high rates of pregnancy mortality, there is no proof that pregnant women are more prone to contracting filovirus than other people (Jamieson et al., 2014). Pregnant women who have MVD have an increased risk of stillbirths and spontaneous abortions (Schwartz, 2019). Little information is available on the effects of MVD infection in infants. There have been reports of several MVD clusters in newborns, some of whom had very mild symptoms (Borchert et al., 2002). MV can be present in the blood, organs, and tissues of sick or recovering individuals, suggesting that the virus can be transmitted through transfusion and transplantation. Filoviruses can survive for a very long time in liquid or dried materials (Piercy et al., 2010). They are inactivated by gamma irradiation, heating to 60°C for 60–75 min, or boiling for 5 min and are sensitive to fatty

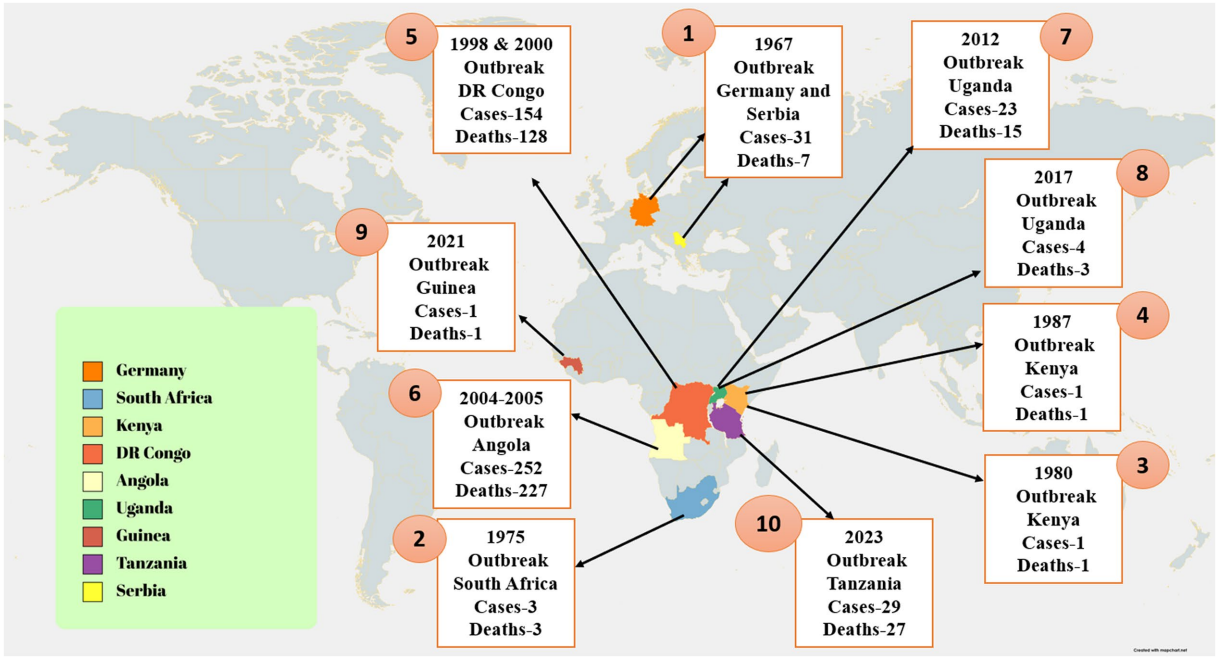

FIGURE 2
The image shows the distribution of confirmed Marburg virus disease (MVD) cases and associated fatalities. The image illustrates that the MVD outbreak in Tanzania was confined to a distinct region, with reported cases concentrated in the Kigoma region. Additionally, the image underscores the ongoing MVD outbreak in Equatorial Guinea, characterized by a broader geographical spread of cases. Moreover, the image also denotes further instances of MVD outbreaks across different African regions (Abir et al., 2022).

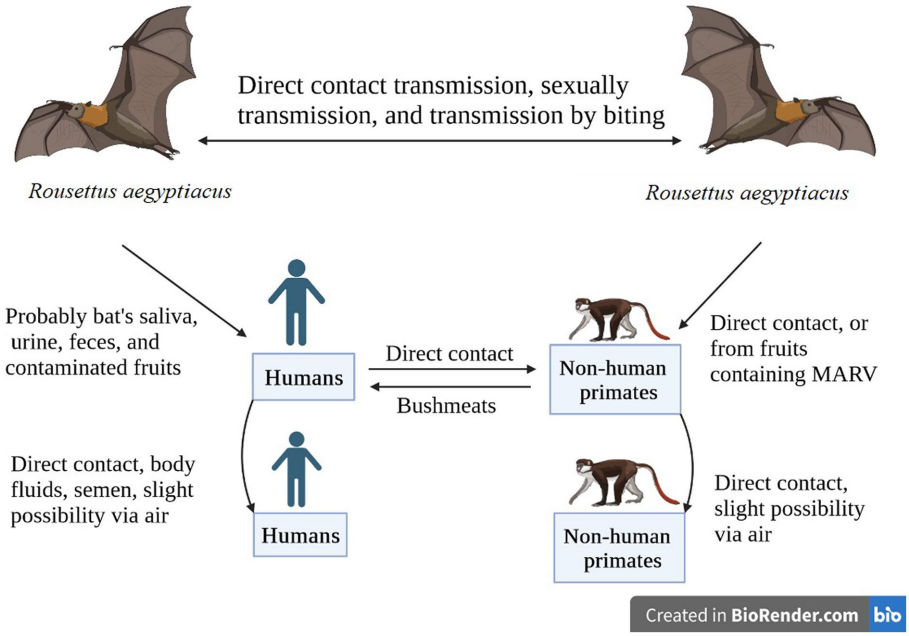

FIGURE 3
African fruit bats serve as reservoirs for the Marburg virus, which is conveyed by direct contact, sexual contact, or biting. Humans and non-human primates can contract the virus through viral-contaminated fruit consumption or direct contact with the reservoir hosts. Disease transmission can also occur through direct contact between NHPs and humans, or from NHPs to humans through bushmeat consumption. The image was created using Bio render software.

solvents, sodium hypochlorite, and other disinfectants (Kuhn, 2008; Feldmann et al., 2019).

5. Clinical signs and disease progression

Marburg virus disease (MVD) has an incubation period of two to 21 days. According to the World Health Organization (WHO), high fever, severe malaise, and headache are some of the sudden symptoms associated with Marburg virus infection. Patients frequently complain of muscle pain and pains at the same time. Patients may experience severe watery diarrhea, cramping in the stomach, nausea, and vomiting on the third day. Up to a week may pass during the phase of diarrhea. Patients frequently exhibit a characteristic appearance during this stage that is characterized by sunken eyes, indifferent facial expressions, and extreme sluggishness. Within 2 to 7 days of the onset of symptoms, a non-itchy rash commonly develops (Elsheikh et al., 2023). Hemorrhagic signs often appear 5 to 7 days after the initial episode, with fatal cases showing several sites of hemorrhage. Bleeding from the gums, nasal passages, and vagina usually accompany fresh blood in vomitus and feces. The problem of spontaneous bleeding at venipuncture sites is particularly difficult. High fevers characterize the illness's severe stage. Involvement with the central nervous system might result in confusion, irritation, and violence. In the later stages of the illness, occasional observations of orchitis, which is defined by inflammation of one or both testicles, have been made (around day 15). Most frequently, death happens 8 to 9 days after the onset, generally after a serious bout of blood loss and a subsequent shock (Elsheikh et al., 2023). Direct contact with the blood, secretions, organs, or other bodily fluids of infected people, as well as with surfaces and objects contaminated with these fluids, can result in human-to-human transmission of the Marburg virus. This contact can happen through cuts, scrapes, or other breaks in the skin or mucous membranes. Exposure to fruit bat species can also cause transmission (Elsheikh et al., 2023). An alternative classification of MV clinical features includes a "Generalization Phase," which is characterized by flu-like symptoms and rash, an "Early Organ Phase," which involves manifestations in specific organs, like encephalitis or hemorrhages, and a "Late Organ/Convalescence Phase," which is characterized by multiorgan failure, shock, coma, and either death or recovery. These phases, in that order, correspond to the first 4 days, the next 9 days, and the time after day 13 (Asad et al., 2020).

5.1. Phase 1 (generalization phase)

Flu-like symptoms such a high fever (>40°C), a strong headache, chills, myalgias, and malaise appear during the generalization phase. The fifth day from the start of the disease is when this phase may last, after which there is a rapid attenuation. There have been reports of exhaustion, general malaise, appetite loss, nausea, vomiting, abdominal pain, and excessively watery diarrhea (Feldmann et al., 2013). Pharyngitis, conjunctivitis, enanthem, dysphagia, and dysphagia are additional frequent problems. Before developing into a maculopapular rash, a rash may also show up on the face, feet, and limbs in the middle to late stages of the generalization phase. Other symptoms include lymphadenopathy, leukopenia, and thrombocytopenia (Leroy, 2009).

5.2. Phase 2 (early organ phase)

A prolonged high temperature and other nonspecific symptoms define the early organ phase, which lasts 5 to 13 days following the onset of symptoms. Patients may also experience conjunctival infections, edoema, tiredness, dyspnea, viral exanthems, and aberrant vascular permeability (Klenk et al., 1999). Neurologic symptoms have also been characterized by patients as causing disorientation, encephalitis, irritability, psychosis, and aggressiveness (Borchert and Van der Stuyft, 2008). About 75% of patients experience hemorrhagic symptoms, including hematemesis, ecchymosis, melena, petechiae, bloody diarrhea, visceral hemorrhagic effusions, uncontrolled leaking from venepuncture sites, and mucosal bleeding. Additionally, complaints of bleeding from the nose, gingiva, and vagina have been made. The kidney, liver, and pancreas are a few of the damaged organs at this point in the illness. Additionally, most infected people displayed elevated serum activity (Kuhn, 2008).

5.3. Phase 3 (late organ/recuperative phase)

There are two distinct outcomes in the late stages of MV infection: either the patient enters a protracted period of recovery or the sickness is fatal. Eight to 16 days after the onset of the initial symptoms, death frequently occurs. Typically, multiorgan failure and shock are the two main causes of demise (Martini et al., 1968). The late organ phase begins in nonfatal cases on day 13 and lasts until day 20 and beyond as the illness develops. Acute metabolic anomalies including convulsions and severe dehydration can cause anuria and multiple organ failure in addition to harming the patient's general health. At this time, orchitis has occasionally been identified. The neurological problems are still there currently. Women who are pregnant who have spontaneous.

6. Pathogenesis of MVD

MVD models, and lab animals can all be used to study host pathophysiology and immune responses, as is widely recognized. Currently, NHPs (mainly cynomolgus and rhesus monkeys, African vervet monkeys, and baboons), hamsters, guinea pigs, and mice have been used to establish four MV disease models. NHPs are the "gold standard" among these models because to their great susceptibility to MV infections, which are almost always fatal, and their specific clinical traits that are like those of human infections. Furthermore, it has been demonstrated (Bente et al., 2009), that NHPs can directly transmit the MV virus through close contact. In the Kenyan case from 1987, MV infection was found in the peripheral blood mononuclear cell population of infected macaques using immunohistochemical, electron microscopy, and flow cytometric investigations (Mehedi et al., 2011). These studies also identified viral antigen and virions in both circulating and tissue-associated macrophages. Thus, the idea that the mononuclear phagocytic

system—which consists of macrophages, monocytes, Kupffer cells, and dendritic cells—is the first cell type that MV infection targets—has been put forth (Brauburger et al., 2012). The lymph nodes, liver, and spleen all displayed the most severe necrotic lesions. Reticuloendothelial cells are abundant in the tissues, allowing infected cells to spread and infect more organs. At the organ level, the liver is a key site for MV replication, and the virus preferentially targets lymphoid tissues there (Shifflett and Marzi, 2019). There has been monocytoidal, plasma cellular alteration in the lymphatic tissue. Sites of necrosis also contain basophilic entities, either in the form of inclusion bodies in parenchymal cells or near necrotic cells. The other organs, on the other hand, are all affected by infection and show pathological changes, such as isolated or widespread necrosis without obvious inflammatory responses. Patients on MARD typically experience proteinuria, a symptom of renal failure. Grossly pale, swollen, and exhibiting significant parenchymal deterioration as well as indications of tubular insufficiency, the injured kidneys are also enlarged. Plasma cells and monocytes are prevalent in the mucous membranes of the stomach and intestines. Alveolar macrophages are found in hemorrhagic, obstructed alveoli in the lungs, and since fibrin surrounds them, these alveoli occasionally stain with viral antigen. In addition to necrosis (Shifflett and Marzi, 2019). The crimson pulp of the spleen, the lymph nodes' follicles and medulla, as well as the lymphocyte count, are all noticeably necrosed in humans. Surprisingly, bystander apoptosis promotes lymphocyte loss rather than virus infection of cells. Aspartate aminotransferase, alanine aminotransferase, serum glutamic oxaloacetic transaminase, and serum glutamic pyruvic transaminase rise are liver tests that are suggestive of MV infection because the asialoglycoprotein receptor, a receptor specific to the liver, can boost these enzymes. Given that the liver produces multiple clotting factors, the pathological alterations to the liver are probably a contributing factor to the abnormalities in coagulation seen following MV infection. Severe MARD patients that undergo multiorgan failure do so as a result of the fatal virus's increased mass effect. A decrease in the production of the steroid-synthesizing enzyme, involvement of the adrenal gland, and its failure all increase the risk of hypotension and hypovolemia, which finally result in shock (Figure 4; Mehedi et al., 2011). The symptoms of this toxic hemorrhagic fever, which have nothing to do with jaundice, include hemorrhagic diatheses in the skin and mucous membranes. Most of the histological abnormalities in the skin tissue include endothelial cell necrosis, localized hemorrhage, swelling, and variable degrees of cutaneous edoema. Using immunohistochemical stains, it is possible to identify various antigens in epidermal dendritic cells, endothelial cells, and connective tissue fibroblasts. The sebaceous and sweat gland epithelium also contains these antigens. Viral inclusions and particles can be observed inside endothelial cells and connective tissue using electron microscopy. Furthermore, it has been shown that the structural protein VP40 of the MV successfully aids in evading the host immune reaction to IFN (Martines et al., 2015).

6.1. Impact of MV on human organs

Multiple human organs may be harmed by the Marburg virus disease (MVD), which can result in organ failure and death (Abir et al., 2022). The liver and adrenal glands are the primary targets of the virus. Along with lymphocyte depletion, MVD can also harm lymphatic tissues by causing necrosis of the follicles, the medulla of lymph nodes, and the red pulp of the spleen. It is interesting to note that lymphocytes are not infected by the virus, despite the fact that bystander apoptosis causes a decrease in lymphocyte numbers (Mehedi et al., 2011; Abir et al., 2022). Monocytes and macrophages are two examples of mononuclear phagocytic cells that MV targets. By activating these cells, MV causes secondary targets like endothelial cells to get damaged. The advancement of shock, which is the main cause of death in MVD, is caused by the production of cytokines and pro-inflammatory mediators by activated macrophages and monocytes. The virus can also result in hemorrhagic signs, increased vascular permeability, and aberrant coagulation, all of which are interconnected and lead to the emergence of the classic symptoms of viral hemorrhagic fever (Mehedi et al., 2011; Abir et al., 2022). Orchitis (inflammation of the testicles) has been observed in male survivors, and central nervous system involvement can cause disorientation, irritability, and violence (Mehedi et al., 2011).

6.2. Diagnosis of MV

Due to the fact that the symptoms and signs of MVD overlap with those of endemic illnesses like Ebola and Lassa fever as well as infectious diseases like malaria, dengue fever, and typhoid fever, it can be difficult to diagnose. The fact that MVD symptoms cannot be present at first presentation and that fever may even go away entirely during the disease adds to its complexity (CDC, 2023a). This makes MVD prone to misdiagnosis, particularly outside of outbreak situations. Additionally, some women have presented with abortion as a manifestation of the disease, and pregnant females affected by MVD have shown higher mortality rates (CDC, 2023a; Roy et al., 2023). To properly manage the illness, a prompt and correct laboratory diagnosis is essential. PCR, immunoglobulin M Capture ELISA, and enzyme-linked immunosorbent assay (ELISA) are crucial confirming procedures for the diagnosis of MVD (Marburg Virus Disease). While IgG capture ELISA is used for late confirmation or finding recovered cases, the IgM capture ELISA is particularly helpful for early disease confirmation. Testing in Biosafety Level-IV laboratories is required for MVD diagnosis since handling the virus has a high level of risk (Islam et al., 2023b). To optimize efficiency and cost-effectiveness for the Ghanaian government, it is crucial to utilize advanced technologies and efficient transportation methods (CDC, 2023a; Roy et al., 2023). By implementing these measures, a limited number of laboratories can handle many samples quickly, while ensuring all necessary safety protocols are strictly adhered to. This approach will not only accelerate the diagnosis process but also enhance overall containment and protection against the spread of the virus.

7. Control and prevention of MV

To prevent the disease's spread, the WHO has prescribed several measures to manage the virus (Mittler et al., 2018). When caring for patients with suspected or confirmed Marburg virus infections, healthcare professionals should take extra precautions to prevent infection. This means avoiding contaminated things and surfaces

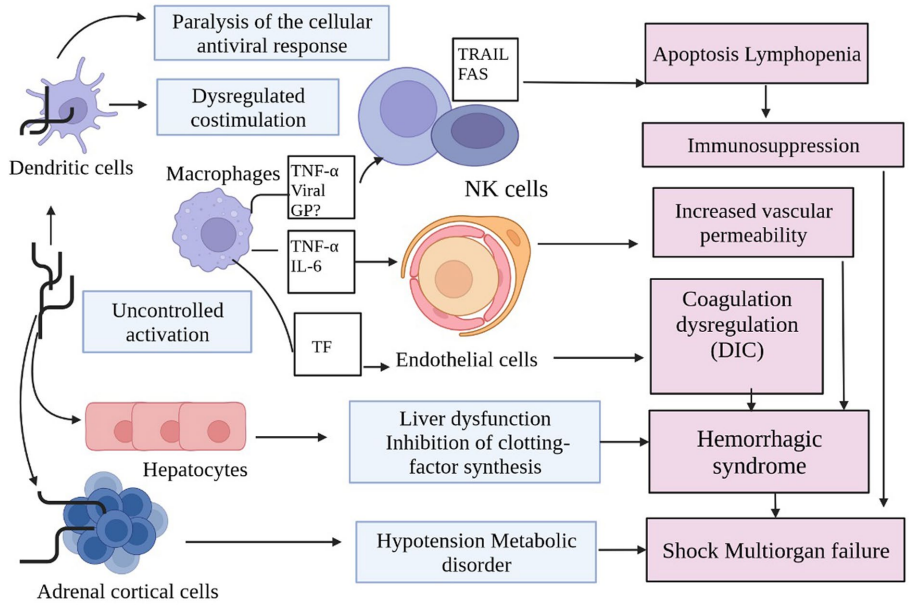

FIGURE 4
The pathogenesis of Marburg virus (MV) hemorrhagic fever in humans involves a complex sequence of interactions with various cell types. MV predominantly targets dendritic cells, monocytes, liver parenchymal cells, adrenocortical cells, and diverse lymphoid tissues. Dendritic cell infection results in compromised T lymphocyte stimulation, inducing lymphocyte apoptosis and subsequent immune suppression. This state amplifies cytokines/chemokines levels, culminating in shock and multiorgan damage. T lymphocytes and endothelial cells continue to suffer damage as a result of macrophage or monocyte infection, which sets off an unchecked cascade of cytokines and chemokines. Hemorrhaging is facilitated by endothelial cell infection, which increases blood vessel permeability and causes disseminated intravascular coagulopathy (DIC). Systemic replication may arise from endothelial cell infection. Parenchymal cell infection within the liver diminishes coagulation factors, potentially leading to later hemorrhage events. Infection of adrenocortical cells within the adrenal gland results in metabolic disturbances and dysregulated blood pressure, which can ultimately culminate in hemorrhage. Lymphoid tissue infections, especially those that affect the lymph nodes and spleen, cause tissue necrosis and impair adaptive immunity. In the later stages of the illness, shock and harm to the lymphoid organs can appear.

including soiled bedding and clothing in addition to the patient's blood and bodily fluids. When near patients with MVD (within 1 m), healthcare staff should wear gloves, a clean, non-sterile long sleeve gown, and facial protection (a face shield or a medical mask and goggles). Residents of the affected areas should endeavor to educate the public about the signs and symptoms of the virus and the precautions that must be taken to prevent a pandemic. Healthcare professionals should think about building isolation units to immediately segregate MV-infected patients and stop person-to-person transmission (Brauburger et al., 2012). With the creation of accurate test diagnoses for suspected instances, the concept of halting transmission will also be strengthened even more. Contrary to previous epidemics, the deployment of barrier nursing techniques and training of hospital staff have benefited the general populace and decreased the incidence of nosocomial infections. Safe burial practices, sanitation standards, and public awareness campaigns are necessary to keep the virus under control since, as previously mentioned, close contact with the remains of infected people also contributes to the transmission of infection (Brauburger et al., 2012). Additionally, it is important to avoid direct contact with bodily fluids like blood, saliva, vomit, urine, and other bodily fluids from infected people. Additionally, care must be taken when handling vegetative items, such as infected needles and pins. It is also advisable to stay away from prospective carriers who are still alive and those who have passed away (such as monkeys, chimps, gorillas, fruit bats, and pigs; Government of Canada, 2023). Additionally, it is imperative that visitors to fruit bat colonies' mines and caves wear gloves and other protective gear, including masks. The WHO further advises male MV disease survivors to practice safe sex and hygiene for 12 months from the onset of symptoms or until their semen has tested negative for MV twice (WHO, 2021a). Infection combat for Viral Hemorrhagic Fevers in the African Health Care Setting is a set of useful, hospital-based guidelines that the CDC and WHO have created in order to combat this deadly infection. Using locally accessible materials and minimal resources, this guideline intends to assist healthcare facilities in identifying cases and preventing the transmission of nosocomial diseases (CDC, 2023b). The European Network for Infectious Diseases (EUNID) outlines strategies for containing group 3 and 4 pathogen infections. Handling highly infectious diseases (HID) like MV requires cautious procedures in labs and hospitals. EUNID recommends initiating treatment for MV cases in high-level isolation units (HLIU), emphasizing isolation and cautious management. It advocates constructing specialized HLIUs for HID patients. Emergency departments must follow protocols for suspected MV cases. Laboratory personnel should inactivate samples, perform bedside tests, and adhere to safety measures. Intensive care for MV patients demands extra precautions and well-supported negative-pressure breathing apparatus. Careful management, including mask treatments and intubation, is crucial. Children with MV require careful handling to prevent spread. EUNID also offers guidelines for investigational interventions, emphasizing patient bedside procedures to minimize transmission risks (Brouqui et al., 2009).

7.1. MV's surveillance strategy

The World Health Organization (WHO) advocates the implementation of vigilant surveillance for Marburg virus disease (MVD) as a preventive measure against outbreaks, alongside aiding countries at risk in formulating preparedness plans (WHO, 2021a). The subsequent recommendations, grounded in empirical evidence, delineate the optimal approaches for Marburg virus surveillance:

a. Healthcare practitioners are advised to assess individuals exhibiting illness for the presence of Marburg virus disease, especially if they have been in close proximity to a person with suspected or confirmed MVD within the preceding 21 days or have visited an area with an ongoing Marburg outbreak during the same period (CDC, 2023c).
b. Healthcare providers should exercise heightened vigilance and conduct evaluations for patients displaying symptoms suggestive of MVD (CDC, 2023d).
c. Health care personnel tending to patients with presumed or confirmed Marburg virus infections are to implement supplementary infection control measures to avert contact with the patient's blood, bodily fluids, and contaminated surfaces or items such as garments and bedding (WHO, 2023b).
d. A variety of precautions can be taken by those who live in or travel to areas where the Marburg virus may be present to protect themselves and prevent the virus from spreading. These precautions include avoiding contact with the bodily fluids of those who are ill, delaying interaction with the semen of those who have recovered from MVD until the virus has been proven to be absent, and avoiding animals that may be carriers (CDC, 2023e).
e. Marburg virus infection is categorized as a notifiable condition, necessitating the implementation of rigorous isolation precautions in instances of suspected infection. It is imperative to emphasize that Marburg virus disease is classified as a notifiable condition, mandating healthcare professionals to promptly report any confirmed case or suspected instances (CDC, 2023e).

7.2. Public awareness campaigns for MV

The Marburg virus infection can be addressed by departmental cooperation and public awareness efforts. Public education efforts can increase understanding of the disease's severity and methods of prevention, influencing people to adopt healthy habits and seek the right medical care (Blasi et al., 2015). To effectively spread information and encourage safety precautions, these campaigns can make use of a variety of techniques, including media coverage, educational initiatives, and social campaigns (Raj, 2008; Akdim et al., 2021). In order to successfully use resources and knowledge, departmental coordination is crucial for a coordinated response to the disease (Kortepeter et al., 2020). The reach and impact of public awareness campaigns can be increased by cooperation across many ministries, including the Federal Ministry of Information, Federal Ministry of Health, and non-governmental organizations (Chagutah, 2009). Together, these initiatives can help to prevent, treat, and control the Marburg virus disease, thereby reducing its effects on people and communities.

7.3. Case studies in MV outbreak management

Several strategies are crucial in controlling Marburg virus (MV) outbreaks, as evidenced by various scientific studies and expert recommendations. Case isolation has been identified as a potent measure; a study published by the National Center for Biotechnology Information (NCBI) emphasizes that timely case isolation can effectively contain a MV outbreak (Ajelli and Merler, 2012). Successful outbreak control demands a multifaceted approach, involving case management, surveillance, and contact tracing, as advocated by the World Health Organization (WHO, 2021a). A robust laboratory service also plays a pivotal role in outbreak management, with WHO stressing its significance. Thorough evaluation of PCR-based methods, focusing on detection limits, proves essential for reliable diagnostics during monitoring phases (Timen et al., 2009). Ensuring safe and dignified burials for the deceased is another critical aspect of outbreak containment, as emphasized by WHO (2021a). Community engagement and social mobilization are integral to outbreak control. WHO underscores the importance of raising awareness about Marburg infection risk factors and protective measures to mitigate human transmission (WHO, 2021a). In terms of intervention, the development of effective vaccines, antivirals, and other therapeutic approaches, alongside appropriate mitigation strategies, emerges as paramount. This priority is affirmed by a bibliometric study published in Frontiers in Tropical Diseases (Islam et al., 2023a). Collectively, these strategies constitute a comprehensive framework for mitigating and controlling MV outbreaks.

8. Vaccine strategy of Marburg virus

The illness is caused by a virus that has no known cure and can only be passed from person to person or animal to animal through direct contact. Getting vaccinated is the greatest way to prevent the Marburg virus from spreading. Unfortunately, there is no Marburg virus vaccine available for use in the prevention of infection currently. Despite this, researchers have been working hard to create a vaccine for the Marburg virus, and several potential strategies have been assessed. Vaccination strategies, including the use of inactivated or destroyed Marburg virus particles, have been studied and assessed (Hunegnaw et al., 2021; Cross et al., 2022). This approach involves growing the virus in a petri dish and then killing it with heat or chemicals. The inactivated viral particles are then employed to create a vaccine. Vaccines against numerous viruses, including polio and hepatitis A, have been successfully developed using this method. One approach that has been studied is the use of a live-attenuated strain of the Marburg virus as a vaccine. This method involves making the virus less infectious or virulent by laboratory manipulation. After then, the engineered virus is used to make a vaccine. Measles and mumps can be prevented by the use of vaccines that include reduced forms of the infectious agent. The third sort of vaccination strategy that has been researched is the use of vaccines that are based on viral vectors. The core of this method is to deliver genetic material from the Marburg

virus into the body via a non-pathogenic virus. An immune response will be triggered by the presence of the genetic material, protecting the body from the Marburg virus (Matassov et al., 2018; Cross et al., 2020). Infectious diseases like Ebola can be prevented and treated by vaccines that use viruses as "vectors." A fourth method that has been tried and tested is the use of protein-based vaccines. The purpose of this method, which involves the use of a protein isolated from the Marburg virus, is to provoke an immune response. Vaccines frequently include the protein, which has been created using recombinant DNA technology. Protein-based vaccines have proven to be effective, leading to the development of preventative measures against diseases like human papillomavirus (HPV). Vaccines against Marburg virus are currently in development, although there are other choices. Possible vaccine targets include the use of vesicular stomatitis virus (VSV) as a vector, the VSV-EBOV-MV vaccine is a viral vector-based vaccination that protects against both Ebola and Marburg (Woolsey et al., 2022). The vaccine is currently being tested in clinical settings after displaying encouraging outcomes in preclinical research. The Ad26.ZEBOV/MV vaccine delivers antigens against the Ebola and Marburg viruses using an adenovirus as a vector. The NIH oversees developing this vaccine. After showing promising results in preclinical tests, the vaccine is currently being studied in clinical settings. The vesicular stomatitis virus (VSV) serves as a vector to transmit genetic material from the Ebola and Marburg viruses for the rVSVG-ZEBOV-GP/MV-GP viral vector-based immunization. Researchers from the University of Maryland created this vaccination. The vaccine is currently being tested in clinical settings after displaying encouraging outcomes in preclinical studies. A Marburg virus vaccine known as mRNA-1,360 creates an antiviral protein using mRNA technology. The vaccine is currently being tested in clinical settings after displaying encouraging outcomes in preclinical studies. The Marburg Vax vaccine is a dead virus-based immunization since it is made from inactivated Marburg virus particles. Its main goal is to provide protection (Jones et al., 2005; Marzi et al., 2019, 2021). The vaccine is currently being tested in clinical settings after displaying encouraging outcomes in preclinical studies. The creation of a Marburg virus vaccine is essential for stopping future epidemics. Although there are many ways to make vaccines, the relevant authorities have not yet approved any treatments or vaccines for MV. Prior to the 2013–2016 EBOV pandemic, there was a paucity of significant public sector investment for the development of pharmaceutical countermeasures, despite the catastrophic effects of filovirus infections on public health. However, funding for basic and translational studies of filoviruses has increased since 2016 as a result of biodefense and research grants. As a result, the licensing procedure for EBOV vaccines and medications to be used in suppressing outbreaks has advanced. With the help of this financing, MV was able to expand its study of animal models and preventative measures, both of which are essential before the start of clinical testing. In NHP research, several approaches have showed promise, and these approaches are now being developed via Phase I clinical trials for the clinical development of vaccines and antivirals (Marzi et al., 2015; Krause et al., 2020). Since almost the moment the virus was identified, a MV vaccine has been under development, but results have been patchy. Only a few of the prospective MV vaccination platforms have shown protective efficacy in NHPs, despite being extensively tested in rodent models. The MV glycoprotein (GP) is used by all presently available successful vaccine candidates as their primary antigen. It offers defense against a variety of RAVV and MV strains. As MV vaccines, fast-acting, live-attenuated, non-replicating, and replicating viral vector regimens may be utilized in multidose, single-dose, and other forms. In the event of an outbreak, reactive vaccination campaigns would make use of single-dose, quick-acting vaccinations. There are, however, a number of candidate vaccines that could be employed for at-risk groups' regular vaccination. The duration of the acquired immunity created by the vaccine will determine whether additional immunizations are required (Dean et al., 2020; WHO, 2023c).

8.1. Vaccine status and WHO guideline

The two-day-old vaccine that prevents illness is supported by the National Institute of Health. In this investigation, a deadly dose of the Marburg virus vaccine was given to rhesus macaques. After 48 h, just two of the five to six monkeys that had received the vaccine were still alive (Geisbert, 2015). These infections can only be treated in laboratories with the utmost level of safety and containment because there are not any licensed immunizations that have been approved for use in humans. As indicated in Table 3 (Grant-Klein et al., 2015), several vaccination approaches had been developed for the treatment of MV in NHP models. There is not a licensed vaccination or antiviral medication for MVD now. Supportive therapy that restores lost blood and clotting elements while also preserving blood pressure, oxygen levels, and electrolyte balance may be helpful. There are several MV vaccines developed. For instance, the VSV-MV vaccine, a recombinant VSV-based immunization that produces the MV glycoprotein, instantly shields hosts from MVD in animal models (Marzi et al., 2021). Another strategy for prevention against both hemorrhagic viruses is the vaccine candidate MVABN-Filo, which contains antigens from the Marburg and the Ebola viruses (Barry et al., 2021). A phase 3 trial that appears to create a powerful defense against the Ebola virus is currently being carried out. In addition to developing preventive vaccines, researchers are currently striving to develop effective postexposure therapies for MVD, such as small molecule antivirals and monoclonal antibodies (mAbs) specific to the MV. Researchers combined a monoclonal antibody (MR186-YTE) with an antiviral (remdesivir) using a non-human primate model of MVD (Cross et al., 2021). The statistics show that this combination was very effective in treating the condition. A summary of the advancement of MVD vaccines and experimental therapies is shown in Table 4 (Baby et al., 2022).

9. T-705 and remdesivir: promising antiviral strategies for Marburg virus disease

Two antiviral agents, T-705 (favipiravir) and remdesivir, have exhibited efficacy against Marburg virus disease (MVD) through preclinical investigations. These agents function as RNA polymerase inhibitors, impeding viral replication and transcription processes (Furuta et al., 2013; Bixler et al., 2018; Marlin et al., 2022). T-705 (favipiravir), a pyrazinecarboxamide derivative, boasts comprehensive antiviral activity across diverse viruses and holds clinical approval in Japan for addressing influenza (Zhu et al., 2018; Zadeh et al., 2022). A

research study disseminated by the National Center for Biotechnology Information (NCBI) proposes T-705 as a viable therapeutic candidate against Marburg virus, particularly valuable for outbreak scenarios due to its prompt and secure oral administration following exposure (Zhu et al., 2018; Zadeh et al., 2022). Angola, a mouse-adapted Marburg virus strain, was used to infect mice in a different investigation, and T-705 showed excellent survivability in these mice (Zhu et al., 2018; Zadeh et al., 2022). Oral dosing that began 1 or 2 days after infection and continued for 8 days resulted in full mouse survival. Remdesivir functions as a monophosphoramidate nucleoside prodrug, which undergoes intracellular metabolic alteration into an active nucleoside triphosphate form, thereby inhibiting viral RNA polymerase (Malin et al., 2020). Notably, a study revealed the curative effectiveness of remdesivir in nonhuman monkeys infected with the Marburg virus experimentally, particularly when therapy started 5 days after inoculation (Porter et al., 2020). Remdesivir was demonstrated to be effective against a variety of RNA viruses *in vitro* and using macaque models, including the Ebola virus, Lassa virus, and Marburg virus (Malin et al., 2020). This research was published in Clinical Microbiology Reviews. It is imperative to acknowledge that the efficacy and safety of these agents in human MVD cases remain untested. Moreover, the application of antiviral drugs necessitates integration with supplementary control measures, including case isolation, surveillance, contact tracing, laboratory services, secure burials, and community mobilization, to ensure the effective management of MVD outbreaks (Cross et al., 2018; Zhu et al., 2018). T-705, also known as Favipiravir, has demonstrated effectiveness *in vitro* and *in vivo* against Marburg virus infection (Zhu et al., 2018). Mice that had been intraperitoneally infected with Marburg virus that had been modified for mice completely survived when given T-705 beginning 1 or 2 days after infection and continuing for 8 days (Zhu et al., 2018). Vero E6 cells showed no negative effects (Zhu et al., 2018). A broad-spectrum antiviral drug called Remdesivir has previously shown antiviral effectiveness against filoviruses including the Marburg virus (Levien and Baker, 2021). Respiratory failure and organ malfunction, including low albumin, low potassium, low red blood cell count, low platelet count, which aids clots, and yellow skin coloring, are the most frequent side events in Remdesivir trials for COVID-19 (Zadeh et al., 2021). Pyrexia, sleeplessness, multi-organ malfunction, DVT, and hypersensitivity/anaphylactic reactions connected to the infusion are additional negative consequences (Levien and Baker, 2021). A combination therapy of monoclonal antibodies (mAbs) and remdesivir has been shown to induce an 80% protection rate against Marburg virus in rhesus macaques (Cross et al., 2021; Rees, n.d.). The combination therapy was initiated 5 days post-inoculation with Marburg virus (Cross et al., 2021). High temperature, severe headaches, severe malaise, muscle aches and pains, gastrointestinal problems, migraines, and dizziness are all signs of Marburg virus sickness (Kortepeter et al., 2020; WHO, 2021b,c). Marburg virus sickness has a case fatality ratio that can reach 88%, but it can be significantly reduced with proper patient care (WHO, 2021b). In summary, Remdesivir has shown antiviral activity against filoviruses like Marburg virus, whereas T-705 has showed efficacy against Marburg virus infection *in vitro* and *in vivo*. In rhesus macaques, monoclonal antibody and remdesivir combination therapy has been reported to result in an 80% protection rate against Marburg virus. High temperature, severe headaches, severe malaise, muscle aches and pains, gastrointestinal problems, migraines, and disorientation are all signs of Marburg virus sickness.

10. Emerging therapeutic agents in clinical trials

Clinical trials have been conducted for some drugs to treat MV; some of these trials have been completed and others are ongoing. MV drug development has progressed much more slowly than preclinical and clinical trials for the treatment of EBOV. Antiviral effectiveness against MV infections in nonhuman primates (NHPs) has long been regarded as the gold standard to assess prospective efficacy in humans and support subsequent clinical trials, much like EBOV. Following exposure in NHPs with advanced disease, several promising strategies, such as pan-filoviral small-molecule antivirals and MV-specific monoclonal antibodies, have shown excellent success. Table 5 shows the biologics currently being tested in clinical trials, along with their current status and research center location (Citeline Clinical, 2023).

11. Conclusion

The emergence of Marburg virus (MV) has presented a complex global challenge characterized by fatal outbreaks and significant clinical hurdles. The extensive analysis conducted in this study sheds light on the multifaceted nature of MV, encompassing its origin, transmission dynamics, clinical manifestations, and the intricate interplay between the virus and its human hosts. The documented outbreaks underscore the

TABLE 3 Vaccine efficacy on the non-human primate model.

S. no.	Vaccine type	Dose	Survival %	References
1	Virus like particles + RIBI (Vaccine adjuvant)	3	100	Hevey et al. (1998)
2	EBOV GP + SUDV GP + MV GP + RAVV GP	3	100	Ashique et al. (2023)
3	rAD5 (vector) + MV GP + DNA MV GP	4	100	Barry et al. (2021)
4	Intact MV, RAVV	2	50	Swenson et al. (2004)
5	VEEV + MV GP + VEEV-MV NP	3	67–100	Marzi et al. (2021)
6	Cad Vax-Pan Filo	2	100	Cross et al. (2021)
7	MV GP	3	67	Geisbert (2015)
8	VSV + MV	1	100	Grant-Klein et al. (2015)

TABLE 4 Development of a vaccine and advancements in experimental therapies for Marburg virus sickness.

Vaccine	Description	Animal studies	Clinical trials	References
MVA-BN-Filo	A multivalent vaccination formulation called Mvabea (MVA-BN-Filo) is intended to give active acquired immunity to the Sudan virus, Ebola virus, Marburg virus, and Tai Forest virus.	No data.	Eight months after immunization, phase 1 results showed persistent GP immunity against Ebola. No MV-related findings were reported.	Marzi et al. (2015)
rVSV-MVGP	A vesicular stomatitis virus vector that is recombinant and expresses the MV glycoprotein (GP).	100% of animal studies are successful. One year after the shot	No data.	Henao-Restrepo et al. (2017)
cAd3-MV	In this immunization, a modified chimpanzee adenovirus known as cAD3 is utilized.	No data for cAd3-MV	Four weeks following a single vaccination, 95% of individuals exhibited a glycoprotein-specific antibody response, which persisted in 70% of them at 48 weeks.	Dean et al. (2020)
CAdVax-panFilo	The complex encodes GPs from EBOV, SUDV, and MV as well as GPs from EBOV and MV Musoke nucleoproteins.	Antibodies were tested against all five filoviruses, and no macaques displayed symptoms of a clinical disease.	No data.	Dean and Longini (2022)
DNA plasmid vaccine	MV Angola DNA is expressed by a Marburg DNA plasmid.	A DNA prime/boost vaccine in macaques provided protection, although all of the animals eventually became ill.	In a phase 1 experiment, 10 participants showed 90% antibody responses.	Cross et al. (2022)

TABLE 5 Ongoing clinical trials for therapeutics.

S. no	Research study	Research place	Disease	Interceding	Status of trial	References
1.	Healthy Adults Receiving the CAd3-Marburg Vaccine	WRAIR-clinical trials center, silver spring, US	Marburg virus	Biological: cAd3 vaccine	Completed	Ashique et al. (2023)
2.	Single Administration Safety Study Treatment for the Marburg Virus Post-exposure Prophylaxis	American West Coast, California	Marburg Hemorrhagic Fever	Drug:AVI-6003 Drug: Placebo	Completed	Ashique et al. (2023)
3.	Filo and Ad26 from MVA-BN(R). On healthy volunteers, ZEBOV vaccines are being tested for safety.	Atlanta, Georgia, US	Marburg Hemorrhagic Fever Ebola virus disease	Biological: Ad26 Zaire Ebola Vaccine. Biological: MVA Multi-Filo Ebola Vaccine	Completed	Ashique et al. (2023)
4.	An investigation on the safety, tolerability, and pharmacokinetics of a single dose of IV BCX4430	US-Kansas City, Lenexa, PRA Health Sciences	Marburg Virus	Drug: Galidesivir Drug: Placebo	Active, not recruiting	Ashique et al. (2023)
5.	Avi-7,288 Pharmacokinetics, Safety, and Tolerability Study in Healthy Adult Volunteers	Clinical Pharmacology Center at SNBL. USA, Baltimore	Marburg Hemorrhagic Fever	Drug: AVI-7288 Other: Placebo	Completed	Ashique et al. (2023)
6.	Marburg and Ebola virus vaccines	9,000 Rockville Pike, National Institutes of Health Clinical Center, Bethesda, Maryland (USA)	Marburg Virus Illness Ebola Virus Illness	Drug: VRC-EBODNA023-00-VP Drug: VRC-MARDNA025-VP	Completed	Ashique et al. (2023)

urgency of understanding and effectively addressing the threat posed by MV to global health security. Throughout this investigation, it has become evident that the clinical challenges posed by MV are substantial, with its virulent nature leading to high mortality rates and a range of severe symptoms. The lack of specific antiviral therapies or vaccines further amplifies the urgency of comprehensive prevention and control strategies. The cases studied emphasize the need for rapid, coordinated responses involving healthcare providers, researchers, and governmental bodies to curtail the impact of MV outbreaks. The global perspective on MV's emergence emphasizes the need for proactive, multidisciplinary approaches to prevent and mitigate its devastating impact. The lessons learned from past outbreaks underscore the importance of preparedness, collaboration, and innovation in addressing this ongoing threat to public health. Through these concerted efforts, we can hope to avert future MV outbreaks and minimize their toll on human lives.

12. Future perspectives

Looking ahead, several crucial research and intervention directions emerge from our analysis. First, continued efforts are imperative to elucidate the intricate mechanisms of MV transmission from its reservoir hosts to humans, allowing for the identification of potential intervention points. Collaborative studies integrating virology, epidemiology, and ecology will be pivotal in achieving a comprehensive understanding of the virus's life cycle. Second, the development of effective preventative measures remains paramount. Advances in vaccine technologies offer promise for the creation of MV-specific vaccines, analogous to strategies employed against related pathogens. In parallel, research should focus on identifying small molecule antiviral compounds that can impede MV replication and spread. Third, bolstering healthcare infrastructure in regions susceptible to MV outbreaks is essential. Strengthening diagnostic capabilities, training healthcare workers in effective infection control measures, and establishing rapid response protocols are vital components of managing MV cases and preventing wider disseminations.

Author contributions

SSr, DS, SK, and AS: concept and original draft. RR, AA, SA, SR, SSa, ZA-q, PB, AM, AR-M, and RS: reviewing and editing. RS: supervision. All authors contributed to the article and approved the submitted version.

Conflict of interest

The authors declare that the research was conducted in the absence of any commercial or financial relationships that could be construed as a potential conflict of interest.

Publisher's note

All claims expressed in this article are solely those of the authors and do not necessarily represent those of their affiliated organizations, or those of the publisher, the editors and the reviewers. Any product that may be evaluated in this article, or claim that may be made by its manufacturer, is not guaranteed or endorsed by the publisher.

References

Abir, M. H., Rahman, T., Das, A., Etu, S. N., Nafiz, I. H., Rakib, A., et al. (2022). Pathogenicity and virulence of Marburg virus. *Virulence* 13, 609–633. doi: 10.1080/21505594.2022.2054760

Aborode, A. T., Wireko, A. A., Bel-Nono, K. N., Quarshie, L. S., Allison, M., and Bello, M. A. (2022). Marburg virus amidst COVID-19 pandemic in Guinea: fighting within the looming cases. *Int. J. Health Plann. Manage.* 37, 553–555. doi: 10.1002/hpm.3332

Ajelli, M., and Merler, S. (2012). Transmission potential and design of adequate control measures for Marburg hemorrhagic fever. *PLoS One* 7:e50948. doi: 10.1371/journal.pone.0050948

Akdim, K., Ez-Zetouni, A., and Zahid, M. (2021). The influence of awareness campaigns on the spread of an infectious disease: a qualitative analysis of a fractional epidemic model. *Model Earth Syst Environ* 8, 1311–1319. doi: 10.1007/s40808-021-01158-9

Alfson, K. J., Avena, L. E., Delgado, J., Beadles, M. W., Patterson, J. L., Carrion, R., et al. (2018). A single amino acid change in the Marburg virus glycoprotein arises during serial cell culture passages and attenuates the virus in a macaque model of disease. *Msphere* 3, e00401–e00417. doi: 10.1128/msphere.00401-17

Amiar, S., Husby, M. L., Wijesinghe, K. J., Angel, S., Bhattarai, N., Gerstman, B. S., et al. (2021). Lipid-specific oligomerization of the Marburg virus matrix protein VP40 is regulated by two distinct interfaces for virion assembly. *J. Biol. Chem.* 296:100796. doi: 10.1016/j.jbc.2021.100796

Amman, B. R., Carroll, S. A., Reed, Z. D., Sealy, T. K., Balinandi, S., Swanepoel, R., et al. (2012). Seasonal pulses of Marburg virus circulation in juvenile Rousettus aegyptiacus bats coincide with periods of increased risk of human infection. *PLoS Pathog.* 8:e1002877. doi: 10.1371/journal.ppat.1002877

Amman, B. R., Jones, M. E. B., Sealy, T. K., Uebelhoer, L. S., Schuh, A. J., Bird, B. H., et al. (2015). Oral shedding of Marburg virus in experimentally infected Egyptian fruit bats (Rousettus aegyptiacus). *J. Wildl. Dis.* 51, 113–124. doi: 10.7589/2014-08-198

Asad, A., Aamir, A., Qureshi, N. E., Bhimani, S., Jatoi, N. N., Batra, S., et al. (2020). Past and current advances in Marburg virus disease: a review. *Infez. Med.* 28, 332–345.

Ashique, S., Chaudhary, V., Pal, S., Panwar, J., Kumar, M., Pramanik, S., et al. (2023). Marburg virus—a threat during SARS-CoV-2 era: a review. *Infect. Disord. Drug Targets* 23:845. doi: 10.2174/1871526523666230228103845

Baby, B., Rajendran, R., Nair, M. M., and Raghavan, R. P. (2022). Sagacious perceptive on Marburg virus foregrounding the recent findings: a critical review. *Infect. Disord. Drug Targets* 22, 13–18. doi: 10.2174/1871526522666220510103618

Bale, S., Julien, J. P., Bornholdt, Z. A., Kimberlin, C. R., Halfmann, P., Zandonatti, M. A., et al. (2012). Marburg virus VP35 can both fully coat the backbone and cap the ends of dsRNA for interferon antagonism. *PLoS Med.* 8:e1002916. doi: 10.1371/journal.ppat.1002916

Bamberg, S., Kolesnikova, L., Möller, P., Klenk, H. D., and Becker, S. (2005). VP24 of Marburg virus influences formation of infectious particles. *J. Virol.* 79, 13421–13433. doi: 10.1128/JVI.79.21.13421-13433.2005

Barry, H., Mutua, G., Kibuuka, H., Anywaine, Z., Sirima, S. B., Meda, N., et al. (2021). Safety and immunogenicity of 2-dose heterologous Ad26. ZEBOV, MVA-BN-filo Ebola vaccination in healthy and HIV-infected adults: a randomised, placebo-controlled phase II clinical trial in Africa. *PLoS Med.* 18:e1003813. doi: 10.1371/journal.pmed.1003813

Bausch, D. G., Nichol, S. T., Muyembe-Tamfum, J. J., Borchert, M., Rollin, P. E., Sleurs, H., et al. (2006). Marburg hemorrhagic fever associated with multiple genetic lineages of virus. *N. Engl. J. Med.* 355, 909–919. doi: 10.1056/NEJMoa051465

Bebell, L. M., and Riley, L. E. (2015). Ebola virus disease and Marburg disease in pregnancy: a review and management considerations for filovirus infection. *Obstet. Gynecol.* 125:1293. doi: 10.1097/AOG.0000000000000853

Becker, S., Rinne, C., Hofsäß, U., Klenk, H. D., and Mühlberger, E. (1998). Interactions of Marburg virus nucleocapsid proteins. *Virology* 249, 406–417. doi: 10.1006/viro.1998.9328

Bente, D., Gren, J., Strong, J. E., and Feldmann, H. (2009). Disease modeling for Ebola and Marburg viruses. *Dis. Model. Mech.* 2, 12–17. doi: 10.1242/dmm.000471

Bertherat, E., Talarmin, A., and Zeller, H. (1999). Democratic Republic of the Congo: between civil war and the Marburg virus. International Committee of Technical and Scientific Coordination of the Durba epidemic. *Med. Trop.* 59, 201–204.

Bixler, S. L., Bocan, T. M., Wells, J., Wetzel, K. S., van Tongeren, S. A., Dong, L., et al. (2018). Efficacy of favipiravir (T-705) in nonhuman primates infected with Ebola virus or Marburg virus. *Antiviral Res.* 151, 97–104. doi: 10.1016/j.antiviral.2017.12.021

Blasi, P. R., King, D., and Henrikson, N. B. (2015). HPV vaccine public awareness campaigns: an environmental scan. *Health Promot. Pract.* 16, 897–905. doi: 10.1177/1524839915596133

Borchert, M., Muyembe-Tamfum, J. J., Colebunders, R., Libande, M., Sabue, M., and van der Stuyft, P. (2002). A cluster of Marburg virus disease involving an infant. *Trop. Med. Int. Health* 7, 902–906. doi: 10.1046/j.1365-3156.2002.00945.x

Borchert, M., and Van der Stuyft, P. (2008). Epidemiology and control of Marburg haemorrhagic fever epidemics in Central Africa. *Afrika Focus* 22, 118–119. doi: 10.1163/2031356X-02201011

Brainard, J., Pond, K., Hooper, L., Edmunds, K., and Hunter, P. (2016). Presence and persistence of Ebola or Marburg virus in patients and survivors: a rapid systematic review. *PLoS Negl. Trop. Dis.* 10:e0004475. doi: 10.1371/journal.pntd.0004475

Brauburger, K., Deflubé, L. R., and Mühlberger, E. (2015). "Filovirus transcription and replication" in *Biology and pathogenesis of rhabdo-and filoviruses*. eds. A. K. Pattnaik and M. A. Whitt (World Scientific Publishing Boston University), 515–555.

Brauburger, K., Hume, A. J., Mühlberger, E., and Olejnik, J. (2012). Forty-five years of Marburg virus research. *Viruses* 4, 1878–1927. doi: 10.3390/v4101878

Brouqui, P., Puro, V., Fusco, F. M., Bannister, B., Schilling, S., Follin, P., et al. (2009). Infection control in the management of highly pathogenic infectious diseases: consensus of the European network of infectious disease. *Lancet Infect. Dis.* 9, 301–311. doi: 10.1016/S1473-3099(09)70070-2

Bruhn, J. F., Kirchdoerfer, R. N., Urata, S. M., Li, S., Tickle, I. J., Bricogne, G., et al. (2017). Crystal structure of the Marburg virus VP35 oligomerization domain. *J. Virol.* 91:e01085. doi: 10.1128/jvi.01085-16

Bukreyev, A. A., Chandran, K., Dolnik, O., Dye, J. M., Ebihara, H., Leroy, E. M., et al. (2014). Discussions and decisions of the 2012–2014 international committee on taxonomy of viruses (ICTV) filoviridae study group, January 2012–June 2013. *Arch. Virol.* 159, 821–830. doi: 10.1007/s00705-013-1846-9

Carette, J. E., Raaben, M., Wong, A. C., Herbert, A. S., Obernosterer, G., Mulherkar, N., et al. (2011). Ebola virus entry requires the cholesterol transporter Niemann–pick C1. *Nature* 477, 340–343. doi: 10.1038/nature10348

CDC. (2023a). Diagnosis. Available at: https://www.cdc.gov/vhf/marburg/diagnosis/index.html

CDC. (2023b). Prevention.

CDC. (2023c). Guide for clinicians evaluating an ill person for Marburg virus disease; Available at: https://www.cdc.gov/vhf/marburg/clinicians/guide-evaluating-mvd-patient.html

CDC. (2023d). Screening Patients. Available at: https://www.cdc.gov/vhf/marburg/clinicians/screening-patients.html

CDC. (2023e). Marburg (Marburg Virus Disease) Available at: https://www.cdc.gov/vhf/marburg/prevention/index.html CDC

Chagutah, T. (2009). Towards improved public awareness for climate related disaster risk reduction in South Africa: a participatory development communication perspective. *Jàmbá J Disaster Risk Stud* 2, 113–126. doi: 10.4102/jamba.v2i2.19

Chakraborty, S., Chandran, D., Mohapatra, R. K., Alagawany, M., Yatoo, M. I., Islam, M. A., et al. (2022). Marburg virus disease–a mini-review. *J. Exp. Biol. Agric. Sci* 10, 689–696. doi: 10.18006/2022.10(4).689.696

Citeline Clinical. (2023). C. Citeline clinical is the world's most comprehensive provider of real-time trial intelligence to the pharmaceutical industry. Available at: https://pages.intelligence.informa.com/Citeline-Clinical-Solutions?utm_source=google&utm_medium=cpc&utm_term=clinical%20trial%20search|&utm_campaign=SO-Clinical-APAC&gclid=CjwKCAjw5remBhBiEiwAxL2M9-oSilo-oYZXTr4qOjLw0wu8ORhC2HS0GZjYN4mPD9vidmogDPFu8xoCWB8QAvD_BwE

Coffin, K. M., Liu, J., Warren, T. K., Blancett, C. D., Kuehl, K. A., Nichols, D. K., et al. (2018). Persistent Marburg virus infection in the testes of nonhuman primate survivors. *Cell Host Microbe* 24, 405–416.e3. e3. doi: 10.1016/j.chom.2018.08.003

Colebunders, R., Tshomba, A., van Kerkhove, M. D., Bausch, D. G., Campbell, P., Libande, M., et al. (2007). Marburg hemorrhagic fever in Durba and Watsa, Democratic Republic of the Congo: clinical documentation, features of illness, and treatment. *J Infect Dis* 196, S148–S153. doi: 10.1086/520543

Cross, R. W., Bornholdt, Z. A., Prasad, A. N., Borisevich, V., Agans, K. N., Deer, D. J., et al. (2021). Combination therapy protects macaques against advanced Marburg virus disease. *Nat. Commun.* 12:1891. doi: 10.1038/s41467-021-22132-0

Cross, R. W., Longini, I. M., Becker, S., Bok, K., Boucher, D., Carroll, M. W., et al. (2022). An introduction to the Marburg virus vaccine consortium, MARVAC. *PLoS Pathog.* 18:e1010805. doi: 10.1371/journal.ppat.1010805

Cross, R. W., Mire, C. E., Feldmann, H., and Geisbert, T. W. (2018). Post-exposure treatments for Ebola and Marburg virus infections. *Nat. Rev. Drug Discov.* 17, 413–434. doi: 10.1038/nrd.2017.251

Cross, R. W., Xu, R., Matassov, D., Hamm, S., Latham, T. E., Gerardi, C. S., et al. (2020). Quadrivalent VesiculoVax vaccine protects nonhuman primates from viral-induced hemorrhagic fever and death. *J. Clin. Invest.* 130, 539–551. doi: 10.1172/JCI131958

Dean, N. E., Gsell, P. S., Brookmeyer, R., Crawford, F. W., Donnelly, C. A., Ellenberg, S. S., et al. (2020). Creating a framework for conducting randomized clinical trials during disease outbreaks. *Mass Medical Soc* 382, 1366–1369. doi: 10.1056/NEJMsb1905390

Dean, N. E., and Longini, I. M. (2022). The ring vaccination trial design for the estimation of vaccine efficacy and effectiveness during infectious disease outbreaks. *Clin. Trials* 19, 402–406. doi: 10.1177/17407745211073594

Deb, N., Roy, P., Jaiswal, V., Mohanty, A., Sah, S., and Sah, R. (2023). Marburg virus disease in Tanzania: the most recent outbreak. *New Microbes New Infect* 53:101123. doi: 10.1016/j.nmni.2023.101123

DiCarlo, A., Biedenkopf, N., Hartlieb, B., Klußmeier, A., and Becker, S. (2011). Phosphorylation of Marburg virus NP region II modulates viral RNA synthesis. *J Infect Dis* 204, S927–S933. doi: 10.1093/infdis/jir319

Edwards, M. R., Johnson, B., Mire, C. E., Xu, W., Shabman, R. S., Speller, L. N., et al. (2014). The Marburg virus VP24 protein interacts with Keap1 to activate the cytoprotective antioxidant response pathway. *Cell Rep.* 6, 1017–1025. doi: 10.1016/j.celrep.2014.01.043

Edwards, M. R., Liu, G., Mire, C. E., Sureshchandra, S., Luthra, P., Yen, B., et al. (2016). Differential regulation of interferon responses by Ebola and Marburg virus VP35 proteins. *Cell Rep.* 14, 1632–1640. doi: 10.1016/j.celrep.2016.01.049

Elsheikh, R., Makram, A. M., Selim, H., Nguyen, D., le, T. T. T., Tran, V. P., et al. (2023). Reemergence of Marburgvirus disease: update on current control and prevention measures and review of the literature. *Rev. Med. Virol.* 33:e2461. doi: 10.1002/rmv.2461

Enterlein, S., Volchkov, V., Weik, M., Kolesnikova, L., Volchkova, V., Klenk, H. D., et al. (2006). Rescue of recombinant Marburg virus from cDNA is dependent on nucleocapsid protein VP30. *J. Virol.* 80, 1038–1043. doi: 10.1128/JVI.80.2.1038-1043.2006

Feldmann, H. (2018). Virus in semen and the risk of sexual transmission. *N. Engl. J. Med.* 378, 1440–1441. doi: 10.1056/NEJMe1803212

Feldmann, H., Mühlberger, E., Randolf, A., Will, C., Kiley, M. P., Sanchez, A., et al. (1992). Marburg virus, a filovirus: messenger RNAs, gene order, and regulatory elements of the replication cycle. *Virus Res.* 24, 1–19. doi: 10.1016/0168-1702(92)90027-7

Feldmann, H., Sanchez, A., and Geisbert, T. (2013). "Filoviridae: Marburg and ebola viruses" in *Fields Virology*. ed. H. Feldmann *6th edn*. (Wolters Kluwer Health Adis (ESP))

Feldmann, F., Shupert, W. L., Haddock, E., Twardoski, B., and Feldmann, H. (2019). Gamma irradiation as an effective method for inactivation of emerging viral pathogens. *Am. J. Trop. Med. Hyg.* 100, 1275–1277. doi: 10.4269/ajtmh.18-0937

Feldmann, H., Will, C., Schikore, M., Slenczka, W., and Klenk, H. D. (1991). Glycosylation and oligomerization of the spike protein of Marburg virus. *Virology* 182, 353–356. doi: 10.1016/0042-6822(91)90680-A

Furuta, Y., Gowen, B. B., Takahashi, K., Shiraki, K., Smee, D. F., and Barnard, D. L. (2013). Favipiravir (T-705), a novel viral RNA polymerase inhibitor. *Antiviral Res.* 100, 446–454. doi: 10.1016/j.antiviral.2013.09.015

Gear, J. S., Cassel, G. A., Gear, A. J., Trappler, B., Clausen, L., Meyers, A. M., et al. (1975). Outbreake of Marburg virus disease in Johannesburg. *Br. Med. J.* 4, 489–493. doi: 10.1136/bmj.4.5995.489

Geisbert, T. W. (2015). Marburg and Ebola hemorrhagic fevers (filoviruses). *Mandell Douglas Bennetts Principles Pract Infect Dis*:1995. doi: 10.1016/B978-1-4557-4801-3.00166-1

Government of Canada. (2023). Marburg virus disease; Available at: https://www.canada.ca/en/public-health/services/infectious-diseases/viral-haemorrhagic-fevers/marburg-virus-disease-prevention.html

Grant-Klein, R. J., Altamura, L. A., Badger, C. V., Bounds, C. E., van Deusen, N. M., Kwilas, S. A., et al. (2015). Codon-optimized filovirus DNA vaccines delivered by intramuscular electroporation protect cynomolgus macaques from lethal Ebola and Marburg virus challenges. *Hum. Vaccin. Immunother.* 11, 1991–2004. doi: 10.1080/21645515.2015.1039757

Heeney, J. L. (2015). Hidden reservoirs. *Nature* 527, 453–455. doi: 10.1038/527453a

Henao-Restrepo, A. M., Camacho, A., Longini, I. M., Watson, C. H., Edmunds, W. J., Egger, M., et al. (2017). Efficacy and effectiveness of an rVSV-vectored vaccine in preventing Ebola virus disease: final results from the Guinea ring vaccination, open-label, cluster-randomised trial (Ebola Ça Suffit!). *Lancet* 389, 505–518. doi: 10.1016/S0140-6736(16)32621-6

Hevey, M., Negley, D., Pushko, P., Smith, J., and Schmaljohn, A. (1998). Marburg virus vaccines based upon alphavirus replicons protect guinea pigs and nonhuman primates. *Virology* 251, 28–37.

Hunegnaw, R., Honko, A., Wang, L., Carr, D., and Murray, T., W. Shiet al. (2021). Rapid and durable protection against Marburg virus with a single-shot ChAd3-MARV GP vaccine. bioRxiv [Preprint].

Islam, M. A., Adeiza, S. S., Amin, M. R., Kaifa, F. H., Lorenzo, J. M., Bhattacharya, P., et al. (2023a). A bibliometric study on Marburg virus research with prevention and control strategies. *Front Trop Dis* 3:1068364. doi: 10.3389/fitd.2022.1068364

Islam, M. A., Rahman, M. A., Jakariya, M., Bahadur, N. M., Hossen, F., Mukharjee, S. K., et al. (2023b). A 30-day follow-up study on the prevalence of SARS-COV-2 genetic markers in wastewater from the residence of COVID-19 patient and comparison with clinical positivity. *Sci. Total Environ.* 858:159350. doi: 10.1016/j.scitotenv.2022.159350

Jamieson, D. J., Uyeki, T. M., Callaghan, W. M., Meaney-Delman, D., and Rasmussen, S. A. (2014). What obstetrician–gynecologists should know about Ebola: a perspective from the Centers for Disease Control and Prevention. *Obstet. Gynecol.* 124, 1005–1010. doi: 10.1097/AOG.0000000000000533

Johnson, E., Johnson, B. K., Silverstein, D., Tukei, P., Geisbert, T. W., Sanchez, A. N., et al. (1996). *Imported virus infections*. Wien, New York: Springer.

Jones, S. M., Feldmann, H., Ströher, U., Geisbert, J. B., Fernando, L., Grolla, A., et al. (2005). Live attenuated recombinant vaccine protects nonhuman primates against Ebola and Marburg viruses. *Nat. Med.* 11, 786–790. doi: 10.1038/nm1258

Kirchdoerfer, R. N., Wasserman, H., Amarasinghe, G. K., and Saphire, E. O. (2017). Filovirus structural biology: The molecules in the machine. *Curr. Top. Microbiol. Immunol.* 411, 381–417. doi: 10.1007/82_2017_16

Klenk, H.-D., Slenczka, W., and Feldmann, H.. (1999). *Marburg and Ebola viruses (filoviridae)*. Switzerland: Brigitte Beer

Koehler, A., Kolesnikova, L., and Becker, S. (2016). An active site mutation increases the polymerase activity of the Guinea pig-lethal Marburg virus. *J. Gen. Virol.* 97, 2494–2500. doi: 10.1099/jgv.0.000564

Koehler, A., Pfeiffer, S., Kolesnikova, L., and Becker, S. (2018). Analysis of the multifunctionality of Marburg virus VP40. *J. Gen. Virol.* 99, 1614–1620. doi: 10.1099/jgv.0.001169

Kolesnikova, L., Bamberg, S., Berghöfer, B., and Becker, S. (2004). The matrix protein of Marburg virus is transported to the plasma membrane along cellular membranes: exploiting the retrograde late endosomal pathway. *J. Virol.* 78, 2382–2393. doi: 10.1128/JVI.78.5.2382-2393.2004

Kolesnikova, L., Mittler, E., Schudt, G., Shams-Eldin, H., and Becker, S. (2012). Phosphorylation of Marburg virus matrix protein VP40 triggers assembly of nucleocapsids with the viral envelope at the plasma membrane. *Cell. Microbiol.* 14, 182–197. doi: 10.1111/j.1462-5822.2011.01709.x

Kortepeter, M. G., Dierberg, K., Shenoy, E. S., and Cieslak, T. J.Medical Countermeasures Working Group of the National Ebola Training and Education Center's (NETEC) Special Pathogens Research Network (SPRN) (2020). Marburg virus disease: a summary for clinicians. *Int. J. Infect. Dis.* 99, 233–242. doi: 10.1016/j.ijid.2020.07.042

Krause, P., Fleming, T. R., Longini, I., Henao-Restrepo, A. M., Peto, R., Dean, N. E., et al. (2020). COVID-19 vaccine trials should seek worthwhile efficacy. *Lancet* 396, 741–743. doi: 10.1016/S0140-6736(20)31821-3

Kuhn, J. (2008). Filoviruses: A compendium of 40 years of epidemiological, clinical, and laboratory studies. *Arch. Virol. Suppl.* 20, 313–360. doi: 10.1007/978-3-211-69495-41

Languon, S., and Quaye, O. (2019). Filovirus disease outbreaks: a chronological overview. *Virology* 10:1178122X19849927. doi: 10.1177/1178122X19849927

Languon, S., and Quaye, O. (2021). Impacts of the filoviridae family. *Curr. Opin. Pharmacol.* 60, 268–274. doi: 10.1016/j.coph.2021.07.016

Leroy, E. (2009). "FILOVIRAL HEMORRHAGIC FEVER: MARBURG AND EBOLA VIRUS FEVERS" in *Feigin and Cherry's textbook of Pediatric infectious diseases* (Elsevier), 2524–2531.

Levien, T. L., and Baker, D. E. (2021). Remdesivir. *Hosp. Pharm.* 56:001857872199980. doi: 10.1177/0018578721999804

Liu, B., Dong, S., Li, G., Wang, W., Liu, X., Wang, Y., et al. (2017). Structural insight into nucleoprotein conformation change chaperoned by VP35 peptide in Marburg virus. *J. Virol.* 91:e00825. doi: 10.1128/jvi.00825-17

Liu, N., Tao, Y., Brenowitz, M. D., Girvin, M. E., and Lai, J. R. (2015). Structural and functional studies on the Marburg virus GP2 fusion loop. *J Infect Dis* 212, S146–S153. doi: 10.1093/infdis/jiv030

Magassouba, D. N. F. (2021). Marburg virus sequence from Guinea, 2021; Available at: https://virological.org/t/marburg-virus-sequence-from-guinea-2021/755

Makenov, M. T., Boumbaly, S., Tolno, F. R., Sacko, N., N'Fatoma, L. T., Mansare, O., et al. (2023). Marburg virus in Egyptian Rousettus bats in Guinea: investigation of Marburg virus outbreak origin in 2021. *PLoS Negl. Trop. Dis.* 17:e0011279. doi: 10.1371/journal.pntd.0011279

Malik, S., Dhasmana, A., Bora, J., Uniyal, P., Slama, P., Preetam, S., et al. (2023). Ebola virus disease (EVD) outbreak re-emergence regulation in East Africa: preparedness and vaccination perspective. *Int. J. Surg.* 109, 1029–1031. doi: 10.1097/JS9.0000000000000175

Malin, J. J., Suárez, I., Priesner, V., Fätkenheuer, G., and Rybniker, J. (2020). Remdesivir against COVID-19 and other viral diseases. *Clin. Microbiol. Rev.* 34:e00162. doi: 10.1128/CMR.00162-20

Manohar, M. P. M., Lee, V. J., Chinedum Odunukwe, E. U., Singh, P. K., Mpofu, B. S., and Oxley Md, C. (2023). Advancements in Marburg (MARV) virus vaccine research with its recent Reemergence in Equatorial Guinea and Tanzania: a scoping review. *Cureus* 15:e42014. doi: 10.7759/cureus.42014

Marlin, R., Desjardins, D., Contreras, V., Lingas, G., Solas, C., Roques, P., et al. (2022). Antiviral efficacy of favipiravir against zika and SARS-CoV-2 viruses in non-human primates. *Nat. Commun.* 13:5108. doi: 10.1038/s41467-022-32565-w

Martines, R. B., Ng, D. L., Greer, P. W., Rollin, P. E., and Zaki, S. R. (2015). Tissue and cellular tropism, pathology and pathogenesis of Ebola and Marburg viruses. *J. Pathol.* 235, 153–174. doi: 10.1002/path.4456

Martini, G., Knauff, H. G., Schmidt, H. A., Mayer, G., and Baltzer, G. (1968). Über eine bisher unbekannte, von affen eingeschleppte infektionskrankheit: Marburg-virus-krankheit. *DMW-Deutsche Medizinische Wochenschrift* 93, 559–571. doi: 10.1055/s-0028-1105098

Marzi, A., Jankeel, A., Menicucci, A. R., Callison, J., O'Donnell, K. L., Feldmann, F., et al. (2021). Single dose of a VSV-based vaccine rapidly protects macaques from Marburg virus disease. *Front. Immunol.* 12:774026. doi: 10.3389/fimmu.2021.774026

Marzi, A., Menicucci, A. R., Engelmann, F., Callison, J., Horne, E. J., Feldmann, F., et al. (2019). Protection against Marburg virus using a recombinant VSV-vaccine depends on T and B cell activation. *Front. Immunol.* 9:3071. doi: 10.3389/fimmu.2018.03071

Marzi, A., Robertson, S. J., Haddock, E., Feldmann, F., Hanley, P. W., Scott, D. P., et al. (2015). VSV-EBOV rapidly protects macaques against infection with the 2014/15 Ebola virus outbreak strain. *Science* 349, 739–742. doi: 10.1126/science.aab3920

Matassov, D., Mire, C. E., Latham, T., Geisbert, J. B., Xu, R., Ota-Setlik, A., et al. (2018). Single-dose trivalent VesiculoVax vaccine protects macaques from lethal ebolavirus and Marburgvirus challenge. *J. Virol.* 92:17. doi: 10.1128/jvi.01190-17

Mehedi, M., Groseth, A., Feldmann, H., and Ebihara, H. (2011). Clinical aspects of Marburg hemorrhagic fever. *Futur. Virol.* 6, 1091–1106. doi: 10.2217/fvl.11.79

Mittler, E., Schudt, G., Halwe, S., Rohde, C., and Becker, S. (2018). A fluorescently labeled marburg virus glycoprotein as a new tool to study viral transport and assembly. *J Infect Dis.* 218, S318–S326. doi: 10.1093/infdis/jiy424

Mühlberger, E. (2007). Filovirus replication and transcription. *Future Virol.* 2, 205–215. doi: 10.2217/17460794.2.2.205

Mühlberger, E., Weik, M., Volchkov, V. E., Klenk, H. D., and Becker, S. (1999). Comparison of the transcription and replication strategies of Marburg virus and Ebola virus by using artificial replication systems. *J. Virol.* 73, 2333–2342. doi: 10.1128/JVI.73.3.2333-2342.1999

Nyakarahuka, L., Ojwang, J., Tumusiime, A., Balinandi, S., Whitmer, S., Kyazze, S., et al. (2017). Isolated case of Marburg virus disease, Kampala, Uganda, 2014. *Emerg. Infect. Dis.* 23, 1001–1004. doi: 10.3201/eid2306.170047

Nyakarahuka, L., Shoemaker, T. R., Balinandi, S., Chemos, G., Kwesiga, B., Mulei, S., et al. (2019). Marburg virus disease outbreak in Kween District Uganda, 2017: epidemiological and laboratory findings. *PLoS Negl. Trop. Dis.* 13:e0007257. doi: 10.1371/journal.pntd.0007257

Page, A., Volchkova, V. A., Reid, S. P., Mateo, M., Bagnaud-Baule, A., Nemirov, K., et al. (2014). Marburgvirus hijacks nrf2-dependent pathway by targeting nrf2-negative regulator keap1. *Cell Rep.* 6, 1026–1036. doi: 10.1016/j.celrep.2014.02.027

Peterson, A. T., and Holder, M. T. (2012). Phylogenetic assessment of filoviruses: how many lineages of Marburg virus? *Ecol. Evol.* 2, 1826–1833. doi: 10.1002/ece3.297

Piercy, T., Smither, S. J., Steward, J. A., Eastaugh, L., and Lever, M. S. (2010). The survival of filoviruses in liquids, on solid substrates and in a dynamic aerosol. *J. Appl. Microbiol.* 109, 1531–1539. doi: 10.1111/j.1365-2672.2010.04778.x

Porter, D. P., Weidner, J. M., Gomba, L., Bannister, R., Blair, C., Jordan, R., et al. (2020). Remdesivir (GS-5734) is efficacious in cynomolgus macaques infected with Marburg virus. *J Infect Dis* 222, 1894–1901. doi: 10.1093/infdis/jiaa290

Qiu, X., Wong, G., Audet, J., Cutts, T., Niu, Y., Booth, S., et al. (2014). Establishment and characterization of a lethal mouse model for the Angola strain of Marburg virus. *J. Virol.* 88, 12703–12714. doi: 10.1128/JVI.01643-14

Raj, S. M. (2008). Public awareness and sensitization campaigns on HIV/AIDS in Nigeria. *J Pan Afric Stud* 2:215.

Rees, V. (n.d.). Antibodies and remdesivir used to treat Marburg virus in rhesus macaques. Available at: https://www.drugtargetreview.com/news/87414/antibodies-and-remdesivir-used-to-treat-marburg-virus-in-rhesus-macaques/

Reuben, R. C., and Abunike, S. A. (2023). Marburg virus disease: the paradox of Nigeria's preparedness and priority effects in co-epidemics. *Bull Natl Res Cent* 47:10. doi: 10.1186/s42269-023-00987-1

Roy, S., Iturburu, A., Mukherjee, D., Oduoye, M. O., Paul, A., Akilimali, A., et al. (2023). Marburg virus disease outbreak amid COVID-19 pandemic: an emerging concern in Ghana, West Africa. *Int. J. Surg.* 109, 597–598. doi: 10.1097/JS9.0000000000000190

Sanchez, A., Kiley, M. P., Holloway, B. P., and Auperin, D. D. (1993). Sequence analysis of the Ebola virus genome: organization, genetic elements, and comparison with the genome of Marburg virus. *Virus Res.* 29, 215–240. doi: 10.1016/0168-1702(93)90063-S

Sanchez, A., Kiley, M. P., Klenk, H. D., and Feldmann, H. (1992). Sequence analysis of the Marburg virus nucleoprotein gene: comparison to Ebola virus and other non-segmented negative-strand RNA viruses. *J. Gen. Virol.* 73, 347–357. doi: 10.1099/0022-1317-73-2-347

Schuh, A. J., Amman, B. R., Jones, M. E. B., Sealy, T. K., Uebelhoer, L. S., Spengler, J. R., et al. (2017). Modelling filovirus maintenance in nature by experimental transmission of Marburg virus between Egyptian rousette bats. *Nat. Commun.* 8:14446. doi: 10.1038/ncomms14446

Schwartz, D. A. (2019). *Maternal filovirus infection and death from Marburg and Ravn viruses: highly lethal to pregnant women and their fetuses similar to Ebola virus, in emerging challenges in filovirus infections*. United Nation: IntechOpen.

Shabman, R. S., Jabado, O. J., Mire, C. E., Stockwell, T. B., Edwards, M., Mahajan, M., et al. (2014). Deep sequencing identifies noncanonical editing of Ebola and Marburg virus RNAs in infected cells. *MBio* 5:14. doi: 10.1128/mbio.02011-14

Shifflett, K., and Marzi, A. (2019). Marburg virus pathogenesis–differences and similarities in humans and animal models. *Virol. J.* 16, 1–12. doi: 10.1186/s12985-019-1272-z

Slenczka, W. (2017). Filovirus research: How it began. *Curr. Top. Microbiol. Immunol.* 411, 3–21. doi: 10.1007/82_2017_8

Smith, D., Isaacson, M., Johnson, K. M., Bagshawe, A., Johnson, B. K., Swanapoel, R., et al. (1982). Marburg-virus disease in Kenya. *Lancet* 319, 816–820. doi: 10.1016/S0140-6736(82)91871-2

Swenson, D. L., Warfield, K. L., Kuehl, K., Larsen, T., Hevey, M. C., Schmaljohn, A., et al. (2004). Generation of Marburg virus-like particles by co-expression of glycoprotein and matrix protein. *FEMS Immunol. Med. Microbiol.* 40, 27–31. doi: 10.1016/S0928-8244(03)00273-6

Timen, A., Koopmans, M. P., Vossen, A. C., van Doornum, G. J., Günther, S., van den Berkmortel, F., et al. (2009). Response to imported case of Marburg hemorrhagic fever, the Netherlands. *Emerg. Infect. Dis.* 15, 1171–1175. doi: 10.3201/eid1508.090015

Towner, J. S., Amman, B. R., Sealy, T. K., Carroll, S. A. R., Comer, J. A., Kemp, A., et al. (2009). Isolation of genetically diverse Marburg viruses from Egyptian fruit bats. *PLoS Pathog.* 5:e1000536. doi: 10.1371/journal.ppat.1000536

Towner, J. S., Khristova, M. L., Sealy, T. K., Vincent, M. J., Erickson, B. R., Bawiec, D. A., et al. (2006). Marburgvirus genomics and association with a large hemorrhagic fever outbreak in Angola. *J. Virol.* 80, 6497–6516. doi: 10.1128/JVI.00069-06

van Paassen, J., Bauer, M. P., Arbous, M. S., Visser, L. G., Schmidt-Chanasit, J., Schilling, S., et al. (2012). Acute liver failure, multiorgan failure, cerebral oedema, and activation of proangiogenic and antiangiogenic factors in a case of Marburg haemorrhagic fever. *Lancet Infect. Dis.* 12, 635–642. doi: 10.1016/S1473-3099(12)70018-X

Wan, W., Kolesnikova, L., Clarke, M., Koehler, A., Noda, T., Becker, S., et al. (2017). Structure and assembly of the Ebola virus nucleocapsid. *Nature* 551, 394–397. doi: 10.1038/nature24490

Wei, H., Audet, J., Wong, G., He, S., Huang, X., Cutts, T., et al. (2017). Deep-sequencing of Marburg virus genome during sequential mouse passaging and cell-culture adaptation reveals extensive changes over time. *Sci. Rep.* 7:3390. doi: 10.1038/s41598-017-03318-3

Wenigenrath, J., Kolesnikova, L., Hoenen, T., Mittler, E., and Becker, S. (2010). Establishment and application of an infectious virus-like particle system for Marburg virus. *J. Gen. Virol.* 91, 1325–1334. doi: 10.1099/vir.0.018226-0

WHO. (2021a). Marburg virus disease. Available at: https://www.who.int/news-room/fact-sheets/detail/marburg-virus-disease

WHO. (2021b). Marburg virus disease.

WHO. (2021c). Marburg virus disease—Guinea. Available at: https://www.who.int/emergencies/disease-outbreak-news/item/2021-DON331

WHO. (2023a). Marburg virus disease—Equatorial Guinea. Available at: https://www.who.int/emergencies/disease-outbreak-news/item/2023-DON444

WHO. (2023b). Marburg virus disease. Available at: https://www.who.int/health-topics/marburg-virus-disease#tab=tab_1

WHO. (2023c). Prioritizing diseases for research and development in emergency contexts. Available at: https://www.who.int/activities/prioritizing-diseases-for-research-and-development-in-emergency-contexts

Woolsey, C., Cross, R. W., Agans, K. N., Borisevich, V., Deer, D. J., Geisbert, J. B., et al. (2022). A highly attenuated Vesiculovax vaccine rapidly protects nonhuman primates against lethal Marburg virus challenge. *PLoS Negl. Trop. Dis.* 16:e0010433. doi: 10.1371/journal.pntd.0010433

Yu, Z., Wu, H., Huang, Q., and Zhong, Z. (2021). Simultaneous detection of Marburg virus and Ebola virus with TaqMan-based multiplex real-time PCR method. *J. Clin. Lab. Anal.* 35:e23786. doi: 10.1002/jcla.23786

Zadeh, V. R., Afowowe, T. O., Abe, H., Urata, S., and Yasuda, J. (2022). Potential and action mechanism of favipiravir as an antiviral against Junin virus. *PLoS Pathog.* 18:e1010689. doi: 10.1371/journal.ppat.1010689

Zadeh, N. M., Mashinchi Asl, N. S., Forouharnejad, K., Ghadimi, K., Parsa, S., Mohammadi, S., et al. (2021). Mechanism and adverse effects of COVID-19 drugs: a basic review. *Int J Physiol Pathophysiol Pharmacol* 13:102.

Zhang, A. P., Bornholdt, Z. A., Abelson, D. M., and Saphire, E. O. (2014). Crystal structure of Marburg virus VP24. *J. Virol.* 88, 5859–5863. doi: 10.1128/JVI.03565-13

Zhao, H., Shi, L., Li, Z., Kong, R., Ren, X., Ma, R., et al. (2022). The Yun/Prohibitin complex regulates adult drosophila intestinal stem cell proliferation through the transcription factor E2F1. *Proc. Natl. Acad. Sci.* 119:e2111711119. doi: 10.1073/pnas.2111711119

Zhu, W., Zhang, Z., He, S., Wong, G., Banadyga, L., and Qiu, X. (2018). Successful treatment of Marburg virus with orally administrated T-705 (favipiravir) in a mouse model. *Antiviral Res.* 151, 39–49. doi: 10.1016/j.antiviral.2018.01.011

frontiers | Frontiers in Microbiology

TYPE Original Research
PUBLISHED 26 September 2023
DOI 10.3389/fmicb.2023.1259935

Check for updates

OPEN ACCESS

EDITED BY
Lei Deng,
Harvard Medical School, United States

REVIEWED BY
Sébastien Bontemps-Gallo,
Institut Pasteur de Lille, France
Victor H. Bustamante,
National Autonomous University of Mexico, Mexico
Abraham Loera Muro,
Centro de Investigación Biológica del Noroeste (CIBNOR), Mexico
Ricardo Oropeza,
National Autonomous University of Mexico, Mexico
Jorge Antonio Yañez,
Meritorious Autonomous University of Puebla, Mexico

*CORRESPONDENCE
Feng Liu
✉ liufeng68431@163.com

RECEIVED 17 July 2023
ACCEPTED 12 September 2023
PUBLISHED 26 September 2023

CITATION
Wan J, Zhang R, Jia Y, Xie T, Dai L, Yao Q, Zhang W, Xiao H, Gao X, Huang J, Bei W and Liu F (2023) The two-component system CpxAR is required for the high potassium stress survival of *Actinobacillus pleuropneumoniae*. *Front. Microbiol.* 14:1259935.
doi: 10.3389/fmicb.2023.1259935

COPYRIGHT
© 2023 Wan, Zhang, Jia, Xie, Dai, Yao, Zhang, Xiao, Gao, Huang, Bei and Liu. This is an open-access article distributed under the terms of the Creative Commons Attribution License (CC BY). The use, distribution or reproduction in other forums is permitted, provided the original author(s) and the copyright owner(s) are credited and that the original publication in this journal is cited, in accordance with accepted academic practice. No use, distribution or reproduction is permitted which does not comply with these terms.

The two-component system CpxAR is required for the high potassium stress survival of *Actinobacillus pleuropneumoniae*

Jiajia Wan[1], Rui Zhang[1], Yizhen Jia[1], Tingting Xie[1], Lu Dai[1], Qing Yao[1], Wendie Zhang[1], Huasong Xiao[1], Xuejun Gao[1], Jing Huang[2], Weicheng Bei[3] and Feng Liu[1]*

[1]College of Animal Sciences, Yangtze University, Jingzhou, Hubei, China, [2]College of Arts and Sciences, Yangtze University, Jingzhou, Hubei, China, [3]State Key Laboratory of Agricultural Microbiology, College of Veterinary Medicine, Huazhong Agricultural University, Wuhan, Hubei, China

Introduction: *Actinobacillus pleuropneumoniae* is an important respiratory pathogen, which can cause porcine contagious pleuropneumonia and lead to great economic losses to worldwide swine industry. High potassium is an adverse environment for bacteria, which is not conducive to providing turgor pressure for cell growth and division. Two-component system CpxAR is an important regulatory system of bacteria in response to environmental changes, which is involved in a variety of biological activities, such as antibiotic resistance, periplasmic protein folding, peptidoglycan metabolism and so on.

Methods: However, little is known about the role of CpxAR in high potassium stress in *A. pleuropneumoniae*. Here, we showed that CpxAR is critical for cell division of *A. pleuropneumoniae* under high potassium (K^+) stress.

Results: qRT-PCR analysis found that CpxAR positively regulated the cell division genes *ftsEX*. In addition, we also demonstrated that CpxR-P could directly bind the promoter region of the cell division gene *ftsE* by EMSA.

Discussion: In conclusion, our results described a mechanism where CpxAR adjusts *A. pleuropneumoniae* survival under high-K^+ stress by upregulating the expression of the cell division proteins FtsE and FtsX. These findings are the first to directly demonstrate CpxAR-mediated high-K^+ tolerance, and to investigate the detailed molecular mechanism.

KEYWORDS

Actinobacillus pleuropneumoniae*, two-component system, CpxAR, high-K^+ stress, cell division, *ftsEX

Introduction

Actinobacillus pleuropneumoniae is the aetiological agent of porcine pleuropneumonia, a serious respiratory disease with high morbidity, high lethality and substantial economic losses in the worldwide swine industry (Pattison et al., 1957; Frey, 1995; Sassu et al., 2018). Currently, 19 serovars of *A. pleuropneumoniae* have been identified based on the antigenic diversity of the capsular polysaccharides and lipopolysaccharides (Stringer et al., 2021; Scherrer et al., 2022). To successfully invade the host, *A. pleuropneumoniae* regulates the expression of its metabolism and virulence-related genes to adapt to adverse environments, such as cold, heat and osmotic.

In bacteria, two-component system (TCS) is a fine signal network to sense any change, and regulates the expression of bacterial effectors for adaptation and survival (Zschiedrich et al., 2016). To increase their adaptability, *A. pleuropneumoniae* has encoded five two-component systems (TCS) to detect and respond to diverse environments, such as CpxAR, QseBC, PhoBR, ArcAB and NarPQ (Xu et al., 2008). The CpxAR TCS is found in many bacteria, consisting of CpxA (histidine kinase) and CpxR (transcriptional regulatory protein), and has been implicated in envelope stress responses. In *A. pleuropneumoniae*, the CpxAR plays an important role in heat stress, cold stress, biofilm formation, capsule synthesis, and pathogenesis (Li et al., 2018; Yan et al., 2020; Yao et al., 2022; Liu et al., 2022a,b).

In *A. pleuropneumoniae*, the CpxAR modulates biofilm formation and virulence by regulating the expression of the *pgaABCD* operon through *rpoE* (Li et al., 2018). CpxAR is also found to mediate *A. pleuropneumoniae* stress resistance and virulence by activating the expression of WecA, which is essential for O-antigen biosynthesis (Yan et al., 2020). Moreover, CpxAR responds to heat stress by suppressing the expression of the type IV pilin ApfA, which is prone to misfolding and aggregation and therefore reduces bacterial survival under heat stress (Liu et al., 2022a). In addition, we demonstrated previously that CpxAR contributes to virulence by upregulating the expression of the polysaccharide capsule export system CpxDCBA (Liu et al., 2022b).

Potassium (K^+) is the major cation in bacterial cytoplasm, and essential for maintaining ion homeostasis which is important for regulating pH and membrane potential (Ballal et al., 2007). But, excessive K^+ is cytotoxic to bacteria, affecting turgor pressure which can lead to disturbances in cell growth and division (Sweet et al., 2021). However, most bacteria have evolved several K^+-translocating systems to maintain K^+ homeostasis, such as TrkAH, KtrAB, KtrCD, KdpFABC, KimA, Kup, Kef, YjbQ and KhtSTU (Stautz et al., 2021).

Schmidt and colleagues found that FtsE and FtsX are essential for cell division (Schmidt et al., 2004). In addition, previous studies have shown that FtsE contributes to the translocation of K-pump to the cell membrane including KdpA, TrkH, and Kup (Ukai et al., 1998; Mir et al., 2015). In *E. coli*, disruption of FtsE function exhibited growth defect under high-K^+ stress (Ukai et al., 1998).

In this study, we showed that CpxAR contributes to *A. pleuropneumoniae* growth and cell division under high-K^+ stress. In addition, we confirmed that CpxAR directly activates the expression of cell division genes *ftsEX*. Taken together, our study describes a new mechanism by which CpxAR enables *A. pleuropneumoniae* to adjust its survival by up-regulating the expression of *ftsEX* under high-K^+ stress.

Materials and methods

Strains, plasmid, and growth conditions

In this study, *A. pleuropneumoniae* strain S4074 was used as a representative strain, which was grown at 37°C in tryptic soy broth (TSB; BD, United States) added with 10% FBS and 10% (vol/vol) nicotinamide adenine dinucleotide (NAD; Biofroxx, Germany). The wild-type S4074 and in-frame mutant strain Δ*cpxRA* were donated by Prof. Weicheng Bei (Li et al., 2018). *Escherichia coli β2155* was cultured at 37°C in Luria-Bertani (LB) with 50 μg/mL diaminopimelic acid (DAP; Sigma, USA). The bacterial strains used in this study are listed in Table 1, and primers are described in Table 2. The recombinant plasmid pJFF224-P*ftsEX* with IPTG-inducible promoter was electrically transferred to the Δ*cpxRA* mutant strains to regulate the *ftsEX* gene expression under the different concentrations of IPTG.

SEM

For scanning electron microscopy (SEM), wild-type S4074 and its mutant derivatives were harvested after they were cultured in TSB medium supplemented with 10% FBS and 10% NAD with or without the supplementation of 0.3 mM KCl. Bacterial cells were fixed with 2.5% glutaraldehyde and deposited onto copper grids (200 mesh; Zhongjingkeyi, China). The copper grids were air-dried, mounted on the sample stub and coated with gold. Subsequently, strains were observed by the SEM (VEGA3; TESCAN, Czech) and the bacterial length was measured by Image J (NIH, United States).

RNA extraction, quantitative RT-PCR, and RT-PCR

WT and Δ*cpxRA* mutant strains were cultivated at 37°C shaking in TSB supplemented with 10% FBS and 10% NAD to an OD600 of 0.6, centrifuged (3,000 g, 5 min) to gather cells. Total RNA of strains was

TABLE 1 Bacterial strains and plasmids used in this study.

Strains/plasmids	Characteristics	Source/reference
A. pleuropneumoniae		
S4074	*A. pleuropneumoniae* reference strain of serovar 1; WT strain	From Prof. Weicheng Bei
Δ*cpxRA*	*A. pleuropneumoniae* 4,074 *cpxRA*-deletion mutant	From Prof. Weicheng Bei
CΔ*cpxRA*	Complemented strain of Δ*cpxRA*; Cm^r	From Prof. Weicheng Bei
E. coli		
DH5α	Cloning host for recombinant vector	Takara
BL21	Expression protein for recombinant vector	Takara
Plasmid		
pET-30a	Expression vector; Kan^r	Novagen
pET30a-*cpxR*	pET-30a carrying *cpxR* gene	This study
pJFF224-XN	*E. coli*-APP shuttle vector: RSF1010 replicon; mob oriV, Cm^r	From Prof. Weicheng Bei
p*ftsE-gfp*	pJFF224-XN carrying the *ftsE-gfp* fusions	This study

Cm^r, Chloramphenicol resistance; Amp^r, Ampicillin resistance; Kan^r, Kanamycin resistance.

10.3389/fmicb.2023.1259935

TABLE 2 Primers used in this study.

Primer	Sequence (5′–3′) a	Product	Use
ftsE-F/R	CCGTAGTACCCGCCTGATTA	219	Detection the transcription of *ftsE*
	AAGCGCGTATTGCCTTAGAG		
ftsX-F/R	CGGTATAAAGGAACGGACGA	208	Detection the transcription of *ftsX*
	GATAACGGCTGGTTGGAAAA		
ftsY-F/*R*	CGTCGTCGGCATACCTAAAT	235	Detection the transcription of *ftsY*
	CGAGCTTGAAACGGAAAAAG		
ftsL-F/*R*	ATGGCAAGTAATGAACGTTATCCGC	287	Detection the transcription of *ftsL*
	TTTTTTATCGACTGTAAACCGAA		
ftsI-F/*R*	GTGGAAGGTTATCGTGTGGC	195	Detection the transcription of *ftsI*
	CGAGAATAACGGCGCAGAA		
ftsW-F/*R*	TCGTATTGATTTTCGGGCGC	153	Detection the transcription of *ftsW*
	GTTTGGTGCGCATTTCATCG		
ftsQ-F/*R*	TGCTGTACGGACCTGATACC	169	Detection the transcription of *ftQ*
	TCGCCACGACCTAATCTGAG		
FtsZ-1-F/*R*	TTGCCGATGTGAAAACCGTT	154	Detection the transcription of *ftsZ*
	AAGATACCTTTCGCACCGGA		
FtsZ-2-F/*R*	TTTTGTTGCTGTTCTGCCGA	158	Detection the transcription of *ftsZ*
	ATCGGTATTGGCGAATCAGG		
ftsB-F/*R*	GTTGGAGCGATTATCAAGAAGC	161	Detection the transcription of *ftsB*
	CACCATCTCACGTTCGAAGC		
ftsA-F/*R*	TTTTGTGCTTACGGGTGGTG	200	Detection the transcription of *ftsA*
	TTTCGCCATTGCCCTTTTCA		
ZipA-F/*R*	GCGGTTGCGTTTGATATTGC	217	Detection the transcription of *ZipA*
	CAGACAACAGGACAACACGG		
ftsH-F/*R*	AGTCCTTTGGGTAGTGGTCG	208	Detection the transcription of *ftsH*
	CATCGGCATTACGGTTTGGT		
ftsK-F/*R*	TTACCGGCGTGATTAAAGCG	222	Detection the transcription of *ftsK*
	CTCTTGCACGCCAGTTATCC		
16SrRNA-F/*R*	CCATGCCGCGTGAATGA	58	Detection the transcription of 16SrRNA
	TTCCTCGCTACCGAAAGAACTT		
ftsE-EMSA-F/*R*	CGCCTTTATAAGCTTTACTTACATT	151	Amplification of *ftsE* promoter region for EMSA
	TTATTCGAACACGAAGAATAGCAAT		
ftsY-EMSA-F/*R*	GTATGTTGTTCGGTTTGGA	303	Amplification of *ftsY* promoter region for EMSA
	TTTACTCGGTCGGTGGT		
rpoE-EMSA-F/*R*	TAAAAAGATAAGATAAGCGGTC	273	Amplification of *rpoE* promoter region for EMSA
	AGTGTGTAACAAAAATGAAAAGT		
rpoD-EMSA-F/*R*	GCGGAAGAAAAGCAAGAGTTGGTCA	151	Amplification of *rpoD* promoter region for EMSA
	TCCATAATTGTATCCGTTTTGTGTG		
ftsEX-F/R	CCGCTCGAGACACGAAGAATAGCAATGATTACAA	1737	Amplification of *ftsEX* genes for GFP-*ftsEX* plasmid
	AGCAAGGTCATCTCAGAAATGGTACCGTATTTGGAACCGATTCGGAAT		
GFP-F/R	AGCAAGGTCATCTCAGAAATGGTACCAGTAAAGGAGAAGAACTTTTCAC	2,257	Amplification of GFP gene for GFP-*ftsEX* plasmid
	AAGGAAAAAAGCGGCCGCTTATTTGTATAGTTCATCCATGCC		
IPTG-*ftsEX*-F/*R*	CGGGGTACC AATAGTAGAAAAGGTAAACATAATG	1,650	Expression of *ftsEX* with the inducing of IPTG
	CGGGGTACC AATAGTAGAAAAGGTAAACATAATG		

extracted using Total RNA Extractor kit (Sangon Biotech, China) according to the manufacturer's instruction. DNA impurity was eliminated using DNase I kit (Vazyme, China) according to instruction. To determine the quality, the RNA was electrophoresed on a 1% agarose gel. cDNA was synthesized using reverse transcriptase from Vazyme. Quantitative Real-Time PCR was performed using Real-Time Quantitative PCR detecting System and SYBR qPCR Mix (Vazyme, China). 16S RNA was used as the endogenous control to normalize expression of target genes. The $2^{-\Delta\Delta Ct}$ method was used to calculate and analyze relative expression level of mRNA (Livak and Schmittgen, 2001). RT-PCR across the *cdd-ftsX*, *ftsX-ftsE*, *ftsE-ftsY*, and *ftsY-rsmD* junctions was performed as previously described (Liu et al., 2022a).

Construction of promoter-gfp repoter strains and promoter analyses

A *ftsE-gfp* fusion containing the *ftsE* promoter region and *gfp* gene, was cloned into the Xho I and Not I sites on the pJFF224-XN plasmid. Then, the *ftsE-gfp* reporter plasmid was electroporated into the wild-type S4074 and the Δ*cpxAR* mutant strain. *A. pleuropneumoniae* strains harboring a *ftsE-gfp* reporter plasmid were grown to an OD600 of 0.6 in TSB medium with or without the supplementation of 0.3 mM KCl. The cells were harvested and resuspended in 1 mL of 10 mM PBS. Luminescence was measured in the Spectramax iD3 microplate reader with excitation at 485 nm and emission at 535 nm.

Expression and purification of His-CpxR

The purification of CpxR was conducted as previously described (Liu et al., 2022b). The *E.coli* BL21 containing the expression vector pET30a-CpxR was used to express His-CpxR protein. Expression of His-CpxR was induced by IPTG (0.5 mM) at 16°C overnight, and bacteria were harvested by centrifuging at 12000 rpm for 10 min. The cell pellet was resuspended in binding buffer (50 mM Na_3PO_4, pH 7.4, 500 mM NaCl, 30 mM imidazole), and lysed by sonication. The soluble fraction of the lysate was added to nickel-nitrilotriacetic acid (Ni-NTA) agarose column and mixed on Multipurpose Shaker QB-206 for 3 h. After being washed with binding buffer, the His-CpxR protein was eluted with elution buffer (20 mM Tris–HCl, pH 7.4, 500 mM NaCl, 500 mM imidazole). The purified His-CpxR was then stored at −80°C until use.

Electrophoretic mobility shift assay

The promoter regions of target genes were amplified from the *A. pleuropneumoniae* S4074 genome and tagged with biotin using a EMSA Probe Biotin Labeling Kit (Beyotime, China). CpxR protein was phosphorylated by acetyl phosphate (Sigma, United States) (Pogliano et al., 1997). Biotin-labeled DNA probes (1 μM) were incubated at room temperature for 20 min with 0–4 pmol CpxR protein in binding buffer (Beyotime, China). The reaction mixtures were analyzed by 4% non-denaturing polyacrylamide gel electrophoresis and transferred to nylon membrane. Next, the band was detected using a Chemiluminescent EMSA Kit (Beyotime, China).

Statistical analysis

Experimental data were analyzed by Student's two-tailed t-tests using GraphPad Prism 7.0 (GraphPad lnc.), and shown as mean ± standard deviation (SD). Statistical significance was assumed at a p value of <0.05.

Results

Deletion of the cpxRA genes decreases the growth of *Actinobacillus pleuropneumoniae* under high-K^+ stress

To explore the role of CpxAR in bacterial adaptation to osmotic stress in *A. pleuropneumoniae*, we tested the growth traits of the wild-type S4074 and its *cpxRA* mutant strain grown in solid or liquid medium with or without the supplementation of 0.3 mM KCl or 0.3 mM NaCl. When the cells were grown in solid medium, the growth of the Δ*cpxRA* strain was markedly reduced with the supplementation of 0.3 mM KCl, but similar to that of the WT strain with the supplementation of 0.3 mM NaCl or normal medium (Figure 1A). Optical density and colony forming units showed that the growth rate of the Δ*cpxRA* strain was significantly lower than that of the WT strain when grown with the supplementation of 0.3 mM KCl (Figures 1B,C). These findings suggested that the growth defect of the mutant strain Δ*cpxRA* was significantly increased compared with that of WT and CΔ*cpxRA* strains under high-K^+ stress. These results suggested that CpxAR contributes to *A. pleuropneumoniae* survival under high potassium stress.

Deletion of cpxRA affects the cell division of *Actinobacillus pleuropneumoniae* under high-K^+ stress

To further investigate how the inactivation of *cpxRA* genes affected the growth of *A. pleuropneumoniae* under high-K^+ stress, we used scanning electron microscope (SEM) to observe the bacterial morphology of the WT, Δ*cpxRA* and CΔ*cpxRA* strains when they were grown with or without the supplementation of 0.3 mM KCl. When grown with the supplementation of 0.3 mM KCl, the cell length of Δ*cpxRA* strain showed a 2-fold increase on average compared to the wild-type and CΔ*cpxRA* strains (Figures 2A,B). In addition, we found that the cell length of Δ*cpxRA* strain was also longer than that of the wild-type and CΔ*cpxRA* strains without K^+ stress, but the difference was much smaller than that under K^+ stress (Figures 2A,B). Together, these findings suggested that CpxAR regulates cell division to help *A. pleuropneumoniae* cope with potassium stress.

CpxAR regulates the expression of cell division genes ftsE and ftsX under high-K^+ stress

To gain insight into the mechanism of CpxAR affecting the cell division of *A. pleuropneumoniae*, we compared the transcript levels of cell division genes in the WT and Δ*cpxRA* strains by qRT-PCR. As shown in Figure 3A, the relative transcript levels of *ftsE* and *ftsX* were significantly downregulated in the Δ*cpxRA* strain with or without the supplementation of 0.3 mM KCl, but *ftsY* was not (Figure 3A). However, there were no significant changes in the cell division genes *ftsL*, *ftsI*, *ftsW*, *ftsQ*, *ftsZ*, *ftsB*, *ftsA*, *zipA*, *ftsH*, and *ftsK* in the Δ*cpxRA* strain compared with the WT strain (Supplementary Figure S1).These results suggested that CpxAR regulates the expression of the cell division genes *ftsE* and *ftsX* in *A. pleuropneumoniae*.

The cell division genes *ftsY*, *ftsE*, and *ftsX* are adjacent on the *A. pleuropneumoniae* chromosome (Figure 3B). To characterize the *ftsYEX* locus, we performed RT-PCR across the *cdd-ftsX*, *ftsX-ftsE*, *ftsE-ftsY*, and *ftsY-rsmD* junctions. The RT-PCR analysis indicated that the *ftsY*, *ftsE*, and *ftsX* genes are co-transcribed as a single mRNA and comprise an operon. To verify whether the *ftsEX* operon contributes to *A. pleuropneumoniae* survival under high-K^+ stress,

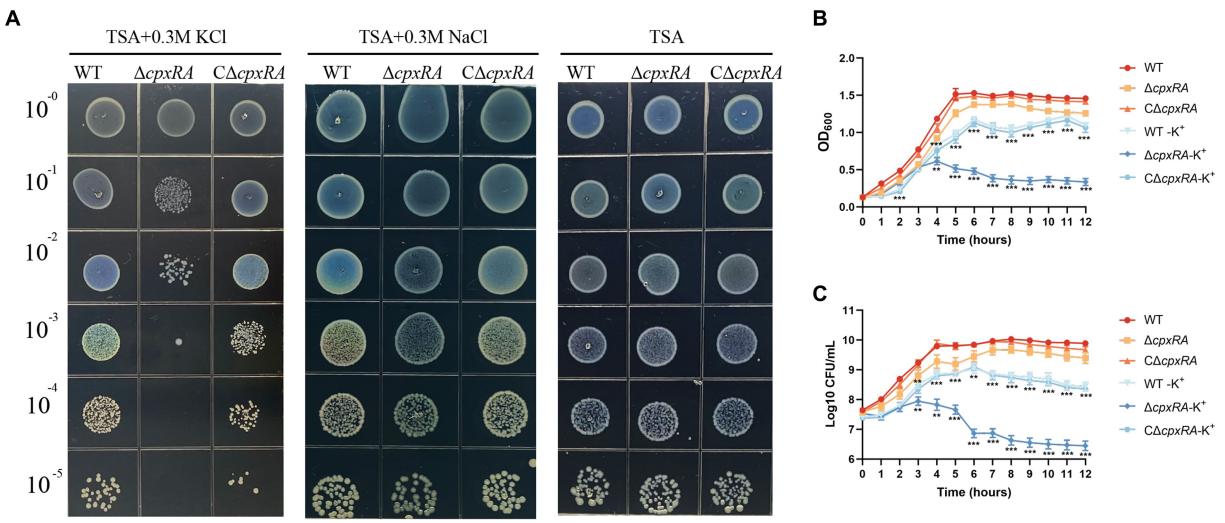

FIGURE 1
CpxAR is required for growth under high-K^+ stress. The growth traits of the WT, Δ*cpxRA* and CΔ*cpxRA* strains with or without 0.3 mM K^+ or 0.3 mM Na^+ were monitored by measurement of spotting on TSA plates **(A)**, OD600 **(B)**, and viable cell counts **(C)**. $^{**}p < 0.01$. $^{***}p < 0.001$.

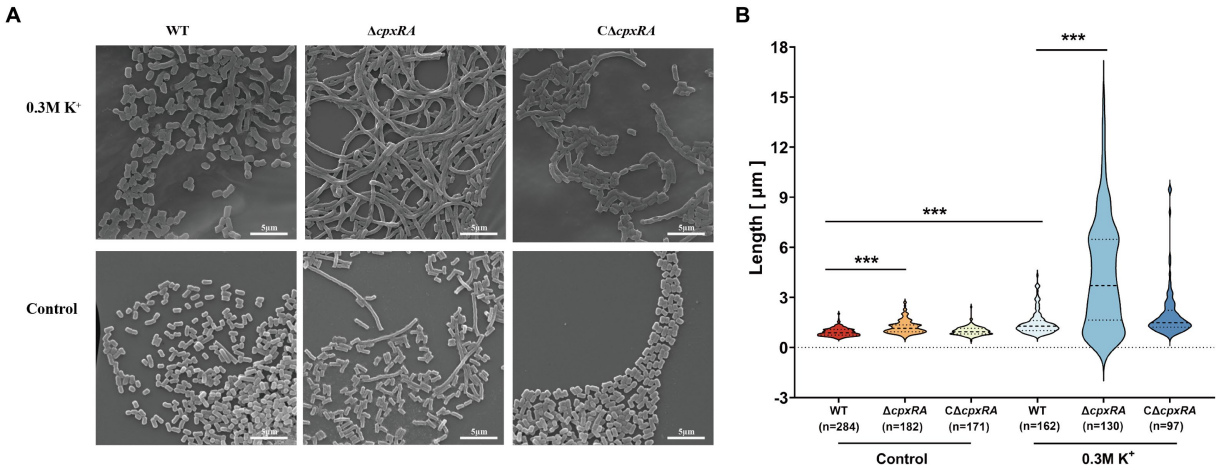

FIGURE 2
CpxAR impacts cell division under high-K^+ stress. **(A)** Observation of bacterial length in the WT, Δ*cpxRA*, and CΔ*cpxRA* strains grown with or without 0.3 mM K^+ by SEM. **(B)** Bacterial length measured for the WT, Δ*cpxRA* and CΔ*cpxRA* strains grown with or without 0.3 mM K^+. The number of bacteria measured is shown in brackets. $^{***}p < 0.001$.

the growth of Δ*cpxRA*/P*ftsEX* was assayed. When the expression of FtsE and FtsX increased with the increase of IPTG concentration, the growth defects of the Δ*cpxRA* strain were significantly rescued (Figure 3C). These observations indicated that the *ftsEX* operon plays an important role in *A. pleuropneumoniae* response to high-K^+ stress.

Here, the prediction results (BDGP)[1] showed that the *ftsYEX* operon has two putative promoter regions, respectively, located upstream of *ftsY* and *ftsE*. To explore the mechanism by which CpxR regulates the *ftsYEX* operon expression, we tested whether CpxR-P binds to the promoter regions of *ftsY* and *ftsE* using gel shift analysis. EMSA analysis showed that CpxR was capable to bind with the promoter regions of *ftsE* and *rpoE* (positive control), but not to the promoter regions of *ftsY* and *rpoD* (negative control) (Figure 3D). In addition, EMSAs showed that phosphorylated CpxR did not bind to the promoter sequence of *ftsE* when 200X of unlabeled probes were added (Figure 3E). To examine the link between CpxR and the expression of the *ftsEX* operon, the GFP reporter strains for *ftsE* gene promoter were constructed. As shown in Figures 3F,G, fluorescence intensities and confocal microscopy analysis showed that the transcrition activity of the promoter was significantly decreased in Δ*cpxRA* strain with or without high-K^+ stress. Together, these data demonstrated that CpxAR directly regulates the expression of *ftsEX* operon.

1 https://www.fruitfly.org/seq_tools/promoter.html

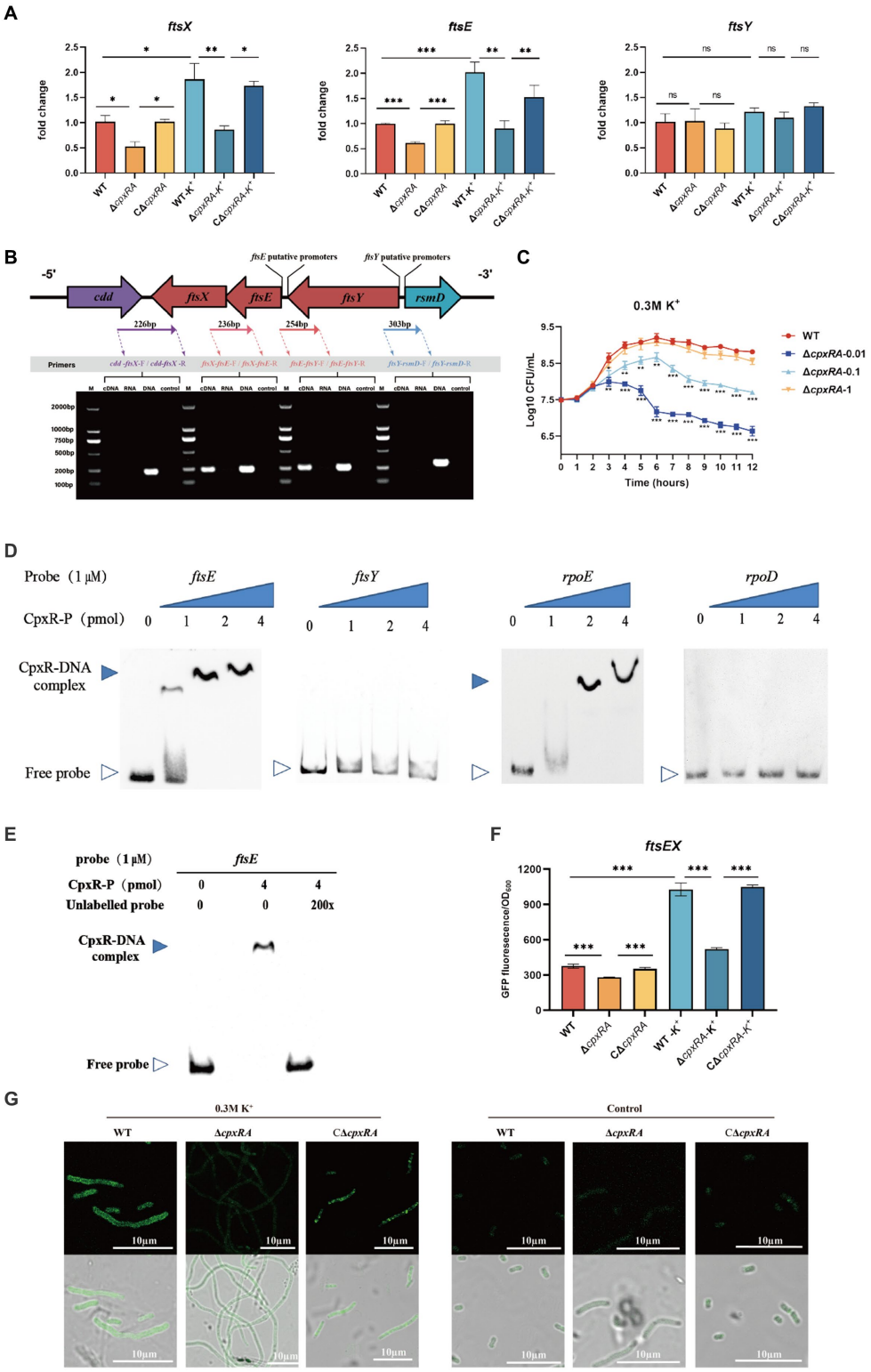

FIGURE 3
CpxAR regulates the expression of cell division genes *ftsE* and *ftsX*. **(A)** qRT-PCR analysis of *ftsE*, *ftsX*, and *ftsY* in WT, Δ*cpxRA*, and CΔ*cpxRA* strains. **(B)** Schematics of organization of genes encoding the cell division proteins. Transcriptional characteristics of the *ftsE*, *ftsX*, and *ftsY* genes measured by RT-PCR. Lane 1, cDNA; lane 2, RNA; lane 3, DNA; and lane 4, negative control. **(C)** The growth analysis of strains expressing *ftsEX* with IPTG at indicated concentrations. **(D)** EMSA analysis of the binding of phosphorylated CpxR to the promoters of *ftsE*, *ftsY*, *rpoE*, and *rpoD*. *rpoE* and *rpoD* served, respectively, as positive and negative control. **(E)** EMSA analysis of the binding of purified CpxR to *ftsE* with or without unlabeled DNA probe. The promoter activity of *ftsE* gene in the WT and Δ*cpxRA* strains was analized by fluorescent microscopy **(F)** and measurement of relative fluorescence units **(G)**. $*p < 0.05$. $**p < 0.01$. $***p < 0.001$.

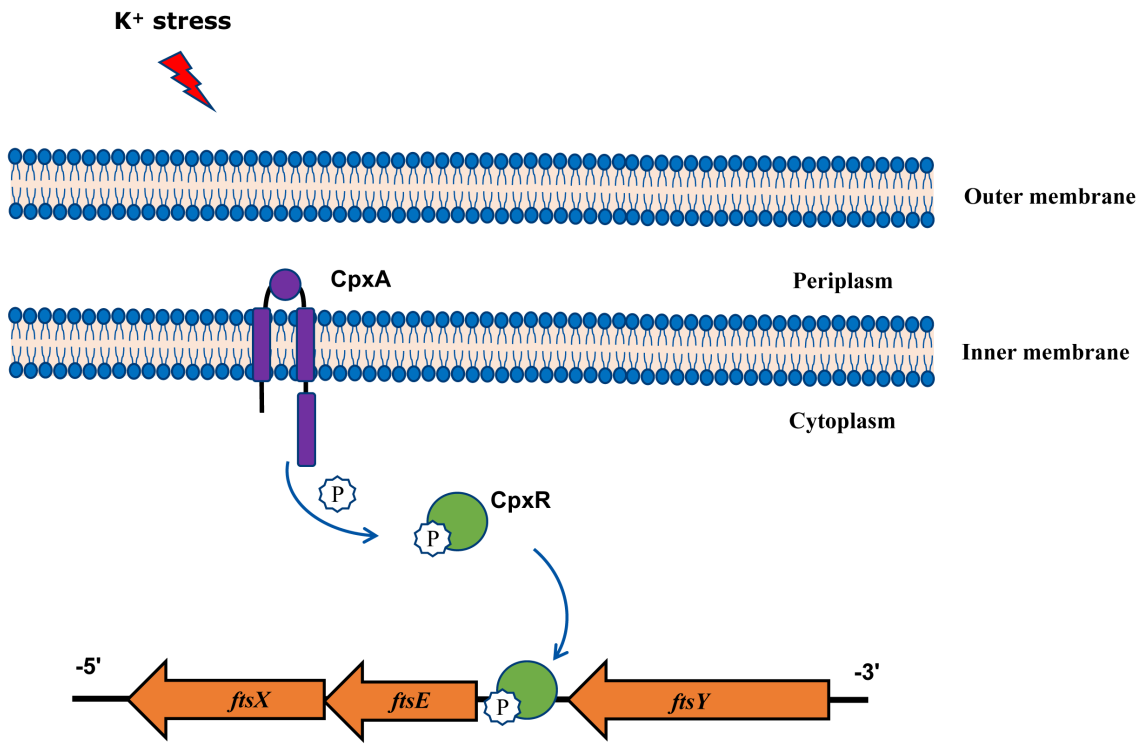

FIGURE 4
Model of CpxAR-*ftsEX* regulatory circuit in *A. pleuropneumoniae*. The high-K+ stress activates the TCS CpxAR which directly induces expression of the *ftsEX* operon.

Discussion

The two-component system is an important group of signal transduction systems in bacteria that interacts with sudden stimulus and responds accordingly to survive in adverse environment (Zhao et al., 2022). Prototypical TCS is composed of a membrane-bound sensor kinase and a cytoplasmic response regulator (Eguchi and Utsumi, 2008). In these systems, the histidine kinase will autophosphorylate when sensing a stimulus, and transfers the phosphoryl group to the response regulator, which then regulates the expression of specific genes by binding these promoters. Previous studies showed that CpxAR plays multiple regulatory roles in *A. pleuropneumoniae* virulence, biofilm formation and stress resistance (Yan et al., 2020). However, the function of the CpxAR system adaptation to other surrounding stresses remains unknown.

Potassium is the major cation in the cytoplasm for bacteria, which is essential for providing turgor pressure for cell growth and division (Sweet et al., 2021). When external K^+ concentrations are high, bacteria adjust their survival by maintaining cellular K^+ homeostasis. However, the mechanism of bacterial survival under high-K^+ stress requires further exploration. In this study, the growth rate of WT strain under K+ stress was significantly lower than that of strain without K+ stress, indicating that high-K^+ stress inhibits cell growth and division of *A. pleuropneumoniae*. Furthermore, we showed that the CpxAR system plays an important role in growth and division of *A. pleuropneumoniae* during high-K^+ stress.

FtsEX is a putative ABC transporter type complex that facilitates the assembly of division proteins and other proteins to the cytoplasmic membrane and is thought to play an important role in cell division (Schmidt et al., 2004; Reddy, 2007). In *E. coli*, disruption of the *ftsE* gene prevents the localization of the K^+-pump proteins to the inner membrane (Ukai et al., 1998). In the present study, qRT-PCR analysis showed that cell division genes *ftsE* and *ftsX* are controlled by CpxAR in *A. pleuropneumoniae*. Indeed, it seemed that FtsE and FtsX are related to the mechanism of CpxAR-mediated potassium stress. In *E. coli*, cell division genes *ftsY*, *ftsE*, and *ftsX* comprise an operon (Gill et al., 1986), which is consistent with our RT-PCR analysis in *A. pleuropneumoniae*. But, we found that the *ftsYEX* operon in *A. pleuropneumoniae* contains two promoter regions by sequence analysis, oneupstream of *ftsY* and the other upstream of *ftsE*.

Previous studies have shown that CpxR can regulate the transcription of a wide range of genes by directly binding to their promoter regions (De Wulf et al., 2002; Vogt and Raivio, 2012). Here, EMSA analysis showed that CpxR can directly interact with *ftsE* promoter. Combined with qRT-PCR analysis, these results confirmed that the *ftsEX* operon is directly and positively regulated by the CpxAR system.

In summary, our findings gain new and important insights into the function of *A. pleuropneumoniae* CpxAR in response to extreme environments, and show that the CpxAR system directly regulates cell division genes to maintain potassium homeostasis (Figure 4). Because the CpxAR system is ubiquitous in many bacteria, our study contribute to the understanding of bacterial environmental adaptability. Future studies will aim to identify more CpxR-regulated genes, which could expand the knowledge of CpxAR function.

Data availability statement

The original contributions presented in the study are included in the article/Supplementary material, further inquiries can be directed to the corresponding author.

Author contributions

JW: Data curation, Investigation, Project administration, Software, Writing – original draft. RZ: Investigation, Writing – original draft. YJ: Investigation, Writing – original draft. TX: Investigation, Writing – original draft. LD: Investigation, Writing – original draft. QY: Investigation, Writing – original draft. WZ: Investigation, Writing – original draft. HX: Investigation, Writing – original draft. XG: Software, Supervision, Writing – original draft. JH: Writing – review & editing. WB: Funding acquisition, Resources, Supervision, Writing – original draft. FL: Conceptualization, Formal analysis, Funding acquisition, Methodology, Supervision, Writing – original draft, Writing – review & editing.

Funding

The author(s) declare financial support was received for the research, authorship, and/or publication of this article. This research was supported by the National Natural Science Foundation of China (32002252) and National Key Research and Development Program of China (2022YFD1800905).

Conflict of interest

The authors declare that the research was conducted in the absence of any commercial or financial relationships that could be construed as a potential conflict of interest.

Publisher's note

All claims expressed in this article are solely those of the authors and do not necessarily represent those of their affiliated organizations, or those of the publisher, the editors and the reviewers. Any product that may be evaluated in this article, or claim that may be made by its manufacturer, is not guaranteed or endorsed by the publisher.

Supplementary material

The Supplementary material for this article can be found online at: https://www.frontiersin.org/articles/10.3389/fmicb.2023.1259935/full#supplementary-material

References

Ballal, A., Basu, B., and Apte, S. K. (2007). The Kdp-ATPase system and its regulation. *J. Biosci.* 32, 559–568. doi: 10.1007/s12038-007-0055-7

De Wulf, P., McGuire, A. M., Liu, X., and Lin, E. C. (2002). Genome-wide profiling of promoter recognition by the two-component response regulator CpxR-P in *Escherichia coli*. *J. Biol. Chem.* 277, 26652–26661. doi: 10.1074/jbc.M203487200

Eguchi, Y., and Utsumi, R. (2008). Introduction to bacterial signal transduction networks. *Adv. Exp. Med. Biol.* 631, 1–6. doi: 10.1007/978-0-387-78885-2_1

Frey, J. (1995). Virulence in Actinobacillus pleuropneumoniae and RTX toxins. *Trends Microbiol.* 3, 257–261. doi: 10.1016/s0966-842x(00)88939-8

Gill, D. R., Hatfull, G. F., and Salmond, G. P. (1986). A new cell division operon in *Escherichia coli*. *Mol. Gen. Genet.* 205, 134–145. doi: 10.1007/BF02428043

Li, H., Liu, F., Peng, W., Yan, K., Zhao, H., Liu, T., et al. (2018). The CpxA/CpxR two-component system affects biofilm formation and virulence in *Actinobacillus pleuropneumoniae*. *Front. Cell. Infect. Microbiol.* 8:72. doi: 10.3389/fcimb.2018.00072

Liu, F., Peng, W., Yan, K., Huang, J., Yuan, F., He, Q., et al. (2022a). CpxAR of *Actinobacillus pleuropneumoniae* contributes to heat stress response by repressing expression of type IV pilus gene apfA. *Microbiol Spectr* 10:e0252322. doi: 10.1128/spectrum.02523-22

Liu, F., Yao, Q., Huang, J., Wan, J., Xie, T., Gao, X., et al. (2022b). The two-component system CpxA/CpxR is critical for full virulence in *Actinobacillus pleuropneumoniae*. *Front. Microbiol.* 13:1029426. doi: 10.3389/fmicb.2022.1029426

Livak, K. J., and Schmittgen, T. D. (2001). Analysis of relative gene expression data using real-time quantitative PCR and the 2(-Delta Delta C(T)) method. *Methods* 25, 402–408. doi: 10.1006/meth.2001.1262

Mir, M. A., Arumugam, M., Mondal, S., Rajeswari, H. S., Ramakumar, S., and Ajitkumar, P. (2015). *Mycobacterium tuberculosis* cell division protein, FtsE, is an ATPase in dimeric form. *Protein J.* 34, 35–47. doi: 10.1007/s10930-014-9593-7

Pattison, I. H., Howell, D. G., and Elliot, J. (1957). A haemophilus-like organism isolated from pig lung and the associated pneumonic lesions. *J. Comp. Pathol.* 67, 320–IN37. doi: 10.1016/s0368-1742(57)80031-9

Pogliano, J., Lynch, A. S., Belin, D., Lin, E. C., and Beckwith, J. (1997). Regulation of *Escherichia coli* cell envelope proteins involved in protein folding and degradation by the Cpx two-component system. *Genes Dev.* 11, 1169–1182. doi: 10.1101/gad.11.9.1169

Reddy, M. (2007). Role of FtsEX in cell division of *Escherichia coli*: viability of ftsEX mutants is dependent on functional SufI or high osmotic strength. *J. Bacteriol.* 189, 98–108. doi: 10.1128/JB.01347-06

Sassu, E. L., Bosse, J. T., Tobias, T. J., Gottschalk, M., Langford, P. R., and Hennig-Pauka, I. (2018). Update on *Actinobacillus pleuropneumoniae*-knowledge, gaps and challenges. *Transbound. Emerg. Dis.* 65, 72–90. doi: 10.1111/tbed.12739

Scherrer, S., Peterhans, S., Neupert, C., Rademacher, F., Bartolomei, G., Sidler, X., et al. (2022). Development of a novel high resolution melting assay for identification and differentiation of all known 19 serovars of *Actinobacillus pleuropneumoniae*. *Microbiology* 11:e1272. doi: 10.1002/mbo3.1272

Schmidt, K. L., Peterson, N. D., Kustusch, R. J., Wissel, M. C., Graham, B., Phillips, G. J., et al. (2004). A predicted ABC transporter, FtsEX, is needed for cell division in *Escherichia coli*. *J. Bacteriol.* 186, 785–793. doi: 10.1128/JB.186.3.785-793.2004

Stautz, J., Hellmich, Y., Fuss, M. F., Silberberg, J. M., Devlin, J. R., Stockbridge, R. B., et al. (2021). Molecular mechanisms for bacterial potassium homeostasis. *J. Mol. Biol.* 433:166968. doi: 10.1016/j.jmb.2021.166968

Stringer, O. W., Bosse, J. T., Lacouture, S., Gottschalk, M., Fodor, L., Angen, O., et al. (2021). Proposal of *Actinobacillus pleuropneumoniae* serovar 19, and reformulation of previous multiplex PCRs for capsule-specific typing of all known serovars. *Vet. Microbiol.* 255:109021. doi: 10.1016/j.vetmic.2021.109021

Sweet, M. E., Larsen, C., Zhang, X., Schlame, M., Pedersen, B. P., and Stokes, D. L. (2021). Structural basis for potassium transport in prokaryotes by KdpFABC. *Proc. Natl. Acad. Sci. U. S. A.* 118:e2105195118. doi: 10.1073/pnas.2105195118

Ukai, H., Matsuzawa, H., Ito, K., Yamada, M., and Nishimura, A. (1998). ftsE(Ts) affects translocation of K+-pump proteins into the cytoplasmic membrane of *Escherichia coli*. *J. Bacteriol.* 180, 3663–3670. doi: 10.1128/JB.180.14.3663-3670.1998

Vogt, S. L., and Raivio, T. L. (2012). Just scratching the surface: an expanding view of the Cpx envelope stress response. *FEMS Microbiol. Lett.* 326, 2–11. doi: 10.1111/j.1574-6968.2011.02406.x

Xu, Z., Zhou, Y., Li, L., Zhou, R., Xiao, S., Wan, Y., et al. (2008). Genome biology of *Actinobacillus pleuropneumoniae* JL03, an isolate of serotype 3 prevalent in China. *PLoS One* 3:e1450. doi: 10.1371/journal.pone.0001450

Yan, K., Liu, T., Duan, B., Liu, F., Cao, M., Peng, W., et al. (2020). The CpxAR two-component system contributes to growth, stress resistance, and virulence of *Actinobacillus pleuropneumoniae* by upregulating wecA transcription. *Front. Microbiol.* 11:1026. doi: 10.3389/fmicb.2020.01026

Yao, Q., Xie, T., Fu, Y., Wan, J., Zhang, W., Gao, X., et al. (2022). The CpxA/CpxR two-component system mediates regulation of *Actinobacillus pleuropneumoniae* cold growth. *Front. Microbiol.* 13:1079390. doi: 10.3389/fmicb.2022.1079390

Zhao, Z., Xu, Y., Jiang, B., Qi, Q., Tang, Y. J., Xian, M., et al. (2022). Systematic identification of CpxRA-regulated genes and their roles in *Escherichia coli* stress response. *mSystems* 7:e0041922. doi: 10.1128/msystems.00419-22

Zschiedrich, C. P., Keidel, V., and Szurmant, H. (2016). Molecular mechanisms of two-component signal transduction. *J. Mol. Biol.* 428, 3752–3775. doi: 10.1016/j.jmb.2016.08.003

frontiers | Frontiers in Microbiology

TYPE Original Research
PUBLISHED 12 October 2023
DOI 10.3389/fmicb.2023.1266583

Check for updates

OPEN ACCESS

EDITED BY
Hong Yin,
Chinese Academy of Agricultural Sciences, China

REVIEWED BY
Rocio Checa,
Complutense University of Madrid, Spain
Lachhman Das Singla,
Guru Angad Dev Veterinary and Animal Sciences University, India

*CORRESPONDENCE
Lin Zhan
✉ zhanlin300@hotmail.com
Jiahong Wu
✉ jiahongw@gmc.edu.cn

†These authors have contributed equally to this work

RECEIVED 25 July 2023
ACCEPTED 25 September 2023
PUBLISHED 12 October 2023

CITATION
Wu S, Meng J, Yu F, Zhou C, Yang B, Chen X, Yang G, Sun Y, Cao W, Jiang J, Wu J and Zhan L (2023) Molecular epidemiological investigation of piroplasms carried by pet cats and dogs in an animal hospital in Guiyang, China.
Front. Microbiol. 14:1266583.
doi: 10.3389/fmicb.2023.1266583

COPYRIGHT
© 2023 Wu, Meng, Yu, Zhou, Yang, Chen, Yang, Sun, Cao, Jiang, Wu and Zhan. This is an open-access article distributed under the terms of the Creative Commons Attribution License (CC BY). The use, distribution or reproduction in other forums is permitted, provided the original author(s) and the copyright owner(s) are credited and that the original publication in this journal is cited, in accordance with accepted academic practice. No use, distribution or reproduction is permitted which does not comply with these terms.

Molecular epidemiological investigation of piroplasms carried by pet cats and dogs in an animal hospital in Guiyang, China

Shengchun Wu[1†], Jiao Meng[1†], Fuxun Yu[2], Caomin Zhou[3], Bin Yang[2], Xingxing Chen[2], Guanghong Yang[4], Yi Sun[5], Wuchun Cao[5], Jiafu Jiang[5], Jiahong Wu[1*] and Lin Zhan[2*]

[1]School of Public Health, The Key Laboratory of Environmental Pollution Monitoring and Disease Control, Ministry of Education, Guizhou Medical University, Guiyang, China, [2]NHC Key Laboratory of Pulmonary Immune-related Diseases, Guizhou Provincial People's Hospital, Guiyang, China, [3]Renal Division, Department of Medicine, Guizhou Provincial People's Hospital, Guizhou Provincial Institute of Nephritic and Urinary Disease, Guiyang, China, [4]Guizhou Center for Disease Control and Prevention, Guiyang, China, [5]Beijing Institute of Microbiology and Epidemiology, Academy of Military Medical Sciences, Beijing, China

Piroplasmosis is a zoonotic disease mainly caused by the *Babesia* and *Theileria* parasites. Piroplasmosis is often a subclinical infection in dogs and cats that is difficult to detect and is often suspected when clinical signs such as anemia are present. It has been reported to be prevalent in China. However, molecular evidence of the disease has not been reported in pet dogs and cats in Guiyang. In this study, we collected 307 anticoagulated blood samples from an animal hospital in the Wudang District of Guiyang during the period March 2021 to November 2021 and extracted DNA from the samples. The 18S rDNA gene was amplified using PCR, and the positive amplification product was sequenced. The sequences were then analyzed for homology and phylogeny. Of the 307 samples collected, 164 were feline and 143 were canine, with a total of 23 amplifying a target band of approximately 400 bp. The percentage of positives of piroplasms infection in pet cats was 4.27% (7/164), with the pathogens being *T. uilenbergi* (3) and *T. luwenshuni* (4). One *Colpodella* sp. and two undetermined species were also detected in the cat samples. The percentage of positives of piroplasms infection in pet dogs was 7.69% (11/143), with the pathogen being *T. uilenbergi* (11). One *Colpodella* sp. was also detected in the dog samples. The results confirmed that *T. uilenbergi* and *T. luwenshuni* are prevalent in pet cats and dogs in this area. In addition, the study found a rare zoonotic pathogen, *Colpodella* sp., in cats and dogs. Therefore, this study is expected to serve as a valuable reference for decision-making regarding animal health management and public health work.

KEYWORDS

dog, cat, phylogenetic studies, piroplasms, *Theileria uilenbergi*, *Theileria luwenshuni*, *Colpodella*, Guizhou

1. Introduction

Piroplasms belong to the phylum Apicomplexa, class Piroplasmea, and order Piroplasmida and include the genera *Babesia* and *Theileria*. They are an order of protozoan parasites that live in macrophages, lymphocytes and red blood cells. Piroplasmosis is a human-animal infectious disease caused by piroplasms (Zhang and Li, 2010), with the main clinical symptoms being fever, anemia and swollen lymph nodes. *Babesia* is widely distributed around the world, and its onset often lacks typical symptoms, making it easy to misdiagnose or overlook. In recent years, the number of reported human cases has been increasing, with the United States, Canada and China having the most reported cases (Yang et al., 2021). The *Babesia* species that most often infect humans are *B. microti*, *B. venatorum*, *B. duncani*, and *B. divergens* (Ord and Lobo, 2015). *Theileria* species are mainly pathogenic to animals and cause serious losses in the livestock industry. Liu et al. (2010) detected *Theileria* sp. in the blood of a hospitalized patient in Suizhou City, Hubei Province (NCBI Accession: HQ844673.1). Although the paper has not yet been published, this finding suggests that *Theileria* sp. may be infectious to humans. Since there are relatively few studies on human *Theileria* infections in China, its study should not be neglected. At this time, none of the canine piroplasm species are zoonotic.

As living standards improve, pet ownership is becoming a normal part of life. Piroplasmosis in dogs and cats can be a chronic or subclinical infection, or it can be a severe acute disease in which the death of infected animals may occur (Irwin and Hutchinson, 1991). When piroplasmosis occurs a subclinical infection in dogs and cats, it is difficult to detect. It is often discovered due to clinical signs such as anemia, fever and lethargy. For example, 36 cases of *B. gibsoni* were seen in a veterinary hospital in Xi'an, and the signs and symptoms were mainly fever, yellow urine and decreased red blood cells and platelets (Feng et al., 2021). Blood transfusions can have an immediate effect, but they are expensive and there is often a shortage of blood available. Therefore, early identification of the pathogen facilitates the diagnosis and treatment of the disease, reducing the animal's suffering as well as the medical burden.

However, there are no reports of piroplasmosis in dogs or cats in Guiyang, southwestern China. Therefore, this study aims to investigate the percentage of infections in pet cats and dogs in an animal hospital in Guiyang, and to provide a scientific basis for the prevention and control of piroplasms infections in pets in the region.

2. Materials and methods

2.1. Sample collection and ethics statement

From March 2021 to November 2021, the anticoagulated blood samples were collected from pet cats and dogs attending an animal hospital in Guiyang, China. The blood samples were stored in EDTA anticoagulation tubes, randomly numbered and then stored at 4°C for later use. For practical reasons, we were unable to obtain basic information about the animals (age, sex, etc.), geographic location of residence, and clinical data information.

This study was approved by the Animal Care Welfare Committee of Guizhou Medical University (Ethical approval number: 2305072). All animals were handled in accordance with the Animal Ethics Procedures and Guidelines of the People's Republic of China. Informed consent was obtained from pet owners to acquire the anticoagulated blood samples from the animals.

2.2. Genomic DNA extraction

Nucleic acids were extracted from 200 μL of blood using the qEx-DNA/RNA Virus Kit (Xi'an Tianlong Science and Technology, Xi'an, China) according to the instructions, and then stored in a refrigerator at −20°C until PCR.

2.3. PCR amplification of the piroplasm 18S rDNA gene

PCR amplification was performed on all genomic DNA samples using the 18S rDNA gene nesting primers for piroplasm parasites (National Health Commission of the People's Republic of China, 2017). A total volume of 25 μl was used for PCR amplification, which included 2.5 μl of 10 × PCR buffer, 2 μl of 2.5 mM dNTP Mixture, 0.5 μl of each primer (10 μM/L), 0.125 μl of Taq polymerase (5 U/μl) (Takara Biotechnology, China), 1 μl of extracted genomic DNA, and double-distilled water to fill the remainder. Genomic DNA from *B. bigemina* stored in our laboratory and sterile double-distilled water were used as positive and negative controls, respectively. The first round of nested PCR reaction procedures included pre-denaturation at 96°C for 2 min, denaturation at 94°C for 30 s, annealing at 54°C for 30 s, extension at 72°C for 40 s, a total of 35 cycles, and a final extension at 72°C for 5 min. The reaction conditions for the second round of Nestor PCR were the same as the reaction procedure for the first round, except that the annealing temperature was changed to 57°C. Finally, 5 μL of PCR products from all samples were taken and subjected to 1.5% agarose gels treated with 4S Green nucleotide stain (Sangon Biotech), and the results were observed using a gel imager (Bio-Rad).

2.4. Sequencing and phylogenetic analysis

The PCR products with amplified target bands were sent to BGI-Chongqing for bi-directional sequencing and sequence splicing. The obtained sequences were aligned with the sequences of registered genes in GenBank using the BLAST tool on the National Center for Biotechnology Information (NCBI) website. After identifying the species, multiple sequence alignments with related genes were conducted using DNAMAN (version 6.0, Lynnon Corporation, Canada) software and representative DNA sequences were taken. The reference sequences were also downloaded from the GenBank database. Representative sequences were selected for evolutionary tree construction, with *Plasmodium berghei* (NCBI Accession: AZ522148.1) and *P. falciparum* (NCBI Accession:

10.3389/fmicb.2023.1266583

DK896461.1) as outgroups. MEGA (version 7.0)[1] software was used to construct a phylogenetic evolutionary tree using the neighbor-joining method and self-extension test 1,000 times for genetic evolutionary analysis.

3. Result

3.1. Prevalence of piroplasms in pets

A total of 307 anticoagulated blood samples were collected, including 164 pet cat samples and 143 pet dog samples. A total of 11 (6.7%) positive amplifications were obtained from the 164 pet cat blood samples, and 12 (8.4%) positives were obtained from 143 pet dog blood samples.

3.2. Genetic evolutionary analysis

A total of 22 target amplicon were successfully sequenced with BLAST homology matching, the piroplasms were sequenced as *T. uilenbergi* (14), *T. luwenshuni* (4) and *Colpodella* sp. (2), with the remaining two sequenced as other eukaryotes (Uncultured *Baldinia* and the Uncultured eukaryote). Specifically, pet cats were found to have *T. uilenbergi* (3), *T. luwenshuni* (4), *Colpodella* sp. (1), Uncultured *Baldinia* (1), and Uncultured eukaryote (1) (Table 1). All sequences were deposited in GenBank (Table 2). The sequences of *T. uilenbergi*, *T. luwenshuni*, *Colpodella* sp., Uncultured *Baldinia*, and Uncultured eukaryote genes detected in the cat samples were the closest to *T. uilenbergi* (NCBI Accession: MG940889.1), *T. luwenshuni* (NCBI Accession: MK685118.1), *Colpodella* sp. (NCBI Accession: JX624256.1), *Uncultured Baldinia clone* (NCBI Accession: MF685332.1), and *Uncultured eukaryote* (NCBI Accession: KU820642.1) in the GenBank database, respectively, while their sequence identities were 100.00, 100.00, 98.23, 99.26, and 98.69%, respectively. In addition, pet dog blood samples were found to have *T. uilenbergi* (11) and *Colpodella* sp. (1). Their gene sequences were closest in the GenBank database to *T. uilenbergi* (NCBI Accession: MG940889.1) and *Colpodella* sp. (NCBI Accession: OQ540589.1) with sequence identities of 100.00 and 94.99%, respectively. The sequence identity of the two *Colpodella* sp. (NCBI Accession: OR226256 and OR226258) was 81.71%, and compared with the reference strain *Colpodella* sp. ATCC50594 strain (NCBI Accession: AY142075) isolated from soil in the United States, the sequence identity was 81.77 and 83.00%, respectively. The sequence of *Colpodella* sp. from cat samples (NCBI Accession: OR226256) was only 79.69%∼83.14% when compared with *Colpodella* sp. strains from suspected clinical cases in China (NCBI Accession: KT364261 and GQ411073), but the sequence identity with another suspected clinical case from China (NCBI Accession: MF594625) was as high as 99.60%. When the sequence of *Colpodella* sp. from dog samples (NCBI Accession: OR226258) was compared with the sequences of *Colpodella* sp. strains from suspected clinical cases (NCBI Accession: KT364261, GQ411073, and MF594625), the sequence identity was only 79.01∼84.39%.

The gene sequences of pet cats (NCBI Accession: OR016205) and pet dogs (NCBI Accession: OR016208) formed a clade with high homology to the sequences of *T. uilenbergi* infecting yaks in the Gansu region, *Dermacentor everestianus* in the Qinghai region, and *Haemaphysalis longicornis* in the Beijing region (NCBI Accession: MG799806.1, MG940889.1, and KC601647.1), with 99.73%∼100.00% homology. The gene sequences of pet cats (NCBI Accession: OR016425) were homopolymerized into a clade with 100.00% homology to the sequences of *T. luwenshuni* infecting sheep in Shandong (NCBI Accession: KJ850935.1) and the United Kingdom (NCBI Accession: KU234526.1). The above *Theileria* gene sequences were clustered with *T. cervi* sequences (NCBI Accession: KT863524.1 and KT863529.1) infecting Sika deer in the Jilin region of China, all of which were *T.* sp. The pet cat gene sequences (NCBI Accession: OR226256) clustered into a single clade with *Colpodellidae* sp. (NCBI Accession: MF594625.1) detected in the blood of a patient with relapsing fever in China, with 99.60% homology. However, pet cat gene sequences (NCBI Accession: OR226256) were distant from *Colpodella* sp. gene sequences detected in ticks (NCBI Accession: OQ540589), horses (NCBI Accession: MW261749), cattle (NCBI Accession: OL848461), and tigers (NCBI Accession: MN640809). The pet dog gene sequences (NCBI Accession: OR226258) clustered into a clade with *Colpodella* sp. (NCBI Accession: OQ540589.1) detected in *H. longicornis* from Yiyuan County, Shandong, China, with a homology of 94.99%. The pet dog gene sequences (NCBI Accession: OR226258) were distant from *Colpodella* sp. gene

TABLE 2 The NCBI Accession of this study gene sequences in GenBank.

NCBI accession	Species	Animals
OR016205	*T. uilenbergi*	Pet cats
OR016425	*T. luwenshuni*	Pet cats
OR226256	*Colpodella* sp.	Pet cats
OR226257	Uncultured *Baldinia*	Pet cats
OR226255	Uncultured eukaryote	Pet cats
OR016208	*T. uilenbergi*	Pet dogs
OR226258	*Colpodella* sp.	Pet dogs

TABLE 1 Different pets carry different numbers of protozoa.

Animals	sample size	*Theileria uilenbergi*	*Theileria luwenshuni*	*Colpodella sp.*	Uncultured *Baldinia*	Uncultured eukaryote
Pet cats	164	3	4	1	1	1
Pet dogs	143	11	—	1	—	—
Total	307	14	4	2	1	1

1 http://www.megasoftware.net/

sequences detected in humans (NCBI Accession: MF594625), horses (NCBI Accession: MW261749), cattle (NCBI Accession: OL848461) and tigers (NCBI Accession: MN640809). In addition, the studied sequences (NCBI Accession: OR226257 and OR226255) were clustered separately and not assigned to a eukaryotic group, occupying an evolutionary position between *Colpodella* sp. and *Theileria* (**Figure 1**).

4. Discussion

The percentage of positives of piroplasms infection in pet dogs in this study was 7.69% (11/143), which was higher than the prevalence of canine-origin piroplasm infections reported in Türkiye (0.13%, 2/757) (Aktas et al., 2015) and China's Hunan Province (4.30%, 5/115) (Wang J. et al., 2020). This may be related to the different geographic locations where the samples were collected, the sensitivity of the diagnostic technique used, and the different clinical statuses of the dogs studied. To the best of our knowledge, this study is the first to report the detection of *T. uilenbergi* in the blood of pet dogs in China. The common hosts of *T. uilenbergi* are sheep and deer (Mans et al., 2015), and host infections may present with fever, diarrhea, respiratory distress and enlarged lymph nodes. However, there are no reports on the pathology and symptoms of *T. uilenbergi* in dogs, and the clinical significance of this is not known. The vectors of *T. uilenbergi* have been confirmed to be *H. longicornis* and *H. qinghaiensis* (Li et al., 2009), and Xiang et al. (2022) reported that *H. longicornis* is the dominant tick species in Guizhou, which increases the likelihood of a *T. uilenbergi* epidemic in the area. The main piroplasms reported to infect dogs in China and abroad are *B. canis*, *B. vogeli*, *B. rossi*, *B. conradae*, *B. vulpes*, and *B. gibsoni* of the genus *Babesia* (Irwin, 2010; He et al., 2017; Niu et al., 2017). Although *Babesia* was not detected in the pet dog samples in this study, *Colpodella* sp. (NCBI Accession: OR226258) was detected in one dog sample, and its pathogenicity requires further investigation. The sequence from the pet dog (NCBI Accession: OR226258) was in close proximity to *Colpodella* sp. (NCBI Accession: MH012043, OQ540589, MH208619, and OQ540590) detected in ticks (**Figure 1**). This result suggests that ticks that may carry *Colpodella* sp. and could be screened for possible *Colpodella* sp. at this site in the future. The Wudang District of Guiyang has many natural scenic spots, and there are a number of parks with dense vegetation and rich ecology distributed around this hospital. When pet owners walk their dogs in the park, their dogs may be bitten by ticks when brushing against vegetation and may be infected with pathogens carried by ticks during the biting process, posing a threat to the animals' health.

The percentage of positives of blood piroplasms in pet cats in this study was 4.27% (7/164), which was lower than the 8.00% (2/25) infection rate reported in Hunan Province (Wang J. et al., 2020). In this study, the pet cat pathogens were more diverse, containing not only *T. uilenbergi*, but also *T. luwenshuni*, *Colpodella* sp. and two unknown species of gene sequences. Reports of piroplasm infections in domestic cats and wild felines include the species such as *B. felis*, *B. cati*, *B. leo*, *B. hongkongensis*, *B. gibsoni*, and *Cytauxzoon* sp. (Hartmann et al., 2013; Palmer et al., 2022; Yin et al., 2022), but there have been no reports on the detection of *T. uilenbergi* and *T. luwenshuni* in blood samples from pet cats. This may be related to the fact that piroplasm in cats is often an asymptomatic infection (Wong et al., 2012), resulting in a lack of research and underreporting. *T. uilenbergi* and *T. luwenshuni* are common *Theileria* in China and are the more pathogenic species (Hao, 2020). They are often found in mixed infections. Studies have reported that *T. luwenshuni* can infect a wide range of host animals, such as goats, sheep, deer and sheepdogs (Ge et al., 2012; Li et al., 2014; Gholami et al., 2016), and it is evident that it may have a wider distribution range. For example, Zhong et al. (2019) and Wang K. L. et al. (2020) investigated the infection of cattle and sheep with *T. luwenshuni* in Aba Prefecture, Sichuan Province and Linyou County, Shanxi Province and found that the infection rates were as high as 75.00 and 61.20%, respectively. The rare *Colpodella* sp., a tick-borne pathogen that has been detected in Qinghai Province (Hu et al., 2022), was also detected in the blood samples of pet cats. *Colpodella* sp. is also a zoonotic pathogen, with the first case of a *Colpodella* sp.-like pathogen infecting a human found in Kunming, Yuan et al. (2012). *Colpodella* sp. was also detected in horses from Jingxi and Napo, Guangxi (Xu et al., 2022; Zhou et al., 2022), as well as being recently detected in the blood of Amur tigers (Chiu et al., 2022). Cui (2013) also amplified *Colpodella* sp. sequences in the blood of febrile patients and in the cerebrospinal fluid of in-patients with neurological symptoms (Jiang et al., 2018). The cat sample *Colpodella* sp. sequence (NCBI Accession: OR226256) clustered with the reference strain ATCC50594 and was closer to the gene sequences of the currently published patients (NCBI Accession: MF594625), with a higher sequence identity (99.60%). The possibility of zoonotic disease transmission to humans in this region cannot be excluded. In this study, it should be noted that *Colpodella* is not a piroplasm. *Colpodella* is a sister group to an apicomplexan clade (Kuvardina et al., 2002). The initial aim of the study was to investigate blood carriage of piroplasms in cats and dogs with 18S rRNA amplification sequencing, but we inadvertently discovered *Colpodella*, which is a significant finding. Therefore, it is not unusual that *Colpodella* was amplified unintentionally with these common primers, which is similar to what has been observed in previous studies (Jiang et al., 2018; Xu et al., 2022). The *Colpodella* sp. pathogen and whether it can infect humans remains controversial and requires further confirmation. The taxonomic statuses of the gene sequences of two unknown species also need to be confirmed.

The PCR molecular biology technique used in this study addresses the morphological difficulty of distinguishing parasites in the blood when the quantity is low. It is able to accurately detect the presence of pathogens. However, there are some limitations to the study, which failed to collect basic information regarding the pet dogs and cats during the sample collection process and failed to analyze the epidemiological characteristics of the hosts in a comprehensive manner. According to the current detection results, the tick-borne pathogens *Theileria* and *Colpodella* sp. were found in the blood samples of dogs and cats. The data suggest that *Theileria* and *Colpodella* sp. were existent in dogs and cats in Guizhou. The *Theileria* and *Colpodella* sp. found in the study are different in their treatments. At the present stage, there is no highly efficient drug for the treatment of piroplasmosis caused by *T. uilenbergi* and *T. luwenshuni*, and the more commonly used drugs include Imidocarb, Diminazene Aceturate, Acriflavine, Atovaquone, Azithromycin, Clindamycin, Quinine, etc. (Hao, 2020). *Colpodella* has been reported in fewer cases in host animals

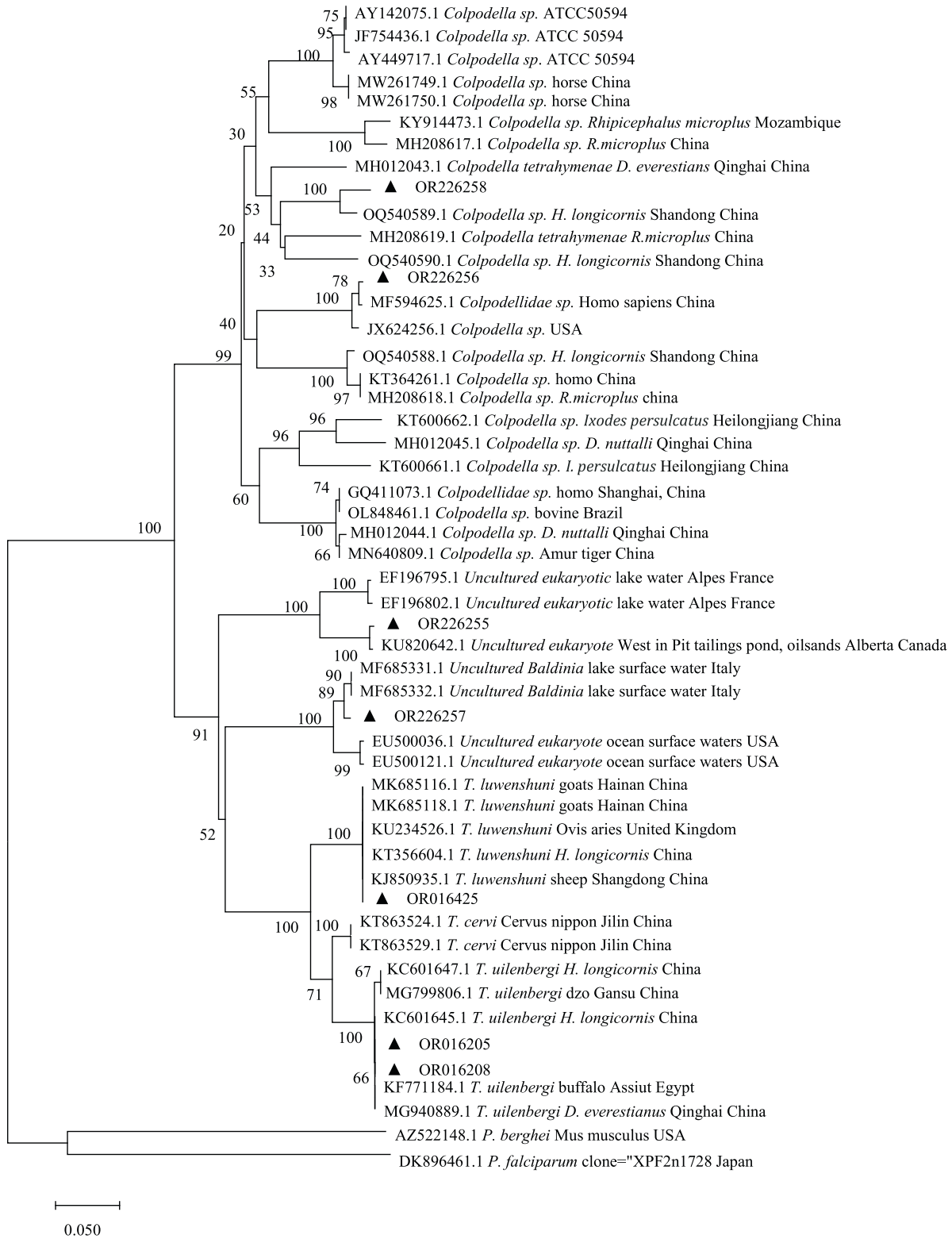

FIGURE 1
Genetic evolutionary analysis of the 18S rDNA piroplasm gene in pet cats and dogs. The 18S rRNA sequences obtained in this study were indicated with black triangles.

and humans. The paucity of case reports makes it difficult to draw conclusions regarding treatment. For example, the patient reported by Yuan et al. showed some common features with *Babesia* cases and responded well to treatment with Atovaquone and Azithromycin (Yuan et al., 2012). The patient reported by Jiang et al. (2018) exhibited neurological symptoms and was treated with

Doxycycline. Neculicioiu et al. (2021) found that a combination regimen of Ceftriaxone and Metronidazole was effective against urinary contamination due to *Colpodella* sp.

In conclusion, this study is the first report of pet dogs and cats infected with *T. uilenbergi*, *T. luwenshuni*, and *Colpodella* sp. in Guiyang, southwestern China, which provides scientific data for the diagnosis of the common piroplasmosis in pet dogs as we as decision-making in the management of animal health and public health.

Data availability statement

The data presented in the study are deposited in the NCBI repository, accession numbers OR016205, OR016425, OR226256, OR226257, OR226255, OR016208, and OR226258.

Ethics statement

The animal studies were approved by the Animal Care Welfare Committee of Guizhou Medical University. The studies were conducted in accordance with the local legislation and institutional requirements. Written informed consent was obtained from the owners for the participation of their animals in this study.

Author contributions

SW: Conceptualization, Data curation, Formal analysis, Investigation, Validation, Visualization, Writing – original draft, Writing – review and editing, Project administration. JM: Investigation, Supervision, Writing – review and editing, Project administration. FY: Funding acquisition, Supervision, Writing – review and editing, Project administration. CZ: Supervision, Writing – review and editing, Project administration. BY: Supervision, Writing – review and editing, Project administration. XC: Supervision, Writing – review and editing, Project administration. GY: Supervision, Writing – review and editing. YS: Supervision, Writing – review and editing. WC: Supervision, Writing – review and editing. JJ: Project administration, Supervision, Writing – review and editing, Validation. JW: Funding acquisition, Project administration, Supervision, Writing – review and editing. LZ: Funding acquisition, Investigation, Project administration, Supervision, Writing – review and editing, Methodology.

Funding

The author(s) declare financial support was received for the research, authorship, and/or publication of this article. This research was financially supported by grants from the National Natural Science Foundation of China (Nos. 82160633 and 81760605), and the GZPH-NSFC-2021-17, the High-level and Innovative Talents of Guizhou Province (QKH-GCC [2022] 033-1).

Acknowledgments

We thank the animal owners for their permission. We also thank the doctors and nurses from the animal hospital in Guizhou for their help in sampling.

Conflict of interest

The authors declare that the research was conducted in the absence of any commercial or financial relationships that could be construed as a potential conflict of interest.

Publisher's note

All claims expressed in this article are solely those of the authors and do not necessarily represent those of their affiliated organizations, or those of the publisher, the editors and the reviewers. Any product that may be evaluated in this article, or claim that may be made by its manufacturer, is not guaranteed or endorsed by the publisher.

References

Aktas, M., Özübek, S., Altay, K., Ipek, N. D., Balkaya, İ, Utuk, A. E., et al. (2015). Molecular detection of tick-borne rickettsial and protozoan pathogens in domestic dogs from Turkey. *Parasit. Vectors* 8:157. doi: 10.1186/s13071-015-0763-z

Chiu, H. C., Sun, X., Bao, Y., Fu, W., Lin, K., Chen, T., et al. (2022). Molecular identification of *Colpodella sp.* of South China tiger *Panthera tigris* amoyensis (Hilzheimer) in the Meihua Mountains, Fujian, China. *Folia Parasitol.* 69:2022019. doi: 10.14411/fp.2022.019

Cui, J. R. (2013). *Animal infection,morphological and molecular identification of a new piroplasma pathogen.* Master's thesis. Naval: Naval Medical University.

Feng, P., Wang, X., Zhang, X. B., Wei, T., Tian, Q. L., Zhang, J., et al. (2021). Diagnosis and treatment of 36 cases of *Babesia gibsonni* infected dogs. *Progress Vet. Med.* 42, 138–141. doi: 10.16437/j.cnki.1007-5038.2021.02.026

Ge, Y., Pan, W., and Yin, H. (2012). Prevalence of *Theileria* infections in goats and sheep in southeastern China. *Vet. Parasitol.* 186, 466–469. doi: 10.1016/j.vetpar.2011.11.066

Gholami, S., Laktarashi, B., Shiadeh, M. M., and Spotin, A. (2016). Genetic variability, phylogenetic evaluation and first global report of *Theileria luwenshuni*, *T. buffeli*, and *T. ovis* in sheepdogs in Iran. *Parasitol. Res.* 115, 2125–2130. doi: 10.1007/s00436-016-5005-6

Hao, G. Y. (2020). Progress in the study of caprine and ovine theileriosis in sheep. *Chin. J. Vet. Sci.* 40, 424–434. doi: 10.16303/j.cnki.1005-4545.2020.02.34

Hartmann, K., Addie, D., Belák, S., Boucraut-Baralon, C., Egberink, H., Frymus, et al. (2013). Babesiosis in cats: ABCD guidelines on prevention and management. *J. Feline Med. Surg.* 15, 643–646. doi: 10.1177/1098612x13489230

He, L., Miao, X., Hu, J., Huang, Y., He, P., He, J., et al. (2017). First Molecular Detection of *Babesia gibsoni* in Dogs from Wuhan, China. *Front. Microbiol.* 8:1577. doi: 10.3389/fmicb.2017.01577

Hu, X. Y., He, Y. C., Kang, M., Li, Z. K., Li, J. X., Sun, Y. L., et al. (2022). Information analysis of ticks and tick-borne pathogens in Qinghai. *Prog. Vet. Med.* 43, 73–79. doi: 10.16437/j.cnki.1007-5038.2022.10.026

Irwin, P. J. (2010). *Canine babesiosis. Vet. Clin. North Am. Small Anim. Pract.* 40, 1141–1156. doi: 10.1016/j.cvsm.2010.08.001

Irwin, P. J., and Hutchinson, G. W. (1991). Clinical and pathological findings of *Babesia* infection in dogs. *Austral. Vet. J.* 68, 204–209. doi: 10.1111/j.1751-0813.1991.tb03194.x

Jiang, J. F., Jiang, R. R., Chang, Q. C., Zheng, Y. C., Jiang, B. G., Sun, Y., et al. (2018). Potential novel tick-borne *Colpodella* species parasite infection in patient with neurological symptoms. *PLoS Neglect. Trop. Dis.* 12:e0006546. doi: 10.1371/journal.pntd.0006546

Kuvardina, O. N., Leander, B. S., Aleshin, V. V., Myl'nikov, A. P., Keeling, P. J., and Simdyanov, T. G. (2002). The phylogeny of colpodellids (Alveolata) using small subunit rRNA gene sequences suggests they are the free-living sister group to apicomplexans. *J. Eukaryotic Microbiol.* 49, 498–504. doi: 10.1111/j.1550-7408.2002.tb00235.x

Li, Y., Chen, Z., Liu, Z., Liu, J., Yang, J., Li, Q., et al. (2014). Molecular identification of *Theileria* parasites of northwestern Chinese Cervidae. *Parasit. Vectors* 7:225. doi: 10.1186/1756-3305-7-225

Li, Y., Luo, J., Guan, G., Ma, M., Liu, A., Liu, J., et al. (2009). Experimental transmission of *Theileria uilenbergi* infective for small ruminants by *Haemaphysalis longicornis* and *Haemaphysalis qinghaiensis*. *Parasitol. Res.* 104, 1227–1231. doi: 10.1007/s00436-009-1347-7

Liu, Z., Ma, M., Peng, Y., Wang, Z., Yang, G., Deng, J., et al. (2010). *Theileria* sp. SZH-human 18S ribosomal RNA gene, complete sequence.

Mans, B. J., Pienaar, R., and Latif, A. A. (2015). A review of *Theileria* diagnostics and epidemiology. *Int. J. Parasitol. Parasites Wildl.* 4, 104–118. doi: 10.1016/j.ijppaw.2014.12.006

National Health Commission of the People's Republic of China (2017). *Diagnosis of Babesiosis*. Beijing: National Health Commission of the People's Republic of China.

Neculicioiu, V. S., Colosi, I. A., Toc, D. A., Lesan, A., and Costache, C. (2021). When a ciliate meets a flagellate: A rare case of *Colpoda spp.* and *Colpodella spp.* isolated from the urine of a human patient. Case report and brief review of literature. *Biology* 10:476. doi: 10.3390/biology10060476

Niu, Q., Yang, J., Liu, Z., Gao, S., Pan, Y., Guan, G., et al. (2017). First molecular detection of piroplasm infection in pet dogs from Gansu, China. *Front. Microbiol.* 8:1029. doi: 10.3389/fmicb.2017.01029

Ord, R. L., and Lobo, C. A. (2015). Human babesiosis: Pathogens, prevalence, diagnosis and treatment. *Curr. Clin. Microbiol. Rep.* 2, 173–181. doi: 10.1007/s40588-015-0025-z

Palmer, J. P., Gazêta, G., André, M., Coelho, A., Corrêa, L., Damasceno, J., et al. (2022). Piroplasm infection in domestic cats in the mountainous region of Rio de Janeiro, Brazil. *Pathogens* 11:900. doi: 10.3390/pathogens11080900

Wang, J., Wang, X., Sun, H., Lv, Z., Li, Y., Luo, J., et al. (2020). Molecular evidence of piroplasm infection in companion animals in Hunan Province, China. *BMC Vet. Res.* 16:297. doi: 10.1186/s12917-020-02500-6

Wang, K. L., Zhou, Y. C., Zhao, S. S., Zhang, Y. J., Yan, Y. Q., Jing, J. C., et al. (2020). Investigation on infection and phylogenetic analysis of *Theileria luwenshuni* in Goats of Linyou, Shanxi. *Prog. Vet. Med.* 41, 123–126. doi: 10.16437/j.cnki.1007-5038.2020.04.026

Wong, S. S., Poon, R. W., Hui, J. J., and Yuen, K. Y. (2012). Detection of *Babesia hongkongensis sp.* nov. in a free-roaming *Felis catus* cat in Hong Kong. *J. Clin. Microbiol.* 50, 2799–2803. doi: 10.1128/JCM.01300-12

Xiang, Y. L., Zhou, J. Z., Liu, Y., Liu, P. T., Hu, Y., and Liang, W. Q. (2022). An investigation of ticks and tick-borne bacteria in some areas of Guizhou province, China. *Chin. J. Vector Biol. Control* 33, 148–152.

Xu, M., Hu, Y., Qiu, H., Wang, J., and Jiang, J. (2022). *Colpodella sp.* (Phylum Apicomplexa) identified in horses shed light on its potential transmission and zoonotic pathogenicity. *Front. Microbiol.* 13:857752. doi: 10.3389/fmicb.2022.857752

Yang, Y., Christie, J., Köster, L., Du, A., and Yao, C. (2021). Emerging Human Babesiosis with "Ground Zero" in North America. *Microorganisms* 9:440. doi: 10.3390/microorganisms9020440

Yin, F., Mu, D., Tian, Z., Li, D., Ma, X., Wang, J., et al. (2022). Molecular Detection of *Babesia gibsoni* in Cats in China. *Animals* 12:3066. doi: 10.3390/ani12223066

Yuan, C. L., Keeling, P. J., Krause, P. J., Horak, A., Bent, S., Rollend, L., et al. (2012). *Colpodella spp.-like* parasite infection in woman, China. *Emerg. Infect. Dis.* 18, 125–127. doi: 10.3201/eid1801.110716

Zhang, X. C., and Li, J. H. (2010). *Veterinary parasitology*. Beijing: Science Press.

Zhong, W., Du, X. M., Hao, L. L., Yuan, D. B., Guo, L., Hou, W., et al. (2019). Investigation on molecular epidemiology of Piroplasma infection in yaks and Tibetan sheep in aba Tibetan autonomous prefecture of Sichuan Province. *Chin. J. Vet. Med.* 55, 20–27.

Zhou, Q. A., Huang, S. B., Mo, S. L., Hu, L. P., Han, Y. H., He, Q. S., et al. (2022). Investigation on molecular epidemiology of piroplasma infection in equine animals in some parts of Guangxi Province. *Chin. J. Vet. Sci.* 42, 78–94. doi: 10.16303/j.cnki.1005-4545.2022.01.13

frontiers | Frontiers in Microbiology

TYPE Review
PUBLISHED 18 October 2023
DOI 10.3389/fmicb.2023.1273870

Check for updates

OPEN ACCESS

EDITED BY
Hong Yin,
Chinese Academy of Agricultural Sciences,
China

REVIEWED BY
Satya Deo Pandey,
University of Louisville, United States
Jayaraman Tharmalingam,
University of Wisconsin-Madison,
United States

*CORRESPONDENCE
Sibo Wang
✉ wangsibowangfei@163.com
Shan Wang
✉ wangshan431141@163.com

†These authors have contributed equally to this work and share first authorship

RECEIVED 07 August 2023
ACCEPTED 27 September 2023
PUBLISHED 18 October 2023

CITATION
Meng Y, Ren Q, Xiao J, Sun H, Huang Y, Liu Y, Wang S and Wang S (2023) Progress of research on the diagnosis and treatment of bone cystic echinococcosis.
Front. Microbiol. 14:1273870.
doi: 10.3389/fmicb.2023.1273870

COPYRIGHT
© 2023 Meng, Ren, Xiao, Sun, Huang, Liu, Wang and Wang. This is an open-access article distributed under the terms of the Creative Commons Attribution License (CC BY). The use, distribution or reproduction in other forums is permitted, provided the original author(s) and the copyright owner(s) are credited and that the original publication in this journal is cited, in accordance with accepted academic practice. No use, distribution or reproduction is permitted which does not comply with these terms.

Progress of research on the diagnosis and treatment of bone cystic echinococcosis

Yibin Meng[1†], Qian Ren[2†], Jun Xiao[2], Haohao Sun[2], Yiping Huang[2], Yaqing Liu[2], Shan Wang[2]* and Sibo Wang[1]*

[1]Department of Spine Surgery, Xi'an Jiaotong University Affiliated HongHui Hospital, Xi'an, China,
[2]Laboratory of Translational Medicine, School of Medicine, Shihezi University, Shihezi, China

Bone cystic echinococcosis (CE) is one of the most complex and dangerous of all echinococcoses. The lack of typical imaging features and clinical manifestations makes diagnosis and treatment of this disease difficult. X-ray and computed tomography (CT) images of bone CE are similar to those of bone cysts, giant-cell bone tumors, and bone metastases, but magnetic resonance imaging (MRI) shows good diagnostic value due to excellent soft-tissue imaging features. Serological tests cannot be used as a definitive diagnostic method for bone CE due to cross-reactivity, which can lead to false-positive or false-negative results. The development of novel antigens can open new frontiers in the diagnosis of the disease. Currently, views conflict on how to diagnose and treat bone CE. Both surgical and pharmacological treatments can be used, but determining which is appropriate is difficult due to the different sites and clinical manifestations of bone CE. Radical resection is not indicated for large-bone injuries, and Pharmacotherapy becomes important. This article reviews the progress of research into the pathogenesis and clinical manifestations of, and diagnostic strategies and treatment options for, bone CE. We aimed to provide a reference for clinical diagnosis and -treatment options.

KEYWORDS

bone cystic echinococcosis, endemic disease, orthopedic surgery, neglected disease, medical advice

1. Introduction

Cystic echinococcosis, commonly called Hydatid disease is caused by the larval form of the parasitic tapeworm, Echinococcus granulosus (*E. granulosus*). Cystic echinococcosis (CE) is found on all continents except Antarctica and is classified by the World Health Organization (WHO) as one of the most neglected and geographically widespread parasitic diseases (World Health Organization, 2015). The lifecycle of *E. granulosus* involves two main hosts, one intermediate and one final. Dogs are common final hosts; the adult larvae adhere to their small intestinal mucosa, and eggs are excreted with feces. In intermediate hosts—which are humans and herbivores (cattle, sheep, goats, camels, horses, and pigs)—the eggs hatch in the body and can reach various sites via the circulatory system (Gnanasekaran et al., 2016).

Musculoskeletal involvement is rare, with an incidence of 0.5–4.0% in all CE cases (Neumayr et al., 2013a). CE can parasitize almost any bone in the body, but half of all cases occur in the spine (Loudiye et al., 2003); the incidence in other bones is lower (Schnepper and Johnson, 2004). Spinal CE was seen in all age groups, both sexes can be affected (Altinörs et al., 2000). Musculoskeletal infection of the spine often results in severe disability or even death (Inayat et al., 2019). By contrast, clinical presentations of patients with nonspinal bone CE are often

nonspecific, with pain and pathological fractures being the most common (Monge-Maillo et al., 2017). Clinical history as well as laboratory, imaging, and serological tests play crucial roles in diagnosing the disease. Radical surgical resection combined with chemotherapy is the current clinical treatment of choice, but the postsurgical recurrence rate can be as high as 40% (Salman et al., 2018). Patients who experience spinal encopresis due to spinal CE often have a high recurrence rate after surgery (Caglar et al., 2019). The prognosis for patients with bone CE is poor: paraplegia, impaired mobility, postoperative disability, and even death (Gdoura et al., 2010; Arkun and Mete, 2011). Because the pathological mechanism of bone CE is unknown, the current literature consists mostly of case studies rather than systematic, comprehensive reports; therefore, consensus is lacking on the diagnosis and treatment of this disease.

2. Possible pathological mechanism of bone CE: hematogenous pathway and secondary infection

The route of parasitic infection in bone CE remains unclear (Cattaneo et al., 2019). In most cases, the disease is confined to the bones and rarely infects other organs (Torricelli et al., 1990). Protoscoleces (PSCs) invade the body and, via blood circulation, usually parasitize organs other than the liver. Commonly parasitized sites are the lungs; spleen; and multiple locations in brain tissue, bones, lymph nodes, and muscles (Petra et al., 2003). Therefore, both primary hematogenous and secondary infections in other organs can cause the development and progression of bone CE.

CE appears mostly in cancellous bone. Cysts lining cancellous bone can fracture bone tissue by attacking it; the disease can also spread to invade exoskeletal structures (Papanikolaou, 2008). Possible pathological mechanisms are as follows. (1) The growing cysts compress bone tissue, causing bones to atrophy (Jacquier and Piroth, 2018). (2) Cysts invade in multiple directions along less-resistant microstructures such as the bone canal; hydatid tissue erodes and replaces bone trabeculae and then destroys and breaks through the bone cortex (Neumayr et al., 2013a,b). (3) Enlarged echinococcal cysts obstruct the vessels that nourish bone, causing ischemic necrosis (Thomas et al., 1997). (4) CE cysts directly activate the proliferation of osteoclasts, causing physiological osteolysis (Song et al., 2007). (5) Cystic invasion decreases host immunity and causes soft-tissue infiltration and fistula formation, while the resulting inflammatory reaction can lead to bone destruction with neurological and joint infection (Morris et al., 2002). (6) CE lesions can spread directly to adjacent bone tissue and destroy its bony structure (Jacquier and Piroth, 2018).

The rigid structure of bone inhibits cysts from forming an exterior membrane therein (Neumayr et al., 2013a,b). Therefore, in the early stage of bone CE, cysts grow invasively along structures that offer the least resistance, such as the bone canal, and lesions appear as irregular branches (Torricelli et al., 1990). However, late-stage intrabony cysts can break through the bone cortex and involve extraosseous structures, which lack rigidity and therefore cannot restrict cystic proliferation. In addition, soft-tissue intracapsular cysts are often accompanied by plasma exudate that invades surrounding tissues. The periosteum and articular cartilage are resistant to parasitic attack; therefore, cartilage infection is rarely reported in cases of bone CE (Morris et al., 2002).

In the spine, particularly in the thoracolumbar region, due to a dense regional vascular network and rich blood supply, cysts infiltrate vertebral cancellous bone via the vertebral artery and develop along the bone marrow cavity toward the epiphyseal plate and articular cartilage in a swollen honeycomb-like or "soap bubble" shape (Arana Iniquez, 1978). Progressive sclerotic cysts compress the vertebral body, pedicle, and lamina to varying degrees, but most of the infected tissue does not attack the intervertebral disc (IVD) due to the periosteal barrier (Schnepper and Johnson, 2004).

3. Clinical manifestations of three types of bone CE

We searched the PubMed database for studies addressing recent treatment and diagnosis of bone CE and found 41 case reports thereof in the last 5 years. As shown in Table 1, the clinical presentation of bone CE is complex, with symptoms depending on the location of the infection, size of the lesion, degree of bone and surrounding-tissue invasion, and complications arising from the cyst and secondary infection (McManus et al., 2012). As shown in Figure 1, cysts can parasitize any bone in the body, but most infect only a single bone (602/721, 83%) (Steinmetz et al., 2014). The results of a European multicenter study showed that 45% of CE cases involved spinal CE and that long bones (femur, 10%; humerus; 2%) were sites of parasitization, while flat bones such as pelvic bones (14%) and ribs (8%) could also be invaded (Cattaneo et al., 2019). Echinococcosis in other parts (such as the skull, sternum, scapula and phalanx) is rare. Therefore, this article focuses on spinal CE, long bone CE and pelvic CE.

3.1. Spinal CE

The thoracic segments (46–50%) have the highest infection rate in spinal CE, and the lumbar (20–29%) and sacral (20–23%) disease also occur. The cervical spine is the least susceptible to infection of the spinal CE (Pamir et al., 2002). Eventually, spinal CE patients usually present with symptoms of spinal cord compression, with back pain in 85%, radicular symptoms in 25%, and cauda equina syndrome or even paralysis in 25–77% (Neumayr et al., 2013a). Neurological infection occurs in 20–80% of cases (Sharma et al., 2020). Patients can present with decreased sensation in one or both legs and the perineum, gradually developing signs of neurological damage such as bilateral lower-limb mobility impairments, urinary and fecal dysfunction, and weakness in urination (Sioutis et al., 2021). Ozek et al. reported that rapid-onset neurological disorders are due to inadequate blood supply caused by vascular injury; in such cases, patient recovery is often slow and incomplete (Ozek, 1994). ROBINSON RG's case report of a female patient with severe neurological symptoms. Despite surgical treatment to remove the cyst, the patient did not have a good prognosis (Robinson, 1959). Paraplegia due to disease recurrence has been reported in as many as 45% of cases (Bhojraj and Shetty, 1999). The recurrence rate of spinal CE is 30–40%, usually due to intraoperative cyst rupture (Johnson and Hobson, 1977). Moreover, the resulting spillage of cyst contents can cause a variety of allergic reactions such as pruritus, urticaria, dyspnea, asthma, vomiting, diarrhea, abdominal cramps, bacterial infection, and even anaphylaxis. This complex clinical presentation poses great difficulties in diagnosis (Pathania et al., 2000).

TABLE 1 The clinical manifestations of bone CE.

Classification of bone CE	Position	Manifestations
Spinal CE	Cranio-vertebral junction	Neck tilt toward the left side, neck pain, and headache along with a low-grade fever and loss of appetite (Kiran et al., 2021).
	Cervical vertebra	Sensory loss in limbs (Majmundar et al., 2019).
	Cervical and thoracic vertebrae	Walking disorders; Dull backache with paresthesia radiating down the legs (Bouattour et al., 2021); Paraparesis (Cavus et al., 2018).
	Thoracic vertebrae	Chronic back pain (Saul et al., 2020); Mid-back pain and intermittent history of fever (Das et al., 2021); Increasing thoracic pain (Depré et al., 2019); Back pain (Dighe et al., 2018); An isolated mass in the T5 vertebral body with the compression of the spinal cord (Zhang et al., 2021); Difficulty with walking and feet had no sense of cold and hot (Zhang et al., 2017). Weakness (Safari et al., 2021); Paraparesis (Akhaddar and Boucetta, 2018); Back swelling, loss of lower extremity strength, complete motor function loss, paraplegia, and immobilization (Alkan Çeviker et al., 2022); Back pain, significant weight loss, and paralysis of both lower limbs (Zhang et al., 2021).
	Thoracic vertebrae + Chest wall + Ribs	Left-sided infraclavicular chest pain and numbness in the left forearm (Hans et al., 2019); Paraparesis and back pain (Kassimi et al., 2021); Weakness and numbness of the left lower limb (Agnihotri et al., 2017).
	Lumbar vertebra	Right lower back pain and weakness in both lower limbs (Tian et al., 2020); Progressive bilateral, poorly systematized, paralyzing lumbar radiculopathy associated with urinary urgency (Staouni et al., 2020).
	Lumbar vertebra and sacral vertebra	Low-back pain (Majmundar et al., 2019); Pus discharge from the lower back; back pain; weakness of the left foot (Sharma et al., 2020); Progressive weakness of lower limbs, frequency, and urinary incontinence (Trifa and Maamri, 2021).
Long bones CE	Humeral bone	Diaphyseal humerus fracture (Patino and Ramos Vertiz, 2019).
	Radial bone	Elbow swelling (Bağcıer and Tufanoğlu, 2020).
	Ulna	Multiple swellings on the right forearm (Reddy et al., 2017).
	Femoral bone	A painful mass in the right thigh and perineal area with progressed pain and paresthesia to the right thigh and shin (Ahmady-Nezhad et al., 2022); Left groin pain and swelling in the left thigh (Salman et al., 2018); Non-union of the fracture (Gautam et al., 2018); Swelling and fracture of the left upper end of the femur; difficulty in walking and swelling in the right inguinal region (Ramteke et al., 2019); Right hip pain (Oueslati et al., 2020); Pain and swelling over her right knee region (Dathik et al., 2019); Hip pain (Masmoudi et al., 2019); Persistent thigh pain in the former fractured hip (Fröschen et al., 2019).
	Tibia bone	Pain and edema in her left upper leg (Nascimento et al., 2018).
Pelvic CE	Iliac bone	Left pelvic pain (Govindasamy et al., 2021).
	Ischiopubic branch acetabulum	Inguinal pain (Daniel et al., 2017).
	Inferior pubic ramus, ischium, and iliac bone	Left buttock pain (Dehghan Manshadi et al., 2017).
	Trochanteric region	Left hip pain (Boussaid et al., 2021).
	Pelvic bone	Progressive para-coxalgia and lower limb weakness of the left leg; pathological bone fracture (Wang et al., 2019).
	Joint space; supra-acetabular region and superior pubic ramus	Left hip pain and limp (Bhatnagar et al., 2017).
	Sacroiliac joint	Pain and paresthesia in the left gluteus (Peña Huertas et al., 2022); Left sciatica and mechanical hip pain (Akremi et al., 2022).

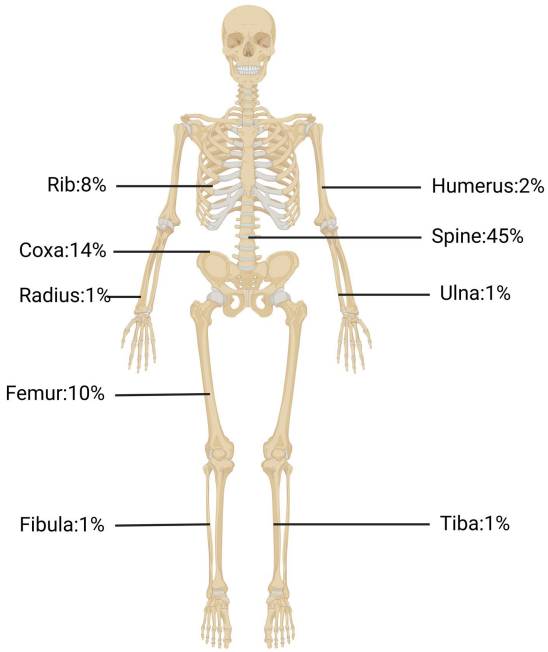

FIGURE 1
The occurrence rates of bone CE in the spine, pelvic bone, tibia bone, ribs, and other locations.

3.2. Pelvic CE

The incidence of pelvic CE is second only to that of spinal CE. A study included 31 patients with pelvic encopresis from 1991 to 2017, with the ilium being the most common (21/31), followed by the acetabulum (7/31), pubis (6/31), sciatica (5/31), and sacrum (5/31) (Inayat et al., 2019). The pelvic bone is densely packed with cancellous bones and is rich in blood supply, providing highly favorable conditions for parasitization by *E. granulosus*. Hemipelvic infection has commonly been reported in recent years; the hip joint easily becomes infected, impairing mobility. Pelvic CE can lie latent for several years and gradually become symptomatic as the disease progresses, generally manifesting as symptoms of lumbosacral-nerve compression (Arik et al., 2015). Generally, the first clinical manifestations appear late in the disease's progression due to the rigid skeletal structure and slow cystic growth. Severe cases are usually associated with late complications such as lumbosacral pain, swelling, fistula formation, and progressive worsening of pain in both legs (Inayat et al., 2019). Although sciatica is often reported as the first symptom of pelvic CE, it must be emphasized that the symptoms of this condition depend on the sizes and locations of cysts.

3.3. Long bones CE

A total of 702 patients with encopresis were included in one study, including 111 patients with long bone encopresis. The highest frequency of infection was in the femur (72/111, 65%), followed by the humerus (11/111, 10%), radius (3/111, 2.7%) and tibia (3/111, 2.7%), with ulna (1/111, 0.9%) and fibula (1/111, 0.9%) cases being rare (Steinmetz et al., 2014). As mentioned above, the femur is the most susceptible to infection. Colonization of these bones by *E. granulosus* mostly involves the epiphysis in the early stages and can initially be asymptomatic. Extensive bony lesions in later stages can lead to pathological hyperplasia of the infected limb, causing swelling and pain that becomes progressively more intense as the burden of activity increases (Song et al., 2007). Local examination of patients with femoral CE can reveal deep pressure pain in the greater trochanter, accompanied by limitation of hip motion, which can lead to late complications such as pathological fracture and fistula formation in severe cases (Kapoor et al., 2013; Inayat et al., 2019). Patients with humeral CE similarly have no obvious symptoms in the early stages. Bone erosion progresses to an advanced stage of severe bone damage, at which point patients often seek medical attention for severe pain. Although the CE of the long bones does not infect the joint surface, advanced pathological bone destruction, inflammation, and infection of the surrounding soft tissues can affect adjacent joints. Therefore, localized masses, restricted mobility, and severe pain can be clinical features of this type of CE.

4. Imaging examination combined with serological results to diagnose bone CE

Because the disease features of bone CE are often atypical, they often pose a diagnostic challenge to clinicians. Given that bone CE progresses very slowly, intrabony cysts can remain quiescent for long periods, even decades (Cattaneo et al., 2019). Spinal CE takes an average of at least 6 months to be diagnosed even after the onset of symptoms (Khazim et al., 2003). Imaging combined with serological testing is now the mainstay of clinical diagnosis.

4.1. Radiographic examination

The most commonly used imaging techniques for bone CE are X-ray, computed tomography (CT), and magnetic resonance imaging (MRI). X-ray is the first diagnostic step when patients present with pain, swelling, and other associated symptoms (Ira et al., 2001). While X-rays often do not show typical imaging features of patients with bone CE (Table 2). In addition, the periosteal reaction is usually not visible on X-ray images; if not, this indicates a pathological fracture caused by an attack on the bone cortex (Chen et al., 2020). Bone infections usually show bone destruction and cystic lesions on imaging. Cystic lesions appear as hypodensities on both CT and X-ray, but CT can show more information on these lesions, including size, extent, location, and degree of bone destruction (Tüzün and Hekimoğlu, 2001). MRI is the most relevant of all imaging modalities for the diagnosis of CE; its excellent soft-tissue resolution clearly shows the relationship between the lesion and adjacent tissues (Pamir et al., 2002).

The most common manifestation of spinal CE is one or more round or oval sockets with indistinct borders that cannot be distinguished from chronic osteomyelitis on imaging (Muscolo et al., 2015). In the early stage, the lesion appears in the vertebral body and can spread to all vertebral structures. When the lesion involves the spinal canal, MRI can show the exact number and sizes of cysts, the integrity of the cyst wall, and the degree of spinal-cord compression (Herrera et al., 2005). Berk et al. reviewed the characteristics of spinal CE on MRI: (World Health Organization, 2015) sausage-like appearance with thin-walled, regular,

TABLE 2 Examination of bone CE.

Classification of bone CE	Positioning	Radiological examination			Serology
		X-ray	CT	MRI	
Spinal CE	Cranio-vertebral junction (Kiran et al., 2021)	Not mentioned	An expansile lytic lesion eroding the vertebra.	Heterogeneously enhancing solid-Multiple cysts.	Not mentioned
	Cervical vertebra (Majmundar et al., 2019)	Not mentioned	Not mentioned	Cystic and enhancing lesions with significant compression.	Not mentioned
	Cervical and thoracic vertebrae (Cavus et al., 2018; Bouattour et al., 2021)	Not mentioned	Not mentioned	Multiple extradural cysts; Dura with spinal cord compression.	Negative
	Thoracic vertebrae (Zhang et al., 2017, 2021; Akhaddar and Boucetta, 2018; Dighe et al., 2018; Depré et al., 2019; Saul et al., 2020; Das et al., 2021; Safari et al., 2021; Alkan Çeviker et al., 2022)	Negative; Paraspinal opacity.	Bony nodules with lysis; The intervertebral foramen is infected and enlarged.	Spinal cord atrophy; DISC infection; Spinal cord compression.	ELISA: +; IHA: +
	Ribs (Hans et al., 2019; Kassimi et al., 2021; Agnihotri et al., 2017)	Not mentioned	Not mentioned	Par costal cyst.	ELISA: +
	Lumbar vertebra (Staouni et al., 2020; Tian et al., 2020)	Not mentioned	Vertebral body and peripheral bone hyperostotic; PET-CT: Cyst lesion on the spine.	Cyst lesion; The intervertebral foramen is infected and enlarged.	Not mentioned
	Lumbar vertebra and sacral vertebra (Majmundar et al., 2019; Sharma et al., 2020; Trifa and Maamri, 2021)	L4-L5 vertebrae were infected	Not mentioned	Multiple extradural cysts; Multiple cysts in the spinal canal.	Raised lymphocytes, eosinophil, and C-reactive proteins.
Long bones CE	Humeral bone (Patino and Ramos Vertiz, 2019)	Pathologic fracture; Multilocular cyst; Osteolytic lesions.	Not mentioned	Pathologic fracture; Multilocular cyst; Osteolytic lesions.	Not mentioned
	Radial bone (Bağcıer and Tufanoğlu, 2020)	Fracture of radius; The bony cortex thins.	Not mentioned	Hyperintense cortical destruction of bone.	Not mentioned
	Ulna (Reddy et al., 2017)	Ulnar cyst; Pathologic fracture; Soft tissue calcification.	Not mentioned	Cyst lesions with Expansive osteolytic lesions.	Not mentioned
	Femoral bone (Gautam et al., 2018; Salman et al., 2018; Dathik et al., 2019; Fröschen et al., 2019; Masmoudi et al., 2019; Ramteke et al., 2019; Oueslati et al., 2020; Ahmady-Nezhad et al., 2022)	Multiple moth-eaten-lytic areas with surrounding sclerosis in greater trochanter lesser trochanter, neck.	Soft tissue infection of bone and joint; Soft tissue calcifications.	Cystic lesions ac-cumulate in the femur; T2 hyperintense lesions.	Haemagglutinin test: positive; ELISA: IgG+
	Tibia bone (Nascimento et al., 2018)	Femoral cyst.	Not mentioned	Not mentioned	Not mentioned

(Continued)

10.3389/fmicb.2023.1273870

TABLE 2 (Continued)

Classification of bone CE	Positioning	Radiological examination			Serology
		X-ray	CT	MRI	
Pelvic CE	Iliac bone (Govindasamy et al., 2021)	Not mentioned	Polycystic lesion of the pelvis.	Not mentioned	Not mentioned
	Ischiopubic branch acetabulum (Daniel et al., 2017)	Osteolytic lesions of the pubic acetabulum	Osteolytic lesions of the pubic acetabulum.	Cysts infect the joints and muscles.	Not mentioned
	Inferior pubic ramus, ischium, and iliac bone (Dehghan Manshadi et al., 2017)	Not mentioned	Not mentioned	Cystic lesions of the pubic ischium and ilium involving the lower limbs.	Not mentioned
	Trochanteric region (Boussaid et al., 2021)	Osteolytic lesions of the pelvis.	Not mentioned	Cystic lesions of soft tissue in the pelvis.	Not mentioned
	Pelvic bone (Wang et al., 2019)	Not mentioned	Cyst destroyed the pelvis and femoral head.	Cyst invades the periarticular muscles of the hip.	Not mentioned
	Joint space; supra-acetabular region and superior pubic ramu s (Bhatnagar et al., 2017)	Destruction of femoral head and acetabulum.	Bony destruction of the acetabular structure.	Not mentioned	ESR: up; absolute eosinophil count: up.
	Sacroiliac joint (Akremi et al., 2022; Peña Huertas et al., 2022)	Osteolytic lesions of the ischium, and fem-oral head osteonecrosis aspect.	Not mentioned	Cyst is compressing the Sciatic nerve.	Not mentioned

*The above cases information is from Table 1.

semicircular terminals; (Gnanasekaran et al., 2016) capsular cavities without septa or fragments, occasionally spherical; (Neumayr et al., 2013a) signal intensity of capsule contents similar to that of CSF; and (Loudiye et al., 2003) capsule wall signal equal to or slightly lower than that of cystic contents on T1-weighted (T1W) images (Berk et al., 1998). In vertebral CE, the most common features are uninjured IVD and vertebral body, while the paraspinal area, subperiosteal bone, and adjacent ribs are more commonly infected (Herrera et al., 2005). Destruction of discs in the advanced stages makes spinal CE difficult to distinguish from inflammatory spinal conditions.

In pelvic CE, osteolytic cystic lesions are the single striking feature located in the ilium but can span the hip and sacroiliac joints. Vertebral osteochondral reactions are uncommon. Calcifications and cysts can be found on imaging after adjacent tissues are invaded (Rangheard et al., 2001). In long-bone CE, the primary cyst begins in the epiphysis (Dathik et al., 2019). The lesion, which can be either monocystic or polycystic, is mostly located in the metaphysis and can expand into the diaphysis and form a fan-shaped cortex; however, dilatation, sclerosis, and periosteal reaction seldom occur. Polycystic lesions are more common, presenting as large round or oval ground areas of bone destruction that collect in the epiphysis or metaphysis and greatly expand the extent of bone destruction.

The progression of bone cysts is characterized by two imaging stages: (World Health Organization, 2015) the microcystic-infiltration stage, in which the cyst creates a cluster of "grape"-like changes; and (Gnanasekaran et al., 2016) the secondary-infection stage, in which inflammatory bone disease casts a grape-like shadow of bone proliferation and destruction (Arias, 1946). In advanced stages of bone CE, the inflammatory stimulation of bone proliferation exceeds the osteolytic process, and imaging has limited specificity to distinguish the disease from bone malignancy. A study by Farrokh Saidi found that "a single cyst only," "lamellar separation," and "cyst degeneration" are independent predictors of good prognosis in hepatic CE (Fathi et al., 2016). However, no studies have determined whether cystic calcification can also predict prognosis in bone CE. In the author's opinion, calcified cysts indicate a lower capacity for cystic growth, a lessened ability to invade surrounding tissues, and a tendency to limit the lesion. Nevertheless, a calcified cyst can act as an intrabony occupying lesion, compressing or even blocking the ability of intrabony trophoblastic vessels to support the bone, thereby causing bone ischemia and compressing nerve tissue in some cases.

4.2. Serology

Serological tests can be used to support bone CE diagnosis and as screening tools. Such tests are divided into two categories: (World Health Organization, 2015) antigen detection using encapsulated cystic fluid and PSC larvae; and (Gnanasekaran et al., 2016) detection of antibodies (aBs) in patient serum. Commonly used antigen indicators in the laboratory include anti–*E. granulosus* cyst fluid (EgCF) antigen, fine-grained echinococcal cestode antigen, epithelial glycoprotein (EGP), semi-purified CE cyst fluid antigen B (AgB), and E2 receptor alpha (Era2) (Siles-Lucas et al., 2017). In antigen-based sensitivity (Sens) and specificity (Sp) experiments, the Sen of antigen detection was 45–92% in both CE patients and healthy populations, while Spc was 70–100%. This means that the surface antigens of both populations contain similar antigenic determinant clusters, which are

thought to be prone to cross-reactivity (Carmena et al., 2006). Some newer antigens, including *E. granulosus* tegumental antigen (EgTeg) and *E. granulosus* alkaline phosphatase (EgAP), have shown >90% Spc and Sen in experiments (Ortona et al., 2005). Although such results still require support from studies with large samples, they provide important reference values for the diagnosis of CE.

The sensitivity of a diagnostic test for bone CE depends on the integrity, growth viability, and locations of cysts (List et al., 2010). In the early stages, intrabony cysts are positive on serological examination due to their inability to form fibrous membranes or due to cystic rupture, infection, or abscess formation (McManus, 2014). Serological tests are mostly negative in the late stages due to cyst aging or calcification, and false-negative results cannot be avoided. The Casoni and indirect-hemagglutination tests also show good diagnostic potential for bone CE (Wang et al., 2019). Ozdemir et al. reported three cases of spinal CE; two were serologically negative but confirmed to have spinal CE via pathology (Ozdemir et al., 2004). Three problems exist with the immune response to serological diagnostic tests for CE: (1) *E. granulosus* antigens cross-react with antigens of other parasitic diseases, which can impair test specificity (2) The strength of the patient's immune system affects serological test results, with both false-positive and -negative results occurring. (3) Test sensitivity decreases to 25–56% in extrahepatic CE (Xiao et al., 2003). Therefore, the serological examination does not provide sufficient evidence for it to be used as the main diagnostic method in bone CE and must hence be combined with other methods for comprehensive analysis.

5. Treatment: radical resection and drug therapy

As shown in Table 3, the treatment of bone CE is site dependent. Currently, the most appropriate treatment is radical surgery or resection of all infected bone (Arkun and Mete, 2011). However, radical surgery is difficult to perform and leaves the patient prone to recurrence, especially when the spine, pelvic bones, and ribs are infected. Therefore, surgery is sometimes combined with other treatments (e.g., radiotherapy) to prevent recurrence.

5.1. Surgery

Before the operation, need to determine the locations and sizes of cysts and the degree to which soft tissues surrounding the bone have been invaded. Surgical recommendations for bone CE are as follows. (1) The bones and surrounding soft tissues infected by CE must be exposed (Luan et al., 2022). (2) Integrity of the cyst wall must be ensured during resection of CE cysts (Das et al., 2021). (3) After such resection, 1–2 cm of parasite-free bone must be removed (Ozdemir et al., 2004). (4) During the operation, the surgical area should be cleaned with a short-term insecticide such as hypertonic saline to avoid recurrence caused by remaining *E. granulosus* (Khazim et al., 2003). (5) Bone grafts can be implanted for functional reconstruction after cyst resection (Thomas et al., 1997). Although many preoperative tests are available to detect osteochondroma-like lesions, bone CE is often found during surgery and confirmed by pathological examination.

Spinal CE should be given higher treatment priority than other types of bone CE. The internationally recognized classification of this disease largely guides the choice of surgical approach (Açikgöz et al., 1996). Complete resection is not possible in extensive intradural CE (Kaen et al., 2009). Intradural CE generally features multiple cysts that can attach to the lumbar-spinal roots, as well as some thin-walled cysts that can easily rupture during surgery (İşlekel et al., 1998). A limited single cyst is associated with better treatment outcomes, and surgery in such cases is considered curative if the cyst is completely removed and does not rupture (Neumayr et al., 2013a). Epidural CE lesions can vary from a single epidural worm cyst to a paravertebral encapsulated cyst to a large, dumbbell-shaped encapsulated cyst with surrounding soft-tissue invasion (Khazim et al., 2003). Patients with these two types of spinal CE are often found to have spinal cord compression. Anterior resection of the cyst is usually performed in these cases; however, if complete resection is not possible, negative-pressure aspiration and partial wall resection are desirable, and drugs with high toxicity should be avoided (Parvaresh et al., 1996). The recurrence rate of epidural CE is high (27%) because multiple cysts cannot be completely excised and the cysts are prone to rupture (Neumayr et al., 2013a).

When bone CE occurs within the vertebral body, microcystic infiltration makes complete resection difficult to achieve. However, surgical intervention can prolong patient survival (Turtas et al., 1980). Complete excision of the cyst with no destruction of the cyst wall is the standard treatment for spinal CE. However, complete cyst removal is difficult in many cases for various reasons: (World Health Organization, 2015) the cyst wall is thin; (Gnanasekaran et al., 2016) the surrounding soft tissue is attached to the cyst wall; Neumayr et al. (2013a) bone CE was not considered preoperatively; (Loudiye et al., 2003) the lesion is extensive, making surgery too invasive for the patient to tolerate; and Schnepper and Johnson (2004) surgery results in bone defects and requires the use of various techniques such as bone grafts, pedicle screw systems, titanium-cage implants, plates, or bone cement to stabilize the spine (Iplikçioğlu et al., 1991). Bone cement might be one of the best options for postoperative vertebral stabilization due to its high-temperature killing effect on PSCs, which reduces postoperative recurrence of bone CE (Yildiz et al., 2001). For large spinal-CE lesions, palliative surgical treatment plus chemotherapy might be more appropriate to limit surgical stress or damage to the patient's neural tissues (Sudo and Minami, 2010).

Pelvic CE is the second-most widespread type of bone CE, which is difficult to treat, and the outcome and prognosis depend on whether the CE has invaded the sacroiliac or hip joints (Martínez et al., 2001). Surgical attempts to remove the lesion can fail, resulting in severe functional disability when the joint is infected. Currently, common surgical treatments for pelvic CE include simple drainage or debridement, complete resection, total hip arthroplasty, bone grafting, pubic fusion, giant prosthesis, arthroplasty, osteotomy, and hemipelvic resection (Liang et al., 2014). Hemipelvic resection is frequently used in patients with extensive pelvic CE who are infected in multiple sites. However, it is accompanied by high mortality and complications such as sepsis, pressure sores, and loss of function, meaning that patients are often resistant to this procedure. Palliative surgical treatment with long-term oral administration of effective anthelmintics such as albendazole (ABZ) is usually a good option for patients with bone CE accompanied by extensive bone destruction (Sudo and Minami, 2010). Daniel et al. reported a case of pelvic CE extending to the hip. After hip resection combined with total hip arthroplasty supplemented by perioperative medication, the patient had no signs of recurrence or sepsis at 1-year postoperative follow-up, but he required a walker as a

TABLE 3 Treatment of bone CE.

Classification of bone hydatid disease	Positioning	Treatment		Result
		Surgery	Drug	
Spinal CE	Cranio-vertebral junction (Kiran et al., 2021)	Decompression; resection of cyst lesion; washing with 20% hypertonic saline solution; occipital-C2- C3 vertebrae fusion	ABZ (400 mg per day for 6 weeks)	Symptoms improved after 3 months
	Cervical vertebra (Majmundar et al., 2019)	Laminectomy + resection of lesions	ABZ (pre-operation and post-operation)	Improved
	Cervical and thoracic vertebrae (Bouattour et al., 2021; Cavus et al., 2018)	Decompression; resection of cyst lesion; washing with 20% hypertonic saline solution	ABZ (15 mg/kg/d, po. For 1 year)	No recurrence after 1 year
	Thoracic vertebrae (Zhang et al., 2017, 2021; Akhaddar and Boucetta, 2018; Dighe et al., 2018; Depré et al., 2019; Saul et al., 2020; Das et al., 2021; Safari et al., 2021; Alkan Çeviker et al., 2022)	Resection of cyst lesion; ashing with betadine solution and hypertonic saline	ABZ (20 mg/kg/day for 6 months)	Improved
	Ribs (Hans et al., 2019; Kassimi et al., 2021; Agnihotri et al., 2017)	Resection of cyst lesion	ABZ	Recurred after 6 months
	Lumbar vertebra (Staouni et al., 2020; Tian et al., 2020)	Resection of cyst lesion; washing with hydrogen peroxide and 5% hypertonic saline; spinal fusion and fixation	ABZ (10-15 mg/kg/day, for at least 6 months)	Improved after 6 months
	Lumbar vertebra and sacral vertebra (Majmundar et al., 2019; Sharma et al., 2020; Trifa and Maamri, 2021)	Debridement; decompression; resection of cyst lesion; washing with hypertonic saline solution	ABZ	No recurrence for 3 years
Long bones CE	Humeral bone (Patino and Ramos Vertiz, 2019)	Oncological resection of the humerus and total replacement of the humerus	ABZ (15 mg/kg/ d) preoperation for 1 month and post-operation for 6 months	Improved
	Radial bone (Bağcıer and Tufanoğlu, 2020)	Surgery	ABZ (400 mg/d) preoperation for 1 month and post-operation for 6 months	No recurrence
	Ulna (Reddy et al., 2017)	Resection of cyst	ABZ (400 mg/d) for 6 weeks	Improved
	Femoral bone (Gautam et al., 2018; Salman et al., 2018; Dathik et al., 2019; Fröschen et al., 2019; Masmoudi et al., 2019; Ramteke et al., 2019; Oueslati et al., 2020; Ahmady-Nezhad et al., 2022)	Resection of the lesion; fixation; resection of the lesion; Reconstruction of the right hip	ABZ (400 mg, bid, proper-operation, and post-operation); praziquantel (300 mg/day post-operation)	Improved
	Tibia bone (Nascimento et al., 2018)	Resection of lesion	ABZ (10-20 mg/kg/day)	Improved
Pelvic CE	Iliac bone (Govindasamy et al., 2021)	Palliative surgery (debridement, cyst resection, 0.1% sodium hypochlorite flushing, drainage)	ABZ (pre-operation for 14 days and post-operation for 6 months)	Non-symptom
	Ischiopubic branch acetabulum (Daniel et al., 2017)	Hemipelvectomy + hip resection + hip reconstruction	ABZ (800 mg,2 doses per day, pre-operation and post-operation)	Improved
	Inferior pubic ramus, ischium, and iliac bone (Dehghan Manshadi et al., 2017)	Not mentioned	ABZ (400 mg, bid, po)	Not mentioned
	Trochanteric region (Boussaid et al., 2021)	Rejected	ABZ	Not mentioned
	Pelvic bone (Wang et al., 2019)	Cystic resection; displacement of artificial hemipelvis and hip joint	ABZ	Improved
	Joint space; supra-acetabular region and superior pubic ramus (Bhatnagar et al., 2017)	Debridement	ABZ (10 mg/kg/day; pre-operation and post-operation)	Improved; no recurrence
	Sacroiliac joint (Akremi et al., 2022; Peña Huertas et al., 2022)	Cyst resection; washing with hypertonic saline; hip replacement	ABZ	Symptom-free; No progress in disease

*The above cases information is from Table 1.

10.3389/fmicb.2023.1273870

mobility aid (Daniel et al., 2017). As can be seen, the outcome of pelvic-joint infection is very serious. Once pelvic CE infects the hip joint, it usually causes weakness in the legs and reduces joint function. Total hip replacement may be considered to restore the function of the joint.

Treatment and prognosis of long-bone CE are better than those of spinal and pelvic CE because the growth of worms is more limited in these bones than in the spine or pelvis. When the infection occurs proximally, femoral CE is more likely to infiltrate the neighboring pelvic bone. When early lesions are limited to a single segment, radical long-bone resection is the treatment of choice. If the lesion is diffusely spread, preserving the limb is not possible; amputation is the only effective treatment (Zlitni et al., 2001). Postoperative bone defects are often treated with different methods, including bone cement filling and bone grafting. Moore et al. reported a case of total femoral-replacement surgery to treat diffuse osteopathy caused by left-femoral CE, using a total femoral prosthesis (MOST Total Femoral System) to reconstruct the defect. The patient's 1-year postoperative prognosis was good, with femoral function mostly restored (Moore et al., 2015). The use of re-aspiration (PAIR) has shown encouraging results in localized cases where surgical removal is not possible or the patient refuses surgery, relapses postoperatively, or does not respond to pharmacological treatment (Peer et al., 2023).

5.2. Pharmacotherapy

If PSCs infection is localized to the axial bone or if the lesion is too large, radical surgical treatment is not possible; instead, palliative surgery plus long-term medication is often the best option for improving symptoms or even curing the patient. Pharmacological treatment of CE is similar to tumor chemotherapy; ABZ can be used preoperatively to inhibit further growth of CE and even reduce cyst size (Horton, 1989), or postoperatively, either alone or in combination with other antiparasitic drugs, to prevent recurrence (Horton, 1989). However, no drugs yet exist that can effectively prevent PSCs from invading and destroying bone and muscle (Togral et al., 2016).

As shown in Table 3, drugs are an important part of perioperative bone CE management, with dosage and duration depending on the site of parasitism and degree of invasion. The action of ABZ is effective in bone CE; 10–15 mg/kg/day for at least 6 continuous months is required for better prognosis as well as a lower relapse rate. To reduce the risk of cystic-fluid rupture and its potential complications, at least 300 mg/day of praziquantel must be given in combination with ABZ. Although ABZ + praziquantel has been reported to have anti-CE activity in some cases, its efficacy remains to be further investigated in subsequent bone CE trials (Gautam et al., 2018). Postoperative chemotherapy plus surgery, a popular form of bone CE treatment in recent years, can be extended for up to 2 years in complicated cases (Agarwal et al., 1992).

One study reported a drug-loaded nanoemulsion to be similar in efficiency to ABZ in inactivating PSCs in subcutaneous tissue. The investigators concluded that the nanoemulsion had high stability, high water solubility, and greater ability to cross biomembranes, thereby proving more efficacious against lesions that were difficult to reach with ABZ (Ahmadi et al., 2020). However, validation was not performed in animal models of bone CE.

6. Discussion

The research reviewed in this paper emphasizes the complexity of diagnosis and treatment of bone echinococcosis. Therefore, to understand the management of bone echinococcosis, the following aspects should be carried out. Bone CE with high rates of recurrence, disability, and paralysis, is a serious parasitic disease that imposes a severe burden on patients and families. Since bone CE mainly exists in pastoral areas, the medical level is not developed, and there is currently no clear consensus on bone CE, how to use convenient and appropriate methods for early diagnosis is undoubtedly the most important. Therefore, special medical examination centers for bone CE should be established to provide regular screening of sensitive populations and to regularly monitor the musculoskeletal conditions of vulnerable individuals. The clinical symptoms of bone CE are less pronounced in the early stages and become apparent in the later stages. Symptoms of bone CE are related to the location of the lesion and its severity. In spinal CE specifically, pain is the earliest symptom and can be accompanied by neurological manifestations. Early diagnosis and treatment are important for improving bone quality and avoiding complications, Figure 2 provides a diagnostic flow chart based on the 2015 Chinese

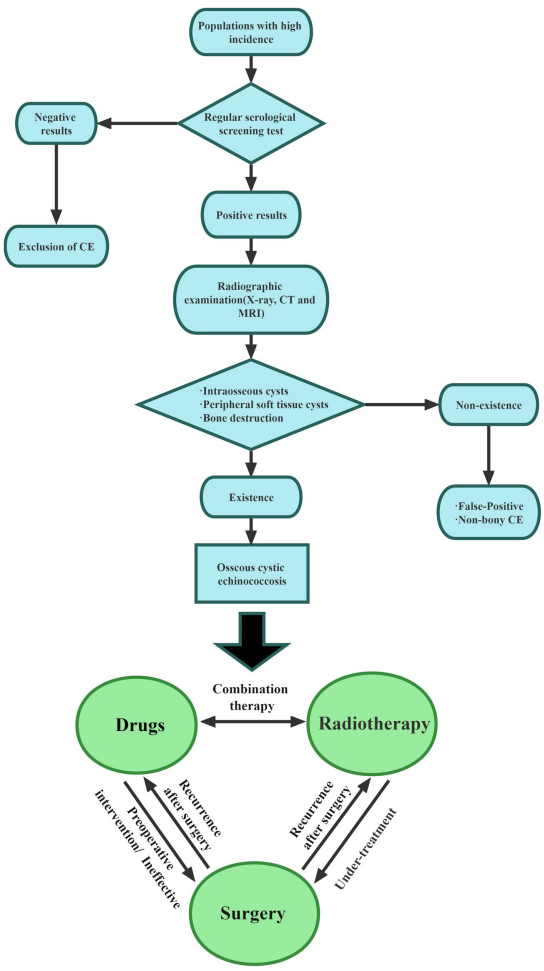

FIGURE 2
Diagnostic flow diagram of bone CE.

Journal of Surgery expert consensus on the diagnosis and treatment of bone CE, hoping to provide a reference for the management of bone CE (Orthopaedics Professional Committee of Xinjiang Medical, 2015). The use of improved serological methods and new antigen development has undoubtedly improved the specificity and sensitivity of diagnosis, but there is a lack of large sample verification, which needs to be combined with imaging results. MRI is undoubtedly the most suitable imaging examination. The 'bone window 'and 'soft tissue window 'are the most sensitive for the diagnosis of bone CE. Therefore, new serological tests combined with imaging results can yield greater diagnostic value. Radical surgery combined with filler PMMA as the treatment of choice for bone CE not only repairs bone defects but can also kill PSCs. However, patients with large-bone defects often refuse radical surgery, and the risk of cystic-fluid leakage is high in such procedures due to cyst location, cyst depth, and degree of bone infiltration. Palliative surgical treatment improves patient survival while relieving the symptoms. Surgery combined with antiparasitic drugs (ABZ, praziquantel) can be used for complex manifestations of bone CE, as a chronic disease management, through systematic treatment, control and avoid complications.

Author contributions

SiW and ShW: Conceptualization, Writing – review & editing. HS, YH and YL: Data curation, Writing – review & editing. YM and QR: Writing – original draft, Writing – review & editing.

Funding

The author(s) declare financial support was received for the research, authorship, and/or publication of this article. This research received no specific grant from any funding agency, commercial or not-for-profit sectors.

Conflict of interest

The authors declare that the research was conducted in the absence of any commercial or financial relationships that could be construed as a potential conflict of interest.

Publisher's note

All claims expressed in this article are solely those of the authors and do not necessarily represent those of their affiliated organizations, or those of the publisher, the editors and the reviewers. Any product that may be evaluated in this article, or claim that may be made by its manufacturer, is not guaranteed or endorsed by the publisher.

References

Açikgöz, B., Sungur, C., Ozgen, T., Camurdanoğlu, M., and Berker, M. (1996). Endoscopic evacuation of sacral hydatid cysts: a case report. *Spinal Cord* 34, 361–364. doi: 10.1038/sc.1996.66

Agarwal, S., Shah, A., Kadhi, S. K., and Rooney, R. J. (1992). Hydatid bone disease of the pelvis. A report of two cases and review of the literature. *Clin. Orthop. Relat. Res.* 280, 251–255. doi: 10.1097/00003086-199207000-00034

Agnihotri, M., Goel, N., Shenoy, A., Rai, S., and Goel, A. (2017). Hydatid disease of the spine: a rare case. *J. Craniovert. Junct. Spine* 8, 159–160. doi: 10.4103/jcvjs.JCVJS_16_17

Ahmadi, A., Moazeni, M., and Shaddel, M. (2020). Subcutaneous hydatid cyst in laboratory mice: is it a suitable method for evaluating therapeutic agents against hydatid cyst? *Arch. Razi. Inst.* 75, 75–81. doi: 10.22092/ari.2018.123382.1245

Ahmady-Nezhad, M., Rezainasab, R., Khavandegar, A., Rashidi, S., and Mohammad-Zadeh, S. (2022). Perineal and right femoral hydatid cyst in a female with regional paresthesia: a rare case report. *BMC Surg.* 22:64. doi: 10.1186/s12893-022-01516-z

Akhaddar, A., and Boucetta, M. (2018). A new surgical technique for the removal of extensive spinal epidural hydatid cyst. *Surg. Neurol. Int.* 9:96. doi: 10.4103/sni.sni_89_18

Akremi, M. S. E., Bellil, M., Souissi, M., Zaibi, M., Balti, W., and Salah, M. B. (2022). Sciatica and femoral head osteonecrosis complicating a gluteal hydatid cyst: a case report. *Int. J. Surg. Case Rep.* 92:106841. doi: 10.1016/j.ijscr.2022.106841

Alkan Çeviker, S., Yüksel, C., Şener, A., Önder, T., Metineren, M. H., Özel, Ç., et al. (2022). Hydatid cyst of the spine: a rare case report. *Turkiye Parazitol. Derg.* 46, 78–81. doi: 10.4274/tpd.galenos.2021.29392

Altinörs, N., Bavbek, M., Caner, H. H., and Erdogan, B. (2000). Central nervous system hydatidosis in Turkey: a cooperative study and literature survey analysis of 458 cases. *J. Neurosurg.* 93, 1–8. doi: 10.3171/jns.2000.93.1.0001

Arana Iniquez, R. E. (1978). "Echinococcus" in *Infections of the nervous system. III. Handbook of clinical neurology am sterdam North-Holland*. eds. P. J. Vinken and G. W. Bruyn, vol. 35, 175–208.

Arias, B. M. (1946). Osteohydatidosis; its radiological features. *Radiology* 47, 569–574. doi: 10.1148/47.6.569

Arik, H. O., Arican, M., Cetin, N. K., and Sarp, U. (2015). Primary intraosseous hydatid cyst of the femur. *Iran Red Crescent Med J* 17:e21070. doi: 10.5812/ircmj.21070

Arkun, R., and Mete, B. D. (2011). Musculoskeletal hydatid disease. *Semin. Musculoskelet. Radiol.* 15, 527–540. doi: 10.1055/s-0031-1293498

Bağcıer, F., and Tufanoğlu, F. H. (2020). A rare presentation of hydatid cyst: a case with radial bone involvement. *Turkiye Parazitol. Derg.* 44, 185–186. doi: 10.4274/tpd.galenos.2020.6416

Berk, C., Ciftçi, E., and Erdoğan, A. (1998). MRI in primary intraspinal extradural hydatid disease: a case report. *Neuroradiology* 40, 390–392. doi: 10.1007/s002340050608

Bhatnagar, N., Kishan, H., Sura, S., Lingaiah, P., and Jaikumar, K. (2017). Pelvic hydatid disease: a case report and review of literature. *J. Orthopaedic Case Rep.* 7, 25–28. doi: 10.13107/jocr.2250-0685.834

Bhojraj, S. Y., and Shetty, N. R. (1999). Primary hydatid disease of the spine: an unusual cause of progressive paraplegia. Case report and review of the literature. *J. Neurosurg.* 91, 216–218. doi: 10.3171/spi.1999.91.2.0216

Bouattour, N., Nabli, F., Nagi, S., Saied, Z., Ben Abdelaziz, I., Hentati, F., et al. (2021). Primary spinal Hydatidosis revealed by spinal cord compression. *Neurol. Clin. Pract.* 11, e37–e39. doi: 10.1212/CPJ.0000000000000763

Boussaid, S., Daldoul, C., Hassayoun, M., Rekik, S., Jammali, S., Sahli, H., et al. (2021). Primitive pelvic bone hydatidosis: what an amazing extension. *Clin. Case Rep.* 9:e05054. doi: 10.1002/ccr3.5054

Caglar, Y. S., Ozgural, O., Zaimoglu, M., Kilinc, C., Eroglu, U., Dogan, I., et al. (2019). Spinal hydatid cyst disease: challenging surgery – an institutional experience. *J. Korean Neurosurg. Soc.* 62, 209–216. doi: 10.3340/jkns.2017.0245

Carmena, D., Benito, A., and Eraso, E. (2006). Antigens for the immunodiagnosis of echinococcus granulosus infection: an update. *Acta Trop.* 98, 74–86. doi: 10.1016/j.actatropica.2006.02.002

Cattaneo, L., Manciulli, T., Cretu, C. M., Giordani, M. T., Angheben, A., Bartoloni, A., et al. (2019). Cystic echinococcosis of the bone: a European Multicenter study. *Am. J. Trop. Med. Hyg.* 100, 617–621. doi: 10.4269/ajtmh.18-0758

Cavus, G., Acik, V., Bilgin, E., Gezercan, Y., and Okten, A. I. (2018). Endless story of a spinal column hydatid cyst disease: a case report. *Acta Orthop. Traumatol. Turc.* 52, 397–403. doi: 10.1016/j.aott.2018.03.004

Chen, Y. W., Aikebaier, A., and Zhao, Y. (2020). Evaluation of imaging features of pelvic echinococcosis based on multimodal images. *J. Orthop. Surg. Res.* 15:493. doi: 10.1186/s13018-020-01912-2

Daniel, C., Matthieu, H., Goulven, R., Jocelyn, M., Valerie, D., and Christophe, H. (2017). Successful pelvic resection for acetabular Hydatidosis. *Case Rep. Orthop.* 2017, 1–4. doi: 10.1155/2017/9495783

Das, G., Nanda, S. N., Sahu, N. K., Kumar, D. S., and Patro, B. P. (2021). Hydatid cyst of dorsal spine masquerading as tubercular infection: a case report and review of literature. *Asian J. Neurosurg.* 16, 886–889. doi: 10.4103/ajns.ajns_199_21

Dathik, S., Chopra, R. K., Talwar, J., Pheroz, M., and Prasad, R. (2019). Primary hydatidosis of distal femur masquerading malignancy -A rare case. *J Clin Orthop Trauma.* 10, 213–220. doi: 10.1016/j.jcot.2017.12.003

Dehghan Manshadi, S. A., Rezahosseini, O., Saberi, S., Salahshour, F., and Mahdavi, I. S. (2017). Collapsed membranes within pelvic cyst: what is the diagnosis? *Clin Case Rep.* 5, 199–200. doi: 10.1002/ccr3.767

Depré, F., Dittmayer, C., and Schneider, T. (2019). Compression of the spinal cord in echinococcus infection. *Int. J. Infect. Dis.* 89, 10–11. doi: 10.1016/j.ijid.2019.09.014

Dighe, M. P., Balasubramaniam, S., and Nadkarni, T. D. (2018). Transthoracic approach for ventrally situated paraspinal extradural hydatid cyst of the dorsal spine. *J. Craniovertebr. Junct. Spine.* 9, 271–273. doi: 10.4103/jcvjs.JCVJS_71_18

Fathi, S., Jalousian, F., Hosseini, S. H., Parsa, H., and Kordafshari, S. (2016). A study of cross-reactivity between recombinant EPC1 antigen of echinococcus granulosus in serum from patients with confirmed cystic echinococcosis infection and other parasitic infections. *Am. J. Trop. Med. Hyg.* 94, 1313–1317. doi: 10.4269/ajtmh.15-0680

Fröschen, F. S., Fischer, H. P., Hischebeth, G. T., Reiter-Owona, I., Randau, T. M., Gravius, S., et al. (2019). Osseous hydatidosis of the proximal femur: a rare diagnosis in revision total hip arthroplasty. *Infection* 47, 301–305. doi: 10.1007/s15010-018-1193-6

Gautam, D., Malhotra, R., and Dubey, S. (2018). Combination drug chemotherapy and massive skeletal allograft in the management of hydatid disease of the femur. *BMJ Case Rep.* 2018, 1–4. doi: 10.1136/bcr-2017-223332

Gdoura, F., Trigui, M., Zribi, W., Ellouze, Z., Bouzidi, R., Ayedi, K., et al. (2010). Pelvic bone hydatidosis. *Orthop. Traumatol. Surg. Res.* 96, 85–89. doi: 10.1016/j.otsr.2009.04.020

Gnanasekaran, K. K., Prabhu, A. J., and George, S. (2016). Osseous hydatidosis of femur in a patient with fracture non-union: an uncommon entity. *J. Clin. Diagn. Res.* 10, ED06–ED08. doi: 10.7860/JCDR/2016/23610.9097

Govindasamy, A., Bhattarai, P. R., and John, J. (2021). Lytic parasitic: a case of bone destructing echinococcosis. *Ther. Adv. Infect. Dis.* 8, 204993612110476–204993612110477. doi: 10.1177/20499361211047664

Hans, B., Gupta, K., Kalra, K., and Suri, J. C. (2019). An unusual case of extrapulmonary hydatid cyst masquerading as a mediastinal tumor. *Cureus* 11:e5612. doi: 10.7759/cureus.5612

Herrera, A., Martínez, A. A., and Rodríguez, J. (2005). Spinal hydatidosis. *Spine (Phila Pa 1976)* 30, 2439–2444. doi: 10.1097/01.brs.0000184688.68552.90

Horton, R. J. (1989). Chemotherapy of echinococcus infection in man with albendazole. *Trans. R. Soc. Trop. Med. Hyg.* 83, 97–102. doi: 10.1016/0035-9203(89)90724-4

Inayat, F., Azam, S., Baig, A. S., Nawaz, G., and Ullah, W. (2019). Presentation patterns, diagnostic modalities, management strategies, and clinical outcomes in patients with hydatid disease of the pelvic bone: a comparative review of 31 cases. *Cureus* 11:e4178. doi: 10.7759/cureus.4178

Iplikçioğlu, C. A., Kökes, F., Bayar, A., Doğanay, S., and Buharali, Z. (1991). Spinal invasion of pulmonary Hydatidosis: computed tomographic demonstration. *Neurosurgery* 29, 467–468. doi: 10.1227/00006123-199109000-00026

Ira, B., Wilson, M., Dukes, K., Greenfield, S., Kaplan, S., and Hillman, B. (2001). Patient's role in the use of radiology testing for common office practice complaints. *Arch. Intern. Med.* 161, 256–263. doi: 10.1001/archinte.161.2.256

İşlekel, S., Zileli, M., and Erşahin, Y. (1998). Intradural spinal hydatid cysts. *Eur. Spine J.* 7, 162–164. doi: 10.1007/s005860050048

Jacquier, M., and Piroth, L. (2018). Vertebral Hydatidosis. *N. Engl. J. Med.* 379:e5. doi: 10.1056/NEJMicm1714206

Johnson, F. W., and Hobson, D. (1977). The effect of penicillin on genital strains of *Chlamydia trachomatis* in tissue culture. *Antimicrobial Chemother.* 3, 46–56. doi: 10.1093/jac/3.1.49

Kaen, A., Lagares, A., Perez-Nunez, A., Rivas, J. J., Ramos, A., and Lobato, R. D. (2009). Intradural extramedullary spinal hydatidosis: case report. *Neurocirugia* 20, 282–287. doi: 10.1016/S1130-1473(09)70169-1

Kapoor, S. K., Kataria, H., Patra, S. R., Bharadwaj, M., Vijay, V., and Kapoor, S. (2013). Multi-organ hydatidosis with extensive involvement of the hemipelvis and ipsilateral femur. *Parasitol. Int.* 62, 82–85. doi: 10.1016/j.parint.2012.08.006

Kassimi, M., Rami, A., Habi, J., Guerroum, H., El Pardya, T. R., Chikhaoui, N., et al. (2021). Recurrent costovertebral hydatidosis with epidural extension. *Radiol Case Rep.* 16, 1712–1714. doi: 10.1016/j.radcr.2021.04.016

Khazim, R., Fares, Y., Heras-Palou, C., and Ruiz, B. P. (2003). Posterior decompression of spinal hydatidosis: long-term results. *Clin. Neurol. Neurosurg.* 105, 209–214. doi: 10.1016/S0303-8467(03)00013-1

Kiran, M., Prasad, C. K., Mrudul, B., and Shishir, K. (2021). An intraoperative surprise! A rare case report of primary craniovertebral junction hydatid disease mimicking a bony tumor. *World Neurosurg.* 146, 171–176. doi: 10.1016/j.wneu.2020.11.072

Liang, Q., Wen, H., Yunus, A., Tian, Z., Jiang, F., and Song, X. (2014). Treatment experiences of pelvic bone hydatidosis. *Int. J. Infect. Dis.* 18, 57–61. doi: 10.1016/j.ijid.2013.09.010

List, C., Qi, W., Maag, E., Gottstein, B., Muller, N., and Felger, I. (2010). Serodiagnosis of echinococcus spp. infection: explorative selection of diagnostic antigens by peptide microarray. *PLoS Negl. Trop. Dis.* 4:e771. doi: 10.1371/journal.pntd.0000771

Loudiye, H., Aktaou, S., Hassikou, H., El-Bardouni, A., El-Manouar, M., Fizazi, M., et al. (2003). Hydatid disease of bone. Review of 11 cases. *Joint Bone Spine* 70, 352–355. doi: 10.1016/S1297-319X(03)00039-3

Luan, H., Liu, K., Deng, Q., Sheng, W., Maimaiti, M., Guo, H., et al. (2022). Multiple debridement of cavity lesions combined with antiparasitic chemotherapy in the treatment of mid or advanced spinal echinococcosis: a retrospective study of 33 patients. *Int. J. Infect. Dis.* 114, 261–267. doi: 10.1016/j.ijid.2021.11.014

Majmundar, N., Patel, P. D., Dodson, V., Tran, A., Goldstein, I., and Assina, R. (2019). Parasitic infections of the spine: case series and review of the literature. *Neurosurg. Focus.* 46:E12. doi: 10.3171/2018.10.FOCUS18472

Martínez, A. A., Herrera, A., Cuenca, J., and Herrero, L. (2001). Hydatidosis of the pelvis and hip. *Int. Orthop.* 25, 302–304. doi: 10.1007/s002640100278

Masmoudi, K., Ben Maitigue, M., Frikha, R., Mouelhi, T., and Cheikhrouhou, H. (2019). Loosening of a Total hip arthroplasty associated with a periprosthetic femoral fracture caused by recurrent Hydatidosis of the hip: a case report. *JBJS Case Connect.* 9:e0044. doi: 10.2106/JBJS.CC.19.00044

McManus, D. P. (2014). Immunodiagnosis of sheep infections with echinococcus granulosus: in 35 years where have we come? *Parasite Immunol.* 36, 125–130. doi: 10.1111/pim.12072

McManus, D. P., Gray, D. J., Zhang, W., and Yang, Y. (2012). Diagnosis, treatment, and management of echinococcosis. *BMJ* 344:e3866. doi: 10.1136/bmj.e3866

Monge-Maillo, B., Chamorro Tojeiro, S., and Lopez-Velez, R. (2017). Management of osseous cystic echinococcosis. *Expert Rev. Anti-Infect. Ther.* 15, 1075–1082. doi: 10.1080/14787210.2017.1401466

Moore, D., Baker, K. C., and Les, K. (2015). Hydatid disease of the femur treated with a Total femoral replacement: a case report. *JBJS Case Connect.* 5:e7. doi: 10.2106/JBJS.CC.M.00279

Morris, B. S., Madiwale, C. V., Garg, A., and Chavhan, G. B. (2002). Hydatid disease of bone: a mimic of other skeletal pathologies. *Australas. Radiol.* 46, 431–434. doi: 10.1046/j.1440-1673.2002.t01-1-01099.x

Muscolo, D. L., Zaidenberg, E. E., Farfalli, G. L., Aponte-Tinao, L. A., and Ayerza, M. A. (2015). Use of massive allografts to manage hydatid bone disease of the femur. *Orthopedics* 38, e943–e946. doi: 10.3928/01477447-20151002-92

Nascimento, G., Silva, C., Marques, R., Silva, C., Oliveira, J. F., Santos, J., et al. (2018). Periprosthetic pathologic fracture following tibial echinococcosis: a case report. *Int. J. Surg. Case Rep.* 51, 231–236. doi: 10.1016/j.ijscr.2018.08.045

Neumayr, A., Tamarozzi, F., Goblirsch, S., Blum, J., and Brunetti, E. (2013a). Spinal cystic echinococcosis--a systematic analysis and review of the literature: part 1. Epidemiology and anatomy. *PLoS Negl. Trop. Dis.* 7:e2450. doi: 10.1371/journal.pntd.0002450

Neumayr, A., Tamarozzi, F., Goblirsch, S., Blum, J., and Brunetti, E. (2013b). Spinal cystic echinococcosis--a systematic analysis and review of the literature: part 2. Treatment, follow-up, and outcome. *PLoS Negl. Trop. Dis.* 7:e2458. doi: 10.1371/journal.pntd.0002458

Orthopaedics Professional Committee of Xinjiang Medical (2015). Expert consensus on the diagnosis and treatment of bone hydatid disease. *Chin. J. Surg.* 53, 922–927. Hydatid Surgery Professional Committee SSB, China Medical Association.

Ortona, E., Margutti, P., Delunardo, F., Nobili, V., Profumo, E., Riganò, R., et al. (2005). Screening of an echinococcus granulosus cDNA library with IgG4 from patients with cystic echinococcosis identifies a new tegumental protein involved in the immune escape. *Clin. Exp. Immunol.* 142, 528–538. doi: 10.1111/j.1365-2249.2005.02939.x

Oueslati, A., Amri, K., Chefi, M. A., Mallat, Y., Znagui, T., and Nouisri, L. (2020). Hydatid disease of proximal femur treated using a mega prosthesis: a case report. *Int. J. Surg. Case Rep.* 68, 67–73. doi: 10.1016/j.ijscr.2020.02.002

Ozdemir, H. M., Ogün, T. C., and Tasbas, B. (2004). A lasting solution is hard to achieve in primary hydatid disease of the spine: long-term results and an overview. *Spine (Phila Pa 1976)* 29, 932–937. doi: 10.1097/00007632-200404150-00022

Ozek, M. M. (1994). Complications of central nervous system hydatid disease. *Pediatr. Neurosurg.* 20, 84–91. doi: 10.1159/000120770

Pamir, M. N., Ozduman, K., and Elmaci, I. (2002). Spinal hydatid disease. *Spinal Cord* 40, 153–160. doi: 10.1038/sj.sc.3101214

Papanikolaou, A. (2008). Osseous hydatid disease. *Trans. R. Soc. Trop. Med. Hyg.* 102, 233–238. doi: 10.1016/j.trstmh.2007.09.012

Parvaresh, M., Moin, H., and Miles, J. B. (1996). Dumbbell hydatid cyst of the spine. *Br. J. Neurosurg.* 10, 211–214. doi: 10.1080/02688699650040403

Pathania, V. P., Kakkar, S., and Sikdar, J. (2000). Hydatid disease of femur. *Med. J. Armed Forces India* 56, 75–76. doi: 10.1016/S0377-1237(17)30103-X

Patino, J. M., and Ramos Vertiz, A. J. (2019). Hydatidosis of the complete humerus. Treated with radical resection and endoprosthesis. Case report. *Int. J. Surg. Case Rep.* 65, 296–300. doi: 10.1016/j.ijscr.2019.10.083

Peer, S., Jabbal, H. S., Singh, P., Ma, P. S., Kakkera, S., and Bhat, P. (2023). A case report of successful percutaneous aspiration, injection, and re-aspiration (PAIR) technique for treatment of retrovesical pelvic hydatid cyst. *Radiol. Case Rep.* 18, 331–334. doi: 10.1016/j.radcr.2022.10.056

Peña Huertas, M., Zafra Martín, J., Álvarez García de Quesada, I., Díaz Gavela, A. A., Guerrero Gómez, L. L., Sánchez García, S., et al. (2022). IJRadiation therapy for recurrent hydatid cyst of the pelvic bone: a case report. *Int. J. Infect. Dis.* 115, 168–170. doi: 10.1016/j.ijid.2021.12.313

Petra, K. B., Bardonnet, K., Renner, E., Auer, H., Pawlowski, Z., Ammann, R. W., et al. (2003). European echinococcosis registry: human alveolar echinococcosis, Europe, 1982-2000. *Emerg. Infect. Dis.* 9, 343–349. doi: 10.3201/eid0903.020341

Ramteke, P., Phulware, R. H., Shende, T., Sahoo, B., and Barwad, A. (2019). Hydatid cyst of the femur, radiologically mimicking a sarcoma. *Diagn. Cytopathol.* 47, 1045–1048. doi: 10.1002/dc.24198

Rangheard, A. S., Vanel, D., Viala, J., Schwaab, G., Casiraghi, O., and Sigal, R. (2001). Synovial sarcomas of the head and neck: CT and MR imaging findings of eight patients. *AJNR Am. J. Neuroradiol.* 22, 851–857.

Reddy, I. V., Kumar, A. H. A., Samorekar, B., Babu, B. A., and Mettu, A. K. (2017). Complicated hydatid cyst of ulna- A rare case report. *J. Clin. Diagn. Res.* 11, RD01–RD03. doi: 10.7860/JCDR/2017/21804.9773

Robinson, R. G. (1959). Hydatid disease of the spine and its neurological complications. *Br. J. Surg.* 47, 301–306. doi: 10.1002/bjs.18004720324

Safari, H., Mirzavand, S., Rafiei, A., and Beiromvand, M. (2021). Twenty-six years of involvement with cystic echinococcosis: a case report. *J. Med. Case Rep.* 15:266. doi: 10.1186/s13256-021-02810-9

Salman, F., Khan, M. I., Hussain, I., and Abdullah, H. M. A. (2018). Pathological fracture of the femoral neck in a middle-aged woman: a rare presentation of primary hydatid cyst disease in humans. *BMJ Case Rep.* 2018. doi: 10.1136/bcr-2017-222980

Saul, D., Seitz, M.-T., Weiser, L., Oberthür, S., Roch, J., Bremmer, F., et al. (2020). Of cestodes and men: surgical treatment of a spinal hydatid cyst. *J. Neurol. Surg. A Cent. Eur. Neurosurg.* 81, 086–090. doi: 10.1055/s-0039-1693707

Schnepper, G. D., and Johnson, W. D. (2004). Recurrent spinal hydatidosis in North America. *Neurosurg. Focus.* 17, 1–6. doi: 10.3171/foc.2004.17.6.8

Sharma, J. K., Tandon, V., Marathe, N. A., Agrahari, Y., Mallepally, A. R., and Chhabra, H. S. (2020). Hydatid cyst of the spine: a rare case report and review of literature. *J. Orthop. Case Rep.* 10, 57–59. doi: 10.13107/jocr.2020.v10.i03.1748

Siles-Lucas, M., Casulli, A., Conraths, F. J., and Müller, N. (2017). Laboratory diagnosis of echinococcus spp. in human patients and infected animals. *Adv. Parasitol.* 96, 159–257. doi: 10.1016/bs.apar.2016.09.003

Sioutis, S., Reppas, L., Bekos, A., Soulioti, E., Saranteas, T., Koulalis, D., et al. (2021). Echinococcosis of the spine. *EFORT Open Rev.* 6, 288–296. doi: 10.1302/2058-5241.6.200130

Song, X. H., Ding, L. W., and Wen, H. (2007). Bone hydatid disease. *Postgrad. Med. J.* 83, 536–542. doi: 10.1136/pgmj.2007.057166

Staouni, I. B., Marzouki, Z., Haloua, M., Lamrani, Y. A., Boubbou, M., Maâroufi, M., et al. (2020). Horse tail syndrome revealing spinal-medullary hydatid disease. *Pan Afr. Med. J.* 36:225. doi: 10.11604/pamj.2020.36.225.21606

Steinmetz, S., Racloz, G., Stern, R., Dominguez, D., Al-Mayahi, M., Schibler, M., et al. (2014). Treatment challenges associated with bone echinococcosis. *J. Antimicrob. Chemother.* 69, 821–826. doi: 10.1093/jac/dkt429

Sudo, H., and Minami, A. (2010). Neurological picture. A widespread echinococcosis of the spine. *J. Neurol. Neurosurg. Psychiatry* 81:892. doi: 10.1136/jnnp.2009.198341

Thomas, M., Keller, M., Schweitzer, J. S., Helfend, L. K., and Chappell, T. (1997). Treatment of progressive cervical spinal instability secondary to hydatid disease. *Spine* 22, 915–919. doi: 10.1097/00007632-199704150-00016

Tian, Y., Jiang, M., Shi, X., Hao, Y., and Jiang, L. (2020). Case report: huge dumbbell-shaped primary hydatid cyst across the intervertebral foramen. *Front. Neurol.* 11:592316. doi: 10.3389/fneur.2020.592316

Togral, G., Arikan, S. M., Ekiz, T., Kekec, A. F., and Eksioglu, M. F. (2016). Musculoskeletal hydatid cysts resembling Tumors: a report of five cases. *Orthop. Surg.* 8, 246–252. doi: 10.1111/os.12246

Torricelli, P., Martinelli, C., Biagini, R., Ruggieri, P., and De Cristofaro, R. (1990). Radiographic and computed tomographic findings in hydatid disease of bone. *Skeletal Radio* 19, 435–439. doi: 10.1007/BF00241799

Trifa, A., and Maamri, K. (2021). Aggressive behavior and recurrent spinal hydatid cyst. *Pan Afr. Med. J.* 40:202. doi: 10.11604/pamj.2021.40.202.32389

Turtas, S., Viale, E. S., and Pau, A. (1980). Long-term results of surgery for hydatid disease of the spine. *Surg. Neurol.* 13, 468–470.

Tüzün, M., and Hekimoğlu, B. (2001). Pictorial essay. Various locations of cystic and alveolar hydatid disease: CT appearances. *J. Comput. Assist. Tomogr.* 25, 81–87. doi: 10.1097/00004728-200101000-00014

Wang, R., Shi, X.-D., and Cao, Y.-P. (2019). Artificial hemipelvis displacement treatment for bone hydatid disease. *Chin. Med. J.* 132, 1621–1622. doi: 10.1097/CM9.0000000000000281

World Health Organization (2015). WHO estimates of the global burden of foodborne diseases burden epidemiology reference group 2007–2015. *J. Diagn. Res.*, Ed06–ed08.

Xiao, N., Mamuti, W., Yamasaki, H., Sako, Y., Nakao, M., Nakaya, K., et al. (2003). Evaluation of use of recombinant Em18 and affinity-purified Em18 for serological differentiation of alveolar echinococcosis from cystic echinococcosis and other parasitic infections. *J. Clin. Microbiol.* 41, 3351–3353. doi: 10.1128/JCM.41.7.3351-3353.2003

Yildiz, Y., Bayrakci, K., Altay, M., and Saglik, Y. (2001). The use of polymethylmethacrylate in the management of hydatid disease of bone. *J. Bone Joint Surg. Br.* 83-B, 1005–1008. doi: 10.1302/0301-620X.83B7.0831005

Zhang, Z., Fan, J., Dang, Y., Xu, R., and Shen, C. (2017). Primary intramedullary hydatid cyst: a case report and literature review. *Eur Spine J.* 26, 107–110. doi: 10.1007/s00586-016-4896-3

Zhang, T., Ma, L.-H., Liu, H., and Li, S.-K. (2021). Incurable and refractory spinal cystic echinococcosis: a case report. *World J. Clin. Cases* 9, 10337–10344. doi: 10.12998/wjcc.v9.i33.10337

Zhang, B., Zhang, L., Zhou, H., Tian, J., and Wang, J. (2021). Progressive compressive myelopathy induced by a rare primary isolated thoracic vertebral hydatid cyst: a case report. *Medicine* 100:e25177. doi: 10.1097/MD.0000000000025177

Zlitni, M., Ezzaouia, K., Lebib, H., Karray, M., Kooli, M., and Mestiri, M. (2001). Hydatid cyst of bone: diagnosis and treatment. *World J. Surg.* 25, 75–82. doi: 10.1007/s002680020010

frontiers | Frontiers in Microbiology

TYPE Original Research
PUBLISHED 15 December 2023
DOI 10.3389/fmicb.2023.1289182

Check for updates

OPEN ACCESS

EDITED BY
Hong Yin,
Chinese Academy of Agricultural Sciences, China

REVIEWED BY
Ioannis A. Giantsis,
University of Western Macedonia, Greece
Dusan Palic,
Ludwig-Maximilians-University Munich, Germany

*CORRESPONDENCE
Sanja Duvnjak
✉ marjanovic@veinst.hr
Bojan Papić
✉ bojan.papic@vf.uni-lj.si

†These authors have contributed equally to this work

RECEIVED 05 September 2023
ACCEPTED 17 November 2023
PUBLISHED 15 December 2023

CITATION
Špičić S, Duvnjak S, Papić B, Reil I, Zrnčić S, Mihaljević Ž, Naletilić Š, Zupičić IG, Kompes G, Habrun B, Mareković I and Zdelar-Tuk M (2023) Description of *Mycobacterium pinniadriaticum* sp. nov., isolated from a noble pen shell (*Pinna nobilis*) population in Croatia. *Front. Microbiol.* 14:1289182. doi: 10.3389/fmicb.2023.1289182

COPYRIGHT
© 2023 Špičić, Duvnjak, Papić, Reil, Zrnčić, Mihaljević, Naletilić, Zupičić, Kompes, Habrun, Mareković and Zdelar-Tuk. This is an open-access article distributed under the terms of the Creative Commons Attribution License (CC BY). The use, distribution or reproduction in other forums is permitted, provided the original author(s) and the copyright owner(s) are credited and that the original publication in this journal is cited, in accordance with accepted academic practice. No use, distribution or reproduction is permitted which does not comply with these terms.

Description of *Mycobacterium pinniadriaticum* sp. nov., isolated from a noble pen shell (*Pinna nobilis*) population in Croatia

Silvio Špičić[1], Sanja Duvnjak[1*†], Bojan Papić[2*†], Irena Reil[1], Snježana Zrnčić[3], Željko Mihaljević[4], Šimun Naletilić[4], Ivana Giovanna Zupičić[3], Gordan Kompes[5], Boris Habrun[5], Ivana Mareković[6] and Maja Zdelar-Tuk[1]

[1]Laboratory for Bacterial Zoonosis and Molecular Diagnostics of Bacterial Diseases, Department of Bacteriology and Parasitology, Croatian Veterinary Institute, Zagreb, Croatia, [2]Veterinary Faculty, Institute of Microbiology and Parasitology, University of Ljubljana, Ljubljana, Slovenia, [3]Laboratory for Fish Pathology, Department for Pathological Morphology, Croatian Veterinary Institute, Zagreb, Croatia, [4]Laboratory for Pathology, Department for Pathological Morphology, Croatian Veterinary Institute, Zagreb, Croatia, [5]Laboratory for General Bacteriology and Mycology, Department of Bacteriology and Parasitology, Croatian Veterinary Institute, Zagreb, Croatia, [6]Department of Clinical and Molecular Microbiology, University Hospital Centre Zagreb, Zagreb, Croatia

Introduction: Shortly before the mass mortality event of the noble pen shell (*Pinna nobilis*) population in the south-eastern Adriatic coast, two rapidly growing *Mycobacterium* strains CVI_P3^T (DSM 114013 T, ATCC TSD-295 T) and CVI_P4 were obtained from the organs of individual mollusks during the regular health status monitoring.

Methods: The strains were identified as members of the genus *Mycobacterium* using basic phenotypic characteristics, genus-specific PCR assays targeting the *hsp65* and 16S rRNA genes and the commercial hybridization kit GenoType Mycobacterium CM (Hain Lifescience, Germany). MALDI-TOF mass spectrometry did not provide reliable identification using the Bruker Biotyper Database.

Results and discussion: Genome-wide phylogeny and average nucleotide identity (ANI) values confirmed that the studied strains are clearly differentiated from their closest phylogenetic relative *Mycobacterium aromaticivorans* and other validly published *Mycobacterium* species (ANI≤85.0%). The type strain CVI_P3^T was further characterized by a polyphasic approach using both phenotypic and genotypic methods. Based on the phenotypic, chemotaxonomic and phylogenetic results, we conclude that strains CVI_P3^T and CVI_P4 represent a novel species, for which the name *Mycobacterium pinniadriaticum* sp. nov. is proposed.

KEYWORDS

noble pen shell, mass mortality event, Croatia, *Mycobacterium*, Adriatic Sea, average nucleotide identity

1 Introduction

The genus *Mycobacterium* (*M.*) was first named in 1896 by Lehmann and Neumann based on phenotypic characteristics such as the presence of mycolic acid in the cell wall, aerobic growth and bacillary cell shape. Currently, the genus comprises nearly 200 validly published species (Parte et al., 2020), including major human pathogens such as *M. tuberculosis* and *M. leprae*. Based on phenotypic and phylogenomic data, the genus can be divided into rapid and

slow growers. A recent study on the genome-wide phylogeny of the genus *Mycobacterium* proposed to split the genus into four new genera (*Mycolicibacterium*, *Mycolicibacter*, *Mycolicibacillus*, and *Mycobacterioides*) and an emended genus *Mycobacterium* (Gupta et al., 2018). However, another recent study using multiple genome-based methods showed that the new genera overlap and therefore suggested that they should be combined into a single genus named *Mycobacterium* (Meehan et al., 2021). Based on clinical manifestation, most *Mycobacterium* species are non-tuberculous mycobacteria (NTM), many of which are important opportunistic pathogens and can be found in various niches and environments (Fedrizzi et al., 2017). To date, many new *Mycobacterium* species have been described, which were first described in different environments such as natural water ecosystems (Zhang et al., 2013; Fogelson et al., 2018; Nouioui et al., 2018) and artificial water systems (Shahraki et al., 2017).

The noble pen shell *Pinna (P.) nobilis* (Linnaeus, 1758) is endemic and the largest bivalve of the Mediterranean Sea, inhabiting soft-bottom coastal areas and seagrass meadows. Occasionally, it also thrives on unvegetated bottoms, maerl beds and boulders (Zavodnik et al., 1991; García-March et al., 2002; Kersting and García-March, 2017; Öndes et al., 2020). Currently, the pen shell populations in the Mediterranean Sea are seriously endangered by *Haplosporidium (H.) pinnae*, a haplosporidian endoparasite that causes mass mortality events (MMEs). Mortality was first reported in the Western Mediterranean, off the coasts of Spain and France in late 2016 (Darriba, 2017; Vázquez-Luis et al., 2017), later expanding along the shores of Turkey, Greece, Albania, and Croatia (Cabanellas-Reboredo et al., 2019; Carella et al., 2019; Panarese et al., 2019; Tiscar et al., 2019; Čižmek et al., 2020; Šarić et al., 2020; Mihaljević et al., 2021). In just 5 years, these MMEs were observed in all parts of the Mediterranean Sea. Although *H. pinnae* is believed to be the main cause of mortality, mycobacteria have also been detected in the affected shell tissue using genetic methods (Carella et al., 2019, 2020; Čižmek et al., 2020; Lattos et al., 2020; Šarić et al., 2020; Mihaljević et al., 2021). To our knowledge, *Mycobacterium* sp. has never been successfully cultured from the tissue of healthy or diseased *P. nobilis*. Finally, the hypothesis that MMEs are caused by multiple pathogens remains uncertain (Scarpa et al., 2020). A pronounced effect of anthropogenic factors related to climate change suggests multifactorial disease as a possible explanation for the MMEs of *P. nobilis* (Šarić et al., 2020; Scarpa et al., 2020). Here, we describe a novel mycobacterial species for which we propose the name *Mycobacterium pinniadriaticum*. Because strains CVI_P3^T and CVI_P4 were both obtained from a single tissue (gills and mantle, respectively) collected a few weeks before the MMEs in Mljet National Park (Croatia) in 2019, its possible involvement in mass mortality events of pen shells remains to be elucidated.

2 Materials and methods

One of the most important habitats of *P. nobilis* in the southern Eastern Adriatic Sea is the Mljet National Park, which is a very productive and biodiverse marine ecosystem and is part of the Natura 2000 European Network of Protected Areas (code HR5000037). It has two lake-like inlets: the Small Lake and the Big Lake. In April 2019, health status control was conducted at five sites in Mljet National Park located in the southeast Adriatic Sea. Healthy shells were collected in April 2019 at a sea temperature of 17.2°C. The deepest points along the transects were from 3.8 m to 7.3 m (Mihaljević et al., 2021). Five sampling sites were selected according to the most abundant pen shell populations. Sampling sites 1 and 2 were located in the Small Lake (Supplementary Figure S1), a lake-like inlet connected by a shallow, narrow channel to the Big Lake (sampling site 3), which was connected to the open sea by a slightly deeper, wider channel. Two additional sampling sites besides these lake-like inlets were Gonoturska Bay (sampling site 4) and Cape Lenga (sampling site 5) (Mihaljević et al., 2021). Five healthy individuals were collected, one for each sampling site (Mihaljević et al., 2021). Samples of digestive glands, mantles and gills were collected for bacteriological examination. All samplings were conducted in April 2019 with permission of the Croatian Ministry of Environmental Protection and Energy (CLASS UP/1-612-17/18-48/172; No. 517-05-1-1-18-4 of 21 December 2018 and CLASS UP/1-612-07/19-48/193; No. 517-05-1-1-19-3 of 11 September 2019).

Samples were homogenized, concentrated and decontaminated as described previously (Kent and Kubica, 1985). The material was inoculated on three standard nutrient media: Löwenstein-Jensen (LJ) slant supplemented with pyruvate, LJ slant supplemented with glycerol, and Stonebrink slant. The inoculated media were incubated at 28, 37, and 45°C under light and dark conditions. Each sample was decontaminated using 5% oxalic acid for 10 min at room temperature. For each sample, 200 µL of homogenized suspension was inoculated on standard nutrient media as described previously. Slants were checked for growth twice a week for 8 weeks. All grown colonies underwent Ziehl-Neelsen (ZN) and Gram staining. Acid-fast bacilli indicative of mycobacteria were subcultured (Figure 1). Growth rate, ability to grow at different temperatures and colony morphology were recorded. Growth, biochemical and phenotypic characterization were performed in parallel at the Croatian Veterinary Institute in Zagreb, Croatia and the Leibniz-Institut Deutsche Sammlung von Microorganismen und Zellkulturen GmbH (DSMZ), Braunschweig, Germany.

Mycolic acid analysis was performed at DSMZ on cultures grown at 28°C for 9 days on M.65 media plates. Mycolic acids were extracted according to the protocol described previously (Vilchèze and Jacobs, 2007) by hydrolyzing mycolic acids from the cell wall by saponification. If the mero-chain contains wax-esters, these are hydrolyzed, resulting in the formation of dicarboxy mycolic acids. Mycolic acids were identified using mass spectrometry-based on the exact masses of mycolic acids. The relative abundance of the mycolic acids was calculated based on the sum of the identified mycolic acids. To test for the presence of long-chain alcohols, the fatty acid methyl ester mixtures were separated by gas chromatography and detected by a flame ionization detector using Sherlock Microbial Identification System (MIS) version 6.4 and myco6 database (MIDI, Microbial ID, Newark, DE, United States). Peaks were automatically integrated and fatty acid names and percentages were calculated by the MIS Standard Software (Microbial ID). Obtained fatty acid profiles were compared with the profiles of other rapidly growing mycobacteria (Vuorio et al., 1999; Hennessee et al., 2009; Tortoli et al., 2009; Musser et al., 2022).

Antimicrobial susceptibility testing (AST) was performed by broth microdilution method using two commercial AST plates, namely Sensititre Myco SLOMYCO (Thermo Scientific) and RAPMYCO (TREK Diagnostic Systems, East Grinstead, UK). Plates

Abbreviations: ANI, Average nucleotide identity; MME, Mass mortality event.

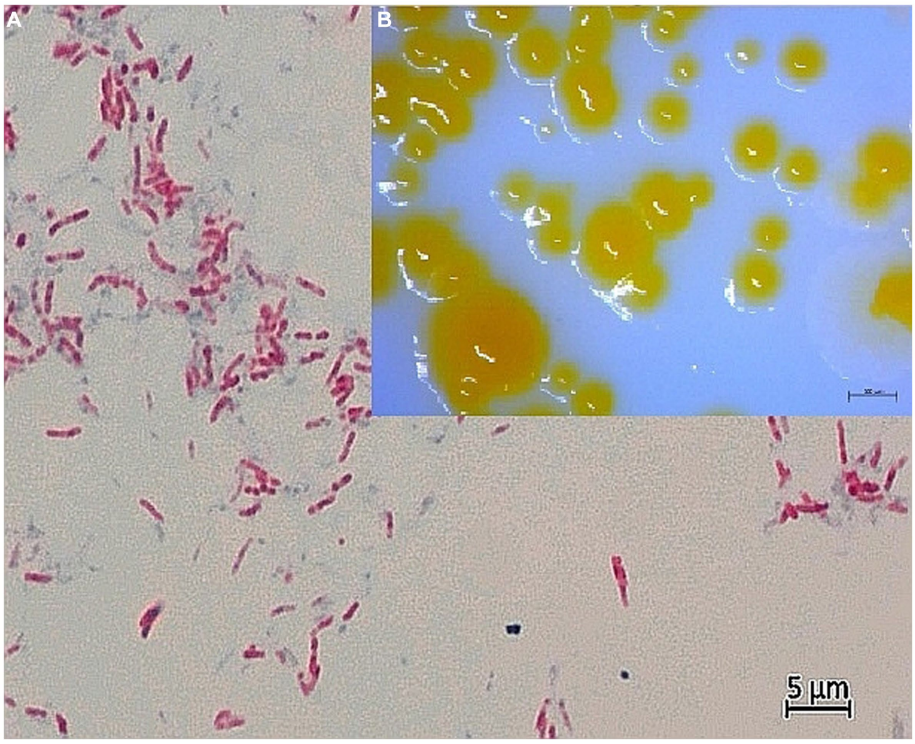

FIGURE 1
(A) Light microscopy of Ziehl-Neelsen-stained strain CVI_P3^T at 1000x magnification with oil immersion. Acid-fast rods, separate and in clusters, are visible. Smear was prepared from bacterial colonies in pure culture on Löwenstein–Jensen agar supplemented with pyruvate. The photo was taken by AxioCam MRC5 with Axio Imager.A2 microscope (CarlZeiss, AG, Germany). **(B)** Colony morphology of CVI_P3^T bacterial colonies in a pure culture grown on Löwenstein–Jensen agar supplemented with pyruvate. The image was taken after 14 days of growth at room temperature (24 ± 1°C) using the stereomicroscope Discovery v20 (Carl Zeiss AG, Germany).

were incubated at 36 ± 1°C and 25°C for 7 days (up to 14 days if bacterial growth was poor).

MALDI-TOF mass spectrometry analysis of the studied strains was performed in parallel at UHCZ and DSMZ. The isolates grown on a solid medium underwent protein extraction as previously described and identification using MALDI Biotyper Mycobacteria Library v6.0 with MALDI Biotyper Microflex LT/SH (Bruker Daltonics GmbH, Bremen, Germany) (O'Connor et al., 2016; Alcaide et al., 2018). The Bacterial Test Standard (Bruker Daltonics GmbH, Bremen, Germany) was used for calibration. The MALDI-TOF analysis did not provide reliable identification using the mycobacterial library mentioned above. In addition, the profiles were analyzed in 24 technical replicates using flexAnalysis 3.4 software. According to the literature and the thresholds used by the manufacturer, scores of ≥1.80 and 1.60 to 1.79 represented high confidence and low confidence identification, respectively. A score of <1.60 is considered unreliable (Rodriguez-Temporal et al., 2020).

DNA extraction was performed by resuspending a loop-full of a bacterial colony in 100 µL of distilled water (AccuGENE, Lonza, Belgium), followed by incubation at 95°C for 20 min with shaking at 350 rpm (Thermomixer comfort, Eppendorf). After centrifugation at 14,000 g for 1 min (SL8, Thermo Scientific, Germany), the supernatant was used as a DNA template for PCR.

Genus identification of strains CVI_P3^T and CVI_P4 was performed using two genus-specific PCR assays for mycobacteria (Supplementary Figures S8, S9). The first assay amplified the *hsp65* gene (encoding the 65-kDa heat shock antigen) with primers TB1 (5′-GAG ATC GAG CTG GAG GAT CC-3′) and TB2 (5′-AGC TGC AGC CCA AAG GTG TT-3′) with an expected product size of 383 bp (Hance et al., 1989). The second assay amplified the 16S rRNA gene with primers 16S rRNA F (5′-ACG GTG GGT ACT AGG TGT GGG TTT C-3′) and 16S rRNA R (5′-TCT GCG ATT ACT AGC GAC TCC GAC TTC A-3′) with an expected product size of 564 bp (Devulder et al., 2005).

For further identification, the studied strains were tested with GenoType Mycobacterium CM (Hain Lifescience, Germany), a commercial molecular genetic assay for the identification of clinically relevant mycobacterial species from cultured material.

For whole-genome sequencing (WGS), DNA was extracted using the NucleoSpin Microbial Mini DNA Kit (Macherey-Nagel, Germany). DNA libraries were prepared using the NEBNext Ultra DNA Sample Prep Master Mix Kit (NEB). Paired-end (2 × 150 bp) sequencing was performed on the NextSeq 6000 System (Illumina) to a minimum coverage of 170×. Genome assembly was performed using Shovill version 1.0.9[1] with SPAdes version 3.13.1 (Bankevich et al., 2012) as the assembler. Assembly quality was assessed using Quast version 5.0.2 (Gurevich et al., 2013). The EDGAR 3.0 platform (Dieckmann et al., 2021) was used to construct nucleotide and amino acid

1 https://github.com/tseemann/shovill

alignments of the core genome comprising 1,198 core genes. The nucleotide and the amino acid-based core genome phylogeny were constructed using RAxML version 8.2.12 (Stamatakis, 2014) with the maximum-likelihood method. Average nucleotide identity values based on the MUMmer algorithm (ANIm) were calculated using pyani version 0.2.11 (Pritchard et al., 2016). For 16S rRNA gene phylogeny, the complete 16S rRNA gene sequences of strains CVI_P3^T and CVI_P4 were extracted from the annotated draft genomes and aligned using Clustal Omega.

3 Results and discussion

Five healthy individuals of the noble pen shell were collected a few weeks before the MMEs in Mljet National Park (Croatia) in 2019, one for each sampling site. Samples of digestive glands, mantles and gills were subjected to bacteriological examination. Growth was detected on the slants seeded with samples of gills and a mantle of a single adult noble pen shell (53 cm long, 18.5 cm wide and 6.6 cm thick) collected at sampling site 1 (Supplementary Figure S1), resulting in the acquisition of strains CVI_P3^T and CVI_P4. Acid-fast bacilli indicative of mycobacteria were subcultured and growth, biochemical and phenotypic characterization were performed (Figure 1). The results of growth rate, ability to grow at different temperatures and colony morphology are summarized and compared with closely related organisms in Table 1.

Mycolic acid analysis was performed on the two strains. Fatty acid names and percentages were calculated using the MIS Standard Software (Microbial ID) and are shown in Supplementary Table S2 and Supplementary Figures S4–S6.

The MALDI-TOF analysis did not provide reliable identification using the mycobacterial library mentioned above. The main spectra profiles (MSPs) generated by FlexAnalysis after smoothing and subtraction are shown in Supplementary Figure S7. According to the literature and the thresholds used by the manufacturer, scores of ≥1,80 and 1,60 to 1,79 represented high and low confidence identification, respectively. A score of <1.60 is considered unreliable (Rodriguez-Temporal et al., 2020). However, MALDI-TOF analysis performed at DSMZ found that the most closely related strain was *M. aurum* DSM 6695 with a score value of 1.37. This strain was isolated from the soil polluted with vinyl chloride in the Netherlands (Hartmans and de Bont, 1992). The most closely matched patterns were also those of *M. pallens* DSM 45404 T DSM b L (score 1.430) and *M. crocinum* DSM 45433 T DSM b L (score 1.220) found by the MALDI-TOF analysis in UHCZ. According to the manufacturer, the matching hints of *M. pallens* and *M. crocinum* were similar to each other. Available data on these two species are scarce. Both were first described from Hawaiian soils in 2009 as rapidly growing mycobacteria, which can degrade polycyclic aromatic hydrocarbons, known organic pollutants (Hennessee et al., 2009).

Antimicrobial susceptibility testing (AST) could not be performed because bacterial growth was insufficient to determine minimum inhibitory concentrations despite several repetitions of the assay.

Genus identification of strains CVI_P3^T and CVI_P4 was performed using two genus-specific PCR assays for mycobacteria, namely *hsp65* and 16S rRNA (Supplementary Figures S8, S9). The

TABLE 1 Phenotypic characteristics of the studied strains CVI_P3^T and CVI_P4 and closely related organisms.

Phenotypic characters	CVI_P3^T/CVI_ P4	*Mycobacterium crocinum**	*Mycobacterium pallens**	*Mycobacterium aromaticivorans**	*Mycobacterium iranicum***
Origin	Pen shell gills	Non-contaminated soil	Non-contaminated soil	Contaminated soil	Various human clinical samples
Pigment production	Yes	Yes	Yes	Yes	Yes
Pigment	Yellow-orange	Yellow-orange	Pale-orange	Yellow-orange	Orange
Pigment classification	Scotochromogenic	Scotochromogenic	Scotochromogenic	Scotochromogenic	Scotochromogenic
Growth rate	Rapid	Rapid	Rapid	Rapid	Rapid
Colony morphology	Smooth	Smooth	–	Smooth	Smooth
Cell morphology	Rod-shaped	Long thin rods	Medium rods	Coccoid and long rod shapes	–
Ziehl Nielsen	Positive	Positive	Positive	Positive	Positive
Gram staining	Weakly positive	Weakly positive	Weakly positive	Weakly positive	Positive
Temperature of growth (°C)	25–37°C, optimal at 28°C	28–37°C, optimal at 37°C	28–37°C	28 and 37°C	25–40°C, optimal at 37°C
NaCl tolerance	Yes, in aerobic conditions	Tolerates 2.5% salinity, not 5%	Negative in 2.5 and 5%	Tolerates 2.5–5.0%	Tolerates 2.5–5.0%
Aerobic growth	Aerobic-microaerophilic	Aerobic	Aerobic	Aerobic	Microaerophilic
Tween 80 hydrolysis	Positive	–	–	–	Negative
Nitrate reduction	Positive	Positive	Positive	Negative	Negative
Urease activity	Negative	Negative	Negative	Positive	Positive
Catalase activity	Negative	Positive	Positive	Positive	Positive

* Hennessee et al. (2009).
** Shojaei et al. (2013).

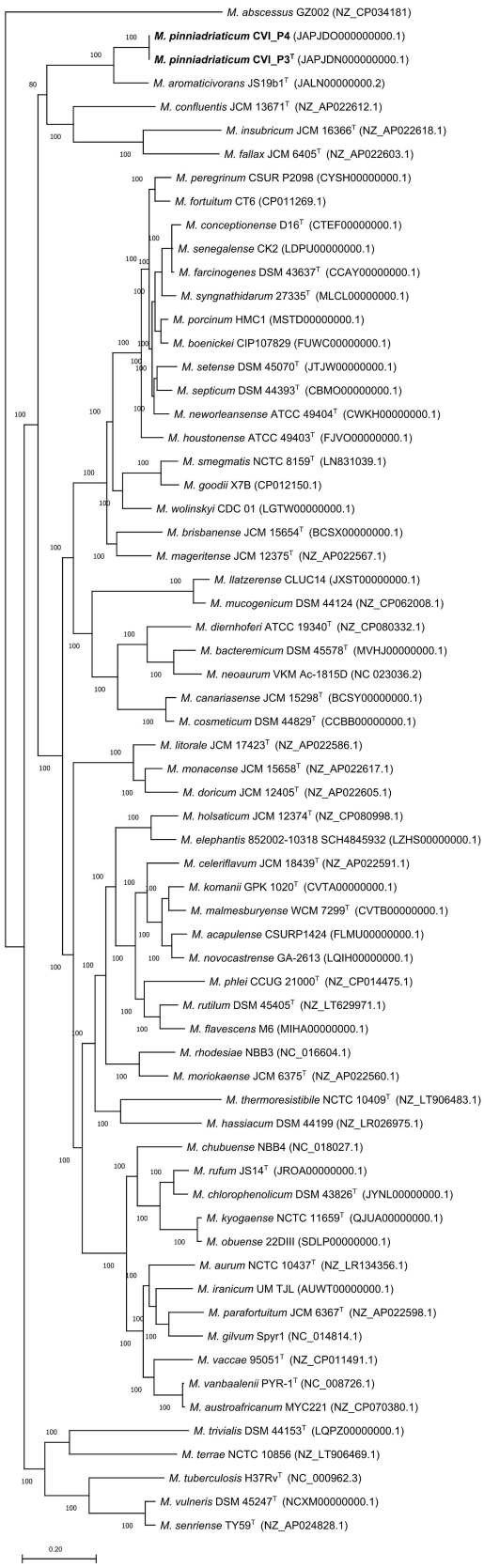

FIGURE 2
Amino acid-based phylogenetic tree of the core genome showing the phylogenetic position of *Mycobacterium pinniadriaticum* sp. nov. (in bold) within the genus *Mycobacterium*. *M. pinniadriaticum* strains

(Continued)

FIGURE 2 (Continued)
CVI_P3^T and CVI_P4 were obtained from the gills and mantle of a noble pen shell, respectively; the shell was collected a few weeks before the mass mortality events in Mljet National Park (Croatia) in 2019. The core genome alignment was constructed using EDGAR 3.0 and comprised 1,198 concatenated core genes and 477,090 amino acid residues per genome. The maximum-likelihood phylogenetic tree was constructed with RAxML version 8.2.12 with the PROTGAMMALGF substitution model. Values on the branches represent bootstrap values. *Mycobacterium abscessus* GZ002 was used as an outgroup and root. Bar, the average number of nucleotide substitutions per site.

assays determined the genus but were not specific enough to determine the species.

The studied strains were also tested with GenoType Mycobacterium CM, a commercial hybridization assay. The assay classified strain CVI_P3^T into the *M. scrofulaceum*/*M. paraffinium*/*M. parascrofulaceum* group (Supplementary Figure S10).

Assembly of the whole genome filtered sequences resulted in draft genomes of the two strains, both 6.9 Mb in size and had a G+C content of 66.3% (Supplementary Table S3). The EDGAR platform used to construct nucleotide and amino acid alignments of the core genome found 1,198 core genes. The core genome alignment had 1,457,448 bp and 485,816 amino acid residues per genome. The nucleotide and the amino acid-based core genome phylogeny showed that the studied strains form a separate clade most closely related to *M. aromaticivorans*, previously described in Hennessee et al. (2009) (Figure 2, Supplementary Figure S2).

A pairwise comparison of the two studied strains revealed a pairwise ANI value of 100%. Pairwise ANI values with the nine selected closely related *Mycobacterium* species are shown in Figure 3. *M. aromaticivorans* JS19b1 had the highest pairwise ANI value of 85.0% with *M. pinniadriaticum*. The calculated ANI values were well below the generally accepted threshold for species delineation of 95–96% ANI (Rosselló-Mora and Amann, 2001; Goris et al., 2007), strongly suggesting that the studied strains are representatives of a new *Mycobacterium* species.

The 16S rRNA gene sequences of both isolates were identical and were phylogenetically most closely related to *M. iranicum* M05T (Shojaei et al., 2013) with a pairwise identity of 98.25% (Supplementary Figure S3). *M. gilvum* SM 35T (Stanford and Gunthorpe, 1971) was the best match identified by the EzBioCloud 16S identification service (Yoon et al., 2017) with 98.88% identity.

The two *Mycobacterium* strains from two different organs of an adult were isolated a few weeks before the MME of the *P. nobilis* population on the eastern coast of the Adriatic Sea. This is the first description of *Mycobacterium* sp. successfully cultured from *P. nobilis* and described to the species level. Its possible involvement in the recent MMEs in Croatia and several other locations along the Mediterranean Sea remains unclear; therefore, further studies are needed to clarify this issue. This hypothesis is supported by the fact that the seawater temperature at the time of sampling was lower (about 17.2°C) than at the time of the highest mortality rate, which occurred later with the increase in seawater temperature to 26°C (Mihaljević et al., 2021), which is optimal for the growth of bacterial colonies. Lower seawater temperatures may have hindered the growth of mycobacteria and/or the establishment of their pathogenic

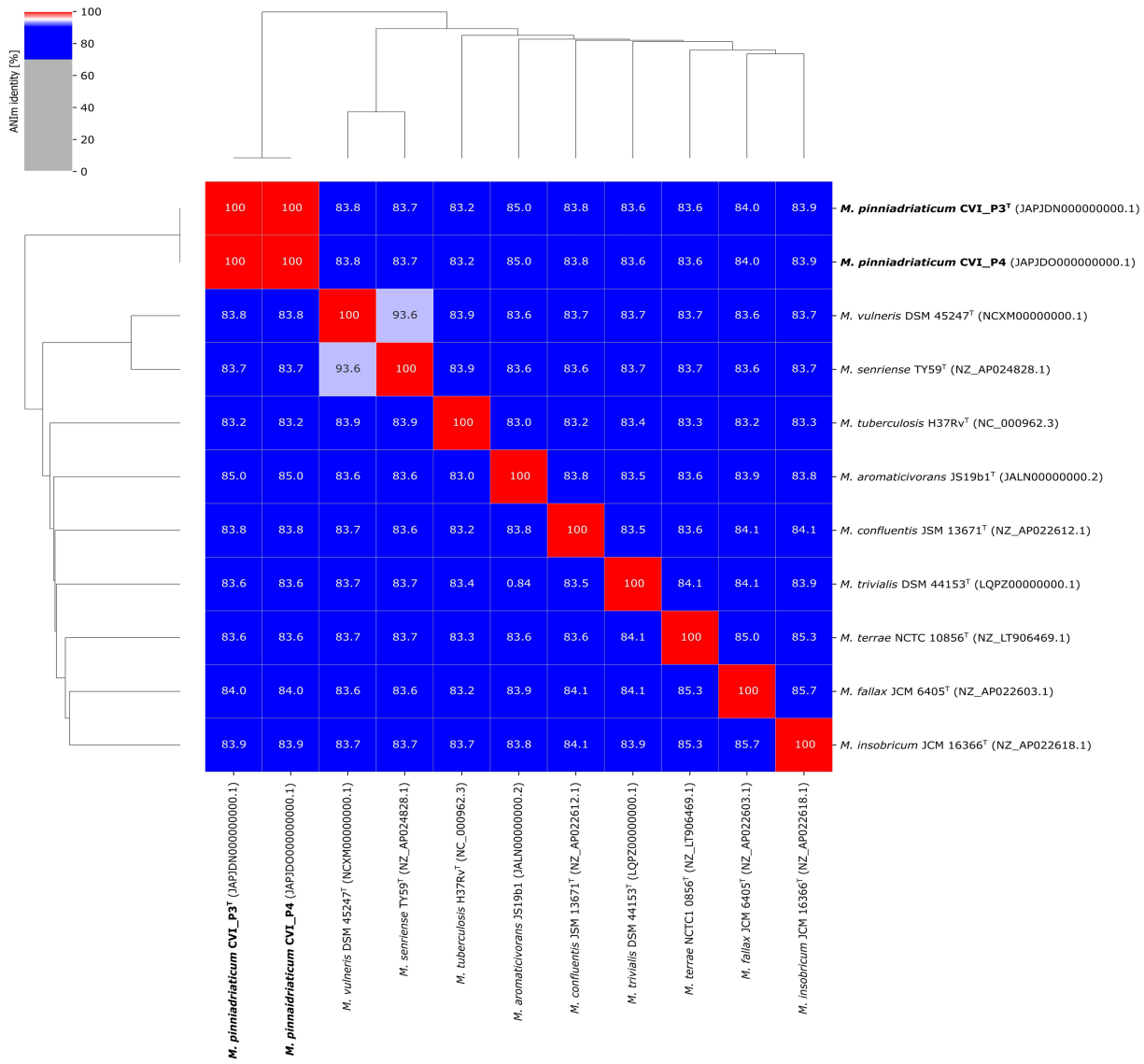

FIGURE 3
Average nucleotide identity (ANI) values of strains CVI_P3^T and CVI_P4 compared with selected closely related mycobacterial species.

potential. In addition, the co-occurrence of different pathogens with the greatest influence of *Mycobacterium* and *Haplosporidium* has been previously suggested (Lattos et al., 2020). Other factors such as seawater temperature, salinity, population density, and age of the pen shell population should also be considered (Carella et al., 2020; Lattos et al., 2020).

4 Description of *Mycobacterium pinniadriaticum* sp. nov.

Mycobacterium pinniadriaticum sp. nov. (pi.ni.ad.ri.ati.kum. L. fem. Adj. pinna, from the name of the bivalve mollusk genus, isolated from a noble pen shell (*Pinna nobilis*); N.L. gen. n. adriaticum, specific epithet of Adriatic Sea).

Generally, rod-shaped, acid-fast, Gram-positive and acid-resistant by Ziehl-Neelsen staining. No spores or filaments were observed by microscopy. This is also the case with its closest relatives which are also rod-shaped with smaller differences considering the size of the rods. The optimal growth temperature is 25–28C in the aerophilic to the microaerophilic atmosphere. Bacteria are unable to grow at 45°C. Its closest relatives grow mostly in an aerobic atmosphere optimally at 37°C. Scotochromogenic, yellowish colonies become visible after 5–7 days on solid media LJ supplemented with pyruvate which is usually the case with its closest relatives. Growth on Stonebrink and LJ supplemented with glycerol was noted in subcultivation. Growth in the presence of 5% NaCl is also observed. The type strain CVI_P3^T is negative for urease and catalase activity. Salinity tolerance and urease activity differ between species that are most closely related. However, catalase activity is negative for *Mycobacterium pinniadriaticum* sp. nov. but usually is positive in its closely related species. Additional phenotypic properties are listed in Supplementary Table S1. Prominent fatty acids (>11%) are C18:1ω9c and C16:1ω6c; the mycolic acid pattern is composed of dicarboxy- or dihydroxy-mycolic acids, α-mycolic acids, wax esters and long-chain alcohols. Comparing its fatty acid profiles to those of its closely related

TABLE 2 Comparison of the whole-cell fatty acid composition of the CVI_P3^T and CVI_P4 strains and closely related strains of rapidly growing mycobacteria.

FAME	1	2	3	4	5	6	7	8	9	10	11	12	13
10:0	0.53	0.23	1.87	ND	ND	ND	ND	ND	ND	ND	ND	ND	ND
12:0	0.88	2.19	0.73	ND	ND	ND	ND	ND	ND	ND	ND	ND	ND
14:0	6.00	9.65	6.95	3.4	3.8	5.4	3.7	7.7	5.0	7.8	3.2	4.8	6.0
15:0	0.64	1.10	1.16	<0.4	<0.4	1.1	<0.4	0.5	0.5	0.2	0.3	<0.4	0.3
16:1ω7c + ω6c	13.48	ND	12.20	ND	ND	ND	ND	ND	ND	ND	ND	ND	ND
16:0	23.59	37.92	23.17	19.6	22.4	19.9	21.9	18.2	19.1	23.7	21.7	23.6	34.1
17:0	0.09	0.86	0.51	ND	ND	ND	ND	ND	ND	ND	ND	ND	ND
18:1ω9c	22.79	26.36	29.69	21.4	20.0	23.5	29.4	18.1	23.2	22.2	17.3	32.4	35.5
18:0	1.36	3.24	1.32	1.3	1.1	0.9	2.7	0.6	3.0	2.1	0.9	1.6	1.0
10Me-18:0	8.54	5.02	3.02	16.6	13.6	13.3	10.6	4.7	3.5	8.4	7.5	2.0	3.9
20:0	0.28	1.15	0.84	<0.4	<0.4	<0.4	0.7	0.6	0.5	0.3	<0.4	1.3	<0.4

1. CVI_P3T; 2. *M. insubricum* FI-06250 T; 3. *M. aromaticivorans* JS19b1; 4. *M. murale* MA112/96 T; 5. *M. aurum* NCTC 10437 T; 6. *M. holderi* DSM 44183 T; 7. *M. gadium* NCTC 10942 T; 8. *M. diernhoferi* DSM 43524 T; 9. *M. vaccae* NCTC 10916 T; 10. *M. komossense* ATCC 33013 T; 11. *M. austroafricanum* DSM 44191 T; 12. *M. neoaurum* NCTC 10818 T; 13. *M. abscessus* NCTC 10882.

species as well as other rapidly growing mycobacteria, the CVI_P3^T strain has a unique profile. Its closest relatives *M. aromaticivorans* JS19b1 and *M. insubricum* have the most similar fatty acid profiles both in composition and percentages. Other rapidly growing species differ significantly in fatty acid composition (Table 2).

Data availability statement

The datasets presented in this study can be found in online repositories. The names of the repository/repositories and accession number(s) can be found in the article/Supplementary material.

Ethics statement

The animal study was approved by Croatian Ministry of Environmental Protection and Energy. The study was conducted in accordance with the local legislation and institutional requirements.

Author contributions

SŠ: Conceptualization, Data curation, Funding acquisition, Investigation, Methodology, Project administration, Supervision, Writing – original draft. SD: Investigation, Methodology, Software, Writing – original draft, Writing – review & editing. BP: Data curation, Investigation, Methodology, Software, Visualization, Writing – original draft, Writing – review & editing. IR: Investigation, Methodology, Writing – original draft. SZ: Investigation, Methodology, Writing – original draft. ŽM: Investigation, Methodology, Writing – original draft. ŠN: Investigation, Methodology, Writing – original draft. IZ: Investigation, Methodology, Writing – original draft. GK: Investigation, Methodology, Writing – original draft. BH: Investigation, Methodology, Writing – original draft. IM: Investigation, Methodology, Writing – original draft. MZ-T: Investigation, Methodology, Writing – original draft.

Funding

The author(s) declare financial support was received for the research, authorship, and/or publication of this article. This work was technically and financially supported by the Croatian Veterinary Institute, Zagreb, Croatia.

Acknowledgments

Prof. Ivan Bekavac Basić is warmly acknowledged for his valuable advice on nomenclature and extensive knowledge of Latin. Dr. Zoran Herljević is acknowledged for processing the MALDI-TOF data using the flexAnalysis software.

Conflict of interest

The authors declare that the research was conducted in the absence of any commercial or financial relationships that could be construed as a potential conflict of interest.

Publisher's note

All claims expressed in this article are solely those of the authors and do not necessarily represent those of their affiliated organizations, or those of the publisher, the editors and the reviewers. Any product that may be evaluated in this article, or claim that may be made by its manufacturer, is not guaranteed or endorsed by the publisher.

Supplementary material

The Supplementary material for this article can be found online at: https://www.frontiersin.org/articles/10.3389/fmicb.2023.1289182/full#supplementary-material

References

Alcaide, F., Amlerová, J., Bou, G., Ceyssens, P. J., Coll, P., Corcoran, D., et al. (2018). European study group on genomics and molecular diagnosis (ESGMD). How to: identify non-tuberculous *Mycobacterium* species using MALDI-TOF mass spectrometry. *Clin. Microbiol. Infect.* 24, 599–603. doi: 10.1016/j.cmi.2017.11.012

Bankevich, A., Nurk, S., Antipov, D., Gurevich, A. A., Dvorkin, M., Kulikov, A. S., et al. (2012). SPAdes: a new genome assembly algorithm and its applications to single-cell sequencing. *J. Comput. Biol.* 19, 455–477. doi: 10.1089/cmb.2012.0021

Cabanellas-Reboredo, M., Vázquez-Luis, M., Mourre, B., Álvarez, E., Deudero, S., Amores, A., et al. (2019). Tracking a mass mortality outbreak of pen shell *Pinna nobilis* populations: A collaborative effort of scientists and citizens. *Sci. Rep.* 9:13355. doi: 10.1038/s41598-019-49808-4

Carella, F., Aceto, S., Pollaro, F., Miccio, A., Iaria, C., Carrasco, N., et al. (2019). A mycobacterial disease is associated with the silent mass mortality of the pen shell *Pinna nobilis* along the Tyrrhenian coastline of Italy. *Sci. Rep.* 9:2725. doi: 10.1038/s41598-018-37217-y

Carella, F., Antuofermo, E., Farina, S., Salati, F., Mandas, D., Prado, P., et al. (2020). In the wake of the ongoing mass mortality events: co-occurrence of *Mycobacterium*, *Haplosporidium* and other pathogens in *Pinna nobilis* collected in Italy and Spain (Mediterranean Sea). *Front. Mar. Sci.* 7:48. doi: 10.3389/fmars.2020.00048

Čižmek, H., Čolić, B., Gračan, R., Grau, A., and Catanese, G. (2020). An emergency situation for pen shells in the Mediterranean: the Adriatic Sea, one of the last *Pinna nobilis* shelters, is now affected by a mass mortality event. *J. Invertebr. Pathol.* 173:107388. doi: 10.1016/j.jip.2020.107388

Darriba, S. (2017). First haplosporidan parasite reported infecting a member of the Superfamily Pinnoidea (*Pinna nobilis*) during a mortality event in Alicante (Spain, Western Mediterranean). *J. Invertebr. Pathol.* 148, 14–19. doi: 10.1016/j.jip.2017.05.006

Devulder, G., Perouse de Montclos, M., and Flandrois, J. P. (2005). A multigene approach to phylogenetic analysis using the genus *Mycobacterium* as a model. *Int. J. Syst. Evol. Microbiol.* 55, 293–302. doi: 10.1099/ijs.0.63222-0

Dieckmann, M. A., Beyvers, S., Nkouamedjo-Fankep, R. C., Hanel, P. H. G., Jelonek, L., Blom, J., et al. (2021). EDGAR3.0: comparative genomics and phylogenomics on a scalable infrastructure. *Nucleic Acids Res.* 49, W185–W192. doi: 10.1093/nar/gkab341

Fedrizzi, T., Meehan, C. J., Grottola, A., Giacobazzi, E., Fregni Serpini, G., Tagliazucchi, S., et al. (2017). Genomic characterization of nontuberculous mycobacteria. *Sci. Rep.* 7:45258. doi: 10.1038/srep45258

Fogelson, S. B., Camus, A. C., Lorenz, W., Phillips, A., Bartlett, P., and Sanchez, S. (2018). *Mycobacterium syngnathidarum* sp. nov., a rapidly growing *Mycobacterium* identified in syngnathid fish. *Int. J. Syst. Evol. Microbiol.* 68, 3696–3700. doi: 10.1099/ijsem.0.002978

García-March, J. R., Garcia-Carrascosa, A. M., and Peña, A. L. (2002). *In situ* measurement of *Pinna nobilis* shells for age and growth studies: A new device. *Mar. Ecol.* 23, 207–217. doi: 10.1046/j.1439-0485.2002.02781.x

Goris, J., Konstantinidis, K. T., Klappenbach, J. A., Coenye, T., Vandamme, P., and Tiedje, J. M. (2007). DNA–DNA hybridization values and their relationship to whole-genome sequence similarities. *Int. J. Syst. Evol. Microbiol.* 57, 81–91. doi: 10.1099/ijs.0.64483-0

Gupta, R. S., Lo, B., and Son, J. (2018). Phylogenomics and comparative genomic studies robustly support division of the genus *Mycobacterium* into an emended genus *Mycobacterium* and four novel genera. *Front. Microbiol.* 9:67. doi: 10.3389/fmicb.2018.00067

Gurevich, A., Saveliev, V., Vyahhi, N., and Tesler, G. (2013). QUAST: quality assessment tool for genome assemblies. *Bioinformatics* 29, 1072–1075. doi: 10.1093/bioinformatics/btt086

Hance, A. J., Grandchamp, B., Lévy-Frébault, V., Lecossier, D., Rauzier, J., Bocart, D., et al. (1989). Detection and identification of mycobacteria by amplification of mycobacterial DNA. *Mol. Microbiol.* 3, 843–849. doi: 10.1111/j.1365-2958.1989.tb00233.x

Hartmans, S., and de Bont, J. A. M. (1992). Aerobic vinyl chloride metabolism in *Mycobacterium aurum* L1. *Appl. Environ. Microb.* 58, 1220–1226. doi: 10.1128/aem.58.4.1220-1226.1992

Hennessee, C. T., Seo, J.-S., Alvarez, A. M., and Li, Q. X. (2009). Polycyclic aromatic hydrocarbon-degrading species isolated from Hawaiian soils: *Mycobacterium crocinum* sp. nov., *Mycobacterium pallens* sp. nov., *Mycobacterium rutilum* sp. nov., *Mycobacterium rufum* sp. nov. and *Mycobacterium aromaticivorans* sp. nov. *Int. J. Syst. Evol. Microbiol.* 59, 378–387. doi: 10.1099/ijs.0.65827-0

Kent, P. T., and Kubica, G. P. (1985) *Public Health Mycobacteriology. A Guide for the Level III Laboratory*. US Department of Health and Human Services, Public Health Service, Centers for Disease Control: Atlanta, GA.

Kersting, D. K., and García-March, J. R. (2017). Long-term assessment of recruitment, early stages and population dynamics of the endangered Mediterranean fan mussel *Pinna nobilis* in the Columbretes Islands (NW Mediterranean). *Mar. Environ. Res.* 130, 282–292. doi: 10.1016/j.marenvres.2017.08.007

Lattos, A., Giantsis, I. A., Karagiannis, D., and Michaelidis, B. (2020). First detection of the invasive *Haplosporidian* and *Mycobacteria* parasites hosting the endangered bivalve *Pinna nobilis* in Thermaikos Gulf. *North Greece. Mar. Environ. Res.* 155:104889. doi: 10.1016/j.marenvres.2020.104889

Linnaeus, C. (1758). Systema Naturae per regna tria naturae, secundum classes, ordines, genera, species, cum characteribus, differentiis, synonymis, locis. Editio decima, reformata [10th revised edition], Laurentius Salvius: Holmiae 824.

Meehan, C. J., Barco, R. A., Loh, Y. H. E., Cogneau, S., and Rigouts, L. (2021). Reconstituting the genus *Mycobacterium*. *Int. J. Syst. Evol. Microbiol.* 71:004922. doi: 10.1099/ijsem.0.004922

Mihaljević, Ž., Pavlinec, Ž., Zupičić, I. G., Oraić, D., Popijač, A., Pećar, O., et al. (2021). Noble pen shell (*Pinna nobilis*) mortalities along the Eastern Adriatic coast with a study of the spreading velocity. *J. Mar. Sci.* 9:764. doi: 10.3390/jmse9070764

Musser, E., Smith, C., Halse, T. A., Kohlerschmidt, D., Rourke, A., Fiero, A., et al. (2022). Characterization of *Mycobacterium salfingeri* sp. nov.: A novel nontuberculous mycobacteria isolated from a human wound infection. *Front. Microbiol.* 13, 1–10. doi: 10.3389/fmicb.2022.992610

Nouioui, I., Brunet, L. R., Simpson, D., Klenk, H. P., and Goodfellow, M. (2018). Description of a novel species of fast-growing *Mycobacterium*: *Mycobacterium kyogaense* sp. nov. a scotochromogenic strain received as *Mycobacterium vaccae*. *Int. J. Syst. Evol. Microbiol.* 68, 3726–3734. doi: 10.1099/ijsem.0.003039

O'Connor, J. A., Lynch-Healy, M., Corcoran, D., O'Reilly, B., O'Mahony, J., and Lucey, B. (2016). Improved matrix-assisted laser desorption ionization-time of flight mass spectrometry (MALDI-TOF MS)-based identification of *Mycobacterium* spp. by use of a novel two-step cell disruption preparatory technique. *J. Clin. Microbiol.* 54, 495–496. doi: 10.1128/JCM.02998-15

Öndes, F., Kaiser, M. J., and Güçlüsoy, H. (2020). Human impacts on the endangered fan mussel, *Pinna nobilis*. Aquatic conservation. *Mar. Freshw. Ecosyst.* 30, 31–41. doi: 10.1002/aqc.3237

Panarese, R., Tedesco, P., Chimienti, G., Latrofa, M. S., Quaglio, F., Passantino, G., et al. (2019). *Haplosporidium pinnae* associated with mass mortality in endangered *Pinna nobilis* fan mussels. *J. Invertebr. Pathol.* 164, 32–37. doi: 10.1016/j.jip.2019.04.005

Parte, A. C., Sardà Carbasse, J., Meier-Kolthoff, J. P., Reimer, L. C., and Göker, M. (2020). List of prokaryotic names with standing in nomenclature (LPSN) moves to the DSMZ. *Int. J. Syst. Evol. Microbiol.* 70, 5607–5612. doi: 10.1099/ijsem.0.004332

Pritchard, L., Glover, R. H., Humphris, S., Elphinstoneb, J. G., and Toth, I. K. (2016). Genomics and taxonomy in diagnostics for food security: soft-rotting enterobacterial plant pathogens. *Anal. Methods* 8, 12–24. doi: 10.1039/C5AY02550H

Rodriguez-Temporal, D., Rodríguez-Sánchez, B., and Alcaide, F. (2020). Evaluation of MALDI biotyper interpretation criteria for accurate identification of nontuberculous mycobacteria. *J. Clin. Microbiol.* 58, e01103–e01120. doi: 10.1128/JCM.01103-20

Rosselló-Mora, R., and Amann, R. (2001). The species concept for prokaryotes. *FEMS Microbiol. Rev.* 25, 39–67. doi: 10.1111/j.1574-6976.2001.tb00571.x

Šarić, T., Župan, I., Aceto, S., Villari, G., Palić, D., De Vico, G., et al. (2020). Epidemiology of noble pen shell (*Pinna nobilis* L. 1758) mass mortality events in Adriatic Sea is characterized with rapid spreading and acute disease progression. *Pathogens* 9:776. doi: 10.3390/pathogens9100776

Scarpa, F., Sanna, D., Azzena, I., Mugetti, D., Cerutti, F., Hosseiniporgham, S., et al. (2020). Multiple non-species-specific pathogens possibly triggered the mass mortality in *Pinna nobilis*. *Life* 10:238. doi: 10.3390/life10100238

Shahraki, A. H., Trovato, A., Droz, S., Haidarieh, P., Borroni, E., Mirsaeidi, M., et al. (2017). *Mycobacterium aquaticum* sp. nov., a rapidly growing species isolated from haemodialysis water. *Int. J. Syst. Evol. Microbiol.* 67, 3279–3282. doi: 10.1099/ijsem.0.002103

Shojaei, H., Daley, C., Gitti, Z., Hashemi, A., Heidarieh, P., Moore, E. R. B., et al. (2013). *Mycobacterium iranicum* sp. nov., a rapidly growing scotochromogenic species isolated from clinical specimens on three different continents. *Int. J. Syst. Evol. Microbiol.* 63, 1383–1389. doi: 10.1099/ijs.0.043562-0

Stamatakis, A. (2014). RAxML version 8: a tool for phylogenetic analysis and post-analysis of large phylogenies. *Bioinformatics* 30, 1312–1313. doi: 10.1093/bioinformatics/btu033

Stanford, J. L., and Gunthorpe, W. J. (1971). A study of some fast-growing scotochromogenic mycobacteria including species descriptions of *Mycobacterium gilvum* (new species) and *Mycobacterium duvalii* (new species). *Br. J. Exp. Pathol.* 52, 627–637.

Tiscar, P. G., Rubino, F., Fanelli, G., Paoletti, B., and Della Salda, L. (2019). Mass mortality of the fan mussel *Pinna nobilis* in Apulia (Ionian Sea) caused by *Haplosporidium pinnae*. *Rapport Commission International pour l'exploration scientifique de la Mer Mediterranée* 42:30.

Tortoli, E., Baruzzo, S., Heijdra, Y., Klenk, H. P., Lauria, S., Mariottini, A., et al. (2009). *Mycobacterium insubricum* sp. nov. *Int. J. Syst. Evol. Microbiol.* 59, 1518–1523. doi: 10.1099/ijs.0.003459-0

Vázquez-Luis, M., Álvarez, E., Barrajón, A., García-March, J. R., Grau, A., Hendriks, I., et al. (2017). SOS *Pinna nobilis*: A mass mortality event in Western Mediterranean Sea. *Front. Mar. Sci.* 4:220. doi: 10.3389/fmars.2017.00220

Vilchèze, C., and Jacobs, W. R. (2007). Isolation and analysis of *Mycobacterium tuberculosis* mycolic acids. *Curr. Protoc. Microbiol.* Chapter 10:Unit 10A.3. doi: 10.1002/9780471729259.mc10a03s05

Vuorio, R., Andersson, M. A., Rainey, F. A., Kroppenstedt, R. M., Kämpfer, P., Busse, H. J., et al. (1999). A new rapidly growing mycobacterial species, *Mycobacterium murale* sp. nov., isolated from the indoor walls of a children's day care centre. *Int. J. Syst. Bacteriol.* 49, 25–35. doi: 10.1099/00207713-49-1-25

Yoon, S. H., Ha, S. M., Kwon, S., Lim, J., Kim, Y., Seo, H., et al. (2017). Introducing EzBioCloud: a taxonomically united database of 16S rRNA gene sequences and whole-genome assemblies. *Int. J. Syst. Evol. Microbiol.* 67, 1613–1617. doi: 10.1099/ijsem.0.001755

Zavodnik, D., Hrs-Brenko, M., and Legac, M. (1991). "Synopsis on the fan shell *Pinna nobilis* L. In the eastern Adriatic Sea" in *Les Espèces Marines à protéger en Méditerranée*. eds. C. F. Boudouresque, M. Avon and V. Gravez (Marseille: GIS Posidonie publications), 169–178.

Zhang, D. F., Chen, X., Zhang, X. M., Zhi, X. Y., Yao, J. C., and Jiang, Y. (2013). *Mycobacterium sediminis* sp. nov. and *Mycobacterium arabiense* sp. nov., two rapidly growing members of the genus *Mycobacterium*. *Int. J. Syst. Evol. Microbiol.* 63, 4081–4086. doi: 10.1099/ijs.0.050567-0

frontiers | Frontiers in Microbiology

TYPE Original Research
PUBLISHED 15 December 2023
DOI 10.3389/fmicb.2023.1283814

Check for updates

OPEN ACCESS

EDITED BY
Hong Yin,
Chinese Academy of Agricultural Sciences,
China

REVIEWED BY
Valentina Virginia Ebani,
University of Pisa, Italy
Marina Eremeeva,
Georgia Southern University, United States

*CORRESPONDENCE
Abid Ali
✉ uop_ali@yahoo.com
Kun-Hsien Tsai
✉ kunhtsai@ntu.edu.tw

RECEIVED 27 August 2023
ACCEPTED 13 November 2023
PUBLISHED 15 December 2023

CITATION
Majid A, Almutairi MM, Alouffi A, Tanaka T, Yen T-Y, Tsai K-H and Ali A (2023) First report of spotted fever group *Rickettsia aeschlimannii* in *Hyalomma turanicum*, *Haemaphysalis bispinosa*, and *Haemaphysalis montgomeryi* infesting domestic animals: updates on the epidemiology of tick-borne *Rickettsia aeschlimannii*.
Front. Microbiol. 14:1283814.
doi: 10.3389/fmicb.2023.1283814

COPYRIGHT
© 2023 Majid, Almutairi, Alouffi, Tanaka, Yen, Tsai and Ali. This is an open-access article distributed under the terms of the Creative Commons Attribution License (CC BY). The use, distribution or reproduction in other forums is permitted, provided the original author(s) and the copyright owner(s) are credited and that the original publication in this journal is cited, in accordance with accepted academic practice. No use, distribution or reproduction is permitted which does not comply with these terms.

First report of spotted fever group *Rickettsia aeschlimannii* in *Hyalomma turanicum*, *Haemaphysalis bispinosa*, and *Haemaphysalis montgomeryi* infesting domestic animals: updates on the epidemiology of tick-borne *Rickettsia aeschlimannii*

Abdul Majid[1], Mashal M. Almutairi[2], Abdulaziz Alouffi[3], Tetsuya Tanaka[4], Tsai-Ying Yen[5], Kun-Hsien Tsai[5]* and Abid Ali[1]*

[1]Department of Zoology, Abdul Wali Khan University Mardan, Mardan, Pakistan, [2]Department of Pharmacology and Toxicology, College of Pharmacy, King Saud University, Riyadh, Saudi Arabia, [3]King Abdulaziz City for Science and Technology, Riyadh, Saudi Arabia, [4]Laboratory of Infectious Diseases, Joint Faculty of Veterinary Medicine, Kagoshima University, Kagoshima, Japan, [5]Department of Public Health, Institute of Environmental and Occupational Health Sciences, College of Public Health, National Taiwan University, Taipei, Taiwan

Tick-borne *Rickettsia* spp. have long been known as causative agents for zoonotic diseases. We have previously characterized *Rickettsia* spp. in different ticks infesting a broad range of hosts in Pakistan; however, knowledge regarding *Rickettsia aeschlimannii* in *Haemaphysalis* and *Hyalomma* ticks is missing. This study aimed to obtain a better understanding about *R. aeschlimannii* in Pakistan and update the knowledge about its worldwide epidemiology. Among 369 examined domestic animals, 247 (66%) were infested by 872 ticks. Collected ticks were morphologically delineated into three genera, namely, *Rhipicephalus*, *Hyalomma,* and *Haemaphysalis*. Adult females were the most prevalent (number = 376, 43.1%), followed by nymphs (303, 34.74%) and males (193, 22.13%). Overall, genomic DNA samples of 223 tick were isolated and screened for *Rickettsia* spp. by the amplification of rickettsial *gltA*, *ompA*, and *ompB* partial genes using conventional PCR. Rickettsial DNA was detected in 8 of 223 (3.58%) ticks including nymphs (5 of 122, 4.0%) and adult females (3 of 86, 3.48%). The rickettsial *gltA*, *ompA*, and *ompB* sequences were detected in *Hyalomma turanicum* (2 nymphs and 1 adult female), *Haemaphysalis bispinosa* (1 nymph and 1 adult female), and *Haemaphysalis montgomeryi* (2 nymphs and 1 adult female). These rickettsial sequences showed 99.71–100% identity with *R. aeschlimannii* and phylogenetically clustered with the same species. None of the tested *Rhipicephalus microplus*, *Hyalomma isaaci*, *Hyalomma scupense*, *Rhipicephalus turanicus*, *Hyalomma anatolicum*, *Rhipicephalus haemaphysaloides*, *Rhipicephalus sanguineus, Haemaphysalis cornupunctata*, and *Haemaphysalis sulcata* ticks were found positive for rickettsial DNA. Comprehensive surveillance studies should be adopted to update the knowledge regarding tick-borne zoonotic *Rickettsia* species, evaluate their risks

to humans and livestock, and investigate the unexamined cases of illness after tick bite among livestock holders in the country.

KEYWORDS

ticks, *Rickettsia aeschlimannii*, *Hyalomma turanicum*, *Haemaphysalis bispinosa*, *Haemaphysalis montgomeryi*

Introduction

Ticks are important ectoparasites due to their capacity to feed on animals including humans (De la Fuente et al., 2017) and transmit various pathogens including viruses, bacteria, and protozoans to their hosts (Boulanger et al., 2019). Among bacteria, *Rickettsia* species are transmitted by ticks, mites, and fleas, causing rickettsioses (Fournier and Raoult, 2009; Labruna, 2009). The main tick genera that are the potential vectors for *Rickettsia* spp. are *Amblyomma*, *Dermacentor*, *Ixodes*, *Hyalomma*, *Rhipicephalus,* and *Haemaphysalis* (Fournier and Raoult, 2009). Several studies have revealed the extensive diversity of the spotted fever group rickettsiae in different tick species and geographic locations (Socolovschi et al., 2009). Approximately 34 species in the genus *Rickettsia* have been validated, and several others are yet to be determined to the species level (El Karkouri et al., 2022). Spotted fever group *Rickettsia* spp. are distributed in Pakistan and have recently been reported in different ticks including *Rh. microplus, Rh. haemaphysaloides, Rh. turanicus, H. kashmirensis,* and *H. cornupunctata* infesting different animals (Ali et al., 2021, 2022; Khan et al., 2023).

Hard ticks are important reservoirs for various *Rickettsia* species including *Rickettsia aeschlimannii* (Parola et al., 2013). Previously, *R. aeschlimannii* has been detected in different tick species belonging to different genera such as *Rhipicephalus, Hyalomma, Amblyomma*, *Haemaphysalis*, and *Ixodes* in Morocco, Spain, Senegal, and Bolivia (Beati et al., 1997; Fernández-Soto et al., 2003; Mediannikov et al., 2010; Tomassone et al., 2010). The first human infection by *R. aeschlimannii* was documented serologically in Morocco (Raoult et al., 2002). Till then, several cases of human infection with tick-borne *R. aeschlimannii* have been reported (Raoult et al., 2002; Znazen et al., 2006; Mokrani et al., 2008; Germanakis et al., 2013; Igolkina et al., 2022). Molecular identification and genetic characterization of *Rickettsia* spp. are based on the *gltA* (citrate synthase gene), *ompA* (outer membrane protein A), *ompB* (outer membrane protein B), and *sca*4 (surface cell antigen 4) genes (Roux et al., 1997; Fournier et al., 2003).

Earlier, we characterized pathogenic and undetermined *Rickettsia* spp. associated with different ticks parasitizing a wide range of vertebrate hosts in Pakistan (Karim et al., 2017; Ali et al., 2021, 2022, 2023; Numan et al., 2022; Aneela et al., 2023; Shehla et al., 2023; Ullah et al., 2023). However, there is a paucity of information regarding the presence of *R. aeschlimannii* in different ticks in the country, and its potential risks to the public and animal's health. Updated knowledge regarding the epidemiology, association with ticks infesting different hosts, and phylogenetic position of spotted fever group (SFG) *R. aeschlimannii* is essential for effective management of infection. This study aimed to molecularly characterize tick-borne *Rickettsia* spp. in selected districts of Pakistan and update the information about the global epidemiology of uncharacterized *Rickettsia* spp.

Materials and methods

Study area

Tick specimens were collected from seven districts of Khyber Pakhtunkhwa (KP), a province in northwest Pakistan, namely, Mohmand (34.5356°N, 71.2874°E), Bajaur (34.7865°N, 71.5249°E), Swabi (34.0719°N, 72.4732°E), Charsadda (34.1682°N, 71.7504°E), Mardan (34.1986°N, 72.0404°E), Dir-Upper (35.3356°N, 72.0468°E), and Dir-Lower (34.9161°N, 71.8097°E). Data regarding the host, ticks, climate, and location were noted. Climatic information was taken from the website climate-data.org. Geo-coordinates of location sites were obtained from the global positioning system and were entered into a spreadsheet, and the study map was designed in ArcGIS10.8.1.3 (ESRI, Redlands, CA, USA) (Figure 1).

Ethical statement

The design of the current study has received approval from the members of the Advanced Study and Research Board (Dir/A&R/AWKUM/2023/0014) and the Faculty of Zoology Department, Abdul Wali Khan University Mardan, Pakistan. Permission was obtained from the owner of the animal before collecting ticks from their animals.

Collection and morphological identification of ticks

Tick specimens were collected conveniently from March 2020 to February 2021 from domestic animals in seven districts of Khyber Pakhtunkhwa, Pakistan. The collection was opportunistic occurring whenever tick-infested animals were found within the survey regions. The whole body of the animal was examined for ticks. With the help of curved forceps, ticks were collected carefully so that the morphological features of ticks were not damaged. Every sample was tagged with its location of collection, date, and species of the animal.

The collected tick specimens were morphologically identified through a stereo microscope (CM100, China) by using standard taxonomic keys (Hoogstraal, 1962, 1966, 1973; Walker et al., 2000; Apanaskevich et al., 2008; 2010; Geevarghese and Mishra, 2011; Ali et al., 2022).

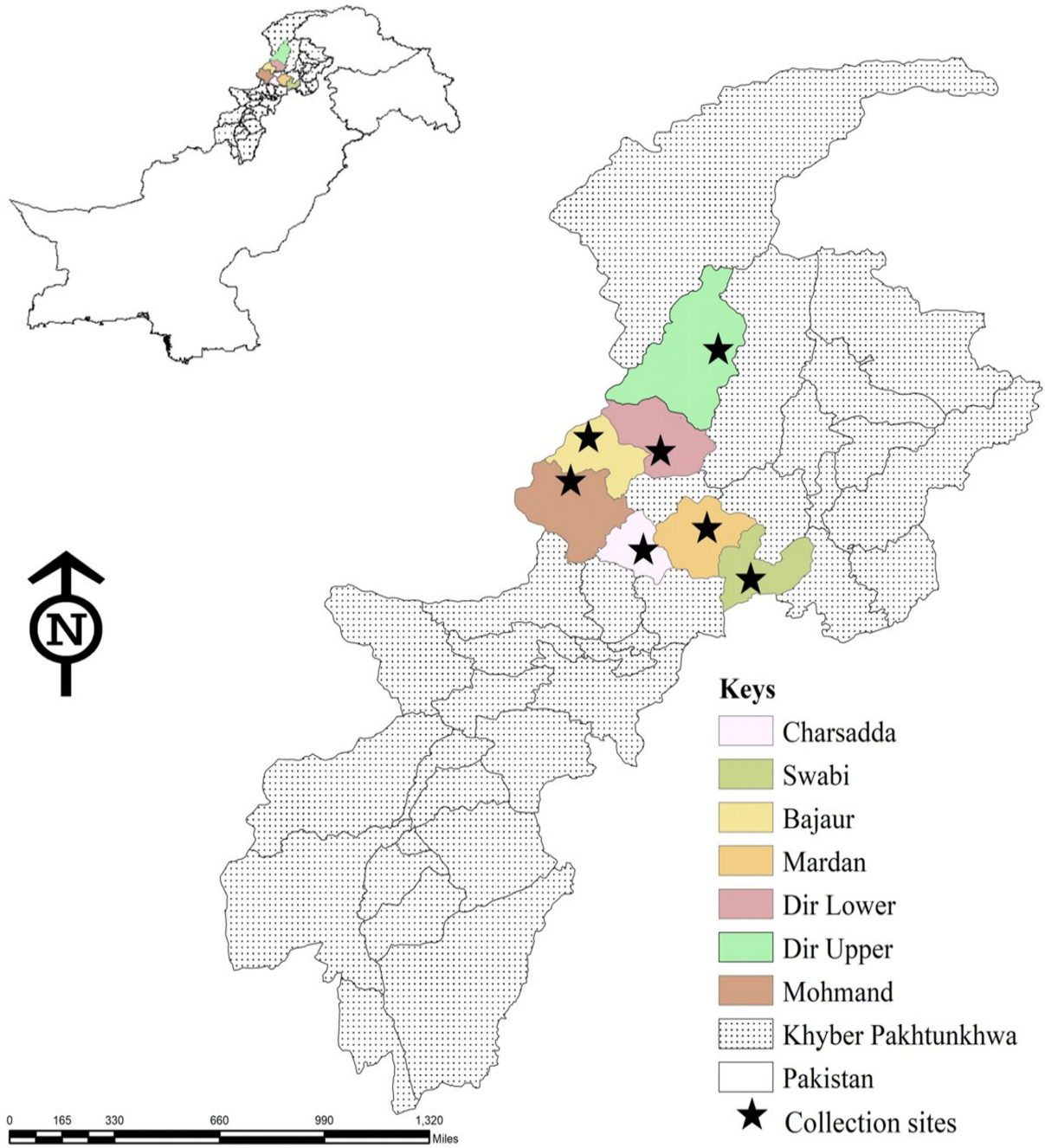

FIGURE 1
Map showing locations in seven districts of Khyber Pakhtunkhwa, where ticks were collected from domestic animals.

Genomic DNA extraction

All ticks were identified morphologically, and genomic DNA was individually extracted from a subset of 223 (122N, 86F, and 15M) ticks. Ticks were cleaned with 70% ethanol, followed by distilled water and phosphate-buffered saline for the elimination of surface contaminants. Each rinsed tick was separately kept in a 1.5 mL tube and subjected to drying within an incubator for 30 min. Using a sterilized scalpel, the samples were cut into pieces inside the Eppendorf tube. The phenol-chloroform method was used for the extraction of genomic DNA from the ticks (Sambrook et al., 1989). The DNA concentration in each extracted sample was quantified with Nanodrop (OPTIZEN, Daejeon, South Korea).

Amplification of targeted rickettsial DNA

The extracted DNA was used in conventional PCR (Thermo Fisher Scientific, and Walham, MA, USA), to amplify fragments of three genes of *Rickettsia,* namely, *gltA* (citrate synthase gene), *ompA* (outer membrane protein A), and *ompB* (outer membrane protein B). PCR was conducted in a 25 μL reaction mixture, containing 1 μL of

each primer (forward and reverse primers), 8.5 μL of PCR water, 2 μL of template DNA, and 12.5 μL of DreamTaq PCR Master Mix (2×) (Thermo Scientific, Waltham, MA, USA). The primers used in the current study are presented in Table 1, and thermocycling conditions were set as previously used (Regnery et al., 1991; Roux and Raoult 2000; Labruna et al., 2004). Positive and negative control samples were *Rickettsia massiliae* DNA and "nuclease-free" water, respectively (Shehla et al., 2023). The amplified products of each PCR were observed by electrophoresis on 2% agarose gel and stained with ethidium-bromide, and the results were visualized on the Gel Doc system (BioDoc-It™ Imaging Systems, Upland, CA, USA).

Sequencing and phylogenetic analysis

The amplified DNA fragments were purified using the GENECLEAN II Kit (Qbiogene, Illkirch, France) and sequenced using the Sanger sequencing (Macrogen, Inc., Seoul, South Korea) in both forward and reverse directions. Poor-quality sequences were removed by trimming all the obtained sequences using SeqMan v 5.00 (DNASTAR, Inc.), and a consensus sequence was generated. Sequences with the highest identity were selected from GenBank using the Basic Local Alignment Search Tool (BLAST) on the user interface of National Center for Biotechnology Information, and these sequences were aligned with the obtained sequences by BioEdit v. 7.0.5 using CLUSTALW multiple alignments (Thompson et al., 1994), followed by MUSCLE alignment (Edgar, 2004). The Neighbor-Joining method was applied for obtaining phylogenies with 1,000 bootstrap replicates in Molecular Evolutionary Genetic Analysis (MEGA-X) software (Kumar et al., 2018). The sequences that were obtained made up the final positions in the dataset.

Data analysis

The recorded data of tick-infested hosts and tick distribution were described with frequency and percentage using descriptive statistics. Fisher's exact test was used to determine the association between host, tick species, rickettsial species, and locations in GraphPad Prism software (V 5.0). p-value <0.05 was considered as significant standard.

Literature-based search

The literature-based search was carried out by using different databases including ScienceDirect, PubMed, Web of Sciences, and Google Scholar to collect published data regarding *Rickettsia aeschlimannii* in different tick species, wild and domestic animals, humans, environment, and vegetation. The search was conducted by using some keywords, such as ticks, tick-borne pathogens, domestic animals, small ruminants, zoonosis, livestock, and *Rickettsia aeschlimannii*. Complete research articles, short communication, review papers, and conference articles were downloaded by using a combination of the above mentioned keywords. Lists of references from downloaded studies were examined to relevant articles (Table 2).

Results

Identified ticks

A total of 369 domestic animals were examined in 7 districts including Mohmand (23 cattle, 14 goats, and 12 sheep), Dir Upper (20 cattle, 15 goats, 12 sheep, and 7 dogs), Dir lower (26 cattle, 17 goats, 13 sheep, and 5 dogs), Bajaur (19 cattle, 16 goats, 13 sheep, and 11 dogs), Charsadda (17 cattle, 15 goats, 13 sheep, and 5 dogs), Mardan (16 cattle, 13 goats, 20 sheep, and 5 dogs), and Swabi (17 cattle, 13 goats, 10 sheep, and 4 dogs) ($p = 0.248$). Of the examined hosts, 66% (247 of 369) of hosts were parasitized by 872 ticks of various life stages (Table 3), having a mean intensity of 3.5 ticks/infested host while the mean abundance was 2.3 ticks/examined host. The highest tick infestation was found on goats (74 of 103, 71.8%) compared with cattle (99 of 138, 71.7%), sheep (62 of 91, 60%), and dogs (12 of 37, 32.4%) ($p < 0.0001$). All collected ticks belonged to three different genera of ixodid ticks, namely, *Rhipicephalus, Hyalomma,* and *Haemaphysalis.* Adult female including engorged ticks were the most prevalent (376, 43.1%), followed by nymphs (303, 34.74%) and males (193, 22.13%) (Table 3) ($p < 0.0001$). The highest tick burden was observed on domestic animals in the Bajaur district (19.3%), followed by Mardan (15%), Swabi (14.9%), Charsadda (13.9%), Mohmand (13.3%), Dir Upper (12.7%), and Dir Lower (10.6%) ($p < 0.0001$). The most dominant species was *Rhipicephalus microplus* (19.0%), followed by *Hyalomma anatolicum* (15.7%), *Rhipicephalus turanicus* (11.5%), *Haemaphysalis sulcata* (10.6%), *Haemaphysalis bispinosa* (9.8%), *Haemaphysalis montgomeryi* (9.1%), *Rhipicephalus sanguineus* (8.8%), *Hyalomma scupense* (4.9%), *Rhipicephalus haemaphysaloides* (3.8%), *Haemaphysalis cornupunctata* (2.7%) *Hyalomma isaaci* (1.9%), and *Hyalomma turanicum* (1.60%) ($p < 0.0001$).

TABLE 1 Primers used for the amplification of rickettsial DNA in the current study.

Gene	Primer	Sequence(5′-3′)	Amplicon size	Annealing Temperatures	Reference
gltA	CS-78	GCAAGTATCGGTGTGAGGATGTAAT	401 bp	56°C	Labruna et al. (2004)
	CS-323	GCTTCCTTAAAATTCAATAAATCAGGAT			
ompA	Rr190.70p	ATGGCGAATATTTCTCCAAAA	532 bp	55°C	Regnery et al. (1991)
	Rr190.602n	AGTGCAGCATTCGCTCCCCCT			
ompB	120-M59	CCGCAGGGTTGGTAACTGC	862 bp	50°C	Roux and Raoult (2000)
	120–807	CCTTTTAGATTACCGCCTAA			

TABLE 2 Global epidemiology of *Rickettsia aeschlimannii* detected in different ticks and vertebrate hosts including human.

Continents	Country	Tick specie/Source	Host	Reference
Africa	Algeria	*Hy. scupense*	Sheep	Bitam et al. (2006)
		Hy. marginatum marginatum	Cattle, sheep	Bitam et al. (2006)
		Hy. aegyptium	Tortoises	Bitam et al. (2009)
		Hy. marginatum rufipes	Camels	Djerbouh et al. (2012)
		Hy. scupense, *Hy. anatolicum*	Cattle	Leulmi et al. (2016)
		Hy. marginatum, *Hy. scupense*, *Hy. impeltatum*	Cattle, goats, sheep, and equids	Sadeddine et al. (2020)
	Angola	*Hy. turncatum*	Cattle	Palomar et al. (2022)
	Benin	*A. variegatum*, *Rh. microplus*, *Hy. rufipes*	Cattle	Yessinou et al. (2023)
	Cameroon	*Hy. rufipes*, *Hy. truncatum*	Cattle	Vanegas et al. (2018)
		Hy. rufipes, *Hy. turncatum*	Nile Monitor, Hedgehog	Paguem et al. (2023)
	Chad	*Hy. marginatum rufipes*	Camels	Mura et al. (2008b)
	Egypt	*Hy. dromedarii*	Camels	Loftis et al. (2006)
		Hy. marginatum rufipes	Cows	
		Hy. impeltatum	Cows	
		Hy. anatolicum excavatum, *Hy. impeltatum*, *Hy. dromedarii*, *Hy. marginatum marginatum*	Ruminants, camels, sheep, and cattle	Allam et al. (2018)
	Ethiopia	*Hy. marginatum rufipes*	Cattle	Mura et al. (2008a)
	Ghana	*A. variegatum*, *Hy. rufipes*, *Rh. evertsi*, *Rhipicephalus* sp.	Cattle, goats, and sheep	Addo et al. (2023)
	Kenya	*Hy. truncatum*, *Hy. marginatum*, *Rh. pulchellus*, *A. variegatum*, *Hy. truncatum*, *Hyalomma* spp.	Camel, cattle, and goat	Koka et al. (2017)
		Hy. truncatum, *Hy. marginatum rufipes*, *Rh. pulchellus*	Sheep and goats	Omondi et al. (2017)
		Hy. truncatum	Domestic animals	Mutai et al. (2013)
		Rh. sanguineus, *Hy. truncatum*, *Hy. marginatum rufipes*	Domestic animals	Diarra et al. (2017)
		Rh. pulchellus, *Hy. dromedarii*, *Hy. rufipes*, *Hy. truncatum*, *Hy. impeltatum*	Camels and sheep	Getange et al. (2021)
		A. gemma	Cattle	Godani et al. (2022)
	Mali	*Hy. marginatum rufipes*	Cattle	Parola et al. (2001)
	Morocco	Unknown	Human	Raoult et al. (2002)
		Hy. marginatum	Cattle	Beati et al. (1997)
	Niger	*Hy. marginatum rufipes*	Cattle	Parola et al. (2001)
	Nigeria	*Hy. impeltatum*, *Hy. rufipes*	Camels	Kamani et al. (2015)
		Hy. dromedarii, *Hy. truncatum*, *Hy. rufipes*, *Hy. impeltatum*	Camels	Onyiche et al. (2020)
	Senegal	*Hy. marginatum rufipes*, *Hy. truncatum*, *Rh. evertsi evertsi*	Cows, donkeys, sheep, goats, and horses	Mediannikov et al. (2010)
		Hy. m. rufipes, *Rh. evertsi*, *Hy. impeltatum*	Domestic animals	Sambou et al. (2014)
	South Africa	*Rh. appendiculatus*	Human	Pretorius and Birtles (2002)
		Hy. marginatum	Domestic animals	Sarih et al. (2008)
		Rh. appendiculatus	Cattle	Pretorius and Birtles (2002)
		Hy. rufipes, *Rh. appendiculatus*, *Rh. evertsi*	Donkeys	Halajian et al. (2018)
	Sudan	*Hy. dromedarii*, *Hy. truncatum*	Camels	Morita et al. (2004)
		Rh. evertsi, *Hy. rufipes*	Domestic animals	Springer et al. (2020)
		Hy. rufipes, *Hy. dromedarii*	Camels	Shuaib et al. (2020)
	Tunisia	*Hy. dromedarii*	Camel	Demoncheaux et al. (2012)
		Unknown	Human	Znazen et al. (2006)
		Rh. sanguineus	Dogs	Khrouf et al. (2014)
		Hy. impeltatum, *Hy. dromedarii*	Camels	Selmi et al. (2020)
		Hy. marginatum, *Rh. sanguineus*	Cattle	Kratou et al. (2023)

(Continued)

TABLE 2 (Continued)

Continents	Country	Tick specie/Source	Host	Reference
	Zambia	*Hy. truncatum*	Dogs and cattle	Qiu et al. (2022)
		Hyalomma spp.	Cattle	Chitanga et al. (2021)
Asia				
		H. punctata	Cattle, sheep	Song et al. (2018)
		Rh. turanicus	Sheep	Wei et al. (2015)
		Hy. marginatum	Yaks	Jiao et al. (2022)
	Iran	*Rh. sanguineus, Hy. rufipes,*	Unknown	Saman and Chegeni (2022)
		Hy. marginatum, Rh. sanguineus	Dogs, sheep	Ghasemi et al. (2022)
	Israel	*Hy. turanicum, Hy. dromedarii, Hy. excavatum*	Camel	Kleinerman et al. (2013)
		Rh. sanguineus	Dogs	Mumcuoglu et al. (2022)
		Hy. marginatum	Horse	Azagi et al. (2017)
	Kazakhstan	*H. punctata*	Vegetation	Shpynov et al. (2004)
	Lebanon	*Rh. annulatus, Hy. anatolicum, Rh. sanguineus*	Farms	De Mera et al. (2018)
Europe	Austria	*Hy. marginatum*	Migratory birds	Duscher et al. (2018)
	Bulgaria	*Hy. anatolicum, Hy. marginatum, Hy. excavatum, Rhipicephalus* spp.	Dogs and cattle	Nader et al. (2018)
	Croatia	*Hy. marginatum*	Cattle	Punda-Polic et al. (2003)
	England	*Hy. marginatum*	Human	McGinley et al. (2021)
	France	*Hy. marginatum*	Sheep, humans, cattle, vegetation, wild boar, cattle, sheep, humans (on clothes), and vegetation	Matsumoto et al. (2004)
		Hyalomma sp.	Migratory birds	Socolovschi et al. (2011)
		Hy. marginatum rufipes	Migratory birds	Matsumoto et al. (2004)
		Hy. marginatum, Rh. sanguineus, Hy. scupense, Rh. bursa	Domestic and wild animals	Grech-Angelini et al. (2020)
	Germany	*Hy. marginatum*	Migratory birds	Rumer et al. (2011)
		Hy. marginatum, Hy. rufipes	Sheep, horse, and cat	Chitimia-Dobler et al. (2019)
	Georgia	*H. sulcata, Hy. scupense, Hy. marginatum, H. punctata,*	Cows and dogs	Sukhiashvili et al. (2020)
	Greece	*Hy. aegyptium*	Wild birds	Diakou et al. (2016)
		Hy. anatolicum	Sheep	Psaroulaki et al. (2006)
	Greece and Italy	*Hy. marginatum, Hy. rufipes, I. frontalis, Haemaphysalis* sp.	Migratory birds	Wallmenius et al. (2014)
	Serbia	*I. ricinus*	Humans	Banović et al. (2022)
	Italy	*Hy. lusitanicum*	Humans	Otranto et al. (2014)
		Hy. lusitanicum, Hy. marginatum, D. marginatus, I. ricinus	Humans	Blanda et al. (2017)
		I. ricinus, Rh. turanicus	Insugherata Natural Reserve	Mancini et al. (2015)
		Hy. marginatum, Hy. lusitanicum	Humans, domestic mammals, and wildlife	Chisu et al. (2018)
		Hy. marginatum	Herbivores (donkeys, cattle, and sheep)	Beninati et al. (2005)
		D. marginatus	Dogs	Sgroi et al. (2022)
		Hy. marginatum	Vegetation	Tomassone et al. (2013)
		Hy. marginatum, Hy. truncatum, Hy. rufipes, Hyalomma sp.	Great reed warbler, Reed warbler, Icterine warbler, Western yellow wagtail, Whinchat, Garden warbler, European pied flycatcher, Sedge warbler, Spotted flycatcher, Common whitethroat, Common redstart, Common nightingale, Collared flycatcher, Subalpine warbler, and Northern wheatear	Pascucci et al. (2019a,b)
		Hy. rufipes, A. marmoreum, Hyalomma sp.	Black redstart, Pied flycatcher, Redstart, Tree pipit, Whinchat, Whitethroat, Collared flycatcher, European robin, Northern weathear, Redstart, Song thrush, Whinchat, Whitethroat, and Wood warbler	Battisti et al. (2020)

(Continued)

TABLE 2 (Continued)

Continents	Country	Tick specie/Source	Host	Reference
		Hy. rufipes	Whitethroat tree pipit, Northern, Wheatear, and Whinchat	Rollins et al. (2021)
		Human	Human	Tosoni et al. (2016)
		Hy. marginatum	Wild boar	Maioli et al. (2009)
		Hy. m. marginatum, Hyalomma spp., *Amblyomma* sp.	Migratory birds	Toma et al. (2014)
		Hy. truncatum, Hy. rufipes	Cattle	Tomassone et al. (2016)
		Hy. marginatum rufipes	Cattle	Ehounoud et al. (2016)
		Hy. marginatum	Free living	Scarpulla et al. (2016)
		Hy. m. marginatum	Mouflon	Chisu et al. (2018)
		Hy. marginatum	*C. elaphus*	Pascucci et al. (2019a,b)
	Poland	*D. reticulatus*	Human	Koczwarska et al. (2023)
	Portugal	*Hy. marginatum*	Wild birds	Santos-Silva et al. (2006)
	Russia (western Russia)	*Hy. marginatum*	Cattle and vegetation	Shpynov et al. (2009)
	Romania	*Hy. marginatum*	Cattle	Andersson et al. (2018)
		H. concinna	Hedgehogs	Borşan et al. (2021)
	Spain	*H. inermis*	Vegetation	Portillo et al. (2008)
		Hy. marginatum	Humans	Fernández-Soto et al. (2009)
		Hy. marginatum, H. punctata, I. ricinus, Rh. bursa, Rh. turanicus, Rh. sanguineus	Humans	Fernández-Soto et al. (2003)
		Hy. marginatum	Humans and cows	Oteo et al. (2005)
	Spain and Morocco	*Hy. marginatum*	Humans and birds	Palomar et al. (2016)
	Sweden	*Hy. rufipes, Hy. marginatum*	Humans, Horse	Grandi et al. (2020)
	Turkey	*Hy. marginatum*	Humans	Keskin et al. (2016)
		Hy. marginatum	Humans	Keskin and Bursali, 2016
		Rh. bursa, Hy. marginatum, Hyalomma sp.	Humans	Gargili et al. (2012)
		Hy. marginatum	Humans	Bursalı et al. (2017)
		Hy. marginatum, Hy. aegyptium, Rh. turanicus, H. parva, H. punctata, H. sulcata, D. marginatus, I. ricinus, Hyalomma spp.	Humans	Karasartova et al. (2018)
		Hy. scupense, Hy. aegyptium, Hy. marginatum, Hy. excavatum	Humans	Orkun et al. (2014)
		Rh. turanicus, Hy. marginatum	Wild boar	Orkun and Çakmak (2019)
		Hy. aegyptium	Hedgehogs	Orkun and Çakmak (2019)
		Hy. marginatum, Rh. bursa	Cattle, goat	Demir et al. (2020)
		Hy. aegyptium	*Testudo graeca*	Akveran et al. (2020)
	United Kingdom	*Hy. rufipes*	Horse	Hansford et al. (2019)
South America	Bolivia	*A. tigrinum*	Dogs	Tomassone et al. (2010)
North America	Panama	*A. dissimile*	*Boa constrictor, Dasypus novemcinctus*	Bermudez et al. (2021)

Detection of *Rickettsia* spp. in ticks

DNA of a subset of 223 ticks was used for the detection of *Rickettsia* spp. by the amplification of three rickettsial markers, namely, *gltA*, *ompA*, and *ompB* gene fragments. Positive ticks for rickettsial *gltA* were also positive when tested with the primers of *ompA* and *ompB*. In total, 8 out of 223 (3.58%) ticks including 5 of 28 (17.85%) from Mohmand, 2 of 30 (6.6%) from Dir Lower, and 1 of 27 (3.7%) from Bajaur were found positive for *Rickettsia* spp. (P, 0.1621). Rickettsial DNA was found in three tick species, namely, *H. montgomeryi*, *H. bispinosa*, and *H. turanicum,* which was collected from sheep and goats. The overall prevalence of *Rickettsia* spp. was 3.58% (8 of 223). No rickettsial DNA was detected in *Rh. microplus* (27), *Hy. isaaci* (4), *Hy. scupense* (11), *Rh. turanicus* (33), *Hy. anatolicum* (33), *Rh. haemaphysaloides* (12), *Rh. sanguineus* (23), *H. cornupunctata* (7), and *H. sulcata* (23). Information regarding the prevalence of *Rickettsia* spp. in various ticks is shown in Table 3.

TABLE 3 Occurrence of ticks infesting various domestic animals and detection of rickettsial DNA associated with ticks.

District/Areas	Host	No. of examined host	No. of infested host	Collected Tick species	No. of Nymphs/ Female/male	Total No. of ticks	Molecularly screened Ticks*	*Rickettsia* spp. detected via *gltA, ompA, ompB*
Mohmand/ Rural	Cattle	23	15	*Hy. anatolicum*	8 N/3F/2F*/2M	15	3N,1F	0
				Rh. microplus	8 N/7F/3F*/7M	25	3N,1F	0
	Goats	14	9	*Hy. turanicum*	5N/5F/1F*/3M	14	2N,2F	2N,1F
				H. sulcata	6N/7F/3M	16	2N,1F,1M	0
	Sheep	12	8	*Hy. isaaci*	6N/7F/4M	17	2N,2F	0
				H. bispinosa	6N/7F/3M	16	2N,1F,1M	1N,1F
				H. montgomeryi	3N/8F/2M	13	2N,2F	0
Total		49	32 (8.6%)		42N/44F/6F*/24M	116 (13.3%)	16N,10F,2M	3N,2F
Dir Upper/ Rural	Cattle	20	14	*Rh. haemaphysaloides*	2N/6F/2M	10	2N,2F	0
				Rh. microplus	9N/7F/3F*/8M	27	2N,2F	0
	Goats	15	9	*Rh. turanicus*	4N/5F/2M	11	2N,2F	0
				H. montgomeryi	2N/8F/2M	12	2N,2F	0
	Sheep	10	8	*H. sulcata*	5N/6F/2M	13	2N,2F	0
				Hy. scupense	2N/6F/1M	9	2N,2F	0
				Hy. anatolicum	5N/3F/3F*/4M	15	2N,2F	0
	Dogs	7	3	*Rh. sanguineus*	5N/6F/3M	14	2N,2F	0
Total		52	34 (9.2%)		34N/47F/6F*/24M	111 (12.7%)	16N,16F	0
Dir lower/Rural	Cattle	26	18	*Rh. microplus*	10N/6F/4F*/9M	29	2N,2F,1M	0
	Goats	17	11	*H. bispinosa*	2N/8F/2M	12	3N,2F	0
				H. montgomeryi	2N/10F/3M	15	2N,2F,1M	IN,1F
	Sheep	13	7	*H. sulcata*	2N/8F/3M	13	3N,2F	0
	Dogs	5	2	*Rh. turanicus*	4N/5F/3M	12	3N,2F	0
				Rh. sanguineus	5N/3F/2F*/2M	12	3N,2F	0
Total		61	38 (10.2%)		25N/40F/6F*/22M	93 (10.6%)	16N,12F,2M	1N,1F
Bajaur/Rural	Cattle	19	17	*Rh. microplus*	10N/8F/2F*/8M	28	2N,1F	0
				Hy. anatolicum	6N/5F/3F*/7M	21	2N,1F	0
	Goats	16	14	*H. sulcata*	7N/8F/4M	19	2N,1F	0
				H. montgomeryi	7N/8F/3M	18	2N,1F	0
				Rh. turanicus	5N/4F/2M	11	2N,1F	1N
	Sheep	13	10	*Rh. turanicus*	8N/4F/2F*/3M	17	1N,1F,1M	0
				H. sulcata	7N/8F/3M	18	1N,1F,1M	0
				H. bispinosa	8N/9F/5M	22	2N,1F	0
	Dogs	11	2	*Rh. sanguineus*	5N/5F/2F*/3M	15	1N,1F,1M	0
Total		59	43 (11.65%)		63N/59F/9F*/38M	169 (19.3%)	15N,9F,3M	1N

(Continued)

10.3389/fmicb.2023.1283814

TABLE 3 (Continued)

District/Areas	Host	No. of examined host	No. of infested host	Collected Tick species	No. of Nymphs/ Female/male	Total No. of ticks	Molecularly screened Ticks*	*Rickettsia* spp. detected via *gltA, ompA, ompB*
Charsadda/Urban	Cattle	17	9	*Rh. microplus*	8N/4F/4F*/7M	23	2N,2F	0
				Rh. haemaphysaloides	6N/4F/2M	12	3N,1F	0
	Goats	15	12	*Rh. haemaphysaloides*	3N/8F/1M	12	3N,1F	0
				Rh. turanicus	3N/4F/2M	9	2N,2F	0
				Hy. anatolicum	6N/4F/2F*/4M	16	2N,1F,1M	0
	Sheep	13	8	*H. cornupunctata*	2N/5F/1M	8	2N,2F	0
				H. bispinosa	2N/4F/1M	7	2N,2F	0
				Hy. anatolicum	5N/3F/3F*/3M	14	2N,2F	0
	Dogs	5	2	*Rh. turanicus*	4N/5F/2M	11	2N,2F	0
				Rh. sanguineus	4N/4F/2M	10	3N,1F	0
Total		50	31 (8.40%)		43N/45F/9F*/25M	122 (13.9%)	23N,16F,1M	0
Mardan/Urban	Cattle	16	13	*Rh. microplus*	6N/4F/2F*/4M	16	2N,1F	0
				Hy. anatolicum	5N/3F/2F*/4M	14	2N,1F	0
	Goats	13	9	*Rh. turanicus*	4N/3F/2M	10	2N,1F	0
				Hy. anatolicum	4N/5F/2F*/2M	11	2N,1F	0
	Sheep	20	14	*H. cornupunctata*	6N/6F/4M	16	2N,1F	0
				Hy. scupense	5N/8F/3M	18	2N,1F	0
				H. bispinosa	5N/5F/2F*/3M	15	1N,1F,1M	0
				H. montgomeryi	2N/4F/2M	6	1N,1F,1M	0
	Dogs	5	2	*Rh. sanguineus*	5N/6F/3M	14	2N,1F	0
				Rh. turanicus	4N/4F/3M	11	1N,1F,1M	0
Total		54	38 (10.2%)		47N/46F/8F*/30M	131 (15.0%)	17N,10F,3M	0
Swabi/Urban	Cattle	17	13	*Rh. microplus*	6N/5F/3F*/4M	18	3N,1F	0
				Hy. anatolicum	5N/4F/2F*/3M	14	2N,1F,1M	0
				Rh. turanicus	4N/3F/2M	9	2N,1F,1M	0
	Goats	13	10	*H. bispinosa*	5N/5F/4M	14	2N,1F,1M	0
				H. montgomeryi	6N/6F/4M	16	2N,2F	0
	Sheep	10	7	*Hy. scupense*	6N/4F/2F*/4M	16	2N,1F,1M	0
				Hy. anatolicum	7N/4F/2F*/4M	17	2N,2F	0
				H. sulcata	5N/6F/3M	14	2N,2F	0
	Dogs	4	1	*Rh. sanguineus*	5N/5F/2M	12	2N,2F	0
Total		44	31 (8.40%)		49N/42F/9F*/30M	130 (14.90)	19N,13F,4M	0
Overall total		369	(66.65)		303N/323F/53F*/193M	872	122N,86F,15M	5N,3F

N, nymphs; F, Adult females; F*, Engorged females; M, males. *Ticks subjected to PCR to screen for *Rickettsia* spp.

10.3389/fmicb.2023.1283814

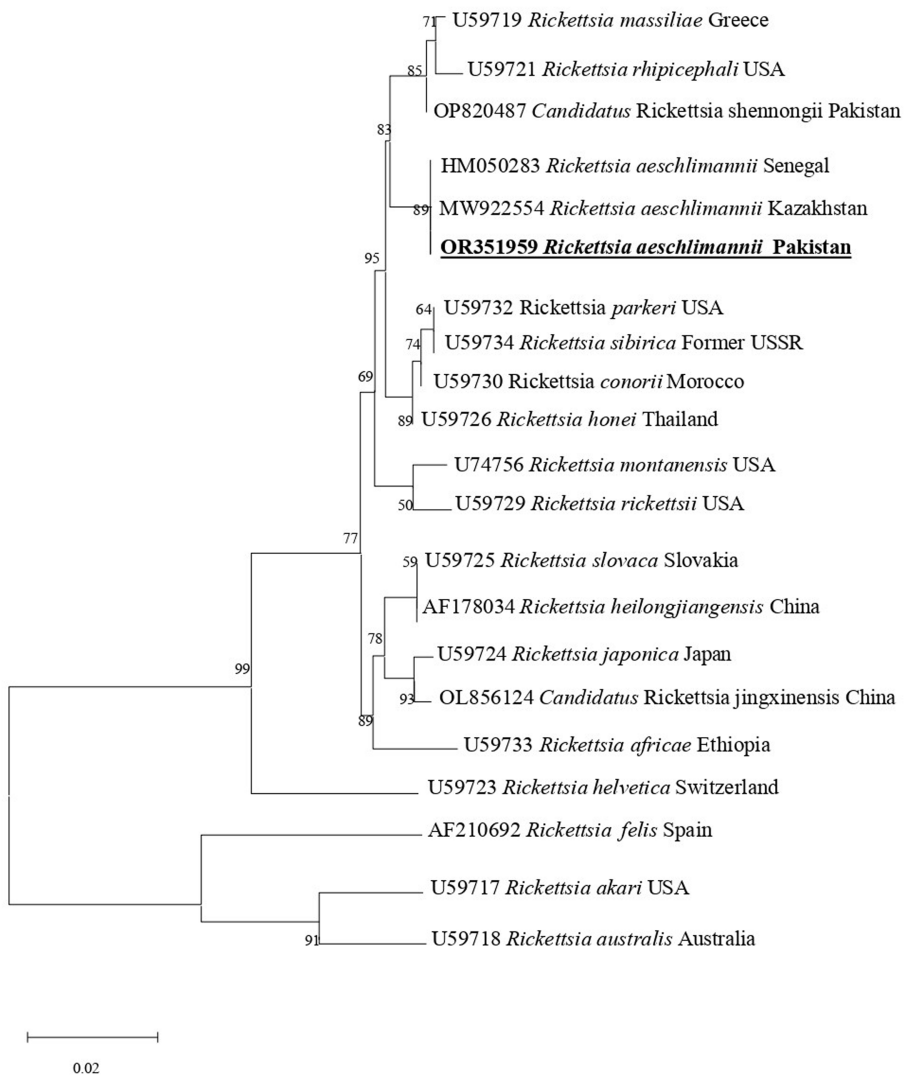

FIGURE 2
Phylogenetic analysis based on the *gltA* sequences of *Rickettsia aeschlimannii*. The obtained sequences of the present study are indicated in bold and underlined fonts. *Rickettsia akari* and *Rickettsia australis* were used as out-group.

Sequence and phylogenetic analysis

Assembled contigs of direct and reverse sequence reads for each PCR-amplified fragment were analyzed. Due to a single haplotype, consensus sequences were generated for each partial gene. The consensus sequence of *gltA* (348 bp) showed 100% identity with *R. aeschlimannii* from Russia, Senegal, and Kazakhstan, followed by 99.71% identity with *R. aeschlimannii*-type strain from Morocco. Similarly, 100% identity was shown by the obtained *ompA* (467 bp) consensus sequence with *R. aeschlimannii* from Russia, Spain, Turkey, and Kazakhstan, followed by 99.79% identity with *R. aeschlimannii*-type strain. Similarly, the *ompB* (764 bp) consensus sequence also showed 100% identity with *R. aeschlimannii* from Kazakhstan, Russia, Italy, and Portugal, followed by 99.74% identity with *R. aeschlimannii*-type strain. In all cases, the query coverage was 100%. The obtained rickettsial *gltA* sequence (accession number: OR351959), *ompA* sequence (accession number: OR351960), and *ompB* sequence (accession number: OR351961) were submitted to GenBank.

In phylogenetic tree based on rickettsial *gltA*, *R. aeschlimannii* clustered with *R. aeschlimannii* reported from Senegal (HM050283) and Kazakhstan (MW922554) (Figure 2). Rickettsial *ompA* clustered with *R. aeschlimannii* reported from Senegal (HM050286), Kazakhstan (MW922585), and Morocco (U43800) (Figure 3), while *ompB* sequence clustered with *R. aeschlimannii* reported from China (MF098413), Senegal (HM050278), and Morocco (AF123705) (Figure 4).

Discussion

Previous studies have recorded the presence of *Rickettsia* spp. in different tick-infesting hosts in Pakistan. However, there was a paucity of information regarding *R. aeschlimannii* in the region. This study presents the first report on molecular detection of *R. aeschlimannii* in *H. bispinosa*, *H. montgomeryi*, and *Hy. turanicum* ticks collected from sheep and goats in Pakistan. The obtained sequences showed maximum

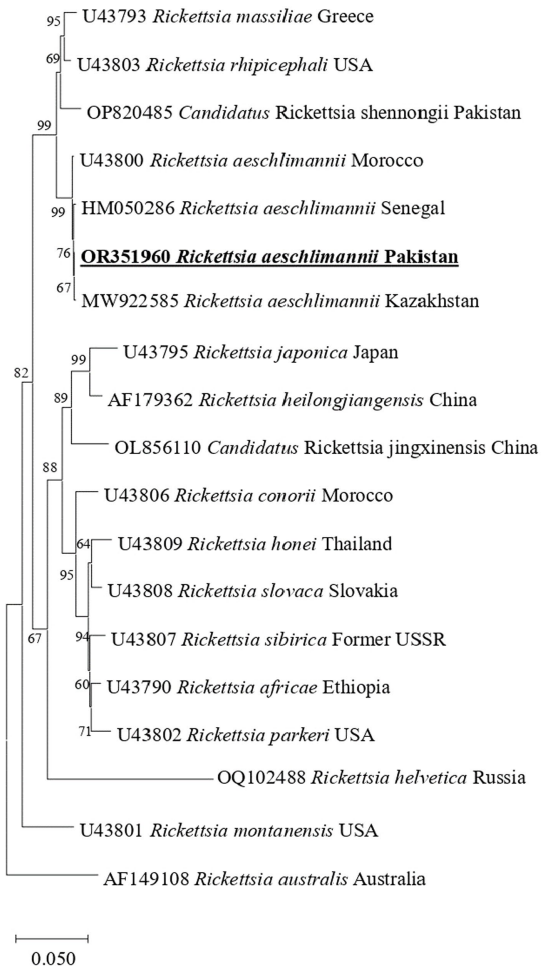

FIGURE 3
Phylogenetic analysis based on the *ompA* sequences of *R. aeschlimannii.* The sequences obtained in this study are indicated in bold and underlined fonts. *Rickettsia australis* is used as an out-group.

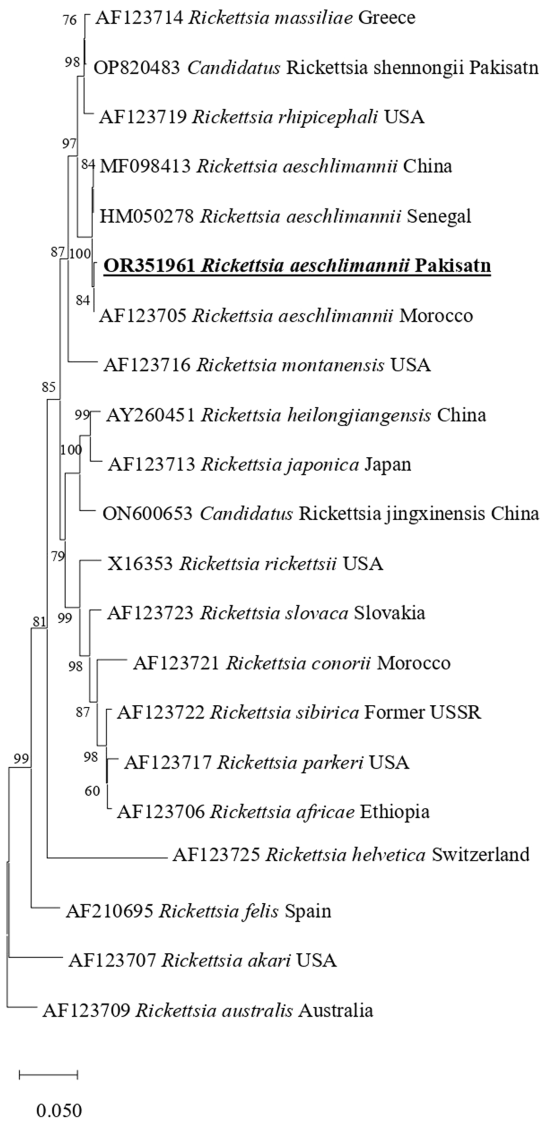

FIGURE 4
Phylogenetic analysis based on the sequences of the *ompB* genes of *R. aeschlimannii.* The obtained sequences in the present study are indicated in bold and underlined fonts. *Rickettsia australis* used as an out-group.

identity and phylogenetically clustered with *Rickettsia aeschlimannii,* which confirms the occurrence of *Rickettsia aeschlimannii* in the regions. *Rickettsia aeschlimannii*, an emerging pathogen with zoonotic potential, has been observed to cause infections in humans across various countries such as Morocco (Raoult et al., 2002), Tunisia (Znazen et al., 2006), Algeria (Mokrani et al., 2008), Greece (Germanakis et al., 2013), and Russia (Igolkina et al., 2022). The detection of *R. aeschlimannii* in tick-parasitizing domestic animals suggests a high exposure of livestock holders to this pathogen.

Small ruminants (goats and sheep), domestic dogs, and cattle were found infested by the ticks of genera *Rhipicephalus, Hyalomma,* and *Haemaphysalis*. Among the collected ticks, *Rh. microplus*, *Hy. anatolicum*, *H. bispinosa* and *H. montgomeryi* were the dominant tick species. These findings mirror the pattern observed in other previous studies conducted in same region (Karim et al., 2017; Ali et al., 2019; Alam et al., 2022; Khan Z. et al., 2022; Tila et al., 2023) underscoring the regional significance of these tick species. Furthermore, it emphasizes the need for further research to comprehensively investigate their prevalence, distribution, and potential implications for public health (Ali et al., 2023).

Ticks of different genera have been reported as carriers for various *Rickettsia* spp. in Pakistan (Ali et al., 2021, 2022; Khan M. et al., 2022; Khan Z. et al., 2022; Numan et al., 2022; Ullah et al., 2023). Herein, *Rickettsia aeschlimannii* was detected in *H. bispinosa*, *H. montgomeryi,* and *Hy. turanicum* ticks using three genetic markers, namely, *gltA*, *ompA*, and *ompB*. To date, there has been a lack of information regarding the detection of *R. aeschlimannii* in *H. bispinosa* and *H. montgomeryi* tick-infesting domestic animals, such as goats and sheep. There is also a possibility that the rickettsial DNA is detected in the ticks may be due to ingesting rickettsemic host blood. Literature search revealed that *R. aeschlimannii* is associated with a variety of tick species belonging to six genera of hard ticks, namely, *Hyalomma*, *Rhipicephalus, Haemaphysalis, Amblyomma, Dermacentor*, and *Ixodes* (Parola et al., 2001; Fernández-Soto et al., 2003; Shpynov et al., 2004; Tomassone et al.,

2010; Karasartova et al., 2018). Furthermore, there are limited reports, which have detected this pathogen in Asia (Wei et al., 2015; Satjanadumrong et al., 2019). This study found its association with two new ticks, expanding its known host and geographical range. The detection of *R. aeschlimannii* in *Hyalomma* and *Haemaphysalis* ticks suggests a potential threat to livestock holders. Additionally, the rate of *R. aeschlimannii* was observed highest in *Haemaphysalis* ticks, which are the primary ticks that infest goats and sheep. This enhances the feasibility of public health risks as these ticks may occasionally infest humans (Guglielmone and Robbins, 2018). *Rickettsia aeschlimannii* has been detected in all life stages of ticks, such as adult females, males, larvae, and nymphs (Raoult et al., 2002; Shpynov et al., 2009; Germanakis et al., 2013; Orkun et al., 2014; Wallmenius et al., 2014; Tosoni et al., 2016). This study presents the first molecular evidence of *R. aeschlimannii* in *H. bispinosa* and *H. montgomeryi* ticks, which suggests that other tick species could also serve as competent vectors for this pathogen in the region.

Molecular methods are considered faster and more accurate for the genetic characterization and phylogenetic analysis of *Rickettsia* spp. (Fournier et al., 1998; Roux and Raoult, 2000). The *gltA*, *ompA, ompB,* and *sca*4 DNA sequences have been used as suitable genetic markers to discriminate different *Rickettsia* spp (Roux and Raoult, 2000; Fournier et al., 2003; Labruna et al., 2004). Herein, these sequences were targeted for molecular characterization and phylogenetic analysis of *R. aeschlimannii* which revealed the close relatedness with corresponding species of the SFG. We assume that human infection caused by rickettsial agents of SFG maybe underreported due to the lack of epidemiological information among health practitioners and laboratory technicians and the lack of diagnostic procedures in Pakistan, given the relevance of the occurrence of these agents in the region. Further studies in the region should be encouraged to obtain information on zoonotic outcomes due to these infectious agents.

Conclusion

This study for the first time contributes to the neglected knowledge and genetic characterization of tick-borne *R. aeschlimannii* in *H. bispinosa*, *H. montgomeryi,* and *Hy. turanicum* ticks in Pakistan. The results of this study also indicated that goats and sheep are exposed to *R. aeschlimannii*. Further molecular studies are important to screen *R. aeschlimannii* in livestock and livestock holders who have close contact with domestic animals.

Data availability statement

We have released your GenBank submissions in OR351959-OR351961. Your sequences will be available for public access within a few days. If you have additional information about your sequences or wish to make further revisions, see: https://www.ncbi.nlm.nih.gov/Genbank/update.html for proper update formats.

Ethics statement

The design of the current work has received an approval from the Advanced Study and Research Board members (Dir/A&R/AWKUM/2023/0014) and the Faculty of Zoology department, Abdul Wali Khan University Mardan, Pakistan. Permissions were obtained from the animal's owner before collecting ticks from their animals. The studies were conducted in accordance with the local legislation and institutional requirements. Written informed consent was obtained from the owners for the participation of their animals in this study.

Author contributions

AM:Datacuration,Investigation,Methodology,Software,Writing–original draft. MA: Data curation, Formal analysis, Funding acquisition, Investigation, Methodology, Writing – original draft, Writing – review & editing. AbdA: Funding acquisition, Investigation, Methodology, Project administration, Resources, Writing – original draft, Writing – review & editing. TT: Data curation, Formal analysis, Investigation, Writing – original draft, Writing – review & editing. T-YY: Formal analysis, Validation, Visualization, Writing – original draft, Writing – review & editing. K-HT: Data curation, Formal analysis, Funding acquisition, Investigation, Writing – original draft, Writing – review & editing. AbiA: Conceptualization, Funding acquisition, Investigation, Methodology, Project administration, Resources, Supervision, Writing –original draft, Writing – review & editing.

Acknowledgments

The authors appreciate the financial support from the Pakistan Science Foundation and Higher Education Commission of Pakistan. The researchers supporting project number (RSP2023R494), King Saud University, Riyadh, Saudi Arabia. This research was also partially funded by the National Science and Technology Council, grant number: 112-2327-B-002-008.

Conflict of interest

The authors declare that the research was conducted in the absence of any commercial or financial relationships that could be construed as a potential conflict of interest.

Publisher's note

All claims expressed in this article are solely those of the authors and do not necessarily represent those of their affiliated organizations, or those of the publisher, the editors and the reviewers. Any product that may be evaluated in this article, or claim that may be made by its manufacturer, is not guaranteed or endorsed by the publisher.

References

Addo, S. O., Bentil, R. E., Baako, B. O. A., Yartey, K. N., Behene, E., Asiamah, B., et al. (2023). Occurrence of *Rickettsia* spp. and *Coxiella burnetii* in ixodid ticks in Kassena-Nankana, Ghana. *Exp. Appl. Acarol.* 90, 137–153. doi: 10.1007/s10493-023-00808-0

Akveran, G. A., Karasartova, D., Keskin, A., Comba, A., Celebi, B., Mumcuoglu, K. Y., et al. (2020). Bacterial and protozoan agents found in *Hyalomma aegyptium* (L., 1758) (Ixodida: Ixodidae) collected from *Testudo graeca* L., 1758 (Reptilia: Testudines) in Corum Province of Turkey. *Ticks Tick-borne Dis.* 11:101458. doi: 10.1016/j.ttbdis.2020.101458

Alam, S., Khan, M., Alouffi, A., Almutairi, M. M., Ullah, S., Numan, M., et al. (2022). Spatio-temporal patterns of ticks and molecular survey of *Anaplasma marginale*, with notes on their phylogeny. *Microorganisms* 10:1663. doi: 10.3390/microorganisms10081663

Ali, A., Khan, M.A., Zahid, H., Yaseen, P. M., Qayash Khan, M., Nawab, J., et al. (2019). Seasonal dynamics, record of ticks infesting humans, wild and domestic animals and molecular phylogeny of *Rhipicephalus microplus* in Khyber Pakhtunkhwa Pakistan. *Frontiers in Physiology* 10:793. doi: 10.3389/fphys.2019.00793

Ali, A., Ullah, S., Numan, M., Almutairi, M. M., Alouffi, A., and Tanaka, T. (2023). First report on tick-borne pathogens detected in ticks infesting stray dogs near butcher shops. *Front. Vet. Sci.* 10:1246871. doi: 10.3389/fvets.2023.1246871

Ali, A., Numan, M., Khan, M., Aiman, O., Muñoz-Leal, S., Chitimia-Dobler, L., et al. (2022). *Ornithodoros (Pavlovskyella)* ticks associated with a *Rickettsia* sp. in Pakistan. *Parasit. Vect.* 15, 1–13. doi: 10.1186/s13071-022-05248-0

Ali, A., Zahid, H., Zeb, I., Tufail, M., Khan, S., Haroon, M., et al. (2021). Risk factors associated with tick infestations on equids in Khyber Pakhtunkhwa, Pakistan, with notes on *Rickettsia massiliae* detection. *Parasit. Vectors* 14, 363–312. doi: 10.1186/s13071-021-04836-w

Allam, N., El Moghazy, F. M., and Abdel-Baky, S. (2018). Molecular epidemiological updates on spotted fever rickettsioses in animal species and their hard ticks settling Egyptian desert. *J. Adv. Pharm. Educat. Res.* 8:65.

Aneela, A., Almutairi, M. M., Alouffi, A., Ahmed, H., Tanaka, T., da Silva Vaz, I., et al. (2023). Molecular detection of *Rickettsia hoogstraalii* in *Hyalomma anatolicum* and *Haemaphysalis sulcata*: updated knowledge on the epidemiology of tick-borne *Rickettsia hoogstraalii*. *Vet. Sci.* 10:605. doi: 10.3390/vetsci10100605

Andersson, M. O., Tolf, C., Tamba, P., Stefanache, M., Radbea, G., Frangoulidis, D., et al. (2018). Molecular survey of neglected bacterial pathogens reveals an abundant diversity of species and genotypes in ticks collected from animal hosts across Romania. *Parasit. Vectors* 11, 1–10. doi: 10.1186/s13071-018-2756-1

Apanaskevich, D. A., Filippova, N. A., and Horak, I. G. (2010). The genus *Hyalomma* Koch, 1844. X. Redescription of all parasitic stages of *Hy. scupense*, 1919 (*Hy. detritum* Schulze) (Acari: Ixodidae) and notes on its biology. *Folia Parasitol.* 57, 69–78. doi: 10.14411/fp.2010.009

Apanaskevich, D. A., Schuster, A. L., and Horak, I. G. (2008). The genus *Hyalomma*: VII. Redescription of all parasitic stages of *Hy. dromedarii* and *Hy. schulzei* (Acari: Ixodidae). *J. Med. Entomol.* 45, 817–831. doi: 10.1093/jmedent/45.5.817

Azagi, T., Klement, E., Perlman, G., Lustig, Y., Mumcuoglu, K. Y., Apanaskevich, D. A., et al. (2017). Francisella-like endosymbionts and *Rickettsia* species in local and imported *Hyalomma* ticks. *Appl. Environ. Microbiol.* 83, e01302–e01317. doi: 10.1128/AEM.01302-17

Banović, P., Díaz-Sánchez, A. A., Simin, V., Foucault-Simonin, A., Galon, C., Wu-Chuang, A., et al. (2022). Clinical aspects and detection of emerging rickettsial pathogens: A "One Health" approach study in Serbia, 2020. *Frontiers in microbiology* 12, p.797399. doi: 10.3389/fmicb.2021.797399

Battisti, E., Urach, K., Hodžić, A., Fusani, L., Hufnagl, P., Felsberger, G., et al. (2020). Zoonotic pathogens in ticks from migratory birds, Italy. *Emerg. Infect. Dis.* 26, 2986–2988. doi: 10.3201/eid2612.181686

Beati, L., Meskini, M., Thiers, B., and Raoult, D. (1997). *Rickettsia aeschlimannii* sp. nov., a new spotted fever group *Rickettsia* associated with *Hyalomma marginatum* ticks. *Int. J. Syst. Evol. Microbiol.* 47, 548–554. doi: 10.1099/00207713-47-2-548

Beninati, T., Genchi, C., Torina, A., Caracappa, S., Bandi, C., and Lo, N. (2005). Rickettsiae in ixodid ticks, Sicily. *Emerg. Infect. Dis.* 11, 509–511. doi: 10.3201/eid1103.040812

Bermudez, S., Martinez-Mandiche, J., Dominguez, L., Gonzalez, C., Chavarria, O., Moreno, A., et al. (2021). Diversity of *Rickettsia* in ticks collected from wild animals in Panama. *Ticks Tick-borne Dis.* 12:101723. doi: 10.1016/j.ttbdis.2021.101723

Bitam, I., Kernif, T., Harrat, Z., Parola, P., and Raoult, D. (2009). First detection of *Rickettsia aeschlimannii* in *Hyalomma aegyptium* from Algeria. *Clin. Microbiol. Infect.* 15, 253–254. doi: 10.1111/j.1469-0691.2008.02274.x

Bitam, I., Parola, P., Matsumoto, K., Rolain, J. M., Baziz, B., Boubidi, S. C., et al. (2006). First molecular detection of *R. conorii*, *R. aeschlimannii*, and *R. massiliae* in ticks from Algeria. *Ann. N. Y. Acad. Sci.* 1078, 368–372. doi: 10.1196/annals.1374.073

Blanda, V., Torina, A., La Russa, F., D'Agostino, R., Randazzo, K., Scimeca, S., et al. (2017). A retrospective study of the characterization of *Rickettsia* species in ticks collected from humans. *Ticks Tick-borne Dis.* 8, 610–614. doi: 10.1016/j.ttbdis.2017.04.005

Borşan, S. D., Ionică, A. M., Galon, C., Toma-Naic, A., Peştean, C., Sándor, A. D., et al. (2021). High diversity, prevalence, and co-infection rates of tick-borne pathogens in ticks and wildlife hosts in an urban area in Romania. *Front. Microbiol.* 12:645002. doi: 10.3389/fmicb.2021.645002

Boulanger, N., Boyer, P., Talagrand-Reboul, E., and Hansmann, Y. (2019). Tick-borne diseases. *Medecine et Maladies Infectieuses* 49, 87–97. doi: 10.13140/RG.2.2.18223.30881

Brouqui, P., Parola, P., Fournier, P. E., and Raoult, D. (2007). Spotted fever rickettsioses in Southern and Eastern Europe. *FEMS* 49, 2–12. doi: 10.1111/j.1574-695X.2006.00138.x

Bursalı, A., Keskin, A., Keskin, A., Kul Köprülü, T., and Tekin, Ş. (2017). Investigation of the presence of Rickettsiae in ticks parasitizing humans in Corum Region. *Turk. Hij. Tecr. Biyol. Derg.* 74, 293–298. doi: 10.5505/TurkHijyen.2017.28291

Chisu, V., Foxi, C., and Masala, G. (2018). First molecular detection of the human pathogen *Rickettsia raoultii* and other spotted fever group rickettsiae in Ixodid ticks from wild and domestic mammals. *Parasitology research*, 17, pp. 3421–3429. doi: 10.1007/s00436-018-6036-y

Chitanga, S., Chibesa, K., Sichibalo, K., Mubemba, B., Nalubamba, K. S., Muleya, W., et al. (2021). Molecular detection and characterization of *Rickettsia* species in Ixodid ticks collected from cattle in Southern Zambia. *Front. Vet. Sci.* 8:684487. doi: 10.3389/fvets.2021.684487

Chitimia-Dobler, L., Schaper, S., Rieß, R., Bitterwolf, K., Frangoulidis, D., Bestehorn, M., et al. (2019). Imported *Hyalomma* ticks in Germany in 2018. *Parasit. Vectors* 12, 134–139. doi: 10.1186/s13071-019-3380-4

Djerbouh, A., Kernif, T., Beneldjouzi, A., Socolovschi, C., Kechemir, N., Parola, P., et al. (2012). The first molecular detection of *Rickettsia aeschlimannii* in the ticks of camels from Southern Algeria. *Ticks Tick Borne Dis.* 3, 374–376. doi: 10.1016/j.ttbdis.2012.10.014

De la Fuente, J., Antunes, S., Bonnet, S., Cabezas-Cruz, A., Domingos, A. G., Estrada-Peña, A., et al. (2017). Tick-pathogen interactions and vector competence: identification of molecular drivers for tick-borne diseases. *Front. Cell. Infect. Microbiol.* 7:114. doi: 10.3389/fcimb.2017.00114

Demoncheaux, J. P., Socolovschi, C., Davoust, B., Haddad, S., Raoult, D., and Parola, P. (2012). First detection of *Rickettsia aeschlimannii* in *Hyalomma dromedarii* ticks from Tunisia. *Ticks Tick Borne Dis.* 3, 398–402. doi: 10.1016/j.ttbdis.2012.10.003

de Mera, I. G. F., Blanda, V., Torina, A., Dabaja, M. F., El Romeh, A., Cabezas-Cruz, A., et al. (2018). Identification and molecular characterization of spotted fever group Rickettsiae in ticks collected from farm ruminants in Lebanon. *Ticks Tick Borne Dis.* 9, 104–108. doi: 10.1016/j.ttbdis.2017.10.001

Demir, S., Erkunt Alak, S., Köseoğlu, A. E., Ün, C., Nalçacı, M., and Can, H. (2020). Molecular investigation of *Rickettsia* spp. and *Francisella tularensis* in ticks from three provinces of Turkey. *Exp. Appl. Acarol.* 81, 239–253. doi: 10.1007/s10493-020-00498-y

Diakou, A., Norte, A. C., Lopes de Carvalho, I., Núncio, S., Nováková, M., Kautman, M., et al. (2016). Ticks and tick-borne pathogens in wild birds in Greece. *Parasitol. Res.* 115, 2011–2016. doi: 10.1007/s00436-016-4943-3

Diarra, A. Z., Almeras, L., Laroche, M., Berenger, J. M., Koné, A. K., Bocoum, Z., et al. (2017). Molecular and MALDI-TOF identification of ticks and tick-associated bacteria in Mali. *PLoS Negl. Trop. Dis.* 11:e0005762. doi: 10.1371/journal.pntd.0005762

Duscher, G. G., Hodžić, A., Hufnagl, P., Wille-Piazzai, W., Schötta, A. M., Markowicz, M. A., et al. (2018). Adult *Hyalomma marginatum* tick positive for *Rickettsia aeschlimannii* in Austria, October 2018. *Eur. Secur.* 23:1800595. doi: 10.2807/1560-7917.ES.2018.23.48.1800595

Edgar, R. C. (2004). MUSCLE: multiple sequence alignment with high accuracy and high throughput. *Nucleic Acids Res.* 32, 1792–1797. doi: 10.1016/j.sbi.2006.04.004

Ehounoud, C. B., Yao, K. P., Dahmani, M., Achi, Y. L., Amanzougaghene, N., Kacou N'Douba, A., et al. (2016). Multiple pathogens including potential new species in tick vectors in Côte d'Ivoire. *PLoS Negl. Trop. Dis.* 10:e0004367. doi: 10.1371/journal.pntd.0004367

El Karkouri, K., Ghigo, E., Raoult, D., and Fournier, P. E. (2022). Genomic evolution and adaptation of arthropod-associated *Rickettsia*. *Sci. Rep.* 12:3807. doi: 10.1038/s41598-022-07725-z

Fernández-Soto, P., Encinas Grandes, A., and Pérez Sánchez, R. (2003). *Rickettsia aeschlimannii* in Spain: molecular evidence in *Hyalomma marginatum* and five other tick species that feed on humans. *Emerg. Infect. Dis.* 9, 889–890. doi: 10.3201/eid0907.030077

Fernández-Soto, P., Díaz Martín, V., Pérez-Sánchez, R., and Encinas-Grandes, A. (2009). Increased prevalence of *Rickettsia aeschlimannii* in Castilla y Leon, Spain. *Eur. J. Clin. Microbiol. Infect. Dis.* 28, 693–695. doi: 10.1007/s10096-008-0667-3

Fournier, P. E., and Raoult, D. (2009). Current knowledge on phylogeny and taxonomy of *Rickettsia* spp. *Ann. N. Y. Acad. Sci.* 1166, 1–11. doi: 10.1111/j.1749-6632.2009.04528.x

Fournier, P. E., Roux, V., and Raoult, D. (1998). Phylogenetic analysis of spotted fever group rickettsiae by study of the outer surface protein rOmpA.. *International Journal of Systematic and Evolutionary Microbiology* 48, 839–849. doi: 10.1099/00207713-48-3-839

Fournier, P. E., Dumler, J. S., Greub, G., Zhang, J., Wu, Y., and Raoult, D. (2003). Gene sequence-based criteria for identification of new *Rickettsia* isolates and description of *Rickettsia heilongjiangensis* sp. nov. *J. Clin. Microbiol.* 41, 5456–5465. doi: 10.1128/JCM.41.12.5456-5465.2003

Gargili, A., Palomar, A. M., Midilli, K., Portillo, A., Kar, S., and Oteo, J. A. (2012). *Rickettsia* species in ticks removed from humans in Istanbul, Turkey. *Vector-Borne Zoonotic Dis.* 12, 938–941. doi: 10.1089/vbz.2012.0996

Germanakis, A., Chochlakis, D., Angelakis, E., Tselentis, Y., and Psaroulaki, A. (2013). *Rickettsia aeschlimannii* infection in a man, Greece. *Emerg. Infect. Dis.* 19:1176. doi: 10.3201/eid1907.130232

Getange, D., Bargul, J. L., Kanduma, E., Collins, M., Bodha, B., Denge, D., et al. (2021). Ticks and tick-borne pathogens associated with dromedary camels (*Camelus dromedarius*) in northern Kenya. *Microorganisms* 9:1414. doi: 10.3390/microorganisms9071414

Ghasemi, A., Latifian, M., Esmaeili, S., Naddaf, S. R., and Mostafavi, E. (2022). Molecular surveillance for *Rickettsia* spp. and *Bartonella* spp. in ticks from Northern Iran. *PLoS One* 17:e0278579. doi: 10.1371/journal.pone.0278579

Godani, S. K., Chengo, M. N., and Muturi, M. W. (2022). Zoonotic pathogens detected in ticks in Kenyan game reserves. *Adv. Entomol.* 11, 1–9. doi: 10.4236/ae.2023.111001

Grandi, G., Chitimia-Dobler, L., Choklikitumnuey, P., Strube, C., Springer, A., Albihn, A., et al. (2020). First records of adult *Hyalomma marginatum* and *H. rufipes* ticks (Acari: Ixodidae) in Sweden. *Ticks Tick-borne Dis.* 11:101403. doi: 10.1016/j.ttbdis.2020.101403

Grech-Angelini, S., Stachurski, F., Vayssier-Taussat, M., Devillers, E., Casabianca, F., Lancelot, R., et al. (2020). Tick-borne pathogens in ticks (Acari: Ixodidae) collected from various domestic and wild hosts in Corsica (France), a Mediterranean island environment. *Transbound. Emerg. Dis.* 67, 745–757. doi: 10.1111/tbed.13393

Guglielmone, A.A., and Robbins, R.G., (2018). *Hard Ticks (Acari: Ixodida: Ixodidae) Parasitizing Humans*. Cham: Springer, 230

Halajian, A., Palomar, A. M., Portillo, A., Heyne, H., Romero, L., and Oteo, J. A. (2018). Detection of zoonotic agents and a new *Rickettsia* strain in ticks from donkeys from South Africa: implications for travel medicine. *Travel Med. Infect. Dis.* 26, 43–50. doi: 10.1016/j.tmaid.2018.10.007

Hansford, K. M., Carter, D., Gillingham, E. L., Hernandez-Triana, L. M., Chamberlain, J., Cull, B., et al. (2019). *Hyalomma rufipes* on an untraveled horse: is this the first evidence of *Hyalomma* nymphs successfully moulting in the United Kingdom? *Ticks Tick-borne Dis.* 10, 704–708. doi: 10.1016/j.ttbdis.2019.03.003

Hoogstraal, H., El Kammah, K.M., Santana, F.J., and Van Peenen, P.D. (1973). Studies on southeast Asian *Haemaphysalis* ticks (Ixodoidea: Ixodidae). *H.(Kaiseriana) lagrangei* Larrousse: identity, distribution, and hosts. *The Journal of Parasitology* , 1118–1129. doi: 10.2307/3278651

Hoogstraal, H., Trapido, H., and Kohls, G. M. (1996). Studies on southeast Asian *Haemaphysalis* ticks (Ixodoidea, Ixodidae). *Speciation in the H.(Kaiseriana) obesa group: H. semermis Neumann, H. obesa Larrousse, H. roubaudi Toumanoff, H. montgomeryi Nuttall, and H. hirsuta sp. n." The Journal of Parasitology* 169–191. doi: 10.2307/3276410

Hoogstraal, H., and Varma, M. G. R. (1962). *Haemaphysalis cornupunctata* sp. n. and *H. kashmirensis* sp. n. from Kashmir, with Notes on *H. sundrai* Sharif and *H. sewelli* Sharif of India and Pakistan (Ixodoidea, Ixodidae). *J. Parasitol.* 48, 185–194. doi: 10.2307/3275561

Geevarghese, G., and Mishra, A.C., (2011). *Haemaphysalis ticks of India*. Waltham, MA: Elsevier.

Igolkina, Y., Rar, V., Krasnova, E., Filimonova, E., Tikunov, A., Epikhina, T., et al. (2022). Occurrence and clinical manifestations of tick-borne rickettsioses in Western Siberia: first Russian cases of *Rickettsia aeschlimannii* and *Rickettsia slovaca* infections. *Ticks Tick-borne Diseases* 13:101927. doi: 10.1016/j.ttbdis.2022.101927

Jian, Y., Li, J., Adjou Moumouni, P. F., Zhang, X., Tumwebaze, M. A., Wang, G., et al. (2020). Human spotted fever group *Rickettsia* infecting yaks (*Bos grunniens*) in the Qinghai-Tibetan plateau area. *Pathogens* 9:249. doi: 10.1016/j.ttbdis.2020.101466

Jiao, J., Yu, Y., He, P., Wan, W., OuYang, X., Wen, B., et al. (2022). *First detection of Rickettsia aeschlimannii in Hyalomma marginatum in tibet*, China. Zoonoses

Kamani, J., Baneth, G., Apanaskevich, D. A., Mumcuoglu, K. Y., and Harrus, S. (2015). Molecular detection of *Rickettsia aeschlimannii* in *Hyalomma* spp. ticks from camels (*Camelus dromedarius*) in Nigeria, West Africa. *Med. Vet. Entomol.* 29, 205–209. doi: 10.1111/mve.12094

Karasartova, D., Gureser, A. S., Gokce, T., Celebi, B., Yapar, D., Keskin, A., et al. (2018). Bacterial and protozoal pathogens found in ticks collected from humans in Corum province of Turkey. *PLoS Negl. Trop. Dis.* 12:e0006395. doi: 10.1371/journal.pntd.0006395

Karim, S., Budachetri, K., Mukherjee, N., Williams, J., Kausar, A., Hassan, M. J., et al. (2017). A study of ticks and tick-borne livestock pathogens in Pakistan. *PLoS Negl. Trop. Dis.* 11:e0005681. doi: 10.1371/journal.pntd.0005681

Keskin, A., and Bursali, A. (2016). Detection of *Rickettsia aeschlimannii* and *Rickettsia sibirica* mongolitimonae in *Hyalomma marginatum* (Acari: Ixodidae) ticks from Turkey. *Acarologia* 56, 533–536. doi: 10.1051/acarologia/20164140

Keskin, A., Bursali, A., Keskin, A., and Tekin, S. (2016). Molecular detection of spotted fever group Rickettsiae in ticks removed from humans in Turkey. *Ticks Tick-borne Dis.* 7, 951–953. doi: 10.1016/j.ttbdis.2016.04.015

Khan, M., Islam, N., Khan, A., Islam, Z. U., Muñoz-Leal, S., Labruna, M. B., et al. (2022). New records of *Amblyomma gervaisi* from Pakistan, with detection of a reptile-associated *Borrelia* sp. *Ticks Tick-borne Dis.* 13:102047. doi: 10.1016/j.ttbdis.2022.102047

Khan, S. M., Khan, M., Alouffi, A., Almutairi, M. M., Numan, M., Ullah, S., et al. (2023). Phylogenetic position of *Haemaphysalis kashmirensis* and *Haemaphysalis cornupunctata*, with notes on *Rickettsia* spp. *Genes* 14:360. doi: 10.3390/genes14020360

Khan, Z., Shehla, S., Alouffi, A., Kashif Obaid, M., Zeb Khan, A., Almutairi, M. M., et al. (2022). Molecular survey and genetic characterization of *Anaplasma marginale* in ticks collected from livestock hosts in Pakistan. *Animals* 12:1708. doi: 10.3390/ani12131708

Khrouf, F., M'Ghirbi, Y., Znazen, A., Ben Jemaa, M., Hammami, A., and Bouattour, A. (2014). Detection of *Rickettsia* in *Rhipicephalus sanguineus* ticks and *Ctenocephalides felis* fleas from southeastern Tunisia by reverse line blot assay. *J. Clin. Microbiol.* 52, 268–274. doi: 10.1128/JCM.01925-13

Kleinerman, G., Baneth, G., Mumcuoglu, K. Y., van Straten, M., Berlin, D., Apanaskevich, D. A., et al. (2013). Molecular detection of *Rickettsia africae*, *Rickettsia aeschlimannii*, and *Rickettsia sibirica* mongolitimonae in camels and *Hyalomma* spp. ticks from Israel. *Vector Borne Zoonotic Dis* 13, 851–856. doi: 10.1089/vbz.2013.1330

Koczwarska, J., Pawełczyk, A., Dunaj-Małyszko, J., Polaczyk, J., and Welc-Falęciak, R. (2023). *Rickettsia* species in *Dermacentor reticulatus* ticks feeding on human skin and clinical manifestations of tick-borne infections after tick bite. *Sci. Rep.* 13:9930. doi: 10.1038/s41598-023-37059-3

Koka, H., Sang, R., Kutima, H. L., and Musila, L. (2017). The detection of spotted fever group *Rickettsia* DNA in tick samples from pastoral communities in Kenya. *J. Med. Entomol.* 54, 774–780. doi: 10.1093/jme/tjw238

Kratou, M., Belkahia, H., Selmi, R., Andolsi, R., Dhibi, M., Mhadhbi, M., et al. (2023). Diversity and phylogeny of cattle ixodid ticks and associated spotted fever group *Rickettsia* spp. in Tunisia. *Pathogens* 12:552. doi: 10.3390/pathogens12040552

Kumar, S., Stecher, G., Li, M., Knyaz, C., and Tamura, K. (2018). MEGA X: molecular evolutionary genetics analysis across computing platforms. *Mol. Biol. Evol.* 35:1547. doi: 10.1093/molbev/msy096/4990887

Labruna, M. B. (2009). Ecology of rickettsia in South America. *Ann. N. Y. Acad. Sci.* 1166, 156–166. doi: 10.1111/j.1749-6632.2009.04516.x

Labruna, M. B., Whitworth, T., Horta, M. C., Bouyer, D. H., McBride, J. W., Pinter, A., et al. (2004). *Rickettsia* species infecting *Amblyomma cooperi* ticks from an area in the state of São Paulo, Brazil, where Brazilian spotted fever is endemic. *J. Clin. Microbiol.* 42, 90–98. doi: 10.1128/JCM.42.1.90-98.2004

Leulmi, H., Aouadi, A., Bitam, I., Bessas, A., Benakhla, A., Raoult, D., et al. (2016). Detection of *Bartonella tamiae*, *Coxiella burnetii* and Rickettsiae in arthropods and tissues from wild and domestic animals in northeastern Algeria. *Parasit. Vectors* 9, 1–8. doi: 10.1186/s13071-016-1316-9

Loftis, A. D., Reeves, W. K., Szumlas, D. E., Abbassy, M. M., Helmy, I. M., Moriarity, J. R., et al. (2006). Rickettsial agents in Egyptian ticks collected from domestic animals. *Exp. Appl. Acarol.* 40, 67–81. doi: 10.1007/s10493-006-9025-2

Maioli, G., Bonilauri, P., Barbieri, I., Calzolari, M., and Francesco, D.F. And Dottori, M., *Detection of spotted fever group Rickettsia and Anaplasma phagocytophilum in ticks removed from wild animals in northern Italy in 2009* (2009).

Mancini, F., Ciccozzi, M., Lo Presti, A., Cella, E., Giovanetti, M., Di Luca, M., et al. (2015). Characterization of spotted fever group Rickettsiae in ticks from a city park of Rome, Italy. *Ann. Ist. Super Sanita* 51, 284–290. doi: 10.4415/ANN_15_04_07

Matsumoto, K., Parola, P., Brouqui, P., and Raoult, D. (2004). *Rickettsia aeschlimannii* in *Hyalomma* ticks from Corsica. *Eur. J. Clin. Microbiol. Infect. Dis.* 23, 732–734. doi: 10.13140/RG.2.2.22971.98080

McGinley, L., Hansford, K. M., Cull, B., Gillingham, E. L., Carter, D. P., Chamberlain, J. F., et al. (2021). First report of human exposure to *Hyalomma marginatum* in England: further evidence of a *Hyalomma* moulting event in North-Western Europe? *Ticks and Tick-borne Diseases* 12:101541. doi: 10.1016/j.ttbdis.2020.101541

Mediannikov, O., Diatta, G., Fenollar, F., Sokhna, C., Trape, J. F., and Raoult, D. (2010). Tick-borne rickettsioses, neglected emerging diseases in rural Senegal. *PLoS Negl. Trop. Dis.* 4:e821. doi: 10.1371/journal.pntd.0000821

Mokrani, N., Parola, P., Tebbal, S., Dalichaouche, M., Aouati, A., and Raoult, D. (2008). *Rickettsia aeschlimannii* infection, Algeria. *Emerg. Infect. Dis.* 14, 1814–1815. doi: 10.3201/eid1411.071221

Morita, C., El Hussein, A. R. M., Matsuda, E., Abdel Gabbar, K. M. A., Muramatsu, Y., Abdel Rahman, M. B., et al. (2004). Spotted fever group Rickettsiae from ticks captured in Sudan. *Jpn. J. Infect. Dis.* 57, 107–109.

Mumcuoglu, K. Y., Arslan-Akveran, G., Aydogdu, S., Karasartova, D., Koşar, A., Savci, U., et al. (2022). Pathogens in ticks collected in Israel: II. Bacteria and protozoa found in *Rhipicephalus sanguineus* sensu lato and *Rhipicephalus turanicus*. *Ticks Tick-borne Dis.* 13:101986. doi: 10.1016/j.ttbdis.2022.101986

Mura, A., Masala, G., Tola, S., Satta, G., Fois, F., Piras, P., et al. (2008a). First direct detection of rickettsial pathogens and a new rickettsia, '*Candidatus* Rickettsia barbariae', in ticks from Sardinia, Italy. *Clin. Microbiol. Infect.* 14, 1028–1033. doi: 10.1111/j.1469-0691.2008.02082.x

Mura, A., Socolovschi, C., Ginesta, J., Lafrance, B., Magnan, S., Rolain, J. M., et al. (2008b). Molecular detection of spotted fever group rickettsiae in ticks from Ethiopia and Chad. *Trans. R. Soc. Trop. Med. Hyg.* 102, 945–949. doi: 10.1016/j.trstmh.2008.03.015

Mutai, B. K., Wainaina, J. M., Magiri, C. G., Nganga, J. K., Ithondeka, P. M., Njagi, O. N., et al. (2013). Zoonotic surveillance for Rickettsiae in domestic animals in Kenya. *Vector Borne Zoonotic Dis.* 13, 360–366. doi: 10.1089/vbz.2012.0977

Nader, J., Król, N., Pfeffer, M., Ohlendorf, V., Marklewitz, M., Drosten, C., et al. (2018). The diversity of tick-borne bacteria and parasites in ticks collected from the Strandja Nature Park in South-Eastern Bulgaria. *Parasit. Vectors* 11, 165–110. doi: 10.1186/s13071-018-2721-z

Numan, M., Islam, N., Adnan, M., Zaman Safi, S., Chitimia-Dobler, L., Labruna, M. B., et al. (2022). First genetic report of *Ixodes kashmiricus* and associated *Rickettsia* sp. *Parasit. Vectors* 15, 378–312. doi: 10.1186/s13071-022-05509-y

Omondi, D., Masiga, D. K., Fielding, B. C., Kariuki, E., Ajamma, Y. U., Mwamuye, M. M., et al. (2017). Molecular detection of tick-borne pathogen diversities in ticks from livestock and reptiles along the shores and adjacent islands of Lake Victoria and Lake Baringo, Kenya. *Front. Vet. Sci.* 4:73. doi: 10.3389/fvets.2017.00073

Onyiche, T. E., Răileanu, C., Tauchmann, O., Fischer, S., Vasić, A., Schäfer, M., et al. (2020). Prevalence and molecular characterization of ticks and tick-borne pathogens of one-humped camels (*Camelus dromedarius*) in Nigeria. *Parasit. Vectors* 13, 428–416. doi: 10.1186/s13071-020-04272-2

Orkun, Ö., and Çakmak, A. (2019, 2019). Molecular identification of tick-borne bacteria in wild animals and their ticks in Central Anatolia, Turkey. *Comp. Immunol. Microbiol. Infect. Dis.* 63, 58–65. doi: 10.1016/j.cimid.2018.12.007

Orkun, Ö., Karaer, Z., Çakmak, A., and Nalbantoğlu, S. (2014). Identification of tick-borne pathogens in ticks feeding on humans in Turkey. *PLoS Negl. Trop. Dis.* 8:e3067. doi: 10.1371/journal.pntd.0003067

Oteo, J. A., Portillo, A., Blanco, J. R., Ibarra, V., Pérez-Martínez, L., Izco, C., et al. (2005). Low risk of developing human *Rickettsia aeschlimannii* infection in the north of Spain. *Ann. N. Y. Acad. Sci.* 1063, 349–351. doi: 10.1196/annals.1355.057

Otranto, D., Dantas-Torres, F., Giannelli, A., Latrofa, M. S., Cascio, A., Cazzin, S., et al. (2014). Ticks infesting humans in Italy and associated pathogens. *Parasit. Vectors* 7, 1–9. doi: 10.1186/1756-3305-7-3

Paguem, A., Manchang, K., Kamtsap, P., Renz, A., Schaper, S., Dobler, G., et al. (2023). Ticks and rickettsiae associated with wild animals sold in bush meat markets in Cameroon. *Pathogens* 12:348. doi: 10.3390/pathogens12020348

Palomar, A. M., Molina, I., Bocanegra, C., Portillo, A., Salvador, F., Moreno, M., et al. (2022). Old zoonotic agents and novel variants of tick-borne microorganisms from Benguela (Angola), July 2017. *Parasit. Vectors* 15:140. doi: 10.1186/s13071-022-05238-2

Palomar, A. M., Portillo, A., Mazuelas, D., Roncero, L., Arizaga, J., Crespo, A., et al. (2016). Molecular analysis of Crimean-Congo hemorrhagic fever virus and *Rickettsia* in *Hyalomma marginatum* ticks removed from patients (Spain) and birds (Spain and Morocco), 2009–2015. *Ticks Tick-borne Dis.* 7, 983–987. doi: 10.1016/j.ttbdis.2016.05.004

Parola, P., Inokuma, H., Camicas, J. L., Brouqui, P., and Raoult, D. (2001). Detection and identification of spotted fever group Rickettsiae and Ehrlichiae in African ticks. *Emerg. Infect. Dis.* 7, 1014–1017. doi: 10.3201/eid0706.010616

Parola, P., Paddock, C. D., Socolovschi, C., Labruna, M. B., Mediannikov, O., Kernif, T., et al. (2013). Update on tick-borne rickettsioses around the world: a geographic approach. *Clin. Microbiol. Rev.* 26, 657–702. doi: 10.1128/CMR.00032-13

Pascucci, I., Di Domenico, M., Curini, V., Cocco, A., Averaimo, D., D'Alterio, N., et al. (2019a). Diversity of *Rickettsia* in ticks collected in Abruzzi and Molise regions (Central Italy). *Microorganisms* 7:696. doi: 10.3390/microorganisms7120696

Pascucci, I., Di Domenico, M., Dondona, G. C., Di Gennaro, A., Polci, A., Dondona, A. C., et al. (2019b). Assessing the role of migratory birds in the introduction of ticks and tick-borne pathogens from African countries: an Italian experience. *Ticks Tick-borne Dis.* 10:101272. doi: 10.1016/j.ttbdis.2019.101272

Portillo, A., Santibáñez, P., Santibáñez, S., Pérez-Martínez, L., and Oteo, J. A. (2008). Detection of Rickettsia spp. in Haemaphysalis ticks collected in La Rioja, Spain. *Vector-Borne Zoonotic Dis.* 8, 653–658. doi: 10.1089/vbz.2007.0272

Pretorius, A. M., and Birtles, R. J. (2002). *Rickettsia aeschlimannii*: a new pathogenic spotted fever group *Rickettsia*, South Africa. *Emerg. Infect. Dis.* 8, 874a–8874a. doi: 10.3201/eid0808.020199

Psaroulaki, A., Ragiadakou, D., Kouris, G., Papadopoulos, B., Chaniotis, B., and Tselentis, Y. (2006). Ticks, tick-borne Rickettsiae, and *Coxiella burnetii* in the Greek island of Cephalonia. *Ann. N. Y. Acad. Sci.* 1078, 389–399. doi: 10.1196/annals.1374.077

Punda-Polic, V., Petrovec, M., Trilar, T., Duh, D., Bradaric, N., Klismanic, Z., et al. (2003). "Detection and identification of spotted fever group Rickettsiae in ticks collected in southern Croatia" in *Ticks and tick-borne pathogens: Proceedings of the 4th international conference on ticks and tick-borne pathogens the Banff Centre Banff, Alberta, Canada 21–26 July 2002* (Dordrecht: Springer Netherlands), 169–176.

Qiu, Y., Simuunza, M., Kajihara, M., Ndebe, J., Saasa, N., Kapila, P., et al. (2022). Detection of tick-borne bacterial and protozoan pathogens in ticks from the Zambia-Angola border. *Pathogens* 11:566. doi: 10.3390/pathogens11050566

Raoult, D., Fournier, P. E., Abboud, P., and Caron, F. (2002). First documented human *Rickettsia aeschlimannii* infection. *Emerg. Infect. Dis.* 8, 748–749. doi: 10.3201/eid0807.010480

Regnery, R. L., Spruill, C. L., and Plikaytis, B. (1991). Genotypic identification of rickettsiae and estimation of intraspecies sequence divergence for portions of two rickettsial genes. *J. Bacteriol.* 173, 1576–1589. doi: 10.1128/jb.173.5.1576-1589.1991

Rollins, R. E., Schaper, S., Kahlhofer, C., Frangoulidis, D., Strauß, A. F., Cardinale, M., et al. (2021). Ticks (Acari: Ixodidae) on birds migrating to the island of Ponza, Italy, and the tick-borne pathogens they carry. *Ticks Tick-borne Dis.* 12:101590. doi: 10.1016/j.ttbdis.2020.101590

Roux, V., and Raoult, D. (2000). Phylogenetic analysis of members of the genus *Rickettsia* using the gene encoding the outer-membrane protein rOmpB (ompB). *Int. J. Syst. Evol. Microbiol.* 50, 1449–1455. doi: 10.1099/00207713-50-4-1449

Roux, V., Fournier, P. E., and Raoult, D. (1997). Differentiation of spotted fever group Rickettsiae by sequencing and analysis of restriction fragment length polymorphism of PCR-amplified DNA of the gene encoding the protein rOmpA. *J. Clin. Microbiol.* 34, 2058–2065. doi: 10.1128/JCM.34.9.2058-2065.1996

Rumer, L., Graser, E., Hillebrand, T., Talaska, T., Dautel, H., Mediannikov, O., et al. (2011). *Rickettsia aeschlimannii* in *Hyalomma marginatum* ticks, Germany. *Emerging infectious diseases* 17, 325–326. doi: 10.3201/eid1702.100308

Sadeddine, R., Diarra, A. Z., Laroche, M., Mediannikov, O., Righi, S., Benakhla, A., et al. (2020). Molecular identification of protozoal and bacterial organisms in domestic animals and their infesting ticks from North-Eastern Algeria. *Ticks Tick-borne Dis.* 11:101330. doi: 10.1016/j.ttbdis.2019.101330

Saman, E. A. G., and Chegeni, A. H. (2022). Hard ticks (Acari: Ixodidae) infected by Rickettsias: the first record of *Rickettsia aeschlimannii* (Rickettsiales: Rickettsiaceae) in Iran. *Syst. Appl. Acarol.* 27, 749–762. doi: 10.11158/saa.27.4.7

Sambou, M., Faye, N., Bassène, H., Diatta, G., Raoult, D., and Mediannikov, O. (2014). Identification of Rickettsial pathogens in ixodid ticks in northern Senegal. *Ticks Tick-borne Dis.* 5, 552–556. doi: 10.1016/j.ttbdis.2014.04.002

Sambrook, J., Fritsch, E.F., and Maniatis, T. *Molecular cloning: a laboratory manual, 2nd*; Cold Spring Harbor Laboratory Press: New York, NY, USA, (1989)

Santos-Silva, M. M., Sousa, R., Santos, A. S., Melo, P., Encarnação, V., and Bacellar, F. (2006). Ticks parasitizing wild birds in Portugal: detection of *Rickettsia aeschlimannii*, *R. helvetica* and *R. massiliae*. *Exp. Appl. Acarol.* 39, 331–338. doi: 10.1007/s10493-006-9008-3

Sarih, M., Socolovschi, C., Boudebouch, N., Hassar, M., Raoult, D., and Parola, P. (2008). Spotted fever group Rickettsiae in ticks, Morocco. *Emerg. Infect. Dis.* 14, 1067–1073. doi: 10.3201/eid1407.070096

Satjanadumrong, J., Robinson, M. T., Hughes, T., and Blacksell, S. D. (2019). Distribution and ecological drivers of spotted fever group *Rickettsia* in Asia. *EcoHealth* 16, 611–626. doi: 10.1007/s10393-019-01409-3

Scarpulla, M., Barlozzari, G., Marcario, A., Salvato, L., Blanda, V., De Liberato, C., et al. (2016). Molecular detection and characterization of spotted fever group Rickettsiae in ticks from Central Italy. *Ticks Tick-borne Dis.* 7, 1052–1056. doi: 10.1016/j.ttbdis.2016.06.003

Selmi, R., Ben Said, M., Ben Yahia, H., Abdelaali, H., and Messadi, L. (2020). Molecular epidemiology and phylogeny of spotted fever group *Rickettsia* in camels (*Camelus dromedarius*) and their infesting ticks from Tunisia. *Transbound. Emerg. Dis.* 67, 733–744. doi: 10.1111/tbed.13392

Sgroi, G., Iatta, R., Lia, R. P., Napoli, E., Buono, F., Bezerra-Santos, M. A., et al. (2022). Tick exposure and risk of tick-borne pathogens infection in hunters and hunting dogs: a citizen science approach. *Transbound. Emerg. Dis.* 69, e386–e393. doi: 10.1111/tbed.14314

Shehla, S., Ullah, F., Alouffi, A., Almutairi, M. M., Khan, Z., Tanaka, T., et al. (2023). Association of SFG *Rickettsia massiliae* and *Candidatus* Rickettsia shennongii with different hard ticks infesting livestock hosts. *Pathogens* 12:1080. doi: 10.3390/pathogens12091080

Shpynov, S., Fournier, P. E., Rudakov, N., Tankibaev, M., Tarasevich, I., and Raoult, D. (2004). Detection of a rickettsia closely related to *Rickettsia aeschlimannii*, "*Rickettsia heilongjiangensis*," *Rickettsia* sp. strain RpA4, and *Ehrlichia muris* in ticks collected in Russia and Kazakhstan. *J. Clin. Microbiol.* 42, 2221–2223. doi: 10.1128/JCM.42.5.2221-2223.2004

Shpynov, S., Rudakov, N., Tohkov, Y., Matushchenkso, A., Tarasevich, I., Raoult, D., et al. (2009). Detection of *Rickettsia aeschlimannii* in *Hyalomma marginatum* ticks in western Russia. *Clin. Microbiol. Infect.* 15, 315–316. doi: 10.1111/j.1469-0691.2008.02256.x

Shuaib, Y. A., Elhag, A. M. A. W., Brima, Y. A., Abdalla, M. A., Bakiet, A. O., Mohmed-Noor, S. E. T., et al. (2020). Ixodid tick species and two tick-borne pathogens in three areas in the Sudan. *Parasitol. Res.* 119, 385–394. doi: 10.1007/s00436-019-06458-9

Socolovschi, C., Mediannikov, O., Raoult, D., and Parola, P. (2009). The relationship between spotted fever group Rickettsiae and ixodid ticks. *Vet. Res.* 40:34. doi: 10.1051/vetres/2009017

Socolovschi, C., Reynaud, P., Raoult, D., and Parola, P. (2011). "Rickettsiae and Borrelia in ticks on migratory birds from the Camargue National Park, France" in *Abstract book of the 6th international meeting on Rickettsiae and Rickettsial diseases* (Heraklion, Crete, Greece)

Song, S., Chen, C., Yang, M., Zhao, S., Wang, B., Hornok, S., et al. (2018). Diversity of *Rickettsia* species in border regions of northwestern China. *Parasit. Vectors* 11, 634–637. doi: 10.1186/s13071-018-3233-6

Springer, A., Shuaib, Y. A., Isaa, M. H., Ezz-Eldin, M. I. E., Osman, A. Y., Yagoub, I. A., et al. (2020). Tick fauna and associated *Rickettsia*, *Theileria*, and *Babesia* spp. in domestic animals in Sudan (North Kordofan and Kassala States). *Microorganisms* 8:1969. doi: 10.3390/microorganisms8121969

Sukhiashvili, R., Zhgenti, E., Khmaladze, E., Burjanadze, I., Imnadze, P., Jiang, J., et al. (2020). Identification and distribution of nine tick-borne spotted fever group Rickettsiae in the country of Georgia. *Ticks Tick-borne Dis.* 11:101470. doi: 10.1016/j.ttbdis.2020.101470

Thompson, J. D., Higgins, D. G., and Gibson, T. J. (1994). CLUSTAL W: improving the sensitivity of progressive multiple sequence alignment through sequence weighting, position-specific gap penalties and weight matrix choice. *Nucleic Acids Res.* 22, 4673–4680. doi: 10.1093/nar/22.22.4673

Tila, H., Khan, M., Almutairi, M. M., Alouffi, A., Ahmed, H., Tanaka, T., et al. (2023). First report on detection of Hepatozoon ayorgbor in *Rhipicephalus haemaphysaloides* and *Hepatozoon colubri* in *Haemaphysalis sulcata* and *Hyalomma anatolicum*: risks of spillover of *Hepatozoon* spp. from wildlife to domestic animals. *Front. Vet. Sci.* 10:1255482. doi: 10.3389/fvets.2023.1255482

Toma, L., Mancini, F., Di Luca, M., Cecere, J. G., Bianchi, R., Khoury, C., et al. (2014). Detection of microbial agents in ticks collected from migratory birds in Central Italy. *Vector-borne Zoonotic Dis.* 14, 199–205. doi: 10.1089/vbz.2013.1458

Tomassone, L., Conte, V., Parrilla, G., and De Meneghi, D. (2010). Rickettsia infection in dogs and *Rickettsia parkeri* in *Amblyomma tigrinum* ticks, Cochabamba department, Bolivia. *Vector-Borne and Zoonotic Diseases* 10, 953–958. doi: 10.1089/vbz.2009.0126

Tomassone, L., De Meneghi, D., Adakal, H., Rodighiero, P., Pressi, G., and Grego, E. (2016). Detection of *Rickettsia aeschlimannii* and *Rickettsia africae* in ixodid ticks from Burkina Faso and Somali Region of Ethiopia by new real-time PCR assays. *Ticks Tick-borne Dis.* 7, 1082–1088. doi: 10.1016/j.ttbdis.2016.09.005

Tomassone, L., Grego, E., Auricchio, D., Iori, A., Giannini, F., and Rambozzi, L. (2013). Lyme borreliosis spirochetes and spotted fever group Rickettsiae in ixodid ticks from Pianosa island, Tuscany archipelago, Italy. *Vector Borne Zoonotic Dis.* 13, 84–91. doi: 10.1089/vbz.2012.1046

Tosoni, A., Mirijello, A., Ciervo, A., Mancini, F., Rezza, G., Damiano, F., et al. (2016). Human *Rickettsia aeschlimannii* infection: first case with acute hepatitis and review. *Eur. Rev. Med. Pharmacol. Sci.* 20, 2630–2633.

Ullah, S., Alouffi, A., Almutairi, M. M., Islam, N., Rehman, G., Ul Islam, Z., et al. (2023). First report of *Rickettsia conorii* in *Hyalomma kumari* ticks. *Animals* 13:1488. doi: 10.3390/ani13091488

Vanegas, A., Keller, C., Krüger, A., Manchang, T. K., Hagen, R. M., Frickmann, H., et al. (2018). Molecular detection of spotted fever group Rickettsiae in ticks from Cameroon. *Ticks Tick Borne Dis.* 9, 1049–1056. doi: 10.1016/j.ttbdis.2018.03.022

Walker, J.B., Keirans, J.E., and Horak, I.G. (2000) *The genus Rhipicephalus (Acari, Ixodidae): a guide to the brown ticks of the world*. Cambridge, NY Cambridge University Press

Koponen, S., and Niemi, R. (2000). Review: Brown ticks of the world. *Entomol. Fennica* 11:124. doi: 10.33338/ef.84056

Wallmenius, K., Barboutis, C., Fransson, T., Jaenson, T. G., Lindgren, P. E., Nyström, F., et al. (2014). Spotted fever *Rickettsia* species in *Hyalomma* and Ixodes ticks infesting migratory birds in the European Mediterranean area. *Parasit. Vectors* 7, 1–20. doi: 10.1186/1756-3305-7-318

Wei, Q. Q., Guo, L. P., Wang, A. D., Mu, L. M., Zhang, K., Chen, C. F., et al. (2015). The first detection of *Rickettsia aeschlimannii* and *Rickettsia massiliae* in *Rhipicephalus turanicus* ticks, in Northwest China. *Parasit. Vectors* 8, 631–634. doi: 10.1186/s13071-015-1242-2

Yessinou, R. E., Cazan, C. D., Panait, L. C., Mollong, E., Biguezoton, A. S., Bonnet, S. I., et al. (2023). New geographical records for tick-borne pathogens in ticks collected from cattle in Benin and Togo. *Vet. Med. Sci.* 9, 345–352. doi: 10.1002/vms3.1022

Znazen, A., Rolain, J. M., Hammami, N., Hammami, A., Ben Jemaa, M., and Raoult, D. (2006). *Rickettsia felis* infection, Tunisia. *Emerg. Infect. Dis.* 12, 138–140. doi: 10.3201/eid1201.050876

frontiers | Frontiers in Microbiology

TYPE Original Research
PUBLISHED 05 January 2024
DOI 10.3389/fmicb.2023.1329772

Check for updates

OPEN ACCESS

EDITED BY
Lei Deng,
Harvard Medical School, United States

REVIEWED BY
Ziyao Zhou,
Sichuan Agricultural University, China
Silvia Di Lodovico,
"G. d'Annunzio" University of Chieti, Italy

*CORRESPONDENCE
Yipeng Jin
✉ yipengjin@cau.edu.cn
Jiahao Lin
✉ jiahao_lin@cau.edu.cn

RECEIVED 30 October 2023
ACCEPTED 07 December 2023
PUBLISHED 05 January 2024

CITATION
Song P, Hao Y, Lin D, Jin Y and Lin J (2024) Evaluation of the antibacterial effect of Epigallocatechin gallate on the major pathogens of canine periodontal disease and therapeutic effects on periodontal disease mice.
Front. Microbiol. 14:1329772.
doi: 10.3389/fmicb.2023.1329772

COPYRIGHT
© 2024 Song, Hao, Lin, Jin and Lin. This is an open-access article distributed under the terms of the Creative Commons Attribution License (CC BY). The use, distribution or reproduction in other forums is permitted, provided the original author(s) and the copyright owner(s) are credited and that the original publication in this journal is cited, in accordance with accepted academic practice. No use, distribution or reproduction is permitted which does not comply with these terms.

Evaluation of the antibacterial effect of Epigallocatechin gallate on the major pathogens of canine periodontal disease and therapeutic effects on periodontal disease mice

Peijia Song[1,2], Yibing Hao[3], Degui Lin[1], Yipeng Jin[1]* and Jiahao Lin[1,2]*

[1]Country National Key Laboratory of Veterinary Public Health and Safety, College of Veterinary Medicine, China Agricultural University, Beijing, China, [2]China Veterinary Medicine Innovation Center, China Agricultural University, Beijing, China, [3]China Agricultural University Veterinary Teaching Hospital, Beijing, China

Background: Periodontal disease (PD) is a prevalent oral affliction in canines, with limited therapeutic options available. The potential transmission of oral bacteria from canines to humans through inter-species contact poses a risk of zoonotic infection. Epigallocatechin gallate (EGCG), the principal catechin in green tea polyphenols, exhibits antibacterial properties effective against human PD. Given the clinical parallels between canine and human PD, this study explores the feasibility of employing EGCG as a therapeutic agent for canine PD.

Methods and results: Initially, a survey and statistical analysis of bacterial infection data related to canine PD in China were conducted. Subsequently, the primary pathogenic bacteria of canine PD were isolated and cultivated, and the *in vitro* antibacterial efficacy of EGCG was assessed. Furthermore, verify the therapeutic effect of EGCG on a mouse PD model *in vivo*. The high-throughput 16S rRNA gene sequencing identified *Porphyromonas, Fusobacterium, Treponema, Moraxella,* and *Capnocytophaga* as the genera that distinguishing PD from healthy canines' gingival crevicular fluid (GCF) samples in China. The anaerobic culture and drug susceptibility testing isolated a total of 92 clinical strains, representing 22 species, from 72 canine GCF samples, including *Porphyromonas gulae*, *Prevotella intermedia*, *Porphyromonas macacae*, etc. The minimum inhibitory concentration (MIC) ranging of EGCG was from 0.019 to 1.25 mg/mL. Following a 7 days oral mucosal administration of medium-dose EGCG (0.625 mg/mL), the abundance of periodontal microorganisms in PD mice significantly decreased. This intervention ameliorated alveolar bone loss, reducing the average cementoenamel junction to the alveolar bone crest (CEJ-ABC) distance from 0.306 mm ± 0.050 mm to 0.161 mm ± 0.026 mm. Additionally, EGCG (0.3125 mg/mL) markedly down-regulated the expression of inflammatory factor IL-6 in the serum of PD mice.

Conclusion: Our research demonstrates the significant antibacterial effects of EGCG against the prevalent bacterium *P. gulae* in canine PD. Moreover, EGCG exhibits anti-inflammatory properties and proves effective in addressing bone loss in a PD mouse model. These findings collectively

suggest the therapeutic potential of EGCG in the treatment of canine PD. The outcomes of this study contribute valuable data, laying the foundation for further exploration and screening of alternative antibiotic drugs to advance the management of canine PD.

KEYWORDS

canine PD, anaerobic bacteria, antibacterial treatment, EGCG, alveolar bone loss

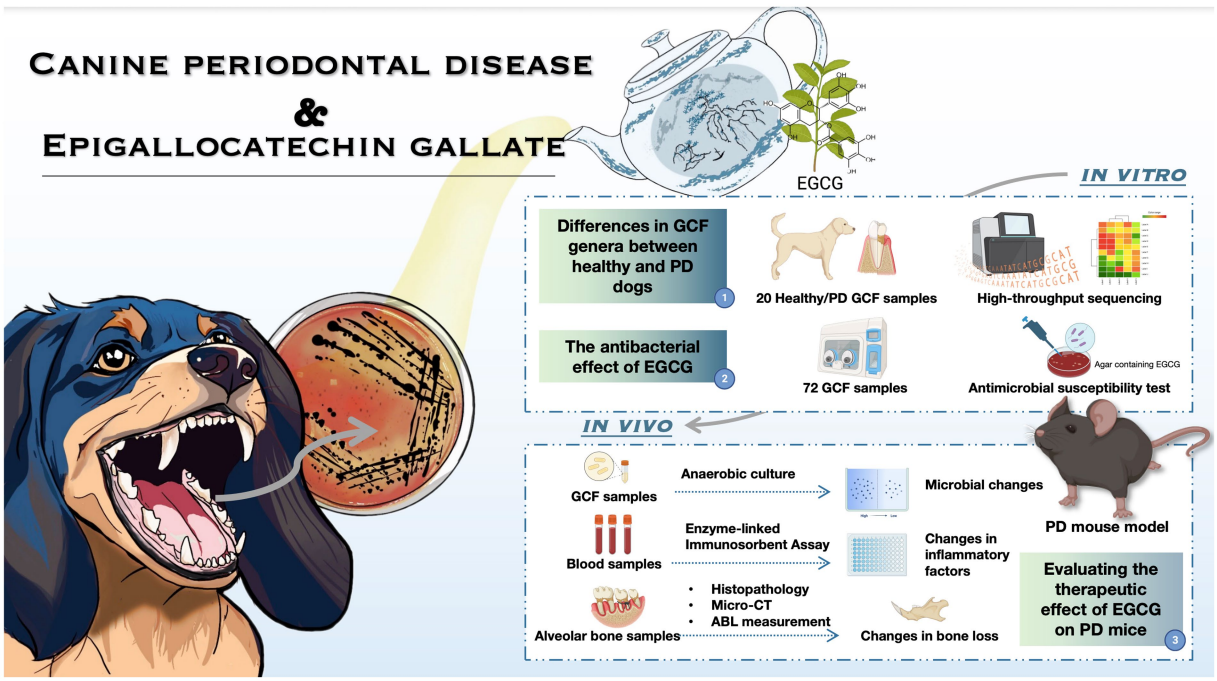

GRAPHICAL ABSTRACT

1 Introduction

Periodontal disease (PD) is a prevalent, age-related oral disease in canines caused by infectious, inflammatory processes (Kortegaard et al., 2008). While gingivitis is a treatable condition marked by red and inflamed gums, PD involves inflammation of the tissues supporting the tooth, leading to attachment loss through the destruction of the periodontal ligament, cementum, and alveolar bone. In canines, a notable tendency to neglect daily oral hygiene practices contributes to a substantial incidence of PD, affecting approximately 80% of adult canines (Lobprise, 2018; Wallis et al., 2021). This disease can persist, recur, cause discomfort, impede normal canine activities, and diminish overall well-being, with potential correlations to systemic health issues in canines, highlighting the need for effective management.

Comparing human PD with canine PD offers valuable insights due to similarities in clinical presentations. Canine PD, especially its natural-onset form, serves as a relevant animal model for studying human PD (Mangione et al., 2022; Choi et al., 2023). Despite these parallels, the pathogens differ, with *Porphyromonas gingivalis* being the primary pathogen in human PD and *Porphyromonas gulae* in canine PD. But there are similarities in the bacterial structure (Hamada et al., 2008). Because of the close relationship between dogs and humans, it has been demonstrated that canine *P. gulae* may be transferred to the human oral cavity through close contact (Yamasaki et al., 2012; Bai et al., 2023) and may be hazardous (Inaba et al., 2019, 2020; Urmi et al., 2021; Shimizu et al., 2022). This proves that the prevention and control of periodontal disease and the suppression of the spread of the pathogen are of public health and safety significance. However, there are also differences in the oral microbiota of humans and dogs (Dewhirst et al., 2012; Cunha et al., 2018), so we need to study the pathogenic microbiota of canine PD in more depth. Dental plaque microbes play a crucial role in PD development (Abdulkareem et al., 2023). In the Chinese research landscape, dominant bacterial genera in canines with PD are not extensively documented, and geographical variations in bacterial microbiota associated with PD suggest the need for a deeper understanding within the Chinese context (Nath et al., 2022).

The potential risk of transferring antibiotic-resistant bacteria from dogs to humans underscores the need for careful consideration in

selecting therapeutic agents for canine PD (Šakarnytė et al., 2023). This aligns with the global issue of antibiotic resistance, emphasizing the importance of finding alternative treatment options. Epigallocatechin gallate (EGCG), a key component of green tea polyphenols' catechins, exhibits antibacterial, antioxidant, anti-inflammatory, and anti-tumor effects (Asahi et al., 2014; Chakrawarti et al., 2016). Various catechin components of tea polyphenols have demonstrated efficacy in human PD treatment (Sitheeque et al., 2009; Cui et al., 2012). Given analogous clinical manifestations of PD in canines and humans, the hypothesis that EGCG could serve as a viable alternative to antibiotics is reasonable, addressing the potential risk of antibiotic resistance transfer and exploring a natural compound for managing PD in canines.

Building upon our laboratory's established research foundation (Bai et al., 2023), our current study aims to collect canine gingival crevicular fluid (GCF) samples for comprehensive microbiota characterization in Beijing using high-throughput 16S rRNA gene sequencing. Subsequent steps involve isolating dominant bacteria from the oral cavities of canines affected by PD and exploring EGCG's inhibitory potential on these bacteria through *in vitro* antimicrobial sensitivity tests. We plan to construct a PD mice model to evaluate the *in vivo* therapeutic effects of EGCG, assessing alveolar bone loss (ABL), alterations in inflammatory factor expression, and shifts in bacterial microbiota. Our study aimed to assess whether EGCG could serve as a preliminary treatment to potentially become an effective drug in treating canine PD, upon identification of the primary pathogens of canine PD in China.

2 Materials and methods

2.1 Sample collection

Gingival crevicular fluid (GCF) samples were procured using dental absorbent paper points (0.04 taper, GAPADENT, China) from a cohort of 96 canines, with or without PD, attending the China Agricultural University Veterinary Teaching Hospital from December 2020 to February 2022. Among these, 24 samples (ranging from 8 months to 15 years of age) were utilized for the acquisition of bacterial genera exhibiting high abundance in canine GCF through high-throughput 16S rRNA gene sequencing. The remaining 72 samples were dedicated to bacterial culture. Importantly, none of the canines had undergone antibiotic treatment or exhibited systemic chronic diseases in the 3 months preceding the sampling period.

2.2 High-throughput sequencing

GCF samples were gathered, and DNA extraction was performed utilizing a nucleic acid extraction kit (Fast DNA Stool KitM, The Beijing Genomics Institute, China). The resulting DNA samples underwent a nucleic acid concentration assay using the Equalbit 1 × dsDNA HS Assay Kit (Vazyme, Nanjing, China), and the nucleic acid concentration and quality were determined using a Qubit fluorometer (Thermo Fisher Scientific, United States) with the dsDNA high sensitivity assay program. Samples exhibiting superior DNA concentration and quality were prioritized for subsequent Illumina MiSeq sequencing. The ensuing data underwent both statistical and biological analyses using Quantitative Insights into Microbial Ecology (QIIME, V 1.9.1), yielding operational taxonomic unit (OTU) analysis results.

2.3 Strains and culture conditions

The collected GCF samples were vortex shaken and isolated using disposable loops (Biologix, Shandong, China) on 10% brain-heart infusion (BHI) sheep blood plates (Solarbio, Beijing, China) containing 5 μg/mL hemoglobin chloride, 1 μg/mL vitamin K1 (VK1), 0.4 mg/mL L-cysteine hydrochloride and 5 mg/mL yeast extract (Solarbio, Beijing, China). The incubation took place at 37°C with 80% humidity under anaerobic conditions (10% CO2, 10% H2, and 80% N2) within an anaerobic culture vessel (YY-s Plus, LongFuJia Biotechnology, Beijing, China) for a culture period of 7–15 days. Single colonies were meticulously chosen and subjected to purification once more. The resulting single colonies were inoculated with a 5% fetal bovine serum (FBS) BHI liquid medium containing hemoglobin chloride and VK1 to be enriched and stored at −80°C. American Type Culture Collection (ATCC) 51700 *P. gulae* was purchased as a quality control bacterium.

2.4 16S rRNA sequencing

Polymerase chain reaction (PCR) was performed using KOD-one Mix (25 μL, TOYOBO, Japan) with bacterial universal primers 27F and 1492R. Following agarose gel electrophoresis, the band size and uniqueness of the PCR products were determined, and the PCR products were sent to GENEWIZ[1] for sequencing based on the Sanger sequencing method. The obtained sequences were compared with those available from the GenBank database using the Ape program on The Basic Local Alignment Search Tool (BLAST).[2] The results of the comparison with known sequences of strains with >99% similarity were considered as the same bacteria, and the results were accurate to the species level.

2.5 Antimicrobial susceptibility testing *In vitro*

Referring to the 9th edition of the standard Methods for Antimicrobial Susceptibility Test of Anaerobic Bacteria published by the Clinical & Laboratory Standards Institute (CLSI) in 2018, drug susceptibility tests were performed according to the procedures of the test for anaerobic bacteria, and the minimum inhibitory concentration (MIC) for EGCG was determined for the clinically dominant isolate and ATCC 51700 standard bacteria in canine GCF samples. EGCG with purity (HPLC) ≥98% were purchased from Sigma (USA). A stock solution of 12.5 mg/mL was prepared by adding 50 mg of EGCG powder to 4 mL of ultrapure water. The drug concentrations in the EGCG-containing drug-sensitive plates were 1.250 mg/mL, 0.625 mg/mL, 0.312 mg/mL, 0.156 mg/mL, and 0.078 mg/mL from highest to lowest.

1 https://www.genewiz.com.cn

2 https://blast.ncbi.nlm.nih.gov/Blast.cgi

2.6 PD model construction

The research was conducted by internationally accepted principles for laboratory animal use and care. All animal studies were reviewed and approved by the China Agricultural University Laboratory Animal Welfare and Animal Experimental Ethical Committee (Approval ID: AW31103202-2-4). Thirty-three male C57BL/6 mice (Beijing Vital River Laboratory Animal Technology Co., Ltd.), 7–8 weeks old were prepared. The mice were anesthetized by intraperitoneal injection of 10% chloral hydrate (Wabcan, Fujian, China), and the PD model was established by ligating the maxillary second molars using the silk ligature method (Rafael et al., 2018; Chipashvili and Bor, 2022). Group A: saline negative control group, group B: chlorhexidine (Maidihai, Beijing, China) positive control group, group C: low-dose EGCG (0.312 mg/mL) dosing group, group D: medium-dose EGCG (0.625 mg/mL) dosing group, and group E: high-dose EGCG (1.250 mg/mL) dosing group. On the eighth day after modeling, sterile cotton swabs soaked with the drug were inserted into the mouths of the mice and held for 2 min for oral mucosal administration. After 7 days of continuous administration mice were sacrificed and whole blood and bilateral maxillae were collected for subsequent testing.

2.7 Evaluation of ABL

Unilateral mouse maxillary bone specimens were soaked and rinsed in hydrogen peroxide and saline (Solarbio, Beijing, China), and the soft tissues attached to the bone tissue were removed as much as possible under a dissecting microscope (Olympus GX71, Japan). The specimens were stained with 0.1% methylene blue (Solarbio, Beijing, China) for 45 s and dried. Unilaterally isolated mouse maxillary specimens were photographed under a dissecting microscope. The distance from the cementum-enamel junction to the alveolar bone crest (CEJ-ABC) was measured using ImageJ software (V 1.47), and measurements were repeated three times at each site.

2.8 Microbial evolution in the oral cavity of PD mice

Two filaments filled with GCF for modeling were carefully cut from both sides of the maxillary second molars of mice and placed in 1 mL of BHI liquid medium and vortex shocked. The quantitative liquid was aspirated for anaerobic incubation and colony counting, and individual clones with similar colony morphology and staining characteristics were selected for strain identification.

2.9 Morphometric of micro-CT analysis and dental X-ray examination

X-ray micro-computed tomography (Skyscan 1,276, Bruker, Belgium) was used. The mouse maxilla was scanned at a voltage of 60 kV and a current of 200 μA with a scan resolution of 6.5 μm. As the filament was placed on the second molar, the region of interest (ROI) for 3D reconstruction was defined as the area above the root tip below the crown of the second molar, with a volume of 0.5 mm × 0.25 mm × 0.4 mm. Three-dimensional image reconstruction was performed using N-Recon software (V 1.7.4.6). Three-dimensional analysis was performed using CT-AN software (V 1.19.11.1+).

2.10 Enzyme-linked immunosorbent assay

Mouse whole blood samples were stored at 4°C overnight, centrifuged at 1000 x g for 20 min, and the supernatant removed to obtain serum samples. The supernatants were then collected and the concentrations of interleukin (IL)-6 and tumor necrosis factor (TNF)-α were determined using enzyme-linked immunosorbent assay (ELISA) kits (Mlbio, Shanghai, China) according to the manufacturer's protocols. The 96-well plate was read at 450 nm on an enzyme marker for result interpretation (Thermo Scientific, Multiskan Go, United States). All assays were performed in triplicate.

2.11 Histological analysis for alveolar bone

The unilateral mouse maxilla was dissected free of soft tissues, immersed in 4% paraformaldehyde fixative (Solarbio, Beijing, China), and fixed at room temperature for 48 h. After decalcification with 10% ethylene diamine tetraacetic acid (EDTA) (Solarbio, Beijing, China) at pH 7.4 for 14 days, the tissues were dehydrated, transparentized, embedded, sectioned, dewaxed, stained with hematoxylin–eosin (HE) and sealed with neutral gum. The samples were ready for microscopic examination and photography.

2.12 Statistical analysis

Data were analyzed and measurements were expressed as mean ± standard deviation (SD). Significant differences were determined by *T*-test between two groups and one-way analysis of variance (ANOVA) for more than two groups in Prism (GraphPad Software, V 9.0, United States). $p < 0.01$ was considered significant for differences.

3 Results

3.1 The bacterial composition of GCF samples from canines based on 16S rRNA high-throughput sequencing

GCF samples were collected from 24 canines. A total of 24 samples of GCF were initially tested for this study and 19 samples were ultimately suitable for the machine based on quality control. It was found that among the 19 samples, operational taxonomic unit (OTU) 1 (*Fusobacterium*), OTU2 (*Porphyromonas*), and OTU15 (*Treponema*) exhibited higher abundances, with OTU2 (*Porphyromonas*) being the darkest in the plot and showing the highest relative abundance. The relative abundance of *Moraxella* spp., *Clostridium phagocytophilum, Neisseria* spp., *and Pseudomonas* spp. in the GCF of group A (healthy canines) was observed to be higher and the relative abundance of *Porphyromonas* spp., *Dictyostelium* spp., *Fretibacterium* spp., *Mycobacterium* spp., and *Archaea* spp. in the GCF of group B (PD canines) was higher (Figure 1).

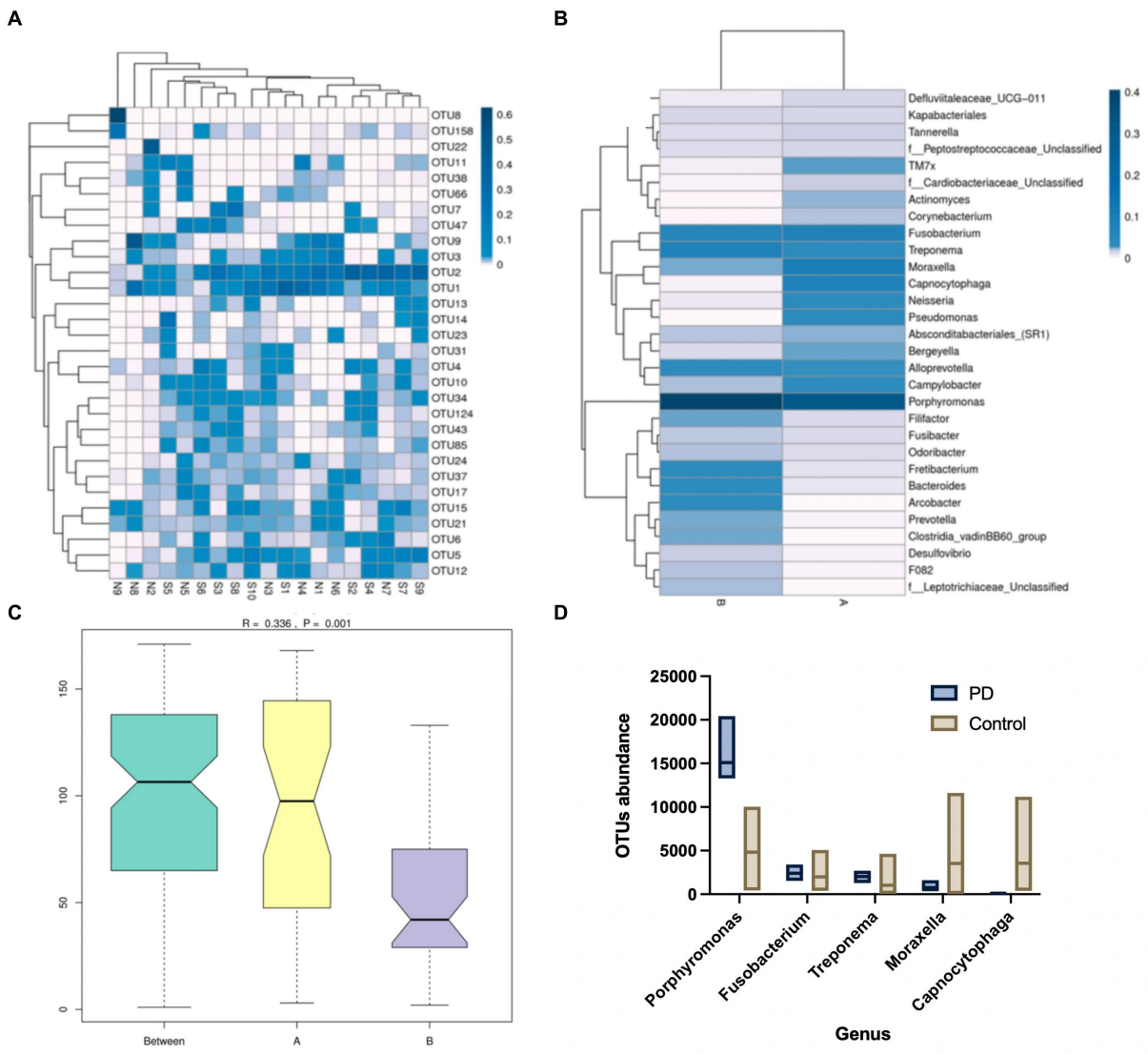

FIGURE 1
(A) Operational taxonomic units (OTU) enrichment clustering heat map. The 30 OTUs with the highest abundance in the sample sequencing results were plotted in R. The corresponding OTU abundance of the 19 samples of gingival crevicular fluid (GCF) were collected. **(B)** Species relative abundance graphs. The samples were grouped accordingly, and the abundance of genera was compared between the two groups. **(C)** Analysis of similarities (Anosim). The size of the between-group and within-group differences were compared between the two sample groups by Anosim analysis. **(D)** Metastatic difference analysis. A comparison of the abundance of the five genera between the two groups of samples has been shown.

3.2 Clinically isolated strains of PD canines

GCF samples from 72 canines with PD were collected for anaerobic culture between December 2020 and February 2022, and a total of 22 species and 92 strains of anaerobic bacteria were isolated and purified. Included *P. gulae, Prevotella intermedia, Porphyromonas crevioricanis, Porphyromonas macacae,* and other bacteria from the oral cavity of canines (Figures 2A,B). As the most academically suspected causative agent of canine PD, the detection rate of *P. gulae* was 31.52% (29/92) (Table 1). A total of 110 h of absorbance values were measured of ATCC 51700 *P. gulae* in modified BHI liquid medium, entering the logarithmic growth phase after 12 h, the stationary phase after 24 h, and the death phase after 72 h (Figure 2C). The bacterium entered the logarithmic phase (12 h) with an optical density (OD) of 0.41 and the end of the logarithmic phase (24 h) with an OD of 0.11.

3.3 Inhibitory effect of EGCG on the growth of clinical isolate strains

An inhibition test using the Wadsworth method *in vitro* on clinical anaerobic isolates from PD canines showed that EGCG was effective against the major human and canine periodontal pathogen, *Porphyromonas gingivalis W83*, and *P. gulae* ATCC 51700 with MICs of 0.078 mg/mL and 0.019 mg/mL (Figure 3). EGCG was also effective against other canine PD isolates. However, 0.05% chlorhexidine, commonly used in veterinary clinical scaling and extraction procedures, showed poor inhibition against some clinical isolates

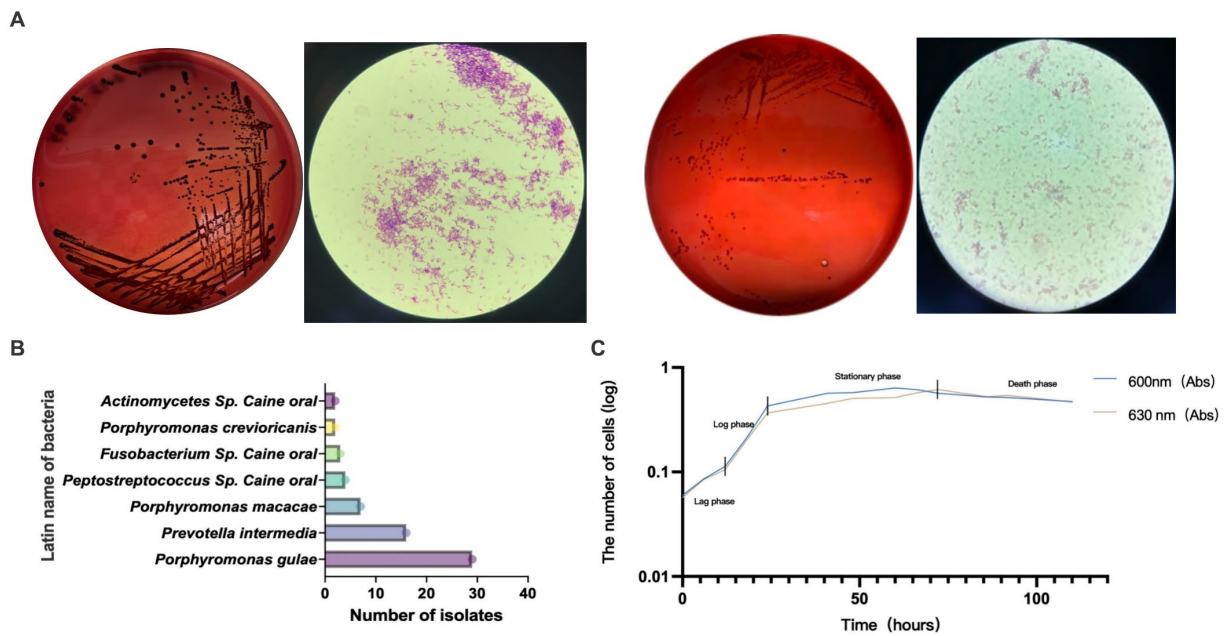

FIGURE 2
(A) Isolated and purified melanin-producing bacteria from the oral cavity of canines with periodontal disease (PD). The modified brain-heart infusion (BHI) plates were incubated anaerobically, then cells were Gram-stained and examined by microscopy (100 X magnification). **(B)** Abundance of various bacteria detected in clinical isolates from the GCF of canines with PD. **(C)** The growth curve of *Porphyromonas gulae* (*P. gulae*) standard bacteria ATCC 51700.

TABLE 1 Isolation and purification of melanin-producing bacteria from the oral cavity of canines with PD.

Species	Number (N = 92)	Detection rates (%)
Porphyromonas gulae	29	31.52
Prevotella intermedia	16	17.39
Porphyromonas macacae	7	0.07
Peptostreptococcus spp. Caine oral	4	0.04
Fusobacterium spp. Caine oral	3	0.03
Porphyromonas crevioricanis	2	0.02
Actinomycetes spp. Caine oral	2	0.02

(*SY10B Porphyromonas crevioricanis, 6 L32 uncultured bacterial clone*) (Table 2).

3.4 Inhibitory effects of EGCG on the alveolar bone resorption and destruction *in vivo*

The animal protocol to assess the therapeutic effect of EGCG on PD *in vivo* involved model establishment on the first day, body weight testing from the second to sixth days, administration initiation on the seventh day, and mouse euthanasia on the fourteenth day. Took GCF samples and maxillary alveolar bone samples from the mice for subsequent tests (Figure 4A). There was no significant change in the body weight of mice before and after administration (Figure 4B). The procedure in the PD mouse model included exposure to the surgical field, expansion of the periodontal space, wire ligation around the maxillary second molar, and repetition of the procedure on the opposite side (Figure 4C). The first row was the isolated tissue of normal mouse maxillary molars, and the second row was the three-dimensional tissue of mouse maxillary molars used to construct a PD model.

The bone volume (BV) in the selected area of the control mice was 0.03333 mm^3 and the bone mineral density (BMD) was 0.58952 g/cm^3. The bone volume (BV) in the selected area of the PD mice was 0.00961 mm^3 and the BMD was 0.18359 g/cm^3 (Figures 4D,E).

The mean CEJ-ABC of three molars in the chlorhexidine group was 0.372 mm ± 0.033 mm, the mean CEJ-ABC of three molars in the EGCG group for three concentrations were 0.317 mm ± 0.044 mm, 0.161 mm ± 0.026 mm, and 0. 238 mm ± 0.035 mm in order. The mean CEJ-ABC of the three molars in the saline group was 0.306 mm ± 0.050 mm. There was no significant difference in the CEJ-ABC distance between the saline and chlorhexidine groups (p-value = 0.68), and there was also a significant difference in the CEJ-ABC distance between the EGCG and chlorhexidine groups in the mid-dose group (p-value = 0.0001). The mid-dose EGCG group was the most effective in improving bone loss and was superior to the chlorhexidine group, an antibacterial rinse commonly used in clinical dentistry (Figure 5A).

The maxillary alveolar bone of the mice was sectioned, cleaned of periodontal soft tissue, and then stained with 0.1% methylene blue to visualize the ABL. Following the treatment of mice with different periodontal drugs, the effect of the drugs on the ABL was observed using a stereomicroscope. As shown in Figure 6, the morphology of the alveolar bone was found to be intact in the control group, whereas the saline group showed the exposure of the buccal root bifurcation of the second molar and a cup-shaped depression of the resorption

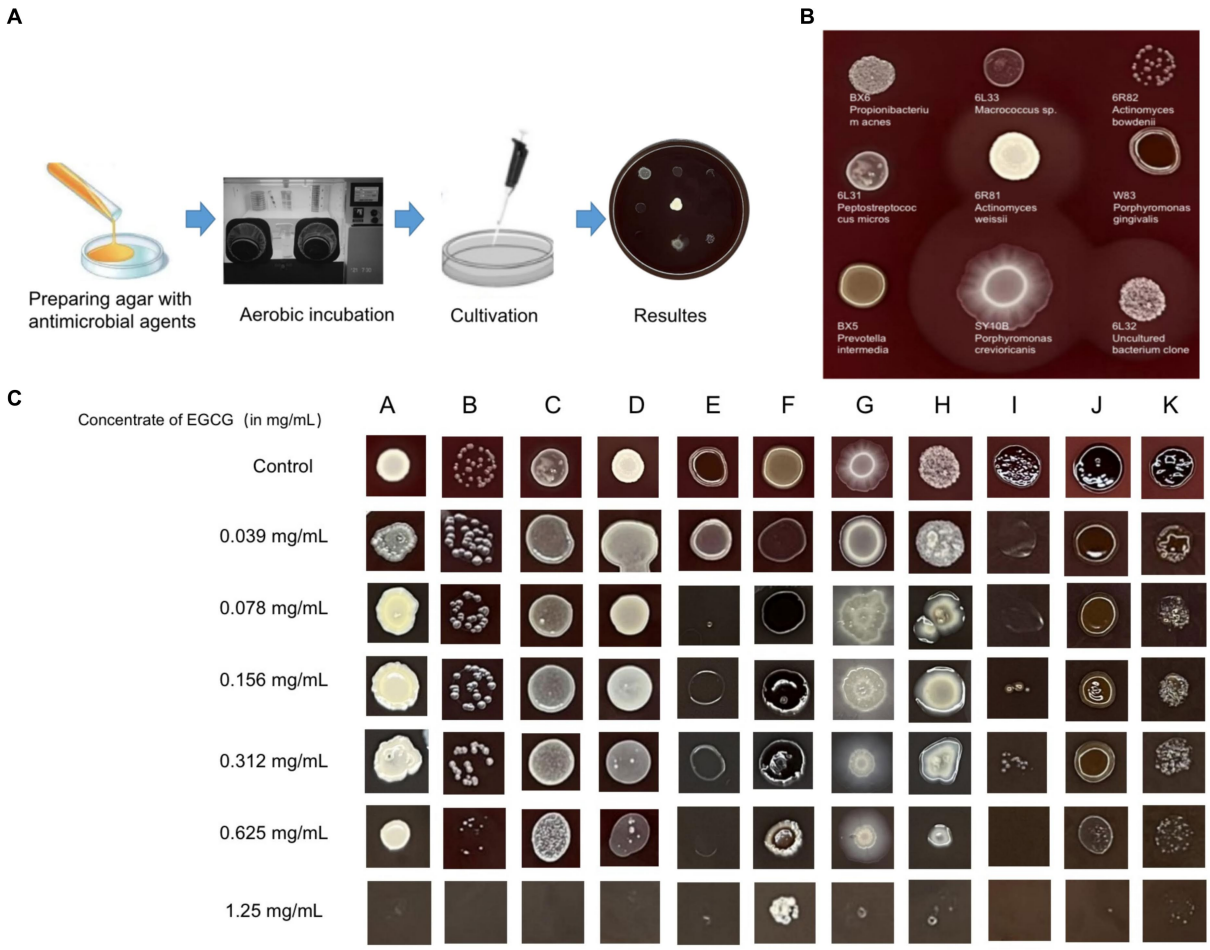

FIGURE 3
(A) Drug sensitivity test used agar dilution method (Wadsworth method) *in vitro*. The drug-containing agar plates were prepared after anaerobic pretreatment. **(B)** For the drug-free control plates, both clinical isolates and standard strains were able to grow well on the enriched Brucella medium. **(C)** Results of the *in vitro* inhibition test for anaerobic bacteria used the Wadsworth method. The lowest drug concentration at which the bacterium was strongly reduced was the minimum inhibitory concentration (MIC) for the bacterium. The graph showed the *in vitro* drug susceptibility results of 11 canine PD-associated strains to EGCG. A: BX6 *Propionibacterium acnes*, B: 6R82 *Actinomyces bowdenii*, C: 6 L31 *Peptostreptococcus micros*, D: 6R81 *Actinomyces weissii*, E: W83 *Porphyromonas gingivalis*, F: BX5 *Prevotella intermedia*, G: SY10B *Porphyromonas crevioricanis*, H: Y1 Uncultured bacterium clone, I: ATCC 51700 *Porphyromonas gulae*, J: SB41 *Prevotella intermedia*, K: SB40 *Porphyromonas gulae*.

surface of the bone centered on the second molar. In the chlorhexidine group, there was severe horizontal ABL in the maxillary molars, with root resorption in the third molar reaching the apical 1/2 area. The effect on ABL varied less between samples for the low, medium, and high EGCG dose groups in the second row (Figure 5B).

3.5 Inhibitory effects of EGCG on periodontal inflammatory cytokines and changes in bacterial microbiota *in vivo*

The average number of microorganisms detected in the oral cavity of the mice was 2.6×10^5 CFU/mL, predominantly comprising *Streptococcus dani*, a gram-positive coccus (Figure 6A). In contrast, the average number of microorganisms detected in the oral cavity of the mice without treatment was 3.64×10^6 CFU/mL, mainly *Escherichia coli* and *Enterococcus faecalis*, with a higher proportion of Gram-negative bacteria. After EGCG treatment, the average number of microorganisms detected was 3.61×10^6 CFU/mL, mainly *E. coli, Staphylococcus aureus, Enterococcus faecalis,* and *Streptococcus aureus*, mainly gram-positive coccus. In the high-dose EGCG group, the average number of microorganisms detected was 3.93×10^6 CFU/mL, mainly *E. coli, E. faecalis,* and *Staphylococcus aureus*, mainly gram-positive cocci. These findings indicate that the medium dose of EGCG has a substantial inhibitory effect on oral bacteria in PD mice. Additionally, the microbial community in the oral cavity of mice gradually shifted towards that of healthy mice after EGCG administration (Figure 6A).

Seven days after modeling, mice were grouped for drug treatment. Figure 6B illustrates that both 0.05% chlorhexidine (50 mg/mL) and three different concentrations of EGCG led to a down-regulation of the expression of the inflammatory factors IL-6 and TNF-α in the serum of periodontopathic mice compared to the saline control group. However, only the low-dose EGCG group (0.3125 mg/mL) exhibited a significant difference in the expression of IL-6 compared to the control group (p-value < 0.05), with no significant differences observed between the other groups.

TABLE 2 Inhibition of 17 clinical isolates of canine periodontal disease and 2 standard strains of bacteria by 6 drugs *in vitro*.

Clinical strains of PD canines	EGCG (mg/mL)	CD (mg/mL)	MDZ (μg/mL)	CC (μg/mL)	MER (μg/mL)	AC (μg/mL)
BX6 *Propionibacterium acnes*	1.25	12.5	R	R	0.8	1.28
6 L33 *Macrococcus* spp.	1.25	6.25	R	12.8	0.8	0.64
6R82 *Actinomyces bowdenii*	0.5	3.125	R	3.2	0.8	0.16
6 L31 *Peptostreptococcus micros*	1.25	6.25	R	3.2	0.8	0.16
6R81 *Actinomyces weissii*	1.25	50	R	3.2	0.8	R
BX5 *Prevotella intermedia*	1	12.5	1.6	3.2	0.8	2.56
SY10B *Porphyromonas crevioricanis*	1.25	R	R	3.2	0.8	R
6 L32 Uncultured bacterium clone	1.25	R	R	R	0.8	0.16
W83 *Porphyromonas gingivalis*	0.078	1.56	1.6	6.4	0.8	0.16
Y1 *Fusobacterium* spp. canine oral taxon	1.25	1.56	R	25.6	1.6	R
SY10B *Porphyromonas crevioricanis*	1.25	1.56	1.6	R	0.8	R
6MN *Propionibacterium acnes*	1.25	12.5	1.6	R	6.4	R
SB45 *Prevotella intermedia*	1.25	3.125	R	25.6	1.6	0.16
SB46 *Prevotella intermedia*	1.25	3.125	R	1.6	0.8	0.64
ATCC 51700 *Porphyromona gulae*	0.019	1.56	1.6	1.6	0.8	0.16
SB40 *Porphyromonas gulae*	0.625	6.25	1.6	1.6	0.8	0.16
SB41 *Prevotella intermedia*	0.0625	12.5	1.6	1.6	0.8	0.16
SB42 *Porphyromonas gulae*	0.019	3.125	1.6	1.6	0.8	0.16
SB43 *Prevotella intermedia*	1.25	12.5	1.6	1.6	0.8	0.16

Chlorhexidine, CD; Metronidazole, MDZ; Clindamycin, CC; Meropenem, MER; Amoxicillin and Clavulanate Potassium, AC.

3.6 Histological analysis for periodontal tissues

The histological analysis of periodontal tissues in healthy mice (Figures 7A,B) revealed intact gingival structures with a slight infiltration of inflammatory cells under the junctional epithelium (JE). This phenomenon is commonly observed clinically around perfectly healthy teeth, representing the body's defense against the invasion of pathogenic bacteria into the GCF. The gingiva was composed of epithelium and connective tissue, and in the figure, the circumferential fibers (*CF*) and gingival fibers were both composed of collagen type 1. *CF* was present in the connective tissue of the free gingiva and gingival papillae, forming a ring around the cervical part of the tooth. In contrast, PD mice (Figures 7C,D) exhibited osteoblasts and multinucleated giant cells differentiated within the marrow cavity. These cellular components led to a progressive thinning of the bone trabeculae that composed the alveolar bone, accompanied by an increase in the size of the marrow cavity, ultimately resulting in bone loss. The presence of multinucleated giant cells indicated the occurrence of chronic inflammation.

4 Discussion

EGCG has been reported to exert anti-inflammatory and antibacterial effects in periodontitis. However, its exact mechanism of action has yet to be determined. Some evidence suggests that EGCG in hPDLFs and hPDLSCs may exert anti-inflammatory effects against *P. gingivalis* lipopolysaccharide, a major pathogen of human periodontitis (Jung et al., 2012). Several studies have demonstrated that EGCG inhibits bone resorption induced by lipopolysaccharides (LPS) by either inhibiting the production of IL-1β or directly impeding osteoclastogenesis (Yun et al., 2004, 2007). Additionally, it has been discovered that EGCG can reduce periapical lesions by inhibiting the expression of cysteine-rich 61 in osteoblasts (Lee et al., 2009). In the field of human dentistry, EGCG has been shown to enhance host conditions in periodontitis and periapical lesions. Such effects stem from EGCG's bactericidal impact on periodontal pathogens, as well as its inhibitory effect on the cytokine production and inflammatory pathways of gingival fibroblasts or osteoblasts (Okagu et al., 2022; Kováč et al., 2023).

On the suitability of the drug EGCG, it exhibits antioxidant properties by minimizing oxygen radicals and stabilizing compounds (Minnelli et al., 2020). Furthermore, its antitumor effects have been highlighted, elucidating how EGCG inhibits tumor cell growth and induces apoptosis through various cellular pathways, such as regulating the cell cycle, gene expression, signal transduction, and transcription factors (Chen et al., 2019). The role of Nrf2 in regulating detoxifying and antioxidant enzymes, and EGCG's impact on the Nrf2-ARE signal for inducing antioxidant enzyme expression, leading to an anti-toxic effect, has been emphasized (Na and Surh, 2008). Additionally, EGCG's antiviral activity, particularly its ability to inhibit the proliferation of the influenza virus in Madin-Darby canine kidney (MDCK) cells, has been underscored (Zhang et al., 2020). However, its relatively underexplored potential in the treatment of canine periodontal disease (PD). Since EGCG has been less studied in this aspect of canine PD, in

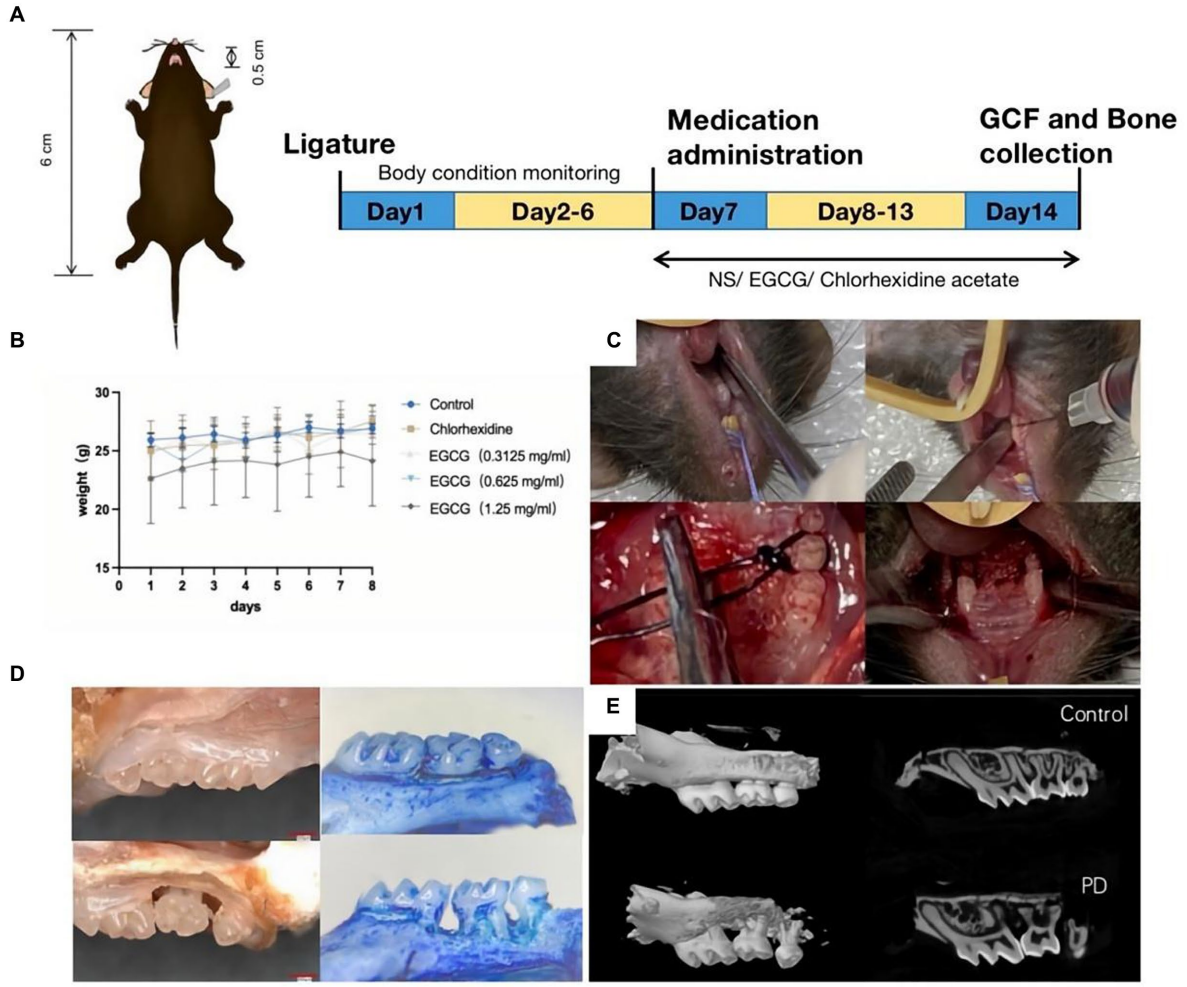

FIGURE 4
(A) Procedure for constructing a PD model in C57BL/6 mice. **(B)** The curve of body weight change curve of the mice after modeling and drug administration. **(C)** Steps of PD modeling by wire ligation. **(D)** Observation of isolated alveolar bone specimens (20X) before and after modeling using a stereomicroscope. **(E)** Observation of alveolar bone loss (ABL) and measurement of bone density using micro-CT.

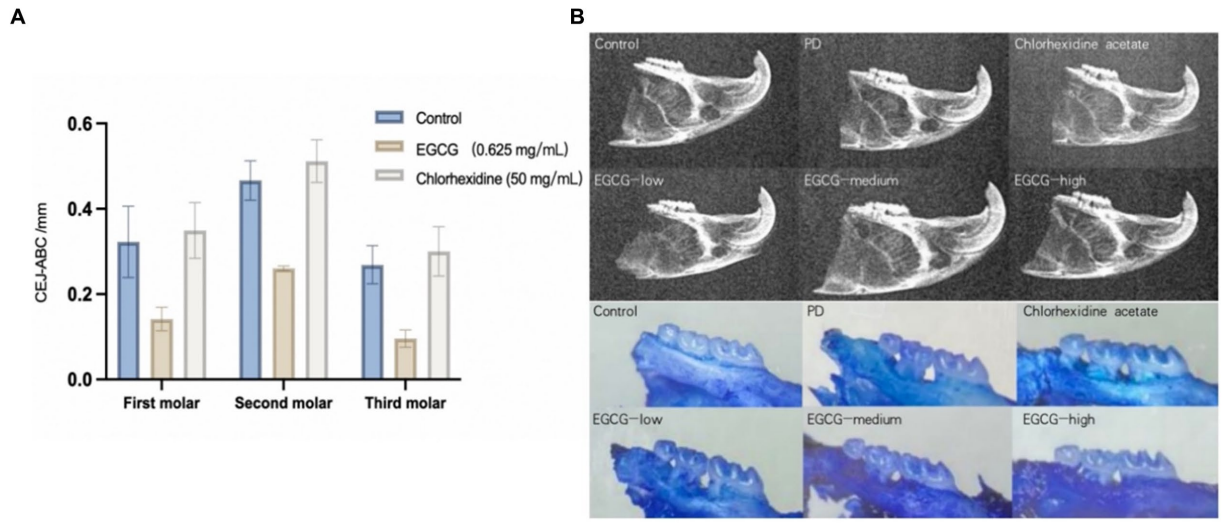

FIGURE 5
(A) Comparison of bone loss distances in PD mice after administration. **(B)** Observation of isolated alveolar bone samples by X-ray versus stereomicroscope.

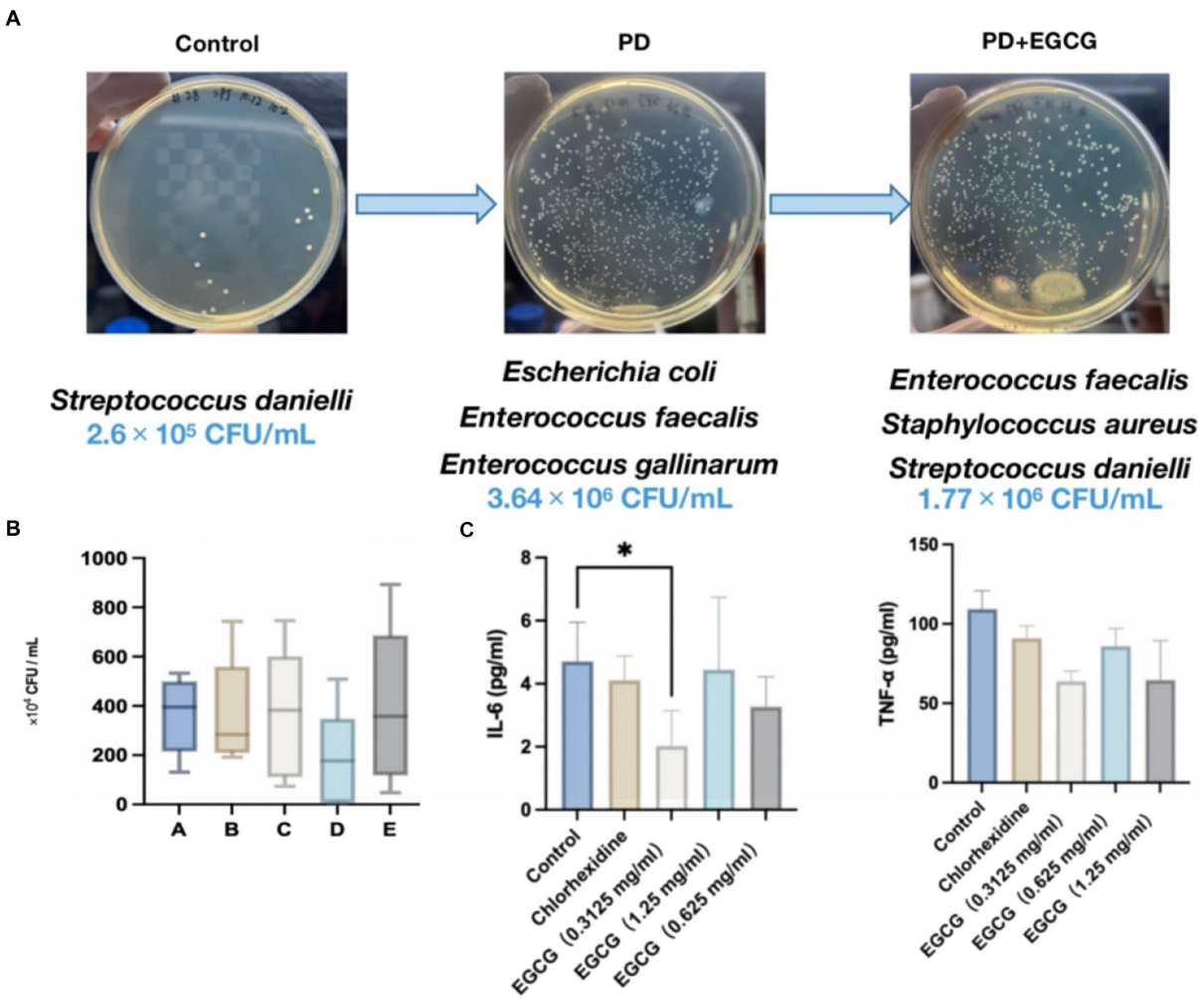

FIGURE 6
(A) Changes in the abundance and species of bacteria in the GCF in the oral cavity of mice before and after modeling. **(B)** Changes in the number of bacteria in the oral cavity of mice after administration. **(C)** Expression levels of the cytokines IL-6, and TNF-α in the serum of mice after administration.

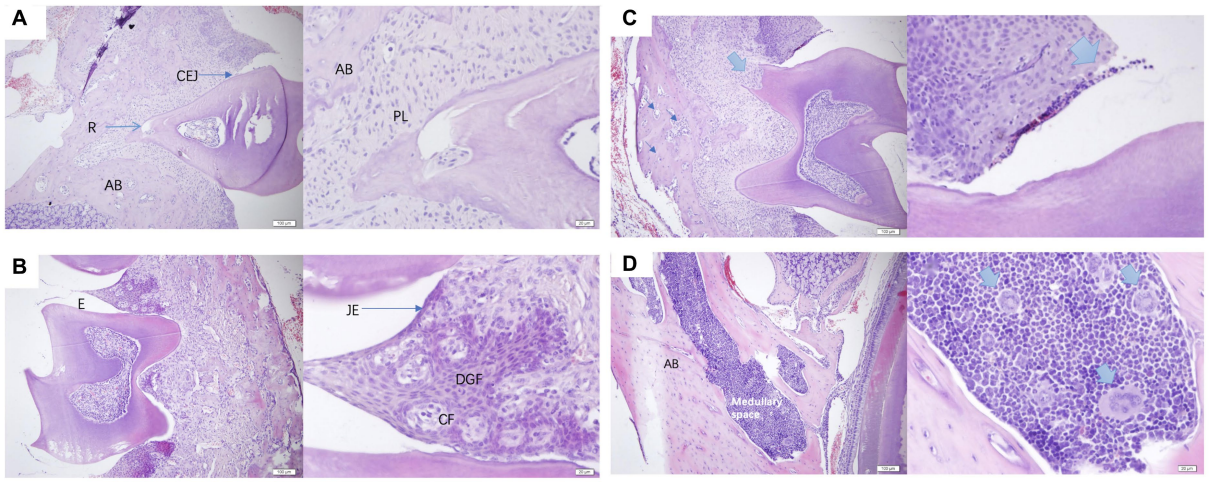

FIGURE 7
(A,B) were normal periodontal sections of mice at a scale of 100 μm and 20 μm. AB, alveolar bone; R, root; CEJ, cementoenamel junction enamel tooth bone boundary; PL, periodontal ligament; E, enamel tooth enamel; JE, junctional epithelium binding epithelium; *CF*, circular fibers; DGF, dentoperiosteal gingival fibers. **(C,D)** were pathological sections of the constructed PD mouse at a scale of 100 μm and 20 μm, alveolar bone, medullary space bone marrow cavity.

this study we chose to test EGCG, a natural compound that has not yet been used to treat canine PD, with positive results.

The identified genera that exhibited variations between PD and healthy canines in China include *Porphyromonas*, *Fusobacterium*, *Treponema*, *Moraxella,* and *Capnocytophaga.* A comparative analysis with previous studies underscores noteworthy differences. Notably, at the phylum level, the oral microbiota of healthy canines predominantly comprised *Thickworm* (45.9%), *Anaplasma* (14.7%), *Methanobacterium* (12.2%), *Helicobacter* (10.5%), *Coelenterata* (3.7%), *Actinobacteria* (3.4%), and *Clostridium* (2.8%) (Riggio et al., 2011). Examining the genus level, *Pasteurella, Bergeyella, Porphyromonas*, and *Actinobacter.* exhibited the highest detection rates in healthy canines (Davis et al., 2013). Further, at the species level, dominant species in healthy canines, canines with gingivitis, and those with periodontitis included specific species of *Pseudomonas* (30.9%), *Porphyromonas cangingivalis* (16.1%), and oral desulfurization bacteria (12.0%), respectively (Riggio et al., 2011). Noteworthy species associated with PD encompassed *Moraxella* spp. COT-396, *Bergeyella zoohelcum*, *Neisseria shayeganii*, *Pasteurellaceae* spp. COT-080, *Capnocytophaga* spp. COT-339, and *Stenotrophomonas* spp. COT-224 (Lenzo et al., 2016).

Comparing these findings with past research and incorporating the outcomes of the current high-throughput sequencing study, it is evident that the canine oral cavity harbors a diverse array of microorganisms. Some of these microorganisms remain unexplored and unidentified, underscoring the importance of microbial culture techniques in understanding the etiology of PD in canines, particularly given the historical limitations associated with anaerobic culture methods. This insight further emphasizes the necessity of ongoing studies to elucidate and characterize the oral microbiota in canines comprehensively.

In the subsequent phase of our study, we successfully isolated the clinical strain of *Porphyromonas gulae*. Additionally, the standard bacterium ATCC 51700 *P. gulae* thrived under the established test conditions, affirming the feasibility of its culture. Extensive research findings consistently underscore *Porphyromonas gulae* as the primary causative agent of PD in dogs. Recent studies, including those referenced (Dewhirst et al., 2012), substantiate the pivotal role and pathogenicity of *P. gulae* in canine PD.

The intricate interplay of various bacteria, exemplified by *Porphyromonas* spp., and their byproducts, contributes to the detrimental impact on periodontal tissues. This microbial colonization initiates on the tooth surface and within periodontal pockets, proliferating before progressing to invade the periodontal tissues and potentially entering the bloodstream (Özavci et al., 2019; Urmi et al., 2021; Shimizu et al., 2022). *Porphyromonas* spp. were detected in substantial quantities in the plaque of both healthy and periodontally affected dogs, emphasizing their ubiquitous presence. Notably, the abundance of *Porphyromonas* spp. in the oral cavity of dogs with periodontal issues significantly exceeded that in their healthy counterparts. This aligns seamlessly with the heightened prevalence of *Porphyromonas* spp. observed in both anaerobic culture results and the outcomes of high-throughput sequencing conducted in our study. This consistent correlation reinforces the association between *Porphyromonas* spp., particularly *P. gulae*, and the manifestation of PD in canines.

Furthermore, our investigation demonstrated the inhibitory potential of EGCG against a diverse array of principal pathogens associated with canine PD, notably *Porphyromonas gulae*. EGCG, as a natural active ingredient, boasts a multitude of applications. The discerned antimicrobial and therapeutic efficacy of EGCG surpassed that of the conventional 0.05% chlorhexidine acetate rinse commonly employed in small animal dentistry. This revelation suggests the promising utility of EGCG as a superior alternative for combatting canine PD, offering a potential avenue for enhanced treatment modalities in veterinary oral health.

Moreover, the application of EGCG exhibited significant efficacy within the *in vivo* milieu of our constructed PD mouse model, manifesting notable antibacterial, anti-inflammatory, and bone loss mitigation effects. However, it is imperative to acknowledge two challenges associated with utilizing mice as a method for constructing PD models. Firstly, operational challenges within a confined space posed difficulties, and secondly, the initial high mortality rate of molded mice. Addressing these concerns, strategic modifications such as the reduction of the operation duration, timely rewarming post-operation, and vigilant daily monitoring of body weight contributed to an improved survival rate among the mice. Despite these challenges, the observed therapeutic effects of EGCG, encompassing anti-inflammatory properties, antibacterial activity, and mitigation of bone loss in PD mice, are highly encouraging. These findings provide a foundation for considering the potential therapeutic applications of EGCG in managing PD in canines, extrapolating from the positive outcomes observed in the murine model.

Although there are important discoveries revealed by these studies, there are also limitations. While our study has made noteworthy contributions, we acknowledge certain limitations. The sample size remains constrained, necessitating expansion in subsequent studies for more robust conclusions. Furthermore, our investigation employed a singular mode of drug administration and a specific drug dosage form. To enhance clinical relevance, future studies should explore diverse drug carriers and dosage forms, conducting direct tests on the target animal, the canine. Ongoing modifications, such as nanoparticle preparation and temperature-sensitive hydrogel formulations, are in the pipeline to extend drug retention in the oral cavity of mice, thus improving bioavailability and therapeutic efficacy.

Despite the limitations, we achieved the successful isolation and cultivation of *P. gulae*, the primary causative agent of canine PD. Our laboratory's accomplishment in isolating a clinical strain of *P. gulae*, a significant breakthrough under strict anaerobic conditions, provides crucial technical support and invaluable strain material for subsequent experiments. Additionally, our study fills a critical gap by elucidating the microbiota differences between PD and healthy canines in China, serving as a foundational resource for future research on the pathogenesis of canine PD and drug screening.

5 Conclusion

Our research demonstrates the significant antibacterial effects of Epigallocatechin-3-gallate (EGCG) against the prevalent bacterium *P. gulae* in canine periodontal disease (PD). Moreover, EGCG exhibits anti-inflammatory properties and proves effective in addressing bone loss in a PD mouse model. These findings collectively suggest the therapeutic potential of EGCG in the treatment of canine PD. The outcomes of this study contribute valuable data, laying the foundation for further exploration and screening of alternative antibiotic drugs to advance the management of canine PD.

Data availability statement

The original contributions presented in the study are included in the article/supplementary materials, further inquiries can be directed to the corresponding authors.

Ethics statement

The animal studies were approved by China Agricultural University Laboratory Animal Welfare and Animal Experimental Ethical Committee (Approval ID: AW31103202-2-4). The studies were conducted in accordance with the local legislation and institutional requirements. Written informed consent was obtained from the owners for the participation of their animals in this study.

Author contributions

PS: Writing – original draft, Writing – review & editing. YH: Formal analysis, Writing – review & editing. DL: Project administration, Writing – review & editing. YJ: Funding acquisition, Project administration, Supervision, Writing – review & editing. JL: Conceptualization, Funding acquisition, Supervision, Writing – review & editing.

Funding

The author(s) declare financial support was received for the research, authorship, and/or publication of this article. This work was supported by the 14th Five-Year Plan National Key Research and Development Program of China (2022YFD1801104); and the National Natural Science Foundation of China (Grant nos. 3227190332 and 31972730).

Conflict of interest

The authors declare that the research was conducted in the absence of any commercial or financial relationships that could be construed as a potential conflict of interest.

Publisher's note

All claims expressed in this article are solely those of the authors and do not necessarily represent those of their affiliated organizations, or those of the publisher, the editors and the reviewers. Any product that may be evaluated in this article, or claim that may be made by its manufacturer, is not guaranteed or endorsed by the publisher.

References

Abdulkareem, A. A., Al-Taweel, F. B., Al-Sharqi, A. J. B., Gul, S. S., Sha, A., and Chapple, I. L. C. (2023). Current concepts in the pathogenesis of periodontitis: from symbiosis to dysbiosis. *J. Oral Microbiol.* 15:2197779. doi: 10.1080/20002297.2023.2197779

Asahi, Y., Noiri, Y., Miura, J., Maezono, H., Yamaguchi, M., Yamamoto, R., et al. (2014). Effects of the tea catechin epigallocatechin gallate on *Porphyromonas gingivalis* biofilms. *J. Appl. Microbiol.* 116, 1164–1171. doi: 10.1111/jam.12458

Bai, Y., Song, P., Shen, Z., Shi, H., Jiang, Z., Lin, J., et al. (2023). *Porphyromonas gulae* infection in canines, pet owners and veterinarians in China: an epidemiological study and risk factor analysis. *One Health Adv.* 1, 1–13. doi: 10.1186/s44280-023-00007-x

Chakrawarti, L., Agrawal, R., Dang, S., Gupta, S., and Gabrani, R. (2016). Therapeutic effects of EGCG: a patent review. *Expert Opin. Ther. Pat.* 26, 907–916. doi: 10.1080/13543776.2016.1203419

Chen, C. Y., Lin, Y. J., Wang, C. C. N., Lan, Y. H., Lan, S. J., and Sheu, M. J. (2019). Epigallocatechin-3-gallate inhibits tumor angiogenesis: involvement of endoglin/Smad1 signaling in human umbilical vein endothelium cells. *Biomed. Pharmacother.* 120:109491. doi: 10.1016/j.biopha.2019.109491

Chipashvili, O., and Bor, B. (2022). Ligature-induced periodontitis mouse model protocol for studying Saccharibacteria. *STAR Protoc.* 3:101167. doi: 10.1016/j.xpro.2022.101167

Choi, W., Mangal, U., Park, J., Kim, J., Jun, T., Jung, J. W., et al. (2023). Occlusive membranes for guided regeneration of inflamed tissue defects. *Nat Commun* 14:7687. doi: 10.1038/s41467-023-43428-3

Cui, Y., Oh, Y. J., Lim, J., Youn, M., Lee, I., Pak, H. K., et al. (2012). AFM study of the differential inhibitory effects of the green tea polyphenol (−)-epigallocatechin-3-gallate (EGCG) against gram-positive and gram-negative bacteria. *Food Microbiol.* 29, 80–87. doi: 10.1016/j.fm.2011.08.019

Cunha, E., Trovão, T., Pinheiro, A., Nunes, T., Santos, R., Moreira da Silva, J., et al. (2018). Potential of two delivery systems for nisin topical application to dental plaque biofilms in dogs. *BMC Vet. Res.* 14:375. doi: 10.1186/s12917-018-1692-9

Davis, I. J., Wallis, C., Deusch, O., Colyer, A., Milella, L., Loman, N., et al. (2013). A cross-sectional survey of bacterial species in plaque from client owned dogs with healthy gingiva, gingivitis or mild periodontitis, *PLoS One8*, e83158. doi: 10.1371/journal.pone.0083158

Dewhirst, F. E., Klein, E. A., Thompson, E. C., Blanton, J. M., Chen, T., Milella, L., et al. (2012). The canine oral microbiome. *PLoS One* 7, –e36067. doi: 10.1371/journal.pone.0036067

Hamada, N., Takahashi, Y., Watanabe, K., Kumada, H., Oishi, Y., and Umemoto, T. (2008). Molecular and antigenic similarities of the fimbrial major components between porphyromonas gulae and *P. gingivalis*. *Vet. Microbiol.* 128, 108–117. doi: 10.1016/j.vetmic.2007.09.014

Inaba, H., Nomura, R., Kato, Y., Takeuchi, H., Amano, A., Asai, F., et al. (2019). Adhesion and invasion of gingival epithelial cells by *Porphyromonas gulae*. *PLoS One* 14, 14, –e0213309. doi: 10.1371/journal.pone.0213309

Inaba, H., Yoshida, S., Nomura, R., Kato, Y., Asai, F., Nakano, K., et al. (2020). *Porphyromonas gulae* lipopolysaccharide elicits inflammatory responses through toll-like receptor 2 and 4 in human gingivalis epithelial cells. *Cell. Microbiol.* 22, 1–11. doi: 10.1111/cmi.13254

Jung, I. H., Lee, D. E., Yun, J. H., Cho, A. R., Kim, C. S., You, Y. J., et al. (2012). Anti-inflammatory effect of (−)-epigallocatechin-3-gallate on *porphyromonas gingivalis* lipopolysaccharide-stimulated fibroblasts and stem cells derived from human periodontal ligament. *J. Periodontal Implant Sci.* 42, 185–195. doi: 10.5051/jpis.2012.42.6.185

Kortegaard, H. E., Eriksen, T., and Baelum, V. (2008). Periodontal disease in research beagle dogs – an epidemiological study. *J. Small Anim. Pract.* 49, 610–616. doi: 10.1111/j.1748-5827.2008.00609.x

Kováč, J., Slobodníková, L., Trajčíková, E., Rendeková, K., Mučaji, P., Sychrová, A., et al. (2023). Therapeutic potential of flavonoids and tannins in management of oral infectious diseases—a review. *Molecules* 28:158. doi: 10.3390/molecules28010158

Lee, Y. L., Hong, C. Y., Kok, S. H., Hou, K. L., Lin, Y. T., Chen, M. H., et al. (2009). An extract of green tea, Epigallocatechin-3-Gallate, reduces periapical lesions by inhibiting cysteine-rich 61 expression in osteoblasts. *J. Endod.* 35, 206–211. doi: 10.1016/j.joen.2008.11.015

Lenzo, J. C., O'Brien-Simpson, N. M., Orth, R. K., Mitchell, H. L., Dashper, S. G., and Reynolds, E. C. (2016). Porphyromonas gulae has virulence and immunological characteristics similar to those of the human periodontal pathogen Porphyromonas gingivalis, *Infect. Immun.* 84, 2575–2585. doi: 10.1128/IAI.01500-15

Lobprise, H. B. (2018). *Oral surgery – general, Wiggs's Vet* Dent Wiley, 247–263.

Mangione, F., Salmon, B., Ezeldeen, M., Jacobs, R., Chaussain, C., and Vital, S. (2022). Characteristics of large animal models for current cell-based oral tissue regeneration. *Tissue Eng. Part B Rev.* 28, 489–505. doi: 10.1089/ten.teb.2020.0384

Minnelli, C., Galeazzi, R., Laudadio, E., Amici, A., Rusciano, D., Armeni, T., et al. (2020). Mon oalkylated epigallocatechin-3-gallate (C18-EGCG) as novel lipophilic EGCG derivative: characterization and antioxidant evaluation. *Antioxidants (Basel)* 9, 1–16. doi: 10.3390/antiox9030208

Na, H. K., and Surh, Y. J. (2008). Modulation of Nrf2-mediated antioxidant and detoxifying enzyme induction by the green tea polyphenol EGCG. *Food Chem. Toxicol.* 46, 1271–1278. doi: 10.1016/j.fct.2007.10.006

Nath, S., Pulikkotil, S. J., Weyrich, L., Zilm, P., Kapellas, K., and Jamieson, L. (2022). Effect of periodontal interventions on characteristics of the periodontal microbial profile: a systematic review and meta-analysis. *Microorganisms* 10:1582. doi: 10.3390/microorganisms10081582

Okagu, I. U., Ezeorba, T. P. C., Aguchem, R. N., Ohanenye, I. C., Aham, E. C., Okafor, S. N., et al. (2022). A review on the molecular mechanisms of action of natural products in preventing bone diseases. *Int. J. Mol. Sci.* 23:8468. doi: 10.3390/ijms23158468

Özavci, V., Erbas, G., Parin, U., Yüksel, H. T., and Kirkan, Ş. (2019). Molecular detection of feline and canine periodontal pathogens. *Vet. Anim. Sci.* 8:100069. doi: 10.1016/j.vas.2019.100069

Rafael, S. D. M., Chan, H., Jin, Q., Sugai, J., and Cirelli, J. A. (2018). Characterization of ligature-induced experimental periodontitis. *Microsc. Res. Tech.* 81, 1412–1421. doi: 10.1002/jemt.23101

Riggio, M. P., Lennon, A., Taylor, D. J., and Bennett, D. (2011). Molecular identification of bacteria associated with canine periodontal disease, *Vet. Microbiol.* 150, 394–400. doi: 10.1016/j.vetmic.2011.03.001

Šakarnytė, L., Šiugždinienė, R., Žymantienė, J., and Ruzauskas, M. (2023). Comparison of oral microbial composition and determinants encoding antimicrobial resistance in dogs and their owners. *Antibiotics (Basel)* 12:1554. doi: 10.3390/antibiotics12101554

Shimizu, M., Miyawaki, S., Kuroda, T., Umeta, M., Kawabe, M., and Watanabe, K. (2022). Erythritol inhibits the growth of periodontal-disease-associated bacteria isolated from canine oral cavity. *Heliyon* 8:e10224. doi: 10.1016/j.heliyon.2022.e10224

Sitheeque, M. A. M., Panagoda, G. J., Yau, J., Amarakoon, A. M. T., Udagama, U. R. N., and Samaranayake, L. P. (2009). Antifungal activity of black tea polyphenols (catechins and theaflavins) against candida species. *Chemotherapy* 55, 189–196. doi: 10.1159/000216836

Urmi, A. S., Inaba, H., Nomura, R., Yoshida, S., Ohara, N., Asai, F., et al. (2021). Roles of *Porphyromonas gulae* proteases in bacterial and host cell biology. *Cell. Microbiol.* 23:e13312. doi: 10.1111/cmi.13312

Wallis, C., Milella, L., Colyer, A., O'Flynn, C., Harris, S., and Holcombe, L. J. (2021). Subgingival microbiota of dogs with healthy gingiva or early periodontal disease from different geographical locations. *BMC Vet. Res.* 17, 1–19. doi: 10.1186/s12917-020-02660-5

Yamasaki, Y., Nomura, R., Nakano, K., Naka, S., Matsumoto-Nakano, M., Asai, F., et al. (2012). Distribution of periodontopathic bacterial species in dogs and their owners, *Arch. Oral Biol.* 57, 1183–1188. doi: 10.1016/j.archoralbio.2012.02.015

Yun, J. H., Kim, C. S., Cho, K. S., Chai, J. K., Kim, C. K., and Choi, S. H. (2007). (−)-epigallocatechin gallate induces apoptosis, via caspase activation, in osteoclasts differentiated from RAW 264.7 cells. *J. Periodontal Res.* 42, 212–218. doi: 10.1111/j.1600-0765.2006.00935.x

Yun, J. H., Pang, E. K., Kim, C. S., Yoo, Y. J., Cho, K. S., Chai, J. K., et al. (2004). Inhibitory effects of green tea polyphenol (−)-epigallocatechin gallate on the expression of matrix metalloproteinase-9 and on the formation of osteoclasts. *J. Periodontal Res.* 39, 300–307. doi: 10.1111/j.1600-0765.2004.00743.x

Zhang, Y., Lin, H., Liu, C., Huang, J., and Liu, Z. (2020). A review for physiological activities of EGCG and the role in improving fertility in humans/mammals. *Biomed. Pharmacother.* 127:110186. doi: 10.1016/j.biopha.2020.110186

frontiers | Frontiers in Microbiology

TYPE Original Research
PUBLISHED 08 January 2024
DOI 10.3389/fmicb.2023.1329609

Check for updates

OPEN ACCESS

EDITED BY
Lei Deng,
Harvard Medical School, United States

REVIEWED BY
Zhijun Zhong,
Sichuan Agricultural University, China
Mingcheng Liu,
Lund University, Sweden

*CORRESPONDENCE
Fengyang Li
✉ fylee1987@outlook.com;
✉ fengyangli@jlu.edu.cn
Liancheng Lei
✉ leiliancheng@163.com

†These authors have contributed equally to this work and share first authorship

RECEIVED 29 October 2023
ACCEPTED 14 December 2023
PUBLISHED 08 January 2024

CITATION
Wu Z, Li N, Li Z, Wang J, Liu M, Qi M, Wei S, Wu T, Guo Y, Zhu J, Jiang H, Xue R, Sun C, Feng X, Gu J, Han W, Li F and Lei L (2024) Development and application of an indirect ELISA and nested PCR for the epidemiological analysis of *Klebsiella pneumoniae* among pigs in China. *Front. Microbiol.* 14:1329609. doi: 10.3389/fmicb.2023.1329609

COPYRIGHT
© 2024 Wu, Li, Li, Wang, Liu, Qi, Wei, Wu, Guo, Zhu, Jiang, Xue, Sun, Feng, Gu, Han, Li and Lei. This is an open-access article distributed under the terms of the Creative Commons Attribution License (CC BY). The use, distribution or reproduction in other forums is permitted, provided the original author(s) and the copyright owner(s) are credited and that the original publication in this journal is cited, in accordance with accepted academic practice. No use, distribution or reproduction is permitted which does not comply with these terms.

Development and application of an indirect ELISA and nested PCR for the epidemiological analysis of *Klebsiella pneumoniae* among pigs in China

Zengshuai Wu[1†], Na Li[1†], Ziheng Li[1], Jianlong Wang[2], Mengmeng Liu[3], Mengzhu Qi[4], Shaopeng Wei[1], Tong Wu[1], Yu Guo[2], Junhui Zhu[1], Hexiang Jiang[1], Ruixue Xue[5], Changjiang Sun[1], Xin Feng[1], Jingmin Gu[1], Wenyu Han[1], Fengyang Li[1]* and Liancheng Lei[1,6]*

[1]State Key Laboratory for Zoonotic Diseases, College of Veterinary Medicine, Jilin University, Changchun, China, [2]Animal Disease Control Center of Inner Mongolia, Hohhot, China, [3]Department of First Hospital, Jilin University, Changchun, China, [4]College of Veterinary Medicine, Shandong Agricultural University, Taian, China, [5]Animal Disease Control Center of Shandong, Jinan, China, [6]College of Animal Science, Yangtze University, Jingzhou, China

Introduction: *Klebsiella pneumoniae* (*K. pneumoniae*) is an important opportunistic and zoonotic pathogen which is associated with many diseases in humans and animals. However, the pathogenicity of *K. pneumoniae* has been neglected and the prevalence of *K. pneumoniae* is poorly studied due to the lack of rapid and sensitive diagnosis techniques.

Methods: In this study, we infected mice and pigs with *K. pneumoniae* strain from a human patient. An indirect ELISA was established using the KHE protein as the coating protein for the detection of *K. pneumoniae* specific antibody in clinical samples. A nested PCR method to detect nuclei acids of *K. pneumoniae* was also developed.

Results: We showed that infection with *K. pneumoniae* strain from a human patient led to mild lung injury of pigs. For the ELISA, the optimal coating concentration of KHE protein was 10 μg/mL. The optimal dilutions of serum samples and secondary antibody were 1:100 and 1:2500, respectively. The analytical sensitivity was 1:800, with no cross-reaction between the coated antigen and porcine serum positive for antibodies against other bacteria. The intra-assay and inter-assay reproducibility coefficients of variation are less than 10%. Detection of 920 clinical porcine serum samples revealed a high *K. pneumoniae* infection rate by established indirect ELISA (27.28%) and nested PCR (19.13%). Moreover, correlation analysis demonstrated infection rate is positively correlated with gross population, Gross Domestic Product (GDP), and domestic tourists.

Discussion: In conclusion, *K. pneumoniae* is highly prevalent among pigs in China. Our study highlights the role of *K. pneumoniae* in pig health, which provides a reference for the prevention and control of diseases associated with *K. pneumoniae*.

KEYWORDS

***Klebsiella pneumoniae*, ELISA, nested PCR, *khe*, pig serum**

1 Introduction

Klebsiella pneumoniae (*K. pneumoniae*) is a rod-shaped gram-negative and opportunistic bacterium belongs to the *Enterobacteriaceae* family. This organism inhabits diverse environments including soil, water, plants, animals and humans (Yang Y. et al., 2019; Ribeiro et al., 2022). As an important opportunistic pathogen, it resides in the respiratory tract and intestinal tract of humans and animals and causes serious infections including pneumonia, septicemia, urinary tract infection, and traumatic infection (Paczosa and Mecsas, 2016).

In recent years, hypervirulent *K. pneumoniae* (hvKP) and multi-drug resistant *K. pneumoniae*, such as carbapenem-resistant *K. pneumoniae* (CRKP), have emerged and led to serious life-threatening community-and hospital-acquired infections worldwide, which makes it a global public health threat (Wang et al., 2020; Jin et al., 2022). In veterinary medicine, there are only a few reports on infections caused by *K. pneumoniae*. For example, *K. pneumoniae* causes respiratory distress in minks (Jian-Li et al., 2017), pneumonia in sheep and goats (Mahrous et al., 2023), clinical mastitis in cow (Yang Y. et al., 2019), and septicemia in pigs (Bowring et al., 2017; Bidewell et al., 2018). However, the virulence and prevalence of *K. pneumoniae* infection in pigs are rarely reported. With the isolation of hvKP and CRKP from pig farms in many countries recently (Lalruatdiki et al., 2018; Liu et al., 2019; Mobasseri et al., 2019; Leangapichart et al., 2021; Zhao et al., 2021), whether there is a *K. pneumoniae* epidemic circulation between human beings and pigs has attracted people's attention. And because the infections with *K. pneumoniae* are usually not fatal and sporadically in most cases (Bowring et al., 2017), pigs may tolerate or only a few are severely infected, the pathogenicity and prevalence of *K. pneumoniae* in pigs have been neglected in veterinary medicine. Considering that *K. pneumoniae* may transmit between humans and animals, the domestic animals may represent a source of the pathogenic and multidrug-resistant *K. pneumoniae* to humans (Yang F. et al., 2019; Leangapichart et al., 2021). Thus, clarifying the pathogenicity and prevalence of *K. pneumoniae* in pig herds has significant public health importance.

Many methods for the detection of *K. pneumoniae* have been reported. Conventional phenotype-based methods including microscopic examination, biochemical identification, and automatic bacterial identification apparatus such as the VITEK 2 system, are time-consuming and have low sensitivity (Dong et al., 2015; Ko et al., 2017). On the other hand, genotype-based techniques including conventional PCR (Liu et al., 2008; Turton et al., 2010), triplex PCR (Jeong et al., 2013), real-time PCR (Barbier et al., 2020; Lim et al., 2021), as well as other novel methods including matrix-assisted laser desorption/ionization time of flight mass spectrometry (MALDI-TOF MS) (Huang et al., 2022) and the loop mediated isothermal amplification (LAMP) (Dong et al., 2015; Poirier et al., 2021) have also been developed for the detection of *K. pneumoniae* in hospitals and laboratories with high sensitivity and specificity. However, some of these techniques have their own drawbacks, such as the requirement of expensive instruments, trained personnel, could not be conducted on-site, or not ideally suitable for detection of *K. pneumoniae* from serum samples (Kim et al., 2022).

Enzyme-linked immunosorbent assay (ELISA) is one of the commonly utilized serological detection methods in veterinary medicine. Although this method also has certain disadvantages listed above, it is an efficient, sensitive, specific, and convenient tool for detection of antigen or antibody levels in serum samples. However, establishment of ELISA and its application to detect *K. pneumoniae* in pigs has not been reported. A gene designated *khe*, which encodes a hemolysin of *K. pneumoniae*, has been proposed as a potential species-specific gene probe (Yin-Ching et al., 2002) and was utilized to detect the signature for clinical *K. pneumoniae* isolates from hospitals (Escobar Pérez et al., 2013; Chen et al., 2014; He et al., 2016). Li et al. (2020) designed a multiplex PCR method to detect *K. pneumoniae* in minks with the *khe* gene. These studies suggested that *khe* is a specific gene of *K. pneumoniae*.

Since there are few severely clinical symptoms, infections with *K. pneumoniae* in pigs are rarely reported and the potential harmfulness to pig health are neglected. Thus, *K. pneumoniae* may be overlooked by conventional methods for pathogen isolation and identification. Moreover, there are no vaccines against *K. pneumoniae* in pigs in China. To clarify the virulence and prevalence of *K. pneumoniae* in pigs in China, infection model by a human origin *K. pneumoniae* was constructed both in mice and pigs and an indirect ELISA was successfully established using recombinant KHE protein as the primary coating antigen. We demonstrated that *K. pneumoniae* infection led to mild lung injury in mice and pigs. In combination with a nested PCR targeting *khe*, the established methods demonstrated a high infection of *K. pneumoniae* in pigs, which is positively correlated with gross population, Gross Domestic Product (GDP), and domestic tourists, indicating a potential transmission of *K. pneumoniae* from humans to pigs.

2 Materials and methods

2.1 Bacterial strains and growth conditions

Supplementary Table S1 contains a list of every strain utilized in this investigation. Mass spectrometry and PCR were used to identify the *K. pneumoniae* strains KP-Q1 (Strain number: CCTCC PB 2023065, ampicillin resistant) and K36 (Strain number: CCTCC PB 2023066) (Cai et al., 2018), which were isolated from First Hospital of Jilin University. *K. pneumoniae* KP-Q1 was cloned by cultivating it overnight at 37°C in Luria-Bertani (LB) liquid medium supplemented with antibiotics (ampicillin, 100 μg/mL). *K. pneumoniae* K36 was cultivated in LB without antibiotics.

2.2 Animal experiment

Six 4-week-old female KM mice (weighing 18–20 g, free from *K. pneumoniae*, purchased from Changsheng Biotechnology) were objectively randomized into two groups ($n = 3$): a healthy control group and a *K. pneumoniae* K36 infection group. In healthy control group, mice received 40 μL PBS via intranasal injection, while mice of K36 infection group received 40 μL PBS with 8×10^4 CFU *K. pneumoniae* K36. Clinical symptoms including weight, appetite and mental status were observed for 72 h post infection. A portion of the lung tissue was taken for hematoxylin–eosin staining.

Eight 45-day-old healthy Rongchang pigs (12 ~ 14 kg, free from *K. pneumoniae*, purchased from Harbin Veterinary Research Institute) were randomly assigned to two groups ($n = 4$): a healthy

control group and a *K. pneumoniae* K36 infection group. In healthy control group, pigs received 1 mL PBS, while K36 infection group pigs received 1 mL PBS with 2×10^7 CFU *K. pneumoniae* K36, both via intranasal injection. Clinical symptoms including appetite, mental status and body weight were continuously monitored for 96 h post infection. A portion of the lung tissue was taken for hematoxylin–eosin staining.

All mice and pigs were housed in the laboratory animal room and maintained on a 14/10-h light–dark cycle with food and water *ad libitum*. All animal experiments were approved by the Institutional Animal Care and Use Committee of Jilin University and conducted in accordance with the Chinese Laboratory Animal Administration Act 1988.

2.3 Serum samples collection

A total of 920 serum samples, including 434 samples from 10 pig farms located in Jinan, Shandong, China, and 486 samples from 6 cities in Inner Mongolia, China, were collected. The *K. pneumoniae* antibody-positive and-negative clinical samples for the determination of cut-off value, sensitivity, and reproducibility analysis, and the positive serums of *Actinobacillus pleuropneumoniae* (APP), *Strptococcus suis* (*S. suis*), *Staphylococcus aureus* (*S. aureus*), and *Escherichia coli* (*E. coli*) for specificity analysis of the established ELISA were collected and confirmed using PCR and sequencing and were stored at −80°C in our laboratory.

2.4 Purification of recombinant KHE protein

For plasmid construction, *khe* gene was amplified by PCR from the *K. pneumoniae* KP-Q1 chromosome using the primer pair KHE-F and KHE-R, which were designed by SnapGene software.[1] Subsequently, the PCR products were digested with HindIII/XhoI restriction enzymes (Takara, Beijing, China) and ligated into the pET28a expression vector using T4 DNA Ligase (Takara, Beijing, China) and transformed into *E. coli* BL21 (DE3) cells (Sangon Biotech, Shanghai, China). Inserted DNA sequences were confirmed by DNA sequencing. Primers and plasmids used in this study are listed in Supplementary Table S1.

For protein purification, cells were cultured in LB medium at 37°C to an optical density at 600 nm (OD_{600}) of 0.6 ~ 0.8, treated with 0.1 mM isopropyl β-D-1-thiogalactopyranoside (IPTG) and further incubated at 16°C for 24 h. The cells were lysed in lysis buffer (50 mM Na_2HPO_4 pH 7.5, 300 mM NaCl, 1 mM phenylmethylsulfonyl fluoride) by sonication. After centrifugation, the supernatant was passed through a nickel-nitrilotriacetic acid (Ni-NTA) column (GeneScript, Nanjing, China). Subsequently, the resin was washed with a 5-bed volume of washing buffer (50 mM imidazole, 50 mM Na_2HPO_4 pH 7.5, 300 mM NaCl) and the bound proteins were eluted with elution buffer (500 mM imidazole, 50 mM Na_2HPO_4 pH 7.5, 300 mM NaCl). The eluted protein was dialyzed against washing buffer using Amicon Ultra-15 filter units (Merck, New Jersey, USA) (10 kDa cut-off) and then stored in aliquots at −80°C. The entire purification process was performed on ice. The concentration of target protein was determined by a BCA protein quantification kit (Thermo Fisher Scientific, Waltham, USA). The purified proteins were analyzed using Coomassie Blue stained SDS-PAGE. Purified recombinant His-tagged KHE (rKHE) protein was further identified using anti-His antibody and *K. pneumoniae* antibody-positive serum as the primary antibody by Western blot.

2.5 Western blot analysis

Western blot was used to identify the purified rKHE. Firstly, purified rKHE was resuspended in SDS sample buffer and heated to 95°C for 10 min before being fractionated by SDS-PAGE electrophoresis (5% stacking gel and 12% resolving gel). Then, the proteins in the resolving gel were transferred onto a polyvinylidene fluoride (PVDF) membrane (Millipore, Massachusetts, USA). The membrane was blocked with 5% skim milk (Becton, New Jersey, USA) overnight. After that, it was incubated with mouse anti-His monoclonal antibody (1:2000; Proteintech, Chicago, USA) followed by incubation with horseradish peroxidase (HRP)-conjugated goat anti-mouse IgG (1:5000; Abconal, Wuhan, China) secondary antibody; or *K. pneumoniae* antibody positive serum (1:200) followed by incubation with goat anti-pig IgG/HRP (1:5000; Solarbio, Beijing, China) secondary antibody. Finally, the targeted proteins were visualized using the ECL reagent (Millipore, Massachusetts, USA) and a Chemiluminescent Imaging System (Tanon 5,200 multi, Shanghai, China).

2.6 Establishment and optimization of *Klebsiella pneumoniae* serum IgG-ELISA

The *K. pneumoniae* serum IgG-ELISA was optimized. To begin with, 100 μL of rKHE protein (1.25 μg/mL ~ 20 μg/mL) diluted with coating buffer (0.05 M carbonate buffer, pH 9.6) was coated on microtiter plates (Nest, Wuxi, China) at 4°C overnight. The unbounded protein was discarded and the wells were washed five times with phosphate buffered saline (PBS) containing 0.05% Tween-20 (PBST). The plates were blocked with 200 μL of 5% bovine serum albumin (BSA) in PBST and incubated at 37°C for 2 h. Then 100 μL of serum (diluted from 1:100 to 1:800) was added into the wells and incubated at 37°C for 0.5 h or 1 h after washing 5 times with PBST. Similarly, 100 μL of goat anti-pig IgG/HRP secondary antibody (Solarbio, Beijing, China) (diluted from 1:2500 to 1:10000 in PBS) was added and incubated at 37°C for 0.5 h or 1 h after the same washing procedure. Subsequently, the plates were washed for 5 times and 100 μL of 3,3′,5,5′-tetramethylbenzidine (TMB) (TIANGEN BIOTECH, Beijing, China) was added and incubated at room temperature for 10 min. Lastly, the reaction was terminated by addition of 50 μL of 2 M H_2SO_4. An ELISA plate reader (BioTek ELx800, Vermont, USA) was used to measure the optical density at 450 nm (OD_{450}). Each experiment was performed at least twice, and all samples were assayed in triplicate.

1 www.snapgene.com

2.7 Determination of cut-off value, sensitivity, repeatability, and specificity of the established ELISA

Twenty standard *K. pneumoniae* antibody-negative samples were selected for ELISA detection based on the optimized coating and reaction conditions. The mean value ($\bar{x}$) and the standard deviation (SD) of OD_{450} values of the negative samples were calculated. The cut-off value was determined using the mean value ($\bar{x}$) plus 3SD of the negative samples.

The coefficient of variation (CV) of intra-and inter-assay variabilities was used to assess the reproducibility of the developed ELISA. Briefly, 6 sera were randomly selected. Three replicates of each sample were run in one batch to evaluate intra-assay (within plate) variation and 3 plates were run as separate batches to evaluate inter-assay (between runs) variation.

To evaluate the sensitivity of the developed ELISA, *K. pneumoniae* positive serum diluted at 1:100, 1:200, 1:400, 1:800, 1:1600, 1:3200, and 1:6400 in PBS were tested using the optimized working conditions. To assess the specificity of the developed ELISA, positive serum samples from APP, *S. suis*, *S. aureus*, *K. pneumoniae*, and *E. coli* were detected. *K. pneumoniae* antibody-negative and-positive serum were served as negative and positive controls, respectively.

2.8 Development of nested PCR

According to the gene sequence of *khe* (GenBank: KX842080.1), two pairs of primers for nested PCR were designed using Primer 5 software (Premier Biosoft, Palo Alto, CA, USA) and synthesized commercially (Kumei Biotechnology, Changchun, China) (Supplementary Table S1). For nested PCR, the nucleic acids in serum samples were isolated according to a previous study (Mayoral et al., 2005). Briefly, the serum was diluted tenfold with 0.1 M HCl–Tris buffer (pH 8.0) and incubated at 100°C for 14 min. Then, it was centrifuged at 10,000 g for 5 min and the supernatant containing nucleic acids was collected for PCR analysis.

The total volume of the two rounds of PCR reaction was 20 μL: 10 μL Premix Taq polymerase (Takara, Beijing, China), 8.6 μL ddH_2O, 0.3 μL forward and reverse primers each, and 0.8 μL DNA template. Thermal cycler conditions consisted of pre-denaturation at 95°C for 5 min, 30 cycles of 95°C for 30 s, 60°C for 30 s, 72°C for 30 s and a final extension was performed at 72°C for 10 min; stored at 4°C in a Thermal Cycler (Life ECO, Bioer Technology, Hangzhou, China). For the second round, the product of the first round was used as the DNA template. Thermal cycler conditions consisted of pre-denaturation at 95°C for 5 min, 30 cycles of 95°C for 30 s, 55°C for 30 s, 72°C for 12 s and a final extension was performed at 72°C for 10 min; stored at 4°C. The length of the targeting sequence is 210 bp. The PCR products were analyzed on a 2% agarose gel (Biowest, Loire Valley, France) containing 0.01% Gold View I (NOVON Scientific, Beijing, China) in TAE buffer (40 mM Tris–HCl pH 8.0, 1.18 mL acetic acid, 2 mM EDTA) and visualized using a Gel Doc XR+ Gel Documentation System (Bio-Rad, Hercules, CA, USA).

2.9 Statistical analysis

Experimental data were statistically analyzed by GraphPad Prism (version 9.0, San Diego, CA, USA). Data are presented as the mean ± SD from three independent replicates. Repeatability analysis of the established ELISA was assessed using CV (CV = SD/mean). CV values less than 15% for the intra-plate assay was considered as accepted repeatability level for the analysis. Spearman correlation coefficient was calculated to determine the relationship between ELISA positive rate and other factors. For all analyses, a p-value <0.05 was regarded as statistically significant.

2.10 Ethical approval

All animal experiments in this study were conducted in accordance with the Chinese Laboratory Animal Administration Act 1988. The animal experiments were approved by the Institutional Animal Care and Use Committee of Jilin University in compliance with the Jilin Laboratory Animal Welfare and Ethics guidelines.

3 Results

3.1 Clinical and pathological features upon *Klebsiella pneumoniae* infection in mice

After intranasal infection with *K. pneumoniae*, the weight change of mice was significantly different at 48 h and 72 h. The weight of *K. pneumoniae* group increased slowly while the control group raised rapidly (Figure 1A). In order to further investigate the pathogenic effect of *K. pneumoniae* on mice, we euthanized the mice at 72 h. Compared with the control group of mice, the *K. pneumoniae* group exhibited significant hemorrhage, neutrophil infiltration, and alveolar septum thickening in the lungs (Figures 1B,C). These data indicate that *K. pneumoniae* can infect mice and result in lung injury.

3.2 Clinical and pathological features upon *Klebsiella pneumoniae* infection in pigs

After *K. pneumoniae* infection, only mild clinical symptoms of respiratory system, such as occasional cough and panting was were observed under our experimental condition (data not shown). However, the body weight of pigs was gradually lost during 72 h post infection, and recovered to normal at 96 h post infection (Figure 2A). To further evaluate the pathological features of *K. pneumoniae* infection, pigs were sacrificed at 96 h post infection and the lung was excised. Compared to healthy control, the lungs of *K. pneumoniae* infected pigs displayed with bilateral fleshy lesions located in the caudal lobes and cardiac notches of both lungs, without obvious boundaries between the lesions and the healthy parts. Moreover, a large number of petechial hemorrhage spots were randomly distributed on the lung surface, but not in transverse sections (Figures 2B,C). Pulmonary pathological sections indicated that *K. pneumoniae* infection group showed more obvious alveolar capillary congestion and dilation, septal thickening and inflammatory

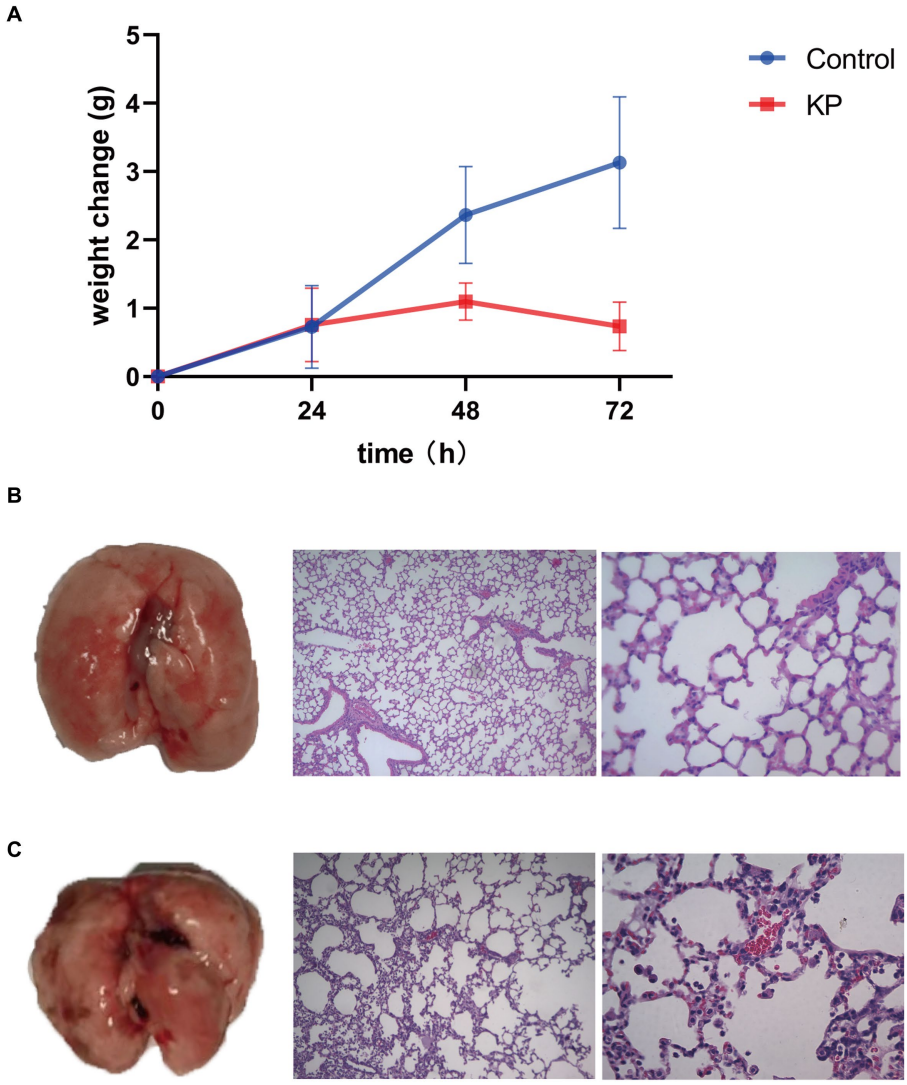

FIGURE 1
Virulence of *Klebsiella pneumoniae* in mice. **(A)** Body weight change upon infection with *K. pneumoniae* for 72 h in mice. **(B)** Left: Lung without *K. pneumoniae* infection. Middle: Hematoxylin–eosin staining of lungs of control group (100×). Right: Hematoxylin–eosin staining of lungs of control group (400×). **(C)** Left: Lung with *K. pneumoniae* infection. Middle: Hematoxylin–eosin staining of lungs of *K. pneumoniae* infection group (100×). Right: Hematoxylin–eosin staining of lungs of *K. pneumoniae* infection group (400×).

cell infiltration compared with the control group (Figures 2D,E). According to our knowledge, this is the first report on the virulence of *K. pneumoniae* on lung of pigs. These results suggest that *K. pneumoniae* infection lead to lung injury in pigs, though no obvious clinical symptoms observed.

3.3 Expression and purification of recombinant KHE protein

The expression profile of the KHE recombinant protein (rKHE, 24 kDa) was analyzed by SDS-PAGE. The results showed that it was successfully expressed and purified with high purity using a Ni-NTA resin, which was also further confirmed by Western blot analysis of purified protein using anti-His primary antibody (Figures 3A,B). Subsequently, the antigen reactivity of rKHE protein was assessed by Western blot analysis. The result showed that the rKHE protein could react specifically with the *K. pneumoniae*-positive serum (Figure 3C), indicating that the purified rKHE protein can be used as the antigen to screen specific antibodies for establishment of ELISA.

3.4 Establishment and optimization of the ELISA

Checkerboard titration was performed for the optimization of the coating concentration of rKHE antigen, the dilution and incubation time of serum and the IgG-HRP secondary antibody. The results showed that the OD_{450} value gave the maximum difference between the positive serum and negative serum (P/N value of 3.170) when the coating concentration of antigen was 10 μg/well and the dilution of serum was 1:100 (Figures 4A,B). Similarly, the optimal

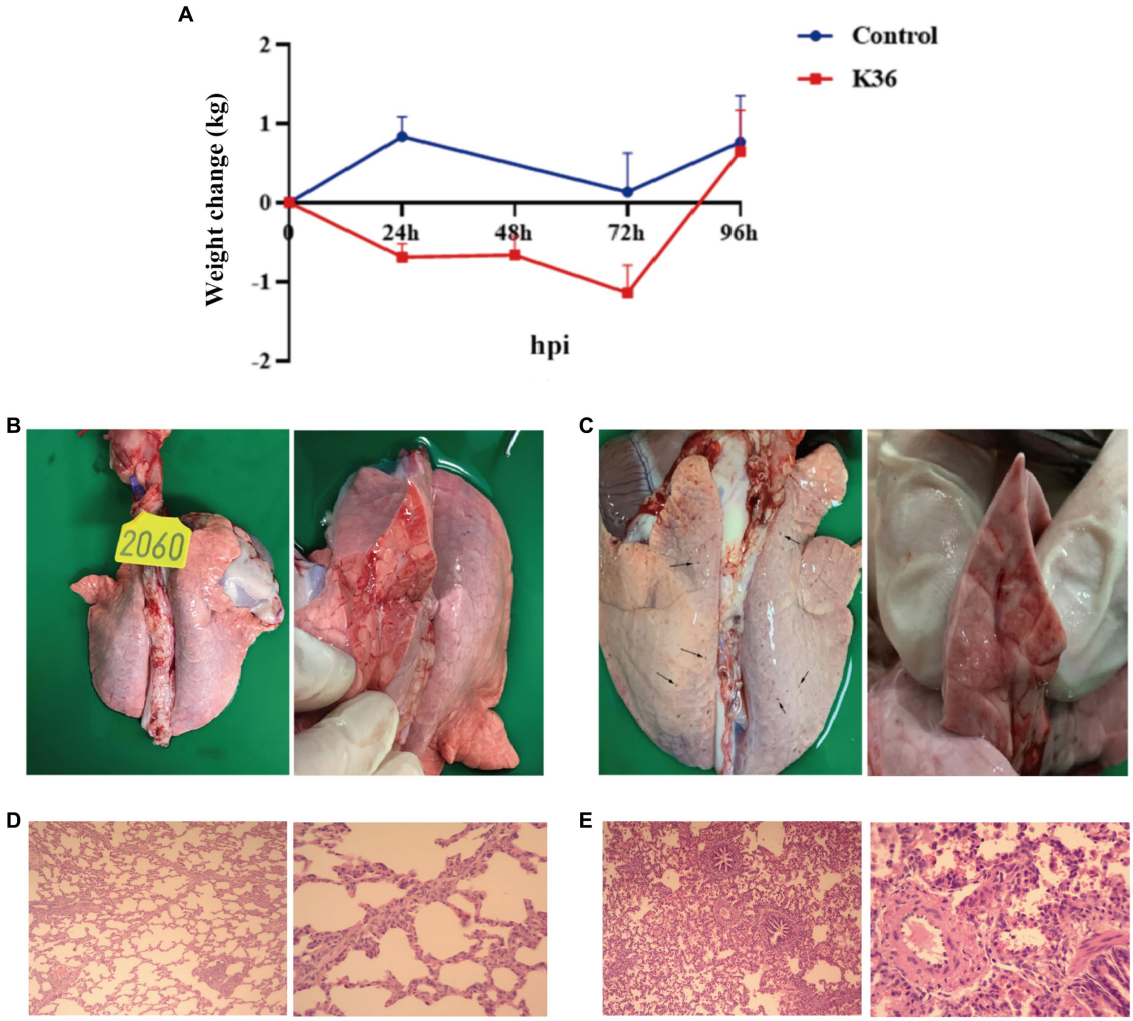

FIGURE 2
Virulence of *K. pneumoniae* in pigs. **(A)** Body weight change upon infection with *K. pneumoniae* for 96 h in Rongchang pigs. **(B,C)** Pathological examination of lung without **(B)** and with **(C)** *K. pneumoniae* infection for 96 h in Rongchang pigs. Typical petechial hemorrhage spots were indicated by black arrows. **(D)** Hematoxylin–eosin staining of lungs of control group. Left: 100×; right: 400×. **(E)** Hematoxylin–eosin staining of lungs with *K. pneumoniae* infection. Left: 100×; right: 400× .

incubation time with the sample was 1 h (Figure 4C); the optimal dilution and the optimal incubation time of the HRP-conjugated goat anti-pig IgG secondary antibody were 1:2500 and 1 h, respectively. (Figures 4D,E).

3.5 Determination of cut-off value of established ELISA

The cut-off value of the established ELISA was determined by measuring the OD_{450} values of 20 standard *K. pneumoniae* antibody-negative serum samples. The results showed that the mean of percent inhibition (PI) ($\bar{x}$) of the negative serum samples was 0.231, and the SD was 0.0526. After calculation, the cut-off value of the established ELISA was 0.389. So, sample was regarded as *K. pneumoniae* antibody-positive and-negative at PI $\geq$0.389 and PI <0.389, respectively.

3.6 Determination of sensitivity, reproducibility, and specificity of established ELISA

The sensitivity of the established ELISA was assessed by measuring the OD_{450} values of serial dilutions of *K. pneumoniae* antibody-positive serums. The results showed that serum at a dilution of 1:800 was still *K. pneumoniae* antibody-positive, while dilution at 1:1600 was *K. pneumoniae* antibody-negative, indicating that the established indirect ELISA had a high sensitivity (Figure 5A). The CVs of intra-and inter-plate variation was used to determine the reproducibility of the established ELISA. The CVs of intra-and inter-assay ranged from 1.10 to 4.32% and 1.46 to 8.03%, respectively (Tables 1, 2), suggesting a good reproducibility. Moreover, to detect the specificity of the established ELISA, cross-reactivities with confirmed positive sera to other common swine pathogens, including APP, *S. suis*, *S. aureus*, and *E. coli*, were detected. The results showed

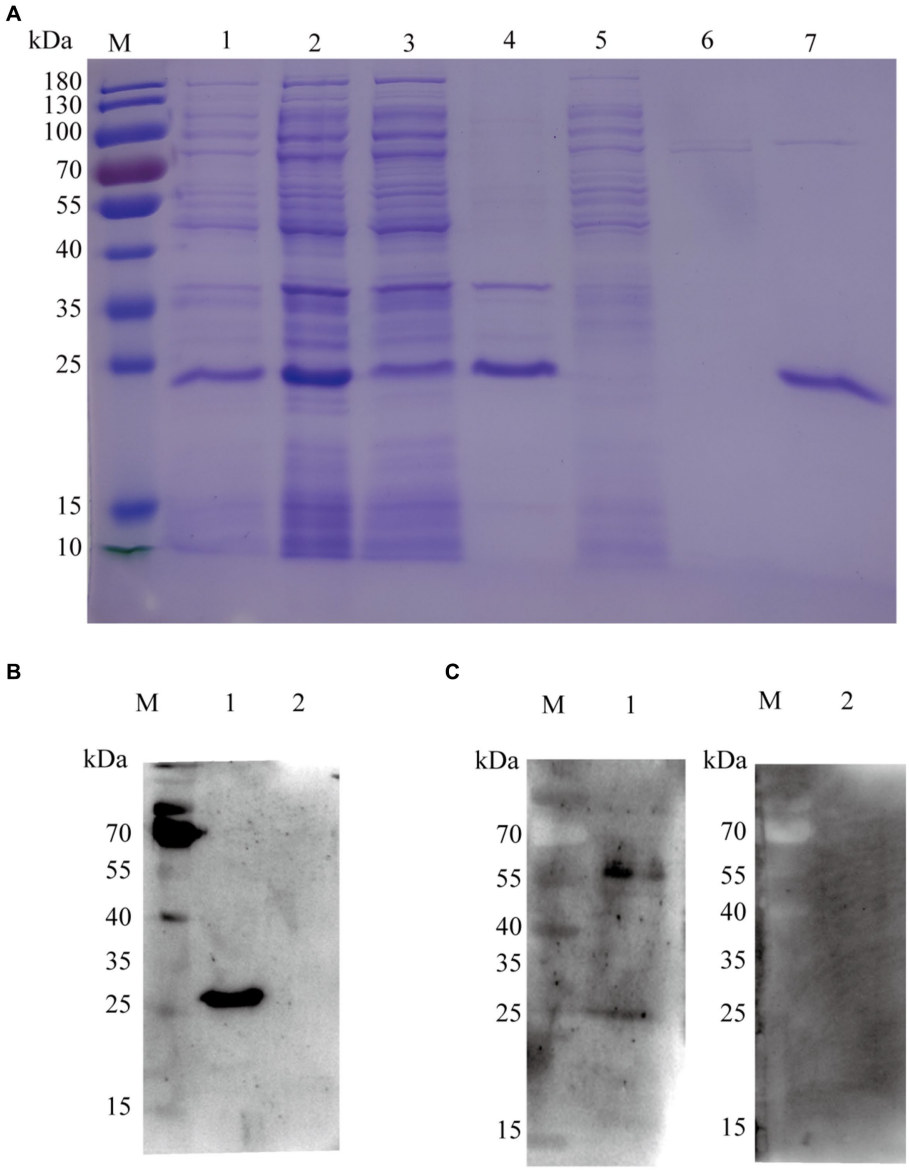

FIGURE 3
SDS-PAGE and Western blot analysis of purified rKHE. **(A)** Assessment of rKHE expression in *E. coli* by SDS-PAGE. M, Protein marker; 1, total protein without IPTG induction; 2, total protein after IPTG induction; 3, supernatant of *E. coli* lysed cells; 4, sediments of *E. coli* lysed cells; 5, 20 mM imidazole effluent; 6, 50 mM imidazole effluent; 7, purified protein; **(B)** rKHE was identified using anti-His monoclonal antibody by Western blot. M, protein marker; 1, BL21 pET28a::KHE upon IPTG induction; 2, BL21 pET28a upon IPTG induction; **(C)** Analysis of antigen reactivity of rKHE protein by Western blot. M, protein marker; 1, *K. pneumoniae*-positive serum; 2, *K. pneumoniae*-negative serum.

that all gave values, except for positive control, were below the defined cut-off point (Figure 5B), indicating there's no cross-reactivities with sera-containing antibodies against other pathogens.

3.7 Detection of the prevalence of *Klebsiella pneumoniae* in pigs by established ELISA

A total of 920 serum samples from pig farms in Shandong and Inner Mongolia of China were investigated using the established ELISA (Figure 6A). In general, the results showed that among these samples, 251 displayed *K. pneumoniae* antibody-positive and 669 displayed *K. pneumoniae* antibody-negative, with a positive rate of 27.28% (251/920) (Figure 6B). Specifically, 179 samples from Jinan and 72 samples from Inner Mongolia showed *K. pneumoniae* antibody-positive, accounting for 41.24% (179/434) and 14.81% (72/486), respectively (Supplementary Tables S2, S3). Moreover, the positive rates of *K. pneumoniae* antibody in different cities were also different, indicating the prevalence of *K. pneumoniae* varies in different pig farms even in the same area. In pig farms of Jinan, the positive rates of *K. pneumoniae* antibody ranged from 0 to 100% (Supplementary Table S2). Interestingly, most of the pig farms from where less serum samples were collected showed a high *K. pneumoniae* antibody-positive rate of over 50%, while the pig farms from where more than 100 serum samples were collected showed a *K. pneumoniae* antibody-positive rate of 35%, approximately. The positive rates of *K. pneumoniae* antibody in serum samples from pig farms of Inner

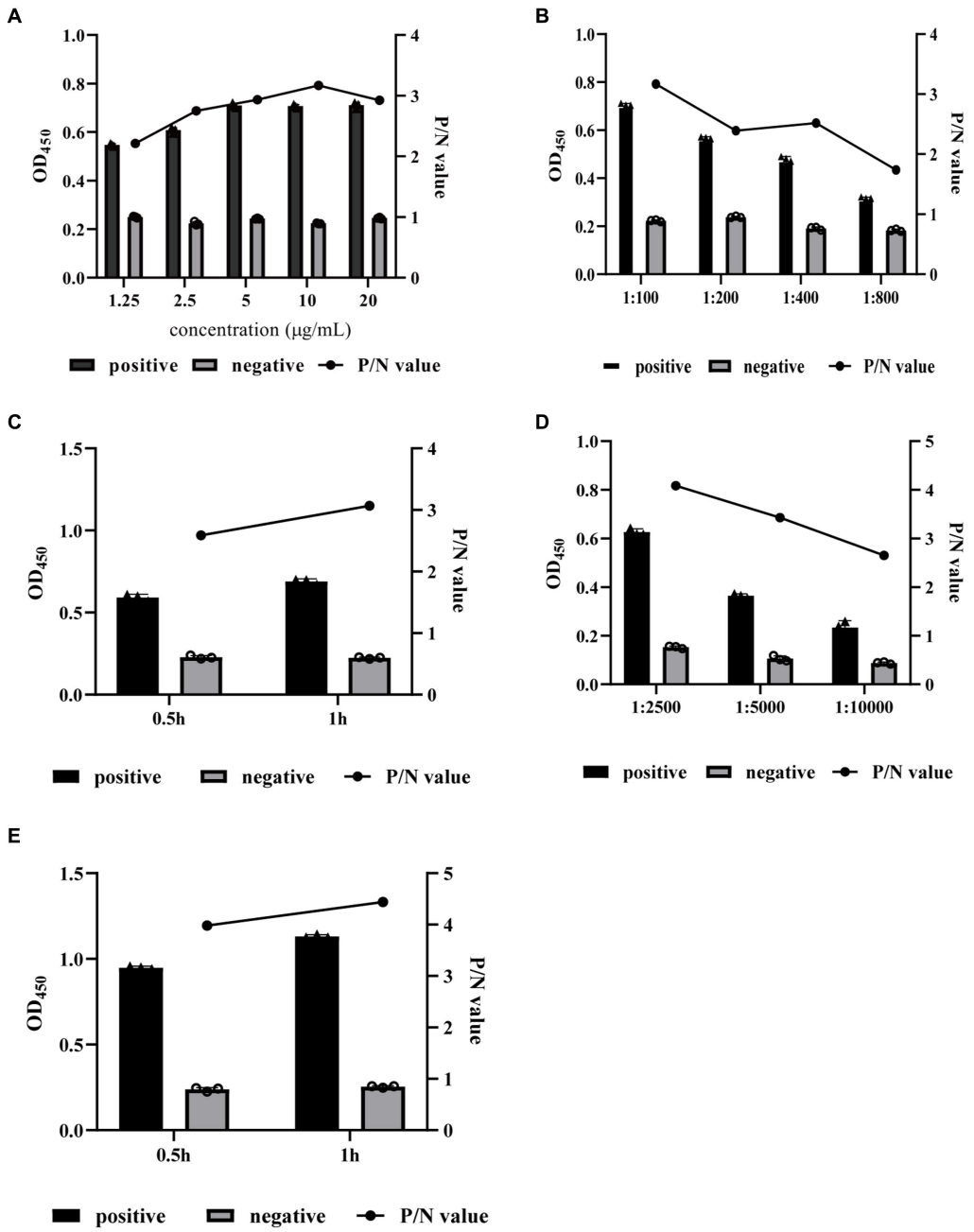

FIGURE 4
Optimization of indirect ELISA conditions. The coating concentration of rKHE antigen **(A)**, the dilution and incubation time of serum **(B,C)**, and the IgG-HRP secondary antibody **(D,E)** were optimized by checkerboard titration and selected according to the P/N value. Data are presented as the mean ± SD from three independent replicates.

Mongolia ranged from 0 to 32.23%, which were mainly concentrated in Chifeng (32.23%), Hohhot (31.58%), and Ordos (18.46%), while the positive rates of *K. pneumoniae* antibody in other areas were lower than 2% (Figure 6A; Supplementary Table S3).

3.8 Detection of the prevalence of *Klebsiella pneumoniae* in pigs by nested PCR

The 920 serum samples from pig farms in Jinan, Shandong and different cities of Inner Mongolia were also investigated using established nested PCR. In general, the results showed that among these samples, clear bands with expected size were observed in 176 *K. pneumoniae* serum samples, but not in other 744 samples (Supplementary Figure S1). The positive rate was 19.13% (176/920) (Figure 6B). Specifically, the positive rates in Jinan and Inner Mongolia were 35.48% (154/434) and 4.53% (22/486), respectively (Supplementary Tables S4, S5). Moreover, the positive rates in different areas of Shandong and Inner Mongolia were also different. In pig farms of Jinan, Shandong, the positive rates ranged from 13.33 to 73.33% (Supplementary Table S4). In pig farms of Inner Mongolia, the positive rates ranged from 0 to 7.02% (Figure 6A; Supplementary Table S5).

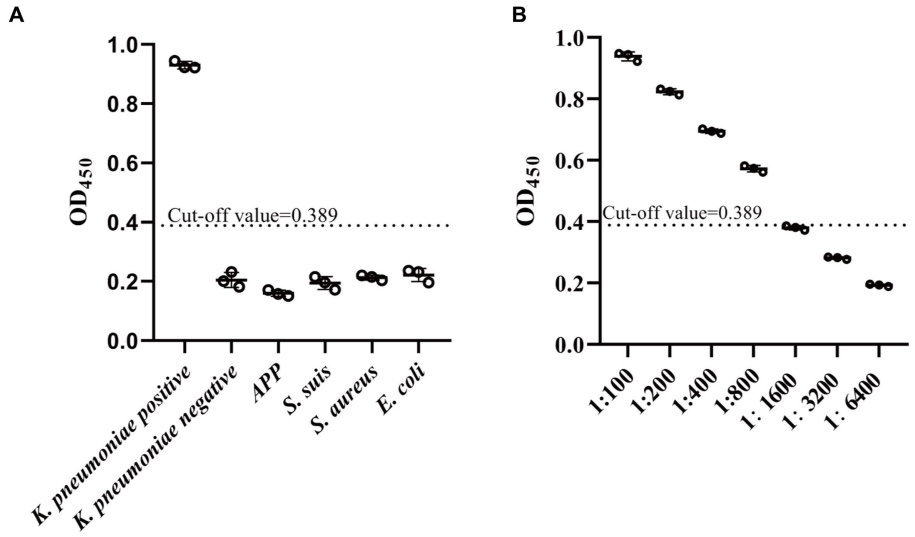

FIGURE 5
Specificity and sensitivity analysis of established indirect ELISA. **(A)** The specificity of established ELISA was evaluated by detection of cross reactions with serum containing antibodies against four common pathogens in swine, including APP (*Actinobacillus pleuropneumoniae*), *S. suis* (*Strptococcus suis*), *S. aureus* (*Staphylococcus aureus*), and *E. coli* (*Escherichia coli*). **(B)** The sensitivity of established ELISA was determined by assessment of serial dilutions of *K. pneumoniae*-positive serum. The cut-off value was determined using the mean value ($\bar{x}$) plus 3SD of the *K. pneumoniae*-negative samples. Values above cut-off was accepted as *K. pneumoniae* antibody-positive. Data are presented as the mean ± SD from three independent replicates.

TABLE 1 Intra-assay of established indirect ELISA.

Serum No.	Number of repetitions (OD_{450} values)			X†	SD†	CV%†
	1	2	3			
1	0.913	0.925	0.905	0.914	0.010	1.101%
2	0.179	0.171	0.175	0.175	0.004	2.286%
3	0.442	0.474	0.479	0.465	0.020	4.317%
4	0.237	0.244	0.233	0.238	0.006	2.339%
5	0.189	0.185	0.183	0.186	0.003	1.645%
6	0.165	0.161	0.173	0.166	0.006	3.673%

†X, average; SD, standard deviation; CV, coefficient of variation, calculated by SD divided by mean values.

TABLE 2 Inter-assay of established indirect ELISA.

Serum No.	Number of repetitions (OD_{450} values)			X†	SD†	CV%†
	1	2	3			
1	0.742	0.728	0.721	0.730	0.011	1.464%
2	0.169	0.147	0.148	0.155	0.012	8.032%
3	0.811	0.854	0.856	0.840	0.025	3.025%
4	0.393	0.367	0.384	0.381	0.013	3.462%
5	0.153	0.152	0.143	0.149	0.006	3.688%
6	0.425	0.443	0.446	0.438	0.009	2.055%

†X, average; SD, standard deviation; CV, coefficient of variation, calculated by SD divided by mean values.

3.9 Determination of factors correlated to *Klebsiella pneumoniae* infection rate

The *K. pneumoniae* infection rate in pig's serum from Jinan, Shandong is much higher than that from other cities of Inner Mongolia (Figure 6A). Since the cities with higher positivity rates such as Jinan and Hohhot tend to be more developed, we wonder if the *K. pneumoniae* infection rate is associated with human activities including gross population, population mobility, Gross Domestic Product (GDP), and breeding density (number of pigs/population).

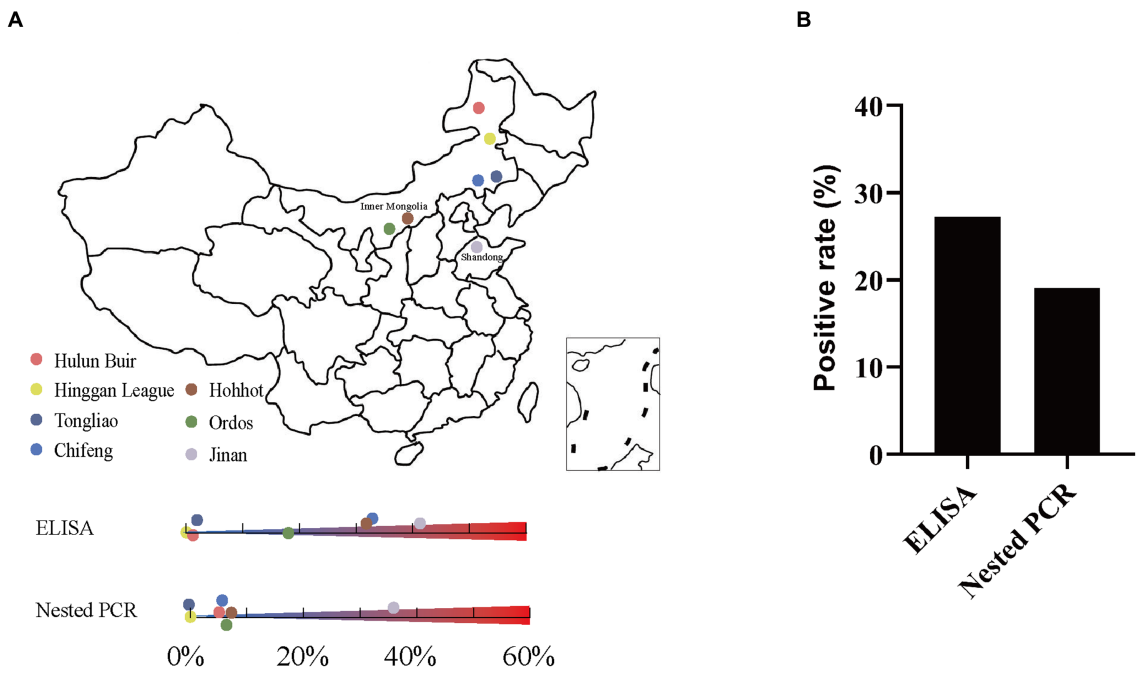

FIGURE 6
Detection of *K. pneumoniae* in serum samples by established indirect ELISA and nested PCR. **(A)** Geographic locations of pig serum samples collected from pig farms in Shandong and Inner Mongolia, China; the original map is downloaded from DataV (https://datav.aliyun.com/portal/school/atlas/area_selector). **(B)** Overall *K. pneumoniae* positive rate by established indirect ELISA and nested PCR.

As expected, high infection rates were mainly observed in Jinan, Chifeng, Hohhot, and Ordos, which have higher gross population, GDP, and population mobility (the number of tourists) than other cities (Table 3). Accordingly, Spearman correlation analysis demonstrated a strong positive correlation between *K. pneumoniae* infection rate and gross population, GDP, and the number of tourists. On the other hand, a moderate negative correlation between *K. pneumoniae* infection rate and breeding density was observed (Table 3; Figure 7). Overall, these results suggest that the prevalence of *K. pneumoniae* in pigs is positively associated with indicated human activities. The more frequent human activities, the higher incidence of *K. pneumoniae* infection in pigs.

3.10 Comparison of results between the established ELISA and nested PCR

We found that the consistency between positive samples identified by ELISA and nested PCR was not high. As shown in Supplementary Table S6, there were 559 negative samples as detected by both methods, indicating that 60.76% of pigs have never been infected with *K. pneumoniae*. There were 66 positive samples as detected by both methods, indicating that 7.17% of pigs are infected with *K. pneumoniae*. Moreover, there were 110 samples showed *K. pneumoniae* antibody negative as detected by established ELISA, but identified as positive by nested PCR, which may indicate that 11.96% of pigs might be infected by *K. pneumoniae* at an early-stage. Identified as positive by established ELISA, while negative by nested PCR were observed in 185 samples, which may indicate that 20.11% of pigs have endured the infection of *K. pneumoniae*.

4 Discussion

Klebsiella pneumoniae is an important opportunistic and zoonotic pathogen that causes various diseases in humans and animals (Bowring et al., 2017; Bidewell et al., 2018). However, the pathogenicity and epidemiology of *K. pneumoniae* in pigs is still unknown due to the lack of rapid and sensitive diagnosis techniques. In this study, we show that infection by a human origin *K. pneumoniae* led to mild lung injury of pigs. Epidemic detection of *K. pneumoniae* by an established indirect ELISA and nested PCR demonstrate a high infection rate in pigs, which is associated with local population, GDP, human activities, and breeding density. These results provide valuable information for the illustration of transmission and control of diseases caused by *K. pneumoniae* both in humans and pigs.

Though *K. pneumoniae*-induced septicemia have been observed, infections by *K. pneumoniae* in pigs are usually not fatal and rarely reported in veterinary medicine (Bowring et al., 2017; Bidewell et al., 2018). The effect of *K. pneumoniae* infection on pig health have been neglected. However, we speculate that *K. pneumoniae* infection may also impair pig health, especially in lung, even though the symptoms are subclinical or even asymptomatic. As expected, we observed mild lung injury and body weight loss upon *K. pneumoniae* infection in pigs (Figure 2). Importantly, the *K. pneumoniae* strain used in infection experiment in pigs is an hypervirulent serotype K2 strain that was isolated from human. According to our knowledge, this is the first report on the virulence of *K. pneumoniae* from a human origin on lung of pigs. Moreover, *K. pneumoniae* have been isolated from lung samples together with other common pathogens that cause pneumoniae in pigs, such as *E. coli* (Lai et al., 2018) and porcine reproductive and respiratory syndrome virus (PRRSV) (Yan et al.,

TABLE 3 Correlation coefficient of ELISA and different factors by Spearman correlation analysis.

Cities	Positive rate		GDP†	Population†	Domestic tourists†	Pig number	Breeding density
	ELISA	Nested PCR	(0.1 billion)	(10,000 person)	(10,000 person-times)	(10,000)	(Pig number/ population)
Jinan	41.24%	35.48%	10140.9	920.24	6037.9	131.95	6.97416
Chifeng	32.23%	5.79%	1763.6	403.13	1383.92	139.19	2.89626
Hohhot	31.58%	7.02%	2800.68	345.42	1820.36	41.03	8.41872
Ordos	18.46%	6.15%	3533.66	215.56	1580.84	28.29	7.61965
Tongliao	1.61%	0.00%	1276.64	286.75	1158.32	157.83	1.81683
Hulun Buir	1.55%	5.43%	1172.2	223.63	781.16	34.53	6.4764
Hinggan League	0.00%	0.00%	547.92	141.32	681.1	53.04	2.6644
Correlation coefficient	1	0.829	0.857	0.893	0.893	0.109	−0.6
P	0.0004	0.03	0.023	0.012	0.012	0.816	0.154

†GDP, population, and domestic tourists are calculated using the data in the year 2020. Data of Jinan is obtained from the Jinan statistical yearbook 2021 published by Jinan government (http://jntj.jinan.gov.cn/art/2021/10/11/art_27523_4743879.html). Data of others cities is obtained from the Statistical Bureau of Inner Mongolia (http://tj.nmg.gov.cn/datashow/easyquery/easyquery.htm?cn=B0103). GDP, Gross Domestic Product.

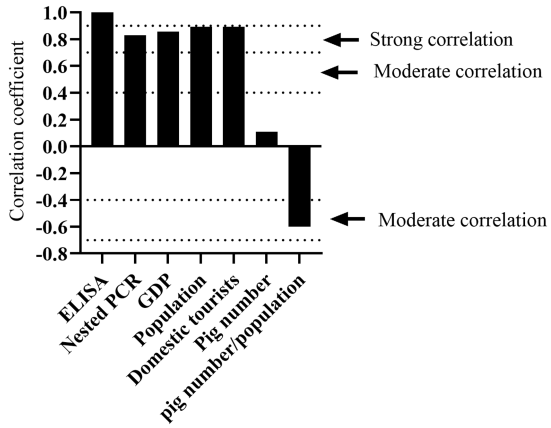

FIGURE 7
Determination of factors correlated to *K. pneumoniae* infection rate by Spearman correlation analysis. Correlation coefficient between 0.00–0.10, negligible correlation; 0.10–0.39, weak correlation; 0.40–0.69, moderate correlation; 0.70–0.89, strong correlation; 0.90–1.00, very strong correlation.

2020). We assume that *K. pneumoniae* may contributes to the pathogeneses of these pathogens.

According to our knowledge, there's no commercial kits for the rapid detection of *K. pneumoniae* antibodies in pig serum. Conventional techniques including PCR are commonly utilized for detection and identification of *K. pneumoniae* (Chen et al., 2021). ELISA is a sensitive, specific, and one of the most common serological methods for the pathogen detection in veterinary medicine. Compared to conventional PCR techniques, it does not require expensive instruments, which makes it a convenient tool for rapid detection of pathogens. In this study, we have established an indirect ELISA method which displayed high sensitivity, reproducibility, and specificity in the assays. Since there's no vaccines for pigs in China against *K. pneumoniae* infection, the established ELISA can be utilized for the diagnosis of *K. pneumoniae* infection by detecting whether the serum contain the specific antibodies. However, a major drawback of this method is that it may requires large amounts of rKHE protein as coating antigens for large-scale serum detections. Thus, a developed protein purification method might be needed. Moreover, evaluation of the prevalence of *K. pneumoniae* might be inadequate since the established ELISA detects anti-rKHE antibody which takes certain time to be produced during infection process by host. Thus, infections at an early stage might be overlooked.

To overcome these drawbacks, a nested PCR that detects nucleic acids of *khe* was developed. Compared conventional PCR, nested PCR has higher sensitivity and specificity in terms of amplifying a cDNA copy of an mRNA present at very low abundance in samples (Green and Sambrook, 2019). In line with these speculations, ELISA and nested PCR gave different results of positive rates in serum samples from both areas, suggesting the pigs were infected with *K. pneumoniae* at different infection stages (Pinedo et al., 2008). ELISA-positive results indicated that the pigs have been infected with *K. pneumoniae* for some time or at a late stage of infection, while nested PCR-positive results indicated that the animal are infected with *K. pneumoniae* at present. Analysis of the results from the both established methods may be needed to better evaluate the prevalence of *K. pneumoniae* in animals.

Most of the infections caused by *K. pneumoniae* have been observed in diverse animals including cattle, goat, horse, and cat, but not many in pigs (Brisse and Duijkeren, 2005; Ribeiro et al., 2022). In this study, a total of 920 serum samples from Shandong and Inner Mongolia of China were detected using the established methods. The positive rates of *K. pneumoniae* antibody in both areas were quite high (Figure 6B), indicating *K. pneumoniae* is a major emerging pathogen that prevalent in pigs. Our result is consistent with a previous study which showed *K. pneumoniae* was the sixth most frequently encountered pathogen in swine (Zou et al., 2011). Considering the fact that *K. pneumoniae* can be transmitted between humans and animals via food chain and occupational contact (Founou et al., 2018; Yang F. et al., 2019; Leangapichart et al., 2021), we hypothesize that the

domestic animals may represent a source of the pathogenic and multidrug-resistant *K. pneumoniae* to humans or vice versa.

Moreover, we observed that the *K. pneumoniae* infection rate varied dramatically in different regions and pig farms (Supplementary Tables S2–S5). Regions with high population density and GDP had higher infection rate than that with low population density and GDP. Moreover, *K. pneumoniae* infection rate is positively correlated with gross population, GDP, and the number of tourists (Figure 7), but negatively correlated with breeding density, suggesting that the prevalence of *K. pneumoniae* in pigs is associated with human activities.

In conclusion, our study demonstrated that *K. pneumoniae* infection impaired pig health. Rapid detection of *K. pneumoniae* by the established indirect ELISA and nested PCR indicated a high infection rate in pigs, which is correlated with local population, GDP, human activities and breeding density. These results suggested the established methods can be applied for rapid clinical diagnoses to evaluate the prevalence of *K. pneumoniae* infection both in animals and humans, and highlighted the effect of *K. pneumoniae* infection on pig health to which needs to be paid more attentions in veterinary medicine.

Data availability statement

The original contributions presented in the study are included in the article/Supplementary material, further inquiries can be directed to the corresponding authors.

Ethics statement

The animal study was approved by the Institutional Animal Care and Use Committee of Jilin University. The study was conducted in accordance with the local legislation and institutional requirements.

Author contributions

ZW: Writing – original draft, Writing – review & editing. NL: Writing – original draft, Writing – review & editing. ZL: Writing – original draft. JW: Writing – original draft. ML: Writing – original draft. MQ: Writing – original draft. SW: Writing – review & editing. TW: Methodology, Writing – original draft. YG: Resources, Writing – original draft. JZ: Methodology, Writing – original draft. HJ: Methodology, Writing – original draft. RX: Resources, Writing – original draft. CS: Resources, Writing – original draft. XF: Writing – original draft. JG: Methodology, Supervision, Writing – review & editing. WH: Writing – review & editing. FL: Writing – original draft, Writing – review & editing. LL: Writing – original draft, Writing – review & editing.

Funding

The author(s) declare financial support was received for the research, authorship, and/or publication of this article. This work was supported by the Key Project of Chinese National Programs for Research and Development (2022YFD1800905), and the National Natural Science Foundation of China (32102670, 32102686).

Acknowledgments

We thank Mengshi Xu (Jilin University, Changchun, China) for the technical assistance on the *Klebsiella pneumoniae* infection experiment in pigs.

Conflict of interest

The authors declare that the research was conducted in the absence of any commercial or financial relationships that could be construed as a potential conflict of interest.

Publisher's note

All claims expressed in this article are solely those of the authors and do not necessarily represent those of their affiliated organizations, or those of the publisher, the editors and the reviewers. Any product that may be evaluated in this article, or claim that may be made by its manufacturer, is not guaranteed or endorsed by the publisher.

Supplementary material

The Supplementary material for this article can be found online at: https://www.frontiersin.org/articles/10.3389/fmicb.2023.1329609/full#supplementary-material

References

Barbier, E., Rodrigues, C., Depret, G., Passet, V., Gal, L., Piveteau, P., et al. (2020). The ZKIR assay, a real-time PCR method for the detection of *Klebsiella pneumoniae* and closely related species in environmental samples. *Appl. Environ. Microbiol.* 86:2711. doi: 10.1128/aem.02711-19

Bidewell, C. A., Williamson, S. M., Rogers, J., Tang, Y., Ellis, R. J., Petrovska, L., et al. (2018). Emergence of *Klebsiella pneumoniae* subspecies pneumoniae as a cause of septicaemia in pigs in England. *PLoS One* 13:e0191958. doi: 10.1371/journal.pone.0191958

Bowring, B. G., Fahy, V. A., Morris, A., and Collins, A. M. (2017). An unusual culprit: *Klebsiella pneumoniae* causing septicaemia outbreaks in neonatal pigs? *Vet. Microbiol.* 203, 267–270. doi: 10.1016/j.vetmic.2017.03.018

Brisse, S., and Duijkeren, E. (2005). Identification and antimicrobial susceptibility of 100 Klebsiella animal clinical isolates. *Vet. Microbiol.* 105, 307–312. doi: 10.1016/j.vetmic.2004.11.010

Cai, R., Wu, M., Zhang, H., Zhang, Y., Cheng, M., Guo, Z., et al. (2018). A smooth-type, phage-resistant *Klebsiella pneumoniae* mutant strain reveals that OmpC is indispensable for infection by phage GH-K3. *Appl. Environ. Microbiol.* 84:1585. doi: 10.1128/aem.01585-18

Chen, Z., Liu, M., Cui, Y., Wang, L., Zhang, Y., Qiu, J., et al. (2014). A novel PCR-based genotyping scheme for clinical *Klebsiella pneumoniae*. *Future Microbiol.* 9, 21–32. doi: 10.2217/fmb.13.137

Chen, R., Shang, H., Niu, X., Huang, J., Miao, Y., Sha, Z., et al. (2021). Establishment and evaluation of an indirect ELISA for detection of antibodies to goat *Klebsiella pneumonia*. *BMC Vet. Res.* 17:107. doi: 10.1186/s12917-021-02820-1

Dong, D., Liu, W., Li, H., Wang, Y., Li, X., Zou, D., et al. (2015). Survey and rapid detection of *Klebsiella pneumoniae* in clinical samples targeting the rcsA gene in Beijing, China. *Front. Microbiol.* 6:519. doi: 10.3389/fmicb.2015.00519

Escobar Pérez, J. A., Olarte Escobar, N. M., Castro-Cardozo, B., Valderrama Márquez, I. A., Garzón Aguilar, M. I., Martinez de la Barrera, L., et al. (2013). Outbreak of NDM-1-producing *Klebsiella pneumoniae* in a neonatal unit in Colombia. *Antimicrob. Agents Chemother.* 57, 1957–1960. doi: 10.1128/aac.01447-12

Founou, L. L., Founou, R. C., Allam, M., Ismail, A., Djoko, C. F., and Essack, S. Y. (2018). Genome sequencing of extended-Spectrum β-lactamase (ESBL)-producing *Klebsiella pneumoniae* isolated from pigs and abattoir Workers in Cameroon. *Front. Microbiol.* 9:188. doi: 10.3389/fmicb.2018.00188

Green, M. R., and Sambrook, J. (2019). Nested polymerase chain reaction (PCR). *Cold Spring Harb. Protoc.* 2019:pdb.prot095182. doi: 10.1101/pdb.prot095182

He, Y., Guo, X., Xiang, S., Li, J., Li, X., Xiang, H., et al. (2016). Comparative analyses of phenotypic methods and 16S rRNA, khe, rpoB genes sequencing for identification of clinical isolates of *Klebsiella pneumoniae*. *Antonie Van Leeuwenhoek* 109, 1029–1040. doi: 10.1007/s10482-016-0702-9

Huang, Y., Li, J., Wang, Q., Tang, K., and Li, C. (2022). Rapid detection of KPC-producing *Klebsiella pneumoniae* in China based on MALDI-TOF MS. *J. Microbiol. Methods* 192:106385. doi: 10.1016/j.mimet.2021.106385

Jeong, E. S., Lee, K. S., Heo, S. H., Seo, J. H., and Choi, Y. K. (2013). Rapid identification of *Klebsiella pneumoniae*, *Corynebacterium kutscheri*, and *Streptococcus pneumoniae* using triplex polymerase chain reaction in rodents. *Exp. Anim.* 62, 35–40. doi: 10.1538/expanim.62.35

Jian-Li, W., Yuan-Yuan, S., Shou-Yu, G., Fei-Fei, D., Jia-Yu, Y., Xue-Hua, W., et al. (2017). Serotype and virulence genes of *Klebsiella pneumoniae* isolated from mink and its pathogenesis in mice and mink. *Sci. Rep.* 7:17291. doi: 10.1038/s41598-017-17681-8

Jin, Z., Wang, Z., Gong, L., Yi, L., Liu, N., Luo, L., et al. (2022). Molecular epidemiological characteristics of carbapenem-resistant *Klebsiella pneumoniae* among children in China. *AMB Express* 12:89. doi: 10.1186/s13568-022-01437-3

Kim, H., Jang, J. H., Jung, I. Y., and Cho, J. H. (2022). A novel peptide as a specific and selective probe for *Klebsiella pneumoniae* detection. *Biosensors (Basel)* 12:153. doi: 10.3390/bios12030153

Ko, J. H., Baek, J. Y., Peck, K. R., Cho, S. Y., Ha, Y. E., Kim, S. H., et al. (2017). Discrepant susceptibility to gentamicin despite amikacin resistance in *Klebsiella pneumoniae* by VITEK 2 represents false susceptibility associated with the armA 16S rRNA methylase gene. *J. Med. Microbiol.* 66, 1448–1450. doi: 10.1099/jmm.0.000583

Lai, C. C., Lin, Y. T., Lin, Y. T., Lu, M. C., Shi, Z. Y., Chen, Y. S., et al. (2018). Clinical characteristics of patients with bacteraemia due to the emergence of mcr-1-harbouring Enterobacteriaceae in humans and pigs in Taiwan. *Int. J. Antimicrob. Agents* 52, 651–657. doi: 10.1016/j.ijantimicag.2018.08.015

Lalruatdiki, A., Dutta, T. K., Roychoudhury, P., and Subudhi, P. K. (2018). Extended-spectrum β-lactamases producing multidrug resistance *Escherichia coli*, Salmonella and *Klebsiella pneumoniae* in pig population of Assam and Meghalaya, India. *Vet. World* 11, 868–873. doi: 10.14202/vetworld.2018.868-873

Leangapichart, T., Lunha, K., Jiwakanon, J., Angkititrakul, S., Järhult, J. D., Magnusson, U., et al. (2021). Characterization of *Klebsiella pneumoniae* complex isolates from pigs and humans in farms in Thailand: population genomic structure, antibiotic resistance and virulence genes. *J. Antimicrob. Chemother.* 76, 2012–2016. doi: 10.1093/jac/dkab118

Li, P., Zhang, D., Li, H., Pang, J., Guo, H., and Qiu, J. (2020). Establishment and application of multiplex PCR for simultaneously detecting *Escherichia coli*, Salmonella, Klebsiella pneumoniae, and *Staphylococcus aureus* in minks. *Front. Vet. Sci.* 7:588173. doi: 10.3389/fvets.2020.588173

Lim, H. J., Kang, E. R., Park, M. Y., Kim, B. K., Kim, M. J., Jung, S., et al. (2021). Development of a multiplex real-time PCR assay for the simultaneous detection of four bacterial pathogens causing pneumonia. *PLoS One* 16:e0253402. doi: 10.1371/journal.pone.0253402

Liu, Y., Liu, C., Zheng, W., Zhang, X., Yu, J., Gao, Q., et al. (2008). PCR detection of *Klebsiella pneumoniae* in infant formula based on 16S-23S internal transcribed spacer. *Int. J. Food Microbiol.* 125, 230–235. doi: 10.1016/j.ijfoodmicro.2008.03.005

Liu, D., Yang, Y., Gu, J., Tuo, H., Li, P., Xie, X., et al. (2019). The Yersinia high-pathogenicity island (HPI) carried by a new integrative and conjugative element (ICE) in a multidrug-resistant and hypervirulent *Klebsiella pneumoniae* strain SCsl1. *Vet. Microbiol.* 239:108481. doi: 10.1016/j.vetmic.2019.108481

Mahrous, S. H., El-Balkemy, F. A., Abo-Zeid, N. Z., El-Mekkawy, M. F., El Damaty, H. M., and Elsohaby, I. (2023). Antibacterial and anti-biofilm activities of cinnamon oil against multidrug-resistant *Klebsiella pneumoniae* isolated from pneumonic sheep and goats. *Pathogens* 12:1138. doi: 10.3390/pathogens12091138

Mayoral, C., Norona, M., Baroni, M. R., Giani, R., and Zalazar, F. (2005). Evaluation of a nested-PCR assay for *Streptococcus pneumoniae* detection in pediatric patients with community-acquired pneumonia. *Rev. Argent. Microbiol.* 37, 184–188.

Mobasseri, G., Teh, C. S. J., Ooi, P. T., Tan, S. C., and Thong, K. L. (2019). Molecular characterization of multidrug-resistant and extended-Spectrum Beta-lactamase-producing *Klebsiella pneumoniae* isolated from swine farms in Malaysia. *Microb. Drug Resist.* 25, 1087–1098. doi: 10.1089/mdr.2018.0184

Paczosa, M. K., and Mecsas, J. (2016). *Klebsiella pneumoniae*: going on the offense with a strong defense. *Microbiol. Mol. Biol. Rev.* 80, 629–661. doi: 10.1128/mmbr.00078-15

Pinedo, P. J., Rae, D. O., Williams, J. E., Donovan, G. A., Melendez, P., and Buergelt, C. D. (2008). Association among results of serum ELISA, faecal culture and nested PCR on milk, blood and faeces for the detection of paratuberculosis in dairy cows. *Transbound. Emerg. Dis.* 55, 125–133. doi: 10.1111/j.1865-1682.2007.01009.x

Poirier, A. C., Kuang, D., Siedler, B. S., Borah, K., Mehat, J. W., Liu, J., et al. (2021). Development of loop-mediated isothermal amplification rapid diagnostic assays for the detection of Klebsiella pneumoniae and Carbapenemase genes in clinical samples. *Front. Mol. Biosci.* 8:794961. doi: 10.3389/fmolb.2021.794961

Ribeiro, M. G., de Morais, A. B. C., Alves, A. C., Bolanos, C. A. D., de Paula, C. L., Portilho, F. V. R., et al. (2022). Klebsiella-induced infections in domestic species: a case-series study in 697 animals (1997-2019). *Braz. J. Microbiol.* 53, 455–464. doi: 10.1007/s42770-021-00667-0

Turton, J. F., Perry, C., Elgohari, S., and Hampton, C. V. (2010). PCR characterization and typing of *Klebsiella pneumoniae* using capsular type-specific, variable number tandem repeat and virulence gene targets. *J. Med. Microbiol.* 59, 541–547. doi: 10.1099/jmm.0.015198-0

Wang, G., Zhao, G., Chao, X., Xie, L., and Wang, H. (2020). The characteristic of virulence, biofilm and antibiotic resistance of *Klebsiella pneumoniae*. *Int. J. Environ. Res. Public Health* 17:6278. doi: 10.3390/ijerph17176278

Yan, X., Zeng, J., Li, X., Zhang, Z., Din, A. U., Zhao, K., et al. (2020). High incidence and characteristic of PRRSV and resistant bacterial co-infection in pig farms. *Microb. Pathog.* 149:104536. doi: 10.1016/j.micpath.2020.104536

Yang, F., Deng, B., Liao, W., Wang, P., Chen, P., and Wei, J. (2019). High rate of multiresistant *Klebsiella pneumoniae* from human and animal origin. *Infect. Drug Resist.* 12, 2729–2737. doi: 10.2147/IDR.S219155

Yang, Y., Higgins, C. H., Rehman, I., Galvao, K. N., Brito, I. L., Bicalho, M. L., et al. (2019). Genomic diversity, virulence, and antimicrobial resistance of *Klebsiella pneumoniae* strains from cows and humans. *Appl. Environ. Microbiol.* 85:2654. doi: 10.1128/aem.02654-18

Yin-Ching, C., Jer-Horng, S., Ching-Nan, L., and Ming-Chung, C. (2002). Cloning of a gene encoding a unique haemolysin from Klebsiella pneumoniae and its potential use as a species-specific gene probe. *Microb Pathog* 33, 1–6. doi: 10.1006/mpat.2002.0499

Zhao, W., Li, S., Schwarz, S., Li, A., Yao, H., and Du, X. D. (2021). Detection of a NDM-5-producing *Klebsiella pneumoniae* sequence type 340 (CG258) high-risk clone in swine. *Vet. Microbiol.* 262:109218. doi: 10.1016/j.vetmic.2021.109218

Zou, L. K., Wang, H. N., Zeng, B., Zhang, A. Y., Li, J. N., Li, X. T., et al. (2011). Phenotypic and genotypic characterization of β-lactam resistance in *Klebsiella pneumoniae* isolated from swine. *Vet. Microbiol.* 149, 139–146. doi: 10.1016/j.vetmic.2010.09.030

frontiers | Frontiers in Microbiology

TYPE Original Research
PUBLISHED 11 January 2024
DOI 10.3389/fmicb.2023.1331434

Check for updates

OPEN ACCESS

EDITED BY
Hong Yin,
Chinese Academy of Agricultural Sciences, China

REVIEWED BY
Tian Luo,
University of Texas Medical Branch at Galveston, United States
ThankGod Emmanuel Onyiche,
University of Maiduguri, Nigeria
David H. Walker,
University of Texas Medical Branch at Galveston, United States

*CORRESPONDENCE
Tian Qin
✉ qintian@icdc.cn
Dongli Liu
✉ ldl029@foxmail.com

RECEIVED 01 November 2023
ACCEPTED 08 December 2023
PUBLISHED 11 January 2024

CITATION
Zhang X, Lv W, Teng Z, Zhao N, Zhou Y, Ma D, Ma L, Cheng Y, Wei J, He J, Ma W, Liu D and Qin T (2024) Molecular detection of Rickettsiales and a potential novel *Ehrlichia* species closely related to *Ehrlichia chaffeensis* in ticks (Acari: Ixodidae) from Shaanxi Province, China, in 2022 to 2023. *Front. Microbiol.* 14:1331434. doi: 10.3389/fmicb.2023.1331434

COPYRIGHT
© 2024 Zhang, Lv, Teng, Zhao, Zhou, Ma, Ma, Cheng, Wei, He, Ma, Liu and Qin. This is an open-access article distributed under the terms of the Creative Commons Attribution License (CC BY). The use, distribution or reproduction in other forums is permitted, provided the original author(s) and the copyright owner(s) are credited and that the original publication in this journal is cited, in accordance with accepted academic practice. No use, distribution or reproduction is permitted which does not comply with these terms.

Molecular detection of Rickettsiales and a potential novel *Ehrlichia* species closely related to *Ehrlichia chaffeensis* in ticks (Acari: Ixodidae) from Shaanxi Province, China, in 2022 to 2023

Xue Zhang[1], Wen Lv[2], Zhongqiu Teng[1], Na Zhao[1], Yue Zhou[3], Di Ma[4], Lin Ma[2], Yuqing Cheng[1], Jianjun Wei[5], Jia He[1], Wenke Ma[6], Dongli Liu[2]* and Tian Qin[1]*

[1]National Key Laboratory of Intelligent Tracking and Forecasting for Infectious Diseases, National Institute for Communicable Disease Control and Prevention, Chinese Center for Disease Control and Prevention, Beijing, China, [2]Shaanxi Provincial Center for Disease Control and Prevention, Xi'an, China, [3]Long County Center for Disease Control and Prevention, Baoji, China, [4]Mei County Center for Disease Control and Prevention, Baoji, China, [5]HanZhong Center for Disease Control and Prevention, Hanzhong, China, [6]Zhenba County Center for Disease Control and Prevention, Hanzhong, China

Important tick-borne diseases include spotted fever group *Rickettsia* (SFGR), *Anaplasma*, and *Ehrlichia*, which cause harm to animal and human health. Ixodidae are the primary vectors of these pathogens. We aimed to analyze the prevalence and genetic diversity of SFGR, Anaplasma, and *Ehrlichia* species in the Ixodidae in Shaanxi Province, China. Herein, 1,113 adult Ixodidae ticks were collected from domestic cattle and goats, and detected using nested PCR. A total of four Ixodidae species were collected and *Ca.* R. jingxinensis (20.58%, 229/1113), *A. bovis* (3.05%, 34/1113), *A. capra* (3.32%, 37/1113), *A. marginale* (0.18%, 2/1113), *E.* sp. Yonaguni138 (0.18%, 2/1113), and a potent novel *Ehrlichia* species named *E.* sp. Baoji96 (0.09%, 1/1113) were detected. *A. marginale* was detected for the first time in *Rhipicephalus microplus*. *E.* sp. Baoji96 was closely related to *E. chaffeensis* and was first identified in *Haemaphysalis longicornis*. In addition, co-infection with two Rickettsiales pathogens within an individual tick was detected in 10 (1.54%) ticks. This study provides a reference for the formulation of biological control strategies for ticks and tick-borne diseases in Shaanxi Province, and could lead to an improved control effect.

KEYWORDS

SFGR, *Anaplasma*, *Ehrlichia*, Ixodidae, Shaanxi Province

1 Introduction

Rickettsiales are a class of bacteria that are gram-negative obligate intracellular bacteria that can infect humans and different vertebrates via the bite of an arthropod vector. Recognized important Rickettsiales pathogens include spotted fever group *Rickettsia* (SFGR), *Anaplasma*, and *Ehrlichia*, and Ixodidae are their primary vectors (Qin et al., 2019). The initial symptoms are similar to those of a cold, such as high fever, weakness, pain, chills, etc., and there are also signature clinical features, rash and eschar. SFGR consists of over 30 species distributed worldwide, and at least 18 species have been identified as human pathogens in China (Robinson et al., 2019; Teng et al., 2023b). For example, *Rickettsia rickettsii* is the most pathogenicSFGR, which causes Rocky Mountain spotted fever (RMSF) in North America. *Rickettsia conorii* causes Mediterranean spotted fever (MSF) in some regions of Europe, Africa, and Asia (Robinson et al., 2019). In addition, disease names associated with pathogens often reflect the region where they are found; however, the actual endemic region is often much larger (Labruna et al., 2014). *Rickettsia japonica* causes Japanese spotted fever (JSF). It was first described in Japan in 1984 in three patients with high fever and rash (Mahara, 1997). But outside Japan, cases have been reported in China, South Korea, the Philippines, and Thailand (Teng et al., 2023a). At present, the genera *Anaplasma* and *Ehrlichia* contain eight known bacterial species that infect humans: *A. phagocytophilum*, *A. platys*, *A. ovis*, *A. bovis*, *A. capra*, *E. chaffeensis*, *E. ewingii*, and *E. muris* (Bakken et al., 1994; Paddock and Childs, 2003; Thomas et al., 2009; Chochlakis et al., 2010; Johnson et al., 2015; Li et al., 2015; Lu et al., 2022). Furthermore, *E. chaffeensis* causes human monocytotropic ehrlichiosis (HME), and *A. phagocytophilum* is responsible for human granulocytotropic anaplasmosis (HGA). Both HME and HGA have fairly high infection rates in the United States, and cases have also been reported in China (Ismail et al., 2010). Rickettsiales are potential pathogenic factors for numerous diseases, which can lead to rash, post-infectious arthritides, interstitial pneumonia, meningoencephalitis, acute kidney injury, multiple organ failure, and even death after human infection (Pasquale Mansueto et al., 2012; Zeidler and Hudson, 2021; Sebastian et al., 2022). Moreover, in recent years, a number of emerging and re-emerging Rickettsiales species have been discovered to infect humans (Qin et al., 2019). Thus, Rickettsiales diseases will continue to be a threat to human health.

The epidemiology of tick-borne Rickettsial disease reflects the geographic and seasonal distribution of the pathogen and transmission is mainly related to the following: the tick vector and its host, and the human behavior of people bitten after their skin is exposed to the tick (Beati et al., 1997). The distribution of tick-borne Rickettsial disease is geographically similar to that of ticks and their hosts, which tells us that understanding the distribution and changes of vectors is very important for the prevention and control of tick-borne rickettsial disease. Ticks are found in a wide range of areas, ranging from forests to roadside bushes, and even in areas without vegetation (Piotrowski and Rymaszewska, 2020). This makes us aware of the potential dangers of tick bites when we travel.

Ixodidae, the primary vectors of pathogens belonging to the Rickettsiales, comprise 111 species from 7 genera in China (Zhang et al., 2019). Ticks are found in all regions of China and infect every class of terrestrial vertebrates, including mammals, birds, reptiles, and even amphibians (Lu et al., 2019). With more and more attention being paid to the construction of urban landscaping, the contact area between man and nature has been greatly increased. This overlaps human, animal and tick habitats, greatly increasing the risk of human tick bites. Despite their ubiquity in nature, these organisms are often overlooked as an important cause of disease around the world. Treatment is easily delayed because of a lack of awareness of tick-borne diseases. Due to misdiagnosis, the best antibiotic treatment time is missed, which may lead to serious complications and even death. Hence, investigation of local tick-borne Rickettsiales pathogen prevalence is helpful for the early diagnosis and treatment of related diseases.

The terrain of Shaanxi province consists of mountains, plains, and basins, spanning three climatic zones. Southern Shaanxi is humid, central Guanzhong is semi-humid, and northern Shaanxi is semi-arid; therefore, it is rich in species and diverse in vegetation types. The Qinling Mountains are even known as a "biological gene bank." Different ticks have different habitats. *Ixodes* prefer cool, moist environments, but *Rhipicephalus sanguineus* are adapted to high temperatures and dry environments. And, Different ticks prefer different hosts (Piotrowski and Rymaszewska, 2020). Here, ticks always find the right living conditions and plenty of hosts. In the past, Rickettsiales studies in Shaanxi Province mainly focused on *Anaplasma*, especially *A. capra* (Guo et al., 2019b). In this study, we aimed to analyze the prevalence and genetic diversity of SFGR, *Anaplasma*, and *Ehrlichia* species in Ixodidae collected from Shaanxi Province, China.

2 Materials and methods

2.1 Sample collection

From 2022 to 2023, adult ticks were collected from locations in Shaanxi Province, China: Zhenba County of Hanzhong city (32°08′ ~ 32°50′N, 107°25′ ~ 108°16′E), Baoji City (33°35′ ~ 35°06′N, 106°18′ ~ 108°03′E), and Shangluo District of Shangluo City (33°06′ ~ 33°44′N, 10°24′ ~ 111°01′E) (Figure 1). Two methods of collecting ticks were used: the tweezers were used to pick up ticks on the body surface of domestic animals (cattle and goats), and the cloth flag method was used to collect ticks in grassland. All ticks were identified by observing their structure under a light microscope and referring to the tick classification search table (Teng and Jiang, 1991).

2.2 DNA extraction

The ticks were removed from −80°C storage, and washed successively using 0.1% Bromo-Germaine, 75% alcohol, and phosphate-buffered saline (PBS) for 10–15 min. This step is to remove impurities from the surface of ticks. The ticks were individually homogenized in PBS, and then centrifuged for 3 min at 2,500 × g. Total nucleic acids from the tick homogenates were extracted using a

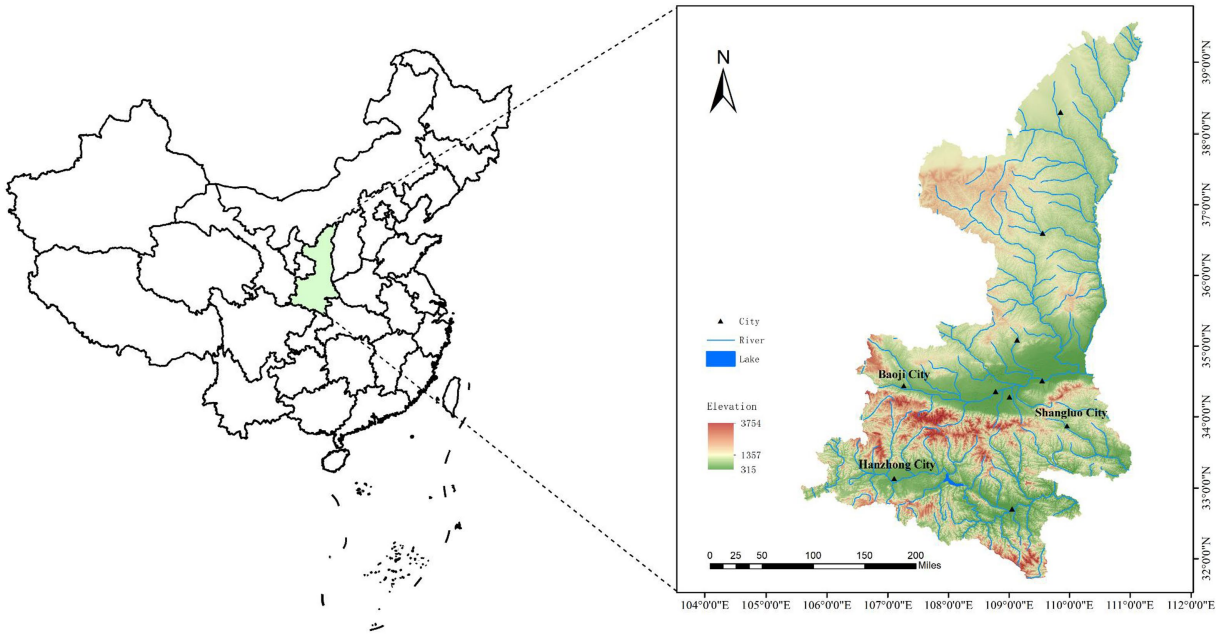

FIGURE 1
Map of Shaanxi Province showing the locations of the study sites.

QIAamp DNA Mini Kit (Qiagen, Hilden, Germany) and diluted to 100 μL. All the DNA extracts were stored at −20°C until use.

2.3 PCR amplification and sequencing

All ticks were further confirmed by PCR amplification and DNA sequencing of the mitochondrial cytochrome oxidase I (*CO* I) gene (Peng-Fei et al., 2018). *Rickettsia* in the ticks were simultaneously detected using nested or semi-nested PCR targeting a 440 bp region of the 17-kDa antigen-encoding (17kD) gene, a 1,100 bp region of the citrate synthase (*glt*A) gene, and a 1,200 bp region of the 16S rRNA (*rrs*) gene. A 500 bp sequence generated using universal primers of the *rrs* gene was used to detect *Anaplasma* and *Ehrlichia*. The clones positive for *Anaplasma* were further amplified using primers amplifying *gro*EL (encoding the 60 kDa heat shock protein), *glt*A, and a longer fragment (1,200 bp) of the *rrs* gene. The clones positive for *Ehrlichia* were further amplified with primers for *gro*EL, *glt*A, *dsb* (encoding the disulfide bond formation protein), *fts*Z (encoding a cell division protein), and a longer fragment of the *rrs* gene. For the potential novel agents, positive specimens a 1,200 bp fragment of the *rrs* gene was amplified, and two nested PCR assays were used to amplify the 5′-end and 3′-end fragments of the *rrs* gene to assemble a complete gene (Wen et al., 2002). All the primers used for PCR are shown in Supplementary Table S1. All primers were synthesized by Sangon Biotech (Shanghai) Co., Ltd. And PCR was performed using Premix Taq Version 2.0 plus dye (Takara, Dalian, China). These sequences were amplified by nested or semi-nested PCR according to Lu et al. (2022). Tm is 50°C.

The PCR products were electrophoresed through 1.0% agarose gels. The target amplicons were purified using a QIAquick PCR Purification Kit (Qiagen). The purified PCR products were sent to Beijing De'aoping Biotechnology Co., Ltd. (Beijing, China) for bi-directional sequencing.

2.4 Genetic and phylogenetic analysis

The sequences obtained from the target genes were modified and assembled using the EditSeq and SeqMan programs (in DNAStar, Ver. 7.0, DNASTAR Inc., Madison, WI, United States) to make them accurate and complete. For confirmation, these sequences were compared with those uploaded to GenBank[1] using the Basic Local Alignment Search Tool (BLASTn). Multiple sequence alignments of these sequences were performed using the Clustal W method (with default parameters) as implemented in the MegAlign program (DNAStar, Ver. 7.0). The evolutionary history of these sequences was inferred using the maximum likelihood method in MEGA version 7 (Bakken et al., 1994; Kumar et al., 2016). The robustness of the resultant phylogenetic trees was assessed based on bootstrap support values obtained from 1,000 replicates; values more than 70% were considered to indicate significant differences.

2.5 Nucleotide sequence accession number

The GenBank accession numbers of the nucleotide sequences obtained in this study are presented in Supplementary Table S2.

1 http://blast.ncbi.nlm.nih.gov/

3 Results

3.1 Tick collection and identification

A total of 1,113 adult ticks were collected from three different locations in Shaanxi Province (365 from Zhenba County, 691 from Baoji City, 57 from Shangluo District) (Figure 1). Based on the tick classification characteristics and further confirmed by amplification of the *COI* gene, three tick species were identified: *Haemaphysalis longicornis* (87.42%, 973/1113), *Rhipicephalus microplus* (11.77%, 131/1113), *Haemaphysalis flava* (0.81%, 9/1113) (Table 1). The *COI* gene sequences of all the ticks obtained in this study showed 99–100% identities with those of the above three ticks in GenBank (OR574171–OR574179).

3.2 Detection and phylogenic analysis of Rickettsia

PCR amplification results showed that 130 ticks were positive for *rrs*, *glt*A, and 17kD, and the prevalence of *Rickettsia* in the ticks was 20.58% (229/1113). *Rickettsia* was detected in *Haemaphysalis longicornis* (20.04%, 195/973), *Rhipicephalus microplus* (23.66%, 31/131), and *Haemaphysalis flava* (33.33%, 3/9). Table 1 shows the situation of ticks and *Rickettsia* (SFGR), *Anaplasma*, and *Ehrlichia* carried by ticks in different areas of Shaanxi Province. Based on these three genes, only one spotted fever group *Rickettsia* was detected. Among all the amplified *Rickettsia* strains, there were three representative strains (*rrs*: OR513096–OR513098; 17KD: OR526945–OR526947; *glt*A: OR526950–OR526952), and other *Rickettsia* strains were 100% identical with these three strains. As shown in the phylogenetic tree in Figure 2, and nucleotide alignment showed that their *rrs* gene, *glt*A gene, and *17*kD gene were 100, 99.89%, 99.54–100% similar to "*Candidatus* Rickettsia jingxinensis" (*Ca.* R. jingxinensis) strains (*rrs*: MH500204, MH923226; *glt*A: MH500217, OQ702260; 17kD: MH932037-MH932038, OQ702257), respectively. Figures 2–4 shows phylogenetic trees constructed with different genes, which can be used to observe the evolutionary relationships between species and to better understand the diversity of species.

3.3 Detection and phylogenic analysis of Anaplasma

Three *Anaplasma* species (*A. bovis, A. capra, A. marginale*) were detected in *H. longicornis* and *Rh. microplus*. *A. bovis* detected in this study was found in *H. longicornis* from Zhenba County and Baoji City with a prevalence of (3.05%, 34/1113). As shown in Figure 3, in the phylogenetic analysis based on the *rrs* gene, the 14 sequences were clustered together with those of *A. bovis* strains obtained from cattle (MH255914) and goats (MH594292, MH255920) found in other provinces of China. The topologies of *gro*EL and *glt*A gene-based phylogenetic trees were similar to that of the *rrs* gene-based phylogenetic tree. The *rrs*, *glt*A, and *gro*EL gene sequences from the strains amplified in this study shared 99.92–100%, 99.35–100%, and 99.87–100% identity with previously reported *A. bovis* sequences, respectively. *A. capra* was detected in *H. longicornis* in Baoji City and Shangluo District, with a positive rate of (3.32%, 37/1113). In the *rrs*, *glt*A, *gro*EL phylogenetic tree, the sequences obtained in this study showed a close relationship with *A. capra* isolate JZT12 (OQ185246) detected in Anhui province in China. DNA sequencing of the partial *rrs* and *glt*A gene showed 100% identity to *A. capra* isolate JZT12, while the *gro*EL gene showed 99.88–100% similarity. The positive rate of *A. marginale* was (0.18%, 2/1113), which was amplified from *H. longicornis* from Shangluo District. Sequence analysis showed that the sequences of the two samples were consistent, and were closely related to that of the known *A. marginale* found in *Rh. microplus* from wild goats and cattle (Lu et al., 2017). The sequences of their partial *rrs* gene showed 100% identity to that of the *A. marginale* strain WHBMXZ-130 (KX987367), and their *glt*A and *gro*EL gene showed 99.70 and 99.88% identity to *A. marginale* strain WHBMXZ-130, respectively.

TABLE 1 Detection of *Rickettsia*, *Anaplasma*, and *Ehrlichia* in ticks from different areas in Shaanxi Province, China.

Locality			Ticks				
Province	County	Geographic coordinates	Species	No. tested	*Rickettsia* (No. of positive)	*Anaplasma* (No. of positive)	Ehrlichia (No. of positive)
Shaanxi	Zhenba	32°08′ ~ 32°50′N, 107°25′ ~ 108°16′E	*Haemaphysalis longicornis*	230	*Ca.* R. jingxinensis (29)	*A. bovis* (11)	*E.* sp. Yonaguni138 (2)
			Rhipicephalus microplus	131	*Ca.* R. jingxinensis (31)	*A. marginale* (2)	0
			Haemaphysalis flava	4	*Ca.* R. jingxinensis (3)	0	0
	Baoji	33°35′ ~ 35°06′N, 106°18′ ~ 108°03′E	*Haemaphysalis longicornis*	686	*Ca.* R. jingxinensis (165)	*A. bovis* (23) *A. capra* (36)	*E.* sp. Baoji96 (1)
			Haemaphysalis flava	5	0	0	0
	Shangluo	33°06′ ~ 33°44′N, 110°24′ ~ 111°01′E	*Haemaphysalis longicornis*	57	*Ca.* R. jingxinensis (1)	*A. capra* (1)	0
Total				1,113	229 (20.58%)	73 (6.56%)	3 (0.27%)

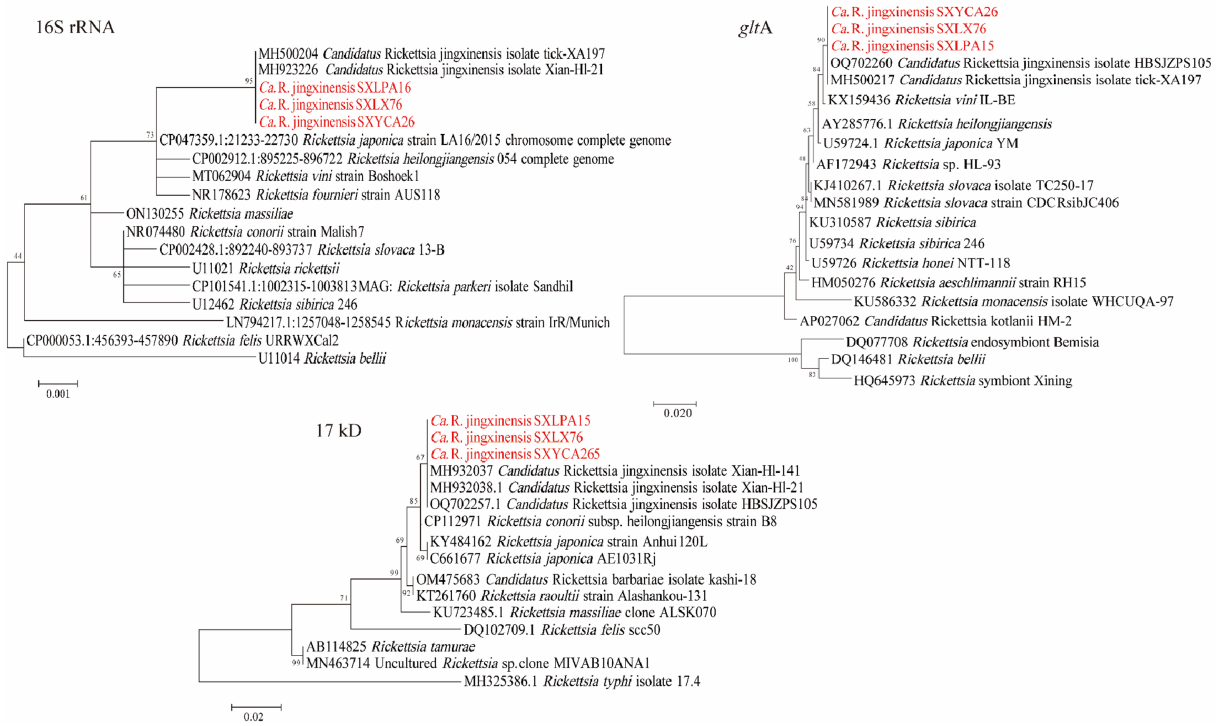

FIGURE 2
Phylogenetic trees of *Rickettsia* strains. The tree was constructed using MEGA 7.0 based on the nucleotide sequences of the 16S rRNA (1,188 bp), gltA (1,000 bp; encoding citrate synthase), and 17kD (440 bp, encoding the 17-kDa antigen) genes. Sequences obtained in this study are marked in red.

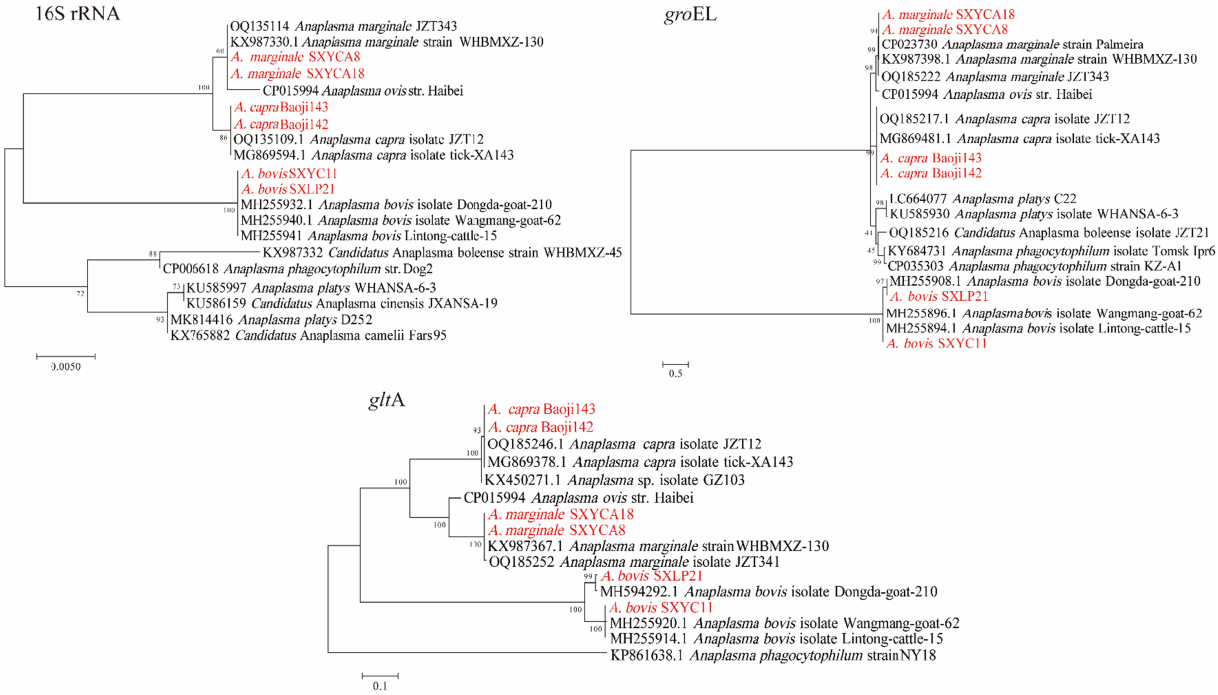

FIGURE 3
Phylogenetic trees of *Anaplasma* strains. The tree was constructed using MEGA 7.0 based on the nucleotide sequences of the 16S rRNA (1,200 bp), gltA (1,000 bp), and groEL (800 bp, encoding the 60 kDa heat shock protein) genes. Sequences obtained in this study are marked in red.

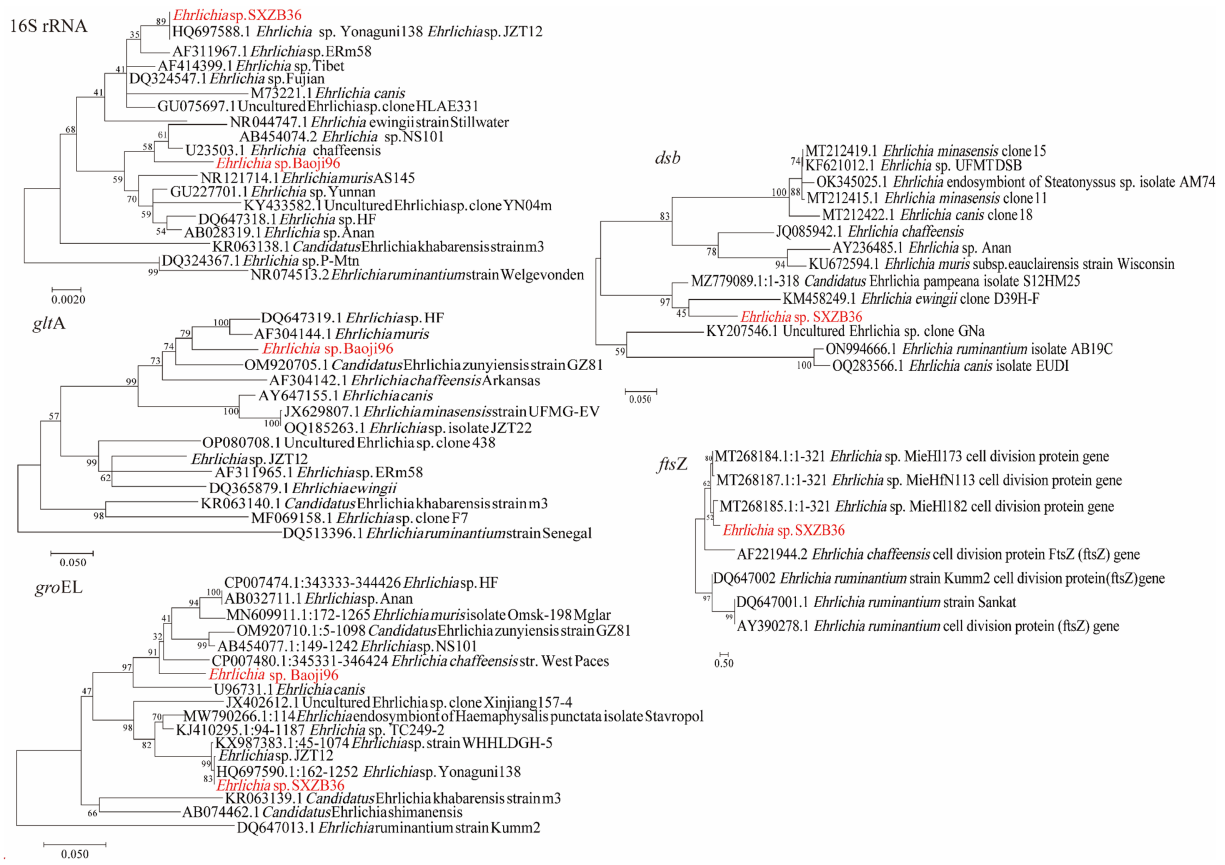

FIGURE 4
Phylogenetic trees of *Ehrlichia* strains. The tree was constructed using MEGA 7.0 based on the nucleotide sequences of the 16S rRNA (1,110 bp), gltA (804 bp), groEL (1,030 bp), dsb (400 bp; encoding the disulfide bond formation protein) and ftsZ (343 bp; encoding a cell division protein) genes. Sequences obtained in this study are marked in red.

3.4 Detection and phylogenic analysis of Ehrlichia

Two *Ehrlichia* species were detected in *H. longicornis* (0.27%, 3/1113). As shown in Figure 4, phylogenetic analysis of the *rrs* and *groEL* gene sequences of one detected from Zhenba revealed that it was most closely related to *E.* sp. *Yonaguni138* (HQ697588) found in Japan (Matsumoto et al., 2011). Its *rrs* and *groEL* genes were 100% identical to that of *Ehrlichia* sp. Yonaguni138. However, its *dsb* gene showed the highest identity (90.28%) to *Ca. E. pampeana* isolate S12HM25, and the *ftsZ* gene showed the highest identity (90.28%) to *Ehrlichia* sp. MieHfN113. This was probably because of the absence of the counterparts of *dsb* and *ftsZ* gene sequences from *Ehrlichia* sp. Yonaguni138 in the GenBank database.

Nucleotide alignment showed that the other *Ehrlichia* species from Baoji City was 99.20% identical to *E. chaffeensis* strain Arkansas (NR_074500) based on the *rrs* gene, 89.69% to *Ehrlichia muris* AS145 (CP006917) based on the *glt*A gene, and 94.91% to *Ehrlichia* sp. NS101 (AB454077) based on the *gro*EL gene. Thus, we believed it represented a putative novel species, which we named as "*Ehrlichia* sp. Baoji96" according to the site where it was detected. To identify Ehrlichial agents at the species level, the 5′-end and 3′-end fragments of the *rrs* gene of *Ehrlichia* sp. Baoji96 was amplified and assembled with the parts already acquired into a complete gene of 1,504 bp. The whole 16S rRNA gene sequence of this novel species was compared with those of other species of *Anaplasma* family using the Clustal W method in the multiple sequence alignment program of DNAStar. It showed that there were interspecific differences between *Ehrlichia* sp. Baoji96 and other *Ehrlichia* species in the hypervariable region at the first 200 bp of the 5′-end of the 16S rRNA gene (Figure 5). The levels of sequence divergences and similarities between the novel species and the strains of Anaplastidae are shown in Figure 6. As can be seen from the table, the entire sequence was most similar to the 16S rRNA gene sequences of *E. chaffeensis*. The similarity is 99.2%, which is less than 99.7%, and is thus in the range for a new species (Qin et al., 2019).

3.5 Co-infection of Rickettsiales in ticks

As is shown in Table 2, co-infection with two Rickettsiales pathogens within an individual tick was detected in 10 (0.90%, 10/1113) ticks. Five (0.45%, 5/1113) ticks were co-infected with *Ca.* R. jingxinensis and *A. bovis*, two (0.18%, 2/1113) ticks were co-infected with *Ca.* R. jingxinensis and *A. capra*, two (0.18%, 2/1113) ticks were co-infected with *Ca.* R. jingxinensis and *A. marginale*, and only one tick was co-infected with *Ca.* R. jingxinensis and *Ehrlichia* spp.

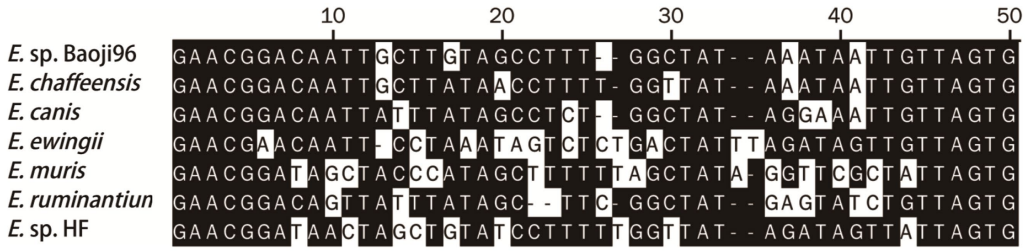

FIGURE 5
The differences in the 16S rRNA gene sequences of *E*. sp. Baoji96 and representative strains of *Ehrlichia* in a 50 bp hypervariable region located at the 5′-end of the 16S rRNA gene after multiple sequence alignment.

Percent Identity

Divergence	1	2	3	4	5	6	7	8	9	10	11	12	13	14	15	16	17	18	19	20	21		
1		99.2	98.1	98.0	97.9	98.2	97.4	94.0	93.7	92.6	92.4	92.4	92.3	92.3	92.2	91.5	84.4	84.6	84.4	86.9	82.4	1	*E.* sp. Baoji96
2	0.8		98.3	98.1	98.0	98.3	97.4	93.9	93.7	92.1	92.1	92.2	91.8	91.8	91.8	91.1	84.1	84.2	83.9	86.5	82.1	2	*E. chaffeensis*
3	1.9	1.7		97.2	98.4	97.6	96.5	93.9	93.9	92.1	92.0	92.1	92.0	92.0	91.9	91.4	84.0	83.7	83.6	86.8	81.7	3	*E.* sp. HF
4	2.1	1.9	2.9		97.2	98.0	97.1	93.4	93.1	92.1	91.9	92.1	92.0	92.0	91.5	91.0	84.0	84.0	83.7	86.5	81.9	4	*E. canis*
5	2.2	2.0	1.6	2.9		97.6	97.0	93.9	94.1	92.2	92.1	92.1	91.8	91.8	91.9	91.4	84.0	84.2	83.9	86.6	82.0	5	*E. muris*
6	1.8	1.7	2.5	2.0	2.5		97.5	94.2	93.6	92.0	91.7	92.1	91.7	91.7	91.6	90.8	83.7	84.0	83.6	86.8	82.3	6	*E. ewingii*
7	2.7	2.7	3.6	2.9	3.1	2.5		94.3	94.2	91.8	91.6	92.1	91.8	91.8	91.7	90.8	84.0	84.2	84.2	86.6	82.1	7	*E. ruminantium*
8	6.3	6.5	6.5	7.0	6.5	6.1	6.0		98.5	91.8	91.7	92.4	92.2	92.2	91.8	91.2	83.9	84.1	83.9	87.4	82.7	8	*Ca.* Neoehrlichia lotoris
9	6.7	6.7	6.5	7.3	6.2	6.7	6.1	1.5		91.4	91.5	92.1	91.7	91.7	91.9	91.1	83.3	83.3	83.2	87.6	82.7	9	*Ca.* Neoehrlichia mikurensis
10	7.8	8.4	8.4	8.4	8.3	8.6	8.7	8.8	9.2		99.2	96.5	98.1	98.2	96.2	95.3	84.2	84.9	84.8	87.0	83.0	10	*A. marginale*
11	8.2	8.5	8.6	8.7	8.4	8.9	9.1	9.0	9.2	0.7		96.1	97.7	97.7	96.0	95.3	84.0	84.7	84.6	86.7	82.6	11	*A. ovis*
12	8.2	8.3	8.4	8.4	8.5	8.5	8.5	8.1	8.4	3.5	4.0		96.1	96.1	98.4	96.8	84.4	85.0	84.7	87.9	83.3	12	*A. phagocytophilum*
13	8.3	8.8	8.6	8.6	8.8	9.0	8.9	8.4	8.9	1.8	2.4	4.1		99.9	95.8	94.6	83.8	84.5	84.3	87.1	83.1	13	*A. centrale*
14	8.3	8.8	8.6	8.6	8.8	9.0	8.9	8.4	8.9	1.8	2.3	4.1	0.1		95.8	94.7	83.8	84.5	84.3	87.1	83.1	14	*A. capra*
15	8.3	8.9	8.7	9.1	8.7	9.0	8.9	8.8	8.7	3.8	4.1	1.6	4.3	4.3		96.8	84.3	84.8	84.6	87.6	83.7	15	*A. platys*
16	9.2	9.6	9.3	9.8	9.3	10.0	9.9	9.5	9.6	4.8	4.9	3.3	5.6	5.5	3.3		83.7	84.0	83.9	86.6	83.4	16	*A. bovis*
17	16.6	17.0	17.1	17.1	17.1	17.5	17.2	17.3	18.0	16.9	17.1	16.6	17.4	17.4	16.7	17.5		94.3	94.4	83.7	80.3	17	*Neorickettsia helminthoeca*
18	17.6	18.0	18.7	18.3	18.1	18.3	18.0	18.2	19.3	17.1	17.4	17.0	17.7	17.7	17.3	18.3	4.9		99.2	83.9	81.3	18	*Neorickettsia sennetsu*
19	17.8	18.4	18.9	18.7	18.6	18.9	18.1	18.4	19.5	17.3	17.7	17.4	18.0	18.0	17.5	18.5	4.8	0.8		83.7	81.0	19	*Neorickettsia risticii*
20	14.7	15.2	14.8	15.2	15.1	14.8	15.1	14.1	13.8	14.6	15.0	13.4	14.5	14.5	13.8	15.1	17.6	18.5	18.9		82.5	20	*Wolbachia pipientis*
21	20.2	20.6	21.1	20.8	20.7	20.3	20.6	19.9	19.9	19.5	20.0	19.0	19.2	19.2	18.5	18.9	21.9	21.8	22.2	20.2		21	*W. melophagi*
	1	2	3	4	5	6	7	8	9	10	11	12	13	14	15	16	17	18	19	20	21		

FIGURE 6
Levels of genetic identity and divergence between *E*. sp. Baoji96 and Anaplasmataceae species in the 16S rRNA gene. Twenty one sequences of representative strains of all genera of Anaplasmataceae were selected. The Clustal W algorithm was used to compare these 21 sequences in pairs and to calculate the genetic distance between them. The values on the upper right are the corrected levels of nucleotide identities for 1,390 bases.

4 Discussion

In the present study, the prevalence and genetic diversity of SFGR, *Anaplasma*, and *Ehrlichia* species in Ticks (Ixodidae) in Shaanxi Province was analyzed using molecular methods. A total of 1,113 ticks, including *H. longicornis*, *Rh. microplus* and *H. flava*, were collected in Shaanxi Province from 2022 to 2023. Among these ticks, one species of *Rickettsia*, two species of *Ehrlichia*, and three species of *Anaplasma* were identified.

The *Rickettsia* species detected in this study was *Ca.* R. jingxinensis, which was first found in Japan (Ishikura et al., 2003) and named in 2016 in Jingxin city, Jilin Province, China (Liu et al., 2016). In recent years, it has been found in both *H. longicornis* and *Rh. microplus* from Liaoning, Hebei, Shaanxi, Anhui, Hubei, and Yunnan provinces of China (Dong et al., 2014; Liu et al., 2016; Wang et al., 2021b; Jin et al., 2023). In addition to *H. longicornis* and *Rh. microplus*, it was also detected in *H. flava* in Shaanxi Province in the present study. The prevalence of *Ca.* R. jingxinensis in the ticks was as high as 20.58%. And our study showed that the *glt*A genes of *Ca.* R. jingxinensis in *H. longicornis*, *Rh. microplus*, and *H. flava* were 100% identical with the *glt*A gene of *R.* sp. strain WHBMXZ-80 and *Ca.* R. longicornii, suggesting an identification of the two organisms as one species, which is consistent with previous reports (Jiang et al., 2018; Jiao et al., 2021). This suggests that *Ca.* R. jingxinensis has a much wider distribution than previously realized and might be emerging as a dominant SFG species in the epidemic distribution of the vector species. Moreover, the *glt*A gene sequence of *Ca.* R. jingxinensis was found in a patient (KU853023) (Guo et al., 2018; Guo et al., 2019a). Furthermore, we found that it can coexist with pathogenic *A. bovis* and *A. capra* in ticks. Hence, we should pay continuous attention to the agent and raise awareness of its potential pathogenicity.

A. bovis, *A. capra*, and *A. marginale* discovered in this study have been identified as human or animal pathogens. *A. bovis* and *A. capra* have emerged as known zoonoses in recent years, which cause considerable harm to both humans and animals (Li et al., 2015; Lu et al., 2019). In 2017, *A. bovis* was reported to be capable of infecting cattle as well as humans (Lu et al., 2019). The emergence of *A. capra* as a human pathogen was observed in Heilongjiang Province in 2015 (Li et al., 2015). Patients infected with these two pathogens have

TABLE 2 Coinfection of *Rickettsia*, *Anaplasma*, and *Ehrlichia* in ticks in Shaanxi Province, China.

Ticks			Coinfection with		
Species	County	No.	*Rickettsia*	*Anaplasma*	*Ehrlichia*
Haemaphysalis longicornis	Zhenba	1	*Ca.* R. jingxinensis		*E.* sp. Yonaguni138
		2	*Ca.* R. jingxinensis	*A. marginale*	
		3	*Ca.* R. jingxinensis	*A. marginale*	
		4	*Ca.* R. jingxinensis	*A. bovis*	
		5	*Ca.* R. jingxinensis	*A. bovis*	
		6	*Ca.* R. jingxinensis	*A. bovis*	
	Baoji	7	*Ca.* R. jingxinensis	*A. bovis*	
		8	*Ca.* R. jingxinensis	*A. bovis*	
		9	*Ca.* R. jingxinensis	*A. capra*	
		10	*Ca.* R. jingxinensis	*A. capra*	

similar clinical symptoms, such as fever, chills, headache, dizziness, myalgia, rash, eschar, and lymphadenopathy (Li et al., 2015; Lu et al., 2019). A previous study showed that infections with *A. bovis* and *A. capra* in goats of Shaanxi Province were frequent in summer, perhaps because the vector ticks were more active in summer (Wang et al., 2021a). In this study, the prevalence of *A. bovis* and *A. capra* were 3.05 and 3.32%, respectively. Although there were not many *A. bovis* and *A. capra* found in this study, combined with previous studies in Shaanxi Province, *A. bovis* and *A. capra* have always existed in Shaanxi Province, suggesting that we should strengthen the investment in vector monitoring and control. Additionally, in Asia, the most important rickettsial disease for cattle is bovine anaplasmosis caused by *A. marginale* (Rodríguez et al., 2009). *A. marginale* is a pathogen belonging to the Rickettsiales, which can cause progressive anemia in ruminants, resulting in huge economic losses (Kumar et al., 2015). A study showed the presence of the disease in more than 50% of cattle sampled in tropical and subtropical regions of Mexico (Rodríguez et al., 2009). The main vectors of *A. marginale* were *Dermacentor* and *Rhipicephalus* ticks (Rodríguez et al., 2009). In this study, the DNA of *A. marginale* was detected for the first time in two *Rh. Microplus* (0.18%) collected in Zhenba County, Shaanxi Province, which proved the prevalence of *A. marginale* in Shaanxi Province. Zhenba County has both a subtropical climate and shows the presence of *A. marginale*, which reminds us that the health of cattle in this area might be facing the problem of *A. marginale* infection.

In recent decades, with the widespread use of laboratory diagnostic methods, the number of new Rickettsiales and their associated diseases has increased, and many bacteria that were previously considered non-pathogenic are now associated with human disease (Lu et al., 2017). For example, the first infection caused by *Rickettsia parkeri* was reported 70 years after it was first identified in *Amblyomma maculatum* ticks (Piotrowski and Rymaszewska, 2020). *Rickettsia slovaca* was first isolated from *Dermacentor marginatus* ticks in Czechoslovakia, several years before the first human cases were reported (Piotrowski and Rymaszewska, 2020). And, in 2021, our research group found an emerging tick-borne pathogen, named as *Ca. Ehrlichia erythraense*, which is associated with human febrile illness discovered in the Dabieshan mountain area of China. The bacteria obtained from the ticks was described as *Ehrlichia* sp. JZT12 (Lu et al., 2023). In the present study, a putative novel *Ehrlichia* species closely related to *E. chaffeensis* was first identified by gene analysis of 16S rRNA in Ixodidae from Shaanxi Province. It was named *Ehrlichia* sp. Baoji96, which showed genetic similarities for the *rrs*, *glt*A, and *gro*EL genes of 99.20% with *E. chaffeensis* strain Arkansas, 89.69% with *Ehrlichia muris* AS145, and 94.91% with *Ehrlichia* sp. NS101, respectively. In addition, the similarities of the *rrs*, *glt*A and *gro*EL genes of *Ehrlichia* sp. Baoji96 and *Ehrlichia* sp. JZT12 were 98.23, 84.24 and 91.39%, respectively. Further research is needed to determine whether this bacteria can cause disease in animals or humans.

5 Conclusion

In this study, we detected Ixodidae parasitized on cattle and goats in warm temperate and subtropical areas of Shaanxi Province, and analyzed the prevalence and genetic diversity of SFGR, *Anaplasma*, and *Ehrlichia* species in Ixodidae in these regions. Shaanxi Province has a diverse terrain and climate, and we have made some new discoveries: *A. marginale* was detected for the first time in *Rh. microplus* collected in Zhenba County, and a novel *Ehrlichia* species closely related to *E. chaffeensis* was first identified in *H. longicornis*. For tick-borne diseases, tick prevention is the key to avoiding infection. Hence, continuous surveillance of Rickettsiales pathogens in Chinese ticks should be conducted to assess the potential risk of transmission to animals and humans by colonizing species in disease-causing pathogens or vectors. This study provides a reference for the formulation of biological control strategies for ticks and tick-borne diseases in this area, and could improve the control effect.

Data availability statement

The original contributions presented in the study are publicly available. This data can be found at: https://www.ncbi.nlm.nih.gov/; OR513096-OR513098, OR520945- OR520951, OR526930- OR526952.

Ethics statement

The manuscript presents research on animals that do not require ethical approval for their study.

Author contributions

XZ: Methodology, Writing – original draft, Writing – review & editing. WL: Methodology, Writing – original draft, Writing – review & editing. ZT: Investigation, Methodology, Writing – review & editing. NZ: Investigation, Methodology, Writing – review & editing. YZ: Investigation, Methodology, Writing – review & editing. DM: Investigation, Methodology, Writing – review & editing. LM: Investigation, Methodology, Writing – review & editing. YC: Data curation, Software, Writing – review & editing. JW: Data curation, Software, Writing – review & editing. JH: Conceptualization, Data curation, Software, Writing – review & editing. WM: Writing – review & editing. DL: Writing – original draft, Writing – review & editing. TQ: Writing – original draft, Writing – review & editing.

Funding

The author(s) declare financial support was received for the research, authorship, and/or publication of this article. This work was supported by grants from the National Natural Science Foundation of China (grant number 81671985), the Science Foundation for the State Key Laboratory for Infectious Disease Prevention and Control of China (grant numbers 2022SKLID209 and 2019SKLID403), and the Public Health Service Capability Improvement Project of the National Health Commission of the People's Republic of China (grant number 2100409002).

Conflict of interest

The authors declare that the research was conducted in the absence of any commercial or financial relationships that could be construed as a potential conflict of interest.

Publisher's note

All claims expressed in this article are solely those of the authors and do not necessarily represent those of their affiliated organizations, or those of the publisher, the editors and the reviewers. Any product that may be evaluated in this article, or claim that may be made by its manufacturer, is not guaranteed or endorsed by the publisher.

Supplementary material

The Supplementary material for this article can be found online at: https://www.frontiersin.org/articles/10.3389/fmicb.2023.1331434/full#supplementary-material

References

Bakken, J. S., Dumler, J. S., Chen, S. M., Eckman, M. R., Van Etta, L. L., and Walker, D. H. (1994). Human granulocytic ehrlichiosis in the upper Midwest United States. A new species emerging? *JAMA* 272, 212–218. doi: 10.1001/jama.1994.03520030054028

Beati, L., Meskini, M., Thiers, B., and Raoult, D. (1997). *Rickettsia aeschlimannii* sp. nov., a new spotted fever group rickettsia associated with *Hyalomma marginatum* ticks. *Int. J. Syst. Bacteriol.* 47, 548–554. doi: 10.1099/00207713-47-2-548

Chochlakis, D., Ioannou, I., Tselentis, Y., and Psaroulaki, A. (2010). Human anaplasmosis and *Anaplasma ovis* variant. *Emerg. Infect. Dis.* 16, 1031–1032. doi: 10.3201/eid1606.090175

Dong, X., Chen, X.-P., Liu, N., Dumler, S. J., and Zhang, Y.-Z. (2014). Co-circulation of multiple species of Rickettsiales bacteria in one single species of hard ticks in Shenyang, China. *Ticks Tick Borne Dis.* 5, 727–733. doi: 10.1016/j.ttbdis.2014.05.011

Guo, W.-P., Huang, B., Zhao, Q., Xu, G., Liu, B., Wang, Y.-H., et al. (2018). Human-pathogenic Anaplasma spp., and Rickettsia spp. in animals in Xi'an, China. *PLoS Negl. Trop. Dis.* 12:e0006916. doi: 10.1371/journal.pntd.0006916

Guo, W.-P., Wang, Y.-H., Lu, Q., Xu, G., Luo, Y., Ni, X., et al. (2019a). Molecular detection of spotted fever group rickettsiae in hard ticks, northern China. *Transbound. Emerg. Dis.* 66, 1587–1596. doi: 10.1111/tbed.13184

Guo, W.-P., Zhang, B., Wang, Y.-H., Xu, G., Wang, X., Ni, X., et al. (2019b). Molecular identification and characterization of Anaplasma capra and *Anaplasma platys*-like in *Rhipicephalus microplus* in Ankang, Northwest China. *BMC Infect. Dis.* 19:434. doi: 10.1186/s12879-019-4075-3

Ishikura, M., Ando, S., Shinagawa, Y., Matsuura, K., Hasegawa, S., Nakayama, T., et al. (2003). Phylogenetic analysis of spotted fever group rickettsiae based on gltA, 17-kDa, and rOmpA genes amplified by nested PCR from ticks in Japan. *Microbiol. Immunol.* 47, 823–832. doi: 10.1111/j.1348-0421.2003.tb03448.x

Ismail, N., Bloch, K. C., and McBride, J. W. (2010). Human ehrlichiosis and anaplasmosis. *Clin. Lab. Med.* 30, 261–292. doi: 10.1016/j.cll.2009.10.004

Jiang, J., An, H., Lee, J. S., O'Guinn, M. L., Kim, H.-C., Chong, S.-T., et al. (2018). Molecular characterization of *Haemaphysalis longicornis*-borne rickettsiae, Republic of Korea and China. *Ticks Tick Borne Dis.* 9, 1606–1613. doi: 10.1016/j.ttbdis.2018.07.013

Jiao, J., Zhang, J., He, P., OuYang, X., Yu, Y., Wen, B., et al. (2021). Identification of tick-borne pathogens and genotyping of *Coxiella burnetii* in *Rhipicephalus microplus* in Yunnan Province, China. *Front. Microbiol.* 12:736484. doi: 10.3389/fmicb.2021.736484

Jin, X., Liao, J., Chen, Q., Ding, J., Chang, H., Lyu, Y., et al. (2023). Diversity of Rickettsiales bacteria in five species of ticks collected from Jinzhai County, Anhui Province, China in 2021-2022. *Front. Microbiol.* 14:1141217. doi: 10.3389/fmicb.2023.1141217

Johnson, D. K. H., Schiffman, E. K., Davis, J. P., Neitzel, D. F., Sloan, L. M., Nicholson, W. L., et al. (2015). Human infection with *Ehrlichia muris*-like pathogen, United States, 2007-2013(1). *Emerg. Infect. Dis.* 21, 1794–1799. doi: 10.3201/eid2110.150143

Kumar, S., Stecher, G., and Tamura, K. (2016). MEGA7: molecular evolutionary genetics analysis version 7.0 for bigger datasets. *Mol. Biol. Evol.* 33, 1870–1874. doi: 10.1093/molbev/msw054

Kumar, T., Sindhu, N., Charaya, G., Kumar, A., Kumar, P., Chandratere, G., et al. (2015). Emerging status of anaplasmosis in cattle in Hisar. *Vet. World* 8, 768–771. doi: 10.14202/vetworld.2015.768-771

Labruna, M. B., Santos, F. C. P., Ogrzewalska, M., Nascimento, E. M. M., Colombo, S., Marcili, A., et al. (2014). Genetic identification of rickettsial isolates from fatal cases of Brazilian spotted fever and comparison with *Rickettsia rickettsii* isolates from the American continents. *J. Clin. Microbiol.* 52, 3788–3791. doi: 10.1128/JCM.01914-14

Li, H., Zheng, Y.-C., Ma, L., Jia, N., Jiang, B.-G., Jiang, R.-R., et al. (2015). Human infection with a novel tick-borne Anaplasma species in China: a surveillance study. *Lancet Infect. Dis.* 15, 663–670. doi: 10.1016/S1473-3099(15)70051-4

Liu, H., Li, Q., Zhang, X., Li, Z., Wang, Z., Song, M., et al. (2016). Characterization of rickettsiae in ticks in northeastern China. *Parasit. Vectors* 9:498. doi: 10.1186/s13071-016-1764-2

Lu, M., Chen, Q., Qin, X., Lyu, Y., Teng, Z., Li, K., et al. (2022). *Anaplasma bovis* infection in fever and thrombocytopenia patients - Anhui Province, China, 2021. *China CDC Week.* 4, 249–253. doi: 10.46234/ccdcw2022.053

Lu, M., Li, F., Liao, Y., Shen, J.-J., Xu, J.-M., Chen, Y.-Z., et al. (2019). Epidemiology and diversity of Rickettsiales Bacteria in humans and animals in Jiangsu and Jiangxi provinces, China. *Sci. Rep.* 9:13176. doi: 10.1038/s41598-019-49059-3

Lu, M., Qin, X.-C., Jiang, Y.-Z., Guo, Q., Jin, X.-J., Teng, Z.-Q., et al. (2023). Emergence of ehrlichiosis by a new tick-borne Ehrlichia species in China. *Int. J. Infect. Dis.* 131, 32–39. doi: 10.1016/j.ijid.2023.03.038

Lu, M., Tian, J.-H., Yu, B., Guo, W.-P., Holmes, E. C., and Zhang, Y.-Z. (2017). Extensive diversity of rickettsiales bacteria in ticks from Wuhan, China. *Ticks Tick Borne Dis.* 8, 574–580. doi: 10.1016/j.ttbdis.2017.03.006

Mahara, F. (1997). Japanese spotted fever: report of 31 cases and review of the literature. *Emerg. Infect. Dis.* 3, 105–111. doi: 10.3201/eid0302.970203

Matsumoto, K., Takeuchi, T., Yokoyama, N., Katagiri, Y., Ooshiro, M., Zakimi, S., et al. (2011). Detection of the new Ehrlichia species closely related to *Ehrlichia ewingii* from *Haemaphysalis longicornis* in Yonaguni Island, Okinawa, Japan. *J. Vet. Med. Sci.* 73, 1485–1488. doi: 10.1292/jvms.11-0007

Paddock, C. D., and Childs, J. E. (2003). *Ehrlichia chaffeensis*: a prototypical emerging pathogen. *Clin. Microbiol. Rev.* 16, 37–64. doi: 10.1128/CMR.16.1.37-64.2003

Pasquale Mansueto, G. V., Cascio, A., Seidita, A., Pepe, I., Carroccio, A., di Rosa, S., et al. (2012). New insight into immunity and immunopathology of Rickettsial diseases. *Clin. Dev. Immunol.* 2012, 1–26. doi: 10.1155/2012/967852

Peng-Fei, Y., Qing-Li, Y., Qi, S. U., Fang, H. E., Li, T., Ya-Dong, X., et al. (2018). Application of DNA barcoding technolodge based on the mitochondrial gene COI to identify *Haemaphysalis longicornis* along the Yangtse River in Jiangsu province. *Jiangsu J. Prevent. Med.* doi: 10.3724/sp.j.1035.2009.00271

Piotrowski, M., and Rymaszewska, A. (2020). Expansion of tick-borne rickettsioses in the world. *Microorganisms* 8. doi: 10.3390/microorganisms8121906

Qin, X. R., Han, H. J., Han, F. J., Zhao, F. M., Zhang, Z. T., Xue, Z. F., et al. (2019). Rickettsia japonica and novel Rickettsia species in ticks, China. *Emerg. Infect. Dis.* 25, 992–995. doi: 10.3201/eid2505.171745

Robinson, M. T., Satjanadumrong, J., Hughes, T., Stenos, J., and Blacksell, S. D. (2019). Diagnosis of spotted fever group Rickettsia infections: the Asian perspective. *Epidemiol. Infect.* 147:e286. doi: 10.1017/S0950268819001390

Rodríguez, S. D., Ortiz, M. Á. G., Ocampo, R. J., and Murguía, C. A. V. Y. (2009). Molecular epidemiology of bovine anaplasmosis with a particular focus in Mexico. *Infect. Genet. Evol.* 9, 1092–1101. doi: 10.1016/j.meegid.2009.09.007

Sebastian, S. A., Co, E. L., Mehendale, M., Sudan, S., Manchanda, K., and Khan, S. (2022). Challenges and updates in the diagnosis and treatment of infective endocarditis. *Curr. Probl. Cardiol.* 47:101267. doi: 10.1016/j.cpcardiol.2022.101267

Teng, K.F., and Jiang, Z.J. (1991). Economic insect fauna of China, Fasc 39 Acari: Ixodidae (in Chinese).

Teng, Z., Gong, P., Wang, W., Zhao, N., Jin, X., Sun, X., et al. (2023a). Clinical forms of Japanese spotted fever from case-series study, Zigui County, Hubei Province, China, 2021. *Emerg. Infect. Dis.* 29, 202–206. doi: 10.3201/eid2901.220639

Teng, Z., Shi, Y., Zhao, N., Zhang, X., Jin, X., He, J., et al. (2023b). Molecular detection of tick-borne bacterial and protozoan pathogens in *Haemaphysalis longicornis* (Acari: Ixodidae) Ticks from free-ranging domestic sheep in Hebei Province, China. *Pathogens (Basel, Switzerland)* 12. doi: 10.3390/pathogens12060763

Thomas, R. J., Dumler, J. S., and Carlyon, J. A. (2009). Current management of human granulocytic anaplasmosis, human monocytic ehrlichiosis and *Ehrlichia ewingii* ehrlichiosis. *Expert Rev. Anti-Infect. Ther.* 7, 709–722. doi: 10.1586/eri.09.44

Wang, K., Yan, Y., Zhou, Y., Zhao, S., Jian, F., Wang, R., et al. (2021a). Seasonal dynamics of Anaplasma spp. in goats in warm-temperate zone of China. *Ticks Tick Borne Dis.* 12:101673. doi: 10.1016/j.ttbdis.2021.101673

Wang, Q., Guo, W.-B., Pan, Y.-S., Jiang, B.-G., Du, C.-H., Que, T.-C., et al. (2021b). Detection of novel spotted fever group Rickettsiae (Rickettsiales: Rickettsiaceae) in ticks (Acari: Ixodidae) in southwestern China. *J. Med. Entomol.* 58, 1363–1369. doi: 10.1093/jme/tjaa294

Wen, B., Jian, R., Zhang, Y., and Chen, R. (2002). Simultaneous detection of Anaplasma marginale and a new Ehrlichia species closely related to *Ehrlichia chaffeensis* by sequence analyses of 16S ribosomal DNA in *Boophilus microplus* ticks from Tibet. *J. Clin. Microbiol.* 40, 3286–3290. doi: 10.1128/JCM.40.9.3286-3290.2002

Zeidler, H., and Hudson, A. P. (2021). Reactive arthritis update: spotlight on new and rare infectious agents implicated as pathogens. *Curr. Rheumatol. Rep.* 23:53. doi: 10.1007/s11926-021-01018-6

Zhang, Y.-K., Zhang, X.-Y., and Liu, J.-Z. (2019). Ticks (Acari: Ixodoidea) in China: geographical distribution, host diversity, and specificity. *Arch. Insect Biochem. Physiol.* 102:e21544. doi: 10.1002/arch.21544

frontiers | Frontiers in Microbiology

TYPE Original Research
PUBLISHED 26 February 2024
DOI 10.3389/fmicb.2024.1365356

Check for updates

OPEN ACCESS

EDITED BY
Guang-hui Zhao,
Northwest A&F University, China

REVIEWED BY
Wen-Ping Guo,
Chengde Medical University, China
Yuan Fang,
National Institute of Parasitic Diseases (China), China
Shaoqiang Wu,
Chinese Academy of Inspection and Quarantine (CAIQ), China
Si-Yang Huang,
Yangzhou University, China

*CORRESPONDENCE
Ze Chen
✉ chenze@yeah.net
Xiaolong Yang
✉ yangxl@hebtu.edu.cn

RECEIVED 04 January 2024
ACCEPTED 01 February 2024
PUBLISHED 26 February 2024

CITATION
Xu X, Gao Z, Wu Y, Yin H, Ren Q, Zhang J, Liu Y, Yang S, Bayasgalan C, Tserendorj A, Yang X and Chen Z (2024) Discovery and vertical transmission analysis of Dabieshan Tick Virus in *Haemaphysalis longicornis* ticks from Chengde, China.
Front. Microbiol. 15:1365356.
doi: 10.3389/fmicb.2024.1365356

COPYRIGHT
© 2024 Xu, Gao, Wu, Yin, Ren, Zhang, Liu, Yang, Bayasgalan, Tserendorj, Yang and Chen. This is an open-access article distributed under the terms of the Creative Commons Attribution License (CC BY). The use, distribution or reproduction in other forums is permitted, provided the original author(s) and the copyright owner(s) are credited and that the original publication in this journal is cited, in accordance with accepted academic practice. No use, distribution or reproduction is permitted which does not comply with these terms.

Discovery and vertical transmission analysis of Dabieshan Tick Virus in *Haemaphysalis longicornis* ticks from Chengde, China

Xiaofeng Xu[1], Zhihua Gao[1], Youhong Wu[1], Hong Yin[2], Qiaoyun Ren[2], Jie Zhang[3], Yongsheng Liu[3], Shunli Yang[3], Chimedtseren Bayasgalan[4], Ariunaa Tserendorj[4], Xiaolong Yang[1]* and Ze Chen[1]*

[1]Hebei Key Laboratory of Animal Physiology, Biochemistry and Molecular Biology, Hebei Collaborative Innovation Center for Eco-Environment, Ministry of Education Key Laboratory of Molecular and Cellular Biology, College of Life Sciences, Hebei Normal University, Shijiazhuang, China, [2]State Key Laboratory of Animal Disease Prevention and Control, Key Laboratory of Veterinary Parasitology of Gansu Province, Lanzhou Veterinary Research Institute, Chinese Academy of Agricultural Science, Lanzhou, Gansu, China, [3]Hebei Key Laboratory of Preventive Veterinary Medicine, College of Animal Science and Technology, Hebei Normal University of Science and Technology, Qinhuangdao, China, [4]School of Veterinary Medicine, Mongolian University of Life Sciences, Ulaanbaatar, Mongolia

Introduction: Ticks are important blood-sucking ectoparasites that can transmit various pathogens, posing significant threats to the wellbeing of humans and livestock. Dabieshan tick virus (DBTV) was initially discovered in 2015 in *Haemaphysalis longicornis* ticks from the Dabieshan mountain region in Hubei Province, China. In recent years, DBTV has been discovered in various regions of China, including Shandong, Zhejiang, Liaoning, Hubei, Yunnan, and Guizhou Provinces. However, the researches on tick-borne transmission of DBTV are scarce.

Methods: This study utilized the small RNA sequencing (sRNA-seq) method to identify tick-associated viruses in ticks collected from Chengde in Hebei Province and Yongcheng in Henan Province, leading to the discovery of a new DBTV strain in Hebei. The complete coding genome of DBTV Hebei strain was obtained through RNA-seq and Sanger sequencing. Furthermore, the transmission experiment of DBTV in *H. longicornis* was examined in laboratory for the first time.

Results: DBTV was detected in newly molted adult *H. longicornis* ticks collected in Chengde, Hebei Province. Additionally, DBTV was also detected in both unfed nymphs and engorged females of *H. longicornis* collected from Chengde, with a positive rate of 20% and 56.25%, respectively. The complete coding genome of DBTV (OP682840 and OP716696) were obtained, and phylogenetic analysis revealed that the DBTV Hebei strain clustered with previously reported DBTV strains. Furthermore, this virus was observed in engorged females, eggs, and larvae of the subsequent generation.

Discussion: It is necessary to expand the scope of DBTV investigation, particularly in northern China. This study demonstrated that DBTV can be transmitted from engorged females to larvae of the next generation. Moreover, the detection of DBTV in unfed nymphs and adults (which moulted from engorged nymphs) collected from the filed of Chengde suggests that *H. longicornis* serves as a potential transmission host and reservoir for DBTV through transstadial and transovarial transmission. However, there remains a lack of research on the isolation and pathogenicity of DBTV, highlighting the need for further studies to mitigate potential harm to the health of animals and humans.

KEYWORDS

Haemaphysalis longicornis, Dabieshan Tick Virus, ticks, transstadial transmission, transovarial transmission, Hebei Province

Introduction

Ticks are important zoonotic ectoparasites that not only feed on blood but also carry viruses, bacteria, rickettsia, protozoa, and other pathogens, leading to the transmission of a variety of diseases (Chen and Yang, 2021). With economic development and the increasing human activity, tick-borne viruses (TBVs) are increasingly regarded as a major threat to the health of animals and humans (Contreras et al., 2015). Since the first tick-borne virus that Louping ill virus was identified in 1918 (Stockman, 1919), more than 100 TBVs have been identified and classified into two orders, nine families, at least 12 genera, as well as some unassigned TBVs (Shi et al., 2018). With the reduction of the cost of high-throughput sequencing and the upgrade of high-throughput data analysis software, metatranscriptomic (metavirome) is widely used to detect TBVs. Consequently, numerous novel viral sequences have been discovered and described in ticks worldwide in recent years (Damian et al., 2020). However, it is important to note that while these viruses are found in ticks, they may originate from the host blood, so they should be called tick carry viruses (Migné et al., 2022). Tick-borne viruses differ from tick carry viruses in that can replicate in host cells and tick cells. To determine a specific tick species as a transmission vector of a tick-borne virus, it is necessary to confirm that ticks can be infected with the virus from the bloodmeal, and that the virus can persist in tick tissues and be transmitted to the next developmental stage. Additionally, ticks can transmit the virus to host animals during the parasitic stage (Nuttall, 2009). In recent years, some transmission experiments have shown that *Haemaphysalis longicornis* may be a competent vector for some deadly viral pathogens. *Haemaphysalis longicornis* maintains and transmits severe fever with thrombocytopenia syndrome virus (SFTSV), which is an effective carrier for transmitting this virus in transovarial and transstadial modes (Zhuang et al., 2018). In 2022, it was reported that Heartland virus (HRTV) can infect *H. longicornis* after microinjection under laboratory conditions, and be transmitted vertically through eggs (Raney et al., 2022). Mice can be employed as a basis for forming direct tick infection or as a model for the secondary evaluation of these and other feasible natural vertebrate host candidates for HRTV transmission (Bosco-Lauth et al., 2016). Furthermore, studies have shown successful infection of adult *H. longicornis* with Langat virus (LGTV) which was successfully transmitted to susceptible mice.

Dabieshan Tick Virus (DBTV) was initially discovered in 2015 in *H. longicornis* ticks from Dabieshan mountain region in Hubei Province, China (Li et al., 2015). This tick-associated virus is a member of the genus *Uukuvirus* within the family *Phenuiviridae* of the order *Bunyavirales*. Most of the viruses in the *Uukuvirus* genus were newly identified, such as Yongjia virus and Pacific coast tick virus. Their potential threat to humans and livestock is still unclear. However, in 2019, Tacheng tick virus 2 (TCTV-2) was detected in humans, causing fever, headache, and multiple clinical symptoms in China (Dong et al., 2021). The RNA genome of DBTV consists of two segments: small (S) and large (L) segments. The L segment encodes the virus RNA-dependent RNA polymerase, and the S segment encodes nucleocapsid protein (N) and nonstructural protein (NSs) (Bouloy and Weber, 2010). As of now, the full-length coding genomes of the L and S segments of the DBTV have been published. In recent years, DBTV has been discovered in various regions of China, including Shandong (Shao et al., 2021), Zhejiang (He et al., 2022), Liaoning (Yang et al., 2021), Hubei, Yunnan, and Guizhou Provinces (Wang et al., 2021). Epidemiological investigations have shown that DBTV is widely disseminated in Linyi, Tai'an, Weifang, Yantai (Ma et al., 2022), and Rizhao city of Shandong Province (Shao et al., 2020) and phylogenetic analysis revealed distinct lineages of DBTV (Ma et al., 2022). The results of PCR showed that the prevalence rate of DBTV was 30.3% in Zhoushan of Zhejiang Province (Zhu et al., 2020). Furthermore, the L segment of Dabieshan Tick Virus, DBTV was detected in *H. longicornis* ticks collected in South Korea in 2021 by high-throughput sequencing technique (Pérez-Sautu et al., 2021). In 2023, a survey by qRT-PCR of tick-associated pathogens found that DBTV exists in both larvae and adults of *H. longicornis* ticks in Cape Toi, Japan with a positive rate of 37.0 and 23%, respectively (Mekata et al., 2023). Other tick species such as *Rhipicephalus microplus* and *R. haemaphysaloides*, have also been discovered to carry DBTV (Ma et al., 2022). However, researchers have failed to isolate DBTV from positive tick sample (Wang et al., 2021). The available literature shows that research on ticks in DBTV transmission is scarce.

In 2009, Kreuze developed a virus detection technology based on small RNA (sRNA) deep sequencing (Kreuze et al., 2009). This method has been successfully applied to detect *Rickettsia*, *Coxiella*, and *Aspergillus* in wild *H. longicornis* ticks (Zhuang et al., 2014). Our previous study has also demonstrated the reliability and sensitivity of sRNA-seq in detecting tick-associated viruses, and founded Mogiana tick virus in *Amblyomma testudinarium* ticks (Xu et al., 2020). In this study, sRNA-seq method was used to detect the presence of tick-associated viruses in *H. longicornis* ticks collected from Chengde of Hebei Province and Yongcheng of Henan Province. Additionally, PCR amplification was used to examine the eggs and larvae of DBTV-infected ticks in a laboratory setting, aiming to elucidate the transmission dynamics of DBTV in *H. longicornis*.

Materials and methods

Tick collection and identification

Free-living ticks on vegetation were collected by dragging flags, and parasitic ticks were collected from sheep by using tweezers. The morphological features of ticks were examined under a stereomicroscope morphologically, following to a reference book (Chen and Yang, 2021). Engorged nymphs of *H. longicornis* ticks were collected from sheep (*Ovis aries*) in Chengde, Hebei Province in 2021. The engorged nymphs were placed in a climatic incubator [(25 ± 1°C), 90% RH, 12 h daylight] in the laboratory and molted to adults. In 2022, unfed adult *H. longicornis* ticks were collected from Yongcheng in Henan Province. Additionally, bloated blood-filled adult ticks of *H. longicornis* were collected from sheep, and the unfed nymphs were collected from vegetation in Chengde, Hebei province. Blood-filled adult *H. longicornis* ticks collected in Chengde, Hebei Province were placed in a climate incubator to lay eggs, which then hatched into

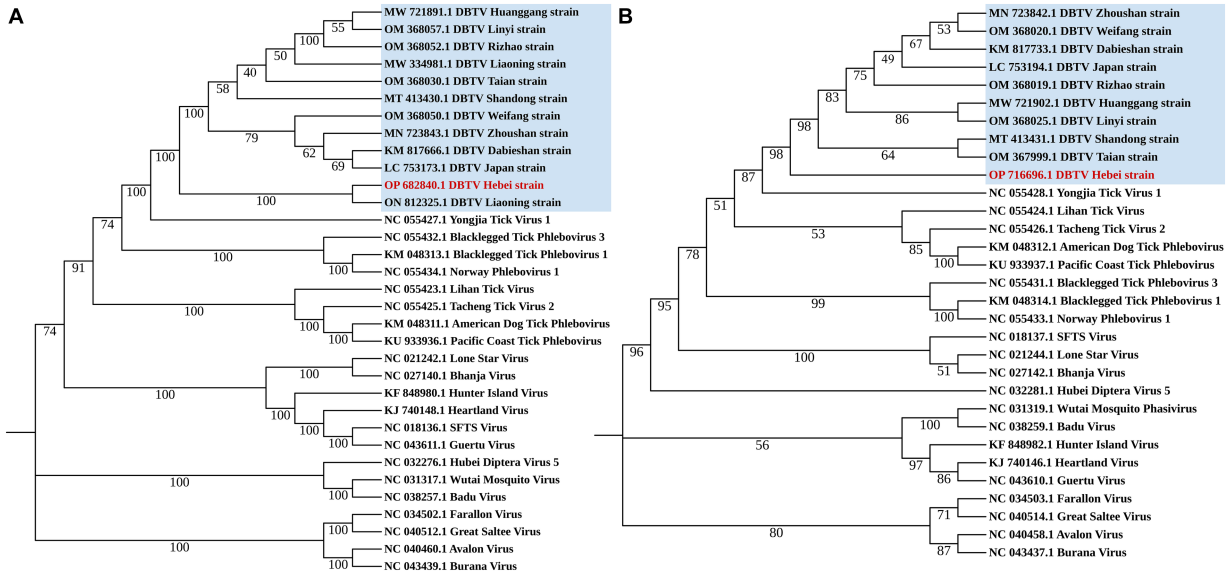

FIGURE 1
Phylogenetic analysis Dabieshan Tick Virus Hebei strain. Maximum Likelihood phylogenetic trees were build based on a 6,182 bp nucleotide sequence of the L segment **(A)** and a 993 bp nucleotide sequence of the S segment **(B)**.

larvae. Furthermore, newly molted adult ticks, bloated blood-filled adult ticks, eggs and larvae of *H. longicornis* from Chengde were utilized for further research. All sample information in this study is available in Supplementary Table 1.

RNA extraction and DBTV detection by RNA-seq

Ticks were frozen in liquid nitrogen or stored at −80°C until total RNA was extracted. The total RNA was extracted by RNAiso Plus* (Takara, Code No.9109). Subsequently, the quality and quantity of total RNA were assessed using Agilent 2000 Bioanalyzer and Agarose gel electrophoresis. The RNA samples were then sent to BGI-Wuhan, China for sRNA sequencing using HiSeq 2500 platform of Illumina. According to the guidelines for building the sRNA library provided by Illumina, the special reagent Ribo-Zero-Gold (Human-Mouse-Rat) Kit (Illumina) was used to remove ribosomal RNA. The sequencing strategy was Single-end (50 bp) of each small RNA library. Raw data assessment and quality control were performed using the software FASTQC (v0.11.5). Adapter and other illumina-specific sequences were removed and low-quality reads were filtered using the software Trimmomatic (Version 0.32). The detection of DBTV was performed by using pipeline VirusDetect[1] software package (Zheng et al., 2017). Genome coverage was calculated as the proportion of positions covered by reads divided by the length of the genome, while average depth was determined by dividing the total number of base pairs in aligned reads by the number of read-covered positions in the reference genome. Statistical calculations and drawings were performed using R v4.3.2 software and the Bioconductor package.

1 http://bioinfo.bti.cornell.edu/tool/VirusDetect/

DBTV complete coding genome acquisition and phylogenetic analysis of DBTV

The small RNA sequence were mapped to the reference genome of DBTV Dabieshan strain (KM817666 and KM817733) by BWA (Li and Durbin, 2009). The .sam file generated by BWA was converted to a .pileup file using SAMtools (Danecek et al., 2021). A perl script was used to obtain sequences that are consistent with the reference genome. Four pairs of specific primers were designed for PCR amplification to fill the gaps in the sequence (Supplementary Table 2). Then, according to the latest Virus Metadata Resource (VMR) released by International Committee on Taxonomy of Viruses (ICTV) 2023, several viruses of *Bunyavirales* were downloaded from NCBI. All sequences were aligned using BioEdit 7.0 software. To determine the phylogenetic status of DBTV Hebei strain, a phylogenetic tree was constructed based on polymorphisms from the L and S segments of the DBTV and some other viruses in *Bunyavirales* (Figure 1). The rate of evolutionary divergence between sequences was modeled with a gamma distribution (shape parameter = 1). MEGA 11 was also used to build Maximum-Likelihood (ML) trees (Koichiro et al., 2021). The L and S segments were analyzed with GTR + G + I and K2 + G models, respectively. The bootstrap values were calculated from 1,000 replicates.

Detection of DBTV transmission in *Haemaphysalis longicornis* by PCR

RNA from female ticks that survived after 7 days of oviposition, eggs and larvae were extracted using Trizol, respectively. RNA was extracted from 200 free-living nymphs of *H. longicornis* collected on vegetation in Chengde, of which 20 individuals were taken as a sample. All RNA was reverse transcribed into cDNA using the

RevertAid First Strand cDNA Synthesis Kit (Thermo Scientific, Code No. K1622). Primer sets DBSV-F (AGG ATG TGG AGC CAG TGA TC) and DBSV-R (ATC TGG TCC TGG AAG TGC TC) were designed to detect DBTV in ticks by PCR amplification. The PCR reaction mixture was incubated at 95°C for 1 min, followed by 35 PCR cycles (30 s at 95°C, 30 s at 55°C, and 20 s at 72°C for each cycle). In order to confirm the positive samples, the PCR amplification products were recovered by Wizard® SV Gel and PCR Clean-Up System (Promega, Code No. A9281) and subsequent sequencing.

Results

Tick collection and DBTV detection by RNA-seq

The ticks were morphologically identified as *H. longicornis* ticks in this study. The RNA of 27 newly molted adult *H. longicornis* ticks collected in Chengde and 44 unfed adult ticks in Yongcheng was extracted and subjected to library construction and small RNA sequencing, respectively. The raw data generated from high-throughput sequencing were uploaded to the NCBI Sequence Read Archive database (SAMN27533436). VirusDetect results revealed that recently molted adult *H. longicornis* ticks collected from Chengde, Hebei Province were infected with DBTV. The sRNA-seq analysis of this DBTV Hebei strain revealed that 95.67% of RNA-dependent RNA polymerase protein gene of DBTV Dabieshan strain (KM817666.1) was covered with an average depth of 309.8. Furthermore, 46.6% of the nucleopasid protein and nonstructural protein genes of DBTV Dabieshan strain (KM817733.1) were covered with an average depth of 18.0 (Figure 2A). However, the virus was not detected in *H. longicornis* collected from Yongcheng City (Figure 2B).

Complete coding genome and phylogenetic analysis of DBTV Hebei strain

The small RNA data were mapped to the reference genomes of DBTV Dabieshan strain (KM817666.1, KM817733.1) using the BWA software. The sRNA sequencing results were combined with the results of Sanger sequencing to obtain the complete coding genome of DBTV Hebei strain. The L and S segments of DBTV Hebei strain, with lengths of 6,549 and 1,789 bp were submitted to the NCBI GenBank database with project accession numbers OP682840 and OP716696, respectively. Nucleotide-level nucleic acid sequence alignment revealed that DBTV Hebei strain and DBTV Dabieshan strain (KM817666.1) showed 95.79% identity in the L segment, with the highest identity of 99.69% observed in DBTV Liaoning strain (ON812325.1). DBTV Hebei strain and DBTV Dabieshan

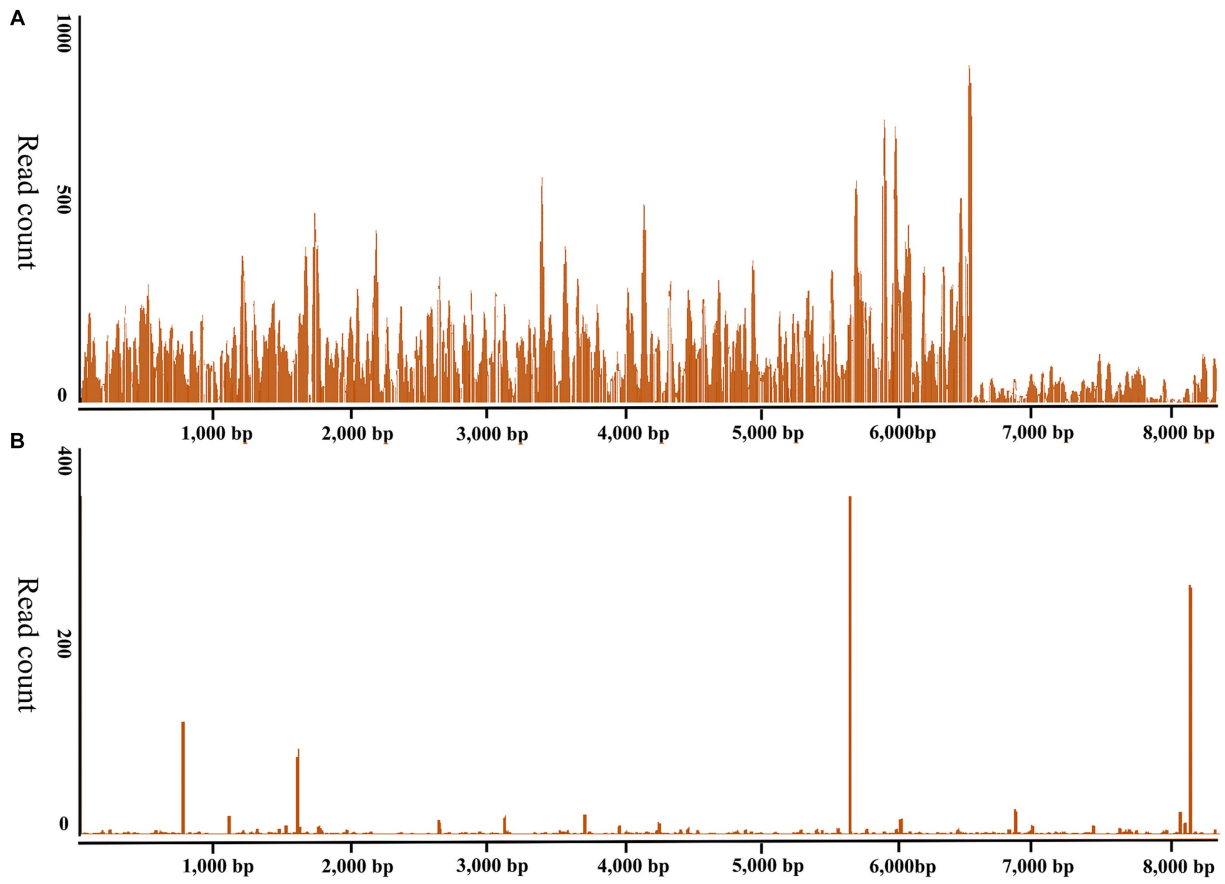

FIGURE 2
Genome coverage of the Dabieshan Tick Virus Hebei strain. The *y*-axis displays the read-counts for each position on the genome, while the *x*-axis shows the positions on the reference genome of the DBTV strain Hubei (GenBank: KM817666.1, KM817733.1). **(A)** *Haemaphysalis longicornis* ticks from Chengde, Hebei Province were used to produce the sRNA-seq data. **(B)**. *Haemaphysalis longicornis* ticks from Yongcheng, Henan Province were used to produce the sRNA-seq data for negative control.

strain (KM817733.1) showed 94.31% identity in the S segment, with the highest identity of 94.53% observed in DBTV Shandong strain (MT413431.1). The results of the genetic distance analysis of the L and S sequences are shown in Tables 1, 2. Among them, the genetic distance between Hebei strain and Liaoning strain (ON812325.1) of L fragment is the smallest, which is 0.0031, and the genetic distance between Hebei strain and other strains is 0.0369–0.0434. Regarding the S segment, the genetic distance between the DBTV Hebei strain and other strains (no record of Liaoning strain) was 0.0255–0.0328. Phylogenetic analysis revealed that the Hebei strain of DBTV, along with previously reported DBTV strains, could be classified into the same cluster. Furthermore, the phylogenetic analysis of the L segment indicated that the DBTV Hebei strain grouped together with the Liaoning strain (Figure 1A).

DBTV transmission in *Haemaphysalis longicornis*

In May 2022, 16 engorged female *H. longicornis* ticks were collected from sheep in Chengde City, Hebei Province, and 200 free-living nymphs of *H. longicornis* were collected from the vegetation of the same pastures in August that year. Two hundred free-living nymphs of *H. longicornis* divided into 10 pools for detection. PCR result showed that two out of the 10 pools tested positive for DBTV. PCR amplification and Sanger sequencing revealed that nine out of 16 females tested positive for DBTV with 56.25% positive rate. Under controlled laboratory conditions, 14 out of 16 female ticks produced eggs. Six pools of eggs were laid by seven DBTV-negative female ticks, resulting in the hatching of larvae with a hatch rate of 83.33%. All eggs laid by the seven DBTV-infected female ticks tested positive for the virus. However, only two out of seven egg clutches successfully hatched into larvae, resulting in a hatch rate of 28.5%. Further analysis showed that only one next generation of larvae pool carried DBTV (Table 3). The infection rate in the offspring of DBTV-negative female ticks was 0% and the infection rate in the offspring of DBTV-infected female ticks was 14.28%.

Discussion

In this research, Dabieshan Tick Virus was identified from adult *H. longicornis* ticks collected in Chengde, Hebei province of China by high-throughput small RNA sequencing (Figure 2). Since its initial detection in Hubei Province in 2015, this virus has been discovered in five other provinces of China (Shao et al., 2020; Zhu et al., 2020; Wang et al., 2021; Yang et al., 2021). Additionally, neighboring countries such as South Korea and Japan have reported identifying the virus in 2021 and 2023, respectively (Li et al., 2015; Pérez-Sautu et al., 2021; Mekata et al., 2023). It is worth noting that all studies reporting DBTV positivity are related to *H. longicornis*, which is consistent with the results of this study. *Haemaphysalis longicornis* is capable of parasitizing certain avian species, particularly migratory birds (Pandey et al., 2022), which suggests that these ticks may contribute to the transmission of both this virus and other tick-borne viruses over long distances. This study reveals that *H. longicornis* ticks detected positive for DBTV in a village located in Chengde City, Hebei Province.

Chengde city neighbors Liaoning province and is separated by the Yanshan mountain range. DBTV Hebei strain L segment nucleic acid with the highest identity of 99.69% was observed in the DBTV Liaoning strain (ON812325.1). Moreover, the analysis of the genetic distance of the L fragment demonstrated that the genetic distance between the

TABLE 1 Distance values based on the DBTV L segment sequences between various strains analyzed in this study.

Virus strain	1	2	3	4	5	6	7	8	9	10	11	12	13	14
1. OP682840.1 DBTV Hebei strain														
2. ON812325.1 DBTV Liaoning strain	0.0031													
3. MW334981.1 DBTV Liaoning strain	0.0430	0.0425												
4. KM817666.1 DBTV Dabieshan strain	0.0425	0.0420	0.0158											
5. MW721891.1 DBTV Huanggang strain	0.0403	0.0398	0.0128	0.0145										
6. MN723843.1 DBTVstrain Zhoushan	0.0420	0.0424	0.0158	0.0129	0.0141									
7. MT413430.1 DBTV Shandong strain	0.0369	0.0367	0.0088	0.0094	0.0075	0.0090								
8. OM368030.1 DBTV Taian strain	0.0415	0.0413	0.0145	0.0153	0.0122	0.0158	0.0075							
9. OM368050.1 DBTV Weifang strain	0.0410	0.0412	0.0136	0.0107	0.0126	0.0107	0.0065	0.0136						
10. OM368052.1 DBTV Rizhao strain	0.0419	0.0413	0.0121	0.0141	0.0071	0.0138	0.0075	0.0122	0.0119					
11. OM368057.1 DBTV Linyi strain	0.0395	0.0390	0.0116	0.0136	0.0056	0.0133	0.0066	0.0117	0.0114	0.0053				
12. LC753173.1 DBTV Japan strain	0.0434	0.0432	0.0155	0.0116	0.0131	0.0119	0.0087	0.0155	0.0104	0.0131	0.0126			
13. NC_055434.1 Norway phlebovirus 1	0.5434	0.5434	0.5444	0.5456	0.5436	0.5444	0.5442	0.5453	0.5454	0.5447	0.5439	0.5453		
14. NC_018136.1 SFTS virus	0.5264	0.5265	0.5248	0.5245	0.5253	0.5260	0.5242	0.5247	0.5255	0.5253	0.5248	0.5240	0.5687	

TABLE 2 Distance values based on the DBTV S segment sequences between various strains analyzed in this study.

Virus strain	1	2	3	4	5	6	7	8	9	10	11	12
1. OP716696.1 DBTV Hebei strain												
2. KM817733.1 DBTV Dabieshan strain	0.0279											
3. MW721902.1 DBTV Huanggang strain	0.0267	0.0073										
4. MN723842.1 DBTV Zhoushan strain	0.0279	0.0049	0.0073									
5. MT413431.1 DBTV Shandong strain	0.0255	0.0073	0.0085	0.0073								
6. OM367999.1 DBTV Taian strain	0.0328	0.0109	0.0146	0.0133	0.0097							
7. OM368020.1 DBTV Weifang strain	0.0255	0.0024	0.0049	0.0024	0.0049	0.0109						
8. OM368019.1 DBTV Rizhao strain	0.0291	0.0061	0.0085	0.0061	0.0085	0.0146	0.0036					
9. OM368025.1 DBTV Linyi strain	0.0279	0.0061	0.0036	0.0061	0.0073	0.0133	0.0036	0.0073				
10. LC753194.1 DBTV Japan strain	0.0255	0.0024	0.0049	0.0024	0.0049	0.0109	0.0000	0.0036	0.0036			
11. NC 055433.1 Norway phlebovirus 1	0.5825	0.5898	0.5922	0.5898	0.5886	0.5874	0.5910	0.5947	0.5922	0.5910		
12. NC 018137.1 SFTS virus	0.5837	0.5874	0.5850	0.5862	0.5862	0.5850	0.5862	0.5886	0.5837	0.5862	0.5910	

TABLE 3 PCR test results of DBTV in *Haemaphysalis longicornis* collected from Chengde, Hebei Province.

Stage	Pools number and results											
Engorged adult female	A1	A2–A6	A7	A8	A9	A10	A11	A12	A13	A14	A15	A16
	+	–	+	–	+	+	+	+	+	–	+	+
Egg pool	E1	E2–E6	E7	E8	E9	E10	E11	E12	E13	E14	/	/
	+	–	+	–	+	+	+	+	+	/	/	
Larva pool	/	L2–L6	L7	L8	L9	/	/	/	/	/	/	/
	/	–	–	–	+	/	/	/	/	/	/	/

"+" and "–" means positive and negative, respectively; "/" means a lack of samples and test result.

DBTV Hebei strain and the Liaoning strain (ON812325.1) was notably insignificant in comparison to the genetic distance between these strains and other local strains from Japan, Shandong, and elsewhere (Table 1). This finding implies potential correlation between virus transmission and infection in these two regions, which could be attributed to either wildlife activities or other factors. Apart from the Liaoning strain, Tables 1, 2 display that the genetic distance between the DBTV Hebei strain and the DBTV Shandong strain is the smallest. The phylogenetic trees constructed from the L and S segments indicated that, compared to other related viruses, the DBTV Hebei strain clustered with other DBTV strains. These findings are consistent with other studies (Ma et al., 2022). However, there is no observed correlation between these groups and their geographical distribution. Further research should be warranted to investigate the mechanisms underlying the differentiation between these distinct groups. It is imperative to enhance the monitoring and investigation of DBTV to gain a comprehensive understanding of its spread and evolution, which will provide a more scientific basis for prevention, control, and treatment.

Furthermore, we observed a significant difference in hatching rates between DBTV positive infected eggs (28.57%) and DTBV negative eggs (83.33%) during the transmission experiment of DTBV in *H. longicornis*. It is generally known that tick-borne virues (TBVs) do not have discernible adverse effects on the rates of oviposition, hatching, feeding in tick vectors (Sonenshine, 2014). However, some feeding experiments have found increased mortality rates in adult *Ornithodoros* ticks fed on African swine fever virus -infected bloodmeal compared to ticks fed on uninfected bloodmeal (Hess et al., 1989; Rennie et al., 2000). In our study, the ticks used were acquired during their parasitic stage and were not completely engorged. Some study demonstrated a markedly positive correlation between the weight of the engorged female and the quantity of egg masses laid (Chen et al., 2012). This suggests that the number of eggs produced by female ticks in this study was limited, and half of them are employed for RNA extraction, potentially affecting their hatching capacity. Although the oviposition rate and hatching rate of ticks infected with DBTV were found to be low in this study, it remains unclear whether these rates were affected by the virus. Regrettably, we were unsuccessful in feeding the DBTV positive larvae of *H. longicornis* to the subsequent generation. To validate the impact of DBTV on both tick and its host, it is imperative to broaden the DBTV positive population of *H. longicornis* and conduct a comprehensive life history analysis in the upcoming investigation.

The positivity rate of DBTV in adult *H. longicornis* ticks obtained from *Ovis aries* in 2022 was 56.25%, which was significantly higher than that of *H. longicornis* ticks in grass (20%), as reported in Shandong (Shao et al., 2021), Zhoushan (Zhu et al., 2020), and Japan (Mekata et al., 2023). The high positivity rate may be attributed to tick aggregation or co-feeding transmission between ticks (Johnstone-Robertson et al., 2020), resulting in an increased prevalence among full-blood female *H. longicornis* tick samples.

Dabieshan Tick Virus was identified in newly molted adult *H. longicornis* through small RNA sequencing, suggesting that the virus can be transmitted from nymphs to adults and that there is a possibility of transstadial transmission. Furthermore, the hungry nymph we collected from the grass at the same site was positive for

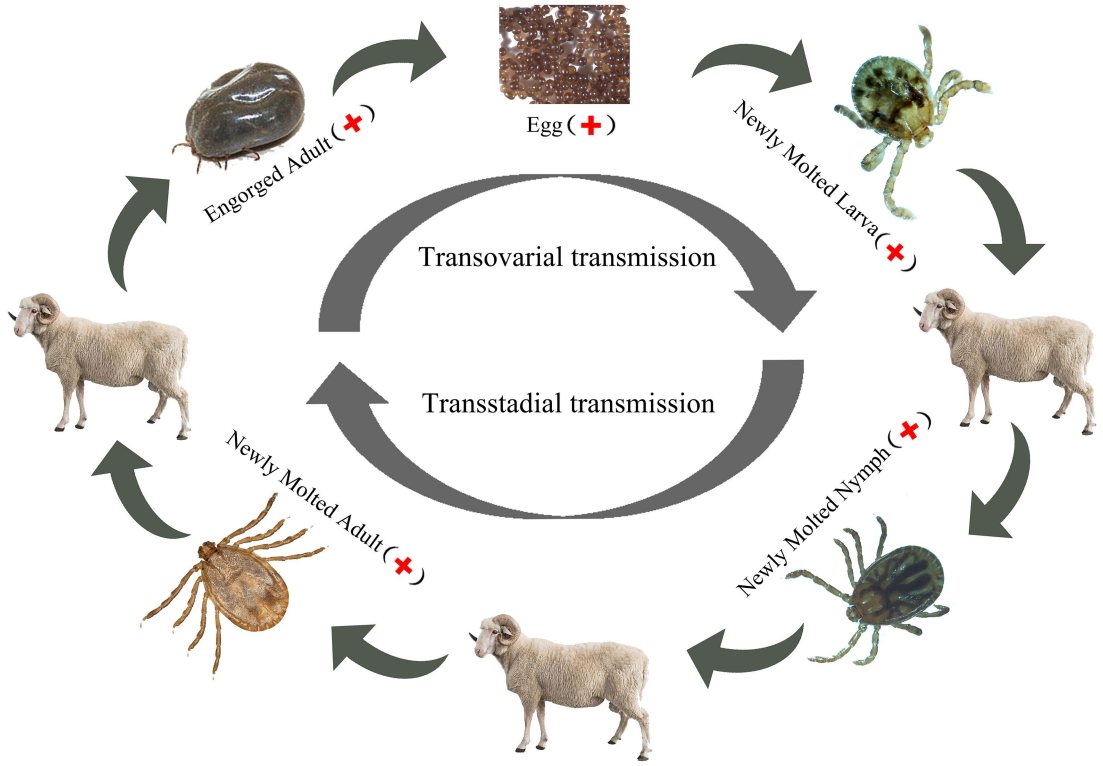

FIGURE 3
DBTV transmission in *Haemaphysalis longicornis*.

DBTV, indicating that the virus can spread from larvae to nymphs. In the follow-up study, the presence of DBTV in female ticks, as well as their eggs and larvae (Table 3), provides additional evidence supporting the virus's transovarial and transstadial transmission potential within *H. longicornis*. Based on the discovery that DBTV RNA is commonly found in Shandong sheep, with a prevalence rate of approximately 10% (Shao et al., 2021). Combining all the above experimental results, we inferred that ticks serve as a vector for transmitting DBTV to host animals (sheep), thus completing the cycle between ticks and livestock in the natural focus of Chengde (Figure 3). The vertical transmission of DBTV in *H. longicornis* makes virus long lasting in the host and extends the transmission route of the virus. Recombination events have been shown to occur in Bunyavirales in both co-infected cell cultures and arthropod hosts (Mhamadi et al., 2023), which may influence the evolution of direction and transmission capability of the viruses (Gerrard et al., 2004). The transmission of DBTV through eggs will lead to the formation of a stable population of the virus in *H. longicornis*, which will increase the probability of virus recombination and reassortment. We need to strengthen the monitoring and management of vector animals, such as the *H. longicornis*, as well as the research and analysis of viral genomes to understand the patterns and effects of these changes.

Conclusion

Our research discovered DBTV in Chengde, Hebei Province for the first time, providing valuable epidemiological data on its distribution. We also suggested that *H. longicornis* might be the vector and reservoir host of DBTV, further supporting the hypothesis that DBTV is a tick-borne virus. However, there is still a deficiency of the research surrounding the isolation and pathogenicity of DBTV, highlighting the need for further studies to prevent potential harm to the health of animals and humans.

Data availability statement

The datasets presented in this study can be found in online repositories. The names of the repository/repositories and accession number(s) can be found below: https://www.ncbi.nlm.nih.gov/genbank/, OP682840; https://www.ncbi.nlm.nih.gov/genbank/, OP716696; and https://www.ncbi.nlm.nih.gov/, SAMN27533436.

Ethics statement

The manuscript presents research on animals that do not require ethical approval for their study.

Author contributions

XF: Investigation, Software, Writing – original draft, Writing – review & editing, Validation, Visualization. ZG: Writing – review & editing, Investigation, Validation. YW: Writing – review & editing, Data curation, Resources. HY: Writing – review & editing, Funding acquisition. QR: Writing – review & editing, Investigation, Validation, JZ: Writing – review & editing, Resources. YL: Writing – review &

editing, Resources. SY: Writing – review & editing. CB: Writing – review & editing, Data curation. AT: Writing – review & editing, Data curation. XY: Funding acquisition, Supervision, Writing – review & editing. ZC: Funding acquisition, Project administration, Supervision, Writing – review & editing, Methodology, Writing – original draft.

Funding

The author(s) declare financial support was received for the research, authorship, and/or publication of this article. This study was financially supported by the Science Foundation of Hebei Normal University (L2023J02), the State Key Laboratory of Veterinary Etiological Biology, Lanzhou Veterinary Research Institute, Chinese Academy of Agricultural Sciences (SKLVEB2021KFKT006), Natural Science Fund of Hebei Province (C2023205011), and National key R&D Program of China Intergovernmental International S&T Innovation Cooperation Program (2023YFE0199900). The funding bodies played no role in the design of the study and collection, analysis, and interpretation of data and in writing the manuscript. The funding bodies played no role in the design of the study and collection, analysis, and interpretation of data and in writing the manuscript.

Acknowledgments

We would like to express our gratitude to Songbo Zhang for providing us with information regarding the collection location of the experimental sample. Additionally, we extend our appreciation to the herdsmen in Chengde City, Hebei Province for their generous assistance during the sampling process.

Conflict of interest

The authors declare that the research was conducted in the absence of any commercial or financial relationships that could be construed as a potential conflict of interest.

The author(s) declared that they were an editorial board member of Frontiers, at the time of submission. This had no impact on the peer review process and the final decision.

Publisher's note

All claims expressed in this article are solely those of the authors and do not necessarily represent those of their affiliated organizations, or those of the publisher, the editors and the reviewers. Any product that may be evaluated in this article, or claim that may be made by its manufacturer, is not guaranteed or endorsed by the publisher.

Supplementary material

The Supplementary material for this article can be found online at: https://www.frontiersin.org/articles/10.3389/fmicb.2024.1365356/full#supplementary-material

References

Bosco-Lauth, A. M., Calvert, A. E., Root, J. J., Gidlewski, T., Bird, B. H., Bowen, R. A., et al. (2016). Vertebrate host susceptibility to heartland virus. *Emerg. Infect. Dis.* 22, 2070–2077. doi: 10.3201/eid2212.160472

Bouloy, M., and Weber, F. (2010). Molecular biology of rift valley fever virus. *Open Virol. J.* 4, 8–14. doi: 10.2174/1874357901004020008

Chen, Z., Li, Y., Liu, Z., Yang, J., and Yin, H. (2012). The life cycle of *Hyalomma rufipes* (acari: ixodidae) under laboratory conditions. *Exp. Appl. Acarol.* 56, 85–92. doi: 10.1007/s10493-011-9490-0

Chen, Z., and Yang, X. (2021). *Systematics and Taxonomy of Ixodida (First Pressed)*. Beijing: Science Press. 653

Contreras, M., De La Fuente, J., and Kocan, K. M. (2015). Prevention and control strategies for ticks and pathogen transmission. *Rev. Sci. Tech.* 34, 249–264. doi: 10.20506/rst.34.1.2357

Damian, D., Maghembe, R., Damas, M., Wensman, J. J., and Berg, M. (2020). Application of viral metagenomics for study of emerging and reemerging tick-borne viruses. *Vect. Borne Zoo. Dis.* 20, 557–565. doi: 10.1089/vbz.2019.2579

Danecek, P., Bonfield, J. K., Liddle, J., Marshall, J., Ohan, V., Pollard, M. O., et al. (2021). Twelve years of SAMtools and BCFtools. *Gigascience* 10:8. doi: 10.1093/gigascience/giab008

Dong, Z., Yang, M., Wang, Z., Zhao, S., Xie, S., Yang, Y., et al. (2021). Human Tacheng tick virus 2 infection, China, 2019. *Emerg. Infect. Dis.* 27, 594–598. doi: 10.3201/eid2702.191486

Gerrard, S. R., Li, L., Barrett, A. D., and Nichol, S. T. (2004). Ngari virus is a Bunyamwera virus reassortant that can be associated with large outbreaks of hemorrhagic fever in Africa. *J. Virol.* 78, 8922–8926. doi: 10.1128/JVI.78.16.8922-8926.2004

He, T., Zhu, C., Li, Z., Ai, L., Hu, D., Wang, C., et al. (2022). Virome analysis of ticks in Zhoushan archipelago, China. *J. Vet. Med. Sci.* 84, 847–854. doi: 10.1292/jvms.22-0058

Hess, W. R., Endris, R. G., Lousa, A., and Caiado, J. M. (1989). Clearance of African swine fever virus from infected tick (acari) colonies. *J. Med. Entomol.* 26, 314–317. doi: 10.1093/jmedent/26.4.314

Johnstone-Robertson, S. P., Diuk-Wasser, M. A., and Davis, S. A. (2020). Incorporating tick feeding behaviour into r (0) for tick-borne pathogens. *Theor. Popul. Biol.* 131, 25–37. doi: 10.1016/j.tpb.2019.10.004

Koichiro, T., Glen, S., and Sudhir, K. (2021). Mega11: molecular evolutionary genetics analysis version 11. *Mol. Biol. Evol.* 38, 3022–3027. doi: 10.1093/molbev/msab120

Kreuze, J. F., Perez, A., Untiveros, M., Quispe, D., Fuentes, S., Barker, I., et al. (2009). Complete viral genome sequence and discovery of novel viruses by deep sequencing of small RNAs: a generic method for diagnosis, discovery and sequencing of viruses. *Virology* 388, 1–7. doi: 10.1016/j.virol.2009.03.024

Li, H., and Durbin, R. (2009). Fast and accurate short read alignment with burrows-wheeler transform. *Bioinformatics* 25, 1754–1760. doi: 10.1093/bioinformatics/btp324

Li, C., Shi, M., Tian, J., Lin, X., Kang, Y., Chen, L., et al. (2015). Unprecedented genomic diversity of RNA viruses in arthropods reveals the ancestry of negative-sense RNA viruses. *elife* 4:e5378. doi: 10.7554/eLife.05378

Ma, C., Zhang, R., Zhou, H., Yu, G., Yu, L., Li, J., et al. (2022). Prevalence and genetic diversity of Dabieshan tick virus in Shandong province, China. *J. Inf. Secur.* 85, 90–122. doi: 10.1016/j.jinf.2022.04.002

Mekata, H., Kobayashi, I., and Okabayashi, T. (2023). Detection and phylogenetic analysis of Dabieshan tick virus and Okutama tick virus in ticks collected from cape Toi, Japan. *Ticks Tick Borne Dis.* 14:102237. doi: 10.1016/j.ttbdis.2023.102237

Mhamadi, M., Dieng, I., Dolgova, A. S., Touré, C. T., Ndiaye, M., Diagne, M. M., et al. (2023). Whole genome sequencing analysis of African Orthobunyavirus isolates reveals naturally interspecies segments recombinations between Bunyamwera and Ngari viruses. *Viruses* 15:550. doi: 10.3390/v15020550

Migné, C. V., Hönig, V., Bonnet, S. I., Palus, M., Rakotobe, S., Galon, C., et al. (2022). Evaluation of two artificial infection methods of live ticks as tools for studying interactions between tick-borne viruses and their tick vectors. *Sci. Rep.* 12:491. doi: 10.1038/s41598-021-04498-9

Nuttall, P. A. (2009). Molecular characterization of tick-virus interactions. *Front. Biosci.* 14, 2466–2483. doi: 10.2741/3390

Pandey, M., Piedmonte, N. P., Vinci, V. C., Falco, R. C., Daniels, T. J., and Clark, J. A. (2022). First detection of the invasive Asian longhorned tick (acari: Ixodidae) on migratory passerines in the Americas. *J. Med. Entomol.* 59, 2176–2181. doi: 10.1093/jme/tjac144

Pérez-Sautu, U., Wiley, M. R., Prieto, K., Chitty, J. A., Haddow, A. D., Sánchez-Lockhart, M., et al. (2021). Novel viruses in hard ticks collected in the Republic of Korea unveiled by metagenomic high-throughput sequencing analysis. *Ticks Tick Borne Dis.* 12:101820. doi: 10.1016/j.ttbdis.2021.101820

Raney, W., Perry, J., and Hermance, M. (2022). Transovarial transmission of heartland virus by invasive Asian longhorned ticks under laboratory conditions. *Emerg. Infect. Dis.* 28, 726–729. doi: 10.3201/eid2803.210973

Rennie, L., Wilkinson, P. J., and Mellor, P. S. (2000). Effects of infection of the tick *Ornithodoros moubata* with African swine fever virus. *Med. Vet. Entomol.* 14, 355–360. doi: 10.1046/j.1365-2915.2000.00251.x

Shao, L., Chang, R., Liu, L., Wang, Y., Gao, Y., Wang, S., et al. (2021). Detection and phylogenetic analysis of a novel tick-borne virus in *Haemaphysalis longicornis* ticks and sheep from Shandong, China. *Virol. J.* 18:233. doi: 10.1186/s12985-021-01704-y

Shao, L., Pang, Z., Fu, H., Chang, R., and Niu, G. (2020). Identification of recently identified tick-borne viruses (Dabieshan tick virus and SFTSV) by metagenomic analysis in ticks from Shandong province, China. *J. Inf. Secur.* 81, 973–978. doi: 10.1016/j.jinf.2020.10.022

Shi, J., Hu, Z., Deng, F., and Shen, S. (2018). Tick-borne viruses. *Virol. Sin.* 33, 21–43. doi: 10.1007/s12250-018-0019-0

Sonenshine, D. E. (2014). *Biology of Ticks*. New York: Oxford University Press. 491

Stockman, S. (1919). Louping-ill duration of the infectivity of the ticks. *J. Comp. Pathol. Ther.* 32, 283–285. doi: 10.1016/S0368-1742(19)80028-0

Wang, A., Pang, Z., Liu, L., Ma, Q., Han, Y., Guan, Z., et al. (2021). Detection and phylogenetic analysis of a novel tick-borne virus in Yunnan and Guizhou provinces, southwestern China. *Pathogens* 10:1143. doi: 10.3390/pathogens10091143

Xu, X., Bei, J., Xuan, Y., Chen, J., Chen, D., Barker, S. C., et al. (2020). Full-length genome sequence of segmented RNA virus from ticks was obtained using small RNA sequencing data. *BMC Genomics* 21, 641–648. doi: 10.1186/s12864-020-07060-5

Yang, Z., Zhang, J., Yang, S., Wang, X., Shen, Q., Sun, G., et al. (2021). Virome analysis of ticks in a forest region of Liaoning, China: characterization of a novel Hepe-like virus sequence. *Virol. J.* 18:163. doi: 10.1186/s12985-021-01632-x

Zheng, Y., Gao, S., Padmanabhan, C., Li, R., and Fei, Z. (2017). Virusdetect: an automated pipeline for efficient virus discovery using deep sequencing of small RNAs. *Virology* 500, 130–138. doi: 10.1016/j.virol.2016.10.017

Zhu, C., He, T., Wu, T., Ai, L., Hu, D., Yang, X., et al. (2020). Distribution and phylogenetic analysis of Dabieshan tick virus in ticks collected from Zhoushan, China. *J. Vet. Med. Sci.* 82, 1226–1230. doi: 10.1292/jvms.20-0081

Zhuang, L., Sun, Y., Cui, X. M., Tang, F., Hu, J. G., Wang, L. Y., et al. (2018). Transmission of severe fever with thrombocytopenia syndrome virus by *Haemaphysalis longicornis* ticks, China. *Emerg. Infect. Dis.* 24, 868–871. doi: 10.3201/eid2405.151435

Zhuang, L., Zhang, Z., An, X., Fan, H., Ma, M., Anderson, B. D., et al. (2014). An efficient strategy of screening for pathogens in wild-caught ticks and mosquitoes by reusing small RNA deep sequencing data. *PLoS One* 9:e90831. doi: 10.1371/journal.pone.0090831

frontiers | Frontiers in Microbiology

TYPE Original Research
PUBLISHED 26 March 2024
DOI 10.3389/fmicb.2024.1359492

Check for updates

OPEN ACCESS

EDITED BY
Hong Yin,
Chinese Academy of Agricultural Sciences, China

REVIEWED BY
Mohamed Abdo Rizk,
Mansoura University, Egypt
Roland Eric Yessinou,
University of Abomey-Calavi, Benin
ThankGod Emmanuel Onyiche,
University of Maiduguri, Nigeria

*CORRESPONDENCE
Xiaohu Han
✉ hxh8849@syau.edu.cn
Zeliang Chen
✉ zeliangchen@126.com

†These authors have contributed equally to this work

RECEIVED 04 January 2024
ACCEPTED 04 March 2024
PUBLISHED 26 March 2024

CITATION
Jamil A, Yu Z, Wang Y, Xin Q, Gao S, Abdul Wahab M, Han X and Chen Z (2024) Tick-borne *Rickettsia, Anaplasma*, *Theileria*, and enzootic nasal tumor virus in ruminant, PET, and poultry animals in Pakistan. *Front. Microbiol.* 15:1359492. doi: 10.3389/fmicb.2024.1359492

COPYRIGHT
© 2024 Jamil, Yu, Wang, Xin, Gao, Abdul Wahab, Han and Chen. This is an open-access article distributed under the terms of the Creative Commons Attribution License (CC BY). The use, distribution or reproduction in other forums is permitted, provided the original author(s) and the copyright owner(s) are credited and that the original publication in this journal is cited, in accordance with accepted academic practice. No use, distribution or reproduction is permitted which does not comply with these terms.

Tick-borne *Rickettsia, Anaplasma*, *Theileria*, and enzootic nasal tumor virus in ruminant, PET, and poultry animals in Pakistan

Anjum Jamil[1], Ze Yu[1†], Yuxin Wang[1†], Qing Xin[1], Shan Gao[2], Muhammad Abdul Wahab[3], Xiaohu Han[1]* and Zeliang Chen[1,2]*

[1]Key Laboratory of Livestock Infectious Diseases, Ministry of Education, Shenyang Agriculture University, Shenyang, China, [2]Department of Epidemiology, School of Public Health, Sun Yat-sun University, Guangzhou, China, [3]Department of Veterinary Parasitology, University of Agriculture Faisalabad, Faisalabad, Pakistan

Introduction: Pakistan is an agricultural country; most of its income is based on livestock rearing. The increasing prevalence of tick-borne pathogens among animals may affect the animal production and livelihood of owners, which eventually derange the economy of a country.

Methodology: To further comprehend TBPs, 213 ticks were collected from different animals, including ruminants, pets, and poultry. After molecular and phylogenetic analysis identification, ticks were managed into different pools based on their species level (*Hyalomma anatolicum* = 80, *Rhipicephalus microplus* = 35, *Hyalomma scupense* = 23, *Rhipicephalus turanicus* = 70, and *Rhipicephalus sanguineus* = 5).

Results and discussion: After tick species identification, further molecular PCR amplification was carried out to screen out the pathogens for the presence of *Theileria*, *Rickettsia*, *Anaplasma*, and enzootic nasal tumor virus (ENTV). The following pathogens were detected: 11 (5.16%) for *Anaplasma*, 1 (0.47%) for *Rickettsia*, and 9 (4.23%) for *Theileria*. Nevertheless, other TBPs that had not been reported so far in Pakistan 3 (1.41%), were positive for enzootic nasal tumor virus (ENTV). Besides, phylogenetic analysis of the enzootic nasal tumor virus (ENTV) strain confirmed its resemblance to the Chinese strain, while Anaplasma has comparability with Pakistan and China, *Rickettsia* with Pakistan, China, and Iran, and *Theileria* with India, South Africa, United States, Japan, and Spain.

Conclusion: This study reveals that there is a considerably wider range of TBPs held in Pakistan that take in various contagious zoonotic pathogens than was previously thought. This information advances TBP epidemiology and will contribute to upgrade future control measure.

KEYWORDS

enzootic nasal tumor virus (ENTVs), *Theileria*, *Anaplasma*, *Rickettsia*, TBPs

1 Introduction

Pakistan is an agricultural country with a profitable environment for the production of livestock. Various livestock species are sheep, goats, cattle, and buffalo, with populations of 28.8, 64.9, 38.3, and 33.7 million, respectively. Sheep play a pivotal role in the dairy sector in Pakistan, following China and India, which have consequential goat and sheep-raising sectors. The financial results of bringing up livestock in Pakistan fail to achieve their maximum potential (Jabbar et al., 2015). Among the vector-borne diseases, the more bonafide complications emanate due to tick-borne disease, which is prevalent in the

world and may lead to severe complications. It has been reported that about 1 million deaths are observed annually due to tick-borne pathogens (WHO, 2014). Ticks are an immense source of spreading zoonotic diseases such as tularemia, tick-borne relapsing fever, Rocky Mountain spotted fever, anaplasmosis, and ehrlichiosis (Bratton and Corey, 2005; Hussain N. et al., 2023). Developing countries like tropical and subtropical countries are in consensus due to TBDs exerting economic challenges on the worldwide livestock sector. Piroplasmosis is the protozoal disease caused by *Babesia* and *Theileria*, although anaplasmosis and rickettsiosis are caused by *Anaplasma* and *Rickettsia*, respectively, and have consequential prestige in the dairy sector. Ruminants are highly vulnerable to tick-borne pathogens. The most commonly reported diseases are anaplasmosis, theileriosis, and piroplasmosis, which affect the reproductive status of the livestock population (Saeed et al., 2015; Sajid et al., 2017; Khan et al., 2022).

ENA is a tumor of sheep and goats, and it is chronic and contagious in nature. It is summarized as the proliferation and thickening of the lining of secretory epithelial cells in the nasal cavity (De las Heras et al., 2003; Svara et al., 2006; Özmen et al., 2010). This tumor is caused by ENTV, a retrovirus, an enzootic nasal tumor virus in small ruminants (Leroux and Mornex, 2008). The retroviruses are highly complicated in structure and are mostly RNA viruses, which are distributed in various vertebrate and non-vertebrate species. Some instances include the small ruminant jaagsiekte sheep retrovirus (JSRV), lentiviruses, and the most contagious ENTV, which cause infections in sheep and goats. ENA was first reported in Germany in 1939 and, in due course, proclaimed in all major livestock farming sectors, especially sheep and goat rearing sites (De las Heras et al., 1995). The tumor is widespread globally and has been identified across many countries, particularly in Turkey, in recent years (Özmen and Serpin, 2016). Pathogenesis of ENTV is similar to another tumor-causing beta retrovirus, JSRV, which causes respiratory issues such as pulmonary adenocarcinoma in sheep and goats (Monot et al., 2015). Both ENTVs have two types in nature: ENTV 1 affects goats and ENTV 2 affects sheep. Both have drastic effects and may cause severe complications (Cousens et al., 1999; Ortín et al., 2003; Bratton and Corey, 2005; WHO, 2014), such as depression, anorexia, exudative nasal discharge with bleeding, and difficulty breathing may lead to stretching the neck, eventually facial complications, and even death due to chronic respiratory blockage (De las Heras et al., 1995; Walsh et al., 2013).

Pakistan's subtropical geography provides a perfect environment for the growth and proliferation of tick populations, which are significant testimony to hemoparasitic diseases. Various tick species, particularly *Boophilus*, *Ixodidae*, *Hyalomma*, and *Rhipicephalus*, have a consequence role in imparting hemoparasitic diseases (Eshetu, 2015), with *Hyalomma* species being the most abundant in Pakistan (Atif et al., 2012).

Most etiological surveys diligently use conventional standard methods, such as reviewing stained blood smears under a microscope. Regardless of its affordability, this approach requires technical proficiency and may lack specificity when addressing morphologically similar TBPs that coexist. In addition, its sensitivity is limited in cases of low parasitemia. To date, there has been no confirmation of tick-borne ENTV in Pakistan. Prior research was defined to certain geographic areas and overlooked to contemplate agroecological areas, methods of production, and sample strategies. These factors can greatly impact the solidity of estimates of the prevalence of diseases transmitted via ticks. The lack of accurate data on the epidemiology of tick-borne diseases (TBDs) makes it difficult to map current affluence as well as the distribution of tick-borne pathogens (TBPs) in Pakistan.

This study made an effort to locate the tick-borne pathogens circulating in Pakistan due to the limited molecular diagnostic-based information available on their epidemiology. Our results suggest the prevalence of *Anaplasma*, *Theileria*, and *Rickettsia* among livestock populations in Pakistan. Furthermore, we reported ENTV for the first time from ticks of sheep and goats, where small ruminant farming is highly pronounced. These findings may expedite the development of various productive strategies for controlling TBDs in Pakistan.

2 Materials and methods

2.1 Study area

To expedite the ticks collection, 13 districts were selected based on livestock population, including Sahiwal (30.677717° N, 73.6245232'°E), Okara (30.8138°N, 73.4534°E), Faisalabad (31.4504° N, 73.1350° E), Pakpattan (*30.34314*° N, *73.38944*° E), Kabola (30.1763° N, 73.0700° E), Lodhran (*29.5339*° N, *71.63244*° E), Mianwali (32.5839° N, 71.5370° E) of Punjab, Karachi (24.8607° N, 67.0011° E), Hyderabad (17.4065° N, 78.4772° E), Nawabshah (36.2447° N, 68.3935° E) of Sindh, Bagh (33.9794° N, 73.7772° E), and Mirpur (33.1480° N, 73.7537° E) of Kashmir and Quetta (30.1798° N, 66.9750° E) of Balochistan from Pakistan. The average temperature of Punjab districts is 5–15°C and 40–50°C, while the Sindh districts are 10–20°C and 30–50°C. In the case of Balochistan districts, 25–35°C and 5–18°C, and in Kashmir districts, 10–20°C and 2–15°C in winter and summer seasons, respectively. Tick specimens were collected from a variety of hosts that were present in easily accessible areas of the research location. Using a Global Positioning System (GPS), Figure 1 illustrates the location and distribution of the study area.

2.2 Study design

A cross-sectional research investigation was conducted to explore the prevalence and geographic distribution of ticks infesting ruminant species on livestock farms. The sample size was calculated based on substantial populations, considering a prevalence of 50% with a 95% confidence level and a desired precision of 10%. At least 70 dairy farms need to be sampled according to this data processing (Jabbar et al., 2015). The number of animal farms was raised to 105, based on the administrative units. In the initial phase, five districts, which accounted for 25% of the total 32 districts, were chosen. Figure 2 shows the district and its relevant villages for tick sampling and pathogen burden.

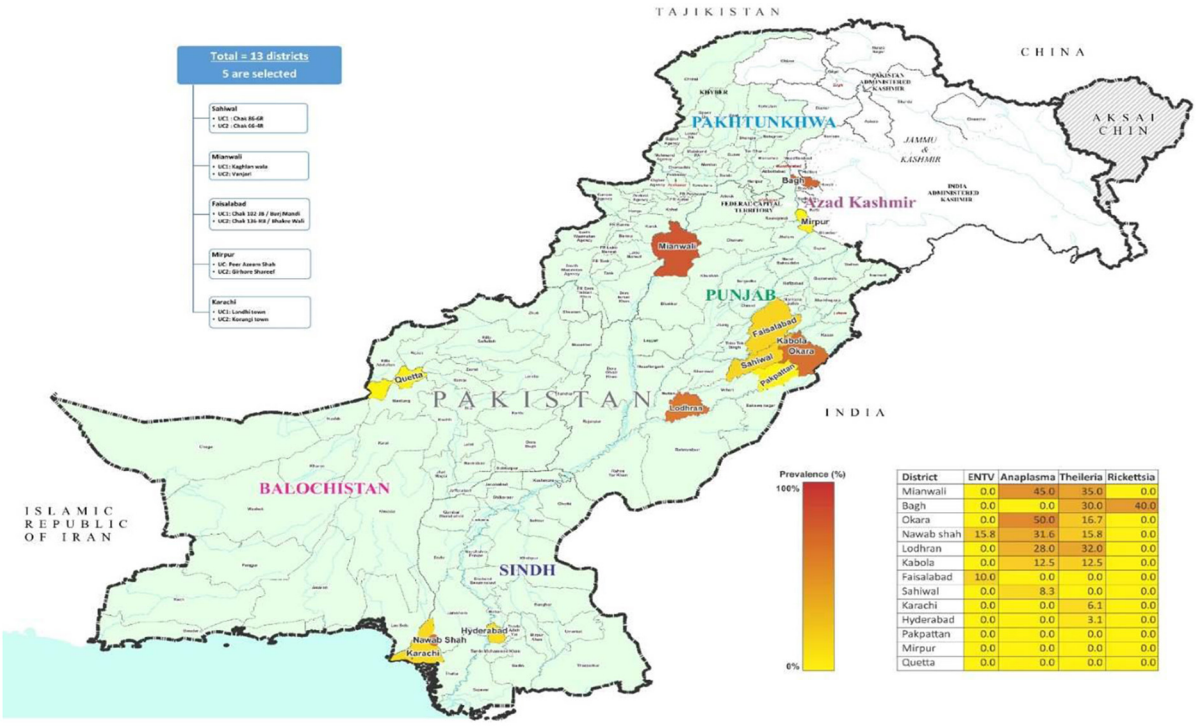

District	ENTV	Anaplasma	Theileria	Rickettsia
Mianwali	0.0	45.0	35.0	0.0
Bagh	0.0	0.0	30.0	40.0
Okara	0.0	50.0	16.7	0.0
Nawab shah	15.8	31.6	15.8	0.0
Lodhran	0.0	28.0	32.0	0.0
Kabola	0.0	12.5	12.5	0.0
Faisalabad	10.0	0.0	0.0	0.0
Sahiwal	0.0	8.3	0.0	0.0
Karachi	0.0	0.0	6.1	0.0
Hyderabad	0.0	0.0	3.1	0.0
Pakpattan	0.0	0.0	0.0	0.0
Mirpur	0.0	0.0	0.0	0.0
Quetta	0.0	0.0	0.0	0.0

FIGURE 1
Location and distribution of the study area.

2.3 Tick collection

Tick surveys were conducted on domestic animals in 2021–2022. Tick samples were collected during the tick active period of March–May and August–October. In a simple cross-sectional survey, we studied goats ($n = 51$), sheep ($n = 44$), cattle ($n = 43$), buffalo ($n = 46$), poultry ($n = 5$), dogs ($n = 21$), and cats ($n = 3$) among domestic animals. The assessed animals were traditional livestock from nomadic and local small farms with varied housing systems and had never been vaccinated or parasitized. The animals' ears, udder, scrotum, tail base, neck, and chest were checked for ticks. Ticks on small and large ruminants took 3–5 and 7–15 min to be found, respectively. All ticks were placed in 2 ml vials. For further laboratory work, ticks were preserved at −80°C. Ticks specimens were collected in glass vials with 70% ethyl alcohol and taken to the parasitology lab for identification. Morphological keys identify tick species under a stereomicroscope (Jamil et al., 2023).

2.4 Tick genomic DNA extraction

After the preservation of ticks, further tick DNA was extracted from morphologically recognized ticks (20 per species). The ticks were taken and dissected horizontally into segments for sample analysis. The tick sample was cut into six different sections and placed in a Falcon tube filled with RNA-free water for extraction. The tick fragments were washed three times with RNA-free water. Tick specimens of each species were cut into pieces using a new scalpel blade and then placed in a 1.5-ml microcentrifuge tube for DNA extraction using the manufacturer's kit instructions.

2.5 Polymerase chain reaction for 16s rRNA amplification

After DNA extraction, further PCR amplification was carried out by amplifying the ∼460-bp fragment of the 16S rRNA gene by managing with a set of primers (forward) 5′-CTGCTCAATGATTTTTTAAATTGCTGTGG-3′ and (reverse) 5′-CCGGTCTGAACTCAGATCAAGT-3′. PCR reactions were performed in a 30-µl reaction mixture, including 2.5 µl of genomic DNA, 1 µl of each primer (10 pmol), 10.5 µl of PCR grade water, and 15 µl of master mix. PCR reactions were conducted with the following parameters: initial denaturation at 95°C for 5 min, followed by 40 cycles of denaturation at 95°C for 45 s, annealing at 50°C for 45 s, extension at 72°C for 1 min, and final extension at 72°C for 5 min.

2.6 Gene amplification for detection of *Theileria, Rickettsia, Anaplasma*, and ENTV

2.6.1 PCR amplification of *Theileria*

PCR amplification was implemented to ascertain the *Theileria* in tick DNA, following base pair 426–430 of the

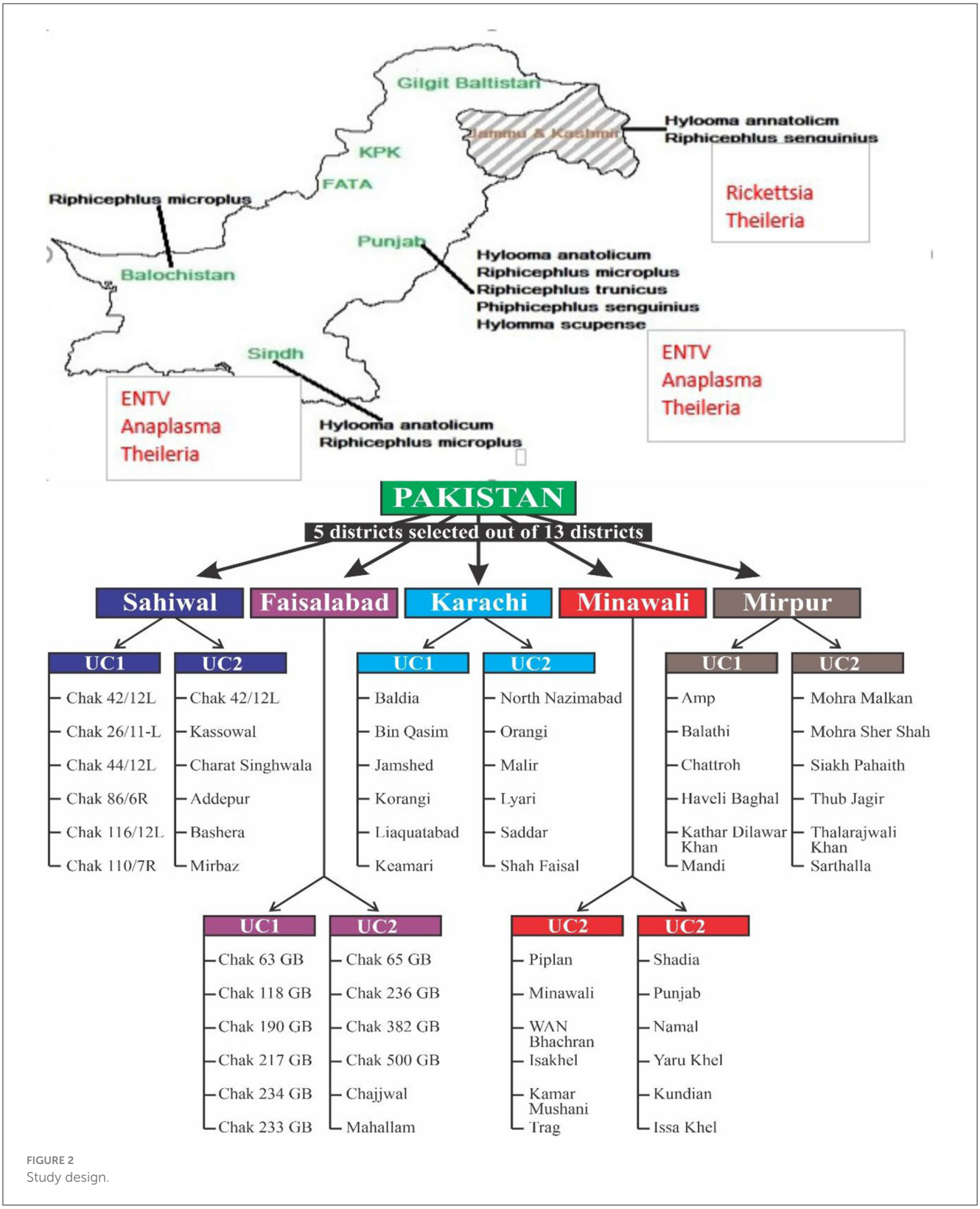

FIGURE 2
Study design.

18S rRNA gene of *Theileria*, which was targeted through the use of previously reported primers (Mwamuye et al., 2017): (forward) 5′-CACAGGGAGGTAGTGACAAG-3′ and (reverse) 5′-AAGAATTTCACCTCTGACAG-3′. The master mixture for the PCR volume mixture is composed of 25 µl (Taq polymerase enzyme, 0.5 µl; PCR buffer, 2.5 µl; extracted DNA, about 3 µl;

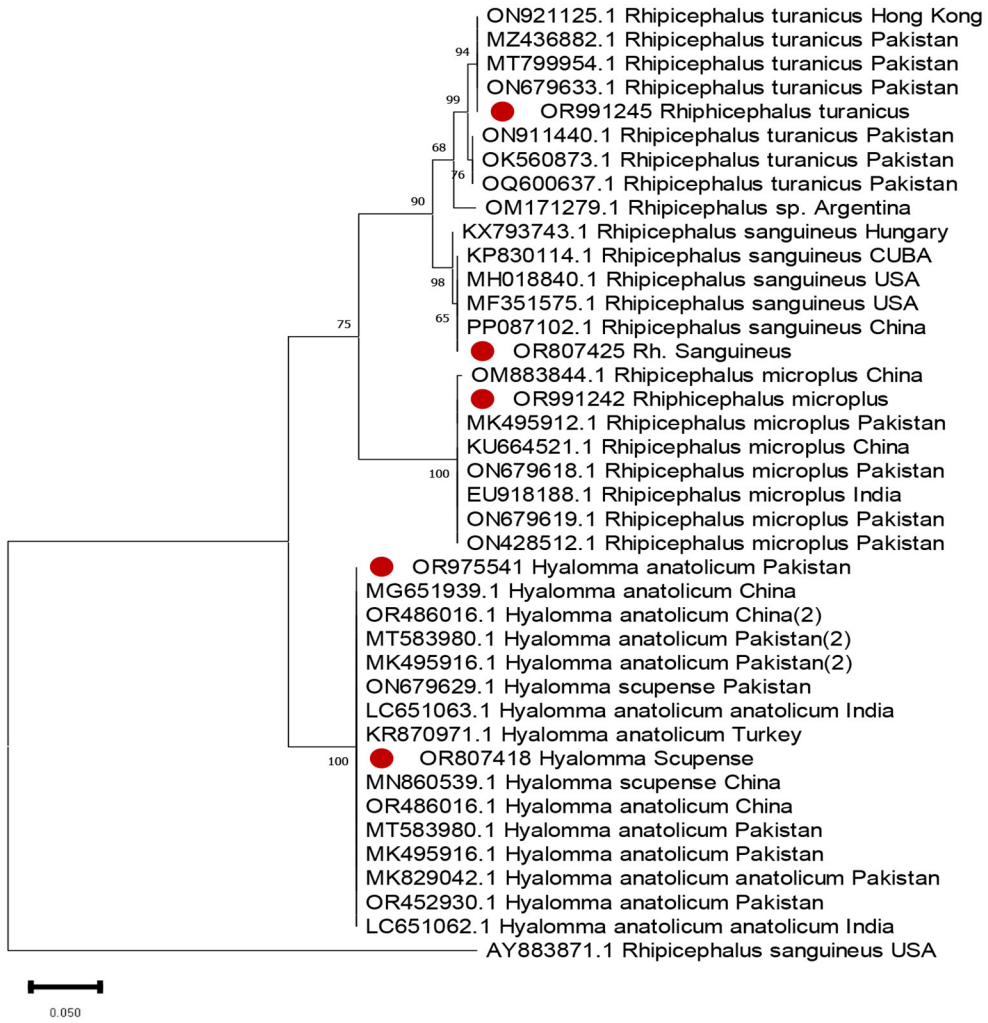

FIGURE 3
Molecular identification and phylogenetic analysis of ticks.

primers, 1 µl; double distilled H_2O, 15 µl; dNTPs, 0.5 µl; and $MgCl_2$, 1 µl). After preparation of the volume, PCR amplifications were performed with the following conditions: the first step of initial denaturation lasted for 5 min at 95°C, followed by 30 cycles of denaturation lasting for 15 s at 95°C, followed by primer annealing lasting for around 15 s at 54°C, and two extensions lasted from 30 s at 72°C to 5 min at 72°C.

2.6.2 PCR amplification of *Anaplasma*

A 309-base pair fragment from the 16S rRNA gene of *Anaplasma* was targeted using previously described primer sequences (Xu et al., 2011): (forward) 5′-GGTACCYACAGAAGAAGTCC-3′ and (reverse) 5′-TAGCACTCATCGTTTACAGC-3′. After having a set of primers, the volume of the master mixture and chemicals used are kept in the same proportion as discussed in the *Theileria* section. After making the volume, the PCR protocol was set up as follows: initial denaturation was performed for 5 min at 95°C, followed by denaturation for about 15 s at 95°C, subsequently annealing for primer lasted for 15 s at 54°C, and finally, two extensions were performed for 30 s at 72°C and 5 min at 72°C.

2.6.3 PCR amplification of *Rickettsia*

To detect *Rickettsia*, conventional PCR primers targeting the citrate synthase gene (*gltA*) of 1,178 bp were used (Xue et al., 2023). The reaction mixture is composed of 25 µl (almost 1 µl of $MgCl_2$, 0.5 µl of enzyme, 3 µl of extracted DNA, moreover, buffer 2.5 µl), and dNTPs, primers, and double distilled H_2O about 0.5, 1, and 15 µl used, respectively. For the PCR, the following protocols were set up. An initial denaturation step lasted for 5 min at 95°C, 30 cycles of denaturation at 95°C for 30 s, primer annealing for 15 s at 50°C, extension for 37 s at 72°C, and the final extension for 5 min at 72°C and for *ompB* gene (Segura et al., 2023). The reaction consisted of the same protocol as had been used for the citrate synthase gene (*gltA*). After making volume, further PCR was performed with the following conditions: initial denaturation step lasted for 5 min at 95°C, followed by 30 cycles of denaturation that persisted for 30 s at

10.3389/fmicb.2024.1359492

95°C; primer annealing was performed for 30 s at 53°C, and finally, extension lasted for 37 s at 72°C.

2.6.4 PCR amplification of enzootic nasal tumor virus

To pinpoint an 832-bp fragment of ENTV from tick DNA, primers with the subsequent sequences were designed [(forward) 5′-CCTTGGTTCCCCAGAGAAGG-3′ and (reverse) 5′-TGGGTATTATARRCACGAGGA-3′]. The amplifications were conducted in 25 μl with 15 μl of double distilled H_2O, 1 μl of primers, 0.5 μl of dNTPs, 2.5 μl of PCR buffer, 1 μl of $MgCl_2$ 0.5 μl of enzyme, and 3 μl DNA. After making volume, the next step for PCR cycling was set up with the following protocol: initial denaturation lasted about 5 min at 95°C, followed by 30 cycles with the succeeding denaturation step for 15 s at 95°C, primer annealing for 15 s at 52°C, and the final step extension for 60 s at 72°C.

All the PCR products are kept at 4°C. Then, the amplified product was added to a 1.5% agarose gel from Biowest in Shanghai, China, using 5 μl per sample. The bands were then observed using a gel documentation system from JUNYI in Beijing, China. Following purification with the QIAquick® PCR Purification Kit (Qiagen, Hilden, Germany) according to the manufacturer's recommendations, the PCR-amplified products were then transferred to Sangon Company (Guangzhou, China) for Sanger sequencing.

2.7 Sequence and phylogenetic analyses

The generated sequences were edited in Geneious Prime Software v.2022.01. BLAST was performed on isolated sequences, and comparisons were done on various sequences that were previously deposited in the GenBank. High similar sequences were downloaded for further phylogenetic analysis. After that, alignment was performed using CLUSTALX. Aligned sequences were checked on the basis of their same length; gaps and extra length were trimmed. Finally, after making manageable alignment, the MEGA v.11.0 software was used for making phylogenetic trees based on the maximum likelihood method (Swofford, 2003). The bootstrap consensus tree inferred from 1,000 replicates (Swofford, 2003) was taken to represent the evolutionary history of the taxa analyzed.

2.8 Data analysis

The data were subjected to analysis using the SPSS software (version 16). The variables were compared using chi-squared, Fisher's exact, and logistic regression tests. A $p < 0.05$ was deemed to be statistically significant.

2.9 Accession numbers

In the current research, different sequences were generated and submitted to the GenBank for accession numbers.

TABLE 1 Positive rate of TBPs among different species of ticks.

Genus	Species	Total samples	Positive ENTV in species	Positive ENTV in genus	Positive *Anaplasma* in species	Positive *Anaplasma* in genus	Positive *Rickettsia* in species	Positive *Rickettsia* in genus	Positive *Theileria* in genus	Positive *Theileria* in species	Total positive
Hyalomma	*Hy. anatolicum*	80	1 (1.25%)	1 (1.25%)	8 (10.00%)	8 (10.00%)	1 (1.25%)	1 (1.25%)	3 (3.75%)	3 (3.75%)	26 (32.50%)
	Hy. scupense	23	0 (0.00%)	0 (0.00%)	0 (0.00%)	0 (0.00%)	0 (0.00%)	0 (0.00%)	0 (0.00%)	0 (0.00%)	0 (0.00%)
Rhipicephalus	*Rh. turanicus*	70	2 (2.86%)	2 (2.86%)	2 (2.86%)	3 (4.29%)	0 (0.00%)	0 (0.00%)	4 (5.71%)	6 (8.57%)	19 (27.14%)
	Rh. sanguineus	5	0 (0.00%)	0 (0.00%)	0 (0.00%)	0 (0.00%)	0 (0.00%)	0 (0.00%)	0 (0.00%)	0 (0.00%)	0 (0.00%)
	Rh. microplus	35	0 (0.00%)	0 (0.00%)	1 (2.86%)	0 (0.00%)	0 (0.00%)	0 (0.00%)	2 (5.71%)	0 (0.00%)	3 (8.57%)
Total		213	3 (1.41%)	3 (1.41%)	11 (5.16%)	11 (5.16%)	1 (0.47%)	1 (0.47%)	9 (4.23%)	9 (4.23%)	48 (22.54%)
Chi-square			1.97^{NS}	1.97^{NS}	6.49^{NS}	7.36^{NS}	1.67^{NS}	1.67^{NS}	1.86^{NS}	6.09^{NS}	17.45**
P-value			0.741	0.741	0.166	0.118	0.796	0.796	0.762	0.192	0.002

NS, non-significant ($P < 0.05$); * significant ($P > 0.05$); **highly significant ($P < 0.01$).

TABLE 2 Positive rate of TBPs among districts and provinces.

Provinces	Districts	Samples to be tasted	ENTV Positive among districts	*Anaplasma* Positive among districts	*Theileria* positive among districts	*Rickettsia* positive among districts	Total positive
Sindh	Nawab shah	19	3 (15.79%)	6 (31.58%)	3 (15.79%)	0 (0.00%)	12 (63.16%)
	Karachi	33	0 (0.00%)	0 (0.00%)	2 (6.06%)	0 (0.00%)	2 (6.06%)
	Hyderabad	32	0 (0.00%)	0 (0.00%)	1 (3.13%)	0 (0.00%)	1 (3.13%)
Punjab	Lodhran	25	0 (0.00%)	7 (28.00%)	8 (32.00%)	0 (0.00%)	15 (60.00%)
	Sahiwal	12	0 (0.00%)	1 (8.33%)	0 (0.00%)	0 (0.00%)	1 (8.33%)
	Okara	12	0 (0.00%)	6 (50.00%)	2 (16.67%)	0 (0.00%)	8 (66.67%)
	Mianwali	20	0 (0.00%)	9 (45.00%)	7 (35.00%)	0 (0.00%)	16 (80.00%)
	Kabola	8	0 (0.00%)	1 (12.50%)	1 (12.50%)	0 (0.00%)	2 (25.00%)
	Pakpattan	8	0 (0.00%)	0 (0.00%)	0 (0.00%)	0 (0.00%)	0 (0.00%)
	Faisalabad	10	1 (10.00%)	0 (0.00%)	0 (0.00%)	0 (0.00%)	1 (10.00%)
Kashmir	Bagh	10	0 (0.00%)	0 (0.00%)	3 (30.00%)	4 (40.00%)	7 (70.00%)
	Mirpur	14	0 (0.00%)	0 (0.00%)	0 (0.00%)	0 (0.00%)	0 (0.00%)
Baluchistan	Quetta	10	0 (0.00%)	0 (0.00%)	0 (0.00%)	0 (0.00%)	0 (0.00%)
Total		213	4 (1.88%)	30 (14.08%)	27 (12.68%)	4 (1.88%)	65 (30.52%)
Chi-square			27.06**	56.92**	32.27**	82.75**	97.21**
P-value			0.008	0.000	0.001	0.000	0.000

NS, non-significant ($P < 0.05$); *significant ($P > 0.05$); **highly significant.

Supplementary Table S1 illustrates pathogens with their accession numbers.

3 Results

3.1 Tick collection and species identification

Both livestock and pets were examined for ticks. The animals examined included 43 cattle, 46 buffalo, 51 goats, and 44 sheep from different livestock farms. The pet animals included 21 dogs and 3 cats. Five samples were collected from poultry. In total, 213 ticks were collected from these animals. Tick samples were collected from different districts, and DNA was extracted. The ticks were identified by sequencing their rRNA sequences and aligning them with known sequences. Two other tick genera were also identified. The prevalence of these genera differed significantly. Among the collected ticks, the genus *Hyalomma* exhibited the highest prevalence, followed by *Rhipicephalus. Five* tick species were identified in this study, among which *H. anatolicum* was the most prevalent, followed by *Rh. turanicus*, with a prevalence rate of 16%. *Rhipicephalus microplus* was the third most common species, accounting for only 2% of the samples. The prevalence of *Rh. sanguineus* was found to be extremely low. Figure 3 shows the evolutionary tree based on the 16s rRNA gene of the obtained sequences. The created phylogenetic tree is divided into four different clades, and the expressed sequences are designated with red circles.

Tick species identification is based on PCR amplification, including phylogenetic analysis targeting the 16s ribosomal gene. The study sequence was analyzed for tick identification, designated with red dots.

3.2 Detection of tick-borne protozoa, virus, and bacterial pathogens

A comprehensive PCR analysis was conducted on 213 ticks, encompassing ticks from five distinct species, to detect the presence of prevalent tick-borne protozoan, bacterial, and viral pathogens. Of the 49 tick pools examined, 28.99% tested positive for tick-borne infections. The infection rate was determined using a comprehensive statistical analysis, yielding a calculated value of 17.45, 0.002 (Table 1). Of the 213 tick samples that were combined, 3 (1.41%) tested positive for ENTV, 11 (5.16%) tested positive for *Anaplasma*, 1 (0.47%) tested positive for *Rickettsia*, and 9 (4.23%) tested positive for *Theileria*. The prevalence of ENTV in the tick genus *Rhipicephalus* was significantly higher (1.82%) than that in other tick genera. Similarly, the bacterial pathogen *Rickettsia* had a significantly higher prevalence rate of 1 (0.97%) in the tick genus *H. anatolicum* than in the other tick genera. Additionally, the bacterial pathogen *Anaplasma* was found to have a higher prevalence of 8 (7.77%) in *Hyalomma* ticks than in other tick genera. Furthermore, *Theileria* was more prevalent in the tick genus *Rhipicephalus*. No tick-borne pathogenic DNA was detected in *Hy. scupense*.

3.3 Distribution of tick-borne pathogens among districts and provinces

After surveying the positivity rate of TBPs among different ticks, we evaluated the distribution of positive ticks among different districts, which is important for evaluating risk in terms of spatial distribution. First, we compared the distribution of TBP-positive rates among different provinces. As shown in Table 2, the

TABLE 3 Positive rate of TBPs among animals.

Animals	Samples to be tasted	Positive for ENTV	Positive for *Anaplasma*	Positive for *Theileria*	Positive for *Rickettsia*	Total positive
Goat	51	3 (5.88%)	12 (23.53%)	12 (23.53%)	3 (5.88%)	30 (58.82%)
Sheep	44	4 (9.09%)	11 (25.00%)	6 (13.64%)	0 (0.00%)	21 (47.73%)
Cattle	43	0 (0.00%)	2 (4.65%)	2 (4.65%)	0 (0.00%)	4 (9.30%)
Buffalo	46	0 (0.00%)	1 (2.17%)	2 (4.35%)	0 (0.00%)	3 (6.52%)
Poultry	5	0 (0.00%)	1 (20.00%)	0 (0.00%)	0 (0.00%)	1 (20.00%)
Dog	21	0 (0.00%)	0 (0.00%)	0 (0.00%)	0 (0.00%)	0 (0.00%)
Cat	3	0 (0.00%)	0 (0.00%)	0 (0.00%)	1 (33.33%)	1 (33.33%)
Total	213	7 (3.29%)	27 (12.68%)	22 (10.33%)	4 (1.88%)	60 (28.17%)
Chi-square		9.76^{NS}	22.27**	16.73*	23.59**	58.66**
P-value		0.135	0.001	0.010	0.001	0.000

NS, non-significant ($P < 0.05$); *significant ($P > 0.05$); **highly significant ($P < 0.01$).

positive rates between the provinces differed significantly (or non-significantly). Samples were collected from several districts in the provinces of Sindh and Punjab. Although different rates of TBPs were identified, no significant differences were observed between the districts of the two provinces. The higher the positivity rate of TBPs, the greater the risk. Therefore, provinces with higher positivity rates face a higher risk of developing TBPs.

3.4 Distribution of tick-borne pathogens among animals

After analyzing the positivity rate among different districts and ticks, we analyzed the TBP positivity rates among different species of livestock. As shown in Table 3, the positivity rate of TBPs was significantly different among the tested animals ($\chi^2 = 58.66$, $P = 0.000$). Among the animal species, goats had the highest positive rate, and all four types of bacteria, virus, and protozoan pathogens were found in the ticks from goats, followed by sheep (21, 47.73%), cattle (4, 9.30%), and buffalo (3, 6.52%). The prevalence of *Theileria* and *Anaplasma* was high. In the case of cats, one (33.33%) *Rickettsia* species was identified, and in poultry, one (20.00%) *Anaplasma* species was detected. Combined with the distribution of ticks from different animals, these results indicate that TBPs are differentially distributed between different species of ticks and animals.

3.5 Phylogenetic analysis of TBPs

The phylogenetic analysis of *Anaplasma marginale*, *Rickettsia canadensis*, *Theileria*, and ENTV delineates our findings in Figures 4–7. After completing all three *Anaplasma marginale* sequences, it has been documented that all three partial sequences formed a different clade and were partially related to other sequences from China and Pakistan (Figure 4). The results of the phylogenetic analysis based on the outer surface protein of *Rickettsia canadensis* showed a close clustering pattern close to two sequences, specifically OR825418 and OR825419, which were obtained from different ticks. These sequences exhibited a close clustering pattern with sequences from Pakistan, China, and Iran. The sequences acquired from GenBank were derived from various tick species. The sequence with the identifier OR8254820 was identified to form a separate clade, as shown in Figure 5. The partial sequences of *Theileria* of different ticks, including *Hyalomma* and *Rhipicephalus*, were collected from various locations in Pakistan, such as Punjab, Sindh, Balochistan, and AJK. Phylogenetic analysis of three partial *Theileria* sequences revealed distinct clades from other sequences in GenBank. *Theileria* (OR804202) is similar to sequences from the United States and India. *Theileria* (OR804200) showed a close relationship to sequences from India. Furthermore, *Theileria* (OR804201) showed 100% similarity with a South African isolate (Figure 6).

The phylogenetic analysis of the current whole-genome sequence of ENTV isolated from *Rh. Turanicus* and *Hy. anatolicum* (OR991120) in sheep and goats from various districts of Pakistan revealed a relatively high homology (100%) with ENTV from the United States (NC004994). The lowest divergence ratios (30%) were detected with ENTV isolated from goats in Canada (FJ744146) (Figure 7).

4 Discussion

In this study, 213 tick species from two genera, namely, *Rhipicephalus* and *Hyalomma*, with five species ascertained, namely, *R. turanicus*, *R. sanguineus, R. microplus, Hy. anatolicum*, and *Hy. scupense,* were assembled from the Punjab, Balochistan, Kashmir, and Sindh provinces in Pakistan. According to these studies, the provinces that share common borders with Afghanistan are inaugurating delving ticks in Pakistan. Our finding proclaimed that nine (4.23%) clarify that *Theileria* were detected in all the surveyed tick species, except *Hy. scupense* and *R. sanguineus*. *Theileria* infections have been investigated using various techniques in different regions worldwide, including Pakistan. For example, in Egypt, the prevalence of *T. annulata* in buffaloes is 15.49% (El-Ashker et al., 2015). Few reports concluded that in Pakistan, the prevalence of *T. annulata* was reported to be 16.3% and

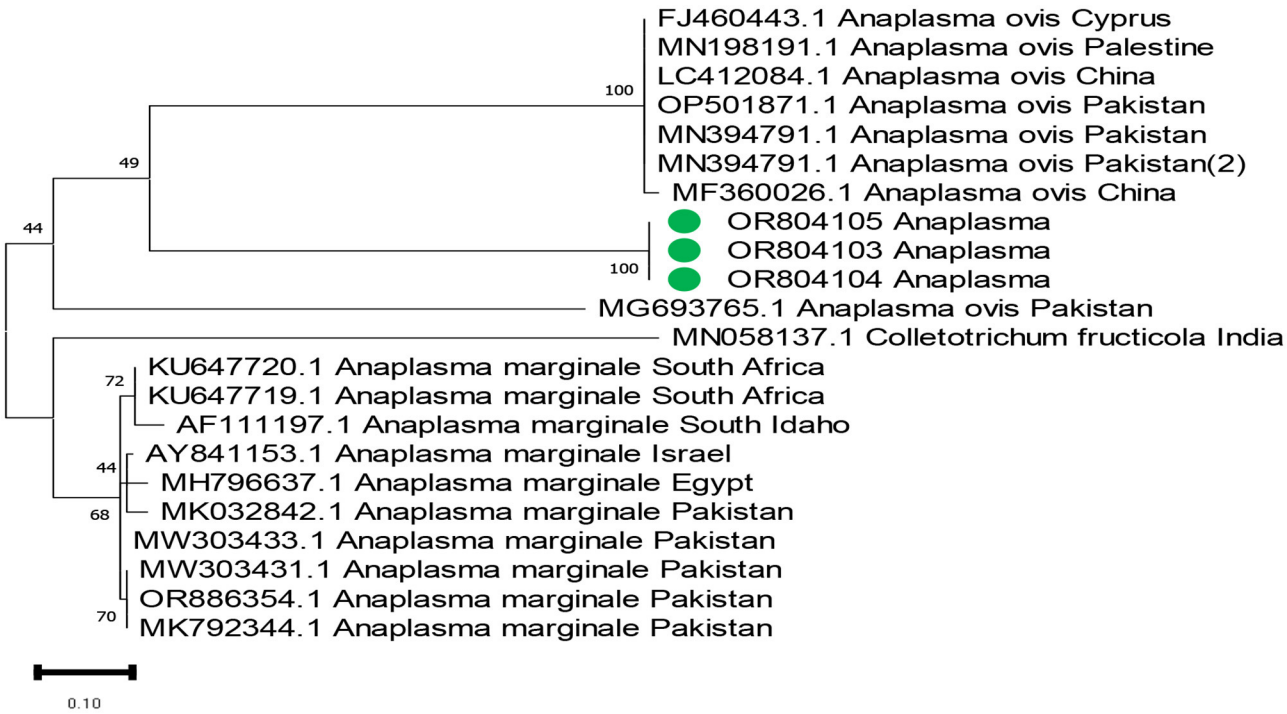

FIGURE 4
Phylogenetic tree based on the 16s rRNA of *Anaplasma marginale* partial sequence. Targeted sequences are expressed in green circles. Supporting bootstrap values were used, and *Anaplasma marginale* from Pakistan was set up as an outgroup.

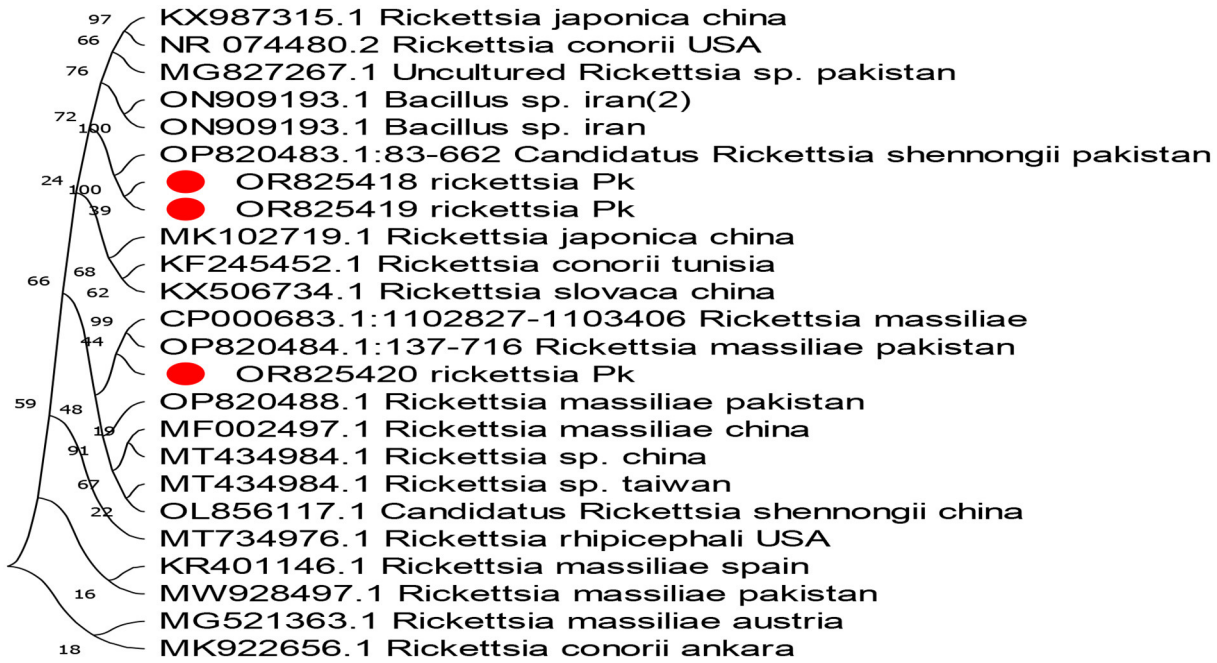

FIGURE 5
Evolutionary tree based on the outer membrane surface protein sequence of *Rickettsia*. The bootstrap values were kept standard, and substitutions were based on scale bar values. As an outgroup, *Rickettsia conorii* from Ankara and *Rickettsia massiliae* were used. The obtained sequences are expressed in red circles.

29.9% in ruminants (Zeb et al., 2020). Our findings align with worldwide research, including those in Pakistan, with a slight difference in the prevalence rate. Differences in prevalence could be due to changes in temperature, humidity, agriculture methods, and vector populations across different locations globally (Zafar et al., 2022) with a high prevalence in the southern part of

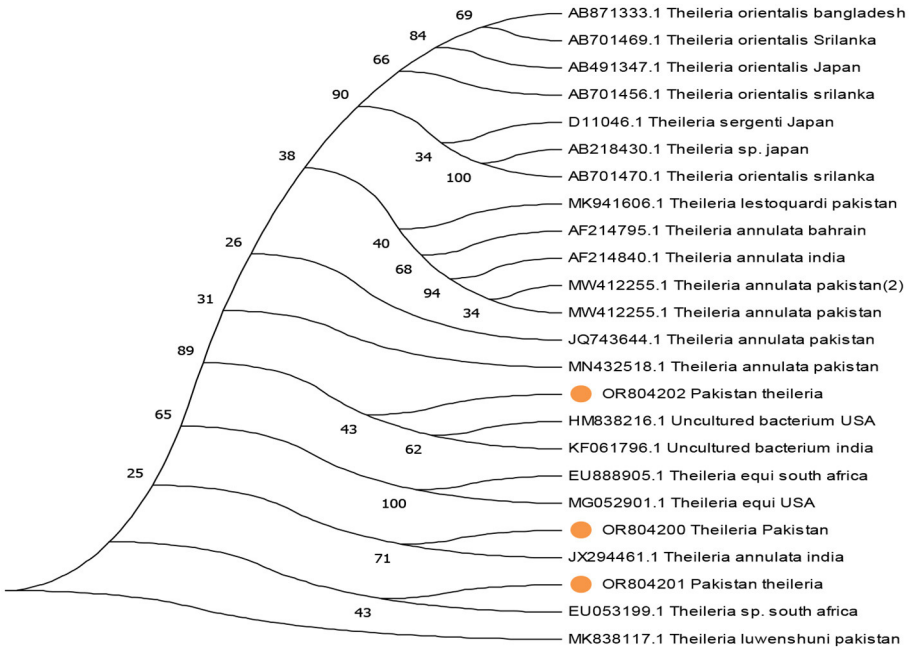

FIGURE 6
Evolutionary tree based on the 18s rRNA of *Theileria*, with the *Theileria luwenshuni* used as an outgroup. Standard values of bootstrap considered along with the scale bar stipulate substitution at each branch site. The extracted sequences are expressed in yellow circles.

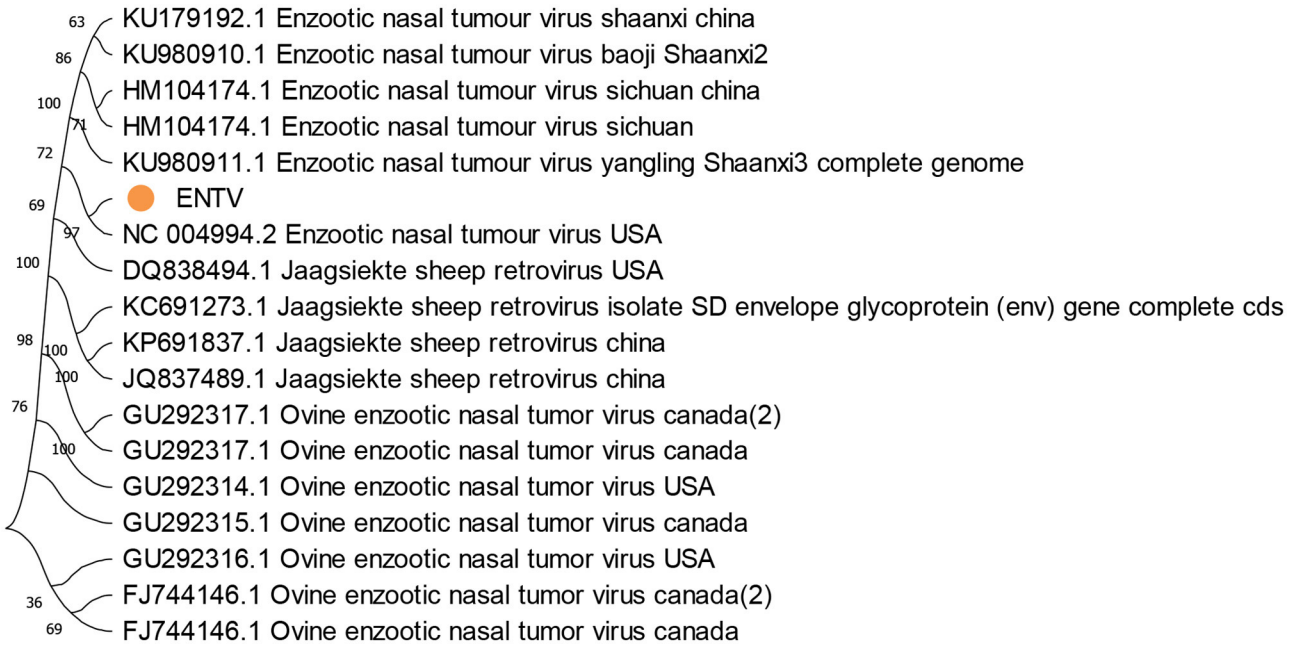

FIGURE 7
Evolutionary tree of the whole-genome sequence analysis of ENTV obtained from goats in Pakistan. The obtained genomes are expressed in yellow circles and shown in the middle of the figure. The ovine enzootic nasal tumor virus in Canada was set as an outgroup. The standard bootstrap value was used, and the maximum likelihood method was applied for evolutionary tree construction.

Lahore district of Punjab Province, where *Theileria* was detected to be 65% prevalent in both *Rhipicephalus* and *Hyalomma* in sheep (Durrani et al., 2011). Research conducted in the following countries, Turkey, Pakistan, and China, indicated that *Theileria* has been detected to be the most abundant species, with a prevalence rate of 34.56%, 79%, and 78%, respectively (Durrani et al., 2011). Besides, the *Theileria* prevalence rate in the present study is lower than the previous studies, which detected *Theileria* from

various mammalian hosts in preference to ticks; hence, the results were found to be inconsistent with our findings. In addition, the ascertained three partial 18s rRNA sequences of *Theileria* are highly pathogenic in nature due to their correspondence with other *Theileria* spp., which were determined from different regions in Pakistan.

In this study, *A. marginale* was detected in 8 (10.00%) *Hy. anatolicum* species and 3 (4.29%) *R. turanicus* species using molecular methods. Few reports suggest that 20 different kinds of ticks are the reservoir host of *A. marginale*, which leads to oppressive complications, for instance, bovine anaplasmosis (Pothmann et al., 2016). In Pakistan, conventional methods such as microscopy analysis are used for detecting *A. marginale*; molecular approaches for detecting such a pathogen in ticks are meager (Khan et al., 2017). The results revealed that *A. marginale* is dominant in *Hy. anatolicum*. Our finding is contrary to the study that identified *R. microplus* as a consequential host for spreading *A. marginale* in various developing countries (Kocan et al., 2010). Our finding contradict the report of Ramzan et al., whose verified research in Multan districts proclaimed the prevalence of *A. marginale* in cattle and buffalo (Ramzan et al., 2020). Our results suggested that small ruminants are utterly more infected with *A. marginale* than large ruminants, which is in accordance with the discrepancy in the susceptibility of cattle and buffalo breeds to anaplasmosis (Sajid et al., 2014).

Our findings concluded that *R. canadensis* was detected in 1 (1.25%) *Hy. anatolicum* tick collected from cats and domestic goats. Candidatus *Rickettsia*, an agent of unknown pathogenicity, is a common vector in cat fleas (Mediannikov et al., 2015; Legendre and Macaluso, 2017). SFGR infections in cats could also be caused by tick-borne SFGR (Jabbar et al., 2015). These findings are contrary to other research conducted in the tribal areas of Rawalpindi, Pakistan, showing that *Rickettsia* is predominant in different tick species such as *Rh. turanicus*, *Rh. microplus, Rh. haemaphysaloides, and Rhipicephalus* species (Ali et al., 2021). Few investigations have reported that *Rh. sanguineus, Rh. sulcatus, Rh. lunulatus, Rh. muhsamae*, and *Rh. senegalensis* are the reservoir hosts of this pathogen (Eremeeva et al., 2006).

Our findings suggested that ENTV was detected in 2 (2.86%) *Rh. turanicus* and 1 (1.25%) *Hy. anatolicum* ticks were collected from a total of 3 (5.88%) small ruminant goats and 4 (9.09%) sheep in the Nawabshah and Faisalabad districts of Pakistan. In Pakistan, there are no reports of ticks infesting ruminants equated with ENTV infection, and to our knowledge, this is the first report of ENTV associated with small ruminant ticks. Research has concluded that ENTV isolated from goats and sheep belongs to ENTV-1 and ENTV-2, respectively (Ortín et al., 2003). Oncogenic retroviruses transform epithelial cells through their envelope (Monot et al., 2015). ENTV may cause severe complications in animals in terms of clinical manifestations such as dry and productive cough, exudative nasal discharge, difficulty breathing, stretching neck breathing, and ultimately facial deformities (De las Heras et al., 1995). Gradually, the animals lose weight and die. A small ruminant population is highly affected by this tumor worldwide; most recent cases have been reported in Turkey (Ajayi et al., 2013; Özmen and Serpin, 2016).

There is a varying route of ENTV transmission among animals, but the most common exploration route is the respiratory route via nasal and cough exudate. It has been reported that ENTV is reproduced experimentally by nebulization (Walsh et al., 2013). Other routes of transmission, such as milk, colostrum, or intrauterine or perinatal infections, as have been reported for JSRV and ENTV, should also be considered (Caporale et al., 2005; Grego et al., 2008). Infected animals are the more common cause of ENTV transmission among disease-free flocks.

Our findings showed that 3 (6.52%) buffaloes, 4 (9.30%) cattle, 30 (58.82%) goats, 21 (47.73%) sheep, 1 (20.00%) poultry, 1 (33.33%) cat, and 21 (0%) dogs were infested with TBPs. Cattle comprised the highest proportion of livestock infested with TBPs. This may be due to the thin skin and other supporting conditions for the growth of ticks in Pakistan, like temperature, humidity, and habitat (Ghafar et al., 2020). Our findings indicate lower rates of tick infestation in buffaloes than in cattle, which aligns with previous research that also found comparable findings (Ghafar et al., 2020; Ramzan et al., 2020; Hussain S. et al., 2023).

Sheep have a lower TBPs infestation rate than goats. Several studies conducted in Pakistan have consistently demonstrated a prevalent trend of tick infestation in livestock, revealing that sheep manifest a lower infection rate (11.1%) than goats (60.0%) (Alessandra and Santo, 2012). In contrast, another study reported that infestation was higher in sheep than in goats (Rashid et al., 2018; Ramzan et al., 2019). The main reason for low infestation may be the presence of wool on the sheep's body. Wool may be a better protective factor against tick attachment in sheep. Our results agree with those of previous findings on tick infestation (Atif, 2012; Monfared et al., 2015).

Our findings among various districts concluded that Mianwali, Lodhran, and Okara in Punjab Province are more highly affected by TBPs than other districts due to the humid environmental conditions, as most of the rice crop is reared in that area (Ashraf et al., 2021). The maximum levels of egg-laying and hatching of Hyalomma ticks are observed at 32–34°C with 85% humidity (Durrani and Shakoori, 2009).

5 Conclusion

In the present study, we performed an etiological survey of tick-borne pathogens among livestock and pet animals in Pakistan. The results showed that various tick-borne pathogens were identified in both livestock and pet animals, and these pathogens are greatly differentially distributed among ticks and animals, which implied a risk for both animals and humans. Furthermore, a new virus, ENTV, was identified in animals in Pakistan. Further studies involving a larger number of ticks sampled across the country and detailed transmission studies should be conducted to further evaluate the prevalence of tick-borne pathogens of veterinary and medical importance.

Data availability statement

The datasets presented in this study have been deposited to the NCBI Genebank Repository. The accession numbers can be found in the Supplementary material.

Ethics statement

The animal studies were approved by the Research Institute of Veterinary Medicine in Shenyang Agriculture University. The studies were conducted in accordance with the local legislation and institutional requirements. Written informed consent was obtained from the owners for the participation of their animals in this study.

Author contributions

AJ: Conceptualization, Writing—original draft, Writing—review & editing, Data curation, Formal analysis, Funding acquisition, Investigation, Methodology, Project administration, Resources, Software, Supervision, Validation, Visualization. ZY: Software, Writing—original draft, Writing—review & editing. YW: Data curation, Formal analysis, Writing—original draft, Methodology. QX: Methodology, Writing—review & editing. MA: Methodology, Writing—review & editing. SG: Data curation, Formal analysis, Methodology, Writing—review & editing. XH: Conceptualization, Data curation, Formal analysis, Funding acquisition, Investigation, Methodology, Project administration, Resources, Software, Supervision, Validation, Visualization, Writing—review & editing, Writing—original draft. ZC: Conceptualization, Data curation, Formal analysis, Funding acquisition, Investigation, Methodology, Project administration, Resources, Software, Supervision, Validation, Visualization, Writing—original draft, Writing—review & editing.

Funding

The author(s) declare that financial support was received for the research, authorship, and/or publication of this article. This study was supported by the Science and Technology Partnership Program, Ministry of Science and Technology of China (no. KY201901014).

Acknowledgments

We would like to thank all the researchers, professors, students, and field members of the Shenyang Agriculture University, China, and a few people from Pakistan who helped us with pleasure and quickness to obtain the study data and cared for it.

Conflict of interest

The authors declare that the research was conducted in the absence of any commercial or financial relationships that could be construed as a potential conflict of interest.

Publisher's note

All claims expressed in this article are solely those of the authors and do not necessarily represent those of their affiliated organizations, or those of the publisher, the editors and the reviewers. Any product that may be evaluated in this article, or claim that may be made by its manufacturer, is not guaranteed or endorsed by the publisher.

Supplementary material

The Supplementary Material for this article can be found online at: https://www.frontiersin.org/articles/10.3389/fmicb.2024.1359492/full#supplementary-material

References

Ajayi, O. L., Oyewusi, I. K., Olaniyi, M. O., Oyekunle, M. A., Jagun, A. T., Omotainse, S. O., et al. (2013). Enzootic nasal adenocarcinoma: cytological and clinicopathological observations in a West African Dwarf goat. *Bull. Anim. Health Prod. Afr* 61, 331–336.

Alessandra, T., and Santo, C. (2012). Tick-borne diseases in sheep and goats: clinical and diagnostic aspects. *Small Rum. Res.* 106, S6–S11. doi: 10.1016/j.smallrumres.2012.04.026

Ali, A., Zahid, H., Zeb, I., Tufail, M., Khan, S., Haroon, M., et al. (2021). Risk factors associated with tick infestations on equids in Khyber Pakhtunkhwa, Pakistan, with notes on Rickettsia massiliae detection. *Parasites Vectors* 14, 1–12. doi: 10.1186/s13071-021-04836-w

Ashraf, S., Parveen, A., Muhammad Awais, M., Gillani, Q., Aktas, M., Ozubek, S., et al. (2021). A report on molecular detection and phylogenetic evaluation of Anaplasma marginale in ticks and blood samples collected from cattle in district Layyah in Punjab (Pakistan). *Curr. Microbiol.* 78, 274–281. doi: 10.1007/s00284-020-02256-0

Atif, F. A. (2012). Prevalence of cattle tick infestation in three districts of the Punjab, Pakistan. *Pakistan J. Sci.* 64:1–15. doi: 10.57041/pjs.v64i1.463

Atif, F. A., Khan, M. S., Iqbal, H. J., Arshad, G. M., Ashraf, E., Ullah, S., et al. (2012). Prevalence of Anaplasma marginale, Babesia bigemina and Theileria annulata infections among cattle in Sargodha District, Pakistan. *Afr. J. Agric. Res* 7, 3302–3307. doi: 10.5897/AJAR11.2051

Bratton, R. L., and Corey, G. R. (2005). Tick-borne disease. *Am. Family Phys.* 71, 2323–2330.

Caporale, M., Centorame, P., Giovannini, A., Sacchini, F., Ventura, D., De, M., et al. (2005). Infection of lung epithelial cells and induction of pulmonary adenocarcinoma is not the most common outcome of naturally occurring JSRV infection during the commercial lifespan of sheep. *Virology* 338, 144–153. doi: 10.1016/j.virol.2005.05.018

Cousens, C., Minguijon, E., Dalziel, R. G., Ortin, A., Garcia, M., Park, J., et al. (1999). Complete sequence of enzootic nasal tumor virus, a retrovirus associated with transmissible intranasal tumors of sheep. *J. Virol.* 73, 3986–3993. doi: 10.1128/JVI.73.5.3986-3993.1999

De las Heras, M., Garcia de Jalon, J. A., Minguijon, E., Gray, E. W., Dewar, P., and Sharp, J. M. (1995). Experimental transmission of enzootic intranasal tumors of goats. *Vet. Pathol.* 32, 19–23. doi: 10.1177/030098589503200103

De las Heras, M., Ortin, A., Cousens, C., Minguijon, E., and Sharp, J. M. (2003). Enzootic nasal adenocarcinoma of sheep and goats. *Jaagsiekte Sheep Retrovirus Lung Cancer* 12, 201–223. doi: 10.1007/978-3-642-55638-8_8

Durrani, A. Z., and Shakoori, A. R. (2009). Study on ecological growth conditions of cattle Hyalomma ticks in Punjab, Pakistan. *Iran. J. Parasitol.* 4, 19–25.

Durrani, A. Z., Younus, M., Kamal, N., Mehmood, N., and Shakoori, A. R. (2011). Prevalence of ovine Theileria species in district Lahore, Pakistan. *Pakistan J. Zool.* 43:1–14.

El-Ashker, M., Hotzel, H., Gwida, M., El-Beskawy, M., Silaghi, C., Tomaso, H., et al. (2015). Molecular biological identification of *Babesia, Theileria, and Anaplasma* species in cattle in Egypt using PCR assays, gene sequence analysis and a novel DNA microarray. *Vet. Parasitol.* 207, 329–334. doi: 10.1016/j.vetpar.2014.12.025

Eremeeva, M. E., Bosserman, E. A., Demma, L. J., Zambrano, M. L., Blau, D. M., Dasch, G. A., et al. (2006). Isolation and identification of Rickettsia massiliae from *Rhipicephalus sanguineus* ticks collected in Arizona. *Appl. Environ. Microbiol.* 72, 5569–5577. doi: 10.1128/AEM.00122-06

Eshetu, E. (2015). A review on the diagnostic and control challenges of major tick-borne haemoparasite diseases of cattle. *J. Biol. Agric. Health* 5, 160–172.

Ghafar, A., Gasser, R. B., Rashid, I., Ghafoor, A., and Jabbar, A. (2020). Exploring the prevalence and diversity of bovine ticks in five agro-ecological zones of Pakistan using phenetic and genetic tools. *Ticks Tick-Borne Dis.* 11:101472. doi: 10.1016/j.ttbdis.2020.101472

Grego, E., Meneghi, D. e., Alvarez, D., Benito, V., Minguijón, A. A., Ortín, E., et al. (2008). Colostrum and milk can transmit jaagsiekte retrovirus to lambs. *Vet. Microbiol.* 130, 247–257. doi: 10.1016/j.vetmic.2008.01.011

Hussain, N., Shabbir, R. M. K., Ahmed, H., Afzal, M. S., Ullah, S., Ali, A., et al. (2023). Prevalence of different tick species on livestock and associated equines and canine from different agro-ecological zones of Pakistan. *Front. Vet. Sci.* 9:1089999. doi: 10.3389/fvets.2022.1089999

Hussain, S., Hussain, A., Aziz, M. U., Song, B., Zeb, J., Hasib, F. Y., et al. (2023). First molecular confirmation of multiple zoonotic vector-borne diseases in pet dogs and cats of Hong Kong SAR. *Ticks Tick-Borne Dis.* 14:102191. doi: 10.1016/j.ttbdis.2023.102191

Jabbar, A., Abbas, T., Sandhu, Z. U. D., Saddiqi, H. A., Qamar, M. F., Gasser, R. B., et al. (2015). Tick-borne diseases of bovines in Pakistan: major scope for future research and improved control. *Parasites Vectors* 8, 1–13. doi: 10.1186/s13071-015-0894-2

Jamil, M., Ali, S., Gul, J., Kashif, M., Ullah, N., Ali, M., et al. (2023). Taxonomical and epidemiological study of tick species on domesticated animals. *Pure Appl. Biol.* 12, 523–530 doi: 10.19045/bspab.2023.120054

Khan, A., Muhammed, A. A., Nasreen, N., Iqbal, F., and Cossio-Bayugar, R. (2022). Tick-borne haemoparasitic diseases in small ruminants in Pakistan: current knowledge and future perspectives. *Saudi J. Biol. Sci.* 29, 2014–2025. doi: 10.1016/j.sjbs.2021.12.046

Khan, M. I., Shah, S. S. A., Khan, H., Irshad, M., and Aziz, U. (2017). Determination of parasitic load in government cattle breeding and dairy farm, Charsadda, Khyber Pakhtunkhwa-Pakistan. *Adv. Anim. Vet. Sci.* 5, 174–178. doi: 10.14737/journal.aavs/2017/5.4.174.178

Kocan, K. M., de la Fuente, J., Blouin, E. F., Coetzee, J. F., and Ewing, S. A. (2010). The natural history of Anaplasma marginale. *Vet. Parasitol.* 167, 95–107. doi: 10.1016/j.vetpar.2009.09.012

Legendre, K. P., and Macaluso, K. R. (2017). Rickettsia felis: a review of transmission mechanisms of an emerging pathogen. *Tropical Med. Inf. Dis.* 2:64. doi: 10.3390/tropicalmed2040064

Leroux, C., and Mornex, J. F. (2008). Retroviral infections in sheep and the associated diseases. *Small Rum. Res.* 76, 68–76. doi: 10.1016/j.smallrumres.2007.12.010

Mediannikov, O., Aubadie-Ladrix, M., and Raoult, D. (2015). Candidatus '*Rickettsia senegalensis*' in cat fleas in Senegal. *New Microbes New Inf.* 3, 24–28. doi: 10.1016/j.nmni.2014.10.005

Monfared, A. L., Mahmoodi, M., and Fattahi, R. (2015). Prevalence of ixodid ticks on cattle, sheep and goats in Ilam County, Ilam Province, Iran. *J. Paras. Dis. Off. Organ Ind. Soc. Parasitol.* 39:37. doi: 10.1007/s12639-013-0267-8

Monot, M., Archer, F., Gomes, M., Mornex, J. F., and Leroux, C. (2015). Advances in the study of transmissible respiratory tumours in small ruminants. *Vet. Microbiol.* 181, 170–177. doi: 10.1016/j.vetmic.2015.08.008

Mwamuye, M. M., Kariuki, E., Omondi, D., Kabii, J., Odongo, D., Masiga, D., et al. (2017). Novel Rickettsia and emergent tick-borne pathogens: a molecular survey of ticks and tick-borne pathogens in Shimba Hills National Reserve, Kenya. *Ticks Tick-Borne Dis.* 8, 208–218. doi: 10.1016/j.ttbdis.2016.09.002

Ortín, A., Cousens, C., Minguijon, E., Pascual, Z., Villarreal, M. P. D., Sharp, J. M., et al. (2003). Characterization of enzootic nasal tumour virus of goats: complete sequence and tissue distribution. *J. Gen. Virol.* 84, 2245–2252. doi: 10.1099/vir.0.19125-0

Özmen, Ö., Sahinduran, S., Haligür, M., and Demir, N. (2010). *Clinical, pathological, immunohistochemical and ultrastructural observations on enzootic nasal adenocarcinoma in five goats*. 16, 633–639. doi: 10.9775/kvfd.2009.1340

Özmen, Ö., and Serpin, N. (2016). First case of Enzootic Nasal Adenocarcinoma (ENA) in a sheep in Turkey. *Vet. J. Mehmet Akif Ersoy Univ.* 1, 87–90. doi: 10.24880/maeuvfd.260794

Pothmann, D., Poppert, S., Rakotozandrindrainy, R., Hogan, B., Mastropaolo, M., Thiel, C., et al. (2016). Prevalence and genetic characterization of Anaplasma marginale in zebu cattle (Bos indicus) and their ticks (Amblyomma variegatum, Rhipicephalus microplus) from Madagascar. *Ticks Tick-Borne Dis.* 7, 1116–1123. doi: 10.1016/j.ttbdis.2016.08.013

Ramzan, M., Naeem-Ullah, U., Abbas, H., Adnan, M., Rasheed, Z., Khan, S., et al. (2019). Diversity of hard ticks in goats and sheep in Multan, Punjab, Pakistan. *Int. J. Agric. Biol. Res.* 35, 7–9.

Ramzan, M., Naeem-Ullah, U., Saba, S., Iqbal, N., and Saeed, S. (2020). Prevalence and identification of tick species (Ixodidae) on domestic animals in district Multan, Punjab Pakistan. *Int. J. Acarol.* 46, 83–87. doi: 10.1080/01647954.2020.1711803

Rashid, M., Godara, R., Yadav, A., and Katoch, R. (2018). Prevalence of ticks in sheep and goats of Jammu region. *Ind. J. Small Rum.* 24, 183–186. doi: 10.5958/0973-9718.2018.00019.3

Saeed, S., Jahangir, M., Fatima, M., Shaikh, R. S., Khattak, R. M., Ali, M., et al. (2015). PCR based detection of Theileria lestoquardi in apparently healthy sheep and goats from two districts in Khyber Pukhtoon Khwa (Pakistan). *Trop. Biomed.* 32, 225–232.

Sajid, M. S., Iqbal, Z., Shamim, A., Siddique, R. M., Hassan, M. J. U., Rizwan, H. M., et al. (2017). Distribution and abundance of ticks infesting livestock population along Karakorum highway from Mansehra to Gilgit, Pakistan. *J. Hellenic Vet. Med. Soc.* 68, 51–58. doi: 10.12681/jhvms.15556

Sajid, M. S., Siddique, R. M., Khan, S. A., Iqbal, Z., and Khan, M. N. (2014). Prevalence and risk factors of anaplasmosis in cattle and buffalo populations of district Khanewal, Punjab, Pakistan. *Global Vet.* 12, 146–153. doi: 10.5829/idosi.gv.2014.12.01.8252

Segura, A., Rafael, M., Vaz-Rodrigues, R., Rodríguez, O., and Gortázar, C., and de la Fuente, J. (2023). Tick infestation in spur-thighed tortoise population: a pilot study for unraveling epidemiological patterns and demographic consequences. *Exp. Appl. Acarol.* 91, 661–679. doi: 10.1007/s10493-023-00863-7

Svara, T., Gombac, M., Vrecl, M., Juntes, P., Kostanjsek, R., Pogacnik, A., et al. (2006). Enzootic nasal adenocarcinoma of sheep in Slovenia. *J. Vet. Med. Series A* 53, 26–29. doi: 10.1111/j.1439-0442.2006.00784.x

Swofford, D. L. (2003). *PAUP* Phylogenetic Analysis Using Parsimony (* and Other Methods). Version 4.* Available online at: http://paupcsit.fsu.edu/ (accessed October 20, 2003).

Walsh, S. R., Linnerth-Petrik, N. M., Yu, D. L., Foster, R. A., Menzies, P. I., Diaz-Méndez, A., et al. (2013). Experimental transmission of enzootic nasal adenocarcinoma in sheep. *Vet. Res.* 44, 1–13. doi: 10.1186/1297-9716-44-66

WHO (2014). *A global brief on vector-borne diseases*. Geneva: World Health Organization.

Xu, B., Liu, L., Huang, X., Ma, H., Zhang, Y., Du, Y., et al. (2011). Metagenomic analysis of fever, thrombocytopenia and leukopenia syndrome (FTLS) in Henan Province, China: discovery of a new bunyavirus. *PLoS Pathogens* 7:e1002369. doi: 10.1371/journal.ppat.1002369

Xue, J., Ren, Q., Yang, X. L., Wang, J., Xie, G., Du, L., et al. (2023). Human pathogens in ticks removed from humans in Hebei, China. *Heliyon* 9:e13859. doi: 10.1016/j.heliyon.2023.e13859

Zafar, S. N. U. A., Khan, A., Niaz, S., Aktas, M., Ozubek, S., Farooq, M., et al. (2022). Prevalence of Anaplasma marginale in cattle blood samples collected from two important livestock regions in Punjab (Pakistan) with a note on epidemiology and phylogeny of parasite. *Saudi J. Biol. Sci.* 29, 1515–1520. doi: 10.1016/j.sjbs.2021.11.020

Zeb, J., Shams, S., Din, I. U., Ayaz, S., Khan, A., Nasreen, N., et al. (2020). Molecular epidemiology and associated risk factors of Anaplasma marginale and Theileria annulata in cattle from North-western Pakistan. *Vet. Parasitol.* 279:109044. doi: 10.1016/j.vetpar.2020.109044

frontiers | Frontiers in Microbiology

TYPE Original Research
PUBLISHED 28 March 2024
DOI 10.3389/fmicb.2024.1359797

Check for updates

OPEN ACCESS

EDITED BY
Kevin S. W. Tan,
National University of Singapore, Singapore

REVIEWED BY
Clifton McKee,
Johns Hopkins University, United States
Miriam Maas,
National Institute for Public Health and the Environment (Netherlands), Netherlands

*CORRESPONDENCE
Wen-Ping Guo
✉ guowenping@nwsuaf.edu.cn

RECEIVED 22 December 2023
ACCEPTED 11 March 2024
PUBLISHED 28 March 2024

CITATION
Xue J, Chen S-S, Xu Z-Y, Wang F-N, Wang J, Diao D, Du L, Xie G-C and Guo W-P (2024) *Anaplasma*, *Bartonella*, and *Rickettsia* infections in Daurian ground squirrels (*Spermophilus dauricus*), Hebei, China. *Front. Microbiol.* 15:1359797. doi: 10.3389/fmicb.2024.1359797

COPYRIGHT
© 2024 Xue, Chen, Xu, Wang, Wang, Diao, Du, Xie and Guo. This is an open-access article distributed under the terms of the Creative Commons Attribution License (CC BY). The use, distribution or reproduction in other forums is permitted, provided the original author(s) and the copyright owner(s) are credited and that the original publication in this journal is cited, in accordance with accepted academic practice. No use, distribution or reproduction is permitted which does not comply with these terms.

Anaplasma, *Bartonella*, and *Rickettsia* infections in Daurian ground squirrels (*Spermophilus dauricus*), Hebei, China

Jing Xue[1], Si-Si Chen[1], Ze-Yun Xu[1], Fang-Ni Wang[1], Jiangli Wang[2], Danhong Diao[2], Luanying Du[1], Guang-Cheng Xie[1] and Wen-Ping Guo[1]*

[1]College of Basic Medicine, Chengde Medical University, Chengde, China, [2]Chengde Center for Disease Control and Prevention, Chengde, China

Rodents have been confirmed as hosts of various vector-borne zoonotic pathogens and are important for the maintenance of these microbes in nature. However, surveillance for zoonotic pathogens is limited for many wild rodent species in China, so our knowledge of pathogen ecology, genetic diversity, and the risk of cross-species transmission to humans is limited. In this study, 165 spleen samples of Daurian ground squirrels (*Spermophilus dauricus*) were collected from Weichang Manchu and the Mongolian Autonomous County of Hebei Province, China, and *Rickettsia*, *Bartonella*, and *Anaplasma* were identified by DNA detection using polymerase chain reaction (PCR). Sequence analysis identified eight bacterial pathogens: *R. raoultii*, *R. sibirica*, *Candidatus* R. longicornii, *B. washoensis*, *B. grahamii*, *B. jaculi*, *A. capra*, and *Candidatus* Anaplasma cinensis. Co-infection of *B. grahamii* and *R. raoultii* in one sample was observed. Our results demonstrated the genetic diversity of bacteria in Daurian ground squirrels and contributed to the distribution of these pathogens. Six species, *A. capra*, *R. raoultii*, *R. sibirica*, *Candidatus* R. longicornii, *B. washoensis*, and *B. grahamii*, are known to be pathogenic to humans, indicating a potential public health risk to the local human population, especially to herders who frequently have close contact with Daurian ground squirrels and are thus exposed to their ectoparasites.

KEYWORDS

Daurian ground squirrel, *Anaplasma*, *Bartonella*, *Rickettsia*, genetic diversity

Introduction

Rodents are the most diverse taxa of mammals (Huchon et al., 2002; Wilson and Reeder, 2005) and serve as reservoirs of many important zoonotic pathogens (Meerburg et al., 2009; Han et al., 2015). These pathogens consist of bacteria, viruses, and parasites. They comprise 66 identified zoonotic pathogens harbored by a minimum of 217 rodent species as reservoirs. Additionally, at least 79 rodent species can host between 2 and 11 zoonotic causative agents (Han et al., 2015). In recent years, an increasing number of viruses have been discovered by next-generation sequencing technology in rodents, some of which possess zoonotic potential (Chen et al., 2023). Furthermore, most of these zoonotic pathogens are indirectly transmitted from rodents to humans via arthropod vectors (Meerburg et al., 2009).

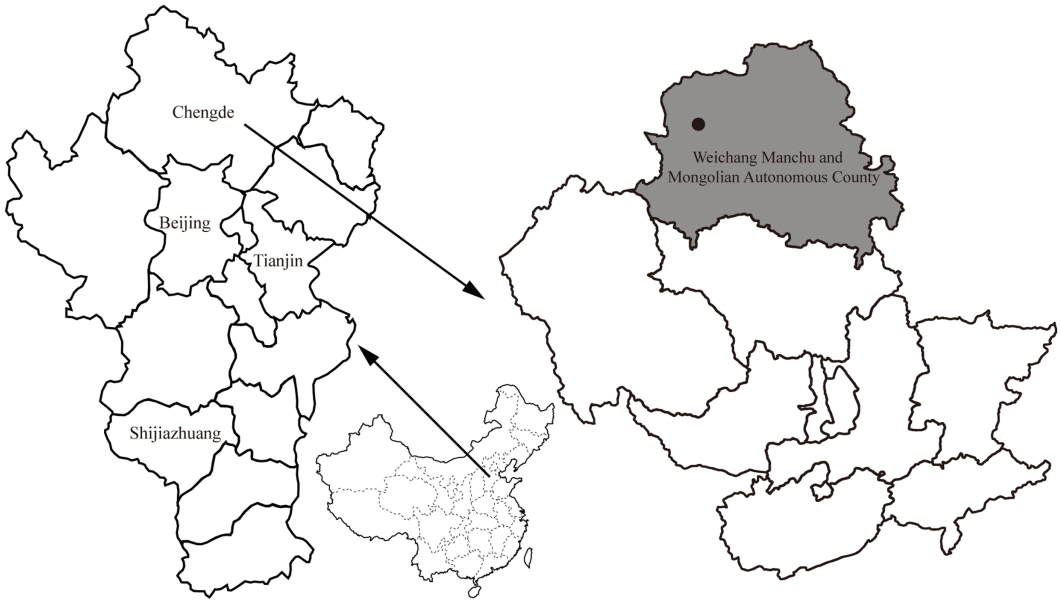

FIGURE 1
Map with the location of the sampling site (black circle) in Weichang Manchu and Mongolian Autonomous County (shown in gray), Hebei, China.

Rickettsia and *Anaplasma* (Order Rickettsiales) are obligate intracellular bacteria that are transmitted by ticks (Darby et al., 2007). Some *Rickettsia* species have been detected in rodents, although the role that rodents play in their life cycle is unclear (Schex et al., 2011; Kuo et al., 2015; Lu et al., 2019). Unlike *Rickettsia*, *Anaplasma* cannot be transmitted transovarially in ticks; therefore, vertebrate mammals such as rodents are required to complete their life cycle (Battilani et al., 2017). Bacteria belonging to the genus *Bartonella* include several zoonotic species that can be transmitted from animals to humans through the bites of infected bloodsucking arthropods (Deng et al., 2012), as well as through the scratch of an infected cat or by contact with the infected feces of a vector (Krügel et al., 2022). Although *Bartonella* DNA has been detected in ticks, the role of ticks as vectors in the transmission of *Bartonella* spp. remains unclear (Telford and Wormser, 2010). As the natural hosts, more than half of all *Bartonella* species, including human pathogens, have been identified in rodents to date (Jian et al., 2022).

The Daurian ground squirrel (*Spermophilus dauricus*) may be a potential reservoir of tick-borne pathogens. In China, a tentative *Ehrlichia* species was identified from this ground squirrel in Inner Mongolia (Li et al., 2023a). In addition, *B. rochalimae* and *B. washoensis* were detected in Inner Mongolia (Li et al., 2023b). Except for the three above-mentioned bacterial species and *Y. pestis*, no other vector-borne intracellular bacteria have been found in Daurian ground squirrels. In our preliminary studies, herders parasitized by ticks were found in the Bashang area of Weichang Manchu and the Mongolian Autonomous County of Hebei Province, China. Therefore, when herders enter the habitat of Daurian ground squirrels, they may come into contact with the rodents and be exposed to their ectoparasites. A previous study showed that intracellular bacterial pathogens, including *R. raoultii* and *Candidatus* R. tarasevichiae, were identified in 26 ticks collected from humans (Xue et al., 2023) in Weichang County, as well as *A. ovis* with zoonotic potential. Therefore, to better understand the genetic diversity of intracellular bacterial pathogens, Daurian ground squirrels were collected from the Bashang area to screen for the presence of neglected vector-borne *Anaplasma*, *Bartonella*, and *Rickettsia*. The results will help to assess the potential transmission risk of these pathogens to humans.

Materials and methods

Sample collection of rodents and DNA extraction

From April to October 2021, rodents were captured alive using baited cages with a treadle release mechanism from one sampling site (approximately 3 km^2) located in the Bashang area of Weichang Manchu and Mongolian Autonomous County, Hebei Province, China (Figure 1). The cages were set at night and then retrieved the following day. Two hundred cages were used in each trapping session, and two or three trapping sessions were conducted each month. Based on the standard taxonomic characteristics (Wang, 2003), the rodents were first identified morphologically at the species level. After species identification, the sampled rodents were euthanized with an isoflurane overdose before surgery to minimize suffering. Spleen tissue samples were aseptically collected from each individual and stored on dry ice. A volume of 200 μL of spleen tissue suspension was prepared by homogenizing a 30 mg sample in 200 μL of TL buffer. DNA was isolated from the spleen suspension of each rodent using a Tissue DNA Kit (Omega, Norcross, GA, United States) according to the manufacturer's protocol. The extracted DNA was eluted in 80 μL of elution buffer and stored at −20°C before pathogen detection and confirmation of rodent species by molecular methods. All samples tested negative for *Yersinia pestis* by detecting immunoglobulin (IgG) antibodies against the F1 antigen and *caf1* and *pla* genes before screening for other pathogens (Zhao et al., 2017). The rodent species was

TABLE 1 Primer sequences used in this study.

Pathogens	Target gene	Primer	Oligonucleotide sequences (5′–3′)	Size (bp)	References
Rickettsia	*ompA*	Rr190k.70p	TGGCGAATATTTCTCCAAAA (+)	532	Ishikura et al. (2003)
		Rr190k.720n	TGCATTTGTATTACCTATTGT (−)		
		Rr190k.602n	AGTGCAGCATTCGCTCCCCCT (−)		
Bartonella	*gltA*	Bar-gltA-FM	GCHGATCAYGARCAAAATGC (+)	476	Jian et al. (2022)
		Bar-gltA-R1	CYTCRATCATTTCTTTCCAYTG (−)		
		Bar-gltA-R2	GCAAAVAGAACMGTRAACAT (−)		
Candidatus Anaplasma cinensis	*gltA*	Platys-glta-F	GATGTGTGGGAAAGAAGAAAT (+)	641	This study
		Pglt-R1	TCATGRTCTGCATGCATKATG (−)		Guo et al. (2019)
		Pglt-R2	CATGCATKATGAARATCGCRT (−)		
	groEL	Platys-groEL-F1	GAGTATTAASCCTGAGGAAC (+)	439	This study
		Platys-groEL-F2	AGAGTGCATCGCAATGTAAT (+)		
		Platys-groEL-R	AGGAATATGTAYGGRTTYTC (−)		
Anaplasma	16S rRNA	fD1	AGAGTTTGATCCTGGCTCAG (+)	639	Weisburg et al. (1991) and Wen et al. (2002)
		Eh-out2	AGTAYCGRACCAGATAGCCGC (−)		
		Eh-gs2	CTAGGAATTCCGCTATCCTCT (−)a		

confirmed by sequence analysis of the mitochondrial cytochrome b (mt-*cyt b*) gene (Guo et al., 2013). This study was approved by the Scientific Ethics Committee of the Chengde Medical University (No. 202004).

Molecular detection of *Rickettsia*, *Anaplasma*, and *Bartonella*

Rickettsia, *Anaplasma*, and *Bartonella* were detected for the presence of DNA using polymerase chain reaction (PCR). *Rickettsia* was screened using semi-nested PCR targeting a conserved region of the outer membrane protein (*ompA*) (Ishikura et al., 2003). The DNA of *Bartonella* was detected by amplifying a fragment of the citrate synthase (*gltA*) gene (Jian et al., 2022). *Anaplasma* was detected by semi-nested PCR using the primer pairs fD1/Eh-out2 and fD1/Eh-gs1 for primary and secondary rounds, targeting the 16S rRNA (Weisburg et al., 1991; Wen et al., 2002). In addition, the DNA of *Candidatus* Anaplasma cinensis was detected to confirm its presence by amplifying the partial *gltA* gene using primers designed for this study. The partial *groEL* gene of *Candidatus* Anaplasma cinensis was amplified to better characterize its genetic characteristics. The primers used in the present study are listed in Table 1. For *Candidatus* A. cinensis, the PCR for the primary round of semi-nested PCR was performed in a 20 μL reaction volume containing 10 μL of Premix Taq (Takara, Dalian, China), 1.6 μL of DNA, 1.0 μL of each primer (10 pmol), and 5.4 μL of water. The secondary round consisted of a final volume of 50 μL that contained 25 μL of PCR mixture Premix Taq (Takara, Dalian, China), 3 μL of the first round PCR products, 2 μL of each primer (10 pmol), and 18 μL of water. The same thermal cycling conditions were used for both rounds and were as follows: pre-denaturation at 94°C for 5 min; 35 cycles of denaturation at 94°C for 40 s; annealing at 56°C for 40 s; elongation at 72°C for 1 min; and a final extension at 72°C for 7 min. Double-distilled water was used as a negative control. In addition, positive controls were included in the reactions using DNA deposited in our laboratory.

The PCR products were separated by electrophoresis using 1% agarose gels, and the bands were observed after staining. The PCR products of the expected size were purified using a MiniBEST Agarose Gel DNA Extraction Kit Ver.4.0 (TaKaRa, Dalian, China). Due to the sequences being less than 700 bp, the amplicons were bidirectionally sequenced using the primers for the secondary round of the PCR after purification. If double peaks were visible on the sequencing chromatograms, the amplicons were cloned into pMD19-T vectors (Takara, Dalian, China) for further sequencing with the universal primers RV-M and M13-47 (Sangon, Beijing, China).

Nucleotide sequence identity and phylogenetic analyses

All the newly generated sequences were searched against the GenBank database using the Basic Local Alignment Search Tool (BLAST). The nucleotide sequence identities between the sequences in this study and reference sequences were determined using the MegAlign program in Lasergene (Burland, 2000). A maximum likelihood (ML) tree used to identify the pathogens by species was reconstructed using PhyML 3.0 (Guindon et al., 2010) based on the optimal nucleotide substitution model (GTR + Γ + I) estimated by MEGA 6.0.6 (Tamura et al., 2013). The reliability of the tree was evaluated by bootstrap analysis with 1,000 replicates.

Statistical analysis

The differences between positive rates of *Anaplasma*, *Bartonella*, and *Rickettsia* infections in Daurian ground squirrels were compared using a χ^2 test with a *p*-value of 0.05 as the threshold.

Results

Rodent sample collection

A total of 165 rodents were captured in Weichang Manchu and Mongolian Autonomous County, Hebei Province, China. Based on both morphological and molecular methods, all of the rodents were identified as Daurian ground squirrels, belonging to the family Sciuridae. The *cytb* gene sequences shared 99.3–100% nucleotide identity with each other and displayed 98.5–99.7% nucleotide identity with known corresponding sequences from Daurian ground squirrels in the GenBank database.

Molecular detection of pathogens

After electrophoresis, 35 PCR products of expected size were subjected to sequencing, and the results were further subjected to BLAST searches. In total, 34 rodent samples tested positive for at least one causative agent, and one co-infection of two pathogens was found. Furthermore, eight pathogens were identified. Specifically, 13 rodent samples tested positive for the genus *Rickettsia*, with a positive rate of 7.9%, including 7 *R. raoultii*, 3 *R. sibirica*, and 3 *Candidatus* R. longicornii. Fifteen rodent samples tested positive for the genus *Bartonella*, with a positive rate of 9.1%, including 10 *B. washoensis*, 3 *B. grahamii*, and 2 *B. jaculi*. Co-infection of *B. grahamii* and *R. raoultii* was observed in one sample. Six samples tested positive for *Candidatus* A. cinensis, with a positive rate of 3.6%. When using the primer pairs fD1/Eh-out2 and fD1/Eh-gs1 targeting the 16S rRNA of the genus *Anaplasma*, none of the six samples mentioned above tested positive. Instead, an additional sample yielded a positive result. After sequencing, BLASTn analysis based on this partial 16S rRNA sequence indicated that this agent could be identified as *A. capra*, with a low positive rate of 0.6%. Unfortunately, we failed to get other genes. *Rickettsia* and *Bartonella* infections in Daurian ground squirrels had no significant difference ($\chi^2 = 0.16$, $p = 0.69$). The positive rate of *Bartonella* infection in Daurian ground squirrels was higher than that of *Anaplasma* ($\chi^2 = 4.12$, $p = 0.04$). However, no significant difference was observed between *Rickettsia* and *Anaplasma* infections ($\chi^2 = 2.74$, $p = 0.10$).

Molecular characterization of identified vector-borne intracellular bacterial pathogens

For the genus *Bartonella*, 10 partial *gltA* gene sequences of *B. washoensis* in this study shared 99.3–100% nucleotide identity with each other and the highest nucleotide identity of 99.7–100% with *Bartonella* sp. DR 1–1, also in Daurian ground squirrels from China (Inoue et al., 2009). Specifically, the *gltA* gene sequences recovered in this study shared 97.1–97.9% nucleotide identity with those of strain 085-0475 isolated from humans. In addition, the *gltA* gene sequences in this study shared 97.0–99.7% nucleotide identity with known ones of *B. washoensis* from ground squirrels and 96.4–98.8% nucleotide identity with known *B. washoensis* variants from other reservoirs. In the phylogenetic tree, all *B. washoensis* variants in this study clustered with the reference *B. washoensis* strain 085-0475, and then with *B. washoensis* isolate human_1487_18, also from humans (Figure 2). However, these newly generated sequences only shared 91.1–92.0% nucleotide identity with the *gltA* gene sequence of isolate human_1487_18. In addition, another three partial *gltA* gene sequences of *B. grahamii* in this study shared 99.1–99.8% nucleotide identity with each other, and 96.6–98.9% with known ones of *B. grahamii*. In the phylogenetic tree, all three newly generated *gltA* gene sequences clustered with those of *B. grahamii* (Figure 2). Two partial *gltA* gene sequences of *B. jaculi* recovered in this study shared 95.7% nucleotide identity with each other and 96.3–99.7% nucleotide identity with known ones of *B. jaculi*. In the phylogenetic tree, these two sequences clustered with that of a known *B. jaculi* isolate (Figure 2).

The partial 16S rRNA gene sequence in this study presented a 100% similarity with some sequences of *A. capra* variants, suggesting a possible *A. capra* infection in Daurian ground squirrels. Using the primers designed in this study, *Candidatus* A. cinensis was detected by amplifying its *gltA* gene in six samples. All six of these partial *gltA* gene sequences in this study shared 99.0–99.7% nucleotide identity and shared 98.7–99.7% nucleotide identity with known ones of *Candidatus* A. cinensis. In addition, a partial *groEL* gene sequence was obtained and showed the highest nucleotide identity of 98.4% with that of known *Candidatus* A. cinensis variants. Moreover, the *groEL* and *gltA* gene sequences herein shared 82.8% and 74.0–74.7% nucleotide identity, respectively, with those of the *A. platys* reference strain S3. Consistently, these variants in the present study clustered with other known *Candidatus* A. cinensis rather than specific *A. platys*. Specifically, the *Candidatus* A. cinensis variants herein clustered within lineages 2 and 4 of Guo et al. (2019) for the *gltA* and *groEL* genes, respectively (Figure 3).

For the genus *Rickettsia*, seven partial *ompA* gene sequences of *R. raoultii* in this study shared 99.2–100% nucleotide identity with each other and 97.7–99.4% with known *R. raoultii* variants. In addition, three partial *ompA* gene sequences of *R. sibirica* in this study shared 98.1–100% nucleotide identity with the known ones of *R. sibirica* variants. Another three partial *ompA* gene sequences of *Candidatus* R. longicornii in this study shared 98.8–100% nucleotide identity with each other and 96.6–100% nucleotide identity with known *Candidatus* R. longicornii variants. Interestingly, the *ompA* gene sequence of isolate Weichang-Sd-87 had an insertion of three bases (GAC) compared to the other four isolates, the same as isolates CCBF8, GXS12, and GXS34 identified from rodents in Guangxi, China. In the phylogenetic tree, 19 *ompA* gene sequences were classified into three groups, corresponding to *R. raoultii*, *R. sibirica*, and *Candidatus* R. longicornii (Figure 4).

Discussion

Rodents are the main hosts of many human pathogens and can indirectly transmit vector-borne intracellular bacteria to humans, such as Rickettsiales and *Bartonella* (Han et al., 2015). The Daurian ground squirrel is a wild rodent species mainly distributed in northern China, Mongolia, and Russia and is a host of *Yersinia pestis* (Zhou et al., 2004a,b; Tian, 2018). Daurian ground squirrels frequently come into contact with herders, which can increase the risk of plague transmission in humans. To date, the diversity of vector-borne intracellular bacterial pathogens carried by Daurian ground squirrels

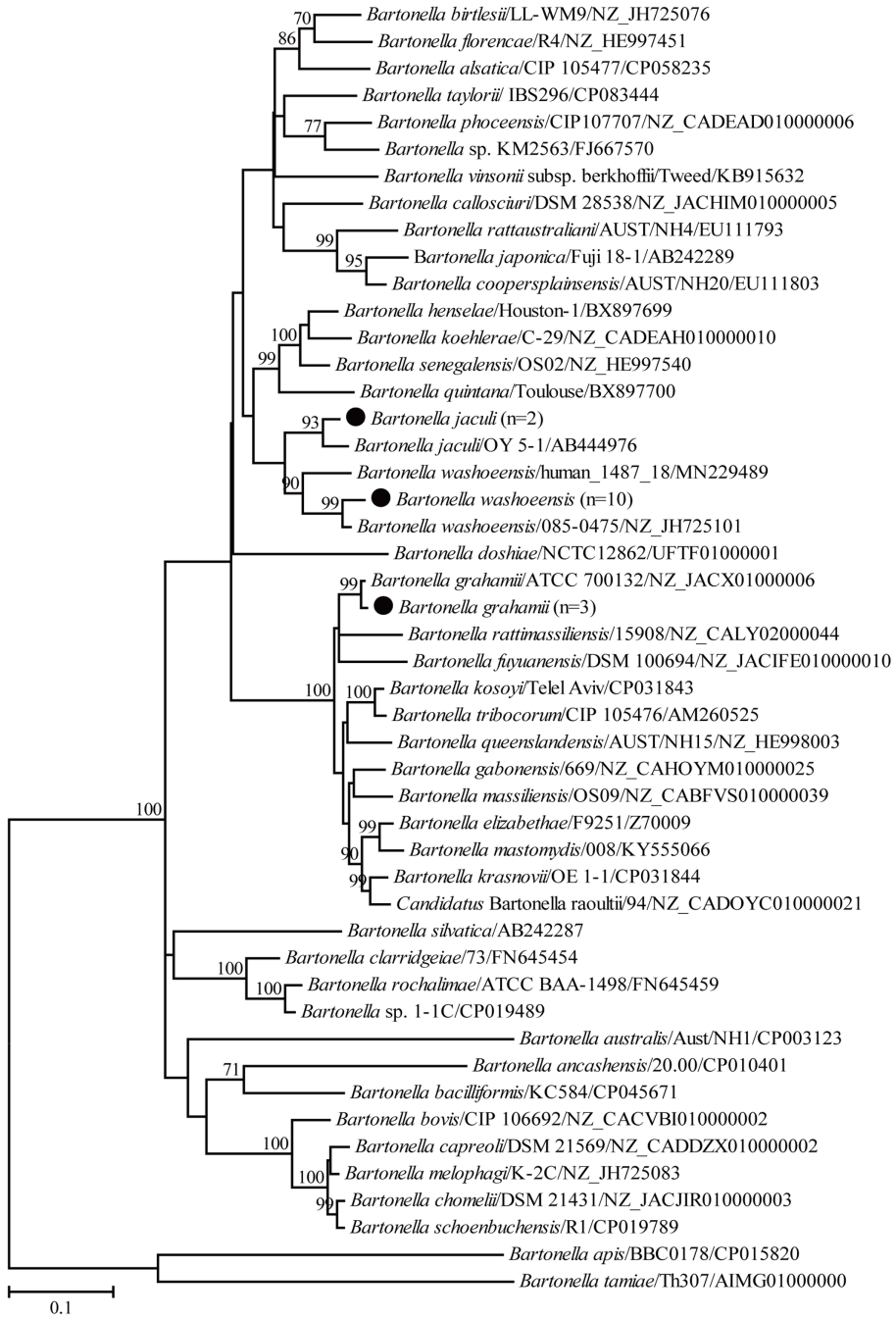

FIGURE 2
Phylogenetic tree based on the partial *gltA* gene sequences of the genus *Bartonella*. Numbers at each node indicate bootstrap values. The tree was mid-point rooted for clarity, and the scale bar represents the number of nucleotide substitutions per site. The representative sequence obtained in this study was used to reconstruct the tree and is marked with circles.

has been unclear, although the ground squirrels are known to be hosts of ticks. In this study, eight intracellular bacterial species were discovered, namely two *Anaplasma* species, three *Rickettsia* species, and three *Bartonella* species. Specifically, these eight species were *A. capra*, *Candidatus* A. cinensis, *R. raoultii*, *R. sibirica*, *Candidatus* R. longicornii, *B. washoensis*, *B. grahamii*, and *B. jaculi*. Importantly, *A. capra*, *R. raoultii*, *R. sibirica*, *Candidatus* R. longicornii, *B. washoensis*, and *B. grahamii* are pathogenic to humans, suggesting potential threats to public health. In this study, a low rate of co-infection between *B. grahamii* and *R. raoultii* was observed. In a previous study, co-infection of *Rickettsia* and *Bartonella* was found to be prevalent in rodents in Vietnam (Anh et al., 2021), although the bacterial species within *Rickettsia* and *Bartonella* were not identified. All these results imply that the co-infection of *Rickettsia* and *Bartonella* in rodents does not interfere with each other. Our results give important insights into the distribution of these vector-borne pathogens and the genetic diversity of vector-borne pathogens in Daurian ground squirrels in the local area.

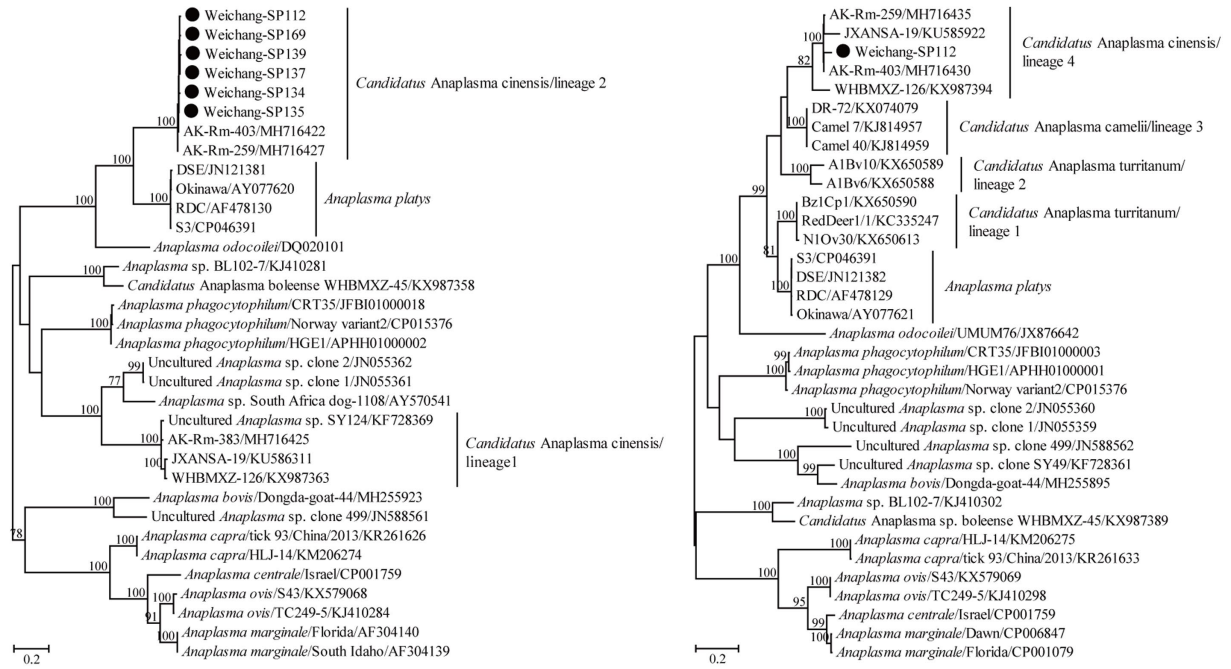

FIGURE 3
Phylogenetic tree based on the partial *gltA* (left) and *groEL* (right) gene sequences of the genus *Anaplasma*. Numbers at each node indicate bootstrap values. The tree was mid-point rooted for clarity, and the scale bar represents the number of nucleotide substitutions per site. The representative sequence obtained in this study was used to reconstruct the tree and is marked with circles.

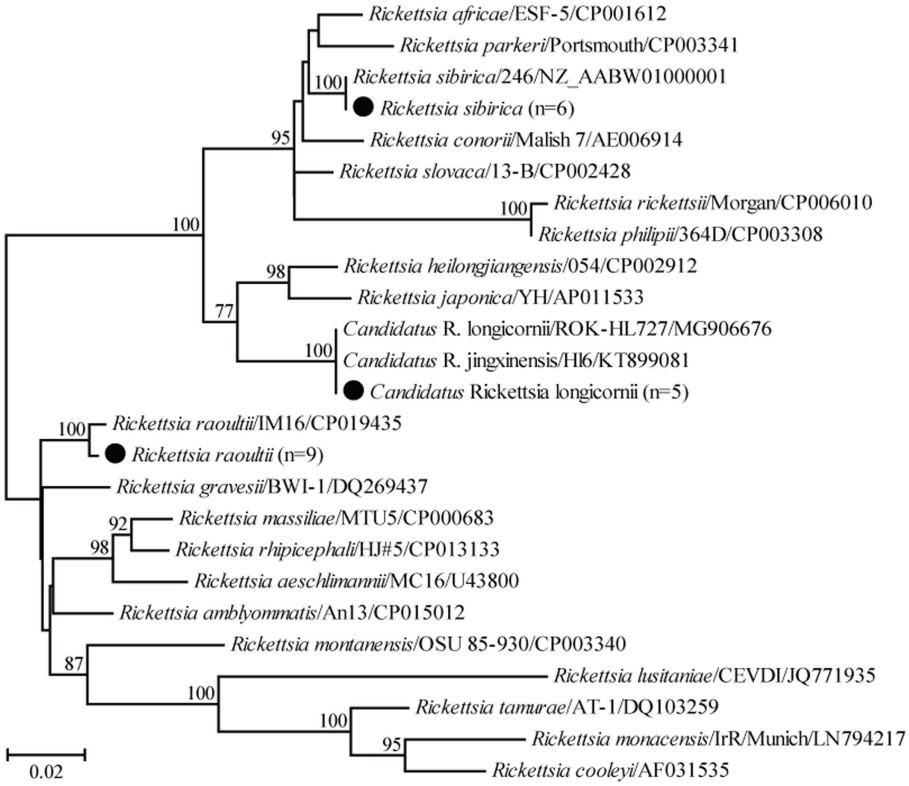

FIGURE 4
Phylogenetic tree based on the partial *ompA* gene sequences of the genus *Rickettsia*. Numbers at each node indicate bootstrap values. The tree was mid-point rooted for clarity, and the scale bar represents the number of nucleotide substitutions per site. The representative sequence obtained in this study was used to reconstruct the tree and is marked with circles.

To date, *Rickettsia* has been found in many rodent species, even in single rodent species collected from a single location (Schex et al., 2011; Kuo et al., 2015; Lu et al., 2019). In previous studies, *R. heilongjiangensis*, *R. japonica*, and an unidentified *Rickettsia* species were detected in *Apodemus agrarius* in China (Lu et al., 2019); *R. felis* and *R. helvetica* were found in *A. flavicollis* in Germany (Schex et al., 2011); and seven *Rickettsia* species were identified in *Rattus losea* in Taiwan (Kuo et al., 2015). Similar to these results, three *Rickettsia* species, namely *R. raoultii*, *R. sibirica*, and *Candidatus* R. longicornii, were identified in Daurian ground squirrels in the present study, indicating that there is genetic diversity in *Rickettsia* hosted by a rodent species in a single location. In our previous studies, two uncultured *Rickettsia* species, *Candidatus* R. tarasevichiae, and *Candidatus* R. principis, were detected in ticks from the same county (Xue et al., 2023). However, neither was recovered in this study, although *Candidatus* R. tarasevichiae was detected in *R. norvegicus* and *Clethrionomys rufocanus* in Dashigou around Mudanjiang City, Heilongjiang Province, Northeast China (Yuan et al., 2021). This may be due to differences in sampling sites or because the Daurian ground squirrel is not the primary host. Our previous study also showed that at least three tick species, *Ixodes persulcatus*, *Dermacentor silvarum*, and *Haemaphysalis concinna*, were present in local areas, and *R. raoultii* has been identified in those ticks (Xue et al., 2023). However, *R. sibirica* and *Candidatus* R. longicornii were not identified, although *R. sibirica* has been detected in the same tick species from other parts of China (Zhao et al., 2021). Hence, ticks should be collected to determine their circulation and prevent further threats to human health.

As the main hosts, rodents are infected by many species within the genus *Bartonella*. Among the rodent-associated *Bartonella* species, eight detected in Daurian ground squirrels, including *B. rochalimae* and *B. washoensis*, are pathogenic to humans (Jian et al., 2022). In addition to *B. washoensis*, which was identified in Daurian ground squirrels in a previous study (Inoue et al., 2009; Li et al., 2023b), *B. grahamii* and *B. jaculi* were detected in Daurian ground squirrels in the present study. Combining the data from previous and our studies, four *Bartonella* species have been recovered in Daurian ground squirrels, indicating that this rodent species is an important host of *Bartonella*. *Bartonella jaculi* was first identified in *Jaculus orientalis* from Egypt (Sato et al., 2013) and then only detected in *Allactaga sibirica* from the Qaidam Basin of China (Rao et al., 2021). These results demonstrated the worldwide geographical distribution of *B. jaculi*, and it has a wide range of rodent hosts. In this study, *B. washoensis* was the predominant *Bartonella* species, followed by *B. grahamii*. Considering their pathogenicity to humans, the ectoparasites (including fleas, mites, lice, and ticks) of Daurian ground squirrels should be collected to determine those that can act as potential vectors of both *B. washoensis* and *B. grahamii* in future studies.

Anaplasma capra was first confirmed to be a human pathogen in 2015 (Li et al., 2015) and has been mainly identified in livestock based on sequences deposited in GenBank and previous studies (Guo et al., 2018; Amer et al., 2019; He et al., 2021; Remesar et al., 2022; Sahin et al., 2022). In this study, only one partial 16S rRNA sequence was obtained, and we conjectured that this may have resulted from a low bacterial load or DNA degradation by some enzymes in the host. Alternatively, rodents may not be a competent reservoir of *A. capra*. *Anaplasma platys* is considered a potential human pathogen because its DNA was detected in two female patients from Venezuela (Arraga-Alvarado et al., 2014). Unlike other *Anaplasma* species, *A. platys* showed a high level of great genetic diversity, manifested by the 16S rRNA gene forming a monophyletic group and the *gltA* and *groEL* genes forming polyphyletic groups (Ben Said et al., 2017; Guo et al., 2019; Nguyen et al., 2020; Zobba et al., 2022). In China, *A. platys*-like variants formed a lineage in the *groEL* tree, while they were classified into two lineages in the *gltA* tree (Guo et al., 2019). In Thailand, similar *A. platys*-like variants were also identified, and they clustered together with the above-mentioned variants in China in the *groEL* tree (Nguyen et al., 2020). At present, this lineage is named *Candidatus* A. cinensis. In addition, another two genetically related lineages of *A. platys*-like in ruminants from Tunisia were named *Candidatus* A. turritanum (Ben Said et al., 2017). Moreover, *Candidatus* A. camelii fell into the genetic diversity of *A. platys* and *A. platys*-like (Guo et al., 2019). In this study, *Candidatus* A. cinensis was identified in Daurian ground squirrels, and this is the first molecular evidence of its infection in rodents. In detail, the *gltA* gene sequences presented the closest genetic relationship with known sequences belonging to lineage 2 rather than those of lineage 1 from Guo et al. (2019), while the *groEL* gene sequences clustered together and formed one lineage. The data from this and previous studies suggest that *Candidatus* A. cinensis is widely distributed and infects a greater variety of potential hosts than suggested by previous studies (Ben Said et al., 2017; Guo et al., 2019; Nguyen et al., 2020). Therefore, its pathogenicity should be given more attention.

There were several limitations to this study. First, we did not check for the presence of blood-sucking vectors on the bodies of the ground squirrels in this study. Therefore, the real risks of the pathogens identified in this study to the local population and the association between the presence of vectors and infected Daurian ground squirrels could not be determined. As such, human cases should be identified in future studies to reveal the risks to the local population. Second, we did not record the age or gender of the captured rodents or the rodent numbers in each month because the aim of this study was to better understand the genetic diversity of vector-borne *Anaplasma*, *Rickettsia*, and *Bartonella*. Therefore, the assessment of the prevalence of each pathogen over time or across age groups or sexes of Daurian ground squirrels could not be determined. Moreover, rodent samples were collected from one sampling site for this study; therefore, potential spatial differences could not be determined, resulting in an incomplete picture of the intracellular bacterial pathogens in Daurian ground squirrels.

In summary, eight vector-borne bacterial species, including six that are pathogenic to humans, were molecularly identified in Daurian ground squirrels. Our results contributed to the characterization of the genetic diversity of bacterial species associated with Daurian ground squirrels, such as *Rickettsia*, *Anaplasma*, and *Bartonella*. Our results also provided evidence that Daurian ground squirrels were potential bacterial hosts. In addition, the results suggested that the pathogens could pose threats to public health in the local population. Considering that there could be an indirect transmission of the above-mentioned bacteria from Daurian ground squirrels to humans, potential vectors should be identified in future studies.

Data availability statement

The datasets presented in this study can be found in online repositories. The nucleotide sequences recovered in this study were deposited in GenBank (https://www.ncbi.nlm.nih.gov/genbank) under the accession numbers OR976065 and OR988094–OR988128.

Ethics statement

The animal study was approved by the ethical committee of Chengde Medical University. The study was conducted in accordance with the local legislation and institutional requirements.

Author contributions

JX: Writing – original draft, Data curation, Formal analysis, Investigation. S-SC: Data curation, Investigation, Methodology, Writing – review & editing. Z-YX: Investigation, Resources, Writing – review & editing. F-NW: Investigation, Writing – review & editing. JW: Funding acquisition, Resources, Writing – review & editing. DD: Investigation, Resources, Writing – review & editing. LD: Supervision, Validation, Writing – review & editing. G-CX: Writing – review & editing. W-PG: Conceptualization, Funding acquisition, Methodology, Project administration, Supervision, Writing – original draft, Writing – review & editing.

Funding

The author(s) declare that financial support was received for the research, authorship, and/or publication of this article. This study was supported by the Hebei Natural Science Foundation (No. C2022406003), the Young Talent Program of Higher School in Hebei Province (No. BJ2020024), the Scientific Research Foundation for High-level Talents of Chengde Medical University (No. 202001), and the Hebei Medical Science Research Project (No. 20210234).

Conflict of interest

The authors declare that the research was conducted in the absence of any commercial or financial relationships that could be construed as a potential conflict of interest.

Publisher's note

All claims expressed in this article are solely those of the authors and do not necessarily represent those of their affiliated organizations, or those of the publisher, the editors and the reviewers. Any product that may be evaluated in this article, or claim that may be made by its manufacturer, is not guaranteed or endorsed by the publisher.

Supplementary material

The Supplementary material for this article can be found online at: https://www.frontiersin.org/articles/10.3389/fmicb.2024.1359797/full#supplementary-material

References

Amer, S., Kim, S., Yun, Y., and Na, K. J. (2019). Novel variants of the newly emerged Anaplasma capra from Korean water deer (Hydropotes inermis argyropus) in South Korea. *Parasit. Vectors* 12:365. doi: 10.1186/s13071-019-3622-5

Anh, L. T. L., Balakirev, A. E., and Chau, N. V. (2021). Investigation of multiple infections with zoonotic pathogens of rodents in northern Vietnam. *J. Vector Borne Dis.* 58, 47–53. doi: 10.4103/0972-9062.321750

Arraga-Alvarado, C. M., Qurollo, B. A., Parra, O. C., Berrueta, M. A., Hegarty, B. C., and Breitschwerdt, E. B. (2014). Case report: molecular evidence of Anaplasma platys infection in two women from Venezuela. *Am J Trop Med Hyg* 91, 1161–1165. doi: 10.4269/ajtmh.14-0372

Battilani, M., De Arcangeli, S., Balboni, A., and Dondi, F. (2017). Genetic diversity and molecular epidemiology of Anaplasma. *Infect. Genet. Evol.* 49, 195–211. doi: 10.1016/j.meegid.2017.01.021

Ben Said, M., Belkahia, H., El Mabrouk, N., Saidani, M., Alberti, A., Zobba, R., et al. (2017). Anaplasma platys-like strains in ruminants from Tunisia. *Infect. Genet. Evol.* 49, 226–233. doi: 10.1016/j.meegid.2017.01.023

Burland, T. G. (2000). DNASTAR's Lasergene sequence analysis software. *Methods Mol. Biol.* 132, 71–91. doi: 10.1385/1-59259-192-2:71

Chen, Y. M., Hu, S. J., Lin, X. D., Tian, J. H., Lv, J. X., Wang, M. R., et al. (2023). Host traits shape virome composition and virus transmission in wild small mammals. *Cell* 186, 4662–4675.e12. doi: 10.1016/j.cell.2023.08.029

Darby, A. C., Cho, N. H., Fuxelius, H. H., Westberg, J., and Andersson, S. G. (2007). Intracellular pathogens go extreme: genome evolution in the Rickettsiales. *Trends Genet.* 23, 511–520. doi: 10.1016/j.tig.2007.08.002

Deng, H., Le Rhun, D., Buffet, J. P., Cotté, V., Read, A., Birtles, R. J., et al. (2012). Strategies of exploitation of mammalian reservoirs by Bartonella species. *Vet. Res.* 43:15. doi: 10.1186/1297-9716-43-15

Guindon, S., Dufayard, J. F., Lefort, V., Anisimova, M., Hordijk, W., and Gascuel, O. (2010). New algorithms and methods to estimate maximum-likelihood phylogenies: assessing the performance of PhyML 3.0. *Syst. Biol.* 59, 307–321. doi: 10.1093/sysbio/syq010

Guo, W. P., Huang, B., Zhao, Q., Xu, G., Liu, B., Wang, Y. H., et al. (2018). Human-pathogenic Anaplasma spp., and Rickettsia spp. in animals in Xi'an, China. *PLoS Negl. Trop. Dis.* 12:e0006916. doi: 10.1371/journal.pntd.0006916

Guo, W. P., Lin, X. D., Wang, W., Tian, J. H., Cong, M. L., Zhang, H. L., et al. (2013). Phylogeny and origins of hantaviruses harbored by bats, insectivores, and rodents. *PLoS Pathog.* 9:e1003159. doi: 10.1371/journal.ppat.1003159

Guo, W. P., Tie, W. F., Meng, S., Li, D., Wang, J. L., Du, L. Y., et al. (2020). Extensive genetic diversity of Anaplasma bovis in ruminants in Xi'an. *China. Ticks Tick Borne Dis* 11:101477. doi: 10.1016/j.ttbdis.2020.101477

Guo, W. P., Zhang, B., Wang, Y. H., Xu, G., Wang, X., Ni, X., et al. (2019). Molecular identification and characterization of Anaplasma capra and Anaplasma platys-like in Rhipicephalus microplus in Ankang. *Northwest China. BMC Infect Dis* 19:434. doi: 10.1186/s12879-019-4075-3

Han, B. A., Schmidt, J. P., Bowden, S. E., and Drake, J. M. (2015). Rodent reservoirs of future zoonotic diseases. *Proc. Natl. Acad. Sci. USA* 112, 7039–7044. doi: 10.1073/pnas.1501598112

He, Y., Chen, W., Ma, P., Wei, Y., Li, R., Chen, Z., et al. (2021). Molecular detection of Anaplasma spp., Babesia spp. and Theileria spp. in yaks (Bos grunniens) and Tibetan sheep (Ovis aries) on the Qinghai-Tibetan plateau, China. *Parasit. Vectors* 14:613. doi: 10.1186/s13071-021-05109-2

Huchon, D., Madsen, O., Sibbald, M. J., Ament, K., Stanhope, M. J., Catzeflis, F., et al. (2002). Rodent phylogeny and a timescale for the evolution of Glires: evidence from an extensive taxon sampling using three nuclear genes. *Mol. Biol. Evol.* 19, 1053–1065. doi: 10.1093/oxfordjournals.molbev.a004164

Inoue, K., Maruyama, S., Kabeya, H., Hagiya, K., Izumi, Y., Une, Y., et al. (2009). Exotic small mammals as potential reservoirs of zoonotic Bartonella spp. *Emerg. Infect. Dis.* 15, 526–532. doi: 10.3201/eid1504.081223

Ishikura, M., Ando, S., Shinagawa, Y., Matsuura, K., Hasegawa, S., Nakayama, T., et al. (2003). Phylogenetic analysis of spotted fever group rickettsiae based on gltA, 17-kDa, and rOmpA genes amplified by nested PCR from ticks in Japan. *Microbiol. Immunol.* 47, 823–832. doi: 10.1111/j.1348-0421.2003.tb03448.x

Jian, R., Ren, Q., Xue, J., Xie, G. C., Wang, J., Chen, G. Q., et al. (2022). Genetic diversity of Bartonella infection in residential and field rodents in Hebei. *China. Front Microbiol* 13:1039665. doi: 10.3389/fmicb.2022.1039665

Kuo, C. C., Shu, P. Y., Mu, J. J., and Wang, H. C. (2015). High prevalence of Rickettsia spp. infections in small mammals in Taiwan. *Vector Borne Zoonotic Dis.* 15, 13–20. doi: 10.1089/vbz.2014.1584

Krügel, M., Król, N., Kempf, V. A. J., Pfeffer, M., and Obiegala, A. (2022). Emerging rodent-associated Bartonella: A threat for human health? *Parasit. Vectors* 15:113. doi: 10.1186/s13071-022-05162-5

Li, J., Zhang, C., Lu, M., Wang, Y., Liu, F., Wang, W., et al. (2023a). Infection by a previously uncharacterized Ehrlichia species in rodents from Inner Mongolia. *Northern China. Ticks Tick Borne Dis* 14:102116. doi: 10.1016/j.ttbdis.2022.102116

Li, J., Zhang, C., Lu, M., Wang, Y., Wang, W., Liu, F., et al. (2023b). The diverse genetic genotypes of Bartonella species circulating in rodents from Inner Mongolia. *Northern China. PLoS Negl Trop Dis* 17:e0011462. doi: 10.1371/journal.pntd.0011462

Li, H., Zheng, Y. C., Ma, L., Jia, N., Jiang, B. G., Jiang, R. R., et al. (2015). Human infection with a novel tick-borne Anaplasma species in China: a surveillance study. *Lancet Infect. Dis.* 15, 663–670. doi: 10.1016/S1473-3099(15)70051-4

Lu, M., Li, F., Liao, Y., Shen, J. J., Xu, J. M., Chen, Y. Z., et al. (2019). Epidemiology and diversity of Rickettsiales Bacteria in humans and animals in Jiangsu and Jiangxi provinces. *China. Sci Rep* 9:13176. doi: 10.1038/s41598-019-49059-3

Meerburg, B. G., Singleton, G. R., and Kijlstra, A. (2009). Rodent-borne diseases and their risks for public health. *Crit. Rev. Microbiol.* 35, 221–270. doi: 10.1080/10408410902989837

Nguyen, A. H. L., Tiawsirisup, S., and Kaewthamasorn, M. (2020). Molecular detection and genetic characterization of Anaplasma marginale and Anaplasma platys-like (Rickettsiales: Anaplasmataceae) in water buffalo from eight provinces of Thailand. *BMC Vet. Res.* 16:380. doi: 10.1186/s12917-020-02585-z

Rao, H., Li, S., Lu, L., Wang, R., Song, X., Sun, K., et al. (2021). Genetic diversity of Bartonella species in small mammals in the Qaidam Basin, western China. *Sci. Rep.* 11:1735. doi: 10.1038/s41598-021-81508-w

Remesar, S., Prieto, A., García-Dios, D., López-Lorenzo, G., Martínez-Calabuig, N., Díaz-Cao, J. M., et al. (2022). Diversity of Anaplasma species and importance of mixed infections in roe deer from Spain. *Transbound. Emerg. Dis.* 69, e374–e385. doi: 10.1111/tbed.14319

Sahin, O. F., Erol, U., and Altay, K. (2022). Buffaloes as new hosts for Anaplasma capra: molecular prevalence and phylogeny based on gtlA, groEL, and 16S rRNA genes. *Res. Vet. Sci.* 152, 458–464. doi: 10.1016/j.rvsc.2022.09.008

Sato, S., Kabeya, H., Fujinaga, Y., Inoue, K., Une, Y., Yoshikawa, Y., et al. (2013). Bartonella jaculi sp. nov., Bartonella callosciuri sp. nov., Bartonella pachyuromydis sp. nov. and Bartonella acomydis sp. nov., isolated from wild Rodentia. *Int. J. Syst. Evol. Microbiol.* 63, 1734–1740. doi: 10.1099/ijs.0.041939-0

Schex, S., Dobler, G., Riehm, J., Müller, J., and Essbauer, S. (2011). Rickettsia spp. in wild small mammals in lower Bavaria, south-eastern Germany. *Vector Borne Zoonotic Dis.* 11, 493–502. doi: 10.1089/vbz.2010.0060

Tamura, K., Stecher, G., Peterson, D., Filipski, A., and Kumar, S. (2013). MEGA6: molecular evolutionary genetics analysis version 6.0. *Mol. Biol. Evol.* 30, 2725–2729. doi: 10.1093/molbev/mst197

Telford, S. R., and Wormser, G. P. (2010). Bartonella spp. transmission by ticks not established. *Emerg. Infect. Dis.* 16, 379–384. doi: 10.3201/eid1603.090443

Tian, L. (2018). Relationship between environmental factors and the spatial distribution of Spermophilus dauricus during 2000-2015 in China. *Int. J. Biometeorol.* 62, 1781–1789. doi: 10.1007/s00484-018-1580-9

Wang, Y.X. (2003) *A complete checklist of mammal species and subspecies in China - a taxonomic and geographic reference*. Beijing: China Forestry Publishing House

Weisburg, W. G., Barns, S. M., Pelletier, D. A., and Lane, D. J. (1991). 16S ribosomal DNA amplification for phylogenetic study. *J. Bacteriol.* 173, 697–703. doi: 10.1128/jb.173.2.697-703.1991

Wen, B., Jian, R., Zhang, Y., and Chen, R. (2002). Simultaneous detection of Anaplasma marginale and a new Ehrlichia species closely related to Ehrlichia chaffeensis by sequence analyses of 16S ribosomal DNA in Boophilus microplus ticks from Tibet. *J. Clin. Microbiol.* 40, 3286–3290. doi: 10.1128/JCM.40.9.3286-3290.2002

Wilson, D.E., and Reeder, D.M. (2005) *Mammal species of the world. A taxonomic and geographic reference. 3rd ed.* Johns Hopkins University Press; Baltimore, Maryland

Xue, J., Ren, Q., Yang, X. L., Wang, J., Xie, G., Du, L., et al. (2023). Human pathogens in ticks removed from humans in Hebei. *China. Heliyon* 9:e13859. doi: 10.1016/j.heliyon.2023.e13859

Yuan, T. T., Ma, L., Jiang, B. G., Fu, W. M., Sun, Y., Jia, N., et al. (2021). First confirmed infection of Candidatus Rickettsia Tarasevichiae in rodents collected from northeastern China. *Vector Borne Zoonotic Dis.* 20, 88–92. doi: 10.1089/vbz.2019.2443

Zhao, S. S., Pulati, Y., Yin, X. P., Li, W., Wang, B. J., Yang, K., et al. (2017). Wildlife plague surveillance near the China-Kazakhstan border: 2012–2015. *Transbound. Emerg. Dis.* 64, e48–e51. doi: 10.1111/tbed.12603

Zhao, G. P., Wang, Y. X., Fan, Z. W., Ji, Y., Liu, M. J., Zhang, W. H., et al. (2021). Mapping ticks and tick-borne pathogens in China. *Nat. Commun.* 12:1075. doi: 10.1038/s41467-021-21375-1

Zhou, D., Han, Y., Song, Y., Huang, P., and Yang, R. (2004b). Comparative and evolutionary genomics of Yersinia pestis. *Microbes Infect.* 6, 1226–1234. doi: 10.1016/j.micinf.2004.08.002

Zhou, D., Han, Y., Song, Y., Tong, Z., Wang, J., Guo, Z., et al. (2004a). DNA microarray analysis of genome dynamics in Yersinia pestis: insights into bacterial genome microevolution and niche adaptation. *J. Bacteriol.* 186, 5138–5146. doi: 10.1128/JB.186.15.5138-5146.2004

Zobba, R., Schianchi, E., Ben Said, M., Belkahia, H., Messadi, L., Piredda, R., et al. (2022). gltA typing of Anaplasma strains related to A. platys: taxonomical and one health implications. *Ticks Tick Borne Dis* 13:101850. doi: 10.1016/j.ttbdis.2021.101850

frontiers | Frontiers in Microbiology

TYPE Systematic Review
PUBLISHED 04 April 2024
DOI 10.3389/fmicb.2024.1329683

Check for updates

OPEN ACCESS

EDITED BY
Hong Yin,
Chinese Academy of Agricultural Sciences, China

REVIEWED BY
Kirk Douglas,
The University of the West Indies, Barbados
Yuki Takamatsu,
Nagasaki University, Japan

*CORRESPONDENCE
Wen Tian
✉ tianwen0492@163.com
Lin Kuang
✉ yangmimi06@163.com

RECEIVED 17 November 2023
ACCEPTED 21 March 2024
PUBLISHED 04 April 2024

CITATION
Lu W, Kuang L, Hu Y, Shi J, Li Q and Tian W (2024) Epidemiological and clinical characteristics of death from hemorrhagic fever with renal syndrome: a meta-analysis. *Front. Microbiol.* 15:1329683. doi: 10.3389/fmicb.2024.1329683

COPYRIGHT
© 2024 Lu, Kuang, Hu, Shi, Li and Tian. This is an open-access article distributed under the terms of the Creative Commons Attribution License (CC BY). The use, distribution or reproduction in other forums is permitted, provided the original author(s) and the copyright owner(s) are credited and that the original publication in this journal is cited, in accordance with accepted academic practice. No use, distribution or reproduction is permitted which does not comply with these terms.

Epidemiological and clinical characteristics of death from hemorrhagic fever with renal syndrome: a meta-analysis

Wei Lu[1], Lin Kuang[1]*, Yuxing Hu[1], Jialing Shi[1], Qi Li[1] and Wen Tian[2]*

[1]School of Integrated Chinese and Western Medicine, Hunan University of Chinese Medicine, Changsha, China, [2]College of Chinese Medicine, Beijing University of Chinese Medicine, Beijing, China

Introduction: Hemorrhagic fever with renal syndrome (HFRS) is an acute infectious disease comprising five stages: fever, hypotension, oliguria, diuresis (polyuria), and convalescence. Increased vascular permeability, coagulopathy, and renal injury are typical clinical features of HFRS, which has a case fatality rate of 1–15%. Despite this, a comprehensive meta-analyses of the clinical characteristics of patients who died from HFRS is lacking.

Methods: Eleven Chinese- and English-language research databases were searched, including the China National Knowledge Infrastructure Database, Wanfang Database, SinoMed, VIP Database, PubMed, Embase, Scopus, Cochrane Library, Web of Science, Proquest, and Ovid, up to October 5, 2023. The search focused on clinical features of patients who died from HFRS. The extracted data were analyzed using STATA 14.0.

Results: A total of 37 articles on 140,295 patients with laboratory–confirmed HFRS were included. Categorizing patients into those who died and those who survived, it was found that patients who died were older and more likely to smoke, have hypertension, and have diabetes. Significant differences were also observed in the clinical manifestations of multiple organ dysfunction syndrome, shock, occurrence of overlapping disease courses, cerebral edema, cerebral hemorrhage, toxic encephalopathy, convulsions, arrhythmias, heart failure, dyspnea, acute respiratory distress syndrome, pulmonary infection, liver damage, gastrointestinal bleeding, acute kidney injury, and urine protein levels. Compared to patients who survived, those who died were more likely to demonstrate elevated leukocyte count; decreased platelet count; increased lactate dehydrogenase, alanine aminotransferase, and aspartate aminotransferase levels; prolonged activated partial thromboplastin time and prothrombin time; and low albumin and chloride levels and were more likely to use continuous renal therapy. Interestingly, patients who died received less dialysis and had shorter average length of hospital stay than those who survived.

Conclusion: Older patients and those with histories of smoking, hypertension, diabetes, central nervous system damage, heart damage, liver damage, kidney damage, or multiorgan dysfunction were at a high risk of death. The results can be used to assess patients' clinical presentations and assist with prognostication.

Systematic review registration: https://www.crd.york.ac.uk/prospero/, (CRD42023454553).

KEYWORDS

hemorrhagic fever with renal syndrome, hantavirus, death patients, epidemiological features, clinical features, meta-analysis

1 Introduction

Hemorrhagic fever with renal syndrome (HFRS) is an acute zoonotic infectious disease transmitted by rodents and is mainly caused by the *Orthohantavirus* genus of the Bunyavirus order *Bunyavirales* (Jonsson et al., 2010). More than 50 hantaviruses have been identified, among which Old World hantaviruses such as the Hantaan virus (HTNV), Dobrava-Belgrade virus (DOBV), Seoul virus (SEOV), Amur virus, and Puumala virus (PUUA) viruses are known to cause HFRS (Zuo et al., 2011; Jiang et al., 2017; Laenen et al., 2019).

Orthohantavirus has a single-stranded negative-sense RNA composed of an S fragment that encodes and forms a nucleocapsid protein, an M fragment that encodes a glycoprotein precursor, and an L fragment that is synthetically dependent on RNA polymerase and other reverse transcriptase (Afzal et al., 2023). It mainly attacks the vascular endothelial cells of the human body, resulting in multiorgan cell damage; however, the pathogenesis of the disease is not fully understood (Vaheri et al., 2013a; Manigold and Vial, 2014). Moreover, the clinical symptoms of HFRS caused by different viruses are different. PUUV causes mild HFRS symptoms, SEOV causes moderate symptoms, and HTNV and DOBV cause severe HFRS symptoms (Sehgal et al., 2023).

HFRS first attracted attention in North Korea in 1953. In 1978, the virus was isolated by scholars and officially named HTNV (Jiang et al., 2017). HFRS is endemic in Europe and Asia, with approximately 100,000 HFRS cases were reported each year, 90% of which occur in China (Vaheri et al., 2013a). Its clinical features include acute kidney injury, severe thrombocytopenia, coagulopathy, bleeding, and flu-like symptoms, which can manifest as mild, severe, or critical (Tariq and Kim, 2022). Clinically, the disease comprises five phases: fever, hypotension, oliguria, diuresis (polyuria), and convalescence (Jiang et al., 2016). During the febrile phase, the patient presents with nonspecific symptoms, including fever, chills, nausea and vomiting, and headache (Sehgal et al., 2023). Symptoms of hypotension, leukocytosis, and thrombocytopenia predominate during the hypotensive phase, and shock can also occur in patients with severe disease (Sehgal et al., 2023). The oliguric phase presents with reduced urine output or even anuria, hematuria, or proteinuria. Patients are at increased risk of acute renal injury, and > 50% of patients die in this period (Sehgal et al., 2023). In the polyuria phase, there is an increase in urine output and recovery from kidney damage, while in the recovery phase, symptoms such as fatigue and weakness are recovered (Jiang et al., 2016; Sehgal et al., 2023). HFRS has a high case fatality rate ranging 1–15%, with PUUA mainly caused in Europe and HTNV in Asia (Vaheri et al., 2013b; Shirai et al., 2016).

HFRS is a zoonotic disease transmitted through contact with water sources, food, and aerosols contaminated with rodent feces, urine, saliva, or direct bites (Douron et al., 1984; Shirai et al., 2016). Human-to-human transmission has also been reported (Vaheri et al., 2013a). Hantavirus is unusually stable and can survive at room temperature for over 10 days (Kallio et al., 2006; Hardestam et al., 2007). Unfortunately, the disease currently lacks specific antiviral therapies or vaccines and can only be treated with supportive care (Zou et al., 2016).

HFRS is associated with high mortality; however, there exists little summative evidence-based research on the epidemiology and clinical characteristics of HFRS-induced deaths. Therefore, this article presents a meta-analysis of the epidemiology and clinical symptoms of patients who died from HFRS. The findings may help improve clinical understanding and ability to treat patients with HFRS.

2 Methods

2.1 Data sources and searches

On October 5, 2023, English-and Chinese-language databases, including PubMed, Scopus, Embase, Web of Science, Proquest, Cochrane Library, Ovid, China National Knowledge Infrastructure Database, VIP Database, Wanfang Database, and SinoMed, were carefully searched. Using search strings such as "Hemorrhagic Fever with Renal Syndrome," "HFRS," "Hantavirus," "Epidemic Hemorrhagic Fever," and "Korean Hemorrhagic Fever." The literature search process and results are shown in Figure 1. The study was registered to the PROSPERO platform (CRD42023454553).

2.2 Selection criteria

To be included in this meta-analysis, the study had to feature patients that met one or more of the following diagnostic criteria: (1) serum-specific IgM positive or serum-specific IgG titers were more than four times higher during convalescence than during the acute phase, or hantavirus RNA was detected from patient specimens or isolation of hantavirus from patient specimens; (2) the study must be prospective or retrospective; (3) study results should include the total number of deaths and survivors and must provide laboratory data for the deceased and survival groups, respectively. Additionally, (1) non-Chinese or non-English studies, (2) conferences and literature reviews, and (3) duplicate publications were excluded.

2.3 Data extraction and quality assessment

Two independent reviewers (Lu and Tian) carefully reviewed and selected all included articles separately. In cases where the inclusion or exclusion of a particular study was in question, the reviewers reviewed the publication and arrived at a consensus decision. If unable to agree, the final decision was made by the third author/reviewer (Kuang).

For all available studies, two independent reviewers evaluated the quality of the included studies using the Newcastle–Ottawa Scale (NOS). Then, using the sorted table, the two jointly extracted data about authors, years, sample size, the patients' epidemiological and personal histories, signs and symptoms, laboratory test results, treatment, and final length of hospital stay from all included studies. Articles with available full text were carefully read before selection for inclusion. Disputes over the data in this study were resolved at the discretion of the third reviewer (Kuang).

2.4 Meta–analysis

Statistical analysis was performed using Stata 14.0 software. Continuous data are presented as standardized mean differences (SMDs), categorical data are expressed as odds ratios (ORs), and 95% confidence intervals (CIs). Cochran's Q and I^2 tests were used for heterogeneity assessment as follows:

$$Q = \sum_{i=1}^{K} w_i \left(x_i - \bar{x}_w \right)^2$$

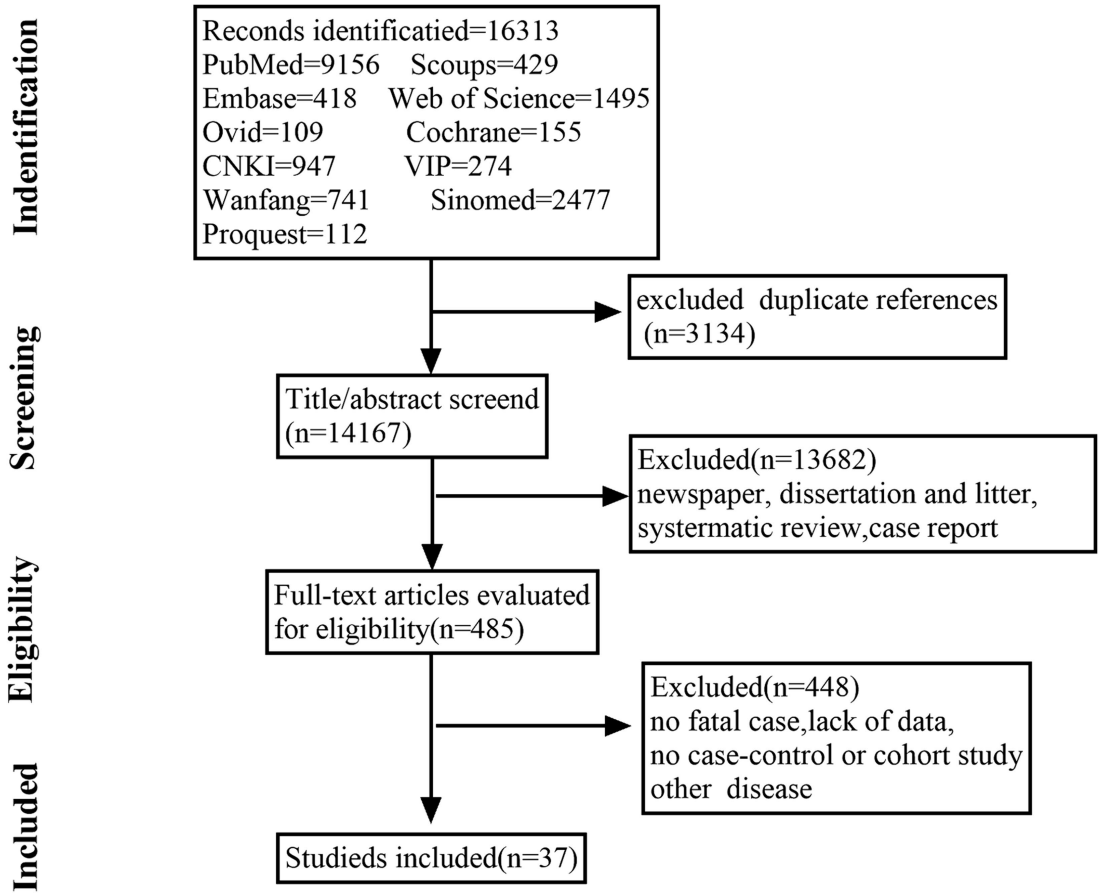

FIGURE 1
Flowchart of the literature screening process.

Here, x_i represents study I, s_i (i = 1, 2…, k).s_i represents the corresponding estimation standard error, $\bar{x}_w$ represents the reciprocal of the x_i variance estimate, and $w_i = 1/s_i^2$. I^2 was calculated as follows: $I^2 = 100\% \times (Q - df)/Q$, where Q denotes Cochran's Q heterogeneity statistic, and df denotes the degree of freedom (Hoaglin, 2016). Because a value of 0 is considered when I^2 is negative, the value of I^2 ranges between 0 and 100%. A p–value of >0.1 and I^2 of <50% indicate insignificant between-study heterogeneity, a fixed-effect model was subsequently used for analysis. Otherwise, sensitivity and subgroup analyses were used to determine the source of the heterogeneity. If the heterogeneity could not be resolved, a random-effects model was used. Funnel plots were used to indicate publication bias.

3 Results

3.1 Literature search, basic information, and quality assessment

A total of 16,313 candidate studies were identified. After removing those that did not meet the inclusion criteria, the full text of 485 articles was read. Finally, 37 articles were included in this study, resulting in a total sample size of 140, 295 cases. The quality of all included studies was scored using the NOS scale. Information on the studies and NOS scale scores are detailed in Table 1. All included studies were ≥ 6 stars.

3.2 Sex

A total of 16 articles contain sex-based analyses. The heterogeneity test revealed an I^2 of 0.00% and p-value of <0.1, indicating low heterogeneity between patients who died and those who survived. A fixed-effect model was chosen for this study. Ultimately, no significant sex-based differences were found between the two groups (OR = 0.991, 95% CI: 0.809–1.212, $p = 0.927$; Supplementary Figure S1A). The funnel plot appeared symmetric after the decompression of publication bias (Supplementary Figure S1B).

3.3 Age

On examining the 11 studies that collected age data, I^2 was 74% and the p-value was <0.1. A random-effects model revealed that patients who died tended to be older than those who survived (SMD = 0.478, 95% CI: 0.21–0.745, $p < 0.001$; Supplementary Figure S2A). After grouping the total number of cases in the included studies, subgroup analysis showed that heterogeneity was mainly attributable to studies with a total number greater than 300

TABLE 1 Basic information and quality assessment of the included literature.

Author	Year	Type	Survival	Death	NOS			
					Selection	Comparability	Outcome	Scores
Zhu et al. (2014)	2014	Case–control study	171	31	☆☆☆	☆☆☆	☆☆	8☆
Wang et al. (2023)	2023	Case–control study	233	75	☆☆☆	☆☆☆	☆☆☆	9☆
Wu et al. (1996)	1996	Case–control study	13	8	☆☆	☆☆	☆☆	6☆
Li et al. (2017)	2017	Case–control study	90	4	☆☆	☆☆	☆☆	6☆
Tang et al. (2005)	2005	Case–control study	93	10	☆☆☆	☆☆	☆☆	7☆
Tian and Li (2009)	2009	Case–control study	72	16	☆☆☆	☆☆	☆☆☆	8☆
Fan (2000)	2000	Case–control study	129	41	☆☆	☆☆	☆☆	6☆
Zong and Li (2001)	2001	Case–control study	160	9	☆☆	☆☆	☆☆	6☆
Du et al. (2023)	2023	Case–control study	78	13	☆☆☆	☆☆☆	☆☆☆	9☆
Tian et al. (2022)	2022	Case–control study	137	12	☆☆☆	☆☆☆	☆☆☆	9☆
Du et al. (2021)	2021	Case–control study	91	14	☆☆☆	☆☆☆	☆☆☆	9☆
Du et al., (2014d)	2014	Cohort study	46	29	☆☆☆	☆☆☆	☆☆☆	9☆
Fan et al. (2018)	2018	Case–control study	133	13	☆☆☆	☆☆☆	☆☆☆	9☆
Xiong and He (2006)	2006	Case–control study	180	33	☆☆☆	☆☆	☆☆☆	8☆
Che et al. (2022)	2022	Case–control study	359	14	☆☆☆	☆☆☆	☆☆☆	9☆
Li et al. (2016)	2016	Case–control study	107	22	☆☆☆	☆☆☆	☆☆☆	9☆
Pan et al. (2001)	2001	Case–control study	127	32	☆☆☆	☆☆	☆☆	7☆
Du et al. (2014b)	2014	Case–control study	27	21	☆☆☆	☆☆☆	☆☆☆	9☆
Ma et al. (2018)	2018	Case–control study	116	19	☆☆☆	☆☆☆	☆☆☆	9☆
Willemann and Oliveira (2014)	2014	Case–control study	281	158	☆☆☆	☆☆☆	☆☆☆	9☆
Luo et al. (2006)	2006	Case–control study	93	14	☆☆☆	☆☆☆	☆☆☆	9☆
Yang (2022)	2022	Case–control study	458	12	☆☆☆	☆☆	☆☆☆	8☆
Zhang et al. (2015)	2015	Case–control study	375	85	☆☆☆	☆☆	☆☆	7☆
Hu et al. (2023)	2023	Case–control study	2,113	132	☆☆☆	☆☆	☆☆☆	8☆
Li (2016)	2016	Case–control study	274	51	☆☆☆	☆☆☆	☆☆☆	9☆
Guo et al. (2012)	2012	Case–control study	90	30	☆☆☆	☆☆	☆☆☆	8☆
Du et al. (2014b)	2014	Case–control study	46	31	☆☆☆	☆☆	☆☆☆	8☆
Ye (2003)	2003	Case–control study	26	5	☆☆	☆☆	☆☆☆	7☆
Shang et al. (2009)	2009	Case–control study	78	19	☆☆	☆☆☆	☆☆☆	8☆
Yang (2012)	2012	Case–control study	45	7	☆☆☆	☆☆	☆☆	7☆
Qin (2015)	2015	Case–control study	26	10	☆☆	☆☆	☆☆	6☆
Xiong et al. (2012)	2012	Case–control study	348	21	☆☆	☆☆	☆☆	6☆
Fu and Yang, (2014)	2014	Case–control study	122,085	1,391	☆☆☆	☆☆	☆☆☆	8☆
Liu et al. (2017)	2017	Case–control study	1,536	7	☆☆☆	☆	☆☆☆	7☆
Du et al. (2014c)	2014	Case–control study	29	26	☆☆	☆☆	☆☆	6☆
Wu et al. (2014)	2014	Case–control study	7,220	78	☆☆☆	☆☆	☆☆	7☆
He et al. (2023)	2023	Case–control study	302	15	☆☆☆	☆☆☆	☆☆	8☆

(Supplementary Figure S2B). In the nine studies that included patients >60 years, the heterogeneity test revealed an I^2 of 47.8 and p-value of <0.1, indicating some heterogeneity in the selected literature (Supplementary Figure S2C). The sensitivity analyses indicated that the Fu et al. study may have been a major source of the observed heterogeneity (Fu and Yang, 2014; Supplementary Figure S2D). After removing this study, patients who died were found to be 2.409 times more likely to be aged >60 years compared to those who survived (95% CI: 1.895–3.063, $p < 0.001$; Supplementary Figure S2E).

3.4 Epidemiology and personal history

Five studies examined onset season (whether the onset occurred in October through December) and found no significant between-group difference (OR = 1.194, 95% CI: 0.699–2.039, $p = 0.517$; Supplementary Figure S3A). In the eight articles that included data on patient occupation (farmer or non-farmer), there were no significant between-group differences (OR = 1.047, 95% CI: 0.522–2.098, $p = 0.897$; Supplementary Figure S3B). In the study on patients' personal histories, significantly more patients who died were smokers than those who survived [the smoking rate was 1.357 times higher among those who died than among those who survived (95% CI: 1.030–1.787, $p = 0.030$; Supplementary Figure S3C)]. There was no significant between-group difference in alcohol consumption (OR = 1.007, 95% CI: 0.715–1.42, $p = 0.966$; Supplementary Figure S3D).

3.5 Hospital admissions

Basic information collected from patients on admission included their temperature at admission and the onset time. A total of seven studies analyzed the time from onset to hospital stay. Using a fixed-effect model, it was found that the onset time among patients who died was lower than that among those who survived (SMD = −0.391, 95% CI: −0.521 to −0.260, $p < 0.001$; Supplementary Figure S4A). However, four studies on body temperature at admission found no significant difference between the two groups (SMD = −0.006, 95% CI: −0.202 to 0.190, $p = 0.951$; Supplementary Figure S4B).

3.6 Comorbidities

The patients' main comorbidities included diabetes, hypertension, and coronary heart disease. Five articles included data on patients with diabetes, and the incidence of comorbid diabetes was 1.991 times higher among patients who died than among those who survived (95% CI: 1.080–3.670, $p = 0.027$; Supplementary Figure S5A). Five studies collected data on hypertension; the incidence of hypertension was 2.811 times higher among patients who died than among those who survived (95% CI: 2.009–3.933, $p < 0.001$; Supplementary Figure S5B). Three studies who examined patients with coronary disease were included, and no significant between-group differences were observed (OR = 6.849, 95% CI: 0.547–76.951, $p = 0.138$; Supplementary Figure S5C).

3.7 Clinical manifestations

Four studies collected data on multiple organ dysfunction syndrome (MODS). Patients who died were 76.93 times more likely to demonstrate MODS complications (95% CI: 12.689–466.432, $p < 0.001$; Supplementary Figure S6A) than those who survived. A total of four studies analyzed shock symptoms, and it was found that shock was 24.075 times more likely in patients who died than in those who survived (95% CI: 8.941–64.825, $p < 0.001$; Supplementary Figure S6B). Four studies described overlapping disease courses, and it was found that the probability of death was 4.412 times higher than that of survival (95% CI: 1.744–11.158, $p = 0.002$; Supplementary Figure S6C). Eleven studies collected data on bacteremia; there was no significant between-group difference in the incidence of concurrent bacteremia (OR = 1.997, 95% CI: 0.953–4.185, $p = 0.067$; Supplementary Figure S6D).

In studies involving patients with craniocerebral injuries, six analyzed symptoms of cerebral edema. Patients who died had 12.566 times higher incidence of cerebral edema than those who survived (95% CI: 4.428–35.659, $p < 0.001$; Supplementary Figure S7A). Three studies analyzed toxic encephalopathy, and patients who died had 9.71 times higher incidence than those who survived (95% CI: 2.847–33.12, $p < 0.001$; Supplementary Figure S7B). Three studies analyzed symptoms of brain hemorrhage; the incidence was 88.652 times higher among patients who died than among those who survived (95% CI: 31.454–249.863, $p < 0.001$; Supplementary Figure S7C). In three studies that analyzed twitch, the incidence was 9.341 times higher among those who died than among those who survived (95% CI: 1.721–50.397, $p = 0.010$; Supplementary Figure S7D).

Among patients with concurrent cardiac injuries, four had arrhythmia. Patients who died had a 4.337 times higher incidence of arrhythmia than those who survived (95% CI: 1.046–18.307, $p = 0.043$; Supplementary Figure S8A). Further, the incidence of heart failure was 5.55 times higher among those who died than among those who survived (95% CI = 3.638–9.609, $p < 0.001$; Supplementary Figure S8B).

Four studies analyzed patients with symptoms of lung injury. The incidence of dyspnea was 2.916 times higher (95% CI: 1.377–6.176, $p = 0.005$; Supplementary Figure S9A), the incidence of acute respiratory distress syndrome (ARDS) was 19.068 times higher (95% CI: 8.105–44.86, $p < 0.001$; Supplementary Figure S9B), and the incidence of lung infections was 3.58 times higher among those who died than among those who survived (95% CI: 1.399–9.158, $p = 0.008$; Supplementary Figure S9C).

Four studies analyzed digestive complications—including liver injury; here, the mortality rate was 3.905 times higher among those who died than among those who survived (95%CI: 1.98–7.703, $p < 0.001$; Supplementary Figure S10A). Of the 10 studies that analyzed gastrointestinal bleeding, the incidence was 2.784 times higher among those who died than among those who survived (95% CI: 1.602–4.839, $p < 0.001$; Supplementary Figure S10B).

Five studies on urinary system injuries included patients with acute kidney injury (AKI). The incidence of acute kidney injury was 0.323 times lower among those who died (95% CI: 0.114–0.911, $p = 0.033$; Supplementary Figure S11A) than among those who survived. Three studies analyzed urine protein levels; patients who died were 2.117 times more likely to demonstrate abnormal urine protein levels (95% CI: 1.602–4.839, $p < 0.001$; Supplementary Figure S11B) than those who survived.

3.8 Laboratory test results

Eleven studies analyzed white blood cell counts (WBC); elevated WBC counts were more common among patients who died (SMD = 0.717, 95% CI: 0.279–1.154, $p = 0.001$; Supplementary Figure S12A) than among those who survived. Thirteen studies analyzed platelet counts; here, patients who died were more likely to demonstrate reduced platelet counts (SMD = −1.072, 95% CI: −1.806 to −0.377, $p = 0.004$; Supplementary Figure S12B) than those who survived. Six studies analyzed hemoglobin levels, collectively revealing

no significant between-group differences (SMD = −0.157, 95% CI: −0.586 to 0.273, $p = 0.475$; Supplementary Figure S12C).

Three studies assessed lactate dehydrogenase levels. Patients who died were more likely to have elevated lactate dehydrogenase levels (SMD = 2.015, 95% CI: 0.524–3.506, $p = 0.008$; Supplementary Figure S13A) than those who survived. Similar results were found for aspartate aminotransferase (AST) (SMD = 1.067, 95% CI: 0.645–1.490, $p < 0.001$; Supplementary Figure S13B) and alanine aminotransferase (ALT) levels (SMD = 0.829, 95% CI: 0.258–0.936, $p = 0.002$; Supplementary Figure S13C). Five studies analyzed prothrombin time (PT), revealing that PT prolongation was more common among patients who died (SMD = 1.145, 95% CI: 0.426–1.827, $p < 0.001$; Supplementary Figure S13D) than among those who survived. Five studies analyzed activated partial thromboplastin time (APTT). Here, patients who died had significantly higher APTT levels than those who survived (SMD = 1.154, 95% CI: 0.436–1.873, $p = 0.002$; Supplementary Figure S13E). Nine studies included data on albumin levels. Patients who died had lower albumin levels than those who survived (SMD = −0.574, 95% CI: −0.855 to −0.293, $p < 0.001$; Supplementary Figure S13F). Patients who died were significantly more likely to demonstrate lower chloride ions (SMD = −0.449, 95% CI: −0.875 to −0.024, $p = 0.038$; Supplementary Figure S13G) and fibrinogen levels (SMD = −0.626, 95% CI: −0.8285 to −0.242, $p < 0.001$; Supplementary Figure S13H) than those who survived.

Across all examined studies, no significant differences were found in urea nitrogen (SMD = 0.362, 95% CI: −0.016 to 0.741, $p = 0.061$; Supplementary Figure S14A), serum creatinine (SMD = −0.007, 95% CI: −1.146 to 1.133, $p = 0.991$; Supplementary Figure S14B), sodium ions (SMD = −0.537, 95% CI: −1.09 to 0.015, $p = 0.057$; Supplementary Figure S14C), potassium ions (SMD = 1.147, 95% CI: −0.475 to 2.769, $p = 0.166$; Supplementary Figure S14D), and total bilirubin (SMD = 0.454, 95% CI: −0.028 to 0.936, $p = 0.065$; Supplementary Figure S14E) levels between those who died with those who survived.

3.9 Treatment

Interestingly, patients who died used more continuous renal replacement therapy (OR = 4.487, 95% CI: 1.186–16.981, $p = 0.027$; Supplementary Figure S15A) and less dialysis than those who survived (OR = 0.304, 95% CI: 0.201–0.459, $p < 0.001$; Supplementary Figure S15B). Four studies noted rates of mechanical ventilation, identifying no significant between-group differences (OR = 4.709, 95% CI: 0.471–47.118, $p = 0.187$; Supplementary Figure S15C).

3.10 Hospitalization

Nine studies included length of hospital stay as a dependent variable, with $I^2 > 50\%$ and p-value <0.1. Consequently, a random-utility model was used to determine that patients who died had a shorter average length of hospital stay than those who survived (SMD = −1.426, 95% CI: −2.168 to −0.685, $p < 0.001$; Supplementary Figure S16A). The source of this heterogeneity comprised literature published between 2018 and 2022 after subgroup analysis (Supplementary Figure S16B).

4 Discussion

HFRS is an infectious disease mainly endemic to Asia and Europe, with China and South Korea being the main endemic regions (Jiang et al., 2016; Dong et al., 2019); however, its incidence throughout Europe and Asia is increasing. Consequently, HFRS is a serious public health concern in its endemic regions.

Although HFRS is more common in men than in women, women are at a higher risk of death from the condition (Klein et al., 2011). Surprisingly, we found no significant sex-based was found between patients who died and those who survived; however, older patients were at a higher risk of death. Fu et al.'s well-powered study found that patients aged >60 years were at a higher risk of death (Fu and Yang, 2014). The present study's sensitivity analysis revealed considerable heterogeneity in results, possibly attributed to the large sample size of the Fu et al. study; however, the risk of death in patients aged >60 years remained high even after the removal of this study. This disparity may be related to older patients' immune statuses, underlying medical conditions, and the prevalence of immunization among adolescents (He et al., 2013).

Studies that reported personal history data found that smokers were at a higher risk of death than nonsmokers. Other studies found smoking to be a risk factor for HFRS infection, given the ability of nicotine to increase oxidative stress and damage the kidneys (Laine et al., 2012; Arany et al., 2013; Tervo et al., 2015; Latronico et al., 2018). However, no significant between-group difference in alcohol consumption was observed, similar to the findings reported by Tervo et al. (2022). Mantula et al. (2017) showed that hyperglycemia is a risk factor for poor prognosis in patients with HFRS. In these studies, patients with diabetes were at a higher risk of death (Mantula et al., 2017; Tietavainen et al., 2019, 2021). It is hypothesized that this may be related to the ability of diabetes to increase endothelial dysfunction through oxidative stress (Karan et al., 2020). More patients with hypertension died, and studies have also shown that hypertension affects long-term prognosis in patients with HFRS (Latus et al., 2015), likely because of the association between vascular endothelial damage and aggravated hypertension.

Similar to Jiang et al.'s findings, patients who died were more likely to demonstrate multistage overlap (Jiang et al., 2016), including shock and multiorgan damage, central nervous system damage, and injuries to the lungs, heart, liver, and kidneys. These effects could be caused by the invading hantavirus's effects on the endothelial cells of the host's organs, eliciting a strong immune response (Liu et al., 2019). Patients who died also had a higher rate of ARDS than those who survived, potentially attributable to acute progressive noncardiogenic pulmonary edema (Zou et al., 2016).

Similarly, our studies on patients' cardiovascular systems showed higher rates of heart failure and arrhythmias among those who died than among those who survived. A Swedish study also showed that cardiovascular disease frequently causes HFRS-related deaths (Connolly-Andersen et al., 2013). Patients in the concomitant death group were more likely to demonstrate proteinuria, typical of HFRS. Additionally, proteinuria is a known risk factor for HFRS complicated by acute pancreatitis (Wang et al., 2023).

Furthermore, laboratory analyses results revealed that patients who died had lower platelet counts than those who survived. This could have resulted from impaired platelet production, impaired thrombin aggregation during hantavirus infection, and

hantavirus-guided resting platelets adhering to infected endothelial cells, leading to circulating thrombocytopenia (Gavrilovskaya et al., 2010; Laine et al., 2015). Thrombocytopenia is associated with HFRS and severe kidney damage and is frequently considered when diagnosing HFRS (Denecke et al., 2010). Similarly, patients who died had prolonged PT and APTT, potentially resulting from tissue factor upregulation caused by the inflammatory storm, leading to coagulation dysfunction and ultimately increasing endothelial cell permeability (Puhlmann et al., 2005). Among patients who died, elevated WBC count was associated with inflammation; the cytokine storm in HFRS patients could also lead to leukocyte extravasation by affecting the permeability of endothelial cells (Nourshargh and Alon, 2014). Decreased fibrinogen in patients with HFRS who died may be due to the lysis of prothrombin into fibrin monomers during coagulation (Koskela et al., 2021; Sehgal et al., 2023). Patients who died had higher AST and ALT levels than those who survived (routinely measured in patients with HFRS). Hantaviruses can invade multiple organ systems, and AST abnormalities are associated with a poorer prognosis (He et al., 2023).

In the present study, patients who died while receiving supportive care for HFRS were more likely to receive renal replacement therapy. Sargianou et al. showed that timely and correct supportive care improved survival with HFRS (Sargianou et al., 2012). Furthermore, continuous renal therapy was previously deemed suitable for patients with severe HFRS, those with multiorgan damage, and those with encephalopathy and other complications, consistent with the present study results (Jiang et al., 2016). Interestingly, it was found that AKI was more pronounced in patients who survived than in those who died. Outinen et al.'s (2015) study also reported that severe AKI is not a risk factor for HFRS-induced death in patients. This is because patients who died are more likely to have overlapping stages of fever, hypotension, and oliguria, and are in a critical condition that might result in death from other fatal comorbidities, such as ARDS (Du et al., 2014a). The overlapping phase of HFRS usually occurs early in the course of the disease, when acute renal failure, one of the severe stages of AKI, has not yet developed or been detected. Timely dialysis treatment can also improve the prognosis of patients with acute renal failure (Mehta et al., 2007; Zhu et al., 2014). In contrast, urine protein appears significantly earlier than acute kidney failure and has been shown to be a risk factor for the prognosis of HFRS (Mantula et al., 2017).

This study has several limitations that should be considered. First, only English and Chinese articles were reviewed; studies in Spanish, French, or other languages were not included, potentially introducing bias. Second, between-group comparisons of viral loads were lacking. Third, the study data were insufficient for meta-analyzing patients' inflammatory factor storms, resulting in some heterogeneity in the study results, and the possibility of bias. Therefore, additional well-powered investigations are needed in the future.

5 Conclusion

The present meta-analysis results demonstrated a significant difference between patients who died and those who survived. Specifically, patients who died demonstrated more severe disease than those who survived. Patients with personal histories of smoking, diabetes, and high blood pressure were at a higher risk of death than those who survived. Patients who died also demonstrated more severe damage to the central nervous system, lungs, and heart, and significantly fewer platelets and higher urine protein levels than those who survived (Supplementary Table S1). These findings can be used to assess clinical practice methods and to ascertain prognosis.

Data availability statement

The original contributions presented in the study are included in the article/Supplementary material, further inquiries can be directed to the corresponding author.

Author contributions

WL: Writing – original draft. LK: Writing – review & editing. YH: Writing – review & editing, Methodology. JS: Methodology, Writing – review & editing. QL: Methodology, Writing – original draft. WT: Methodology, Writing – review & editing.

Funding

The author(s) declare financial support was received for the research, authorship, and/or publication of this article. This work was supported by the National Natural Science Foundation of China (82174391) and received funding from the Hunan Key Subject of Integrated Traditional Chinese and Western Medicine.

Conflict of interest

The authors declare that the research was conducted in the absence of any commercial or financial relationships that could be construed as a potential conflict of interest.

Publisher's note

All claims expressed in this article are solely those of the authors and do not necessarily represent those of their affiliated organizations, or those of the publisher, the editors and the reviewers. Any product that may be evaluated in this article, or claim that may be made by its manufacturer, is not guaranteed or endorsed by the publisher.

Supplementary material

The Supplementary material for this article can be found online at: https://www.frontiersin.org/articles/10.3389/fmicb.2024.1329683/full#supplementary-material

References

Afzal, S., Ali, L., Batool, A., Afzal, M., Kanwal, N., Hassan, M., et al. (2023). Hantavirus: an overview and advancements in therapeutic approaches for infection. *Front. Microbiol.* 14:1233433. doi: 10.3389/fmicb.2023.1233433

Arany, I., Clark, J., Reed, D. K., and Juncos, L. A. (2013). Chronic nicotine exposure augments renal oxidative stress and injury through transcriptional activation of p66shc. *Nephrol. Dial. Transplant.* 28, 1417–1425. doi: 10.1093/ndt/gfs596

Che, L., Wang, Z., Du, N., Li, L., Zhao, Y., Zhang, K., et al. (2022). Evaluation of serum ferritin, procalcitonin, and c-reactive protein for the prediction of severity and mortality in hemorrhagic fever with renal syndrome. *Front. Microbiol.* 13:865233. doi: 10.3389/fmicb.2022.865233

Connolly-Andersen, A. M., Ahlm, K., Ahlm, C., and Klingstrom, J. (2013). Puumala virus infections associated with cardiovascular causes of death. *Emerg. Infect. Dis.* 19, 126–128. doi: 10.3201/eid1901.111587

Denecke, B., Bigalke, B., Haap, M., Overkamp, D., Lehnert, H., and Haas, C. S. (2010). Hantavirus infection: a neglected diagnosis in thrombocytopenia and fever? *Mayo Clin. Proc.* 85, 1016–1020. doi: 10.4065/mcp.2009.0040

Dong, Y., Ma, T., Zhang, X., Ying, Q., Han, M., Zhang, M., et al. (2019). Incorporation of cd40 ligand or granulocyte-macrophage colony stimulating factor into hantaan virus (htnv) virus-like particles significantly enhances the long-term immunity potency against htnv infection. *J. Med. Microbiol.* 68, 480–492. doi: 10.1099/jmm.0.000897

Douron, E., Moriniere, B., Matheron, S., Girard, P. M., Gonzalez, J. P., Hirsch, F., et al. (1984). Hfrs after a wild rodent bite in the haute-savoie--and risk of exposure to hantaan-like virus in a Paris laboratory. *Lancet* 1, 676–677. doi: 10.1016/s0140-6736(84)92187-1

Du, H., Hu, H., Li, J., Wang, X., Jiang, H., Lian, J., et al. (2023). High levels of exfoliated fragments following glycocalyx destruction in hemorrhagic fever with the renal syndrome are associated with mortality risk. *Front Med (Lausanne)* 10:1096353. doi: 10.3389/fmed.2023.1096353

Du, H., Hu, H., Wang, P., Wang, X., Zhang, Y., Jiang, H., et al. (2021). Predictive value of pentraxin-3 on disease severity and mortality risk in patients with hemorrhagic fever with renal syndrome. *BMC Infect. Dis.* 21:445. doi: 10.1186/s12879-021-06145-0

Du, H., Li, J., Jiang, W., Yu, H., Zhang, Y., Wang, J., et al. (2014a). Clinical study of critical patients with hemorrhagic fever with renal syndrome complicated by acute respiratory distress syndrome. *PLoS One* 9:e89740. doi: 10.1371/journal.pone.0089740

Du, H., Li, J., Wang, P., and Bai, X. (2014b). Application of renal replacement therapy in critical patients with hemorrhagic fever and renal syndrome. *Med. J. Chin. Peoples Liber. Army* 26, 42–45. doi: 10.3969/j.issn.2095-140X.2014.04.013

Du, H., Li, J., Yu, H. T., and Rong, Z. (2014c). Application of continuous renal replacement therapy and intermittent hemodialysis in patients with severe hemorrhagic fever with renal syndrome. *Infect. Dis. Inf.* 27, 18–21.

Du, H., Wang, P. Z., Li, J., Bai, L., Li, H., Yu, H. T., et al. (2014d). Clinical characteristics and outcomes in critical patients with hemorrhagic fever with renal syndrome. *BMC Infect. Dis.* 14:191. doi: 10.1186/1471-2334-14-191

Fan, H. (2000). Analysis of factors related to secondary shock secondary to hemorrhagic fever with renal syndrome. *Chin. Crit. Care Med.* 12:239. doi: 10.3760/j.issn:1003-0603.2000.04.021

Fan, X., Deng, H., Sang, J., Li, N., Zhang, X., Han, Q., et al. (2018). High serum procalcitonin concentrations in patients with hemorrhagic fever with renal syndrome caused by hantaan virus. *Front. Cell. Infect. Microbiol.* 8:129. doi: 10.3389/fcimb.2018.00129

Fu, M., and Yang, H. (2014). Analysis of epidemic haemorrhagic fever epidemic characteristics in China from 2004 to 2012. *China Health Ind.* 11, 35–36. doi: 10.16659/j.cnki.1672-5654.2014.28.042

Gavrilovskaya, I. N., Gorbunova, E. E., and Mackow, E. R. (2010). Pathogenic hantaviruses direct the adherence of quiescent platelets to infected endothelial cells. *J. Virol.* 84, 4832–4839. doi: 10.1128/JVI.02405-09

Guo, N., Cui, S., Wang, X., and Cui, H. (2012). Role of hemorrhagic fever with renal syndrome(hfrs) critical score in predicting the prognosis for patients with hfrs. *J. Shandong Univ.* 50, 67–70. doi: 10.6040/j.issn.1671-7554.2012.11.014

Hardestam, J., Simon, M., Hedlund, K. O., Vaheri, A., Klingstrom, J., and Lundkvist, A. (2007). Ex vivo stability of the rodent-borne hantaan virus in comparison to that of arthropod-borne members of the bunyaviridae family. *Appl. Environ. Microbiol.* 73, 2547–2551. doi: 10.1128/AEM.02869-06

He, S., Han, Q., Wang, X., Zhang, X., Li, N., and Liu, Z. (2023). Aspartate aminotransferase to platelet ratio at admission can predict the prognosis of patients with hemorrhagic fever with renal syndrome. *J. Med. Virol.* 95:e29126. doi: 10.1002/jmv.29126

He, X., Wang, S., Huang, X., and Wang, X. (2013). Changes in age distribution of hemorrhagic fever with renal syndrome: an implication of China's expanded program of immunization. *BMC Public Health* 13:394. doi: 10.1186/1471-2458-13-394

Hoaglin, D. C. (2016). Misunderstandings about q and 'cochran's q test' in meta-analysis. *Stat. Med.* 35, 485–495. doi: 10.1002/sim.6632

Hu, H. F., Zhan, J. Y., Du, H., and Yang, Y. Y. (2023). Clinical epidemiological characteristics and prognostic risk factors in 2 245 patients with hemorrhagic fever with renal syndrome. *Chin. J. Infect. Dis.* 41, 70–76. doi: 10.3760/cma.j.cn311365-20220422-00141

Jiang, H., Du, H., Wang, L. M., Wang, P. Z., and Bai, X. F. (2016). Hemorrhagic fever with renal syndrome: pathogenesis and clinical picture. *Front. Cell. Infect. Microbiol.* 6:1. doi: 10.3389/fcimb.2016.00001

Jiang, H., Zheng, X., Wang, L., Du, H., Wang, P., and Bai, X. (2017). Hantavirus infection: a global zoonotic challenge. *Virol. Sin.* 32, 32–43. doi: 10.1007/s12250-016-3899-x

Jonsson, C. B., Figueiredo, L. T., and Vapalahti, O. (2010). A global perspective on hantavirus ecology, epidemiology, and disease. *Clin. Microbiol. Rev.* 23, 412–441. doi: 10.1128/CMR.00062-09

Kallio, E. R., Klingstrom, J., Gustafsson, E., Manni, T., Vaheri, A., Henttonen, H., et al. (2006). Prolonged survival of puumala hantavirus outside the host: evidence for indirect transmission via the environment. *J. Gen. Virol.* 87, 2127–2134. doi: 10.1099/vir.0.81643-0

Karan, A., Bhakkiyalakshmi, E., Jayasuriya, R., Sarada, D., and Ramkumar, K. M. (2020). The pivotal role of nuclear factor erythroid 2-related factor 2 in diabetes-induced endothelial dysfunction. *Pharmacol. Res.* 153:104601. doi: 10.1016/j.phrs.2019.104601

Klein, S. L., Marks, M. A., Li, W., Glass, G. E., Fang, L. Q., Ma, J. Q., et al. (2011). Sex differences in the incidence and case fatality rates from hemorrhagic fever with renal syndrome in China, 2004-2008. *Clin. Infect. Dis.* 52, 1414–1421. doi: 10.1093/cid/cir232

Koskela, S., Makela, S., Strandin, T., Vaheri, A., Outinen, T., Joutsi-Korhonen, L., et al. (2021). Coagulopathy in acute puumala hantavirus infection. *Viruses* 13:1553. doi: 10.3390/v13081553

Laenen, L., Vergote, V., Calisher, C. H., Klempa, B., Klingstrom, J., Kuhn, J. H., et al. (2019). Hantaviridae: current classification and future perspectives. *Viruses* 11:788. doi: 10.3390/v11090788

Laine, O., Joutsi-Korhonen, L., Lassila, R., Koski, T., Huhtala, H., Vaheri, A., et al. (2015). Hantavirus infection-induced thrombocytopenia triggers increased production but associates with impaired aggregation of platelets except for collagen. *Thromb. Res.* 136, 1126–1132. doi: 10.1016/j.thromres.2015.10.003

Laine, O., Joutsi-Korhonen, L., Makela, S., Mikkelsson, J., Pessi, T., Tuomisto, S., et al. (2012). Polymorphisms of pai-1 and platelet gp ia may associate with impairment of renal function and thrombocytopenia in puumala hantavirus infection. *Thromb. Res.* 129, 611–615. doi: 10.1016/j.thromres.2011.11.007

Latronico, F., Maki, S., Rissanen, H., Ollgren, J., Lyytikainen, O., Vapalahti, O., et al. (2018). Population-based seroprevalence of puumala hantavirus in Finland: smoking as a risk factor. *Epidemiol. Infect.* 146, 367–371. doi: 10.1017/S0950268817002904

Latus, J., Schwab, M., Tacconelli, E., Pieper, F. M., Wegener, D., Dippon, J., et al. (2015). Clinical course and long-term outcome of hantavirus-associated nephropathia epidemica, Germany. *Emerg. Infect. Dis.* 21, 76–83. doi: 10.3201/eid2101.140861

Li, Q. (2016). Analysis of prognostic factors influencing patients with hemorrhagic fever with renal syndrome and early warning intervention countermeasures. *Chin. J. Control Endem. Dis.* 31, 690–691.

Li, S., Tian, Y., Zhao, G., and Ma, J. (2016). Analysis on risk factors of 22 cases of hemorrhagic fever with renal syndrome. *China Mod. Doct.* 54, 81–84.

Li, X., Zhang, S., and Cao, H. H. (2017). Relationship between blood changes and prognosis in patients with hemorrhagic fever with renal syndrome. *J. Trop. Med.* 17, 772–775. doi: 10.3969/j.issn.1672-3619.2017.06.021

Liu, J., Deng, A., and Peng, Z. (2017). Analysis of epidemiologic characteristics of hemorrhagic fever patients with renal syndrome (hfrs) in Guangdong from 2009 to 2013. *J. Med. Pest Control* 33, 606–609. doi: 10.7629/yxdwfz201706005

Liu, R., Ma, H., Shu, J., Zhang, Q., Han, M., Liu, Z., et al. (2019). Vaccines and therapeutics against hantaviruses. *Front. Microbiol.* 10:2989. doi: 10.3389/fmicb.2019.02989

Luo, R., Chen, Y., and Zhang, Y. (2006). Prognosis of hemorrhagic fever with renal syndrome used by roc curves and discriminant analysis. *Chin. J. Zoonoses* 5, 481–482. doi: 10.3969/j.issn.1002-2694.2006.05.028

Ma, X., Li, F., Yang, H., Wang, F., and Zhao, H. (2018). The timing of treatment and prognostic factors by continuous renai repiacement therapy in severe hemorrhagic fever with renai svndrome. *China Trop. Med.* 20, 927–930. doi: 10.1186/s12879-020-05638-8

Manigold, T., and Vial, P. (2014). Human hantavirus infections: epidemiology, clinical features, pathogenesis and immunology. *Swiss Med. Wkly.* 144:w13937. doi: 10.4414/smw.2014.13937

Mantula, P. S., Outinen, T. K., Clement, J., Huhtala, H., Porsti, I. H., Vaheri, A., et al. (2017). Glomerular proteinuria predicts the severity of acute kidney injury in puumala hantavirus-induced tubulointerstitial nephritis. *Nephron* 136, 193–201. doi: 10.1159/000459634

Mehta, R. L., Kellum, J. A., Shah, S. V., Molitoris, B. A., Ronco, C., Warnock, D. G., et al. (2007). Acute kidney injury network: report of an initiative to improve outcomes in acute kidney injury. *Crit. Care* 11:R31. doi: 10.1186/cc5713

Nourshargh, S., and Alon, R. (2014). Leukocyte migration into inflamed tissues. *Immunity* 41, 694–707. doi: 10.1016/j.immuni.2014.10.008

Outinen, T. K., Makela, S., Clement, J., Paakkala, A., Porsti, I., and Mustonen, J. (2015). Community acquired severe acute kidney injury caused by hantavirus-induced hemorrhagic fever with renal syndrome has a favorable outcome. *Nephron* 130, 182–190. doi: 10.1159/000433563

Pan, T., Xiu, T., Gong, Q., and Zhang, S. C. (2001). Analysis of causes of death from hemorrhagic fever with renal syndrome in 32 cases. *Jiangsu Med. J.* 27:465. doi: 10.3969/j.issn.0253-3685.2001.06.040

Puhlmann, M., Weinreich, D. M., Farma, J. M., Carroll, N. M., Turner, E. M., and Alexander, H. J. (2005). Interleukin-1beta induced vascular permeability is dependent on induction of endothelial tissue factor (tf) activity. *J. Transl. Med.* 3:37. doi: 10.1186/1479-5876-3-37

Qin, G. (2015). Clinical analysis of blood sodium and urea nitrogen values in oliguric phase in 169 patients with hemorrhagic fever. *Yianbian Med. J.* 43:44.

Sargianou, M., Watson, D. C., Chra, P., Papa, A., Starakis, I., Gogos, C., et al. (2012). Hantavirus infections for the clinician: from case presentation to diagnosis and treatment. *Crit. Rev. Microbiol.* 38, 317–329. doi: 10.3109/1040841X.2012.673553

Sehgal, A., Mehta, S., Sahay, K., Martynova, E., Rizvanov, A., Baranwal, M., et al. (2023). Hemorrhagic fever with renal syndrome in asia: history, pathogenesis, diagnosis, treatment, and prevention. *Viruses* 15:561. doi: 10.3390/v15020561

Shang, Q., Yu, J., and Wang, Y. (2009). Analysis of prognostic factors of severe renal syndrome. *Pract. J. Med. Pharm.* 26, 19–20. doi: 10.3969/j.issn.1671-4008.2009.01.009

Shirai, H., Yashima, J., Tojimbara, T., and Honda, K. (2016). Thrombotic microangiopathy caused by oral contraceptives in a kidney transplant recipient. *Nephrology (Carlton)* 21, 41–43. doi: 10.1111/nep.12769

Tang, Z., Ye, X., and Liao, Y. (2005). Clinical observation of liver damages in epidemic hemorrhagic fever. *J. First Mil. Med. Univ.* 5, 593–594. doi: 10.3321/j.issn:1673-4254.2005.05.029

Tariq, M., and Kim, D. M. (2022). Hemorrhagic fever with renal syndrome: literature review, epidemiology, clinical picture and pathogenesis. *Infec. Chemother.* 54, 1–19. doi: 10.3947/ic.2021.0148

Tervo, L., Makela, S., Syrjanen, J., Huttunen, R., Rimpela, A., Huhtala, H., et al. (2015). Smoking is associated with aggravated kidney injury in puumala hantavirus-induced haemorrhagic fever with renal syndrome. *Nephrol. Dial. Transplant.* 30, 1693–1698. doi: 10.1093/ndt/gfv273

Tervo, L., Outinen, T. K., Makela, S., Mustalahti, J., Huhtala, H., Porsti, I., et al. (2022). Alcohol consumption and its influence on the clinical picture of puumala hantavirus infection. *Viruses* 14:500. doi: 10.3390/v14030500

Tian, X., and Li, H. (2009). Clinical analysis of the treatment of hemorrhagic fever with renal syndrome. *J. Qiqihar Univ. Med.* 30, 924–925. doi: 10.3969/j.issn.1002-1256.2009.08.015

Tian, Z., Yao, N., Wu, Y., Wang, F., and Zhao, Y. (2022). Serum superoxide dismutase level is a potential biomarker of disease prognosis in patients with hemorrhagic fever with renal syndrome caused by the hantaan virus. *BMC Infect. Dis.* 22:446. doi: 10.1186/s12879-022-07394-3

Tietavainen, J., Makela, S., Huhtala, H., Porsti, I. H., Strandin, T., Vaheri, A., et al. (2021). The clinical presentation of puumala hantavirus induced hemorrhagic fever with renal syndrome is related to plasma glucose concentration. *Viruses* 13:1177. doi: 10.3390/v13061177

Tietavainen, J., Mantula, P., Outinen, T., Huhtala, H., Porsti, I. H., Niemela, O., et al. (2019). Glucosuria predicts the severity of puumala hantavirus infection. *Kidney Int. Rep.* 4, 1296–1303. doi: 10.1016/j.ekir.2019.05.770

Vaheri, A., Henttonen, H., Voutilainen, L., Mustonen, J., Sironen, T., and Vapalahti, O. (2013a). Hantavirus infections in europe and their impact on public health. *Rev. Med. Virol.* 23, 35–49. doi: 10.1002/rmv.1722

Vaheri, A., Strandin, T., Hepojoki, J., Sironen, T., Henttonen, H., Makela, S., et al. (2013b). Uncovering the mysteries of hantavirus infections. *Nat. Rev. Microbiol.* 11, 539–550. doi: 10.1038/nrmicro3066

Wang, T., Du, H., and Zhao, Y. (2023). Analysis of clinical characteristics and construction of death risk model of severe patients with hemorrhagic fever with renal syndrome. *Infect. Dis. Inf.* 36, 43–50. doi: 10.3969/j.issn.1007-8134.2023.01.06

Willemann, M. C., and Oliveira, S. V. (2014). Risk factors associated with hantavirosis fatality: a regional analysis from a case-control study in Brazil. *Rev. Soc. Bras. Med. Trop.* 47, 47–51. doi: 10.1590/0037-8682-0243-2013

Wu, W., Guo, J. Q., and Guan, P. (2014). Analysis of epidemiological features of hemorrhagic fever with renal syndrome and associated environmental risk factors in Liaoning province, China during 2005-2007. *Chin. J. Vector Biol. Control* 25, 39–42. doi: 10.11853/j.issn.1003.4692.2014.01.011

Wu, A. H., Tan, D. M., and Ren, P. S. (1996). Study of serum ldh and hbd levels in patients with hemorrhagic fever with renal syndrome. *J. Central South Univ.* 1, 75–77.

Xiong, X., Cheng, H., and Shi, G. (2012). Analysis on death risk of severe cases of hemorrhagic fever with renal syndrome in gaoan city, Jiangxi province in 2010. *Pract. Prev. Med.* 19, 1650–1652. doi: 10.3969/j.issn.1006-3110.2012.11.015

Xiong, Q., and He, S. (2006). Univariate analysis affecting the prognosis of hemorrhagic fever with renal syndrome. *J. Chin. Phys.* 8, 537–538. doi: 10.3760/cma.j.issn.1008-1372.2006.04.059

Yang, L. (2012). Cases of 52 severe hemorrhagic fever with renal syndrome and multiple organ dysfunction syndrome analysis. *Chin. J. Zoonoses* 28, 410–411. doi: 10.3969/j.issn.1002-2694.2012.04.023

Yang, K. (2022). Investigation and analysis of risk factors of death in patients with epidemic hemorrhagic fever. *Nurs. Pract. Res.* 19, 200–203. doi: 10.3969/j.issn.1672-9676.2022.02.009

Ye, P. (2003). Clinical nursing of secondary infection of hemorrhagic fever with severe and critical renal syndrome. Shanghai journal of. *Prev. Med.* 15:405:411. doi: 10.3969/j.issn.1004-9231.2003.08.025

Zhang, J., Zheng, X., Wang, X., and Xie, F. (2015). The clinical analysis of 460 cases of hemorrhagic fever with renal syndrome complicated by multiple organ dysfunction syndrome. *J. North Sichuan Med. Coll.* 30, 626–629. doi: 10.3969/j.issn.1005-3697.2015.05.13

Zhu, W., Zhang, X., Ran, X., Hu, X., and Xu, R. (2014). Analysis of prognostic factors affecting 202 cases of hemorrhagic fever with severe renal syndrome. *Chin. J. Clin. Res.* 27, 299–301. doi: 10.13429/j.cnki.cjcr.2014.03.019

Zong, R., and Li, C. (2001). Detection and analysis of epidemic hemorrhagic fever complicated by liver damage. *Heihe Sci. Technol.* 3:53.

Zou, L. X., Chen, M. J., and Sun, L. (2016). Haemorrhagic fever with renal syndrome: literature review and distribution analysis in China. *Int. J. Infect. Dis.* 43, 95–100. doi: 10.1016/j.ijid.2016.01.003

Zuo, S. Q., Fang, L. Q., Zhan, L., Zhang, P. H., Jiang, J. F., Wang, L. P., et al. (2011). Geo-spatial hotspots of hemorrhagic fever with renal syndrome and genetic characterization of Seoul variants in Beijing, China. *PLoS Negl. Trop. Dis.* 5:e945. doi: 10.1371/journal.pntd.0000945

Frontiers in Microbiology

Explores the habitable world and the potential of microbial life

The largest and most cited microbiology journal which advances our understanding of the role microbes play in addressing global challenges such as healthcare, food security, and climate change.

Discover the latest Research Topics

See more →

Frontiers

Avenue du Tribunal-Fédéral 34
1005 Lausanne, Switzerland
frontiersin.org

Contact us

+41 (0)21 510 17 00
frontiersin.org/about/contact